Advances in Biochemistry in Health and Disease

Sajal Chakraborti
Naranjan S. Dhalla *Editors*

Regulation of Ca^{2+}-ATPases, V-ATPases and F-ATPases

Springer

Advances in Biochemistry in Health and Disease

Series Editor: Naranjan S. Dhalla
Winnipeg, Manitoba, Canada

Volume 1: S. K. Cheema (ed), *Biochemistry of Atherosclerosis*

Volume 2: S. W. Schaffer and M-Saadeh Suleiman (eds), *Mitochondria: The Dynamic Organelle*

Volume 3: A. K. Srivastava and M. B. Anand-Srivastava (eds), *Signal Transduction in the Cardiovascular System in Health and Disease*

Volume 4: B. Ostadal and N. S. Dhalla (eds), *Cardiac Adaptations-Molecular Mechanisms*

Volume 5: B. I. Jugdutt and N. S. Dhalla (eds), *Cardiac Remodeling-Molecular Mechanisms*

Volume 6: Jawahar L. Mehta and N. S. Dhalla (eds), *Biochemical Basis and Therapeutic Implications of Angiogenesis*

Volume 7: S. Chakraborti and N. S. Dhalla (eds), *Proteases in Health and Disease*

Volume 8: S. Chakraborti and N. S. Dhalla (eds), *Role of Proteases in Cellular Dysfunction*

Volume 9: B. Turan and N. S. Dhalla (eds), *Diabetic Cardiomyopathy: Biochemical and Molecular Mechanisms*

Volume 10: P. S. Tappia and N. S. Dhalla (eds), *Phospholipases in Heaith and Disease*

Volume 11: G. D. Lopaschuk and N. S. Dhalla (eds), *Cardiac Energy Metabolism in Health and Disease*

Volume 12: K. Ahmed, O.-G. Issinger, and R. Szyszka (eds), *Protein Kinase CK2 Cellular Function in Normal and Disease States*

Volume 13: I. M. C. Dixon and J. Wigle (eds), *Cardiac Fibrosis and Heart Failure: Cause or Effect?*

Volume 14: S. Chakraborti and N. S. Dhalla (eds), *Regulation of Ca^{2+}-ATPases, V-ATPases and F-ATPases*

More information about this series at http://www.springer.com/series/7064

Sajal Chakraborti • Naranjan S. Dhalla
Editors

Regulation of Ca^{2+}-ATPases, V-ATPases and F-ATPases

Springer

Editors
Sajal Chakraborti
Biochemistry and Biophysics
University of Kalyani
Kalyani, West Bengal, India

Naranjan S. Dhalla
St. Boniface Hospital Research
Institute of Cardiovascular Science
Winnipeg, MB, Canada

Advances in Biochemistry in Health and Disease
ISBN 978-3-319-24778-6 ISBN 978-3-319-24780-9 (eBook)
DOI 10.1007/978-3-319-24780-9

Library of Congress Control Number: 2015956768

Springer Cham Heidelberg New York Dordrecht London

Printed on acid-free paper

Springer International Publishing AG Switzerland is part of Springer Science+Business Media (www.springer.com)

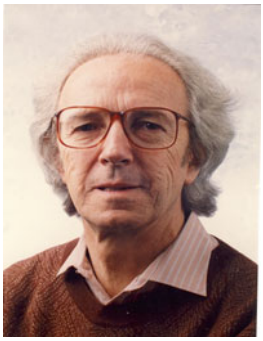

Ernesto Carafoli

This book on the Regulation of Ca^{2+}-ATPases, V-ATPases, and F-ATPases is dedicated to Professor Ernesto Carafoli for his outstanding leadership in the field of membrane biology. Dr. Ernesto Carafoli was born in 1932 in Italy. He received his M.D. from the University of Modena, Italy, in the year 1957 and thereafter joined as an Assistant Professor of General Pathology in the same University. He was a Fogarty International postdoc fellow in the laboratory of Dr. Albert Lehninger at the Johns Hopkins University School of Medicine, Baltimore, during 1963–1965 and he was Visiting Lecturer in the same Laboratory in 1968–1969. In 1973, he moved

to the Swiss Federal Institute of Technology, Zurich, as a Professor of Biochemistry. After serving the Department for 25 years, he returned to Italy in 1998 and joined the University of Padova as Professor of Biochemistry and later as the Director of the Venetian Institute of Molecular Medicine (VIMM) at Padova of which he was a co-founder. Currently he is associated with the VIMM, Italy.

Dr. Carafoli's research earned him a good number of International honors and awards. He is the fellow of the International Society of Heart Research, member of the European Molecular Biology Organization (EMBO), Honorary Member of the American Society of Biochemistry and Molecular Biology, and has been Welcome visiting Professor at the Case Western Reserve University, Ohio (1996). He is a fellow of the International Academy of Cardiovascular Sciences (2002) and "Grande Ufficiale" of Order of Merit of the Republic of Italy (2006). He was awarded the "Medal of Merit," the highest honor by the International Academy of Cardiovascular Sciences in 2009. He served as editor of numerous internationally reputed journals. Currently, he is the chief editor of Biochemical and Biophysical Research Communications.

Dr. Carafoli is an expert of the Ca^{2+}*ATPase (pump) of plasma membrane (PMCA). His important contributions include the discovery that the enzyme is activated by the acidic phospholipids in the membrane, isolation and purification of the enzyme using a calmodulin affinity procedure, its reconstitution in liposomes,*

the determination of its Ca^{2+} vs. charge stoichiometry, the finding that the isolated enzyme is activated by limited proteolysis. His further work has led to the discovery that the pump is regulated by a phosphorylation/ dephosphorylation cycle.

Dr. Carafoli has cloned the human PMCA pump and has established the chromosomal localization of the four human genes encoding its basic isoforms. He used synthetic, photoactivatable version of the C-terminal calmodulin domain of PMCA and revealed that the domain functions are auto-inhibitory. The domain inhibits by interacting with two "receptor" sites in the pump located in close proximity to the active site. Another important contribution of Dr. Carafoli was the discovery that single amino acid mutations in one of its transmembrane domains render the PMCA very similar to sarcoplasmic reticulum Ca^{2+} pump (SERCA). An extension of the work on the pump is the finding of a striking isoform specific effect of Ca^{2+} on the transcription of its genes in neurons. Of particular interest was the finding of a very rapid, calcineurin-mediated downregulation of transcription of the gene for isoform 4. Another important accomplishment has been the total synthesis of functionally competent phospholamban and the elucidation of its complete tertiary structure by NMR methods.

More recently, his research interest has turned to the characterization of mutant forms of PMCA. Mutations in the gene of PMCA2, which is expressed in the stereocilia of the hair cells of the Corti organ, have been found in some forms of hereditary

deafness, and mutations of PMCA3 gene have been found to be associated with a cerebellar ataxia phenotype.

Dr. Carafoli has published about 500 research articles in internationally peer-reviewed high impact factor journals on the topics of muscle biochemistry, membrane biochemistry, mitochondrial bioenergetics, membrane transport of Ca^{2+} (specifically PMCA), and regulation of Ca^{2+} metabolism. They have more than 35,000 citations. He wrote about 100 book chapters and 70 invited research articles on the above-mentioned topics.

Dr. Carafoli undoubtedly is a legendary figure especially in the field of the plasma membrane Ca^{2+} ATPase. He has excellent ability to motivate young researchers. His insight to explore and amalgamate classical studies with modern notions is amazing. He is truly a genius. We feel honored to dedicate this book to Dr. Ernesto Carafoli and wish him good health and success in his long fruitful activities.

Preface

> This is my delight, thus to wait and watch at the wayside where shadow chases light and rain comes in the wake of summer. Messengers with tidings from unknown skies greet me and speed along the road. My heart is glad within and breath of the passing breeze is sweet.
>
> Rabindranath Tagore
> (Gitanjali: Song of offerings)

The biological membranes of cellular organization enfold an important group of membrane proteins called the ATPases, which not only are versatile in maintaining chemical gradient and electrical potential across the membrane but also bring metabolites necessary for cell metabolism and drive out toxins, waste products, and solutes that otherwise can curb cellular functions. ATPases are distributed virtually in all forms starting from unicellular to multicellular and also in viruses. There are different types of ATPases, which differ in function and structure and in the type of ions they transport. The three main types of the ion pump ATPase family are (1) P-type ATPases that transport different ions across membranes. Plasma membrane Ca^{2+}ATPase (PMCA) utilizes ATP as the energy to extrude Ca^{2+} from the cells. The main calcium controlling organelle in the cell is within the sarco(endo)plasmic reticulum (SERCA). This pump transports Ca^{2+} from the cytosol to the lumen of the SR (or ER). The involvement of phospholamban in the regulation of SERCA by phosphorylation has been described. Interactions of SR Ca^{2+}ATPase with phospholamban was shown to have functional roles in different types of diseases, for example, pulmonary hypertension; (2) F-type ATPase in mitochondria, chloroplasts, and bacterial plasma membranes produce ATP using the proton gradient; and (3) V-type ATPase catalyzes ATP hydrolysis to transport solutes and maintains acidic pH in organelles like lysosomes. Genetic defects in either of the ATPases cause several diseases. For example, mutations expressed in osteoclasts and intercalated cells lead to diseases such as osteoporosis, tumor cell invasion, and renal tubule acidosis. Furthermore, H^+-ATPase gene mutations cause distal renal tubular acidosis, a condition characterized by impaired renal acid secretion resulting in metabolic acidosis. A number of

researches have demonstrated the involvement of several members of the ATPase family in the cell pathology and diseases, thereby penetrating exciting new areas of our understanding.

In this book, the authors summarize recent knowledge about the molecular mechanisms associated with Ca^{2+}-ATPase, V-ATPase, and F-ATPase in intracellular and extracellular Ca^{2+} transport, mitochondrial ATP synthase, vesicular H^+ transport, and lysosomal pH regulation. This book thereby bridges the gap between fundamental research and biomedical and pharmaceutical applications. It also provides an informative resource to improve ATPase research and modern therapeutic approaches toward different life-threatening diseases that are associated with dysregulation of the ATPases.

This book contains 29 chapters, which have been arranged under four parts, namely: (1) Plasma Membrane Ca^{2+}-ATPases; (2) Sarco(endo)plasmic Reticulum ATPases; (3) Vacuolar ATPases; and (4) F_1,F_o- and other ATPases, for the convenience of our readers. It is hoped that the readers will find each chapter stimulating and thought inciting, which will add new dimensions of future ATPase research. It is well said that: all endings are also beginnings, we just don't know it at the time!

As editors of the book, we are indebted to the authors for the time and energy they spent in shaping the book, an advancement of knowledge in the field that it bears. We would like to thank Prof. Rattan Lal Hangloo, Vice Chancellor, University of Kalyani for his encouragement. We remain thankful to Dr. Vijayan Elimban and Ms. Eva Little (St. Boniface Hospital Research Centre, University of Manitoba, Winnipeg, Canada) for all their meticulous work helping to get this book into print. Finally, we express our gratitude to Dr. Meran Owen (Senior Publishing Editor, Springer—London) as well as Ms. Lesley Poliner (Project Coordinator, Springer—New York) for their understanding, cooperation, and support during the preparation of this book.

Kalyani, India — Sajal Chakraborti
Winnipeg, MB, Canada — Naranjan S. Dhalla

Contents

Part I
Plasma Membrane ATPases

Chapter 1
The Plasma Membrane Calcium ATPase: Historical Appraisal and Some New Concepts

Ernesto Carafoli

Abstract The plasma membrane calcium ATPase (PMCA pump) was discovered nearly 50 years ago. Among its functional properties, the wealth of regulatory mechanisms singles it out from all other members of the P-type ion pumps superfamily. The cytosolic C-terminal tail of the protein contains a binding domain for calmodulin, which binds to sites near the active site and maintains the enzyme autoinhibited in the resting state. Calmodulin removes the C-terminal domain from these docking sites, relieving the inhibition. Other pump regulators are the acidic phospholipids of the inner leaflet of the membrane, which are in principle sufficient for 50 % of maximal pump activity. The activation by acidic phospholipids could perhaps also be involved in the process of apoptosis, which is known to transfer the activatory phosphatidylserine to the outer leaflet of the membrane bilayer: the decreased Ca^{2+} ejection activity of the pump could amplify the cytosolic Ca^{2+} overload frequently involved in apoptosis. Another novel concept on the PMCA pump is the conclusion that its Ca^{2+} ejection activity is less important to the total regulation of cytosolic Ca^{2+} than that of the SERCA pump and the plasma membrane Na/Ca exchanger. The main role of the PMCA pump is instead the regulation of Ca^{2+} in restricted cytosolic domains in which it interacts with numerous important enzymes. The local regulation of Ca^{2+} necessarily confers to the activation by calmodulin an oscillatory character: as Ca^{2+} decreases in the local pump environment, calmodulin will leave the pump, terminating its activation.

Keywords Calcium signaling • Calcium ATPases • Calcium pumps • Calmodulin • Acidic phospholipids • Local calcium homeostasis

E. Carafoli (✉)
Venetian Institute of Molecular Medicine, University of Padova,
Via Orus, 2, 35129 Padova, Italy
e-mail: ernesto.carafoli@unipd.it

S. Chakraborti, N.S. Dhalla (eds.), *Regulation of Ca^{2+}-ATPases,V-ATPases and F-ATPases*, Advances in Biochemistry in Health and Disease 14,
DOI 10.1007/978-3-319-24780-9_1

1 Introduction

The plasma membrane Ca^{2+} ATPase (PMCA pump) was discovered nearly 50 years ago [1]. Studies in the following years have characterized it as the most complex member of the superfamily of P-type ion pumps [2]. One of its properties should be mentioned at the outset, as it has seriously complicated the study of the pump: it is its great propensity to aggregate in the purified state. The pump dimerizes through its C-terminal calmodulin-binding domain [3], but in the isolated state, aggregates are invariably formed which are much larger. They have so far defeated all attempts to monomerize the pump in a functionally active state. Perhaps the most important structural property that sets the PMCA pump apart from all other members of the superfamily is the presence of a long cytosolic C-terminal tail, which has an essential role in the regulation of the activity of the enzyme: it is the locus of interaction of regulatory partners, chief among them calmodulin, and is the structure responsible for the mechanism of autoinhibition, which is a distinctive properties of the PMCA pump. Another distinctive property is the wealth of regulatory mechanisms, which act with different and still incompletely understood mechanisms. Traditionally, the most important among them have been calmodulin and acidic phospholipids, but others have recently emerged, e.g., protein partners that may interact with the pump in a spatially confined cell environment.

2 General Properties of the Plasma Membrane Ca^{2+} Pump: A Succinct Summary

The tertiary structure of the PMCA pump is not available, but molecular modeling work on the SERCA pump template (Fig. 1.1) shows a topology of ten transmembrane domains and three main cytosolic protrusions that correspond to the A, N, and P cytosolic domains of the SERCA pump. It also shows that, as in the case of the SERCA pump, a large conformational change occurs when the pump binds Ca^{2+}: the change affects both the transmembrane helices and the cytosolic portion, but is most evident in the latter, which becomes far more "open" in the presence of Ca^{2+}. The PMCA pump has long been known to have a unique, unstructured C-terminal cytosolic tail of about 150 residues that contains a canonical calmodulin-binding domain (a second, lower-affinity domain that binds calmodulin and has recently been identified downstream of the first in some splicing variants of the pump [4]). The C-terminal tail also contains consensus sites for two activatory kinases: that for PKA is isoform specific and is located downstream of the calmodulin-binding domain [5], whereas PKC has two target sites that are not isoform specific [6], a Thr within the calmodulin-binding domain and a Ser further downstream. One early finding on the PMCA pump which was made before its purification is its activation by acidic phospholipids [7]. The finding was extended to the purified pump [8], and it was calculated that the amount of acidic phospholipids in the environment of the

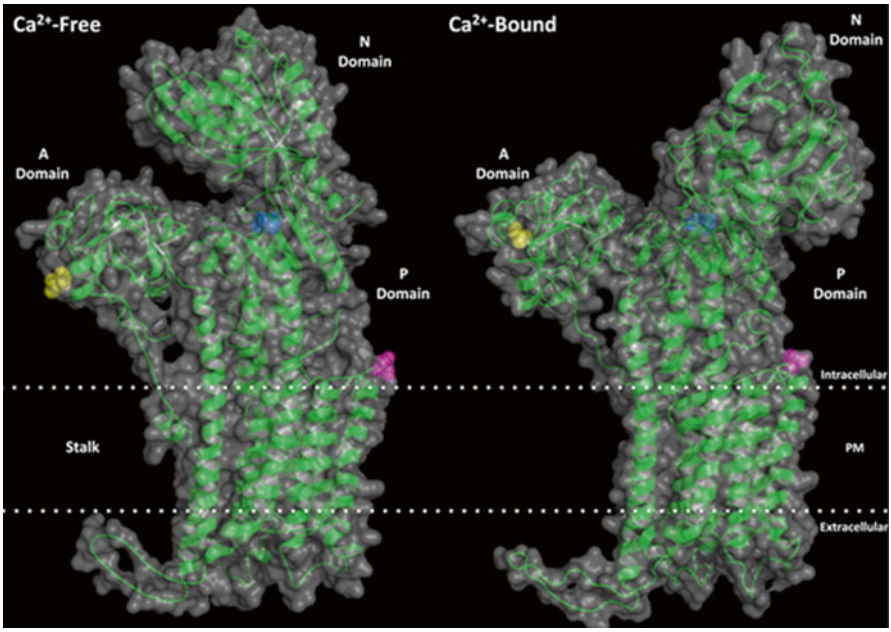

Fig. 1.1 Structure of the PMCA pump (isoform 3): Ca^{2+}-induced structural changes). Cartoon representation (*green*), superimposed on a space filling representation (*gray*) of the Ca^{2+}-free (*left*) and Ca^{2+}-bound (*right*) structures of the pump, were built on the basis of the respective SERCA structures (PDB 3W5B and 1SU4, respectively). The *blue dots* represent the catalytic aspartate. The N-terminus and the C-terminus of the pump are shown as *yellow* and *magenta dots*, respectively

erythrocyte membrane was in principle sufficient for about 50 % of maximal pump activity [9]. The mechanism of the activation by acidic phospholipids is still not understood, but it has been found that they reduce the K_m Ca^{2+} to even lower levels than calmodulin does [10] and that they interact with the calmodulin-binding domain and the first loop that protrudes into the cytosol between transmembrane domains 2 and 3 [11].

As all P-type pumps, the PMCA pump conserves temporarily the energy of the ATP that is hydrolyzed during the reaction cycle in the form of an aspartyl-phosphate. Interestingly, the PMCA pump transfers one Ca^{2+} across the membrane for each hydrolyzed ATP, instead of the two Ca^{2+} per ATP transferred by the SERCA pump: thus, it has only one Ca^{2+}-binding site, which corresponds to site two of the SERCA pump; this is so because one conserved acidic residue in transmembrane domain 5, which is essential for the formation of Ca^{2+}-binding site 1 in the SERCA pump, is absent in the PMCA pump—its insertion by mutagenesis in transmembrane domain 5 evidently completes the missing binding site for Ca^{2+}, restoring the Ca^{2+}/ATP stoichiometry of the PMCA pump to 2 [12].

The PMCA pump was cloned in 1988 [13, 14]. At the time of the cloning, some of its important domains had been already recognized and sequenced, e.g., the

calmodulin-binding domain [5]. Other domains were identified after the cloning, including the sites that interact with acidic phospholipids [11] and the sites that are responsible for the process of autoinhibition [15, 16], in which the C-terminal tail of the pump folds over under resting conditions of low Ca^{2+} and binds with its calmodulin-binding domain to two sites in the main body of the pump. One is close to the active site in the main cytosolic protruding unit, and the other is located in the large cytosolic unit that protrudes between transmembrane domains 2 and 3. When Ca^{2+} in the environment increases, calmodulin becomes associated with its binding domain, somehow removing it from the main body of the pump and restoring activity.

Soon after its successful cloning, it was found that four separate mammalian genes produce four distinct basic isoforms of the pump [see [17] for a comprehensive review]. The four basic pumps have a sequence identity of about 80 %: the differences do not concern the catalytic core of the pumps, but the regions that are involved in the regulation of their activity [18]. Two of the basic pumps are expressed ubiquitously (PMCA1 and 4), and two (PMCA2 and 3) are restricted to some tissues, with preference for the brain. Until a few years ago it was assumed that both ubiquitous isoforms were housekeeping pumps, but recent work has instead shown that isoform 4 has specific roles in some tissues, e.g., the testis [19]. As expected, the catalytic properties of the four pumps are the same, but the rate of activation by Ca^{2+} (and also the rate of inactivation by its removal) is slower in the two ubiquitous isoforms, which are therefore characterized as "slow" pumps: their role correlates with the type of Ca^{2+} signals in tissues, which could be slow or fast [20]. A striking difference between the ubiquitous and the tissue restricted isoforms if the affinity for calmodulin, which is significantly higher in the latter pumps. Concerning calmodulin, one striking property of PMCA2 which is not yet molecularly understood is its peculiar ability to express high activity in the absence of calmodulin [21, 22]. PMCA2, therefore, continuously pumps Ca^{2+} very effectively irrespective of the presence of its most important activator: this property may respond to particular Ca^{2+} homeostasis demands of specialized cell types, e.g., the outer hair cells of the inner ear [23]. The sustained Ca^{2+} ejection ability of the PMCA2 pump in the absence of calmodulin does not reflect differences in the C-terminal calmodulin-binding domain, the sequence of which is the same in the four basic pump variants in the portion. It evidently reflects differences in the domain(s) of the main body of the PMCA2 molecule that mediate(s) the autoinhibition process. In addition to the four basic isoforms, a large number of additional pump variants are produced by the alternative splicing of the primary transcripts of the four genes. The splicing inserts, naturally, do not involve the catalytic portion of the pump. They occur at site A in the cytosolic loop protruding between transmembrane domains 2 and 3 and at site C within the C-terminal calmodulin-binding domain. The number of the inserted exons, at both site A and site C, varies with the pump and the tissues: it confers to the variants properties that satisfy the functional Ca^{2+} homeostasis requirements of given cell types, and may be responsible for their targeting to particular domains of the plasma membrane [24]. The alternative spicing process is peculiarly complex in the PMCA2 pump, adding to it another property that singles it out from the other three basic pumps.

3 Emerging New Concepts on the Regulation and Function of PMCA Pumps

3.1 Local or General Action of the PMCA Pumps

The correct functioning of PMCA pumps is essential to all animal cells: this is clearly underlined by the increasing number of pathologies of numerous tissues that recognize the malfunction of PMCA pumps as the causative factor. Naturally, the mechanistic function of PMCA pumps is to eject Ca^{2+} from cells: however, in most cells this function of the PMCA pumps is quantitatively overshadowed by that of more powerful systems, i.e., the SERCACa^{2+} pump of the endo(sarco)plasmic reticulum and—in excitable cells—the Na^+/Ca^{2+} exchanger of the plasma membrane (cells like the erythrocytes are obviously exceptions). Prima facie, then, considering the quantitative aspects of the cytosolic homeostasis of Ca^{2+}, the coexistence of PMCA pumps alongside the other systems does not have a logical rationale. The simplest way out of the conundrum would be by proposing that the *raison d'être* of PMCA pumps would not be the bulk homeostasis of cytosolic Ca^{2+}, but its selective regulation in the microdomains surrounding the cytosolic portion of the pump. The concept, in essence, proposes that the role of the PMCA pump in the total extrusion of cell Ca^{2+} in many—perhaps most—cell types could be minor or even quantitatively irrelevant: its main function would be the locally restricted regulation of cytosolic Ca^{2+}. Ca^{2+} can still be used as a signaling agent even in cells that experience large physiological oscillations in its concentration because the pools controlled by the activity of the PMCA pumps would be spatially restricted: for instance, in the cardiomyocytes the general Ca^{2+} pool to be used for contractility is separated from the pool used for signaling purposes [25]. Mohamed et al. [26] have nicely shown that the PMCA 4 pump is indeed only involved in heart Ca^{2+} signaling, not in its general the beat-to-beat control in the contraction/relaxation process. A necessary prerequisite of such signaling role of the PMCA pump would be its localization to spatially restricted microdomains of the plasma membrane in which the pump would preferentially interact with enzyme partners. That the PMCA pump is specifically localized to caveolae has indeed been shown more than 20 years ago [27]. Others have confirmed the finding [28] and have extended it to show that in the subplasma membrane domain of caveolae, which are important sites of cell signaling [29], the PMCA pump indeed interacts specifically with important signaling partners [30]. In the heart, the interaction with neuronal nitric oxide synthase (nNOS) regulates indirectly cardiac contractility by acting on a spatially confined cyclic nucleotide microdomain [26].

3.2 Acidic Phospholipids

The preferred localization of the PMCA pump to the caveolae, or to similar domains like rafts and dendritic spines, brings back the matter of the regulation of the pump by phospholipids. These specialized plasma membrane domains have particular

phospholipid composition and fluidity and could modulate the activity of the PMCA pumps by their lateral mobility [31–33]. It has also been shown that the association of the PMCA pumps with caveolae or rafts, and thus its regulation, could be isoform specific [34]. But the regulation of the activity of the PMCA pumps by acidic phospholipids could come into play in a condition of wider general significance: the apoptotic death of cells [35]. As is well known, an early event of apoptosis is the externalization of phosphatidylserine by scramblases (one of which is Ca^{2+} dependent) to make cells recognizable by phagocytes [36, 37]. Phosphatidylserine is mostly localized to the inner leaflet of the plasma membrane bilayer, where its concentration around the PMCA pump (see above) has been calculated to activate it to about 50 % of maximal [9]. An interesting mechanism could thus be proposed in which scramblases would become activated in apoptotic cells in response to the increase of cytosolic Ca^{2+}. They would transfer phosphatidyl serine to the external lipid monolayer, depriving the PMCA pump of an important activating factor and amplifying the cytosolic Ca^{2+} overload that would eventually execute the apoptotic death of the cell.

The matter of the activation of the PMCA pump by phospholipids deserves some additional discussion: the (acidic) phospholipids of the inner leaflet of the plasma membrane bilayer are supposed to be physically separated from the catalytic core of the pump that protrudes into the cytosol. Therefore, their direct involvement in the operation of the reaction cycle of the pump cannot be easily envisaged, as it would demand that the cytosolic portions of the pump somehow establish contact with the surface of the lipid bilayer. The activatory effects of acidic phospholipids could instead be linked to something structural, i.e., to the modulation of the access of Ca^{2+} to its binding site within the membrane. Surprisingly, however, a report has appeared in which acidic phospholipids have been shown to act on the reaction cycle proper, as they accelerate the dephosphorylation of the pump [38].

Another issue in the matter of the activation by phospholipids is the time scale of their effects: changes of the phospholipid environment of the pump are unlikely to be as rapid as those, for instance, of calmodulin, suggesting that phospholipids could be longer range modulators of pump activity. One possible exception would be the doubly phosphorylated product of phosphatidylinositol (PIP2), which is the only phospholipid that changes rapidly concentration in response to plasma membrane agonists. A reversible, rapid activation of the PMCA pump by PIP2 has actually been proposed [39].

One last point on acidic phospholipids deserves some discussion: its functional interplay with the activation by protein kinases. Both PKA and PKC (see above) activate the PMCA pump (the effect of PKC has aspects that are somewhat controversial). The activity of PKC requires diacylglycerol (DAG), which comes from the hydrolysis of PIP2, and the most important adenylyl cyclase is activated by Ca^{2+}, the increase of which in the cytosol is promoted by InsP3, which also comes from the hydrolysis of PIP2. So, here we have a seemingly paradoxical situation: the activation of the PMCA pump by the protein kinases demands the disappearance of PIP2, which is the most powerful pump activatory phospholipid: possibly, as suggested elsewhere [35] one should consider temporal, or even spatial, factors in the effect of the kinases with respect to the suppression of the effect of PIP2.

3.3 The Autoinhibition of the Pump

The first indication that the PMCA pump at rest was in an autoinhibited state mediated by the C-terminal CaM-binding domain came from experiments in which the proteolytic removal of the C-terminal tail of the pump, including its CaM-binding domain by calpain, irreversibly removed the autoinhibition [5, 9]. The indication was directly verified by experiments in which the autoinhibited state was induced by adding synthetic peptides corresponding to the CaM-binding domain to the pump that had been made fully active by C-terminal truncation [15]. The proposal that the C-terminal tail of the pump would "close" the access route to the active site was provided by experiments in which blue and green fluorescent proteins were fused to the N- and C-termini of the pump [40]. The distance between the two fluorophores was about 45 A in the autoinhibited state and became greater when the pump was activated by CaM (or acidic phospholipids). Other pump regions distant from the CaM-binding domain and from the C-terminal tail could also have a role in the autoinhibition process, i.e., the "stalk" region, in which Asp-170 could help in the stabilization of the autoinhibited state [40, 41]. The "stalk" region has been proposed to form basic pockets that would be suitable for the binding of the head groups of PIP2, which would be protected from the degradation by phospholipase C.

3.4 The Regulation of the PMCA Pump by Calmodulin

The built-in stop mechanism in the activation of the PMCA pump discussed for the effect of the protein kinases has more general significance and can be extended to the case of CaM. Once Ca^{2+} increases in the microenvironment of the autoinhibited pump, CaM becomes bound by the pump and activates the ejection of Ca^{2+}. However, as this occurs, Ca^{2+} decreases in the microenvironment of the pump, leading to the detachment of CaM and to the restoration of the autoinhibited state. Thus, by definition, the activation of the pump by CaM cannot be permanent, but must necessarily follow an oscillatory pattern, in which bursts of activation are followed by periods of relative inactivity. Only conditions of sustained cytosolic Ca^{2+} overload, as frequently occurring in pathology, can produce permanent activations of the pump. These conditions would probably also activate calpains, which would cleave out the C-terminal tail of the pump, contributing to its permanent state of maximal activation and to the amplification of the Ca^{2+} overload condition.

4 Conclusions

The PMCA pumps stand out from all other pumps of the P-type superfamily because of the wealth and complexity of their regulatory mechanisms. They have been discussed in this contribution, which has tried to put them in their respective roles and functional perspectives. The discussion has emphasized aspects of the regulation of

the pump which have not been considered so far: the most interesting concept that has emerged is that the pump, in the physiological conditions prevailing in the cell cytosol, can only be activated by its most important partner, calmodulin, in temporarily limited bursts. The contribution has also underlined the concept that the main role of the PMCA pumps is not to contribute a quantitatively important fraction of the total Ca^{2+} ejection activity of cells: it is the regulation of Ca^{2+}, and of the partners of the pumps sensitive to it, in selected microdomains within the cells.

References

1. Schatzmann HJ (1966) ATP-dependent Ca^{++} -extrusion from human red cells. Experientia 22:364–365
2. Pedersen PL, Carafoli E (1987) Ion motive ATPases. I. Ubiquity, properties, and significance to cell function. Trends Biochem Sci 12:146–150
3. Vorherr T, Kessler T, Hofmann F et al (1991) The calmodulin-binding domain mediates the self-association of the plasma membrane Ca^{2+} pump. J Biol Chem 266:22–27
4. Tidow H, Poulsen LR, Andreeva A et al (2012) A bimodular mechanism of calcium control in eukaryotes. Nature 491:468–472
5. James P, Maeda M, Fischer R et al (1988) Identification and primary structure of a calmodulin binding domain of the Ca^{2+} pump of human erythrocytes. J Biol Chem 263:2905–2910
6. Wang KK, Wright LC, Machan CL et al (1991) Protein kinase C phosphorylates the carboxyl terminus of the plasma membrane Ca^{2+} ATPase from human erythrocytes. J Biol Chem 266:9078–9085
7. Ronner P, Gazzotti P, Carafoli E (1977) A lipid requirement for the (Ca^{2+} + Mg^{2+})-activated ATPase of erythrocyte membranes. Arch Biochem Biophys 179:578–583
8. Niggli V, Penniston JT, Carafoli E (1979) Purification of the (Ca^{2+} + Mg^{2+})-ATPase from human erythrocyte membranes using a calmodulin affinity column. J Biol Chem 254:9955–9958
9. Niggli V, Adunyah ES, Carafoli E (1981) Acidic PL, unsaturated fatty acids, and limited proteolysis mimic the effect of calmodulin on the purified erythrocyte Ca^{2+} ATPase. J Biol Chem 256:8588–8592
10. Enyedi A, Flura M, Sarkadi B et al (1987) The maximal velocity and the calcium affinity of the red cell calcium pump may be regulated independently. J Biol Chem 262:6425–6430
11. Brodin P, Falchetto R, Vorherr T et al (1992) Identification of two domains which mediate the binding of activating PL to the plasma-membrane Ca^{2+} pump. Eur J Biochem 204:939–946
12. Guerini D, Zecca-Mazza A, Carafoli E (2000) Single amino acid mutations in trans membrane domain 5 confer to the plasma membrane Ca^{2+} pump properties typical of the Ca^{2+} pump of endo(sarco)plasmic reticulum. J Biol Chem 275:31361–31368
13. Shull GE, Greeb J (1988) Molecular cloning of two isoforms of the plasma membrane Ca^{2+} -transporting ATPase from rat brain. Structural and functional domains exhibit similarity to Na^{+}, K^{+}- and other cation transport ATPases. J Biol Chem 263:8646–8657
14. Verma AK, Filoteo AG, Stanford DR et al (1988) Complete primary structure of a human plasma membrane Ca^{2+} pump. J Biol Chem 263:14152–14159
15. Falchetto R, Vorherr T, Brunner J et al (1991) The plasma membrane Ca^{2+} pump contains a site that interacts with its calmodulin-binding domain. J Biol Chem 266:2930–2936
16. Falchetto R, Vorherr T, Carafoli E (1992) The calmodulin-binding site of the plasma membrane Ca^{2+} pump interacts with the transduction domain of the enzyme. Protein Sci 1:1613–1621
17. Brini M, Carafoli E (2009) Calcium pumps in health and disease. Physiol Rev 89:1341–1378
18. Strehler EE, Zacharias DA (2001) Role of alternative splicing in generating isoform diversity among plasma membrane calcium pumps. Physiol Rev 81:21–50

19. Schuh K, Cartwright EJ, Jankevics E (2004) Plasma membrane Ca^{2+} ATPase 4 is required for sperm motility and male fertility. J Biol Chem 279:28220–28226
20. Caride AJ, Filoteo AG, Penheiter AR et al (2001) Delayed activation of the plasma membrane calcium pump by a sudden increase in Ca^{2+}: fast pumps reside in fast cells. Cell Calcium 30:49–57
21. Hilfiker H, Guerini D, Carafoli E (1994) Cloning and expression of isoform 2 of the human plasma membrane Ca^{2+} ATPase. Functional properties of the enzyme and its splicing products. J Biol Chem 269:26178–26183
22. Elwess NL, Filoteo AG, Enyedi A et al (1997) Plasma membrane Ca^{2+} pump isoforms 2a and 2b are unusually responsive to calmodulin and Ca^{2+}. J Biol Chem 272:17981–17986
23. Giacomello M, De Mario A, Primerano S et al (2012) Hair cells, plasma membrane Ca^{2+} ATPase and deafness. Int J Biochem Cell Biol 44:679–683
24. Chicka MC, Strehler EE (2003) Alternative splicing of the first intracellular loop of plasma membrane Ca^{2+} -ATPase isoform 2 alters its membrane targeting. J Biol Chem 278:18464–18470
25. Molkentin JD (2006) Dichotomy of Ca^{2+} in the heart: contraction versus intracellular signaling. J Clin Invest 116:623–626
26. Mohamed TMA, Oceandy D, Zi M et al (2011) Plasma membrane calcium pump (PMCA4)-neuronal nitric-oxide synthase complex regulates cardiac contractility through modulation of a compartmentalized cyclic nucleotide microdomain. J Biol Chem 286:41520–41529
27. Fujimoto T (1993) Calcium pump of the plasma membrane is localized in caveolae. J Cell Biol 120:1147–1157
28. Hammes A, Oberdorf-Maass S, Rother T et al (1998) Overexpression of the sarcolemmal calcium pump in the myocardium of transgenic rats. Circ Res 83:877–888
29. Cohen AW, Hnasko R, Schubert W et al (2004) Role of caveolae and caveolins in health and disease. Physiol Rev 84:1341–1379
30. Cartwright EJ, Oceandy D, Neyses L (2007) Plasma membrane calcium ATPase and its relationship to nitric oxide signaling in the heart. Ann N Y Acad Sci 1099:247–253
31. Pang Y, Zhu H, Wu P et al (2005) The characterization of plasma membrane Ca^{2+} ATPase in rich sphingomyelin-cholesterol domains. FEBS Lett 579:2397–2403
32. Tang D, Dean WL, Borchman D et al (2006) The influence of membrane lipid structure on plasma membrane Ca^{2+} ATPase activity. Cell Calcium 39:209–216
33. Jiang L, Fernandes D, Mehta N et al (2007) Partitioning the plasma-membrane Ca^{2+} ATPase into lipid rafts in primary neurons: effects of cholesterol depletion. J Neurochem 102:378–388
34. El-Yazbi AF, Cho WJ, Schulz R et al (2008) Calcium extrusion by plasma membrane calcium pump is impaired in caveolin-1 knockout mouse small intestine. Eur J Pharmacol 591:80–87
35. Lopreiato R, Giacomello M, Carafoli E (2014) The plasma membrane calcium pump: new ways to look at an old enzyme. J Biol Chem 289:10261–10268
36. Fadok VA, Voelker DR, Campbell PA et al (1992) Exposure of phosphatidylserine on the surface of apoptotic lymphocytes triggers specific recognition and removal by macrophages. J Immunol 148:2207–2216
37. Verhoven B, Schlegel RA, Williamson P (1995) Mechanisms of phosphatidylserine exposure, a phagocyte recognition signal, on apoptotic T lymphocytes. J Exp Med 182:1597–1601
38. Filomatori CV, Rega AF (2003) On the mechanism of activation of the plasma membrane Ca^{2+} -ATPase by ATP and acidic PL. J Biol Chem 278:22265–22271
39. Choquette D, Hakim G, Filoteo AG et al (1984) Regulation of plasma membrane Ca^{2+} ATPases by lipids of the phosphatidylinositol cycle. Biochem Biophys Res Commun 125:908–915
40. Corradi GR, Adamo HP (2007) Intramolecular fluorescence resonance energy transfer between fused autofluorescent proteins reveals rearrangements of the N- and C-terminal segments of the plasma membrane Ca^{2+} pump involved in the activation. J Biol Chem 282:35440–35448
41. Bredeston LM, Adamo HP (2004) Loss of autoinhibition of the plasma membrane Ca^{2+} pump by substitution of aspartic 170 by asparagines. Activation of plasma membrane calcium ATPase 4 without disruption of the interaction between the catalytic core and the C-terminal regulatory domain. J Biol Chem 279:41619–41625

Chapter 2
The Plasma Membrane Ca^{2+} ATPases: Isoform Specificity and Functional Versatility

Tito Calì, Denis Ottolini, and Marisa Brini

Abstract Plasma membrane Ca^{2+} ATPases are single polypeptides of about 1100–1250 amino-acid residues with a molecular mass of 125–140 kDa. They contain ten membrane spanning segments and their N- and C-terminals are both on the cytosolic side. The bulk of their mass is also in the cytoplasm and contains three major intracellular domains: the A (actuator), N (nucleotide-binding), and P (catalytic phosphorylation) domains. Four basic isoforms are encoded by four distinct genes, and their transcripts originated a huge number of alternative splicing variants that in most cases are also translated in the corresponding protein variants. Emerging evidence underlines that PMCA pumps, in addition to maintain resting cytosolic Ca^{2+} levels against a steep concentration gradient (i.e., nM versus mM), play a local control in specific sub-plasma membrane domains by tethering Ca^{2+}-/calmodulin-dependent enzymes and reducing their activity, i.e., by decreasing Ca^{2+} concentration in the microenvironment where they are confined. This aspect of pump activity confers to PMCA pump a key role as signal transducer and justifies the existence of so many PMCA variants that could be specialized in tuning the activity of different partners with different Ca^{2+} sensitivity.

Keywords Plasma membrane Ca^{2+} pump • Isoforms • Ca^{2+} signaling

1 Introduction

Ca^{2+} controls the most important cell functions in all eukaryotic organisms. Fertilization, muscle contraction, secretion, several phases of metabolism, gene transcription, apoptotic death, etc. are finely orchestrated by the functional versatility

T. Calì
Department of Biomedical Sciences, University of Padova, Via Ugo Bassi 58b, 35131 Padova, Italy

D. Ottolini • M. Brini (✉)
Department of Biology, University of Padova, Via Ugo Bassi 58b, 35131 Padova, Italy
e-mail: marisa.brini@unipd.it

S. Chakraborti, N.S. Dhalla (eds.), *Regulation of Ca^{2+}-ATPases,V-ATPases and F-ATPases*, Advances in Biochemistry in Health and Disease 14,
DOI 10.1007/978-3-319-24780-9_2

of Ca^{2+} signaling and its exquisite spatial and temporal regulation. The specificity of cellular Ca^{2+} signals depends on the coordinated interplay between numerous soluble Ca^{2+}-binding proteins and membrane Ca^{2+} transporters which differ both in their mechanism and sensitivity for Ca^{2+} handling, in their distribution in the intracellular compartments and in their regulation. Ca^{2+}-transporting proteins include ion channels, pumps, and exchangers that drive Ca^{2+} ions across the plasma membrane and across the membranes of intracellular organelles [1].

Three differently located Ca^{2+} ATPase types (pumps) have been described in animal cells: the sarcoplasmic/endoplasmic Ca^{2+} ATPase (SERCA pump) located in the membranes of endo(sarco)plasmic reticulum (including the nuclear envelope), the secretory pathway Ca^{2+} ATPase (SPCA pump) in those of the Golgi network, and the plasma membrane Ca^{2+} ATPase (PMCA pump) in the plasma membrane.

Animal Ca^{2+} pump types belong to the family of P-type ATPases. The name comes from their mechanism for Ca^{2+} transport: the energy from ATP hydrolysis is conserved in the form of a phosphorylated enzyme intermediate (hence P-type) where ATP phosphorylation of an invariant aspartate residue in a highly conserved sequence S**D**KTGT[L/I/V/M][T/I/S] allows the translocation of Ca^{2+} across the membrane [2]. Structural works on the SERCA pump and the solution of its three-dimensional structure have better elucidated the reaction cycle of P-type ATPases. The polypeptide chain of the pump folds in four main domains: one transmembrane domain M (composed by ten transmembrane helices) and three cytosolic domains — the actuator domain A and the phosphorylation domain P (both connected with the M domain) and the nucleotide-binding domain N, which is connected to the domain P [3]. Upon binding of Ca^{2+} and its translocation, a series of structural changes involving both the protruding cytoplasmic portion and the transmembrane domain results in the "opening" of the "compact" structure of the cytosolic portion (Fig. 2.1). The mechanism of action is the same for all the Ca^{2+} pumps, with the difference that SERCA pump transports two Ca^{2+} ions instead of one and that SPCA is also able to transport Mn^{2+} in addition to Ca^{2+}. Despite of the common mechanism for Ca^{2+} transport, the existence of a multitude of variants for each of the three Ca^{2+} pumps, either encoded by different genes or generated by alternative splicing mechanisms, suggests that the cell needs to differentiate their action in Ca^{2+} extrusion, possibly by activating the proper Ca^{2+} pump in a precise moment or cell district.

In this chapter the focus will be on the plasma membrane Ca^{2+} pumps (PMCA) and the specificity and functional versatility of its isoforms.

2 General Properties of the Plasma Membrane Ca^{2+} Pumps

The PMCA pump has high Ca^{2+} affinity and low transport capacity, with a 1:1 Ca^{2+}/ATP stoichiometry. It was cloned in 1988 [4, 5], and its sequence revealed the same essential membrane organization and topology properties of the SERCA pump. Later, molecular modeling work based on the structure of the SERCA pump predicts the same general features, with ten transmembrane domains and the large cytosolic

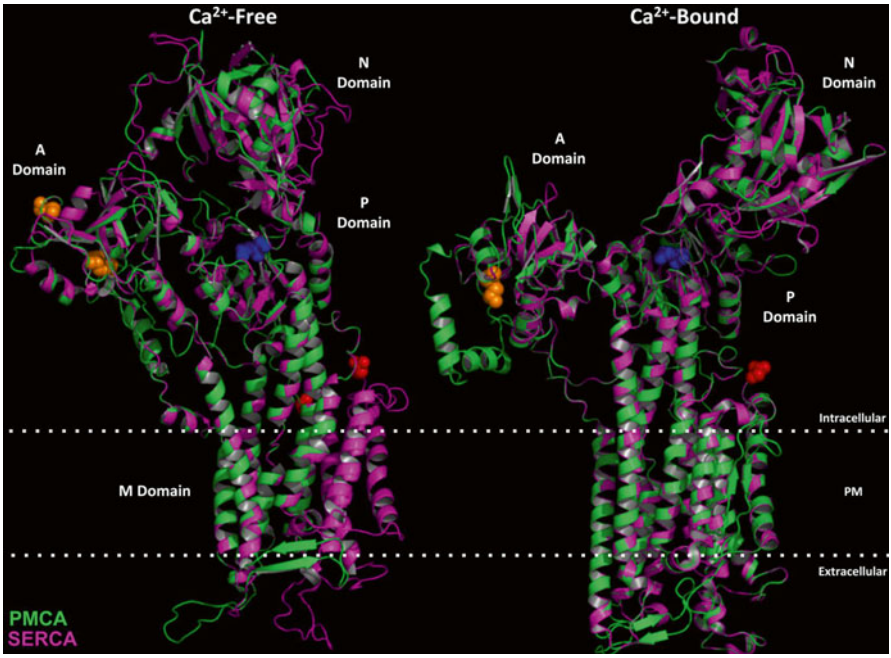

Fig. 2.1 Three-dimensional structure of the PMCA pump. The structure of the PMCA (in *green*) was deduced from that of the SERCA pump (PDB3W5B and 1SU4) and superimposed on it (in *purple*). The structure is shown in the two conformational forms: the Ca^{2+}-free (closed) and the Ca^{2+}-bound (open) form. Upon Ca^{2+} binding, the cytosolic portion of the pump undergoes to a transition from a compact arrangement in the absence of Ca^{2+} to a looser one in its presence. The transmembrane domain M and the three cytosolic domains A, N, and P are shown. The aspartic catalytic residue position is shown as *blue sphere*. The *orange* and the *red spheres* represent the N- and C-terminals, respectively, of the two pumps. In the Ca^{2+}-bound conformation, those of the PMCA and the SERCA pumps perfectly overlap

headpiece divided into the three main cytosolic A, N, and P domains (Fig. 2.2). The catalytic phosphorylation site (S**D**KTGLT) and other important consensus domains are conserved, but the existence of two prominent domains makes the PMCA pump different with respect to the other two Ca^{2+} ATPases. Specifically, a 40-residue-long domain responsible for the binding of activatory phospholipids is present in the first cytosolic loop between transmembrane domains 2 and 3, and a 120-amino-acid-long tail protruding from transmembrane domain 10 and containing the domain that binds calmodulin, i.e., the natural activator of the pump, is present in the C-terminal region [6]. Under nonactivated conditions, the C-terminal tail of the pump is proposed to interact with two sites in the first and second cytosolic loops of the enzyme to maintain the pump auto-inhibited [7, 8]. Calmodulin interacts with its binding domain removing it from the docking sites next to the active center, freeing the pump from autoinhibition [9, 10]. A second calmodulin-binding domain has recently been identified in some splicing variants of the pump [11], and it has been suggested

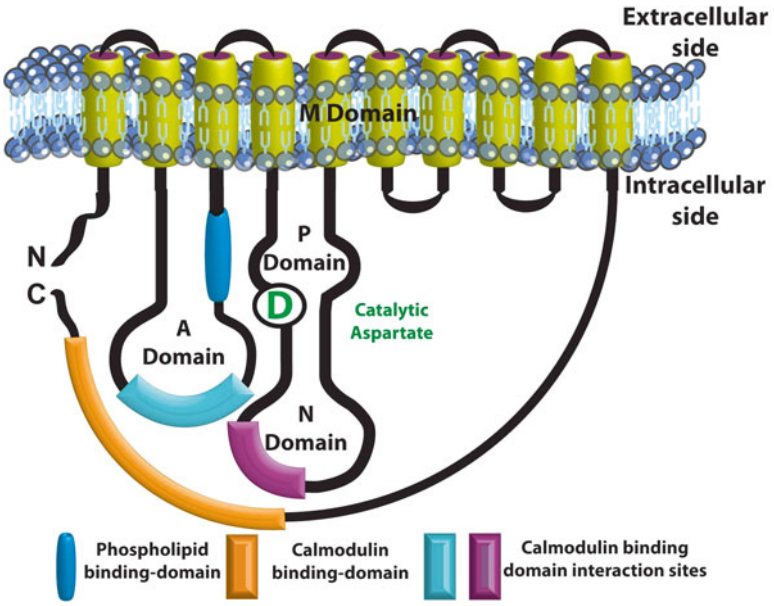

Fig. 2.2 Topology model of PMCA. The pump is organized in the membrane with ten transmembrane domains connected on the external side by short loops. The cytosolic portion of the pump contains the catalytic center and other functionally important domains. The ATP binding site, the acidic phospholipid-binding domain, and the calmodulin-binding domain are shown with different colors

that, together with the original calmodulin-binding domain, it permits the regulation of the pump both in the nanomolar range and in the micromolar range of Ca^{2+} concentration, according to a bi-modular mechanism of control [11].

In addition to calmodulin binding, the PMCA pump has other mechanisms of activation. Among them are the ability of the calmodulin-binding domain to bind also acidic phospholipids [12], the presence of Ca^{2+}-binding motifs upstream and downstream of the calmodulin-binding domain [13], an oligomerization (polymerization) process involving the calmodulin-binding sequence in the C-terminal tail of the pump, the cleavage by calpain, and phosphorylation by protein kinase C and protein kinase A (the latter only occurs in one of the isoforms). The cleavage by calpain occurs immediately upstream of the C-terminal calmodulin-binding domain [14] and activates the pump irreversibly, making it calmodulin insensitive. This irreversible mechanism of activation could become significant in conditions of pathological Ca^{2+} overload that would demand increased Ca^{2+} exporting ability [15]. PKC and PKA consensus sequences have been found in the C-terminal tail of the pump, and regulation of PMCA by PKC has been reported in a variety of cell types [16, 17]. The physiological relevance of the mechanism of phosphorylation is still unclear; however, a number of studies suggest that it could affect various PMCA isoforms and splicing variants in different ways according to their C-terminal sequence characteristics (for a review, refer to [18]).

3 Isoforms of the PMCA Pump

The PMCA pump is the product of a multigene family. In mammals four basic genes (*ATP2B1–ATP2B4*) exist, and their transcripts undergo a complex alternative splicing process that increases the total number of isoforms to about 30 [18–20]. The four gene products (isoforms 1–4) differ in tissue distribution and calmodulin affinity. Pumps 1 and 4 are ubiquitous and have lower calmodulin affinity ($K_d \sim 30$–50 nM), pumps 2 and 3 have higher calmodulin sensitivity ($K_d \sim 2$–8 nM), and their expression is restricted to some tissues: PMCA2 is expressed prominently in the nervous system and in the mammary gland, PMCA3 in the nervous and muscle system [18].

All the four PMCA transcripts undergo alternative splicing at two sites (site A and site C), thus originating a large number of variants which differ for distribution, interaction with different proteins, and calmodulin affinity. Site A is located upstream of the phospholipid-binding domain in the first cytosolic loop of the pump, site C in the C-terminal calmodulin-binding domain.

The splicing process at site A leads to the insertion of one exon (in the case of PMCA1, PMCA3, and PMCA4) or up three exons in PMCA2, thus generating variants *w* (three exons included), *x* (two exons included), and *y* (only one exon). The site A inserts are always in frame: they affect the properties of the pumps, but do not substantially alter their structure. The *z* variants display no insertion. Variant *z* is not found in PMCA1, as all mature transcripts of this isoform invariably contain an exon.

The splicing process at site C is characterized by the inclusion of one (in the case of PMCA1, PMCA3, and PMCA4) or two (in the case of PMCA2) full extra exons that results in changes in reading frame and in the introduction of premature stop codons. The mature proteins are truncated and they are designated as *a* variant. The insertion of portions of exon can also occur leading to variants *c*, *d*, *e*, and *f* according to the different isoforms, but their existence and significance at protein levels is not clear. Pumps in which no insertions occur at site C are designated as *b* or full-length variants. In the case of PMCA2 and PMCA3, site C splicing is more complex: two or three, and not only one, novel exons can be included or excluded, thus generating additional C-terminal variants. For a detailed description of splicing variants, the reader could refer to [6].

Differential activity of the splice variants has been studied mainly for those variants generated by the splicing occurring at the C-terminal and focusing on distinguishing the full length from the truncated variants.

Studies on the pump activity performed both on microsomal fraction enriched in specific isoforms or, in vitro, on specific PMCA isoforms purified from eukaryotic overexpression systems such as recombinant baculovirus-infected insect Sf9 cells have revealed some differences between the isoforms. These studies are adequate to define isoform functional characteristics with respect to enzyme kinetics (V_{max}, K_m for Ca^{2+}) and regulation by calmodulin, phosphorylation, and phospholipids. They have revealed that the C-terminal truncation determined by the C inserts in the *a* variants lowers, as expected, the affinity of the pumps for calmodulin [21, 22] and that phospholipids mimic the effect of calmodulin [23].

Unfortunately, these studies can provide only limited information concerning the true physiological properties of the isoforms that should be investigated in living cells. One of the major problems in studying PMCA activity in intact cells is that in most cell lines more than one PMCA isoform is expressed (most cells express at least PMCA1 and PMCA4) and multiple splice variants may be present simultaneously. Therefore, assignment of Ca^{2+} extrusion characteristics to a particular isoform or splice variant is not readily possible in vivo. In addition, the absence of specific PMCA inhibitors further complicates this type of analysis. A few studies, however, were informative.

Ca^{2+} measurements performed in intact cells overexpressing the different isoforms and comparing the ability of *a* and *b* variants in counteracting the cytosolic transients generated upon cell stimulation have revealed that the neuron-specific PMCA2 and PMCA3 isoforms were much more effective in counteracting cytosolic transients generated by cell stimulation than the ubiquitously expressed PMCA1 and PMCA4 isoforms [22]. Instead, they have not shown major differences in Ca^{2+} extrusion ability between truncated and full-length variants of PMCA3 and PMCA4 isoforms, thus suggesting that either in intact cells calmodulin was not a limiting factor or their differences in calmodulin affinity were overcome under condition of their maximal activation [22]. The analysis of the joint contribution of site A and site C splicing on the Ca^{2+}-handling ability of PMCA2 pump has instead revealed that *z*/*a*, *w*/*b*, and *z*/*b* splicing variants are all very active, with difference to the doubly inserted *w*/*a* variant that had only limited ability to rapidly increase activity when challenged with a Ca^{2+} pulse, but had about the same highly non-stimulated (basal) activity of the full-length *z*/*b* variant [24]. This finding opened the question on whether site A splicing could have an effect in the modulation of phospholipid activation by altering the overall conformation of the second cytosolic loop of the pump. By measuring the ATPase activity in microsomal membranes of transfected CHO cells, we have found that the PMCA2*w*/*a* variant, as expected, was much less sensitive to calmodulin than the *z*/*b* and *w*/*b* isoforms. However, it was also less sensitive to phosphatidylserine, thus underlining the role of the calmodulin-binding domain in the regulation of pump activity by acidic phospholipids. The finding that the *z*/*b* and *w*/*b* isoforms had the same response to phosphatidylserine stimulation had indicated that the splicing insertion upstream of the phospholipid-binding domain failed to modify the phospholipid sensitivity of the pump [25].

As to the possible physiological meaning of the splicing at site A, an interesting suggestion comes from the finding that, in the case of PMCA2, the insertion of the three exons at site A (which corresponds to a 45-amino-acid insertion, the *w* form) targets the pump to the apical domain of polarized cells, whereas smaller inserts sort the protein to the basolateral domain of the plasma membrane [26]. Interestingly, it has been later demonstrated that the splicing differentially affects the lipid interactions of PMCA pump with the membrane and that the apical localization of this PMCA variant is lipid raft-dependent and sensitive to cholesterol depletion [27].

A recent elegant analysis performed in intact cells has shed light on the action of three PMCA isoforms (PMCA4a, PMCA4b, and PMCA2b) on regulating the pattern of the store-operated Ca^{2+} entry (SOCE), i.e., the influx of Ca^{2+} from the extracellular ambient induced as a consequence of store depletion [28]. The study has shown that the slow activating PMCA4b isoform produced long-lasting Ca^{2+} oscillations in response to SOCE, whereas the activation of the fast PMCA2b isoform resulted in rapid and highly PMCA abundance-sensitive clearance of SOCE-mediated Ca^{2+} transients. At variance, the activation of the PMCA4a variant reduced cytosolic Ca^{2+} transient induced by Ca^{2+} entry, but resulted in the establishment of a basal cytosolic Ca^{2+} concentration higher than that before SOCE activation, indicating that this isoform is suitable to respond to repeated stimuli. The mathematical modeling indicated that the distinct properties of PMCA isoforms are well suited to differentially affect the shape and the kinetics of the Ca^{2+} transients generated by SOCE activation and thus their relative abundance in different cell types may lead to different activation of downstream signaling pathways [28].

At the end of this paragraph discussing the properties of the different PMCA isoforms and splicing variants, it is important to underline that the expression of some PMCA variants changes during embryonic development and during differentiation both in vivo and in vitro. In muscle, the alternative splicing events occur during myogenic differentiation, and, even in L6 myoblasts cell lines, they can be induced by the application of the muscle differentiation factor myogenin [29]. Interestingly, the induction of the splice form 1c of PMCA1 occurs upon myotube formation [30, 31]. Nerve growth factor treatment of PC12 pheochromocytoma cells leads to the appearance of the "differentiation-specific" splice variants of PMCAs 1, 2, and 4 (i.e., 1c, 2a, 4a) [29]. Similarly, a marked upregulation of PMCA1a, PMCA2, and PMCA3 at the mRNA and protein level occurs in rat cerebellar granule cells kept under depolarizing conditions for several days (leading to increased Ca^{2+} influx) [32]. In contrast, elevation of intracellular Ca^{2+} resulted in a rapid (within hours) and specific downregulation of the PMCA4a splice variant by a process mediated by the Ca^{2+}-/calmodulin-sensitive phosphatase calcineurin [33]. In the human neuroblastoma cell line IMR32, differentiation is accompanied by a marked upregulation of PMCA isoforms 2 and 4 (and to a lesser extent, of PMCA1) which in turn leads to an improved Ca^{2+} extrusion efficiency [34]. Another interesting example is the upregulation of PMCA4b expression occurring during colon and gastric cancer cell differentiation that closely correlates with the induction of established differentiation markers, suggesting that an increase in the PMCA-dependent Ca^{2+} transport activity characterizes the differentiation of these cancer cells [35].

In the last years another important distinguishing aspect of the isoforms has received increasing interest: the identification of a number of protein partners that specifically interact with them has opened the discussion on the possibility that PMCA Ca^{2+} extrusion may be locally tuned to control specific microdomains and thus the activity of the resident enzymes/proteins. These aspects are discussed in detail in the next two paragraphs.

4 Why So Many PMCA Variants?

Emerging evidence suggests that in addition to their function as calcium transporters, PMCAs also participate in the regulation of calcium-dependent signal transduction pathways via the interaction with partner proteins. The existence of so many PMCA pump isoforms, including the splice variants, could be rationalized by the finding that they are selectively recruited to plasma membrane compartments/domains by the interaction with specific proteins and that, through a local control of Ca^{2+} concentration, they may regulate the activity of enzymes recruited in functional complexes. Thus, the meaning of the interaction is double: by one side, specific interactors engage PMCA to sub-plasma membrane domains, and by the other, the Ca^{2+}-ejection properties of PMCA, by maintaining intracellular calcium low in cellular microdomains where the tethering with calcium-dependent signaling proteins occurs, negatively modulate Ca^{2+}-sensitive transduction pathways (Fig. 2.3). In agreement with this interpretation, different regulatory interactions have been identified. The identification of some protein partners has, however, only partially reflected differences among isoforms. The preferential site of interaction is the PDZ-binding domain in the C-terminal tail of the *b* variants. PMCA2 and PMCA4 have been shown to interact with several members of the MAGUK (membrane-associated guanylate kinases, or SAP) family of protein kinases which contain PDZ domains and are associated with the cortical actin cytoskeleton [36, 37].

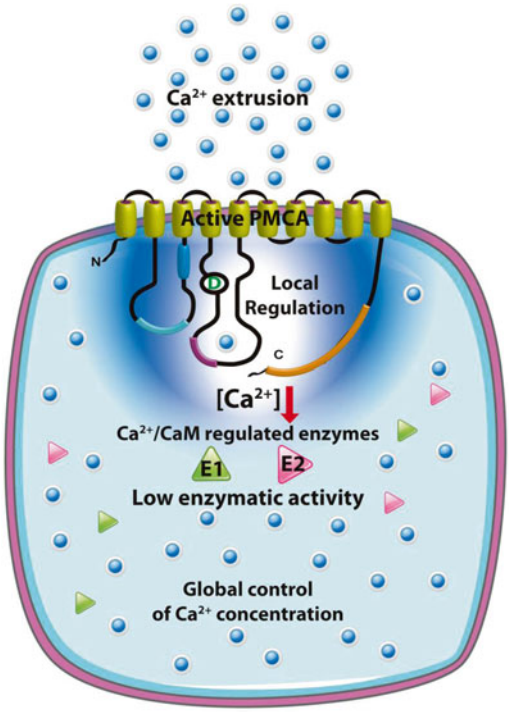

Fig. 2.3 A schematic cartoon showing the double physiological role of PMCA Ca^{2+} extrusion activity. PMCA contributes both to the global regulation of cytosolic Ca^{2+} levels and to the generation of restricted low-calcium microenvironments, where different Ca^{2+}-/calmodulin-dependent enzymes can be tethered by the interaction with the PMCA and their activity downregulated by the very low Ca^{2+} levels. *CaM*, calmodulin

Another PDZ domain-containing protein, NHERF2 (Na^+/H^+ exchanger regulatory factor 2), has been shown to interact with PMCA2*b*, but not with PMCA4*b* [38]. Interestingly, the specific interaction with NHERF2 enhances the apical concentration of PMCA2*w*/*b* by anchoring the pump to the apical membrane cytoskeleton [39]. The PDZ-binding domain of PMCA4*b* also interacts with neuronal nitric oxide synthase (nNOS, NOS-1) in a complex in which alpha-syntrophin [40] and both the PMCA4 and PMCA2 interact through a portion located between transmembrane domains 4 and 5 with endothelial NOS (eNOS, NOS-3) [41]. The decrease in Ca^{2+} concentrations in the immediate vicinity of the enzyme downregulates the production of NO by synthase, thus playing a crucial role in the pathophysiology of the cardiovascular system.

In addition to the C-terminal domain, other regions of the pumps also interact with protein partners. The main intracellular loop joining transmembrane domains 4 and 5, as mentioned above, interacts with eNOS, but also binds RASSF1 (tumor suppressor RAS-associated factor 1), inhibiting the epidermal growth factor-mediated activation of the RAS signaling pathway [42]. The main intracellular loop interacts with alpha-syntrophin (see above) and with the catalytic subunit of the Ca^{2+}-sensitive signal transduction phosphatase calcineurin. Both PMCA2 and PMCA4 have been shown to functionally interact with it, but the strongest interaction was observed with PMCA2, and it results in inhibition of the calcineurin/nuclear factor of activated T-cell signaling pathway [41]. No interaction was instead detected with PMCA1 [43].

Another important interaction is that occurring between the N-terminal cytosolic region of the PMCA1, PMCA3, and PMCA4, but not of the PMCA2 pump and the epsilon isoform of 14-3-3 protein [44, 45]. This interaction is peculiar since it affects pump activity rather than that of the partner as in the case of the other described interactors.

Finally, it is worth to mention that a novel role for the plasma membrane Ca^{2+} ATPase in the regulation of Ca^{2+} signaling is recently emerged in a paper describing the action of PMCA in the control of phosphatidylinositol 4,5-bisphosphate levels [46]. It has been found that PMCAs protect PtdIns(4,5)P_2 in the plasma membrane from the hydrolysis by phospholipase C (PLC). Two mechanisms have been proposed for this action: the first one is that Ca^{2+} extrusion operated by the PMCA was responsible for limiting Ca^{2+} availability to sustain PLC activity, and the second one is that PMCA binds to PtdIns(4,5)P_2 and thus reduces the accessibility for PLC and leads to less inositol 1,4,5-triphosphate ($InsP_3$) production and consequently diminished Ca^{2+} release from intracellular Ca^{2+} stores [46].

5 Functional Versatility

Transgenic animals with altered expression of PMCAs are being used to evaluate the physiological significance of the different isoforms. The identification/generation of mice harboring mutations in the gene coding for PMCA pumps has permitted a better understanding of the involvement of specific PMCA isoforms in the regulation of

Ca^{2+} homeostasis of the cells that express them. In the last 10 years, the discovery of human diseases linked to defects in specific isoforms has also contributed to dissect the importance of PMCA isoforms for specific tissues or organs, since the clinical phenotypes linked to PMCA mutations are generally more restricted than their distribution and abundance.

As mentioned, PMCA1 and PMCA4 have wide tissue distribution and have traditionally been considered as the housekeeping enzymes: however, they have now been shown to play a critical and exquisite signal transduction role. For instance, ablation of PMCA4 gene in mice has profound effect on the reproductive function, since it greatly limits sperm motility and generates male infertility [47]. PMCA4 ablation has also a specific effect on the heart-pumping activity: by failing to modulate the activity of NOS-1, it profoundly affects the process of the excitation/contraction coupling of the cardiomyocyte and thus leads to cardiac hypertrophy and alteration in cardiac rhythm [48, 49].

A genome-wide association study aimed at identifying genetic factors that influence blood pressure and hypertension risk has located the most significant single nucleotide polymorphism in the gene for the PMCA1 pump [50, 51], thus ensuring also for this isoform a possible role in sudden cardiac death, blood pressure control, and hypertension.

At variance with PMCA1 and PMCA4, the PMCA2 and PMCA3 pumps have restricted tissue distribution: they are particularly abundant in neurons. PMCA2 ablation in mice generates cerebellar ataxia and hearing loss [52–54]. PMCA3 knockout mice have not been reported so far, possibly because PMCA3 ablation is embryonically lethal.

Several genetic pathologies linked to the dysfunction of the PMCA pumps have now been described in humans. The first described disease phenotype related to a PMCA pump defect is a form of hereditary deafness that involves the PMCA2 isoform of the pump, which is abundantly expressed in the stereocilia of the hair cells of the Corti organ in the inner ear. The tight control of the homeostasis of Ca^{2+} in the endolymph is essential for the functioning of the stereocilia bundle that gates mechanoelectrical channels through which K^+ (and Ca^{2+}) flow into the hair cell to generate (or modulate) the acoustic signals. Two human families with a hereditary deafness phenotype caused by two different point mutations in the PMCA2 gene were described [24, 55], and curiously, at variance with mice, in humans the PMCA mutations act as modifier of a phenotype caused by mutations in other genes (i.e., cadherin 23) or through a digenic mechanism, where both mutations in cadherin 23 and in PMCA2 genes are necessary to develop the hearing loss phenotype.

Interestingly, mutations in PMCA3 gene have been recently identified in two families affected by cerebellar ataxia [56, 57]: their mechanism of action is possibly different since in the first family the mutation is responsible per se of the X-linked phenotype [56] and in the second one the phenotype was developed only when the patient also inherited mutations in the *LAMA1* gene, which encodes the extracellular matrix protein laminin subunit 1α [57].

Molecular studies of the mutant PMCA3 pumps expressed in model cells have shown that the mutations impaired pump ability to extrude Ca^{2+} both in resting condition

and upon cell stimulation [56, 57]. A missense mutation (Tyr543Met) in the PMCA3 pump gene has also been detected in human pancreatic cancer cells [58], but the effects of the mutation on the activity of the pump have not been investigated.

6 Conclusions

The data from several groups largely support the view that the PMCA pumps are not uniquely in place to keep resting cytosolic Ca^{2+} concentration and counteract Ca^{2+} transients generated by cell stimuli and thus turn off activatory signals, but that they can themselves regulate the activity of specific enzymatic complexes by locally controlling Ca^{2+} environments. Surprisingly and interestingly, defects in pump activity, generally, do not lead to global cell impairment that conduces to cell death but originated disease conditions that compromise only specific cell populations or tissues, despite the distribution of mutated isoform is not confined to them. This aspect is particularly fascinating and suggests that the expression of specific PMCA isoforms could be orchestrated by the cell to finely tune Ca^{2+} homeostasis in specific environments and according to specific requirements. A lot of work is still necessary to profoundly understand the complexity of the system and to develop specific drugs that could modulate PMCA activity in an isoform-specific manner and could thus be suitable to therapeutical approaches to target PMCA inactivating mutations.

Acknowledgments We are deeply grateful to Ernesto Carafoli who has greatly contributed during the years to clarify the mechanisms of action and regulation of the plasma membrane Ca^{2+} pump and has trained us in this field of investigation with enthusiasm and passion. T.C is supported by the Scientific Independence of Young Researchers (SIR) grant (Bando SIR 2014 n. RBSI14C65Z) from the Italian Ministry of University and Research (MIUR).

References

1. Berridge MJ, Bootman MD, Roderick HL (2003) Calcium signalling: dynamics, homeostasis and remodelling. Nat Rev Mol Cell Biol 4:517–529
2. Pedersen P, Carafoli E (1987) Ion motive ATPases. I. Ubiquity, properties, and significance to cell function. Trends Biochem Sci 12:146–150
3. Toyoshima C (2009) How Ca^{2+}-ATPase pumps ions across the sarcoplasmic reticulum membrane. Biochim Biophys Acta 1793:941–946
4. Shull GE, Greeb J (1988) Molecular cloning of two isoforms of the plasma membrane Ca2 + -transporting ATPase from rat brain. Structural and functional domains exhibit similarity to Na+, K + - and other cation transport ATPases. J Biol Chem 263:8646–8657
5. Verma AK, Filoteo AG, Stanford DR et al (1988) Complete primary structure of a human plasma membrane Ca^{2+} pump. J Biol Chem 263:14152–14159
6. Brini M, Carafoli E (2009) Calcium pumps in health and disease. Physiol Rev 89:1341–1378
7. Falchetto R, Vorherr T, Brunner J, Carafoli E (1991) The plasma membrane Ca^{2+} pump contains a site that interacts with its calmodulin-binding domain. J Biol Chem 266:2930–2936
8. Falchetto R, Vorherr T, Carafoli E (1992) The calmodulin-binding site of the plasma membrane Ca^{2+} pump interacts with the transduction domain of the enzyme. Protein Sci 1:1613–1621

9. Elshorst B, Hennig M, Forsterling H et al (1999) NMR solution structure of a complex of calmodulin with a binding peptide of the Ca^{2+} pump. Biochemistry 38:12320–12332
10. Guerini D, Krebs J, Carafoli E (1984) Stimulation of the purified erythrocyte Ca^{2+}-ATPase by tryptic fragments of calmodulin. J Biol Chem 259:15172–15177
11. Tidow H, Poulsen LR, Andreeva A et al (2012) A bimodular mechanism of calcium control in eukaryotes. Nature 491:468–472
12. Brodin P, Falchetto R, Vorherr T, Carafoli E (1992) Identification of two domains which mediate the binding of activating phospholipids to the plasma-membrane Ca^{2+} pump. Eur J Biochem 204:939–946
13. Hofmann F, James P, Vorherr T, Carafoli E (1993) The C-terminal domain of the plasma membrane Ca^{2+} pump contains three high affinity Ca^{2+} binding sites. J Biol Chem 268: 10252–10259
14. James P, Vorherr T, Krebs J et al (1989) Modulation of erythrocyte Ca^{2+}-ATPase by selective calpain cleavage of the calmodulin-binding domain. J Biol Chem 264:8289–8296
15. Salamino F, Sparatore B, Melloni E et al (1994) The plasma membrane calcium pump is the preferred calpain substrate within the erythrocyte. Cell Calcium 15:28–35
16. Monteith GR, Roufogalis BD (1995) The plasma membrane calcium pump--a physiological perspective on its regulation. Cell Calcium 18:459–470
17. Penniston JT, Enyedi A (1998) Modulation of the plasma membrane Ca^{2+} pump. J Membr Biol 165:101–109
18. Strehler EE, Zacharias DA (2001) Role of alternative splicing in generating isoform diversity among plasma membrane calcium pumps. Physiol Rev 81:21–50
19. Ortega C, Ortolano S, Carafoli E (2007) The plasma membrane calcium pump. In: Krebs J, Michalak M (eds) Calcium: a matter of life or death, vol 41. Springer, New York, NY, pp 179–197, Chapter 7
20. Guerini D, Carafoli E (1999) The calcium pumps. In: Carafoli E, Klee C (eds) Calcium as a cellular regulators, vol 10. Oxford University Press, Oxford, pp 249–278
21. Preiano BS, Guerini D, Carafoli E (1996) Expression and functional characterization of isoforms 4 of the plasma membrane calcium pump. Biochemistry 35:7946–7953
22. Brini M, Coletto L, Pierobon N et al (2003) A comparative functional analysis of plasma membrane Ca^{2+} pump isoforms in intact cells. J Biol Chem 278:24500–24508
23. Niggli V, Adunyah ES, Penniston JT, Carafoli E (1981) Purified (Ca^{2+}-Mg^{2+})-ATPase of the erythrocyte membrane. Reconstitution and effect of calmodulin and phospholipids. J Biol Chem 256:395–401
24. Ficarella R, Di Leva F, Bortolozzi M et al (2007) A functional study of plasma-membrane calcium-pump isoform 2 mutants causing digenic deafness. Proc Natl Acad Sci U S A 104: 1516–1521
25. Brini M, Di Leva F, Ortega CK et al (2010) Deletions and mutations in the acidic lipid-binding region of the plasma membrane Ca^{2+} pump: a study on different splicing variants of isoform 2. J Biol Chem 285:30779–30791
26. Chicka MC, Strehler EE (2003) Alternative splicing of the first intracellular loop of plasma membrane Ca^{2+}-ATPase isoform 2 alters its membrane targeting. J Biol Chem 278:18464–18470
27. Xiong Y, Antalffy G, Enyedi A, Strehler EE (2009) Apical localization of PMCA2w/b is lipid raft-dependent. Biochem Biophys Res Commun 384:32–36
28. Paszty K, Caride AJ, Bajzer Z et al (2015) Plasma membrane Ca^{2+}-ATPases can shape the pattern of Ca^{2+} transients induced by store-operated Ca^{2+} entry. Sci Signal 8:ra19
29. Hammes A, Oberdorf S, Strehler EE et al (1994) Differentiation-specific isoform mRNA expression of the calmodulin-dependent plasma membrane Ca^{2+}-ATPase. FASEB J 8:428–435
30. Brandt P, Ibrahim E, Bruns GA, Neve RL (1992) Determination of the nucleotide sequence and chromosomal localization of the ATP2B2 gene encoding human Ca^{2+}-pumping ATPase isoform PMCA2. Genomics 14:484–487
31. De Jaegere S, Wuytack F, De Smedt H et al (1993) Alternative processing of the gene transcripts encoding a plasma-membrane and a sarco/endoplasmic reticulum Ca^{2+} pump during differentiation of BC3H1 muscle cells. Biochim Biophys Acta 1173:188–194

32. Guerini D, Garcia-Martin E, Gerber A et al (1999) The expression of plasma membrane Ca^{2+} pump isoforms in cerebellar granule neurons is modulated by Ca^{2+}. J Biol Chem 274:1667–1676
33. Guerini D, Wang X, Li L et al (2000) Calcineurin controls the expression of isoform 4CII of the plasma membrane Ca^{2+} pump in neurons. J Biol Chem 275:3706–3712
34. Usachev YM, Toutenhoofd SL, Goellner GM et al (2001) Differentiation induces up-regulation of plasma membrane Ca^{2+}-ATPase and concomitant increase in Ca^{2+} efflux in human neuroblastoma cell line IMR-32. J Neurochem 76:1756–1765
35. Ribiczey P, Tordai A, Andrikovics H et al (2007) Isoform-specific up-regulation of plasma membrane Ca^{2+}ATPase expression during colon and gastric cancer cell differentiation. Cell Calcium 42:590–605
36. DeMarco SJ, Strehler EE (2001) Plasma membrane Ca^{2+}-atpase isoforms 2b and 4b interact promiscuously and selectively with members of the membrane-associated guanylate kinase family of PDZ (PSD95/Dlg/ZO-1) domain-containing proteins. J Biol Chem 276:21594–21600
37. Schuh K, Uldrijan S, Gambaryan S et al (2003) Interaction of the plasma membrane Ca^{2+} pump 4b/CI with the Ca^{2+}/calmodulin-dependent membrane-associated kinase CASK. J Biol Chem 278:9778–9783
38. DeMarco SJ, Chicka MC, Strehler EE (2002) Plasma membrane Ca^{2+} ATPase isoform 2b interacts preferentially with Na+/H+ exchanger regulatory factor 2 in apical plasma membranes. J Biol Chem 277:10506–10511
39. Padanyi R, Xiong Y, Antalffy G et al (2010) Apical scaffolding protein NHERF2 modulates the localization of alternatively spliced plasma membrane Ca^{2+} pump 2B variants in polarized epithelial cells. J Biol Chem 285:31704–31712
40. Williams JC, Armesilla AL, Mohamed TM et al (2006) The sarcolemmal calcium pump, alpha-1 syntrophin, and neuronal nitric-oxide synthase are parts of a macromolecular protein complex. J Biol Chem 281:23341–23348
41. Holton M, Yang D, Wang W et al (2007) The interaction between endogenous calcineurin and the plasma membrane calcium-dependent ATPase is isoform specific in breast cancer cells. FEBS Lett 581:4115–4119
42. Armesilla AL, Williams JC, Buch MH et al (2004) Novel functional interaction between the plasma membrane Ca^{2+} pump 4b and the proapoptotic tumor suppressor Ras-associated factor 1 (RASSF1). J Biol Chem 279:31318–31328
43. Buch MH, Pickard A, Rodriguez A et al (2005) The sarcolemmal calcium pump inhibits the calcineurin/nuclear factor of activated T-cell pathway via interaction with the calcineurin A catalytic subunit. J Biol Chem 280:29479–29487
44. Rimessi A, Coletto L, Pinton P et al (2005) Inhibitory interaction of the 14-3-3{epsilon} protein with isoform 4 of the plasma membrane Ca^{2+}-ATPase pump. J Biol Chem 280:37195–37203
45. Linde CI, Di Leva F, Domi T et al (2008) Inhibitory interaction of the 14-3-3 proteins with ubiquitous (PMCA1) and tissue-specific (PMCA3) isoforms of the plasma membrane Ca^{2+} pump. Cell Calcium 43:550–561
46. Penniston JT, Padanyi R, Paszty K et al (2014) Apart from its known function, the plasma membrane Ca^{2+} ATPase can regulate Ca^{2+} signaling by controlling phosphatidylinositol 4,5-bisphosphate levels. J Cell Sci 127(Pt 1):72–84
47. Schuh K, Cartwright EJ, Jankevics E et al (2004) Plasma membrane Ca^{2+} ATPase 4 is required for sperm motility and male fertility. J Biol Chem 279:28220–28226
48. Mohamed TM, Oceandy D, Zi M et al (2011) Plasma membrane calcium pump (PMCA4)-neuronal nitric-oxide synthase complex regulates cardiac contractility through modulation of a compartmentalized cyclic nucleotide microdomain. J Biol Chem 286:41520–41529
49. Cartwright EJ, Oceandy D, Austin C, Neyses L (2011) Ca^{2+} signalling in cardiovascular disease: the role of the plasma membrane calcium pumps. Sci China Life Sci 54:691–698
50. Cho YS, Go MJ, Kim YJ et al (2009) A large-scale genome-wide association study of Asian populations uncovers genetic factors influencing eight quantitative traits. Nat Genet 41:527–534
51. Hong KW, Go MJ, Jin HS et al (2010) Genetic variations in ATP2B1, CSK, ARSG and CSMD1 loci are related to blood pressure and/or hypertension in two Korean cohorts. J Hum Hypertens 24:367–372

52. LA Kurnellas MP, Li H, Deng L, Ehrlich DJ, Elkabes S (2007) Molecular alterations in the cerebellum of the plasma membrane calcium ATPase 2 (PMCA2)-null mouse indicate abnormalities in Purkinje neurons. Mol Cell Neurosci 34:178–188
53. Kurnellas MPNA, Shull GE, Elkabes S (2005) Plasma membrane calcium ATPase deficiency causes neuronal pathology in the spinal cord: a potential mechanism for neurodegeneration in multiple sclerosis and spinal cord injury. FASEB J 19:298–300
54. Kozel PJ, Friedman RA, Erway LC et al (1998) Balance and hearing deficits in mice with a null mutation in the gene encoding plasma membrane Ca^{2+}-ATPase isoform 2. J Biol Chem 273:18693–18696
55. Schultz JM, Yang Y, Caride AJ et al (2005) Modification of human hearing loss by plasma-membrane calcium pump PMCA2. N Engl J Med 352:1557–1564
56. Zanni G, Calì T, Kalscheuerc V, Ottolini D, Barresia S, Lebrune N, Montecchi-Palazzi L, Chellye J, Bertini E, Brini M, Carafoli E (2012) A mutation of plasma membrane ca^{2+} atpase isoform 3 in a family with x-linked congenital cerebellar ataxia impairs ca^{2+} homeostasis. Proc Natl Acad Sci U S A 109:14514
57. Calì T, Lopreiato R, Shimony J et al (2015) A novel mutation in isoform 3 of the plasma membrane Ca^{2+} pump impairs cellular Ca^{2+} homeostasis in a patient with cerebellar ataxia and laminin subunit 1alpha mutations. J Biol Chem 290:16132
58. Jones S, Zhang X, Parsons DW et al (2008) Core signaling pathways in human pancreatic cancers revealed by global genomic analyses. Science 321:1801–1806

Chapter 3
PMCA2*w/a* Splice Variant: A Key Regulator of Hair Cell Mechano-transduction Machinery

Mario Bortolozzi and Fabio Mammano

Abstract Sensory hair cells of the inner ear detect sound stimuli, inertial or gravitational forces. These mechanical inputs cause deflection of the cell stereociliary bundle and activate a small number of cation-selective mechano-transduction (MET) channels that admit K^+ and Ca^{2+} ions into the cytoplasm. Stereociliary Ca^{2+} levels are homeostatically regulated by an unusual splicing isoform (*w/a*) of plasma membrane calcium-pump isoform 2 (PMCA2*w/a*), ablation or missense mutations of which cause deafness and loss of balance in humans and mice. At variance with other PMCA2 isoforms, PMCA2*w/a* expressed in CHO transfectants increases only marginally its activity in response to a rapid increase of the cytoplasmic free Ca^{2+} concentration ($[Ca^{2+}]_c$). In this expression system, deafness-related mutations of PMCA2*w/a* decrease the pump ability to extrude Ca^{2+} both at steady state and in response to a $[Ca^{2+}]_c$ rise. Consistent with these findings, mouse strains in which the pump is genetically ablated or mutated show hearing impairment correlated with defects in homeostatic regulation of stereociliary Ca^{2+}, decreased sensitivity of the MET channels to hair bundle displacement, and morphological abnormalities in the organ of Corti. These results highlight a critical role played by PMCA2*w/a* in the control of hair cell function and survival and provide mechanistic insight into the etiology of deafness and vestibular disorders.

M. Bortolozzi
Department of Physics and Astronomy "G. Galilei", University of Padua,
Via Marzolo 8, 35131 Padua, Italy

Venetian Institute of Molecular Medicine (VIMM), Via Orus 2, 35129 Padua, Italy

F. Mammano (✉)
Department of Physics and Astronomy "G. Galilei", University of Padua,
Via Marzolo 8, 35131 Padua, Italy

Venetian Institute of Molecular Medicine (VIMM), Via Orus 2, 35129 Padua, Italy

CNR Institute of Cell Biology and Neurobiology, Via E. Ramarini, 32, 00015
Monterotondo, Scalo Roma, Italy
e-mail: fabio.mammano@cnr.it

S. Chakraborti, N.S. Dhalla (eds.), *Regulation of Ca^{2+}-ATPases,V-ATPases and F-ATPases*, Advances in Biochemistry in Health and Disease 14,
DOI 10.1007/978-3-319-24780-9_3

Keywords Inner ear • Utricle • Hair cell stereocilia • Ca^{2+} imaging • Ca^{2+} uncaging • Patch clamp • Immunofluorescence • Confocal microscopy • Electron microscopy

1 Introduction

Two Ca^{2+} exporting systems maintain cytosolic Ca^{2+} of eukaryotic cells at the low concentration demanded by the signaling function. In cardiomyocytes and possibly in other excitable cells as well, the larger capacity Na^{+}/Ca^{2+} exchanger is the most important system, whereas the plasma membrane Ca^{2+}-ATPase (PMCA) pump has the primary role in most other cell types [1]. Of the four basic isoforms of the PMCA pump, two operate in all tissues (PMCA1 and PMCA4) while the other two (PMCA2 and PMCA3) in specialized tissues, such as the muscle and, especially, brain [1, 2]. PMCA2 is expressed at high levels in vestibular and outer hair cell stereocilia and apical membranes and at moderate levels in inner hair cell stereocilia and in the spiral ganglion [3–7]. This pump has properties that set it apart from all other PMCAs [8]: it has very high affinity for the activator calmodulin, yet its activity is only modestly activated by it [8, 9]. Unlike the other three PMCA basic isoforms, PMCA2 has peculiarly high activity in the absence of the activator calmodulin, i.e., it pumps Ca^{2+} out of cells at a relatively high constant rate.

Several splice variants of the four PMCAs have been detected in inner ear cDNAs [3]. Alternative splicing is peculiarly complex in PMCA2 (Fig. 3.1a), as it involves the insertion of up to three novel exons at site A, in the cytosolic loop connecting transmembrane domains 2 and 3, and of two at site C in the C-terminal tail of the pump [10]. The site A insertions are in frame, creating variant *w* when three exons are inserted or the normal variant *z* without site A inserts. The expression of the splice variant PMCA2x is induced only by a transient rise of intracellular Ca^{2+}, indicating that phosphorylation/dephosphorylation is an essential mechanism for the function of various spliceosomal proteins [11, 12]. The insert at site C creates instead

Fig. 3.1 (continued) form are indicated by *red dashed lines*. The sizes of alternatively spliced exons are given as nucleotide numbers. PL = phospholipid-binding domain; P = location of the aspartyl phosphate formation. (**b**) Schematics of the hair cell stereociliary bundle in the resting and deflected state. The *boxed area* is magnified to illustrate the prevailing view of the molecular composition of the transduction complex, which includes a tip link connecting the top of a shorter stereocilium and the side wall of its taller neighbour, upper tip-link densities (tripartite complex of myosin-7a, harmonin-b, and sans) and the lower tip-link densities (myosin XVa, whirlin, Eps8, and CIB2) [18]. Cadherin-23 and protocadherin-15 form the upper and lower parts of the tip link, respectively. The molecular machinery of the MET complex is anchored to the cytoplasmic region of protocadherin-15 [64–66]. Stereociliary Ca^{2+} concentration is regulated by the extrusion activity of the PMCA2*w*/*a* pump.

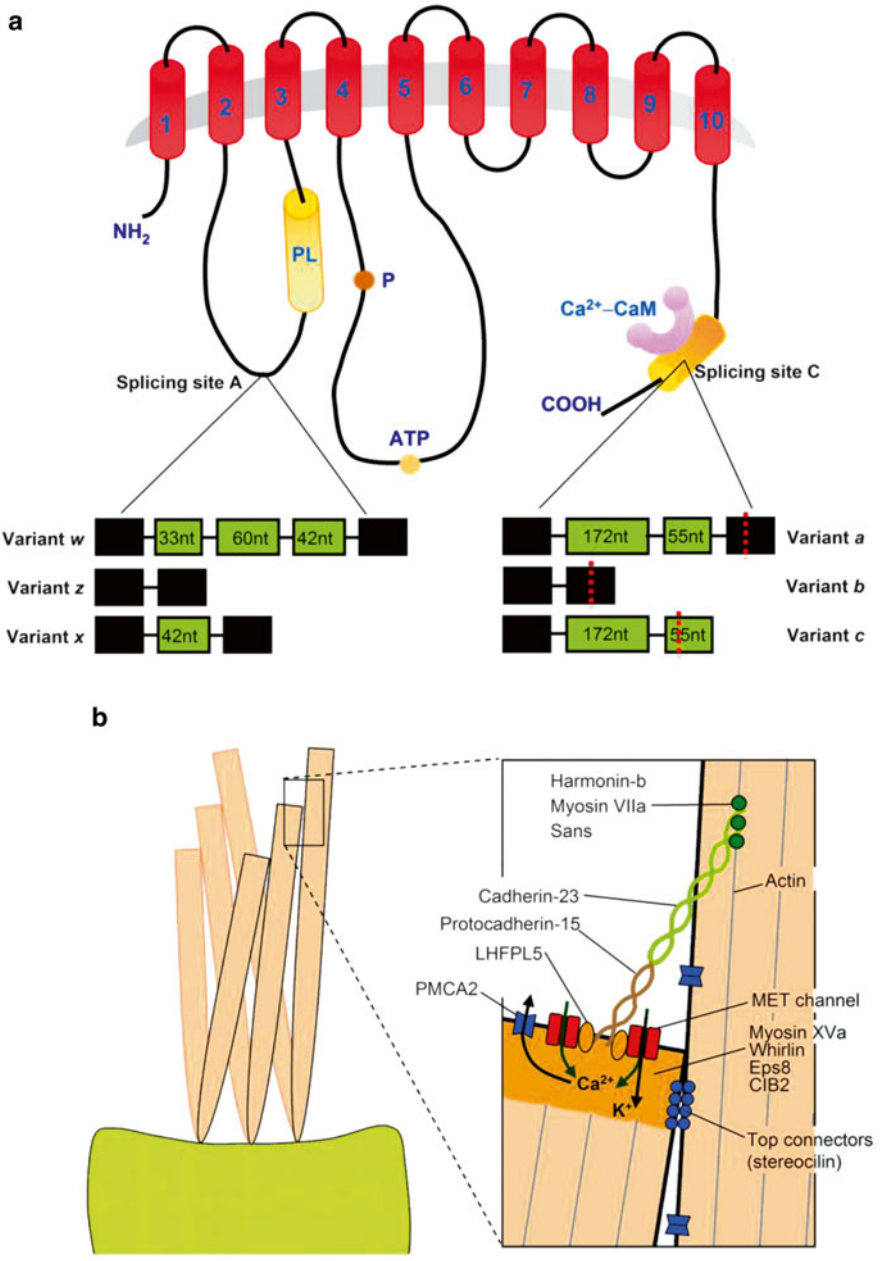

Fig. 3.1 PMCA2 and the hair cell mechano-transduction machinery. (**a**) Topology domains and splicing variants of the human PMCA2 isoforms. Splice site "C" lies within the calmodulin-binding domain (*yellow cylinder*; CaM = calmodulin). Constitutively spliced exons are indicated as *black boxes*; alternatively inserted exons are shown in *green*; the resulting splice variants are labeled by their *lower case* symbols; the positions of the translation stop codons for each splice

a novel stop codon, leading to truncation of the pump in variant *a*, variant *b* being the normal full-length pump and *c* a C-terminal shortened version due to a change in the reading frame. The site C insertions eliminate about half of the calmodulin-binding domain; those at site A occur next to a domain that binds activatory acidic phospholipids, which, however, also bind to the calmodulin-binding domain [13]. As expected, the site C insertions lower the affinity of PMCA pumps for calmodulin [14], but do not compromise the activation by acidic phospholipids, which is alternative to that by calmodulin [15]. The site A insertion, by contrast, could impair the activation by acidic phospholipids, particularly in the C-terminally truncated pump variants, in which the C-terminal phospholipid-binding domain is also compromised. PMCA1*b* prevails in basolateral membranes, whereas the C-terminally truncated PMCA2*a* is the only isoform detected in the stereocilia of hair cells [4]. Recent work has shown that the truncated isoform in the stereocilia of cochlear outer hair cells (OHCs; [16]) is also spliced at site A and is thus the *w/a* variant [17].

A few words are in order here to summarize the basics of mechano-transduction in hair cells [18] and the role played by PMCA2*w/a* in hearing [19] (Fig. 3.1b). It is currently thought that deflection of the stereociliary bundle in the direction of the taller stereocilia increases tension in the tip link, a filament stretched between the tops of stereocilia. This mechanical stimulus is conveyed to MET channels, which open to allow cations to flow into the cell [20]. The apical surface of hair cells is bathed in endolymph, which is rich in K^+ but low in Na^+ and Ca^{2+} [21]; thus, K^+ carries most of the transduction current. However, due to the high permeability of MET channels to Ca^{2+}, its influx is significant despite the low Ca^{2+} levels of the endolymph, which are much lower than those of other extracellular fluids [22–26]: 20–23 μM in the rodent cochlea [27, 28] and 200–250 μM in the vestibular system, possibly due to the presence there of calcium carbonate crystals [29, 30]. Irrespective of the hair cell type, Ca^{2+} entering through MET channels is rapidly sequestered by buffers in the stereocilia [31, 32]. Ca^{2+} is then shuttled back to endolymph by the PMCA2*w/a* pump [33, 34]. Various laboratories estimated the density of this pump in stereocilia membrane at 2000–2200/μm^2 [5, 34–37], from which a figure of about 200 ions/s per pump has been inferred for the extrusion rate [5]. PMCA2*w/a* action is thought to increase Ca^{2+} in the immediate proximity of the hair bundle [34], possibly with the complicity of the acellular structures overlying the hair cells in the cochlea [38] and, particularly, in the vestibular system [30], where the pump would also contribute to the formation and maintenance of the otoconia [39].

Mutations of the *ATP2b2* gene, coding for PMCA2, have been causally linked to hereditary deafness, loss of balance, and ataxia in mice [39–45] and humans [46, 47]. In some cases, these mutations lead to the truncation of the protein product and to its eventual disappearance from the stereocilia of hair cells. Other mutations, which do not compromise the reading frame of the gene and are thus compatible with the expression of the full-length PMCA2*w/a* variant of the pump, affect residues that are highly conserved in all PMCA isoforms across species and in other P-type pumps.

Here, we recapitulate work carried out in our laboratory to analyze the functional consequences of PMCA2*w/a* mutations in expression systems as well as in vestibular

and cochlear hair cells derived from mutant mice, in collaboration with research teams led by Ernesto Carafoli, Marisa Brini, Paolo Gasparini, Karen Steel, Steve Brown, and the late Edoardo Arslan. A limited number of key results generated by other laboratories are also reviewed, aiming to convey a broader message to the reader.

2 Comparative Analysis of the Ca^{2+} Handling Activity of PMCA2 Splice Variants and Mutants Expressed in Transiently Transfected CHO Cells

Historically, the first deafness-linked point mutation of PMCA2*w/a* is a G-S replacement at amino acid 283, PMCA2*w/a*(G283S) [40] in the first cytosolic loop of the pump (Fig. 3.1a), which was identified in the *deafwaddler* (*dfw*) mouse strain [48]. The same amino acidic change at nearby position 293, PMCA2*w/a*(G293S), was later found in a human family with hearing defects [47]. In the *N*-ethyl-*N*-nitrosourea-induced *Oblivion* (*Obl*) mouse mutant, S is replaced by F at position 922 of PMCA2*w/a*(S922F) in the sixth transmembrane domain [44]. The *Tommy* mouse mutant carries the mutation PMCA2*w/a*(E629K), which affects a highly conserved residue located in the second intracellular loop of the pump [45]. In the *z/b* nomenclature of the pump, the *Tommy* mutation is classified as p.E584K and occurs only two residues upstream the site of the human mutation p.V586M reported in Ref. [46].

Mammalian expression plasmids for the wild-type (wt) pump, the *dfw* mouse mutation PMCA2*w/a*(G283S) and the human PMCA2*w/a*(G293S) mutation, and *z/b*, *z/a*, and *w/b* splice isoforms were generated and transfected in CHO cells [47]. Appropriate controls (Western blots and quantitative immunocytochemistry) established that all variants of the pump were expressed at equivalent levels and were correctly delivered to the plasma membrane (Fig. 3.2a–g). CHO cells were co-transfected with the Ca^{2+}-sensitive photoprotein aequorin [49] and stimulated with ATP, an $InsP_3$-linked agonist that acts on P2Y purinergic receptors (Fig. 3.2h, i). We think that, under these experimental conditions, the height of the Ca^{2+} transient generated by the opening of the $InsP_3$ receptor is controlled primarily by the PMCA pumps and not by the SERCA pump. Indeed, in control experiments, the latter was silenced using the specific inhibitor 2,5-di-*tert*-butyl-1,4 benzohydroquinone, with marginal changes in the height of the Ca^{2+} peak and in the kinetics of the return of the traces to baseline. The post-peak decay kinetics of the traces is expected to be influenced by Ca^{2+} influx through store-operated calcium channels. No efforts were made to eliminate their contribution to the shape of the Ca^{2+} curves, as it was felt that the effects would have been the same for all pump variants.

Two of the splice variants (*z/a* and *w/b*) have essentially the same effect on the Ca^{2+} peak of the full-length, non-spliced PMCA2*z/b* pump, which is a very active PMCA isoform [8] (Fig. 3.2h). By contrast, the doubly spliced variant PMCA2*w/a* is less able to control the peak height, meaning that it reacts less to the surge of the Ca^{2+} pulse. However, when the function of the pump becomes the long-term control

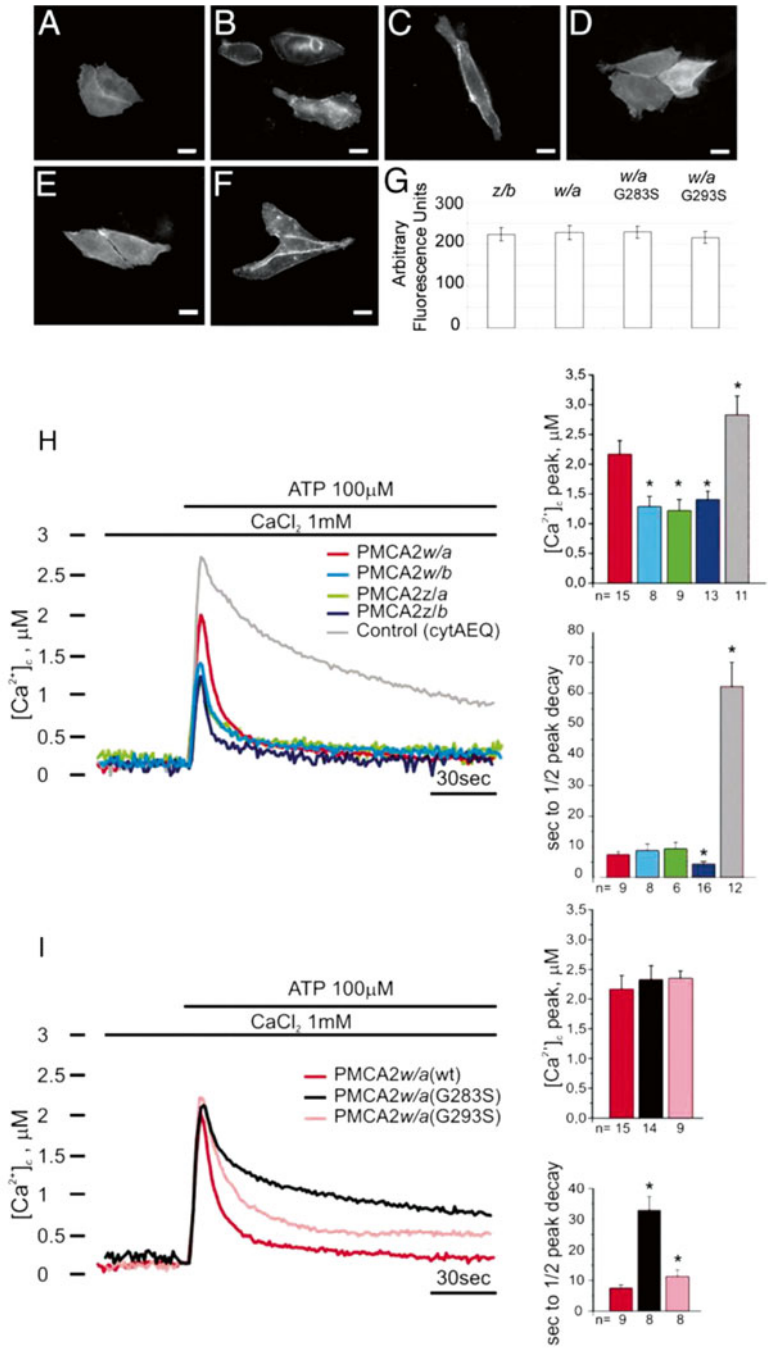

Fig. 3.2 Immunolocalization and activity of recombinant PMCA2 pumps in transiently transfected CHO cells. (**a**–**d**) Expression of PMCA2 variants in CHO cells *w/b* (**a**), *z/a* (**b**), *z/b* (**c**), and *w/a* (**d**). Pump immunoreactivity to the 5F10 antibody was revealed by an Alexa Fluor 488-conjugated secondary antibody. (**e** and **f**) PMCA mutants on the *w/a* construct G283S (**e**) and G293S (**f**) were stained with the primary 2N antibody, and the interaction was visualized by an

of post-peak Ca^{2+}, i.e., when only nonactivated pumping is presumably required, all variants, including PMCA2*w/a*, are equivalent (the *z/b* is slightly more efficient; see histograms in Fig. 3.2h).

The *dfw* mutant PMCA2*w/a*(G283S) and the human mutant PMCA2*w/a*(G293S) are as ineffective as the wt PMCA2*w/a* in handling the Ca^{2+} peak (Fig. 3.2i). Instead, the declining phase of the Ca^{2+} curve, measured by the half peak decay time, was much slower in the PMCA2*w/a*(G283S) and PMCA2*w/a*(G293S) mutants than in the wt PMCA2*w/a* (wt, 7.4 ± 1.0 s; PMCA2*w/a*(G283S), 32.9 ± 4.4 s; PMCA2*w/a*(G293S), 11.3 ± 2.3; $p < 0.01$). The defect is more pronounced in the PMCA2*w/a*(G283S) than in the PMCA2*w/a*(G293S) mutant, and these differences are exacerbated if the mutations are inserted in the backbone of the full-length pump (PMCA2*z/b*).

The resting activity of the *Obl* and *Tommy* mutant pumps, i.e., PMCA2*w/a*(S922F) [44] and PMCA2*w/a*(E629K) [45], is lower than that of the *dfw* pump, i.e., PMCA2*w/a*(G283S), and both exhibit a half peak decay time which is significantly longer than that of the wt PMCA2*w/a* pump (wt, 6.7 ± 0.7 s; Obl, 39.4 ± 6.7 s; Tommy, 45.5 ± 6.0 s; $p < 0.01$).

3 Ca^{2+} Homeostasis in Hair Cells of Mutant Mice

To substantiate the above results, the PMCA2 ability to extrude Ca^{2+} was investigated in situ using neonatal organotypic cultures of utricle sensory epithelium collected between postnatal days 0 and 3 (P0–P3) and observed between P1 and P4. The choice of utricles for these experiments was dictated, on the one hand, by the larger dimension of the sensory hair bundle in vestibular hair cells compared to cochlear hair cells and, on the other hand, by the ease with which the utricular preparation can be mounted to acquire confocal images with the cell main axis resting in the focal plane (Fig. 3.3a). In this preparation, hair cells were stimulated by the rapid photorelease of Ca^{2+} from a cytosolic caged precursor (*o-nitrophenyl-EGTA*, Fig. 3.3b). The hair cell dissipates this sudden increase of $[Ca^{2+}]_c$ by the action of endogenous buffers, uptake by mitochondria [50], and transport by Ca^{2+}-ATPases [39]. The ability of PMCA2 to extrude Ca^{2+} depends, among other things, also on the $[Ca^{2+}]_c$ levels; thus, we decided to select only experiments with similar $\Delta f/f_0 = (f - f_0)/f_0$ transients, where f is fluorescence at time t and f_0 is pre-stimulus

Fig. 3.2 (continued) Alexa Fluor 488-conjugated secondary antibody (scale bars, 20 μm). (**g**) Quantification of PMCA2 concentration in the plasma membrane by immunofluorescence levels. Standard deviations are indicated by the bars. (**h**) CHO cells transiently transfected with the indicated PMCA2 variants, with or without the cytAEQ Ca^{2+} reporter, were stimulated by bath application of 100 μM ATP to produce a transient increase of $[Ca^{2+}]_c$. The histograms show the means ± SD of $[Ca^{2+}]_c$ peaks and half peak decay times. (**i**) CHO cells transiently transfected with the normal PMCA2*w/a* and the PMCA2*w/a*(G283S) and the human PMCA2*w/a*(G293S) mutants. The traces are representative of at least eight experiments. *, $p < 0.01$ estimated with respect to PMCA2*w/a*

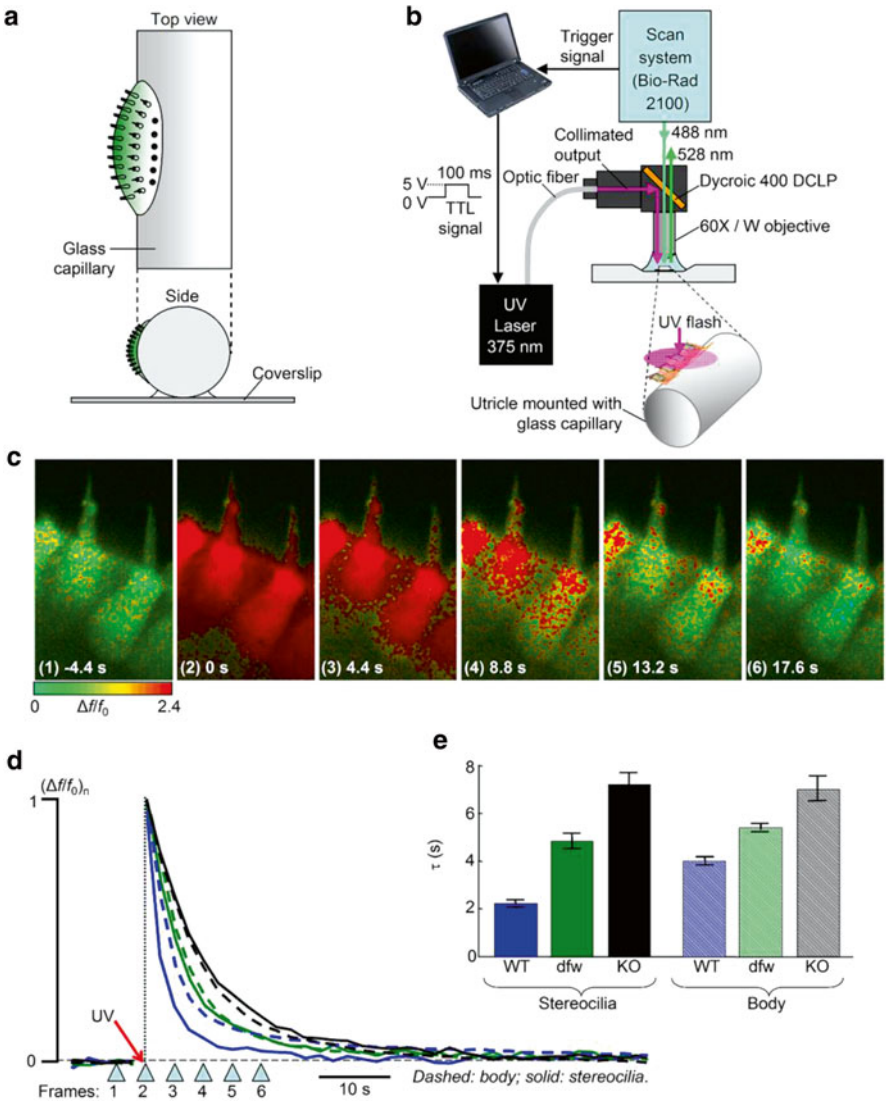

Fig. 3.3 Ca^{2+} imaging in vestibular hair cells of wt and mutant mice. (**a**) Fixing a mouse utricular macula to the lateral side of a glass capillary permits to visualize hair bundles in the focal plane of the microscope objective and to estimate $[Ca^{2+}]_c$ changes in the stereocilia and cell body by Ca^{2+} imaging. (**b**) UV laser light (375 nm), controlled by a transistor–transistor logic (TTL) signal generated by a computer connected to the scanning system of a confocal microscope (Bio-Rad 2100), was delivered for 100 ms to elicit a homogeneous $[Ca^{2+}]_c$ increase in an area covering a few hair cells. $[Ca^{2+}]_c$ was detected by Fluo-4 (excitation wavelength, 488 nm; emission, 528 nm). (**c**) Time sequence of confocal images acquired before and after UV photolysis of caged Ca^{2+} in hair cells of a utricle culture (P2) from a PMCA2 KO mouse. Timing relative to the onset of the UV light delivery is shown on each numbered frame; the amplitude of the $\Delta f/f_0$ signal is encoded by the color scale bar beneath frame 1. (**d**) Time course of normalized fluorescence ratio changes $(\Delta f/f_0)_n$

Table 3.1 Activities of PMCA2*w/a* in hair cells of mutant mice

Mouse	Stereociliary Ca^{2+} clearance time constant (τ)	Ca^{2+} clearance ratio ($\tau_{mutant}/\tau_{background}$)
Strain genetic background	2.2 ± 0.2 s (*dfw*)	1
	2.8 ± 0.4 s (*Obl*)	
	2.8 ± 0.3 s (*Tommy*)	
Tommy heterozygous	3.8 ± 0.8 s	1.4 ± 0.3
Obl heterozygous	4.2 ± 1 s	1.5 ± 0.4
Tommy homozygous	4.5 ± 0.9 s	1.6 ± 0.3
dfw homozygous	4.8 ± 0.6 s	2.2 ± 0.6
Obl homozygous	6.9 ± 1.3 s	2.5 ± 0.5
PMCA2 KO	7.2 ± 0.8 s	3.3 ± 0.4

Ca^{2+} clearing rate of the stereocilia in the case of PMCA2 ablation or impairment of its activity. For each mouse strain, the corresponding genetic background was taken as reference

fluorescence (Fig. 3.3c). To quantify the recovery of $[Ca^{2+}]_c$ after Ca^{2+} uncaging, we used the time constant τ of a single-exponential fit to the $\Delta f/f_0$ trace obtained by spatially averaging the Ca^{2+} transient within the stereocilia and body compartments (Fig. 3.3d; solid lines, stereocilia; dashed lines, cell body; [47]). In wt mice, the recovery to baseline Ca^{2+} was slightly, but significantly ($p < 10^{-4}$), faster in the stereocilia (time constant $\tau = 2.2 \pm 0.2$ s, $n = 18$) than in the cell body ($\tau = 4.0 \pm 0.3$ s, $n = 18$) (Fig. 3.3e). This result confirms the hypothesis that stereocilia act as Ca^{2+} microdomains [32] in which Ca^{2+} gradients generated during mechano-transduction [25] are dissipated independently from the cell body [33]. τ was significantly larger in *dfw* than in wt and, particularly, in PMCA2 KO mice. These results show that ablation of PMCA2, or impairment of its activity, decreased the Ca^{2+} clearing rate of the stereocilia, making it similar to the slower rate of cell soma. Similar experiments were performed also for *Obl* [44] and *Tommy* [45] mutant mice, and the results are summarized in Table 3.1.

Hearing the lowest sounds requires hair cell stereocilia to detect displacements of atomic dimensions, of the order of 0.2 nm [51]. In the mouse cochlea, their operating range is about 500 nm [52]. To assay the impact of PMCA2*w/a* dysfunction on mechano-transduction, organotypic cochlear cultures from wt and mutant P0–P3 mice were studied between P1 and P4 ([47]) by a combination of patch-clamp recording and mechanical stimulation of the hair cell stereocilia (Fig. 3.4a). The amplitude and kinetics of MET channel currents in PMCA2 KO and homozygous *dfw* hair cells were qualitatively similar to those of wt controls. However, the curves

Fig. 3.3 (continued) evoked by UV photolysis of caged Ca^{2+}. Each data point is averaged over $n > 13$ cells in 2–4 mice of each type for wt controls (*blue traces*), homozygous *dfw* (*green traces*), and PMCA2 KO mice (*black traces*); *solid lines*, stereocilia; *dashed lines*, cell body, excluding stereocilia. The *arrowheads* below the time axis show the time of frame capture in (**c**). (**e**) Decay time constants τ were derived by a single-exponential fit. ANOVA test yielded $p < 10^{-4}$ and $p = 0.03$ for compatibility of stereociliary τ of wt-*dfw* and *dfw*-KO, respectively

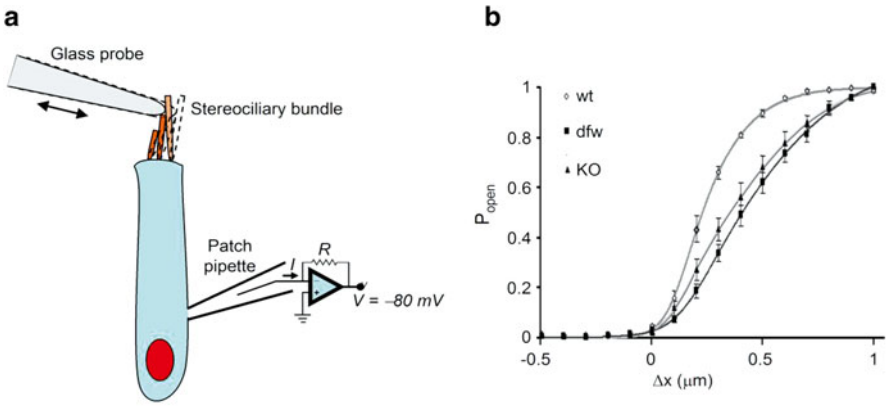

Fig. 3.4 Open probability of MET channels in outer hair cells. (**a**) Schematic diagram of hair bundle stimulation by a glass probe and simultaneous recording of membrane current by patch clamp. (**b**) Plots of peak MET current versus displacement, Δx, of hair bundle tip. Positive Δx steps indicate (excitatory) glass probe movements toward the highest stereocilia. Peak current was measured as the difference in current relative to that obtained with a large negative displacement, where all transducer channels are assumed to be closed and normalized to yield a measure of channel open probability (P_{open}, ordinates). For fitting formula and parameters, see Ref. [47]

relating bundle displacement (X) to MET channel open probability, P_{open} (X), were shifted positively in *dfw* and PMCA2 KO mice with respect to wt controls (Fig. 3.4b). The shift was more pronounced in the KO mice (175 nm) than in the *dfw* mice (117 nm). These results are consistent with those obtained with vanadate, which blocks Ca^{2+} extrusion in auditory hair cells [53] and induces a similar (~200 nm) shift in the P_{open} (X) curve [54].

4 Measurements of Auditory-Evoked Brainstem Responses

Auditory-evoked potentials originating from the brainstem (ABRs) in mice are similar to those of humans, reflecting the synchronous short-latency synaptic activity of successive nuclei along the peripheral afferent auditory neural pathway. In the mouse, the normal response to suprathreshold stimuli appears as a series of four to five consecutive robust potentials, labeled with Roman numerals I–V [55].

Hearing threshold was measured from the IV wave ABR evoked by click and tone bursts at different sound frequencies in wt, heterozygous, and homozygous *Tommy* mice aged between P18 and P45 (Fig. 3.5a, [45]). Profound hearing impairment was found in the homozygote from P18 (measurements at younger stages were not performed due to difficulties intrinsic in the ABR technique; the reader should be aware that wt mice acquire hearing around P12). A significant difference ($p < 0.001$, $n = 5$) between wild-type and *Tommy* heterozygote thresholds was observed with clicks as well as tone bursts at frequencies of 14 kHz and above (Fig. 3.5b). We also measured auditory thresholds in *Obl* mice at different ages (Fig. 3.5b shows only

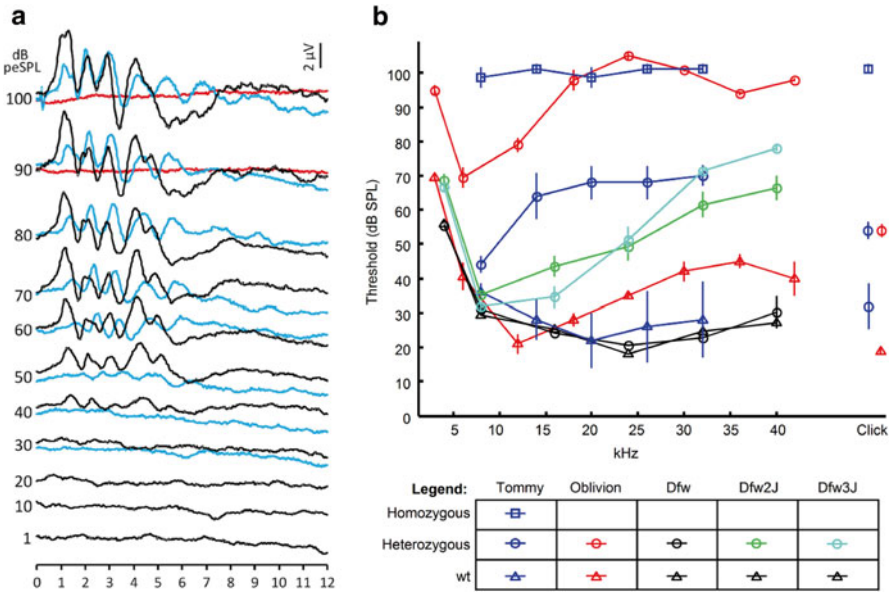

Fig. 3.5 Hearing performance of wild-type and mutant mice assessed by ABR. (**a**) Representative ABR recordings in response to click stimuli from wt (P31, *black traces*), heterozygous (P27, *blue traces*), and homozygous (P24, *red traces*) *Tommy* mice. (**b**) ABR thresholds for click and tone bursts at different frequencies obtained from several mutant mice. At 100 dB, PMCA2 KO mice, as well as homozygous dfw, dfw2J, and dfw3J mice were completely deaf at every frequency [39] [42]. *Bars* represent standard error of the mean. Note that click responses are plotted at an arbitrary point on the frequency axis (the position does not reflect the frequency content of click stimuli)

data between P59 and P62). Hearing impairment in heterozygous (*Obl*/+) mice increased from P20 to P90, whereas ABRs were absent in homozygous siblings (*Obl*/*Obl*) of all ages. In addition, *Obl*/*Obl* mutants were small and affected by severe vestibular dysfunction from the second postnatal week. Mutant *dfw* mice were analyzed by McCullog and Tempel (Ref. [42]), together with two functional null allele mice, *dfw*2J and *dfw*3J. ABRs were normal in heterozygous *dfw*/+ mice (at P37), whereas *dfw*2J/+ and *dfw*3J/+ mice showed large auditory threshold shifts particularly at high frequencies (>24 kHz); *dfw*/*dfw* mice were profoundly deaf [42].

5 Organ of Corti Degeneration due to PMCA2 Mutations

We performed confocal imaging immunoassays to monitor the progressive degeneration of the organ of Corti, which correlates with the lack of auditory function in the heterozygote and homozygote mutant mice we have studied. By immunolabeling transversal and orthogonal sections of the cochlea, we observed a progressive base to apex loss of PMCA2 in the hair cells of homozygous *Tommy* mice after P40. At P60, PMCA2 immunofluorescence signal was virtually absent in the basal part

of the cochlea, and signs of hair cell degeneration were evident by the lack of several nuclei stained with DAPI (Fig. 3.6a, [45]).

In *Obl* mutants, the gross morphology of the middle ear ossicles and inner ear appeared normal. Scanning electron microscopy in mutants at 3–4 months of age showed degeneration of hair cells, with the basal turn more severely affected than the apex and OHCs more affected than IHCs, a pattern that is commonly reported in damaged cochleas (Fig. 3.6b, [44]). *Obl*/*Obl* homozygotes were more severely affected than heterozygotes. However, there were many remaining hair cells with relatively normal appearance in the mutants, including a W-shaped arrangement of stereocilia, especially in the apical turn. Stereocilia fusion was seen in some, an early indicator of hair cell degeneration. At P20, no significant hair cell loss was detected in *Obl*/+ mutants compared to their littermate controls, despite the fact that these mice did show significantly raised ABR thresholds (Fig. 3.5b). Hair cell counts from the basal and middle turns at P75 showed no significant OHC degeneration in the middle turn and no significant IHC loss throughout the cochlea in *Obl*/+ heterozygotes. By P121, there was significant OHC and IHC loss in basal and middle turns in *Obl*/+. This suggests that the hair cell loss seen in these mutants is a secondary consequence of the hair cell not functioning correctly, rather than being the primary cause of raised thresholds in *Obl*/+ mutants.

In *Obl*/*Obl* mutants at P30, there was highly variable hair cell degeneration, both within and between animals. In some regions there was scattered hair cell loss with a pattern similar to that seen in heterozygotes (Fig. 3.6b, G′, H′), while in some regions toward the base, there was complete degeneration of the organ of Corti with a complete absence of specialized cells, including supporting cells such as pillar cells (Fig. 3.6b, I′).

6 Mutations in Humans

A mutational screening of the PMCA2 gene (GenBank accession number NM_001001331.1) on samples of 450 subjects coming from different countries identified a missense mutation associated with autosomal dominant hearing loss [47]. The mutated allele was a G to A transition at position 877 in exon 5 of the

Fig. 3.6 (continued) (Alexa Fluor 488-conjugated, *green*), and nuclei were stained with DAPI (*blue*). *Scale bar*, 15 μm. (**b**) At 3–4 months of age, *Obl* wt mice (genetic background) show three rows of OHCs and one row of IHCs in the apex (**a**′), middle (**b**′), and base (**c**′) of the cochlea. *Obl*/+ mice exhibit extensive OHC loss and some IHC loss in the base of the cochlea (**f**′) and a few missing OHC in the middle of the cochlea (**e**′). The apex appears normal (**d**′). At 1 month of age, the phenotype of *Obl*/*Obl* mice is extremely variable. In some regions of the base, middle, and apex, the phenotype is similar to that seen in *Obl*/+ mice. However, in other parts of the apex (**g**′) and middle (**h**′) regions of the cochlea, there are missing patches of OHCs. In some regions of the base, there is a complete degeneration of the organ of Corti, with no IHC, OHC, or supporting cells such as pillar cells present (**i**′). Scale bar, 10 μm

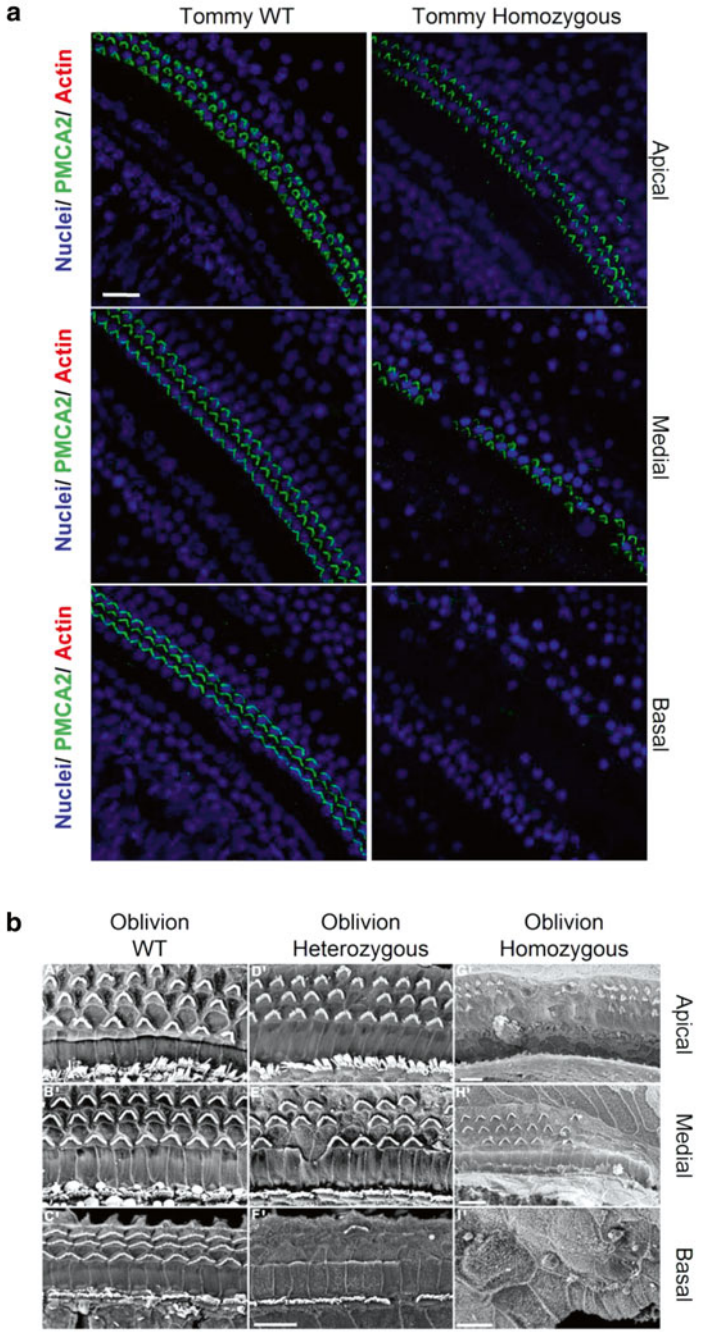

Fig. 3.6 Organ of Corti morphological analysis by confocal immunofluorescence and scanning electron microscopy. (**a**) Shown are cochlea whole mounts (horizontal sections, orthogonal to the modiolus) from P60 wt (*left column*) and homozygous (*right column*) *Tommy* mice. Images from apical, medial, and basal regions were obtained by maximal back projection of 20 confocal optical sections from a 2 μm step z-stack. PMCA2 expression was probed by a PMCA2 selective antibody

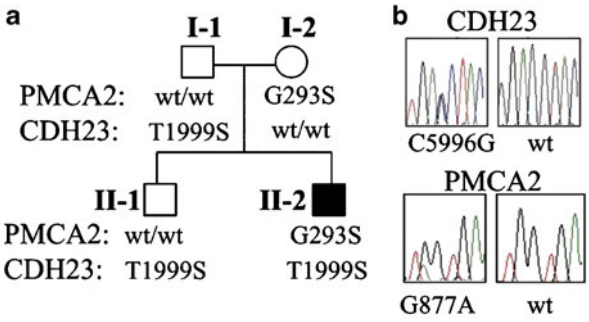

Fig. 3.7 Association of digenic mutations of PMCA2 and CDH23 with hearing loss. (**a**) Pedigree of an Italian family. *Black symbols* denote the family members affected. Genotypes of PMCA2 and CDH23 are indicated for each individual [47]. (**b**) Representative chromatogram of CDH23 C5996G and PMCA2 G877A, respectively, which were identified from the family

nucleotide sequence, leading to the replacement of a highly conserved glycine with a serine at position 293 in the cytosolic loop connecting transmembrane domains 2 and 3 (the region in which the mutation G283S of *dfw* maps). The mutated allele was detected in an Italian patient affected by severe bilateral sensorineural hearing impairment without vestibular involvement. Two hundred chromosomes of individuals coming from the same geographical area of the patient were negative for the presence of the mutated allele. The G293S mutation was inherited from the mother who had normal hearing. The father and a brother of the patient, with normal hearing, were also negative for the G293S mutation. Considering the recent finding of a contribution of the PMCA2 gene mutation as a modifier of the hearing loss phenotype [46], the whole family was analyzed for the presence of mutations in other genes which are also frequently involved in hereditary hearing loss [47], connexin 30 (GJB6), Myosin 6 (MYO6), and CDH23; mitochondrial DNA was also screened. The screening on the CDH23 gene (GenBank accession number NM_022124.2) identified a T to S substitution at position 1999 (C5996G) in the affected son but not in the mother (Fig. 3.7). This mutated allele, which had already been described in a mutation database as a polymorphism, was inherited by the patient from his healthy father and was also present in the healthy brother. Negative results were obtained for the other DNA sequences analyzed.

As ablation [39] or missense mutations of the PMCA2 Ca^{2+} pump of the stereocilia cause deafness and loss of balance, Ca^{2+} concentration in endolymph is expected to fall causing an alteration of the mechano-transduction process. This may provide a clue as to why, both in humans [47] and mice [56], PMCA2 mutations potentiated the deafness phenotype induced by coexisting mutations of cadherin-23 (*Usher syndrome type* 1D), a single-pass membrane Ca^{2+}-binding protein that is abundantly expressed in the stereocilia (Fig. 3.1b).

The cooperation of the cadherin-23 and the PMCA2 pump is evidently critical in the molecular events that ultimately permit the neural encoding of the acoustic signal. It is thus easy to appreciate the importance of their mutations in the generation

of the hearing loss phenotype: indeed, a G753A polymorphism of cadherin-23 was detected in the original *dfw* mice [57]. Furthermore, in one human family, a homozygous mutation in cadherin-23 (F1888S) caused the hearing loss in five siblings, whereas a coexistent heterozygous PMCA2 pump mutation (V586M in the *z/b* nomenclature) was associated with increased loss in the three most severely affected siblings [46].

The link between cadherin-23 and the PMCA2 pump, therefore, is important. However, it is not obligatory, as shown by the results of the *Tommy* mutant described here and those on the *Obl* mutant [44]. Evidently, the biochemical defect of the homeostasis of Ca^{2+} in the stereocilia of OHCs has different degrees of severity. Homozygous cadherin-23 mutations that impair the ability of the protein to bind Ca^{2+}, as detected in one of the human families described [46], may be sufficient to disrupt the opening properties of the MET channels, generating the hearing loss phenotype, which is then only exacerbated by the concomitant PMCA2 pump mutation. On the other hand, homozygous PMCA2 pump mutations, as was the case for the *Obl* mutant and is the case for the *Tommy* mutant, may per se be sufficient to decrease the Ca^{2+} concentration in the endolymph to a degree that would affect the function of the otherwise normal cadherin-23 in the tip links and to generate the hearing loss phenotype, without the contribution of cadherin-23 mutations.

7 Conclusions

Isoform 2 of the PMCA pump (Fig. 3.1a) has properties that distinguish it from other PMCA isoforms: when tested in the cellular environment, it is two to three times more active than the two ubiquitous pumps in pumping Ca^{2+} out of the cell [8]. In the isolated state, it shows very high calmodulin affinity (K_d, 2–4 nM) [14], i.e., it becomes fully activated under conditions (e.g., calmodulin and/or Ca^{2+} concentration) that would activate very poorly isoforms 1 and 4. PMCA2 also has peculiarly high activity in the absence of activators [9]. But the property that distinguishes PMCA2 most clearly is the complexity of alternative splicing. Mutant PMCA2*w/a* pumps are unable to handle a sudden surge of $[Ca^{2+}]_c$ by increasing their activity (Fig. 3.2) and also fail to operate efficiently at the nonactivated level.

Within the hair cell stereocilia, the control of Ca^{2+} is vital to a number of aspects of the mechano-transduction process, e.g., the regulation of adaptation, the ability to sense the deflection of the ciliary bundle with high sensitivity [51, 58], and the breaking and regeneration of tip links [59]. These peculiar functions of the Ca^{2+} signal have in all likelihood dictated the choice of the PMCA2*w/a* isoform (Figs. 3.3 and 3.4). Since resting stereociliary Ca^{2+} is very low [25, 33], it makes sense to control it with a pump variant which decreases Ca^{2+} to lower concentrations than other isoforms [14] even if it is insensitive to calmodulin (and, presumably, to acidic phospholipids). The relative insensitivity of the *w/a* pump to calmodulin makes good sense, as its very high concentration in the stereocilia (70 μM [60]) would produce permanent maximal activation of pump isoforms normally sensitive to it.

These properties evidently satisfy the Ca^{2+} homeostasis demands of the endolymph and of the stereocilia, controlling hearing function (Fig. 3.5). Even if Ca^{2+} in the endolymph is very low, the measured value of 23 μM [28] is considerably higher than that necessary for the integrity of the tip links, which is only compromised below 1 μM [61]. In fact, even the inactivating *dfw* mutation only lowers the endolymph Ca^{2+} concentration to about 6 μM [28]. However, a number of in vitro studies have shown that the generation of MET currents, for instance, in chickens, requires a minimum of 20 μM extracellular Ca^{2+} and is not elicited at 10 μM [23]. A diminished Ca^{2+} removal from the hair cell affects MET currents and adaptation, the process by which hair cells continuously readjust their sensitivity to the ciliary bundle displacements [34, 35, 62, 63]. Indeed, the pharmacological blockade of the PMCA2 pump shifted the current-displacement (*I–X*) curve in the positive direction and reduced its slope considerably [50]. Similar effects have been reported by *dfw* mutation or PMCA2 KO in Fig. 3.4.

PMCA2 mutation might therefore completely disrupt Ca^{2+} homeostasis, with the basal turn of the cells more severely affected than the apex and with OHCs more affected than IHCs, as found in both the *Obl* and *Tommy* mice (Fig. 3.6). As the only cochlear PMCA2 exposed to endolymph is that of the stereocilia [4, 28], this may provide a clue as to why, in some cases, mutations in the gene of the PMCA2 pump potentiated the deafness phenotype induced by coexisting mutations of cadherin-23 (USH1D).

Acknowledgments The work summarized here was carried out by the authors' team in collaboration with research teams led by Ernesto Carafoli, Marisa Brini, Paolo Gasparini, Karen Steel, Steve Brown, and the late Edoardo Arslan. For grant support, see Refs. [44, 45, 47].

References

1. Carafoli E, Santella L, Branca D et al (2001) Generation, control, and processing of cellular calcium signals. Crit Rev Biochem Mol Biol 36:107–260
2. Guerini D, Coletto L, Carafoli E (2005) Exporting calcium from cells. Cell Calcium 38:281–289
3. Crouch JJ, Schulte BA (1996) Identification and cloning of site C splice variants of plasma membrane Ca-ATPase in the gerbil cochlea. Hear Res 101:55–61
4. Dumont RA, Lins U, Filoteo AG et al (2001) Plasma membrane Ca2+-ATPase isoform 2a is the PMCA of hair bundles. J Neurosci 21:5066–5078
5. Chen Q, Mahendrasingam S, Tickle JA et al (2012) The development, distribution and density of the plasma membrane calcium ATPase 2 calcium pump in rat cochlear hair cells. Eur J Neurosci 36:2302–2310
6. Grati M, Aggarwal N, Strehler EE et al (2006) Molecular determinants for differential membrane trafficking of PMCA1 and PMCA2 in mammalian hair cells. J Cell Sci 119(Pt 14):2995–3007
7. Grati M, Schneider ME, Lipkow K et al (2006) Rapid turnover of stereocilia membrane proteins: evidence from the trafficking and mobility of plasma membrane Ca(2+)-ATPase 2. J Neurosci 26:6386–6395

8. Brini M, Coletto L, Pierobon N et al (2003) A comparative functional analysis of plasma membrane Ca2+ pump isoforms in intact cells. J Biol Chem 278:24500–24508
9. Hilfiker H, Guerini D, Carafoli E (1994) Cloning and expression of isoform 2 of the human plasma membrane Ca2+ ATPase. Functional properties of the enzyme and its splicing products. J Biol Chem 269:26178–26183
10. Krebs J (2015) The plethora of PMCA isoforms: alternative splicing and differential expression. Biochim Biophys Acta 1853:2018. doi:10.1016/j.bbamcr.2014.12.020, pii: S0167-4889(14)00448-0
11. Zacharias DA, Strehler EE (1996) Change in plasma membrane Ca2(+)-ATPase splice-variant expression in response to a rise in intracellular Ca2+. Curr Biol 6:1642–1652
12. Stamm S (2008) Regulation of alternative splicing by reversible protein phosphorylation. J Biol Chem 283:1223–1227
13. Brodin P, Falchetto R, Vorherr T et al (1992) Identification of two domains which mediate the binding of activating phospholipids to the plasma-membrane Ca2+ pump. Eur J Biochem 204:939–946
14. Elwess NL, Filoteo AG, Enyedi A et al (1997) Plasma membrane Ca2+ pump isoforms 2a and 2b are unusually responsive to calmodulin and Ca2+. J Biol Chem 272:17981–17986
15. Niggli V, Adunyah ES, Penniston JT et al (1981) Purified (Ca2+-Mg2+)-ATPase of the erythrocyte membrane. Reconstitution and effect of calmodulin and phospholipids. J Biol Chem 256:395–401
16. Lim DJ (1986) Functional structure of the organ of Corti: a review. Hear Res 22:117–146
17. Hill JK, Williams DE, LeMasurier M et al (2006) Splice-site A choice targets plasma-membrane Ca2+-ATPase isoform 2 to hair bundles. J Neurosci 26:6172–6180
18. Fettiplace R, Kim KX (2014) The physiology of mechanoelectrical transduction channels in hearing. Physiol Rev 94:951–986
19. Carafoli E (2011) The plasma membrane calcium pump in the hearing process: physiology and pathology. Sci China Life Sci 54:686–690
20. Corey DP, Sotomayor M (2004) Hearing: tightrope act. Nature 428:901–903
21. Anniko M, Wroblewski R (1986) Ionic environment of cochlear hair cells. Hear Res 22:279–293
22. Corey DP, Hudspeth AJ (1979) Ionic basis of the receptor potential in a vertebrate hair cell. Nature 281:675–677
23. Ohmori H (1985) Mechano-electrical transduction currents in isolated vestibular hair cells of the chick. J Physiol 359:189–217
24. Lumpkin EA, Marquis RE, Hudspeth AJ (1997) The selectivity of the hair cell's mechanoelectrical-transduction channel promotes Ca2+ flux at low Ca2+ concentrations. Proc Natl Acad Sci U S A 94:10997–11002
25. Denk W, Holt JR, Shepherd GM et al (1995) Calcium imaging of single stereocilia in hair cells: localization of transduction channels at both ends of tip links. Neuron 15:1311–1321
26. Jorgensen F, Kroese AB (1995) Ca selectivity of the transduction channels in the hair cells of the frog sacculus. Acta Physiol Scand 155:363–376
27. Bosher SK, Warren RL (1978) Very low calcium content of cochlear endolymph, an extracellular fluid. Nature 273:377–378
28. Wood JD, Muchinsky SJ, Filoteo AG et al (2004) Low endolymph calcium concentrations in deafwaddler2J mice suggest that PMCA2 contributes to endolymph calcium maintenance. J Assoc Res Otolaryngol 5:99–110
29. Corey DP, Hudspeth AJ (1983) Kinetics of the receptor current in bullfrog saccular hair cells. J Neurosci 3:962–976
30. Marquis RE, Hudspeth AJ (1997) Effects of extracellular Ca2+ concentration on hair-bundle stiffness and gating-spring integrity in hair cells. Proc Natl Acad Sci U S A 94:11923–11928
31. Hackney CM, Mahendrasingam S, Penn A et al (2005) The concentrations of calcium buffering proteins in mammalian cochlear hair cells. J Neurosci 25:7867–7875

32. Ricci AJ, Wu YC, Fettiplace R (1998) The endogenous calcium buffer and the time course of transducer adaptation in auditory hair cells. J Neurosci 18:8261–8277
33. Lumpkin EA, Hudspeth AJ (1998) Regulation of free Ca2+ concentration in hair-cell stereocilia. J Neurosci 18:6300–6318
34. Yamoah EN, Lumpkin EA, Dumont RA et al (1998) Plasma membrane Ca2+-ATPase extrudes Ca2+ from hair cell stereocilia. J Neurosci 18:610–624
35. Ricci AJ, Fettiplace R (1998) Calcium permeation of the turtle hair cell mechanotransducer channel and its relation to the composition of endolymph. J Physiol 506(Pt 1):159–173
36. Crouch JJ, Schulte BA (1995) Expression of plasma membrane Ca-ATPase in the adult and developing gerbil cochlea. Hear Res 92:112–119
37. Wu YC, Tucker T, Fettiplace R (1996) A theoretical study of calcium microdomains in turtle hair cells. Biophys J 71:2256–2275
38. Shah DM, Freeman DM, Weiss TF (1995) The osmotic response of the isolated, unfixed mouse tectorial membrane to isosmotic solutions: effect of Na+, K+, and Ca2+ concentration. Hear Res 87:187–207
39. Kozel PJ, Friedman RA, Erway LC et al (1998) Balance and hearing deficits in mice with a null mutation in the gene encoding plasma membrane Ca2+-ATPase isoform 2. J Biol Chem 273:18693–18696
40. Street VA, McKee-Johnson JW, Fonseca RC et al (1998) Mutations in a plasma membrane Ca2+-ATPase gene cause deafness in deafwaddler mice. Nat Genet 19:390–394
41. Takahashi K, Kitamura K (1999) A point mutation in a plasma membrane Ca(2+)-ATPase gene causes deafness in Wriggle Mouse Sagami. Biochem Biophys Res Commun 261:773–778
42. McCullough BJ, Tempel BL (2004) Haplo-insufficiency revealed in deafwaddler mice when tested for hearing loss and ataxia. Hear Res 195:90–102
43. Tsai YS, Pendse A, Moy SS et al (2006) A de novo deafwaddler mutation of Pmca2 arising in ES cells and hitchhiking with a targeted modification of the Pparg gene. Mamm Genome 17:716–722
44. Spiden SL, Bortolozzi M, Di Leva F et al (2008) The novel mouse mutation Oblivion inactivates the PMCA2 pump and causes progressive hearing loss. PLoS Genet 4:e1000238
45. Bortolozzi M, Brini M, Parkinson N et al (2010) The novel PMCA2 pump mutation Tommy impairs cytosolic calcium clearance in hair cells and links to deafness in mice. J Biol Chem 285:37693–37703
46. Schultz JM, Yang Y, Caride AJ et al (2005) Modification of human hearing loss by plasma-membrane calcium pump PMCA2. N Engl J Med 352:1557–1564
47. Ficarella R, Di Leva F, Bortolozzi M et al (2007) A functional study of plasma-membrane calcium-pump isoform 2 mutants causing digenic deafness. Proc Natl Acad Sci U S A 104:1516
48. Lane PW (1987) New mutants and linkages: deafwaddler (dfw). Mouse News Lett 77:129
49. Brini M, Marsault R, Bastianutto C et al (1995) Transfected aequorin in the measurement of cytosolic Ca2+ concentration ([Ca2+]c). A critical evaluation. J Biol Chem 270:9896–9903
50. Beurg M, Nam JH, Chen Q et al (2010) Calcium balance and mechanotransduction in rat cochlear hair cells. J Neurophysiol 104:18–34
51. Fettiplace R, Ricci AJ (2006) Mechanoelectrical transduction in auditory hair cells. In: Eatock RA, Fay RR, Popper AN (eds) Vertebrate hair cells. Springer Science Inc., New York, NY, pp 154–203
52. Beurg M, Evans MG, Hackney CM, Fettiplace R (2006) A Large-Conductance Calcium-Selective Mechanotransducer Channel in Mammalian Cochlear Hair Cells. J Neurosci 26:10992–11000
53. Tucker T, Fettiplace R (1995) Confocal imaging of calcium microdomains and calcium extrusion in turtle hair cells. Neuron 15:1323–1335
54. Wu YC, Ricci AJ, Fettiplace R (1999) Two components of transducer adaptation in auditory hair cells. J Neurophysiol 82:2171–2181
55. Scimemi P, Santarelli R, Selmo A et al (2014) Auditory brainstem responses to clicks and tone bursts in C57 BL/6J mice. Acta Otorhinolaryngol Ital 34:264–271

56. Watson CJ, Tempel BL (2013) A new Atp2b2 deafwaddler allele, dfw(i5), interacts strongly with Cdh23 and other auditory modifiers. Hear Res 304:41–48
57. Noben-Trauth K, Zheng QY, Johnson KR (2003) Association of cadherin 23 with polygenic inheritance and genetic modification of sensorineural hearing loss. Nat Genet 35:21–23
58. Corns LF, Johnson SL, Kros CJ et al (2014) Calcium entry into stereocilia drives adaptation of the mechanoelectrical transducer current of mammalian cochlear hair cells. Proc Natl Acad Sci U S A 111:14918–14923
59. Zhao Y, Yamoah EN, Gillespie PG (1996) Regeneration of broken tip links and restoration of mechanical transduction in hair cells. Proc Natl Acad Sci U S A 93:15469–15474
60. Walker RG, Hudspeth AJ, Gillespie PG (1993) Calmodulin and calmodulin-binding proteins in hair bundles. Proc Natl Acad Sci U S A 90:2807–2811
61. Assad JA, Shepherd GM, Corey DP (1991) Tip-link integrity and mechanical transduction in vertebrate hair cells. Neuron 7:985–994
62. Assad JA, Hacohen N, Corey DP (1989) Voltage dependence of adaptation and active bundle movement in bullfrog saccular hair cells. Proc Natl Acad Sci U S A 86:2918–2922
63. Eatock RA, Corey DP, Hudspeth AJ (1987) Adaptation of mechanoelectrical transduction in hair cells of the bullfrog's sacculus. J Neurosci 7:2821–2836
64. Kazmierczak P, Sakaguchi H, Tokita J et al (2007) Cadherin 23 and protocadherin 15 interact to form tip-link filaments in sensory hair cells. Nature 449:87–91
65. Lefevre G, Michel V, Weil D et al (2008) A core cochlear phenotype in USH1 mouse mutants implicates fibrous links of the hair bundle in its cohesion, orientation and differential growth. Development 135:1427–1437
66. Maeda R, Kindt KS, Mo W et al (2014) Tip-link protein protocadherin 15 interacts with transmembrane channel-like proteins TMC1 and TMC2. Proc Natl Acad Sci U S A 111: 12907–12912

Chapter 4
PMCA3: A Mysterious Isoform of Calcium Pump

Tomasz Boczek and Ludmila Zylinska

Abstract Calcium ion as a powerful, universal extracellular and intracellular carrier of information involves precise controlling system to convey proper signals to the cells. The most sensitive for changes in cytosolic Ca^{2+} concentration is a family of plasma membrane calcium (PMCA) pump encoded by four independent genes (PMCA1–4). Differences in tissue-specific expression of the isoforms and splicing variants in excitable and non-excitable cells are considered to reflect a unique profile of calcium signaling in particular cells. Among PMCA isoforms, PMCA3 appears to be the least known, although it was cloned in 1989. Using different techniques, its developmental and cell- and tissue-dependent expression has been reported in a number of studies; nonetheless, our knowledge about PMCA3 role in the cells is still scarce. Low expression and restricted localization may indicate less important role of PMCA3 in comparison with other isoforms. However, its high Ca^{2+} and calmodulin affinity, low sensitivity to calpain degradation, and resistance to the stress conditions could offer some unique function. The present article focuses on the PMCA3 characteristics, especially in the light of new findings suggesting that this isoform could be critical for the maintenance of cytosolic Ca^{2+} concentration acting as a second line of defense against calcium overload.

Keywords Plasma membrane calcium pump • Gene • Isoforms • Calcium homeostasis • Brain • Tissues • PC12 cells

1 Introduction

Since first cloning data were released, it became apparent that PMCA3 belongs to multigene family of four distinct members (PMCA1-4) recognized in mammals, responsible for ATP-dependent Ca^{2+} extrusion to the extracellular milieu. The amino

T. Boczek • L. Zylinska (✉)
Department of Molecular Neurochemistry, Medical University,
6/8 Mazowiecka Street, 92-215 Lodz, Poland
e-mail: ludmila.zylinska@umed.lodz.pl

S. Chakraborti, N.S. Dhalla (eds.), *Regulation of Ca^{2+}-ATPases,V-ATPases and F-ATPases*, Advances in Biochemistry in Health and Disease 14,
DOI 10.1007/978-3-319-24780-9_4

acid sequence of PMCA3 shares 70–80 % homology with other PMCA isoforms [1] and high conservancy of critical functional region with other P-type ATPases [2].

PMCA3 due to its specific kinetic parameters is classified as fast responsive isoform and thus may be of great importance for cellular protection from Ca^{2+} overload. Studies on C-terminally truncated PMCA3 variants revealed that COOH tail is critical for key properties of the isoform, e.g., calmodulin (CaM) sensitivity, Ca^{2+} affinity, or sensitivity to other regulatory molecules. The truncation at the 1117th residue [3], which is located within CaM-binding domain [4], generated the pump surprisingly reacting with CaM with an affinity (K_M of 5–10 nM) similar to that for PMCA2 which has the highest CaM affinity among all PMCAs [5]. Basic ATPase activity of partially purified truncated enzyme (~200 nmol ATP/min/mg protein) was stimulated about threefold by CaM in the presence of Ca^{2+} [3]. Moreover, the shortened PMCA3 was as effective in controlling of cytosolic Ca^{2+} concentration ($[Ca^{2+}]_c$) as the corresponding full-length protein (K_M for CaM of 8 nM). On the other hand, truncation after the 15th residue of the CaM-binding domain produced an enzyme only negligibly stimulated by CaM (K_M of 15 nM) [6]. For this PMCA3 variant, the average ATPase activity was increased only by 1.41-fold by CaM, but the pump was activated by Ca^{2+} at the rates even faster than for the full-length variants of PMCA2 or PMCA4 [7]. PMCAs activity can be also modulated by several independent mechanisms, but this has not been rigorously tested for PMCA3. Despite extensive studies aimed to resolve the sense of existence of four isoforms of one protein, up to date no unifying explanations of this paradox have been proposed. In contrast to other three PMCA isoforms, these studies provided only parsimonious insight into the function of PMCA3 which still remains the most mysterious isoform of calcium pump. This review continues the earlier discussion on calcium pump started by E. Carafoli in the 1980s of the last century [8] but also gives a special emphasis on the latest progress regarding the unique aspects of PMCA3 functioning.

2 PMCA3 Gene Structure and Chromosomal Localization

Several recent reports indicate that regulation of PMCA3 gene expression may be of great importance for developmental progression, tissue specificity, and alternative splicing patterns. The ATP2B3 gene encoding isoform 3 of plasma membrane Ca^{2+}-ATPase in human is located from base pair 153.518.446 to 153.582.928 on the long arm of the X chromosome at position 28 (Fig. 4.1) [9]. The gene has 22 exons of the total length of about 6.4 kbp. The smallest in size exon 6 consists as little as 42 bp. The first exon specifies 126 nucleotides of the 5′ untranslated region and the codons for 69 amino acids of N-terminal tail [10]. The introns range in size from about 100 bp to 14.8 kbp and have boundaries with consensus sites for splice junctions. A single gene product of approximately 7 kbp was originally detected in the hybridization studies [10].

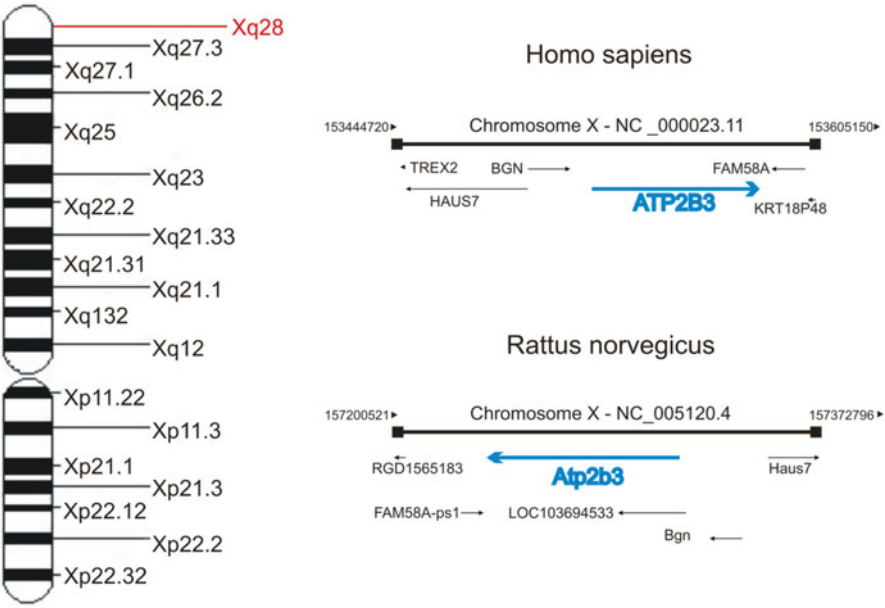

Fig. 4.1 Localization of ATP2B3 on human X chromosome (*left*) and the genomic context of PMCA3 gene in human and rat (*right*)

Rat *Atp2b3* gene consists of 24 exons ranging in size from 42 bp (exon 8) to 945 bp (exon 24) and is also located on the X chromosome [11]. The exons with the total known length of ~5.3 kbp are distributed across all of 75.629 bp of the gene. The 5′ untranslated region is separated by two introns dispersing this untranslated sequence across 20 kbp of genomic DNA. The polyadenylation signal is located following exon 23 and about 2 kbp downstream from exon 24 to produce mRNA of 4.5 kbp or 7.5 kbp, respectively.

The human and rat PMCA3 genes share high sequence similarity. The pairwise alignment revealed 89 % identity in the coding region, 66 % identity in the first 250 bp of 3′ untranslated region, and 77 % identity within available 125 bp located in 5′ untranslated sequence. Additionally, first 6 exons of the human ATP2B3 gene exactly correspond to exons 3–8 of the rat sequence, and the positions of introns are nearly identical in both species [10, 11].

3 PMCA3 Splicing Variants

The *Atp2b3* transcripts are affected by alternative splicing at two major sites called A and C sites [12]. The A site is located upstream of the phospholipid-sensitive basic region of PMCA in the first cytosolic loop. The C site is found in the COOH-terminal tail within the calmodulin-binding domain; therefore, it specifies the

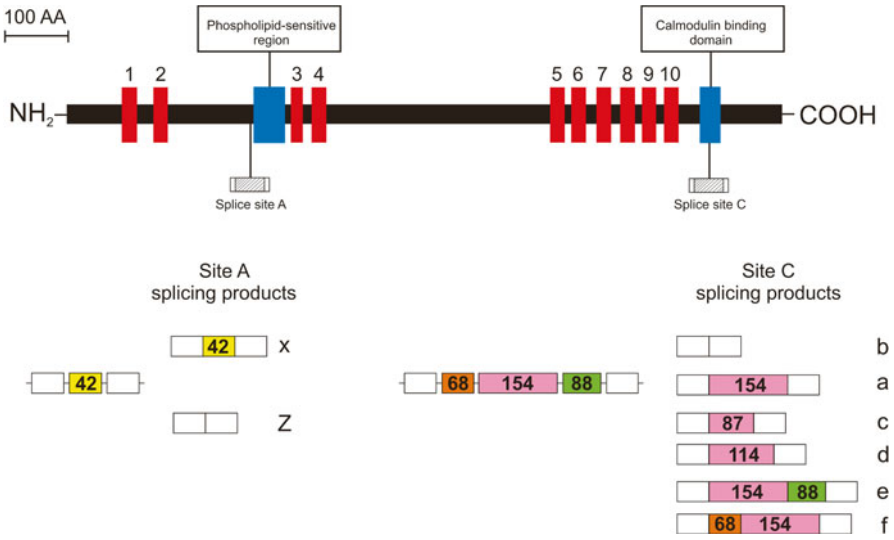

Fig. 4.2 Schematic model of PMCA (*upper panel*) showing localization of splice A and C sites. The ten putative transmembrane regions are numbered and indicated as *red boxes*. Alternative splicing products (*lower panel*) of rat *Atp2b3* gene. Exons are shown as *boxes* with the *numbers* representing the length of each exon. Human ATP2B3 presents virtually identical splicing pattern

affinity of PMCA for Ca^{2+}/calmodulin complex. The alternative splicing at A site affects a single exon (exon 8 in the rat PMCA3 gene) encoding 13 amino acids of the first intracellular loop. This exon can be either inserted or excluded from the mature transcripts yielding two splice variants: PMCA3x (exon included) and PMCA3z (exon excluded) [13]. In both human and rat, the size of this exon is 42 nucleotides [10, 11] (Fig. 4.2).

In contrast to splice site A, the splicing at site C is much more complex and involves additional splice sites located inside the exons, read-through of the penultimate exon, and incorporation of full extra exons [10–15]. In PMCA3, at least two exons are subject to alternative splicing. These are 68 bp exon (exon 22 in the rat) and 154 bp exon (exon 23 in the rat) containing multiple internal donor sites. PMCA3 pump with no insertion at C site is designated as 3b. The insertion of full 154 bp exon leads to the generation of variant 3a or either 3c or 3d when internal splice donors within this exon at positions of 87 or 114, respectively, are utilized. Variant 3e is formed when 88 bp of the following intron and a poly(A) tail are added to 154 bp exon. This read-through affects the reading frame which terminates three codons into the intron. As a result, PMCA3e has the calmodulin-binding domain as PMCA3a but also has an alternative C-terminal sequence in which three amino acids, Ser-Glu-Ser, replace the last eight amino acids in PMCA3a. The mRNA encoding PMCA3f version contains 68 bp exon located in the 5′ to 154 bp exon, and, in most of the cases, the alternative 3′ sequence is derived from the intron following 154 bp exon similar to PMCA3e. Because the unique 68 bp exon contains an in-frame translocation termination codon after 45 bp, the second part of

calmodulin-binding domain is replaced by a sequence not found in the a or b variants, and the pump is truncated 15 residues downstream of the splice. Therefore, each of the mRNAs where 68 bp exon was inserted before (or instead) of 154 bp exon at C site encodes the shortest C-terminus among all PMCA isoforms [11, 13].

The combinatorial splicing possibilities at both splicing sites may theoretically generate a large number of PMCA3 variants including PMCA3x/b, PMCA3x/a, PMCA3z/a, PMCA3z/b, PMCA3x/c, PMCA3x/f, etc. Despite yet unresolved functional consequences of alterations in C-terminus of PMCA3, given the widespread occurrence of variations in COOH-terminal tail among other Ca^{2+}-transporting ATPase, it is unlikely that these, sometimes only minor sequence variations, have only little if any significance.

4 PMCA3 Expression in Cells and Tissues

4.1 The Brain

Among all main PMCA isoforms, PMCA3 is the least known one. From the available data the general observation is that the expression of particular PMCA3 splice variants strongly depends on developmental steps of the selected cells, finally being restricted to only few tissues [14]. As a general phenomenon, upregulation of PMCA3 during neuronal differentiation was shown in several reports, and this appears to be independent of the in vivo or in vitro conditions. Ca^{2+} itself can also affect PMCA3 expression in neurons, and this effect seems to be an essential component of differentiation and survival following Ca^{2+} overload.

In rat brain changes in PMCA3 expression during development were observed, and PMCA3a variant became visible on embryonic day 18, reaching steady-state level at postnatal day 3, whereas mRNA of PMCA3b was detected on embryonic day 10 and reached steady-state expression on embryonic day 18 [16].

PMCA3 protein was also first identified in the brain, and both splice variants—a and b—were the major forms detected in nervous tissue [17]. The abundant presence was shown in the granule layer of cerebellum, the brain region primarily involved in motor and cognitive functions [18]. PMCA3 was expressed throughout the neuropil, in the plasma membrane of granule cells, in cerebellar glomeruli, and in the presynaptic terminals of parallel excitatory fibers [19, 20]. Although PMCA3 is expressed in large amount in the cerebellum of adult rats, it is only minimally present in the neonatal cerebellum. In granule cells it became highly expressed after 7–9 days of culturing under membrane-depolarizing conditions, and the expression was strongly dependent on the activity of L-type Ca^{2+} channel and glutamate-operated Ca^{2+} channels [21].

In developing chick cerebellum, both variants, PMCA3a and PMCA3b, were expressed in the membrane fraction from the embryonic day 10 and did not change significantly after hatching [22]. PMCA3 was detected in the soma and dendritic branches of Purkinje cells, and its level correlated with cell maturation. Also, a high

expression was observed in interneurons of the molecular and granular layers, which may indicate some relation to different requirements of Ca^{2+} at definite stages of development.

In mouse, determination of PMCA3 protein examined in the cortex, cerebellum, and hippocampus during postnatal development (P0, P8, P15, P30) revealed that its presence was comparatively lower at all examined stages in relation to other PMCA isoforms [23]. PMCA3 displayed similar expression pattern during development in three brain areas, being the highest in hippocampus. This correlated with functional cell maturation, mainly with the formation of synapses. Developmental diversity of PMCA3 expression and its functional specialization was studied at tissue and cellular levels in vitro and in vivo [18, 23–25]. In the rat hippocampus at postnatal day 1 PMCA3 was very weakly visible, but increased markedly at 30 days of age being the strongest in the neuropil of CA3 and dentate gyrus.

Also, a specific shift from ubiquitous splice form "a" to a neuro-specific form "b" was observed [25]. This process occurred in parallel with synaptic development suggesting rearrangement of Ca^{2+} signaling necessary for synaptic transmission. In the human hippocampus, in situ hybridization assays showed that PMCA3 mRNA was weakly detected throughout the hippocampal formation that could reflect its lesser functional significance in Ca^{2+} handling [26]. The potential role of PMCA3 in the hippocampus was studied by analyzing the changes in PMCA expression after kainate-induced neurodegeneration [27]. Interestingly, in opposite to PMCA1 and PMCA2, mRNA level for PMCA3 was not altered what suggests its unusual resistance to toxic conditions. In gerbil brain, a distribution pattern of PMCA3 protein was found to be enriched in the membrane preparations from hippocampus and cerebellum, but not in cerebral cortex [28]. Interestingly, PMCA3 appeared to be less sensitive to ischemia/reperfusion-induced degradation in both the hippocampus and the cerebral cortex.

PMCA3 transcripts as well as PMCA3 protein were detected in the rat spinal cord, with significant presence in all of the layers of gray matter [29]. Additionally, its amount remained unaffected during spinal cord injury indicating an unaltered function of this isoform under given pathological conditions.

In the choroid plexus of mouse embryo, PMCA3 was seen after day 16, but large quantity of this isoform was found in the adult rats, mouse, and humans, where it putatively participated in the regulation of cerebrospinal fluid production [18, 30, 31].

4.2 The Eye

In the mouse retina, PMCA3 was predominantly localized in the plasma membrane of third-order neurons, which are used for Ca^{2+} clearance from retinal spiking neurons during large depolarization [32]. In postnatal and adult rat retina, PMCA3 expression showed spatial and temporal changes [33]. It was upregulated during postnatal development and prominently expressed in the inner retina. Since PMCA3 co-localized with the cholinergic amacrine cell marker—choline acetyltransferase—the authors

suggested that PMCA3 could play a role in the cholinergic activity of the developing retina. The presence of PMCA3 transcripts was detected in human corneal epithelium, and PMCA3 immunoreactivity was located in basal cell nuclei in the central cornea, but in the limbal, basal, and wing cells, a perinuclear location was revealed [34]. Further study showed a presence of PMCA3a splice variant in the corneas of five different donors, although its level varied in individual samples [35]. The significance of this result remains unresolved yet.

4.3 Other Tissues

The presence of PMCA3 at mRNA and protein level was also examined in several other tissues, but few studies showing a physiological significance of this isoform are available. Generally, low amount of PMCA3 in relation to other isoforms may indicate its complementary action during calcium-induced signaling; however, a possible protective role, especially under stress conditions, cannot be ruled out.

In the rat skeletal muscle, PMCA3f is the main isoform and exhibits a fast reaction to calcium increase [36]. Although PMCA3 possesses high affinity for CaM (K_M of 5–10 nM), its activity is relatively independent of CaM [6, 37].

PMCA3 at mRNA level was shown to be expressed in cultured trophoblasts isolated from human term placenta that could play some role in placental transfer of maternal calcium during fetal development [38]. A statistically significant positive relationships between PMCA3 mRNA amount and neonatal bone mineral content, bone area, placental weight, and birth weight were observed by Martin et al. [39]. Increased levels of PMCA3 might thereby enhance placental calcium transfer and mineralization of the fetal skeleton.

A remarkable combination of PMCA3 variants—3z/a and 3z/c—was revealed in the rat pancreatic insular cells, and they were detected at both mRNA and protein levels [40]. The presence of this fast-reacting calcium isoform in non-neuronal cells may indicate its peculiar contribution to Ca^{2+}-regulated function of pancreas.

PMCA3 presence was examined in three major zones of the rat kidney—the cortex, outer medulla, and inner medulla [41]. Only in the cortex and outer medulla, the presence of PMCA 3a and 3c variants was detected, and the mRNAs were largely abundant in descending thin limb of Henle. However, they were also found in the glomeruli and cortical thin ascending limb that may suggest specific function of PMCA3 in distinct kidney zones.

4.4 Cell Lines

Developmental expression of PMCA3 was also examined using different cell lines, where chemically induced differentiation is allowed to elucidate the importance of specific growth conditions on gene expression profile. In neuroblastoma cell line,

IMR-32 differentiation induced by 1 mM dibutyryl-cAMP in combination with 2.5 μM 5-bromouridine caused a large increase in PMCA3, showing its role in maintenance of calcium balance as well as in synaptic transmission [42].

PC12 cell line is a neoplastic counterpart of chromaffin cells originally derived from transplantable pheochromocytoma of rat adrenal medulla [43]. Upon the neurotrophin exposure, PC12 cells differentiate into sympathetic-like neurons, become electrically excitable, express neuronal markers, and extend neurites; thereby, this line is frequently used as a model for the study of neuronal functions. Both forms, undifferentiated and differentiated cells, express 3a, 3b, and 3c variants of PMCA, but the physiological significance of these variants remains still unclear [44].

5 Functional Study of PMCA3

The studies from last few years revealed that besides main Ca^{2+}-transporting function, calcium pumps play an important role in forming of multiprotein signaling complexes in the specific plasma membrane domains. However, PMCA3 isoform appears to interact scarcely. Among proteins, which were recognized to interact with PMCAs, a small-sized, cytosolic protein named PISP (PMCA-interacting single-PDZ protein) was shown to bind to all PMCA b-spliced forms including PMCA3b variant [45]. Interestingly, binding to the C-terminal tail of the pump did not alter the activity of the enzyme. Formation of this complex was proposed to act as a "chaperone" during the transit from the endoplasmic reticulum to the plasma membrane.

In the brain, Ca^{2+}-regulated synaptic function depends on controlled calcium currents, which include the action of *N*-methyl-D-aspartate (NMDA) and metabotropic glutamate receptors (mGluR). A family of Homer scaffolding proteins was shown to participate in this regulation, and one of them, Ania-3, expressed in close proximity to the postsynaptic density, binds to the b-spliced variants of PMCA and also to PMCA3b, and the PDZ domain was required for this interaction [46]. Inhibitory effect on calcium pump activity was exerted by binding of 14-3-3 proteins that belong to the small acidic modulatory proteins regulating many vital cell functions such as transcription, cell cycle, signal transduction, cellular spreading and migration, and many others. Up to now, more than 200 signaling proteins have been described as 14-3-3 ligands [47]. Using a two-hybrid screening system, it was found that PMCA3 interacted not only with ε isoform of 14-3-3 protein but with ζ isoform as well [48].

Although, as described above, protein-protein interactions were detected for PMCA3, their physiological and biological significance remains unclear. In opposite, the recent report has shown the local functional coupling between neuronal presynaptic glycine transporter (GlyT2), PMCA3, and Na^+/Ca^{2+} exchanger 1 (NCX1) [49]. The authors suggest that this association may help in correcting the local imbalance of Na^+ produced during high activity periods of glycine-$3Na^+$

co-transport by GlyT2, after neurotransmitter release. In contrast to PISP and Ania-3 proteins, PMCA3-GlyT2 interaction does not require PDZ-domain presence. Interestingly, the formation of this complex occurs in lipid raft domains, where the highest presence of PMCAs protein was identified [50]. Also, the association of nearly 60 % of PMCAs with lipid rafts in synaptic membranes of the rat cortex exhibited higher activity than non-raft PMCAs [51]. Due to higher level of cholesterol in aging brain, which is suggested to create a lipid domain more ordered, a stabilization of the active conformation of the enzyme may represent a novel CaM-independent mechanism of PMCA regulation. Since PMCAs amount and activity decline with age, the potential protective action of cholesterol could be particularly important, at least in some biologically meaningful range. Even if PMCA3 represents a minor fraction of total PMCA protein in raft and non-raft domains, its high Ca^{2+} and CaM affinity, as well as low sensitivity for calpain-mediated degradation, may place this isoform among cellular second-line defense systems against Ca^{2+} overload.

6 PMCA3 Mutations

Recently, several reports described some mutations in ATP2B3 gene in human, which could help to clarify the function of PMCA3 isoform in controlling of calcium homeostasis.

Using X-exome sequencing, Zanni et al. [52] identified a missense mutation (Gly at 1107 was replaced by Asp) in CaM-binding domain of PMCA3 in a family with X-linked congenital cerebellar ataxia. The functional consequence of this mutation was analyzed on model cells (HeLa) co-transfected with expression plasmids encoding mutated pump, and the reduced PMCA3 transport activity, as well as a delayed return of Ca^{2+} to baseline, was detected. The authors suggested a possible inability of the mutant pump to form multiprotein complexes; thereby, the regulation of local calcium concentration could be disturbed.

Somatic hotspot mutations in ATP2B3 were identified in approximately 7 % of aldosterone-producing adenomas (APAs) using exome sequencing technique [53]. Thus, a direct inactivation of PMCA3 could increase intracellular Ca^{2+} concentration, thereby leading to altered calcium- and aldosterone-induced signaling. Under ex vivo conditions, electrophysiological studies on primary cultured adenoma cells with different underlying mutations showed substantially higher levels of depolarization in ATP2B3-mutant cells (7 cells from 2 cases) compared to cells from normal adjacent tissue. This indicates that adenoma cells with mutations in ATPase gene have profoundly altered electrophysiological properties.

Further study showed that among 112 screened APAs, somatic mutations in ATP2B3 were present in 0.9 % of samples, and three additional different in-frame DNA deletions leading to either p.Leu425_Val426del or p.Val426_ Val427del were identified [54].

7 PMCA3 Downregulation Assays

As was stated above, data on PMCA3 are fairly limited in comparison to the other three basic isoforms. For instance, its gene has never been knocked out suggesting an important contribution of *Atp2b3* products in the early development. Our work on pheochromocytoma-derived PC12 cells which originate from the neural crest, a tissue that further develops into sympathetic and parasympathetic ganglia, sheds some light on the mysterious aspects of PMCA3 functioning. In a model of stable transfection, knockdown of *Atp2b3* in non-differentiated PC12 cells by an antisense mRNA had profound consequences on Ca^{2+} homeostasis. PMCA3-deficient cells maintained permanently higher resting $[Ca^{2+}]_c$, enhanced Ca^{2+} uptake upon stimulation, and were unable to remove Ca^{2+} efficiently following membrane depolarization [55]. Impaired Ca^{2+} clearing potency and the resulting prolonged calcium signal did not, however, lead to the initiation of death cascades. Although it is thought that PMCA isoforms cannot fully compensate for each other, an increased synthesis of PMCA4 in response to PMCA3 downregulation seems to efficiently protect cells from Ca^{2+} overload and subsequent death. Taking multidirectional action of calcium into consideration, PMCA3-dependent Ca^{2+}-activated transduction pathways, or even elevated $[Ca^{2+}]_c$ by itself, could trigger a spontaneous neuritogenesis-like transformation observed in PMCA3-deficient line [56]. Reconstructed 3D micrographs of these cells showed the extension of neuronal protrusions and appearance of growth cone-like areas with accompanying upregulation of growth-associated protein 43 (GAP43), a neuronal growth cones marker. This apparent shift toward neuronal phenotype involved a significant rearrangement of gene expression pattern involving genes engaged in, e.g., differentiation, signaling and neurogenesis, or transcriptional regulation [57]. Among the genes affected by PMCA3 knockdown, the transcripts of calmodulin gene I and II were found to be increased giving rise to higher calmodulin (CaM) protein level. This observation is of particular importance since CaM is a protein activator of PMCA and may indicate PMCA3 participation in CaM gene expression regulation.

In PC12 line, differentiation is mediated by signaling pathways triggered by mitogen-activated protein kinases (MAPKs) [58]. However, in our PMCA3-depleted model, neurogenesis seems to be driven by different, so far unidentified, signaling pathways as the activity of extracellular signal-regulated kinases 1 and 2 (ERK1/2) and p38 MAPK was markedly inhibited [57]. Strong, but yet plausible, candidate bringing together higher $[Ca^{2+}]_c$, intracellular signaling and modified gene expression profile seems to be calcineurin (CaN). The synthesis and activity of this protein phosphatase was elevated in PMCA3-deficient cells, and intensification of CaN/PMCA4 complex formation was assumed to regulate CaN activity and dopamine release [55]. The observation of dopamine secretion recovery after inhibition of CaN activity pointed out an existence of a feedback mechanism based on the interplay between Ca^{2+}/PMCA4/CaN by which PMCA3 may be involved in coordination of secretory pathways.

Further studies showed that CaN-dependent nuclear factor of activated T cells (NFAT) signaling is largely responsible for reduction in dopamine secretion in

PMCA3-downregulated cells. In these cells, NFAT overactivation and subsequent nuclear translocation led to repression of *Vamp1* and *Vamp2* encoding proteins involved in neurotransmitter release [59]. Therefore, NFAT signaling in our model line may regulate exocytosis by limiting the membrane fusion step. These findings reinforce the hypothesis on the existence of PMCA3/NFAT regulatory loop. Our recent report has revealed that this relationship may also involve transcriptional regulation of *Atp2b3* [60]. Regarding the PMCA3 splicing pattern, a brain-specific variant PMCA3x/a was predominant upon NFAT inhibition, while the expression of other splicing forms generated at C site was completely abolished. It is therefore very likely that higher NFAT activity in PMCA3-deficient cells is involved in PMCA3 alternative splicing and NFAT-mediated transcription is necessary for the formation of PMCA3e,f,c,b variants.

In the next set of experiments, we used unique capacity of PC12 line to change their phenotype into sympathetic-like neurons to resolve any potential role of PMCA3 in differentiation process. Stimulation of PMCA3-deficient cells with cAMP derivative induced prominent neurite sprouting and resulted in more intensive differentiation during 2-day period as assessed by the number of cells bearing neurites and the neurite length [61]. However, retraction of growth cones and preferable formation of varicosities were observed as morphological response to PMCA3 depletion.

The knockdown of PMCA3 in differentiated cells reduced the ability to control cellular homeostasis of Ca^{2+} and led to significant increase in resting $[Ca^{2+}]_c$ [61] in a manner similar to non-differentiated line. However, upon differentiation, the efficient protection from consequences of abnormally prolonged calcium signal had to be provided by much more sophisticated adaptive mechanisms. In addition to previously observed upregulation of PMCA4, which seems to play a role of "main cellular bodyguard," PMCA3-deficient cells were equipped with higher level of PMCA1. Another compensatory change involved increased level of *sarco-/endoplasmic* reticulum Ca^{2+}-ATPase 2 and 3 (SERCA 2 and 3), thereby giving the ability for more effective Ca^{2+} packing into the endoplasmic reticulum (ER). Our experimental verification with SERCA inhibitor—thapsigargin—revealed higher Ca^{2+} accumulation in the ER as another mechanism by which PMCA3-downregulated cells aimed to decrease $[Ca^{2+}]_c$. The partial loss of PMCA3 also potentiated Ca^{2+} influx through the plasma membrane voltage-dependent calcium channels (VDCCs) and slowed the return to baseline of the Ca^{2+} transients induced by depolarizing KCl concentration [61]. Our functional studies with VDCCs inhibitors showed that observed KCl-evoked increase in Ca^{2+} influx was due to higher content of P/Q and L-type channels. Of particular interest is the prominent upregulation of P/Q channels that may be related to acquisition of specific secretory properties of PMCA3-deficient cells, since this type of VDCCs is closely related to neurotransmitter release. These findings strengthen our hypothesis regarding the contribution of PMCA3 to regulation of secretory pathways and, in overall, indicate that this isoform is apparently involved in the control of differentiation process.

PMCA3, like other PMCA isoforms, operates as Ca^{2+}/H^+ countertransporter linking the extrusion of Ca^{2+} to the inward proton transport. Based on the kinetic properties, one may expect that PMCA3 action generates large quantities of protons

leading to cellular acidification. If this is true, then partial deprivation of PMCA3 activity should reduce the amount of H^+ entering cytosol potentially altering organellar pH homeostasis. Indeed, our differentiated PMCA3-deficient cells maintained resting mitochondrial pH at 7.62 ± 0.01 and cytosolic at 7.49 ± 0.02, values in both compartments higher than in naive cells [62]. Mitochondrial pH decrease during cytosolic Ca^{2+} elevations evoked by Ca^{2+} influx through VDCCs was, however, partially attenuated even despite potentiation of $[Ca^{2+}]_c$ transients in our model line. In such conditions, pH gradient across the inner mitochondrial membrane followed the changes in mitochondrial/cytosolic H^+ fluxes which were largely driven by the electron transport chain. Because SERCA and Na^+/Ca^{2+} exchanger modulated pH response in a neglectable manner during Ca^{2+} loads, PMCA3 can be considered as an important regulator of intracellular pH of differentiated PC12 cells.

The increase in steady-state mitochondrial pH could indicate higher capacity of mitochondria to produce ATP. Nonetheless, our further studies on energy metabolism of PMCA3-deficient cells, as well as the experiments with oligomycin, indicated rather low rate of ATP turnover and state of mitochondria close to state 4 [62]. In parallel, we demonstrated higher glucose consumption and concomitant lactate release in these cells but also a compensatory ATP generation via the Pasteur effect in the presence of oligomycin [63]. Increased percentage of necrotic cells observed following short-time hexokinase inhibition seems to additionally support our presumption of paramount importance of anaerobic glycolysis for ATP supply in PMCA3 downregulated line. Mitochondrially generated ATP in this line is critical to sustain neuronal differentiation as the inhibition of ATP synthase decreased the expression of neuronal marker βIII-tubulin and initiated massive cell death. These results provide an evidence for an important role of PMCA3 in the regulation of bioenergetic pathways and maintenance of ATP level during differentiation process.

Using rat pituitary GH3 line, a model system of excitable endocrine cells, we next confirmed that disturbance of Ca^{2+} homeostasis caused by PMCA3 downregulation is not restricted only to (pseudo)neuronal lines but may represent a more general phenomenon [64]. The most prominent finding in GH3 cells with decreased PMCA3 level was an upregulation of glutamate decarboxylase 65 kDa isoform (GAD65) expression, which correlated with augmented protein amount. Glutamate decarboxylase (GAD) is responsible for γ-aminobutyric acid (GABA) synthesis, and, in addition to 65 kDa isoform, it also exists as GAD67. Although the expression of the latter was not affected by PMCA3 downregulation, the total enzymatic activity of GAD was lower than in naive cells. This suggests a functional connection between PMCA3 and GAD65, which is thought to preferentially produce GABA for secretion. In view of our findings, PMCA3 function could be related to the regulation of GABA synthesis and degradation that additionally highlights its involvement in the process of neurotransmitters synthesis and release.

Our studies on *Atp2b3* knockdown cell models clearly demonstrate that PMCA3 function is not only limited to Ca^{2+} extrusion but may be extended on many important processes. Therefore, it is of high priority to make efforts for generating knockout animals to elucidate the role of PMCA3 in the early development. On the

other hand, the overexpression studies in cells lacking PMCA3 may also provide valuable data regarding such restricted localization and sophisticated function of this isoform.

8 Conclusions

The expression of PMCA3 determined under a wide range of experimental conditions and during developmental stages of the cells seems to reflect its unique characteristic and function. Based on the available data, PMCA3 seems to be a defined component of the plasma membrane signal-processing machinery, although its precise role is far to be fully clarified. The regulatory function of PMCA3 could be recognized to operate through the action of subcellular microdomains, several of which exist in a single cell. The expressional level appears to be not only gene specific but even transcript specific and strongly depends on the cell type. PMCA3 colocalization with other isoforms, as well as with some proteins modulating calcium-induced events, suggests that it may enable the cells to govern their vital activities. Being a fast-acting calcium pump with relative resistance to the stress conditions, as was shown in several studies, PMCA3 may significantly contribute to the maintaining of cellular calcium homeostasis when other isoforms are less effective.

Acknowledgments This work was supported by the Medical University of Lodz grant nos. 503/6-086-02/503-01 and 502-03/6-086-02/502-64-061 and, in part, by National Science Centre grant (to T. Boczek) based on decision UMO-2012/05/D/NZ4/02982.

References

1. Strehler EE, Heim R, Carafoli E (1991) Molecular characterization of plasma membrane calcium pump isoforms. Adv Exp Med Biol 307:251–261
2. Kühlbrandt W (2004) Biology, structure and mechanism of P-type ATPases. Nat Rev Mol Cell Biol 5:282–295
3. Brini M, Coletto L, Pierobon N et al (2003) A comparative functional analysis of plasma membrane Ca^{2+} pump isoforms in intact cells. J Biol Chem 278:24500–24508
4. Strehler EE, Strehler-Page MA, Vogel G et al (1989) mRNAs for plasma membrane calcium pump isoforms differing in their regulatory domain are generated by alternative splicing that involves two internal donor sites in a single exon. Proc Natl Acad Sci U S A 86:6908–6912
5. Hilfiker H, Guerini D, Carafoli E (1994) Cloning and expression of isoform 2 of the human plasma membrane Ca^{2+} ATPase. Functional properties of the enzyme and its splicing products. J Biol Chem 269:26178–26183
6. Filoteo AG, Enyedi A, Verma AK et al (2000) Plasma membrane Ca^{2+} pump isoform 3f is weakly stimulated by calmodulin. J Biol Chem 275:4323–4328
7. Caride AJ, Penheiter AR, Filoteo AG et al (2001) The plasma membrane calcium pump displays memory of past calcium spikes. Differences between isoforms 2b and 4b. J Biol Chem 276:39797–39804

8. Carafoli E (1984) Calcium-transporting systems of plasma membranes, with special attention to their regulation. Adv Cyclic Nucleotide Protein Phosphorylation Res 17:543–549
9. Wang MG, Yi H, Hilfiker H et al (1994) Localization of two genes encoding plasma membrane Ca^{2+} ATPases isoforms 2 (ATP2B2) and 3 (ATP2B3) to human chromosomes 3p26 → p25 and Xq28, respectively. Cytogenet Cell Genet 67:41–45
10. Brown BJ, Hilfiker H, DeMarco SJ et al (1996) Primary structure of human plasma membrane Ca^{2+}-ATPase isoform 3. Biochim Biophys Acta 1283:10–13
11. Burk SE, Shull GE (1992) Structure of the rat plasma membrane Ca^{2+}-ATPase isoform 3 gene and characterization of alternative splicing and transcription products. Skeletal muscle-specific splicing results in a plasma membrane Ca^{2+}-ATPase with a novel calmodulin-binding domain. J Biol Chem 267:19683–19690
12. Strehler EE, Zacharias DA (2001) Role of alternative splicing in generating isoform diversity among plasma membrane calcium pumps. Physiol Rev 81:21–50
13. Keeton TP, Burk SE, Shull GE (1993) Alternative splicing of exons encoding the calmodulin-binding domains and C termini of plasma membrane Ca^{2+}-ATPase isoforms 1, 2, 3, and 4. J Biol Chem 268:2740–2748
14. Brini M, Carafoli E (2009) Calcium pumps in health and disease. Physiol Rev 89:1341–1378
15. Brini M, Calì T, Ottolini D et al (2013) The plasma membrane calcium pump in health and disease. FEBS J 280:5385–5397
16. Brandt P, Neve RL (1992) Expression of plasma membrane calcium-pumping ATPase mRNAs in developing rat brain and adult brain subregions: evidence for stage-specific expression. J Neurochem 59:1566–1569
17. Stauffer TP, Guerini D, Celio MR et al (1997) Immunolocalization of the plasma membrane Ca^{2+} pump isoforms in the rat brain. Brain Res 748:21–29
18. Eakin TJ, Antonelli MC, Malchiodi EL et al (1995) Localization of the plasma membrane Ca^{2+}-ATPase isoform PMCA3 in rat cerebellum, choroid plexus and hippocampus. Brain Res Mol Brain Res 29:71–80
19. Burette A, Rockwood JM, Strehler EE et al (2003) Isoform-specific distribution of the plasma membrane Ca^{2+} ATPase in the rat brain. J Comp Neurol 467:464–476
20. Burette A, Weinberg RJ (2007) Perisynaptic organization of plasma membrane calcium pumps in cerebellar cortex. J Comp Neurol 500:1127–1135
21. Guerini D, Garcia-Martin E, Gerber A et al (1999) The expression of plasma membrane Ca^{2+} pump isoforms in cerebellar granule neurons is modulated by Ca^{2+}. J Biol Chem 274:1667–1676
22. Sepulveda MR, Hidalgo-Sanchez M, Marcos D et al (2007) Developmental distribution of plasma membrane Ca^{2+}-ATPase isoforms in chick cerebellum. Dev Dyn 236:1227–1236
23. Marcos D, Sepulveda MR, Berrocal M et al (2009) Ontogeny of ATP hydrolysis and isoform expression of the plasma membrane Ca^{2+}-ATPase in mouse brain. BMC Neurosci 10:112
24. Stauffer TP, Guerini D, Carafoli E (1995) Tissue distribution of the four gene products of the plasma membrane Ca^{2+} pump. A study using specific antibodies. J Biol Chem 270: 12184–12190
25. Kip SN, Gray NW, Burette A et al (2006) Changes in the expression of plasma membrane calcium extrusion systems during the maturation of hippocampal neurons. Hippocampus 16:20–34
26. Zacharias DA, DeMarco SJ, Strehler EE (1997) mRNA expression of the four isoforms of the human plasma membrane Ca^{2+}-ATPase in the human hippocampus. Brain Res Mol Brain Res 45:173–176
27. Garcia ML, Murray KD, Garcia VB et al (1997) Seizure-induced alterations of plasma membrane ATPase isoforms 1, 2 and 3 mRNA and protein in the rat hippocampus. Mol Brain Res 45:230–238
28. Lehotsky J, Kaplan P, Racay P et al (1999) Distribution of plasma membrane Ca^{2+} pump (PMCA) isoforms in the gerbil brain: effect of ischemia-reperfusion injury. Neurochem Int 35:221–227

29. Tachibana T, Ogura H, Tokunaga A et al (2004) Plasma membrane calcium ATPase expression in the rat spinal cord. Brain Res Mol Brain Res 131:26–32
30. Stahl WL, Eakin TJ, Owens JWM et al (1992) Plasma membrane Ca^{2+}-ATPase isoforms: distribution of mRNAs in rat brain by in situ hybridization. Mol Brain Res 16:223–231
31. Zacharias DA, Kappen C (1999) Developmental expression of the four plasma membrane calcium ATPase (Pmca) genes in the mouse. Biochim Biophys Acta 1428:397–405
32. Krizaj D, Demarco SJ, Johnson J et al (2002) Cell-specific expression of plasma membrane calcium ATPase isoforms in retinal neurons. J Comp Neurol 451:1–21
33. Rentería RC, Strehler EE, Copenhagen DR et al (2005) Ontogeny of plasma membrane calcium ATPase isoforms in the neural retina of the postnatal rat. Vis Neurosci 22:263–274
34. Talarico EF Jr, Kennedy BG, Marfurt CF et al (2005) Expression and immunolocalization of plasma membrane calcium ATPase isoforms in human corneal epithelium. Mol Vis 11:169–178
35. Talarico EF Jr, Mangini NJ (2007) Alternative splice variants of plasma membrane calcium-ATPases in human corneal epithelium. Exp Eye Res 85:869–879
36. Caride AJ, Filoteo AG, Penheiter AR et al (2001) Delayed activation of the plasma membrane calcium pump by a sudden increase in Ca^{2+}: fast pumps reside in fast cells. Cell Calcium 30:49–57
37. Strehler EE, Filoteo AG, Penniston JT et al (2007) Plasma-membrane Ca(2+) pumps: structural diversity as the basis for functional versatility. Biochem Soc Trans 35:919–922
38. Moreau R, Daoud G, Masse A et al (2003) Expression and role of calcium-ATPase pump and sodium-calcium exchanger in differentiated trophoblasts from human term placenta. Mol Reprod Dev 65:283–288
39. Martin R, Harvey NC, Crozier SR et al (2007) Placental calcium transporter (PMCA3) gene expression predicts intrauterine bone mineral accrual. Bone 40:1203–1208
40. Kamagate A, Herchuelz A, Bollen A et al (2000) Expression of multiple plasma membrane Ca^{2+}-ATPases in rat pancreatic islet cells. Cell Calcium 27:231–246
41. Caride AJ, Chini EN, Homma S et al (1998) mRNA encoding four isoforms of the plasma membrane calcium pump and their variants in rat kidney and nephron segments. J Lab Clin Med 132:149–156
42. Usachev YM, Toutenhoofd SL, Goellner GM et al (2001) Differentiation induces upregulation of plasma membrane Ca^{2+}-ATPase and concomitant increase in Ca^{2+} efflux in human neuroblastoma cell line IMR-32. J Neurochem 76:1756–1765
43. Greene LA, Kaplan DR (1995) Early events in neurotrophin signalling via Trk and p75 receptors. Curr Opin Neurobiol 5:579–587
44. Hammes A, Oberdorf S, Strehler EE et al (1994) Differentiation-specific isoform mRNA expression of the calmodulin-dependent plasma membrane Ca^{2+}-ATPase. FASEB J 8:428–435
45. Goellner GM, DeMarco SJ, Strehler EE (2003) Characterization of PISP, a novel single-PDZ protein that binds to all plasma membrane Ca^{2+} -ATPase b-splice variants. Ann N Y Acad Sci 986:461–471
46. Sgambato-Faure V, Xiong Y, Berke JD et al (2006) The Homer-1 protein Ania-3 interacts with the plasma membrane calcium pump. Biochem Biophys Res Commun 343:630–637
47. Mhawech P (2005) 14-3-3 proteins--an update. Cell Res 15:228–236
48. Linde CI, Di Leva F, Domi T et al (2008) Inhibitory interaction of the 14-3-3 proteins with ubiquitous (PMCA1) and tissue-specific (PMCA3) isoforms of the plasma membrane Ca^{2+} pump. Cell Calcium 43:550–561
49. de Juan-Sanz J, Núñez E, Zafra F et al (2014) Presynaptic control of glycine transporter 2 (GlyT2) by physical and functional association with plasma membrane Ca^{2+} -ATPase (PMCA) and Na^{+}- Ca^{2+} exchanger (NCX). J Biol Chem 289:34308–34324
50. Jiang L, Fernandes D, Mehta N et al (2007) Partitioning of the plasma membrane Ca^{2+}-ATPase into lipid rafts in primary neurons: effects of cholesterol depletion. J Neurochem 102:378–388

51. Jiang L, Bechtel MD, Galeva NA et al (2012) Decreases in plasma membrane Ca^{2+}-ATPase in brain synaptic rafts from aged rats. J Neurochem 123:689–699
52. Zanni G, Calìb T, Kalscheuercet VM et al (2012) Mutation of plasma membrane Ca^{2+} ATPase isoform 3 in a family with X-linked congenital cerebellar ataxia impairs Ca^{2+} homeostasis. Proc Natl Acad Sci U S A 109:14514–14519
53. Beuschlein F, Boulkroun S, Osswald A et al (2013) Somatic mutations in ATP1A1 and ATP2B3 lead to aldosterone-producing adenomas and secondary hypertension. Nat Genet 45:440–444
54. Williams TA, Monticone S, Schack VR et al (2014) Somatic ATP1A1, ATP2B3, and KCNJ5 mutations in aldosterone-producing adenomas. Hypertension 63:188–195
55. Kosiorek M, Podszywalow-Bartnicka P, Zylinska L et al (2011) Interaction of plasma membrane Ca^{2+}-ATPase isoform 4 with calcineurin A: implications for catecholamine secretion by PC12 cells. Biochem Biophys Res Commun 411:235–240
56. Zylinska L, Kozaczuk A, Szemraj J et al (2007) Functional importance of PMCA isoforms in growth and development of PC12 cells. Ann N Y Acad Sci 1099:254–269
57. Boczek T, Kozaczuk A, Ferenc B et al (2012) Gene expression pattern in PC12 cells with reduced PMCA2 or PMCA3 isoform: selective up-regulation of calmodulin and neuromodulin. Mol Cell Biochem 360:89–102
58. Muroi Y, Ishii T, Teramoto K et al (2004) Calcineurin contributes to the enhancing effect of adenosine on nerve growth factor-induced neurite outgrowth via the decreased duration of p38 mitogen-activated protein kinase phosphorylation. J Pharmacol Sci 95:124–131
59. Kosiorek M, Zylinska L, Zablocki K et al (2014) Calcineurin/NFAT signaling represses genes Vamp1 and Vamp2 via PMCA-dependent mechanism during dopamine secretion by Pheochromocytoma cells. PLoS One 9:e92176
60. Kosiorek M, Podszywalow-Bartnicka P, Zylinska L et al (2014) NFAT1 and NFAT3 cooperate with HDAC4 during regulation of alternative splicing of PMCA isoforms in PC12 cells. PLoS One 9:e99118
61. Boczek T, Lisek M, Kowalski A et al (2012) Downregulation of PMCA2 or PMCA3 reorganizes Ca^{2+} handling systems in differentiating PC12 cells. Cell Calcium 52:433–444
62. Boczek T, Lisek M, Ferenc B et al (2014) Plasma membrane Ca^{2+}-ATPase isoforms composition regulates cellular pH homeostasis in differentiating PC12 cells in a manner dependent on cytosolic Ca^{2+} elevations. PLoS One 9:e102352
63. Boczek T, Lisek M, Ferenc B et al (2014) Silencing of plasma membrane Ca^{2+}-ATPase isoforms 2 and 3 impairs energy metabolism in differentiating PC12 cells. Biomed Res Int 2014:735106
64. Kowalski A, Zylinska L, Boczek T et al (2011) GABA-shunt enzymes activity in GH3 cells with reduced level of PMCA2 or PMCA3 isoform. Biochem Biophys Res Commun 411:815–820

Chapter 5
The ATP2B Plasma Membrane Ca^{2+} ATPase Family: Regulation in Response to Changing Demands of Cellular Calcium Transport

Emanuel E. Strehler

Abstract The mammalian ATP2B family of plasma membrane calcium ATPases (PMCAs) consists of over 30 members generated from four genes and via complex alternative RNA splicing. Regulation occurs at the level of ATP2B gene transcription, splicing, translation, and posttranslational modification. PMCA isoforms and splice variants vary in their functional properties and are differentially regulated by intrinsic factors such as calmodulin and lipids, as well as by dynamic interaction with a large number of scaffolding and signaling proteins. A major emerging theme is the functional integration of different PMCAs in multiprotein complexes to allow reciprocal cross talk between localized PMCA-mediated Ca^{2+} control and the function of other members in the complex. The same PMCA isoform may be responsible for bulk calcium export in the cells of one tissue but control the local activity of a signaling microdomain in the cells of another. Regulation of the PMCAs must therefore be understood in the physiological context of the tissues and cells where they are expressed.

Keywords Alternative splicing • ATP2B ion pumps • Calcium microdomain • Calcium signaling • Plasma membrane calcium ATPase • PMCA • Signaling cross talk

1 Introduction

Calcium is an abundant and essential element in all living systems, and is used for both structural (skeleton, teeth) and signaling purposes. Cells expend a large amount of energy to control calcium fluxes and to maintain calcium homeostasis. As an

E.E. Strehler (✉)
Department of Biochemistry and Molecular Biology, Mayo Clinic College of Medicine, 200 First Street SW, Rochester, MN 55905, USA
e-mail: strehler.emanuel@mayo.edu

S. Chakraborti, N.S. Dhalla (eds.), *Regulation of Ca^{2+}-ATPases,V-ATPases and F-ATPases*, Advances in Biochemistry in Health and Disease 14,
DOI 10.1007/978-3-319-24780-9_5

important signaling agent, ionized free calcium (Ca^{2+}) must be very tightly regulated. Accordingly, cells have evolved membrane-intrinsic transport systems specifically dedicated to Ca^{2+} transport across biological membranes [1, 2]. Plasma membrane Ca^{2+} ATPases (PMCAs) are present in all eukaryotic cells and belong to the large superfamily of P-type ATP-driven ion pumps characterized by the formation of a phosphorylated enzyme intermediate [3]. Among the P-type ion pumps, the PMCAs are classified as ATP2B subfamily of Ca^{2+} pumps, with ATP2A and ATP2C representing the Ca^{2+} pumps of the sarco/endoplasmic reticulum and the Golgi compartment, respectively [4, 5]. Following the early realization that PMCAs represent a dedicated Ca^{2+} extrusion system capable of removing "excess" Ca^{2+} across the plasma membrane to maintain long-term intracellular Ca^{2+} balance, subsequent studies have shown a remarkable complexity not only in the number of PMCA isoforms expressed in different cells and tissues but also in the mechanisms by which these calcium pumps are regulated. This review will start with an overview of the molecular complexity of the mammalian PMCA family and then highlight different mechanisms of regulation of these proteins and their integration in the physiological demands of cellular Ca^{2+} handling.

2 Overview of the Mammalian ATP2B Gene Family Coding for Plasma Membrane Ca^{2+} ATPases (PMCAs)

The known mammalian genomes contain four separate PMCA genes (nomenclature for the human genes: ATP2B1, ATP2B2, ATP2B3, ATP2B4) located on different chromosomes (12q21.3, 3p25.3, Xq28, and 1q32.1 for human ATP2B1–4, respectively). The genes are large, with ~20–25 protein-coding exons spread over 50 to >100 kb, and additional 5′ untranslated exons separated by large introns in the 5′ region [6]. The human genes, for example, are ~120 kb for ATP2B1, ~380 kb for ATP2B2, ~ 65 kb for ATP2B3, and ~120 kb for ATP2B4 (Fig. 5.1). Several exons are subject to alternative splicing resulting in a multitude of PMCA splice variants differing in specific regions of the protein. The two major regions affected by alternative splicing are located in the first intracellular loop (site A) and the C-terminal tail (site C; see scheme in Fig. 5.2). A remarkable feature of all PMCA genes is the presence of at least one exon containing only 5′ untranslated (5′ UTR) sequence; the ATP2B2 gene has at least four separate upstream exons specifying 5′ UTR sequences (Fig. 5.1). In addition, some of these upstream exons are alternatively spliced and incorporated due to alternative promoters [7]. The complex upstream gene structure and multiple transcriptional start sites are suggestive of complex transcriptional regulation of the ATP2B genes.

The PMCAs contain ~1200 amino acid residues and have molecular masses of ~125–140 kDa [8]. Alternative splicing (at site A) of one to three small exons coding for integer multiples of triplet codons leads to changes in the length of the first intracellular loop, which can thus differ by up to 45 residues (comparing human

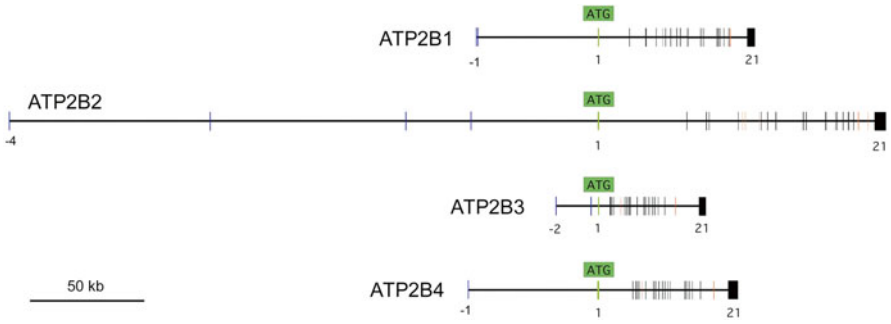

Fig. 5.1 Exon–intron structure of the human ATP2B genes. The four genes are aligned with respect to their ATG initiation codon in exon 1 and their length is shown to scale. Upstream exons (*blue boxes*) have negative numbers, the last exon (exon 21) containing the bulk of the 3′ UTR is also labeled. Constitutively spliced exons are shown as *black boxes*. A scale bar (50 kb) is indicated on the *lower left*

PMCA2 splice variants 2z and 2w). The PMCA site-A variants are indicated by lower case letters w, x, y, z [9]; a splice variant inserting yet a fourth optional exon coding for an additional 12 amino acids has been identified in the bullfrog and has been named variant "v" [10]. The cytosolic loop affected by site-A splicing is part of the A (actuator) domain of the pumps and as such, is intimately involved in the structural transitions that accompany the Ca^{2+} pumping reaction cycle [11]. This loop also contains a region sensitive to acidic phospholipids and participates in the autoregulation (auto-inhibition) of the pump in the basal state, i.e., at low $[Ca^{2+}]_i$ and in the absence of calmodulin (CaM) [12, 13]. Interestingly, however, the site A splice variants have not been found to differ significantly in their in vitro functional properties [14] or acidic lipid sensitivity when over-expressed in transfected CHO cells [15]. The effect of alternative splicing at site A on PMCA regulation may instead be indirect, e.g., by altering membrane targeting [16] and lipid partitioning, or by affecting signaling cross talk via specific lipid sequestration [17] or as yet unknown protein interactions.

Alternative splicing at site C is complex and can either insert additional amino acids into the C-terminal tail (splice variants c, d) or truncate the C-tail due to a shift in reading frame and the earlier occurrence of a stop codon (splice variants a, e, f) [9, 18]. The alternative splicing affects a major regulatory region of the PMCAs, i.e., the CaM-binding domain [19]. In addition, the splice variants with an altered reading frame and earlier stop codon also show major differences in their regulation by other proteins, most notably by PDZ domain-containing signaling and scaffolding proteins (see below) [20]. Because of the potential for combinatorial use of the alternative splice options at sites A and C, over 30 PMCA isoform variants can be generated from the four mammalian genes and >20 of these have been detected at various levels in different tissues [21]. Tables summarizing the various splice options have been published in many recent reviews [18, 19, 21, 22] and the reader is referred to these for further information.

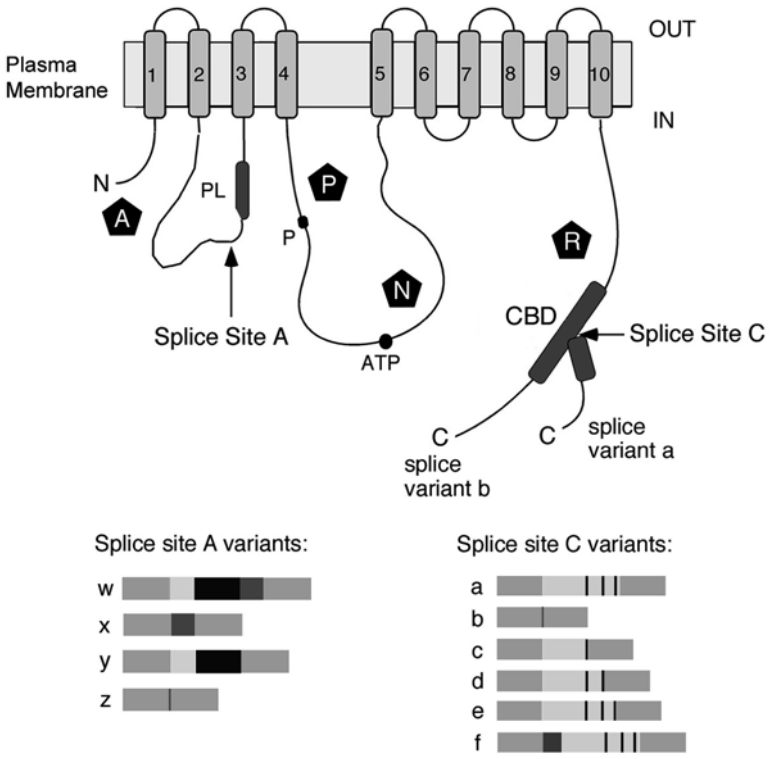

Fig. 5.2 Scheme of the mammalian PMCA and alternative splice options. A model of the PMCA in the plasma membrane is shown on the *top*. The cytosolic (IN) and extracellular (OUT) sides are indicated. The ten membrane-spanning regions of the PMCA are numbered, and the N- and C-terminus are labeled. The phospholipid-binding region in the first cytosolic loop (PL), the obligatory aspartate residue phosphorylated during the enzyme reaction cycle (P), the ATP binding region (ATP), and the CaM-binding domain (CBD) are also indicated. Major functional domains of the PMCA are labeled in *black pentagons* as A (actuator), P (phosphorylation), N (nucleotide-binding), and R (regulatory). *Arrows* indicate where alternative splicing results in isoform variability in the first cytosolic loop (splice site A) and the C-terminal tail (splice site C). Splicing at site C can result in a change in reading frame, this is exemplified by two different C-termini shown for variants a and b. Exon arrangements resulting in splice variants at site A and site C are shown on the *bottom. Flanking gray boxes* represent constitutively spliced exons, alternatively spliced exons are shown as separate *boxes* in different shades of *gray*, and the resulting splice variants are labeled by their *lowercase symbol* on the *left*. Note that splice options c, d, and e use different splice donor sites within the same exon (indicated by *black vertical lines*); complete insertion of this exon gives rise to splice variant a

3 ATP2B Gene Regulation

The transcriptional regulation of ATP2B genes is not well understood, but they are clearly differentially regulated during embryonic development and in different organs and cell types in response to numerous stimuli [23, 24]. In situ hybridization

studies during mouse embryogenesis have shown that *Atp2b1* is transcribed very early on, including in embryonic stem cells [25], and continues to be expressed in virtually all tissues throughout life, albeit at varying levels [26]. It is therefore not surprising that germ-line knockout of both copies of the Atp2b1 gene is embryonic lethal [27]. However, although PMCA1 is often referred to as "housekeeping" isoform, the ATP2B1 gene is subject to tight regulation at the transcriptional and post-transcriptional level. The early response transcription factor c-myb, for example, was shown to repress *Atp2b1* transcription during the G1/S phase of the cell cycle in mouse vascular smooth muscle cells, likely by interacting with myb-binding sites in the promoter region of the gene [28]. Similarly, c-myc can bind directly to a regulatory region in the Atp2b4 gene promoter and mediates transcriptional downregulation of PMCA4 during B lymphocyte differentiation [29]. Early promoter studies on the mouse Atp2b1 gene identified numerous general and specific transcription factor binding sites [30] and showed both protein kinase C (PKC) and protein kinase A (PKA) dependent transcriptional (up)regulation of PMCA1 expression [31]. These kinases are mediators of hormone-induced second messenger (Ca^{2+}, cAMP) regulation of PMCA expression and likely work through transcription factors such as CREB. The ATP2B1 gene is also subject to transcriptional regulation by the active form of vitamin D, 1,25-$(OH)_2$-D3, which strongly induces PMCA1 expression in the small intestine, kidney distal tubules, and osteoblasts [32–36].

The transcriptional regulation of the ATP2B genes is evidently tissue-specific and may change with the differentiation state and in response to external stimuli. Thus, depolarization and a rise in Ca^{2+} in cerebellar granule cells result in opposite regulation of ATP2B1–B3 and ATP2B4: ATP2B4 is downregulated at the transcriptional level in a calcineurin-dependent manner, presumably via calcineurin-mediated increased nuclear translocation of the transcription factor NFAT [37]. By contrast, ATP2B2 is upregulated in cerebellar development by a transcription factor generated from an internal ribosomal entry site in the voltage-gated calcium channel gene CACNA1A [38]. Another striking example of tissue-specific and (likely) hormonal control of transcription of a PMCA gene is that of *Atp2b2* in the lactating mammary gland: the transcript and protein levels of PMCA2 are induced up to 100-fold starting at parturition and during lactation in mice [39, 40]. Interestingly, the mammary gland PMCA2 transcripts are generated by using an alternative promoter and incorporating alternatively spliced 5′ UTR exons of the ATP2B2 gene different from the promoter and 5′ UTR exons used by neuronal cells [7]. As mentioned above, alternative promoters and alternatively spliced 5′ exons may be present in other ATP2B genes (e.g., ATP2B1), further broadening the potential for tissue-specific and physiological context-specific regulation [41].

4 Regulation at the Level of Alternative Splicing and RNA Stability

Alternative splicing of the ATP2B primary transcripts must be carefully regulated because the amino acid changes due to alternative exon usage at sites A and C result in significant changes in the functional properties of the encoded PMCA isoforms.

Evidence for cell-type and differentiation-specific alternative splicing of ATP2B transcripts is widespread. Cochlear outer hair cells almost exclusively express the w/a splice variant of PMCA2, whereas lactating mammary cells express only the w/b variant [10, 40, 42]. In differentiating hippocampal neurons, splicing of ATP2B1, B2, and B3 transcripts shifts from the b- to the a-variant [43], and a recent study in a mouse carotid artery injury model showed that ATP2B4 splicing shifted from the a- to the b-variant in the injured carotids [44]. The factors and mechanisms regulating alternative splicing of ATP2B pre-mRNAs are still incompletely understood. Changes in second messengers, including Ca^{2+} as an important feedback regulator, are clearly playing a role (see for example Ref. [45]), and these likely impact different components of the spliceosome or specific RNA-binding proteins that either promote or repress the use of specific splice sites [46, 47]. In one example Ca^{2+}, working through CaM kinase IV, has been shown to affect alternative splicing in neuronal cells via CaMKIV-responsive RNA elements (CaRREs) [48]. CaRREs are indeed present in relevant regions of ATP2B genes [47] and may be recognized by the RNA binding protein hnRNP-L which is directly phosphorylated by CaMKIV [49]. The transcription factors NFAT1 and NFAT3, possibly working with the histone deacetylase HDAC4, were also recently shown to affect alternative splicing of several ATP2B transcripts in PC12 cells [50]: Inhibition of NFAT1/3 resulted in an increased expression of the "fast" PMCA2x/c, 3x/a, and 4x/a variants primarily at the expense of the "b" variants. For a more detailed discussion of the regulation of alternative splicing in the ATP2B gene family, the reader is referred to a recent review by J. Krebs [18].

The pattern of alternative splicing also depends on the RNA secondary structure, which may be influenced by the length and sequence of the 5′ and 3′ UTR regions. Because several ATP2B genes contain alternative promoters and multiple transcription initiation sites, the promoter and first exon choice could influence the splicing of downstream exons. Similarly, alternative poly-adenylation sites have been documented in the ATP2B genes, resulting in vastly different lengths of 3′ UTR sequences as demonstrated in Northern blots from various tissues [51, 52]. However, no experimental evidence has as yet been provided for a role of the untranslated regions in alternative splicing of the ATP2B pre-mRNAs.

Posttranscriptional regulation of PMCA expression at the level of mRNA stability also deserves attention but has not yet been carefully evaluated. The differences mentioned above in the 3′ UTR regions and poly-adenylation sites of several ATP2B mRNAs may play an important role in the control of their half-lives. In rat aortic and brain vessel endothelial cells ATP2B1 transcripts have been estimated to have a short half-life of 2–3 h [31, 53], a finding that is corroborated by the significant changes in ATP2B1 mRNA levels during the cell cycle in proliferating vascular smooth muscle cells [54]. Thus, when rapid turnover of a specific PMCA isoform is required such as during cell proliferation or in response to external stimuli demanding altered basal Ca^{2+} levels, regulation at the level of ATP2B mRNA stability may be particularly important. However, systematic analyses of the correlation between the 3′ UTR length, poly-A site choice, and mRNA stability have not yet been performed for any of the ATP2B genes.

5 Regulation at the Level of Protein Translation and Stability

The vast majority of studies in which ATP2B expression was determined at the mRNA (Northern blots, in situ hybridization, RT-PCR) and at the protein level (Western blots, immunohistochemistry) report a tight correlation, i.e., PMCA protein levels generally reflect RNA abundance for the particular PMCA. This holds true for most overexpression studies where recombinant cDNAs (usually comprised of only the protein-coding sequence) are transiently or stably transfected into recipient cells. Antisense knockdown (siRNA) studies similarly show a good correlation between decreased RNA levels and loss of the specific PMCA protein, although the analysis of the effects of such treatment requires consideration of the PMCA half-life and is therefore usually performed at least 24–48 h after (transient) mRNA knockdown [55–58]. However, as in the case of ATP2B RNA stability, very little information is available on the half-lives of the endogenous PMCA isoforms in physiological conditions.

The translational regulation of ATP2B mRNAs is another area that has not yet received appropriate attention in the field. The incorporation of alternative 5′ UTR sequences (as well as of alternative exon sequences) may profoundly influence the efficiency of translation initiation due to different secondary RNA structures in the vicinity of the AUG start codon. Specific sequences in the 5′ or 3′ UTR may also play a role in targeting some ATP2B mRNAs to cellular compartments for local translation; this could be of particular relevance for ATP2B2 and ATP2B3, which are mainly expressed in neurons and where specific splice variants are concentrated in membrane microdomains such as presynaptic boutons or postsynaptic spines [59–61].

Information on posttranslational regulation of PMCA stability is also scarce although several recent studies have begun to shed some light on this issue. As already mentioned, early half-life estimates from pulse-chase experiments in endothelial cells showed that the PMCA1 isoform is comparatively unstable. A similar finding was reported by Guerini and coworkers who noted that PMCA1b was remarkably unstable due to its high susceptibility to degradation by the calcium-sensitive protease calpain [62]. Proteolytic cleavage of the PMCA by calpain allows rapid regulation of the Ca^{2+} extrusion capacity of a cell. For example, upon platelet activation by thrombin 50 % of PMCA4b was found to be cleaved by calpain within ~5 min [63]. Initially, this may result in a constitutively active 124 kDa fragment capable of preventing Ca^{2+} overload, but a subsequent reduction in active PMCA at the membrane is required to allow normal progression of clot formation. A similar Ca^{2+}-dependent feedback regulation of the PMCA by calpain appears to be operative in physiological stimulation as well as (NMDA/Ca^{2+}-induced) excitotoxicity in neurons: Limited cleavage of the PMCA is required for normal Ca^{2+} signal control, but excessive calpain cleavage will lead to excitotoxicity and cell death [64–66].

The examples above illustrate instances of the regulated degradation of specific PMCAs. Much less is known about the “constitutive” pathways of PMCA turnover

and the mechanisms of their degradation. Several reports have shown that PMCAs may be "flagged" for destruction, e.g., by posttranslational modifications such as oxidation and glycation, and these modifications result in PMCA inhibition [67–71]. The most plausible routes for the eventual demise of the pumps involve endocytosis followed by lysosomal degradation. Alternatively, PMCA turnover may also occur by shedding of PMCA-enriched membrane vesicles, as appears to be the case at the apical membrane of lactating mammary epithelial cells [40] or in the male and female reproductive tract [72, 73].

6 Regulation by (Reversible) Posttranslational Modification

Besides proteolytic cleavage and generally irreversible modifications such as oxidation and glycation mentioned above, the PMCAs are highly regulated by phosphorylation in an isoform- and splice variant-specific manner. Ser/Thr phosphorylation by prominent signaling kinases including PKA and PKC has been shown to enhance the activity of most isoforms; however, the precise effect (stimulation or decrease of pump activity) is dependent on the isoform and splice variant under study [74–80]. Phosphorylation of a specific tyrosine residue (Tyr-1176) in PMCA4, likely by the focal adhesion kinase FAK, is operative in platelet activation and results in an inhibition of PMCA activity [81–83]. The regulation of different PMCAs by phosphorylation has been extensively covered in many earlier reviews [84–86] and will therefore not be further discussed here. It is worth mentioning, however, that virtually nothing is known about the "off" mechanism of PMCA phosphorylation, i.e., about the specific Ser/Thr- and Tyr-phosphatases that are required for removal of the phosphates to make this type of regulation truly reversible.

7 Regulation by Calmodulin, the Lipid Environment, and Oligomerization

The "mother of all regulation" for the PMCAs is that by CaM, as evidenced by the extensive literature dealing with the affinity, Ca^{2+} dependence, kinetics, mechanism of action, regulation, and functional outcomes of CaM interaction with the PMCAs (see for example Refs. [84, 87–89] for early reviews). All PMCA isoforms and splice variants are sensitive to CaM and in all instances, the binding of Ca^{2+}-CaM activates the pump by releasing auto-inhibitory intramolecular interactions of the C-tail with the two major cytosolic loops in the pump [13, 86]. However, there are large differences in the extent of activation of the basal activity of the various PMCA isoforms by CaM, and perhaps more importantly in the kinetics of CaM regulation. The differences in the rates of activation and termination of CaM regulation profoundly affect how different PMCA isoforms impact the timing and shape of Ca^{2+} signals, and have allowed the distinction of "fast" and "slow" PMCAs with different "memory" for past activation [90–92]. The specific expression pattern of these pumps

reflects the physiological demands and the type of Ca^{2+} signaling in different cells: Fast pumps such as PMCA2x/b are prominent in excitable cells with frequent and rapid Ca^{2+} swings whilst slow pumps (PMCA4x/b) are dominant in non-excitable cells with very different demands on the shape and timing of Ca^{2+} signals.

As integral membrane proteins, the PMCAs are highly sensitive to their lipid environment. Numerous studies have investigated the effect of membrane phospholipids, free fatty acids and cholesterol on the activity and CaM regulation of PMCAs, with most studies focusing on the (erythrocyte) PMCA4x/b [87, 93–96]. Acidic phospholipids, notably the multiply charged phosphatidylinositol bisphosphate (PIP_2), are potent activators of PMCA4b and have been shown to directly bind to two distinct regions in the pump, one within the C-tail overlapping the CaM-binding domain and one in the first intracellular loop close to the third membrane-spanning segment [12]. Although the precise mechanism of direct phospholipid regulation of the PMCA is not fully understood, it likely involves lipid binding to membrane-proximal regions of the C-tail and intracellular loop to "loosen" autoinhibitory interactions, thereby facilitating access of substrates or conformational changes during the reaction cycle [97–99]. The type and shape of lipids surrounding the PMCAs in the lipid bilayer obviously affect pump function; on a longer time-scale PMCAs may thus also be regulated by changes in the lipid composition of the membrane. The fatty acid chain length, degree of unsaturation, type of head groups, as well as the cholesterol content impact the thickness and fluidity of the bilayer, which will impose conformational constraints on the membrane domain of the PMCAs and modulate their activity [100–102]. The membrane lipid composition plays an essential role in the partitioning of different PMCAs into membrane micro- or nano-domains (lipid rafts). Several studies have investigated the relative distribution and activity of different PMCA isoforms in sphingolipid- and cholesterol-rich lipid rafts in various cell types [103, 104]. PMCA4b is specifically concentrated in caveolae, which are specific membrane compartments found in many cell types including cardiomyocytes and endothelial cells [105–108]. The local enrichment of the PMCA in specific lipid microdomains may also facilitate the dimerization/oligomerization of pump molecules, which has been shown to happen via their regulatory C-tails and is thought to result in CaM-independent activation of pump function [109–112]. This could serve to maintain a high constitutive Ca^{2+} efflux activity in these specific membrane domains, allowing the cell to create and maintain local areas of low [Ca^{2+}] without compromising its bulk cytosolic Ca^{2+} level.

8 Integrated Regulation of PMCA Function in Cellular Calcium Signaling

Many of the studies on the regulation and functional properties of individual PMCA isoforms have been carried out on purified or highly enriched preparations of the pump in vitro. While these studies were and still are necessary to gain a detailed understanding of the structural and functional characteristics of each isoform or splice variant, they fail to address the integrated role played by the PMCAs in their

physiological context. This gap is now rapidly being filled, in part due to improved technology to analyze calcium signaling with high spatial and temporal resolution in living cells, but also because of the increased use of cell, organ and animal models amenable to genetic and environmental manipulation. The emerging concept shows that a crucial function of the PMCAs is their tightly integrated participation in all aspects of cellular calcium signaling [102, 113, 114]. In fact, it may be argued that the original role ascribed to the PMCA, i.e., that of maintaining the basal resting level of intracellular [Ca^{2+}], is secondary to their other roles in cellular Ca^{2+} handling. In some physiological contexts such as during lactation, a specific PMCA isoform (PMCA2w/b) has as its main function the massive export of Ca^{2+} into the milk from the apical (luminal) side of breast epithelial cells. Similarly, in enterocytes of the small intestine, PMCA1x/b is responsible for the bulk transport of Ca^{2+} into the blood at the basolateral side to maintain dietary calcium absorption. The expression, splicing, targeting, local regulation, and eventual removal of the PMCA2w/b and PMCA1x/b in these tissues are under tight control by external factors including sex steroids and 1,25-$(OH)_2$ D3, respectively. In other cell types, the same or a different PMCA isoform/splice variant may have an entirely different function, e.g., to control the spiking frequency and signal shape of local Ca^{2+} signals in presynaptic nerve terminals or postsynaptic spines. In these latter cases, the PMCAs have little, if any, effect on bulk cytosolic Ca^{2+}; other PMCA(s) or different calcium extrusion systems such as the Na^+/Ca^{2+} exchangers (NCX) may instead perform this function in the cell.

It is now amply clear that the PMCAs are not working in isolation but are constantly "sensing" the physiological state of the cell by dynamically interacting with other proteins and lipids. Besides CaM, a large and growing number of proteins have been shown to interact with the PMCAs [113–115]. Some of these proteins bind specifically only to a certain isoform or type of splice variant, whereas others interact promiscuously with most isoforms and splice variants. The C-terminus of all b(c/d) splice variants contains a consensus sequence for interaction with PDZ domain proteins, and many different PDZ proteins are now known to bind to the PMCA b splice variants [20, 115]. These PDZ proteins have different functional modalities including scaffolding, membrane trafficking/recycling, and signaling. Other proteins involved in signaling cross talk or direct activation or inhibition regulate several PMCA isoforms by interacting with the N-terminal tail or intracellular loops of the molecule [116]. These include inhibitory interactions of 14-3-3e and Homer-2 with sequences in the N-tail of multiple PMCAs [117–119]. The interaction of a PPXXF motif in the N-tail of PMCA4 with Homer-2 at the apical pole of parotid gland acinar cells illustrates the tight cross talk between a specific PMCA isoform and its signaling partner: Knockdown of Homer-2 results in a parallel increase in PMCA4 expression and Ca^{2+} extrusion activity in acinar cells, whereas increased expression of Homer-2 downregulates PMCA4 expression and activity [119].

Numerous examples of the integrated regulation of PMCA function by differential and dynamic protein–protein interactions have been reported in the recent literature. In rat coagulating (prostate) gland epithelial cells, PMCA1b, but not 4b, was found to be localized in the apical membrane and released by apocrine secretion in a process controlled by androgens: Upon androgen deprivation, the PMCA1b was

no longer released in aposomes and instead accumulated in a cytoplasmic compartment [120]. Rapid agonist-induced recruitment of PMCA1b to the plasma membrane has also been demonstrated in HT29 human colorectal carcinoma cells. Muscarinic G-protein coupled receptor activation by acetylcholine resulted in a significant increase in PMCA1b in the plasma membrane, and this effect was dependent on Ca^{2+} and the PDZ protein NHERF2 [121]. Here, G-protein coupled receptor activation leads to phospholipase C activation, IP3 release, and Ca^{2+} influx from the ER, promoting the targeting of NHERF2 to recruit and retain the PMCA1b in the plasma membrane. The role of NHERF2 as a "recruiter" of specific PMCA isoforms to a particular membrane domain has also been demonstrated for PMCA2w/b: Co-expression of NHERF2 increased the amount of PMCA2w/b in the apical membrane of polarized kidney epithelial cells and reduced its internalization likely via anchoring the pump to the underlying membrane cytoskeleton [122, 123]. Anchoring to the membrane cytoskeleton appears to be important for sustained PMCA function, as actin polymerization increased and disruption of polymerization decreased PMCA-mediated Ca^{2+} efflux during T-cell stimulation [124]. The polymerization state of actin may itself regulate PMCA activity [125], but the major role of anchoring of the PMCA is likely the maintenance of sufficient efflux capacity within a particular membrane domain. During immunological synapse formation preceding T-cell stimulation, the PMCA (4b) is retargeted to a different membrane microdomain by stimulus-induced interaction with other molecules involved in cellular Ca^{2+} signaling, i.e., STIM1 [126, 127], providing an example for Ca^{2+} dependent feedback regulation of PMCA localization and activity.

Integration of specific PMCAs in multi-protein signaling complexes to provide local Ca^{2+} control has also been demonstrated in rod photoreceptor synaptic terminals, where the proper localization and function of PMCA1b was shown to depend on the two PDZ domain containing proteins MPP4 and PSD95 [128, 129]. Recent examples of the importance of the integration of PMCAs in multiprotein complexes for local signaling include the finding of a tight functional coupling of PMCA isoforms 2 and 3 and the Na^+/Ca^{2+} exchanger NCX1 with the presynaptic glycine transporter GlyT2 in lipid raft subdomains in rat brainstem and spinal cord neurons [130]. In the most recent example, PMCA4b was found to cross talk with the G-protein coupled estrogen receptor GPER1/GPR30 in endothelial cells: Receptor stimulation resulted in PMCA4b inhibition by tyrosine phosphorylation and independently by physical interaction mediated by the PDZ protein PSD95. Conversely, the interaction stimulated receptor signaling, demonstrating a tightly connected interplay between Ca^{2+} signaling and GPER-mediated downstream phosphorylation of ERK1/2 via the formation of a heteromeric complex [131].

9 Conclusions

It is ironic that we may have been slow in recognizing the most important functions of the PMCAs because the initial identification and all successful biochemical characterizations were made on the pump from red blood cells, yet in these cells much

of the signaling complexity found elsewhere is absent. It is now abundantly clear that most PMCAs are not acting as "isolated" pumps dedicated solely to maintaining low bulk cytosolic Ca^{2+}; rather they are tightly integrated with scaffolding and other signaling proteins in specific membrane domains to provide "holistic" calcium control in the context of changing cellular demands, which are under external regulation by hormones, neurotransmitters and other factors impacting the cell. The regulation of PMCAs includes dynamic changes in their abundance by (1) changing transcription, splicing, and translation, (2) controlling the forward trafficking, lipid partitioning, anchoring and retention in membrane domains, and (3) recycling, shedding to the extracellular milieu, or removal followed by degradation. In addition, the activity of the PMCAs is regulated by posttranslational modification including phosphorylation, oxidation, and partial proteolysis, by direct interaction with stimulatory or inhibitory proteins and lipids, and by redistribution and association with different protein complexes. Different PMCA isoforms and splice variants are differently impacted by these regulatory mechanisms and show inherent differences in their functional properties including in their basal rates and stimulation kinetics. An important emerging concept is that many PMCAs work as integrated members of teams where they both regulate and are regulated by other members of the signaling/scaffolding protein complex. Thus, replacement of one isoform by another in a specific cell type will generally not correct the pathology caused by the absence or mutation of the former. Systems-level approaches will be needed to fully understand the unique role played by each PMCA isoform in cell physiology and pathophysiology, and may contribute to the development of specific modifiers of the pumps to address the many diseases involving these important calcium transporters.Acknowledgements I am grateful to M.-A. Strehler-Page for help with the preparation of Fig. 5.1. This work was supported in part by the Mayo Foundation for Medical Research.

References

1. Berridge MJ, Lipp P, Bootman MD (2000) The versatility and universality of calcium signalling. Nat Rev Mol Cell Biol 1:11–21
2. Brini M, Carafoli E (2000) Calcium signalling: a historical account, recent developments and future perspectives. Cell Mol Life Sci 57:354–370
3. Pedersen PL, Carafoli E (1987) Ion motive ATPases. I. Ubiquity, properties, and significance to cell function. Trends Biochem Sci 12:146–150
4. Palmgren MG, Nissen P (2011) P-type ATPases. Annu Rev Biophys 40:243–266
5. Thever MD, Saier MH (2009) Bioinformatic characterization of P-type ATPases encoded within the fully sequenced genomes of 26 eukaryotes. J Membr Biol 229:115–130
6. Strehler EE, Treiman M (2004) Calcium pumps of plasma membrane and cell interior. Curr Mol Med 4:323–335
7. Silverstein RS, Tempel BL (2006) Atp2b2, encoding plasma membrane Ca^{2+}-ATPase type 2, (PMCA2) exhibits tissue-specific first exon usage in hair cells, neurons, and mammary glands of mice. Neuroscience 141:245–257
8. Carafoli E (1992) The Ca^{2+} pump of the plasma membrane. J Biol Chem 267:2115–2118

9. Strehler EE, Zacharias DA (2001) Role of alternative splicing in generating isoform diversity among plasma membrane calcium pumps. Physiol Rev 81:21–50
10. Dumont RA, Lins U, Filoteo AG et al (2001) Plasma membrane Ca^{2+} ATPase isoform 2a is the PMCA of hair bundles. J Neurosci 21:5066–5078
11. Bublitz M, Poulsen H, Morth JP, Nissen P (2010) In and out of the cation pumps: P-type ATPase structure revisited. Curr Opin Struct Biol 20:431–439
12. Brodin P, Falchetto R, Vorherr T, Carafoli E (1992) Identification of two domains which mediate the binding of activating phospholipids to the plasma-membrane Ca^{2+} pump. Eur J Biochem 204:939–946
13. Carafoli E (1994) Biogenesis: plasma membrane calcium ATPase: 15 years of work on the purified enzyme. FASEB J 8:993–1002
14. Hilfiker H, Guerini D, Carafoli E (1994) Cloning and expression of isoform 2 of the human membrane Ca^{2+} ATPase. J Biol Chem 269:26178–26183
15. Brini M, Di Leva F, Ortega CK et al (2010) Deletions and mutations in the acidic lipid-binding region of the plasma membrane Ca^{2+} pump. J Biol Chem 285:30779–30791
16. Chicka MC, Strehler EE (2003) Alternative splicing of the first intracellular loop of plasma membrane Ca^{2+}-ATPase isoform 2 alters its membrane targeting. J Biol Chem 278: 18464–18470
17. Penniston JT, Padányi R, Pászty K et al (2014) Apart from its known function, the plasma membrane Ca^{2+} ATPase can regulate Ca^{2+} signaling by controlling phosphatidylinositol 4,5-bisphosphate levels. J Cell Sci 127:72–84
18. Krebs J (2015) The plethora of PMCA isoforms: alternative splicing and differential expression. Biochim Biophys Acta 1853:2018-2024
19. Brini M, Carafoli E (2009) Calcium pumps in health and disease. Physiol Rev 89: 1341–1378
20. Strehler EE, Filoteo AG, Penniston JT, Caride AJ (2007) Plasma-membrane Ca^{2+}-pumps: structural diversity as the basis for functional versatility. Biochem Soc Trans 35:919–922
21. Strehler EE (2013) Plasma membrane calcium ATPases as novel candidates for therapeutic agent development. J Pharm Pharm Sci 16:190–206
22. Giacomello M, De Mario A, Scarlatti C et al (2013) Plasma membrane calcium ATPases and related disorders. Int J Biochem Cell Biol 45:753–762
23. Ritchie MF, Zhou Y, Soboloff J (2011) Transcriptional mechanisms regulating Ca^{2+} homeostasis. Cell Calcium 49:314–321
24. Naranjo JR, Mellstrom B (2012) Ca^{2+}-dependent transcriptional control of Ca^{2+} homeostasis. J Biol Chem 287:31674–31680
25. Yanagida E, Shoji S, Hirayama Y et al (2004) Functional expression of Ca^{2+} signaling pathways in mouse embryonic stem cells. Cell Calcium 36:135–146
26. Zacharias DA, Kappen C (1999) Developmental expression of the four plasma membrane calcium ATPase (Pmca) genes in the mouse. Biochim Biophys Acta 1428:397–405
27. Okunade GW, Miller ML, Pyne GJ et al (2004) Targeted ablation of plasma membrane Ca^{2+}-ATPase (PMCA) 1 and 4 indicates a major housekeeping function for PMCA1 and a critical role in hyperactivated sperm motility and male fertility for PMCA4. J Biol Chem 279:33742–33750
28. Afroze T, Husain M (2000) c-myb-Binding sites mediate G_1/S-associated repression of the plasma membrane Ca^{2+}-ATPase-1 promoter. J Biol Chem 275:9062–9069
29. Habib T, Park H, Tsang M et al (2007) Myc stimulates B lymphocyte differentiation and amplifies calcium signaling. J Cell Biol 179:717–731
30. Du Y, Carlock L, Kuo TH (1995) The mouse plasma membrane Ca^{2+} pump isoform 1 promoter: cloning and characterization. Arch Biochem Biophys 316:302–310
31. Kuo TH, Liu B-F, Diglio C, Tsang W (1993) Regulation of the plasma membrane calcium pump gene expression by two signal transduction pathways. Arch Biochem Biophys 305:428–433
32. Zelinski JM, Sykes DE, Weiser MW (1991) The effect of Vitamin D on rat intestinal plasma membrane Ca-pump mRNA. Biochem Biophys Res Commun 179:749–755

33. Cai Q, Chandler JS, Wasserman RH et al (1993) Vitamin D and adaptation to dietary calcium and phosphate deficiencies increase intestinal plasma membrane calcium pump expression. Proc Natl Acad Sci U S A 90:1345–1349
34. Pannabecker TL, Chandler JS, Wasserman RH (1995) Vitamin-D-dependent transcriptional regulation of the intestinal plasma membrane calcium pump. Biochem Biophys Res Commun 213:499–505
35. Glendenning P, Ratajczak T, Dick IM, Prince RL (2000) Calcitriol upregulates expression and activity of the 1b isoform of the plasma membrane calcium pump in immortalized distal kidney tubular cells. Arch Biochem Biophys 380:126–132
36. Glendenning P, Ratajczak T, Dick IM, Prince RL (2001) Regulation of the 1b isoform of the plasma membrane calcium pump by 1,25-dihydroxyvitamin D3 in rat osteoblast-like cells. J Bone Miner Res 16:525–534
37. Guerini D, Wang X, Li L, Genazzani A, Carafoli E (2000) Calcineurin controls the expression of isoform 4CII of the plasma membrane Ca^{2+} pump in neurons. J Biol Chem 275:3706–3712
38. Du X, Wang J, Zhu H et al (1999) Second cistron in *CACNA1A* gene encodes a transcription factor mediating cerebellar development and SCA6. Cell 154:118–133
39. Reinhardt TA, Horst RL (1999) Ca^{2+}-ATPases and their expression in the mammary gland of pregnant and lactating rats. Am J Physiol 276:C796–C802
40. Reinhardt TA, Filoteo AG, Penniston JT, Horst RL (2000) Ca^{2+}-ATPase protein expression in mammary tissue. Am J Physiol Cell Physiol 279:C1595–C1602
41. Ayoubi TA, Van de Ven WJM (1995) Regulation of gene expression by alternative promoters. FASEB J 10:453–460
42. Hill JK, Williams DE, LeMasurier DE et al (2006) Splice-site A choice targets plasma-membrane Ca^{2+}-ATPase isoform 2 to hair bundles. J Neurosci 26:6172–6180
43. Kip SN, Gray NW, Burette A et al (2006) Changes in the expression of plasma membrane calcium extrusion systems during the maturation of hippocampal neurons. Hippocampus 16:20–34
44. Afroze T, Ge Y, Khoshbin A et al (2014) Calcium efflux activity of plasma membrane Ca^{2+} ATPase-4 (PMCA4) mediates cell cycle progression in vascular smooth muscle cells. J Biol Chem 289:7221–7231
45. Zacharias DA, Strehler EE (1996) Change in plasma membrane Ca^{2+}-ATPase splice-variant expression in response to a rise in intracellular Ca^{2+}. Curr Biol 6:1642–1652
46. Grabowski PJ, Black DL (2001) Alternative RNA splicing in the nervous system. Prog Neurobiol 65:289–308
47. Li Q, Lee J-A, Black DL (2007) Neuronal regulation of alternative pre-mRNA splicing. Nat Rev Neurosci 8:819–831
48. Xie J, Black DL (2001) A CaMK IV-responsive RNA element mediates depolarization-induced alternative splicing of potassium channels. Nature 410:936–939
49. Liu G, Razanau A, Hai Y et al (2012) A conserved serine of heterogeneous nuclear ribonucleoprotein L (hnRNPL) mediates depolarization-regulated alternative splicing of potassium channels. J Biol Chem 287:22709–22716
50. Kosiorek M, Podszywalow-Bartnicka P, Zylinska L, Pikula S (2014) NFAT1 and NFAT3 cooperate with HDAC4 during regulation of alternative splicing of PMCA isoforms in PC12 cells. PLoS One 9:e99116
51. Greeb J, Shull GE (1989) Molecular cloning of a third isoform of the calmodulin-sensitive plasma membrane Ca^{2+}-transporting ATPase that is expressed predominantly in brain and skeletal muscle. J Biol Chem 264:18569–18576
52. De Jaegere S, Wuytack F, Eggermont JA et al (1990) Molecular cloning and sequencing of the plasma-membrane Ca^{2+} pump of pig smooth muscle. Biochem J 271:655–660
53. Kuo TH, Wang KKW, Carlock L et al (1991) Phorbol ester induces both gene expression and phosphorylation of the plasma membrane Ca^{2+} pump. J Biol Chem 266:2520–2525
54. Husain M, Jiang L, See V et al (1997) Regulation of vascular smooth muscle cell proliferation by plasma membrane Ca^{2+}-ATPase. Am J Physiol 272:C1947–C1959

55. Sasamura S, Furukawa K-I, Shiratori M et al (2002) Antisense-inhibition of plasma membrane Ca^{2+} pump induces apoptosis in vascular smooth muscle cells. Jpn J Pharmacol 90:164–172
56. Szemraj J, Kawecka I, Bartkowiak J, Zylinska L (2004) The effect of antisense oligonucleotide treatment of plasma membrane Ca^{2+}-ATPase in PC12 cells. Cell Mol Biol Lett 9:451–464
57. Kurnellas MP, Li H, Jain MR et al (2010) Reduced expression of plasma membrane calcium ATPase 2 and collapsin response mediator protein 1 promotes death of spinal cord neurons. Cell Death Differ 17:1501–1510
58. Curry MC, Luk NA, Kenny PA et al (2012) Distinct regulation of cytoplasmic calcium signals and cell death pathways by different plasma membrane calcium ATPase isoforms in MDA-MB-231 breast cancer cells. J Biol Chem 287:28598–28608
59. Jensen TP, Filoteo AG, Knöpfel T, Empson RM (2007) Presynaptic plasma membrane Ca^{2+} ATPase isoform 2a regulates excitatory synaptic transmission in rat hippocampal CA3. J Physiol 579(1):85–99
60. Burette AC, Strehler EE, Weinberg RJ (2009) "Fast" plasma membrane calcium pump PMCA2a concentrates in GABAergic terminals in the adult rat brain. J Comp Neurol 512:500–513
61. Burette AC, Strehler EE, Weinberg RJ (2010) A plasma membrane Ca^{2+} ATPase isoform at the postsynaptic density. Neuroscience 169:987–993
62. Guerini D, Pan B, Carafoli E (2003) Expression, purification, and characterization of isoform 1 of the plasma membrane Ca^{2+} pump. J Biol Chem 278:38141–38148
63. Brown CS, Dean W (2007) Regulation of plasma membrane Ca^{2+}-ATPase in human platelets by calpain. Platelets 18:207–211
64. Lehotsky J, Kaplan P, Murin R, Raeymaekers L (2002) The role of plasma membrane Ca^{2+} pump (PMCA) in pathologies of mammalian cells. Front Biosci 7:d53–d84
65. Pottorf WJ II, Johanns TM, Derrington SM et al (2006) Glutamate-induced protease-mediated loss of plasma membrane Ca^{2+} pump activity in rat hippocampal neurons. J Neurochem 98:1646–1656
66. Ferragamo MJ, Reinardy JL, Thayer SA (2009) Ca^{2+}-dependent, stimulus-specific modulation of the plasma membrane Ca^{2+} pump in hippocampal neurons. J Neurophysiol 101:2563–2571
67. Zaidi A, Michaelis ML (1999) Effects of reactive oxygen species on brain synaptic plasma membrane Ca^{2+}-ATPase. Free Radic Biol Med 27:810–821
68. Jiang L, Bechtel MD, Galeva NA et al (2012) Decreases in plasma membrane Ca^{2+}-ATPase in brain synaptic membrane rafts from aged rats. J Neurochem 123:689–699
69. Zaidi A (2010) Plasma membrane Ca^{2+}-ATPases: targets of oxidative stress in brain aging and neurodegeneration. World J Biol Chem 1:271–280
70. González Flecha FL, Castello PR, Gagliardino JJ, Rossi JP (1999) Molecular characterization of the glycated plasma membrane calcium pump. J Membr Biol 171:25–34
71. Horakova L, Strosova MK, Spickett CM, Blaskovic D (2013) Impairment of calcium ATPases by high glucose and potential pharmacological protection. Free Radic Res 47:81–92
72. Patel R, Al-Dossary AA, Stabley DL et al (2013) Plasma membrane Ca^{2+}-ATPase 4 in murine epididymis: secretion of splice variants in the luminal fluid and a role in sperm maturation. Biol Reprod 89:1–11
73. Al-Dossary AA, Strehler EE, Martin-DeLeon PA (2013) Expression and secretion of plasma membrane Ca^{2+}-ATPase 4a (PMCA4a) during murine estrus: association with oviductal exosomes and uptake in sperm. PLoS One 8:e80181
74. James PH, Pruschy M, Vorherr T et al (1989) Primary structure of the cAMP-dependent phosphorylation site of the plasma membrane calcium pump. Biochemistry 28:4253–4258
75. Wang KKW, Wright LC, Machan C et al (1991) Protein kinase C phosphorylates the carboxyl terminus of the plasma membrane Ca^{2+}-ATPase from human erythrocytes. J Biol Chem 266:9078–9085

76. Hofmann F, Anagli J, Carafoli E, Vorherr T (1994) Phosphorylation of the calmodulin binding domain of the plasma membrane Ca^{2+} pump by protein kinase C reduces interaction with calmodulin and with its pump receptor site. J Biol Chem 269:24298–24303
77. Enyedi A, Elwess NL, Filoteo AG et al (1997) Protein kinase C phosphorylates the "a" forms of plasma membrane Ca^{2+} pump isoforms 2 and 3 and prevents binding of calmodulin. J Biol Chem 272:27525–27528
78. Enyedi A, Verma AK, Filoteo AG, Penniston JT (1996) Protein kinase C activates the plasma membrane Ca^{2+} pump isoform 4b by phosphorylation of an inhibitory region downstream of the calmodulin-binding domain. J Biol Chem 271:32461–32467
79. Verma AK, Paszty K, Filoteo AG et al (1999) Protein kinase C phosphorylates plasma membrane Ca^{2+} pump isoform 4a at its calmodulin binding domain. J Biol Chem 274:527–531
80. Zylinska L, Guerini D, Gromadzinska E, Lachowicz L (1998) Protein kinases A and C phosphorylate purified Ca^{2+}-ATPase from rat cortex, cerebellum and hippocampus. Biochim Biophys Acta 1448:99–108
81. Dean WL, Chen D, Brandt PC, Vanaman TC (1997) Regulation of platelet plasma membrane Ca^{2+}-ATPase by cAMP-dependent and tyrosine phosphorylation. J Biol Chem 272:15113–15119
82. Wan TC, Zabe M, Dean WL (2003) Plasma membrane Ca^{2+}-ATPase isoform 4b is phosphorylated on tyrosine 1176 in activated human platelets. Thromb Haemost 89:122–131
83. Dean WL (2010) Role of platelet plasma membrane Ca^{2+}-ATPase in health and disease. World J Biol Chem 1:265–270
84. Wang KKW, Villalobo A, Roufogalis BD (1992) The plasma membrane calcium pump: a multiregulated transporter. Trends Cell Biol 2:46–52
85. Monteith GR, Roufogalis BD (1995) The plasma membrane calcium pump—a physiological perspective on its regulation. Cell Calcium 18:459–470
86. Penniston JT, Enyedi A (1998) Modulation of the plasma membrane Ca^{2+} pump. J Membr Biol 165:101–109
87. Schatzmann HJ (1982) The plasma membrane calcium pump of erythrocytes and other animal cells. In: Carafoli E (ed) Membrane transport of calcium. Academic, London, pp 41–108
88. Penniston JT (1983) Plasma membrane Ca^{2+}-ATPases as active Ca^{2+} pumps. In: Cheung WY (ed) Calcium and cell function. Academic, New York, pp 99–147
89. Carafoli E (1991) Calcium pump of the plasma membrane. Physiol Rev 71:129–153
90. Caride AJ, Filoteo AG, Penheiter AR et al (2001) Delayed activation of the plasma membrane calcium pump by a sudden increase in Ca^{2+}: fast pumps reside in fast cells. Cell Calcium 30:49–57
91. Caride AJ, Penheiter AR, Filoteo AG et al (2001) The plasma membrane calcium pump displays memory of past calcium spikes. Differences between isoforms 2b and 4b. J Biol Chem 276:39797–39804
92. Caride AJ, Filoteo AG, Penniston JT, Strehler EE (2007) The plasma membrane Ca^{2+} pump isoform 4a differs from isoform 4b in the mechanism of calmodulin binding and activation kinetics. J Biol Chem 282:25640–25648
93. Niggli V, Adunyah ES, Carafoli E (1981) Acidic phospholipids, unsaturated fatty acids and proteolysis mimic the effect of calmodulin on the purified erythrocyte Ca^{2+}-ATPase. J Biol Chem 256:8588–8592
94. Missiaen L, Raeymaekers L, Wuytack F et al (1989) Phospholipid-protein interactions of the plasma-membrane Ca^{2+}-transporting ATPase. Biochem J 263:287–294
95. Rossi JP, Delfino JM, Caride AJ, Fernándes HN (1995) Interaction of unsaturated fatty acids with the red blood cell Ca^{2+}-ATPase. Studies with a novel photoactivatable probe. Biochemistry 34:3802–3812
96. Tang D, Dean WL, Borchman D, Paterson CA (2006) The influence of membrane lipid structure on plasma membrane Ca^{2+}-ATPase activity. Cell Calcium 39:209–216
97. Lehotsky J (1995) Plasma membrane Ca^{2+}-pump functional specialization in the brain. Complex of isoform expression and regulation by effectors. Mol Chem Neuropathol 25:175–187

98. Duan J, Zhang J, Zhao Y et al (2006) Ganglioside GM2 modulates the erythrocyte Ca^{2+}-ATPase through its binding to the calmodulin-binding domain and its "receptor". Arch Biochem Biophys 434:155–159
99. Perez-Gordones MC, Lugo MR, Winkler M et al (2009) Diacylglycerol regulates the plasma membrane calcium pump function from human erythrocytes by direct interaction. Arch Biochem Biophys 489:55–61
100. Mangialavori IC, Caride AJ, Rossi RC et al (2011) Diving into the lipid bilayer to investigate the transmembrane organization and conformational state transitions of P-type ion ATPases. Curr Chem Biol 5:118–129
101. Mangialavori I, Villamil Giraldo AM, Pignataro MF et al (2011) Plasma membrane calcium pump (PMCA) differential exposure of hydrophobic domains after calmodulin and phosphatidic acid activation. J Biol Chem 286:18397–18404
102. Lopreiato R, Giacomello M, Carafoli E (2014) The plasma membrane calcium pump: new ways to look at an old enzyme. J Biol Chem 289:10261–10268
103. Sepúlveda MR, Berrocal-Carrillo M, Gasset M, Mata AM (2006) The plasma membrane Ca^{2+}-ATPase isoform 4 is localized in lipid rafts of cerebellum synaptic plasma membranes. J Biol Chem 281:447–453
104. Jiang L, Fernandes D, Mehta N et al (2007) Partitioning of the plasma membrane Ca^{2+}-ATPase into lipid rafts in primary neurons: effects of cholesterol depletion. J Neurochem 102:378–388
105. Fujimoto T (1993) Calcium pump of the plasma membrane is localized in caveolae. J Cell Biol 120:1147–1157
106. Schnitzer JE, Oh P, Jacobson BS, Dvorak AM (1995) Caveolae from luminal plasmalemma of rat lung endothelium: microdomains enriched in caveolin, Ca^{2+}-ATPase, and inositol triphosphate receptor. Proc Natl Acad Sci U S A 92:1759–1763
107. Tortelote GG, Valverde RHF, Lemos T et al (2004) The plasma membrane Ca^{2+} pump from proximal kidney tubules is exclusively localized and active in caveolae. FEBS Lett 576:31–35
108. Zhang J, Xiao P, Zhang X (2009) Phosphatidylserine externalization in caveolae inhibits Ca^{2+} efflux through plasma membrane Ca^{2+}-ATPase in ECV304. Cell Calcium 45:177–184
109. Kosk-Kosicka D, Bzdega T (1998) Activation of the erythrocyte Ca^{2+}-ATPase by either self-association or interaction with calmodulin. J Biol Chem 263:18184–18189
110. Kosk-Kosicka D, Bzdega T, Wawrzynow A (1989) Fluorescence energy transfer studies of purified erythrocyte Ca^{2+}-ATPase. Ca^{2+}-regulated activation by oligomerization. J Biol Chem 264:19495–19499
111. Vorherr T, Kessler T, Hofmann F, Carafoli E (1991) The calmodulin-binding domain mediates the self-association of the plasma membrane Ca^{2+} pump. J Biol Chem 266:22–27
112. Levi V, Rossi JPFC, Castello PR et al (2002) Structural significance of the plasma membrane calcium pump oligomerization. Biophys J 82:437–446
113. Strehler EE, Caride AJ, Filoteo AG et al (2007) Plasma membrane Ca^{2+} ATPases as dynamic regulators of cellular calcium handling. Ann N Y Acad Sci 1099:226–236
114. Holton ML, Wang W, Emerson M et al (2010) Plasma membrane calcium ATPases as novel regulators of signal transduction pathways. World J Biol Chem 1:201–208
115. Di Leva F, Domi T, Fedrizzi L et al (2008) The plasma membrane Ca^{2+} ATPase of animal cells: structure, function and regulation. Arch Biochem Biophys 476:65–74
116. Oceandy D, Mohamed TM, Cartwright EJ, Neyses L (2011) Local signals with global impacts and clinical implications: lessons from the plasma membrane calcium pump (PMCA4). Biochim Biophys Acta 1813:974–978
117. Rimessi A, Coletto L, Pinton P et al (2005) Inhibitory interaction of the 14-3-3e protein with isoform 4 of the plasma membrane Ca^{2+}-ATPase pump. J Biol Chem 280:37195–37203
118. Linde CI, Di Leva F, Domi T et al (2008) Inhibitory interaction of the 14-3-3 proteins with ubiquitous (PMCA1) and tissue-specific (PMCA3) isoforms of the plasma membrane Ca^{2+} pump. Cell Calcium 43:550–561

119. Yang Y-M, Lee J, Jo H et al (2014) Homer2 protein regulates plasma membrane Ca^{2+}-ATPase-mediated Ca^{2+} signaling in mouse parotid gland acinar cells. J Biol Chem 289:24971–24979
120. Post H, Gutberlet J, Wiche R et al (2008) The localization of PMCA1b in epithelial cells and aposomes of the rat coagulating gland is influenced by androgens. Prostate 68:1076–1085
121. Kruger WA, Yun CC, Monteith GR, Poronnik P (2009) Muscarinic-induced recruitment of plasma membrane Ca^{2+}-ATPase involves PSD-95/Dlg/Zo-1-mediated interactions. J Biol Chem 284:1820–1830
122. Padányi R, Xiong Y, Antalffy G et al (2011) Apical scaffolding protein NHERF2 modulates the localization of alternatively spliced plasma membrane Ca^{2+} pump 2b variants in polarized epithelial cells. J Biol Chem 285:31704–31712
123. Enyedi A, Strehler EE (2011) Regulation of apical membrane enrichment and retention of plasma membrane Ca^{2+} ATPase splice variants by the PDZ-domain protein NHERF2. Commun Integr Biol 4:340–343
124. Rivas FV, O'Keefe JP, Alegre M-L, Gajewski TF (2004) Actin cytoskeleton regulates calcium dynamics and NFAT nuclear duration. Mol Cell Biol 24:1628–1639
125. Dalghi MG, Fernandez MM, Ferreira Gomes M et al (2013) Plasma membrane calcium ATPase activity is regulated by actin oligomers through direct interaction. J Biol Chem 288:23380–23393
126. Quintana A, Pasche M, Junker C et al (2011) Calcium microdomains at the immunological synapse: how ORAI channels, mitochondria and calcium pumps generate local calcium signals for efficient T-cell activation. EMBO J 30:3895–3912
127. Ritchie MF, Samakai E, Soboloff J (2012) STIM1 is required for attenuation of PMCA-mediated Ca^{2+} clearance during T-cell activation. EMBO J 31:1123–1133
128. Yang J, Pawlyk B, Wen X-H et al (2007) Mpp4 is required for proper localization of plasma membrane calcium ATPases and maintenance of calcium homeostasis at the rod photoreceptor synaptic terminals. Hum Mol Genet 16:1017–1029
129. Aartsen WM, Arsanto J-P, Chauvin J-P et al (2009) PSD95b regulates plasma membrane Ca(2+) pump localization at the photoreceptor synapse. Mol Cell Neurosci 41:156–165
130. deJuan-Sanz J, Nunez E, Zafra F et al (2014) Presynaptic control of glycine transporter 2 (GlyT2) by physical and functional association with plasma membrane Ca^{2+}-ATPase (PMCA) and Na^{+}-Ca^{2+} exchanger (NCX). J Biol Chem 289:34308–34324
131. Tran Q-K, Ver Meer M, Burghard MA et al (2015) Hetero-oligomeric complex between the G protein-coupled estrogen receptor 1 and the plasma membrane Ca^{2+} ATPase 4b. J Biol Chem 290:13293–13307

Chapter 6
The Plasma Membrane Ca^{2+} ATPase and the Na/Ca Exchanger in β-cell Function and Diabetes

André Herchuelz and Nathalie Pachera

Abstract The rat pancreatic β cell expresses six splice variants of the plasma membrane Ca^{2+} ATPase (PMCA) and two splice variants of the Na/Ca exchanger 1 (NCX1). In the β cell, Na/Ca exchange displays a high capacity, contributes to both Ca^{2+} outflow and inflow, and participates to the control of insulin release. Gain-of-function studies show that overexpression of PMCA2 or NCX1 leads to endoplasmic reticulum (ER) Ca^{2+} depletion with subsequent ER stress, decrease in β-cell proliferation, and β-cell death by apoptosis. Loss-of-function studies show, on the contrary, that heterozygous inactivation of NCX1 ($Ncx1^{+/-}$) leads to an increase in β-cell function and a fivefold increase in both β-cell mass and proliferation. The mutation also increases β-cell resistance to hypoxia, and *Ncx1*$^{+/-}$ islets show a 2–4 times higher rate of diabetes cure than $Ncx1^{+/+}$ islets when transplanted in diabetic animals. Thus, downregulation of the Na/Ca exchanger leads to various changes in β-cell function that are opposite to the major abnormalities seen in diabetes. Preliminary data indicate that heterozygous inactivation of PMCA2 leads to related though not completely similar results. These provide two unique models for the prevention and treatment of β-cell dysfunction in diabetes and following islet transplantation. In addition, the β-cell includes the mutually exclusive exon B in the alternative splicing region of NCX1, which confers a high sensitivity of its NCX splice variants (NCX1.3 and 1.7) to the inhibitory action of compounds like KBR-7943. Hence, it is possible to develop NCX1 inhibitors acting preferentially on the β-cell to stimulate its proliferation in diabetes.

Keywords Plasma membrane Ca^{2+}-ATPase • PMCA • Sodium–calcium exchange • Na/Ca exchange • Calcium • Ca^{2+} • B cell • Diabetes

A. Herchuelz (✉) • N. Pachera
Laboratoire de Pharmacodynamie et de Thérapeutique, Faculté de Médicine, Université Libre de Bruxelles (ULB), Route de Lennik, 808-Bâtiment GE B-1070, Bruxelles, Belgium
e-mail: herchu@ulb.ac.be

S. Chakraborti, N.S. Dhalla (eds.), *Regulation of Ca^{2+}-ATPases,V-ATPases and F-ATPases*, Advances in Biochemistry in Health and Disease 14,
DOI 10.1007/978-3-319-24780-9_6

1 Introduction

Calcium (Ca^{2+}) plays an important role in the process of glucose-induced insulin release from the pancreatic β-cell. When stimulated by glucose, the β-cell displays a complex series of events that leads to a rise in cytosolic free Ca^{2+} concentration ($[Ca^{2+}]_i$) that triggers insulin release.

The β-cell is equipped with a double system responsible for Ca^{2+} extrusion: the plasma membrane Ca^{2+} ATPase (PMCA) and the Na/Ca exchanger (NCX) [1, 2]. The PMCA belongs to the P-type family of transport ATPases which form a phosphorylated intermediate during the reaction cycle [3]. The β-cell expresses the four main isoforms of the PMCA, namely, PMCA1, PMCA2, PMCA3, and PMCA4 [4]. Six alternative splice mRNA variants, characterized at splice sites A and C, were detected in the β-cell (rPMCA1xb, 2yb, 2wb, 3za, 3zc, 4xb), plus one additional variant in pancreatic islet cells (PMCA4za). At the mRNA and protein level, five variants predominated (1xb, 2wb, 3za, 3zc, 4xb), while one additional isoform (4za) predominated at the protein level only. This provides evidence for the presence of PMCA2 and PMCA3 isoforms at the protein level in nonneuronal tissue. Hence, the pancreatic β-cell is equipped with multiple PMCA isoforms with possible differential regulation, providing a full range of PMCAs for $[Ca^{2+}]_i$ regulation [4].

The Na/Ca exchanger is an electrogenic transporter located at the plasma membrane that couples the exchange of three Na^+ for one Ca^{2+}. The Na/Ca exchanger has been cloned in 1990 [5], and four isoforms have been identified : NCX1, NCX2, NCX3, and NCX4 [6, 7]. The rat β-cell expresses two splice variants of the isoform NCX1, namely, NCX1.3 and NCX1.7, the mouse β-cell expressing in addition NCX1.2 [8]. PCR amplification did not yield any DNA fragment for NCX2, and NCX3 was not looked for [9]. In the rat pancreatic β-cell, Na/Ca exchange displays a quite high capacity and participates in the control of $[Ca^{2+}]_i$ and of insulin release [10].

In previous work, by performing loss- and gain-of-function studies (use of antisense oligonucleotides targeting NCX1 or overexpression of NCX1), we observed that the Na/Ca exchanger contributed significantly to Ca^{2+} outflow from the cell (70 %) but also to Ca^{2+} entry in the β-cell. Indeed, during the upstroke of the action potentials, the Na/Ca exchanger may reverse and contribute to Ca^{2+} entry (about 25 % of the initial peak) [11, 12].

By performing PMCA overexpression studies, we could demonstrate that the PMCA also contributes to Ca^{2+} outflow out of the cell [13]. Surprisingly, in the clone showing the highest level of overexpression, the rise in $[Ca^{2+}]_i$ induced by membrane depolarization (K^+: 50 mM) was almost completely abolished. This is striking because the PMCA is considered as a high-affinity, low-capacity system at variance with the Na/Ca exchanger which is a low-affinity, high-capacity system. Hence, the overexpression of a low-capacity system was not expected to reduce the rise in $[Ca^{2+}]_i$ to such an extent.

Different lines of evidence suggest that glucose, the main physiological stimulus of insulin release, stimulates β-cell Na/Ca exchange activity [12, 14]. Previous work on the PMCA shows, on the contrary, that glucose inhibits PMCA activity [15].

To understand the respective role of these two mechanisms, we studied the effect of glucose on PMCA and NCX transcription, expression, and activity in rat pancreatic islet cells [16]. Glucose (11.1 and 22.2 mM) induced a parallel decrease in PMCA transcription, expression, and activity. In contrast the sugar induced a parallel increase in NCX transcription, expression, and activity. The effects of the sugar were mimicked by the metabolizable insulin secretagogue α-ketoisocaproate and persisted in the presence of the Ca^{2+} channel blocker nifedipine. The above results are compatible with the view that when stimulated by glucose, the β-cell switches from a low-efficiency Ca^{2+}-extruding mechanism, the PMCA, to a high-capacity system, the Na/Ca exchanger, in order to better face the increase in Ca^{2+} inflow. These effects of glucose do not result from a direct effect of the sugar itself and are not mediated by the increase in intracellular free Ca^{2+} concentration induced by the sugar [16].

2 NCX and PMCA in Diabetes

Evidences suggest that programmed cell death (apoptosis) represents the main mechanism of β-cell death in animal models of type 1 diabetes mellitus (T1DM) and possibly also in human T1DM [17]. On the other hand, type 2 diabetes mellitus (T2DM) is a complex disease characterized by both insulin resistance and β-cell dysfunction. One of the earliest abnormality occurring in this disease is the alteration in pulsatile insulin release with the suppression of the first phase of insulin response to glucose, both defects being present well before the development of overt hyperglycemia and clinical diabetes [18]. The second phase of insulin release is also diminished, and a number of abnormalities of continuous insulin release have been observed [19, 20]. In addition to a defect in β-cell function, a reduction in islet and β-cell mass has been observed [21, 22]. This reduction could be related to increased programmed cell death (apoptosis), to a decrease in β-cell replication, or both [23].

Ca^{2+} is not solely of importance in cell signaling but may also trigger programmed cell death (apoptosis) and regulate death-specific enzymes. Therefore, the development of strategies to control Ca^{2+} homeostasis may represent a potential approach to prevent or enhance cell apoptosis. To test this hypothesis, the Na/Ca exchanger (NCX1.7 isoform) was stably overexpressed in insulin-secreting tumoral cells [24]. NCX overexpression increased apoptosis induced by sarco-endoplasmic reticulum (ER) Ca^{2+} ATPase (SERCA) inhibitors but not by agents increasing $[Ca^{2+}]_i$ through opening of plasma membrane Ca^{2+} channels. NCX overexpression reduced the rise in $[Ca^{2+}]_i$ induced by all agents, depleted ER Ca^{2+} stores, sensitized the cells to Ca^{2+}-independent proapoptotic signaling pathways, and reduced cell proliferation by about 40 %. ER Ca^{2+} stores depletion was accompanied by the activation of the ER-specific caspase (caspase-12), the activation being enhanced by SERCA inhibitors. Hence, Na/Ca exchanger overexpression, by depleting ER Ca^{2+} stores, triggers the activation of caspase-12 and increases apoptotic cell death [24]. By increasing apoptosis and decreasing cell proliferation, overexpression of Na/Ca exchanger

may represent a new potential approach in cancer gene therapy. On the other hand, the latter results open the way to the development of new strategies to control cellular Ca^{2+} homeostasis that could on the contrary prevent the process of apoptosis that mediates, in part, β-cell destruction in T1DM and T2DM [24].

Type 1 cytokines, such as interleukin-1β (IL-1β), tumor necrosis factor-α (TNF-α), and interferon-γ (IFN-γ), are early mediators of β-cell death in type 1 diabetes mellitus [17], and a combination of IL-1β+IFN-γ has been shown to decrease the expression of the ER Ca^{2+}-pump SERCA2b in the β cell [25–27]. Therefore, we wondered whether cytokines could not induce β-cell death by depleting ER Ca^{2+} stores, namely, by a mechanism similar to that induced by Na/Ca overexpression. By using fura-2 and furaptra to monitor cytosolic and ER free Ca^{2+} concentration, we could show that cytokines, like NCX overexpression, induce a severe depletion of ER Ca^{2+} stores with activation of ER stress [28].

Chronic exposure to high free fatty acid (FFA) concentrations causes β-cell apoptosis [23, 29, 30] and may contribute to the increased β-cell apoptosis rates in T2D [31], a phenomenon called lipotoxicity [32]. Interestingly, we could recently show that saturated FFAs also induce ER stress via ER Ca^{2+} depletion with resulting β-cell apoptosis [33].

In summary, ER Ca^{2+} depletion with resulting ER stress appears as a mechanism common to various conditions leading to β-cell death. In order to further evaluate such a view, we examined whether PMCA overexpression may lead to a similar picture and explored in further details the pathways triggered by ER stress. On the other hand, our data also suggest that the opposite effect, namely, a reduction in Na/Ca exchange or PMCA activity, may lead to an increase in ER Ca^{2+} stores and perhaps reduce β-cell apoptosis. These hypotheses have been tested and are presented in the following paragraphs [34, 35].

3 Effect of PMCA Overexpression on β-Cell Death

In this study, clonal β-cells (BRIN-BD11) were examined for the effect of PMCA overexpression on cytosolic, ER, and mitochondrial [Ca^{2+}] using a combination of aequorins with different Ca^{2+} affinities and on the ER and mitochondrial pathways of apoptosis [34]. Overexpression of PMCA decreased [Ca^{2+}] in the cytosol, the ER, and the mitochondria and induced apoptosis. Figure 6.1 shows that PMCA2-overexpressing clones displayed an increased rate of basal apoptosis (Fig. 6.1a). The sarco-endoplasmic reticulum Ca^{2+} ATPase (SERCA) inhibitors cyclopiazonic acid (CPA, 50 μM) and thapsigargin (500 nM) increased apoptosis levels in all clones, but this was more marked in PMCA2-overexpressing cells (Fig. 6.1a). The rate of apoptosis induced by CPA was significantly higher in clone 2 than in clone 5, namely, in the clone showing the highest level of PMCA2 overexpression (Fig. 6.1a) indicating that Ca^{2+} depletion in itself is instrumental. PMCA2-overexpressing cells also displayed increased levels of caspase 3 cleavage

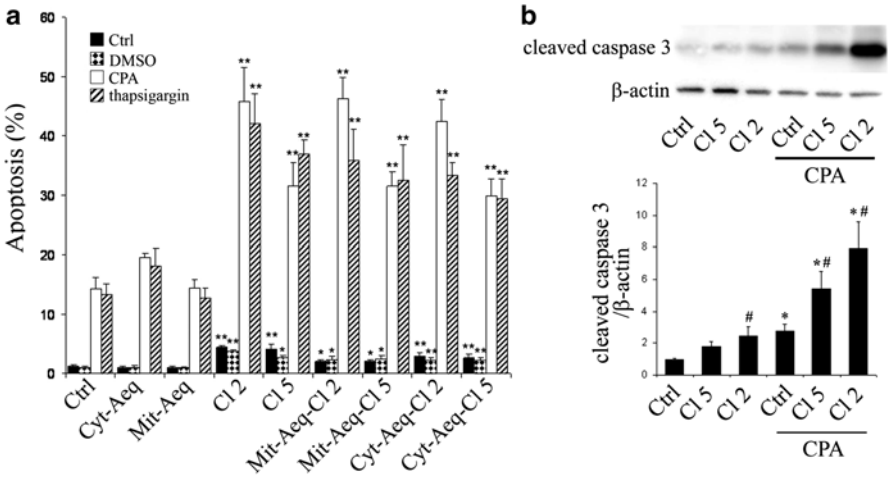

Fig. 6.1 Effect of PMCA2 overexpression on cells viability and caspase 3 cleavage. (**a**) Cell viability. Non-transfected BRIN BD-11 cells (Ctrl) or different clones of BRIN cells transfected with PMCA2, clone 2 (Cl 2) or 5 (Cl 5), and/or aequorin targeted to the cytosol (Cyt-Aeq) or the mitochondria (Mit-Aeq) were untreated (*black bars*) or treated for 24 h with CPA (*white bars*), thapsigargin (*stripe bars*), or the solvent DMSO (*dotted bars*). Apoptosis levels were evaluated by observation under a microscope after HO-PI staining. The data are expressed as the percentage of apoptotic cells over the total number of cells counted ± SEM. Results are means of three to five independent experiments. $*P<0.05$; $**P<0.01$; vs. respective non-transfected control. (**b**) Caspase 3 cleavage. Western blot analyses of non-transfected (Ctrl) and PMCA2-transfected cells, clone 2 (Cl 2) or clone 5 (Cl 5) using an antibody directed against the cleaved caspase 3 fragment. *Upper panel*: representative blot of caspase 3 and β-actin expression. *Lower panel*: quantitative assessment of cleaved caspase 3 levels normalized to the β-actin levels. Results are means of five independent experiments. $*P<0.05$ vs. respective non-treated control. $\#P<0.05$ vs. respective non-transfected condition. This research was originally published in J. Biol. Chem; Jiang L, Allagnat F, Nguidjoe E, Kamagate A, Pachera A, Vanderwinden J-M, Brini M, Carafoli E,. Eizirik DL, Cardozo AK, Herchuelz A (2010) Plasma membrane Ca^{2+}-ATPase overexpression depletes both mitochondrial and endoplasmic reticulum Ca^{2+} stores and triggers apoptosis in insulin-secreting BRIN-BD11 cells. J Biol Chem 285: 30634–30643, 2010. Reproduced with permission

compared to control cells, in the absence or presence of CPA (Fig. 6.1b). Under these conditions, the rate of caspase 3 cleavage tended to be higher in clone 2 than in clone 5.

PMCA overexpression activated the IRE1α-XBP1s but inhibited the PERK-eiF2α-CHOP and the ATF6-BiP pathways of the ER unfolded protein response. Increased Bax/Bcl-2 expression ratio (proapoptotic/antiapoptotic Bcl-2 family members) was observed in PMCA-overexpressing β-cells. This was followed by Bax translocation to the mitochondria with subsequent cytochrome c release, opening on the permeability transition pore, loss of mitochondrial membrane potential, and apoptosis. Interestingly, $[Ca^{2+}]$ was not solely decreased in the cytoplasm and the ER of PMCA2-overexpressing cells, but also in the mitochondria. Indeed, in

various models of cell death due to ER Ca^{2+} release and ER Ca^{2+} depletion, cell death is attributed to the uptake of Ca^{2+} by the mitochondria with resulting opening of the mitochondrial permeability transition pore (MPTP) and loss of the mitochondrial electrochemical gradient [36]. Although the two latter changes were observed in our cells, they cannot be attributed to mitochondrial Ca^{2+} overload [34].

Thus, Pmca2 overexpression like Ncx1 overexpression induces β-cell Ca^{2+} depletion and β-cell death, but the mechanisms leading to β-cell death could be different.

4 Effect of Ncx1 Heterozygous Inactivation on Pancreatic β-Cell Function

If it is possible to increase apoptosis and to decrease β-cell proliferation by increasing the activity of the Na/Ca exchanger, it may be possible to obtain the opposite effects by downregulating such a mechanism. In order to test this hypothesis, we generated Ncx1 heterozygous deficient mice ($Ncx1^{+/-}$) [35].

Evidence was obtained that the expression of the exchanger in the β-cell was reduced at the mRNA but also at the functional level. For instance, the uptake of ^{45}Ca induced by the removal of extracellular Na^+ (reverse Na/Ca exchange) was reduced by half (Fig. 6.2a), while the increase in cytosolic free Ca^{2+} concentration ($[Ca^{2+}]_i$) induced by the same maneuver (Fig. 6.2b) was reduced by 24 % ($P<0.05$) in $Ncx1^{+/-}$ compared to $Ncx1^{+/+}$ islets.

We then measured the effect of glucose-induced insulin release from pancreatic islets. Figure 6.2c, d shows the effect of an increase in glucose concentration from 2.8 to 11.1 mM on insulin release from perfused islets (c: representative experiment, d: mean of 4–6 experiments). In $Ncx1^{+/+}$ islets, glucose induced an oscillatory increase in insulin release, while in $Ncx1^{+/-}$ islets, the sugar induced a marked first phase followed by a progressive increase in insulin release with less clear oscillations. The amount of insulin released during the initial phase (16–20 min) and the whole period of stimulation (16–60 min) was about 2.6 and 2.4 times higher, respectively, in $Ncx1^{+/-}$ than in $Ncx1^{+/+}$ islets ($P<0.02$). The major increase in insulin release was attended, by an increase in glucose-induced ^{45}Ca uptake (Fig. 6.2e), in islet insulin content (Fig. 6.2f) and in proinsulin immunostaining. The increase in ^{45}Ca uptake induced by 16.7 mM glucose and insulin content was twice as high in $Ncx1^{+/-}$ than in $Ncx1^{+/+}$ islets. Taken as a whole, the data so far presented show that Ncx1 heterozygous inactivation strongly increases β-cell function including glucose-induced insulin production and release.

We then measured β-cell mass, size, and proliferation. The latter parameters were measured at 4 and 12 weeks, namely, in the young and adult age (Fig. 6.3a–c). As expected, β-cell mass was increased at 12 compared to 4 weeks in both types of islets though the increase was of much larger magnitude in $Ncx1^{+/-}$ than $Ncx1^{++}$ islets (8.8 vs. 1.6-fold increase, respectively, $P<0.001$, Fig. 6.3a). This increase was not due to β-cell or islet hypertrophy since no change in β-cell and islet size was

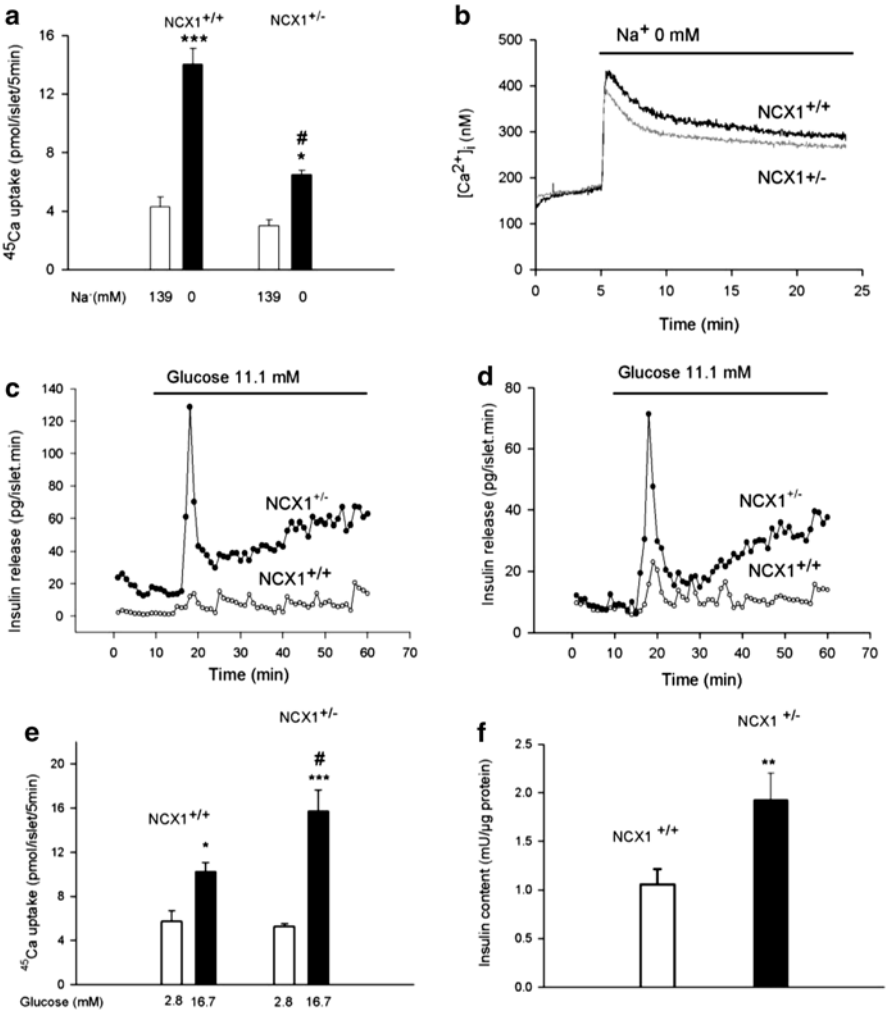

Fig. 6.2 Effect of Ncx1 heterozygous inactivation on Na/Ca exchange activity and on islet function. (**a**) ^{45}Ca uptake in the presence and the absence of extracellular Na^+. Means ± SEM of four experiments, comprising 4–5 replicates each. * $P<0.05$, *** $P<0.001$ vs. Na^+ 139 mM; # $P<0.001$ vs. $Ncx1^{+/+}$. (**b**) Effect of extracellular Na^+ removal on $[Ca^{2+}]_i$ in $Ncx1^{+/+}$ and $Ncx1^{+/-}$ islets. The period of exposure to Na^+-free medium is indicated by a *bar* above the *curves*. The *curves* shown are the mean of seven traces in each case. (**c**, **d**) Effect of 11.1 mM glucose on insulin release from groups of 20 islet (**c**) representative experiment, (**d**) mean of 4 and 6 ($Ncx1^{+/-}$) experiments. The amount of insulin released in response to glucose is about 2.5 times higher in $Ncx1^{+/-}$ than in $Ncx1^{+/+}$ islets ($P<0.05$). (**e**) Effect of glucose on ^{45}Ca uptake in $Ncx1^{+/+}$ and $Ncx1^{+/-}$ islets ($n=4$–6 experiments, * $P<0.05$, *** $P<0.001$ vs. 2.8 mM; # $P<0.01$ vs. $Ncx1^{+/+}$ islets at 16.7 mM glucose). (**f**) Insulin content of batches of ten islets; $n=10$ experiments ** $P<0.01$ vs. $Ncx1^{+/+}$ islets.

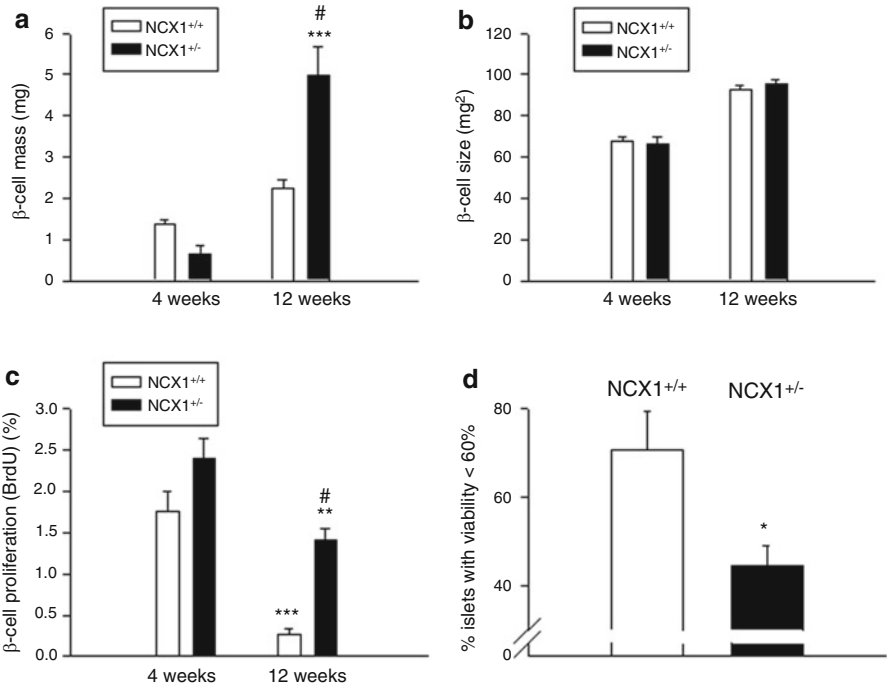

Fig. 6.3 Effect of Ncx1 heterozygous inactivation of Na/Ca exchange on β-cell mass, size, proliferation, and resistance to hypoxia. Changes in β-cell mass (**a**), size (**b**), and proliferation rate (**c**) between weeks 4 and 12 in $Ncx1^{+/+}$ (*open bars*) and $Ncx1^{+/-}$ mice (*closed bars*). Mean ± SEM values from 5 and 6 pancreases, respectively. (**a**) ***$P < 0.001$ vs. 4 weeks values; #$P < 0.001$ vs. $Ncx1^{+/+}$ β-cells at 12 weeks. (**c**) **$P < 0.01$, ***$P < 0.001$ vs. respective value at 4 weeks; #$P < 0.01$ vs. $Ncx1^{+/+}$ islets at 12 weeks. (**d**) Cell viability measured in intact islets using Ho342 and PI staining after 6 h exposure to hypoxia. Mean ± SEM values from four individual experiments. * $P < 0.05$ vs. $Ncx1^{+/+}$ islets. Copyright © 2011, American Diabetes Association, from Diabetes Vol 60: 2076–2085, 2011. Reproduced with permission

observed between $Ncx1^{+/+}$ and $Ncx1^{+/-}$ mice (Fig. 6.3b). It was rather due to an increase in β-cell proliferation rate. Again, as expected, β-cell proliferation was decreased at 12 compared to 4 weeks (Fig. 6.3c), though the decrease was of lower magnitude in $Ncx1^{+/-}$ than $Ncx1^{+/+}$ islets (−40 % vs. −85 %, $P < 0.01$). As a result, a 5.25 times higher proliferation rate was observed at 12 weeks in $Ncx1^{+/-}$ compared to $Ncx1^{+/+}$ mice (Fig. 6.3c).

β-cell apoptosis was also measured, but no difference could be found between $Ncx1^{+/-}$ and $Ncx1^{+/+}$ islets, whether under basal or stimulated conditions (e.g., in the presence of SERCA inhibitors or cytokines) and using different methods (TUNEL method or Ho342 and PI staining). The sole condition under which a difference could be found was when the islets were exposed to hypoxia (6 h). Thus, in $Ncx1^{+/+}$ islets, 71 % of the islets showed a decrease in viability below 60 % compared with 45 % in $Ncx1^{+/-}$ islets when exposed to hypoxia (Fig. 6.3d).

Islets transplantation represents a valuable approach in the treatment of diabetes. However, its applicability is limited by the need to transplant a high number of islets (from two or more donors). In clinical islet transplantation, it has been estimated that up to 70 % of the transplanted β-cell mass is destroyed in the early posttransplant period due to nonimmune-mediated physiological stress, namely, prolonged hypoxia during the revascularization process [37]. Therefore, we transplanted $Ncx1^{+/-}$ islets under the kidney capsule of alloxan-diabetic mice to examine their performances compared to $Ncx1^{+/+}$ islets. The rate of success of a 200 $Ncx1^{+/+}$ islets transplantation was 2/5. In comparison, the rate of success of a 100 $Ncx1^{+/-}$ islet transplantation was 4/5, while the rate of success of a 50 $Ncx1^{+/-}$ islets transplantation was 2/3. This suggests that the $Ncx1^{+/-}$ islets are at least 4–7 times more efficient to cure diabetes than $Ncx1^{+/+}$ islets.

Otherwise, the phenotype of $Ncx1^{+/-}$ mice appeared normal, and their glucose metabolism (in vivo) was similar to that of $Ncx1^{+/+}$ mice except for an increased and earlier initial peak of insulin release during the glucose tolerance test, a finding in agreement with the major increase in glucose-induced first-phase insulin release (Fig. 6.2c, d) in $Ncx1^{+/-}$ islets.

Downregulation of the β-cell Na/Ca exchanger is thus a unique model providing a novel concept for the prevention and treatment of T1D and T2D and to improve the applicability of islet transplantation.

5 Effect of Pmaca2 Heterozygous Inactivation on Pancreatic β-Cell Function

Preliminary data indicate that heterozygous inactivation of PMCA2 leads to apparented, though not completely similar results.

6 Effect of the NCX Inhibitor KB-R7943 on NCX1 Splice Variants and Insulin Release

In a recent study, Hamming et al. [38], using the patch-clamp technique, examined the effect of the NCX inhibitor KB-R7943 on recombinant NCX1 isoforms activity in forward mode. They observed that at variance with NCX1.1, the isoform expressed in the heart, NCX1.3 and NCX1.7, the isoforms expressed in the β-cell, exhibit significant inactivation during forward mode operation and are 15- to 18-fold more sensitive to KB-R7943 inhibition, compared with NCX1.1 ($IC50s = 2.9$ and 2.4 vs. 43 μM, respectively). Because NCX1 splice variants differ only in the exon composition of the alternative splice region (ABCDEF for NCX1.1, BD, and BDF for NCX1.3 and NCX1.7, respectively), the authors replaced exon A by exon B in NCX1.1 generating NCX1.11. This conferred to NCX1.11 the same sensitivity to KB-R7943 than NCX1.3 and NCX1.7. On the contrary replacing exon B with A in

NCX1.3 (NCX1.4) dramatically decreased the activity of the drug. KB-R7943 also increased glucose-induced rise in $[Ca^{2+}]_i$ and insulin release from pancreatic islets. The latter data are in agreement with our own [35]. Taken together, our works suggest that inhibitors of the Na/Ca exchanger may represent new therapeutic agents in diabetes that could prevent the development of T1DM and T2DM (DM) in at-risk patients, preserve residual β-cell function and mass in recent-onset DM, activate endogenous β-cell regeneration by stimulation of β-cell proliferation in DM, and improve the applicability of islet transplantation.

7 Conclusions

Gain of PMCA2 or NCX1 function leads to ER stress, decrease in β-cell proliferation, and β-cell death by apoptosis. Loss of NCX1 function leads on the contrary to an increase in β-cell function, mass, and proliferation, namely, to various changes in β-cell function that are opposite to the major abnormalities seen in diabetes. Preliminary data indicate that heterozygous inactivation of PMCA2 leads to related though not completely similar results. Hence, we identified novel targets to preserve and protect functional β-cell mass in the treatment of both T1DM and T2DM. Because NCX1 splice variants expressed in the β-cell are about 20 times more sensitive to NCX1 inhibitors like KB-R7943 than isoforms expressed in other tissues, future work in the field may lead to the development of new therapeutic agents that could prevent the development of diabetes in at-risk patients, preserve residual β-cell function and mass in recent-onset DM, and activate endogenous β-cell regeneration by stimulation of β-cell proliferation in DM. PMCA2 inhibitors may have related though not completely similar actions, and their actions on β-cell function are worth to be examined.

Acknowledgments The authors thank A. Van Praet, A. Iabkriman, and M-P. Berghmans (Laboratory of Pharmacology; ULB) for excellent technical support. This work has been supported by grants from the Belgian Fund for Scientific Research (FRSM 3.4593.04, 3.4527.08), the EFSD/Novo Nordisk Programme in Diabetes Research (2005/6), and JDRF (award 17-2011-650, USA).

References

1. Carafoli E (1988) Membrane transport of calcium: an overview. Methods Enzymol 157:3–11
2. Blaustein MP, Lederer WJ (1999) Sodium/calcium exchange: its physiological implications. Physiol Rev 79:763–854
3. Carafoli E (1994) Biogenesis: plasma membrane calcium ATPase: 15 years of work on the purified enzyme. FASEB J 8:993–1002
4. Kamagate A, Herchuelz A, Bollen A et al (2000) Expression of multiple plasma membrane Ca^{2+}-ATPases in rat pancreatic islet cells. Cell Calcium 27:231–246
5. Nicoll DA, Longoni S, Philipson KD (1990) Molecular cloning and functional expression of the cardiac sarcolemmal Na^{+}-Ca^{2+} exchanger. Science 250:562–565

6. Hryshko LV, Philipson KD (1997) Sodium-calcium exchange: recent advances. Basic Res Cardiol 92(Suppl 1):45–51
7. On C, Marshall CR, Chen N et al (2008) Gene structure evolution of the Na^{+}-Ca^{2+} exchanger (NCX) family. BMC Evol Biol 8:127–142
8. Van Eylen F, Svoboda M, Herchuelz A (1997) Identification, expression pattern and potential activity of Na/Ca exchanger isoforms in rat pancreatic B-cells. Cell Calcium 21:185–193
9. Van Eylen F, Bollen A, Herchuelz A (2001) NCX1 Na/Ca exchanger splice variants in pancreatic islet cells. J Endocrinol 168:517–526
10. Herchuelz A, Plasman PO (1991) Sodium-calcium exchange in the pancreatic B cell. Ann N Y Acad Sci 639:642–656
11. Van Eylen F, Lebeau C, Herchuelz A (1998) Contribution of Na/Ca exchange to Ca^{2+} outflow and entry in the rat pancreatic beta-cell: studies with antisense oligonucleotides. Diabetes 47: 1873–1880
12. Van Eylen F, Horta OD, Barez A et al (2002) Overexpression of the Na/Ca exchanger shapes stimulus-induced cytosolic Ca^{2+} oscillations in insulin-producing BRIN-BD11 cells. Diabetes 51:366–375
13. Kamagate A, Herchuelz A, Van Eylen F (2002) Plasma membrane Ca^{2+}-ATPase overexpression reduces Ca^{2+} oscillations and increases insulin release induced by glucose in insulin-secreting BRIN-BD11 cells. Diabetes 51:2773–2788
14. Plasman PO, Lebrun P, Herchuelz A (1990) Characterization of the process of sodium-calcium exchange in pancreatic islet cells. Am J Physiol 259:E844–E850
15. Gagliardino JJ, Rossi JP (1994) Ca^{2+}-ATPase in pancreatic islets: its possible role in the regulation of insulin secretion. Diabetes Metab Rev 10:1–17
16. Ximenes HM, Kamagate A, Van Eylen F et al (2003) Opposite effects of glucose on plasma membrane Ca^{2+}-ATPase and Na/Ca exchanger transcription, expression, and activity in rat pancreatic beta-cells. J Biol Chem 278:22956–22963
17. Eizirik DL, Mandrup-Poulsen T (2001) A choice of death – the signal-transduction of immune-mediated beta-cell apoptosis. Diabetologia 44:2115–2133
18. Utzschneider KM, Kahn SE (2003) In International Textbook of Diabetes Mellitus: DeFronzo RA, Ferrannini E, Keen H, Zimmet P (eds) β-cell dysfunction in type 2 diabetes. Hoboken, NJ: John Wiley & Sons. 375–388
19. Porte D Jr (1991) Banting lecture 1990. Beta-cells in type II diabetes mellitus. Diabetes 40: 66–180
20. Kahn SE, Zraika S, Utzschneider KM et al (2009) The beta cell lesion in type 2 diabetes: there has to be a primary functional abnormality. Diabetologia 52:1003–1012
21. Maclean N, Ogilvie RF (1955) Quantitative estimation of the pancreatic islet tissue in diabetic subjects. Diabetes 4:367–376
22. Rahier J, Guiot Y, Goebbels RM et al (2008) Pancreatic beta-cell mass in European subjects with type 2 diabetes. Diabetes Obes Metab 10(Suppl 4):32–42
23. Cnop M, Welsh N, Jonas JC et al (2005) Mechanisms of pancreatic beta-cell death in type 1 and type 2 diabetes: many differences, few similarities. Diabetes 54(Suppl 2):S97–S107
24. Diaz-Horta O, Kamagate A, Herchuelz A et al (2002) Na/Ca exchanger overexpression induces endoplasmic reticulum-related apoptosis and caspase-12 activation in insulin-releasing BRIN-BD11 cells. Diabetes 51:1815–1824
25. Cardozo AK, Heimberg H, Heremans Y et al (2001) A comprehensive analysis of cytokine-induced and nuclear factor-kappa B-dependent genes in primary rat pancreatic beta-cells. J Biol Chem 276:48879–48886
26. Kutlu B, Cardozo AK, Darville MI (2003) Discovery of gene networks regulating cytokine-induced dysfunction and apoptosis in insulin-producing INS-1 cells. Diabetes 52:2701–2719
27. Cardozo AK, Kruhoffer M, Leeman R et al (2001) Identification of novel cytokine-induced genes in pancreatic beta-cells by high-density oligonucleotide arrays. Diabetes 50:909–920
28. Cardozo AK, Ortis F, Storling J et al (2005) Cytokines downregulate the sarcoendoplasmic reticulum pump Ca^{2+} ATPase 2b and deplete endoplasmic reticulum Ca^{2+}, leading to induction of endoplasmic reticulum stress in pancreatic beta-cells. Diabetes 54:452–461

29. Cnop M, Hannaert JC, Hoorens A et al (2001) Inverse relationship between cytotoxicity of free fatty acids in pancreatic islet cells and cellular triglyceride accumulation. Diabetes 50: 1771–1777
30. Maedler K, Spinas GA, Dyntar D et al (2001) Distinct effects of saturated and monounsaturated fatty acids on beta-cell turnover and function. Diabetes 50:69–76
31. Butler AE, Janson J, Bonner-Weir S et al (2003) Beta-cell deficit and increased beta-cell apoptosis in humans with type 2 diabetes. Diabetes 52:102–110
32. El-Assaad W, Buteau J, Peyot ML et al (2003) Saturated fatty acids synergize with elevated glucose to cause pancreatic beta-cell death. Endocrinology 144:4154–4163
33. Cunha DA, Hekerman P, Ladriere L et al (2008) Initiation and execution of lipotoxic ER stress in pancreatic beta-cells. J Cell Sci 121:2308–2318
34. Jiang L, Allagnat F, Nguidjoe E et al (2010) Plasma membrane Ca^{2+}-ATPase overexpression depletes both mitochondrial and endoplasmic reticulum Ca^{2+} stores and triggers apoptosis in insulin-secreting BRIN-BD11 cells. J Biol Chem 285:30634–30643
35. Nguidjoe E, Sokolow S, Bigabwa S et al (2011) Heterozygous inactivation of the Na/Ca Exchanger increases glucose-induced insulin release, beta-cell proliferation, and mass. Diabetes 60:2076–2085
36. Orrenius S, Zhivotovsky B, Nicotera P (2003) Regulation of cell death: the calcium-apoptosis link. Nat Rev Mol Cell Biol 4:552–565
37. Emamaulee JA, Shapiro AM (2006) Perpectives in diabetes. Interventional strategies to prevent β-cell apoptosis in islet transplantation. Diabetes 55:1907–1914
38. Hamming KS, Soliman D, Webster NJ et al (2010) Inhibition of beta-cell sodium-calcium exchange enhances glucose-dependent elevations in cytoplasmic calcium and insulin secretion. Diabetes 59:1686–1693

Chapter 7
Long-Range Allosteric Regulation of Pumps and Transporters: What Can We Learn from Mammalian NCX Antiporters?

Daniel Khananshvili

Abstract The Ca^{2+}-dependent allosteric regulation of ion-channels, pumps, and transporters is still a subject of multidisciplinary research due to its fundamental significance. The mammalian Na^{+}/Ca^{2+} exchangers (NCX1–3) and their splice-variants are expressed in a tissue-specific manner to extrude Ca^{2+} in diverse cell types. Since NCX proteins are involved in regulating numerous physiological and pathophysiological events, their selective pharmacological targeting is a long-wanted objective, although this intervention remains challenging due to our poor understanding of the underlying mechanisms. Eukaryotic NCXs are strongly regulated by cytosolic [Ca^{2+}] oscillations, where Ca^{2+} interacts with the regulatory domains, CBD1 and CBD2. Recent evidence suggests that the CBD1–CBD2 interface controls Ca^{2+}driven tethering of CBDs, which is associated with Ca^{2+} occlusion (and slow dissociation) at the primary Ca^{2+} sensor (Ca3–Ca4 sites), thereby driving the dynamic coupling of CBDs. This mechanism seems to be common for all isoform/splice variants. The primary allosteric Ca^{2+} sensor on CBD1 is highly conserved among all NCX variants, whereas the "tissue-specific" splicing segment located on CBD2 modifies not only the affinity and kinetic properties of Ca3–Ca4 sites but also the essence of the primary signal, resulting either the activation, inhibition, or no response to regulatory Ca^{2+} in a given variant. By using hydrogen-deuterium exchange mass-spectrometry (HDX-MS), small-angle X-ray scattering (SAXS), equilibrium $^{45}Ca^{2+}$ binding, and stopped-flow techniques, we found that Ca^{2+} binding to CBD1 rigidifies the backbone flexibility of CBD2 (but not for CBD1), whereas CBD2 stabilizes the apo-CBD1 structure. The extent and strength of Ca^{2+}-dependent rigidification of CBD2 is splice-variant dependent, where the backbone rigidification spans from Ca3–Ca4 sites of CBD1 up to the tip of CBD2 (>50 Å), or alternatively, it stops at the CBD2 helix in the splice variant exhibiting inhibitory response to Ca^{2+}. These findings provide a structure-dynamic basis by

D. Khananshvili, Ph.D. (✉)
Department of Physiology and Pharmacology, Sackler School of Medicine, Tel-Aviv University, Ramat-Aviv, Tel-Aviv 69978, Israel
e-mail: dhanan@post.tau.ac.il

S. Chakraborti, N.S. Dhalla (eds.), *Regulation of Ca^{2+}-ATPases,V-ATPases and F-ATPases*, Advances in Biochemistry in Health and Disease 14,
DOI 10.1007/978-3-319-24780-9_7

which alternative splicing diversifies responses to Ca^{2+} and controls the propagation of allosteric signals over long distances.

Keywords NCX • Allosteric regulation • Regulatory domains • Calcium • Signal propagation

1 Introduction

1.1 Ca^{2+} Homeostasis, PM Ca^{2+} ATPase, and NCX

A fundamental feature of the living cell is to maintain resting levels of cytosolic free [Ca^{2+}] as low as 0.1 μM, whereas in specific cell types (e.g., excitable tissues) the oscillations of cytosolic Ca^{2+} have to take place in the right place and within the right timeslot [1, 2]. This very complex process requires the dynamic regulation and coordination of ion channels, pumps, and transporters. The PM (plasma membrane) Ca^{2+}-ATPase and Na^+/Ca^{2+} exchanger (NCX) are two exclusive systems that extrude Ca^{2+} from the cell, although their partial contributions to Ca^{2+} homeostasis differ among distinct cell types, depending on functional specialization and regulatory specificity possessed by a given cell type [1, 3, 4].

As established by Carafoli in the 1980s, PM Ca^{2+}-ATPase is a "high-affinity/low-capacity" system that maintains a primary Ca^{2+} gradient across the cell membrane, whereas the Na^+/Ca^{2+}exchanger is a "low-affinity/high-capacity" system that rapidly responds to dynamic (transient) swings in cytosolic $[Ca^{2+}]_i$ under ever-varying regulatory conditions (e.g., in cardiomyocytes) [1, 5, 6]. In mammalian NCX, the "low affinity" represents K_m values of ~5 μM, whereas the "high capacity" refers to rapid turnover rates of 2500–5000 s^{-1} for the ion transport cycle [7–9]. Notably, the turnover rates of mammalian NCX1–NCX3 are 10^3–10^4 times faster than those of prokaryotic NCX_Mj [3, 4, 10], although the ion binding/transport residues within the membrane-embedded part of the proteins are highly conserved among the NCX orthologs [11–14]. Notably, the major difference between the NCX1–3 and NCX_Mj proteins is that the mammalian NCXs contain the Ca^{2+}-binding regulatory domains CBD1 and CBD2 [15–19], whereas NCX_Mj lacks these regulatory domains [20].

1.2 Brief Background and Significance

The NCX proteins utilize the electrochemical gradient of Na^+ while catalyzing the exchange of $3Na^+$ ions with $1Ca^{2+}$, thereby extruding the Ca^{2+} from the cytosol or organelle (e.g., nuclei or mitochondria) matrix [1–3, 21–23]. The existence of the Na^+/Ca^{2+} exchanger was discovered in late 1960s in the heart [24] and squid giant axon preparations [25], by demonstrating a countercurrent (antiporter) type exchange of Na^+ with Ca^{2+} in an electrogenic fashion. Since then, the central role of the Na^+/

Ca^{2+} exchanger (NCX) in excitable and non-excitable tissues has been established and its key role in regulating cell calcium in health and disease has been widely accepted [2, 3, 11, 22]. Three mammalian genes (*SLC8A1*, *SLC8A2*, and *SLC8A3*) and their splice variants are expressed in a tissue-specific manner [11–14, 26] to modulate fundamental physiological events, such as excitation-contraction coupling, long-term potentiation of the brain and learning, blood pressure, immune response, neurotransmitter and insulin secretion, mitochondrial bioenergetics, among others [2, 3, 22, 23]. Altered expression/regulation of NCXs contribute to distorted Ca^{2+}-homeostasis in heart failure, arrhythmia, cerebral ischemia, hypertension, diabetes, renal Ca^{2+} reabsorption, muscle dystrophy, and other maladies [2, 3, 11, 22].

Shortly after the discovery of the cell membrane NCX, the activity of the mitochondrial Na^+/Ca^{2+} exchanger was discovered by Carafoli and collaborators more than 40 years ago, while revealing a unique feature of mitochondrial NCX (in sharp contrast with all other NCX orthologs) transporting either the Li^+ or Na^+ ion (but not K^+) in exchange with Ca^{2+} [27]. This unique feature in ion-transport selectivity appears to be a crucial criterion for disclosure of the molecular identity of mitochondrial NCX, currently termed NCLX, because of its capacity to transport Li^+ [28]. Our understanding of the basic mechanisms underlying the ion selectivity and regulation of NCLX remains of primary interest due to the importance of NCLX in shaping cellular and mitochondrial Ca^{2+} homeostasis to regulate the cytosolic Ca^{2+} SR/ER Ca^{2+} content, the rates of ATP synthesis, hormonal secretion, synaptic transmission and release of apoptotic factors in response to death signals [28–30].

1.3 Dynamic Regulation of Ca^{2+}-Extruding Proteins and Isoform/Splice Variants

For dynamic adjustment of Ca^{2+}-extrusion rates, both the PM Ca^{2+}-ATPase and Na^+/Ca^{2+} exchanger must be "secondarily" regulated by dynamic oscillations of cytosolic Ca^{2+} with the respective regulatory sites of the pump or exchanger, thereby representing the feedback mechanism underlying regulation [1–5, 31]. The pioneering works of Carafoli and collaborators provided first-hand information on the existence of the isoform/splice in variants of PM Ca^{2+}-ATPase proteins as well as primary information on the autoinhibitory segment [5, 6, 31, 32], the structural prototype of which was later found in NCX and termed XIP (e*X*changer *I*nhibitory *P*eptide) [33]. The XIP turned out to be very instrumental for studying the regulatory mechanisms underlying NCX in intact cell systems when added from the cytosolic side.

Both, the PM Ca^{2+}-ATPase [5, 6, 31, 32] and NCX [11–14, 34–36] proteins express numerous isoform/splice variants in a tissue-specific manner, although the underlying mechanisms remain poorly understood. The dynamic regulation of NCX is especially diverse and complex, since it must remove large amounts of Ca^{2+} within a limited time, where the Ca^{2+}-extrusion rates via NCX must change within milliseconds to match the dynamic changes in cytosolic Ca^{2+} [3, 4, 37, 38]. For example, Ca^{2+} interaction with regulatory CBD domains (located 70–80 Å from the transport sites) of cardiac NCX enhances the turnover rates up to 25-fold, where the

Ca^{2+} extrusion rates change in response to dynamic changes in membrane potential and cytosolic Na^+ and Ca^{2+} concentrations during the action potential [39].

Recently, high-resolution X-ray structures of regulatory CBD domains of eukaryotic NCX [16, 17, 40] and of full-size prokaryotic NCX [20] have become available (Fig. 7.1) and the dynamic properties of isolated proteins have been analyzed using advanced biophysical approaches [41–45]. Despite this progress, there are several major open questions: Why are diverse cell types needed to express so many isoform/splice variants and why does each cell type express a specific set of variants? What are the exact mechanisms underlying the function and regulation of diverse isoform/splice variants? How do distinct variants partially contribute to general and specific functions in a given cell type? How profitable (if at all) would be the development of mechanism-based blockers/agonists for selective pharmacological targeting of predefined isoform/splice variants and how could this challenging intervention be approached? [2, 3, 41]. During the last few years huge progress has been made in better understanding the molecular mechanisms underlying NCX regulation in tissue-specific isoform/splice variants [41–48]. The goal of the present article is to highlight the recent achievements in understanding the molecular mechanisms underlying mammalian NCX proteins, which may be of general significance.

2 Structure-Functional Basis of Ion-Transport and Regulation

2.1 General Features of NCX Proteins

The NCX (SLC8) gene family is one of five families belonging to the CaCA (Ca^{2+}/Cation Antiporter) superfamily [2, 3, 14]. Briefly, members of the CaCA superfamily share similar topology, comprising two clusters; each cluster contains five or six transmembrane helices (TM) and two clusters are joined by a cytoplasmic loop of varying length [11–14, 49–51]. Interestingly, prokaryotic NCX_Mj and mitochondrial NCLX lack the regulatory CBD domains, whereas all eukaryotic NCX1–3 proteins contain CBD domains located on the cytosolic loop-f between TM5 and TM6 [15–20]. The CaCA proteins possess a conserved sequence motif in each cluster (α_1 and α_2 segments), which are involved in the ion transport events [14, 49–51]. Despite the overall structural similarity within the CaCA superfamily, the NCX, NCXK, CAX, and NCLX gene families possess high selectivity for Na^+, Ca^{2+}, K^+, H^+, and Li^+ transport [2, 3, 11, 14].

Three mammalian gene products (NCX1–3) and their splice variants are expressed in a tissue-specific manner: NCX2 and NCX3 are expressed in the brain and skeletal muscle, and NCX1 is universally distributed, practically in every mammalian cell [26, 34–36]. At the post-transcriptional level, at least 17 NCX1 and 5 NCX3 proteins are produced through alternative splicing of the primary nuclear *SLC8A1* and *SLC8A3* transcripts; however, no splice variants have been identified

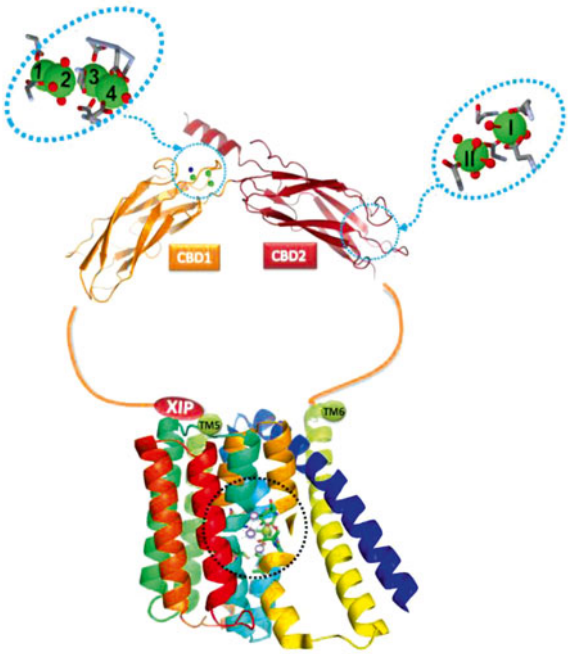

Fig. 7.1 The principal structure of mammalian NCX proteins. The crystal structure (3V5U) of archaebacterial *Methanococcus jannaschii* (NCX_Mj), containing ten transmembrane helices (TM1–10), can be used as a template for mammalian NCX proteins also some structural differences may exist, causing 10^3–10^4-fold differences in the turnovers rates. The cytosolic regulatory f-loop (~500 amino acids) contains the two-domain tandem of Ca^{2+}-binding CBD1 and CBD2 domains (3US9), which are connected with the TM5 and TM6, respectively, though the long linkers. The auto-inhibitory segment, XIP (20 amino acids), is connected to the C-terminal of TM5. The CBD1 domain contains four Ca^{2+} binding site (Ca1–Ca4), where the high affinity Ca3–Ca4 sites represent a primary allosteric sensor which is highly conserved among NCX isoform/splice variants. The CBD2 domain contains two Ca^{2+} binding sites (CaI–CaII), where the CaI site is responsible for alleviation of Na^+-dependent inactivation. Under physiological relevant conditions the low affinity Ca^{2+} binding sites on CBD1 (Ca1–Ca2) and on CBD2 (CaII) can bind either the Mg^{2+} ion and/or protons, which can secondarily (indirectly) modulate the affinity and kinetics of the primary Ca^{2+} sensors. *Green* and *red spheres* represent the Ca^{2+} ions and water molecules, respectively

for *SLC8A2* [11–14, 34–36]. These splice variants arise from a combination of six small exons (A, B, C, D, E, and F) located on a restricted region of the large intracellular loop-f (Fig. 7.2); all splice variants include a mutually exclusive exon, either A or B in order to maintain an open reading frame [11, 13, 14]. Notably, excitable tissues contain exon A, whereas kidney, stomach, and skeletal muscle tissues comprise NCX with exon B. The cardiac (NCX1.1), kidney (NCX1.3), brain (NCX1.4), and β-cell (NCX1.7) splice variants exhibit distinct properties for Ca^{2+}-dependent allosteric regulation of NCX activity, which may have physiological relevance [52–55]. Moreover, there are striking differences in allosteric responses to regulatory Ca^{2+} among eukaryotic NCX orthologs. For example, elevating the

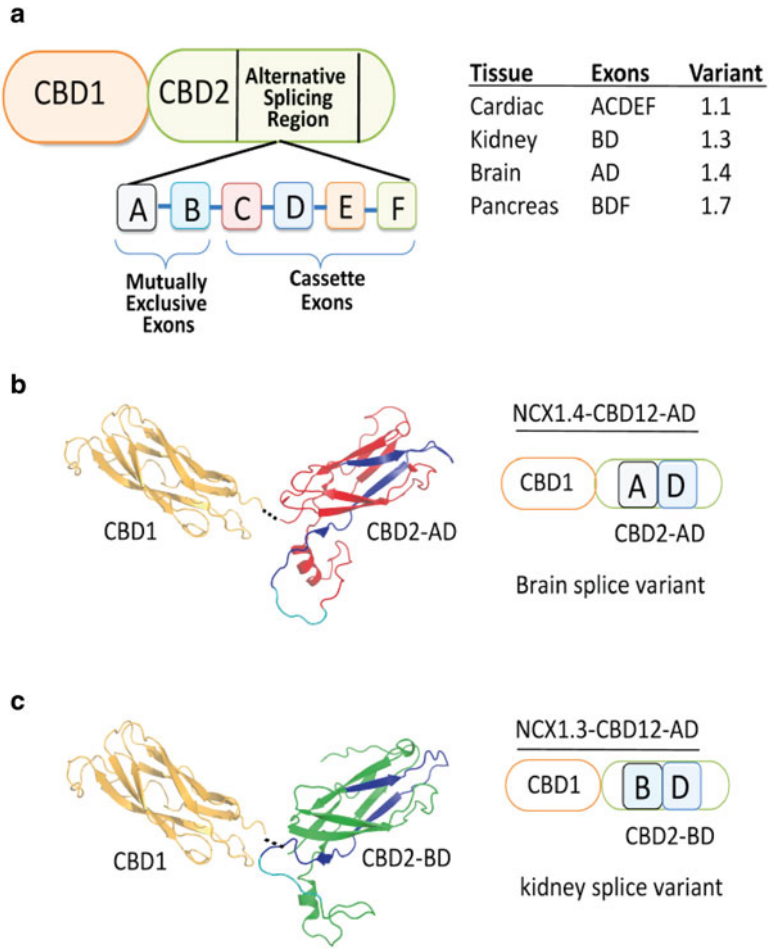

Fig. 7.2 Alternating splicing in NCX variants. The mammalian NCX1–3 proteins contain a splice segment, which is exclusively located on CBD2. (**a**) Tissue-specific splice variants arise from a combination of six small exons A, B, C, D, E, and F, whereas a mutually exclusive exon (either A or B) shows up in every splice variant. (**b**) and (**c**) The NMR structures of CBD1 (PDB 2FWS, *orange*), CBD2-AD (PDB 2FWU, *red*), and CBD2-BD (PDB code 2KLT, *green*) structures were superimposed on the template of the CBD12-E454K crystal structure (PBD 3US9) to show the position of the splice segment. Residues encoded by exons A and B are shown in *blue* and residues encoded by exon D are *cyan*

cytosolic Ca^{2+} activates the brain (AD), cardiac (ACDEF), and kidney (BD) variants, although the Ca^{2+}-induced alleviation of Na^{+}-dependent inactivation is observed only in the cardiac and brain variants [52, 53]. In contrast, the allosteric interaction of Ca^{2+} with a *Drosophila* NCX (CALX1.1) results in inhibition of the exchanger activities, whereas Ca^{2+} has no effect on the CALX1.2 ortholog [54, 55]. These regulatory differences are especially interesting in light of structural similarities in CBD domains among the NCXs.

2.2 *Crystal Structure of NCX_Mj and Ion-Transport Machinery in NCXs*

The crystal structure of archaebacterial *Methanococcus jannaschii* (NCX_Mj) was discovered in 2012 [20], thereby offering new opportunities for elucidating the molecular mechanisms underlying the ion selectivity, transport catalysis, and alternating access in NCX and similar proteins. The outward-facing (extracellular) conformation of NCX_Mj (Fig. 7.2) depicts ten transmembrane helices (TM1–10) that appear to be the similar in mammalian NCX proteins [20, 56]. The ion-binding pocket of NCX_Mj contains four ion-binding sites S_{Ca}, S_{ext}, S_{mid}, S_{int}, and S_{Ca}, arranged in a diamond-shaped configuration, where 12 residues contribute to Na^+ and Ca^{2+} ligation (4 in TM2 and TM7, and 2 in TM3 and TM8). In sharp contrast with eukaryotic NCX, the cytosolic loop between TM5 and TM6 is extremely short (12 residues) in NCX_Mj, meaning that this loop cannot be a prototype for a large cytosolic f-loop (~500 residues) of eukaryotic NCX bearing the regulatory CBD domains. Eight helices of NCX_Mj (TM2–5 and TM7–10) generate a tightly packed hub (which is perpendicularly inserted in the membrane), whereas two long/slanting helices (TM1 and TM6) are loosely packed in front of a rigid eight-helix core [20, 49–51]. The sliding of the gating bundle (TM1/TM6) toward the rigid core of eight helices may represent a major conformational change associated with alternating access, which could to be a general feature not only for NCX proteins but also for other gene families belonging to the Ca/CA superfamily [20, 49–51]. Interestingly, the turnover rate of NCX_Mj is ~0.5 s^{-1} [10, 57], which is 10^3–10^4 slower than the turnover rates of mammalian NCX and NCKX proteins [7–9]. These differences in transport kinetics are especially interesting in light of the structural similarities shared by the NCX_Mj and NCX1–3 proteins. Namely, 11 ion-coordinating residues (among 12) are highly conserved in organisms ranging from bacteria to humans, whereas in eukaryotic NCXs, D240 is consistently replaced by glutamine [11–14, 20]. Interestingly, the turnover rates of the ion-exchange reactions increase five to ten-times in the D240N mutant of NCX_Mj, thus suggesting that the aspartate to asparagine replacement in eukaryotic species may represent an evolutionary improvement of catalytic power in mammalian NCX orthologs [57].

Previous kinetic studies provided strong evidence that the $3Na^+$ ion and $1Ca^{2+}$ ion are transported in separate steps throughout the transport cycle [58]. In agreement with this, the crystal structure of NCX_Mj revealed that the simultaneous occupation of all four sites by $3Na^+$ and $1Ca^{2+}$ is thermodynamically forbidden [20]. According to the original interpretation of the crystallographic data, S_{ext}, S_{mid}, and S_{int} are occupied by $3Na^+$ ions, and S_{Ca} is occupied by $1Ca^{2+}$ [20]. Recent MD simulations and ion flux analyses revealed that $3Na^+$ ions occupy S_{ext}, S_{int}, and S_{Ca}, whereas the Ca^{2+} ion occupies S_{Ca} [57]. According to this interpretation, S_{mid} does not bind either the Na^+ or Ca^{2+} ions, where one water molecule is bound to protonated D240. To date, no systematic studies have been undertaken to resolve the catalytic status of putative ion-coordinating residues belonging to S_{mid} or any other site. Despite this progress, it remains unclear how partial occupation of four sites by Ca^{2+}

or three Na^+ ions drives the sliding of TM1/TM6 to initiate alternating access and how the ion transport cycle becomes accelerated by Ca^{2+} interaction with regulatory CBD residues in eukaryotic NCX orthologs.

2.3 Structural Organization of Regulatory CBD Domains

All eukaryotic NCX orthologs (including CALX) contain a huge cytosolic f-loop between TM5 and TM6, bearing the Ca^{2+}-binding regulatory domains, CBD1 and CBD2 [11–19]. The CBD1 and CBD2 domains are connected in a head-to-tail fashion through a very short linker (five residues) to form a two-domain (CBD12) tandem [15, 40]. It was proposed that charged auto-inhibitory XIP sequence (20 amino acids), exhibiting an α-helix structure [33], located at the N-terminus of the f-loop, is involved in both Na^+ and PIP_2-dependent regulation [58–60].

High-resolution X-ray and NMR studies of isolated CBD1 and CBD2 domains revealed an immunoglobulin-like β-sandwich structure with seven antiparallel β-strands containing four Ca^{2+} binding sites (Ca1–Ca4) on CBD1 and two Ca^{2+} sites (CaI–CaII) on CBD2 [41–43, 61]. The CBD domains share a common core structure typical of C_2-type domain folding, which occurs in many regulatory proteins (synaptotagmins, $cPLA_2$, PKC, titin, fibronectin, neuronal cell adhesion factors, among others), although the underlying mechanisms are poorly understood. In general, such C_2 domains are known to interact with diverse effectors (e.g., Ca^{2+}, PIP_2, lipids, and other proteins), although so far, the two CBD domains in NCX only appear to interact with Ca^{2+}.

In the cardiac, brain, and kidney variants the Ca3 and Ca4 sites of CBD1 have high affinity for Ca^{2+} binding (K_d = 0.05–0.2 μM), whereas the remaining two sites of CBD1, Ca1, and Ca2 possess low affinity for Ca^{2+} (K_d > 20 μM) [41–43, 61]. In the cardiac and brain variants, the CaI site of CBD2 binds Ca^{2+} with a K_d of ~10 μM, whereas the CaII site of CBD2 exhibits lower affinity for Ca^{2+} binding [41–43, 61]. Mutant analysis of full-size NCX revealed that in the cellular system only three of the six Ca^{2+} sites (Ca3 and Ca4 on CBD1 and CaI on CBD2) contribute to $[Ca^{2+}]$-dependent allosteric regulation of NCX [62–65]. Namely, the Ca3–Ca4 sites are responsible for primary allosteric regulation with a $K_{0.5}$ value of 0.2–0.4 μM, whereas the CaI site is involved in $[Ca^{2+}]$-dependent alleviation of Na^+-dependent inactivation with a $K_{0.5}$ value of ~10 μM [41–43, 61]. Most probably, the low affinity sites (Ca1, Ca2, and CaII) are the Mg^{2+} rather than the Ca^{2+} sites, which are constitutively occupied by Mg^{2+} under physiologically relevant ionic conditions [66]. Interestingly, the occupation of Ca1–Ca2 sites by Mg^{2+} decreases the affinity of the primary sensor (Ca3–Ca4 sites), whereas the occupation of the CaII site by Mg^{2+} increases the affinity of the CaI site [23, 46, 47]. The physiological significance underlying this is to keep the primary and secondary Ca^{2+} sensors within a physiologically relevant range, thereby covering the effective concentration range of 0.2–10 μM Ca^{2+}. Thus, CBD1 contains a high-affinity allosteric Ca^{2+} sensor (Ca3–Ca4 sites), the affinity and kinetics of which are modulated by a spliced segment on CBD2 [62–65].

3 CBD Domains as Highly Sensitive Sensors of Ca^{2+} and H^+, but not of Na^+

3.1 *Ionic Modes of NCX Regulation by Cytosolic Ca^{2+}, H^+, and Na^+*

In mammalian tissues the cytosolic Ca^{2+} activates NCX, whereas the cytosolic Na^+ and H^+ inhibit NCX activities [23, 67–70]. Recent electrophysiological studies revealed that in cardiac NCX1.1 both CBDs can contribute to $[Ca^{2+}]$-dependent regulation of NCX, where the Ca3–Ca4 sites of CBD1 largely govern allosteric activation, with $K_{0.5} \sim 0.3$ μM, whereas the CaI site of CBD2 alleviates Na^+-dependent inactivation, with $K_{0.5} \sim 5$ μM [62–65]. Notably, 100 mM Na^+ has no effect on Ca^{2+} binding affinity or stoichiometry regarding CBD domains, thereby suggesting that Na^+ and Ca^{2+} ions do not compete for occupation of function sites on CBDs [39, 43, 61]. This is consistent with the claim that Na^+-dependent inactivation is due to Na^+ binding to transport sites, whereas the Ca^{2+} binding to the CaI site of CBD2 somehow relieves the inhibitory effect [62–65]. However, it has been known for a long time that eukaryotic NCX is extremely sensitive to mild cytosolic acidification (a pH decrease from 7.2 to 6.9 results in nearly 90 % inactivation of NCX), thereby suggesting the physiological relevance of NCX "proton block" under acidosis and ischemia conditions [23, 39, 71, 72]. In general, H^+ may interact with transport and/or regulatory domains, although there is no evidence that within the physiological range of pH the protons affect the ionization of ion-binding transport sites. Recent progress on these issues is summarized below.

3.2 *Unusually High Degree of Cooperativity for Allosteric Regulation of Cardiac NCX*

Owing to large and rapid changes in cytosolic $[Ca^{2+}]$ during the action potential, the $[Ca^{2+}]$-dependent allosteric activation of NCX is especially important in excitable tissues [22, 37, 38, 73]. Namely, in cardiomyocytes, only ~5 % of the maximal NCX current is detected at resting $[Ca^{2+}]_i$ levels, whereas the rise of $[Ca^{2+}]_i$ from 0.1 μM to 1–2 μM recruits nearly 100 % of NCX-mediated current [39, 73, 74]. The "surprising" finding is the very large Hill-coefficient ($n_H = 8$) for Ca^{2+}-dependent activation of NCX1.1 in intact cardiomyocytes [39, 73]. It is impossible to explain the observed high values of cooperativity, even so, one assumes the involvement of all six Ca^{2+} binding sites of CBD12 (which apparently is not the case). Therefore, some additional mechanisms should be considered for such a high Ca^{2+}-dependent allosteric activation. For example, the recently discovered Ca^{2+}-dependent dimerization of NCX molecules could be a relevant mechanism in intact cells [47], although more dedicated experimentation is required to demonstrate the physiological relevance of this putative mechanism. Nevertheless, the extreme cooperativity of NCX

does have important physiological implications, thereby indicating a high sensitivity of the Ca^{2+} extrusion to changes in $[Ca^{2+}]_i$. This would be highly consistent with the remarkable role of NCX in regulating $[Ca^{2+}]_i$.

3.3 Regulatory CBD Domains as Cytosolic pH/Ca^{2+} Sensors

Since among the six Ca^{2+} binding sites of CBDs, only three sites (Ca3, Ca4, and CaI) actually contribute to $[Ca^{2+}]$-dependent regulation of NCX1, it is reasonable to determine the functional role of the remaining three low affinity sites (K_d>20 μM) [39, 61–65]. Notably, the low-affinity Ca^{2+} sites are located in very near (3–4 Å) the "functionally active" high-affinity Ca^{2+} sites [16, 40, 48]; therefore, it is possible that these "invalid" low-affinity Ca^{2+} sites act as the pH and not the Ca^{2+} sensor. Recent multidisciplinary studies by using the intact cardiomyocytes as well as the isolated preparations of CBD1, CBD2, and CBD12 proteins clearly demonstrate that Ca^{2+} and protons can compete with each other for functional sites on CBDs [39, 43, 61]. Interestingly, high cooperativity for Ca^{2+}-dependent activation of NCX currents was observed at both pH 7.2 and 6.9; however, the concentration dependence of the Ca^{2+}-activation curve was dramatically shifted to the higher concentration of Ca^{2+}. Notably, the close adjacency of Ca^{2+} sites in CBDs is consistent with the sharp dependence of Ca^{2+} binding on pH, thereby suggesting the cooperative nature of binding domain folding. More specifically, the binding of the first Ca^{2+} ion may partially (or fully) deprotonate the coordinating residue(s), thereby enabling the next Ca^{2+} ion to bind to the remaining site(s). A similar mechanism was proposed for the C2 domain of phospholipase A2, in which two Ca^{2+} sites are separated by 4.1 Å [75]. The physiological significance of these findings is that an acidic pH may shut down NCX to prevent an NCX-mediated high risk of generating the arrhythmias under ischemia/acidosis conditions.

4 Synergistic Interactions between CBDs and Dynamic Coupling

4.1 The CBD2 Domain Shapes the Ca^{2+}-Sensing Properties of the Allosteric Sensor on CBD1

Recent studies with the brain, cardiac, and kidney splice variants of an isolated two-domain tandem (CBD12) have demonstrated that two CBDs communicate with each other, thereby increasing 10–50 times the affinity for Ca^{2+} at high-affinity Ca3–Ca4 sites, while concomitantly decelerating Ca^{2+} off-rates [40–43]. The slow dissociation of "occluded" Ca^{2+} (observed in isolated CBD12, but not in isolated CBD1 or CBD2) is the most characteristic hallmark for the functional coupling of the two CBD domains [40, 43–45, 61], thereby representing the physical

basis for slow inactivation (I_1 and/or I_2 states) of full-size NCX proteins, observed in electrophysiological experiments [52–55, 61–73]. Interestingly, the synergistic interactions between the two CBD domains are stronger in the kidney and cardiac splice variants than in the brain splice variant, thereby suggesting that the relevant mechanisms may contribute to regulatory specificity of NCX variants [42–44]. These findings are in a good agreement with the results of FRET experiments using the isolated preparations of CBD12 and full-size NCX [46, 47] as well as with the results of whole-cell patch-clamp experiments [62–65, 70–73]. The striking finding is that the interdomain CBD1–CBD2 linker plays a critical role in controlling the synergistic interactions between CBDs, thereby affecting the dynamic properties of a primary Ca^{2+} sensor involved in allosteric regulation [42–45]. Crucial mechanistic questions that have emerged from these studies are: how does Ca^{2+} binding couple with regulatory conformational transitions to decode the allosteric signal and, in turn, how does this coupling contribute to the transmission of regulatory information to ion transport domains. Since previous studies have shown that both CBD domains contribute to allosteric regulation of NCX through interdomain coupling (see above), the emerging goal is to elucidate how the Ca^{2+} binding to CBD1 is decoded and propagated to ion transport domains. These questions are especially interesting in light of the fact that the structure of a primary sensor on CBD1 is extremely well preserved among all isoform/splice variants [15, 19, 40, 76].

4.2 A Two-Domain Interface-Structure Encodes Ca^{2+}-Driven Tethering of CBDs

Although the identification of synergistic interactions between the two CBD domains provided convincing evidence for CBD2-dependent modification of the affinity and kinetic properties of Ca^{2+} sensing at the primary Ca^{2+} sensor (Ca3–C4 sites) on CBD1 [42, 43, 61], only the recently derived crystal structures of the two-domain CBD12 tandem [40] (Fig. 7.2), in conjunction with advanced biophysical approaches (NMR, SAXS, HDX-MS, and stopped-flow mixing), have revealed the underlying mechanisms of Ca^{2+}-dependent interactions between the CBDs [77]. The CBD12 crystal structures of NCX1.4 (CBD12-AD, brain splice variant) [40] and CALX1.1 and CALX1.2 [77] have shown a strikingly similar interface between the two CBD domains, where the Ca^{2+} binding to the primary sensor (Ca3–Ca4 sites) on CBD1 results in interdomain tethering of CBDs through the residues located on CBD1 (Asp499 and Asp500) and CBD2 (Arg532 and Asp565). Interestingly, the buried R532 of CBD2 is a central residue in the network, tethering D565 in CBD2 and D499 and D500 in CBD1 (Fig. 7.3b, c). Most importantly, this interdomain bifurcated salt-bridge supports Ca^{2+} coordination with D499 and D500, since it is a part of the Ca3–Ca4 sites [40, 76]. Thus, Ca^{2+} binding to Ca3–Ca4 couples CBDs to the interface, consequently restricting interdomain flexibility. Consistent with this observation, mutant analyses of isolated CBDs suggest that the two-domain interface governs Ca^{2+}-driven conformational alignment of CBDs, resulting in slow

dissociation of "occluded" Ca^{2+} from CBD12 (Fig. 7.3), thereby mediating the Ca^{2+}-induced conformational transitions associated with allosteric signal transmission [40–45, 61, 77]. More specifically, occupation of Ca3–Ca4 sites by Ca^{2+} induces disorder-to-order transition owing to charge neutralization and coordination, thereby constraining CBD conformational freedom, thus rigidifying the NCX1 f-loop and triggering allosteric signal transmission [43–45, 77]. This newly found Ca^{2+}-driven "interdomain switch" is highly conserved among all NCX isoform/splice variants comprising the regulatory CBD domains on the loop-f [76, 77].

4.3 The Critical Role of the Interdomain Linker in Ca^{2+}-Driven CBD Coupling

The CBD12 crystal structures of NCX1.4, CALX1.1, and CALX1.2 reveal a relatively small contact area (~360 $Å^2$) between the CBDs [76, 77], thereby confirming the previous claim suggesting that such a brief domain-domain contact cannot occur in solution without the interdomain linker [39, 43, 44, 61]. Moreover, several lines of evidence reveal that the linker selectively retains, modifies, and integrates the intrinsic dynamic features of the Ca3, Ca4, and CaI sites, thereby allowing NCX regulation within the physiologically relevant dynamic range [40–48]. For example, in the brain splice variant, the linker-dependent constraints decelerate up to 50 times the Ca^{2+} off-rates of occluded Ca^{2+} and increase up to 10 times the affinity at the primary allosteric sensor of Ca^{2+} on CBD1, while the linker largely retains the intrinsic properties of the CaI site on CBD2 in the CBD12 tandem [42, 43]. The "alanine-walk" substitutions in the CBD1–CBD2 linker (501-HAGIFT-506) have shown that among all linker residues, only G503 is obligatory for Ca^{2+}-induced reorientations of CBDs and slow dissociation of occluded Ca^{2+} [43, 44]. Moreover, swapping between positions A502 and G503 in the CBD1–CBD2 linker results in the complete loss of slow dissociation of occluded Ca^{2+}, meaning that dynamic coupling of CBDs requires an exact pose of glycine at position 503, which is absolutely required for Ca^{2+}-driven tethering of CBDs, thereby limiting the linker's flexibility and restricting the interdomain movements of CBDs [43–45]. According to the crystal structure of CBD12 [40, 76], the dihedral φ/ψ angles at position 503 are only allowed for glycine and any other residue in that specific position will

Fig. 7.3 (continued) clearly acts as the principal linchpin holding the two CBDs together. (**c**) The two CBD domains are tethered in a Ca^{2+}-dependent manner, involving amino acids from both CBD1 and CBD2. The buried R532, located in CBD2, is a central residue in the interface, tethering D565 in CBD2 and D499 and D500 in CBD1. Thus, Ca^{2+} binding to the Ca3–Ca4 sites couples directly to the interdomain interface to restrict the interdomain flexibility of the CBDs. Consistent with biophysical studies the Ca3–Ca4 sites are obligatory for robust interdomain interactions upon Ca^{2+} binding, since D499 and D500 are disordered in the apo-form. (**d**) The interface residues are colored according to their conservation score, thereby demonstrating that most residues at the two-domain interphase are highly conserved among the mammalian NCX1–3 and CALX variants

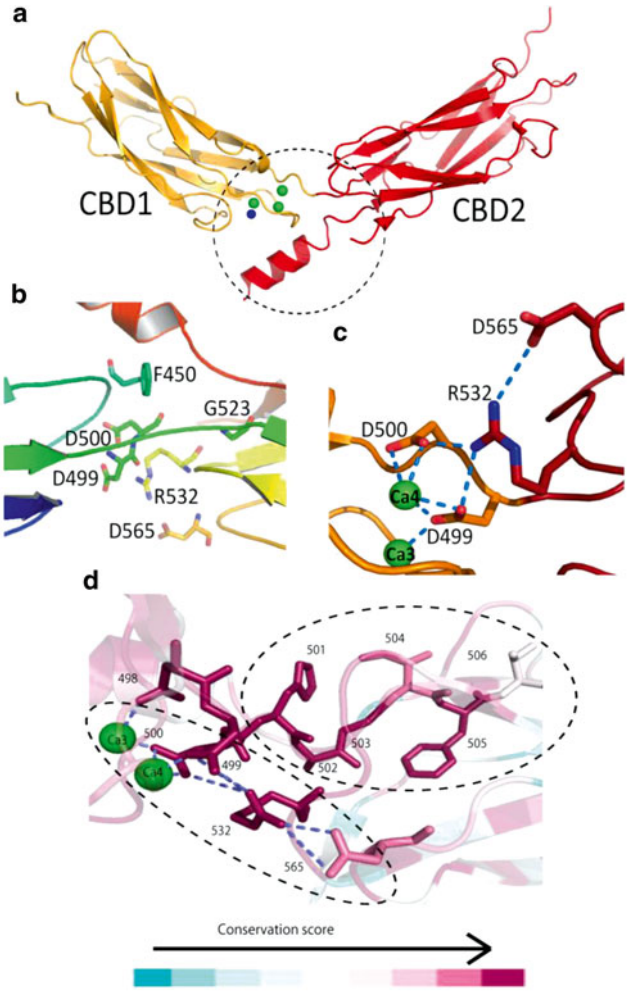

Fig. 7.3 The interface structure of the two-domain CBD12 tandem. (**a**) Crystal structure of the NCX1.4-CBD12-E454K mutant (3US9), which largely retains the wild-type phenotype in ion-transport activities and regulation as well as the Ca^{2+} binding affinities and Ca^{2+} off-rates in isolated CBD2 and CBD12 protein preparations. CBD1 and CBD2 are colored *orange* and *red*, respectively. The *rectangles* frame a zoom perspective as depicted in panels **b** (*blue*), **c** (*magenta*), and **d** (*green*). *Green* and *blue spheres* depict Ca^{2+} ions and water molecules, respectively. (**b**) The interface involves mainly interactions of the CBD1 Ca^{2+} binding loops with the interdomain linker, the CBD2 flexible FG loop and the strictly conserved CBD2 BC loop. Although more than 20 residues are buried in the interface, only a few prominent interactions between residues from both domains are observed. The interface may be subdivided into three regions, two hydrophilic and one hydrophobic. The first hydrophilic region includes a pivotal interdomain electrostatic network centered at R532 in CBD2. This arginine takes a conformation that forms bifurcated hydrogen-bonded and non-hydrogen bonded salt-bridges with D499, D500 in CBD1 and D565 in CBD2. D499 and D500 also participate in the coordination of the Ca3–Ca4 sites, thereby playing a direct role at the primary Ca^{2+} sensor while concomitantly stabilizing the tandem domain interface. This network

require rotation around the Cα of this residue, resulting in steric clashes in the protein structure. Strikingly enough, electrophysiological experiments revealed that mutations of either G503 in intact (full-size) NCX1 (owing to activation by regulatory Ca^{2+}) or analogues G555 in CALX1.1 (owing to inhibition by regulatory Ca^{2+}) largely lose the [Ca^{2+}]-dependent regulation in a cellular system [78, 79], thereby underscoring the conclusions reached by structure-dynamic studies [40, 77]. All these findings are consistent with a general theory suggesting that in multidomain regulatory proteins the linker's structure encodes successive conformational transitions in managing allosteric signal transfer and thus, the proteins behave as "vehicles" [80, 81].

4.4 Structure-Functional Comparison of the CBD12 Interface with Other Proteins

The conservation and structural composition of the two-domain interface point to a general mechanism that governs the NCX family [40]. Importantly, the architecture of this interface differs from the tandem C2 domains of synaptotagmin and PKC [82, 83], implying a different mode of action [82–84]. Rather, motif searches [83, 84] of the PDB reveal a striking similarity with the cadherin extracellular domain, which bears multiple β-sandwich domains bridged by small interfaces, and which contains three Ca^{2+} sites [85]. Cadherin studies demonstrated that Ca^{2+} rigidifies the protein [86], enabling cell–cell interactions. Furthermore, in vivo studies suggest that extracellular Ca^{2+} fluctuations may physiologically regulate cadherin activity [86, 87], suggesting the relevance of Ca^{2+}-dependent rigidification as a principal mechanism. In addition, the tandem architecture is reminiscent of the arrestin family, where tandem β sandwiches are opposed by a polar core of buried charged residues [87]. Disruption of this polar core activates arrestin for high-affinity binding to its GPCR target [87]. A similar mechanism may occur in CBD12, where the deeply buried F450 prevents Ca^{2+}-dependent rigidification of specific segments on CBD1 [70, 76, 77]. These parallel actions share a common denominator of interfaces with charge interactions within the polar environment, wherein charged ligands induce structural transitions, imparting a certain regulatory message. Analogously with CBD12 [40, 47], the Ca^{2+} binding to a two-domain construct of cadherin restricts the linker motions substantially [85]. Nevertheless, the Ca^{2+} binding modes of cadherins and CBD12 are dissimilar. Namely, the Ca^{2+} binding to the two-domain cadherin construct involves direct interactions with residues in the linker region, whereas the binding of Ca^{2+} to sites Ca3 and Ca4 in CBD1 involves ligation with residues 498–500 that directly precede linker residues 501–503 [40–43]. Analogously to CBD12, in Rabphilin-3A the C2A–C2B linker results in ~10-fold increase in Ca^{2+} affinity through interdomain interactions [83]. However, in contrast to CBD12, the linker of Rabphilin-3A itself contributes to the ligation sphere.

5 Conformational Possessions Associated with Allosteric Signaling

5.1 *A Common Mechanism Underlies Signal Decoding upon Ca^{2+} Binding to Ca3–Ca4 Sensor*

Recently, the crystal structures of Ca^{2+} bound CBD12 tandems from the two CALX splice variants, CALX1.1 and CALX1.2, were resolved [40, 76], where these two splice variants exhibit different responses to regulatory Ca^{2+}. Namely, the Ca^{2+} binding to CBDs of CALX1.1 inactivates the exchanger activities, whereas the regulatory Ca^{2+} has no effect on the exchanger's activity in the CALX-1.2 variant [53–55, 78, 79]. According to the original interpretation of this work, the regulatory differences between the two CALX splice variants arise from different hinge angles between the CBD domains, showing 118° and 110.5° for CALX1.1 and CALX1.2, respectively [76]. However, this interpretation was challenged by a more recently derived crystal structure of a Ca^{2+}-bound CBD12 tandem from the brain splice variant (NCX1.4) [40], since the hinge angle of NCX1.4 (113°) and CALX1.1 (118°) are quite similar in these variants, taking into account the overall structural similarities (r.m.s.d of 1.86 Å for 214 Cα atoms) [40]. These findings are especially interesting in the context of the regulatory differences in these variants, since NCX1.4 is activated by regulatory Ca^{2+}, whereas CALX1.1 is inhibited by allosteric interactions with Ca^{2+} [53–55]. Thus, the structural similarities between CBD12 from NCX and CALX imply that the different responses to regulatory Ca^{2+} cannot be attributed solely to the orientation of CBDs in the CBD12 tandem. Moreover, the X-ray crystallography, NMR, FRET, and SAXS techniques failed to identify any changes in the interdomain orientation of CBDs upon Ca^{2+} binding to the CBD12 tandem in any isoform/splice variant tested to date [40–48]. Since the primary allosteric sensor on CBD1 (Ca3–Ca4 sites) and the two-domain interface in the CBD12 tandem are nearly identical among eukaryotic NCXs, including CALX, the Ca^{2+}-driven local conformational changes might represent a general mechanism for initial decoding of regulatory signals in NCX variants (Fig. 7.3d). After the initial decoding of regulatory information upon Ca^{2+} binding to Ca3–Ca4 sites, the allosteric signal is further modified (transformed) and propagated by the CBD2 domain, which in turn, is controlled by a splice-variant segment (see below).

5.2 *Population Shift Underlies the Ca^{2+} Induced Dynamic Changes in the CBD Domains*

It was previously suggested that an electrostatic switch at CBD1 underlies Ca^{2+}-dependent activation of NCX; also it remains unclear how this may induce conformational changes that are relevant to regulatory activities [19]. A recent analysis

revealed that Ca^{2+} interaction with the primary allosteric sensor is not merely an electrostatic switch rather than a Ca^{2+}-switch situated at the interface of CBDs, although no global conformational changes in the CBDs' alignment are observed concerning either the interdomain angle or the distance between the CBD domains [40, 45, 77].

In general terms, "induced fit" and "conformational selection" (population shift) hypotheses were proposed as the principal mechanisms underlying ligand-induced dynamic coupling in proteins. In addition, both mechanisms may exist in a given protein at different stages of the activity cycle [80, 81]. Accumulating data obtained by NMR [48], FRET [46, 47], and SAXS [45] analyses suggest a model whereby Ca^{2+} binding to the primary allosteric sensor (Ca3–Ca4 sites) induces a population shift rather than global conformational changes in CBDs [45]. The presence of a putative population shift mechanism presumes that numerous conformational transitions occur over relatively small energetic barriers [45, 80, 81]. According to the population shift mechanisms all conformational states already preexist in apo protein, where the ligand binding to protein shifts the fractional distribution of preexisting conformational states [80, 81]. Recent findings reveal that Ca^{2+} binding to the Ca3–Ca4 sites results in a "population shift", where more constraint conformational states become highly populated at dynamic equilibrium in the absence of global conformational transitions in the CBDs' alignment [45]. The mechanism underlying the population shift may have physiological significance for NCX proteins, since an induced fit can take place under one of two scenarios: a high concentration of ligand or a high affinity of protein to ligand. However, neither of these regulatory conditions seems to take place in the cell. Moreover, induced fit is much faster than population shift, which needs to overcome a barrier (a higher barrier leading to a slower population shift), so the observed slow rate constants for dissociation of occluded Ca^{2+} ($k_{obs} \sim 0.5\ s^{-1}$) from CBD12 [40–44] and slow I_2 inactivation ($t_{0.5} \sim 2$ s) of intact NCX, observed in electrophysiological experiments [52–55, 62–68], are compatible with a population shift mechanism [45].

5.3 Allosteric Signal Propagation in NCX Isoform/Splice Variants

Previous studies have suggested a common mechanism for decoding the initial signal upon Ca^{2+} interaction with Ca3–Ca4 sites on CBD1, although neither of them addressed the pathway by which the allosteric signal is conveyed, nor explained how the regulatory responses are diversified in different ortholog/splice variants, even though the isoform/splice variants share very common structural motifs. Only recent studies using HDX-MS techniques provided a breakthrough in understanding the mechanistic insights regarding both aspects of allosteric NCX regulation [77]. The advantage of the HDX-MS technique is that relatively small variations in the backbone conformational dynamics can be identified even in the absence of global conformational changes. Surprisingly enough, slight nuances in

splicing-derived structural differences at the domains' interface result in major variations in the dynamic properties of the backbone, which may underlie either positive (NCX-1.4), negative (CALX-1.1), or no response (CALX-1.2) to regulatory Ca^{2+} [52–55]. Interestingly, F450 (which is deeply buried in the interface, interacting with the interdomain linker and with the helical segment of CBD2's FG-loop), prevents the signal transfer toward CBD1, while stabilizing the apo-CBD1 and directing the signal propagation upon Ca^{2+} binding through the linker toward CBD2 over a distance of 50 Å [77] (Fig. 7.4). Most importantly, the Ca^{2+}-induced decrease in backbone flexibility at CBD2 segments correlates with regulatory specificity (negative, positive, or no response to Ca^{2+}) in a given splice variant. Namely, for CALX1.1, in which a minimal response to Ca^{2+} occurs, the exchanger remains inhibited; for NCX1.4, in which a maximal response to Ca^{2+} occurs, the exchanger is activated; an intermediate phenotype is observed for CALX-1.2, which also exhibits intermediate changes in backbone flexibility in response to Ca^{2+} [77]. Therefore, the fastening of the CBD2 FG loop helix (which is a part of the alternative splicing segment) to the CBD1 Ca^{2+} binding region (which involves hydrophobic interactions centered at F450) can rigidify the F and G strands of CBD2 up to the domain tip [77]. This may represent the principal mechanism of allosteric signal propagation upon Ca^{2+} binding to the primary sensor (Ca3–Ca4 sites). Based on these observations, it has been proposed that specific structure-dynamic determinants balance between the translational and rotational movements within CBD12 to shape the dynamic domains' coupling, thereby yielding either positive, negative, or no response to regulatory Ca^{2+} [77]. These findings provide a structure-dynamic basis by which alternative splicing diversifies responses to regulatory Ca^{2+} in NCX isoform/splice variants and controls the propagation of allosteric signals over long distances. The next challenge is to elucidate how the allosteric signal propagates from the CBD2 domain to transport sites of NCX.

6 Conclusions

Recent structural and biophysical studies revealed a common module for decoding the Ca^{2+} induced allosteric signal in NCX proteins at the interface of the two CBD domains and identified the structure-dynamic determinants that govern the phenotype variances in response to regulatory Ca^{2+} in a given isoform/splice variant exhibiting either positive, negative, or no response to regulatory cytosolic Ca^{2+}. The major conclusions of recent achievements can be summarized as follows:

1. The high-affinity Ca3–Ca4 sites of CBD1 serve as the primary allosteric sensors for Ca^{2+} and their structures are highly conserved among all NCX variants, whereas the CaI site on CBD2 secondarely modifies the regulatory properties of the primary allosteric sensor on CBD1 and is responsible for Ca^{2+}-dependent alleviation of Na^{+}-dependent inactivation.
2. An alternating segment, exclusively located on CBD2, is in proximity to the primary allosteric sensor on CBD1 and in conjunction with other structural

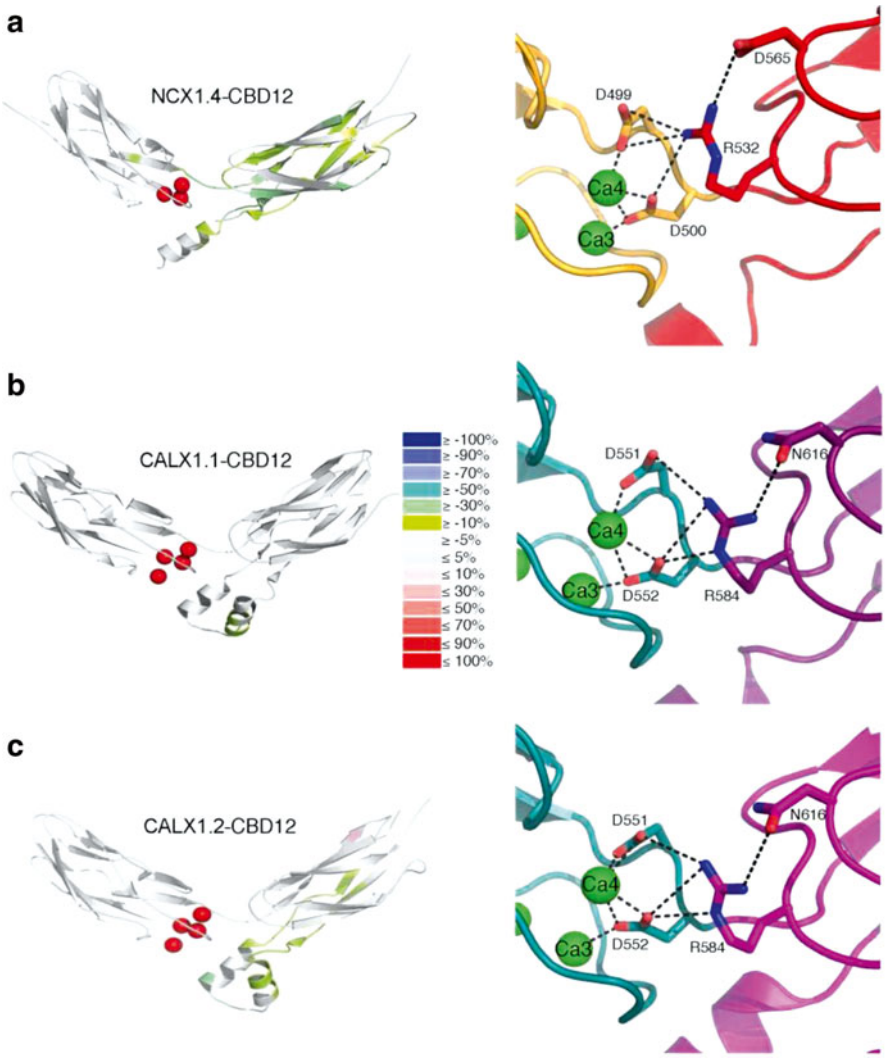

Fig. 7.4 Characteristic differences in Ca^{2+}-dependent rigidification of the CBD2 backbone in diverse isoform/splice variants. The difference between the HDX-MS profiles of the apo and Ca^{2+}-bound forms are depicted for diverse variants showing the positive (NCX1.4-CBD12) (**a**), negative (CALX1.1-CBD12) (**b**) and no response (CALX1.2-CBD12) (**c**) to regulatory Ca^{2+} The HDX-MS data points are overlaid onto the crystal structure (PDB 3US9) of CBD12-1.4-E454K. Ca^{2+} is indicated as *red spheres*. The color legend shows the differential HDX after Ca^{2+} binding

components, at the interface of CBDs; it shapes the Ca^{2+} binding affinity and dissociation rates of "occluded" Ca^{2+} in the cardiac, brain, and kidney splice variants of NCX1.

3. The short interdomain linker plays a critical role in Ca^{2+}-driven coupling of CBD domains by two different means: On the one hand, the linker directs Ca^{2+}-driven tethering of CBDs to form an interdomain Ca^{2+} saltbridge, whereas, on the other

hand, the relay of CBDs (upon Ca^{2+} binding and formation of interdomain Ca^{2+} saltbridge) stabilizes stochastic oscillations of the linker to restrict CBD movements.

4. The two-domain interface controls Ca^{2+}-induced tethering of CBDs and slow dissociation of occluded Ca^{2+}, where the occupation of the primary allosteric sensor (Ca3–Ca4 sites) by Ca^{2+} rigidifies the interdomain linker and thus, the dynamic movements of CBDs. This represents a common mechanism for decoding the initial information upon Ca^{2+} binding for all NCX isoform/splice variants.
5. In Ca^{2+}-bound conformations, the interdomain angle of CBD12 is very similar for NCX1.4 and CALX1.1, meaning that the interdomain angle (and/or distance) between the two domains cannot account for the regulatory diversity in NCX1.4 and CALX1.1, thus showing the positive and negative responses to regulatory Ca^{2+}.
6. Ca^{2+} binding to the Ca3–Ca4 sites results in a "population shift", where more constraint conformational states become highly populated at dynamic equilibrium in the absence of global conformational transitions in the CBDs' alignment.
7. Upon Ca^{2+} binding to Ca3–Ca4 sites of CBD1 the conformational states with rigidified backbone flexibility of CBD2 (but not of CBD1) become populated, where the extent and strength of Ca^{2+}-dependent rigidification of CBD2 is diversified by the splice-variant segment on CBD2. The newly fond conformational states correlate with disparate regulatory responses to Ca^{2+} observed in diverse variants of eukaryotic NCXs exhibiting either positive, negative or no response to regulatory Ca^{2+}.

Acknowledgements I express my most sincere gratitude to Ernesto Carafoli for thoughtful, didactic and unforgettable talks on scientific and on non-scientific (still very important) issues. This work was partially funded by the USA-Israel Binational Foundation Research Grant #2009-334, and the Israel Science Foundation Grant #825/14. The support of the Fields Estate Foundation is highly appreciated.

References

1. Carafoli E (1987) Intracellular calcium homeostasis. Annu Rev Biochem 56:395–433
2. Berridge MJ, Bootman MD, Roderick HL (2003) Calcium signalling: dynamics, homeostasis and remodelling. Nat Rev Mol Cell Biol 4:517–529
3. Khananshvili D (2013) The SLC8 gene family of sodium-calcium exchangers (NCX)—structure, function, and regulation in health and disease. Mol Aspects Med 34:220–235
4. Khananshvili D (2014) Sodium-calcium exchangers (NCX): molecular hallmarks underlying the tissue-specific and systemic functions. Pflugers Arch 466:43–60
5. Brini M, Calì T, Ottolini D, Carafoli E (2014) The plasma membrane calcium pump in health and disease. FEBS J 280:5385–5397
6. Lopreiato R, Giacomello M, Carafoli E (2015) The plasma membrane calcium pump: new ways to look at an old enzyme. J Biol Chem 289:10261–10268
7. Baazov D, Wang X, Khananshvili D (1999) Time-resolved monitoring of electrogenic Na^{+}-Ca^{2+} exchange in the isolated cardiac sarcolemma vesicles by using a rapid-response fluorescent probe. Biochemistry 38:1435–1445

8. Niggli E, Lederer WJ (1991) Molecular operations of the sodium-calcium exchanger revealed by conformational currents. Nature 349:621–624
9. Hilgemann DW, Nicoll DA, Philipson KD (1991) Charge movement during Na^+-translocation by native and cloned Na^+/Ca^{2+} exchanger. Nature 352:715–718
10. Almagor L, Giladi M, van Dijk L, Buki T, Hiller R, Khananshvili D (2014) Functional asymmetry of bidirectional Ca^{2+}-movements in an archaeal sodium-calcium exchanger (NCX_Mj). Cell Calcium 56:276–284
11. Philipson KD, Nicoll DA (2000) Sodium-calcium exchange: a molecular perspective. Annu Rev Physiol 62:111–133
12. Nicoll DA, Longoni S, Philipson KD (1990) Molecular cloning and functional expression of the cardiac sarcolemmal Na^+-Ca^{2+} exchanger. Science 250:562–565
13. Cai X, Lytton J (2004) The cation/Ca^{2+} exchanger superfamily: phylogenetic analysis and structural implications. Mol Biol Evol 21:1692–1703
14. Lytton J (2007) Na^+/Ca^{2+} exchangers: three mammalian gene families control Ca^{2+}-transport. Biochem J 406:365–382
15. Hilge M, Aelen J, Vuister GW (2006) Ca^{2+} regulation in the Na^+/Ca^{2+} exchanger involves two markedly different Ca^{2+} sensors. Mol Cell 22:15–25
16. Nicoll DA, Sawaya MR, Kwon S, Cascio D, Philipson KD, Abramson J (2006) The crystal structure of the primary Ca^{2+} sensor of the Na^+/Ca^{2+} exchanger reveals a novel Ca^{2+} binding motif. J Biol Chem 281:21577–21581
17. Besserer GM, Ottolia M, Nicoll DA, Chaptal V, Cascio D, Philipson KD, Abramson J (2007) The second Ca^{2+}-binding domain of the Na^+/Ca^{2+} exchanger is essential for regulation: crystal structures and mutational analysis. Proc Natl Acad Sci U S A 104:18467–18472
18. Chaptal V, Ottolia M, Mercado-Besserer G, Nicoll DA, Philipson KD, Abramson J (2009) Structure and functional analysis of a Ca^{2+} sensor mutant of the Na^+/Ca^{2+} exchanger. J Biol Chem 284:14688–14692
19. Hilge M, Aelen J, Foarce A, Perrakis A, Vuister GW (2009) Ca^{2+} regulation in the Na^+/Ca^{2+} exchanger features a dual electrostatic switch mechanism. Proc Natl Acad Sci U S A 106:14333–14338
20. Liao J, Li H, Zeng W, Sauer DB, Belmares R, Jiang Y (2012) Structural insight into the ion-exchange mechanism of the sodium/calcium exchanger. Science 335:686–690
21. Reeves JP, Hale CC (1984) The stoichiometry of the cardiac sodium-calcium exchange system. J Biol Chem 259:7733–7739
22. Blaustein MP, Lederer WJ (1999) Sodium/calcium exchange: its physiological implications. Physiol Rev 79:763–854
23. DiPolo R, Beauge L (2006) Sodium/calcium exchanger: influence of metabolic regulation on ion carrier interactions. Physiol Rev 86:155–203
24. Reuter H, Seitz N (1968) The dependence of calcium efflux from cardiac muscle on temperature and external ion composition. J Physiol 195:451–470
25. Baker PF, Blaustein MP, Hodgkin AL, Steinhardt RA (1969) The influence of calcium on sodium efflux in squid axons. J Physiol 200:431–458
26. Linck B, Qiu Z, He Z, Tong Q, Hilgemann DW, Philipson KD (1998) Functional comparison of the three isoforms of the Na^+/Ca^{2+} exchanger (NCX1, NCX2, NCX3). Am J Physiol 274:C415–C423
27. Carafoli E, Tiozzo R, Lugli G, Crovetti F, Kratzing C (1974) The release of calcium from heart mitochondria by sodium. J Mol Cell Cardiol 6:361–371
28. Palty R, Silverman WF, Hershfinkel M, Caporale T, Sensi SL, Parnis J, Nolte C, Fishman D, Shoshan-Barmatz V, Herrmann S, Khananshvili D, Sekler I (2010) NCLX is an essential component of mitochondrial Na^+/Ca^{2+} exchange. Proc Natl Acad Sci U S A 107:436–441
29. Verkhratsky A, Parpura V (2014) Calcium signaling and calcium channels: evolution and general principles. Eur J Pharmacol 739:1–3
30. Pizzo P, Drago I, Filadi R, Pozzan T (2012) Mitochondrial Ca^{2+} homeostasis: mechanism, role, and tissue specificities. Pflugers Arch 464:3–17
31. Carafoli E (1991) Calcium pump of the plasma membrane. Physiol Rev 71:129–153

32. Brini M, Carafoli E (2009) Calcium pumps in health and disease. Physiol Rev 89:1341–1378
33. Li Z, Nicoll DA, Collins A, Hilgemann DW et al (1991) Identification of a peptide inhibitor of the cardiac sarcolemmal Na^+-Ca^{2+} exchanger. J Biol Chem 266:1014–1020
34. Lee SL, Yu AS, Lytton J (1994) Tissue-specific expression of Na^+-Ca^{2+} exchanger isoforms. J Biol Chem 269:14849–14852
35. Kofuji P, Lederer WJ, Schulze DH (1994) Mutually exclusive and cassette exons underlie alternatively spliced isoforms of the Na/Ca exchanger. J Biol Chem 269:5145–5149
36. Herchuelz A, Kamagate A, Ximenes H, Van Eylen F (2007) Role of Na/Ca exchange and the plasma membrane Ca^{2+}-ATPase in beta cell function and death. Ann N Y Acad Sci 1099:456–467
37. Bers DM (2002) Cardiac excitation-contraction coupling. Nature 415:198–205
38. Bers DM (2008) Calcium cycling and signaling in cardiac myocytes. Annu Rev Physiol 70:23–49
39. Boyman L, Hagen BM, Giladi M, Hiller R, Lederer WJ, Khananshvili D (2011) Proton-sensing Ca^{2+} binding domains regulate the cardiac Na^+/Ca^{2+} exchanger. J Biol Chem 286:28811–28820
40. Giladi M, Sasson Y, Fang X, Hiller R, Buki T, Wang Y-X, Hirsch JA, Khananshvili D (2012) A common Ca^{2+}-driven interdomain module governs eukaryotic NCX regulation. PLoS One 7(6):e39985
41. Giladi M, Khananshvili D (2013) Molecular determinants of allosteric regulation in NCX proteins. Adv Exp Med Biol 961:35–48
42. Giladi M, Bohbot H, Buki T, Schulze DH, Hiller R, Khananshvili D (2012) Dynamic features of allosteric Ca^{2+} sensor in tissue-specific NCX variants. Cell Calcium 51:478–485
43. Giladi M, Boyman L, Mikhasenko H, Hiller R, Khananshvili D (2010) Essential role of the CBD1-CBD2 linker in slow dissociation of Ca^{2+} from the regulatory two-domain tandem of NCX1. J Biol Chem 285:28117–28125
44. Giladi M, Friedberg I, Fang X, Hiller R, Wang YX, Khananshvili D (2012) G503 is obligatory for coupling of regulatory domains in NCX proteins. Biochemistry 51:7313–7320
45. Giladi M, Hiller R, Hirsch JA, Khananshvili D (2013) Population shift underlies Ca^{2+}-induced regulatory transitions in the sodium-calcium exchanger (NCX). J Biol Chem 288: 23141–23149
46. John SA, Liao J, Jiang Y, Ottolia M (2013) The cardiac Na^+-Ca^{2+} exchanger has two cytoplasmic ion permeation pathways. Proc Natl Acad Sci U S A 110:7500–7505
47. John SA, Ribalet B, Weiss JN, Philipson KD, Ottolia M (2011) Ca^{2+}-dependent structural rearrangements within Na^+-Ca^{2+} exchanger dimers. Proc Natl Acad Sci U S A 108:1699–1704
48. Salinas PK, Brüschweiler-Li L, Johnson E, Brüschweiler R (2011) Ca^{2+} binding alters the inter-domain flexibility between the cytoplasmic Ca-binding domains in the Na/Ca exchanger. J Biol Chem 286:32123–32131
49. Waight AB, Pedersen BP, Schlessinger A, Bonomi M, Chau BH, Roe-Zurz Z, Risenmay AJ, Sali A, Stroud RM (2013) Structural basis for alternating access of a eukaryotic calcium/proton exchanger. Nature 499:107–110
50. Nishizawa T, Kita S, Maturana AD, Furuya N, Hirata K, Kasuya G, Ogasawara S, Dohmae N, Iwamoto T, Ishitani R, Nureki O (2013) Structural basis for the counter-transport mechanism of a H^+/Ca^{2+} exchanger. Science 341:168–172
51. Wu M, Tonga S, Walterspergerb S, Diederichsc K, Wang M, Zheng L (2013) Crystal structure of Ca^{2+}/H^+ antiporter protein YfkE reveals the mechanisms of Ca^{2+} efflux and its pH regulation. Proc Natl Acad Sci U S A 110:11367–11372
52. Dunn J, Elias CL, Le HD, Omelchenko A, Lytton J (2002) The molecular determinants of ionic regulatory differences between brain and kidney Na^+/Ca^{2+} exchanger (NCX1) isoforms. J Biol Chem 277:33957–33962
53. Dyck C, Omelchenko A, Elias CL, Quednau BD, Philipson KD, Hnatowich M, Hryshko LV (1999) Ionic regulatory properties of brain and kidney splice variants of the NCX1 Na^+-Ca^{2+} exchanger. J Gen Physiol 114:701–711

54. Omelchenko A, Dyck C, Hnatowich M, Buchko J, Nicoll DA et al (1998) Functional differences in ionic regulation between alternatively spliced isoforms of the Na^+-Ca^{2+} exchanger from *Drosophila melanogaster*. J Gen Physiol 111:691–702
55. Hryshko LV, Matsuoka S, Nicoll DA, Weiss JN, Schwarz EM et al (1996) Anomalous regulation of the *Drosophila* Na^+-Ca^{2+} exchanger by Ca^{2+}. J Gen Physiol 108:67–74
56. Ren X, Philipson K (2013) The topology of the cardiac Na^+/Ca^{2+} exchanger, NCX1. J Mol Cell Cardiol 57:68–71
57. Marinelli F, Almagor L, Hiller R, Giladi M, Khananshvili D, Faraldo-Gómez JD (2014) Sodium recognition by the Na^+/Ca^{2+} exchanger in the outward-facing conformation. Proc Natl Acad Sci U S A 50:E5354–E5362
58. Khananshvili D (1990) Distinction between the two basic mechanisms of cation transport in the cardiac Na^+-Ca^{2+} exchange system. Biochemistry 29:2437–2442
59. Reeves JP, Condrescu M (2008) Ionic regulation of the cardiac sodium-calcium exchanger. Channels 2:322–328
60. Hryshko L (2008) What regulates Na^+/Ca^{2+} exchange? Focus on "Sodium-dependent inactivation of sodium/calcium exchange in transfected Chinese hamster ovary cells". Am J Physiol Cell Physiol 295:C869–C871
61. Boyman L, Mi khasenko H, Hiller R, Khananshvili D (2009) Kinetic and equilibrium properties of regulatory calcium sensors of NCX1 protein. J Biol Chem 284:6185–6193
62. Ottolia M, Nicoll DA, John S, Philipson KD (2010) Interactions between Ca^{2+} binding domains of the Na^+-Ca^{2+} exchanger and secondary regulation. Channels 4:1–4
63. Ottolia M, Nicoll DA, Philipson KD (2009) Roles of two Ca^{2+}-binding domains in regulation of the cardiac Na^+-Ca^{2+} exchanger. J Biol Chem 284:32735–32741
64. Ottolia M, Torres N, Bridge JH, Philipson KD, Goldhaber JI (2013) Na/Ca exchange and contraction of the heart. J Mol Cell Cardiol 61:28–33
65. Chaptal V, Besserer GM, Ottolia M, Nicoll DA, Cascio D, Philipson KD, Abramson J (2007) How does regulatory Ca^{2+} regulate the Na^+-Ca^{2+} exchanger? Channels 1:397–403
66. Breukels V, Konijnenberg A, Nabuurs SM, Touw WG, Vuister GW (2011) The second Ca^{2+}-binding domain of NCX1 binds Mg^{2+} with High affinity. Biochemistry 50:8804–8812
67. Hilgemann DW, Matsuoka S, Nagel GA, Collins A (1992) Steady-state and dynamic properties of cardiac sodium-calcium exchange. Sodium-dependent inactivation. J Gen Physiol 100:905–932
68. Hilgemann DW (1990) Regulation and deregulation of cardiac Na^+-Ca^{2+} exchange in giant excised sarcolemmal membrane patches. Nature 344:242–245
69. Matsuoka S, Nicoll DA, Reilly RF, Hilgemann DW, Philipson KD (1993) Initial localization of regulatory regions of the cardiac sarcolemmal Na^+-Ca^{2+} exchanger. Proc Natl Acad Sci U S A 90:3870–3874
70. Matsuoka S, Nicoll DA, He Z, Philipson KD (1997) Regulation of cardiac Na^+-Ca^{2+} exchanger by the endogenous XIP region. J Gen Physiol 109:273–286
71. Doering AE, Eisner DA, Lederer WJ (1996) Cardiac Na-Ca exchange and pH. Ann N Y Acad Sci 779:182–198
72. Doering AE, Lederer WJ (1994) The action of Na^+ as a cofactor in the inhibition by cytoplasmic protons of the cardiac Na^+-Ca^{2+} exchanger in the guinea-pig. J Physiol 480:9–20
73. Ginsburg KS, Weber CR, Bers DM (2013) Cardiac Na^+–Ca^{2+} exchanger: dynamics of Ca^{2+}-dependent activation and deactivation in intact myocytes. J Physiol 591:2067–2086
74. Shattock MJ, Ottolia M, Bers DM et al (2015) Na^+/Ca^{2+} exchange and Na^+/K^+-ATPase in the heart. J Physiol 593:1361–1382
75. Malmberg NJ, Varma S, Jakobsson E, Falke JJ (2004) Ca^{2+} activation of the cPLA2 C2 domain: ordered binding of two Ca^{2+} ions with positive cooperativity. Biochemistry 43:16320–16328
76. Wu M, Tong S, Gonzalez J, Jayaraman V, Spudich JL, Zheng L (2011) Structural basis of the Ca^{2+} inhibitory mechanism of Drosophila Na/Ca exchanger CALX and its modification by alternative splicing. Structure 19:1509–1517
77. Giladi M, Lee SY, Hiller R, Chung KY, Khananshvili D (2015) Structure-dynamic determinants governing a mode of regulatory response and propagation of allosteric signal in splice variants of Na^+/Ca^{2+} exchange (NCX) proteins. Biochem J 465:489–501

78. Matsuoka S, Nicoll DA, Hryshko LV, Levitsky DO, Weiss JN, Philipson KD (1995) Regulation of the cardiac Na^+-Ca^{2+} exchanger by Ca^{2+}. Mutational analysis of the Ca^{2+} binding domain. J Gen Physiol 105:403–420
79. Dyck C, Maxwell K, Buchko J, Trac M, Omelchenko A, Hnatowich M, Hryshko LV (1998) Structure-function analysis of CALX1.1, a Na^+-Ca^{2+} exchanger from Drosophila. Mutagenesis of ionic regulatory sites. J Biol Chem 273:12981–12987
80. Ma B, Tsai C-J, Haliloğlu T, Nussinov R (2011) Dynamic allostery: linkers are not merely flexible. Structure 19:907–917
81. Tsai CJ, del Sol A, Nussinov R (2008) Allostery: absence of a change in shape does not imply that allostery is not at play. J Mol Biol 378:1–11
82. Rizo J, Südhdof TC (1998) C2-domains, structure and function of a universal Ca^{2+}-binding domain. J Biol Chem 273:15879–15882
83. Montaville P, Schlicker C, Leonov A, Zweckstetter M, Sheldrick GM, Becker S (2007) The C2A-C2B linker defines the high affinity Ca^{2+} binding mode of Rabphilin-3A. J Biol Chem 282:5015–5025
84. Stahelin RV, Wang J, Blatner NR, Rafter JD, Murray D, Cho W (2005) The origin of C1A-C2 interdomain interactions in protein kinase C. J Biol Chem 280:36452–36463
85. Häussinger D, Ahrens T, Sass HJ, Pertz O, Engel J, Grzesiek S (2002) Calcium-dependent homoassociation of E-cadherin by NMR spectroscopy: changes in mobility, conformation and mapping of contact regions. J Mol Biol 324:823–839
86. Baumgartner W, Golenhofen N, Grundhofer N, Wiegand J, Drenckhahn D (2003) Ca^{2+} dependency of N-cadherin function probed by laser tweezer and atomic force microscopy. J Neurosci 23:11008–11014
87. Hirsch JA, Schubert C, Gurevich VV, Sigler PB (1999) The 2.8 Å crystal structure of visual arrestin: a model for arrestin's regulation. Cell 97:257–269

Chapter 8
Regulation of Ca^{2+}/Mg^{2+} Ecto-ATPase in the Heart

Subburaj Kannan, Vijayan Elimban, Pascal Bogaert, Monika Bartekova, and Naranjan S. Dhalla

Abstract The plasma membrane Ca^{2+}/Mg^{2+} ecto-ATPase is an acidic glycoprotein, which hydrolyzes different nucleoside triphosphates and is activated by millimolar concentrations of various divalent cations. Unlike transport ATPases, it does not require Mg-ATP as a substrate and is different from the mitochondrial, myofibrillar, and sarcoplasmic reticulum ATPases. This enzyme is present in all tissues of the body including liver, brain, heart, kidney, blood, platelets, endothelium, and smooth muscles. The Ca^{2+}/Mg^{2+} ecto-ATPase is considered to play diverse physiological roles such as termination of purinergic transmission, regulation of extracellular ATP concentration, gating mechanism for Ca^{2+} and Mg^{2+} fluxes, ATP-driven proton pump, cell-to-cell communication as well as cellular differentiation and transformation in a tissue specific manner. The activity of Ca^{2+}/Mg^{2+} ecto-ATPase is altered by a wide variety of physiological, pharmacological, and pathological interventions which change membrane fluidity and its composition with respect to cholesterol and phospholipid contents. The molecular weight of this enzyme varies from tissue to tissue in the range of 180–240 kDa with subunits of 90, 80, 67, 20, and 10 kDa. The cDNA sequence for the plasma membrane Ca^{2+}/Mg^{2+} ecto-ATPase from different tissues show homology with different adhesion molecules including CD36, CD39, and CD70. The evidence in the existing literature suggests that the Ca^{2+}/Mg^{2+} ecto-ATPase is a multifunctional adhesion molecule which exists in different isoforms in various tissues.

Keywords Ca^{2+}/Mg^{2+} ecto-ATPase • Ca^{2+}-dependent ATPase • Mg^{2+}-dependent ATPase • Membrane ATPases • Adhesion molecules • Cellular function • Sarcolemmal Ca^{2+}/Mg^{2+} ecto-ATPase

S. Kannan • V. Elimban • P. Bogaert • N.S. Dhalla (✉)
Department of Physiology and Pathophysiology, Faculty of Health Sciences, Institute of Cardiovascular Sciences, St. Boniface Hospital Research Centre, University of Manitoba, 351 Tache Avenue, Winnipeg, MB, Canada R2H 2A6
e-mail: nsdhalla@sbrc.ca

M. Bartekova
Institute for Heart Research, Slovak Academy of Sciences, Bratislava, Slovak Republic

S. Chakraborti, N.S. Dhalla (eds.), *Regulation of Ca^{2+}-ATPases,V-ATPases and F-ATPases*, Advances in Biochemistry in Health and Disease 14,
DOI 10.1007/978-3-319-24780-9_8

1 Introduction

ATP was discovered in 1929 and has been demonstrated to serve as energy source for maintaining cellular function [1–6]. When the nutrient molecules such as glucose and fatty acids are metabolized by oxidation, the free energy is conserved by the synthesis of ATP from ADP and Pi. On the other hand, the energy dependent activities of the cell are sustained by the energy released from the ATP hydrolysis [1–6]. The enzymes which catalyze the breakdown of ATP to form ADP and Pi have been identified as ATPases in many subcellular organs and plasma membrane [1–13]. Some of these ATPases include enzymes such as Ca^{2+}/Mg^{2+} ecto-ATPase, plasma membrane Ca^{2+}-pump ATPase, sarcoplasmic reticulum Ca^{2+}-pump ATPase, dynein ATPase, alkaline phosphatase, ATP diphosphohydrolase, Na^+/K^+ ATPase, proton-pump ATPase, actomyosin ATPase, and H^+/K^+ ATPase. Although there is a wealth of information available on ATPases of different species ranging from prokaryotes to eukaryotes, this review is focused mainly on the structural and functional properties of Ca^{2+}/Mg^{2+} ecto-ATPase in the plasma membrane. Additionally, some of the features which may distinguish this enzyme from other ATPases are highlighted.

The enzyme referred to as Ca^{2+}/Mg^{2+} ecto-ATPase, Ca^{2+}/Mg^{2+} ATPase, Ca^{2+}-activated ATPase, Mg^{2+}-activated ATPase, plasma membrane E-type ATPase, or basal ATPase was first identified in 1957 in the liver. However, this enzyme is now shown to be present in the plasma membrane of different organs and its activation has been demonstrated to require millimolar concentrations of either Ca^{2+} or Mg^{2+} for the maximal hydrolysis of ATP and several other nucleotide triphosphates [1, 14]. Nearly six decades of research on Ca^{2+}/Mg^{2+} ecto-ATPase from different organ systems originating from different species has provided information on its biochemistry and molecular biology without ascribing any definitive physiological functional role to this enzyme [1, 14, 15]. The intent of this article is to summarize the experimental evidence for membrane Ca^{2+}/Mg^{2+} ecto-ATPase to understand its role in animal cell function.

2 Classification and Distinguishing Features of Ca^{2+}/Mg^{2+} Ecto-ATPase

Based on the following criterion, Ca^{2+}/Mg^{2+} ecto-ATPase has been classified as an E-type ATPase (E.C.3.6.1.15) [16]: (1) Ca^{2+}/Mg^{2+} ecto-ATPase has a catalytic site located on the extracellular surface; (2) Ca^{2+}/Mg^{2+} ecto-ATPase is insensitive to inhibitors of P-type ion transporting ATPases (Na^+/K^+ ATPase as well as Ca^{2+}-pump ATPase of the sarcolemma and sarcoplasmic reticulum) such as ouabain and vanadate, F-type ATPases (F_1F_0 mitochondrial proton pump) such as NaN_3 and oligomycin, and V-type ATPases (vacuolar proton pumps) such as *N*-ethylmaleimide and fluoride; (3) Ca^{2+}/Mg^{2+} ecto-ATPase is inactivated by detergents; (4) Ca^{2+}/Mg^{2+} ecto-ATPase does not form phosphoprotein intermediates during substrate hydrolysis; (5) $Ca^{2+}/$

Mg^{2+} ecto-ATPase is dependant upon millimolar (mM) concentrations of Ca^{2+} or Mg^{2+} as a cofactor; (6) Ca^{2+}/Mg^{2+} ecto-ATPase hydrolyzes nucleoside triphosphates but not nucleoside diphosphates or nucleoside monophosphates; (7) Ca^{2+}/Mg^{2+} ecto-ATPase has an alkaline pH optimum (pH 7.5–8.5); (8) Ca^{2+}/Mg^{2+} ecto-ATPase exhibits a high turnover (formation/breakdown) rate with a calculated turnover number of 500,000 min^{-1} [17]; and (9) Ca^{2+}/Mg^{2+} ecto-ATPase is present in low abundance in most tissues.

Ca^{2+}/Mg^{2+} ecto-ATPase has been shown to be distinctly different from other enzymes which are known to hydrolyze ATP [1, 18]. It is pointed out that Na^{+}-K^{+} ATPase, a marker for the plasma membrane, maintains the intracellular concentration of Na^{+} and K^{+}, and requires Mg^{2+} for its activity. Ouabain, a specific inhibitor of Na^{+}-K^{+} ATPase has no effect on Ca^{2+}/Mg^{2+} ecto-ATPase activity of the plasma membranes from different species. The Ca^{2+}-pump ATPase, which is referred as high affinity Ca^{2+} ATPase or Ca^{2+}-stimulated ATPase, is present in both the plasma membrane and sarcoplasmic reticulum, requires micromolar concentrations of Ca^{2+} and utilizes MgATP as a substrate. The plasma membrane Ca^{2+}-stimulated ATPase plays a role in Ca^{2+}-efflux whereas the sarcoplasmic reticulum Ca^{2+}-stimulated ATPase sequesters Ca^{2+} and plays a role in lowering the intracellular concentration of Ca^{2+}. On the other hand, the proton ATPase (F_1F_0-ATPase), resides on the inner membrane of the mitochondria; the mitochondrial ATPase is inhibited by specific inhibitors like oligomycin and NaN_3, which have no effect on Ca^{2+}/Mg^{2+} ecto-ATPase.

The alkaline phosphatase is a nonspecific phosphatase which hydrolyzes ATP to ADP and Pi. The Ca^{2+}/Mg^{2+} ecto-ATPase is different from alkaline phosphatase because: (1) plasma membrane-bound alkaline phosphatase exhibits optimal activity at pH 10.3 whereas the Ca^{2+}/Mg^{2+} ecto-ATPase is optimally active at pH 7.4–7.5; (2) unlike Ca^{2+}/Mg^{2+} ecto-ATPase, alkaline phosphatase does not require Ca^{2+} or Mg^{2+} as a cofactor for its catalytic activity. Vanadate and cysteine inhibit alkaline phosphatase but these agents have no effect on Ca^{2+}/Mg^{2+} ecto-ATPase activity [1]. It should be mentioned that ATP diphosphohydrolase catalyzes the hydrolysis of triphosphonucleosides and diphosphonucleosides to yield nucleoside monophosphate and inorganic phosphate [19]. It hydrolyses both nucleoside triphosphate and nucleoside diphosphate at equal rates while Ca^{2+}/Mg^{2+} ecto-ATPase hydrolyzes nucleoside diphosphate at much lower rate in comparison to that of the nucleoside triphosphate.

3 Functional and Regulatory Properties of Ca^{2+}/Mg^{2+} Ecto-ATPase

A variety of functions have been proposed for Ca^{2+}/Mg^{2+} ecto-ATPase [1, 14, 15] including: (1) termination of purinergic signaling in smooth muscle cells [20]; (2) neurotransmission [21], (3) non-synaptic information transfer [22, 23]; (4) cellular secretion [24, 25]; (5) vesicular trafficking [26]; (6) Ca^{2+}-influx and Mg^{2+}-efflux from cardiac myocytes [2]; (7) regulation of ectokinase substrate concentration [27];

(8) cell adhesion [28–37]; (9) bicarbonate transport [38]; (10) tumourigenesis [39]; (11) mesentric artery functions [40]; and (12) mechanochemical functions involving cell motility in HeLa cells and Ehrlich ascites tumor cells [41, 42].

Differential regulation of ecto-ATPase activity due to leukocytes was observed during differentiation and maturation [43]. Epidermal growth factor-dependent enhancement in ecto-ATPase activity in human hepatoma xenograft requires hydrocortisone and cholera toxin while the xenograft tissue growth was inhibited [44]. Hennighausen and Lange [45] proposed that the ecto-ATPase activity in rodent thymocytes is related to the maturation of the cells. Based on the inhibitory data obtained from the mammalian brain tissue synaptosomes (rat, mouse, gerbil, and human), it was suggested that Ca^{2+}-dependent ecto-ATPase and Mg^{2+}-dependent ecto-ATPase may represent two different enzymes and they may be regulated independently [46]. Still et al. [47] have shown that concanavalin A (conA) causes inactivation of ecto-ATPase present in the intact frog skeletal muscles. Mouse macrophage cell line J774 was reported to possess an ATP receptor promoting Ca^{2+} influx which is limited by the presence of ecto-ATPases for the hydrolysis of ATP [48]. It was found that there was no correlation between ecto-ATPase inhibition and changes in contractile force development in guinea pig urinary bladder and vas deferens in response to different divalent cations [49]. In human brain, the posterior part of epileptic hippocampus has been shown to exhibit a marked increase in the ecto-ATPase activity, which has been suggested to be involved in the epileptic seizure development and sustenance of epilepsy [50].

It has been shown that the ecto-ATPase was lost from the external side of the myelin sheath where the focal separation of myelin lamellae occurs after the stretch injury in the nerve fibers; this event became apparent 1 and 4 h after the injury and has been characterized as a loss of regular axonal structure [51]. It has been reported that ecto-ATPase inactivation occurs after the ATP hydrolysis in brain synaptosomes; however, ATP hydrolytic products, ADP, AMP, adenosine, and inorganic phosphates did not affect the ecto-ATPase inactivation [52]. Furthermore, con A confers partial protection to ATP hydrolysis-induced inactivation of ecto-ATPase which was suggested to be partly due to the phosphorylation of membrane-bound proteins [52]. The adenosine nucleosides (ATP, ADP, AMP, and adenosine) have been shown to stimulate the proliferation of the endothelial LLC-MK2 cells whereas the inhibition of ecto-ATPase, 5′-nucleotidase or alkaline phosphatase reduced the proliferation of the LLC-MK2 cells, suggesting that different purines and pyrimidines may contribute to the proliferation of the LLC-MK2 cells [53]. A novel purinoceptor (P_1), where both adenosine and ATP act as agonists, was found to be present on the surface of follicular oocytes of *Xenopus laevis* [54]. Since the ecto-ATPase confers low rate of ATP hydrolysis, it was argued that the ecto-ATPase may not seem to generate sufficient ligand (Ado/AMP) to function as a P_1 purinoceptor [54].

The Ca^{2+}/Mg^{2+} ecto-ATPase is expressed upon cell activation and is inhibited by non-hydrolyzable ATP analogues [55]. The inhibition of this enzyme was observed to occur by regulating the influx of Ca^{2+}, which was necessary to maintain lymphocyte cellular activation. The increase in the expression of mesangial cell ecto-ATPase

after the treatment with polyamines such as spermine and spermidine was suggested to increase the production of adenosine, which plays a role in mesangial inflammatory processes [56]. Since ecto-ATPase gene expression is increased in human hepatoma and its activity is inhibited by detergents and high temperature, which decrease the membrane protein interaction, it has been suggested that this enzyme is regulated by both enzymatic and transcriptional alterations [57]. Partial sequence of a genomic DNA clone indicated that the CD39L1 gene corresponds to an alternative spliced form of the human ecto-ATPase [58]. Similarities with respect to metabolic control as well as regulatory and catalytic properties between both ecto-ATPase and CD39L1 have been described in the literature [59–61].

The cardiac Ca^{2+}/Mg^{2+} ecto-ATPase was found to show a significant amino sequence homology with human platelet CD36 and the activities of both are regulated by phosphorylation due to the activation of protein kinase A [62]. It should be noted that ischemia induced by medial artery occlusion and a novel ecto-ATPase inhibitor, PV4, was found to increase the concentration of extracellular ATP in the rat striatum [63]. The ecto-ATPase activity in the porcine renal proximal tubula cell line was also inhibited by ischemia [64]. Heat shock of *Trypanosoma cruzi* Y strain epimastigotes was also observed to stimulate the Mg^{2+}-dependent ecto-ATPase activity [65]. However, when the plasma membrane from epimastigotes did not show any increase in the ecto-ATPase activity upon heat shock treatment, suggesting that some cytoplasmic components may be involved in influencing the enzyme activation by heat shock stress [65]. The strong localization of Ca^{2+} ecto-ATPase on the luminal surface of the blood–brain barrier has been suggested to account for the physiological homeostasis of Ca^{2+} across the blood–brain interface [66]. Thus it appears that the Ca^{2+}/Mg^{2+} ecto-ATPase is regulated by a wide variety of mechanisms.

4 Structural Properties of the Ca^{2+}/Mg^{2+} Ecto-ATPase

Western (immuno) blots with polyclonal antibodies for Ca^{2+}/Mg^{2+} ecto-ATPase indicated that the liver Ca^{2+}/Mg^{2+} ecto-ATPase was more enriched in the canalicular domain [67]. Three different anti-Ca^{2+}/Mg^{2+} ecto-ATPase antibodies have been reported: (a) The antibody #669 raised against SDS-PAGE purified Ca^{2+}/Mg^{2+} ecto-ATPase, only recognized the denatured Ca^{2+}/Mg^{2+} ecto-ATPase; (b) Antibody #708 was generated for chromatographically purified enzyme (i.e., non-denatured protein), and recognized both the native and denatured Ca^{2+}/Mg^{2+} ecto-ATPase. This antibody has been extensively employed in immunoprecipitation analysis [67] and; (c) Antipeptide #36 was generated against a sequence obtained from tryptic digestion of purified liver Ca^{2+}/Mg^{2+} ecto-ATPase. It recognized the reduced form of Ca^{2+}/Mg^{2+} ecto-ATPase but not the non-reduced form [68, 69]. A rat liver hepatocyte protein with 100 kDa has been characterized as Ca^{2+}/Mg^{2+} ecto-ATPase. It is present in two isoforms with different C terminals viz. 10 AA and 70 AA, while the ATP binding domain localized on the extracellular domain. Furthermore, the sequence homology

analysis of the liver ecto-ATPase showed that it has three immunoglobulin-like domains that are homologous to those present in the human biliary glycoprotein-l (BGP 1). There are 16 potential asparagine-linked N-glycosylation sites in this protein [70].

The primary structure of the rat liver plasma membrane ecto-ATPase has the nucleotide and amino acid sequence homology with BGP 1. However it should be noted that this cDNA sequence has no Walker motives (I $GX_1X_2X_3X_4$-GK or II R/K-$X_1X_2X_3$-L; X = hydrophobic residues) which represents the ATP binding domain in the ion motive ATPases. The lack of Walker ATP binding domain sequence was attributed to the insensitivity of ecto-ATPase to vanadate, which has been identified as a characteristic feature of the ion motive ATPases to form aspartyl phosphoprotein intermediates [38]. However, the rat liver Ca^{2+}/Mg^{2+} ecto-ATPase cDNA has been shown to detect the transcripts of a biliary glycoprotein and carcinoembryonic antigen, but not the mercurial insensitive ecto-ATPase in small cell lung cancer cell lines [39]. Furthermore, the expression product of the liver ecto-ATPase cDNA has been shown to be functioning as a cell adhesion molecule without E-type ATPase (ecto-ATPase) activity [71]. Hydropathy plot analysis of rat liver ecto-ATPase cDNA sequence showed that it has two hydrophobic stretches. One is located at the NH_2-terminal and forms part of a membrane signal sequence and the other is located near the COOH-terminal.

The overall structural arrangement (amino acid) predicts that most of the liver ecto-ATPase protein mass is in the extracellular space and that the COOH terminal of the protein is intracellular. This structural information is consistent with the fact that the liver Ca^{2+}/Mg^{2+} ATPase protein is an ecto-ATPase [68]. The two stretches of the amino acid sequence (consisting of amino acids 92–100 and 335–348) are similar to the consensus sequences for nucleotide-binding domains of other ATP-binding proteins. The expression construct containing the coding region of the rat liver Ca^{2+}/Mg^{2+} ecto-ATPase, cloned in front of the cytomegalovirus promoter and SV 40 origin of replication (pEXP), was expressed in the mouse L cell line and the HeLa cell line. The lysate obtained from the cells transfected with the plasmid pEXP had a higher Ca^{2+}-activated ATPase activity compared to that of the control [68]. There are two rat liver cell-CAM 105 isoforms (long and short) which have been cloned and characterized. The short isoform is predominant on the external surface of the rat liver plasma membrane. The longer isoform has more potential phosphorylation sites than the shorter isoform. Differential phosphorylation could be one of the mechanisms for differential isoform function. Both long and short isoforms are localized in the canalicular domain of hepatocytes. The difference in the sequence of the two isoform suggests that these are probably derived from different genes rather than being formed by alternative splicing [72]. Mg^{2+} ATPase (85 kDa glycoprotein), purified from the traverse tubules of chicken skeletal muscle, has been shown to have the amino acid sequence homologous to T cadherin, which shares many biochemical properties of the traverse tubule Mg^{2+} ATPase of chicken skeletal muscle [29].

The ecto-nucleotidase activity profile (ecto-ATPase; ecto-ADPase) of human umbilical vein endothelial cells was similar to that of the enzyme from leukocytes.

Fillipini et al. [73] postulated that the presence of ecto-ATPase on the cytolytic thymus derived lymphocytes confers protection from the deleterious effect mediated by extracellular ATP. An antiserum directed against bovine aortic endothelial smooth muscle cell ATP diphosphohydrolase showed marked inhibition on both ecto-ATPase and ecto-ADPase of bovine aortic endothelial smooth muscle cells. It was suggested that both enzyme activities are probably conferred by one enzyme referred to as ATP diphosphohydrolase. Sequential hydrolysis of ATP and ADP in the adult rat cerebral cortex synaptosomes was attributed to the presence of an ATP diphosphohydrolase [74]. An ecto-ATPase requiring millimolar concentration of Ca^{2+} or Mg^{2+} has been localized on the taste bud of the cells and it is suggested to be involved either in neurotransmission or in the energy supply mechanism in the taste bud function [75].

Kurihara et al. [76] demonstrated that the ecto-ATPases hydrolyzing nucleoside triphosphates in A-431(epidermal carcinoma) cells were different from P2 purinergic receptors. Based on in vitro studies on ecto-ATPase (Ca^{2+} or Mg^{2+}-dependent ecto-ATPase) in Langerhans cells, it was suggested that this ATPase confers protection against membrane lytic effect mediated by extracellular ATP [77]. Beukers et al. [78] demonstrated that human platelets possess ecto-ATPase with high affinity for ATP, as well as for ADP which causes the platelet aggregation. It was thus indicated that the role of ecto-ATPase activity in platelet aggregation may be minimal because breakdown of ATP to ADP occurs slowly. 8-Azido-ATP has been shown to be a substrate for ecto-ATPase in cultures of chromaffin cells with a Km of ~256 mM and Vmax of 14.3 nmol/min × 10^6 cells [79]. An ATPase isolated from bovine synaptosome membranes with a molecular weight 50 kDa was considered as an ecto-ATPase due to the fact that the active site was exposed to external environment [80]. It has been demonstrated that Ca^{2+}/Mg^{2+} ecto-ATPase activity is associated with neural cell adhesion molecule (NCAM) purified from rat brain microsomes; however, it has been shown that the Mg^{2+} ATPase activity and neural cell adhesion molecule could be separated in the partially purified rat and chicken brain microsomes [81]. The Ca^{2+} or Mg^{2+}-activated ATPase from the bovine brain synaptosomal plasma membranes has a molecular weight 50 kDa and requires millimolar concentration of Ca^{2+} or Mg^{2+} for maximal hydrolysis with an optimum pH between 7.5 and 8.5. Sippel et al. [82] showed that bile acid efflux and Ca^{2+}/Mg^{2+} ecto-ATPase activities were two distinct properties of a single rat liver hepatocyte canalicular membrane protein; however, introduction of mutations in the consensus sequence at amino acids Gly 97 and Arg 98 in the Ca^{2+}/Mg^{2+} ecto-ATPase abrogated ATPase activity but did not affect its bile acid transport activity [83]. Kast et al. [84] reported that electrogenic taurocholate transport resides entirely in the endoplasmic reticulum, whereas ATP-dependent bile acid transport is an intrinsic function of the canalicular membrane as well as a yet unidentified intracellular membrane-bound compartment. Therefore the two transport activities were most probably mediated by two different bile acid transporting polypeptides.

By using an antipeptide antibody, it was identified that chicken gizzard Ca^{2+}/Mg^{2+} ecto-ATPase and T-cadherin are different proteins [85]. It should be mentioned that these proteins were localized on the luminal surfaces and intercellular

canaliculi of the acinar cells of both parotid and submandibular glands [86]. It was suggested that these may play a major role in ATP-breakdown, stabilization of microvillar membranes, cell adhesion, and secretory mechanisms in the rat parotid and submandibular glands [86]. Rat hepatocytes were shown to possess both mercurial sensitive and mercurial insensitive ecto-ATPase. During the hepatoma tumor formation, the mercurial sensitive ecto-ATPase was increased whereas the latter was decreased. It was also found that the mercurial-sensitive ecto-ATPase was expressed at high level in three lines of human small-cell lung carcinoma cells compared to the normal cells [87].

When the rat glomerular mesangial cells were cultured without serum, a reduction in the ecto-ATPase activity was evident [88]. A unique, ecto-ATPase partly sensitive to dicyclohexylcarbodiimide was demonstrated to be present on the surface of the human placental brush border membranes [89]. Suramin, Ni^{2+} and S-ATP, showed inhibitory effect on the human blood cells ecto-ATPase activity [89]. By utilizing specific monoclonal antibodies, an ecto-ATPase protein was immunoprecipitated. This protein was shown to have amino acid sequence homology with integrins, a group of proteins involved in contact between the cell adhesion molecules [90]. An ecto-ATPase localized on the rat small intestinal brush border membrane was proposed to play a major role in the nutrient break down [91]. It has been shown that the purinergic receptor antagonists, pyridoxalphosphate-6-azophenyl-2′,4′-disulfonic acid, suramin, and reactive blue, inhibited the ecto-ATPase activity in the bovine pulmonary artery endothelium, glial cells, and macrophages [92]. A human plasma factor 100 KF, which reduced expression of ecto-ATPase, has been shown to increase the permeability of human endothelium for macromolecules in a dose-dependent fashion [93]. It was shown that this plasma constituent may be important in the pathogenesis of glomerular disease [93].

Partially purified rat liver plasma membrane and lysosomal Ca^{2+}/Mg^{2+} ATPases have been shown to have similarity with an ecto-ATPase in the following characteristics: broad pH-activity profiles, Km values for ATP being 21–27 μM (at pH 4.5) and 18–14 μM (at pH 7.0) (in the presence of Ca^{2+}), hydrolysis of both ATP and ADP, inhibition by vanadate and 4,4′-diisothiocyanatostilbene 2,2′-disulfonic acid, as well as cross-reactivity against an antibody to the N-terminal peptide of ecto-ATPase [94]. By inhibiting the ecto-ATPase activity by an inhibitor, ARL67156 (6-*N*,*N*-diethyl-D-β,γ,-dibromo methylene ATP), it has been shown that there was an increase in nerve stimulation and neurogenic contractions in the isolated guinea pig vas deferens [95]. Based on observations such as differences in the pH, divalent cation requirement, and the absence of inhibitory effect of ADP on degradation of ATP during ATP hydrolysis on the surface of oocytes of *Xenopus laevis*, it was suggested that the degradation of ATP and ADP are mediated by two separate Ca^{2+} or Mg^{2+} dependent ecto-ATPase and Ca^{2+}/Mg^{2+}-dependent ecto-ADPase [12].

Following demyelination, there was a continuous expression of the ecto-ATPase activity in the internodal axolemma of exposed axons, and specifically the ecto-ATPase activity was prominent at the sites of axonal contacts and glial-cell processes. However, upon remyelination, the area of the axonal surface exhibiting the ecto-ATPase activity decreased in direct proportion to the thickening of the new

myelin sheath. Thus the differential expression of the ecto-ATPase activity was considered to play a role in the axo-glial recognition and founding of axo-glial contacts [96]. The cross-linking agents, 3,3′-dithiobis (sulfosuccinimidylpropionate) and dithiobis (succinimidylpropionate), resulted an oligomeric state (130 kDa immunoreactive band) and an increase in the ecto-ATPase activity, whereas the destabilizing agents showed inhibition of ecto-ATPase activity in chicken gizzard smooth muscle [97]. A novel membrane associated ecto-ATPase was identified in rat Sertoli cells. This enzyme was considered to be an ecto-ATPase due to the fact that it was activated by either Mg^{2+} or Ca^{2+}, and it hydrolyzed other nucleoside triphosphates, but not ADP [98]. A soluble E-type ecto-ATPase was also purified from the single-celled eukaryote, *Tetrahymena thennophila* [99]. This enzyme shared immune-cross-reactivity with the membrane-bound chicken gizzard smooth muscle ecto-ATPase (66 kDa). This ecto-ATPase enzymev was proposed to act as an inactivator of the purinergic signals (chemorepulsion responses to extracellular ATP and GTP) and also in the clearance of the extracellular nucleotides. Apyrase, an enzyme with ecto-ATPase activity, abolished the ATP-mediated cytotoxicity in the human tumor cells [100].

The cDNA sequence of chicken gizzard smooth muscle ecto-ATPase was found to have considerable homology with mouse and human CD39 and it was suggested to be involved in the homotypic cell adhesion process [32]. It should be noted that CD39 is a lymphoid cell (B cell) differentiation marker present in the Epstein Barr virus transformed immunocompetent cells and this molecule has been shown to have apyrase activity; the CD39 molecule was demonstrated to be an ecto-Ca^{2+} or Mg^{2+}-dependent apyrase [101]. It has been suggested that E-type ATPase activity may be tightly bound to proteins having adhesion characteristics. This conclusion was based on studies conducted on both ecto-ATPases and cell adhesion molecules. It was observed that the sequence for the ecto-ATPase purified from rat liver is homologous to the BGP 1 I [28]. Furthermore, it was noted that the liver ecto-ATPase cDNA sequence does not contain the Walker motives and it is implied that aspartyl phosphate intermediate formation is not required for ATP hydrolysis by this ecto-ATPase [102]. Expression of the rat liver ecto-ATPase eDNA, however, demonstrated that this clone coded for a protein in *E. coli* had the properties of a cell adhesion protein [30]. Similar to the rat liver enzyme, cloning of the chicken gizzard smooth muscle ecto-ATPase produced a cDNA with a sequence that has a considerable sequence homology with mouse and human CD39 [32]. Interestingly, CD39 is a cell adhesion protein that has been found to have an ecto-$Ca2^{+}/Mg^{2+}$ apyrase activity capable of hydrolyzing both ATP and ADP [32, 101, 103]. While there is no direct or indirect evidence to prove or disprove that ecto-ATPase/E-type ATPase activity is associated with adhesion molecules, it is intriguing to note that β_2 subunit of the Na^{+}/K^{+} ATPase has been shown to possess homology with cell adhesion molecule of glia [104]. Similarly, ecto 5′ nucleotidase (hydrolyzes AMP to adenosine) has also been demonstrated to harbor and/or function as an adhesion molecule, CD73 [105]. Thus, there is considerable evidence to indicate that E-type ATPases are directly or indirectly associated with the cell adhesion proteins in different organs of the body.

5 Sarcolemmal Ca^{2+}/Mg^{2+} Ecto-ATPase in the Heart

Extensive efforts were made in our laboratory to examine the presence, localization and role of Ca^{2+}/Mg^{2+} ecto-ATPase in the cardiac sarcolemmal membrane [1, 2, 106–109]. The properties of Ca^{2+}-dependent and Mg^{2+}-dependent ATPase activities in the sarcolemmal membrane for myocardium revealed that this enzyme possesses characteristics which are similar to those seen in different tissues such as brain, liver, kidney and skeletal muscle [1, 2, 110–112]. The Ca^{2+}/Mg^{2+} ecto-ATPase was stimulated by a wide variety of divalent cations, hydrolyzed various nucleoside triphosphates and was different from Ca^{2+}-stimulated ATPase (Ca^{2+}-pump ATPase) and Na^{+}-K^{+} ATPases. Although sarcolemmal Ca^{2+}/Mg^{2+} ecto-ATPase showed some similarities with mitochondrial, sarcoplasmic reticulum and myofibrillar ATPases, most of the biochemical characteristics of this enzyme were different from those for other subcellular organelles [113–115]. Phospholipid N-methylation was observed to be involved in the regulation of sarcolemmal Ca^{2+}/Mg^{2+} ecto-ATPase [116]. The activities of this enzyme in the presence of Ca^{2+} or Mg^{2+} were altered differentially by treatments with phospholipases A and C as well as with various detergents such as deoxycholate and lubrol [117, 118]. These observations are consistent with the view that the activities of Ca^{2+}/Mg^{2+} ecto-ATPase are modified upon changes in the microenvironment of the membrane with respect to phospholipid composition and fluidity, and that Ca^{2+}-dependent ATPase and Mg^{2+}-dependent ATPase may be two different enzymes.

It needs to be emphasized that the sarcolemmal phosphorylation mediated by cyclic AMP and protein kinase A was found to increase the Ca^{2+}/Mg^{2+} ecto-ATPase activity [119]. Furthermore, electrical stimulation of the cardiac sarcolemmal membrane increases the activity of this enzyme [120, 121]. In addition, the activation of sarcolemmal Ca^{2+}-dependent ATPase by different concentrations of Ca^{2+} was linearly related to the development of contractile activity in isolated perfused hearts [122]. Different cardiodepressing agents and anti-arrhythmic agents as well as some divalent cations were found to decrease the sarcolemmal Ca^{2+}/Mg^{2+} ecto-ATPase activity [123–125]. The activity of this enzyme was also altered in different pathophysiological conditions depending upon the stage of cardiac contractile function [126–130]. These studies are taken to suggest that sarcolemmal Ca^{2+}/Mg^{2+} ecto-ATPase play an important role in maintaining cardiac function during health and disease. Furthermore, there is ample evidence to suggest that the Ca^{2+}/Mg^{2+} ecto-ATPase may be involved in the fluxes of Ca^{2+} and Mg^{2+} across the sarcolemmal membrane [1, 2].

Treatment of the heavy sarcolemmal membrane containing a fuzzy coat of basement membrane with trypsin not only increased the Ca^{2+}-dependent ATPase activity without any changes in Mg^{2+}-dependent ATPase activity but also released Ca^{2+}-dependent ATPase in the supernatant [131]. Purification of this Ca^{2+}-dependent ATPase showed that the molecular weight of this enzyme was 67 kDa with two subunits of 55 and 12 kDa molecular weights [132]. This Ca^{2+}-dependent ATPase was markedly inhibited by Na^{+} and was suggested to be involved in Ca^{2+}-entry into cardiomyocyte and serve as a site for Na^{+}-Ca^{2+} antagonism in the sarcolemmal

membrane [132]. The Ca^{2+}/Mg^{2+} ecto-ATPase, remaining in the trypsin treated sarcolemmal preparation [133], was also solubilized and purified, showing a molecular weight of 240 kDa [134, 135]. This enzyme was found to have five subunits with molecular weight of 90, 80, 67, 20, and 10 kDa, and was not inhibited by Na^{+} [134]. Since the heavy sarcolemmal membrane was subjected to trypsin treatment before isolating Ca^{2+}-dependent ATPase and Ca^{2+}/Mg^{2+} ecto-ATPase from the hearts [132, 135], it is likely that the polypeptide composition of these enzymes may be a consequence of proteolysis and that both Ca^{2+}-dependent ATPase and Ca^{2+}/Mg^{2+} ecto-ATPase isolated in our laboratory [132, 135] are the components of the same ecto-ATP hydrolyzing system in the myocardial cell membrane.

In order to gain further information regarding the molecular structure and function of cardiac Ca^{2+}/Mg^{2+} ecto-ATPase, a light plasma membrane fraction was obtained from the myocardial tissue by the sucrose gradient method [136–138]. No Ca^{2+}-dependent ATPase activity was detected in the supernatant when the light sarcolemmal membrane, unlike the heavy sarcolemmal fraction, was subjected to trypsin treatment. However, the ATP hydrolysis by the light membrane was stimulated by various divalent cations and the Ca^{2+}/Mg^{2+} ecto-ATPase activities were inhibited by some divalent cations similar to that seen with the heavy sarcolemmal membrane [136]. The Ca^{2+}/Mg^{2+} ecto-ATPase was specifically stimulated by Con A indicating the role of membrane fluidity in the activation of sarcolemmal ATP hydrolysis due to Ca^{2+} or Mg^{2+} by ecto-ATPase [137]. On the other hand, gramicidin S was observed to depress the sarcolemmal Ca^{2+}/Mg^{2+} ecto-ATPase activity, and this effect was shown to be associated with the cardio-depressant action of this agent [138].

The purified Ca^{2+}/Mg^{2+} ecto-ATPase from the cardiac plasma membrane showed a molecular weight of 18 kDa with two subunits of 90 kDa molecular weight each [139]. The purified enzyme was found to be associated with phospholipids, cholesterol and polysaccharides indicating the glycoprotein nature of Ca^{2+}/Mg^{2+} ecto-ATPase. Further studies indicated that the purified Ca^{2+}/Mg^{2+} ecto-ATPase was found to bind a considerable amount of Ca^{2+} and showed low and high affinities for ATP binding; phospholipids associated with purified enzyme were found to be required for maximal activity [140]. Mass spectroscopic analysis of the enzyme showed the presence of multi-components indicating the micro-heterogeneity in the protein structure [141]. Amino acid sequence of tryptic fragment of purified Ca^{2+}/Mg^{2+} ecto-ATPase indicated the enzyme to be an adhesion molecule as monoclonal antibody directed against human CD36 cross-reacted with this enzyme [31]. Polyclonal antiserum raised against the purified cardiac Ca^{2+}/Mg^{2+} ecto-ATPase also cross-reacted with human CD36 [31]. Molecular cloning of cardiac sarcolemmal Ca^{2+}/Mg^{2+} ecto-ATPase involving the isolation of cDNA clone provided a single gene that was homologous to the adhesion molecule, CD36 [142]. Immunofluorescence of cardiac tissue sections stained with Ca^{2+}/Mg^{2+} ecto-ATPase antibodies revealed the localization of this enzyme at the plasma membrane of cardiomyocytes [143]. Staining of Ca^{2+}/Mg^{2+} ecto-ATPase was not cardiac specific since these antibodies also detected the presence of membrane proteins in sections from skeletal muscle, brain, liver and kidney. These studies support the view that the Ca^{2+}/Mg^{2+} ecto-ATPase is a transmembrane glycoprotein having homology with CD36 adhesion molecule.

6 Conclusions

From the foregoing discussion regarding the properties of Ca^{2+}/Mg^{2+} ecto-ATPase, it is evident that this is a transmembrane enzyme whose catalytic site is exposed to extracellular space and is considered to maintain the extracellular concentration of ATP. This enzyme is a glycoprotein in nature and its activity is determined by alterations in membrane fluidity and cholesterol as well as phospholipid composition. It is present in the plasma membranes of all tissues in the body and has been suggested to play a role in the maintenance of a wide variety of cellular functions. The Ca^{2+}/Mg^{2+} ecto-ATPase has been purified from different tissues and its molecular weight varies in a wide range with several subunits. The sequence of cDNA for Ca^{2+}/Mg^{2+} ecto-ATPase shows homology with different isoforms of adhesion molecules such as CD36, CD39, and CD70; this is dependent upon its presence in different cell types from various tissues. Several studies have suggested that Ca^{2+}/Mg^{2+} ecto-ATPase is a multiple functional enzyme and its role in maintaining cellular function is tissue and organ specific.

Acknowledgements The infrastructure for the preparation of this chapter was provided by the St. Boniface Hospital Research Foundation.

References

1. Dhalla NS, Zhao D (1988) Cell membrane Ca^{2+}/Mg^{2+} ATPase. Prog Biophys Mol Biol 52:1–37
2. Dhalla NS, Zhao D (1989) Possible role of sarcolemmal Ca^{2+}/Mg^{2+} ATPase in heart function. Magnes Res 2:161–172
3. Carafoli E (1991) The calcium pumping ATPase of the plasma membrane. Annu Rev Physiol 53:531–547
4. Chacko S, Miyata H, Horiuchi KY (1987) Modulation of actomyosin ATPase by thin filament-associated proteins. Prog Clin Biol Res 245:143–158
5. Chow D, Forte J (1995) Functional significance of the beta-subunit for heterodimeric P-type ATPases. J Exp Biol 198:1–17
6. Forgac M (1992) Structure and properties of the coated vesicle (H^+)-ATPase. J Bioenerg Biomembr 24:341–350
7. Sweadner KJ (1989) Isozymes of the Na^+/K^+-ATPase. Biochim Biophys Acta 988:185–220
8. Knowles AF (2011) The CDA1_CD39 superfamily: NTPDases with diverse functions. Purinergic Signal 7:21–45
9. Sansom FM (2012) The role of the NTPDase enzyme family in parasites: what do we know, and where to from here? Parasitology 16:1–18
10. Sansom FM, Robson SC, Hartland EL (2008) Possible effects of microbial ecto-nucleotide triphosphate diphosphohydrolases on host-pathogen interactions. Microbiol Mol Biol Rev 72:765–781
11. Zimmermann H (2000) Extracellular metabolism of ATP and nucleotides. Naunyn Schmiedebergs Arch Pharmacol 362:299–309
12. Zimmermann H, Zebish M, Stratar N (2012) Cellular function and molecular structure of ecto-nucleotidases. Purinergic Signal 8:437–502

13. Horisberger JD, Lemas V, Kraehenbuhl JP, Rossier BC (1991) Structure-function relationship of Na, K-ATPase. Annu Rev Physiol 53:565–584
14. Plesner L (1995) Ecto ATPases: identities and functions. Int Rev Cytol 158:141–214
15. Plesner L, Kirley TL, Knowles AF (eds) (1997) Ecto-ATPases. Plenum, New York
16. Webb E (1992) Enzyme nomenclature. International Union of Biochemistry and Molecular Biology Academic Press, San Diego
17. Treuheit MJ, Vagy PL, Kirley TL (1992) Mg^{2+} ATPase from rabbit skeletal muscle transverse tubules is 67-kilodalton glycoprotein. J Biol Chem 267:11777–11782
18. Dhalla NS, Pierce GN, Elimban V (1984) Involvement of the sarcolemmal membrane in cardiac contraction and relaxation. In: Abe H, Ito Y, Tada M, Opie LH (eds) Regulation of cardiac function. Japan Science Press, Tokyo, pp 11–22
19. Knowles AF, Isler RE, Reece JF (1983) The common occurrence of ATP diphosphohydrolase in mammalian plasma membranes. Biochim Biophys Acta 731:88–96
20. Su C (1983) Purinergic neurotransmission and neuromodulation. Annu Rev Pharmacol Toxicol 23:397–411
21. Burnstock G (1996) Introduction-purinergic transmission. Semin Neurosci 8:171–174
22. Edwards FA, Gibb AJ, Colquhoun D (1992) ATP receptor-mediated synaptic currents in the central nervous system. Nature 359:144–147
23. Trams EG, Lauter CJ (1974) On the sidedness of plasma membrane enzymes. Biochim Biophys Acta 345:180–197
24. Beaudoin AR, Vachereau A, Grondin G et al (1986) Microvesicular secretion, a mode of cell secretion associated with the presence of an ATP-diphosphohydrolase. FEBS Lett 203:1–2
25. Strobel R, Rosenberg M (1992) Immunoaffinity chromatographic purification of chicken ecto ATP diphosphohydrolase. Ann N Y Acad Sci 671:487–489
26. Kittel A, Bacsy E (1994) Ecto-ATPases and 5′-nucleotidases in the caveolae of smooth muscle. Enzyme histochemical evidence may indicate a role for caveolae in neurotransmission. Cell Biol Int 18:875–879
27. De Souza LR, Reed JK (1991) The involvement of ecto-ATPase activity in the phosphorylation of intracellular proteins by the addition of extracellular [^{32}P] ATP in PC12 cells. Neurochem Int 19:581–592
28. Lin SH, Guidotti G (1989) Cloning and expression of a cDNA coding for a rat liver plasma membrane ecto-ATPase. The primary structure of the ecto-ATPase is similar to that of the human biliary glycoprotein 1. J Biol Chem 264:14408–14414
29. Cunningham HB, Yazaki PJ, Domingo RC et al (1993) The skeletal muscle transverse tubular Mg^{2+}-ATPase: identity with Mg-ATPases of smooth muscle and brain. Arch Biochem Biophys 303:32–43
30. Cheung PH, Thompson NL, Earley K et al (1993) Cell-CAM105 isoforms with different adhesion functions are co-expressed in adult rat tissues and during liver development. J Biol Chem 268:6139–6146
31. Kannan S, Elimban V, Fandrich R et al (1997) Evidence that the rat cardiac sarcolemmal Ca^{2+}/Mg^{2+} ectoATPase (Myoglein) is a cell adhesion molecule. Cardiovasc Pathobiol 2:3–9
32. Kirley TL (1997) Complementary DNA cloning and sequencing of the chicken muscle ecto-ATPase. Homology with the lymphoid cell activation antigen CD39. J Biol Chem 272: 1076–1081
33. Dzhandzhugazyan K, Bock E (1993) Demonstration of Ca^{2+}-Mg^{2+} ATPase activity of the neural cell adhesion molecule. FEBS Lett 336:279–283
34. Dzhandzhugazyan K, Bock E (1997) Relationship of NCAM to E-type ATPases of rat synaptosomes Ecto-ATPases. In: Plesner L, Kirley T, Knowles AF (eds) EctoATPases: recent progress on structure and function. Plenum Press, New York, pp 277–282
35. Dzhandzhugazyan K, Bock E (1997) Demonstration of an ATP-binding site in NCAM: functional implications of nucleotide binding. Biochemistry 36:15381–15395
36. Tingstrom A, Blikstad I, Aurivillius M, Obrink B (1990) C-CAM (Cell-CAM 105) is an adhesive cell surface glycoprotein with hemophilic binding properties. J Cell Sci 96:17–25

37. Knowles AF, Gao JP, Murray S (1997) Is the rat liver ectoATPase identical to C-CAMJppI20, a cell adhesion molecule? In: Plesner L, Kirley T, Knowles AF (eds) Ecto-ATPases: recent progress on structure and function. Plenum Press, New York, pp 277–282
38. Martin SS, Senior AE (1980) Membrane adenosine triphosphatase activities in rat pancreas. Biochim Biophys Acta 602:401–418
39. Knowles AF (1995) The rat liver ecto-ATPase/C-CAM cDNA detects induction of carcinoembryonic antigen but not the mercurial-insensitive ecto-ATPase in human hepatoma Li-7A cells treated by epidermal growth factor and cholera toxin. Biochem Biophys Res Commun 207:529–535
40. Juul B, Plesner L, Aalkjaer C (1993) Effects of ATP and related nucleotides on the tone of isolated rat mesenteric resistance arteries. J Pharmacol Exp Ther 264:1234–1240
41. Epstein MA, Holt SJ (1963) Electron microscope observations on the surface adenosine triphosphatase like enzymes of HeLa cells infected with herpes virus. J Cell Biol 19:337–347
42. Stewart CC, Gasic G, Hempling HG (1969) Effect of exogenous ATP on the volume of TA3 ascites tumor cells. J Cell Physiol 73:125–131
43. Hehl EM, Hennighausen G, Lange P (1985) Ecto-ATPases in leukocytes and its modification by drugs. Allerg Immunol (Leipz) 31:17–23
44. Knowles AF, Salas Prato M, Villela J (1985) Epidermal growth factor inhibits growth while increasing the expression of an ecto Ca^{2+}-ATPase of a human hepatoma cell line. Biochem Biophys Res Commun 126:8–14
45. Hennighausen G, Lange P (1985) Activity of ecto-ATPase in different populations of mouse and rat lymphocytes. Biomed Biochim Acta 44:1269–1272
46. Nagy AK, Shuster TA, Delgado Escueta AV (1986) Ecto-ATPase of mammalian synaptosomes: identification and enzymic characterization. J Neurochem 47:976–986
47. Still JS, Manery JF, Dryden EE (1986) The inactivation by concanavalin A of the ecto-ATPase and ectoacetylcholinesterase of intact skeletal muscles. Biochem Cell Biol 64:1272–1280
48. Steinberg TH, Silverstein SC (1987) Extracellular ATP4-promotes cation fluxes in the J774 mouse macrophage cell line. J Biol Chem 262:3118–3122
49. Ziganshin AU, Ziganshina LE, Hoyle CH, Burnstock G (1995) Effects of divalent cations and La^{3+} on contractility and ecto-ATPase activity in the guinea-pig urinary bladder. Br J Pharmacol 114:632–639
50. Nagy AK, Houser CR, Delgado Escueta AV (1990) Synaptosomal ATPase activities in temporal cortex and hippocampal formation of humans with focal epilepsy. Brain Res 529: 192–201
51. Maxwell WL, McCreath BJ, Graham DI, Gennarelli TA (1995) Cytochemical evidence for redistribution of membrane pump Ca^{2+} ATPase and ecto-Ca^{2+} ATPase activity, and calcium influx in myelinated nerve fibres of the optic nerve after stretch injury. J Neurocytol 24:925–942
52. Romero M, Guizouarn H, Pellissier B et al (1996) The erythrocyte Na^+/H^+ exchangers of eel (Anguilla anguilla) and rainbow trout (Oncorhynchus mykiss): a comparative study. J Exp Biol 199:415–426
53. Lemmens R, Vanduffel L, Teuchy H, Culic O (1996) Regulation of proliferation of LLC-MK2 cells by nucleosides and nucleotides: the role of ecto-enzymes. Biochem J 316:551–557
54. King BF, Pintor J, Wang S et al (1996) A novel P1 purinoceptor activates an outward K^+ current in follicular oocytes of Xenopus laevis. J Pharmacol Exp Ther 276:93–100
55. Dombrowski KE, Ke Y, Brewer KA, Kapp JA (1998) Ecto-ATPase: an activation marker necessary for effector cell function. Immunol Rev 161:111–118
56. Stefanovic V, Mitic-Zlatkovic M, Savic V, Vlahovic P (2002) Effect of polyamines on mesangial cell ecto-5′-nucleotidase and ecto-ATPase activity. Nephron 92:216–218
57. Knowles AF, Chiang WC (2003) Enzymatic and transcriptional regulation of human ecto-ATPase/E-NTPDase 2. Arch Biochem Biophys 418:217–227
58. Mateo J, Harden TK, Boyer JL (1999) Functional expression of a cDNA encoding a human ecto-ATPase. Br J Pharmacol 128:396–402
59. Marcus AJ, Broekman MJ, Drosopoulos JHF (2003) Metabolic control of excessive extracellular nucleotide accumulation by CD39/ecto-nucleotidase-1: implications for ischemic vascular diseases. J Pharmacol Exp Ther 305:9–16

60. Zimmermann H (1999) Two novel families of ectonucleotidases: molecular structures, catalytic properties and a search for function. Trends Pharmacol Sci 20:231–236
61. Zimmermann H (1999) Nucleotides and cd39: principal modulatory players in hemostasis and thrombosis. Nat Med 5:987–988
62. Kannan S (2003) E-NTPase/E-NTPDase: a potential regulatory role in E-kinase/PKA-mediated CD36 activation. Cell Biol Int 27:153–163
63. Melani A, Corti F, Stephan H et al (2012) Ecto-ATPase inhibition: ATP and adenosine release under physiological and ischemic in vivo conditions in the rat striatum. Exp Neurol 233: 193–204
64. Ribeiro MC, Costa-Alves MS, Wengert M et al (2012) Characterization of ecto-ATPase activity in the surface of LLC-PK1 cells and its modulation by ischemic conditions. Biochim Biophys Acta 1820:2030–2036
65. Giarola NL, de Almeida-Amaral EE, Collopy-Junior I et al (2013) Trypanosoma cruzi: effects of heat shock on ecto-ATPase activity. Exp Parasitol 133:434–441
66. Manoonkitiwongsa PS, Whitter EF, Chavez JN, Schultz RL (2010) Blood-brain barrier Ca^{2+}-ATPase cytochemistry: incubation media and fixation methods for differentiating Ca^{2+}-specific ATPase from ecto-ATPase. Biotech Histochem 85:257–268
67. Lin SH (1989) Localization of the ecto-ATPase (ecto-nucleotidase) in the rat hepatocyte plasma membrane. Implications for the functions of the ecto-ATPase. J Biol Chem 264:14403–14407
68. Lin SH (1990) Liver plasma membrane ecto-ATPase. Ann N Y Acad Sci 603:394–400
69. Buxton DB, Robertson SM, Olson MS (1986) Stimulation of glycogenolysis by adenine nucleotides in the perfused rat liver. Biochem J 237:773–780
70. Lin SH, Culic O, Flanagan D, Hixson DC (1991) Immunochemical characterization of two isoforms of rat liver ecto-ATPase that show an immunological and structural identity with a glycoprotein cell adhesion molecule with Mr 105,000. Biochem J 278:155–161
71. Cheung PH, Luo W, Qiu Y et al (1993) Structure and function of C-CAM1. The first immunoglobulin domain is required for intercellular adhesion. J Biol Chem 268:24303–24310
72. Culic O, Huang QH, Flanagan D et al (1992) Molecular cloning and expression of a new rat liver cell-CAM 105 isoforms. Differential phosphorylation of isoforms. Biochem J 285: 47–53
73. Filippini A, Taffs RE, Agui T, Sitkovsky MV (1990) Ecto-ATPase activity in cytolytic T-lymphocytes. Protection from the cytolytic effects of extracellular ATP. J Biol Chem 265: 334–340
74. Battastini AM, da Rocha JB, Barcellos CK et al (1991) Characterization of an ATP diphosphohydrolase (EC 3.6.1.5) in synaptosomes from cerebral cortex of adult rats. Neurochem Res 16:1303–1310
75. Barry MA (1992) Ecto calcium dependent ATPase activity of mammalian taste bud cells. J Histochem Cytochem 40:1919–1928
76. Kurihara K, Hosoi K, Ueha T (1992) Characterization of ecto-nucleoside triphosphatase on A-431 human epidermoidal carcinoma cells. Enzyme 46:213–220
77. Girolomoni G, Santantonio ML, Bergstresser PR et al (1992) Membrane ecto-ATPase on epidermal Langerhans cells. J Invest Dermatol 99:18S–19S
78. Beukers MW, Pirovano IM, van Weert A et al (1993) Characterization of ecto-ATPase on human blood cells. A physiological role in platelet aggregation? Biochem Pharmacol 46:1959–1966
79. Rodriguez Pascual F, Torres M, Miras-Portugal MT (1993) 8-Azido-adenine nucleotides as substrates of ecto-nucleotidases in chromaffin cells: inhibitory effect of photoactivation. Arch Biochem Biophys 306:420–426
80. Hohmann J, Kowalewski H, Vogel M, Zimmermann H (1993) Isolation of a Ca^{2+} or Mg^{2+}-activated ATPase (ecto-ATPase) from bovine brain synaptic membranes. Biochim Biophys Acta 1152:146–154
81. Stout JG, Brittsan A, Kirley TL (1994) Brain ecto Mg^{2+}-ATPase is not the neural cell adhesion molecule. Biochem Mol Biol lnt 33:1091–1098

82. Sippel CJ, Suchy FJ, Ananthanarayanan M, Perlmutter DH (1993) The rat liver ecto-ATPase is also a canalicular bile acid transport protein. J Biol Chem 268:2083–2091
83. Sippel CJ, Fallon RJ, Perlmutter DH (1994) Bile acid efflux mediated by the rat liver canalicular bile acid transport ecto-ATPase protein requires serine 503 phosphorylation and is regulated by tyrosine 488 phosphorylation. J Biol Chem 269:19539–19545
84. Kast C, Stieger B, Winterhalter KH, Meier PJ (1994) Hepatocellular transport of bile acids. Evidence for distinct subcellular localizations of electrogenic and ATP-dependent taurocholate transport in rat hepatocytes. J Biol Chem 269:5179–5186
85. Stout J, Kirley TL (1994) Purification and characterization of the ecto-Mg-ATPase of chicken gizzard smooth muscle. J Biochem Biophys Methods 29:61–75
86. Murphy HC, Hand AR, Dowd FJ (1994) Localization of an ecto-ATPase/cell-CAM 105 (C-CAM) in the rat parotid and submandibular glands. J Histochem Cytochem 42:561–568
87. Shi XJ, Knowles AF (1994) Prevalence of the mercurial-sensitive EctoATPase in human small cell lung carcinoma: characterization and partial purification. Arch Biochem Biophys 315:177–184
88. Stefanovic V, Vlahovic P (1995) Divalent cation-activated ecto-ATPase activity of rat glomerular mesangial cells. Arch Physiol Biochem 103:15–20
89. Beukers MW, Kerkhof CJ, van Rhee MA (1995) Suramin analogs, divalent cations and ATP gamma S as inhibitors of ecto-ATPase. Naunyn Schmiedebergs Arch Pharmacol 351:523–528
90. Stout JG, Strobel RS, Kirley TL (1995) Properties of and proteins associated with the extracellular ATPase of chicken gizzard smooth muscle. A monoclonal antibody study. J Biol Chem 270:11845–11850
91. Schweickhardt C, Sabolic I, Brown D, Burckhardt G (1995) Ecto-adenosine triphosphatase in rat small intestinal brush-border membranes. Am J Physiol 268:G663–G672
92. Chen BC, Lee CM, Lin WW (1996) Inhibition of ecto-ATPase by PPADS, suramin and reactive blue in endothelial cells, C6 glioma cells and RAW 264.7 macrophages. Br J Pharmacol 119:1628–1634
93. Cheung PK, Baller JF, Bakker WW (1996) Impairment of endothelial and subendothelial sites by a circulating plasma factor associated with minimal change disease. Nephrol Dial Transplant 11:2185–2191
94. Adachi T, Arai K, Ohkuma S (1996) A comparative study of (Ca^{2+}-Mg^{2+})-ATPase on the lysosomal membrane and ecto-ATPase on the plasma membrane from rat liver. Biol Pharm Bull 19:1291–1297
95. Westfall TO, Kennedy C, Sneddon P (1996) Enhancement of sympathetic purinergic neurotransmission in the guinea·pig isolated vas deferens by the novel ectoATPase inhibitor ARL 67156. Br J Pharmacol 117:867–872
96. Felts PA, Smith KJ (1996) Changes in the distribution of a calcium-dependent ATPase during demyelination and remyelination in the central nervous system. J Neurocytol 25:171–180
97. Stout JG, Kirley TL (1996) Control of cell membrane ecto-ATPase by oligomerization state: intermolecular cross-linking modulates ATPase activity. Biochemistry 35:8289–8298
98. Barbacci E, Filippini A, De Cesaris P, Ziparo E (1996) Identification and characterization of an ecto-ATPase activity in rat Sertoli cells. Biochem Biophys Res Commun 222:273–279
99. Smith TM Jr, Kirley TL, Hennessey TM (1997) A soluble ecto-ATPase from Tetrahymena thennophila: purification and similarity to the membrane-bound ecto-ATPase of smooth muscle. Arch Biochem Biophys 337:351–359
100. Correale P, Tagliaferri P, Guarrasi R et al (1997) Extracellular adenosine 5′ triphosphate involvement in the death of LAK-engaged human tumor cells via P2x-receptor activation. Immunol Lett 55:69–78
101. Wang TF, Guidotti G (1996) CD39 is an ecto, (Ca^{2+}, Mg^{2+}) apyrase. J Biol Chem 271: 9898–9901
102. Lin SH (1985) The rat liver plasma membrane high affinity (Ca^{2+}-Mg^{2+}) ATPase is not a calcium pump. J Biol Chem 260:10076–10980

103. Beaudoin AR, Sevigny J, Grondin G et al (1997) Purification, characterization, and localization of two ATP diphosphohydrolase isoforms in bovine heart. Am J Physiol 273:H673–H681
104. Gloor S, Antonicek H, Sweadner KJ et al (1990) The adhesion molecule of glia (AMOG) is a homologue of the beta subunit of the Na, K-ATPase. J Cell Biol 110:165–174
105. Airas L, Jalkanen S (1996) CD73 mediates adhesion of B cells to follicular dendritic cells. Blood 88:1755–1764
106. Sulakhe PV, Dhalla NS (1971) Excitation-contraction coupling in heart. VI. Demonstration of calcium activated ATPase in the dog heart sarcolemma. Life Sci 10:185–191
107. Slezak T, Okruhlicova L, Tribulova N et al (1995) Renaissance of cytochemical localization on membrane ATPases in the myocardium. Mol Cell Biochem 147:169–172
108. McNamara DB, Singh JN, Dhalla NS (1974) Properties of some heart sarcolemmal-bound enzymes. J Biochem 76:603–609
109. Takeo S, Duke P, Taam GML et al (1979) Effects of lanthanum on the heart sarcolemmal ATPase and calcium binding activities. Can J Physiol Pharmacol 57:496–503
110. Anand-Srivastava MB, Panagia V, Dhalla NS (1982) Properties of Ca^{2+}- or Mg^{2+}-dependent ATPase in rat heart sarcolemma. Adv Myocardiol 3:359–371
111. Dhalla NS, Anand MB, Harrow JAC (1976) Calcium binding and ATPase activities of heart sarcolemma. J Biochem 79:1345–1350
112. McNamara DB, Sulakhe PV, Dhalla NS (1971) Properties of the sarcolemmal calcium stimulated ATPase of the hamster skeletal muscle. Biochem J 125:525–530
113. Anand MB, Chauhan MS, Dhalla NS (1977) Ca^{2+}/Mg^{2+} ATPase activities of heart sarcolemma, microsomes and mitochondria. J Biochem 82:1731–1739
114. Tuana BS, Kutryk MJB, Elimban V et al (1984) Influence of myosin antiserum on heart Ca^{2+} or Mg^{2+} ATPase activity. Res Commun Chem Pathol Pharmacol 45:297–300
115. Elimban V, Zhao D, Dhalla NS (1987) A comparative study of the rat heart sarcolemmal Ca^{2+}-dependent ATPase and myosin ATPase. Mol Cell Biochem 77:143–152
116. Panagia V, Elimban V, Ganguly PK, Dhalla NS (1987) Decreased Ca^{2+} binding and Ca^{2+}-ATPase activities in heart sarcolemma upon phospholipid methylation. Mol Cell Biochem 78:65–71
117. Anand-Srivastava MB, Dhalla NS (1987) Alterations in Ca^{2+}/Mg^{2+} ATPase activity upon treatment of heart sarcolemma with phospholipases. Mol Cell Biochem 77:89–96
118. Panagia V, Lamers JMJ, Singal PK, Dhalla NS (1982) $Ca^{2+}$and Mg^{2+}-dependent ATPase activities in the deoxycholate-treated rat heart sarcolemma. Int J Biochem 14:387–397
119. Ziegelhoffer A, Anand-Srivastava MB, Khandelwal RL, Dhalla NS (1979) Activation of heart sarcolemmal Ca^{2+}/Mg^{2+} ATPase by cyclic AMP-dependent protein kinase. Biochem Biophys Res Commun 84:1073–1081
120. Ziegelhoffer A, Anand-Srivastava MB, Dhalla NS (1984) Possible role of Ca^{2+}-ATPase in the mechanism of calcium influx through cardiac sarcolemma. In: Will-Shahab L, Krause E-G, Schulze W (eds) Cellular and molecular aspects of regulation of the heart. Akademia, Berlin, pp 99–106
121. Ziegelhoffer A, Dhalla NS (1987) Activation of Ca^{2+}/Mg^{2+} ATPase in heart sarcolemma upon electrical stimulation. Mol Cell Biochem 77:135–141
122. Dhalla NS, Pierce GN, Panagia V et al (1982) Calcium movements in relation to heart function. Basic Res Cardiol 77:117–139
123. Dhalla NS, Lee SL, Anand MB, Chauhan MS (1977) Effects of acebutolol, practolol and propranolol on the rat heart sarcolemma. Biochem Pharmacol 26:2055–2060
124. Dhalla NS, Harrow JAC, Anand MB (1978) Actions of some antiarrhythmic agents on heart sarcolemma. Biochem Pharmacol 27:1281–1283
125. Harrow JAC, Das PK, Dhalla NS (1978) Influence of some divalent cations on heart sarcolemmal bound enzymes and calcium binding. Biochem Pharmacol 27:2605–2609
126. Heyliger CE, Dhalla NS (1986) Sarcolemmal Ca^{2+} binding and Ca^{2+}-ATPase activities in hypertrophied heart. J Appl Cardiol 1:447–467
127. Daly MJ, Dzurba A, Tuana BS, Dhalla NS (1986) Sarcolemmal Ca^{2+}-binding and enzyme activities in myocardium from hypothyroid rat. Can J Cardiol 2:356–361

128. Kaneko M, Singal PK, Dhalla NS (1990) Alterations in heart sarcolemmal Ca^{2+}-ATPase and Ca^{2+}-binding activities due to oxygen free radicals. Basic Res Cardiol 85:45–54
129. Alto LE, Elimban V, Dhalla NS (1999) Alterations in sarcolemmal Ca^{2+}/Mg^{2+} ecto-ATPase activity in hearts subjected to calcium paradox. Exp Clin Cardiol 4:29–34
130. Pierce GN, Dhalla NS (1987) The association of membrane alterations with heart dysfunction during experimental diabetes mellitus. In: Dhalla NS, Singal PK, Beamish RE (eds) Pathophysiology of heart disease. Martinus Nijhoff Publishing, Boston, pp 177–184
131. Dhalla NS, Anand-Srivastava MB, Tuana BS, Khandelwal RL (1981) Solubilization of a calcium dependent adenosine triphosphatase from rat heart sarcolemma. J Mol Cell Cardiol 13:413–423
132. Tuana BS, Dhalla NS (1982) Purification and characterization of a Ca^{2+}-dependent ATPase from rat heart sarcolemma. J Biol Chem 257:14440–14445
133. Anand-Srivastava MB, Dhalla NS (1987) Characteristics of Ca^{2+}/Mg^{2+} ATPase in heart sarcolemma treated with trypsin. In: Dhalla NS, Pierce GN, Beamish RE (eds) Heart function and metabolism. Martinus Nijhoff Publishing, Boston, pp 191–203
134. Tuana BS, Dhalla NS (1987) Solubilization of a divalent cation dependent ATPase from dog heart sarcolemma. Mol Cell Biochem 77:79–87
135. Tuana BS, Dhalla NS (1988) Purification and characterizations of a Ca^{2+}/Mg^{2+} ecto-ATPase from rat heart sarcolemma. Mol Cell Biochem 81:75–88
136. Zhao D, Dhalla NS (1988) Characterization of rat heart plasma membrane Ca^{2+}/Mg^{2+} ATPase. Arch Biochem Biophys 263:281–292
137. Zhao D, Makino N, Dhalla NS (1989) Specific stimulation of heart sarcolemmal Ca^{2+}/Mg^{2+} ATPase by concanavalin A. Arch Biochem Biophys 268:40–48
138. Zhao D, Dhalla NS (1989) Influence of gramicidin S on cardiac membrane Ca^{2+}/Mg^{2+} ATPase activities and contractile force development. Can J Physiol Pharmacol 67:546–552
139. Zhao D, Dhalla NS (1991) Purification and composition of Ca^{2+}/Mg^{2+} ATPase from rat heart plasma membrane. Mol Cell Biochem 107:135–149
140. Zhao D, Elimban V, Dhalla NS (1991) Characterization of the purified rat heart plasma membrane Ca^{2+}/Mg^{2+} ATPase. Mol Cell Biochem 107:151–160
141. Kannan S, Elimban V, Dakshinamurti K, Dhalla NS (1998) Biophysical characterization of rat cardiac Ca^{2+}/Mg^{2+} ecto-ATPase (Myoglein). Mol Cell Biochem 183:153–157
142. Kannan S, Lalonde C, Zahradka P, Dhalla NS (1998) Molecular cloning of rat cardiac sarcolemmal Ca^{2+}/Mg^{2+} ectoATPase (Myoglein). J Mol Cell Cardiol 30:2261–2268
143. Kannan S, Elimban V, Fandrich RR et al (1999) Immunolocalization of the sarcolemmal Ca^{2+}/Mg^{2+} ecto-ATPase (Myoglein) in rat myocardium. Mol Cell Biochem 197:187–194

Part II
Sarco(endo)plasmic Reticulum ATPases

Chapter 9
The Ca^{2+} ATPase of the Sarco-/Endoplasmic Reticulum (SERCA): Structure and Control

Giuseppe Zanotti

Abstract The SERCA pump, a membrane protein of about 110 kDa, transports two Ca^{2+} ions per ATP hydrolyzed, from the cytoplasm to the lumen of the sarcoplasmic reticulum. In muscle cells its ability to remove Ca^{2+} from the cytosol induces relaxation. The transport mechanism employed by SERCA1a from rabbit skeletal muscle has been dissected at the molecular level by several crystal structures that represent nearly all the different conformational states of the catalytic cycle of Ca^{2+} transport. The structure of the complexes of SERCA with sarcolipin or phospholamban, two small membrane proteins responsible of the control of the pump activity in the skeletal muscle and in the heart, has also been determined, allowing the understanding of the molecular aspects of the control. All these structural data, along with extensive molecular dynamics calculations and functional characterization in vitro, have allowed a detailed understanding at the atomic level of the process of transport of calcium from the cytoplasm to the reticulum. SERCA1 represents perhaps, among the P-type ATPases, the best described at the atomic level.

Keywords Calcium pumps • Ca^{2+} ATPases • SERCA • Calcium transport • Endoplasmic reticulum

1 Introduction

The Ca^{2+} ATPase of the sarco(endo)plasmic reticulum (SERCA) is a single polypeptide chain protein of approximately 110 kDa and about 1000 residues [1]. SERCA is an integral membrane protein located in the membrane of the reticulum that, thanks to ATP hydrolysis, pumps back into the sarcoplasmic reticulum the calcium ions that have been previously released in the muscle cells during contraction, allowing in such a way the muscle to relax [2] (for a general review, see [3]). Three different

G. Zanotti (✉)
Department of Biomedical Sciences, University of Padua,
Viale G. Colombo 3, 35131 Padua, Italy
e-mail: giuseppe.zanotti@unipd.it
http://tiresia.bio.unipd.it/zanotti

S. Chakraborti, N.S. Dhalla (eds.), *Regulation of Ca^{2+}-ATPases,V-ATPases and F-ATPases*, Advances in Biochemistry in Health and Disease 14,
DOI 10.1007/978-3-319-24780-9_9

types of SERCA exist in mammals, encoded in three different genes, and each of them gives rise, by alternative splicing, to different isoforms: three for SERCA1 and SERCA2 and six for SERCA3 (they are called SERCA1a, SERCA1b, and so on, till SERCA3f) [4]. This alternative splicing gives rise to proteins that differ in length at the C-terminus, being SERCA1a the shortest and SERCA3a the longest with 994 and 1052 residues, respectively. They are present in different amounts in various tissues, and the functional differences among isoforms have not been fully clarified yet. SERCA1a is the only form present in fast-twitch skeletal muscle, while isoforms 2a and 2b are predominant in the heart.

Sequences of SERCA are very well conserved in mammals, but SERCA-like Ca^{2+} ATPases have been found in many lower species, including bacteria. The best structurally characterized among SERCA pumps is SERCA1a from rabbit skeletal muscle. 44 coordinate files of this protein have been deposited at the Protein Data Bank (PDB) since the first crystal structure was determined in 2000 [5], mostly in different conformational states [6–21]. Only one structure from other species was determined, bovine SERCA [22], discussed in paragraph 5. General reviews on the structural basis of the Ca^{2+} pumping by SERCA can be found in [23–25]. In this chapter a general description of SERCA three-dimensional structure and its mechanism of calcium transport are summarized.

2 Overall Crystal Structure of SERCA from Rabbit Muscle

The structure of SERCA1a from rabbit muscle can be described as consisting of three cytoplasmic domains, labeled A, N, and P for actuator, nucleotide-binding, and phosphorylation domain, respectively, by the M domain consisting of ten transmembrane helices (from M1 to M10) and by a small lumenal portion, made of few loops that connect some of the transmembrane helices. Domains A and P are connected to the M domain, while domain N is not, being close in space to domain P (Fig. 9.1a).

Domain **P** includes two separate parts of the amino acid sequence: residues from 330 to 359 and from 604 to 737 (beginning and end of each domain are approximate, assigned by visual inspection of the 3D model). The beginning and the end of domain P are connected to helices M4 and M5 of domain M, while the sequence included between the two segments of domain P, from amino acid 360–603, constitutes domain N, which is continuous along the polypeptide chain. Domain P is arranged as a classical Rossmann fold, a seven-stranded parallel β-strand surrounded by eight α-helices (Fig. 9.1b). The Rossmann fold in proteins is often associated with the binding of nucleotides, and, in fact, domain P participates in the binding of ATP and contains Asp351, the residue that is phosphorylated.

Domain **N** comprises a seven-stranded antiparallel β-sheet with two helix bundles on each side (Fig. 9.1b). It contains most of the residues implicated in the binding of ATP, in particular Phe487, Ly515, and Lys492.

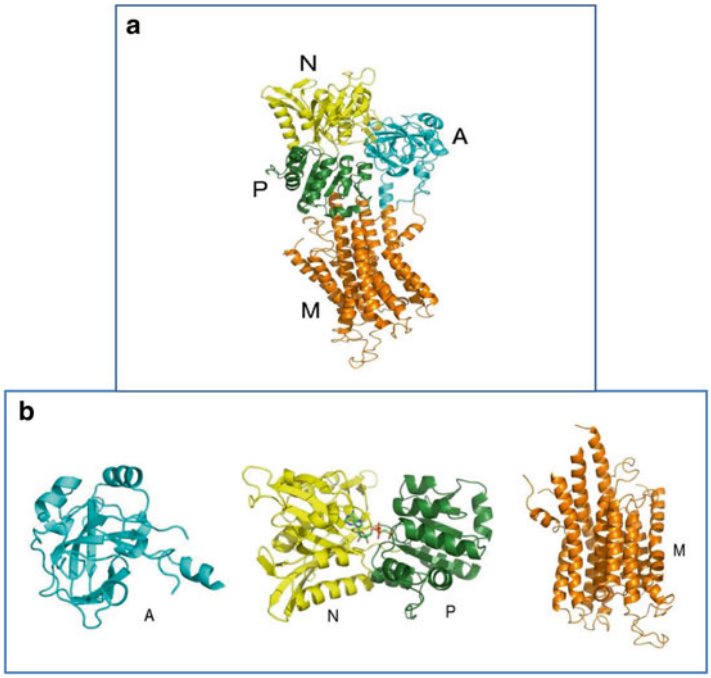

Fig. 9.1 (**a**) Cartoon view of E1 state of SERCA pump. The actuator domain (A) is *cyan* (residues 1–43 and 115–241), the phosphorylation (P) domain *green* (residues 330–359 and 604–737), the nucleotide-binding (N) domain *yellow* (residues 360–603), and the transmembrane (M) domain *orange* (residues 44–114, 242–329, and 738–994). Coordinates from fitE1AMPPCP.pdb. (**b**) Cartoon view of the four separated domains (not in scale). The AMPPCP analogue of ATP is shown as stick model bound in between domains N and P. Coordinates from fitE1AMPPCP.pdb

Domain **A**, the smallest among the SERCA domains, like domain P is not continuous in the amino acid sequence, including residues from the N-terminus to 40/43 and from 115/118 to 241. The C-terminus of domain A is connected to helix M1 of domain M, and the remaining portion is in between helices M2 and M3. Its fold can be described as a jellyroll structure, plus two α-helices located in the N-terminal portion of the domain (Fig. 9.1b).

Domain **M** is the largest of domain of SERCA, including ten transmembrane helices and few luminal loops, for a total of more than 400 residues. The helices, numbered from M1 to M10, not only span the membrane, but some of them also expand in the cytoplasm. All these helices move considerably during the reaction cycle, as described below, and in doing so they contribute to the transport of calcium ions from the cytoplasm to the reticulum.

The enzyme has two binding sites for calcium, one for ATP and magnesium and others for effectors and inhibitors. The two calcium-binding sites, located closed-by in domain M, have a cooperative behavior with two binding constants for the rabbit enzyme, measured in vitro, of 1.2×10^5 and 5.0×10^7 for site I and II, respectively

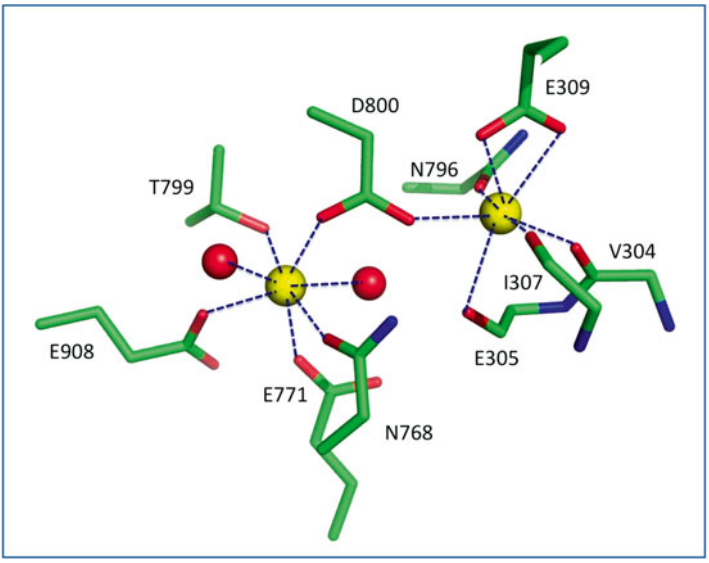

Fig. 9.2 Detail of the two calcium-binding sites (coordinates E1Mfit). Ca^{2+} ions are shown as *yellow spheres*, solvent molecules as *red spheres*. Only side or main chain atoms of SERCA residues coordinating calcium are shown. Distances of oxygen atoms range from 2.22 to 2.68 Å

[26]. In the Ca^{2+} high-affinity conformation of the pump (see below), both Ca^{2+} sites have seven coordinating oxygen atoms: in site I the ion interacts with one oxygen of Thr99, Glu771 and 908, Asn768, Asp800, and of two water molecules; in site II Ca^{2+} is surrounded by the two oxygen atoms of Glu309, one oxygen of Asn796 and Asp800 (the latter bridges the two calcium ions, interacting with both), and the carbonyl oxygen of Val304, Glu305, and Ile307. The distances between Ca^{2+} and oxygen atoms range from 2.2 to 2.7 Å (Fig. 9.2).

The ATP-binding site (Fig. 9.3) is in between domains N and P: the nucleotide-binding domain contains most of the residues that interacts with the adenosine moiety, in particular Arg589, 515, 560 and 678, Glu442, Asn627, Thr625, and Phe487. The latter is the only hydrophobic residue in contact with the nucleotide, and it is responsible of a π-π stacking interaction with the purine ring of ATP. Only the γ-phosphate of the nucleotide and Mg^{2+} ion interact with domain P through the residue that is phosphorylated, Asp351, and Thr353.

3 The Reaction Cycle: Conformations of Different States

The reaction cycle (Fig. 9.4a) can be describe in terms of two major conformational states, called E1 and E2, the former being the state with the highest affinity for calcium, while E2 has the lowest. Large conformational movements that explain the

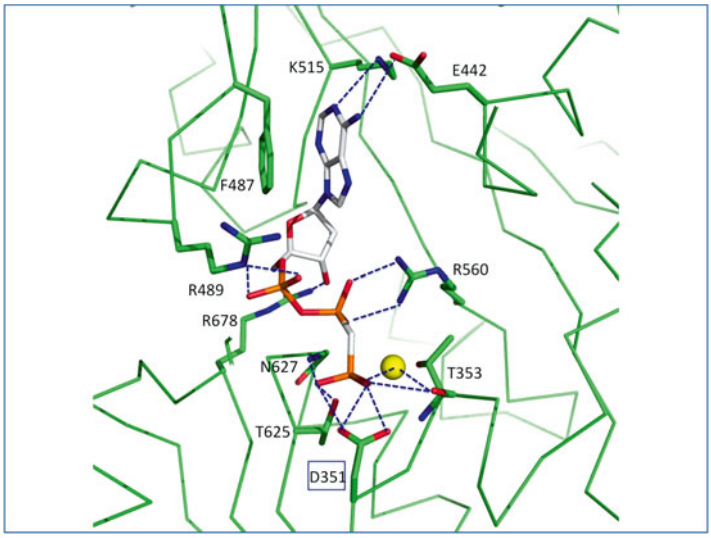

Fig. 9.3 The ATP analogue AMPPCP bound to the E1 state of SERCA (structure fitE1AMPPCP). Only residue side chains in contract with the nucleotide are shown, and potential hydrogen bond interactions are indicated by *dashed lines*. Most of the residues interacting with the nucleotide belong to domain N, while only the γ-phosphate is close to residues of domain P, Thr353, and Asp351. The latter, the residue that becomes phosphorylated, is *boxed*

different affinities for calcium ions take place in the transition between the two states. These two states can be in turn subdivided in substates, characterized by minor conformational differences.

The **E2** conformation, without calcium or ATP bound, is considered the ground state of the pump. In it, the calcium-binding cavity is filled with water molecules and H^+ ions that protonate carboxyl groups, in order to compensate for the absence of the four positive charges of the two Ca^{2+}. The structure of the pump in the E2 conformation is quite compact, with domains A, N, and P in contact (Fig. 9.4b). This situation cannot last for long at pH 7, and protons present in the Ca^{2+}-binding cavity are dissipated through the membrane. This event induces the binding of a Mg^{2+} ion in the calcium-binding cavity and places the enzyme in the **E1-Mg^{2+}** state. The carboxyl groups present in the calcium-binding cavity are deprotonated, and the cavity assumes a high affinity for Ca^{2+}. Only when the concentration of Ca^{2+} in the cytoplasm is low, the site with the highest affinity for calcium is occupied by Mg^{2+}. In the E1 conformation, the structure of SERCA is much less compact with respect to E2 state, and the calcium-binding cavity is accessible from the cytoplasmic space. As soon as the calcium concentration in the cytoplasm rises, Ca^{2+} binds to the calcium-binding cavity, displacing Mg^{2+} and placing SERCA in the **E1·2Ca^{2+}** state. The two Ca^{2+} ions enter sequentially, Ca^{2+} II after Ca^{2+} I. The next step is the binding of ATP-Mg^{2+}, which binds to the site in between domains N and P. The interactions

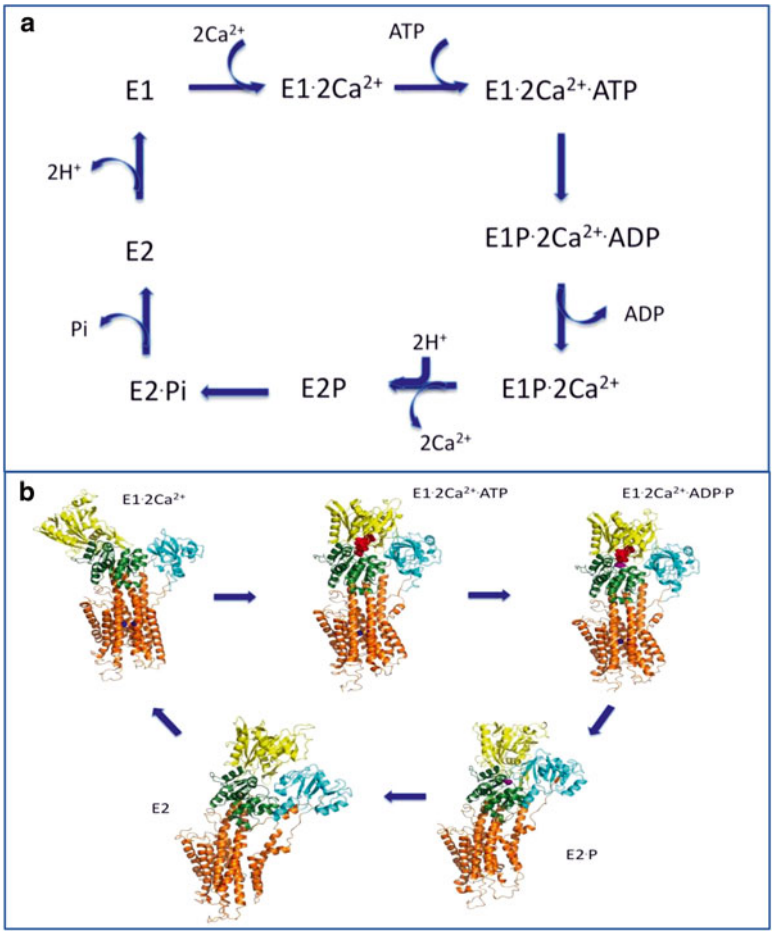

Fig. 9.4 (**a**) Scheme of the SERCA cycle. The scheme was adapted from Ref. [59]. (**b**) Representative structures of the SERCA cycle. The four domains N, A, P, and M are colored *yellow*, *cyan*, *dark green*, and *orange*, respectively. ATP or ADP is shown as *red spheres*, Ca^{2+} ions as *blue spheres*. AlF_3^- or BeF_3^-, mimicking the phosphate, as *magenta spheres*

of ATP with the protein place it in a highly strained conformation and at the same time close the gate of the calcium-binding site, so that the two calcium ions are occluded inside the SERCA transmembrane domain.

The key event at this point is phosphorylation: the transfer of the γ phosphate to Asp351 triggers the transition from the **E1·2Ca^{2+}** to the **E1P** state and, through a series of small interactions described in great detail in [27], the transition to the **E2P** state. The latter involves a general rearrangement of the domains, the largest being a rotation of about 90° of domain A. These movements make the overall structure of the pump much more compact, but at the same time they cause a drastic rearrangement of the transmembrane helices, in particular M1 to M6, altering the geometry of the

calcium-binding cavity and triggering the opening of luminal gate: the two calcium ions are released into the lumen. The opening of the gate allows H^+ and water to enter the empty calcium-binding cavity and fill it.

The final step of the cycle is represented by the hydrolysis of the phosphate from Asp351. A further rearrangement of domain A places a water molecule in a position where Glu183 can assist its attack to the aspartyl phosphate and catalyze its hydrolysis, pushing the enzyme back into the **E2** ground state, where SERCA is ready to start a new cycle.

4 SERCA Regulation; Binding of Phospholamban and Sarcolipin

Phospholamban (PLB), a mediator of the β-adrenergic signal in the heart [28], is a small protein, 52 amino acids long, consisting of a long hydrophobic helix and a small cytoplasmic domain. It is prevalently present in cardiac muscle, and it is believed to regulate the activity of SERCA in the heart [29]. Its counterpart in striated skeletal muscle is represented by sarcolipin (SLN), another small regulatory membrane protein of 31 amino acids present in both fast-twitch skeletal and atrial cardiac muscles [30, 31]. Sarcolipin and phospholamban share 50 % identity in the transmembrane helix, and they both control the activity of the pump, since their binding to SERCA blocks or depress the transport of calcium. The β-adrenergic control regulates phosphorylation of PLB at Ser13 and/or Thr17. SLN is phosphorylated at Thr in position 5. In both cases phosphorylation induces dissociation of the protein from the pump, releasing the inhibition.

Several modeling studies of the binding to SERCA of these two regulator molecules have been produced [32–37], including molecular dynamics [38, 39] and time-resolved FRET [36], but only very recently the crystal structure of both complexes, SERCA/SLN [20, 21] and SERCA/PLB [32], have been determined. In all cases the ATPase used to produce crystals was SERCA1a from rabbit skeletal muscle, which probably is the natural target of sarcolipin, but not of phospholamban, whose main target is the SERCA2 isoform, present mostly in the heart. Nevertheless, crystal structures clearly show that both sarcolipin and phospholamban share the same binding site, in a grove defined by transmembrane helices M2, M6, and M9 (Fig. 9.5). In both sarcolipin complexes, the crystallized sample was extracted from the rabbit skeletal muscle, while the SERCA/PLB complex was prepared in vitro by mixing SERCA extracted from rabbit sarcoplasmic reticulum with recombinant PLB.

Sarcolipin consists of a single continuous transmembrane helix, slightly curved, with few residues at both ends. It is associated with SERCA in a previously undescribed E1 state, and the binding of SLN stabilizes this E1 state, deprived of bound calcium, and prevents the transition of SERCA to the E2 state. The cleft formed by M2, M6, and M9 helices where SLN is embedded becomes quite narrow in proximity of Thr5 of SLN, so that phosphorylation of Thr5 induces repulsion of

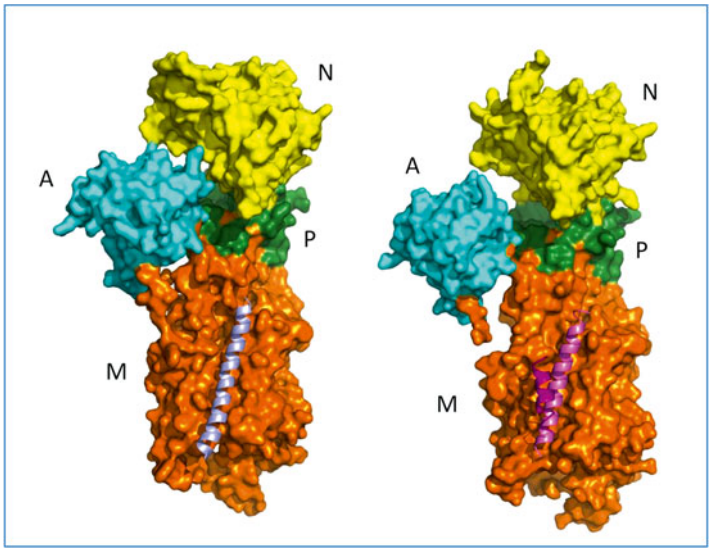

Fig. 9.5 The complex SERCA/sarcolipin (*left*) and SERCA/phospholamban (*right*). Coordinates from 4H1W and 4KYT, respectively

the bound SLN, with consequent dissociation of the complex and reactivation of the enzyme normal activity.

In the crystal structure of SERCA/PLB complex, only one transmembrane helix of PLB, residues from 21 to 49, and a small portion of a second one are visible in the electron density in the crystal, while the cytoplasmic domain is disordered and not visible. In the complex the pump is present in an E2-Ca^{2+}-free conformation. The binding of PLB in between helices M4, M5, M6, and M8 of SERCA disrupts the two high-affinity calcium-binding sites, stabilizing the E2 state of SERCA and blocking the transition from the E2 to the E1 conformation of the pump.

5 SERCA from Other Species

The only known crystal structure of SERCA from species other than rabbit is that of the bovine enzyme, determined at 2.9 Å resolution in the E1 state [22]. The structure, as expected from the similarity of the amino acid sequences between rabbit and bovine enzymes (the two differ only for 22 amino acid positions and 1 deletion), is very similar to that of the rabbit enzyme in the corresponding state, with a r.m.s.d. for the superposition of equivalent Cα atoms of 0.82 Å. Structural differences are confined to few loop regions, mostly in the luminal area where loops that connect transmembrane helices are often found flexible (Fig. 9.6). Calcium-binding and nucleotide-binding sites are structurally very well conserved, and this

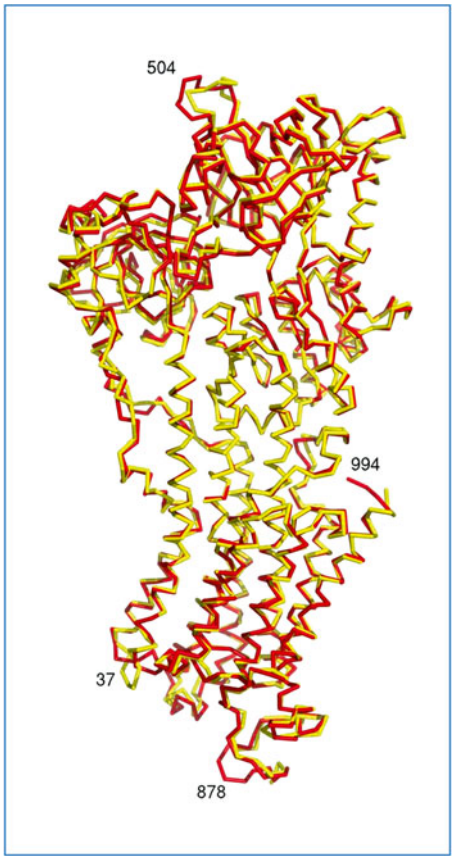

Fig. 9.6 Superposition of Cα chain trace of bovine SERCA (*yellow*, PDB ID 3TLM) to rabbit SERCA (*red*, PDB ID 1T5S [9]). Both structures correspond to the E1 state

reflects in a similar $K_{0.5}$ for Ca^{2+} activation of the pump: the pCa has been measured in the range 6–6.6 for rabbit, bovine, and human enzymes [40–42]. Despite that, the bovine enzyme shows a catalytic activity, measured in isolated membranes, reduced of about 30 % with respect to the rabbit enzyme [22]. The most relevant structural differences are present in the long loop that connects α-helices M7 and M8. Since the transition from the E1 to the E2 conformational state perturbs the region of the intermembrane helices and involves the area that protrudes into the lumen, these structural differences could influence the transition E1 → E2, justifying the reduced catalytic activity.

Another characterized SERCA-type pump is the enzyme from the gram-negative pathogen *Listeria monocytogenes*, which exhibits a high sequence similarity with mammalian SERCA1a. Despite the absence of a crystal structure, the enzyme has been purified and characterized in solution and a molecular model built by homology with the rabbit enzyme [43]. Despite the significant similarity in the amino acid sequence and in the three-dimensional architecture, significant

differences can be detected in the bacterial enzyme, in particular the presence of 1 Ca^{2+}-binding site only, corresponding to site II of SERCAa1, and the transport of 1 Ca^{2+} and possibly $1H^{+}$ per ATP hydrolyzed.

6 SERCA Inhibitors

SERCA, being an ATPase, can be fully inhibited in vitro by classical ATP analogues or by inhibitors that bind to the ATP-binding site. Since ATP binding is common to an extremely large number of enzymes, including all protein kinases, these classes of inhibitors are generally not specific and not useful as SERCA inhibitors in vivo. A different group of SERCA inhibitors is represented by ligands that bind preferentially to one of the SERCA state and freeze the enzyme in that conformation, blocking the cycle.

The most characterized and specific among these inhibitors is thapsigargin [44] (the structural formula of thapsigargin is reported in Fig. 9.7a), a molecule that binds preferentially to the E2 conformation of the pump at a transmembrane site located at the protein-lipid interphase in between helices M3, M5, and M7 (Fig. 9.7b) [6, 11]. Several studies on the effects of thapsigargin on SERCA have been performed [45–48], and various thapsigargin analogues have been proposed as SERCA pump inhibitors and tested [18].

7 Dynamical Studies

The picture of a protein molecule given by a crystal structure is a sort of "static" one, despite dynamical aspects can be derived by an accurate analysis of thermal parameters. In the case of SERCA, a protein that undergoes drastic conformational change during its pumping cycle, the knowledge of the structures of nearly all the possible states of the catalytic cycle gives a very clear picture of the dynamics of the cycle, in a sort of movie where we can observe only a limited number of photograms of some steps of the process. Molecular dynamics simulations can allow filling in the gap in between these steps.

Several molecular dynamics calculations have been performed, in order to mimic the movements of SERCA molecule during its catalytic cycle. Coarse-grained simulations were able to reproduce the transitions from E2 to E1, in wild type and mutants, showing compensation of relative changes of enthalpy and entropy along the transition [49]. Another approach has used a full-atom dynamics, including lipid bilayer, water molecules, and ions to dissect the molecular events that trigger the transition from a conformation to another. A 500 ns molecular dynamics starting from the E1 conformation, with and without calcium, suggests that the presence of Ca^{2+} and not of ATP is necessary for the activation of the transition from the open to the activated close conformation of the pump [50]. Another dynamics of E1 form in

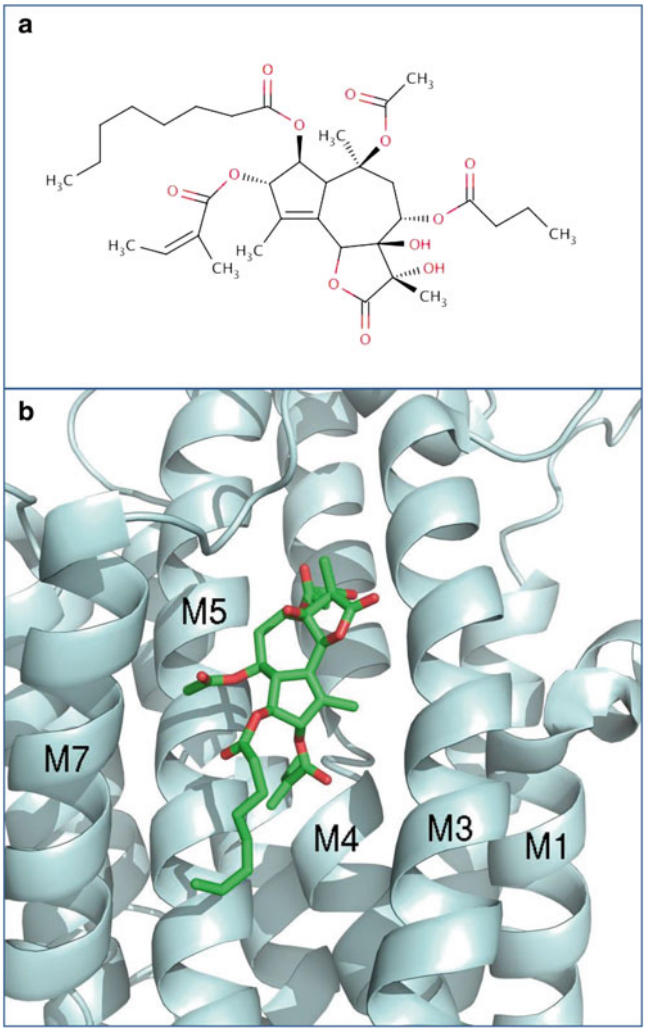

Fig. 9.7 (**a**) Thapsigargin chemical formula. (**b**) Detail of the transmembrane helices region with thapsigargin bound. The model corresponds to the E2 state of the pump. Coordinates from PDB ID 1XP5 [11]

the presence and absence of Mg^{2+} bound, but in absence of Ca^{2+}, suggests that the E1 state with Mg^{2+} or K^{+} bound facilitates the E2 to E1·Ca^{2+} transition [51]. Finally, principal components analysis has allowed to partition the SERCA structure into multiple catalytically distinct states and to dissect the role of single residues in the process of binding and release of calcium [52].

Experimental dynamics data sometimes suggest a slightly different view of the transition. A fast-scanning atomic force microscopy study has analyzed the behavior of single SERCA molecules contained in SR vesicles immobilized on a mica surface [53].

Results are quite puzzling and contrasting in different experimental conditions: at 10 nM ATP and 100 μM Ca^{2+} concentration, shape changes of SERCA can be interpreted as corresponding to the conformations observed during the ATP-mediated cycle, while at more physiological conditions (1.0 mM ATP and 100 μM Ca^{2+}), the more compact conformation was not observed, at least with the time resolution of 50 μs.

Dynamics of phospholamban has also been investigated by NMR, either alone [54–57] or in complex with SERCA [58].

8 Conclusions

Thanks to a large mass of structural data, possibly unparalleled among membrane proteins, the mechanism of transport of calcium ions by the Ca^{2+} ATPase of the sarco-/endoplasmic reticulum has been dissected at atomic level in great details. Using a technique, protein crystallography, that gives essentially static images, we have now a complete picture of a complex dynamical phenomenon. This is particularly relevant in this case, where the subject is not a water-soluble, small protein, but a large and complex membrane protein. Nevertheless, several questions on SERCA are still open. All the studies were performed on SERCA1a, and since the other (iso) forms differ for a very limited numbers of residues, it is reasonable to assume that the general mechanism proposed is valid for all of them. Nevertheless, since three forms of SERCA, each of them with several isoforms, are present in the different tissues, they must have their own specificity and functionality. Another aspect not at well studied is the effect of the membrane environment, and on environment in general, on the pump functionality. Possibly the different phospholipid, and other molecules, composition of the membrane affects the efficiency and the behavior of the enzyme. Finally, control mechanisms of the pump in different organs are probably also different. All these aspects require studies in vivo that can be performed only on animal models. More in general, the reductionist approach of molecular and structural biology is fundamental to the understanding of the general aspects of molecular mechanisms, but these studies must be coupled to others, at cellular and tissue level, where molecules works in a complex environment, in contact with a large number of other molecules that may influence activities and performances.

Acknowledgments I would like to thank Ernesto Carafoli for introducing me to the world of SERCA and PMCA and also for comments and criticisms on this manuscript.

References

1. MacLennan DH, Brandl CJ, Korczak B, Green NM (1985) Amino-acid sequence of a Ca^{2+} + Mg^{2+}-dependent ATPase from rabbit muscle sarcoplasmic reticulum, deduced from its complementary DNA sequence. Nature 316:696–700
2. de Meis L, Hasselbach W (1971) Acetyl phosphate as substrate for Ca^{2+} uptake in skeletal muscle microsomes. Inhibition by alkali ions. J Biol Chem 246:4759–4763

3. Brini M, Carafoli E (2009) Calcium pumps in health and disease. Physiol Rev 89:1341–1378
4. Martonosi A, Pikula S (2003) The structure of the Ca2+-ATPase of sarcoplasmic reticulum. Acta Biochim Pol 50:337
5. Toyoshima C, Nakasako M, Nomura H, Ogawa H (2000) Crystal structure of the calcium pump of sarcoplasmic reticulum at 2.6 A resolution. Nature 405:647–655
6. Toyoshima C, Nomura H (2002) Structural changes in the calcium pump accompanying the dissociation of calcium. Nature 418:605–611
7. Hua S, Ma H, Lewis D et al (2002) Functional role of "N" (nucleotide) and "P" (phosphorylation) domain interactions in the sarcoplasmic reticulum (SERCA) ATPase. Biochemistry 41:2264–2272
8. Toyoshima C, Mizutani T (2004) Crystal structure of the calcium pump with a bound ATP analogue. Nature 430:529–535
9. Sørensen TL, Møller JV, Nissen P (2004) Phosphoryl transfer and calcium ion occlusion in the calcium pump. Science 304:1672–1675. doi:10.1126/science.1099366
10. Xu C, Ma H, Inesi G et al (2004) Specific structural requirements for the inhibitory effect of thapsigargin on the Ca^{2+} ATPase SERCA. J Biol Chem 279:17973–17979
11. Olesen C, Sorensen T, Nielsen R et al (2004) Dephosphorylation of the calcium pump coupled to counterion occlusion. Science 306:2251
12. Obara K, Miyashita N, Xu C et al (2005) Structural role of countertransport revealed in Ca(2+) pump crystal structure in the absence of Ca(2+). Proc Natl Acad Sci U S A 102:14489–14496. doi:10.1073/pnas.0506222102
13. Jensen A-ML, Sorensen TL-M, Olesen C et al (2006) Modulatory and catalytic modes of ATP binding by the calcium pump. EMBO J 25:2305–2314
14. Olesen C, Picard M, Winther A-ML et al (2007) The structural basis of calcium transport by the calcium pump. Nature 450:1036–1042
15. Picard M, Jensen A-ML, Sørensen TL-M et al (2007) Ca2+ versus Mg^{2+} coordination at the nucleotide-binding site of the sarcoplasmic reticulum Ca^{2+}-ATPase. J Mol Biol 368:1–7
16. Marchand A, Winther A-ML, Holm PJ et al (2008) Crystal structure of D351A and P312A mutant forms of the mammalian sarcoplasmic reticulum Ca(2+) -ATPase reveals key events in phosphorylation and Ca(2+) release. J Biol Chem 283:14867–14882
17. Laursen M, Bublitz M, Moncoq K et al (2009) Cyclopiazonic acid is complexed to a divalent metal ion when bound to the sarcoplasmic reticulum Ca^{2+}-ATPase. J Biol Chem 284:13513–13518
18. Winther A-ML, Liu H, Sonntag Y et al (2010) Critical roles of hydrophobicity and orientation of side chains for inactivation of sarcoplasmic reticulum Ca^{2+}-ATPase with thapsigargin and thapsigargin analogs. J Biol Chem 285:28883–28892
19. Toyoshima C, Yonekura S-I, Tsueda J, Iwasawa S (2011) Trinitrophenyl derivatives bind differently from parent adenine nucleotides to Ca^{2+}-ATPase in the absence of Ca^{2+}. Proc Natl Acad Sci 108:1833–1838
20. Winther A-ML, Bublitz M, Karlsen JL et al (2013) The sarcolipin-bound calcium pump stabilizes calcium sites exposed to the cytoplasm. Nature 495:265–269. doi:10.1038/nature11900
21. Toyoshima C, Iwasawa S, Ogawa H et al (2013) Crystal structures of the calcium pump and sarcolipin in the Mg^{2+}-bound E1 state. Nature 495:260–264
22. Sacchetto R, Bertipaglia I, Giannetti S et al (2012) Crystal structure of sarcoplasmic reticulum Ca(2+)-ATPase (SERCA) from bovine muscle. J Struct Biol 178:38–44
23. Toyoshima C, Nomura H, Sugita Y (2003) Structural basis of ion pumping by Ca^{2+}-ATPase of sarcoplasmic reticulum. FEBS Lett 555:106–110
24. Toyoshima C, Inesi G (2004) Structural basis of ion pumping by CA(2+)-ATPase of the sarcoplasmic reticulum. Annu Rev Biochem 73:269–292
25. Møller JV, Nissen P, Sørensen TL-M, Le Maire M (2005) Transport mechanism of the sarcoplasmic reticulum Ca^{2+}-ATPase pump. Curr Opin Struct Biol 15:387–393
26. Inesi G, Kurzmack M, Coan C, Lewis DE (1980) Cooperative calcium binding and ATPase activation in sarcoplasmic reticulum vesicles. J Biol Chem 255:3025–3031
27. Toyoshima C (2009) How Ca^{2+}-ATPase pumps ions across the sarcoplasmic reticulum membrane. Biochim Biophys Acta 1793:941–946

28. Lindemann JP, Jones LR, Hathaway DR et al (1983) beta-Adrenergic stimulation of phospholamban phosphorylation and Ca^{2+}-ATPase activity in guinea pig ventricles. J Biol Chem 258:464–471
29. Trieber CA, Afara M, Young HS (2009) Effects of phospholamban transmembrane mutants on the calcium affinity, maximal activity, and cooperativity of the sarcoplasmic reticulum calcium pump. Biochemistry 48:9287–9296
30. Wawrzynow A, Theibert JL, Murphy C et al (1992) Sarcolipin, the "proteolipid" of skeletal muscle sarcoplasmic reticulum, is a unique, amphipathic, 31-residue peptide. Arch Biochem Biophys 298:620–623
31. Asahi M, Sugita Y, Kurzydlowski K et al (2003) Sarcolipin regulates sarco(endo)plasmic reticulum Ca^{2+}-ATPase (SERCA) by binding to transmembrane helices alone or in association with phospholamban. Proc Natl Acad Sci U S A 100:5040–5045
32. Akin BL, Hurley TD, Chen Z, Jones LR (2013) The structural basis for phospholamban inhibition of the calcium pump in sarcoplasmic reticulum. J Biol Chem 288:30181–30191
33. Chen LTL, Yao Q, Soares TA et al (2009) Phospholamban modulates the functional coupling between nucleotide domains in Ca-ATPase oligomeric complexes in cardiac sarcoplasmic reticulum. Biochemistry 48:2411–2421
34. Gorski PA, Glaves JP, Vangheluwe P, Young HS (2013) Sarco(endo)plasmic reticulum calcium ATPase (SERCA) inhibition by sarcolipin is encoded in its luminal tail. J Biol Chem 288:8456–8467
35. Gustavsson M, Verardi R, Mullen DG et al (2013) Allosteric regulation of SERCA by phosphorylation-mediated conformational shift of phospholamban. Proc Natl Acad Sci 110: 17338–17343
36. Dong X, Thomas DD (2014) Time-resolved FRET reveals the structural mechanism of SERCA-PLB regulation. Biochem Biophys Res Commun 449:196–201
37. Abrol N, Smolin N, Armanious G et al (2014) Phospholamban C-terminal residues are critical determinants of the structure and function of the calcium ATPase regulatory complex. J Biol Chem 289:25855–25866
38. Sugita Y, Miyashita N, Yoda T et al (2006) Structural changes in the cytoplasmic domain of phospholamban by phosphorylation at Ser16: a molecular dynamics study. Biochemistry 45:11752–11761
39. Lian P, Wei D-Q, Wang J-F, Chou K-C (2011) An allosteric mechanism inferred from molecular dynamics simulations on phospholamban pentamer in lipid membranes. PLoS One 6:e18587
40. Maruyama K, MacLennan DH (1988) Mutation of aspartic acid-351, lysine-352, and lysine-515 alters the Ca^{2+} transport activity of the Ca2+-ATPase expressed in COS-1 cells. Proc Natl Acad Sci U S A 85:3314–3318
41. Sacchetto R, Testoni S, Gentile A et al (2009) A defective SERCA1 protein is responsible for congenital pseudomyotonia in Chianina cattle. Am J Pathol 174:565–573
42. Odermatt A, Barton K, Khanna VK et al (2000) The mutation of Pro789 to Leu reduces the activity of the fast-twitch skeletal muscle sarco(endo)plasmic reticulum Ca^{2+} ATPase (SERCA1) and is associated with Brody disease. Hum Genet 106:482–491
43. Faxén K, Andersen JL, Gourdon P et al (2011) Characterization of a Listeria monocytogenes Ca(2+) pump: a SERCA-type ATPase with only one Ca(2+)-binding site. J Biol Chem 286:1609–1617
44. Vandecaetsbeek I, Vangheluwe P, Raeymaekers L et al (2011) The Ca^{2+} pumps of the endoplasmic reticulum and Golgi apparatus. Cold Spring Harb Perspect Biol 3:a004184
45. Sagara Y, Inesi G (1991) Inhibition of the sarcoplasmic-reticulum Ca^{2+} transport ATPase by thapsigargin at subnanomolar concentrations. J Biol Chem 266:13503–13506
46. Wictome M, Henderson I, Lee AG, East JM (1992) Mechanism of inhibition of the calcium pump of sarcoplasmic reticulum by thapsigargin. Biochem J 283(Pt 2):525–529
47. Inesi G, Sagara Y (1992) Thapsigargin, a high affinity and global inhibitor of intracellular Ca^{2+} transport ATPases. Arch Biochem Biophys 298:313–317

48. Seekoe T, Peall S, McIntosh DB (2001) Thapsigargin and dimethyl sulfoxide activate medium P(i)↔HOH oxygen exchange catalyzed by sarcoplasmic reticulum Ca^{2+}-ATPase. J Biol Chem 276:46737–46744
49. Nagarajan A, Andersen JP, Woolf TB (2012) Coarse-grained simulations of transitions in the E2-to-E1 conformations for Ca ATPase (SERCA) show entropy–enthalpy compensation. J Mol Biol 422:575–593
50. Espinoza-Fonseca LM, Thomas DD (2011) Atomic-level characterization of the activation mechanism of SERCA by calcium. PLoS One 6:e26936
51. Espinoza-Fonseca LM, Autry JM, Thomas DD (2014) Microsecond molecular dynamics simulations of Mg^{2+}- and K+- bound E1 intermediate states of the calcium pump. PLoS One 9:e95979
52. Kekenes-Huskey PM, Metzger VT, Grant BJ, Andrew McCammon J (2012) Calcium binding and allosteric signaling mechanisms for the sarcoplasmic reticulum Ca^{2+}ATPase. Protein Sci 21:1429–1443
53. Yokokawa M, Takeyasu K (2011) Motion of the Ca2+-pump captured. FEBS J 278: 3025–3031
54. Chu S, Coey AT, Lorigan GA (2010) Solid-state (2)H and (15)N NMR studies of side-chain and backbone dynamics of phospholamban in lipid bilayers: investigation of the N27A mutation. Biochim Biophys Acta 1798:210–215
55. Traaseth NJ, Veglia G (2010) Probing excited states and activation energy for the integral membrane protein phospholamban by NMR CPMG relaxation dispersion experiments. Biochim Biophys Acta 1798:77–81
56. Traaseth NJ, Shi L, Verardi R et al (2009) Structure and topology of monomeric phospholamban in lipid membranes determined by a hybrid solution and solid-state NMR approach. Proc Natl Acad Sci 106:10165–10170
57. Traaseth N, Buffy J, Zamoon J, Veglia G (2006) Structural dynamics and topology of phospholamban in oriented lipid bilayers using multidimensional solid-state NMR. Biochemistry 45:13827–13834
58. Seidel K, Andronesi OC, Krebs J et al (2008) Structural characterization of Ca(2+)-ATPase-bound phospholamban in lipid bilayers by solid-state nuclear magnetic resonance (NMR) spectroscopy. Biochemistry 47:4369–4376
59. Toyoshima C (2008) Structural aspects of ion pumping by Ca^{2+}-ATPase of sarcoplasmic reticulum. Arch Biochem Biophys 476:3–11

Chapter 10
Functional and Structural Insights into Sarcolipin, a Regulator of the Sarco-Endoplasmic Reticulum Ca^{2+}-ATPases

Thomas Barbot, Cédric Montigny, Paulette Decottignies, Marc le Maire, Christine Jaxel, Nadège Jamin, and Veronica Beswick

Abstract Sarcolipin (SLN), a transmembrane peptide from sarcoplasmic reticulum, is one of the major proteins involved in the muscle contraction/relaxation process. A number of enzymological studies have underlined its regulatory role in connection with the SERCA1a activity. Indeed, SLN folds as a unique transmembrane helix and binds to SERCA1a in a groove close to transmembrane helices M2, M6, and M9, as proposed initially by cross-linking experiments and recently detailed in the 3D structures of the SLN–Ca^{2+}-ATPase complex. In addition, association of SLN with SERCAs may depend on its phosphorylation. SLN possesses a peculiar C-terminus (RSYQY) critical for the regulation of the ATPases. This luminal tail appears to be essential for addressing SLN to the ER membrane. Moreover, we recently demonstrated that some SLN isoforms are acylated on cysteine 9, a feature which remained unnoticed so far even in the recent crystal structures of the SLN–SERCA1a complex. The removal of the fatty acid chain was shown to increase the activity of the membrane-embedded Ca^{2+}-ATPase by about 20 %. The exact functional and structural

T. Barbot • C. Montigny • M. le Maire • C. Jaxel • N. Jamin
Institute for Integrative Biology of the Cell (I2BC), Commissariat à l'Energie Atomique et aux Energies Alternatives (CEA), Centre National de la Recherche Scientifique (CNRS), Université Paris-Sud, iBiTec-S/SB2SM/Laboratoire des Protéines et Systèmes Membranaires, CEA-Saclay, 91191 Gif-sur-Yvette CEDEX, France

P. Decottignies
Pharmacologie et biochimie de la synapse, Neuro PSI, UMR9197, CNRS, Université Paris-Sud, 91405 Orsay CEDEX, France

V. Beswick (✉)
Institute for Integrative Biology of the Cell (I2BC), Commissariat à l'Energie Atomique et aux Energies Alternatives (CEA), Centre National de la Recherche Scientifique (CNRS), Université Paris-Sud, iBiTec-S/SB2SM/Laboratoire des Protéines et Systèmes Membranaires, CEA-Saclay, 91191 Gif-sur-Yvette CEDEX, France

Physics Department, Université d'Evry-Val-d'Essonne, 91025 Evry CEDEX, France
e-mail: veronica.beswick@cea.fr

S. Chakraborti, N.S. Dhalla (eds.), *Regulation of Ca^{2+}-ATPases,V-ATPases and F-ATPases*, Advances in Biochemistry in Health and Disease 14,
DOI 10.1007/978-3-319-24780-9_10

role of this post-translational modification is presently unknown. Recent data are in favor of a key regulator role of SLN in muscle-based thermogenesis in mammals. The possible link of SLN to heat production could occur through an uncoupling of the SERCA1a-mediated ATP hydrolysis from calcium transport. Considering those particular features and the fact that SLN is not expressed at the same level in different tissues, the role of SLN and its exact mechanism of regulation remain sources of interrogation.

Keywords Sarcolipin • Calcium ATPase • NMR • X-Ray crystallography • Molecular dynamics • Phosphorylation • Protein acylation • Oligomerization • Regulatory peptides • Membrane protein

Abbreviations

SRER	Sarco-endoplasmic reticulumEndoplasmic reticulum
ER	Endoplasmic reticulum
SERCA1a or 2a	Sarco-Endoplasmic Reticulum Ca^{2+}-ATPase isoform 1a or 2a
SLN	Sarcolipin
hSLN	Human isoform of SLN
rSLN	Rabbit isoform of SLN
mSLN	Mouse isoform of SLN
PLN	Phospholamban
DDM	*n*-Dodecyl-β-D-maltopyranoside
$C_{12}E_8$	Octaethylene glycol monododecyl ether
DOC	Deoxycholate
SDS	Sodium dodecyl sulfate
DPC	*n*-Dodecylphosphocholine or Fos-choline-12
SEC	Size exclusion chromatography
MS	Mass spectrometry
MALDI-TOF	Matrix-assisted laser desorption ionization—time of flight
NMR	Nuclear magnetic resonance
ssNMR	Solid state nuclear magnetic resonance
MD	Molecular dynamics
POPC	1-Palmitoyl-2-oleoyl-sn-glycero-3-phosphocholine
DOPC	1,2-Dioleoyl-sn-glycero-3-phosphocholine
DOPE	1,2-Dioleoyl-sn-glycero-3-phosphoethanolamine
EYPC	Egg yolk phosphatidylcholine
EYPA	Egg yolk phosphatic acid
RyR	Ryanodine Receptor
FCCP	Carbonyl cyanide-p-trifluoromethoxyphenylhydrazone

1 Introduction

Sarcolipin is a transmembrane peptide (SLN, 31 amino acids) [1] which was first isolated from rabbit fast-twitch skeletal muscle during the extraction of sarco-endoplasmic reticulum (SR) membranes [2]. Purification and solubility analysis of SLN revealed strong interactions with lipids and the presence of fatty acids. Therefore, considering its amino acid sequence similarity with phospholamban (PLN), a Ca^{2+}-ATPase regulatory peptide, it was suggested that SLN interacts both with lipids and the sarco-endoplasmic reticulum Ca^{2+}-ATPase (SERCA1a) [3, 4].

The main role of SERCAs is to control cytosolic calcium by maintaining SR/ER calcium stores in cells. Calcium is the primary regulator of the contractile machinery and a second messenger in the signal transduction pathways that control, e.g. muscle growth, metabolism, and pathological remodeling. Upon muscle stimulation, Ca^{2+} release by the ryanodine receptor (RyR) localized at the SR membrane transiently increases Ca^{2+} level in the cytosol, triggering actomyosin cross-bridge formation within the sarcomere to generate contractile force. Re-uptake of Ca^{2+} into the SR by SERCAs is necessary for muscle relaxation and restores the Ca^{2+} level for subsequent contraction–relaxation cycles. Several SERCA isoforms have been described with different expression profiles depending on the species, tissues, and even the developmental stage. SERCA1a and SERCA2a isoforms are predominant, and are mainly expressed in the fast-twitch muscle and in the slow-twitch muscle, respectively [5] (Table 10.1 and references herein).

The main steps of the calcium transport cycle are well understood (Fig. 10.1). However, its regulation and especially, the exact role of sarcolipin are still a matter of debate as reviewed below. As a matter of fact, SLN is one of known regulators of SERCA activity in vertebrates as well as phospholamban (PLN, 52 amino acids; [6]) and most probably myoregulin (MLN, 46 amino acids; [7]) (Fig. 10.2). Contrary to SLN and MLN, PLN has been extensively characterized during the last two decades. In invertebrate, an ortholog of these proteins has also been discovered recently and is named sarcolamban (SCL, 28 amino acids; [7, 8]).

In order to contribute to a better understanding of the specific regulator role of SLN upon SERCA activities, we propose, in this review, some critical readings of the published data as well as some additional data. First, SLN gene characterization, its localization in species and tissues and its differential expression during muscle development are presented. Secondly, SLN implications in diseases and thermogenesis are discussed. Then, structural and functional data, including the role of particular amino acid sequence features (phosphorylation, luminal tail, acylation) are reviewed to give a general and new outlook on the topic. Finally, the hypothesis of SLN oligomer formation and SLN interaction with PLN are considered.

Table 10.1 Expression of SLN, PLN, MLN, SERCA1a and SERCA2a in various species and tissues

		Levels of expression (mRNA and proteins) of peptides and SERCA								
		SLN		PLN		MLN	SERCA1a		SERCA2a	
Species	Tissues	mRNA	Proteins	mRNA	Proteins	mRNA	mRNA	Proteins	mRNA	Proteins
Mouse	Atria	++[a] +++[e]	+++[b]	++[a]+++[e]	+/−[b]	−[e]	−[a]		+++[a] +++[e]	+++[b]
	Ventricle	−[a] −[e]	−[b]	+++[a] +++[e]	+++[b]	−[e]	−[a]		+++[a] ++[e]	+++[b]
	Slow-twitch muscle	+[a]	+/−[b]	+/−[a] −[e]	+/−[b]	+[e]	++[a]	+[b]	++[a] +[e]	++[b]
	Fast-twitch muscle	−[a]	++[b]	+/−[a] −[e]	+/−[b]	+++[e]	+++[a]	++[b]	+/−[a] −[e]	+[b]
Rat	Atria	++[a]	+++[b]	++[a]	+[b]		−[a]		+++[a]	+++[b]
	Ventricle	−[a]	−[b]	+++[a]	+++[b]		−[a]		+++[a]	+++[b]
	Slow-twitch muscle	+/−[a]	+/−[b]	−[a]	−[b]		+[a]		++[a]	++[b]
	Fast-twitch muscle	−[a]	++[b]	−[a]	−[b]		+++[a]		+/−[a]	+[b]
Rabbit	Atria	++[a]	+/−[b]	++[a]	+[b]		−[a]		+++[a]	+++[b]
	Ventricle	−[a]	−[b]	+++[a]	+++[b]		−[a]		+++[a]	+++[b]
	Slow-twitch muscle	++[a]	++[b]	+[a]	−[b]		++[a]		++[a]	+[b]
	Fast-twitch muscle	+++[a]	+++[b]	+/−[a]	−[b]		++[a]		+[a]	+[b]
Pig	Atria	+[a]		+[a]			−[a]		+++[a]	
	Ventricle	+/−[a]		+[a]			−[a]		+++[a]	
	Slow-twitch muscle	+++[a]		+/−[a]			+[a]		++[a]	
	Fast-twitch muscle	+++[a]		+/−[a]			++[a]		++[a]	

Dog	Atria		+/−[b]		+/−[b]					+++[b]
	Ventricle		−[b]		+++[b]					+++[b]
	Slow-twitch muscle		++[b]		−[b]					+[b]
	Fast-twitch muscle		+++[b]		−[b]					+[b]
Human	Atria		+++[c]		+++[c]					+++[c]
	Ventricle									
	Slow-twitch muscle		+[d]		+++[d]			+[d]		+++[d]
	Fast-twitch muscle		+++[d]		++[d]			+++[d]		−[d]

Relative evaluations were performed by measuring the mRNA levels (RT PCR) and the proteins levels (western-blots). Selected references are [12][a], [13][b], [16][c], [14][d] and [7][e]

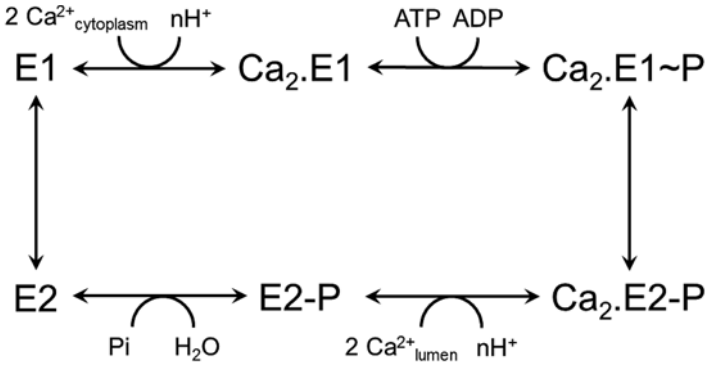

Fig. 10.1 Ca^{2+}-ATPase catalytic cycle. Sarcoplasmic reticulum calcium ATPases catalyze calcium transport from the cytosol to the lumen, coupled with ATP hydrolysis. The main steps of the catalytic cycle are shown here. At physiological pH, two cytoplasmic calcium ions bind to the "E1" high-affinity states. Binding of one Mg.ATP triggers calcium occlusion and it results in autophosphorylation of the ATPase ("Ca_2.E1~P" occluded state). Then, large conformational changes occur, leading to the calcium deocclusion, the release of the calcium into the lumen, and protonation of the transport sites. The Ca^{2+}-free "E2-P" state is finally hydrolyzed to the "E2" ground state

```
hSLN                              MGINTRELFLNFTIVLITVILMWLLVRSYQY
hPLN   MEKVQYLTRSAIRRASTIEMPQQARQKLQNLFINFCLILICLLLICIIVMLL
hMLN        MTGKNWILISTTTPKSLEDEIVGRLLKILFVIFVDLISIIYVVITS
dSCL                              MSEARNLFTTFGILAILLFFLYLIYAVL
                                  *  *  ...  .  .  ..
```

Fig. 10.2 Transmembrane peptides that putatively interact with SERCAs. Alignment of human sarcolipin (hSLN), human phospholamban (hPLN), human myoregulin (hMLN), and their invertebrate ortholog *Drosophila melanogaster* sarcolamban (dSCL). Sequences were aligned with the SEAVIEW program [100]. *Boxed* residues are expected to match with the hydrophobic part of the lipid bilayer. Identical residues are indicated by a *star* and similar residues are *dotted*

2 Sarcolipin Gene Characterization

In human, SLN gene is mapped to chromosome 11q22-q23 [4]. SLN gene (5.6 kb) has two small exons, with the entire coding sequence lying in exon 2 and a large intron (3.9 kb) separating the two segments. Several box elements upstream of the transcription initiation site may correspond to DNA binding sites for transcriptional activators such as (a) the binding site for the myocyte enhancer factor MEF2 in combination with MEF3-like element involved in muscle-specific induction of the aldolase A gene, and (b) the E box-paired sites for MyoD bound in the muscle creatine kinase enhancer [9] and in the acetylcholine receptor α-subunit enhancer [10]. Thus, these DNA binding elements might be responsible for the muscle-specific expression of the SLN gene. The 3′ end of the gene contains multiple polyadenylation signals and two transcripts may be produced, one being preferential.

Comparison of human, rabbit, and mouse SLN cDNAs revealed 84 % nucleotide sequence identity between human and rabbit, 44 % nucleotide sequence identity between human and mouse, and 41 % sequence identity between mouse and rabbit SLN cDNAs. The higher level of nucleotide sequence identity between human and rabbit SLN cDNAs is reflected in their identical length and in their use of the same polyadenylation signal sequence for the major transcript. This polyadenylation site is lacking in the mouse SLN gene, which contains another consensus polyadenylation signal sequence downstream. Thus, the mouse cDNA is longer. In terms of translation, nucleotides including the translation initiation signal sequence [11] are not well conserved among the three species [4].

The two other membrane peptides, PLN and MLN, have a similar gene organization. As a matter of fact, the human PLN gene, as the SLN gene, contains two exons and one large intron (6 kb), the entire coding sequence being located in exon 2. The 3′ end of the PLN gene also contains multiple polyadenylation signals. Recent genome-wide studies have suggested that hundreds of functional peptides may be also encoded in vertebrate long noncoding RNAs (lncRNAs) notably in humans and mice. While analyzing the evolutionary conservation of lncRNA, Anderson et al. recently identified an annotated skeletal muscle-specific lncRNA and a short 138 nucleotides ORF with the potential to encode a highly conserved 46 amino acid peptide, myoregulin (MLN) [7]. The human and mouse MLN genes consist of three exons that span 16.5 kb and 15 kb, respectively, with the ORF located in exon 3. MLN, the skeletal muscle-specific isoforms of SERCA and the Ryanodine receptor (RyR) are co-regulated by MyoD, suggesting that they comprise a core genetic module important for Ca^{2+} handling in skeletal muscle. Analysis of the 5′ flanking region of the MLN gene revealed highly conserved binding sites for the myogenic transcription factors MyoD (E-box) and MEF2. Thus, the MLN gene is a direct target of the transcription factors that activate skeletal myogenesis as the SLN gene [7, 9].

3 Expression of Sarcolipin in Species and Tissues

3.1 Expression of mRNA Encoding Sarcolipin

In order to describe SLN expression at the mRNA level, Odermatt et al. have performed Northern blots analyses by using a human probe against the 3′ untranslated region of the cDNA [4]. Using this method, no expression of SLN was found in various human tissues such as brain, placenta, lung, liver, kidney, uterus, colon, small intestine, bladder, and stomach. Only trace amounts were detected in prostate and pancreas. Yet, the SLN transcript was highly expressed in skeletal muscle at least 50-fold more abundant than in heart muscle. By using a similar rabbit probe, a ninefold higher level of the SLN transcript was found in rabbit fast-twitch skeletal muscle (*psoas*) than in slow-twitch skeletal muscle (*soleus*).

SLN expression at the mRNA level and in various species was more recently determined by RT-PCR experiments. Vangheluwe et al. have shown a difference of

SLN mRNA level in small mammals (mouse and rat) as compared to large mammals (rabbit and pig) [12]. Indeed, SLN mRNA was found in *atria* for rodents, while it was detected in *atria*, *soleus* and *extensor digitorum longus* (EDL) for rabbit, and at very high level in *soleus* and EDL for pig. By comparison, PLN mRNA was detected at very high level in ventricles for rodents and rabbit (at lower level for pig), in *atria* for all the species and also in *soleus* for rabbit. In terms of SERCA1a and SERCA2a mRNA, SERCA2a is the only isoform found in heart (ventricle and *atria*) for all studied species, SERCA2a is more expressed than SERCA1a in *soleus* for all the species, and SERCA1a is largely the major form in EDL for all the species except for pig (where SERCA2a is more abundant than SERCA1a) (see Table 10.1).

The SLN expression was also studied at the protein level. To perform such studies, the authors have generated an antibody targeted to a peptide corresponding to the N-terminal sequence (12 residues) of mouse SLN [12]. This antibody reacts to mouse SLN as expected but the authors noticed that this antibody could also cross-react with PLN and, has a very low affinity for rabbit and pig SLN, probably due to sequence diversity at the N-terminus of SLN between small and larger mammals. Consequently, the use of this antibody was restricted to rodents (see Fig. 10.3a for sequences). Western blot analyses of SLN abundance confirmed the expression of SLN in *atria* for rodents. Using a highly specific antibody, targeting the C-terminal sequence (6 residues) of SLN which is conserved among most of the species (see below), Babu et al. have shown that SLN is more abundant in rodent *atria* (mouse, rat) than in *atria* of larger mammals (rabbit, dog) [13]. In rodents' *atria* and ventricles, the high levels of expression of SLN and SERCA2a are correlated, whereas in rabbit and dog, SLN is predominantly expressed in muscle tissues although SERCA2a expression is moderate (see Table 10.1). Recently, SLN was found in human *vastus lateralis* skeletal muscle only in the presence of SERCA1a and, in fast-twitch muscle fibers while PLN is expressed in fast-twitch and slow-twitch fibers, with a preference for slow-twitch fibers, where SERCA2a is predominant [14] (see Table 10.1).

3.2 Differential Expression of Sarcolipin during Muscle Development

Babu et al. have studied whether SLN expression may be developmentally regulated [13]. The authors analyzed the temporal pattern of SLN expression in rat *atria*, ventricle, quadriceps, and tongue during embryonic and neonatal development. SLN was detected in the *atria* and its expression level increases throughout development, whereas in the ventricle, its expression level was below detection. At the same development stage, PLN was detected only in heart tissues and the expression level was higher in the ventricles. During embryonic development, the fast-twitch muscle undergoes several transitions from slow- to fast-twitch fibers. Thus, in rat fast-twitch skeletal muscles as the quadriceps muscles, SLN and SERCA2a are expressed at

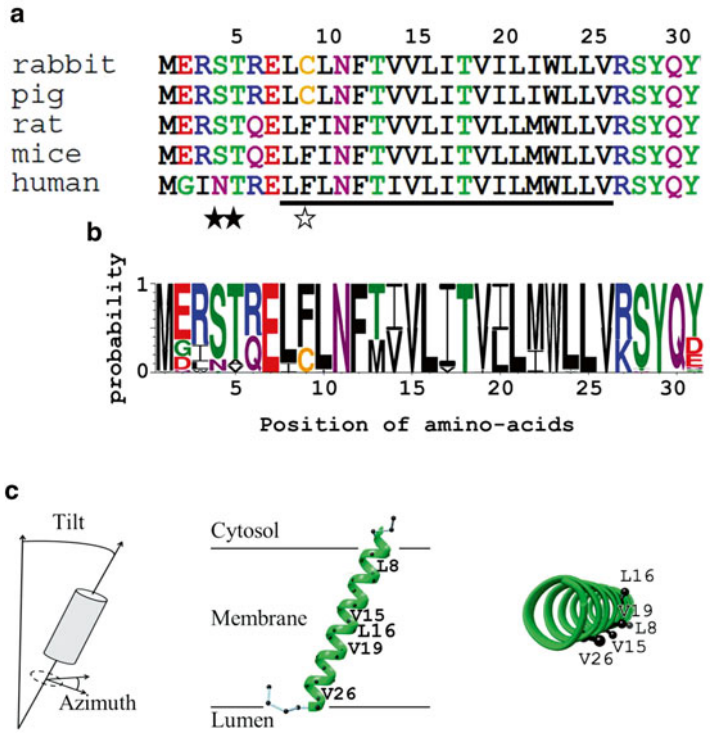

Fig. 10.3 Sarcolipin. (**a**) The alignment of selected sequences was obtained with the SEAVIEW program [100]. Serine 4 and Threonine 5 were identified as putative phosphorylation sites for Ca^{2+}-calmodulin-dependent kinases or STK16 kinases (*black stars,* [32, 33]). In rabbit and pig, cysteine 9 is constitutively acylated (*white star*, [31]). The region of SLN predicted to match with the hydrophobic part of the lipid bilayer is *underlined*. (**b**) A sequence logo [101, 102] was obtained from the alignment of 110 sarcolipin sequences (for detailed procedure, see [31]). Color code for panels **a** and **b** is the following: acidic residues in *red*, basic residues in *blue*, cysteine in *yellow*, Q and N in *pink*, other polar residues and glycine in *green*, and *black* for hydrophobic residues. The *height of the letters* corresponds to the relative frequency of each amino acid at a given position. (**c**) *left*, definition of the tilt and azimuthal angles; *middle*, hSLN helical structure and its orientation within the bilayer, with the N-terminus pointing in the cytosol and the C-terminus pointing in the lumen; *right*, hSLN helix viewed from the luminal side of the membrane [39]. Only the residues of the helix side oriented toward the lumen are depicted. For the sake of clarity, only α and β carbons are represented by *small black spheres* on *right panel*

high levels throughout embryonic development. After birth, SLN and SERCA2a protein levels decline and disappear after 21 days. In contrast, SERCA1a expression increases and SERCA1a becomes the predominant SERCA isoform in the adult. In parallel, during mouse embryogenesis, MLN might be expressed in the precursors of skeletal muscle as estimated from the mRNA levels (using northern-blot analysis with a probe specific to the full-length MLN transcript). During fœtal and adult stages, MLN mRNA is found in all skeletal muscles, similarly to the expression pattern of SERCA1a, and is not detected in cardiac or smooth muscles [7].

4 Sarcolipin in Health and Diseases

As human SLN is highly expressed in *atria* and mediates β-adrenergic responses, its involvement in various heart diseases has been investigated. Both at mRNA and protein levels, SLN expression has been shown to be altered in the atrial myocardium disease [15] so SLN is proposed to be a key regulator of cardiac SERCAs. SLN mRNA levels are decreased in *atria* of patients with chronic atrial fibrillation (AF). SLN protein expression level is also significantly decreased both in patients with atrial fibrillation (AF) and in those with heart failure (HF). Although PLN protein level is not altered, PLN phosphorylation is significantly decreased in the atrial tissues of patients with AF and HF compared to control patients. The Ca^{2+} sensitivity as well as the V_{max} of SR Ca^{2+} uptake is significantly increased in human *atria* from AF patients [16]. In children with congenital heart defects (tetralogy of Fallot), at the mRNA level, SLN and PLN expressions were decreased relatively to SERCA2a and RyR2 expressions [17].

In large mammals and human, SLN is also highly expressed in fast-twitch muscle fibers associated with SERCA1a. Thus, diseases related to muscle dysfunctions have been studied. The Brody disease is an inherited disorder of skeletal muscle function characterized by exercise-induced impairment of muscle relaxation. Studies of the sarcoplasmic reticulum from Brody patients have shown a decrease of the Ca^{2+} uptake and the Ca^{2+}-dependent ATP hydrolysis. As a matter of fact, SERCA1a activity was reduced by 50 % even if the SERCA1a content was reported to be normal in all patients. Mutations in the *ATP2A1* gene encoding SERCA1a have been associated with the Brody disease in some families (called Brody disease with *ATP2A1* mutations), but not in other families (called Brody syndrome without *ATP2A1* mutations) [18]. As SLN interacts with SERCA1a, it was proposed that SLN gene could be altered in Brody disease, because a mutation of SLN could increase inhibition of SERCA1a function. However, no alteration in coding, splice junctions or promoter sequences was found in the SLN gene [4].

The SERCAs and more recently SLN have been proposed to play a key role in non-shivering thermogenesis (reviewed in [19, 20]). Animals lacking brown adipose tissues produce heat from ATP hydrolysis to maintain their body temperature [19, 21]. Moreover, regulation of thermogenesis is critical for cold acclimation [19]. There are functional similarities in the use of the skeletal muscle for thermogenesis across several animals, like fishes, birds, and mammals [19]. De Meis et al. suggested that part of the energy released from the hydrolysis of ATP at the SR, i.e. by the Ca^{2+}-ATPase, could be dissipated as heat, while the other part of the energy would be used to drive the transport of calcium ions through the membrane [22]. As suggested by de Meis et al. this process could involve the release of calcium from the $Ca_2.E_2$-P state in the cytosol instead of in the lumen, yielding a futile hydrolysis of ATP since all the energy would be dissipated as heat. This phenomenon was named slippage or uncoupling [23–25]. Interestingly, the rate of slippage is affected by the presence of sarcolipin. SLN when co-reconstituted with SERCA1a, increases the rate of uncoupling, resulting in an increase of the heat production whereas the

accumulation of calcium decreases [20]. Using isothermal calorimetry, it was shown that the amount of heat production is maximal at a SLN:SERCA1a 15:1 mol:mol ratio [26]. As reported in Table 10.1, the SLN content of SR depends on the muscle type. Therefore, SLN expression level could vary with the involvement of a given muscle in thermogenesis. This hypothesis gave rise to several studies in order to demonstrate the specific in vivo role of SLN in thermogenesis [27]. Recently, SLN was shown to have a protective role against hypothermia and obesity induced by high fat diet using a knock-out mouse model [28, 29]. As a matter of fact, it is suggested that this protective role results from an increase in the uncoupling of the SERCA1a, but also that the ryanodine receptor 1 Ca^{2+} channel may play a role in thermogenesis [28, 30].

5 Structure of Sarcolipin

5.1 Primary Structure

Sarcolipin possesses 31 residues and is composed of three regions (Fig. 10.3a). For most of the species, the N-terminus (1–7) is rich in polar and charged residues as illustrated by Fig. 10.3b. For some species ([31], see also Fig. 10.3b), several charged residues are replaced by neutral or hydrophobic residues, for example ^{1}MERST for rabbit is replaced by ^{1}MGINT for human. The N-terminus, oriented toward the cytosol [3], contains potential phosphorylation sites (Ser4 and Thr5) [32, 33]. On the contrary to the N-terminus, the C-terminus amino acid sequence, ^{27}RSYQY, is highly conserved. The central region, from Leu8 to Val26, is mainly composed of hydrophobic residues and possesses, in some species, a cysteine at position 9 that was recently shown to be acylated ([31], see below).

5.2 3D Structure of Isolated Human Sarcolipin

Human sarcolipin structure, at atomic resolution, has been extensively studied by solution and solid-state NMR spectroscopies. Solution NMR spectroscopy is performed on membrane proteins solubilized in detergent micelles. This technique is limited to small membrane proteins due to the large size of protein-detergent complexes and to the internal dynamics of membrane protein within the complex. NMR data yield spatial information, such as range of distances between atoms, which is then applied as experimental constraint during molecular modeling. A set of 3D structures compatible with the NMR data is finally obtained. Solid-state NMR (ssNMR) allows the study of membrane proteins in lipid environments such as lipid vesicles or oriented bilayer systems. ssNMR provides information on the secondary structure adopted by the protein and on the orientation of the helices inside the

bilayer (tilt angle of the helix relative to the direction of the magnetic field and the rotation angle around the helix axis, i.e. azimuthal angle, Fig. 10.3c). It can also give high-resolution information on the side-chain conformations [34, 35].

The solution and ssNMR experiments performed on hSLN solubilized in SDS [36] or DPC [37, 38] micelles as well as embedded in DOPC/DOPE bilayers [39] have revealed that hSLN folds as a unique transmembrane helix. The protein adopts a helical structure from residue Glu7 to Arg27 when solubilized in DPC micelles but extends up to residue Ile3 when embedded in a lipid bilayer. This later result is in agreement with results from molecular dynamics (MD) simulations performed on hSLN inserted in a pure DOPC bilayer [40]. It is noteworthy that the sole structure of human SLN found in the PDB (PDB ID: 1jdm) comes from the oldest data obtained by solution NMR experiments performed on hSLN solubilized in the presence of SDS and are consistent with a shorter α-helix structure defined from residue Phe9 to residue Arg27 [36]. The somewhat shorter helical structure observed in the presence of SDS demonstrates the influence of the nature of the detergent headgroup, used to solubilize the protein, on the structure of the N-terminus of hSLN. The transmembrane domain of hSLN solubilized in the presence of DPC encompasses a flexible helix up to residue Ile14 and a more rigid ideal alpha-helix from residue Val15 to residue Arg27 [37, 38]. MD simulation of hSLN in DOPC bilayer confirms the presence of these two different helical flexible regions, responsible for a curved structure [40]. However, Veglia and co-workers have recently proposed that hSLN adopts a helical conformation closer to an ideal helix for the whole sequence from Ile3 to Arg27 when applying solid-state NMR experimental restrained in their simulations [41]. Besides, ssNMR showed that hSLN helix is tilted with respect to the membrane normal. In DOPC/DOPE lipid mixture, the tilt angle is 23 ± 2° [39, 42] in good agreement with the value derived from MD simulations of hSLN in DOPC bilayers which is 28 ± 6° [40] and also with the value obtained by solid-state NMR of hSLN in pure DOPC bilayer [43]. Moreover, experiments and MD simulations have revealed that the residues Leu8, Val15, Leu16, Val19, and Val26 located on the same side of the tilted helix point toward the lumen [39, 40] (Fig. 10.3c). This tilt and this azimuthal position of the helix are driven by the N- and C-terminal residues which undergo specific interactions with the lipid membrane at the water/lipid interfaces. As a matter of fact, MD simulation showed that the N-terminal residues Met1 and Ile3 are located outside the cytosolic interface, the polar residue Thr5, a putative phosphorylation site of SLN [32, 33], interacts with the lipid headgroups as well as Arg6 which forms a salt bridge with the lipid headgroups. On the luminal interface, both C-terminal residues Tyr 29 and Tyr31 interact with lipids via cation–π interactions between the aromatic rings and the lipid choline groups. Arg27 also forms a salt bridge with the lipid headgroups. Moreover, as expected, hydrophobic amino acids are located within the hydrophobic core of the membrane bilayer. The two hydrophilic residues, Thr13 and Thr18, distributed in the center of the lipid bilayer, have their polar hydroxyl groups hydrogen bonded with the backbone carbonyl groups of Phe9 and Ile14, respectively [40].

6 SLN Affects Moderately the Affinity for Ca^{2+} and the V_{max} of SERCA

The possible role of sarcolipin on SERCA isoforms turnover was investigated in various experimental models. One widespread model since the discovery of sarcolipin involves the heterologous expression of SLN and SERCA isoforms in HEK-293 cells [3]. Cells are simultaneously transfected with several genes coding regulatory peptides like SLN or PLN and a SERCA isoform (SERCA1a or 2a). These cell lines, derived from Human Embryonic Kidney cells (HEK cells) [44] do not appear to express endogenously SLN, PLN, SERCA1a and SERCA2a, and are thus good models to assess the role of SLN on SERCA isoforms. Nevertheless, the presence of partners playing a regulatory role is unknown (e.g. RyR, kinases). The coding sequences were inserted in a pMT2 expression vector, under the control of a SV40 strong constitutive promoter, one obvious drawback is the uncontrolled expression level of the different proteins. This lack of control of the protein expression levels of each partner could explain some discrepancies within the published results. MacLennan et al. first showed that co-expression of rabbit SLN with rabbit SERCA1a in HEK-293 cells results in a moderate decrease in the affinity for calcium ($Ca_{1/2}$ rises from 0.3 to 0.5 μM in absence or in presence of sarcolipin, respectively) combined with a huge increase in the V_{max} of about 40 % at micromolar, i.e. saturating, concentrations of calcium [3]. Surprisingly, the same group showed some years later that co-expression in HEK-293 cells of SERCA1a or SERCA2a in presence of SLN resulted in a slight decrease of about 5–10 % of the V_{max} which is far from the initial results [45–47]. However, the authors confirmed that the presence of SLN induces a moderate but reliable decrease in $Ca_{1/2}$ for the two isoforms (0.20 and 0.33 μM for SERCA1a, and 0.13 and 0.37 μM for SERCA2a, in the absence and in the presence of SLN, respectively) [45–47]. As mentioned, the stoichiometry is not tightly controlled during co-expression and this could explain the discrepancies of the results obtained for such heterologous expression systems.

Interestingly, Hughes et al. studied the stoichiometry of the interaction between sarcolipin and SERCA isoforms using rabbit SERCA1a prepared from native sarco-endoplasmic reticulum membranes and a synthetic rabbit SLN co-reconstituted in DOPC bilayers [43, 48]. The authors demonstrated that a 10:1 (SLN:SERCA1a) molar ratio is necessary to observe a moderate decrease in calcium affinity and in V_{max} ($Ca_{1/2}$ rises from 0.2 to 0.5 μM and V_{max} decreases from 1.5 to 1.2 μmol hydrolyzed ATP.mg^{-1} min^{-1}, in absence or in presence of SLN respectively). A 3:1 molar ratio has no effect on SERCA1a turnover. This observation was confirmed in similar studies using a value of the SLN:SERCA1a molar ratio after co-reconstitution in EYPC/EYPA bilayers of about 1:1 to 4.5:1 [49, 50]. At low molar ratio, no effect on V_{max} was found whereas V_{max} decreased by 20 % at the highest molar ratio. A moderate decrease in calcium affinity ($Ca_{1/2}$ rises from 0.4, in absence of SLN, to 0.8 μM, in presence of SLN) was found. Moreover, the presence of endogenous SLN (or PLN) in the samples must be considered as it could affect the stoichiometry. As a matter of fact, native sarco-endoplasmic reticulum membranes prepared from rabbit

fast-twitch skeletal muscle already contains endogenous sarcolipin that could reach about 1:1 SLN:SERCA1a mol:mol [3]. We recently demonstrated that most of the sarcolipin remains associated with SERCA1a even after treating the membranes with deoxycholate (*DOC-extracted SR*) and also even after membrane solubilization by mild detergent [31]. Size exclusion chromatography purification of the DDM-solubilized SR shows that the SLN is mainly co-eluted with SERCA1a at about a 1:1 mol:mol ratio. Some SLN is also detected in the mixed micelles peak suggesting that in the SR membrane, the SLN to SERCA1a ratio is higher than 1:1 mol:mol [31]. Therefore, it is suggested that the results presented above based on co-reconstitution experiments were obtained in presence of misestimated amount of SLN [49, 50, 43, 48, 31]. For example, the lack of effect observed at low molar ratio (proposed to be 1:1 SLN:SERCA1a) is not surprising as it is probably related to a molar ratio higher than 2:1 considering the endogenous SLN content. This point appears to be critical for the interpretation of mutagenesis experiments as both wild-type and mutated SLN are present [50]. In addition, as reported in Table 10.2, some experiments were performed with SERCA and SLN isoforms from different species and sometimes within the same experiment. But, as mentioned previously, the amino acid sequences of SLN differ among species especially the N-terminus (Fig. 10.3a, b) [14, 3, 12]. For example, human SLN reconstituted in presence of rabbit SERCA1a has a lower inhibitory effect than rabbit SLN [38, 49, 50]. In the case of rabbit SLN overexpressed in presence of rat SERCA1a or SERCA2a in rat

Table 10.2 $Ca_{1/2}$and V_{max} estimates in several selected references

SLN [a]	SERCA [a]	Systems used [b] and SLN:SERCA molar ratio [c]	$Ca_{1/2}$ (μM) [d]		V_{max} [e] (% of SERCA alone)	References
			No SLN	+ SLN		
rSLN	rSERCA1a	HEK-293 cells	0.3	0.5	143	[3]
rSLN	rSERCA1a	HEK-293 cells	0.2	0.33	95	[45, 47]
rSLN	rSERCA2a	HEK-293 cells	0.13	0.37	90	[45, 47]
rSLN	rSERCA1a	DOPC bilayers (10:1)	0.2	0.5	80	[43, 48]
hSLN	DOC-extracted rSERCA1a	EYPC-EYPA bilayers (4.5:1)	0.4	0.6	80	[49]
rSLN	DOC-extracted rSERCA1a	EYPC-EYPA bilayers (4.5:1)	0.4	0.8	70	[50]
hSLN	rSERCA1a	DPC micelles	0.25	0.5	100	[38]
rSLN	rat SERCA1a	Slow-twitch myocytes	0.4	0.4	70	[51]

[a]"r" referred to rabbit isoforms, "h" to human isoform

[b]HEK-293 cells and myocytes were used for co-expression and possible microsomes preparation. DOPC or EYPC-EYPA bilayers were obtained from co-reconstitution of SR from native sources with recombinant or synthetic SLN

[c]Molar ratio does not take into account the possible presence of endogenous SLN

[d]$Ca_{1/2}$ corresponds to the amount of calcium necessary to attain half-maximal activity (calcium uptake or turn-over depending on the system used)

[e]Unfortunately, values of V_{max} in $\mu mol.mg^{-1}.min^{-1}$ were not available

myocytes (which are deprived in endogenous SLN) no effect on affinity was detected but a significant decrease of about 30 % in calcium uptake and a reduced contractility were observed [51].

To put it in a nutshell, stoichiometry appears to be one of the critical points to assess diligently the effect of SLN on the SERCA1a catalysis. Neither heterologous expression nor co-reconstitution experiments described here gave an accurate estimate of the SLN:SERCA ratio while yet they all agreed that this ratio is important. Nonetheless, it is widely accepted that sarcolipin is an inhibitor of SERCAs but the detailed mechanism of this inhibition remains unknown at the molecular level.

7 Structural Insights into the SLN–SERCA1a Complex from NMR and X-Ray Diffraction Experiments

7.1 NMR Studies of the Interaction between hSLN and SERCA1a

Studies of the hSLN–SERCA1a interactions were performed using solution NMR spectroscopy of hSLN upon addition of SERCA1a in the presence of DPC. Analysis of both chemical shifts and peak intensities of SLN signals indicate the existence of three different SLN states: the free, the bound, and the intermediate states at the NMR time scale. The effects of the binding were inferred by analyzing the changes occurring in the intermediate form as the bound state of SLN cannot be detected due to the large size of the SLN/SERCA1a/DPC complex.

Changes in ^{1}H chemical shifts were used as reporters for structural changes occurring in hSLN upon interaction with SERCA1a. As a matter of fact, these changes are correlated with variations in hydrogen bond interactions or secondary structures upon interaction [52]. The different flexible regions of isolated hSLN previously identified have distinct properties in the presence of SERCA1a. Concerning the N-terminus, residues Met1 through Arg6, except Asn4, do not exhibit significant chemical shift changes indicating that this region remains highly dynamic in the presence of SERCA1a. In contrast, signals from the helical region spanning residues Glu7 through Val26, which contains two dynamical domains, show large chemical shift changes. Signals from Glu7 to Thr18 (except Thr13) display downfield shifts, whereas signals from the C-terminal portion of the transmembrane helix exhibit an increasing upfield shift for all the residues up to Val26. Buffy et al. have suggested that these chemical shift changes could indicate the formation of tighter hydrogen bonds in the region from Glu7 to Val14 and a slight unwinding of the helix from residues Val15 through Arg27, a mechanism analogous to that proposed for the transmembrane domain of PLN [38]. Concerning the unstructured C-terminal tail, all signals, except those of Arg27, are shifted upfield which could reveal a structural change of this amino acid sequence suggesting an interaction of the tail with either the luminal part of the ATPase or the lipids.

7.2 X-Ray Diffraction of the rSLN–SERCA1a Complex

Two recent crystallographic structures of rabbit SLN in complex with rabbit SERCA1a (PDB ID: 3W5A at a resolution of 3.0 Å [53] and PDB ID: 4H1W at a resolution of 3.1 Å [54]) revealed a previously undescribed conformation of SERCA1a in the presence of SLN. This SERCA1a–rSLN complex was obtained in the presence of high concentration of magnesium (40–75 mM) that appears to be essential to stabilize a Ca^{2+}-deprived form of the enzyme. Considering the relative position of the ATPase sub-domains and the conditions of crystallization, authors from the two groups suggested that this complex corresponds to a genuine E1 intermediate, i.e. between the protonated E2 form and the Ca_2.E1P occluded state (Fig. 10.1). This complex could allow cytoplasmic ion exchange between protons and calcium ions: as a matter of fact, both structures display a large open groove, followed by a deep, funnel-shaped and negatively charged path that leads to the transmembrane Ca^{2+} binding sites, suggesting that this form is prefiguring the Ca^{2+} fixation.

However, the physiological significance of this E1-Mg state is also worth discussion. In both studies mentioned above [53, 54], the structures were solved with the Ca^{2+}-free enzyme solubilized in $C_{12}E_8$, a condition known to cause irreversible enzyme inactivation [55–58]. Besides, the functional role of the E1-Mg state is unclear. On the one hand, Toyoshima et al. concluded that this state is an obligate intermediate in the catalytic cycle of SERCA1a and that Mg^{2+} binding accelerates Ca^{2+} binding by reducing the energy required for formation of a calcium-bound E1 form. On the other hand, Winther et al. concluded differently, that Mg^{2+} binding to the "low-affinity Mg^{2+} sites" actually delays SERCA1a activation by Ca^{2+}. Moreover, Akin et al. [59] concluded that the E1-Mg state obtained at 40–75 mM $MgSO_4$ by Toyoshima et al. and Winther et al. does not exist at a physiological Mg^{2+} concentration (i.e. about 3 mM).

Analyses of both structures [53, 54] reveal that in the complex, rSLN forms a slightly bended membrane-spanning helix, and is associated with SERCA1a within a groove between M2, M6, and M9 transmembrane helices (Fig. 10.4a). Most of the residues located at the interface between rSLN and SERCA1a are hydrophobic amino acids. Those residues form a large hydrophobic cluster (Fig. 10.4b) as represented by the important network of distances less than 4.7 Å between rSLN and SERCA1a hydrophobic side-chains (orange and blue dotted lines). Moreover, rSLN and SERCA1a also show proximities between polar residues. For example, rSLN Asn11 side-chain and SERCA1a Gly801 backbone form a hydrogen bond (Fig. 10.4c), as well as rSLN Glu7 side-chain and SERCA1a Asn111 side-chain (Fig. 10.4d). N-terminal and C-terminal residues of SLN are poorly defined. The local disorder of the electron density maps suggests that no stable interaction involves rSLN C-terminus and SERCA1a in the conditions used for crystallization [54]. These structures are also in agreement with several site-directed mutagenesis experiments: as a matter of fact, MacLennan et al. observed a moderate but significant loss of inhibition after substitution by alanine of SLN Asn11, Val14 and

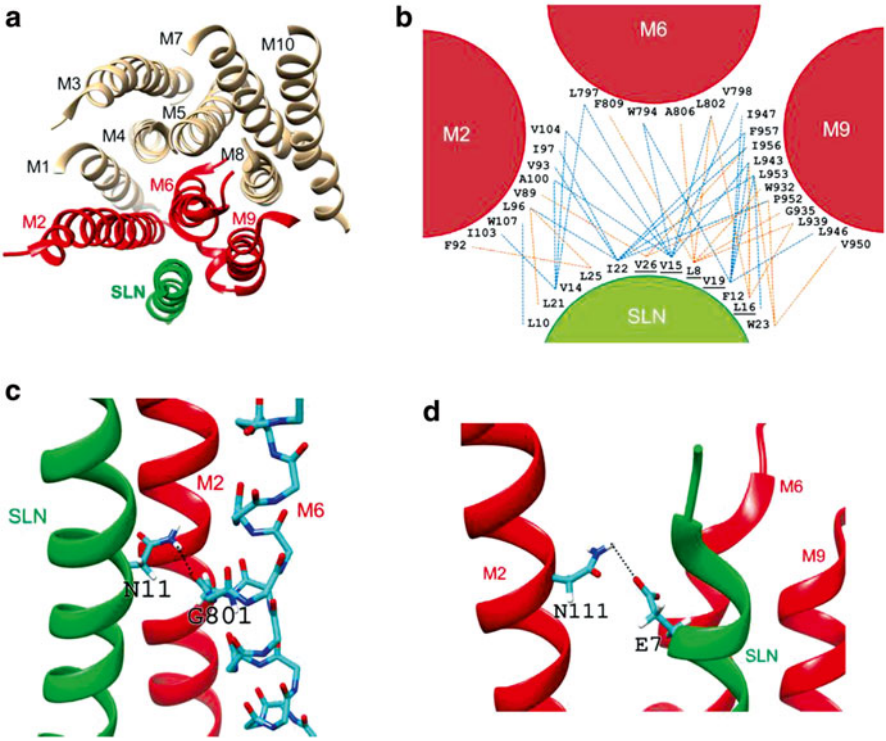

Fig. 10.4 rSLN in interaction with SERCA1a transmembrane domain. (PDB: 4H1W, [54]). (**a**) rSLN is in interaction with SERCA1a within a groove between M2, M6, and M9 transmembrane helices (viewed from the cytosol). Sarcolipin is depicted as a *green ribbon*. SERCA1a transmembrane helices M2, M6, and M9 are depicted as *red ribbons* and the other transmembrane helices are in *grey*. (**b**) Scheme of the hydrophobic interaction network taking place at rSLN/SERCA1a interface (viewed from the cytosol). Only the hydrophobic amino acids involved in the interaction network are displayed. SLN residues previously pinpointed in Fig. 10.3c are underlined. A distance of 4.7 Å or less between side-chains is represented by *blue* or *orange dotted lines* for a sake of clarity. (**c**) rSLN Asn11 side-chain and SERCA1a Gly801 backbone form a hydrogen bond [54]. (**d**) rSLN Glu7 side-chain and SERCA1a Asn111 side-chain form a hydrogen bond [53]. Residues backbone and side-chains are represented as *sticks*. Carbon atoms are in cyan, oxygen in *red*, nitrogen in *blue*, and hydrogen in *white*. Hydrogen bond is represented as a *dotted black line*

Val19 [3]. These authors also showed that substitution by alanine of SERCA1a Leu321 (M4) and Leu802 (M6) trigger SLN dissociation [46]. Additional cross-linking experiments confirmed that the binding sites of SLN and PLN overlap as expected, due to similarities between the SLN transmembrane domain (from Leu8 to Val26) and the membrane-spanning C-terminal segment of PLN [53] (see Fig. 10.2 for sequence similarities).

Because the contacts between rSLN and SERCA1a observed in the E1-Mg structures were similar to PLN–SERCA1a interactions inferred previously from cross-linking experiments [60–64], Toyoshima et al. and Winther et al. postulated

that the E1-Mg state is similar to the state that binds PLN [53, 54]. However, notable structural differences of their respective transmembrane domains indicate that PLN stabilizes a distinct conformation of SERCA1a. The Ca^{2+} binding sites in the E1-Mg structures are partially formed and have a distinctly E1-like appearance. On the other hand, in the metal-free E2 state that binds PLN, the SERCA transmembrane structure is closest to E2 state more than E1 state, leading to the collapse of the Ca^{2+} binding sites [59], suggesting that PLN and rSLN are interacting with different ATPase conformers.

Toyoshima et al. and Winther et al. made hypothesis concerning the binding or not of rSLN to different SERCA1a conformers during the catalytic cycle [53, 54]. Toyoshima et al. proposed that the E1.Mg^{2+} state is the preferred state for binding of rSLN as suggested previously for PLN [65, 46, 60, 64]. These authors suggested that rSLN cannot interact with the Ca_2.E1 and E2 states because, in these states, the position of the helices M2, M4, M6, and M9 leads to a very narrow and a very wide groove, respectively, that will prevent rSLN to bind firmly. Instead, Winther et al. suggested that the E2 state of SERCA1a is compatible with a SERCA1a–rSLN complex as the E2 structure offers a wider binding groove to rSLN [54]. In contrast, in the occluded Ca_2.E1P conformation, the position of the M1, M2, M3, and M4 helices leads to a narrowing of rSLN-binding site thus implicating rSLN dislodgement or a positional rearrangement. Recent cross-linking experiments suggest that rSLN remains in contact with the pump throughout the enzymatic cycle and, are thus in favor of a positional rearrangement of rSLN in interaction with SERCA1a [53]. Bidwell et al. demonstrate that a PLN–SERCA1a interaction remains even in presence of millimolar concentration of calcium or in presence of thapsigargin which may trigger the ATPase in a Ca_2.E1 or E2-like conformation, respectively [66].

8 Focus on Some Particular Features of Sarcolipin

8.1 Phosphorylation

Sequence analysis and site-directed mutagenesis experiments of Ser4 and Thr5 suggested that human, rat, and mouse SLN could be phosphorylated on Thr5 whereas rabbit, cow, and pig could be phosphorylated on Ser4 or Thr5 [33]. In this work, the effect of SLN overexpression and its ability to get phosphorylated were investigated in two different models. Using overexpression of the rabbit SERCA1a isoform in HEK-293 cells, in presence of wild-type (WT), S4A or T5A rabbit SLN, the authors demonstrated that both Ser4 and Thr5 are involved in the ATPase inhibition, Thr5 having probably a more preponderant role than Ser4. It is also shown that phosphorylation could be achieved by the Serine/Threonine-protein Kinase 16 (STK16, [67–70]). The overexpression of mouse SLN in mouse cardiac myocytes obtained from PLN null transgenic mice results in an inhibition of the cardiac function. Treatment with isoproterenol, a β-adrenoreceptor agonist and an activator of the cardiac muscle, resulted in complete restoration of the calcium dynamics in SLN

overexpressing tissues whereas no effect was found in absence of SLN. Therefore, a mechanism for which isoproterenol would act through cAMP signaling to regulate SLN interaction with SERCA isoforms is proposed. Bhupathy et al. demonstrated that a T5A point mutation exerts an inhibitory effect on rat myocyte contractility and calcium transients similar to that of WT SLN, whereas a phosphorylation mimetic mutation, T5E, abolishes the inhibition [32]. The WT and mutated SLN co-localized with SERCA2a in the rat ventricular myocytes sarcoplasmic reticulum. Interestingly, the overexpression of SLN has no effect on SERCA2a and PLN expression levels suggesting that the functional changes observed were really due to SLN. Similar results were obtained previously with PLN null transgenic mice [33], suggesting that SLN may act against SERCA2a independently of PLN (see below). Bhupathy et al. also proposed that SLN phosphorylation depends on the calcium/calmoduline-dependent protein Kinase II (CaMKII) rather on the STK16. The role of STK16 remains unclear whereas the role of CaMKII in heart is better known, especially CaMKII phosphorylates PLN at Thr17 during β-adrenergic-mediated stimulation and could be important for heart function [71–74]. However, no study investigates the possible role of Ser4.

Both Ser4 and Thr5 of SLN are close to SERCA1a Trp932 in the two recent structures of the SLN–SERCA1a complex [53, 54] and, molecular modeling of the phosphorylation of these two residues (Fig. 10.5) shows that in both cases, phosphorylation may induce steric clashes with Trp932 leading most probably to SLN and/or SERCA1a conformational changes. As a consequence, these conformational changes could induce dissociation of the complex as suggested by Toyoshima et al. [53].

Among 67 unique SLN sequences, most of them include a Ser and a Thr residue at positions 4 and 5, respectively, except for the rhinoceros which contains two successive threonines [31]. All the primates (9 species), including human, contain only Thr5, Ser4 being replaced by an asparagine (S4N). Note that Trp932 of SERCA isoforms 1a and 2a are fully conserved among mammals suggesting that some local rearrangement of the ATPase and/or the SLN N-terminus could take place when either Ser4 or Thr5 are substituted. Interestingly, most of the sequences from fishes (7 species among 8) contain only a serine at position 4, the threonine being replaced by an alanine (T5A) or a valine (T5V). Assuming that the regulatory mechanism of SERCA isoforms (and of muscle contraction) is conserved among species, i.e. dissociation of SLN from SERCA1a induced by phosphorylation, Ser4 will be a candidate for phosphorylation in fishes. Indeed, kinases like CaMKII are poorly specific [75] and thus, both Ser4 and Thr5 can be phosphorylation targets.

8.2 The RSYQY Luminal Tail

The C-terminus amino acid sequence of SLN, Arg^{27}-Ser-Tyr-Gln-Tyr (RSYQY tail), appears critical for its proper localization at the endoplasmic reticulum membrane, as it acts as an ER retention signal. Progressive amino acid deletion revealed that removal of the Arg27-Tyr31 sequence results in a misrouting of SLN. Interestingly, when the deleted form of SLN is co-expressed with SERCA2a,

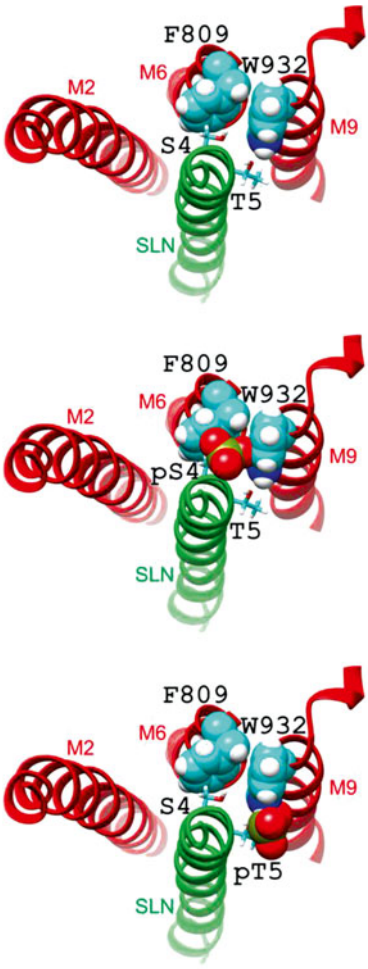

Fig. 10.5 Phosphorylation of rSLN Ser4 and Thr5. View from the cytosol of rSLN surrounded by the transmembrane helices M2, M6, and M9 of SERCA1a (PDB: 4H1W, [54]). *Top*: native rSLN; *middle*: model with rSLN Ser4 phosphorylated (*pS4*); *bottom*: model with rSLN Thr5 phosphorylated (*pT5*). Sarcolipin is depicted as a *green ribbon*. SERCA1a transmembrane helices M2, M6, and M9 are depicted as *red ribbons*. rSLN Ser4 and Thr5 side-chains are depicted as *sticks*. SERCA1a Phe809 and Trp932 side-chains are depicted as Van der Waal's spheres. Phosphorylated side-chains were modeled using UCSF Chimera software [103] and are depicted as Van der Waal's spheres. Carbon atoms are in cyan, oxygen in *red*, nitrogen in *blue*, phosphorus in bronze, and hydrogen in *white*

misrouting is abolished and this shortened form is stably expressed and properly co-localized with SERCA2a at the ER. It suggests that in presence of sufficient amount of a SERCA isoform, SLN can be addressed to the ER independently of its tail. However, it has been reported that in absence of SERCA, SLN may accumulate in the ER via interactions of its luminal tail with another partner [76].

A key role of this C-terminal tail for catalysis was pointed out early by MacLennan et al. [3] who showed that a C-terminally FLAG tagged version of SLN does not affect SERCA1a activities as WT or N-terminally tagged (NF) SLN isoforms. As a matter of fact, human, rat or rabbit SLN (hSLN, rat SLN, and NF-SLN respectively) induce a moderate decrease of $Ca_{1/2}$ (shifted from 0.35 μM in absence of SLN to 0.5 μM when SLN is co-expressed with SERCA1a in HEK-293 cells) and a significant increase of the Ca^{2+} uptake activity up to about 140 %. On the

other hand, co-expression of a C-terminally FLAG tagged rabbit SLN (SLN-FC) and SERCA1a resulted in a significant decrease of both $Ca_{1/2}$ (shifted from 0.35 μM to 1.1 μM) and V_{max} (only 62 % of the SERCA1a alone). To investigate the role of the tail in the regulation of SERCA1a, alanine mutants of the tail were co-reconstituted with native SERCA1a within proteoliposomes (SERCA1a:SLN:lipids 1:4.5:120 m:m:m, i.e. molar ratio close to those of native SR, [49, 50]). This study showed that, compared to the WT SLN, all the alanine mutants induced a lower inhibition of the SERCA1a, i.e. a moderate decrease of the affinity for calcium and a slight decrease of the V_{max}, except the Y31A mutant which induced an increase of the V_{max} despite a poor effect on the $Ca_{1/2}$ [50]. Note that these results are not in agreement with those previously published by MacLennan et al. [3]. Later, this group demonstrated that modifications of the tail sequence could trigger a misrouting of SLN as described above [76] suggesting that in HEK-293 cells, improper trafficking of mutated SLN was not taken into account in previous experiments. As a consequence, the co-reconstitution model seems to be a better model to investigate the effect of a complete amino acid deletion of the tail. Co-reconstitution of a ΔR27SLN with SERCA1a led to a smaller inhibition of the SERCA1a than for entire SLN ($Ca_{1/2}$ and V_{max} are closer to the SERCA1a alone values) [50]. However, in that model, the SERCA1a is from native rabbit SR membrane which already contains endogenous rabbit SLN. As mentioned above, SLN remains associated with the SERCA1a even after deoxycholate extraction or solubilization with mild detergent and subsequent purification [31]. Therefore, results from Gorski et al. were probably obtained in the presence of both endogenous WT SLN and recombinant—WT or mutated—SLN. However, considering the fact that a significant molar excess of SLN was used, those results suggest that SLN luminal tail is essential for the inhibition of the SERCA1a by SLN. The high degree of amino acid conservation of the Arg^{27}-Tyr-Gln residues also suggests a critical functional role of this sequence of SLN, a role that has survived evolutionary divergence [76, 31] (Fig. 10.3b). While SLN inhibition properties may reside in its luminal tail, most of the inhibition properties of PLN depend on its transmembrane region. As a matter of fact, the amino acid C-terminus sequences of SLN and PLN are rather different: Arg^{27}-Ser-Tyr-Gln-Tyr (RSYQY tail) for SLN and Met^{50}-Leu-Leu (MLL tail) for PLN in mammals. Furthermore, myoregulin is deprived of such a tail (Fig. 10.2), suggesting a mechanism of inhibition proper to each regulatory peptide. Recently, a very different amino acid sequence of the luminal tail was reported [77] for a zebrafish isoform of PLN (zfPLN) that comprises additional residues, Leu^{50}-Leu-Ile-Ser-Phe-His-Gly-Met (^{50}LLISPHGM). This luminal tail has different functional properties than those of SLN and other PLN isoforms and can only regulate SERCA1a in the context of the full primary sequence of zfPLN. Deletion of this tail resulted in a loss of inhibition by zfPLN and, a zfPLN–SLN_{tail} chimera restored the inhibition. A chimera composed of the human PLN and the luminal tail of zfPLN shares the same functional properties as human PLN suggesting that this tail is efficient only in a zebrafish context [77]. C-terminal residues are poorly defined in the two published crystal structures of the SLN–SERCA1a complexes due to missing electron density which probably reflects a high flexibility of this region [53, 54].

Thus, the hypothesis concerning the interaction between the luminal tail of SLN and the SERCA1a derived from experimental data [46, 50] could not be confirmed from these structures. However, solid state NMR studies showed that the peptide encompassing the five C-terminal residues (R^{27}SYQY) interacts with SERCA1a. Moreover, this peptide inhibits the ATPase activity, yet it has no effect on the $Ca_{1/2}$. Using various peptides differing by their length and amino acid composition, the authors proposed that the positively charged residue Arg27 may be important in stabilizing the interaction of the luminal tail with the SERCA1a, possibly through salt bridge formation, and that Tyr29 and Tyr31 could participate in π–π or π–cation interactions with residues from the luminal face of SERCA1a [43]. These interactions could not be confirmed by the crystal structures of the SLN–SERCA1a complexes due to the poorly defined structure of the C-terminal residues of SLN and of the luminal loop between M1 and M2.

8.3 S-Palmitoylation and S-Oleoylation of Cysteine 9

Recently, our group showed that native rabbit SLN is modified by a fatty acid anchor on its unique cysteine residue (Cys9) with a palmitic acid or, surprisingly, an oleic acid in a ratio of 60 % and 40 %, respectively [31]. Treatment with hydroxylamine removes the fatty acids from a majority of the SLN pool and apparently without any modification on the SERCA1a. Mass spectrometry analysis of SEC-purified samples after several hours of incubation confirmed that SLN is satisfactorily deacylated and that it remains associated with the SERCA1a even after solubilization by mild detergent like *n*-dodecyl-β-D-maltopyranoside (DDM) or octaethylene glycol monododecyl ether ($C_{12}E_8$) and successive purification of the complex by size exclusion chromatography [31]. This treatment does not modify the affinity of SERCA1a for Ca^{2+} but it results in an increase of the Ca^{2+}-dependent ATPase activity of native SR membranes indicating that the S-acylation is required for full inhibitory effect of rabbit SLN on rabbit SERCA1a (Fig. 10.6). Deacylation does not affect the stability of the Ca^{2+}ATPase over time, neither in a native membranous context nor after solubilization by mild detergent (*unpublished results*).

Sarcolipin is most probably acylated in the crystals [53, 54] as we found SLN acylated when it was purified in conditions very similar to the crystallization procedure [31]. Although no electron density exists to describe the position of the acyl chain (probably a consequence of a local disorder in the crystals), we propose a model of SLN palmitoylated on Cys9 in complex with SERCA1a and embedded in a POPC bilayer (Fig. 10.7). The acyl chain was grafted on the SLN Cys9 within the crystal structure of the complex [54]. As shown in Fig. 10.7, the acyl chain is inserted in the upper leaflet of the membrane and faces the lipids as Cys9 is located on the opposite side of the helix interaction side. It suggests that the acyl chain is probably not directly in contact with the Ca^{2+}-ATPase.

Alignment of 67 SLN amino acid sequences from different species shows that 19 of them contain a cysteine and the remaining sequences a phenylalanine at position 9. As an example, we demonstrated that pig SLN, obtained from *extensor digitorum*

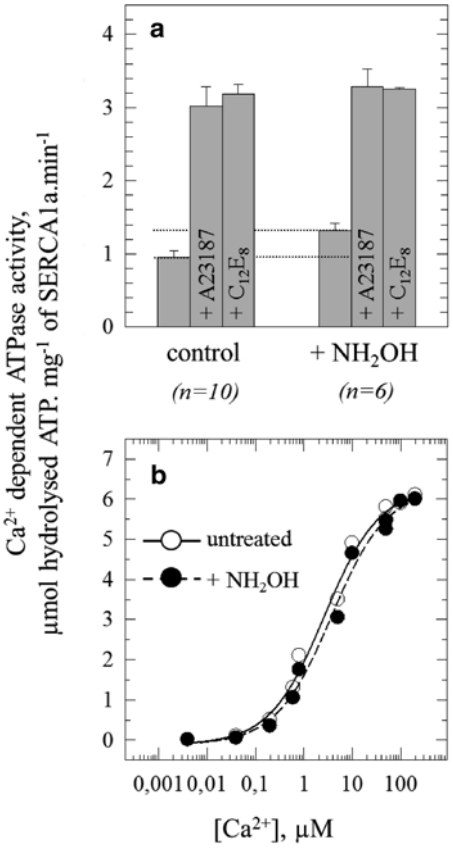

Fig. 10.6 Hydroxylamine treatment of SR membranes results in an increase of calcium ATPase activity but has a moderate effect on the apparent affinity for calcium. (**a**) Effect of hydroxylamine on ATPase activity. Rabbit SR membranes were initially suspended at 4 mg mL^{-1} in the assay buffer and stored on ice. When employed, an equal volume of a freshly prepared 2 M hydroxylamine solution (NH_2OH, pH adjusted at 7.5 with saturated Tris) was added prior to incubation at 20 °C for 1 h. As a control, an equal volume of buffer was added before incubation at 20 °C for 1 h. ATPase activity was estimated by an enzyme coupled assay as described previously [57] at pH 7.5 in presence of 50 µM free calcium (see [31] for further details). (**b**) Ca^{2+} dependency of the ATPase activity. ATPase activity was again measured by a coupled enzyme assay as described previously. The medium was first supplemented with 50 µM Ca^{2+} and subsequently with final Ca^{2+} concentrations of 100 or 200 µM, and then, various concentrations of EGTA were added sequentially, to explore the effect of lower free Ca^{2+} concentrations ($[Ca^{2+}]_{free}$ was estimated according to [104]). The medium also contained 0.1 mg/mL SR vesicles which have been formerly treated with 1 M hydroxylamine for 3 h at 20 °C (*black symbols and dashed line*) or not (3 h at 20 °C in absence of hydroxylamine; *empty symbols* and *continuous line*). Final concentration of hydroxylamine in the cuvette was 5 mM and has no effect on the enzyme coupled assay. These experiments have been done twice, each data point being the mean, and these data were fitted to Hill equations. *Error bars* were not indicated as they were smaller than the size of the symbols. The estimated $Ca_{1/2}$ for untreated and NH_2OH-treated SR are 2.3 ± 0.3 µM (pCa = 5.64) and 3.2 ± 0.5 µM (pCa = 5.49), respectively. Note that our values are higher than those indicated by MacLennan et al. who did the measurements at pH 7 [46], in conditions where the E2 to E1 equilibrium is pulled toward E2 resulting in slightly lower $Ca_{1/2}$ values

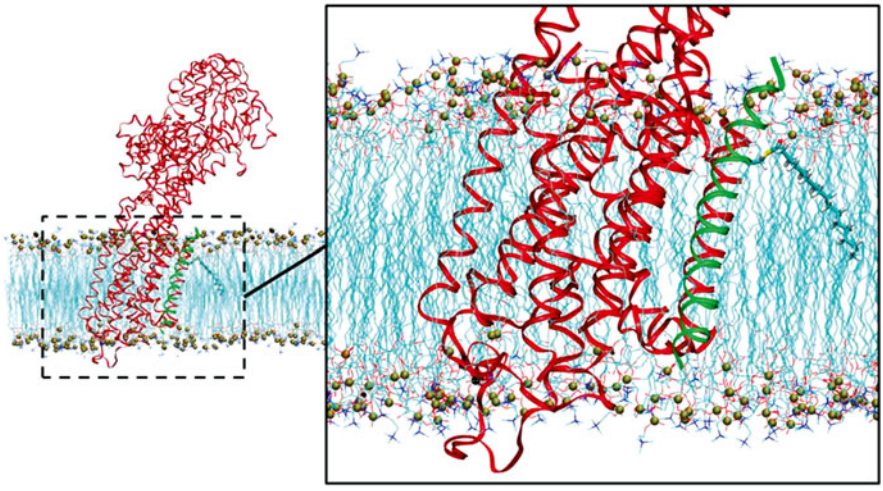

Fig. 10.7 Molecular modeling of Cys9-palmitoylated sarcolipin in interaction with SERCA1a embedded in a POPC bilayer. Molecular modeling of the palmitoylated SLN was made using UCSF Chimera software [103] and the SERCA1a/rSLN complex structure (PDB: 4H1W, [54]) as template. The complex was embedded in a POPC bilayer using the InflateGRO method [105] and data from the OPM database [106]. SERCA1a was tilted by 23° with respect to the membrane normal. Several energy minimization steps were performed using GROMACS [107] with protein atoms harmonically restrained using a force constant of 10,000 kcal mol^{-1} nm^{-2}. Snapshot representations are made using VMD software [108]. rSLN and SERCA1a are depicted as a *green* and a *red ribbon*, respectively. The palmitoyl anchor is represented in licorice and the POPC lipids are in sticks without the hydrogen atoms for the sake of clarity. Phosphorus atoms of POPC are represented as Van der Waal's spheres. Carbon atoms are in cyan, oxygen in *red*, nitrogen in *blue*, phosphorus in bronze, sulfur in *yellow*, and hydrogen in *white*

longus (EDL), is also fully palmitoylated/oleoylated and has the same properties as the rabbit SLN after deacylation. Based on a cladogram, we finally postulated that the phenylalanine mutation to cysteine in some species is the result of an evolutionary convergence. We proposed that, besides phosphorylation, S-acylation/deacylation may also regulate SLN activity [31]. Interestingly, acylation is also a feature that distinguishes sarcolipin from phospholamban: none of the three cysteines of PLN located within the membrane domain is acylated [78].

9 Does Sarcolipin Associate with Itself and with Phospholamban?

9.1 Does Sarcolipin Form Homo-Oligomers?

Considering the high degree of similarities between SLN and PLN transmembrane domain, the homo-oligomerization of SLN has been investigated because PLN forms stable pentamers [79, 80]. Indeed, the high-resolution structure of these

PLN pentamers was solved by NMR in the presence of DPC and reconstituted in a DOPC/DOPE bilayer [81, 82]. It has been proposed that this pentameric state should correspond to an inactive form of the PLN in equilibrium with a monomeric active form, the latter being able to interact with SERCA1a for inhibition. However, this hypothesis is challenged by the recent high-resolution crystal structure of a SERCA1a–PLN complex which shows that a dimeric and even a pentameric form of PLN could also interact with SERCA1a [59]. As a matter of fact, the residues involved in the pentamerization motif are localized at the opposite side of the helix than those implicated in the interaction with SERCA1a. It has been demonstrated that PLN homo-oligomerize via a Leucine zipper motif (Leu-x2-Ile-x3-Leu-x2-Ile-x3-Leu, [80–82]). No such motif can be found in SLN amino acid sequences suggesting that SLN, if able to interact with itself, homo-oligomerize via a different motif.

The oligomeric state of SLN was investigated by several groups [83–86, 43]. The study of the oligomerization of hSLN was performed in the presence of nonionic detergents and by centrifugation analysis and cross-linking experiments [86]. In these experiments, the authors show that both SLN and PLN form oligomers but that these oligomers greatly differ. Sarcolipin does not form SDS-resistant oligomers at concentration close to those used for PLN as shown by SDS-PAGE analysis. On contrary to PLN oligomers which are formed at low concentration reaching a pentameric equilibrium state, SLN oligomers appear only at much higher concentrations and seem to never reach a stable oligomeric state as the size of the oligomer increases linearly as a function of SLN concentration. In addition, SLN oligomers were observed by cross-linking in POPC liposomes but only in the presence of a very large excess of cross-linker. Analysis of SLN oligomer formation after reconstitution in DOPC bilayers by solid-state NMR reveals that SLN remains monomeric at millimolar concentration [43].

It has also been suggested that oligomerization of SLN could result in a pore formation as proposed for PLN [83–85]. To demonstrate the formation of pores, SLN was incorporated into a supported lipid bilayer anchored to a mercury electrode through a hydrophilic tetraethyleneoxy chain. As a matter of fact, lipid bilayers tethered to a metal surface via a hydrophilic "spacer," often called tethered bilayer lipid membranes (tBLMs), may provide a friendly environment to channel-forming peptides and proteins, thus maintaining their functionally active state and allowing an investigation of their putative function. Adding inorganic anions as chloride, sulfate, phosphate, or oxalate in the presence of SLN leads to an increase of the tBLM conductivity whereas the same experiment using inorganic cations does not show a modification of the membrane conductivity. This could suggest that sarcolipin aggregates into an anion-conducting-like pore. But, such a permeabilization cannot occur at physiological pH [84]. The authors suggested that sarcolipin pore activity should participate in the dissipation of the local increase of the luminal transmembrane potential caused by proton counter transport and the translocation in the lumen of the phosphate ions resulting from ATP hydrolysis [83]. Even if the SLN channel permeabilizing effect observed for phosphate ions is modest compared to the ATPase activity, such a translocation of phosphate should improve the

accumulation of calcium in the lumen and limit retro-inhibition of the SERCA1a, resulting in an increase of the turnover at millimolar concentration of calcium as suggested initially by MacLennan et al. [3]. Nevertheless, it has to be considered that SLN oligomerization is observed here in supported DOPC monolayers, an in vitro model which is very different from a natural bilayer. Because SLN is a transmembrane peptide, its insertion in a lipid monolayer instead of a bilayer could artificially favor its oligomerization. Smith et al. have demonstrated that co-reconstitution of SLN with native SR membrane does not permeabilize the membrane neither to calcium nor to proton [20]. Moreover, SERCA1a acts as a Ca^{2+}/H^{+}-ATPase (Fig. 10.1), and since the bilayer is impermeable to protons, addition of FCCP, a protonophore, to the vesicles resulted in an increase of the accumulation of calcium [87]. Smith et al. showed that even in the presence of a SLN:SERCA1a 5:1 mol:mol ratio, the greatest accumulation of calcium observed in the presence of FCCP, remains the same as in the control experiment done in the absence of SLN, demonstrating that SLN does not form oligomers leaky to protons [20]. The divergent results found in the literature suggest that the putative oligomerization of SLN has to be carefully investigated in a natural environment in order to validate the relevancy of such mechanism in the context of the regulation of SERCA isoforms and of the SR calcium homeostasis.

9.2 Do SLN and PLN Interact?

Similarly to the ongoing discussion of homo-oligomerization of SLN, the potential interaction of SLN with PLN is also currently under debate. Since SLN and PLN are co-expressed in the *atria* and in several smooth or fast-twitch muscle [4, 12], possible ternary interactions of those two peptides and the rabbit SERCA1a or rabbit SERCA2a isoforms were investigated [45]. Co-overexpression of SLN, PLN, and SERCA isoforms in HEK-293 cells led to a super-inhibition of the calcium uptake in microsomes: calcium affinity decreased by one order of magnitude (at pH 7, $Ca_{1/2SERCA1a\ alone} = 0.35$ μM, $Ca_{1/2SERCA1a+PLN} = 0.79$ μM, $Ca_{1/2SERCA1a+SLN} = 0.58$ μM, $Ca_{1/2SERCA1a+PLN+SLN} = 3.0$ μM) and the V_{max}, which was not affected by the expression of only one regulatory peptide, decreased by 20 % for SERCA1a and 50 % for SERCA2a. Using molecular modeling, the authors firstly suggested that a SERCA1a/PLN/SLN ternary complex could be formed (E2-like structure used as SERCA1a model, [58]) with both SLN and PLN in close contact with SERCA1a [46]). However, the same authors recently rejected this hypothesis arguing that the binding groove of SLN within the SERCA1a–SLN complex is too narrow to accommodate an additional transmembrane helix like that of PLN [53]. The high-resolution structure of SERCA1a–SLN complex was obtained using native sarcoplasmic reticulum membrane as protein sources. The structure of the groove is conserved in the high-resolution structure of SERCA1a obtained using a recombinant SLN-free source and the same conditions of crystallization [88–90, 53]. Thus, this suggests that the groove size is governed by the state of the ATPase and not induced by the presence of SLN (or PLN).

It has been proposed that SLN could destabilize PLN pentamers and that this destabilization could result in an increase in PLN monomers and in a super-inhibition of SERCAs. As a matter of fact, site-directed mutagenesis study of phospholamban showed that the equilibrium between the pentameric form ("inactive" form) and the monomeric form ("active" inhibitory form) influences the ATPase activity [91]. Mutations of key residues of the leucine zipper motif induced depolymerization of PLN and an increase in its inhibitory effect on SERCA2a. To date, this super-inhibitory activity is not clearly demonstrated in vivo. In addition, in the co-overexpression experiments, the stoichiometry of SLN, PLN or SERCA isoforms which is not indicated could be a source of misinterpretation. It is not demonstrated that the level of expression of the regulatory peptides is sufficient to exert a maximum inhibitory effect on the overexpressed ATPase. As pointed out above, the effect of SLN on the $Ca_{1/2}$ or the V_{max} depends on the system used to characterize the inhibition. Moreover, the expression levels of SLN and PLN in vivo are still a matter of debate [92] so caution should be taken not to misinterpret the in vitro data in a physiological context.

10 Conclusions

The role of sarcolipin in SERCAs regulation is complex and still subject to debate. Sarcolipin is regulated itself at several levels from the gene to the protein. The presence in myocytes of particular transcription factors (myocyte enhancer factor) is probably responsible of its muscle-specific expression. Furthermore, the presence of different polyadenylation signals among species could also result in differences at the final translation level. Several data are now available on the expression level of SLN from different tissues and from different species. It has been clearly demonstrated that SLN is expressed in several tissues, even in the presence of other regulatory peptides like phospholamban. Sarcolipin expression is not restricted to fast-twitch muscle as initially proposed. The level of expression in one particular tissue from one species to another could also greatly vary, for example, the amount of SLN in the mouse skeletal muscle is about one thousand time lower than in rabbit skeletal muscle [92]. All these data indicate that expression of SLN is fine-tuned at many levels, even before its interaction with Ca^{2+}-ATPases or putative other partners. In addition, interaction of SLN with Ca^{2+}-ATPases is regulated by post-translational modifications. Phosphorylation of its N-terminus, via the β-adrenergic calcium regulation pathway, could trigger its dissociation from the Ca^{2+}-ATPases. Recently, it has been demonstrated that sarcolipin is also S-palmitoylated and S-oleoylated. The exact role of these latter modifications is still unknown but it has been reported that acylation could affect membrane protein localization, stabilization within the membrane, and interaction with other proteins [93]. To date, SLN is the only SERCAs regulatory peptide which is acylated. Interestingly, it is now clear that SLN and PLN do not share the same regulatory mechanism. The recent high-resolution structures of the SERCA1a–SLN complex [53, 54] illustrate and give

new insights into how SLN inhibition arises from the stabilization of a Ca^{2+}-free E1 intermediate state. However, these structures and the comparison with the recent structure of SERCA1a–PLN complex [59] raise the following question: what are the structural and dynamic features of both partners (peptides and SERCAs) that are important for the regulation of SERCAs knowing that SLN and PLN are sometimes expressed in the same cells, at the same time, and in similar amounts [12]? Moreover, although rabbit SERCA1a and human SERCA2a share a high degree of identity (about 85 %), it is worth to mention the presence of a small patch of different amino acids in the N-domain. Many residues from this patch belong to the interaction site of the PLN N-terminus with the SERCAs N-domain, so it could explain part of the functional differences between PLN and SLN as SLN has not such an N-terminal extension [94–96]. Furthermore, the life time of the SLN–SERCAs complex during catalysis remains unclear. The hypothesis that SLN could interact only with a particular catalytic state and the hypothesis that SLN could remain bound to the SERCAs during the whole cycle are both considered in the literature. For example, based on a docking analysis, Winther et al. suggest that sarcolipin does not bind to the Ca_2.E1P state as the groove is too narrow [54]. However, we observed that the complex remains formed even in presence of saturating concentration of calcium and of AMPCP which may trigger the ATPase in a Ca_2.E1P-like conformation (*unpublished results*).

Numerous studies have recently documented the role of SLN in muscle-based thermogenesis. It has been shown that expression of SLN increases the uncoupling of the ATPase and, consequently the rate of heat production [24, 25]. Furthermore, knock-out mice ($SLN^{-/-}$) or SLN overexpressing mice (SLN^{OE}) were recently extensively used to determine the possible role of SLN in several metabolic pathways [28, 29, 97]. Knock-out mice have a lower body temperature so it suggests that SLN expression is probably critical for cold-induced muscle-based thermogenesis, probably via its interaction with SERCA1a [28, 29]. Additionally, SLN^{OE} mice displayed a higher oxygen consumption and fatty acid oxidation than wild-type mice suggesting a diet-induced thermogenesis [98]. An increase of SLN expression seems to improve skeletal muscle performance by reducing fatigue during a prolonged activity [97]. However, the use of $SLN^{-/-}$ or SLN^{OE} mice was recently debated due to the low level of SLN expression in wild-type mice skeletal muscles. It is unlikely that deleting SLN would have an assessable effect on thermogenesis by the calcium pumps [92]. As rodents possess brown adipose tissue physiologically essentially dedicated to heat production, they probably do not need another efficient muscle-based heat production pathway. Nevertheless, SLN might have a role in muscle-based thermogenesis in larger mammals, most of them being deprived from such brown adipose tissues [99].

Given the importance of SERCAs pump activity in regulating Ca^{2+} handling and the pathogenesis of skeletal muscle diseases, such as myopathy and muscular dystrophies, the recent discovery of several putative regulatory peptides opens interesting possibilities for the treatment of these diseases [7]. It suggests that expression of the different regulatory peptides could act with compensatory effects as MLN might be expressed in SLN- and PLN-deprived mice tissues [7]. However, at the present

time, myoregulin peptides were not detected in vivo [7, 8]: their expression level compared to SLN and PLN in different species and tissues has to be investigated. Interestingly, the sequence coding MLN was found in a mistakenly annotated noncoding mRNA specific from skeletal muscle. Consequently, several unidentified regulatory peptides could also be encoded in the many mRNA sequences currently annotated as noncoding sequences, and their discovery would open the way to a better knowledge of muscle physiology.

Acknowledgments This work was supported by the French Infrastructure for Integrated Structural Biology (FRISBI) and by grants from the Agence Nationale pour la Recherche and the Ile de France region (Domaine d'Intérêt Majeur Maladies Infectieuses, DIM MALINF).

References

1. Wawrzynow A, Theibert JL, Murphy C et al (1992) Sarcolipin, the "proteolipid" of skeletal muscle sarcoplasmic reticulum, is a unique, amphipathic, 31-residue peptide. Arch Biochem Biophys 298:620–623
2. MacLennan D, Yip C, Iles G et al (1972) Isolation of sarcoplasmic reticulum proteins. Cold Spring Harb Symp Quant Biol 37:469–477
3. Odermatt A, Becker S, Khanna VK et al (1998) Sarcolipin regulates the activity of SERCA1, the fast-twitch skeletal muscle sarcoplasmic reticulum Ca2+-ATPase. J Biol Chem 273:12360–12369
4. Odermatt A, Taschner PE, Scherer SW et al (1997) Characterization of the gene encoding human sarcolipin (SLN), a proteolipid associated with SERCA1: absence of structural mutations in five patients with Brody disease. Genomics 45:541–553
5. Moller JV, Juul B, le Maire M (1996) Structural organization, ion transport, and energy transduction of P-type ATPases. Biochim Biophys Acta 1286:1–51
6. Kirchberber MA, Tada M, Katz AM (1975) Phospholamban: a regulatory protein of the cardiac sarcoplasmic reticulum. Recent Adv Stud Cardiac Struct Metab 5:103–115
7. Anderson DM, Anderson KM, Chang CL et al (2015) A micropeptide encoded by a putative long noncoding RNA regulates muscle performance. Cell 160:595–606
8. Magny EG, Pueyo JI, Pearl FM et al (2013) Conserved regulation of cardiac calcium uptake by peptides encoded in small open reading frames. Science 341:1116–1120
9. Weintraub H, Davis R, Lockshon D et al (1990) MyoD binds cooperatively to two sites in a target enhancer sequence: occupancy of two sites is required for activation. Proc Natl Acad Sci U S A 87:5623–5627
10. Piette J, Bessereau JL, Huchet M et al (1990) Two adjacent MyoD1-binding sites regulate expression of the acetylcholine receptor alpha-subunit gene. Nature 345:353–355
11. Kozak M (1987) At least six nucleotides preceding the AUG initiator codon enhance translation in mammalian cells. J Mol Biol 196:947–950
12. Vangheluwe P, Schuermans M, Zador E et al (2005) Sarcolipin and phospholamban mRNA and protein expression in cardiac and skeletal muscle of different species. Biochem J 389:151–159
13. Babu GJ, Bhupathy P, Carnes CA et al (2007) Differential expression of sarcolipin protein during muscle development and cardiac pathophysiology. J Mol Cell Cardiol 43:215–222
14. Fajardo VA, Bombardier E, Vigna C et al (2013) Co-expression of SERCA isoforms, phospholamban and sarcolipin in human skeletal muscle fibers. PLoS One 8, e84304
15. Uemura N, Ohkusa T, Hamano K et al (2004) Down-regulation of sarcolipin mRNA expression in chronic atrial fibrillation. Eur J Clin Invest 34:723–730

16. Shanmugam M, Molina CE, Gao S et al (2011) Decreased sarcolipin protein expression and enhanced sarco(endo)plasmic reticulum Ca2+ uptake in human atrial fibrillation. Biochem Biophys Res Commun 410:97–101
17. Vittorini S, Storti S, Parri MS et al (2007) SERCA2a, phospholamban, sarcolipin, and ryanodine receptors gene expression in children with congenital heart defects. Mol Med 13:105–111
18. Guglielmi V, Vattemi G, Gualandi F et al (2013) SERCA1 protein expression in muscle of patients with Brody disease and Brody syndrome and in cultured human muscle fibers. Mol Genet Metab 110:162–169
19. Block BA (1994) Thermogenesis in muscle. Annu Rev Physiol 56:535–577
20. Smith WS, Broadbridge R, East JM et al (2002) Sarcolipin uncouples hydrolysis of ATP from accumulation of Ca2+ by the Ca2+-ATPase of skeletal-muscle sarcoplasmic reticulum. Biochem J 361:277–286
21. de Meis L (1998) Control of heat produced during ATP hydrolysis by the sarcoplasmic reticulum Ca(2+)-ATPase in the absence of a Ca2+ gradient. Biochem Biophys Res Commun 243:598–600
22. Mitidieri F, de Meis L (1999) Ca(2+) release and heat production by the endoplasmic reticulum Ca(2+)-ATPase of blood platelets. Effect of the platelet activating factor. J Biol Chem 274:28344–28350
23. de Meis L (2001) Role of the sarcoplasmic reticulum Ca2+-ATPase on heat production and thermogenesis. Biosci Rep 21:113–137
24. de Meis L (2001) Uncoupled ATPase activity and heat production by the sarcoplasmic reticulum Ca2+-ATPase. Regulation by ADP. J Biol Chem 276:25078–25087
25. Lee AG (2002) A calcium pump made visible. Curr Opin Struct Biol 12:547–554
26. Mall S, Broadbridge R, Harrison SL et al (2006) The presence of sarcolipin results in increased heat production by Ca(2+)-ATPase. J Biol Chem 281:36597–36602
27. Stammers AN, Susser SE, Hamm NC et al (2015) The regulation of sarco(endo)plasmic reticulum calcium-ATPases (SERCA). Can J Physiol Pharmacol 19:1–12
28. Bal NC, Maurya SK, Sopariwala DH et al (2012) Sarcolipin is a newly identified regulator of muscle-based thermogenesis in mammals. Nat Med 18:1575–1579
29. Bombardier E, Smith IC, Vigna C et al (2013) Ablation of sarcolipin decreases the energy requirements for Ca2+ transport by sarco(endo)plasmic reticulum Ca2+-ATPases in resting skeletal muscle. FEBS Lett 587:1687–1692
30. Gillard EF, Otsu K, Fujii J et al (1991) A substitution of cysteine for arginine 614 in the ryanodine receptor is potentially causative of human malignant hyperthermia. Genomics 11:751–755
31. Montigny C, Decottignies P, Le Marechal P et al (2014) S-palmitoylation and s-oleoylation of rabbit and pig sarcolipin. J Biol Chem 289:33850–33861
32. Bhupathy P, Babu GJ, Ito M et al (2009) Threonine-5 at the N-terminus can modulate sarcolipin function in cardiac myocytes. J Mol Cell Cardiol 47:723–729
33. Gramolini AO, Trivieri MG, Oudit GY et al (2006) Cardiac-specific overexpression of sarcolipin in phospholamban null mice impairs myocyte function that is restored by phosphorylation. Proc Natl Acad Sci U S A 103:2446–2451
34. Montaville P, Jamin N (2010) Determination of membrane protein structures using solution and solid-state NMR. Methods Mol Biol 654:261–282
35. Warschawski DE, Arnold AA, Beaugrand M et al (2011) Choosing membrane mimetics for NMR structural studies of transmembrane proteins. Biochim Biophys Acta 1808: 1957–1974
36. Mascioni A, Karim C, Barany G et al (2002) Structure and orientation of sarcolipin in lipid environments. Biochemistry 41:475–482
37. Buck B, Zamoon J, Kirby TL et al (2003) Overexpression, purification, and characterization of recombinant Ca-ATPase regulators for high-resolution solution and solid-state NMR studies. Protein Expr Purif 30:253–261

38. Buffy JJ, Buck-Koehntop BA, Porcelli F et al (2006) Defining the intramembrane binding mechanism of sarcolipin to calcium ATPase using solution NMR spectroscopy. J Mol Biol 358:420–429
39. Buffy JJ, Traaseth NJ, Mascioni A et al (2006) Two-dimensional solid-state NMR reveals two topologies of sarcolipin in oriented lipid bilayers. Biochemistry 45:10939–10946
40. Shi L, Cembran A, Gao J et al (2009) Tilt and azimuthal angles of a transmembrane peptide: a comparison between molecular dynamics calculations and solid-state NMR data of sarcolipin in lipid membranes. Biophys J 96:3648–3662
41. De Simone A, Mote KR, Veglia G (2014) Structural dynamics and conformational equilibria of SERCA regulatory proteins in membranes by solid-state NMR restrained simulations. Biophys J 106:2566–2576
42. Traaseth NJ, Ha KN, Verardi R et al (2008) Structural and dynamic basis of phospholamban and sarcolipin inhibition of Ca(2+)-ATPase. Biochemistry 47:3–13
43. Hughes E, Clayton JC, Kitmitto A et al (2007) Solid-state NMR and functional measurements indicate that the conserved tyrosine residues of sarcolipin are involved directly in the inhibition of SERCA1. J Biol Chem 282:26603–26613
44. Shaw G, Morse S, Ararat M et al (2002) Preferential transformation of human neuronal cells by human adenoviruses and the origin of HEK 293 cells. FASEB J 16:869–871
45. Asahi M, Kurzydlowski K, Tada M et al (2002) Sarcolipin inhibits polymerization of phospholamban to induce superinhibition of sarco(endo)plasmic reticulum Ca2+-ATPases (SERCAs). J Biol Chem 277:26725–26728
46. Asahi M, Sugita Y, Kurzydlowski K et al (2003) Sarcolipin regulates sarco(endo)plasmic reticulum Ca2+-ATPase (SERCA) by binding to transmembrane helices alone or in association with phospholamban. Proc Natl Acad Sci U S A 100:5040–5045
47. MacLennan DH, Asahi M, Tupling AR (2003) The regulation of SERCA-type pumps by phospholamban and sarcolipin. Ann N Y Acad Sci 986:472–480
48. Hughes E, Middleton DA (2003) Solid-state NMR reveals structural changes in phospholamban accompanying the functional regulation of Ca2+-ATPase. J Biol Chem 278:20835–20842
49. Douglas JL, Trieber CA, Afara M et al (2005) Rapid, high-yield expression and purification of Ca2+-ATPase regulatory proteins for high-resolution structural studies. Protein Expr Purif 40:118–125
50. Gorski PA, Glaves JP, Vangheluwe P et al (2013) Sarco(endo)plasmic reticulum calcium ATPase (SERCA) inhibition by sarcolipin is encoded in its luminal tail. J Biol Chem 288:8456–8467
51. Tupling AR, Asahi M, MacLennan DH (2002) Sarcolipin overexpression in rat slow twitch muscle inhibits sarcoplasmic reticulum Ca2+ uptake and impairs contractile function. J Biol Chem 277:44740–44746
52. Pardi A, Wagner G, Wuthrich K (1983) Protein conformation and proton nuclear-magnetic-resonance chemical shifts. Eur J Biochem 137:445–454
53. Toyoshima C, Iwasawa S, Ogawa H et al (2013) Crystal structures of the calcium pump and sarcolipin in the Mg2+-bound E1 state. Nature 495:260–264
54. Winther AM, Bublitz M, Karlsen JL et al (2013) The sarcolipin-bound calcium pump stabilizes calcium sites exposed to the cytoplasm. Nature 495:265–269
55. Lund S, Orlowski S, de Foresta B et al (1989) Detergent structure and associated lipid as determinants in the stabilization of solubilized Ca2+-ATPase from sarcoplasmic reticulum. J Biol Chem 264:4907–4915
56. Montigny C, Arnou B, Champeil P (2010) Glycyl betaine is effective in slowing down the irreversible denaturation of a detergent-solubilized membrane protein, sarcoplasmic reticulum Ca2+-ATPase (SERCA1a). Biochem Biophys Res Commun 391:1067–1069
57. Montigny C, Arnou B, Marchal E et al (2008) Use of glycerol-containing media to study the intrinsic fluorescence properties of detergent-solubilized native or expressed SERCA1a. Biochemistry 47:12159–12174

58. Toyoshima C, Nomura H (2002) Structural changes in the calcium pump accompanying the dissociation of calcium. Nature 418:605–611
59. Akin BL, Hurley TD, Chen Z et al (2013) The structural basis for phospholamban inhibition of the calcium pump in sarcoplasmic reticulum. J Biol Chem 288:30181–30191
60. Chen Z, Akin BL, Stokes DL et al (2006) Cross-linking of C-terminal residues of phospholamban to the Ca2+ pump of cardiac sarcoplasmic reticulum to probe spatial and functional interactions within the transmembrane domain. J Biol Chem 28:14163–14172
61. Chen Z, Stokes DL, Jones LR (2005) Role of leucine 31 of phospholamban in structural and functional interactions with the Ca2+ pump of cardiac sarcoplasmic reticulum. J Biol Chem 280:10530–10539
62. Chen Z, Stokes DL, Rice WJ et al (2003) Spatial and dynamic interactions between phospholamban and the canine cardiac Ca2+ pump revealed with use of heterobifunctional cross-linking agents. J Biol Chem 278:48348–48356
63. Jones LR, Cornea RL, Chen Z (2002) Close proximity between residue 30 of phospholamban and cysteine 318 of the cardiac Ca2+ pump revealed by intermolecular thiol cross-linking. J Biol Chem 277:28319–28329
64. Toyoshima C, Asahi M, Sugita Y et al (2003) Modeling of the inhibitory interaction of phospholamban with the Ca2+ ATPase. Proc Natl Acad Sci U S A 100:467–472
65. Akin BL, Chen Z, Jones LR (2010) Superinhibitory phospholamban mutants compete with Ca2+ for binding to SERCA2a by stabilizing a unique nucleotide-dependent conformational state. J Biol Chem 285:28540–28552
66. Bidwell P, Blackwell DJ, Hou Z et al (2011) Phospholamban binds with differential affinity to calcium pump conformers. J Biol Chem 286:35044–35050
67. Berson AE, Young C, Morrison SL et al (1999) Identification and characterization of a myristylated and palmitylated serine/threonine protein kinase. Biochem Biophys Res Commun 259:533–538
68. Kurioka K, Nakagawa K, Denda K et al (1998) Molecular cloning and characterization of a novel protein serine/threonine kinase highly expressed in mouse embryo. Biochim Biophys Acta 1443:275–284
69. Ligos JM, Gerwin N, Fernandez P et al (1998) Cloning, expression analysis, and functional characterization of PKL12, a member of a new subfamily of ser/thr kinases. Biochem Biophys Res Commun 249:380–384
70. Stairs DB, Perry Gardner H, Ha SI et al (1998) Cloning and characterization of Krct, a member of a novel subfamily of serine/threonine kinases. Hum Mol Genet 7:2157–2166
71. MacLennan DH, Kranias EG (2003) Phospholamban: a crucial regulator of cardiac contractility. Nat Rev Mol Cell Biol 4:566–577
72. Simmerman HK, Jones LR (1998) Phospholamban: protein structure, mechanism of action, and role in cardiac function. Physiol Rev 78:921–947
73. Tada M, Kadoma M (1989) Regulation of the Ca2+ pump ATPase by cAMP-dependent phosphorylation of phospholamban. Bioessays 10:157–163
74. Zhao W, Uehara Y, Chu G et al (2004) Threonine-17 phosphorylation of phospholamban: a key determinant of frequency-dependent increase of cardiac contractility. J Mol Cell Cardiol 37:607–612
75. Ubersax JA, Ferrell JE Jr (2007) Mechanisms of specificity in protein phosphorylation. Nat Rev Mol Cell Biol 8:530–541
76. Gramolini AO, Kislinger T, Asahi M et al (2004) Sarcolipin retention in the endoplasmic reticulum depends on its C-terminal RSYQY sequence and its interaction with sarco(endo) plasmic Ca(2+)-ATPases. Proc Natl Acad Sci U S A 101:16807–16812
77. Gorski PA, Trieber CA, Ashrafi G et al (2015) Regulation of the sarcoplasmic reticulum calcium pump by divergent phospholamban isoforms in zebrafish. J Biol Chem 290: 6777–6788
78. Mayer EJ, McKenna E, Garsky VM et al (1996) Biochemical and biophysical comparison of native and chemically synthesized phospholamban and a monomeric phospholamban analog. J Biol Chem 271:1669–1677

79. Arkin IT, Adams PD, Brunger AT et al (1997) Structural perspectives of phospholamban, a helical transmembrane pentamer. Annu Rev Biophys Biomol Struct 26:157–179
80. Simmerman HK, Kobayashi YM, Autry JM et al (1996) A leucine zipper stabilizes the pentameric membrane domain of phospholamban and forms a coiled-coil pore structure. J Biol Chem 271:5941–5946
81. Traaseth NJ, Verardi R, Torgersen KD et al (2007) Spectroscopic validation of the pentameric structure of phospholamban. Proc Natl Acad Sci U S A 104:14676–14681
82. Verardi R, Shi L, Traaseth NJ et al (2011) Structural topology of phospholamban pentamer in lipid bilayers by a hybrid solution and solid-state NMR method. Proc Natl Acad Sci U S A 108(22):9101–9106
83. Becucci L, Foresti ML, Schwan A et al (2013) Can proton pumping by SERCA enhance the regulatory role of phospholamban and sarcolipin? Biochim Biophys Acta 1828:2682–2690
84. Becucci L, Guidelli R, Karim CB et al (2007) An electrochemical investigation of sarcolipin reconstituted into a mercury-supported lipid bilayer. Biophys J 93:2678–2687
85. Becucci L, Guidelli R, Karim CB et al (2009) The role of sarcolipin and ATP in the transport of phosphate ion into the sarcoplasmic reticulum. Biophys J 97:2693–2699
86. Hellstern S, Pegoraro S, Karim CB et al (2001) Sarcolipin, the shorter homologue of phospholamban, forms oligomeric structures in detergent micelles and in liposomes. J Biol Chem 27630845–30852
87. Levy D, Seigneuret M, Bluzat A et al (1990) Evidence for proton countertransport by the sarcoplasmic reticulum Ca2(+)-ATPase during calcium transport in reconstituted proteoliposomes with low ionic permeability. J Biol Chem 265:19524–19534
88. Clausen JD, Bublitz M, Arnou B et al (2014) SERCA mutant E309Q binds two Ca(2+) ions but adopts a catalytically incompetent conformation. EMBO J 32:3231–3243
89. Jidenko M, Nielsen RC, Sorensen TL et al (2005) Crystallization of a mammalian membrane protein overexpressed in Saccharomyces cerevisiae. Proc Natl Acad Sci U S A 102: 11687–11691
90. Marchand A, Winther AM, Holm PJ et al (2008) Crystal structure of D351A and P312A mutant forms of the mammalian sarcoplasmic reticulum Ca(2+) -ATPase reveals key events in phosphorylation and Ca(2+) release. J Biol Chem 283:14867–14882
91. Kimura Y, Kurzydlowski K, Tada M et al (1997) Phospholamban inhibitory function is activated by depolymerization. J Biol Chem 272:15061–15064
92. Butler J, Smyth N, Broadbridge R et al (2015) The effects of sarcolipin over-expression in mouse skeletal muscle on metabolic activity. Arch Biochem Biophys 569:26–31
93. Charollais J, Van Der Goot FG (2009) Palmitoylation of membrane proteins (Review). Mol Membr Biol 26:55–66
94. Toyofuku T, Kurzydlowski K, Tada M et al (1993) Identification of regions in the Ca(2+)-ATPase of sarcoplasmic reticulum that affect functional association with phospholamban. J Biol Chem 268:2809–2815
95. Toyofuku T, Kurzydlowski K, Tada M et al (1994) Amino acids Glu2 to Ile18 in the cytoplasmic domain of phospholamban are essential for functional association with the Ca(2+)-ATPase of sarcoplasmic reticulum. J Biol Chem 269:3088–3094
96. Toyofuku T, Kurzydlowski K, Tada M et al (1994) Amino acids Lys-Asp-Asp-Lys-Pro--Val402 in the Ca(2+)-ATPase of cardiac sarcoplasmic reticulum are critical for functional association with phospholamban. J Biol Chem 269:22929–22932
97. Sopariwala DH, Pant M, Shaikh SA et al (2015) Sarcolipin overexpression improves muscle energetics and reduces fatigue. J Appl Physiol 118:1050–1058
98. Maurya SK, Bal NC, Sopariwala DH et al (2015) Sarcolipin is a key determinant of basal metabolic rate and its overexpression enhances energy expenditure and resistance against diet induced obesity. J Biol Chem 24:840–849
99. Gamu D, Bombardier E, Smith IC et al (2014) Sarcolipin provides a novel muscle-based mechanism for adaptive thermogenesis. Exerc Sport Sci Rev 42:136–142
100. Galtier N, Gouy M, Gautier C (1996) SEAVIEW and PHYLO_WIN: two graphic tools for sequence alignment and molecular phylogeny. Comput Appl Biosci 12:543–548

101. Crooks GE, Hon G, Chandonia JM et al (2004) WebLogo: a sequence logo generator. Genome Res 14:1188–1190
102. Schneider TD, Stephens RM (1990) Sequence logos: a new way to display consensus sequences. Nucleic Acids Res 18:6097–6100
103. Pettersen EF, Goddard TD, Huang CC et al (2004) UCSF Chimera--a visualization system for exploratory research and analysis. J Comput Chem 25:1605–1612
104. Bers DM, Patton CW, Nuccitelli R (2010) A practical guide to the preparation of Ca(2+) buffers. Methods Cell Biol 99:1–26
105. Kandt C, Ash WL, Tieleman DP (2007) Setting up and running molecular dynamics simulations of membrane proteins. Methods 41:475–488
106. Lomize MA, Pogozheva ID, Joo H et al (2012) OPM database and PPM web server: resources for positioning of proteins in membranes. Nucleic Acids Res 40(Database issue):D370–376
107. Pronk S, Pall S, Schulz R et al (2013) GROMACS 4.5: a high-throughput and highly parallel open source molecular simulation toolkit. Bioinformatics 29:845–854
108. Humphrey W, Dalke A, Schulten K (1996) VMD: visual molecular dynamics. J Mol Graph 14(33-38):27–38

Chapter 11
Regulation of Cardiac Sarco(endo)plasmic Reticulum Calcium-ATPases (SERCA2a) in Response to Exercise

Naomi C. Hamm, Andrew N. Stammers, Shanel E. Susser, Michael W. Hlynsky, Dustin E. Kimber, D, Scott Kehler, and Todd A. Duhamel

Abstract Sarco(endo)plasmic reticulum calcium ATPase (SERCA2a) plays an integral role in Ca^{2+} cycling in the heart. After a myocardial contraction has occurred, SERCA2a is primarily responsible for transporting Ca^{2+} out of the cytosol into the sarcoplasmic reticulum. Consequently, SERCA2a is key in determining relaxation time and inotropy of subsequent contractions. There are ten different SERCA isoforms in the body, where SERCA2a is the isoform expressed in the heart. Both SERCA2a expression and activity are reduced in models of disease. As such, a large body of research has examined SERCA2a and how it might be used as a means to restore heart function in models of disease. In this chapter, we examine various regulatory mechanisms of SERCA2a and how these mechanisms affect SERCA2a and cardiac function. Transcriptional, protein (e.g., phospholamban and

N.C. Hamm • A.N. Stammers • M.W. Hlynsky • D.E. Kimber • D.S. Kehler
Health, Leisure & Human Performance Research Institute, Faculty of Kinesiology & Recreation Management, University of Manitoba, Winnipeg, MB, Canada, R3T 2N2

Institute of Cardiovascular Sciences, St. Boniface Hospital Research Centre, Winnipeg, MB, Canada, R3T 2N2

S.E. Susser
Institute of Cardiovascular Sciences, St. Boniface Hospital Research Centre, Winnipeg, MB, Canada, R3T 2N2

Department of Physiology, Faculty of Health Sciences, University of Manitoba, Winnipeg, MB, Canada, R3T 2N2

T.A. Duhamel (✉)
Health, Leisure & Human Performance Research Institute, Faculty of Kinesiology & Recreation Management, University of Manitoba, Winnipeg, MB, Canada, R3T 2N2

Institute of Cardiovascular Sciences, St. Boniface Hospital Research Centre, Winnipeg, MB, Canada, R3T 2N2

Department of Physiology, Faculty of Health Sciences, University of Manitoba, Winnipeg, MB, Canada, R3T 2N2
e-mail: tduhamel@sbrc.ca

S. Chakraborti, N.S. Dhalla (eds.), *Regulation of Ca^{2+}-ATPases,V-ATPases and F-ATPases*, Advances in Biochemistry in Health and Disease 14,
DOI 10.1007/978-3-319-24780-9_11

sarcolipin), hormonal (e.g., thyroid hormone and adiponectin), and posttranslational modification (e.g., nitration, glutathionylation, SUMOylation, acetylation, glycosylation, and O-glcNAcylation) processes as they regulate SERCA2a are discussed. Additionally, exercise and its effect on the regulatory mechanisms of SERCA2a is examined.

Keywords Sarco(endo)plasmic reticulum calcium ATPase • Heart failure • Phospholamban • Sarcolipin • Thyroid hormone • Adiponectin • Posttranslational modifications • Exercise

1 Introduction

1.1 Role of Calcium in Muscular Contractions

Calcium (Ca^{2+}) is a key component of the excitation–contraction coupling (ECC) process in both cardiac and skeletal muscle. When Ca^{2+} is released from the sarcoplasmic reticulum (SR), free intracellular Ca^{2+} in the cytosol increases approximately tenfold. This facilitates Ca^{2+} binding to troponin C, which allows the tropomyosin filament to rotate and expose the myosin-actin binding site [1]. Myosin and actin are then able to interact and initiate cross bridge cycling, where adenosine triphosphate (ATP) hydrolysis moves the myosin along the actin filaments through a series of conformational changes [2]. Cross bridge cycling instigates the power stroke, resulting in muscular contraction. In cardiac muscle, the release of Ca^{2+} is initiated through Ca^{2+} induced Ca^{2+} release, a process where entry of Ca^{2+} through the L-type Ca^{2+} channel causes a further release of Ca^{2+} from the SR [1, 3].

Following contraction, Ca^{2+} must be removed from the cytoplasm to initiate myocardial relaxation. This occurs through four main transporters: the sarcolemmal Ca^{2+} ATPase, the mitochondrial Ca^{2+} uniport, the Na^{+}/Ca^{2+} exchanger, and the Sarco(endo)plasmic reticulum Ca^{2+} ATPase (SERCA) [4]. In the mammalian heart, SERCA2a is primarily responsible for removing Ca^{2+} from the cytoplasm and subsequently transporting it back into the SR [4]. The amount of SERCA2a Ca^{2+} removal varies between species. For example, SERCA2a accounts for 92 %, 75 %, and 70 % of Ca^{2+} removal in rat, rabbit, and human hearts, respectively [4, 5].

SERCA2a is a ~110-kDa transmembrane protein that is part of the P-type ATPase category. As such, it functions to actively transport Ca^{2+} across the SR membrane and into the lumen through ATP hydrolysis [6]. SERCA2a is comprised of three distinct regions: the cytoplasmic head, the transmembrane helices, and the luminal loops [7]. Together, the transmembrane helices and luminal loops create the transmembrane domain [8], while the cytoplasmic head can be

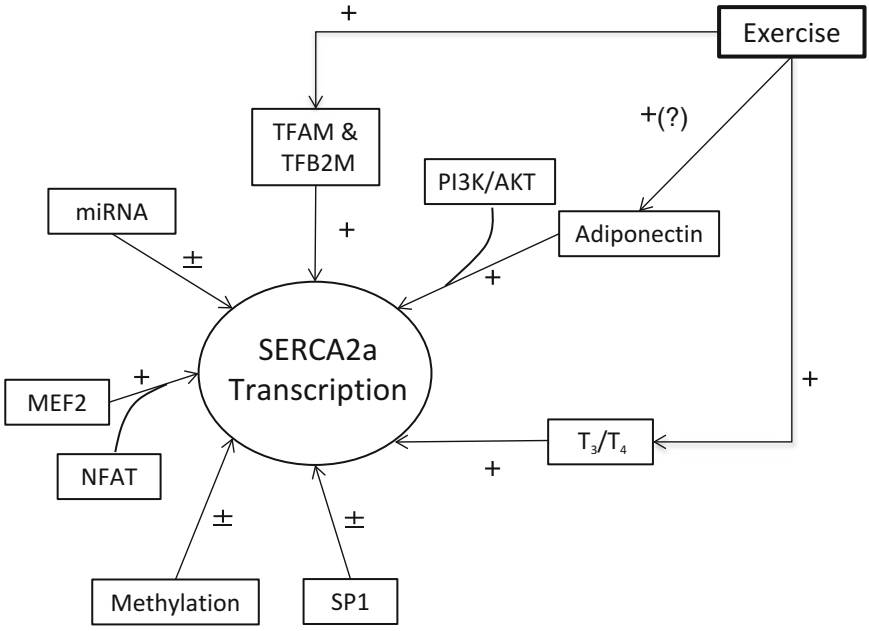

Fig. 11.1 Summary of SERCA2a transcriptional regulation. Factors affected by exercise are also noted. Abbreviations: miRNA, Micro RNA; MEF2, Myocyte enhancing factor-2; NFAT, Nuclear factor of activated T-cells; SP1, Specificity protein 1; T_3/T_4, Thyroid hormone; PI3K/Akt, Phosphatidylinositide 3-kinase/protein kinase 3 pathway; TFAM, Mitochondrial transcription factor A; TFB2M, Mitochondrial transcription factor B2

further subdivided into three different domains: the actuator domain, phosphorylation domain, and nucleotide domain. Each of these domains plays an integral role in the function of SERCA2a. The transmembrane domain contains two binding sites for Ca^{2+}, and depending on protein conformation, these binding sites can exist in a high- or low-affinity state [9]. The actuator domain, which is the smallest domain, facilitates the major conformational changes that occur as Ca^{2+} is transported into the lumen [9]. Lastly, the interface between the phosphorylation and nucleotide domains form the catalytic site where ATP hydrolysis occurs [10].

SERCA2a's major role in Ca^{2+} transport has made it of primary interest when examining cardiomyopathy. This chapter aims to discuss the regulation of SERCA2a in the heart, its role in heart failure and the mechanisms affecting SERCA2a expression and function. It also examines SERCA2a as a therapeutic target for the prevention or treatment of heart failure. Finally, we describe how exercise may affect cardiac function by regulating SERCA2a function. An overall summary of the mechanisms and pathways affecting SERCA2a can be found in Figs. 11.1 and 11.2.

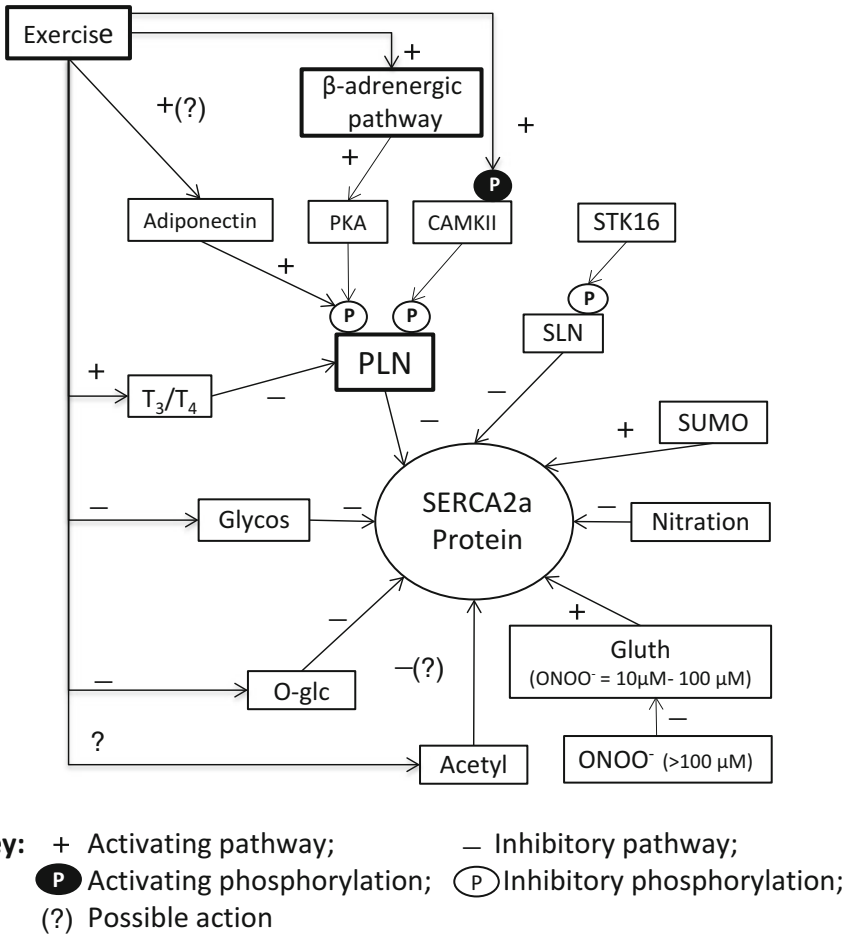

Fig. 11.2 Summary of SERCA2a protein regulation. Factors and pathways affected by exercise are also noted. Abbreviations: T_3/T_4, Thyroid hormone; PLN, Phospholamban; SLN, Sarcolipin; PKA, Protein Kinase A; CAMKII, Ca^{2+}/Calmodulin-dependent protein kinase II; STK16, Serine/threonine kinase 16; SUMO, SUMOylation; Gluth, Glutathionylation; Acetyl, Acetylation; O-glc, O-GlcNAcylation; Glycos, Glycosylation

2 Transcriptional Regulation

Multiple isoforms of SERCA have been identified, all of which are encoded by one of three SERCA genes: ATP2A1, ATP2A2, and ATP2A3. The human *ATP2A2* gene is responsible for encoding the SERCA2a-c isoforms [11], which are expressed in varying quantities throughout the body. *ATP2A2* is located on chromosomal region 12q23-q24.1 and is organized into 22 exons [12, 13]. Alternative splicing at exon 20 produces either SERCA2a or SERCA2b [12], where SERCA2a is expressed predominantly in cardiac and smooth muscle and SERCA2b is expressed in both

muscle and non-muscle cells [14]. In skeletal muscle, this process is partially mediated by a transcriptional factor known as myogenin [15]; however, little research has explored alternative splicing in cardiac muscle. SERCA2c arises from a splice variant inserted between exon 20 and exon 21 and is expressed in confined regions of the cardiomyocyte [9, 12]. The exact role of SERCA2c is yet to be fully elucidated.

Numerous factors regulate the transcription of *ATP2A2*. Two of these factors, mitochondrial transcription factors A (TFAM) and B2 (TFB2M), regulate *ATP2A2* transcription in the heart by binding to the -122 to -114 and the -122 to -117 regions, respectively [16]. Myocardial SERCA2a transcription is significantly correlated to TFAM and TFB2M expression, suggesting TFAM and TFB2M play an essential role in the regulation of SERCA2a gene transcription. In fact, overexpression of TFAM and TFB2M in rat myocardial infarction models increased SERCA2a transcriptional activity twofold and prevented stress-induced reductions of SERCA2a mRNA levels [16]. Furthermore, mutation of *ATP2A2* TFAM and TFB2M binding regions significantly reduced SERCA2 gene transcription [16]. In contrast, diabetic hearts and models of heart failure experience a reduction in TFAM levels [17, 18].

Specificity Protein 1 (SP1) is another transcription factor important to the gene regulation of SERCA2. Evidence suggests SP1 promoter sites are essential for full SERCA2a gene transcription [19, 20]. However, SP1 also mediated the decrease of SERCA2a mRNA seen in pressure overloaded hearts [21]. Therefore, SP1 is partially involved in both the basal and pressure-overloaded induced changes in SERCA2a transcriptional activity.

Myocyte enhancing factor-2 (MEF2) also mediates genetic transcription of SERCA2a. MEF2 is a common target for hypertrophic pathways. Although its exact regulation of SERCA2a is yet to be fully elucidated [22], it appears to upregulate SERCA2a transcription in models of hypertrophy [23, 24]. MEF2C works in conjunction with nuclear factor of activated T-cells (NFAT). In ischemic and dilated hearts removed from transplant patients, MEF2C and NFAT protein levels were significantly correlated [25], where ischemic heart saw a significant increase in both proteins [25]. Additionally, in a study by Vlasblom et al. [23], co-transfection of MEF2C and NFAT stimulated SERCA2a promoter sites, but only when both factors were present. This was accompanied by a 2.5-fold increase in SERCA2a mRNA [23]. In contrast to these findings, diabetic patients with heart failure had significantly decreased MEF2C and SERCA2a protein levels when compared to heart failure patients without diabetes [26]. While more research is needed in this area, MEF2C is another factor to consider when examining the transcriptional regulation of SERCA2a.

MicroRNAs (miRNAs; miR) are a class of small, noncoding mRNA molecules that regulate RNA or protein expression [27, 28]. Since various miRNA recognition sites are located within the 3′ untranslated region of SERCA2, it has been suggested miRNA may affect cardiac function through regulation of SERCA2a protein expression. However, the interaction between SERCA2a and miRNAs is complex, with 43–144 miRNAs affecting SERCA2a expression during heart failure [27–29]. Furthermore, binding sites located on 3′ UTR can bind with multiple miRNAs, and miRNAs themselves can bind with up to 10 different sites [29].

Boštjančič et al. [29] identified ten different miRNAs upregulated in infarcted hearts. Of these 10 miRNAs, miR-25 and -185 have been identified as down regulators of SERCA2a specifically [28–30]. MiR-25 is upregulated 270 % in failing hearts [28], whereas reducing miR-25 expression restored end systolic pressure volume and ejection fraction in pressure-overloaded hearts [28]. Furthermore, miR-25 suppression increased total SERCA2a and SUMOylated SERCA2a levels [28].

In comparison, miR-22 and miR-1 are associated with enhanced SERCA2a expression [27, 31]. MiR-22 knockout mice experienced prolonged Ca^{2+} cytosolic decay and a 25 % lower SR Ca^{2+} load than controls [31]. While SERCA2a protein expression was not significantly altered in healthy knockout mice, 1 week of transverse aortic constriction decreased SERCA2a protein content 2.4-fold [31]. Accompanying this decrease was 50 % greater fibrosis levels, impaired fractional shortening, and increased LV end systolic dimensions [31]. MicroRNAs and their regulation of SERCA2a are yet to be fully understood; however, this remains a promising area of research.

Recent studies have begun investigating SERCA2a methylation and the role it may play in SERCA2a expression and function. Methylation is an epigenetic modification that involves the addition of a methyl group to DNA nucleotide [32]. Murine hearts with transverse aortic constriction (TAC) experienced a significant decrease of SERCA2a [33]. This was accompanied by decreased methylation at *ATP2A2* promoter sites and increased methylation at *ATP2A2* repression sites [33]. Moreover, methylation factors were altered after TAC, with displaced demethylases and recruited methyltransferases at the *ATP2A2* promoter regions [33]. Prenatal environment can affect methylation and SERCA2a expression. For example, female mice exposed to estrogen diethylstilbestrol (DES) in utero had increased levels of DNA methylation at the calsequestrin-2 promoter after swim training [34]. Subsequently, SERCA2a and calsequestrin-2 protein expression increased, and cardiac hypertrophy was prevented in mice treated with DES [34].

3 Regulation of SERCA2a in Models of Disease

SERCA2a is a key factor in regulating cardiac contractility and relaxation. As such, there is a substantial amount of research examining SERCA2a in both animal and human heart models. Defective SERCA2a functioning via reduced mRNA, protein expression or activity levels leads to abnormal Ca^{2+} handling, reduced SR Ca^{2+} uptake and inefficient energy use [11, 35–37]. These traits are commonly characterized in patients with heart failure and eventually lead to impaired systolic and diastolic function of the heart [11, 37, 38]. In fact, a review of the literature reported significant decreases in SERCA2a mRNA and protein levels in various animal models of heart failure [39]. Moreover, failing human myocardium experienced up to a 60 % decrease in SERCA2a mRNA [39]. Decreases in SERCA2a expression in heart failure is accompanied by diminished activity levels. Arai et al. [35] reported a 50 % reduction in Ca^{2+} reuptake in right ventricular tissue removed from failing

human hearts. However, this effect may be partially mediated by increases in circulating levels of myocardial C-type natriuretic peptide, a molecule known to increase in heart failure [40].

Diabetic hearts also experience a decrease in SERCA2a expression an activity. In diabetic sedentary mice, SERCA2a protein content and maximal SERCA2a activity was decreased by 21 % and 32 %, respectively [41]. This was accompanied by impaired diastolic function [41]. Vasanji et al. [42] reported a decrease in SERCA2a protein content and activity in diabetic hearts, but also noted a significant increase in phospholamban (see Sect. 4 for more details on phospholamban) to SERCA2a protein ratio levels. The underlying mechanisms linking diabetes to SERCA2a activity are not yet fully understood; however it may be partially mediated by reduced enzymatic activity of silent information regulation (SIRT) 1 [43].

Given its integral role in cardiac function, SERCA2a presents a promising target for cardiac treatment. In mice with established diabetic cardiomyopathy, conditional expression of SERCA2a restored cardiac function [44]. Furthermore, activation of SIRT1 in diabetic heart models increased SERCA2a protein and mRNA levels to near control values [43]. In turn, functional parameters of the heart were significantly improved [43]. Transgenic mice overexpressing SERCA1a in the heart demonstrated a 170 %, 50 %, and 66 % increase in maximum Ca^{2+} uptake velocity, peak rate of myocyte shortening, and relengthening, respectively [45]. However, Kalyanasundaram et al. [46] cautioned against using SERCA1a therapy as a heart failure treatment, reporting increased apoptosis, dilated cardiomyopathy, and early mortality in calsequestrin deficient mice over expressing SERCA1a in the heart.

SERCA2a therapy in human models of heart failure has also been well received. Overexpression of SERCA2a by adenoviral gene transfer in human ventricle cardiomyocytes increased SERCA2a protein number and activity, induced a faster contraction velocity, and enhanced relaxation [47]. Likewise, the CUPID trial found that patients with advanced heart failure experienced up to an 88 % risk reduction in adverse event occurrence, such as LV assistive device implant, heart transplant and death, 12 months after receiving an intracoronary infusion of SERCA2a [48]. A 3-year follow-up found those who receive high-dose infusions still had an 82 % risk reduction for recurrent cardiovascular events [49]. Thus, SERCA2a gene therapy for the treatment of the diseased human heart appears to be beneficial.

4 Protein Regulation of SERCA2a

Phospholamban (PLN) is a 52 amino acid protein that has been well established as an inhibitor of SERCA2a activity [50]. PLN binds to SERCA2a and decreases its affinity for Ca^{2+} [51]. This binding occurs when cytosolic Ca^{2+} levels are low and PLN is in a dephosphorylated state. In contrast, phosphorylation of PLN prevents PLN from binding to SERCA2a, allowing SERCA2a to remain active [51]. This occurs through two different mechanisms: Ca^{2+}/Calmodulin kinase (CAMKII) phosphorylation and protein kinase A (PKA) phosphorylation [50, 52]. CAMKII is

a serine/threonine protein kinase that is activated by an increase in cytosolic Ca^{2+} and phosphorylates PLN at the Threonine[17] residue [50]. Similarly, PKA phosphorylates PLN at the Serine[16] residue [5, 52]; however, PKA phosphorylation is governed through β-adrenergic stimulation. When β-Agonists bind to receptors, a signal transduction pathway is activated that increases production of cyclic AMP (cAMP) via adenylate cyclase [5, 52]. This ultimately activates PKA, which phosphorylates PLN [5, 52]. Phosphorylation of PLN through either of these mechanisms can increase SERCA2a activity up to threefold, increasing relaxation velocity and contributing to the positive inotropic and lusitropic effects of β-adrenergic stimulation [5, 53].

Due to its major role in SERCA2a regulation, PLN expression is closely related to SERCA2a activity. In fact, when compared to wild-type littermates, PLN knockout mice experienced significantly greater contraction and relaxation rates, accompanied by an increase in SERCA2a affinity for Ca^{2+} [54]. PLN expression varies in quantity throughout the body's tissues. For example, in the murine heart, PLN is expressed threefold higher in right ventricle tissues compared to right atrial tissues [53]. Consequently, the relative ratio of PLN:SERCA2a is 4.2-fold lower in the atrium and is associated with significantly shortened relaxation and contraction times [53]. Similar findings have been found in the human heart. PLN protein expression is 44 % lower in the right atrium, and time to peak tension, time to relax and total contraction time are significantly decreased when compared to right ventricle tissues [55]. These data suggest that PLN expression, along with phosphorylation, plays a large role in cardiac function though regulation of SERCA2a activity in the heart.

In diseased states, both PLNcontent and phosphorylation in the heart are altered. As mentioned previously, PLN:SERCA2a ratio is increased in diabetic hearts [42]. Furthermore, PLN phosphorylation by both CAMKII and PKA is significantly decreased [42]. In ischemic and ischemia-reperfused hearts, CAMKII PLN phosphorylation is reduced, whereas PKA PLN phosphorylation is diminished in ischemia-reperfused hearts only [56]. Reduced PLN phosphorylation in heart failure may be partially due to lower levels of taurine, a beta-amino acid found in high concentrations in the heart [57].

Sarcolipin (SLN) is a homologue to PLN with high amino acid conservation in the transmembrane domain [58, 59]. Because of this, SLN and PLN likely interact with SERCA2a in a similar manner, although the precise regulatory mechanisms of SLN are not yet fully elucidated. SLN is a 31 amino acid protein and is thought to induce its inhibitory effect by binding directly to SERCA2a and reducing its affinity for Ca^{2+} [51, 60]. However, a study suggests SLN acts by reducing the V_{max} of SECA2a Ca^{2+} uptake, and unlike PLN, it can interact with SERCA2a in the presence of high Ca^{2+} concentrations [61]. SLN also functions by interacting with PLN to create a super-inhibition of SERCA2a [58, 62]. SLN forms a complex with PLN that destabilizes PLN pentamers [50]. This promotes the formation of PLN monomers, the inhibitory form of PLN [50]. Thus, by enhancing the effects of PLN, SLN acts to further reduce SERCA2a activity.

Babu et al. [60] demonstrated SLN's effect by over expressing SLN in rat myocytes through adenoviral gene transfer. These myocytes experienced a 31 % reduction in cell shortening compared to control myocytes [60]. SLN's effect can be relieved through phosphorylation. SLN is phosphorylated by serine/threonine kinase 16 (STK 16) at Threonine^{5}, which promotes dissociation of SLN from SERCA2a and subsequently increases SERCA2a activity [63]. This contributes to the relaxant effect of β-adrenergic stimulation [63]. SLN mRNA is mainly expressed in the atrial tissues of the heart [60]. In fact, Babu et al. [60] found SLN mRNA below detectable levels rat heart ventricle tissues. Similar results have been found in humans, with SLN mRNA being expressed only atrial tissues of the heart [64]. Given the different expression of SLN and PLN in cardiac muscle, it is thought that SLN is responsible for mediating SERCA2a activity where PLN is absent. SLN expression is deregulated in conditions of disease, where SLN mRNA and protein levels can be increased up to 12- and 6-fold, respectively in ventricle tissues [65]. Beyond SLN's role in Ca^{2+} regulation, it is also involved in thermoregulation by promoting SERCA2a uncoupling in skeletal muscle [65]. This interaction is unique to SLN [61].

5 Hormonal Regulation of SERCA2a

Thyroid hormone can be found in two different forms in the body: levothyroxine (T_4) and triiodothyronine (T_3), where T_3 is the active form and T_4 is a prohormone that is converted into T_3 or reverse T_3 [66]. While intracellular T_3 is about 20 times more potent than T_4 [66], administration of both forms has been well documented to affect the expression and activity of SERCA2a [67–71]. This effect occurs through positive regulation of SERCA2a gene transcription [72]. Various animal models have demonstrated thyroid hormone's impact on SERCA2a. For example, hypothyroid conditions imposed on rat and rabbit cardiomyocytes decreased SERCA2a mRNA content to 36–72 % of control levels, whereas hyperthyroid conditions increased SERCA2a mRNA up to 167 % of control levels [68, 70, 71, 73]. Furthermore, administration of T_3 to hypothyroid rat hearts significantly increased SERCA2a mRNA levels 2 h after injection, and normalized it 5 h after injection [71]. Similar results have been found with SERCA2a protein levels, with hypothyroid conditions decreasing protein content 11 %–26 % [69, 73], and hyperthyroid conditions increasing content 34 %–88 % [67, 69].

In addition to its direct regulation of SERCA2a, thyroid hormone further affects SERCA2a activity by regulation of PLN. Thyroid hormone affects PLN in an opposite manner to SERCA2a, where a decrease of T_3 or T_4 upregulates PLN, and an increase downregulates PLN. Reed et al. [73] demonstrates this in mice hearts, where hypothyroidism increased PLN mRNA and protein levels 28 % and 20 %, respectively and hyperthyroidism decreased PLN mRNA and protein levels 13 % and 30 %, respectively. Similar findings have been reported with rat and rabbit hearts. Hyperthyroid conditions induced up to a 50 % decrease in PLN mRNA and

a 25 % decrease in protein levels [68–70]. On the other hand, hypothyroid conditions increased PLN protein content 35 % in rat cardiomyocytes [69].

Coinciding to the changes in SERCA2a and PLN expression, thyroid hormone also induces a change in cardiac function. Chang et al. [67] found administering T_4 to rats with aortic banding eliminated abnormal myocardial functioning and increased contractility, relaxation speed, and cytosolic Ca^{2+} removal when compared to controls. Additionally, both rabbit and rat hyperthyroid hearts have greater Ca^{2+} maximal uptake than euthyroid hearts [68, 69]. A review by Novitzky and Cooper [66] presents thyroid hormone as a possible treatment for patients with "stunned myocardium," a condition where myocardial function is depressed due to global or regional ischemic events. These data demonstrate that through regulation of SERCA2a and PLN, thyroid hormone presents a possible means of reversing cardiac dysfunction and inhibiting cellular damage caused by ineffective Ca^{2+} cycling.

Another hormone responsible for the regulation of SERCA2a is adiponectin. Adiponectin is an adipocyte-derived peptide hormone that is inversely related to traditional cardiovascular risk factors, such as blood pressure, heart rate, and cholesterol and triglyceride levels [74, 75]. It also possesses antioxidant and anti inflammatory qualities [75, 76]. These cardioprotective properties are thought to occur through the modulation of SERCA2a activity [74]. Adiponectin appears to affect SERCA2a through PLN phosphorylation and the PI3K/Akt signaling pathway [74]. In a study by Safwat et al. [74], administration of globular adiponectin significantly restored SERCA2a activity in rats with induced ischemia/reperfusion injury. Additionally, the p-PLN/PLN ratio was significantly increased, suggesting PLN phosphorylation may be the mechanism adiponectin uses to increase SERCA2a activity [74]. Accompanying the increase in SERCA2a activity and PLN phosphorylation was a 139 % increase ($p < 0.05$) in p-Akt/Akt ratio [74]. Adiponectin induced benefits to cardiac function were abolished with administration of LY294002, an inhibitor of PI3K, confirming that PI3K/Akt pathway activation is essential for globular adiponectin to exert its effect on SERCA2a [74].

Other studies examining adiponectinand SERCA2a activity have shown similar results to Safwat et al. [74]. Adiponectin gene therapy significantly increased SERCA expression in skeletal muscle of diabetic rats [77]. This restoration was furthered by a 9 week swimming exercise protocol [77]. Additionally, treatment of H9C2 cardiomyoblasts in an adiponectin-enriched medium significantly increased SERCA2a expression and decreased in inflammatory markers compared to cardiomyoblasts in an adiponectin depleted culture [78]. In contrast, induction of ER stress through tunicamycin treatment reduced SERCA2a expression, adiponectin, and adiponectin receptor 1 by as much as 50 % [78].

6 Posttranslational Modification Regulation of SERCA2a

Various posttranslational modifications have been found to affect the activity of SERCA2a. Some of these modifications are currently being researched, and as such, the process and effects of these modifications are yet to be fully elucidated.

This section will examine current knowledge of nitration, glutathionylation, SUMOylation, acetylation, glycosylation and O-glcNAcylation and their role in SERCA2a function.

Nitration is a chemical process where a nitro group is added to a protein. Nitration inhibits SERCA2a activity through the polyol pathway, a pathway that contributes to oxidative stress in hyperglycemic conditions [79, 80]. In fact, levels of nitrotyrosine on SERCA2a were significantly increased in high-glucose perfused rat hearts compared to hearts perfused with normal glucose levels [80]. Studies on the human heart found nitrotyrosine levels to be nearly doubled in idiopathic dilated cardiomyopathic hearts compared to age matched controls [79]. This was accompanied by a significant positive correlation between time to half relaxation and nitrotyrosine to SERCA2a ratio [79]. This suggests SERCA2a nitration can substantially affect cardiac function [79]. However, nitration's exact role in normal regulation of SERCA2a is yet to be defined.

Glutathionylation is the process where a disulfide bond is formed between the cysteine of a protein and glutathione (GSH) [81]. In SERCA2a, glutathionylation occurs predominately on cysteine^{674} [82–84] and subsequently increases SERCA2a activity and Ca^{2+} uptake [82, 84, 85]. It is well documented that nitric oxide (NO) causes muscle relaxation through cGMP and protein kinase G. However, NO appears to induce relaxation by increasing SERCA2a glutathionylation as well [86]. Exposure to low amounts of oxidative species including NO, Perioxynitrate ($ONOO^-$) and nitroxyl can increase SERCA2a activity 45–60 % in cardiac muscle cells [83–86]. However, it should be noted that NO cannot act alone, and must be combined with the superoxide radical to form $ONOO^-$ before it can react with cytosolic GSH and glutathionylate cys^{674} [82].

While low amounts (10–100 μM) of oxidative species increases SERCA2 activity, transgenic mice exposed to high amounts (>100 μM) experienced a decrease SERCA2 activity [82]. Glutathiolyation can normally be reversed either chemically or enzymatically, but in cases such as atherosclerosis where there is a chronic increase in oxidative species, cys ^{674} is irreversibly oxidized to sulfonylation [82, 84–86]. Consequently, further glutathiolation and activation of SERCA2a is prevented [82, 84]. This causes a subsequent decrease in SERCA2a activity, which can lead to heart failure. Substances known to reverse glutathiolation, such as dithiothreitol, can help prevent SERCA2 inactivation, but are unable to reverse oxidation once it has occurred [85, 86].

SUMOylation and its effect on SERCA2a is a promising area of research when examining SERCA2a protein stability and function. SUMOylation occurs through the binding of small ubiquitin-like modifier 1 (SUMO1) to the lysine ^{480} and lysine^{585} residues of SERCA2a [87, 88]. This modification is thought to have cardioprotective properties [87, 88]. In heart failure, there is a 30 %–40 % decrease in SUMO1, which is accompanied by a decrease in total SERCA2a SUMOylation [87]. Moreover, downregulation of SUMO1 using small hairpin RNA reduced SERCA2a protein levels by 40 % [87]. This is likely due to lower levels of SERCA2a SUMOylation reducing SERCA2a half life from 5.9 to 4.9 days [87]. SUMOylation proved to be a potential therapeutic means when injection of SUMO1 to pressure

overloaded hearts significantly improved cardiac performance and restored SERCA2a function and mRNA expression to almost normal levels [87, 88]. The mechanisms SUMOylation uses to rescue SERCA2a function are yet to be fully elucidated. However, it is thought that SUMOylation competes with other posttranslational modifications, such as ubiquitination or acetylation, to increase SERCA2a's stability and prevent degradation [87]. SERCA2a SUMOylation also appears to increase SERCA2a ATPase activity by increasing its sensitivity to ATP [87].

Acetylation/deacetylation involves the attachment, or removal, of an acetyl group from a molecule. Its precise role in SERCA2a regulation has yet to be examined, although it may regulate SERCA2a in a manner opposite to SUMOylation [89]. Three potential acetylation sites were identified within the nucleotide-binding domain of SERCA2a: lysine^{464}, lysine^{510}, and lysine^{533} [90]. Therefore, acetylation/deacetylation could play a role in cardiac muscle Ca^{2+} cycling [90]. Kho et al. [87] reported increased SERCA2a acetylation in failing hearts, which could be reversed with sirtuin-1 deacetylase, but no data was given to validate this statement. Although current evidence is limited, acetylation/deacetylation is a potential regulator of SERCA2a activity.

Glycosylation occurs when a saccharide is attached to a protein. This can be done enzymatically or nonenzymatically, where the nonenzymatic reaction is better known as glycation. An increase in glycosylation has been associated with a 25–45 % decrease in SERCA2a mRNA and protein levels [91, 92] and a 40 % increase in PLN levels [92]. This combination results in an overall decrease in SERCA2a activity, reducing Ca^{2+} transport into the SR. Since elevated levels of glucose appears to increase SERCA2a glycosylation, this area remains of particular interest when examining the relationship between diabetes and heart disease [91, 92].

O-glcNAcylation is a specific form of glycosylation where a single O-linked *N*-acetylglucosamine is either added or removed from a serine or threonine residue [91, 93, 94]. O-glcNAcylation reduces SERCA2a activity through direct regulation SERCA2a and modification of PLN [91, 93, 95]. High-glucose treated rat cardiomyocytes had substantially increased levels of nuclear O-glcNAclyation, accompanied by a 28–37 % and 25 % reduction in SERCA2a mRNA and protein expression, respectively [91]. Additionally, cardiomyocytes injected with an O-glcNAc-transferase had a 47 % decrease in SERCA2a expression when compared to controls [91]. In contrast, reducing cellular O-glcNAcylation through an adenovirus expressing O-glcNAcase increased SERCA2a protein expression 40 %, reduced PLN protein 50 %, and increased PLN phosphorylation twofold [94]. SERCA2a O-glcNAcylation may be partially mediated by SP1, as SP1 is known to be heavily O-glcNAcylated and is directly involved in the transcription of SERCA2a [20, 96].

7 Regulation of SERCA2a in Models of Exercise

It has been well documented that exercise increases cardiac function through enhanced SERCA2a Ca^{2+} uptake, especially in models of cardiovascular disease [97]. This can occur as a result of direct regulation of SERCA2a transcription and

activity, or through modifications of the regulatory processes discussed earlier in this chapter. Here, we examine the various processes by which exercise regulates SERCA2a.

Aerobic exercise in hypertensive rats significantly increased cell contractility and Ca^{2+} transport [97]. These changes were partially due to increased PLN phosphorylation and SERCA2a mRNA expression [97]. Similar results were demonstrated in mice with induced heart failure. Aerobic interval training improved atrial myocyte shortening by 89 % and restored SERCA2a function to near control levels [98]. Additionally, genetic mouse models of sympathetic hyperactivity-induced heart failure experienced greater peak Ca^{2+} transient levels and reduced diastolic Ca^{2+} decay time after 8 weeks of aerobic training [99]. These results were enhanced with administration of carvidilol, a beta-blocker used to treat heart failure [99]. Similar benefits have been demonstrated in diabetic models as well. For example, voluntary wheel running in diabetic mice attenuated the decrease in diastolic function and SERCA2a content and activity [41]. Even when disease is absent, cardiac function increases in response to exercise. Kemi et al. [100] reported a 60 % and 50 % increase in fractional myocyte shortening and Ca^{2+} transient amplitude, respectively, in aerobic interval trained mice. With these adaptations was a 25 % increase in SERCA2a protein content [100]. Wisløff et al. [101] report comparable findings in exercise trained mice, where SERCA2a protein content increased 82 % and Ca^{2+} cycling and sensitivity was significantly increased compared to sedentary mice. The effects of exercise training on SERCA2a require a stimulus to be maintained. For example, Carneiro-Júnior et al. [97] noted cardiac adaptations to exercise were reversed to control levels after 4 weeks of detraining. Despite these data, some studies have reported that exercise training in aging models was not able to change age related degradations to SERCA2a and cardiac function [102].

Exercise may partially mediate its effect of SERCA2a through regulation of TFAM and TFB2M [16]. Aerobic fitness is positively correlated with mitochondrial biogenesis [103], and thus, requires an increase in mitochondrial transcription factors such as TFAM and TFB2M. TFAM protein expression was significantly higher in elite athletes compared to moderately active individuals [103], and in male participants, TFB2M mRNA levels nearly doubled after 10 days of exercise training with restricted blood flow [103]. Moreover, exercise training in hyperglycemic mice restored TFAM protein to control levels [104]. Therefore, it is likely exercise affects SERCA2a transcription through regulation of TFAM and TFB2M.

Exercise also affects SERCA2a activity by regulating PLN phosphorylation [105]. In aged, ovariectomized rats, exercise training reversed reduced PLN phosphorylation at $Threonine^{17}$ and normalized SERCA2a activity [105]. Furthermore, aerobic exercise in hypertensive rats significantly increased PLN phosphorylation at both $Serine^{16}$ and $Threonine^{17}$ [106]. This contributed to an improved inotropic and lusitropic response to β-adrenergic stimulation [106]. Exercise's effect on PLN phosphorylation may be partially mediated through CaMKII phosphorylation [100]. Aerobic interval training increases CaMKII $Threonine^{287}$ phosphorylation, indicating activation [100]; this would contribute to the increase in PLN^{Thr17} phosphorylation observed [100]. Accompanying the

increase in PLN phosphorylation, exercise reduces PLN:SERCA2a expression ratios, further enhancing SERCA2a activity [100].

Exercise has varying effects on circulating thyroid hormone, where intense exercise reduces free T_3 (fT_3) and T_3 and increases T_4, free T_4 (fT_4), and thyroid stimulating hormone [107–109]. These changes are acute and most likely due to suppression of T_4 to T_3 conversion [108]; given proper recovery, thyroid hormone levels are restored within 72 h [108]. In contrast, chronic exercise is associated with a significant increase in thyroid hormone levels. Four weeks of treadmill training increased T_3 and T_4 in hypothyroid rats to near control levels [110]. This would suggest a subsequent upregulation of SERCA2a. In fact, 4 weeks of wheel running in adult male rats significantly increased thyroid hormone receptor β1 mRNA nearly twofold, which would augment transcription of downstream thyroid hormone target genes, such as SERCA2a [111]. As such, it is likely exercise partially mediates SERCA2a expression through thyroid hormone regulation.

More research is needed to fully understand how adiponectin responds to exercise; however, studies suggest physical activity increases adiponectin levels. Cross-sectional studies report positive correlations between physical activity levels and adiponectin [112, 113], and intervention studies produce similar results. For example, obese individuals randomized to a controlled physical activity-behavior-diet-based lifestyle intervention for 3 months experienced a 34 % increase in adiponectin concentration [114]. Nevertheless, not all studies agree with these results. In a systematic review by Simpson & Singh [115], less than half the studies on chronic exercise and adiponectin reported significant results. While this does not mean exercise does not regulate adiponectin, more rigorous and long-term studies are needed.

Researchers examining exercise and posttranslational modifications have mainly focused on O-glcNAcylation. Six weeks of exercise training in mice decreased O-glcNAcylation 40–75 %, which was paired with a 30 % increase in SERCA mRNA [93, 96]. Moreover, mice trained at a high running capacity had a significantly lower O-glcNAcylated SERCA2a to total SERCA2a ratio than mice trained at a low running capacity [116]. Swim-trained mice experienced a reduction in O-glcNAcylated SP1, suggesting SP1 may be involved in exercise regulation of SERCA2a [96]. It is possible physical activity reduces O-glcNAcylation through regulation of glucose levels, as O-glcNAcylation increases in the presence of glucose [91]. Research on exercise's effect of other posttranslational modifications if needed to further understand how exercise regulates SERCA2a.

8 Conclusion

Regulation of SERCA2a is governed by numerous factors, such as gene transcription, posttranslational modifications, and endogenous proteins. Given its critical role in heart function and failure, an abundance of research has focused on SERCA2a'a function, regulation, and how it can be used as a therapeutic target. Some of these areas, such as SUMOylation, acetylation, and microRNAs, have yet

to be fully elucidated. Exercise has also presented itself as a possible means of effective therapy, although more research is needed on the exact mechanisms here as well. Overall, SERCA2a remains a promising target to maintain and restore heart function and enhance longevity and quality of life.

References

1. Bers DM (2002) Cardiac excitation-contraction coupling. Nature 415:198–205
2. Lodish H, Berk A, Zipursky SL et al (2000) Molecular cell biology, 4th edn. W. H Freeman, San Francisco, CA
3. Fabiato A (1983) Calcium-induced release of calcium from the cardiac sarcoplasmic reticulum. Am J Physiol 245:C1–C14
4. Bers DM (1997) Ca transport during contraction and relaxation in mammalian ventricular muscle. Basic Res Cardiol 92(Suppl 1):1–10
5. MacLennan DH, Kranias EG (2003) Phospholamban: a crucial regulator of cardiac contractility. Nat Rev Mol Cell Biol 4:566–577
6. Tran K, Smith NP, Loiselle DS, Crampin EJ (2009) A thermodynamic model of the cardiac sarcoplasmic/endoplasmic Ca(2+) (SERCA) pump. Biophys J 96:2029–2042
7. Martonosi AN, Pikula S (2003) The structure of the Ca2+-ATPase of sarcoplasmic reticulum. Acta Biochim Pol 50:337–365
8. Sacchetto R, Bertipaglia I, Giannetti S et al (2012) Crystal structure of sarcoplasmic reticulum Ca2+-ATPase (SERCA) from bovine muscle. J Struct Biol 178:38–44
9. Wuytack F, Raeymaekers L, Missiaen L (2002) Molecular physiology of the SERCA and SPCA pumps. Cell Calcium 32:279–305
10. Toyoshima C, Inesi G (2004) Structural basis of ion pumping by Ca2+-ATPase of the sarcoplasmic reticulum. Annu Rev Biochem 73:269–292
11. Kawase Y, Hajjar RJ (2008) The cardiac sarcoplasmic/endoplasmic reticulum calcium ATPase: a potent target for cardiovascular diseases. Nat Clin Pract Cardiovasc Med 5:554–565
12. Gélébart P, Martin V, Enouf J, Papp B (2003) Identification of a new SERCA2 splice variant regulated during monocytic differentiation. Biochem Biophys Res Commun 303:676–684
13. Otsu K, Fujii J, Periasamy M et al (1993) Chromosome mapping of five human cardiac and skeletal muscle sarcoplasmic reticulum protein genes. Genomics 17:507–509
14. Loukianov E, Ji Y, Baker DL et al (1998) Sarco(endo)plasmic reticulum Ca2+ ATPase isoforms and their role in muscle physiology and pathology. Ann N Y Acad Sci 853:251–259
15. Van den Bosch L, Eggermont J, De Smedt H et al (1994) Regulation of splicing is responsible for the expression of the muscle-specific 2a isoform of the sarco/endoplasmic-reticulum Ca(2+)-ATPase. Biochem J 302(Pt 2):559–566
16. Watanabe A, Arai M, Koitabashi N et al (2011) Mitochondrial transcription factors TFAM and TFB2M regulate Serca2 gene transcription. Cardiovasc Res 90:57–67
17. Choi YS, Kim S, Pak YK (2001) Mitochondrial transcription factor A (mtTFA) and diabetes. Diabetes Res Clin Pract 54(Suppl 2):S3–S9
18. Ikeuchi M, Matsusaka H, Kang D et al (2005) Overexpression of mitochondrial transcription factor a ameliorates mitochondrial deficiencies and cardiac failure after myocardial infarction. Circulation 112:683–690
19. Baker DL, Dave V, Reed T, Periasamy M (1996) Multiple Sp1 binding sites in the cardiac/slow twitch muscle sarcoplasmic reticulum Ca-ATPase gene promoter Are required for expression in Sol8 muscle cells. J Biol Chem 271:5921–5928
20. Flesch M (2001) On the trail of cardiac specific transcription factors. Cardiovasc Res 50:3–6

21. Takizawa T, Arai M, Tomaru K et al (2003) Transcription factor Sp1 regulates SERCA2 gene expression in pressure-overloaded hearts: a study using in vivo direct gene transfer into living myocardium. J Mol Cell Cardiol 35:777–783
22. Zarain-Herzberg A, Fragoso-Medina J, Estrada-Avilés R (2011) Calcium-regulated transcriptional pathways in the normal and pathologic heart. IUBMB Life 63:847–855
23. Vlasblom R, Muller A, Musters RJP et al (2004) Contractile arrest reveals calcium-dependent stimulation of SERCA2a mRNA expression in cultured ventricular cardiomyocytes. Cardiovasc Res 63:537–544
24. Zhang Z-Y, Liu X-H, Hu W-C et al (2010) The calcineurin-myocyte enhancer factor 2c pathway mediates cardiac hypertrophy induced by endoplasmic reticulum stress in neonatal rat cardiomyocytes. Am J Physiol Heart Circ Physiol 298:H1499–H1509
25. Cortés R, Rivera M, Roselló-Lletí E et al (2012) Differences in MEF2 and NFAT transcriptional pathways according to human heart failure aetiology. PLoS One 7, e30915
26. Razeghi P, Young ME, Cockrill TC et al (2002) Downregulation of myocardial myocyte enhancer factor 2C and myocyte enhancer factor 2C-regulated gene expression in diabetic patients with nonischemic heart failure. Circulation 106:407–411
27. Kumarswamy R, Lyon AR, Volkmann I et al (2012) SERCA2a gene therapy restores microRNA-1 expression in heart failure via an Akt/FoxO3A-dependent pathway. Eur Heart J 33:1067–1075
28. Wahlquist C, Jeong D, Rojas-Muñoz A et al (2014) Inhibition of miR-25 improves cardiac contractility in the failing heart. Nature 508:531–535
29. Boštjančič E, Zidar N, Glavač D (2012) MicroRNAs and cardiac sarcoplasmic reticulum calcium ATPase-2 in human myocardial infarction: expression and bioinformatic analysis. BMC Genomics 13:552
30. Earls LR, Fricke RG, Yu J et al (2012) Age-dependent microRNA control of synaptic plasticity in 22q11 deletion syndrome and schizophrenia. J Neurosci Off J Soc Neurosci 32:14132–14144
31. Gurha P, Abreu-Goodger C, Wang T et al (2012) Targeted deletion of microRNA-22 promotes stress-induced cardiac dilation and contractile dysfunction. Circulation 125:2751–2761
32. Handy DE, Castro R, Loscalzo J (2011) Epigenetic modifications: basic mechanisms and role in cardiovascular disease. Circulation 123:2145–2156
33. Angrisano T, Schiattarella GG, Keller S et al (2014) Epigenetic switch at atp2a2 and myh7 gene promoters in pressure overload-induced heart failure. PLoS One 9, e106024
34. Haddad R, Kasneci A, Sebag IA, Chalifour LE (2013) Cardiac structure/function, protein expression, and DNA methylation are changed in adult female mice exposed to diethylstilbestrol in utero. Can J Physiol Pharmacol 91:741–749
35. Arai M, Alpert NR, MacLennan DH et al (1993) Alterations in sarcoplasmic reticulum gene expression in human heart failure. A possible mechanism for alterations in systolic and diastolic properties of the failing myocardium. Circ Res 72:463–469
36. Mercadier JJ, Lompré AM, Duc P et al (1990) Altered sarcoplasmic reticulum Ca2(+)-ATPase gene expression in the human ventricle during end-stage heart failure. J Clin Invest 85:305–309
37. Park WJ, Oh JG (2013) SERCA2a: a prime target for modulation of cardiac contractility during heart failure. BMB Rep 46:237–243
38. Aronson D, Krum H (2012) Novel therapies in acute and chronic heart failure. Pharmacol Ther 135:1–17
39. Hasenfuss G (1998) Alterations of calcium-regulatory proteins in heart failure. Cardiovasc Res 37:279–289
40. Moltzau LR, Aronsen JM, Meier S et al (2013) SERCA2 activity is involved in the CNP-mediated functional responses in failing rat myocardium. Br J Pharmacol 170:366–379
41. Epp RA, Susser SE, Morissette MP et al (2013) Exercise training prevents the development of cardiac dysfunction in the low-dose streptozotocin diabetic rats fed a high-fat diet. Can J Physiol Pharmacol 91:80–89

42. Vasanji Z, Dhalla NS, Netticadan T (2004) Increased inhibition of SERCA2 by phospholamban in the type I diabetic heart. Mol Cell Biochem 261:245–249
43. Sulaiman M, Matta MJ, Sunderesan NR et al (2010) Resveratrol, an activator of SIRT1, upregulates sarcoplasmic calcium ATPase and improves cardiac function in diabetic cardiomyopathy. Am J Physiol Heart Circ Physiol 298:H833–H843
44. Suarez J, Scott B, Dillmann WH (2008) Conditional increase in SERCA2a protein is able to reverse contractile dysfunction and abnormal calcium flux in established diabetic cardiomyopathy. Am J Physiol Regul Integr Comp Physiol 295:R1439–R1445
45. Loukianov E, Ji Y, Grupp IL et al (1998) Enhanced myocardial contractility and increased Ca2+ transport function in transgenic hearts expressing the fast-twitch skeletal muscle sarcoplasmic reticulum Ca2+-ATPase. Circ Res 83:889–897
46. Kalyanasundaram A, Lacombe VA, Belevych AE et al (2013) Up-regulation of sarcoplasmic reticulum Ca(2+) uptake leads to cardiac hypertrophy, contractile dysfunction and early mortality in mice deficient in CASQ2. Cardiovasc Res 98:297–306
47. del Monte F, Harding SE, Schmidt U et al (1999) Restoration of contractile function in isolated cardiomyocytes from failing human hearts by gene transfer of SERCA2a. Circulation 100:2308–2311
48. Jessup M, Greenberg B, Mancini D et al (2011) Calcium upregulation by percutaneous administration of gene therapy in cardiac disease (CUPID) a phase 2 trial of intracoronary gene therapy of sarcoplasmic reticulum Ca2+-ATPase in patients with advanced heart failure. Circulation 124:304–313
49. Zsebo K, Yaroshinsky A, Rudy JJ et al (2014) Long-term effects of AAV1/SERCA2a gene transfer in patients with severe heart failure: analysis of recurrent cardiovascular events and mortality. Circ Res 114:101–108
50. Bhupathy P, Babu GJ, Periasamy M (2007) Sarcolipin and phospholamban as regulators of cardiac sarcoplasmic reticulum Ca2+ ATPase. J Mol Cell Cardiol 42:903–911
51. Periasamy M, Bhupathy P, Babu GJ (2008) Regulation of sarcoplasmic reticulum Ca2+ ATPase pump expression and its relevance to cardiac muscle physiology and pathology. Cardiovasc Res 77:265–273
52. Levitzki A (1988) From epinephrine to cyclic AMP. Science 241:800–806
53. Koss KL, Ponniah S, Jones WK et al (1995) Differential phospholamban gene expression in murine cardiac compartments. Molecular and physiological analyses. Circ Res 77:342–353
54. Luo W, Grupp IL, Harrer J et al (1994) Targeted ablation of the phospholamban gene is associated with markedly enhanced myocardial contractility and loss of beta-agonist stimulation. Circ Res 75:401–409
55. Bokník P, Unkel C, Kirchhefer U et al (1999) Regional expression of phospholamban in the human heart. Cardiovasc Res 43:67–76
56. Netticadan T, Temsah R, Osada M, Dhalla NS (1999) Status of Ca2+/calmodulin protein kinase phosphorylation of cardiac SR proteins in ischemia-reperfusion. Am J Physiol 277:C384–C391
57. Ramila KC, Jong CJ, Pastukh VM et al (2015) Role of protein phosphorylation in excitation-contraction coupling in taurine deficient hearts. Am J Physiol Heart Circ Physiol 308(3):H232–H239, ajpheart.00497.2014
58. Asahi M, Kurzydlowski K, Tada M, MacLennan DH (2002) Sarcolipin inhibits polymerization of phospholamban to induce superinhibition of sarco(endo)plasmic reticulum Ca2+-ATPases (SERCAs). J Biol Chem 277:26725–26728
59. Asahi M, Sugita Y, Kurzydlowski K et al (2003) Sarcolipin regulates sarco(endo)plasmic reticulum Ca2+-ATPase (SERCA) by binding to transmembrane helices alone or in association with phospholamban. Proc Natl Acad Sci U S A 100:5040–5045
60. Babu GJ, Zheng Z, Natarajan P et al (2005) Overexpression of sarcolipin decreases myocyte contractility and calcium transient. Cardiovasc Res 65:177–186
61. Sahoo SK, Shaikh SA, Sopariwala DH et al (2013) Sarcolipin protein interaction with sarco(endo)plasmic reticulum Ca2+ATPase (SERCA) is distinct from phospholamban

protein, and only sarcolipin Can promote uncoupling of the SERCA pump. J Biol Chem 288:6881–6889
62. Zvaritch E, Backx PH, Jirik F et al (2000) The transgenic expression of highly inhibitory monomeric forms of phospholamban in mouse heart impairs cardiac contractility. J Biol Chem 275:14985–14991
63. Gramolini AO, Trivieri MG, Oudit GY et al (2006) Cardiac-specific overexpression of sarcolipin in phospholamban null mice impairs myocyte function that is restored by phosphorylation. Proc Natl Acad Sci U S A 103:2446–2451
64. Minamisawa S, Wang Y, Chen J et al (2003) Atrial chamber-specific expression of sarcolipin is regulated during development and hypertrophic remodeling. J Biol Chem 278:9570–9575
65. Bal NC, Maurya SK, Sopariwala DH et al (2012) Sarcolipin is a newly identified regulator of muscle-based thermogenesis in mammals. Nat Med 18:1575–1579
66. Novitzky D, Cooper DKC (2014) Thyroid hormone and the stunned myocardium. J Endocrinol 223:R1–R8
67. Chang KC, Figueredo VM, Schreur JH et al (1997) Thyroid hormone improves function and Ca2+ handling in pressure overload hypertrophy. Association with increased sarcoplasmic reticulum Ca2+-ATPase and alpha-myosin heavy chain in rat hearts. J Clin Invest 100:1742–1749
68. Kimura Y, Otsu K, Nishida K et al (1994) Thyroid hormone enhances Ca2+ pumping activity of the cardiac sarcoplasmic reticulum by increasing Ca2+ ATPase and decreasing phospholamban expression. J Mol Cell Cardiol 26:1145–1154
69. Kiss E, Jakab G, Kranias EG, Edes I (1994) Thyroid hormone-induced alterations in phospholamban protein expression. Regulatory effects on sarcoplasmic reticulum Ca2+ transport and myocardial relaxation. Circ Res 75:245–251
70. Nagai R, Zarain-Herzberg A, Brandl CJ et al (1989) Regulation of myocardial Ca2+-ATPase and phospholamban mRNA expression in response to pressure overload and thyroid hormone. Proc Natl Acad Sci U S A 86:2966–2970
71. Rohrer D, Dillmann WH (1988) Thyroid hormone markedly increases the mRNA coding for sarcoplasmic reticulum Ca2+-ATPase in the rat heart. J Biol Chem 263:6941–6944
72. Hartong R, Wang N, Kurokawa R et al (1994) Delineation of three different thyroid hormone-response elements in promoter of rat sarcoplasmic reticulum Ca2+ATPase gene. Demonstration that retinoid X receptor binds 5′ to thyroid hormone receptor in response element 1. J Biol Chem 269:13021–13029
73. Reed TD, Babu GJ, Ji Y et al (2000) The expression of SR calcium transport ATPase and the Na(+)/Ca(2+)Exchanger are antithetically regulated during mouse cardiac development and in Hypo/hyperthyroidism. J Mol Cell Cardiol 32:453–464
74. Guo J, Bian Y, Bai R et al (2013) Globular adiponectin attenuates myocardial ischemia/reperfusion injury by upregulating endoplasmic reticulum Ca^{2+}-ATPase activity and inhibiting endoplasmic reticulum stress. J Cardiovasc Pharmacol 62:143–153
75. Pischon T, Girman CJ, Hotamisligil GS et al (2004) Plasma adiponectin levels and risk of myocardial infarction in men. JAMA 291:1730–1737
76. Villarreal-Molina MT, Antuna-Puente B (2012) Adiponectin: anti-inflammatory and cardioprotective effects. Biochimie 94:2143–2149
77. Safwat Y, Yassin N, Gamal El Din M, Kassem L (2013) Modulation of skeletal muscle performance and SERCA by exercise and adiponectin gene therapy in insulin-resistant rat. DNA Cell Biol 32:378–385
78. Boddu NJ, Theus S, Luo S et al (2014) Is the lack of adiponectin associated with increased ER/SR stress and inflammation in the heart? Adipocyte 3:10–18
79. Lokuta AJ, Maertz NA, Meethal SV et al (2005) Increased nitration of sarcoplasmic reticulum Ca2+-ATPase in human heart failure. Circulation 111:988–995
80. Tang WH, Cheng WT, Kravtsov GM, Tong XY et al (2010) Cardiac contractile dysfunction during acute hyperglycemia due to impairment of SERCA by polyol pathway-mediated oxidative stress. Am J Physiol 299:C643–C653

81. Ghezzi P (2005) Oxidoreduction of protein thiols in redox regulation. Biochem Soc Trans 33:1378
82. Adachi T, Weisbrod RM, Pimentel DR et al (2004) S-Glutathiolation by peroxynitrite activates SERCA during arterial relaxation by nitric oxide. Nat Med 10:1200–1207
83. Lancel S, Zhang J, Evangelista A et al (2009) Nitroxyl activates SERCA in cardiac myocytes via glutathiolation of cysteine 674. Circ Res 104:720–723
84. Tong X, Ying J, Pimentel DR et al (2008) High glucose oxidizes SERCA cysteine-674 and prevents inhibition by nitric oxide of smooth muscle cell migration. J Mol Cell Cardiol 44:361–369
85. Jardim-Messeder D, Camacho-Pereira J, Galina A (2012) 3-Bromopyruvate inhibits calcium uptake by sarcoplasmic reticulum vesicles but not SERCA ATP hydrolysis activity. Int J Biochem Cell Biol 44:801–807
86. Adachi T (2010) Modulation of vascular sarco/endoplasmic reticulum calcium ATPase in cardiovascular pathophysiology. In: Vanhoutte PM (ed) Advances in pharmacology. Academic Press, San Diego, CA, pp 165–195
87. Kho C, Lee A, Jeong D et al (2011) SUMO1-dependent modulation of SERCA2a in heart failure. Nature 477:601–605
88. Tilemann L, Lee A, Ishikawa K et al (2013) SUMO-1 gene transfer improves cardiac function in a large-animal model of heart failure. Sci Transl Med 5:211ra159
89. Van Rechem C, Boulay G, Pinte S et al (2010) Differential regulation of HIC1 target genes by CtBP and NuRD, via an acetylation/SUMOylation switch, in quiescent versus proliferating cells. Mol Cell Biol 30:4045–4059
90. Foster DB, Liu T, Rucker J et al (2013) The cardiac acetyl-lysine proteome. PLoS One 8, e67513
91. Clark RJ, McDonough PM, Swanson E et al (2003) Diabetes and the accompanying hyperglycemia impairs cardiomyocyte calcium cycling through increased nuclear O-GlcNAcylation. J Biol Chem 278:44230–44237
92. Bidasee KR, Zhang Y, Shao CH et al (2004) Diabetes increases formation of advanced glycation End products on sarco(endo)plasmic reticulum Ca2+-ATPase. Diabetes 53:463–473
93. Bennett CE, Johnsen VL, Shearer J, Belke DD (2013) Exercise training mitigates aberrant cardiac protein O-GlcNAcylation in streptozotocin-induced diabetic mice. Life Sci 92:657–663
94. Hu Y, Belke D, Suarez J et al (2005) Adenovirus-mediated overexpression of O-GlcNAcase improves contractile function in the diabetic heart. Circ Res 96:1006–1013
95. Yokoe S, Asahi M, Takeda T, Otsu K, Taniguchi N, Miyoshi E, Suzuki K (2010) Inhibition of phospholamban phosphorylation by O-GlcNAcylation: implications for diabetic cardiomyopathy. Glycobiology 20:1217–1226
96. Belke DD (2011) Swim-exercised mice show a decreased level of protein O-GlcNAcylation and expression of O-GlcNAc transferase in heart. J Appl Physiol 111:157–162
97. Carneiro-Júnior MA, Quintão-Júnior JF, Drummond LR et al (2013) The benefits of endurance training in cardiomyocyte function in hypertensive rats are reversed within four weeks of detraining. J Mol Cell Cardiol 57:119–128
98. Johnsen AB, Høydal M, Røsbjørgen R, Stølen T, Wisløff U (2013) Aerobic interval training partly reverse contractile dysfunction and impaired Ca^{2+} handling in atrial myocytes from rats with post infarction heart failure. PLoS One 8, e66288
99. Vanzelli AS, Medeiros A, Rolim N et al (2013) Integrative effect of carvedilol and aerobic exercise training therapies on improving cardiac contractility and remodeling in heart failure mice. PLoS One 8, e62452
100. Kemi OJ, Ellingsen O, Ceci M, Grimaldi S, Smith GL, Condorelli G, Wisløff U (2007) Aerobic interval training enhances cardiomyocyte contractility and Ca2+ cycling by phosphorylation of CaMKII and Thr-17 of phospholamban. J Mol Cell Cardiol 43:354–361
101. Wisløff U, Loennechen JP, Currie S, Smith GL, Ellingsen Ø (2002) Aerobic exercise reduces cardiomyocyte hypertrophy and increases contractility, Ca2+ sensitivity and SERCA-2 in rat after myocardial infarction. Cardiovasc Res 54:162–174

102. Thomas MM, Vigna C, Betik AC, Tupling AR, Hepple RT (2011) Cardiac calcium pump inactivation and nitrosylation in senescent rat myocardium are not attenuated by long-term treadmill training. Exp Gerontol 46:803–810
103. Norrbom J, Wallman SE, Gustafsson T, Rundqvist H, Jansson E, Sundberg CJ (2010) Training response of mitochondrial transcription factors in human skeletal muscle. Acta Physiol (Oxf) 198:71–79
104. Lumini-Oliveira J, Magalhães J, Pereira CV, Moreira AC, Oliveira PJ, Ascensão A (2011) Endurance training reverts heart mitochondrial dysfunction, permeability transition and apoptotic signaling in long-term severe hyperglycemia. Mitochondrion 11:54–63
105. Bupha-Intr T, Laosiripisan J, Wattanapermpool J (2009) Moderate intensity of regular exercise improves cardiac SR Ca2+ uptake activity in ovariectomized rats. J Appl Physiol (1985) 107:1105–1112
106. MacDonnell SM, Kubo H, Crabbe DL, Renna BF, Reger PO, Mohara J, Smithwick LA, Koch WJ, Houser SR, Libonati JR (2005) Improved myocardial beta-adrenergic responsiveness and signaling with exercise training in hypertension. Circulation 111:3420–3428
107. Ciloglu F, Peker I, Pehlivan A, Karacabey K, Ilhan N, Saygin O, Ozmerdivenli R (2005) Exercise intensity and its effects on thyroid hormones. Neuro Endocrinol Lett 26:830–834
108. Hackney AC, Kallman A, Hosick KP, Rubin DA, Battaglini CL (2012) Thyroid hormonal responses to intensive interval versus steady-state endurance exercise sessions. Horm Athens Greece 11:54–60
109. Neto R, de Souza dos Santos M, Rangel I, Ribeiro M, Cavalcanti-de-Albuquerque J, Ferreira A, Cameron L, Carvalho D, Werneck de Castro J (2013) Decreased serum T3 after an exercise session is independent of glucocorticoid peak. Horm Metab Res 45:893–899
110. Shin M-S, Ko I-G, Kim S-E, Kim B-K, Kim T-S, Lee S-H, Hwang D-S, Kim C-J, Park J-K, Lim B-V (2013) Treadmill exercise ameliorates symptoms of methimazole-induced hypothyroidism through enhancing neurogenesis and suppressing apoptosis in the hippocampus of rat pups. Int J Dev Neurosci 31:214–223
111. Kinugawa K, Yonekura K, Ribeiro RCJ, Eto Y, Aoyagi T, Baxter JD, Camacho SA, Bristow MR, Long CS, Simpson PC (2001) Regulation of thyroid hormone receptor isoforms in physiological and pathological cardiac hypertrophy. Circ Res 89:591–598
112. St-Pierre DH, Faraj M, Karelis AD, Conus F, Henry JF, St-Onge M, Tremblay-Lebeau A, Cianflone K, Rabasa-Lhoret R (2006) Lifestyle behaviours and components of energy balance as independent predictors of ghrelin and adiponectin in young non-obese women. Diabetes Metab 32:131–139
113. Tsukinoki R, Morimoto K, Nakayama K (2005) Association between lifestyle factors and plasma adiponectin levels in Japanese men. Lipids Health Dis 4:27
114. Balagopal P, George D, Yarandi H, Funanage V, Bayne E (2005) Reversal of obesity-related hypoadiponectinemia by lifestyle intervention: a controlled, randomized study in obese adolescents. J Clin Endocrinol Metab 90:6192–6197
115. Simpson KA, Singh MAF (2008) Effects of exercise on adiponectin: a systematic review. Obesity 16:241–256
116. Johnsen VL, Belke DD, Hughey CC, Hittel DS, Hepple RT, Koch LG, Britton SL, Shearer J (2013) Enhanced cardiac protein glycosylation (O-GlcNAc) of selected mitochondrial proteins in rats artificially selected for low running capacity. Physiol Genomics 45:17–25

Chapter 12
Calcium Handling in Pulmonary Vasculature Under Oxidative Stress: Focus on SERCA

Amritlal Mandal, Tapati Chakraborti, and Sajal Chakraborti

Abstract Maintenance of cytoplasmic calcium ($[Ca^{2+}]_i$) at physiological level is a constant challenge for every cell including endothelial and smooth muscle cells of pulmonary vasculature. The cells are equipped with complex regulatory mechanisms to deal with a relatively large Ca^{2+} gradient that exists not only between intracellular and extracellular spaces but also between cytoplasm and sarco(endo) plasmic reticulum [S(ER)]. Cells usually achieve their goal either by using plasma membrane Ca^{2+}-ATPase (PMCA) as an export mechanism or by using S(ER) Ca^{2+}-ATPase (SERCA) as a sequestering mechanism in the S(ER) stores. The S(ER) Na^+/Ca^{2+} exchanger (NCX) also plays an important role along with SERCA in regulating $[Ca^{2+}]_i$. Exposure to air pollutants, cigarette smoke, suspended particulate materials, pesticides and subsequent generation of free radicals especially by inflammatory and vascular cells have been identified as a threat to the normal functioning of pulmonary vasculature. The complete sets of events that lead to activation of inflammatory and vascular cells remain unclear. However, a considerable number of reports suggest that a correlation exists between reactive oxygen species (ROS) and Ca^{2+}-ATPase regulation. This chapter provides a glimpse on oxidant mediated regulation of Ca^{2+}-ATPases in pulmonary vasculature with special attention to SERCA.

Keywords Ca^{2+}-ATPase • Sarco(endo)plasmic reticulum Ca^{2+}-ATPse (SERCA) • Plasma membrane Ca^{2+}-ATPse (PMCA) • Na^+/Ca^{2+} (NCX) • Reactive oxygen species (ROS) • Cytoplasmic calcium ($[Ca^{2+}]_i$)

A. Mandal
Department of Physiology, University of Arizona, Tucson, AZ 85724, USA

T. Chakraborti • S. Chakraborti (✉)
Department of Biochemistry and Biophysics, University of Kalyani, Kalyani 741235, West Bengal, India
e-mail: saj_chakra@rediffmail.com

S. Chakraborti, N.S. Dhalla (eds.), *Regulation of Ca^{2+}-ATPases,V-ATPases and F-ATPases*, Advances in Biochemistry in Health and Disease 14,
DOI 10.1007/978-3-319-24780-9_12

1 Introduction

Physiological cytoplasmic calcium concentration ($[Ca^{2+}]_i$) is ~50–150 nM, while the extracellular Ca^{2+} concentration is relatively high ~1.0–2.5 mM. A large gradient of Ca^{2+} concentration exists between two spaces and also between cytoplasm and intracellular Ca^{2+} stores. Maintenance of low $[Ca^{2+}]_i$ is a challenge for cells for proper physiological function. Cellular Ca^{2+} homeostasis is largely controlled by the plasma membrane Ca^{2+}-ATPase (PMCA) [1, 2], which exports cytoplasmic Ca^{2+} ion and imports extracellular protons at the expense of ATP. SERCA pumps also contribute significantly by controlling the $[Ca^{2+}]_i$ influx into the S(ER) [3, 4]. When $[Ca^{2+}]_i$ is elevated, the plasma membrane Na^+/Ca^{2+} exchanger (NCX) works in forward mode exporting one Ca^{2+} against the import of three Na^+ [5, 6]. Reactive oxygen species (ROS) and reactive nitrogen species (RNS) are mediators of cell signaling in airway, pulmonary epithelial and arterial cells by a variety of toxic agents including cigarette smoke, asbestos, silica, airborne particulate matter, automobile exhaust, and ozone (O_3).

A considerable number of reports suggest a role of ROS in regulating Ca^{2+}-ATPase activity [7–15]. The concentration of ROS in the vasculature is normally balanced mainly by activities of superoxide dismutase (SOD) and catalase, thus converting potentially damaging free radicals into harmless molecules. When the balance is disrupted due to some pathophysiological conditions such as ischemia reperfusion (IR) injury and inflammation or atherosclerotic-lesion formation, an increase in ROS occurs in the vasculature. An increase in ROS such as superoxide ($O_2^{-\bullet}$) and hydroxyl radical ($OH^\bullet$) production may lead to changes in cell signaling. During IR injury, impaired calcium regulation is one of the major consequences observed in blood vessels. Because ROS are increased during ischemia and have been linked to multiple effects on calcium signaling in both the endothelium and smooth muscle, it is likely that the signals affected by ROS are important mediators of vascular injury. The evidence supporting a role of ROS in arterial dysfunction is complicated by differences in the type of radical species examined and variations in pathophysiological conditions [16]. Pesticides [17], air pollution [18, 19] and inhaled ultra fine particles [20] also contribute significantly in developing oxidative stress in pulmonary vasculature.

2 Lung Diseases and Oxidants

Influx of activated inflammatory cells to the lung is a common feature that lung is challenged with air pollution related health hazards. Generation of free radicals by activated inflammatory cells is also involved in the oxidative stress associated with air pollution. Signals, for example, activated lipids may stimulate transcription factors such as nuclear factor-κB (NF-κB) and increased expression of a range of pro-inflammatory chemokines and cytokines. Using molecular oxygen, the NADPH

oxidase produces $O_2^{-\bullet}$ and that becomes modified by SOD resulting in the formation of hydrogen peroxide (H_2O_2). Due to the cell permeable characteristics of H_2O_2, it can easily cross cell membranes and activates different intracellular signaling pathways, or lead to the generation of other potent ROS, for example, $OH^{\bullet}$. Alternatively, myeloperoxidase, which is also released by the neutrophil, uses H_2O_2 as a substrate, and produces hypochlorous acid (HOCl), another potent oxidant. The influx and subsequent activation of inflammatory cells creates a second wave of oxidative stress that severely compromise endogenous antioxidant defenses in the lung [18].

3 Lung Diseases, PAH, and SERCA

Pulmonary arterial hypertension (PAH) is usually associated with high blood pressure in the pulmonary artery (PA) [21]. This often is associated with a variety of lung diseases and/or hypoxemia [22]. PA wall thickening [23], right ventricular hypertrophy and failure [24, 25], PA embolism [22], and some lung diseases such as interstitial lung disease (ILD) [26] and chronic obstructive pulmonary disease (COPD) [22] have been identified in patients with PAH. Idiopathic pulmonary fibrosis (IPF) has also been implicated in developing PAH in humans [27]. Though it is very common in patients suffering from lung diseases are often diagnosed with PAH, no direct evidence is currently available showing relationship between lung diseases and SERCA in the development of PAH.

4 Inhaled Oxidants and Cigarette Smoke

Inhalation of cigarette smoke and airborne pollutants, either oxidant gases such as O_3, NO, sulfur dioxide (SO_2), or H_2O_2 results in direct lung damage as well as in the activation of inflammatory responses in lungs. Cigarette smoke is a complex mixture of over thousands of chemical compounds, including high concentrations of reactive free radicals [28]. Cigarette smoke causes a significant fall in the endogenous anti-proteinases (e.g., α1-PI) activity of bronchoalveolar lavage fluid [29].

5 Sources of ROS in the Pulmonary Vasculature

Vascular insults, such as IR or inflammation, result in the release of H_2O_2 from polymorphonuclear leukocytes (PMNL) or monocytes. In addition, both endothelial cells and smooth muscle cells produce a variety of oxidant species that may have both direct and indirect effects on cell signaling [30]. Substantial amount of research have revealed that ROS are produced in pulmonary artery by fibroblasts [31],

endothelial cells [32, 33] and smooth muscle cells [34]. Following sections briefly states the physiological sources of different ROS in pulmonary artery endothelial and smooth muscle cells.

5.1 Nitric Oxide (NO)

NO plays an important role in maintaining low blood pressure in the pulmonary circulation. NO is produced in pulmonary artery smooth muscle (PASM) by enzymatic oxidation of endogenous substrate L-arginine by nitric oxide synthase (NOS) when exposed to inflammatory cytokines, tumor necrosis factor- α (TNF-α), and interferon-γ (IFN- γ) [35]. Being a gas, NO rapidly diffuses through membranes and activates guanylyl cyclase, which increases cellular cGMP. The resulting activation of cGMP-dependent protein kinase leads to smooth muscle relaxation and thereby decreases pulmonary vascular tone [36]. A simplified cartoon showing NO, oxidative stress and inflammation in PAH is depicted in Fig. 12.1.

5.2 Superoxide ($O_2^{-\bullet}$)

In some pathophysiological conditions, such as in IR injury, excessive production of $O_2^{-\bullet}$ in vascular cells plays an important role in intracellular signaling pathways by affecting NO synthesis. The most important source of $O_2^{-\bullet}$ in the pulmonary vasculature is the NADPH oxidase [34]. Agonists such as angiotensin II and TNF-α increase membrane associated NADPH oxidase derived $O_2^{-\bullet}$ production in vascular smooth muscle cells (VSMCs) [34, 37]. In this context, we have demonstrated stimulatory role of protein kinase C (PKC) in the generation of NADPH oxidase derived $O_2^{-\bullet}$ during treatment of bovine pulmonary artery smooth muscle cells (PASMCs) with the thromboxane A_2 mimetic U46619 [38].

5.3 Peroxynitrite ($ONOO^-$)

$ONOO^-$, a highly reactive species that affects multiple cellular responses and signaling pathways, is formed by a reaction between $O_2^{-\bullet}$ and NO. Under normal circumstances, the balance between the rates of $O_2^{-\bullet}$ and NO formation is modulated by the concentration of both the intracellular and extracellular forms of SOD, which converts $O_2^{-\bullet}$ to H_2O_2 [39]. $ONOO^-$ has been demonstrated as an extremely reactive species and is of significant importance within the vasculature. Recent research has proved that $ONOO^-$ as an important contributor towards various pathophysiological conditions in the lung, for example, PAH [40–42].

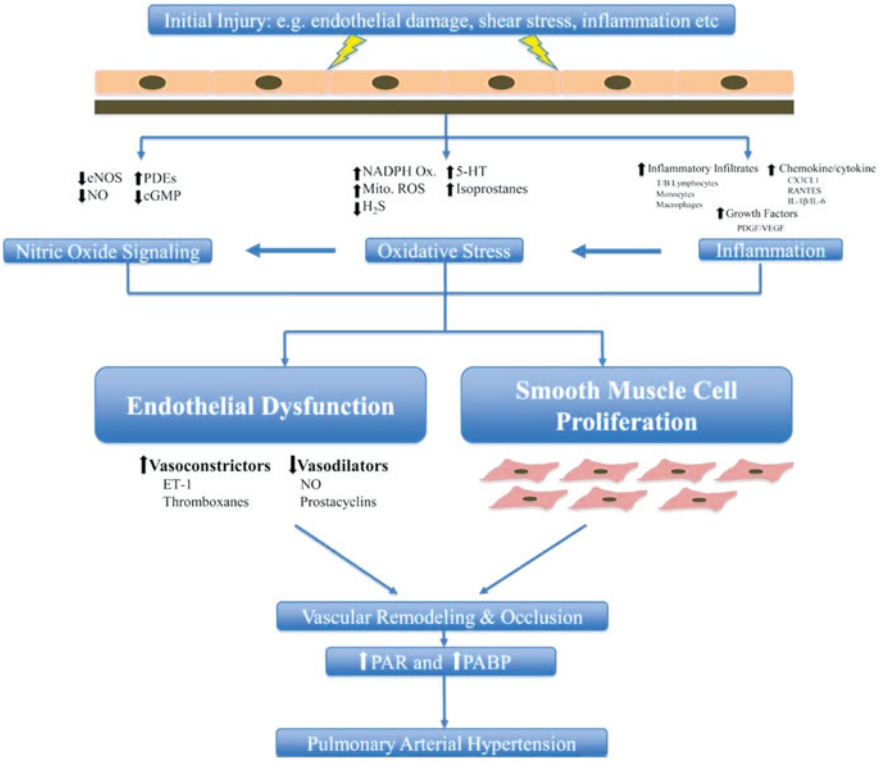

Fig. 12.1 Nitric oxide, oxidative stress, and inflammation in pulmonary hypertension. Despite advancements in PAH research in the last 20 years, the initiating factors in most patients remain unclear. Whatever the initiating insult, endothelial cell activation occurs, leading to an increase in the expression of cell adhesion molecules and production of chemokines and cytokines. Infiltration of inflammatory mediators (lymphocytes, monocytes, and macrophages) occurs as well as production of growth factors. Disturbance of the endothelial cells also results in an alteration of nitric oxide signaling leading to a decrease in eNOS expression and NO production. Shear stress on vascular wall and inflammatory infiltrates can lead to the activation of oxidative stress mechanisms such as superoxide generating NADPH oxidase, mitochondrial reactive oxygen species (ROS) production, decreases in hydrogen sulfide (H_2S) levels and increases in serotonin (5-HT) levels. These mechanisms act cumulatively causing a decrease in vasodilators (NO, prostacyclins) and an increase in vasoconstrictors (ET-1, thromboxanes). This imbalance of vasoactive substance lead to endothelial cell dysfunction and smooth muscle cell proliferation and hyperplasia that eventually causes vascular remodeling and narrowing of the pulmonary arteries. Occlusion of the pulmonary arteries increase pulmonary vascular resistance (PVR) and pulmonary artery blood pressure (PABP) leading to pulmonary arterial hypertension. Taken from Ref. [135] with permission

6 SERCA and Pulmonary Arterial Calcium Homeostasis

SERCA is an important player in developing pathology of pulmonary vasculature [43]. The wide array of research performed on SERCA subtypes and their specific roles in cardiac, vascular and skeletal muscle have identified 14 genes with different

functional characteristics and cell-specific expression patterns [43]. Most of the VSMCs in mature vessels exhibit a quiescent/contractile phenotype and controls the vascular tone. In different types of VSMCs, enormous variations do exist with regard to the mechanisms responsible for generating Ca^{2+} signal. In each VSMC phenotype, the Ca^{2+} signaling mechanism is specifically adapted to its particular function [44].

SERCA is a 110 kDa protein which accumulates calcium into the S(ER) of all cells. SERCA2a and SERCA2b were known to express in rat pulmonary arterial smooth muscle (PASM), whereas SERCA1 or SERCA3 expression remain undetected [45]. Both the isoforms: SERCA2a and SERCA2b were differentially distributed within isolated rat PASM cells and both isoforms seem to participate in the basal calcium uptake [46]. Two isoforms are specifically distributed in two different regions of SR. SERCA2a has been shown to localize in a region comprising ryanodine receptor 3 (RyR3) proximal to the nucleus within PASMCs, whereas SERCA2b is present in a different region of SR compartment proximal to the plasma membrane where ryanodine receptor 1 (RyR1) is localized [45]. A schematic representation of the spatial and functional compartmentalization of the SERCA isoforms in pulmonary arterial smooth muscle cell is shown in Fig. 12.2.

Distinct difference in SERCA gene expression pattern exists between endothelium of veins and arteries. Endothelium from rat coronary artery, coronary vein and aorta were reported to express both SERCA2 and SERCA3 mRNA, whereas smooth muscle cells only express SERCA2 mRNA [47].

Pulmonary circulation is a low pressure and fast flow system with a very thin wall thickness. PAH is a disease of the small pulmonary arteries associated with vascular narrowing due to vascular wall thickening leading to progressive increase of pulmonary vascular resistance. The terminal observation of such disease process is the failure of right ventricle due to intolerance in increased right ventricular afterload [48]. PAH is mainly characterized by dysregulated proliferation of PASMCs leading to abnormal vascular remodeling. New ideas and hypotheses are evolving in an effort to correlate regulation of SERCA, pulmonary vascular remodeling and the development of PAH. Experimental evidences have established SERCA2a regulation and pulmonary vascular remodeling as an important mechanism for PAH pathophysiology [49]. Pulmonary vascular remodeling occurs as a result of pulmonary vascular endothelial dysfunction, PASMC proliferation/migration, hypertrophy, inflammation and thrombosis in situ causes formation of plexiform lesions, which are the hallmarks of the disease [50, 51]. These remodeled vessels, together with an imbalance in vasodilators and vasoconstrictors, contribute to increased pulmonary vascular resistance resulting in right ventricular hypertrophy.

So far pharmacological intervention to treat the disease is pretty much limited, with documentation of meager numbers of survival outcome. When SERCA2a is downregulated, $[Ca^{2+}]_i$ levels are increased resulting in hypertension. In rat vascular injury models, VSMCs isolated from media of the thoracic aorta showed downregulation of SERCA2a expression and an increase in $[Ca^{2+}]_i$ with subsequent VSMC proliferation and an increase in neointima formation [52].

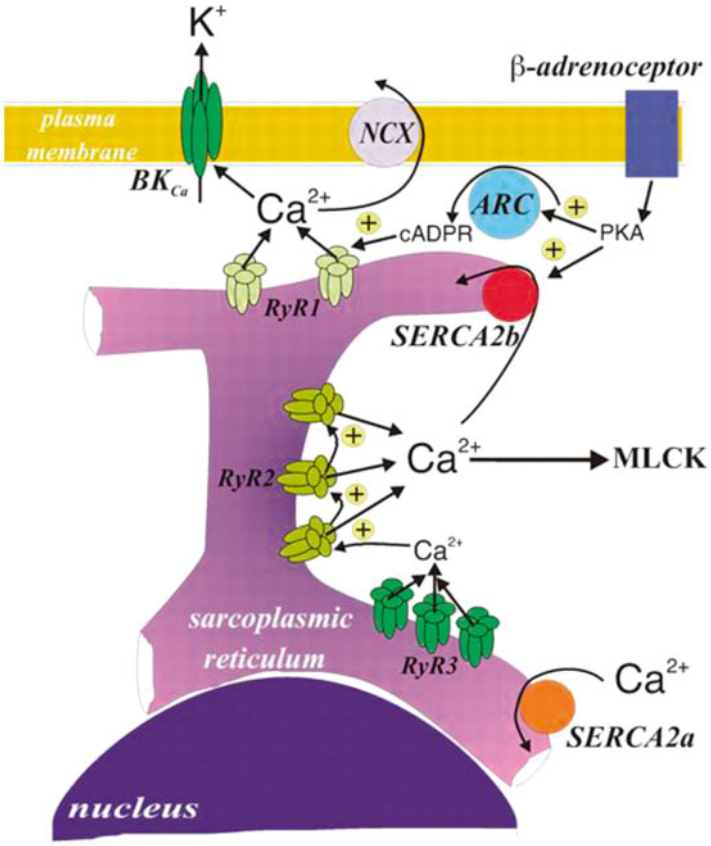

Fig. 12.2 Schematic representation of the spatial and functional compartmentalization of the SERCA isoforms in a pulmonary arterial smooth muscle cells. NCX, sodium/calcium exchanger; PKA, cAMP-dependent protein kinase; ARC, ADP-ribosyl cyclase; cADPR, cyclic adenosine diphosphate-ribose; MLCK, myosin light chain kinase. Taken from Ref. [45] with permission

Gene transfer of SERCA2a to upregulate its protein expression to better handle elevated $[Ca^{2+}]_i$ has been demonstrated in animal models [52, 53]. SERCA2a gene transfer has also been shown to ameliorate endothelial dysfunction by increasing eNOS expression and activity [52, 53]. SERCA2a gene transfer using adeno-associated virus serotype 1 has been studied and validated extensively in the ventricular myocardium and was shown to improve left ventricular systolic function and ventricular remodeling in rat and swine preclinical models of heart failure [54]. It has, therefore, been hypothesized that SERCA2a is downregulated in pulmonary arterioles in PAH and that gene transfer of SERCA2a prevent or ameliorate pulmonary vascular remodeling and right ventricular dysfunction in PAH [49]. The therapeutic potential of SERCA2a gene transfer to target pulmonary vascular dysfunction in human PAH has not yet been ascertained.

7 PASMCs, ROS and SERCA

Most of the effects of ROS on calcium signaling in the pulmonary artery are due to the endothelial effects. There are evidence that ROS generated in the endothelium can directly affect calcium homeostasis in the adjoining smooth muscle cells [7, 55, 56]. Most evidence supports a primary role of ROS in the inactivation of SERCA in smooth muscle [14, 57] and in other cell types [58–62]. The effects of oxidants on SERCA are tissue specific. In cardiac myocytes SERCA has been reported to have a reactive thiolate anion on cysteine-674, which when adducts with glutathione increases Ca^{2+} uptake [12]. The same reactive thiol is quantitatively and irreversibly oxidized in vitro by relatively high dose of $ONOO^{-}$. Despite the requirement for this high concentration, chronically elevated oxidants oxidize SERCA in diseased tissues [13, 15]. Using plasma membrane and ER enriched fractions of coronary artery, Grover and Samson [10] demonstrated inactivation of both the PMCA and SERCA by X/XO system [10]. Preincubation with SOD, but not catalase, ameliorate the inactivation, suggesting involvement of $O_2^{-\bullet}$ in this scenario [10].

The mechanism of SERCA inhibition by $O_2^{-\bullet}$ occurs possibly through the irreversible oxidation of sulfhydryl groups or by direct attack on the ATP binding site. Inhibition of SERCA by oxidation of sulfhydryl groups is supported by the ability of reducing agents and cysteine to prevent inhibition, the decline in sulfhydryl content of oxidized SR, and the ability of sulfhydryl-binding agents to inhibit Ca^{2+}-ATPase activity [63, 64]. Research from our laboratory in pulmonary arterial smooth muscle microsomes revealed that stimulation of Ca^{2+}-ATPase activity occurs through involvement of an aprotinin-sensitive proteinase [56, 65]. Our research also provided evidence for oxidant stimulated Ca^{2+}-ATPase activity and decreased Na^{+} dependent Ca^{2+} uptake (NCX) with a net calcium overload under oxidant triggered conditions in pulmonary arterial cells [7, 65, 66]. These observations were apparently in contrast to previous reports that oxidants depress calcium pump activity in systems such as S(ER) [67] and heart sarcolemma [68]. The difference between other studies and our observation regarding the effect of oxidants on Ca^{2+}-ATPase activity and ATP-dependent Ca^{2+} uptake may be explained considering the differences of the functional responsiveness and biochemical characteristics of pulmonary vessels compared to that of systemic vessels and other nonvascular systems. Because of the differences in the biochemical characteristics and metabolic needs, pulmonary vessel responds differently to stimuli in comparison to systemic vessels. There are examples of tissue specific responsiveness of hypoxia-induced smooth muscle tone. Hypoxia constricts pulmonary vessels, while dilates systemic vessels [69, 70]. Major pathways for calcium handling mechanisms in pulmonary arterial smooth muscle cells are depicted in Fig. 12.3.

Cellular signaling mechanisms linked to calcium mobilization plays significant roles in several signal transduction pathways that control cell proliferation, differentiation, and apoptosis. Recent research suggests that acute hypoxia causes smooth muscle contraction in pulmonary arteries through a direct effect on $[Ca^{2+}]_i$ [71]. Subsequent relaxation depends upon activation of ion transport mechanisms, which

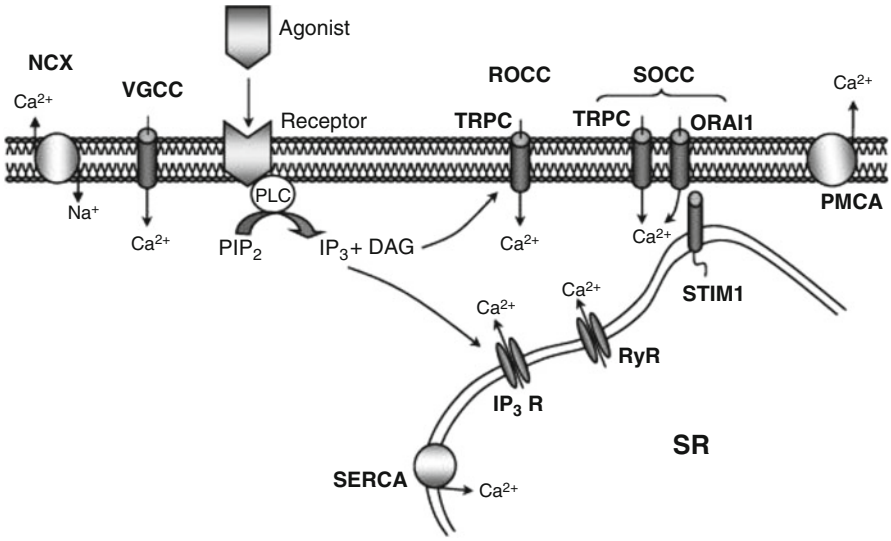

Fig. 12.3 Schematic illustration of calcium handling pathways in pulmonary arterial smooth muscle cells. PMCA: plasma membrane Ca^{2+}-ATPase; NCX: Na^{+}/Ca^{2+} exchange; STIM: stromal interaction molecule; VGCC: voltage-gated calcium channel; TRPC: transient receptor potential cation channels; ORAI1: gene encoding calcium-release activated calcium channel protein-1; PLC: phospholipase C; ROCC: receptor-operated Ca^{2+} channel; SOCC: store-operated Ca^{2+} channel; RyR: ryanodine receptor; PIP2: phosphatidylinositol 4,5-bisphosphate; IP_3R: inositol triphosphate receptor. Taken from Ref. [136] with permission

may be modified by circulating hormones such as the naturally occurring endogenous ouabain [72]. Sustained hypoxia may cause long-term adaptation of pulmonary endothelium. One change is a reduction in NO production, possibly through reduced activity of NOS [73]. In normal physiological condition, synthesis of NO appears important in many species including human in regulating low pulmonary vascular resistance [74]. Downregulation of endothelial NO biosynthesis as a result of long-term hypoxia may accelerate development of secondary PAH [75]. Thus, altered NOS (endothelial or inducible) expression either due to transcriptional or translational regulation seems important for better understanding of cellular cross talk in normal and inflammatory cells.

8 Store-Operated Calcium Entry, SERCA Inhibition, and PAH

Store-operated calcium entry (SOCE) is an important cellular calcium influx mechanism that results as a consequence of depletion of the ER calcium store, which causes opening of plasma membrane calcium channels. This was first described in 1986 by Putney [76] in parotid acinar cells. As the ER/SR cellular Ca^{2+} store (either

IP_3 or ryanodine sensitive) is depleted, the relatively large increase in $[Ca^{2+}]_i$ is controlled by pumping out the Ca^{2+} into the extracellular space by PMCA. To ensure sustained signaling and maintenance of cellular Ca^{2+} homeostasis, the Ca^{2+} that have been extruded must be returned to the cytosol and ultimately reaccumulated by SERCA and this occurs with the involvement of SOCE channels.

Pulmonary vasoconstriction is a result of progressive smooth muscle contraction. An increase in $[Ca^{2+}]_i$ in PASMCs is a major trigger for pulmonary vasoconstriction [77]. Several studies have provided evidence that SERCA inhibitors not only increase Ca^{2+} influx, but also affect vascular tone of different blood vessels [78]. The Ca^{2+} overload induced vascular smooth muscle contraction is tissue specific. For example, in rat aorta the Ca^{2+} induced contraction is nifedipine (L-type calcium channel blocker) sensitive [79–84], whereas rat pulmonary artery shows nifedipine insensitivity [85]. PASM contraction as a result of SERCA inhibition can cause calcium entry via both voltage operated calcium channel (VOCC) and store operated Ca^{2+} channel (SOCC) [78].

9 Calcium Regulation in PAH

Right ventricular hypertrophy and failure has been extensively studied in experimental swine model of PAH [86, 87]. The key finding was a reduction in right ventricular (RV) SERCA2a expression with increased ER stress. ROS concentration has been reported to increase dramatically during cardiac IR injury [88–91]. An increase in ROS levels may lead to aberrant coronary vascular tone, thus producing cardiac dysfunction and arrhythmias [89, 92]. During cardiac IR, one of the major injuries to coronary artery SMCs is a dysregulation of calcium-handling [89]. The activities of the SERCA, NCX, and Na,K-ATPase (NKA) normally help maintain a transmembrane ion balance, but their inhibition may impair Ca^{2+} regulation [93, 94]. Earlier research has provided evidence that acute exposure to ROS causes relaxation of blood vessels of various species [95], whereas prolonged exposure to high levels of ROS produces a loss of utilization of $[Ca^{2+}]_i$ pool in coronary arterial smooth muscle [9–11].

Proliferation of pulmonary arterial smooth muscle cells (PASMCs) associated with sustained vasoconstriction and vascular remodeling are the major pathogenic events in PAH. Increased production of vasoactive and mitogenic agonists and decreased apoptosis of PASMCs are the cause of increased PASMC proliferation. Increased cytosolic Ca^{2+} overload has been found to be an important stimulus for PASMC migration and proliferation. Pulmonary vascular remodeling followed by an increase in pulmonary vascular resistance (PVR) is the final outcome [96–98]. An increase in resting $[Ca^{2+}]_i$, enhanced SOCE and enhanced receptor operated calcium entry (ROCE) were reported in PASMCs isolated from patients with idiopathic pulmonary arterial hypertension (IPAH) [96–98]. The complete set of events for IPAH development is currently unclear [99]. Apart from voltage-dependent Ca^{2+} channels and Ca^{2+}-sensitive ion channels other unidentified Ca^{2+} channels have also been implicated in developing IPAH [100–102].

Primary cultured pulmonary artery smooth muscle cells (PASMC) either isolated from rat [103], rabbit [104] or bovine [56] have gained popularity and has been established as important models for studying oxidant induced cellular calcium mobilization in altered Ca^{2+}-ATPase activity in PAH and associated Ca^{2+} overload. $O_2^{-\bullet}$ has been reported to cause ATP-induced calcium transients in freshly isolated PASMCs from rabbit [73] or was responsible for an increase in ATP-dependent Ca^{2+} uptake in bovine PASMCs [65]. In isolated rat PASMCs, NCX was also reported to play significant role in decreasing the augmented $[Ca^{2+}]_i$ for maintaining physiological level [103]. Interestingly, under oxidant stress, inhibition of NCX has been shown to over ride an increase in ATP dependent Ca^{2+} uptake in microsomes isolated from bovine PASMCs [7].

10 Oxidant-Induced Regulation of SERCA in Relation to PAH Pathophysiology

Due to the importance of the PAH and limited knowledge of the regulation of Ca^{2+} dynamics under oxidant triggered conditions in PASMC, our laboratory has invested significant effort to determine the role that $O_2^{-\bullet}$ plays on Ca^{2+}-ATPase activity and ATP dependent Ca^{2+}-uptake in microsomes of bovine PASM and the involvement of proteases such as an aprotinin sensitive serine protease and matrix metalloprotease-2 (MMP-2) in this scenario. Proteinases have been established as an important player in experimentally induced and physiologically occurring changes in cells and tissues [105, 106]. In the lung, MMP-2 has been shown to produce active vasopressors such as angiotensin (from angiotensinogen) and endothelin (from proendothelin) [107, 108]. This raises the possibility that oxidant-mediated pulmonary hypertension could be mediated by MMP-2. Evidence from other studies supported our findings that $ONOO^-$ induced stimulation of MMP-2 activity play an important role in stimulating Ca^{2+} ATPase activity in bovine PASMC plasma membrane [109]. We have also provided evidence showing similar role of MMP-2 to that of an aprotinin sensitive protease in bovine PASMCs [7, 66, 110].

PKC was implicated to positively affect $O_2^{-\bullet}$ production. In an effort to identify the specific PKC isoform(s) in regulating $O_2^{-\bullet}$ generation and cellular Ca^{2+} regulation, we studied microsomes isolated from bovine pulmonary arterial smooth muscle exposed to the $O_2^{-\bullet}$ generating system (X +XO) and by employing biochemical approach, PKCδ was identified as the important PKC isoform, which regulates $O_2^{-\bullet}$ production [111]. $O_2^{-\bullet}$ has been demonstrated to inhibit Na^+ dependent Ca^{2+} uptake by $ONOO^-$ which is a major contributing mechanism for Ca^{2+} overload in pulmonary smooth muscle under oxidant triggered condition [111].

In IR injury, increased production of $O_2^{-\bullet}$ and NO have been reported [112, 113]. Toxic effects of $ONOO^-$ are mediated by modification and activation of cellular targets such as aprotinin, α1-PI and TIMPs that contains –SH group [7, 114–117]. Additionally, oxidants may dysregulate SERCA itself or its regulators, for example, phospholamban or some other regulatory signaling components [118].

11 Cooperativity of Different Calcium Homeostasis Mechanisms in Pulmonary Vasculature

Cooperative mechanisms generally exist in all cell types for maintaining cellular Ca^{2+} homeostasis and the key players participating in this fine tuning are PMCA, SERCA, and NCX coupled to NKA [119]. The nature and relative contributions of these components for cytosolic Ca^{2+} clearance have long been an important topic for study in smooth muscle, especially in relation to regulation of contractility. Recent advances in gene-targeting and transgenesis have made it possible to add or delete individual components, and importantly specific isoforms from the cell to gain insight into the calcium clearance mechanisms in pulmonary vascular smooth muscle [119, 120]. Transient receptor potential channels (TRPCs) [121–123] and NCX [123–125] have been identified as important players for various forms of hypertension. TRPC1 and TRPC6 were known to play critical roles in hypoxic PAH [126, 127]. TRPC6 [96] and NCX1 [125] both play significant roles in human primary PAH and both are found to be upregulated in this scenario. Both NCX1 and NCX3 mRNA and protein expression were detected in cultured human PASMCs [128].

In human PASMCs, Ca^{2+} entry via reverse mode NCX is a critical pathway for cytoplasmic Ca^{2+} rise, which induces pulmonary vasoconstriction and pulmonary vascular hypertrophy [128]. Devine et al. [129] for the first time reported ~5 % of the cell volume is occupied by SR in aorta and PASM in rabbit compared to only ~2 % in smooth muscle present in mesenteric vein, artery and portal vein. This alone establishes a possible requirement of considerably higher SERCA activity in maintaining physiological Ca^{2+} concentration in PASM. We have studied the cooperative nature of PMCA, SERCA (ATP dependent Ca^{2+} uptake), and NCX (Na^+ dependent Ca^{2+} uptake) activity in microsomes isolated from bovine PASM under oxidant treated conditions [7, 65, 66]. We found that oxidant treatments cause significant increase in both PMCA and SERCA activity with a decrease in NCX activity. MMP-2 activity was found to increase markedly in all these studies [7].

In this regard basal PMCA, SERCA, and NCX activities in cultured endothelial cells (EC) and smooth muscle cells (SMC) isolated from pig coronary artery are worth mentioning. PMCA and SERCA activities were low in EC than SMC. SMC possesses a higher NCX activity than EC [130]. No such comparison has, however, been reported for EC and SMC in pulmonary artery but it appears that NCX plays a significant role in maintaining basal Ca^{2+} homeostasis in microsomes of pulmonary artery smooth muscle [7, 65, 66].

Our knowledge has advanced considerably with the development of specific SERCA inhibitors, such as cyclopyazonic acid (CPA) [131] and thapsigargin (TG) [132]. NCX is often inhibited by replacing extracellular Na^+ or using the reverse mode inhibitor, KB-R7943, or forward mode inhibitor, SEA0400 [124] depending upon directionality of the Ca^{2+} transport. NKA can be specifically inhibited by ouabain, affecting the coupled NKA, NCX, SERCA calcium regulatory mechanisms in pulmonary arterial cells under normal and stimulated conditions. Use of conditional gene-targeted or transgenic mice models with altered Ca^{2+} clearance components is

of particular use in terms of dissecting out the specific function of the multitude of isoforms. Interpretation is limited in the sense that compensatory changes in other components can occur, but often the compensation itself may be the most interesting aspect.

12 Conclusions and Future Direction

A reasonable number of evidence suggest that oxidative stress plays an important role in the injurious and inflammatory responses in pulmonary diseases such as asthma, COPD, and PAH. Air pollutants, cigarette smoke, suspended ultrafine particulate materials and heavy metals, etc. in addition to endogenously generated vasoactive active agents such as thromboxanes, endothelin and cytokines are considered as the major factors that contribute to an increase in oxidative stress in the pulmonary vasculature. There are certain disease conditions such as PAH and *cor pulmonale*, where pulmonary arterial endothelial and smooth muscle cells play pivotal roles and that dysregulation in the activities of SERCA, NKA, NCX, and PMCA contribute to the development of the disease pathology. Under certain stress conditions, dysregulation of cooperative mechanism among SERCA, NKA, and NCX has been observed in pulmonary artery endothelial and smooth muscle cells. Due to availability of specific pharmacological inhibitors such as CPA and TG and the SERCA2 knockout transgenic mice [133], a number of information are now available demonstrating SERCA as a determining factor for such a fine control of intracellular Ca^{2+} into the ER stores [133].

Although oxidative stress has been reported to negatively affect Ca^{2+}-ATPase in systemic vessels, research from our laboratory have established oxidative stress as a positive regulator of Ca^{2+}-ATPase activity in pulmonary artery endothelial and smooth muscle cells and that has later been identified as SERCA2b [110]. The link between selective inhibition of MMP-2 and subsequent increase in Ca^{2+}-ATPase activity and inhibition of Na^{+} dependent Ca^{2+} uptake (NCX) also helped, at least partly, understanding critical Ca^{2+} mediated cross talk between SERCA2b, NCX, aprotinin sensitive serine protease, and MMP-2, which has strong implications in elevating $[Ca^{2+}]_i$. Recent advancements in treating HF with adeno associated viral vector serotype (AAV1) containing SERCA2a gene showed promise in a phase I clinical trial [134] and this suggests that further improvements in vector and delivery method might improve the efficacy of treatment. Similar gene therapy strategy could be promising in treating pulmonary vasculature to restore physiological SERCA activity under oxidant burden in the lung.

Further research warrants understanding of the cellular and molecular adaptation to hypoxia in human that will equip us with better therapeutic intervention in treating patients suffering from COPD and secondary PAH. Irrespective of the source of oxidant species, the underlying signaling mechanisms causing especially SERCA dysregulation has significant implications in pulmonary vascular diseases such as PAH, right ventricular hypertrophy and *cor pulmonale*, which remains as an important area that demands further research.

Acknowledgements Financial assistance from the Department of Science and Technology (Govt. of India) and the Indian Council of Medical Research (I.C.M.R) is greatly acknowledged.

References

1. Strehler EE, Caride AJ, Filoteo AG et al (2007) Plasma membrane Ca^{2+}-ATPases as dynamic regulators of cellular calcium handling. Ann N Y Acad Sci 1099:226–36
2. Strehler EE, Treiman M (2004) Calcium pumps of plasma membrane and cell interior. Curr Mol Med 4:323–35
3. Periasamy M, Huke S (2001) SERCA Pump level is a critical determinant of Ca^{2+} homeostasis and cardiac contractility. J Mol Cell Cardiol 33:1053–63
4. Periasamy M, Kalyanasundaram A (2007) SERCA pump isoforms: their role in calcium transport and disease. Muscle Nerve 35:430–42
5. Fraser LR, Umar G, Sayed S (1993) Na^+-requiring mechanisms modulate capacitation and acrosomal exocytosis in mouse spermatozoa. J Reprod Fertil 97:539–49
6. Blaustein MP, Lederer WJ (1999) Sodium/calcium exchange: its physiological implications. Physiol Rev 79:763–854
7. Chakraborti S, Mandal A, Das S et al (2004) Inhibition of Na^+/Ca^{2+} exchanger by peroxynitrite in microsomes of pulmonary smooth muscle: role of matrix metalloproteinase-2. Biochim Biophys Acta 1671:70–78
8. Zima AV, Blatter LA (2006) Redox regulation of cardiac calcium channels and transporters. Cardiovasc Res 71:310–321
9. Grover AK, Samson SE (1988) Effect of superoxide radical on Ca^{2+} pumps of coronary artery. Am J Physiol Cell Physiol 255:C297–C303
10. Grover AK, Samson SE, Fomin VP (1992) Peroxide inactivates calcium pumps in pig coronary artery. Am J Physiol Cell Physiol 263:H537–H543
11. Grover AK, Samson SE, Fomin VP et al (1995) Effects of peroxide and superoxide on coronary artery: ANG II response and sarcoplasmic reticulum Ca^{2+} pump. Am J Physiol Cell Physiol 269:C546–C553
12. Lancel S, Zhang J, Evangelista A et al (2009) Nitroxyl Activates SERCA in cardiac myocytes via glutathiolation of cysteine 674. Circ Res 104:720–723
13. Qin F, Siwik DA, Lancel S et al (2013) Hydrogen peroxide-mediated SERCA cysteine 674 oxidation contributes to impaired cardiac myocyte relaxation in senescent mouse heart. J Am Heart Assoc 2:1–9
14. Qin F, Siwik DA, Pimentel DR et al (2014) Cytosolic H_2O_2 mediates hypertrophy, apoptosis, and decreased SERCA activity in mice with chronic hemodynamic overload. Am J Physiol Heart Circ Physiol 306:H1453–H1463
15. Cohen RA, Tong X (2010) Vascular oxidative stress: the common link in hypertensive and diabetic vascular disease. J Cardiovasc Pharmacol 55:308–316
16. Lounsbury KM, Hu Q, Ziegelstein RC (2000) Calcium signaling and oxidant stress in the vasculature. Free Radic Biol Med 28:1362–1369
17. Abdollahi M, Ranjbar A, Shadnia S et al (2004) Pesticides and oxidative stress: a review. Med Sci Monit 10:141–147
18. Kelly FJ (2003) Oxidative stress: its role in air pollution and adverse health effects. Occup Environ Med 60:612–616
19. Donaldson K, Stone V, Borm PJA et al (2003) Oxidative stress and calcium signaling in the adverse effects of environmental particles (PM10). Free Radic Biol Med 34:1369–1382
20. Oberdorster G (2001) Pulmonary effects of inhaled ultrafine particles. Int Arch Occup Environ Health 74:1–8
21. Lau EMT, Humbert M, Celermajer DS (2015) Early detection of pulmonary arterial hypertension. Nat Rev Cardiol 12:143–155

22. McLaughlin VV, McGoon MD (2006) Pulmonary arterial hypertension. Circulation 114:1417–1431
23. Yuan JX, Rubin LJ (2005) Pathogenesis of pulmonary arterial hypertension: the need for multiple hits. Circulation 111:534–538
24. Cody RJ, Haas GJ, Binkley PF (1992) Plasma endothelin correlates with the extent of pulmonary hypertension in patients with chronic congestive heart failure. Circulation 85:504–509
25. Galié N, Manes A, Branzi A (2004) The endothelin system in pulmonary arterial hypertension. Cardiovasc Res 61:227–237
26. Behr J, Ryu JH (2008) Pulmonary hypertension in interstitial lung disease. Eur Respir J 31:1357–1367
27. Lettieri CJ, Nathan SD, Barnett SD et al (2006) Revalence and outcomes of pulmonary arterial hypertension in advanced idiopathic pulmonary fibrosis. Chest 129:746–752
28. Church DF, Pryor WA (1985) Free-radical chemistry of cigarette smoke and its toxicological implications. Environ Health Perspect 64:111–126
29. Abboud RT, Fera T, Richter A et al (1985) Acute effect of smoking on the functional activity of alpha1-protease inhibitor in bronchoalveolar lavage fluid. Am Rev Respir Dis 131:79–85
30. Rajagopalan S, Kurz S, Münzel T et al (1996) Angiotensin II-mediated hypertension in the rat increases vascular superoxide production via membrane NADH/NADPH oxidase activation. Contribution to alterations of vasomotor tone. J Clin Invest 97:1916–1923
31. Meier B, Radeke HH, Selle S et al (1989) Human fibroblasts release reactive oxygen species in response to interleukin-1 or tumour necrosis factor-alpha. Biochem J 263:539–545
32. Matsubara T, Ziff M (1986) Superoxide anion release by human endothelial cells: synergism between a Phorbol ester and a calcium ionophore. J Cell Physiol 127:207–210
33. Matsubara T, Ziff M (1986) Increased superoxide anion release from human endothelial cells in response to cytokines. J Immunol 137:3295–3298
34. Griendling KK, Minieri CA, Ollerenshaw JD et al (1994) Angiotensin II stimulates NADH and NADPH oxidase activity in cultured vascular smooth muscle cells. Circ Res 74:1141–1148
35. Thomae KR, Joshi PC, Davies P et al (1996) Nitric oxide produced by cytokine-activated pulmonary artery smooth muscle cells is cytotoxic to cocultured endothelium. Surgery 119:61–66
36. Moncada S, Rees DD, Schulz R et al (1991) Development and mechanism of a specific supersensitivity to nitrovasodilators after inhibition of vascular nitric oxide synthesis in vivo. Proc Natl Acad Sci U S A 88:2166–2170
37. De Keulenaer GW, Alexander RW, Ushio-Fukai M et al (1998) Tumour necrosis factor alpha activates a p22phox-based NADH oxidase in vascular smooth muscle. Biochem J 329:653–657
38. Chakraborti S, Chowdhury A, Kar P et al (2009) Role of protein kinase C in NADPH oxidase derived $O_2^{\cdot-}$-mediated regulation of KV-LVOCC axis under U46619 induced increase in $[Ca^{2+}]_i$ in pulmonary smooth muscle cells. Arch Biochem Biophys 487:123–130
39. Stralin P, Marklund SL (1994) Effects of oxidative stress on expression of extracellular superoxide dismutase, CuZn-superoxide dismutase and Mn-superoxide dismutase in human dermal fibroblasts. Biochem J 298:347–352
40. Tsan MF (2001) Superoxide dismutase and pulmonary oxygen toxicity: lessons from transgenic and knockout mice. Int J Mol Med 7:13–19
41. Beckman DL, Mehta P, Hanks V et al (2000) Effects of peroxynitrite on pulmonary edema and the oxidative state. Exp Lung Res 26:349–359
42. Wedgwood S, McMullan DM, Bekker JM et al (2001) Role for endothelin-1-induced superoxide and peroxynitrite production in rebound pulmonary hypertension associated with inhaled nitric oxide therapy. Circ Res 89:357–364
43. Chemaly ER, Bobe R, Adnot S et al (2013) Sarco (endo) plasmic reticulum calcium ATPases (SERCA) isoforms in the normal and diseased cardiac, vascular and skeletal muscle. J Cardiovasc Dis Diagn 1:2–6

44. Pauly RR, Bilato C, Cheng L et al (1997) Vascular smooth muscle cell cultures. Methods Cell Biol 52:133–154
45. Clark JH, Kinnear NP, Kalujnaia S et al (2010) Identification of functionally segregated sarcoplasmic reticulum calcium stores in pulmonary arterial smooth muscle. J Biol Chem 285:13542–13549
46. Lipskaia L, Limon I, Bobe R et al (2012) In Sugi H (Ed.) Calcium cycling in synthetic and contractile phasic or tonic vascular smooth muscle cells. Current basic and pathological approaches to the function of muscle cells and tissues–from molecules to humans, Rijeka, Croatia, Intech Publishers, Chapter 2: 28–44
47. Khan I, Sandhu V, Misquitta C et al (2000) SERCA pump isoform expression in endothelium of veins and arteries: every endothelium is not the same. Mol Cell Biochem 203:11–15
48. Humbert M, Morrell NW, Archer SL et al (2004) Cellular and molecular pathobiology of pulmonary arterial hypertension. J Am Coll Cardiol 43:S13–S24
49. Hadri L, Kratlian RG, Benard L et al (2013) Therapeutic efficacy of AAV1.SERCA2a in monocrotaline-induced pulmonary arterial hypertension. Circulation 128:512–523
50. Davies RJ, Morrell NW (2008) Molecular mechanisms of pulmonary arterial hypertension: role of mutations in the bone morphogenetic protein type II receptor. Chest 134:1271–1277
51. Voelkel NF, Cool C (2004) Pathology of pulmonary hypertension. Cardiol Clin 22:343–351
52. Lipskaia L, del Monte F, Capiod T et al (2005) Sarco/endoplasmic reticulum Ca^{2+}-ATPase gene transfer reduces vascular smooth muscle cell proliferation and neointima formation in the rat. Circ Res 97:488–495
53. Bobe R, Hadri L, Lopez JJ et al (2011) SERCA2a controls the mode of agonist-induced intracellular Ca^{2+} signal, transcription factor NFAT and proliferation in human vascular smooth muscle cells. J Mol Cell Cardiol 50:621–633
54. Kawase Y, Hajjar RJ (2008) The cardiac sarcoplasmic/endoplasmic reticulum calcium ATPase: a potent target for cardiovascular diseases. Nat Clin Pract Cardiovasc Med 5:554–565
55. Chakraborti T, Das S, Mandal M et al (2002) Role of Ca^{2+}-dependent metalloprotease-2 in stimulating Ca^{2+}ATPase activity under peroxynitrite treatment in bovine pulmonary artery smooth muscle membrane. IUBMB Life 53:167–173
56. Chakraborti T, Ghosh SK, Michael JR et al (1996) Role of an aprotinin-sensitive protease in the activation of Ca^{2+}-ATPase by superoxide radical (O_2^{-}) in microsomes of pulmonary vascular smooth muscle. Biochem J 317:885–890
57. Qin Z, Hou X, Weisbrod RM, Seta F et al (2014) Nox2 mediates high fat high sucrose diet-induced nitric oxide dysfunction and inflammation in aortic smooth muscle cells. J Mol Cell Cardiol 72:56–63
58. Zhang J, Li Y, Jiang S et al (2014) Enhanced endoplasmic reticulum SERCA activity by overexpression of hepatic stimulator substance gene prevents hepatic cells from ER stress-induced apoptosis. Am J Physiol Cell Physiol 306:C279–C290
59. Tang WH, Cheng WT, Kravtsov GM et al (2010) Cardiac contractile dysfunction during acute hyperglycemia due to impairment of SERCA by polyol pathway-mediated oxidative stress. Am J Physiol Cell Physiol 299:C643–C653
60. Kuster GM, Lancel S, Zhang J et al (2010) Redox-mediated reciprocal regulation of SERCA and Na^{+}/Ca^{2+} exchanger contributes to sarcoplasmic reticulum Ca^{2+} depletion in cardiac myocytes. Free Radic Biol Med 48:1182–1187
61. Perrier E, Fournet-Bourguignon M-P, Royere E et al (2009) Effect of uncoupling endothelial nitric oxide synthase on calcium homeostasis in aged porcine endothelial cells. Cardiovasc Res 82:133–142
62. Flesch M, Maack C, Cremers B et al (1999) Effect of β-blockers on free radical-induced cardiac contractile dysfunction. Circulation 100:346–353
63. Scherer N, Deamer D (1986) Oxidative stress impairs the function of sarcoplasmic reticulum by oxidation of sulfhydryl groups in the Ca^{2+}-ATPase. Arch Biochem Biophys 246:589–601

64. Suzuki YJ, Ford GD (1991) Inhibition of Ca^{2+}-ATPase of vascular smooth muscle sarcoplasmic reticulum by reactive oxygen intermediates. Am J Physiol Heart Circ Physiol 261:H568–H574
65. Mandal A, Chakraborti T, Das S et al (2004) Matrix metalloproteinase-2-mediated inhibition of Na^{+}-dependent Ca^{2+} uptake by superoxide radicals (O_2^{-}) in microsomes of pulmonary smooth muscle. IUBMB Life 56:267–276
66. Das S, Chakraborti T, Mandal M et al (2002) Role of membrane-associated Ca^{2+} dependent matrix metalloprotease-2 in the oxidant activation of Ca^{2+}-ATPase by tertiary butylhydroperoxide. Mol Cell Biochem 237:85–93
67. Moreau VH, Castilho RF, Ferreira ST et al (1998) Oxidative damage to sarcoplasmic reticulum Ca^{2+}-ATPase at submicromolar iron concentrations: evidence for metal-catalyzed oxidation. Free Radic Biol Med 25:554–560
68. Grover AK, Samson SE, Robinson S et al (2003) Effects of peroxynitrite on sarcoplasmic reticulum Ca^{2+} pump in pig coronary artery smooth muscle. Am J Physiol Cell Physiol 284:C294–C301
69. Murray PA, Lodato RF, Michael JR (1986) Neural antagonists modulate pulmonary vascular pressure-flow plots in conscious dogs. J Appl Physiol 60:1900–1907
70. Robinson BF, Collier JG, Karim SM et al (1973) Effect of prostaglandins A1, A2, B1, E2 and F2 on forearm arterial bed and superficial hand veins in man. Clin Sci 44:367–376
71. Taggart MJ, Wray S (1998) Hypoxia and smooth muscle function: key regulatory events during metabolic stress. J Physiol 509:315–325
72. Blaustein MP (1996) Endogenous ouabain: role in the pathogenesis of hypertension. Kidney Int 49:1748–1753
73. Wang Y, Zhang L, Shen W et al (1999) Interrelation between nitric oxide and endothelin-1 in an experimental acute hypoxia in rats and its intervention. Chin Med J (Engl) 112:363–365
74. Hampl V, Herget J (2000) Role of nitric oxide in the pathogenesis of chronic pulmonary hypertension. Physiol Rev 80:1337–72
75. Budhiraja R, Tuder RM, Hassoun PM (2004) Endothelial dysfunction in pulmonary hypertension. Circulation 109:1591–65
76. Putney JWJ, Aub DL, Taylor CW et al (1986) Formation and biological action of inositol 1,4,5-trisphosphate. Fed Proc 45:2634–2638
77. Makino A, Firth AL, Yuan JX (2011) Endothelial and smooth muscle cell ion channels in pulmonary vasoconstriction and vascular remodeling. Comp Physiol 1:1555–1602
78. Leung FP, Yung LM, Yao X et al (2008) Store-operated calcium entry in vascular smooth muscle. Br J Pharmacol 153:846–857
79. Kwan CY, Chaudhary R, Zheng XF et al (1994) Effects of sarcoplasmic reticulum calcium pump inhibitors on vascular smooth muscle. Hypertension 23:I156–1160
80. Low AM, Loke JC, Kwan CY et al (1994) Sensitivity to protein kinase C inhibitors of nicardipine-insensitive component of high K^{+} contracture in rat and guinea-pig aorta. Br J Pharmacol 112:604–610
81. Tepel M, Ruess C, Mehring N et al (1994) Effect of inhibition of sarcoplasmic Ca^{2+}-ATPase on vasoconstriction and cytosolic Ca^{2+} in aortic smooth muscle from spontaneously hypertensive and normotensive rats. Clin Exp Hypertens 16:493–506
82. Xuan YT, Glass PS (1996) Propofol regulation of calcium entry pathways in cultured A10 and rat aortic smooth muscle cells. Br J Pharmacol 117:5–12
83. Noguera MA, Ivorra MD, Chuliá S et al (1997) Capacitative Ca^{2+} entry associated with alpha1-adrenoceptors in rat aorta. Naunyn Schmiedebergs Arch Pharmacol 356:83–89
84. Tosun M, Paul RJ, Rapoport RM (1998) Coupling of store-operated Ca^{++} entry to contraction in rat aorta. J Pharmacol Exp Ther 285:759–766
85. Gonzalez DLFP, Savineau JP, Marthan R (1995) Control of pulmonary vascular smooth muscle tone by sarcoplasmic reticulum Ca^{2+} pump blockers: thapsigargin and cyclopiazonic acid. Pflugers Arch 429:617–624

86. Aguero J, Ishikawa K, Hadri L et al (2014) Characterization of right ventricular remodeling and failure in a chronic pulmonary hypertension model. Am J Physiol Heart Circ Physiol 307:H1204–H215
87. Wu J, Luo X, Huang Y et al (2015) Hemodynamics and right-ventricle functional characteristics of a swine carotid artery-jugular vein shunt model of pulmonary arterial hypertension: An 18-month experimental study. Exp Biol Med pii: 1535370214566561. [Epub ahead of print]
88. Baker JE, Felix CC, Olinger GN et al (1988) Myocardial ischemia and reperfusion: direct evidence for free radical generation by electron spin resonance spectroscopy. Proc Natl Acad Sci U S A 85:2786–9
89. Goldhaber JI, Weiss JN (1992) Oxygen free radicals and cardiac reperfusion abnormalities. Hypertension 20:118–127
90. Henry TD, Archer SL, Nelson D et al (1990) Enhanced chemiluminescence as a measure of oxygen-derived free radical generation during ischemia and reperfusion. Circ Res 67:1453–1461
91. Kaul N, Siveski-Iliskovic N, Hill M et al (1993) Free radicals and the heart. J Pharmacol Toxicol Methods 30:55–67
92. Kaneko M, Matsumoto Y, Hayashi H et al (1994) Oxygen free radicals and calcium homeostasis in the heart. Mol Cell Biochem 139:91–100
93. Elmoselhi A, Butcher A, Samson S et al (1994) Free radicals uncouple the sodium pump in pig coronary artery. Am J Physiol Cell Physiol 266:C720–C728
94. Kukreja RC, Weaver AB, Hess ML (1990) Sarcolemmal Na^+-K^+-ATPase: inactivation by neutrophil-derived free radicals and oxidants. Am J Physiol Heart Circ Physiol 259:H1330–H336
95. Rubanyi GM, Vanhoutte PM (1986) Oxygen-derived free radicals, endothelium, and responsiveness of vascular smooth muscle. Am J Physiol Heart Circ Physiol 250:H815–H821
96. Yu Y, Fantozzi I, Remillard CV et al (2004) Enhanced expression of transient receptor potential channels in idiopathic pulmonary arterial hypertension. Proc Natl Acad Sci U S A 101:13861–13866
97. Zhang S, Patel HH, Murray F et al (2007) Pulmonary artery smooth muscle cells from normal subjects and IPAH patients show divergent cAMP-mediated effects on TRPC expression and capacitative Ca^{2+} entry. Am J Physiol Lung Cell Mol Physiol 292:L1202–L210
98. Song MY, Makino A, Yuan JX (2011) STIM2 contributes to enhanced store-operated Ca^{2+} entry in pulmonary artery smooth muscle cells from patients with idiopathic pulmonary arterial hypertension. Pulm Circ 1:84–94
99. Morrell NW, Adnot S, Archer SL et al (2009) Cellular and molecular basis of pulmonary arterial hypertension. J Am Coll Cardiol 54:S20–S31
100. Yamamura A, Yamamura H, Zeifman A et al (2011) Activity of Ca^{2+}-activated Cl^- channels contributes to regulating receptor- and store-operated Ca^{2+} entry in human pulmonary artery smooth muscle cells. Pulm Circ 1:269–279
101. Ko EA, Wan J, Yamamura A et al (2013) Functional characterization of voltage-dependent Ca^{2+} channels in mouse pulmonary arterial smooth muscle cells: divergent effect of ROS. Am J Physiol Cell Physiol 304:C1042–C1052
102. Wan J, Yamamura A, Zimnicka AM et al (2013) Chronic hypoxia selectively enhances L- and T-type voltage-dependent Ca^{2+} channel activity in pulmonary artery by upregulating Cav1.2 and Cav3.2. Am J Physiol Lung Cell Mol Physiol 305:L154–L164
103. Zheng Y-M, Wang Y-X (2007) Sodium–calcium exchanger in pulmonary artery smooth muscle cells. Ann N Y Acad Sci 1099:427–435
104. Wang YP, Oike M, Ito Y (1999) Effects of superoxide anion on intracellular Ca^{2+} concentration in rabbit pulmonary arterial smooth muscle cells. Zhongguo Yao Li Xue Bao 20:10–14
105. Chakraborti S, Michael JR (1991) Involvement of a serine esterase in oxidant-mediated activation of phospholipase A_2 in pulmonary endothelium. FEBS Lett 281:185–7
106. Gipson TS, Bless NM, Shanley TP (1999) Regulatory effects of endogenous protease inhibitors in acute lung inflammatory injury. J Immunol 162:3653–3662

107. Fernandez-Patron C, Zouki C, Whittal R et al (2001) Matrix metalloproteinases regulate neutrophil-endothelial cell adhesion through generation of endothelin-1[1-32]. FASEB J 15:2230–2240
108. Ramchandran R, Kasturi S, Douglas JG et al (1996) Metalloprotease-mediated cleavage secretion of pulmonary ACE by vascular endothelial and kidney epithelial cells. Am J Physiol Heart Circ Physiol 271:H744–H51
109. Liu Y, Huang H, Xia W et al (2010) NADPH oxidase inhibition ameliorates cardiac dysfunction in rabbits with heart failure. Mol Cell Biochem 343:143–153
110. Mandal A, Das S, Chakraborti T et al (2006) Solubilization, purification and reconstitution of Ca^{2+}-ATPase from bovine pulmonary artery smooth muscle microsomes by different detergents: Preservation of native structure and function of the enzyme by DHPC. Biochim Biophys Acta 1760:20–31
111. Chakraborti S, Mandal A, Das S et al (2005) Role of MMP-2 in PKCδ-mediated inhibition of Na^+ dependent Ca^{2+} uptake in microsomes of pulmonary smooth muscle: Involvement of a pertussis toxin sensitive protein. Mol Cell Biochem 280:107–117
112. Beckman JS, Beckman TW, Chen J et al (1990) Apparent hydroxyl radical production by peroxynitrite: implications for endothelial injury from nitric oxide and superoxide. Proc Natl Acad Sci U S A 87:1620–1624
113. Zweier JL, Wang P, Samouilov A et al (1995) Enzyme-independent formation of nitric oxide in biological tissues. Nat Med 1:804–809
114. Radi R, Beckman JS, Bush KM et al (1991) Peroxynitrite oxidation of sulfhydryls. The cytotoxic potential of superoxide and nitric oxide. J Biol Chem 266:4244–4250
115. Ischiropoulos H, Al-Mehdi AB (1995) Peroxynitrite-mediated oxidative protein modifications. FEBS Lett 364:279–82
116. Donnini S, Monti M, Roncone R et al (2008) Peroxynitrite inactivates human-tissue inhibitor of metalloproteinase-4. FEBS Lett 582:1135–1140
117. Frears ER, Zhang Z, Blake DR et al (1996) Inactivation of tissue inhibitor of metalloproteinase-1 by peroxynitrite. FEBS Lett 381:21–24
118. Bigelow DJ, Squier TC (2005) Redox modulation of cellular signaling and metabolism through reversible oxidation of methionine sensors in calcium regulatory proteins. Biochim Biophys Acta 1703:121–134
119. Ishida Y, Paul RJ (2005) Ca^{2+} clearance in smooth muscle: lessons from gene-altered mice. J Smooth Muscle Res 41:235–245
120. Shull GE (2000) Gene knockout studies of Ca^{2+}-transporting ATPases. Eur J Biochem 267:5284–5290
121. Firth AL, Remillard CV, Yuan JX (2007) TRP channels in hypertension. Biochim Biophys Acta 1772:895–906
122. Liu D, Yang D, He H et al (2009) Increased transient receptor potential canonical type 3 channels in vasculature from hypertensive rats. Hypertension 53:70–76
123. Pulina MV, Zulian A, Berra-Romani R et al (2010) Upregulation of Na^+ and Ca^{2+} transporters in arterial smooth muscle from ouabain-induced hypertensive rats. Am J Physiol Heart Circ Physiol 298:H263–H274
124. Iwamoto T, Kita S, Zhang J et al (2004) Salt-sensitive hypertension is triggered by Ca^{2+} entry via Na^+/Ca^{2+} exchanger type-1 in vascular smooth muscle. Nat Med 10:1193–1139
125. Zhang S, Dong H, Rubin LJ et al (2007) Upregulation of Na^+/Ca^{2+} exchanger contributes to the enhanced Ca^{2+} entry in pulmonary artery smooth muscle cells from patients with idiopathic pulmonary arterial hypertension. Am J Physiol Cell Physiol 292:C2297–C2305
126. Lin M-J, Leung GPH, Zhang W-M et al (2004) Chronic hypoxia-induced upregulation of store-operated and receptor-operated Ca^{2+} channels in pulmonary arterial smooth muscle cells: a novel mechanism of hypoxic pulmonary hypertension. Circ Res 95:496–505
127. Weigand L, Foxson J, Wang J et al (2005) Inhibition of hypoxic pulmonary vasoconstriction by antagonists of store-operated Ca^{2+} and nonselective cation channels. Am J Physiol Lung Cell Mol Physiol 289:L5–L13

128. Zhang S, Yuan JX, Barrett KE et al (2005) Role of Na^+/Ca^{2+} exchange in regulating cytosolic Ca^{2+} in cultured human pulmonary artery smooth muscle cells. Am J Physiol Cell Physiol 288:C245–C252
129. Devine CE, Somlyo AV, Somlyo AP (1972) Sarcoendoplasmic reticulum and excitation-contraction coupling in mammalian smooth muscles. J Cell Biol 52:690–718
130. Szewczyk MM, Davis KA, Samson SE et al (2007) Ca^{2+}-pumps and Na^+–Ca^{2+}-exchangers in coronary artery endothelium versus smooth muscle. J Cell Mol Med 11:129–138
131. Luo DL, Nakazawa M, Ishibashi T et al (1993) Putative, selective inhibitors of sarcoplasmic reticulum Ca^{++}-pump ATPase inhibit relaxation by nitroglycerin and atrial natriuretic factor of the rabbit aorta contracted by phenylephrine. J Pharmacol Exp Therap 265:1187–1192
132. Bian JH, Ghosh TK, Wang JC et al (1991) Identification of intracellular calcium pools. Selective modification by thapsigargin. J Biol Chem 266:8801–8806
133. Li L, Louch WE, Niederer SA et al (2011) Calcium dynamics in the ventricular myocytes of SERCA2 knockout mice: a modeling study. Biophys J 100:322–331
134. Zsebo K, Yaroshinsky A, Rudy JJ et al (2014) Long-term effects of AAV1/SERCA2a gene transfer in patients with severe heart failure: Analysis of recurrent cardiovascular events and mortality. Circ Res 114:101–108
135. Crosswhite P, Sun Z (2010) Nitric oxide, oxidative stress and inflammation in pulmonary arterial hypertension. J Hypertens 28:201–212
136. Shimoda LA, Undem C (2010) Interactions between calcium and reactive oxygen species in pulmonary arterial smooth muscle responses to hypoxia. Respir Physiol Neurobiol 174:221–229

Chapter 13
Plant Type 2B Ca^{2+}-ATPases: The Diversity of Isoforms of the Model Plant *Arabidopsis thaliana*

Maria Cristina Bonza, Laura Luoni, Claudio Olivari, and Maria Ida De Michelis

Abstract In plant cells, Ca^{2+} extrusion from the cytoplasm is accomplished either through Ca^{2+}-H^+ antiporters powered by a proton-motive force or through Ca^{2+} pumps powered by ATP hydrolysis. Plants possess two types of Ca^{2+}-pumping ATPase, named ECAs (for ER-type Ca^{2+}-ATPase) and ACAs (for auto-inhibited Ca^{2+}-ATPase), which group respectively with animal sarco-endoplasmic reticulum Ca^{2+}-ATPase in the 2A subgroup of P-type ATPases or with plasma membrane Ca^{2+}-ATPase in the 2B subgroup. Each type comprises different isoforms, localized on different membranes. Here, we summarize available knowledge of the biochemical characteristics and the physiological role of ACAs, focusing on what we have learnt from analysis of the model plant *Arabidopsis thaliana*.

Keywords Ca^{2+}-ATPase • *Arabidopsis thaliana* • Calmodulin • Phosphorylation • Phospholipids • Calcium homeostasis • Development • Stress

1 Introduction

As other eukaryotes, plants use cytosolic Ca^{2+} as a second messenger in the transduction of a variety of endogenous and environmental signals. Fine tuning of cytosolic Ca^{2+} is realized by regulation of Ca^{2+} channels and active Ca^{2+} transport systems localized at the plasma membrane (PM) or at the membranes of intracellular stores as the endoplasmic reticulum (ER) or the vacuole (tonoplast, TP). Stimulus-induced opening of Ca^{2+} channels followed by Ca^{2+} extrusion—to the apoplast or

M.C. Bonza • L. Luoni • C. Olivari • M.I. De Michelis (✉)
Dipartimento di Bioscienze, Università degli Studi di Milano, Istituto di Biofisica del CNR, Sezione di Milano, via G. Celoria 26, 20133 Milan, Italy
e-mail: mariaida.demichelis@unimi.it

S. Chakraborti, N.S. Dhalla (eds.), *Regulation of Ca^{2+}-ATPases,V-ATPases and F-ATPases*, Advances in Biochemistry in Health and Disease 14,
DOI 10.1007/978-3-319-24780-9_13

intracellular stores—generates transient increases of cytosolic calcium concentration (Ca^{2+} waves), whose amplitude, frequency, and localization encode signal specificity [1–8]. Active Ca^{2+} transport systems include both Ca^{2+}/H^+ antiporters driven by the electrochemical H^+ gradient generated by H^+ pumps and Ca^{2+}-ATPases. While Ca^{2+}/H^+ antiporters are low-affinity, high-capacity transporters mainly—if not exclusively—localized at the TP, Ca^{2+}-ATPases are high-affinity, low-capacity pumps resident in the PM, ER, TP, and Golgi membranes [2, 4, 9–14].

Several genes encoding plant Ca^{2+}-ATPases have been cloned since the early 90s and phylogenetic analysis has shown that they group either with animal SERCA (sarco-endoplasmic reticulum Ca^{2+}-ATPase) in the 2A subgroup of P-type ATPases or with PMCA (plasma membrane Ca^{2+}-ATPase) in the 2B subgroup [9–16]. Since in plant cells each Ca^{2+} pump type is not restricted to one particular organelle or membrane, they have been named ECA (ER-type Ca^{2+}-ATPase) and ACA (autoinhibited Ca^{2+}-ATPase) respectively [9–14]. We will focus on ACAs, providing a picture of what we have learnt from biochemical, genetic, and physiological analysis of the model plant *Arabidopsis thaliana*.

2 Common Features

2.1 Structure

Like other members of the type 2 subgroup of P-type ATPases, plant ACAs (Fig. 13.1) are single polypeptides of 1000–1100 aa having 10 transmembrane domains (TM), a cytoplasmic head consisting of a large loop between TM 4 and TM 5—which contains the nucleotide binding and the phosphorylation domain—and a small loop between TM 2 and TM 3, which is part of the actuator domain [12, 15–19]. ACAs contain all the characteristic motifs of the type 2 subgroup of P-type ATPases including the highly conserved sequence DKTGT containing the phosphorylated Asp, the PEGL motif considered to play a central role in energy transduction and the KGAXE sequence involved in nucleotide binding [12, 15–17, 20]. The distinctive feature of ACAs is the extended cytosolic N-terminus preceding the first TM whose regulatory properties are discussed below [9–14].

2.2 Transport Mechanism and Biochemical Properties

The ATP/Ca^{2+} stoichiometry of ACAs has not been determined, but it is reasonable to assume that they operate with a 1:1 stoichiometry as PMCA [15, 16]. In fact—as for PMCA—only residues defining SERCA Ca^{2+}-binding site 2 are conserved in ACAs and their kinetics as a function of Ca^{2+} concentration is simple, with no sign of cooperativity [21–23]. Similar to PMCA, ACAs catalyze a Ca^{2+}/H^+ exchange of unknown stoichiometry [24–26], a mechanistic feature shared by type 2A Ca^{2+}-ATPases as SERCA [15, 27]. Recent analysis based on the crystal structure of

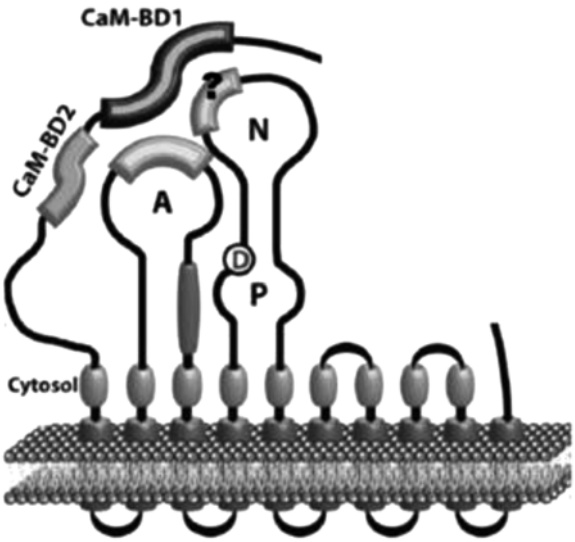

Fig. 13.1 Schematic representation of ACAs. A: actuator domain; N: nucleotide binding domain; P: phosphorylation domain, where D is the Asp phosphorylated in the catalytic cycle; CaM-BD: CaM binding domain. Modified from Lopreiato et al. [19]

SERCA strongly indicates that charges of residues involved in Ca^{2+} binding must be partially or entirely compensated for by other cations once Ca^{2+} is released, making counter-transport mandatory of these pumps [27–29].

ACAs share most biochemical traits of P-type ATPase, but most isoforms (see below for exceptions) are unique for being able to use ITP or GTP as an alternative nucleoside-triphosphate substrate to ATP: this characteristic allows determination of their hydrolytic activities in membrane fractions containing high levels of other P-type ATPases such as, e.g., plant PM H^+-ATPase [30]. ACAs are particularly sensitive to inhibition by fluorescein derivatives, such as erythrosin B or eosin yellow, which are known to bind to the nucleotide binding domain [9, 12, 24, 30–35]. The relation between these two features of the catalytic site is not clear; however ACA12, an *A. thaliana* isoform, which is unable to use ITP as a substrate is also less sensitive to eosin yellow [36].

2.3 Regulation

ACAs share with other type 2B Ca^{2+}-ATPases an extended terminal domain which confers unique regulatory properties. However, while in PMCAs this domain is localized in the extended C-terminus of the protein [15, 19], ACAs have a very short C-terminus after the tenth TM and an extended cytosolic N-terminus preceding the first TM [9–14, 18].

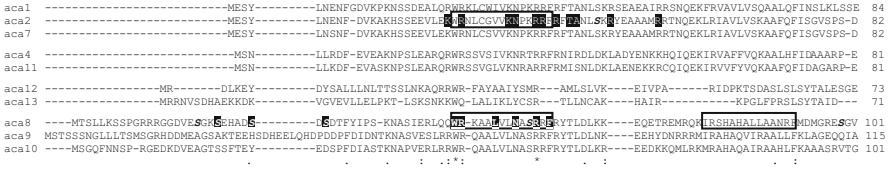

Fig. 13.2 Alignment of *A. thaliana* ACAs N-terminus. CaM binding domains are *boxed*, residues involved in auto-inhibition are *white* on *black background*, phosphorylated Ser are *bold italics* in the N-terminus of ACA2 and ACA8 isoforms

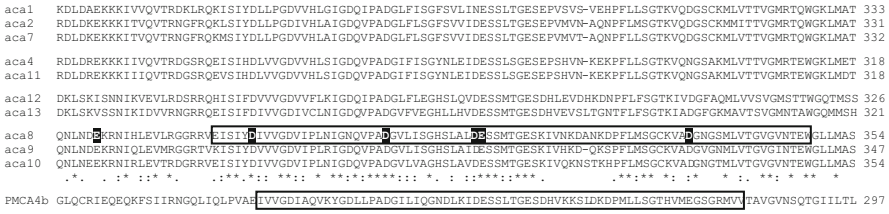

Fig. 13.3 Alignment of the region of *A. thaliana* ACAs small cytoplasmic loop comprising a site of intramolecular interaction of the N-terminal auto-inhibitory domain (*boxed*). The corresponding sequence of PMCA4b is shown for comparison. Acidic residues of ACA8 isoform involved in auto-inhibition are *bold underlined*

Despite the different localization, the N-terminus of ACAs has structural and functional features similar to the C-terminus of PMCAs. In fact (Figs. 13.1 and 13.2) ACAs N-terminus contains an auto-inhibitory domain partially overlapped by a high-affinity calmodulin (CaM) binding domain (CaMBD). A second, lower affinity, CaMBD downstream the first one has been recently identified in the *A. thaliana* isoform ACA8 [37] as well as in different isoforms of PMCA: sequence alignment (Fig. 13.2) suggests that this second site may be present in most, but perhaps not all, ACA isoforms (see below). As for PMCA, in the absence of CaM the regulatory terminal domain of ACAs interacts with the catalytic head of the pump, inhibiting its activity: CaM binding to the high affinity site substantially activates the pump, but complete activation occurs only upon CaM binding to both sites [37, 38].

While the terminal regulatory domain of at least some ACA isoform has been described in detail, less is known on how its auto-inhibitory action is exerted. An interaction domain for the C-terminus of the human isoform PMCA4b and for the N-terminus of *A. thaliana* isoform ACA8 has been identified in the small cytoplasmic loop connecting TM domains 2 and 3 [15, 39–42]. This region is highly conserved between members of the type 2B Ca^{2+}-ATPases group and rich of acidic residues (Fig. 13.3). Mutation to Ala of any of six tested conserved acidic residues in this region of ACA8 originates a partially deregulated enzyme with higher basal activity in the absence of added CaM [42]. Since alanine scanning mutagenesis of the N-terminus of ACAs reveals the involvement of basic residues in the auto-inhibitory domain [21, 43], the negative charge conferred by acidic residues to the

surface area of the small cytoplasmic loop may favor and/or stabilize its auto-inhibitory interaction with the N-terminal auto-inhibitory domain [42].

In *A. thaliana* isoforms ACA2 and ACA8, as in human isoform PMCA4b, mutation of an aspartic residue localized at the cytoplasmic end of the second TM, conserved in most ACA isoforms, generates a deregulated pump that is almost insensitive to further activation by CaM [21, 42, 44]. However, a detailed characterization of the PMCA4b mutant suggests that this mutation does not displace the auto-inhibitory domain, but rather directly changes accessibility of Ca^{2+} to the TM domain [44, 45].

CaM binding is not the only mechanism of regulation of the auto-inhibitory action of ACA N-terminus. Phosphorylation of different Ser residues in the N-terminus of the protein modulates the kinetics and/or the affinity of interaction with CaM as well as the amplitude of the response of the pump to CaM [46, 47]: since the N-terminus of the protein is highly variable between isoforms (Fig. 13.2), phosphorylation likely represents an isoform-specific mechanism of regulation of pump activity. ACAs are also regulated by acidic phospholipids such as phosphatidylserine or phosphatidylinositol-4P [22, 23]. Acidic phospholipids activate *A. thaliana* ACA8 via two distinct mechanisms, involving their binding to different sites: acidic phospholipids binding to a site in the protein N-terminus, overlapping the auto-inhibitory and the high-affinity CaMBD, stimulates ACA8 activity similar to CaM or to cleavage of the N-terminus, while binding to a second, as yet unidentified, site further stimulates ACA8 activity by lowering its $K_{0.5}$ for free Ca^{2+} [23]. This complex regulatory mechanism, only partially overlapping that of CaM, is similar to that reported for PMCA [15] and is likely shared by other ACA isoforms [22, 48].

Overall, despite the different localization of the regulatory terminal domain in ACAs and PMCAs, plant and animal type 2B Ca^{2+}-ATPases share a very similar mechanism of auto-inhibition. Indeed, the auto-inhibitory function of the terminal domain is preserved not only when it is switched from the C- to N-terminus in PMCA or vice versa in ACA, but also when the C-terminus of PMCA is fused to a N-deleted ACA mutant [49, 50].

3 Diversity of *A. thaliana* Isoforms

The genome of *A. thaliana* encodes 10 isoforms of ACA, all expressed at least in some cell type. Phylogenetic analysis indicates that they pertain to four clusters that appear to be conserved in flowering plants [18]. The four clusters (Table 13.1) are characterized, beside by sequence similarity and molecular mass, by the number and position of introns; moreover, current evidence suggests that members of each cluster localize at the same membrane [11, 12, 18]. Cluster 1 comprises three genes, each with 6 introns, encoding isoforms ACA1, ACA2, ACA7 with 77–92 % similarity. ACA1, the first cloned ACA, was originally proposed to be localized at the plastid inner envelope [51, 52], but no Ca^{2+}-ATPase activity has been detected in

Table 13.1 Comparison of *A. thaliana* ACA isoforms

Cluster	1			2		3		4		
	ACA1	ACA2	ACA7	ACA4	ACA11	ACA12	ACA13	ACA8	ACA9	ACA10
ACA1	100	78	77	62	61	43	42	48	47	48
ACA2		100	92	62	63	43	42	48	47	49
ACA7			100	63	63	44	41	48	48	49
ACA4				100	87	42	42	46	47	47
ACA11					100	41	42	48	47	48
ACA12						100	65	51	50	51
ACA13							100	51	51	51
ACA8								100	69	72
ACA9									100	69
ACA10										100
Mol mass (kDa)	111.3	110.4	110.8	112.8	111.9	113.7	112.5	116.2	118.8	116.9
Introns	6	6	6	6	6	0	0	33	31	32
Localization	ER	ER	PM?	TP	TP	PM	PM	PM	PM	PM

Similarities were computed by multiple alignment with ClustlawW

this membrane [53] and ACA1 has been found associated with the ER in a proteomic survey of *A. thaliana* organelles [54]; ACA2, the only isoform of this cluster characterized at the biochemical level, is localized at the ER [55]; ACA7 was found largely associated with the PM upon expression in tobacco leaves under a viral promoter [56], but nothing is known about its localization in *A. thaliana*. Cluster 2 includes two genes, with 6 introns, which encode two isoforms, ACA4 and ACA11, 87 % similar: both have been found localized at the TP [57, 58]. Cluster 3 is unique: it comprises two intron-less genes encoding two isoforms (ACA12 and ACA13) which are only 65 % similar to each other and highly divergent from members of the other clusters specially in the regulatory N-terminus (see below) [11, 18, 36, 59]. Both ACA12 and ACA13 have been found localized at the PM [36, 59, 60]. Cluster 4 comprises 3 genes with 31–33 introns encoding isoforms ACA8, ACA9, and ACA10: these isoforms, which are ca 70 % similar to each other, are all localized at the PM and are characterized by a molecular mass slightly higher than that of the other isoforms, mainly due to a longer N-terminal domain (see Fig. 13.2) [12, 18, 61–63].

While members of the same cluster are 65 to 92 % similar, similarity between members of different clusters ranges between 42 and 62 %. Biochemical characterization has been performed so far only for ACA8, ACA2 and ACA12 [21, 23, 25, 33, 36, 37, 41–43, 46, 47, 50, 55, 61, 64], but the available results indicate that sequence variability generates subtle functional differences which can be physiologically relevant.

Alignment of ACA isoforms shows that the most variable region is the N-terminus, where differences are evident also in the CaMBDs (Fig. 13.2). Members of clusters 1 and 2 share highly similar high-affinity CaMBD with the two hydrophobic residues W and F separated by 13 aa, while in those of cluster 4 they are

separated by 12 aa. This implies a different mode of CaM binding: comparison of the structure of the CaM–CaMBD complex of ACA8 [37] and of BCA1, a cluster 2 isoform of *Brassica oleracea* [65], shows that while in ACA8 the anchor residues are W and F (1:14 binding mode), in BCA1 the C-lobe of CaM is anchored by W, but the N-lobe is anchored by the I residue localized 3 aa downstream F (1:18 binding mode). The high-affinity CaMBD of members pertaining to cluster 3 are markedly divergent [11, 12, 18, 36]; nevertheless, ACA12 binds CaM-agarose matrix and has been successfully purified by affinity chromatography [36]. As to the low-affinity CaMBD, it is poorly conserved among clusters and possibly absent in isoforms of cluster 3 (Fig. 13.2). Thus, diverse ACA isoforms may differ in their affinity and/or kinetics of interaction with CaM. Moreover, plants are unique among eukaryotes for having different isoforms of CaM, very similar to CaMs from other organisms, as well as CaM-like proteins with CaM activity ("divergent CaMs"), with distinct abilities to activate target proteins [66, 67]. ACAs analyzed so far are activated by divergent CaMs, but their affinity for these proteins is lower than that for canonic CaMs [64, 68, 69]: further work is needed to ascertain to what extent the ability to discriminate between different CaM isoforms varies among *A. thaliana* ACA isoforms.

Members of cluster 3 have the lowest similarities to other isoforms. Characterization of ACA12 shows that it has several peculiar biochemical features. First, in contrast with all characterized ACA isoforms of *A. thaliana* and other plants, it is substantially unable to use ITP as an alternative to ATP; second, the effective concentrations of the fluorescein derivative eosin yellow are about 2 order of magnitude higher that those required to inhibit other ACAs [36]. But the most striking difference is that ACA12 is not activated by CaM; coherently, ACA12 complements the Ca^{2+}-sensitive phenotype of yeast strain K616 which, being devoid of endogenous Ca^{2+}-ATPases, is unable to grow in Ca^{2+}-depleted media unless it expresses a deregulated Ca^{2+}-ATPase [21, 33, 36, 43]. This unusual feature might be ascribed to the fact that two conserved acidic residues crucial for auto-inhibition of other type 2B, localized at the edge of the second and of the third TM, are an Asn (N211) and an Arg (R334) in ACA12 sequence. Indeed, in the Ca^{2+}-depleted medium K616 cells expressing ACA12 N211D mutant grow very poorly and those expressing ACA12 R334E mutant or the double mutant N211D-R334E are unable to grow [36]. Surprisingly, ACA13, which has the same substitutions found in ACA12 at those critical positions has been reported to be unable to complement K616 phenotype, unless deleted of the first 65 aa [59]: however, effective expression of ACA13 WT was not checked and K616 does not produce ACA12 under the standard growth conditions used by Iwano and coworkers [36, 59].

The expression pattern of *A. thaliana* ACA isoforms is variegated [http://bar.utoronto.ca/efp_arabidopsis/cgi-bin/efpWeb.cgi, 70]. Some isoforms (ACA1, ACA2, ACA4, ACA11, ACA8, and ACA10) are widely expressed throughout development [57, 63, 71–73] while the expression of others is limited to specific cell types in a single organ: expression of ACA7 is confined to developing pollen grains and ACA9 is expressed primarily in pollen [56, 62]. Members of cluster 3 have the most restricted expression pattern: both are barely detectable throughout

development except in senescent leaves and sepals (ACA12) [http://bar.utoronto.ca/efp_arabidopsis/cgi-bin/efpWeb.cgi, 70] or in the flower stigma and the root tip (ACA13) [59]. Beside by developmental signals, the expression of ACA isoforms is regulated by environmental signals such as biotic and abiotic stresses (see below).

4 Physiological Roles

Three main experimental approaches have been used in the attempt to define the role of *A. thaliana* ACA isoforms in physiology of the plant: (1) analysis of gene expression at different developmental stages and in response to environmental signals; (2) a pharmacological approach exploiting the high sensitivity to fluorescein derivatives of (most) ACAs; (3) phenotypic characterization of knockout (KO) mutants of single or multiple ACA isoforms. Each of these approaches has its pitfalls: (1) up- or down-regulation of gene expression per se does not allow one to draw any solid conclusion, especially when, as in most studies, it is not shown to be associated with a change in protein level and/or enzyme activity; (2) sensitivity to inhibitors, even when sufficiently specific, does not allow to discriminate between different isoforms; (3) due to the largely overlapping expression patterns of different isoforms, the role of a specific isoform can be masked by redundancy in KO mutants of single ACA isoforms; moreover, when a phenotype is observed it may be an indirect, rather than straightforward, consequence of the lack of the protein, which might influence other physiological processes. Nevertheless, the integrated and critical use of the above-mentioned approaches has allowed researchers to ascertain the involvement of an ACA cluster, or even of a single isoform in some developmental process or in the response of the plant to external stimuli.

4.1 Development

Single isoform KO mutants do not show phenotypic alterations up to the rosette stage when grown under standard condition [56, 58–60, 62, 63, 71]. The only exception is an *aca10* KO mutant in a genotype containing a naturally occurring dominant allele of an unlinked gene, which has stunted rosette development [63]. As mentioned above, the lack of a single isoform can be compensated by other isoforms localized at the same membrane and with similar expression pattern; moreover, the absence of one isoform can stimulate the expression of other(s). Mutants lacking multiple isoforms of the same ACA cluster show early phenotypic alterations: the double *aca8-aca10* KO mutant—which lacks the two widely expressed PM isoforms—shows significantly reduced root growth when cultivated in vitro [60] and the *aca4-aca11* KO mutant—which lacks the two TP isoforms—displays a high frequency of hypersensitive response-like lesions suggesting an altered control of a salicylic acid-dependent programmed cell death pathway [58].

Phenotypic alterations become evident in some single mutant at flowering time. In the *A. thaliana* Columbia ecotype the single *aca10* KO mutant and, more so, the double *aca8-aca10* KO have reduced inflorescence height and display increased axillary stem formation: intriguingly, the *aca10* KO mutant has normal flowers in the Wassilewskija or in the Nossen ecotype unless a dominant allele of an unlinked gene is present [60, 63]. The single *aca8* KO mutant does not have phenotypic alterations in any of the ecotypes, but ACA8 overexpression rescues the flowering phenotype of the *aca10* KO mutant: the unique role of ACA10 in flowering probably reflects subtle differences in expression patterns, protein levels, or regulatory properties between isoforms ACA10 and ACA8, which can be overcome or mitigated by overexpression [60, 63]. The most striking phenotype alterations in single mutants are reduced pollen development and/or pollination due to the lack of isoforms ACA7, ACA9, or ACA13, which are mainly or exclusively expressed in flowers. Mutants lacking ACA9, a PM isoform primarily expressed in pollen, display reduced growth of pollen tubes, with high frequency of aborted fertilization leading to a threefold reduction in seed set [62]. Two different insertional *aca7* mutant lines show large amounts of dead pollen grains in mature flowers, due to altered progression from uninucleated microspores to bicellular pollen grains: these results suggest that Ca^{2+} transport outside the cytoplasm of developing pollen grains is essential to support normal pollen development [56]. Finally ACA13, a PM isoform which is primarily expressed in stigmatic papilla cells and induced by pollination, is required for pollen germination and pollen tube growth [59].

4.2 Response to Endogenous/Hormonal and Environmental Signals

The fact that in plant cells cytosolic Ca^{2+} waves are involved in the transmission of a variety of endogenous and environmental signals strongly suggests an important role for ACAs in the transmission of these stimuli: since Ca^{2+} dynamics which encode signal specificity depend also on the rate of Ca^{2+} extrusion, the expression level and regulatory properties of each ACA isoform can influence signal transduction and thus the plant response. However, so far, only in few instances the involvement of specific ACA isoforms in the transduction of a signal has been unequivocally demonstrated and the role specifically played has not been clarified in any instance. In most cases, the involvement of ACA isoforms in the response to a signal has been inferred mainly from the effect of the signal on their mRNA level.

Cold stress stimulates the expression of ACA8, but represses that of ACA10, suggesting once more differential roles for the two more widely expressed PM isoforms [71]; boron starvation has been shown to up-regulate ACA1, ACA10, and ACA13 expression, thus possibly enhancing the ability to extrude Ca^{2+} from the cytoplasm both to the apoplast and to internal stores as the ER or possibly plastids [74]. A role of the TP isoform ACA4 in the response to salt stress is suggested by

the increased level of ACA4 mRNA in *A. thaliana* seedlings exposed to salt stress; in addition, overexpression of ACA4 in yeast improves salt tolerance [57]. Also overexpression of the ER isoform ACA2 improves yeast salt tolerance, but there is no evidence that this isoform plays a role in the response to salt of *A. thaliana* [75]. A role for PM-localized ACAs in ABA signaling has been proposed based on the ABA-induced stimulation of expression of ACA8 and ACA9 in *A. thaliana* seedlings, which at least in the case of ACA8, has been shown to determine an increase in protein amount in the PM. However, the relatively slow induction of ACA8 and ACA9 mRNAs (within 2–4 h) and accumulation of ACA8 protein at the PM (within 8 h) suggest that these events may be involved, rather than in short-term effects of ABA on cytosolic-free Ca^{2+} concentration, in a mechanism for desensitization of the cell to ABA signal when, under stress conditions, ABA is a constant presence [72].

Analysis of the *aca8*, *aca10*, and *aca8-aca10* KO mutants has brought evidence for a role of these PM isoforms in plant antibacterial immunity: all the mutants allow higher bacterial growth and develop stronger symptoms than the WT upon exposure to a virulent bacterium. Upon exposure to the bacterial elicitor flagellin the *aca8-aca10* KO mutant, but not the single mutants, displays a lower cytosolic Ca^{2+} transient and a lower oxidative burst than the WT and exhibits altered transcriptional reprogramming [60]. However, inhibition of ACA-mediated Ca^{2+} efflux with the fluorescein derivative eosin yellow in *A. thaliana* cultured cells which mainly express ACA8 [64] increases the oxidative burst [76]. ACA12 and ACA 13, whose expression is strongly stimulated by bacteria [http://bar.utoronto.ca/efp_arabidopsis/cgi-bin/efpWeb.cgi, 11, 70], may also be involved in the response to pathogen attack. Thus, while the involvement of PM localized ACA isoforms in *A. thaliana* response to biotic stress is well documented, the role they play in this process remains to be elucidated.

5 Conclusions

Despite the different localization of the auto-inhibitory domain and of the CaMBDs in the protein sequence, most ACA isoforms share with PMCAs multiple regulatory properties: regulation by CaM, acidic phospholipids, and phosphorylation of the terminal regulatory domain [12, 15, 19]. Moreover, the findings that the terminal regulatory domains interact with the same part of the catalytic head and are interchangeable between ACA8 and PMCA4b indicate that plant and animal type 2B Ca^{2+}-ATPases share the same mechanism of auto-inhibition [50]. A lot of questions await for an answer, including the role of the recently identified low-affinity CaMBD [37, 38] and the role of the acidic residues localized at the hinges between TM 2 and TM 3 and the small cytoplasmic loop of the pumps [21, 42]. Progress in understanding the mechanism of auto-inhibition of type 2B Ca^{2+}-ATPases heavily relies on solving the structure of these pumps, which promises to be a difficult task.

Gene expression analysis, pharmacological approaches using selective inhibitors such as fluorescent derivatives and phenotyping of single and double KO mutants

converge in indicating that ACAs play important roles in *A. thaliana* development, fertilization, and response to both biotic and abiotic stress [12, 13, 34, 56–60, 62, 63, 72, 74–76]. However, given the high number of isoforms, the role of a single isoform is often hindered by redundancy. Moreover, at present, too little is known about the biochemical characteristics of different ACA isoforms. Characterization of *A. thaliana* isoform ACA12 has highlighted peculiar characteristics of substrate specificity, inhibitor sensitivity, and regulatory properties [36]. Differences in the kinetics of interaction and affinities for CaM of ACA isoforms may arise from the variability of the CaMBDs and regulation by phospho-dephosphorylation of the N-terminus is likely to be isoform-specific since many of the Ser residues which are phosphorylated in ACA8 or ACA2 are not conserved in other isoforms. Phosphorylation has been shown to affect auto-inhibition, CaM affinity and the kinetics of CaM binding and release, thus providing a mechanism of fine tuning of ACAs activation and deactivation. However, so far, scant knowledge on the protein kinases involved in ACAs phosphorylation is available: both ACA2 and ACA8 have been shown to be substrates for members of the calcium-dependent protein kinase (CDPK) family, but nothing is known on which CDPK isoform(s) phosphorylate them in vivo [46, 47].

Once the involvement of an ACA isoform in a physiological process is ascertained, the exact role it plays needs to be determined. This requires dissection of the signal transduction pathway involved in order to define which is the step affected by ACA up- or down-regulation. The use of new imaging and molecular tools for in vivo monitoring of Ca^{2+} dynamics in the cytoplasm and in organels will definitely help to unravel the role of ACAs in plant response to endogenous and environmental stimuli [77, 78]. Moreover, since ACAs catalyze a Ca^{2+}/H^+ exchange, changes in their activity may well affect net proton fluxes across the PM and/or endomembranes and thus the value of $\Delta\mu H^+$ and related transport processes, as well as cytosolic pH homeostasis. Indeed, Ca^{2+}-dependent changes in H^+ fluxes, leading to cytoplasmic acidification, have been observed in response to different developmental and environmental signals which evoke transient increases of cytoplasmic Ca^{2+} concentration [79–81]. While in most cases the underlying mechanism has not been addressed, the use of fluorescein derivatives has highlighted the involvement of ACAs activity in ABA-induced changes of H^+ fluxes in *Egeria densa* leaves [79].

References

1. Sanders D, Pelloux J, Brownlee C et al (2002) Calcium at the crossroads of signaling. Plant Cell 14(Suppl):S401–S417
2. Shigaki T, Hirschi KD (2006) Diverse functions and molecular properties emerging for CAX cation/H^+ exchangers in plants. Plant Biol 8:419–429
3. McAinsh MR, Pittman JK (2009) Shaping the calcium signature. New Phytol 181:275–294
4. Boudsocq M, Sheen J (2010) Stress Signaling II: Calcium Sensing and Signaling. In: Pareek A, S.K. Sopory SK et al (eds) Abiotic Stress Adaptation in Plants: Physiological, Molecular and Genomic Foundation. Springer Science + Business Media B.V. 75–90

5. Dodd AN, Kudla J, Sanders D (2010) The language of calcium signaling. Annu Rev Plant Biol 61:593–620
6. Kudla J, Batistic O, Hashimoto K (2010) Calcium signals: the lead currency of plant information processing. Plant Cell 22:541–563
7. Spalding EP, Harper JF (2011) The ins and outs of cellular Ca^{2+} transport. Curr Opin Plant Biol 14:715–720
8. Batistič O, Kudla J (2012) Analysis of calcium signaling pathways in plants. Biochim Biophys Acta 1820:1283–1293
9. Geisler M, Axelsen KB, Harper JF et al (2000) Molecular aspects of higher plant P-type Ca^{2+}-ATPases. Biochim Biophys Acta 1465:52–78
10. Sze H, Liang F, Hwang I et al (2000) Diversity and regulation of plant Ca^{2+} pumps: Insights from expression in yeast. Annu Rev Plant Physiol Plant Mol Biol 51:433–462
11. Boursiac Y, Harper JF (2007) The origin and function of calmodulin regulated Ca^{2+} pumps in plants. J Bioenerg Biomembr 39:409–414
12. Bonza MC, De Michelis MI (2011) The plant Ca^{2+}-ATPases repertoire: biochemical features and physiological functions. Plant Biol 13:421–430
13. Pittman JK, Bonza MC, De Michelis MI (2011) Ca^{2+} Pumps and Ca^{2+} Antiporters in Plant Development. In: Geisler M, Venema K (eds) Transporters and pumps in plant signalling. Springer-Verlag, Berlin 133–161
14. Huda KMK, Banu MSA, Tuteja R et al (2013) Global calcium transducer P-type Ca^{2+}-ATPases open new avenues for agriculture by regulating stress signaling. J Exp Bot 64:3099–3109
15. Brini M, Carafoli E (2009) Calcium pumps in health and disease. Physiol Rev 89:1341–1378
16. Palmgren MG, Nissen P (2011) P-type ATPases. Annu Rev Biophys 40:243–266
17. Møller JV, Juul B, le Maire M (1996) Structural organization, ion transport, and energy transduction of P-type ATPases. Biochim Biophys Acta 1286:1–51
18. Baxter I, Tchieu J, Sussman MR et al (2003) Genomic comparison of P-type ATPase ion pumps in Arabidopsis and rice. Plant Physiol 132:618–628
19. Lopreiato R, Giacomello M, Carafoli E (2014) The plasma membrane calcium pump: new ways to look at an old enzyme. J Biol Chem 289:10261–10268
20. Palmgren MG, Axelsen KB (1998) Evolution of P-type ATPases. Biochim Biophys Acta 1365:37–45
21. Curran AC, Hwang H, Corbin J et al (2000) Autoinhibition of a calmodulin dependent calcium pump involves a structure in the stalk that connects the transmembrane domain to the ATPase catalytic domain. J Biol Chem 275:30301–30308
22. Bonza MC, Luoni L, De Michelis MI (2001) Stimulation of the plasma membrane Ca^{2+}-ATPase activity by acidic phospholipids. Physiol Plant 112:315–320
23. Meneghelli S, Fusca T, Luoni L et al (2008) Dual mechanism of activation of plant plasma membrane Ca^{2+}-ATPase by acidic phospholipids: Evidence for a phospholipid binding site which overlaps the calmodulin-binding site. Mol Membr Biol 25:539–546
24. Rasi-Caldogno F, Pugliarello MC, De Michelis MI (1987) The Ca^{2+}-transport ATPase of plant plasma membrane catalyzes a nH^+/Ca^{2+} exchange. Plant Physiol 83:994–1000
25. Luoni L, Bonza MC, De Michelis MI (2000) H^+/Ca^{2+} exchange driven by the plasma membrane Ca^{2+}-ATPase of *Arabidopsis thaliana* reconstituted in proteoliposomes after calmodulin-affinity purification. FEBS Lett 482:225–230
26. Zhai J, Xu H, Cong X, Deng Y et al (2013) Ca^{2+}/H^+ exchange in the plasma membrane of Arabidopsis thaliana leaves. Acta Physiol Plant 35:161–173
27. Niggli V, Sigel E (2008) Anticipating antiport in P-type ATPases. Trends Biochem Sci 33(4):156–160
28. Olesen C, Sørensen T, Nielsen RC et al (2004) Dephosphorylation of the calcium pump coupled to counterion occlusion. Science 306:2251–2255
29. Obara K, Miyashita N, Xu C et al (2005) Structural role of countertransport revealed in Ca^{2+} pump crystal structure in the absence of Ca^{2+}. Proc Natl Acad Sci U S A 102:14489–14496
30. Carnelli A, De Michelis MI, Rasi Caldogno F (1992) Plasma-membrane Ca-ATPase of radish seedlings. 1. Biochemical-characterization using ITP as a substrate. Plant Physiol 98:1196–1201

31. Briskin DP (1990) Ca^{2+}-traslocating ATPase of the plant plasma membrane. Plant Physiol 94:397–400
32. De Michelis MI, Carnelli A, Rasi-Caldogno F (1993) The Ca^{2+} pump of the plasma membrane of *Arabidopsis thaliana*: characteristics and sensitivity to fluorescein derivatives. Botanica Acta 106:20–25
33. Bonza MC, Luoni L, De Michelis MI (2004) Functional expression in yeast of an N-depleted form of *At*-ACA8, a plasma membrane Ca^{2+}-ATPase of *Arabidopsis thaliana*, and characterization of a hyperactive mutant. Planta 218:814–823
34. Bonza MC, Loro G, Behera S et al (2013) Analyses of Ca^{2+} accumulation and dynamics in the Endoplasmic Reticulum of Arabidopsis thaliana root cells using genetically encoded Cameleon sensors. Plant Physiol 163:1230–1241
35. Galva C, Virgin GK, Helms JB et al (2013) ATP protects against FITC labeling of Solanum lycopersicon and Arabidopsis thaliana Ca^{2+}-ATPase ATP binding domains. Plant Physiol Biochem 71:261–267
36. Limonta M, Romanowsky S, Olivari C et al (2014) ACA12 Is a deregulated isoform of plasma membrane Ca^{2+}-ATPase of arabidopsis thaliana. Plant Mol Biol 84(4-5):387–397
37. Tidow H, Poulsen LR, Andreeva A et al (2012) A bimodular mechanism of calcium control in eukaryotes. Nature 491:468–472
38. Bonza MC, Luoni L, Olivari C et al (2013) Unravelling the molecular mechanisms of regulation of plant type 2B Ca^{2+}-ATPases using Arabidopsis thaliana plasma membrane isoform ACA8 as a model system. In: Pandalai SG (eds) Recent research development in membrane biology, 3, Research Signpost, Kerala 1–14
39. Falchetto R, Vorherr T, Brunner J et al (1991) The plasma membrane Ca^{2+} pump contains a site that interacts with its calmodulin binding domain. J Biol Chem 266:2930–2936
40. Falchetto R, Vorherr T, Carafoli E (1992) The calmodulin-binding site of the plasma membrane Ca^{2+} pump interacts with the transduction domain of the enzyme. Protein Sci 1:1613–1621
41. Luoni L, Meneghelli S, Bonza MC et al (2004) Auto-inhibition of *Arabidopsis thaliana* plasma membrane Ca^{2+}-ATPase involves an interaction of the N-terminus with the small cytoplasmic loop. FEBS Lett 594:20–24
42. Fusca T, Bonza MC, Luoni L et al (2009) Single point mutations in the small cytoplasmic loop of ACA8, a plasma membrane Ca^{2+}-ATPase of *Arabidopsis thaliana*, generate partially deregulated pumps. J Biol Chem 284:30881–30888
43. Baekgaard L, Luoni L, De Michelis MI et al (2006) The plant plasma membrane Ca^{2+} pump ACA8 contains overlapping as well as physically separated autoinhibitory and calmodulin-binding domains. J Biol Chem 281:1058–1065
44. Bredeston LM, Adamo HP (2004) Loss of autoinhibition of the plasma membrane Ca^{2+} pump by substitution of aspartic 170 by asparagine. Activation of plasma membrane calcium ATPase 4 without disruption of the interaction between the catalytic core and the C-terminal regulatory domain. J Biol Chem 279:41619–41625
45. Corradi GR, Adamo HP (2007) Intramolecular fluorescence resonance energy transfer between fused autofluorescent proteins reveals rearrangements of the N- and C-terminal segments of the plasma membrane Ca^{2+} pump involved in the activation. J Biol Chem 282:35440–35448
46. Hwang I, Sze H, Harper JF (2000) A calcium-dependent protein kinase can inhibit a calmodulin-stimulated Ca^{2+} pump (ACA2) located in the endoplasmic reticulum. Proc Natl Acad Sci U S A 97:6224–6229
47. Giacometti S, Marrano CA, Bonza MC et al (2012) Phosphorylation of serine residues in the N-terminus modulates the activity of ACA8, a plasma membrane Ca^{2+}-ATPase of *Arabidopsis thaliana*. J Exp Bot 63(3):1215–1224
48. Hsieh WL, Pierce WS, Sze H (1991) Calcium-Pumping ATPases in vesicles from carrot cells. Stimulation by calmodulin or phosphatidylserine and formation of a 120 kilodalton phosphoenzyme. Plant Physiol 97:1535–1544
49. Adamo HP, Grimaldi ME (1998) Functional consequences of relocating the C-terminal calmodulin-binding autoinhibitory domains of the plasma membrane Ca^{2+} pump near the N-terminus. Biochem J 331:763–766

50. Bonza MC, Luoni L (2010) Plant and animal type 2B Ca^{2+}-ATPases: evidence for a common auto-inhibitory mechanism. FEBS Lett 584(23):4783–4788
51. Huang L, Berkelman T, Franklin AE et al (1993) Characterization of a gene encoding a Ca^{2+}-ATPase-like protein in the plastid envelope. Proc Natl Acad Sci U S A 90:10066–10070
52. Huang L, Berkelman T, Franklin AE et al (1994) Errata corrige. Proc Natl Acad Sci U S A 91:9664
53. Roh MH, Shingles R, Cleveland MJ et al (1998) Direct measurement of calcium transport across chloroplast inner-envelope vesicles. Plant Physiol 118:1447–1454
54. Dunkley TPJ, Hester S, Shadforth IP et al (2006) Mapping the *Arabidopsis* organelle proteome. Proc Natl Acad Sci U S A 103:6518–6523
55. Hong B, Ichida A, Wang Y et al (1999) Identification of a calmodulin-regulated Ca^{2+}-ATPase in the endoplasmic reticulum. Plant Physiol 119:1165–1175
56. Lucca N, Leon G (2012) Arabidopsis ACA7, encoding a putative auto-regulated Ca^{2+}-ATPase, is required for normal pollen development. Plant Cell Rep 31:651–659
57. Geisler M, Frangne N, Gomès E et al (2000) The ACA4 gene of *Arabidopsis* encodes a vacuolar membrane calcium pump that improves salt tolerance in yeast. Plant Physiol 124:1814–1827
58. Boursiac Y, Lee SM, Romanowsky S et al (2010) Disruption of the vacuolar Calcium-ATPases in Arabidopsis results in the activation of a salicylic acid-dependent programmed cell death pathway. Plant Physiol 154:1158–1171
59. Iwano M, Igarashi M, Tarutani Y et al (2014) A pollen coat-inducible autoinhibited Ca^{2+}-ATPase expressed in stigmatic papilla cells is required for compatible pollination in the Brassicaceae. Plant Cell 26:636–649
60. Frei dit Frey N, Mbengue M, Kwaaitaal M et al (2012) Plasma membrane Calcium ATPases are important components of receptor-mediated signaling in plant immune responses and development. Plant Physiol 159:798–809
61. Bonza MC, Morandini P, Luoni L et al (2000) *At*-ACA8 encodes a plasma membrane-localized Ca^{2+}-ATPase of *Arabidopsis thaliana* with a calmodulin binding domain at the N-terminus. Plant Physiol 123:1495–1505
62. Schiøtt M, Romanowsky SM, Bækgaard L et al (2004) A plasma membrane Ca^{2+} Pump is required for normal pollen tube growth and fertilization. Proc Natl Acad Sci U S A 101:9502–9507
63. George L, Romanowsky SM, Harper JF et al (2008) The ACA10 Ca^{2+}-ATPase regulates adult vegetative development and inflorescence architecture in *Arabidopsis*. Plant Physiol 146:716–728
64. Luoni L, Bonza MC, De Michelis MI (2006) Calmodulin/Ca^{2+}-ATPase interaction at the *Arabidopsis thaliana* plasma membrane is dependent on calmodulin isoform showing isoform-specific Ca^{2+} dependencies. Physiol Plant 126:175–186
65. Ishida H, Vogel HJ (2010) The solution structure of a plant calmodulin and the CaM-binding domain of the vacuolar calcium-ATPase BCA1reveals a new binding and activation mechanism. J Biol Chem 285:38502–38510
66. Snedden WA, Fromm H (1998) Calmodulin, calmodulin-related proteins and plant responses to the environment. Trends Plant Sci 3:299–304
67. Zielinski RE (1998) Calmodulin and calmodulin-binding proteins in plants. Annu Rev Plant Physiol Plant Mol Biol 49:697–725
68. Lee SH, Johnson JD, Walsh MP et al (2000) Differential regulation of Ca^{2+}/calmodulin-dependent enzymes by plant calmodulin isoforms and free Ca^{2+} concentration. Biochem J 350:299–306
69. Yamniuk AP, Vogel HJ (2004) Structurally homologous binding of plant calmodulin isoforms to the calmodulin-binding domain of vacuolar calcium-ATPase. J Biol Chem 279:7698–7707
70. Winter D, Vinegar B, Nahal H et al (2007) An "electronic fluorescent pictograph" browser for exploring and analyzing large-scale biological data sets. PLoS ONE 2(8), e718
71. Schiøtt M, Palmgren MG (2005) Two plant Ca^{2+} pumps expressed in stomatal guard cells show opposite expression patterns during cold stress. Physiol Plant 124:278–283

72. Cerana M, Bonza MC, Harris R et al (2006) Abscisic acid stimulates the expression of two isoforms of plasma membrane Ca^{2+}-ATPase in *Arabidopsis thaliana* seedlings. Plant Biol 8:572–578
73. Lee SM, Kim HS, Han HJ et al (2007) Identification of a calmodulin-regulated autoinhibited Ca^{2+}-ATPase (ACA11) that is localized to vacuole membranes in *Arabidopsis*. FEBS Lett 581:3943–3949
74. Quiles-Pando C, Rexach J, Navarro-Gochicoa MT et al (2013) Boron deficiency increases the levels of cytosolic Ca^{2+} and expression of Ca^{2+}-related genes in Arabidopsis thaliana roots. Plant Physiol Biochem 65:55–60
75. Anil VS, Rjkumar P, Kumar P et al (2008) A plant Ca^{2+} pump, ACA2, relieves salt hypersensitivity in yeast. Modulation of cytosolic calcium signature and activation of adaptive Na^{+} homeostasis. J Biol Chem 283:3497–3506
76. Romani G, Bonza MC, Filippini I et al (2004) Involvement of the plasma membrane Ca^{2+}-ATPase in the short term response of *Arabidopsis thaliana* cultured cells to oligogalacturonides. Plant Biol 6:192–200
77. Monshausen GB (2012) Visualizing Ca^{2+} signatures in plants. Curr Opin Plant Biol 15:1–6
78. Costa A, Kudla J (2014) Colorful insights: advances in imaging drive novel breakthroughs in Ca^{2+} signaling. Mol Plant doi: 10.1016/j.molp.2014.11.020
79. Beffagna N, Romani G, Sforza MC (2000) H^{+} Fluxes at plasmalemma level: In vivo evidence for a significant contribution of the Ca^{2+}-ATPase and for the involvement of its activity in the abscisic Acid-induced changes in egeria densa leaves. Plant Biol 2:168–175
80. Monshausen GB, Bibikova TN, Weisenseel MH et al (2009) Ca^{2+} regulates reactive oxygen species production and pH during mechanosensing in Arabidopsis roots. Plant Cell 21:2341–2356
81. Monshausen GB, Miller ND, Murphy AS et al (2011) Dynamics of auxin-dependent Ca^{2+} and pH signaling in root growth revealed by integrating high-resolution imaging with automated computer vision-based analysis. Plant J 65:309–318

Chapter 14
Regulation of Ca^{2+} Transport ATPases by Amino- and Carboxy-Terminal Extensions: Mechanisms and (Patho)Physiological Implications

Jialin Chen, Susanne Smaardijk, Ilse Vandecaetsbeek, and Peter Vangheluwe

Abstract Ca^{2+} transport ATPases play a vital role in maintaining low cytosolic Ca^{2+} concentrations. Three types of Ca^{2+} ATPases exist: the Sarco/Endoplasmic Reticulum Ca^{2+} ATPases (SERCA), Secretory Pathway Ca^{2+} ATPases (SPCA), and Plasma Membrane Ca^{2+} ATPases (PMCA). The expression of numerous Ca^{2+} ATPase isoforms and splice variants generate a complex toolkit of Ca^{2+} transporters that provide cell type and compartmental specific functions. Still, the basic Ca^{2+} transporting mechanism is highly conserved in all Ca^{2+} ATPase variants, which is related to a highly conserved core structure holding a transmembrane domain for Ca^{2+} binding and transport, and three cytosolic domains, which coordinate ATP hydrolysis. In contrast, the N- and C-terminal stretches of the various isoforms and splice variants display much more variation. They provide additional isoform or splice variant specific functions to the Ca^{2+} pumps, which are reviewed here. The N- and C-termini may regulate the enzymatic properties of the Ca^{2+} pumps via intramolecular interactions, contain targeting signals, recruit other proteins, bind lipids/ions or may be subjected to posttranslational modifications. Insights into the properties and molecular mechanisms of the N- and C-terminal extensions may offer novel therapeutic opportunities to regulate and control specific Ca^{2+} transporter isoforms in a diseased context.

Keywords Ca^{2+} transport ATPase • Lactation • Cardiac contractility • Calmodulin • Alternative splicing

J. Chen • S. Smaardijk • I. Vandecaetsbeek • P. Vangheluwe (✉)
Laboratory of Cellular Transport Systems, Department of Cellular and Molecular Medicine, KU Leuven, Campus Gasthuisberg ON1, Herestraat 49/box 802, 3000 Leuven, Belgium
e-mail: peter.vangheluwe@med.kuleuven.be

S. Chakraborti, N.S. Dhalla (eds.), *Regulation of Ca^{2+}-ATPases,V-ATPases and F-ATPases*, Advances in Biochemistry in Health and Disease 14,
DOI 10.1007/978-3-319-24780-9_14

1 Introduction

Ca^{2+} is an important second messenger in many cellular processes, such as cell growth, apoptosis, muscle contraction, and fertilization. The cytosolic free Ca^{2+} concentration in resting conditions is maintained between 10 and 100 nM, a concentration that is much lower than in the extracellular matrix (1–2 mM) or in most of the intracellular organelles (0.1–0.5 mM). The cytosolic Ca^{2+} concentration is tightly controlled by Ca^{2+} buffering and transporting proteins, since Ca^{2+} ions cannot be formed or degraded, but can only be transported from one compartment to another.

Two modes of Ca^{2+} transport can be recognized in cells: passive flux through Ca^{2+} channels and active transport by carriers against the electrochemical gradient [1]. Extracellular Ca^{2+} passively enters the cell via TRP channels, voltage-gated Ca^{2+} channels and Ca^{2+}-release activated channels, whereas the inositol triphosphate and ryanodine receptors passively release Ca^{2+} into the cytosol from intracellular stores (*e.g.*, the endoplasmic and sarcoplasmic reticulum, ER and SR). In the meantime, active transporters remove Ca^{2+} from the cytosol into organelles or outside of the cell. The secondary active transporter Na^+/Ca^{2+}-exchanger uses the energy stored in the Na^+ gradient to transport 1 Ca^{2+} out of the cell whilst counter-transporting 3 Na^+ ions, extruding Ca^{2+} mainly when the cytosolic Ca^{2+} concentration is elevated [2]. For maintaining a sub-micromolar cytosolic Ca^{2+} concentration, mammalian cells further critically depend on three differently localized primary active Ca^{2+}-ATPase transporters that power Ca^{2+} transport by ATP hydrolysis: the Sarco/Endoplasmic Reticulum Ca^{2+} ATPase (SERCA), the Secretory Pathway Ca^{2+} ATPase (SPCA), and the Plasma Membrane Ca^{2+} ATPase (PMCA) [1]. They belong to the family of P-type ATPases that undergo auto-phosphorylation on a conserved aspartic acid, a feature that controls the Ca^{2+} binding, occlusion, and transport [3, 4].

SERCA1a is currently the only Ca^{2+}-ATPase for which the structure has been resolved [5], but thanks to the overall high degree in sequence similarity and domain organization, predicted homology models of several other Ca^{2+}-ATPases were generated. The topology follows the classical P-type ATPase topology, with 10 common transmembrane (M) helices that form a M-domain, which holds the Ca^{2+}-binding sites and ion entrance/exit pathways. In addition, the cytosolic loops form three distinct functional domains: a nucleotide-binding domain (N), a phosphorylation domain (P), and an actuator domain (A), which make up the core of the Ca^{2+} pumps and which execute the Ca^{2+} transport cycle (Fig. 14.1) [5].

When cytosolic Ca^{2+} rises sufficiently, the P-domain becomes auto-phosphorylated by an ATP molecule that is recruited by the N-domain. Later in the cycle, the pump is dephosphorylated by the A-domain that functions as a built-in protein phosphatase [3, 6]. Four principle conformational states can be recognized in the Ca^{2+} transport cycle: E1, E1P, E2P, and E2. The E1 conformations display high affinity towards cytosolic Ca^{2+}, whereas in the E2 conformations the pump shows a much lower luminal Ca^{2+} affinity. Via an allosteric mechanism, the phosphorylation and dephosphorylation reactions are tightly coupled to the opening and closure of the

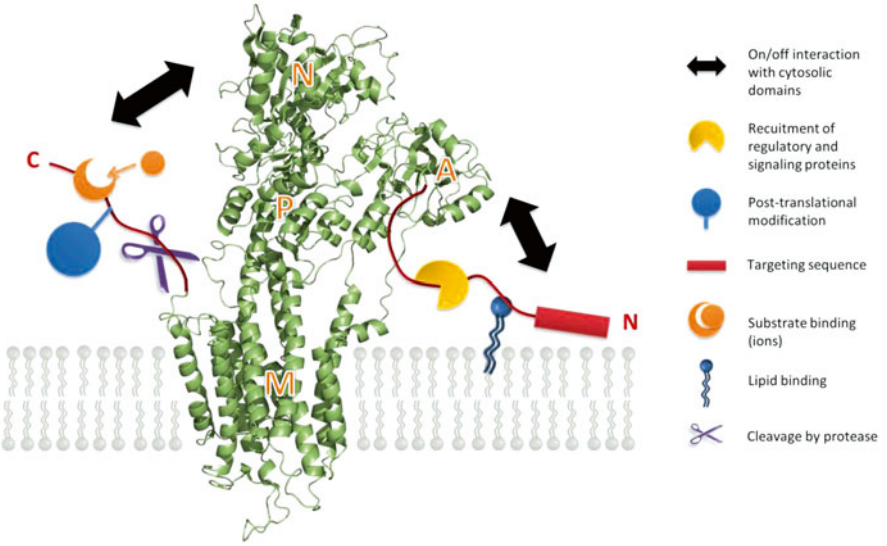

Fig. 14.1 Regulatory mechanisms of P-type transport ATPases by N- and C-terminal extensions. An example of a P-type ATPase structure (*green*) with hypothetical N- and C-termini (*red*). Actuator (A), Nucleotide binding (N), phosphorylation (P), and membrane (M) domains as well as the N- and C-termini are indicated. The extended N- and C-termini are possibly functioning as on/off or regulatory switches of the pumping activity by reversibly interacting with the main body of the pump. The N- and C-termini may also recruit regulatory proteins, lipids, substrates or may be subjected to posttranslational modifications or be prone to protease cleavage. Finally, the N- and C-termini may further contain targeting information

cytosolic/extra-cytosolic Ca^{2+} entrance/exit pathways in the M-domain. The access to the Ca^{2+}-binding sites switches from the cytosol to the extra-cytosolic compartment and a concomitant drop in the Ca^{2+} affinity at the extra-cytosolic side promotes Ca^{2+} release. This results in the unidirectional transport of Ca^{2+} against the electrochemical gradient.

Besides the highly conserved domain architecture and pumping mechanism, the Ca^{2+}-ATPases markedly vary in the N- and C-terminal stretches. The amino- and carboxy-ends of the different Ca^{2+}-ATPase isoforms contain important regulatory features that have evolved to allow a cell-context specific regulation of Ca^{2+} transport. In general, the variable N- and C-termini of P-type ATPases exert one or several of the following possible functions: regulation of the enzymatic properties or transport cycle of the pump, interaction with substrates or lipids, recruitment of modulatory proteins, regulation of the subcellular targeting, or regulation by post-translational modifications (Fig. 14.1).

The Ca^{2+} transporters belong to the family of P-type ATPases that is divided into five subfamilies according to their sequence and function (heavy metal pumps, P1; ions, P2; protons, P3; lipids, P4; unknown substrate, P5) [3]. Members of all P-type ATPase subfamilies are closely regulated by their N- and/or C-termini, thereby modulating essential cellular functions. For instance, the copper ATPases belong to

the P1B heavy metal pumps and their N-terminus holds a membrane associated platform that may recruit copper chaperones for subsequent substrate delivery to the copper binding sites in the N-terminus or to the copper transport sites in the M-domain [7]. The N- [8] and C-termini [9] of the Wilson copper transporter further determine the subcellular localization in a copper-dependent manner. The C-terminus of the Na^+/K^+-ATPase, an important member of the P2-type ATPases, docks into the C-terminal M-domain and regulates the access to a non-canonical Na^+-entrance pathway impacting on the Na^+ affinity on both sides of the membrane [10, 11]. In the P3-type H^+-ATPases, the C-terminus includes an auto-inhibitory domain that upon removal by proteolytic digestion [12] or truncation at the genetic level [13] leads to the release of the auto-inhibitory restraints and a strong activation of proton pumping. The C-terminus works in conjunction with the N-terminus to block the H^+ pump via an intramolecular interaction [14]. Phosphorylation of the C-terminus further recruits the regulatory 14-3-3 protein, which relieves this intramolecular interaction to stimulate proton transport [15]. Also lipid flippases belonging to the P4-type ATPases are controlled by the N- and C-terminal ends. The auto-inhibition of the yeast Drs2p lipid flippase by the C-terminal tail [16] can be relieved by interaction with the Golgi-localized phosphatidylinositol 4-phosphate lipid [17]. Moreover, the C-terminal interaction with ArfGEF synergistically stimulates lipid flippase activity, which activates the vesicle budding machinery of the Golgi at the sites of vesicle formation [17]. Finally, the poorly characterized P5-type ATPases display unique N-terminal stretches that contain unusual membrane spanning segments resembling the N-terminal stretches of the P1-type ATPases [18]. These segments are predicted to be important for the regulation of auto-phosphorylation activity, substrate delivery, or recruitment of modulatory proteins [19].

In this book chapter we provide an overview of how the highly variable N- and C-termini regulate Ca^{2+} transport mediated by the Ca^{2+}-ATPases belonging to the P2-type ATPase subfamily.

2 Regulation of the SERCA Pumps by Amino and Carboxy Termini

2.1 SERCA Isoforms and Splice Variants

In humans, three different genes (*ATP2A1-3*) generate multiple SERCA isoforms and splice variants (SERCA1a-b, SERCA2a-d, and SERCA3a-f) as a result of developmental or tissue-specific gene expression and alternative splicing (Fig. 14.2) [4, 20]. Interestingly, all the splice variants of the SERCA isoforms only differ at their C-terminus [21]. The tightly regulated developmental and cell type-specific expression pattern of the different SERCA isoforms suggests that each isoform is adapted to a specific spatiotemporal function.

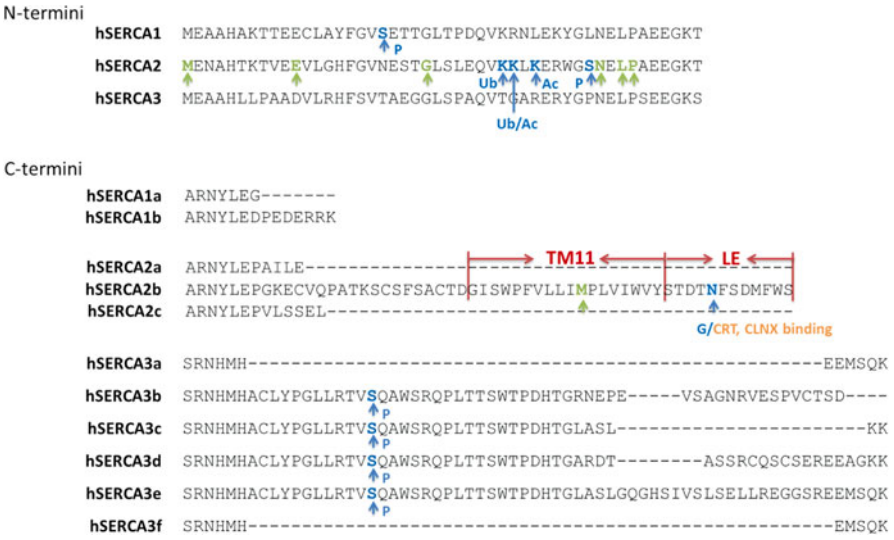

Fig. 14.2 The N- and C-termini of the different human SERCA isoforms and splice variants contain important regulatory sites. The N-terminus is defined as all the residues before M1 and the C-terminus is defined as the sequence stretch after M10. *Green arrows* in hSERCA2 indicate residues that are mutated and associated with Darier Disease. *Blue arrows* indicate posttranslational modifications that are mentioned in the text. P, phosphorylation. Ub, ubiquitination, Ac, acetylation, G, glycosylation. The hSERCA2d is not included, since this variant has not yet been demonstrated at the protein level

2.1.1 SERCA1 Splice Variants

The C-terminus of the fast-twitch skeletal muscle isoform SERCA1a ends with only one specific glycine residue, whereas the SERCA1b splice variant holds a slightly longer C-terminus (ending with –DPEDERRK) and is only expressed in neonatal fibers [22], myoblasts, developing myotubes and regenerating muscle [23]. This suggests that SERCA1b might have an important role in the relaxation of myotubes and/or the growth and development of new fibers, which are typical for neonatal and regenerating muscles. However, the specific physiological role of SERCA1b and its charged C-tail remain elusive [23]. In contrast, the SERCA1a isoform is by far the best characterized SERCA isoform. This 110-kDa protein was the first member of the P-type ATPase family to be cloned [24] and it has been extensively studied by site-directed mutagenesis and crystallography, leading to detailed insights in its structure–function relationship. SERCA1a is responsible for removing Ca^{2+} from the myofilaments in fast- and slow-twitch skeletal muscle and is referred to as the muscle relaxing factor. Interestingly, a shorter, truncated SERCA1 variant (S1T) was detected in different fetal and adult tissues, including spleen, thymus, pancreas, kidney, and liver, but not in adult and fetal skeletal and cardiac muscle [25]. S1T corresponds to a 46 kDa N-terminal fragment of SERCA1a lacking parts of the N- and P-domain and also M5–M10 of the M-domain. S1T only contains one of the

seven Ca^{2+}-binding residues and is thus unable to transport Ca^{2+} [25]. Although its precise physiological role is unclear, S1T promotes ER Ca^{2+} leakage resulting in ER Ca^{2+} depletion. Since S1T is localized in the ER–mitochondria microdomains the Ca^{2+} that leaks from the ER is transferred to the mitochondria triggering the activation of the mitochondrial apoptotic pathway, which may determine cell fate [26].

2.1.2 SERCA2 Splice Variants

The SERCA2 pumps are by far the most widespread of all SERCA isoforms and phylogenetically the oldest [27, 28]. SERCA2 predominantly exists as two splice variants that contain a common 993 amino acid stretch and a variable C-terminus. SERCA2a contains a 2a-tail that ends with four residues, and SERCA2b displays a 49 amino-acid long extension that is responsible for the unique enzymatic properties of this pump (2b-tail) (Fig. 14.2) [29]. Although SERCA1 splicing is developmentally regulated, splicing of SERCA2 is regulated in a tissue-specific manner. SERCA2a is the main isoform found in the SR of cardiac, slow-twitch skeletal and smooth muscle cells [30, 31], but it is also found in some neurons, in particular in the GABAergic neurons like the Purkinje cells [32]. SERCA2b is expressed in the ER of most cell types and can therefore be considered as the housekeeping isoform. In various smooth muscle cell types, SERCA2b is the main SERCA2 isoform with SERCA2a representing only 20–25 % of all SERCA2 [30]. Two additional human-specific SERCA2 splice variants were identified, SERCA2c [33] and SERCA2d [34]. At the mRNA level, SERCA2c was detected in differentiating monocytes [35] and cardiac cells, whereas the existence of the SERCA2c protein was confirmed in the heart [33]. So far, SERCA2d expression was only demonstrated at the mRNA level in human skeletal muscle, which was decreased in myotonic dystrophy type 1 [34].

2.1.3 SERCA3 Splice Variants

In humans at least six different splice variants of SERCA3 are recognized (SERCA3a-f) [27]. SERCA3 has a more restricted tissue expression pattern than the housekeeping Ca^{2+} pump, SERCA2b. With the notable exception of human umbilical vein endothelial cells, SERCA3 seems to be co-expressed with the housekeeping SERCA2b pump, but might be targeted to a different subcellular compartment [36]. SERCA3 splice variants are expressed in hematopoietic cell lineages, endothelial cells [37], monocytes, colon and pancreatic β-cells [38]. A more recent report mentioned the expression of three SERCA3 isoforms (SERCA3a, -3d and -3f) in human cardiomyocytes [21]. Interestingly, SERCA3 pumps differ from the other SERCA isoforms by a remarkably low affinity for cytosolic and luminal Ca^{2+} [39]. Moreover, in contrast to SERCA1 and SERCA2 splice variants, SERCA3 is insensitive to the cardiac SERCA2a regulator phospholamban (PLB) and displays a higher resistance to oxidative damage [40, 41].

2.2 *Regulation of SERCA Splice Variants by N- and C-Terminal Extensions*

In the following sections, we discuss how the alternative N- and C-termini of SERCA1-3 splice variants regulate the enzymatic properties and subcellular targeting. We highlight the role of N-/C-termini in recruiting regulatory proteins or post-translational modifications (PTMs). In addition, some disease-associated mutations can be found in the N- and C-termini. Finally, we address the (patho)physiological implications of the SERCA splice variants for cardiac contractility.

2.2.1 Biochemical Properties

SERCA2b

Two properties discriminate SERCA2b from SERCA1a or SERCA2a: a twofold higher affinity for Ca^{2+} and a lower maximal turnover rate, which are both attributed to the presence of the 2b-tail that comprises an additional membrane segment (M11) and a luminal extension (LE) (Figs. 14.2 and 14.3) [42–44]. SERCA2b is therefore the only Ca^{2+} transporter with 11 membrane segments. Remarkably, fusion of the 2b-tail to SERCA1a or supplying synthetic peptides corresponding to (parts of) the 2b-tail to SERCA2a or SERCA1a, impose SERCA2b-like properties to these Ca^{2+} pumps [44, 45]. This indicates that the 2b-tail can be regarded as a transferable, functional peptide that modulates the Ca^{2+} affinity of the pump by direct interaction. The Ca^{2+} affinity regulation by the 2b-tail peptide thus closely resembles how the single-pass transmembrane proteins PLB or sarcolipin (SLN), a PLB homolog, regulate the Ca^{2+} affinity of the Ca^{2+} pump by direct interaction (Fig. 14.3). However, the functional effect of the 2b-tail on the apparent Ca^{2+} affinity is independent and opposite from PLB or SLN, which can be explained by distinct and independent binding sites for the 2b-tail as compared to PLB or SLN (Fig. 14.3) [46].

M11 and LE are two functional regions in the 2b-tail that operate independently by interacting with sites upstream in the SERCA2b protein (Fig. 14.3b) [44, 45, 47]. Based on the known SERCA1a crystal structures, the solved NMR structure of M11 and mutagenesis, a structural model for SERCA2b was proposed (Fig. 14.3b) [44]. According to that model, M11 interacts with M7 and M10 of SERCA2b, a relatively immobile part of the pump, resembling the binding site of the β subunit on the Na^+/K^+-ATPase. The M11 interaction reduces the maximal turnover rate and increases the apparent Ca^{2+} affinity of SERCA2b by slowing the E2P to E2 and E2 to E1 transitions [45, 47, 48].

The mechanism of LE is quite different from that of M11, which relates to a separate binding site at the luminal side of the pump. A groove between luminal loops L5-6 and L7-8 is opened at the luminal side of M11, for the descent of LE. This displacement allows for a peptide consisting of the last four crucial amino acids of the 2b-tail carboxyl terminus (1039-MFWS) to reach a luminal binding

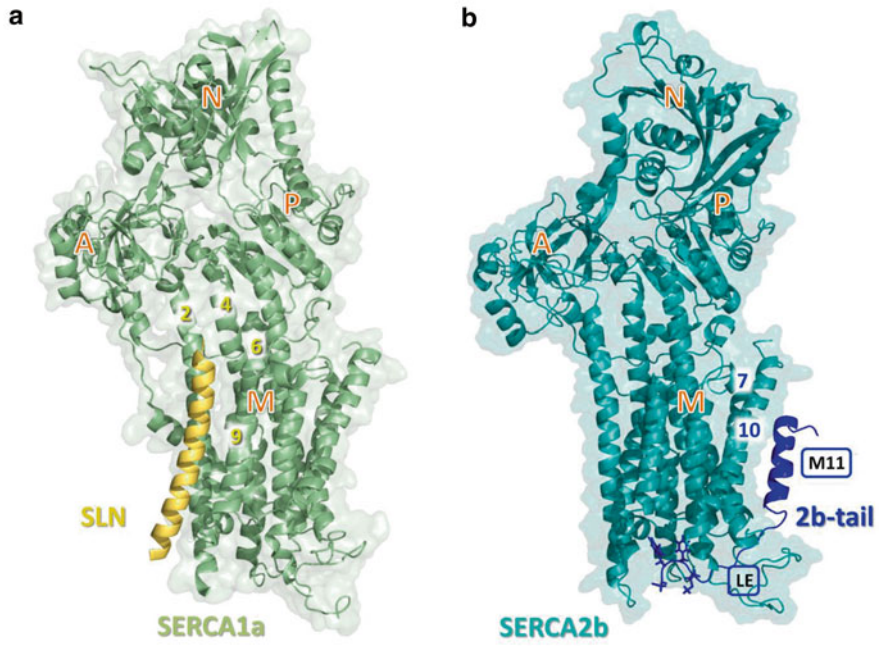

Fig. 14.3 Comparison of the SLN binding site in SERCA1a (**a**) and the 2b-tail binding site in SERCA2b (**b**). (**a**) the SLN binding site in SERCA1a is depicted in *yellow* (E1-SLN state; 4H1W crystal structure [198]). (**b**) The 2b-tail (*dark blue*) consists of an 11th transmembrane helix (M11) and a luminal extension (LE) (homology model of SERCA2b, based on 1SU4 crystal structure in the E1 conformation [44]). The last four residues of the 2b-tail (1039-MFWS) are functionally important and are presented in stick representation. The 2b-tail binding site in the region M7, M10 is distinct from the SLN binding site in M2, M4, M6, M9 in SERCA1a (numbering is indicated on helices). M, membrane region; A, actuator domain; N, nucleotide binding site and P, phosphorylation domain

pocket that is formed by the five luminal loops of the pump [44]. This intramolecular interaction stabilizes the pump in the Ca^{2+}-bound E1 conformation with high-affinity binding sites facing the cytosol [44]. LE mainly reduces the E1P to E1 backwards reaction, thereby slowing the Ca^{2+} dissociation from the SERCA2b pump and increasing the intrinsic Ca^{2+} affinity. LE also slows down the E1P to E2P conversion [47].

SERCA2c

The SERCA2c protein exhibits unique enzymatic properties as compared to SERCA2a and SERCA2b, which is due to the unique six amino acids extension in the carboxyl terminus. The maximal turnover rate of SERCA2c is comparable to SERCA2b, but SERCA2c displays a lower apparent affinity for cytosolic Ca^{2+} than SERCA2a and SERCA2b. SERCA2c may therefore function particularly

in conditions of a high cytosolic Ca^{2+} concentration [33]. In HEK293 cells, overexpression of the SERCA2c protein leads to comparable changes in both the cytosolic Ca^{2+} and ER Ca^{2+} levels [33].

SERCA3a-f

Although the human SERCA3a–f splice variants differ at their C-terminus, they display a similar apparent affinity for cytosolic Ca^{2+} that is three- to fivefold lower than SERCA1a [39, 49, 50]. The lower Ca^{2+} affinity relates to a reduced E2–E1 transition rate and an increased rate of Ca^{2+} dissociation from the Ca^{2+}-bound E1 state [39]. Since SERCA3 is frequently co-expressed in the ER together with the high Ca^{2+} affinity variant SERCA2b, SERCA3 may specifically function in ER regions exposed to local elevated Ca^{2+} concentrations [21, 49].

Despite their similar Ca^{2+} affinities, the different SERCA3 pumps show distinct effects on both the cytosolic and ER Ca^{2+} levels [49]. HEK-293 cells stably expressing SERCA3c and -3f showed the highest cytosolic Ca^{2+} levels whereas SERCA3a and -3d transfected cells displayed the lowest cytosolic Ca^{2+} levels [21, 49, 50]. The ER Ca^{2+} levels of cells overexpressing hSERCA3b, -3d, and -3f were significantly higher than when the other splice variants were overexpressed [21]. These distinct effects coincide with different Ca^{2+} pumping activities of the SERCA3 variants [49], although another study showed that SERCA3a-c may have similar maximal turnover rates that are higher than SERCA1a [39].

Remarkably different from the SERCA1 and SERCA2 isoforms, the SERCA3 ATPase activity is not stimulated by the addition of ionophore to membrane vesicles. This might indicate that the SERCA3 transport activity is insensitive to luminal Ca^{2+} or that SERCA3 itself promotes a Ca^{2+} leak from the ER [39].

2.2.2 Subcellular Targeting

Different compartmentalization of distinct SERCA isoforms and splice variants might be important to allow local Ca^{2+} signaling in Ca^{2+} microdomains of the cell [21, 51].

SERCA2a-c

In human left ventricular tissue and isolated cardiomyocytes, hSERCA2a is targeted to regions close to the transversal T-tubules and to the longitudinal SR, whereas hSERCA2b is preferentially targeted transversally nearby the T-tubules [21]. Similar patterns were observed in mice overexpressing hSERCA2b in the heart [52]. In contrast, the endogenous mSERCA2b and mSERCA2a seem to be targeted to the same sites in mouse cardiomyocytes [53, 54], which is further underscored by the observation that mSERCA2b can replace mSERCA2a in the longitudinal SR of

mice in which the SERCA2a splice variant is substituted by SERCA2b [53]. The hSERCA2c splice variant shows a more distinct pattern and is restricted to a subplasma membrane region and in intercalated discs [21]. This restricted localization together with the specific enzymatic properties may indicate that SERCA2c operates in another Ca^{2+} microdomain than SERCA2a and SERCA2b [21].

SERCA3a-f

hSERCA3a, -3d, and -3f are expressed in human cardiomyocytes [21], whereas mSERCA3a, -3b, and -3c are found in mouse cardiovascular tissue [54]. Interestingly, these SERCA3 variants occupy distinct subcellular sites different from SERCA2a and SERCA2b. In human cardiomyocytes, hSERCA3a presents a uniform distribution and is targeted to the regions of the transversal SR close to the T-tubules and the intercalated discs. hSERCA3d is more restricted to the ER membrane in the perinuclear region, whereas hSERCA3f is mainly observed in the ER membrane near the plasma membrane [21]. In mouse cardiomyocytes mSERCA3b was preferentially expressed in the transversal SR near the T-tubules and the junctional reticulum [54]. However, no specific localization was observed for the mSERCA3a and -3c variants [54].

2.2.3 Interacting Proteins

The Ca^{2+}-binding ER resident chaperones calreticulin (CRT, 46-kDa) and its 90-kDa homolog calnexin (CLNX) may interact with the 2b-tail of SERCA2b. Both proteins contain a globular N-domain involved in oligosaccharide binding, an extended P-domain mediating ERp57 binding and an acidic Ca^{2+}-binding C-domain [51]. CRT can complex over half of all ER luminal Ca^{2+} [55], whereas luminal Ca^{2+} buffering by CLNX is much less pronounced because it contains less Ca^{2+}-binding sites. In *Xenopus* oocytes overexpressing mammalian SERCA2b, CRT, or CLNX may functionally interact with N-linked carbohydrates on N1035 belonging to the LE of the 2b-tail [56]. The interaction of CRT or CLNX with SERCA2b, but not with SERCA2a, exerts an inhibitory effect on the Ca^{2+}-wave propagation in *Xenopus* oocytes in line with a direct functional interaction [56, 57]. These luminal proteins may play a role as luminal Ca^{2+} sensors to adapt the activity of SERCA2b depending of the Ca^{2+} loading state of the ER [56, 57]. It remains unstudied whether the regulation of SERCA2b by CRT or CLNX may also occur in mammalian cells.

2.2.4 Posttranslational Modifications in the N/C-Termini of SERCA Isoforms

According to the PhosphoSitePlus database several posttranslational modifications (PTMs) were identified in the N- and C-termini of the SERCA isoforms. This database comprises literature data and unpublished high-throughput mass spectrometry

data. In human SERCA1a S19 phosphorylation was detected at the N-terminus. Ubiquitination of K7, K30, and K35 in mouse SERCA1a and acetylation of K30 and K35 in rat SERCA1a were indicated. In SERCA2, phosphorylation on S38 was detected in human, mouse, and rat samples and is further described below. The hSERCA2 N-terminus might further be ubiquitinated on K30 and K31 and acetylated on K31 and K33. S17, T19, and S25 in the N-terminus and T1009 in the C-terminus of mouse SERCA3b-e were identified as phosphorylation acceptor sites, whereas human SERCA3b-e may be phosphorylated on S1005. Most of these PTMs remain to be studied to unravel their functional role, and only for a few PTMs information can be found. S38 phosphorylation Several reports documented the phosphorylation of the cardiac SERCA2a pump on residue S38, which is part of a Ca^{2+}/calmodulin-dependent protein kinase II (CaMKII) consensus site (RXXS/T) that is not present in SERCA1a [58, 59]. CaMKII-dependent phosphorylation on S38 increases the maximal turnover rate of SERCA2a without altering its apparent Ca^{2+} affinity [58–60]. Although SERCA2a phosphorylation was observed in isolated perfused intact beating heart [61], no S38-phosphorylated SERCA2a was detected by immunoblotting with a phospho-S38 specific antibody for SERCA2a in kinase-treated SR vesicles or suitably stimulated cardiac myocytes [62]. Some studies question the functional effects of the S38 phosphorylation because of the lack of in vivo information [62, 63]. At least according to the PhosphoSitePlus database, S38 phosphorylation was identified by mass spectrometry techniques in several species. CaMKII may mediate the cardiac frequency-dependent acceleration of relaxation [64] by phosphorylation of SR proteins such as PLB [65] and potentially also SERCA2a [58–60].

N1035 Glycosylation

As mentioned earlier, N1035 is a putative glycosylation site in the 2b-tail of SERCA2b that may be involved in the interaction with CRT or CLNX. However, despite serious efforts, glycosylation of N1035 was never experimentally observed [44, 56, 57]. The lack of glycosylation does however not *a priori* exclude CLNX or CRT binding to SERCA2b because these ER chaperones can occasionally also bind to non-glycosylated targets [57, 66]. The fact that an N1035A SERCA2b mutant displays normal Ca^{2+}-dependent ATPase-activity when overexpressed in COS cells, seems to indicate that glycosylation is not required to obtain the enzymatic properties of SERCA2b. According to a SERCA2b homology model, the 2b-tail may be buried in the luminal loops of the pump [44] making the glycosylation of this site unlikely [56].

2.2.5 Disease Mutations in the N-/C-Termini

Mutations in *ATP2A1* are associated with Brody disease (OMIM 601003), which is characterized by painless muscle cramping and exercise-induced impairment of muscle relaxation. Although Brody myopathy can be caused by mutations in

ATP2A1, there is evidence of genetic heterogeneity. So far no Brody Disease mutations are recognized in the N- or C-termini of SERCA1a.

Heterozygous mutations in *ATP2A2* are implicated in Darier–White disease (OMIM 124200), an autosomal dominant skin disorder characterized by distinctive nail abnormalities and warty papules and plaques mainly on the chest, neck, back, ears, forehead, and groin. The skin disease is characterized by a disruption of cell–cell contacts (acantholysis) in the suprabasal layers of keratinocytes in the epidermis. Currently more than 180 mutations in the *ATP2A2* gene are identified that lead to Darier disease [67], that in many cases result in loss of pumping activity. Only a fraction of the mutated residues are located in the N- and C-termini of SERCA2b (M1V [68, 69], M1T [68], ΔE11 [70], G23E [48, 68, 69, 71], N39T [70, 72], ΔL41 [70], and ΔP42 [70]). M1023I is the only one known Darier disease mutation that is found in the 2b-tail [68]. Recently, Darier disease mutants have been identified that lead to a gain-of-function resulting in a leaky Ca^{2+} pump that dissipates the ER Ca^{2+} gradient, which would explain the dominant phenotype of the disease [73].

2.2.6 Physiological Relevance of the SERCA2 Regulation

The alternative C-terminal extensions of the SERCA pumps have important physiological implications, which are best understood for the SERCA2 splice variants. In mouse cardiomyocytes, the majority of the SERCA2 protein consists of SERCA2a (95 %) and a modest expression of SERCA2b (5 %) is observed [53]. The expression levels of SERCA2c in total human heart are only minor in comparison with SERCA2a and SERCA2b, but they might operate in different subcompartments [21].

In cardiomyocytes, the SERCA2a activity controls the relaxation, the Ca^{2+} concentration of the SR and as a result the amount of Ca^{2+} that can be released for contraction [74, 75]. Since SERCA2a has a profound impact on cardiomyocyte contractility, its activity is tightly controlled, mainly by regulating the apparent Ca^{2+} affinity of the pump [76–79]. Early in cardiac development, alternative splicing of the SERCA2 messengers leads to the replacement of the housekeeping high Ca^{2+} affinity SERCA2b pump by SERCA2a, which displays a lower Ca^{2+} affinity [80]. In normal physiological conditions, the apparent Ca^{2+} affinity of SERCA2a is even further reduced by the expression of PLB decreasing Ca^{2+} transport activity and inhibiting cardiac relaxation and contraction at rest [81]. PLB phosphorylation during β-adrenergic stimulation releases the inhibitory effect of PLB on SERCA2a, which temporarily increases the apparent Ca^{2+} affinity and stimulates cardiac contractility [81, 82]. These findings are well documented and are based on multiple animal models of altered SERCA2a and PLB expression in the heart (reviewed in Ref. [81]). However, these mouse models did not shed light on the physiological relevance of the SERCA2a/b diversity.

In *SERCA2*$^{b/b}$ mice, SERCA2a is replaced by SERCA2b by preventing the alternative splicing of the SERCA2 messengers. The adult *SERCA2*$^{b/b}$ mice developed concentric left-ventricular hypertrophy, showing that SERCA2a is crucial for

normal cardiac growth and function [76]. Remarkably, the high Ca^{2+} affinity of SERCA2b in these *SERCA2*$^{b/b}$ mice is at least partially compensated by a twofold upregulation and a reduced phosphorylation status of PLB, which serves as a cardioprotective effect [79]. The high apparent Ca^{2+} affinity of SERCA2b actually ensures proper contractile parameters of the heart in resting conditions [79], but it becomes limiting at high Ca^{2+} loads due to the compensatory lower expression levels and lower maximal turnover rate of the pump [83]. Together, the studies in the *SERCA2*$^{b/b}$ mice highlight the physiological importance of the SERCA2a/b isoform diversity [4, 78, 84].

In human heart failure, SERCA2a expression is significantly reduced, whereas PLB levels are unchanged (reviewed in Ref. [75] and [81]). This results in a chronic inhibition of SERCA2a marked by a lower apparent Ca^{2+} affinity, which contributes to the impaired contractility of the failing heart. Restoration of the cardiac expression levels of SERCA2a via viral gene transfer is considered as a promising therapeutic approach that currently is explored in clinical trials [85, 86], but alternative interventions aim to increase the apparent Ca^{2+} affinity of SERCA2a [87]. This can be achieved by interfering with PLB expression or activity [88, 89], or by targeting the empty 2b-tail binding site on the SERCA2a pump with 2b-tail mimetics or analogs [77].

3 Regulation of the SPCA Pumps by Amino and Carboxy Termini

3.1 SPCA Isoforms and Splice Variants

The founding member of the Golgi/secretory pathway Ca^{2+} ATPases is PMR1 (plasma membrane-related), which was first described in *Saccharomyces cerevisiae* [90]. Later, the mammalian SPCA isoforms were cloned and characterized [91, 92]. In higher order animals, including amphibians, reptiles, and mammals, two isoforms are recognized, ATP2C1 (SPCA1) and ATP2C2 (SPCA2). SPCA1 is ubiquitously expressed and is considered the housekeeping Golgi Ca^{2+} pump, whereas the expression of SPCA2 is mainly restricted to brain and secretory cells, such as the various segments of the gastrointestinal tract, trachea, thyroid, salivary gland, mammary gland, and prostate [93, 94]. This suggests that SPCA2 may exert a more specialized physiological function than SPCA1a.

Compared to SERCA, SPCA1a has a slightly longer N- and C-terminus (Fig. 14.4). The C-terminus of hSPCA2 contains 17 amino acids and is slightly shorter than the hSPCA1a C-terminus with 21 amino acids. Alternative splicing further gives rise to multiple SPCA1 variants that differ only in their C-termini (SPCA1a-d) [4, 95, 96]. SPCA1c seems to be a truncated form, which is detected at the mRNA, but not protein level. Based on the predicted secondary structure, SPCA1c lacks not only the complete C-terminus but also the last membrane helix

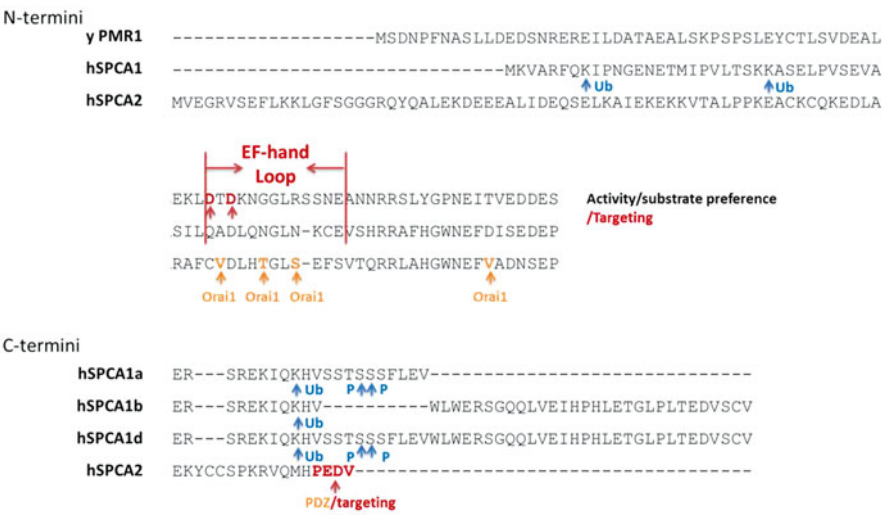

Fig. 14.4 The N- and C-termini of SPCA isoforms and splice variants contain important regulatory sites. hSPCA1c is truncated in M10 and is not displayed. The N-terminus is defined as all the residues before M1 and the C-terminus is defined as the sequence stretch after M10. The EF-hand-like loop regions are indicated for *S. cerevisiae* yPMR1 and human hSPCA1. In yPMR1, the residues indicated in red are present in the EF-hand-like motif and are important for Ca^{2+}/Mn^{2+} preference, transport activity and subcellular targeting. hSPCA2 interacts to the Orai1 channel via its N- and C-termini. The N-terminal hSPCA2 residues important for Orai1 interaction are indicated with *orange arrows*. hSPCA2 contains a PDZ binding domain at the C-terminus, which might be important for targeting. The *blue arrows* indicate residues that might be acceptor sites for posttranslational modifications according to PhosphoSitePlus. P, phosphorylation. Ub, ubiquitination

M10 indicating that the truncated SPCA1c variant might be unstable, questioning its physiological relevance [96]. The other splice variants SPCA1a, SPCA1b, and SPCA1d share a common C-terminus of 11 residues, followed by an alternative sequence stretch. hSPCA1a, the predominant isoform of SPCA1, contains a stretch of ten amino acids, which includes five serine residues, interrupted by one threonine. This motif is substituted for a stretch of 30 amino acids in the SPCA1b variant. SPCA1d is the longest splice variant with a unique C-terminus of 51 amino acids that contains both the SPCA1a and the SPCA1b-specific C-terminal motifs [95, 96].

Interestingly, like the truncated S1T variant of SERCA1a, also a shorter splice variant of SPCA2 has been reported, which in this case corresponds only to the C-terminal part of SPCA2, resulting in an ER-localized 20 kDa protein that can be found in the mouse pancreas and in acinar cell lines [97]. This splice variant is clearly not a functional Ca^{2+} pump since it lacks all of the catalytic domains of SPCA2. Although it includes M6, the Ca^{2+} transport binding sites are incompletely formed and the phosphorylation-, actuator-, and nucleotide-binding domains of the pump are lacking. The regulation of its expression by MIST1, a transcription factor that is required for acinar cell maturation and function, may suggest that the

C-terminal SPCA2 protein fragment might play a so far unrecognized physiological role in the pancreas [97]. For instance, the truncated protein might interact with the Orai1 Ca^{2+} channel, which is discussed in Sect. 3.2.3.

In general, hSPCA1 displays a 29 % sequence identity and 43 % sequence similarity with the rabbit SERCA1a, the best characterized Ca^{2+} pump for which the Ca^{2+} transport mechanism is well understood [4]. Although this suggests that the Ca^{2+} pumping mechanism is highly conserved in SPCA, SPCA also displays distinct enzymatic properties. (1) Unlike SERCA, which transports two Ca^{2+} ions per hydrolyzed ATP, SPCA pumps only one Ca^{2+} ion per cycle. The Ca^{2+}-binding site of SPCA overlaps with the Ca^{2+} binding site II in the SERCA pumps, involving residues in M4 and M6 [4]. (2) Unlike the other Ca^{2+} ATPases, SPCA has in addition to Ca^{2+} the unique ability to transport Mn^{2+}. Transport of Mn^{2+} and Ca^{2+} is mutually exclusive, indicating that both ions are transported via the same substrate binding site II in the M domain [98–100]. SPCA pumps ensure uptake of Mn^{2+} in the lumen of the Golgi compartment, where several Mn^{2+}-depending enzymes reside, such as the glycosyltransferases and sulfotransferases [4]. (3) An important characteristic of SPCA is the considerably higher affinity for cytosolic Ca^{2+} ions than SERCA [96]. The high apparent Ca^{2+} affinity suggests that the Ca^{2+} uptake into the Golgi/secretory pathway is permanently activated and is independent of a transient elevation of the cytosolic Ca^{2+} concentration. The maximal turnover rates of the SPCA isoforms and splice variants are two- to sixfold lower compared to SERCA1a [96]. (4) SPCA is more compact than SERCA with shorter cytosolic and luminal loops [4]. At least some of the longer loops in SERCA contain unique regulatory and interaction sites [101]. For instance, HAX-1 interacts with the unique part of a cytosolic loop in the N-domain [102], whereas ERp57 interacts with the larger luminal L7-8 loop in SERCA [103].

Despite these fundamental differences between SERCAs and SPCAs, their overall sequence similarity clearly demonstrates that they are more closely related than compared to the more distantly related PMCA Ca^{2+} pumps. For this reason, SERCAs and SPCAs belong to the same P2A group in the P2 subfamily, whereas PMCAs are members of the P2B group [4].

3.2 Regulation of SPCA Splice Variants by N- and C-Terminal Extensions

3.2.1 Biochemical Properties

Although the physiological roles of the splice variants of SPCA1 have never been studied in great detail, ATPase activities of these splice variants have been compared in a HEK-293 overexpression system [96]. Only low overexpression levels in HEK-293 cells were observed for SPCA1c and consequently no activity was detected [96]. For the other three SPCA1 splice variants, the K_m values are similar (9–10 nM), but lower than for SPCA2 (25 nM) and SERCA1a (284 nM) [104].

The higher affinity of SPCA1 and SPCA2 compared to SERCA1a is related to a kinetic effect rather than to a true increase of affinity at the Ca^{2+} binding site II, which is composed by identical residues in SERCA and SPCA. The maximal turnover rate is also comparable for SPCA1a, SPCA1b and SPCA1d (20–27 s^{-1}), slightly higher for SPCA2 (40 s^{-1}), but is 4.6–6.4-fold lower than for SERCA1a (130 s^{-1}). Apparently, the alternative C-termini of SPCA1 have little impact on the enzymatic properties of this pump.

3.2.2 Substrate Binding and Specificity

The N-terminus of the *S. cerevisiae* PMR1 holds an unpaired EF-hand-like motif that has been demonstrated to bind Ca^{2+} (Fig. 14.5a) [99]. An EF-hand motif is a helix–loop–helix motif in which a central Ca^{2+} ion is chelated by oxygen atoms arranged in three dimensions. EF-hand motifs may act as sensors of intracellular Ca^{2+} levels (*e.g.*, in calmodulin) or serve as Ca^{2+} buffers (*e.g.*, in parvalbumin [105]). Of interest, the Ca^{2+} binding in the PMR1 motif can be abolished by molar excess of Mn^{2+}, but not Mg^{2+}, suggesting possible competition between Ca^{2+} and Mn^{2+} binding [99]. Disruption of the EF-hand-like motif in PMR1 by either alanine substitution or deletion severely impairs PMR1 Ca^{2+} transport activity. The D51A and D53A single point substitutions in the EF-hand-like motif lead to a lower maximal turnover rate and reduced affinity for Ca^{2+}, whereas the D51A/D53A double mutant is retained in the ER, highlighting the importance of this motif for PMR1 activity and subcellular targeting [99]. Remarkably, the two point mutations have distinct effects on the affinities for Ca^{2+} and Mn^{2+} ions. Overexpression of the D51A mutant fails to rescue the Mn^{2+} hypersensitivity in the Δpmr1 strain, in line with impaired Mn^{2+} transport. However, the D53A single and D51A/D53A double mutants are able to rescue the Mn^{2+} hypersensitivity of the Δpmr1 strain, indicating that only Ca^{2+}, but not Mn^{2+} transport is impaired [99]. Thus, the PMR1 N-terminus, which is distal from the membrane regions that shape the Ca^{2+}/Mn^{2+} pathway, also regulates substrate preference. The N-terminal Ca^{2+} and/or Mn^{2+} binding might regulate intramolecular interactions between the N-terminus and downstream elements of PMR1, since the N-terminal region of PMR1 influences proteolytic stability of the C-terminal part of the protein [99].

It is currently unknown whether the N-terminus of the human isoforms is regulated in a similar manner, but it is interesting to point out that the N-terminal EF-hand-like motif is at least partially conserved in the N-terminus of hSPCA1a (Fig. 14.5a), whereas it is less conserved in SPCA2. Although the SPCA1 N-terminus lacks one of the aspartate residues in the loop of the EF-hand-like region, prediction of the N-terminal structure with iTasser, a folding prediction program, indicates that the N-terminus of hSPCA1 may retain the EF-hand-like helix–loop–helix motif (Fig. 14.5b).

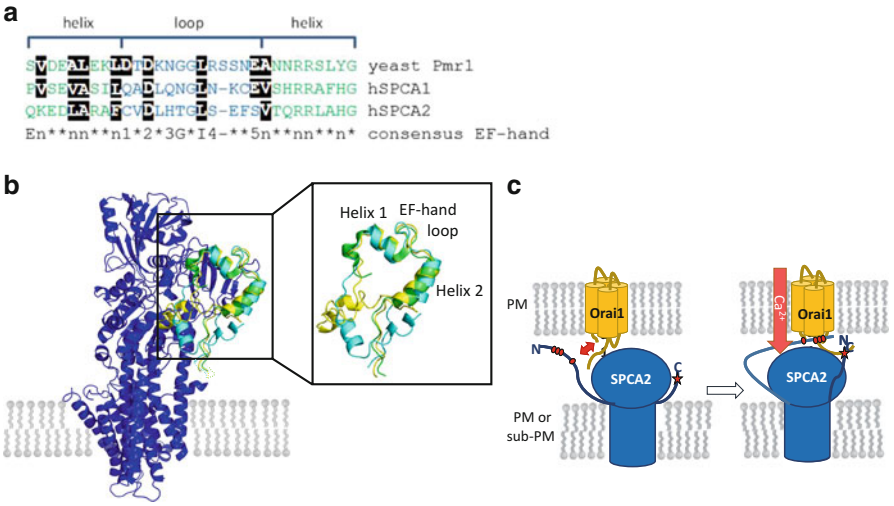

Fig. 14.5 Role of the N- and C-termini of the Secretory Pathway Ca^{2+}-ATPases in Ca^{2+} binding and Orai1 interaction. (**a**) Alignment of the EF-hand-like region of SPCA1, SPCA2 and PMR1. Residues that match the EF-hand consensus motif are indicated in black. Consensus: E = glutamate, * = any amino acid, n = apolar amino acid, 1–5 = negatively charged Ca^{2+} coordinating residues, G = glycine, I = isoleucine or similar. (**b**) A full-length homology model of SPCA1 (*dark blue*, truncated at the start of M1) was overlaid with the crystal structure of the SERCA1a N-terminus (*green*) and the predicted structures of the N-terminus of SPCA1 (*cyan*), PMR1 (*yellow*). N-terminus predictions were performed with iTasser [199]. The SPCA1 homology model was generated with SWISS-MODEL using the SERCA1a E2P crystal structure (3B9B) as a template [200]. (**c**) Proposed model of the interaction between SPCA2 and Orai1. Four critical residues in the N-terminus of SPCA2 interact with the cytosolic parts of Orai1, allowing for an interaction between Orai1 and the C-terminus of SPCA2, which activates the channel. The exact sites of interaction in the SPCA2 C-terminus and Orai1 are not known. The model is adapted from Ref. [111]

Although the precise function of the N-terminal segment of PMR1 remains unclear, the binding of the substrate to the N-terminus is a common regulatory mechanism observed in other P-type ATPases such as PMCA (see Sect. 4) and the Cu^{+} transporters ATP7A and ATP7B [106].

3.2.3 Subcellular Targeting

It remains unknown if the splice variants of SPCA1 are distributed differently, but so far, several differences between the subcellular localization of human SPCA1 and SPCA2 proteins have been observed, which might relate to a dileucine motif and a putative type III PDZ binding motif that is only present in the hSPCA2 C-terminus. The precise localization of SPCA1 and SPCA2 in the Golgi apparatus and secretory pathway further seems to vary between cell types. In non-polarized

cells, SPCA1 showed a distribution consistent with Golgi/TGN localization [107, 108]. In HeLa cells and Human Kidney 2 cells, SPCA1 levels seem to increase along the secretory pathway, with weak co-localization with ER- and intermediate compartment markers, and stronger co-localization with markers of the TGN and secretory vesicles/endosomes [109]. In liver, SPCA1 is found in an endosomal compartment close to the basolateral membrane, which might sequester Mn^{2+} as a mechanism of Mn^{2+} detoxification [108]. SPCA1 and SPCA2 exhibit a markedly different localization in epithelial cells of lactating mammary tissue, with SPCA1 being mostly present in the perinuclear Golgi region, whereas SPCA2 is more located in extra-Golgi vesicles. In the cell body and dendrites of rat hippocampal neurons, the endogenous SPCA2 is present in vesicles derived from the TGN, which is different from a more perinuclear distribution of hSPCA1 [94].

3.2.4 Interacting Proteins

Orai1

Orai1 is a plasma membrane Ca^{2+} channel that is responsible for store-operated Ca^{2+} entry (SOCE). The classical Orai1 activation mechanism occurs through an interaction with STIM1/2 from a sub-plasma membrane ER compartment. The integral membrane ER proteins STIM1/2 are Ca^{2+} sensing proteins that upon Ca^{2+} depletion of the ER store relocalize in clusters that physically interact with Orai1 in the plasma membrane [110]. An alternative, store-independent activation pathway for Orai1 depends on the interaction of Orai1 with SPCA2, which relates to the unique capacity of the SPCA2 N- and C-termini to interact and activate the Ca^{2+} channel. SPCA2 may interact to Orai1 within the plasma membrane [111] or alternatively, from a sub-plasma membrane compartment (Golgi or secretory vesicles) [112]. Specific residues in the N-terminus of SPCA2 first coordinate the interaction with Orai1, ensuring that the C-terminus of SPCA2 is available and maneuvered sufficiently close to Orai1 to activate Orai1 (Fig. 14.5c) [111].

A SPCA2 fragment corresponding to the C-terminal M9-10 region is able to activate Orai1 indicating that the C-terminus contains the Orai1 activation properties [111]. Of interest, a C-terminal M9-10 fragment of SPCA1 also activates Orai1, although the full-length SPCA1 fails to activate Orai1. This remarkable difference between SPCA1 and SPCA2 is explained by differences in the N-terminus of SPCA1 and SPCA2. The N-terminus is therefore able to control the access of the C-terminus to the Orai1 channel for activation [111]. Critical amino acid substitutions in the N-terminus of SPCA1, notably at the position of the predicted EF-hand like motif in SPCA1, prevent the SPCA1-Orai1 interaction (Fig. 14.5a). This suggests that the N- and C-termini are communicating in SPCA1 and SPCA2 via a so far unidentified mechanism. As mentioned in Sect. 3.2.2, also the N-terminus of the yeast PMR1 influences the stability of the C-terminal part of the pump.

3.2.5 Posttranslational Modifications in the N/C-Termini of SPCA Isoforms

PTMs may regulate the function of the SPCA N- and C-terminal stretches. Although no PTMs have been experimentally confirmed in the N- or C-terminus of SPCA1 and 2, evidence for ubiquitination of residues K8 and K25 in SPCA1 is available in the PhosphoSitePlus database. In addition, the C-terminus of SPCA1a and SPCA1d contains a serine/threonine-rich motif that is absent in the C-terminus of SPCA1b, but that is indicated by PhosphoSitePlus as a possible phosphorylation site. No information on the functional importance of these PTMs is currently available.

3.2.6 Disease Mutations

The *ATP2A2* and *ATP2C1* genes are involved in related skin disorders. Mutations in SERCA2 result in Darier disease, whereas mutations in SPCA1 cause Hailey–Hailey disease, a related non-immune mediated acantholytic skin disease with similar symptoms [113]. A remarkable parallel between the two genes was also observed in heterozygous *Atp2a2*+/– [114] and *Atp2c1*+/– mice [115], which both display an increased incidence of squamous tumors. Over 100 different mutations in *ATP2C1* have been identified in Hailey–Hailey disease patients, but so far no mutations in the N- or C-terminus other than frameshifts or nonsense mutations, are known to cause Hailey–Hailey disease.

3.2.7 Implications of the SPCA Regulation for Lactation and Breast Cancer

The activity and expression of multiple Ca^{2+} transporters in the mammary gland is tightly coordinated during pregnancy, lactation at parturition, and the process of involution. These changes are required to support the release of large amounts of Ca^{2+} in the milk (8–60 mM, depending on the species) [116]. SPCA1, SPCA2, and Orai1 levels are highly upregulated in mammary gland during lactation [117, 118], resulting in a 150-fold increase in SPCA2 and a 15-fold increase in SPCA1 protein levels [117]. SPCA2 activates Orai1 via its N- and C-terminal extensions at the basolateral side of the mammary gland luminal epithelial cells, which leads to an increased Ca^{2+} influx. Ca^{2+} is subsequently transferred into the milk at the apical side via two main Ca^{2+} transport routes: via the ER/secretory pathway (SERCA/SPCA) and across the apical plasma membrane via PMCA [117, 119, 120]. PMCA2 knockout mice exhibit 60 % lower Ca^{2+} levels in the milk suggesting the remaining 40 % may be released via the ER/secretory pathway [119].

In the pancreas, the expression of a short 20 kDa splice variant of SPCA2 as well as the full length SPCA2 are controlled by the transcription factor MIST1 [97]. Besides the expression in pancreatic acinar cells, MIST1 is also transiently expressed

during lactation in the epithelial alveolar cells suggesting that MIST1 might also control SPCA2 upregulation in mammary gland [97]. It is therefore tempting to speculate that the C-terminal SPCA2 fragment might interfere or regulate the SPCA2-Orai1 interaction as was already experimentally observed with a M9-10 fragment of SPCA2 [111]. Alternatively, the C-terminal fragment might regulate the targeting of Orai1, *e.g.*, in mammary epithelial cells [117]. Indeed, in mouse mammary epithelial cells mislocalization of Orai1 in SPCA2 knockdown cells could be partially rescued by overexpression of the last 77 amino acids of SPCA2 [117].

The store-independent mechanism of Ca^{2+} influx through the SPCA2-Orai1 interaction may also contribute to the altered Ca^{2+} homeostasis in some types of breast cancer. SPCA2 is upregulated and involved in luminal subtypes of breast cancer [111] and Orai1 expression is dramatically increased in several mammary tumor cell lines like MCF-7 and MDA-MB-231 [118]. Of interest, the Orai1 channel in MCF-7 breast cancer cells remains constitutively activated by SPCA2 leading to pathological Ca^{2+} influx, activation of MAP kinase pathways, high rates of proliferation, and tumorigenesis [111]. Knockdown of SPCA2 in MCF-7 cells attenuated cell proliferation, colony formation in soft agar, and MCF-7-induced tumor formation in mice [111]. In contrast, SPCA2 was not expressed in the highly metastatic cell line MDA-MB-231. In MDA-MB-231 cells, STIM1/Orai1-mediated store-dependent Ca^{2+} entry might be more important [121]. Interestingly, SPCA1 knockdown in MDA-MB-231 cells reduces cell proliferation and impairs the posttranslational modification of IGF1R, a protein important in tumor progression suggesting that also SPCA1 might exert tumor promoting effects [122]. Different from SPCA2, SPCA1 is upregulated in the basal-like breast cancer subtype, *i.e.*, a breast cancer subtype with the worst prognosis, suggesting a specific role of SPCA1 [122].

Thus, SPCA1/2 isoforms play a prominent role in the Ca^{2+} dyshomeostasis of breast cancer cells [111, 112, 122, 123]. Moreover, SPCA1/2 pumps might be potential therapeutic targets for breast cancer therapy. In particular, interfering with the N-/C-terminal dependent activation of Orai1 might be a valuable therapeutic approach, since a 40-amino acid fragment corresponding to the SPCA2 N-terminus interferes with the SPCA2-Orai1 interaction, which may prevent the pathological activation of Ca^{2+}-influx [111]. Such therapeutic strategies should however take into account the different roles of the SPCA1 and SPCA2 isoforms in different breast cancer subtypes [112].

4 Plasma Membrane Ca^{2+} ATPase

4.1 PMCA Isoforms and Splice Variants

PMCA is a low capacity, but high affinity extruder for Ca^{2+} that contributes to maintain a steep Ca^{2+} gradient across the plasma membrane [124]. PMCA was first identified in mammalian erythrocyte membranes [125] and later purified by calmodulin affinity chromatography [126]. PMCA is found in all eukaryotes, including fungi,

plants, and animals, but PMCA-like pumps are also present in Eubacteria and Archaea. PMCA lacks a critical acidic residue in M5 explaining why PMCA, like the SPCA isoforms, only contains one Ca^{2+}-binding site in the M-domain that corresponds to site II of the SERCA1a pump [4]. The Ca^{2+} affinity of PMCA falls in the 10–30 μM range in resting conditions, but changes to 0.2–0.5 μM range in optimal stimulated conditions [124]. Although the Ca^{2+} affinity of the PMCA pump is lower than that of the SPCA and most SERCA pumps, PMCA operates in both resting and stimulated conditions in many cell types to fine-tune the cytosolic and/or microdomain Ca^{2+} concentrations [124]. PMCA pumps further differ from SERCA and SPCA isoforms by the presence of a much longer cytosolic C-terminus, which contains several important regulatory elements, such as a calmodulin binding domain (CaMBD) and an acidic phospholipid binding site [124, 127, 128]. The C-terminal segment of PMCA is an auto-inhibitory domain that interacts with the catalytic core of the pump [129].

Four mammalian genes (*ATP2B1-4*) encoding four PMCA isoforms have been identified, which mainly differ in tissue distribution [130, 131] and calmodulin affinity [132, 133]. Among them, PMCA1 is expressed ubiquitously and is expressed the earliest in development. PMCA2 and PMCA3 show a more tissue specific expression pattern. PMCA2 is highly expressed in the nervous system, liver, kidney, lactating mammary glands, and uterus [134, 135], whereas the expression of PMCA3 is more restricted with expression in brain, muscle, and lung. PMCA4 is expressed ubiquitously and abundantly in human [135], but also performs tissue-specific roles [136]. In addition, PMCA1 and PMCA4 display low calmodulin binding affinity, whereas PMCA2 and PMCA3 are more sensitive to calmodulin. Noteworthy, the calmodulin effect is remarkably different in PMCA2 as compared to the other isoforms since calmodulin only moderately stimulates PMCA2 [124]. This allows a sustained extrusion of Ca^{2+} via PMCA2 even in the absence of activators, which is for instance critical in the outer hair cells of the inner ear, since loss of PMCA2 results in deafness [137].

Furthermore, the four isoforms are subjected to alternative splicing at two hotspots (site A lies within the first cytosolic loop [141] and site C is positioned within the C-terminal tail [130]), leading to a complex array of around 30 PMCA protein variants (reviewed in Refs. [128, 135, 138–140]). Historically, alternative splicing at sites B and D was also considered to generate additional splice variants, but were later recognized as splicing artifacts [128, 135]. The PMCA variability introduced by the A and C regions does not affect the catalytical core of the pump, but is responsible for the differential subcellular targeting to special plasma membrane domains (*e.g.* lipid rafts, caveolae or apical versus basolateral membranes in epithelial cells), the regulation of pumping activity and the interaction with proteins or lipids, offering tissue and cell type dependent ways to respond to cytosolic Ca^{2+} signals and to modulate Ca^{2+}-dependent signal transduction pathways [124]. Although this may rationalize the existence of multiple PMCA variants, the specific role of many splice variants remains unclear.

The alternative splicing site A is located between a putative G protein binding sequence and a phospholipid binding site [135]. Except for PMCA1, which at site

A is only spliced in the *x* form, the other PMCA isoforms undergo alternative splicing at site A generating multiple variants. The different combination of three exons generates the PMCA2 *w*, *x*, *y*, and *z* variants, whereas for PMCA3 and PMCA4, only variants *x* and *z* are recognized [135]. The splicing at site A might modulate the lipid activation [135], G protein regulation [143] and subcellular targeting [144].

In this review, we are unable to completely cover the vast literature on PMCA isoforms and splice variants (for excellent reviews the reader is referred to Refs. [124, 135, 138, 145]), but in analogy to the SERCA and SPCA pumps described above, we here focus on some main properties, mechanisms, and roles of the N- and C-terminal dependent regulation of PMCA. For PMCA1-4, alternative splicing at site C generates multiple human PMCA variants that vary at their C-terminus (termed *a-f*). These segments affect the auto-inhibition properties, are promoting interactions with regulatory molecules such as the Ca^{2+}-binding protein calmodulin, acidic phospholipids, protein kinases, PDZ-domain containing proteins, Ca^{2+} ions and endogenous proteases [124, 135]. Many of these interactions alter the conformation of the C-terminus promoting its release from the catalytic core of the pump [128, 146].

4.2 Regulation of PMCA Splice Variants by N- and C-Terminal Extensions

4.2.1 Biochemical Properties

The presence of multiple Ca^{2+}- and Mg^{2+}-dependent ATPases and multiple PMCA isoforms in most cells and the lack of highly specific inhibitors of PMCA make it complicated to perform functional PMCA studies in intact cells [135]. Therefore, specific information on the functional role of the variable C-termini remains incomplete. Most kinetic studies were performed on PMCA4b, while other studies compared the main splice variants *a* and *b* of PMCA2 and PMCA4 [142, 147]. In COS microsomes overexpressing PMCA isoforms without the further addition of calmodulin, slightly higher values of both Ca^{2+} uptake activity and Ca^{2+} affinity were observed for rat PMCA2b than rat PMCA2a and hPMCA4b, suggesting a higher basal activity (without calmodulin) of PMCA2 compared to PMCA4. Interestingly, a truncated hPMCA4b without a C-terminus resembles rPMCA2b in the Ca^{2+} uptake activity further highlighting that the C-terminus is able to fine-tune the basal enzymatic activity [147].

4.2.2 Subcellular Targeting

Diverse PMCA isoforms not only regulate global intracellular Ca^{2+} homeostasis but also participate in local Ca^{2+} signaling. For both purposes the targeting of particular isoforms of PMCA to specific subcellular localizations is crucial, especially in

polarized cells such as epithelial cells and neurons. Studies in various epithelial cells indicated that the *w* insert promotes apical localization of PMCA, whereas the *x* and *z* inserts promote the targeting to the basolateral membrane [134, 144, 148, 149]. The apical localization of PMCA2w/b also depends on the lipid environment [150], and is promoted by the C-terminal PDZ domain interaction with the apical scaffolding protein NHERF2 [151].

Other studies found that PMCA pumps are enriched in specialized plasma membrane invaginations called caveolae [152, 153], where the local membrane is concentrated with cholesterol, glycosphingolipids and signaling proteins. Fujimoto et al. observed caveolae localization of PMCA in many human and mouse cell types [152]. A later study using synaptosomal plasma membranes vesicles from pig cerebellum further showed that PMCA4, but not PMCA1, -2, or -3 is associated with lipid rafts [154]. In intestinal smooth muscle, PMCA4*b* is associated with caveolin-1, whereas PMCA4*a* is associated with rafts [155], suggesting that the association of PMCA pumps with caveolae or rafts depends on the properties of the C-terminus. The targeting of various PMCA isoforms is further regulated by PDZ-binding proteins, which is discussed in Sect. 4.2.3.

4.2.3 Interacting Proteins

Calmodulin

By far the best understood regulatory mechanism of PMCA is the interaction with calmodulin, which in a Ca^{2+} loaded state binds with high affinity, reducing the K_m of the pump to sub-micromolar values [124]. The CaMBD is located at the C-terminal cytosolic region in mammalian PMCA, but positioned in the N-terminal region of plant PMCA proteins. In the mammalian PMCA, the Ca^{2+} loaded calmodulin binds at a site around 40 amino acids downstream of the last transmembrane helix [156]. In the absence of calmodulin, the long C-terminal tail is positioned close to the main body of the pump and interacts with two parts of the cytosolic loops: one in the A-domain and one in the N-domain between the phosphorylation and ATP binding site [129, 157]. According to an intramolecular FRET study the two termini of hPMCA4x/b are in close proximity in the auto-inhibited state, which limits the substrate access and inhibits pump activity [158]. When the Ca^{2+}-loaded calmodulin binds to the C-terminus of the pump, it induces a conformational change that swings the C-terminus away from the cytosolic loops activating the pump [128, 158]. Once the pump becomes activated by calmodulin, both substrate affinity and pumping rate are increased [159].

Recently, the crystal structure of the regulatory domain of the *Arabidopsis thaliana* PMCA isoform Aca8R in complex with calmodulin unexpectedly revealed two tandem inverted calmodulin binding sites (*i.e.*, CaMBS1 and CaMBS2) that are separated by eight residues [160]. A structural model for Aca8 in the auto-inhibited state was proposed indicating that the CaMBDs may interact with a highly conserved cleft, situated between the A domain and the N and P domains, that is fully exposed in the

E2 conformation and buried in the E1 conformation [160]. CaMBS2 can on itself promote auto-inhibition of PMCA, but when both CaMBDs work together, an additive effect is observed leading to complete auto-inhibition [160]. CaMBD1 would respond to nanomolar Ca^{2+} concentrations in basal conditions, whereas CaMBD2 would be sensitive to higher micromolar Ca^{2+} concentrations in stimulated conditions [160]. Overall, this may result in a two-step activation/inhibition mechanism explaining why PMCA responds to a wide range of cytosolic Ca^{2+} signals. The presence of two CaMBDs is also found in several, but not all, mammalian PMCA variants, including human hPMCA1d and hPMCA4d [138, 160].

Since alternative splicing of site C is located in the middle of the CaMBD, alternative splicing generates a series of splice variants with different calmodulin-dependent properties that alter the calmodulin binding affinity, the pH sensitivity of binding and on/off rates of calmodulin activation (see review [135]). Compared to the *b* variant, the *a* variant contains a frameshift in the middle of the CaMBD. Although the full C-terminus of variant *a* is much shorter, the CaMBD in *a* is longer than in *b* and is composed of two parts that are connected by a loop [161, 162], The PMCA1 and PMCA4 *d* variants contain the second CaMBD2 after the common CaMBD1 [160]. PMCA3f is the shortest splice variant, which is terminated 15 amino acids after splice site C, resulting in a different second half of the CaMBD and the lack of downstream regulatory regions [163].

The variations in the CaMBD result in different calmodulin affinities. In general, the *b* variants display a higher affinity towards calmodulin than the *a* variants [147, 164, 165], which is related to nine residues downstream of splice site C [164]. At site C an IQ-like motif is recognized, which is a sequence stretch for Ca^{2+}-independent calmodulin binding [127]. The motif in the *b* variants corresponds closer to the consensus IQ motif than that in the *a* variants. The lower calmodulin affinity of the short PMCA3f variant might also relate to a low resemblance to the PMCA3f IQ-like motif to the consensus IQ motif [135]. Finally, PMCA2a and PMCA2b present a higher calmodulin affinity than PMCA4b, leading to constitutive activation of PMCA2 in the brain where the calmodulin concentration reaches 50 μM [2, 135].

Although most PMCAs bind calmodulin with high affinity, the activation kinetics may differ significantly. PMCA4b shows an extraordinary slow calmodulin on/off rate, whereas PMCA4a is considerably faster [165]. The slow calmodulin on rate may allow the cytosolic Ca^{2+} to rise to a higher level before PMCA is activated and the slow off rate may result in a longer PMCA activation and a more complete Ca^{2+} extrusion. This may shape the formation of Ca^{2+} spikes [166] or provide a memory function [133].

PDZ Domain Containing Proteins

As mentioned in Sect. 4.2.2, various PMCA isoforms are targeted to specialized membrane domains such as lipid rafts [154] and caveolae [152, 153], which recruit multiple signaling proteins [167]. Many PMCA interacting proteins contain a PDZ domain, an 80–90 amino acid long structural domain that recognizes the C-terminus

of target proteins for complex formation or targeting to a specific region. Especially the *b* splice variants contain C-terminal extensions that end with a sequence stretch ETSL/V enabling PDZ domain binding [168].

Various members of the membrane-associated guanylate kinase (MAGUK) family [168], Ca^{2+}/CaM-dependent serine kinase (CASK) [169], neuronal nitric oxide synthase (nNOS) [140], the Na^+/H^+exchanger regulatory factor-2 (NHERF2) [170], cytoskeletal protein [171], and others [172, 173] interact via their PDZ domains to the C-terminus of PMCA, which can also be isoform specific. It is proposed that by binding, these interacting proteins may target and hold selected PMCA isoforms to spatially defined membrane regions [168], or recruit PMCA into multiprotein signaling complexes [170] for precise spatial and temporal Ca^{2+} signaling.

Calpain

Initiated by μM concentration of Ca^{2+}, calpain cleaves erythrocyte PMCA at the CaMBD, generating a permanently activated pump that loses the sensitivity to calmodulin [174]. Compared to PMCA2 and -4, PMCA1 is most sensitive to calpain cleavage [175]. PMCA is also the target for several other intracellular proteases such as caspases [176, 177], where the functional effect of PMCA depends on the site of cleavage.

14-3-3 Proteins

The N-terminus of PMCA recruits 14-3-3 proteins, which reduces the PMCA activity. 14-3-3 proteins are a family of regulators found in all eukaryotes that interact with a wide range of protein partners and that regulate many cellular processes, such as gene transcription, cell cycle regulation, and apoptosis [178]. The ε isoform of the 14-3-3 proteins interacts with the N-terminus of PMCA1, -3 [179] and -4 [180], whereas PMCA3 also interacts with the ζ isoform of 14-3-3 protein [179]. Only PMCA2 does not interact with 14-3-3 proteins, which might relate to PMCA2 specific residues in the N-terminus that may disrupt the amphipathic α helical structure required for the interaction with 14-3-3 proteins [179].

4.2.4 Stimulation of PMCA by Phospholipids

Two phospholipid binding sites were identified in PMCA, one in the M2 and M3 loop and one in the C-terminal CaMBD. Binding of acidic phospholipids to the C-terminal CaMBD [181, 182] such as phosphatidylserine, phosphatidic acid, phosphatidylinositol bisphosphate, and cardiolipin decrease the K_m of PMCA at least as low as calmodulin [183]. The activation by acidic phospholipids remains however poorly understood, although it is estimated that the local acidic phospholipid concentrations may be sufficiently high to stimulate PMCA up to ~50 % of its maximal activity [181].

4.2.5 Posttranslational Modifications in the N/C-Termini of SERCA Isoforms

PMCA can be phosphorylated by both Ser/Thr and Tyr kinases, which is thought to influence the regulation of the pumps either by activating PMCA or by regulating calmodulin binding. Here, we briefly discuss the best studied phosphorylations mediated by protein kinase A (PKA) and protein kinase C (PKC).

PKA

PKA phosphorylation seems to be specific for a certain subset of PMCA isoforms and splice variants, but variability in the PKA-mediated functional outcome exists, greatly depending on the PMCA isoform type [184]. During ß-adrenergic stimulation PKA can activate cardiac PMCA, which promotes Ca^{2+} extrusion [185].

PKC

The various PMCA isoforms and splice variants are differentially regulated by PKC. PKC readily phosphorylates the C-terminus of PMCA2a, -3a, -4a, and -4b, whereas PMCA2b and -3b are poor substrates for PKC [135, 186]. The functional effect of PKC-dependent phosphorylation also differs: the PMCA4a activity is not affected by PKC phosphorylation, whereas PMCA4b becomes partially activated [135]. In addition, the Ca^{2+}-calmodulin affinity and activating properties are not influenced by PKC in PMCA4a and -4b, whereas they are severely compromised in PMCA2a and -3a [135].

4.2.6 (Patho)Physiological Implications of the PMCA Isoform Diversity

The importance of PMCA isoforms is underscored by their various physiological functions and implications in human disease. Below the major (patho)physiological significance of the different PMCA isoforms is shortly discussed (for excellent reviews on PMCA in health and disease, the reader is referred to [124, 139, 187]).

PMCA2

In lactating mammary gland, PMCA4b is downregulated, whereas PMCA1 expression is moderately increased and PMCA2w/b is dramatically upregulated [188]. As mentioned in Sect. 3.2.7, PMCA2w/b is located at the apical membrane of the secretory cell [119] working together with the SPCA1/2-dependent secretory pathway [117] to load Ca^{2+} into milk. PMCA2 upregulation is also observed in breast

cancer and contributes to an increased resistance to apoptosis, [189], while its downregulation increases apoptosis [189].

High levels of PMCA2 are also found in the apical stereocilia in the hair cells of the Corti organ in the inner ear. Since stereocilia do not contain ER or mitochondria they solely rely on PMCA2 for Ca^{2+} clearance, underscoring the importance of PMCA2 for hearing and balancing. PMCA2 null mice are deaf and show balancing problems, while heterozygous mice show significant hearing loss [190]. Moreover, deafwaddler mice [191] and Wriggle Sagami mice [192] carry PMCA2 mutations [191]. The balance defect is related to the absence of the Ca^{2+} carbonate crystals of the otoconia embedded in the otolithic membrane of the sensory epithelium, which are sensing gravity and linear acceleration [124].

PMCA3

The PMCA3 G1107D substitution in a highly conserved region in the CaMBD is associated with X-linked pinocerebellar ataxia, impairing the Ca^{2+} clearance from the cell [193]. Another PMCA3 mutation, T543M, was identified in human pancreatic cancer cells affecting a residue located in one of the two docking site for the auto-inhibitory CaMBD [194].

PMCA4

In contrast to PMCA1, the genetic ablation of PMCA4 is not embryonically lethal, but produces specific phenotypes such as male sterility as a result of reduced sperm motility [195]. PMCA4b also modulates nNOS signaling in the heart by direct interaction via its PDZ-binding domain. In PMCA4 KO mice, the in vivo contractility and Ca^{2+} amplitude response increases, but relaxation is not altered. The nNOS interaction regulates cardiac contractility through modulation by cyclic nucleotides [196]. The overexpression of the PMCA4 pump in the myocardium of the rat leads to abnormal myocardial growth and hypertrophy [197].

5 Conclusions

Although P-type Ca^{2+} transporters share common domain architectures and similar transport mechanisms, they are differentially regulated by flexible N- and C-terminal extensions providing a multifaceted toolkit of Ca^{2+} transporters. The complex array of Ca^{2+} transporter isoforms and splice variants in various cellular compartments controls the spatiotemporal Ca^{2+} signals in a cell and serves as scaffolds to recruit other proteins. Without any doubt, the existence of so many isoforms and variants provide specific functions in specialized tissues, cell types, and subcellular domains. However, their (patho)physiological functions are only gradually emerging and

information on many splice variants remains limited. But it is becoming increasingly clear that insights into the properties and molecular mechanisms of the N- and C-terminal extensions may provide novel therapeutic opportunities to regulate and control specific Ca^{2+} transporter isoforms in a disease context.

Acknowledgements This work has been funded by the Flanders Research Foundation FWO G.0442.12 and G.0B11.15, the Inter-University Attraction Poles program (P7/13), and the KU Leuven (OT/13/091).

References

1. Berridge MJ, Bootman MD, Roderick HL (2003) Calcium signalling: dynamics, homeostasis and remodelling. Nat Rev Mol Cell Biol 4:517–529
2. Carafoli E (1987) Intracellular calcium homeostasis. Annu Rev Biochem 56:395–433
3. Palmgren MG, Nissen P (2011) P-type ATPases. Annu Rev Biophys 40:243–266
4. Vangheluwe P, Sepulveda MR, Missiaen L et al (2009) Intracellular Ca^{2+}- and Mn^{2+}-transport ATPases. Chem Rev 109:4733–4759
5. Toyoshima C, Nakasako M, Nomura H et al (2000) Crystal structure of the calcium pump of sarcoplasmic reticulum at 2.6 A resolution. Nature 405:647–655
6. Toyoshima C (2009) How Ca^{2+}-ATPase pumps ions across the sarcoplasmic reticulum membrane. Biochim Biophys Acta 1793:941–946
7. Gourdon P, Liu XY, Skjorringe T et al (2011) Crystal structure of a copper-transporting PIB-type ATPase. Nature 475:59–64
8. Braiterman L, Nyasae L, Guo Y et al (2009) Apical targeting and Golgi retention signals reside within a 9-amino acid sequence in the copper-ATPase, ATP7B. Am J Physiol Gastrointest Liver Physiol 296:G433–G444
9. Braiterman L, Nyasae L, Leves F et al (2011) Critical roles for the COOH terminus of the Cu-ATPase ATP7B in protein stability, trans-Golgi network retention, copper sensing, and retrograde trafficking. Am J Physiol Gastrointest Liver Physiol 301:G69–G81
10. Poulsen H, Khandelia H, Morth JP et al (2010) Neurological disease mutations compromise a C-terminal ion pathway in the Na^+/K^+-ATPase. Nature 467:99–102
11. Toustrup-Jensen MS, Holm R, Einholm AP et al (2009) The C terminus of Na^+, K^+-ATPase controls Na^+ affinity on both sides of the membrane through Arg935. J Biol Chem 284:18715–18725
12. Palmgren MG, Sommarin M, Serrano R et al (1991) Identification of an autoinhibitory domain in the C-terminal region of the plant plasma membrane H^+-ATPase. J Biol Chem 266:20470–20475
13. Portillo F, de Larrinoa IF, Serrano R (1989) Deletion analysis of yeast plasma membrane H^+-ATPase and identification of a regulatory domain at the carboxyl-terminus. FEBS Lett 247:381–385
14. Ekberg K, Palmgren MG, Veierskov B et al (2010) A novel mechanism of P-type ATPase autoinhibition involving both termini of the protein. J Biol Chem 285:7344–7350
15. Svennelid F, Olsson A, Piotrowski M et al (1999) Phosphorylation of Thr-948 at the C terminus of the plasma membrane H^+-ATPase creates a binding site for the regulatory 14-3-3 protein. Plant Cell 11:2379–2391
16. Zhou X, Sebastian TT, Graham TR (2013) Auto-inhibition of Drs2p, a yeast phospholipid flippase, by its carboxyl-terminal tail. J Biol Chem 288:31807–31815
17. Natarajan P, Liu K, Patil DV et al (2009) Regulation of a Golgi flippase by phosphoinositides and an ArfGEF. Nat Cell Biol 11:1421–1426
18. Sorensen DM, Buch-Pedersen MJ, Palmgren MG (2010) Structural divergence between the two subgroups of P5 ATPases. Biochim Biophys Acta 1797:846–855

19. van Veen S, Sorensen DM, Holemans T et al (2014) Cellular function and pathological role of ATP13A2 and related P-type transport ATPases in Parkinson's disease and other neurological disorders. Front Mol Neurosci 7:48
20. Hovnanian A (2007) SERCA pumps and human diseases. Subcell Biochem 45:337–363
21. Dally S, Monceau V, Corvazier E et al (2009) Compartmentalized expression of three novel sarco/endoplasmic reticulum Ca^{2+}ATPase 3 isoforms including the switch to ER stress, SERCA3f, in non-failing and failing human heart. Cell Calcium 45:144–154
22. Brandl CJ, deLeon S, Martin DR et al (1987) Adult forms of the Ca^{2+}ATPase of sarcoplasmic reticulum. Expression in developing skeletal muscle. J Biol Chem 262:3768–3774
23. Zador E, Vangheluwe P, Wuytack F (2007) The expression of the neonatal sarcoplasmic reticulum Ca^{2+} pump (SERCA1b) hints to a role in muscle growth and development. Cell Calcium 41:379–388
24. Brandl CJ, Green NM, Korczak B et al (1986) Two Ca^{2+} ATPase genes: homologies and mechanistic implications of deduced amino acid sequences. Cell 44:597–607
25. Chami M, Gozuacik D, Lagorce D et al (2001) SERCA1 truncated proteins unable to pump calcium reduce the endoplasmic reticulum calcium concentration and induce apoptosis. J Cell Biol 153:1301–1314
26. Chami M, Oules B, Szabadkai G et al (2008) Role of SERCA1 truncated isoform in the proapoptotic calcium transfer from ER to mitochondria during ER stress. Mol Cell 32:641–651
27. Wuytack F, Raeymaekers L, Missiaen L (2002) Molecular physiology of the SERCA and SPCA pumps. Cell Calcium 32:279–305
28. Vangheluwe P, Raeymaekers L, Dode L et al (2005) Modulating sarco(endo)plasmic reticulum Ca^{2+} ATPase 2 (SERCA2) activity: cell biological implications. Cell Calcium 38:291–302
29. Lytton J, MacLennan DH (1988) Molecular cloning of cDNAs from human kidney coding for two alternatively spliced products of the cardiac Ca^{2+}-ATPase gene. J Biol Chem 263:15024–15031
30. Lytton J, Zarain-Herzberg A, Periasamy M et al (1989) Molecular cloning of the mammalian smooth muscle sarco(endo)plasmic reticulum Ca^{2+}-ATPase. J Biol Chem 264:7059–7065
31. Zarain-Herzberg A, MacLennan DH, Periasamy M (1990) Characterization of rabbit cardiac sarco(endo)plasmic reticulum Ca^{2+}-ATPase gene. J Biol Chem 265:4670–4677
32. Baba-Aissa F, Raeymaekers L, Wuytack F et al (1996) Distribution of the organellar Ca^{2+} transport ATPase SERCA2 isoforms in the cat brain. Brain Res 743:141–153
33. Dally S, Bredoux R, Corvazier E et al (2006) Ca^{2+}-ATPases in non-failing and failing heart: evidence for a novel cardiac sarco/endoplasmic reticulum Ca^{2+}-ATPase 2 isoform (SERCA2c). Biochem J 395:249–258
34. Kimura T, Nakamori M, Lueck JD et al (2005) Altered mRNA splicing of the skeletal muscle ryanodine receptor and sarcoplasmic/endoplasmic reticulum Ca^{2+}-ATPase in myotonic dystrophy type 1. Hum Mol Genet 14:2189–2200
35. Gelebart P, Martin V, Enouf J et al (2003) Identification of a new SERCA2 splice variant regulated during monocytic differentiation. Biochem Biophys Res Commun 303:676–684
36. Lee MG, Xu X, Zeng W et al (1997) Polarized expression of Ca^{2+} pumps in pancreatic and salivary gland cells. Role in initiation and propagation of $[Ca^{2+}]i$ waves. J Biol Chem 272:15771–15776
37. Mountian I, Manolopoulos VG, De Smedt H et al (1999) Expression patterns of sarco/endoplasmic reticulum Ca^{2+}-ATPase and inositol 1,4,5-trisphosphate receptor isoforms in vascular endothelial cells. Cell Calcium 25:371–380
38. Brouland JP, Gelebart P, Kovacs T et al (2005) The loss of sarco/endoplasmic reticulum calcium transport ATPase 3 expression is an early event during the multistep process of colon carcinogenesis. Am J Pathol 167:233–242
39. Dode L, Vilsen B, Van Baelen K et al (2002) Dissection of the functional differences between sarco(endo)plasmic reticulum Ca^{2+}-ATPase (SERCA) 1 and 3 isoforms by steady-state and transient kinetic analyses. J Biol Chem 277:45579–45591

40. MacLennan DH, Toyofuku T, Lytton J (1992) Structure-function relationships in sarcoplasmic or endoplasmic reticulum type Ca^{2+} pumps. Ann N Y Acad Sci 671:1–10
41. Grover AK, Kwan CY, Samson SE (2003) Effects of peroxynitrite on sarco/endoplasmic reticulum Ca^{2+} pump isoforms SERCA2b and SERCA3a. Am J Physiol Cell Physiol 285:C1537–C1543
42. Lytton J, Westlin M, Burk SE et al (1992) Functional comparisons between isoforms of the sarcoplasmic or endoplasmic reticulum family of calcium pumps. J Biol Chem 267:14483–14489
43. Verboomen H, Wuytack F, Van den Bosch L et al (1994) The functional importance of the extreme C-terminal tail in the gene 2 organellar Ca^{2+}-transport ATPase (SERCA2a/b). Biochem J 303:979–984
44. Vandecaetsbeek I, Trekels M, De Maeyer M et al (2009) Structural basis for the high Ca^{2+} affinity of the ubiquitous SERCA2b Ca^{2+} pump. Proc Natl Acad Sci U S A 106:18533–18538
45. Gorski PA, Trieber CA, Lariviere E et al (2012) Transmembrane helix 11 is a genuine regulator of the endoplasmic reticulum Ca^{2+} pump and acts as a functional parallel of beta-subunit on alpha-Na^+, K^+-ATPase. J Biol Chem 287:19876–19885
46. Verboomen H, Wuytack F, De Smedt H et al (1992) Functional difference between SERCA2a and SERCA2b Ca^{2+} pumps and their modulation by phospholamban. Biochem J 286(Pt 2):591–595
47. Clausen JD, Vandecaetsbeek I, Wuytack F et al (2012) Distinct roles of the C-terminal 11th transmembrane helix and luminal extension in the partial reactions determining the high Ca^{2+} affinity of sarco(endo)plasmic reticulum Ca^{2+}-ATPase isoform 2b (SERCA2b). J Biol Chem 287:39460–39469
48. Dode L, Andersen JP, Leslie N et al (2003) Dissection of the functional differences between sarco(endo)plasmic reticulum Ca^{2+}-ATPase (SERCA) 1 and 2 isoforms and characterization of Darier disease (SERCA2) mutants by steady-state and transient kinetic analyses. J Biol Chem 278:47877–47889
49. Martin V, Bredoux R, Corvazier E et al (2002) Three novel sarco/endoplasmic reticulum Ca^{2+}-ATPase (SERCA) 3 isoforms. Expression, regulation, and function of the membranes of the SERCA3 family. J Biol Chem 277:24442–24452
50. Bobe R, Bredoux R, Corvazier E et al (2004) Identification, expression, function, and localization of a novel (sixth) isoform of the human sarco/endoplasmic reticulum Ca^{2+}ATPase 3 gene. J Biol Chem 279:24297–24306
51. Michalak M, Groenendyk J, Szabo E et al (2009) Calreticulin, a multi-process calcium-buffering chaperone of the endoplasmic reticulum. Biochem J 417:651–666
52. Greene AL, Lalli MJ, Ji Y et al (2000) Overexpression of SERCA2b in the heart leads to an increase in sarcoplasmic reticulum calcium transport function and increased cardiac contractility. J Biol Chem 275:24722–24727
53. Vangheluwe P, Louch WE, Ver Heyen M et al (2003) Ca^{2+} transport ATPase isoforms SERCA2a and SERCA2b are targeted to the same sites in the murine heart. Cell Calcium 34:457–464
54. Lipskaia L, Keuylian Z, Blirando K et al (2014) Expression of sarco (endo) plasmic reticulum calcium ATPase (SERCA) system in normal mouse cardiovascular tissues, heart failure and atherosclerosis. Biochim Biophys Acta 1843:2705–2718
55. Baksh S, Michalak M (1991) Expression of calreticulin in Escherichia coli and identification of its Ca^{2+} binding domains. J Biol Chem 266:21458–21465
56. John LM, Lechleiter JD, Camacho P (1998) Differential modulation of SERCA2 isoforms by calreticulin. J Cell Biol 142:963–973
57. Roderick HL, Lechleiter JD, Camacho P (2000) Cytosolic phosphorylation of calnexin controls intracellular Ca^{2+} oscillations via an interaction with SERCA2b. J Cell Biol 149:1235–1248
58. Xu A, Hawkins C, Narayanan N (1993) Phosphorylation and activation of the Ca^{2+}-pumping ATPase of cardiac sarcoplasmic reticulum by Ca^{2+}/calmodulin-dependent protein kinase. J Biol Chem 268:8394–8397

59. Hawkins C, Xu A, Narayanan N (1994) Sarcoplasmic reticulum calcium pump in cardiac and slow twitch skeletal muscle but not fast twitch skeletal muscle undergoes phosphorylation by endogenous and exogenous Ca^{2+}/calmodulin-dependent protein kinase. Characterization of optimal conditions for calcium pump phosphorylation. J Biol Chem 269:31198–31206
60. Xu A, Narayanan N (1999) Ca^{2+}/calmodulin-dependent phosphorylation of the Ca^{2+}-ATPase, uncoupled from phospholamban, stimulates Ca^{2+}-pumping in native cardiac sarcoplasmic reticulum. Biochem Biophys Res Commun 258:66–72
61. Xu A, Netticadan T, Jones DL et al (1999) Serine phosphorylation of the sarcoplasmic reticulum Ca^{2+}-ATPase in the intact beating rabbit heart. Biochem Biophys Res Commun 264:241–246
62. Rodriguez P, Jackson WA, Colyer J (2004) Critical evaluation of cardiac Ca^{2+}-ATPase phosphorylation on serine 38 using a phosphorylation site-specific antibody. J Biol Chem 279:17111–17119
63. Reddy LG, Jones LR, Pace RC et al (1996) Purified, reconstituted cardiac Ca^{2+}-ATPase is regulated by phospholamban but not by direct phosphorylation with Ca^{2+}/calmodulin-dependent protein kinase. J Biol Chem 271:14964–14970
64. Bassani RA, Mattiazzi A, Bers DM (1995) CaMKII is responsible for activity-dependent acceleration of relaxation in rat ventricular myocytes. Am J Physiol 268(2 Pt 2):H703–H712
65. Zhao W, Uehara Y, Chu G et al (2004) Threonine-17 phosphorylation of phospholamban: a key determinant of frequency-dependent increase of cardiac contractility. J Mol Cell Cardiol 37:607–612
66. Ireland BS, Brockmeier U, Howe CM et al (2008) Lectin-deficient calreticulin retains full functionality as a chaperone for class I histocompatibility molecules. Mol Biol Cell 19:2413–2423
67. Savignac M, Edir A, Simon M et al (2011) Darier disease : a disease model of impaired calcium homeostasis in the skin. Biochim Biophys Acta 1813:1111–1117
68. Ikeda S, Mayuzumi N, Shigihara T et al (2003) Mutations in ATP2A2 in patients with Darier's disease. J Invest Dermatol 121:475–477
69. Ruiz-Perez VL, Carter SA, Healy E et al (1999) ATP2A2 mutations in Darier's disease: variant cutaneous phenotypes are associated with missense mutations, but neuropsychiatric features are independent of mutation class. Hum Mol Genet 8:1621–1630
70. Ringpfeil F, Raus A, DiGiovanna JJ et al (2001) Darier disease--novel mutations in ATP2A2 and genotype-phenotype correlation. Exp Dermatol 10:19–27
71. Sakuntabhai A, Ruiz-Perez V, Carter S et al (1999) Mutations in ATP2A2, encoding a Ca^{2+} pump, cause Darier disease. Nat Genet 21:271–277
72. Jacobsen NJ, Lyons I, Hoogendoorn B et al (1999) ATP2A2 mutations in Darier's disease and their relationship to neuropsychiatric phenotypes. Hum Mol Genet 8:1631–1636
73. Kaneko M, Desai BS, Cook B (2014) Ionic leakage underlies a gain-of-function effect of dominant disease mutations affecting diverse P-type ATPases. Nat Genet 46:144–151
74. Periasamy M, Huke S (2001) SERCA pump level is a critical determinant of Ca^{2+}homeostasis and cardiac contractility. J Mol Cell Cardiol 33:1053–1063
75. Periasamy M, Bhupathy P, Babu GJ (2008) Regulation of sarcoplasmic reticulum Ca^{2+} ATPase pump expression and its relevance to cardiac muscle physiology and pathology. Cardiovasc Res 77:265–273
76. Ver Heyen M, Heymans S, Antoons G et al (2001) Replacement of the muscle-specific sarcoplasmic reticulum Ca^{2+}-ATPase isoform SERCA2a by the nonmuscle SERCA2b homologue causes mild concentric hypertrophy and impairs contraction-relaxation of the heart. Circ Res 89:838–846
77. Vangheluwe P, Wuytack F (2011) Improving cardiac Ca^{2+} transport into the sarcoplasmic reticulum in heart failure: lessons from the ubiquitous SERCA2b Ca^{+}(2) pump. Biochem Soc Trans 39:781–787
78. Vangheluwe P, Sipido KR, Raeymaekers L et al (2006) New perspectives on the role of SERCA2's Ca^{2+} affinity in cardiac function. Biochim Biophys Acta 1763:1216–1228

79. Vangheluwe P, Tjwa M, Van Den Bergh A et al (2006) A SERCA2 pump with an increased Ca^{2+} affinity can lead to severe cardiac hypertrophy, stress intolerance and reduced life span. J Mol Cell Cardiol 41:308–317
80. Anger M, Samuel JL, Marotte F et al (1994) In situ mRNA distribution of sarco(endo)plasmic reticulum Ca^{2+}-ATPase isoforms during ontogeny in the rat. J Mol Cell Cardiol 26:539–550
81. MacLennan DH, Kranias EG (2003) Phospholamban: a crucial regulator of cardiac contractility. Nat Rev Mol Cell Biol 4:566–577
82. Kadambi VJ, Ponniah S, Harrer JM et al (1996) Cardiac-specific overexpression of phospholamban alters calcium kinetics and resultant cardiomyocyte mechanics in transgenic mice. J Clin Invest 97:533–539
83. Antoons G, Ver Heyen M, Raeymaekers L et al (2003) Ca^{2+} uptake by the sarcoplasmic reticulum in ventricular myocytes of the SERCA2b/b mouse is impaired at higher Ca^{2+} loads only. Circ Res 92:881–887
84. Vandecaetsbeek I, Raeymaekers L, Wuytack F et al (2009) Factors controlling the activity of the SERCA2a pump in the normal and failing heart. Biofactors 35:484–499
85. del Monte F, Harding SE, Schmidt U et al (1999) Restoration of contractile function in isolated cardiomyocytes from failing human hearts by gene transfer of SERCA2a. Circulation 100:2308–2311
86. Zsebo K, Yaroshinsky A, Rudy JJ et al (2014) Long-term effects of AAV1/SERCA2a gene transfer in patients with severe heart failure: analysis of recurrent cardiovascular events and mortality. Circ Res 114:101–108
87. Kranias EG, Hajjar RJ (2012) Modulation of cardiac contractility by the phospholamban/SERCA2a regulatome. Circ Res 110:1646–1660
88. Suckau L, Fechner H, Chemaly E et al (2009) Long-term cardiac-targeted RNA interference for the treatment of heart failure restores cardiac function and reduces pathological hypertrophy. Circulation 119:1241–1252
89. Hoshijima M, Ikeda Y, Iwanaga Y et al (2002) Chronic suppression of heart-failure progression by a pseudophosphorylated mutant of phospholamban via in vivo cardiac rAAV gene delivery. Nat Med 8:864–871
90. Rudolph HK, Antebi A, Fink GR et al (1989) The yeast secretory pathway is perturbed by mutations in PMR1, a member of a Ca^{2+} ATPase family. Cell 58:133–145
91. Gunteski-Hamblin AM, Clarke DM, Shull GE (1992) Molecular cloning and tissue distribution of alternatively spliced mRNAs encoding possible mammalian homologues of the yeast secretory pathway calcium pump. Biochemistry 31:7600–7608
92. Wootton LL, Argent CC, Wheatley M et al (2004) The expression, activity and localisation of the secretory pathway Ca^{2+} -ATPase (SPCA1) in different mammalian tissues. Biochim Biophys Acta 1664:189–197
93. Vanoevelen J, Dode L, Van Baelen K et al (2005) The secretory pathway Ca^{2+}/Mn^{2+}-ATPase 2 is a Golgi-localized pump with high affinity for Ca^{2+} ions. J Biol Chem 280:22800–22808
94. Xiang M, Mohamalawari D, Rao R (2005) A novel isoform of the secretory pathway Ca^{2+}, Mn^{2+}-ATPase, hSPCA2, has unusual properties and is expressed in the brain. J Biol Chem 280:11608–11614
95. Fairclough RJ, Dode L, Vanoevelen J et al (2003) Effect of Hailey-Hailey disease mutations on the function of a new variant of human secretory pathway Ca^{2+}/Mn^{2+}-ATPase (hSPCA1). J Biol Chem 278:24721–24730
96. Dode L, Andersen JP, Raeymaekers L et al (2005) Functional comparison between secretory pathway Ca^{2+}/Mn^{2+}-ATPase (SPCA) 1 and sarcoplasmic reticulum Ca^{2+}-ATPase (SERCA) 1 isoforms by steady-state and transient kinetic analyses. J Biol Chem 280:39124–39134
97. Garside VC, Kowalik AS, Johnson CL et al (2010) MIST1 regulates the pancreatic acinar cell expression of Atp2c2, the gene encoding secretory pathway calcium ATPase 2. Exp Cell Res 316:2859–2870

98. Wei Y, Chen J, Rosas G et al (2000) Phenotypic screening of mutations in Pmr1, the yeast secretory pathway Ca^{2+}/Mn^{2+}-ATPase, reveals residues critical for ion selectivity and transport. J Biol Chem 275:23927–23932
99. Wei Y, Marchi V, Wang R et al (1999) An N-terminal EF hand-like motif modulates ion transport by Pmr1, the yeast Golgi Ca^{2+}/Mn^{2+}-ATPase. Biochemistry 38:14534–14541
100. Van Baelen K, Vanoevelen J, Missiaen L et al (2001) The Golgi PMR1 P-type ATPase of Caenorhabditis elegans. Identification of the gene and demonstration of calcium and manganese transport. J Biol Chem 276:10683–10691
101. Kho C, Lee A, Jeong D et al (2011) SUMO1-dependent modulation of SERCA2a in heart failure. Nature 477:601–605
102. Vafiadaki E, Arvanitis DA, Pagakis SN et al (2009) The anti-apoptotic protein HAX-1 interacts with SERCA2 and regulates its protein levels to promote cell survival. Mol Biol Cell 20:306–318
103. Li Y, Camacho P (2004) Ca^{2+}-dependent redox modulation of SERCA 2b by ERp57. J Cell Biol 164:35–46
104. Dode L, Andersen JP, Vanoevelen J et al (2006) Dissection of the functional differences between human secretory pathway Ca^{2+}/Mn^{2+}-ATPase (SPCA) 1 and 2 isoenzymes by steady-state and transient kinetic analyses. J Biol Chem 281:3182–3189
105. Ikura M (1996) Calcium binding and conformational response in EF-hand proteins. Trends Biochem Sci 21:14–17
106. Huster D, Lutsenko S (2003) The distinct roles of the N-terminal copper-binding sites in regulation of catalytic activity of the Wilson's disease protein. J Biol Chem 278:32212–32218
107. Van Baelen K, Vanoevelen J, Callewaert G et al (2003) The contribution of the SPCA1 Ca^{2+} pump to the Ca^{2+} accumulation in the Golgi apparatus of HeLa cells assessed via RNA-mediated interference. Biochem Biophys Res Commun 306:430–436
108. Leitch S, Feng M, Muend S et al (2011) Vesicular distribution of Secretory Pathway Ca^{2+}-ATPase isoform 1 and a role in manganese detoxification in liver-derived polarized cells. Biometals 24:159–170
109. Micaroni M, Perinetti G, Berrie CP et al (2010) The SPCA1 Ca^{2+} pump and intracellular membrane trafficking. Traffic 11:1315–1333
110. Lewis RS (2007) The molecular choreography of a store-operated calcium channel. Nature 446:284–287
111. Feng M, Grice DM, Faddy HM et al (2010) Store-independent activation of Orai1 by SPCA2 in mammary tumors. Cell 143:84–98
112. Cross BM, Breitwieser GE, Reinhardt TA et al (2014) Cellular calcium dynamics in lactation and breast cancer: from physiology to pathology. Am J Physiol Cell Physiol 306:C515–C526
113. Hu Z, Bonifas JM, Beech J et al (2000) Mutations in ATP2C1, encoding a calcium pump, cause Hailey-Hailey disease. Nat Genet 24:61–65
114. Prasad V, Boivin GP, Miller ML et al (2005) Haploinsufficiency of Atp2a2, encoding the sarco(endo)plasmic reticulum Ca^{2+}-ATPase isoform 2 Ca^{2+} pump, predisposes mice to squamous cell tumors via a novel mode of cancer susceptibility. Cancer Res 65:8655–8661
115. Okunade GW, Miller ML, Azhar M et al (2007) Loss of the Atp2c1 secretory pathway Ca^{2+}-ATPase (SPCA1) in mice causes Golgi stress, apoptosis, and midgestational death in homozygous embryos and squamous cell tumors in adult heterozygotes. J Biol Chem 282:26517–26527
116. Neville MC (2005) Calcium secretion into milk. J Mammary Gland Biol Neoplasia 10:119–128
117. Cross BM, Hack A, Reinhardt TA et al (2013) SPCA2 regulates Orai1 trafficking and store independent Ca^{2+} entry in a model of lactation. PLoS One 8, e67348
118. McAndrew D, Grice DM, Peters AA et al (2011) ORAI1-mediated calcium influx in lactation and in breast cancer. Mol Cancer Ther 10:448–460

119. Reinhardt TA, Lippolis JD, Shull GE et al (2004) Null mutation in the gene encoding plasma membrane Ca^{2+}-ATPase isoform 2 impairs calcium transport into milk. J Biol Chem 279:42369–42373
120. Faddy HM, Smart CE, Xu R et al (2008) Localization of plasma membrane and secretory calcium pumps in the mammary gland. Biochem Biophys Res Commun 369:977–981
121. Yang S, Zhang JJ, Huang XY (2009) Orai1 and STIM1 are critical for breast tumor cell migration and metastasis. Cancer Cell 15:124–134
122. Grice DM, Vetter I, Faddy HM et al (2010) Golgi calcium pump secretory pathway calcium ATPase 1 (SPCA1) is a key regulator of insulin-like growth factor receptor (IGF1R) processing in the basal-like breast cancer cell line MDA-MB-231. J Biol Chem 285:37458–37466
123. Monteith GR, Davis FM, Roberts-Thomson SJ (2012) Calcium channels and pumps in cancer: changes and consequences. J Biol Chem 287:31666–31673
124. Brini M, Carafoli E (2009) Calcium pumps in health and disease. Physiol Rev 89:1341–1378
125. Schatzmann HJ (1966) ATP-dependent Ca^{++}-extrusion from human red cells. Experientia 22:364–365
126. Niggli V, Penniston JT, Carafoli E (1979) Purification of the (Ca^{2+}-Mg^{2+})-ATPase from human erythrocyte membranes using a calmodulin affinity column. J Biol Chem 254:9955–9958
127. Penniston JT, Enyedi A (1998) Modulation of the plasma membrane Ca^{2+} pump. J Membr Biol 165:101–109
128. Carafoli E (1994) Biogenesis: plasma membrane calcium ATPase: 15 years of work on the purified enzyme. FASEB J 8:993–1002
129. Falchetto R, Vorherr T, Carafoli E (1992) The calmodulin-binding site of the plasma membrane Ca^{2+} pump interacts with the transduction domain of the enzyme. Protein Sci 1:1613–1621
130. Keeton TP, Burk SE, Shull GE (1993) Alternative splicing of exons encoding the calmodulin-binding domains and C termini of plasma membrane Ca^{2+}-ATPase isoforms 1, 2, 3, and 4. J Biol Chem 268:2740–2748
131. Stauffer TP, Guerini D, Carafoli E (1995) Tissue distribution of the four gene products of the plasma membrane Ca^{2+} pump. A study using specific antibodies. J Biol Chem 270:12184–12190
132. Enyedi A, Filoteo AG, Gardos G et al (1991) Calmodulin-binding domains from isozymes of the plasma membrane Ca^{2+} pump have different regulatory properties. J Biol Chem 266:8952–8956
133. Caride AJ, Filoteo AG, Penheiter AR et al (2001) Delayed activation of the plasma membrane calcium pump by a sudden increase in Ca^{2+}: fast pumps reside in fast cells. Cell Calcium 30:49–57
134. Hill JK, Williams DE, LeMasurier M et al (2006) Splice-site A choice targets plasma-membrane Ca^{2+}-ATPase isoform 2 to hair bundles. J Neurosci 26:6172–6180
135. Strehler EE, Zacharias DA (2001) Role of alternative splicing in generating isoform diversity among plasma membrane calcium pumps. Physiol Rev 81:21–50
136. Okunade GW, Miller ML, Pyne GJ et al (2004) Targeted ablation of plasma membrane Ca^{2+}-ATPase (PMCA) 1 and 4 indicates a major housekeeping function for PMCA1 and a critical role in hyperactivated sperm motility and male fertility for PMCA4. J Biol Chem 279:33742–33750
137. Ficarella R, Di Leva F, Bortolozzi M et al (2007) A functional study of plasma-membrane calcium-pump isoform 2 mutants causing digenic deafness. Proc Natl Acad Sci U S A 104:1516–1521
138. Lopreiato R, Giacomello M, Carafoli E (2014) The plasma membrane calcium pump: new ways to look at an old enzyme. J Biol Chem 289:10261–10268
139. Brini M, Cali T, Ottolini D et al (2013) The plasma membrane calcium pump in health and disease. FEBS J 280:5385–5397

140. Cartwright EJ, Oceandy D, Neyses L (2009) Physiological implications of the interaction between the plasma membrane calcium pump and nNOS. Pflugers Arch 457:665–671
141. Adamo HP, Penniston JT (1992) New Ca^{2+} pump isoforms generated by alternative splicing of rPMCA2 mRNA. Biochem J 283(Pt 2):355–359
142. Hilfiker H, Guerini D, Carafoli E (1994) Cloning and expression of isoform 2 of the human plasma membrane Ca^{2+} ATPase. Functional properties of the enzyme and its splicing products. J Biol Chem 269:26178–26183
143. Lotersztajn S, Pavoine C, Deterre P et al (1992) Role of G protein beta gamma subunits in the regulation of the plasma membrane Ca^{2+} pump. J Biol Chem 267:2375–2379
144. Chicka MC, Strehler EE (2003) Alternative splicing of the first intracellular loop of plasma membrane Ca^{2+}-ATPase isoform 2 alters its membrane targeting. J Biol Chem 278:18464–18470
145. Strehler EE (2013) Plasma membrane calcium ATPases as novel candidates for therapeutic agent development. J Pharm Pharm Sci 16:190–206
146. Chiesi M, Vorherr T, Falchetto R et al (1991) Phospholamban is related to the autoinhibitory domain of the plasma membrane Ca^{2+}-pumping ATPase. Biochemistry 30:7978–7983
147. Elwess NL, Filoteo AG, Enyedi A et al (1997) Plasma membrane Ca^{2+} pump isoforms 2a and 2b are unusually responsive to calmodulin and Ca^{2+}. J Biol Chem 272:17981–17986
148. VanHouten JN, Neville MC, Wysolmerski JJ (2007) The calcium-sensing receptor regulates plasma membrane calcium adenosine triphosphatase isoform 2 activity in mammary epithelial cells: a mechanism for calcium-regulated calcium transport into milk. Endocrinology 148:5943–5954
149. Antalffy G, Mauer AS, Paszty K et al (2012) Plasma membrane calcium pump (PMCA) isoform 4 is targeted to the apical membrane by the w-splice insert from PMCA2. Cell Calcium 51:171–178
150. Xiong Y, Antalffy G, Enyedi A et al (2009) Apical localization of PMCA2w/b is lipid raft-dependent. Biochem Biophys Res Commun 384:32–36
151. Enyedi A, Strehler EE (2011) Regulation of apical membrane enrichment and retention of plasma membrane Ca ATPase splice variants by the PDZ-domain protein NHERF2. Commun Integr Biol 4:340–343
152. Fujimoto T (1993) Calcium pump of the plasma membrane is localized in caveolae. J Cell Biol 120:1147–1157
153. Schnitzer JE, Oh P, Jacobson BS et al (1995) Caveolae from luminal plasmalemma of rat lung endothelium: microdomains enriched in caveolin, Ca^{2+}-ATPase, and inositol trisphosphate receptor. Proc Natl Acad Sci U S A 92:1759–1763
154. Sepulveda MR, Berrocal-Carrillo M, Gasset M et al (2006) The plasma membrane Ca^{2+}-ATPase isoform 4 is localized in lipid rafts of cerebellum synaptic plasma membranes. J Biol Chem 281:447–453
155. El-Yazbi AF, Cho WJ, Schulz R et al (2008) Calcium extrusion by plasma membrane calcium pump is impaired in caveolin-1 knockout mouse small intestine. Eur J Pharmacol 591:80–87
156. James P, Maeda M, Fischer R et al (1988) Identification and primary structure of a calmodulin binding domain of the Ca^{2+} pump of human erythrocytes. J Biol Chem 263:2905–2910
157. Enyedi A, Vorherr T, James P et al (1989) The calmodulin binding domain of the plasma membrane Ca^{2+} pump interacts both with calmodulin and with another part of the pump. J Biol Chem 264:12313–12321
158. Corradi GR, Adamo HP (2007) Intramolecular fluorescence resonance energy transfer between fused autofluorescent proteins reveals rearrangements of the N- and C-terminal segments of the plasma membrane Ca^{2+} pump involved in the activation. J Biol Chem 282:35440–35448
159. Niggli V, Adunyah ES, Penniston JT et al (1981) Purified (Ca^{2+}-Mg^{2+})-ATPase of the erythrocyte membrane. Reconstitution and effect of calmodulin and phospholipids. J Biol Chem 256:395–401

160. Tidow H, Poulsen LR, Andreeva A et al (2012) A bimodular mechanism of calcium control in eukaryotes. Nature 491:468–472
161. Verma AK, Enyedi A, Filoteo AG et al (1996) Plasma membrane calcium pump isoform 4a has a longer calmodulin-binding domain than 4b. J Biol Chem 271:3714–3718
162. Verma AK, Paszty K, Filoteo AG et al (1999) Protein kinase C phosphorylates plasma membrane Ca^{2+} pump isoform 4a at its calmodulin binding domain. J Biol Chem 274:527–531
163. Filoteo AG, Enyedi A, Verma AK et al (2000) Plasma membrane Ca^{2+} pump isoform 3f is weakly stimulated by calmodulin. J Biol Chem 275:4323–4328
164. Enyedi A, Verma AK, Heim R et al (1994) The Ca^{2+} affinity of the plasma membrane Ca^{2+} pump is controlled by alternative splicing. J Biol Chem 269:41–43
165. Caride AJ, Elwess NL, Verma AK et al (1999) The rate of activation by calmodulin of isoform 4 of the plasma membrane Ca^{2+} pump is slow and is changed by alternative splicing. J Biol Chem 274:35227–35232
166. Foder B, Scharff O (1992) Solitary calcium spike dependent on calmodulin and plasma membrane Ca^{2+} pump. Cell Calcium 13:581–591
167. Anderson RG (1993) Caveolae: where incoming and outgoing messengers meet. Proc Natl Acad Sci U S A 90:10909–10913
168. DeMarco SJ, Strehler EE (2001) Plasma membrane Ca^{2+}-ATPase isoforms 2b and 4b interact promiscuously and selectively with members of the membrane-associated guanylate kinase family of PDZ (PSD95/Dlg/ZO-1) domain-containing proteins. J Biol Chem 276:21594–21600
169. Schuh K, Uldrijan S, Gambaryan S et al (2003) Interaction of the plasma membrane Ca^{2+} pump 4b/CI with the Ca^{2+}/calmodulin-dependent membrane-associated kinase CASK. J Biol Chem 278:9778–9783
170. DeMarco SJ, Chicka MC, Strehler EE (2002) Plasma membrane Ca^{2+} ATPase isoform 2b interacts preferentially with Na^+/H^+ exchanger regulatory factor 2 in apical plasma membranes. J Biol Chem 277:10506–10511
171. Bozulic LD, Malik MT, Powell DW et al (2007) Plasma membrane Ca^{2+}-ATPase associates with CLP36, alpha-actinin and actin in human platelets. Thromb Haemost 97:587–597
172. Goellner GM, DeMarco SJ, Strehler EE (2003) Characterization of PISP, a novel single-PDZ protein that binds to all plasma membrane Ca^{2+}-ATPase b-splice variants. Ann N Y Acad Sci 986:461–471
173. Sgambato-Faure V, Xiong Y, Berke JD et al (2006) The Homer-1 protein Ania-3 interacts with the plasma membrane calcium pump. Biochem Biophys Res Commun 343:630–637
174. James P, Vorherr T, Krebs J et al (1989) Modulation of erythrocyte Ca^{2+}-ATPase by selective calpain cleavage of the calmodulin-binding domain. J Biol Chem 264:8289–8296
175. Guerini D, Pan B, Carafoli E (2003) Expression, purification, and characterization of isoform 1 of the plasma membrane Ca^{2+} pump: focus on calpain sensitivity. J Biol Chem 278:38141–38148
176. Schwab BL, Guerini D, Didszun C et al (2002) Cleavage of plasma membrane calcium pumps by caspases: a link between apoptosis and necrosis. Cell Death Differ 9:818–831
177. Paszty K, Verma AK, Padanyi R et al (2002) Plasma membrane Ca^{2+}ATPase isoform 4b is cleaved and activated by caspase-3 during the early phase of apoptosis. J Biol Chem 277:6822–6829
178. Fu H, Subramanian RR, Masters SC (2000) 14-3-3 proteins: structure, function, and regulation. Annu Rev Pharmacol Toxicol 40:617–647
179. Linde CI, Di Leva F, Domi T et al (2008) Inhibitory interaction of the 14-3-3 proteins with ubiquitous (PMCA1) and tissue-specific (PMCA3) isoforms of the plasma membrane Ca^{2+} pump. Cell Calcium 43:550–561
180. Rimessi A, Coletto L, Pinton P et al (2005) Inhibitory interaction of the 14-3-3{epsilon} protein with isoform 4 of the plasma membrane Ca^{2+}-ATPase pump. J Biol Chem 280:37195–37203
181. Niggli V, Adunyah ES, Carafoli E (1981) Acidic phospholipids, unsaturated fatty acids, and limited proteolysis mimic the effect of calmodulin on the purified erythrocyte Ca^{2+}—ATPase. J Biol Chem 256:8588–8592

182. Missiaen L, Raeymaekers L, Wuytack F et al (1989) Phospholipid-protein interactions of the plasma-membrane Ca^{2+}-transporting ATPase. Evidence for a tissue-dependent functional difference. Biochem J 263:687–694
183. Enyedi A, Flura M, Sarkadi B et al (1987) The maximal velocity and the calcium affinity of the red cell calcium pump may be regulated independently. J Biol Chem 262:6425–6430
184. Khan I, Grover AK (1991) Expression of cyclic-nucleotide-sensitive and -insensitive isoforms of the plasma membrane Ca^{2+} pump in smooth muscle and other tissues. Biochem J 277(Pt 2):345–349
185. Bruce JI, Yule DI, Shuttleworth TJ (2002) Ca^{2+}-dependent protein kinase--a modulation of the plasma membrane Ca^{2+}-ATPase in parotid acinar cells. J Biol Chem 277:48172–48181
186. Enyedi A, Elwess NL, Filoteo AG et al (1997) Protein kinase C phosphorylates the "a" forms of plasma membrane Ca^{2+} pump isoforms 2 and 3 and prevents binding of calmodulin. J Biol Chem 272:27525–27528
187. Giacomello M, De Mario A, Scarlatti C et al (2013) Plasma membrane calcium ATPases and related disorders. Int J Biochem Cell Biol 45:753–762
188. Reinhardt TA, Filoteo AG, Penniston JT et al (2000) Ca^{2+}-ATPase protein expression in mammary tissue. Am J Physiol Cell Physiol 279:C1595–C1602
189. VanHouten J, Sullivan C, Bazinet C et al (2010) PMCA2 regulates apoptosis during mammary gland involution and predicts outcome in breast cancer. Proc Natl Acad Sci U S A 107:11405–11410
190. Kozel PJ, Friedman RA, Erway LC et al (1998) Balance and hearing deficits in mice with a null mutation in the gene encoding plasma membrane Ca^{2+}-ATPase isoform 2. J Biol Chem 273:18693–18696
191. Street VA, McKee-Johnson JW, Fonseca RC et al (1998) Mutations in a plasma membrane Ca^{2+}-ATPase gene cause deafness in deafwaddler mice. Nat Genet 19:390–394
192. Takahashi K, Kitamura K (1999) A point mutation in a plasma membrane Ca^{2+}-ATPase gene causes deafness in Wriggle Mouse Sagami. Biochem Biophys Res Commun 261:773–778
193. Zanni G, Cali T, Kalscheuer VM et al (2012) Mutation of plasma membrane Ca^{2+} ATPase isoform 3 in a family with X-linked congenital cerebellar ataxia impairs Ca^{2+} homeostasis. Proc Natl Acad Sci U S A 109:14514–14519
194. Jones S, Zhang X, Parsons DW et al (2008) Core signaling pathways in human pancreatic cancers revealed by global genomic analyses. Science 321:1801–1806
195. Schuh K, Cartwright EJ, Jankevics E et al (2004) Plasma membrane Ca^{2+} ATPase 4 is required for sperm motility and male fertility. J Biol Chem 279:28220–28226
196. Mohamed TM, Oceandy D, Zi M et al (2011) Plasma membrane calcium pump (PMCA4)-neuronal nitric-oxide synthase complex regulates cardiac contractility through modulation of a compartmentalized cyclic nucleotide microdomain. J Biol Chem 286:41520–41529
197. Hammes A, Oberdorf-Maass S, Rother T et al (1998) Overexpression of the sarcolemmal calcium pump in the myocardium of transgenic rats. Circ Res 83:877–888
198. Winther AM, Bublitz M, Karlsen JL et al (2013) The sarcolipin-bound calcium pump stabilizes calcium sites exposed to the cytoplasm. Nature 495:265–269
199. Zhang Y (2008) I-TASSER server for protein 3D structure prediction. BMC Bioinformatics 9:40
200. Arnold K, Bordoli L, Kopp J et al (2006) The SWISS-MODEL workspace: a web-based environment for protein structure homology modelling. Bioinformatics 22:195–201

Part III
Vacuolar ATPases

Chapter 15
Function and Regulation of Mammalian V-ATPase Isoforms

Suhaila Rahman, Ichiro Yamato, and Takeshi Murata

Abstract The vacuolar (H+)-ATPases (V-ATPase) are a family of highly conserved multisubunit ATP-driven nanomotors, responsible for the acidification of a variety of intracellular compartments in eukaryotic cells. Vacuolar (H+)-ATPases are important in both normal physiology and in pathophysiology. These complicated and huge enzymes consist of at least 14 subunits divided into two domains (membrane-bound V_o and cytosolic V_1). The peripheral stalk subunits of eukaryotic or mammalian vacuolar ATPases (V-ATPases) play key roles in regulating the assembly and disassembly of the enzyme. Interestingly, many of the peripheral stalk subunits also possess several homologues, which are known to be tissue-specific and are responsible for the formation of proton pumps with specialized functions within different tissues. Such tissue-specific isoforms/homologues and splice variants cannot complement each other, meaning that tissue/cell-specific regulation of V-ATPases is difficult to understand. In order to understand the structure/function and isoform-specific regulation mechanism of the human V-ATPase, several of the peripheral stalk subunits and their isoforms were expressed and characterized. In this review, we will discuss the binding interaction phenomena specifically at the stalk region, which mediates the reversible assembly and disassembly of V-ATPase in eukaryotic/mammalian cell systems.

Keyword V-ATPase • Peripheral stalk • Subunit-isoform • Cell-free expression system • Kinetics • Affinity • Subunit–subunit interaction • Isoform–isoform interaction

S. Rahman • I. Yamato (✉)
Department of Biological Science and Technology, Tokyo University of Science,
6-3-1 Niijuku, Katsushika-ku, Tokyo 125-8585, Japan
e-mail: iyamato@rs.noda.tus.ac.jp

T. Murata
Department of Chemistry, Graduate School of Science, Chiba University,
1-33 Yayoi-cho, Inage, Chiba 263-8522, Japan

RIKEN Systems and Structural Biology Center,
1-7-22 Suehiro-cho, Tsurumi, Yokohama 230-0045, Japan

JST, PRESTO, 1-33 Yayoi-cho, Inage, Chiba 263-8522, Japan

S. Chakraborti, N.S. Dhalla (eds.), *Regulation of Ca^{2+}-ATPases,V-ATPases and F-ATPases*, Advances in Biochemistry in Health and Disease 14,
DOI 10.1007/978-3-319-24780-9_15

1 Introduction

In order to function correctly, the human cell system requires regulation of the concentrations of ions such as calcium, magnesium, sodium, potassium, and hydrogen. Ion transporting adenosine triphosphatase (ATPase) is an ion-regulating membrane protein that pumps ions across the membrane using chemical energy derived from adenosine triphosphate (ATP) hydrolysis. Cation-transporting ATPases are very important for the maintenance of ion concentrations inside and outside of cells, and are classified into three types (P-type, F-type, and V-type ATPases) according to differences in their structure, function, and biochemical properties. Figure 15.1 shows the localization and function of cation-transporting ATPases in a eukaryotic cell. P-type ATPases form a large protein family in practically all cell types from archaea to humans. They generate essential ion gradients that are the basis for diverse functions such as signaling, energy storage, and secondary transport processes. Members of this family generate and maintain crucial electrochemical gradients across cell membranes by translocating cations, heavy metals, and lipids, a process that requires ATP hydrolysis. On the other hand, proton-pumping F-ATPase (ATP synthase) synthesizes ATP; with the entire reaction (oxidative- or photophosphorylation) carried out in the membranes of mitochondria, bacteria, or chloroplasts. This complex, the F_1F_o-ATPase (F-ATPase), uses proton motive force (the transmembrane movement of protons driven by the electrochemical membrane potential) as an energy source for the endothermic phosphorylation of adenosine diphosphate (ADP). This reaction is catalyzed by F-ATPase operating as a nano-scale machine with a rotary action [1–4]. F-ATPase belongs to a small

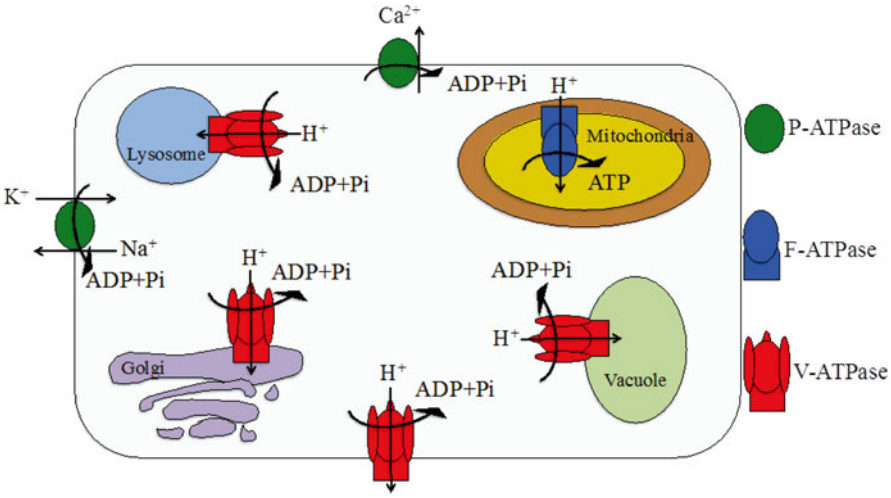

Fig. 15.1 Ion-translocating ATPases in a eukaryotic cell (localization and function). *Green*, *blue*, and *red color* symbols represent P-, F-, and V-ATPase, respectively. *Straight arrows* indicate the directions of ion translocation

family of membrane complexes that includes vacuolar H^+-translocating V_1V_o-ATPase (V-ATPase) and A_1A_o-ATPase (A-ATPase), all of which originated from a common evolutionary ancestor [5, 6]. The V-ATPase operates as an ATP-powered ion pump in the acidic organelles and plasma membranes of eukaryotic cells, whereas the A-ATPases (A-type refers to archaea) are ATP synthases in the cell membrane of archaea and in some bacteria [7–9]. A-ATPases are similar to the F-ATPases functionally, although the structure and subunit composition of A-ATPases are more similar to those of V-ATPases. V-ATPases are also found in bacteria, such as *Thermus thermophilus* [10] and *Enterococcus hirae* [11]. *T. thermophilus* V-ATPase functions as an ATP synthase. Therefore it has sometimes been called an A-ATPase. On the other hand, *E. hirae* V-ATPase acts as a primary ion pump, which transports Na^+ or Li^+ physiologically instead of H^+ [12, 13]. The enzyme is composed of nine subunits having amino acid sequences that are homologous to those of the corresponding subunits of eukaryotic V-ATPases. The molecular mechanisms of *E. hirae* V-ATPase have been proposed on the basis of crystal structures of the parts, and single-molecule observation of the rotation [13–18].

2 Functional and Structural Features of Eukaryotic V-ATPases

Eukaryotic V-ATPases are multiprotein complexes that consist of 14 different polypeptide chains. Electron microscopy and image analysis have provided a general outline for the structural organization of V-ATPase [19–21]. The complex has a bipartite structure consisting of a membrane-integrated V_o domain (subunits a, c, c′, c″, d, and e) and a cytoplasmic extrinsic V_1 domain (subunits A–H) (Fig. 15.2). These two domains are linked by a connecting region that is important for coupling proton translocation in V_o with ATP hydrolysis in V_1 and is involved in regulating the activity of the enzyme by reversible disassembly. The connecting region consists of a central shaft (subunits D, F, and d) and multiple peripheral stator elements (subunits C, E, G, H, and a). Some of the eight different subunits in the V_1 domain are present in multiple copies; the domain contains three copies of the A, B, E, and G subunits, and one copy of the C, D, F, and H subunits. In V_1, the head group contains a trimer of nucleotide-binding A–B dimers that are responsible for ATP hydrolysis. The remaining V_1 subunits are distributed between one of two types of stalks (peripheral and central) that connect the V_1 and V_o domains. These stalks have distinct functions in the rotary mechanism by which V-ATPases couple ATP hydrolysis to proton transport. The central stalk serves as an axis that couples the energy released from ATP hydrolysis to the rotation of a ring of proteolipid subunits in V_o. The peripheral stalks serve to prevent the rotation of the A_3B_3 head during ATP hydrolysis and therefore serve a stator function. The integral V_o domain contains six different subunits. In yeast, these subunits are a, d, e, c, c′, and c″ [22, 23], whereas higher eukaryotes lack subunit c′ but contain the accessory subunit Ac45 [24]. The V_o subunits appear to be present in a stoichiometry of four or five copies of subunit

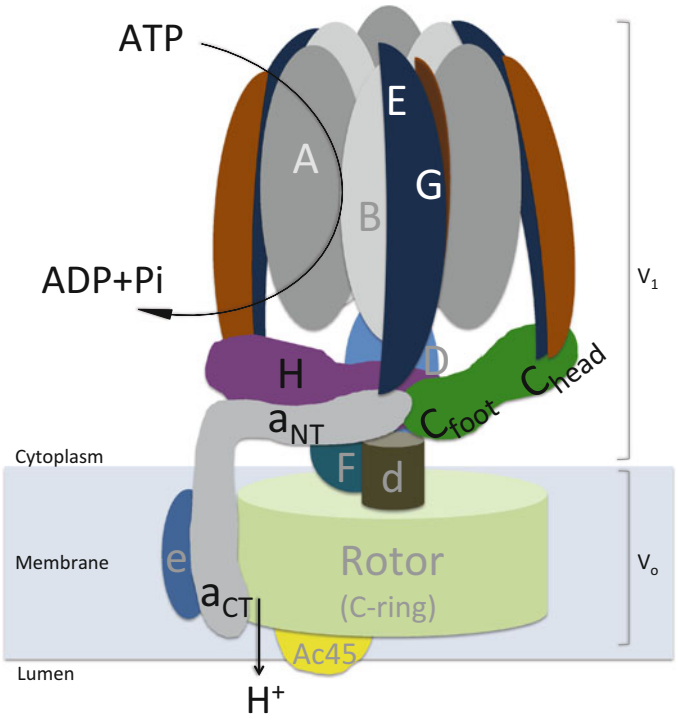

Fig. 15.2 Schematic model of mammalian V-ATPase with subunit composition and organization. Subunits A, B, C, D, E, F, G, and H form the cytosolic domain (V_1), and subunits a, c, d, and e form the transmembrane domain (V_o). The A–B subunit interfaces are the ATP catalytic sites where the ATP hydrolysis is mediated and the protons are transported between subunit a and the proteolipid c-ring. The central stalk is composed of D, F, d subunits, which mediates the rotation; whereas, the peripheral stator elements (C, E, G, H, and a) serve to prevent such rotation of the A_3B_3 head during ATP hydrolysis

c and single copies of the remaining subunits [22, 25]. The proteolipid subunits (c, c′ and c″) are highly hydrophobic proteins that are arranged to form a ring [26].

Crosslinking and electron microscopy studies have provided evidence that C, E, G, H, and the N-terminal domain of the a subunit (a_{NT}) all form part of the peripheral stalk [27]. It is known that in F-type ATP synthase there is only one peripheral stalk, whereas bacterial V-ATPases or A-ATPases contain two pairs of EG in their peripheral stalk, and eukaryotic V-ATPases have three pairs of EG [28]. *Saccharomyces cerevisiae* V-ATPase has been extensively studied and is used as a model for studying eukaryotic V-ATPases. The emerging consensus is that subunits E and G form a stable subcomplex [29–33], that is in contact with subunits C and H [31–35]. In contrast to the stator-forming subunit b in the related F-ATPases, V-ATPase subunits E and G do not have a membrane anchor to support their stator role. Therefore, they require a direct or indirect connection to the static membrane-anchored subunit a. Subunits C and H have been shown to tightly interact, and this interaction provides

a base for the three EG peripheral stalks. The structures of yeast V-ATPase C, H, and EGC (head) subunits have been solved [36–38]. Subunits C and H have no counterparts in bacterial A/V-ATPases. Subunit C has a "dogbone" structure [36] that is approximately 110 Å long and fits into the stator of the V-ATPase, where it contacts with the N-terminal region of subunit E. In addition, subunits C and H play a key role in the regulation process that occurs, for instance, during nutrient shortage [39, 40]. Subunit C is the first to dissociate from the complex, whereas subunit H is responsible for silencing the ATP hydrolysis activity in the free V_1 [27], a process necessary for avoiding wasteful energy consumption.

2.1 Human V-ATPase

Human V-ATPase is the most complicated of all the ATPases characterized in any organisms. The study of human V-ATPase is difficult for reasons such as unavailability of cell systems, the absence of several subunits that are present in yeast and bacteria, and the existence of several tissue-specific isoforms of certain subunits. In higher eukaryotes (mammals), several H^+-ATPase subunits have been shown to have multiple isoforms encoded by different genes with differing tissue expression patterns (Table 15.1). Two isoforms exist for each of the B, C, E, d, and e, subunits, three for the G subunit, and four for the a subunit, allowing many possible permutations of subunit structure in individual proton pumps. It is likely that pumps at different locations have their own unique subunit identities and the existence of different subunit isoforms may play an important role in the localization and activity of proton pumps in specific cell types and subcellular compartments. We assume that the basic subunit structure is the same among all V-ATPases, and that their diverse cellular localizations and functions are determined by subunit isoform composition. Various regulatory mechanisms allow V-ATPases to localize to distinct cellular environments or organ systems. Until now, most research on V-ATPases was carried out in bacteria or yeast. However, several isoforms present in mammals are not found in yeast. Furthermore, sequence similarity between yeast and human subunits is relatively low (identity 31–41 percentage, and similarity 51–60 percentage, depending on subunits and isoforms); hence, the assumption that their structural organization and biochemical properties are alike may not be valid [41]. From the two-protein sequence alignment of human or mouse isoforms, it was found that sequence identity and similarity between isoforms were not high (about 47–80 percentage, depending on subunits and isoforms), which explains the importance of multiple isoforms of each subunit [42]. The areas in which large mismatches occurred were similar for human and mouse V-ATPase, which is indicative of a close evolutionary relationship between these two proteins and also explains the tissue or organ specificity of mammalian V-ATPases.

From the above, some important questions arise: (1) Why do human or mammalian V-ATPases possess several isoforms, especially in their peripheral stalk? (2) Why and how do these isoforms localize at the cellular and subcellular level with

Table 15.1 Peripheral stalk subunit composition of mammalian V-ATPase

Domain	Subunit	MW (KDa)	Subunit functional location	Subunit function	Isoform	Gene	Mammalian splice variant	Tissue localization	Subcellular localization
V_1	C	45	Stator	Regulatory, assembly	C1	*ATP6V1C1*	1	C1-Ubiquitous	
					C2	*ATP6V1C2*	2	C2a-Lung, C2b-Renal, epididymus, placenta, testis	
	E	27	Stator	Regulatory, assembly	E1	*ATP6V1E1*	3	E1-Testis, acrosome, olfactory epithelium	
					E2	*ATP6V1E2*	1	E2-Ubiquitous	
	G	14	Stator	Regulatory, assembly	G1	*ATP6V1G1*	2	G1-Ubiquitous	Lysosomal membrane
					G2	*ATP6V1G2*	2	G2-Neural	Synaptic vesicles
					G3	*ATP6V1G3*	3	G3-Kidney, epididymus, inner ear	
	H	56	Stator	Regulatory		*ATP6V1H*	3		Clathrin-coated vesicles
V_o	a	100	Stator, proton-pore	Assembly, targeting, H+ transport		*ATP6VoA1*	4	a1-Neuronal, brain	Synaptic vesicles
						ATP6VoA2	2	a2-Endothelial, neurons	Golgi
						ATP6VoA3	2	Osteoclasts, pancreatic β-cells	Endosomal and lysosomal
						ATP6VoA4	3	Kidney, epididymis	Plasma membrane

tissue specificity? and (3) What causes such tissue-specific isoforms to carry out specific functions? To answer these questions a detailed study of different human V-ATPase subunit isoforms and their functions in specific tissues, cells, and organelles is required. In order to carry out such studies, different isoforms of human V-ATPase peripheral stalk subunits were expressed using an *Escherichia coli* cell-free protein synthesis system. The subunits expressed were E1, E2, G1, G2, G3, C1, C2, H, and the N-terminal soluble part of the a1 and a2 isoforms, encoded by genes *ATP6V1E1, ATP6V1E2, ATP6V1G1, ATP6V1G2, ATP6V1G3, ATP6V1C1, ATP6V1C2, ATP6V1H, ATP6V0A1,* and *ATP6V0A2*, respectively.

3 Physiological Roles of V-ATPase

ATP-dependent proton pumps known as V-ATPases in eukaryotic cell plays important roles in regulating the pH of intracellular compartments, the extracellular space, and the cytoplasm. V-ATPases within intracellular compartments are important for such normal cellular processes as receptor mediated endocytosis and intracellular membrane traffic, protein processing and degradation, and coupled transport of small molecules and ions [43]. They also facilitate the entry of a number of envelope viruses and bacterial toxins, including influenza virus and anthrax toxin [44, 45]. In tumor cells, V-ATPases targeting the plasma membrane are involved in tumor metastasis by creating an acidic extracellular environment that aids invasion [46]. V-ATPases present in the plasma membranes of cells are also important in normal physiology; they facilitate bone resorption by osteoclasts, acid secretion in the kidney, pH homeostasis, angiogenesis, and sperm maturation and storage [47].

4 Pathophysiology Associated with V-ATPase Dysfunction

In humans, V-ATPases are linked to several genetic or non-genetic diseases. The functional importance of V-ATPase in humans was revealed in patients harboring mutations of some of its subunits. In humans, mutation in any isoform-specific V-ATPase gene has been shown to result in disease within the tissue or organ in which that particular isoform is found. For example, mutations in genes encoding a4 and a3 cause kidney disease and osteopetrosis, respectively. Other studies suggest that V-ATPase is regulated in a much more complex manner than is currently assumed. Mutations of the *ATP6V1B1* and *ATP6V0a4* genes, coding for subunits B1 and a4, respectively, induce recessive distal renal tubular acidosis (dRTA) disease [48]. Interestingly, in many but not all cases, mutations in the B1 or a4 isoform can also lead to sensorineural deafness [49]. This is due to the role of V-ATPases in controlling the ion composition of the hemolymph that surrounds hair cells of the inner ear. Another important human genetic defect directly linked to mutations in the a3 isoform of the a subunit of V-ATPase is osteopetrosis. This disease is

characterized by the thickening of the bones, and skull and skeletal defects due to the inability of osteoclasts to degrade bone. Immunolocalization studies have demonstrated that the a3 isoform is localized to the limited membrane of the extracellular bone-resorbing compartment in mature osteoclasts. Thus, mutations in the a3 isoform result in the inability of osteoclasts to secrete acid and hence to degrade bone [47]. Intracellular V-ATPases function in the entry of various viruses and toxins. V-ATPase-dependent acidification of endosomal compartments is also crucial for the entry of the cytotoxic portions of various envelope viruses and bacterial toxins [27]. Recently, plasma membrane V-ATPases have been implicated in tumor metastasis. These plasma membrane V-ATPases regulate proton transport and have been proposed to both contribute to alkalinization of the tumor cell cytoplasm and to acidification of the extracellular environment. Extracellular acidification may promote tumor cell invasion by providing a low pH environment that is conducive to the activity of secreted cathepsins.

The complexity of the V-ATPase holoenzyme, which is composed of several subunits, some having more than one isoform, may reflect the need for differential regulation of the various functions that the enzyme performs in a variety of cell types and subcellular locations [48]. Therefore, the existence of so many isoforms of a specific subunit may be the main reason for the difficulties in understanding the complex roles of V-ATPase in human disease. Because V-ATPases are involved in a number of human diseases, and because many V-ATPase subunits are expressed in a tissue, cell, and organelle-specific manner, V-ATPases are attractive drug targets.

5 Functional Role of the Peripheral Stalk and the Importance of Its Integrity for Torque Resistance

Peripheral stalk subunits play a significant role in resisting the torque of V-ATPase, and the peripheral stalk is an area of V-ATPase where binding integrity among subunits is thought to differ from species to species. Conversely, it is complicated to understand the overall process consisting of signal transduction, subunit–subunit interaction, isoform specific organellar localization of each subunit, and finally functional implication. Until now, the regulation of the V-ATPase by V_o–V_1 dissociation has been studied primarily in non-mammalian systems such as yeast cells [39, 50] and insect cells [40, 51, 52]. However, there are limited reports about V-ATPase assembly/disassembly in mammalian systems, such as in kidney cells [53] and dendritic cells [54], and fewer details of the mechanism involved have been elucidated in these cases. It has been established from several studies that the C, E, G, and H subunits, and a_{NT} all form part of the peripheral stalk [7, 55, 56]. Bacterial cells lack subunits C and H suggesting that, bacterial A/V-ATPases are not regulated by this type of reversible dissociation. Study of V-ATPase in *E. hirae* [57] and *T. thermophilus* [58] indicates that subunits E, G, and a_{NT} can form a strong complex with a 1:1:1 stoichiometry. However, this phenomenon was not observed in eukaryotic systems. On the other hand, the reconstruction of yeast CE_3G_3H using

cryo-electron microscopy revealed interaction of subunits C and H, acting as a base for three pairs of EG heterodimers [59]. However, no biochemical evidence of this ternary binding interaction between CE_3G_3H subunits has been reported.

However, reconstruction and biochemical interaction studies using human CE3G3H found that the equivalent complex was unstable, due to the lower affinity between the C and H subunits [41]. It is probable that the interaction of the three EG heterodimer and the presence of nucleotides might be necessary to stabilize the C-H complex in vivo, resulting in a stable CE3G3H complex. In a recent study, Gruber and co-workers showed that the binding of the nucleotides ADP and ATP to the C-terminus of subunit C might induce structural changes in the foot region, thereby altering its interaction with other V_1 and V_o subunits [60]. Three peripheral stalks, consisting of three pairs of EG heterodimers along with C, H, and a_{NT} function to resist the torque of rotation by supporting an A_3B_3 hexamer during catalysis (Fig. 15.3). Binary interaction of the peripheral stalk subunits (C, EG, H, and a_{NT}) revealed that only the C-EG and H-EG complexes form with high affinity [41]. Interestingly, in both yeast and human V-ATPase, two EG pairs interact with the C subunit via its head (C_{head}) and foot (C_{foot}) domains with different affinities, and the third EG pair interacts with the H subunit [35, 41, 61, 62]. The interaction of the a_{NT} subunit was found to be less active in all cases, suggesting that the presence of the whole a subunit may be required in order to understand the overall structure of this complex in eukaryotes. However, interaction studies of both yeast and human peripheral stalk subunits strongly suggest that subunits C and EG are core components and two major players in the assembly process of V-ATPase (Fig. 15.3). Without EG and C, complex formation of other subunits was unusual: C-a-H could not interact with each other, and EG-a-H interacted as an EG-H complex only, without a [41]. Thus, assembly of the peripheral stalk subunits seems to be initiated by the EG and C subunits. The C subunit is known to play a critical role in connecting V_1 and V_o. The C_{head} links to one peripheral stator EG heterodimer with high affinity, whilst the C_{foot} links to another peripheral stator EG heterodimer with low affinity, forming a ternary junction point along with a_{NT} [35, 41, 56, 61, 63, 64] (Fig. 15.3). Subunit C is the only subunit that reversibly leaves the enzyme during glucose deprivation, causing dissociation of the V_1–V_o complex [65]. Therefore, the differences in the interaction affinities of the C subunit with E, G, H, and a_{NT} are likely to be essential for this reversible dissociation.

5.1 Subunit–Subunit Binding Interaction Phenomena at the Stator Region

V-ATPase is a large enzyme consisting of several subunits, and reconstitution of the entire enzyme complex in an in vitro system is quite difficult. Since the peripheral stator is the major player in the regulation of eukaryotic/mammalian V-ATPase, we focused our attempts on understanding V-ATPase regulation on the subunits of the peripheral stator. When expressed alone, the E and G subunits were very unstable,

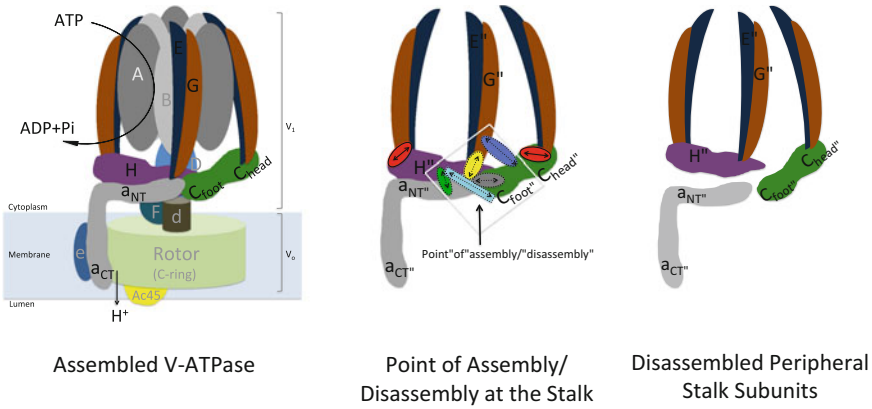

Fig. 15.3 Assembly and disassembly status of mammalian V-ATPase. Left, assembled V-ATPase complex showing the hydrolysis of ATP from the rotation of the enzyme and the *arrow* indicates the direction of proton movement. Mid, point of assembly/disassembly of the V-ATPase at the stalk region during regulation process, which is mediated at the C_{foot}-EG-a_{NT} region (*white color box*). Right, disassembled peripheral stalk subunits of the V-ATPase, dissociated from V_o membrane domain

but the co-expressed human EG subunit complex was found to be very stable, which is consistent with other findings from *S. cerevisiae*, *E. hirae, T. thermophilus,* and *Thermoplasma acidophilum.* This suggests an evolutionarily conserved function for this complex as a stator in all V/A-ATPases [28, 33, 42, 57, 66–69]. The two major regulatory subunits C and H are situated at the V_1–V_o junction, forming a base to hold three pairs of EG heterodimers with different affinities. However, the C and H subunits interact with very low binding affinity [41], which could be crucial for the facile dissociation of the enzyme. From several studies of yeast and human V-ATPase, it is known that the C subunit has two binding sites for two pairs of EG subunits. The C_{foot} region possesses lower affinity for one EG heterodimer; it is possible that this interaction is mediated specifically via the E subunit. The C_{head} region interacts with another EG pair with very high affinity, and yeast crystal structures of C_{head}-EG indicate that C_{head} has a binding site for both the E and G subunits. However, using the surface plasmon resonance technique, we obtained two different binding affinities for the C–EG interaction, which may correspond to the C_{head} and C_{foot} regions of the C subunit, respectively [41, Rahman et al. unpublished results]. We also observed a strong interaction between the EG and H subunits. Cryo-electron microscopic studies in yeast have revealed a CE_3G_3H assembly structure [59]. Therefore, we used various biochemical techniques to examine the possibility of a ternary complex formed by the EG, C, and H subunits in a 3:1:1 EG:C:H molar ratio. However, we found that this ternary complex was not as stable as the two independent stable binary complexes formed by C-EG and H-EG. Thus, we concluded that the putative EG–C–H ternary complex was not formed because of the low binding affinities between C-H and EG-C_{foot}. This finding indicates that the CE_3G_3H complex did not appear to undergo any conformational changes related to

regulation of its binding activity, but that the interaction was controlled by the sum of their individual affinities.

A key feature of the reversible disassembly of eukaryotic V-ATPases is located on the V_1–V_o interface, involving C_{foot}, the distal lobe of a_{NT}, and one EG heterodimer [35, 56, 64, 70] (Fig. 15.3). This inspired us to investigate the EG–a_{NT}–C ternary interaction, revealing that this strong interaction was still mediated by EG-C in spite of the low affinity between C-a and EG-a [41]. Thus, the a subunit possibly interacts via avidity. The next area of investigation is quaternary interaction, which includes the combined interactions of all the peripheral stalk subunits. The quaternary interactions of the EG, C, H, and a_{NT} subunits were found to be slightly more stable than the binary and ternary interactions in different combinations [41]. The cumulative binding of these subunits did not result in any affinity changes, but high avidity was observed, and this may be sufficiently strong to withstand the torque of rotational catalysis in eukaryotic cells. Thus, it is conceivable that multiple variable affinity interactions among stator subunits would be sufficient to allow the overall stator function and facilitate V-ATPase activity. We further speculate that the sum of these individual interactions in the peripheral stalk region is strong enough to withstand the torque of rotational catalysis and maintain the structural integrity of the complex. However, in cell system, there still remain other possibilities to retain strong interaction to resist the torque than the avidity, such as contributions of nucleotides or other protein binding factors.

6 Characterization of Human V-ATPase Peripheral Stalk Isoform

There is no doubt that the subunits of the peripheral stalk are the major players in the assembly and regulation of the enzyme. These subunits exist as several isoforms and are localized to different endomembrane organelles, including lysosomes, endosomes, the Golgi apparatus, chromaffin granules, and coated vesicles. They are also found in the plasma membrane of some specialized cells (Table 15.1). The existence of multiple homologs or isoforms of V-ATPase in mammalian cells adds another level of complexity to the motor. Since several V-ATPase subunits have multiple homologous or paralogous isoforms, some with several splice variants, there are theoretically hundreds of different permutations and combinations of subunit isoforms, which allow the assembly and expression of many variant V-ATPase isoenzymes in the human body. The mechanisms underlying the diverse functions and localizations of V-ATPases are believed to be mediated by the structures of these various isoforms [71]. Until now, isoforms have been identified for the a, d, e, B, C, E, and G subunits, and the specific isoenzymes found in given cell types have been determined by the differential, tissue-specific expression pattern of the subunit isoforms. However, the regulatory mechanism underlying the assembly of the unique combinations of isoforms, and the information necessary to target the enzyme to different cellular destinations, are still not clearly

understood in mammalian cells. Expression pattern analyses together with genetic approaches have demonstrated that specific V-ATPase complexes participate in highly differentiated cellular and tissue functions, including renal acidification, bone resorption, spermatogenesis, and neurotransmitter accumulation [72]. For such sophisticated cellular functions, specific V-ATPases along with specific subunits/isoforms are required, which cannot complement each other. For example, kidney, testis, inner-ear, osteoclast, brain, and lung require the isoform combinations E2G3-a4-C2-H, E1G1-a2-C2-H, E2G1-a3-C2-H, E2G1-a3-C1-H, E2G2-a1-C1-H, and E2G3-a1-C1-H, respectively for their specific functionality (Table 15.1) Unfortunately, in cases of isoform-specific mutations, isoforms cannot complement each other for such specialized functionalities, resulting in disease or dysfunction in the tissue in which that isoform is normally located. Therefore, it is imperative that crystal structures are obtained for different subunits/isoforms and their influence on quaternary subunit–subunit interaction is understood, as this will aid discovery of tissue-specific V-ATPase mechanisms and regulatory processes in mammals. Keeping this notion in our mind, we attempted to characterize human V-ATPase subunits/isoforms utilizing several biochemical techniques in an in vitro system. However, these investigations would be much more promising if we could express all the subunits/isoforms of the central stalk, catalytic domain, peripheral stalk, and rotor, thus allowing us to attempt the reconstitution of an entire active proton pump. However, this is not possible at present, and therefore we focused on one particular major part of the pump, the peripheral stator. This has a major role in assembly/disassembly of the enzyme, and can contain many of several isoforms of each subunit (Table 15.1). The peripheral stalk consists of subunits C, E, G, H, and a_{NT}. Two isoforms for the E and C subunits have been identified, and three for the G subunit [73–76]. Isoform E1 was specifically expressed in the germ cells of the testis, whereas E2 was found ubiquitously in all tissues examined [77]. Among the three G isoforms, G1 was found ubiquitously, whereas G2 was found in the brain and G3 in the kidney and inner ear [76]. Since the E or G subunits cannot be expressed or purified alone, two E and three G isoforms, comprising six different protein complexes (E1G1, E1G2, E1G3, E2G1, E2G2, and E2G3) have been purified using a cell-free co-expression system [42, 78]. In this review, EG-isoforms are considered as a single subunit for all binary, ternary, and quaternary interactions. There are four isoforms of the a subunit, which are thought to direct isoenzymes to specific target organelles via their encoded polypeptide signals. Isoforms a1, a2, and a3 are found ubiquitously in different endomembrane organelles, but a4 is specific to the plasma membrane of kidney-intercalated cells [79–82]. We could express only the N-terminal part of the a1 and a2 isoforms, and failed to express a3 and a4 at all, even after trying several constructs of each. The human C subunit has two isoforms: C1 is expressed ubiquitously, whereas C2 exhibits tissue specificity, with further diversity (C2-a and C2-b) resulting from alternative mRNA splicing. C2-a is predominantly expressed in the lung, whereas C2-b is expressed in the kidney and testis [75, 83]. We were able to express only the C1 and C2-b subunit; expression of the C2-a isoform was not possible. We examined the

in vitro binding interactions of several human V-ATPase subunits and their isoforms with the aim of evaluating structural and functional differences among the isoforms.

6.1 Characterization of the Subunit–Subunit/Isoform–Isoform Binding Interactions at the Stalk Region

As we discussed above, we hypothesized that specific assembly (complex formation) itself is a prerequisite for the V-ATPase isoform-specific localization mechanism, and thus we studied the complex-forming tendencies of such isoforms. E and G alone were unstable and could not be expressed, requiring co-expression and co-purification for their proper folding. Therefore, we expressed and purified six combinations of EG-isoforms: E1G1, E1G2, E1G3, E2G1, E2G2, and E2G3. Isoforms E2G2 and E2G3 tended to aggregate during the concentration and filtration steps of purification, which impeded our investigations of these isoforms. On the other hand, C-isoforms (sequence identity 62 % and similarity 83 %) exhibited differences in their stoichiometry during expression and purification: C1 was expressed as a monomer and C2-b as a dimer–monomer equilibrium [42]. Therefore, we tried qualitative and quantitative examinations expecting to reveal large differences in the binding interactions of these subunits/isoforms. To explore differences among the isoforms, we examined subunit–subunit interactions between the EG and C isoforms. We found that all EG isoforms tested interacted with the C isoforms with high affinity and in a similar manner [41], Rahman et al. unpublished results]. Isoform C2 interacted with the EG isoforms as a monomer, whereas C2 alone existed as a dimer–monomer equilibrium [Rahman et al. unpublished results]. There is no crystal structure of the C2 isoform, and therefore the reasons for such interesting structural differences remain unknown. Out of several EG heterodimer complexes, only E1G1 possessed high affinity for the H subunit [41]. Other EG isoforms had lower affinity for the H subunit [Rahman et al. unpublished result]. Using biochemical techniques, we observed moderate to low binding interactions between other peripheral stalk subunits, such as the H/C-isoforms, EG-isoforms/a-isoforms, C-isoforms/a-isoforms, and H/a-isoforms [Rahman et al. unpublished result].

However, we did not observe any major differences among isoforms, or any strong influence of the affinity among isoforms on the stability of complexes. The critical role that V-ATPases play in normal physiological processes seems to be complicated in eukaryotic cells, and likely accounts for both their structural complexity and the array of regulatory mechanisms, which can be controlled by their isoform-specific activity. These isoform-specific-mechanisms allow V-ATPases to be localized to distinct cellular environments or organ systems, and to be independently regulated. We suggest that the differences of affinity among isoforms could be influenced by several other factors such as organ-specific signals, pH levels, biochemical arrangements, or cell regulation processes. Hence, it is possible that factors other than structural differences play an important role in the assembly of ubiquitous isoforms and tissue-specific isoforms into functional V-ATPase complexes.

7 Conclusions

At this point, we would like to emphasize that at the time of the submission of this review, the high-resolution structure of the mammalian peripheral stalk subunits/isoforms has not been determined. Such structural information, along with the elucidation of the quaternary protein–protein interactions between different subunits and their isoforms, will facilitate the understanding of the proton translocation mechanism and will clarify the regulation mechanism of tissue-specific V-ATPases. Over the last few decades, a wealth of knowledge has been accumulated about this complicated enzyme concerning its molecular mechanisms and the structure of its subunits in bacteria and yeast. However, we are far away from a full understanding of the several tissue-specific isoforms of mammalian V-ATPase. There is increasing interest in V-ATPases because of their involvement in number of human diseases and disease processes, including osteoporosis, renal disease, toxin and viral cell invasion, cancer metastasis, diabetes, and Alzheimer's disease. However, scientists are struggling to achieve new investigational drugs targeting V-ATPase. Few such drugs are already on the horizon, but unfortunately, the new technologies are still in infancy; however, these drugs may make major contributions in the future. Such drug discovery will proceed much faster when the complete V-ATPase atomic structure is elucidated and the many subunit–subunit/isoform–isoform interactions that are important to its function are characterized.

References

1. Duncan TM, Bulygin VV, Zhou Y et al (1995) Rotation of subunits during catalysis by Escherichia coli F1- ATPase. PNAS 92:10964–10968
2. Kinosita K, Yasuda R, Noji H et al (1998) F1-ATPase: a rotary motor made of a single molecule. Cell 93:21–24
3. Noji H, Yasuda R, Yoshida M et al (1997) Direct observation of the rotation of F1-ATPase. Nature 386:299–302
4. Sabbert D, Engelbrecht S, Junge W (1996) Intersubunit rotation in active F-ATPase. Nature 381:623–625
5. Gruber G, Wieczorek H, Harvey WR et al (2001) Structure–function relationships of A-, F- and V-ATPases. J Exp Biol 204:2597–2605
6. Yoshida M, Muneyuki E, Hisabori T (2001) ATP synthase- a marvellous rotary engine of the cell. Nat Rev Mol Cell Biol 2:669–677
7. Forgac M (2007) Vacuolar ATPases: rotary proton pumps in physiology and pathophysiology. Nat Rev Mol Cell Biol 8:917–929
8. Muller V, Gruber G (2003) ATP synthases: structure, function and evolution of unique energy converters. Cell Mol Life Sci 60:474–494
9. Cross RL, Muller V (2004) Evolution of A, F and V-type ATP synthases and ATPases: reversal in function and changes in H+/ATP coupling ratio. FEBS Lett 576:1–4
10. Imamura H et al (2003) Evidence for rotation of V1-ATPase. PNAS 100:2312–2315
11. Murata T, Igarashi K, Kakinuma Y et al (2000) Na^+ binding of V-type Na^+-ATPase in Enterococcus hirae. J Biol Chem 275:13415–13419
12. Murata T, Yamato I, Kakinuma Y et al (2008) Ion binding and selectivity of the rotor ring of the Na+-transporting V-ATPase. PNAS 105(25):8607–8612

13. Murata T, Yamato I, Kakinuma Y et al (2005) Structure of the rotor of the V-Type Na+-ATPase from Enterococcus hirae. Science 308(5722):654–659
14. Mizutani K, Yamamoto M, Suzuki K et al (2011) Structure of the rotor ring modified with N, N'-dicyclohexylcarbodiimide of the Na+-transporting vacuolar ATPase. PNAS 108(33):13474–13479
15. Saijo S, Arai S, Hossain KM et al (2011) Crystal structure of the central axis DF complex of the prokaryotic V-ATPase. PNAS 108(50):19955–19960
16. Arai S, Saijo S, Suzuki K et al (2013) Rotation mechanism of Enterococcus hirae V1-ATPase based on asymmetric crystal structures. Nature 493(7434):703–707
17. Minagawa Y, Ueno H, Hara M et al (2013) Basic properties of rotary dynamics of the molecular motor *Enterococcus hirae* V1-ATPase. J Biol Chem 288(45):32700–32707
18. Ueno H, Minagawa Y, Hara M et al (2014) Torque generation of *Enterococcus hirae* V-ATPase. J Biol Chem 289(45):31212–31223
19. Venzke D, Domgall I, Kocher T et al (2005) Elucidation of the stator organization in the V-ATPase of Neurospora crassa. J Mol Biol 349:659–669
20. Wilkens S, Inoue T, Forgac M (2004) Three-dimensional structure of the vacuolar ATPase: localization of subunit H by difference imaging and chemical cross-linking. J Biol Chem 279:41942–41949
21. Wilkens S, Zhang Z, Zheng Y (2005) A structural model of the vacuolar ATPase from transmission electron microscopy. Micron 36(2):109–126
22. Nishi T, Forgac M (2002) The vacuolar (H^+)-ATPases—nature's most versatile proton pumps. Nat Rev Mol Cell Biol 3:94–103
23. Sambade M, Kane PM (2004) The yeast vacuolar proton-translocating ATPase contains a subunit homologous to the Manduca sexta and bovine e subunits that is essential for function. J Biol Chem 279:17361–17365
24. Supek F, Supekova L, Mandiyan S et al (1994) A novel accessory subunit for vacuolar H^+-ATPase from chromaffin granules. J Biol Chem 269:24102–24106
25. Powell B, Graham LA, Stevens TH (2000) Molecular characterization of the yeast vacuolar H^+-ATPase proton pore. J Biol Chem 275:23654–23660
26. Wilkens S, Forgac M (2001) Three-dimensional structure of the vacuolar ATPase proton channel by electron microscopy. J Biol Chem 276:44064–44068
27. Jefferies KC, Forgac M (2008) Subunit H of the V-ATPase inhibits ATP hydrolysis by the free V1 domain by interaction with the rotary subunit F. J Biol Chem 283:4512–4519
28. Lee LK, Stewart AG, Donohoe M et al (2010) The structure of the peripheral stalk of Thermus thermophilus H+-ATPase/synthase. Nat Struct Mol Biol 17:373–379
29. Tomashek JJ, Graham LA, Hutchins MU et al (1997) V1-situated stalk subunits of the yeast vacuolar proton-translocating ATPase. J Biol Chem 272:26787–26793
30. Xu T, Vasilyeva E, Forgac M (1999) Subunit interactions in the clathrin-coated vesicle vacuolar (H^+)-ATPase complex. J Biol Chem 274:28909–28915
31. Jones RP, Durose LJ, Findlay JB et al (2005) Defined sites of interaction between subunits E (Vma4p), C (Vma5p), and G (Vma10p) within the stator structure of the vacuolar H+-ATPase. Biochemistry 44:3933–3941
32. Féthière J, Venzke D, Diepholz M et al (2004) Building the stator of the yeast vacuolar-ATPase: specific interaction between subunits E and G. J Biol Chem 279:40670–40676
33. Ohira M, Smardon AM, Charsky CMH et al (2006) The E and G subunits of the yeast V-ATPase interact tightly and Are both present at more than one copy per V1 complex. J Biol Chem 281(32):22752–22760
34. Féthière J, Venzke D, Madden DR et al (2005) Peripheral stator of the yeast V-ATPase: stoichiometry and specificity of interaction between the EG complex and subunits C and H. Biochemistry 44:15906–15914
35. Inoue T, Forgac M (2005) Cysteine-mediated cross-linking indicates that subunit C of the V-ATPase is in close proximity to subunits E and G of the V_1 domain and subunit a of the V_o domain. J Biol Chem 280:27896–27903
36. Drory O, Frolow F, Nelson N (2004) Crystal structure of yeast V-ATPase subunit C reveals its stator function. EMBO Rep 5:1148–1152

37. Sagermann M, Stevens TH, Matthews BW (2001) Crystal structure of the regulatory subunit H of the V-type ATPase of Saccharomyces cerevisiae. PNAS 98(13):7134–7139
38. Oot RA, Huang LS, Berry EA et al (2012) Crystal structure of the yeast vacuolar ATPase heterotrimeric EGC(head) peripheral stalk complex. Structure 20(11):1881–1892
39. Kane PM (1995) Disassembly and reassembly of the yeast vacuolar H^+-ATPase in vivo. J Biol Chem 270:17025–17032
40. Sumner JP, Dow JAT, Earley FGP et al (1995) Regulation of plasma membrane V-ATPase activity by dissociation of peripheral subunits. J Biol Chem 270:5649–5653
41. Rahman S, Yamato I, Saijo S et al (2013) Biochemical and biophysical properties of interactions between subunits of the peripheral stalk region of human V-ATPase. PLoS ONE 8(2), e55704
42. Rahman S, Ishizuka-Katsura Y, Arai S (2011) Expression, purification and characterization of isoforms of peripheral stalk subunits of human V-ATPase. Protein Expr Purif 78:181–188
43. Gruenberg J, van der Goot FG (2006) Mechanisms of pathogen entry through the endosomal compartments. Nat Rev Mol Cell Biol 7:495–504
44. Gruenke JA, Armstrong RT, Newcomb WW et al (2002) New insights into the spring-loaded conformational change of influenza virus hemagglutinin. J Virol 76:4456–4466
45. Abrami L, Lindsay M, Parton RG et al (2004) Membrane insertion of anthrax protective antigen and cytoplasmic delivery of lethal factor occur at different stages of the endocytic pathway. J Cell Biol 166:645–651
46. Sennoune SR, Bakunts K, Martinez GM et al (2004) Vacuolar H+-ATPase in human breast cancer cells with distinct metastatic potential: distribution and functional activity. Am J Physiol Cell Physiol 286(2004):C1443–C1452
47. Hinton A, Bond S, Forgac M (2009) V-ATPase functions in normal and disease processes. Eur J Physiol 457:589–598
48. Breton S, Brown D (2007) New insights into the regulation of V-ATPase-dependent proton secretion. Am J Physiol Renal Physiol 292:F1–F10
49. Karet FE, Finberg KE, Nelson RD et al (1999) Mutations in the gene encoding B1 subunit of H+-ATPase cause renal tubular acidosis with sensorineural deafness. Nat Genet 21:84–90
50. Kane PM (2012) Targeting reversible disassembly as a mechanism of controlling V-ATPase activity. Curr Protein Pept Sci 13:117–123
51. Zimmermann B, Dames P, Walz B et al (2003) Distribution and serotonin-induced activation of vacuolar-type H+-ATPase in the salivary glands of the blowfly Calliphora vicina. J Exp Biol 206:1867–1876
52. Wieczorek H, Beyenbach KW, Huss M et al (2009) Vacuolar-type proton pumps in insect epithelia. J Exp Biol 212(11):1611–1619
53. Sautin YY, Lu M, Gaugler A et al (2005) Phosphatidylinositol 3-kinase-mediated effects of glucose on vacuolar H+-ATPase assembly, translocation, and acidification of intracellular compartments in renal epithelial cells. Mol Cell Biol 25:575–589
54. Trombetta ES, Ebersold M, Garrett W et al (2003) Activation of lysosomal function during dendritic cell maturation. Science 299:1400–1403
55. Zhang Z, Charsky C, Kane PM et al (2003) Yeast V1-ATPase: affinity purification and structural features by electron microscopy. J Biol Chem 278:47299–47306
56. Zhang Z, Zheng Y, Mazon H et al (2008) Structure of the yeast vacuolar ATPase. J Biol Chem 283:35983–35995
57. Yamamoto M, Unzai S, Saijo S et al (2008) Interaction and stoichiometry of the peripheral stalk subunits NtpE and NtpF and the N-terminal hydrophilic domain of NtpI of Enterococcus hirae V-ATPase. J Biol Chem 283:19422–19431
58. Yokoyama K, Nagata K, Imamura H et al (2003) Subunit Arrangement in V-ATPase from Thermus thermophilus. J Biol Chem 278:42686–42691
59. Hildenbrand ZL, Molugu SK, Stock D et al (2010) The C-H peripheral stalk base: a novel component in V1-ATPase assembly. PLoS One 5, e12588
60. Armbrüster A, Hohna C, Hermesdorf A et al (2005) Evidence for major structural changes in subunit C of the vacuolar ATPase due to nucleotide binding. FEBS Lett 579:1961–1967

61. Diepholz M, Venzke D, Prinz S et al (2008) A different conformation for EGC stator subcomplex in solution and in the assembled yeast V-ATPase: possible implications for regulatory disassembly. Structure 16:1789–1798
62. Oot RA, Wilkens S (2010) Domain characterization and interaction of the yeast vacuolar ATPase subunit C with the peripheral stator stalk subunits E and G. J Biol Chem 285:24654–24664
63. Zhang Z, Inoue T, Forgac M et al (2006) Localization of subunit C (Vma5p) in the yeast vacuolar ATPase by immuno electron microscopy. FEBS Lett 580:2006–2010
64. Qi J, Forgac M (2008) Function and subunit interactions of the N-terminal domain of subunit a (Vph1p) of the yeast V-ATPase. J Biol Chem 283:19274–19282
65. Curtis KK, Francis SA, Oluwatosin Y et al (2002) Mutational analysis of the subunit C (Vma5p) of the yeast vacuolar H+-ATPase. J Biol Chem 277:8979–8988
66. Lokanath NK, Matsuura Y, Kuroishi C et al (2007) Dimeric core structure of modular stator subunit E of archaeal H+-ATPase. J Mol Biol 366:933–944
67. Kish-Trier E, Briere LK, Dunn SD et al (2008) The stator complex of the A1A0-ATP synthase—structural characterization of the E and H subunits. J Mol Biol 375:673–685
68. Esteban O, Bernal RA, Donohoe M et al (2008) Stoichiometry and localization of the stator subunits E and G in Thermus thermophilus H+-ATPase/synthase. J Biol Chem 283:2595–2603
69. Kish-Trier E, Wilkens S (2009) Domain architecture of the stator complex of the A1A0-ATP synthase from Thermoplasma acidophilum. J Biol Chem 284:12031–12040
70. Oot RA, Wilkens S (2012) Subunit interactions at the V1-Vo interface in the yeast vacuolar ATPase. J Biol Chem 287:13396–13406
71. Imai-Senga Y, Sun-Wada GH, Wada Y et al (2002) A human gene, ATP6E1, encoding a testis specific isoform of H+-ATPase subunit E. Gene 289(1–2):7–12
72. Sun-Wada GH, Wada Y (2010) Vacuolar-type proton pump ATPases: roles of subunit isoforms in physiology and pathology. Histol Histopathol 25(12):1611–1620
73. Sun-Wada GH, Imai-Senga Y, Yamamoto A et al (2002) A Proton pump ATPase with testis-specific E1-subunit isoform required for acrosome acidification. J Biol Chem 277:18098–18105
74. Sun-Wada GH, Murata Y, Namba M, Yamamoto A et al (2003) Mouse proton pump ATPase C subunit isoforms (C2-a and C2-b) specifically expressed in kidney and lung. J Biol Chem 278:44843–44851
75. Sun-Wada GH, Yoshimizu T, Imai-Senga Y et al (2003) Diversity of mouse proton-translocating ATPase: presence of multiple isoforms of the C, d and G subunits. Gene 302:147–153
76. Murata Y, Sun-Wada GH, Yoshimizu T et al (2002) Differential localization of the vacuolar H+ pump with G subunit isoforms (G1 and G2) in mouse neurons. J Biol Chem 277:36296–36303
77. Hayashi K, Sun-Wada GH, Wada Y et al (2008) Defective assembly of a hybrid vacuolar H+-ATPase containing the mouse testis-specific E1 isoform and yeast subunits. Biochim Biophys Acta 1777:1370–1377
78. Terada T, Murata T, Shirouzu M et al (2014) Cell-free expression of protein complexes for structural biology. Methods Mol Biol 1091:151–159
79. Toyomura T, Oka T, Yamaguchi C et al (2000) Three subunit a isoforms of mouse vacuolar H+-ATPase. Preferential expression of the a3 isoform during osteoclast differentiation. J Biol Chem 275:8760–8765
80. Oka T, Murata Y, Namba M et al (2001) a4, a unique kidney-specific isoform of mouse vacuolar H+-ATPase subunit a. J Biol Chem 276:40050–40054
81. Nishi T, Forgac M (2000) Molecular cloning and expression of three isoforms of the 100 kDa a subunit of the mouse vacuolar proton-translocating ATPase. J Biol Chem 275:6824–6830
82. Smith AN, Finberg KE, Wagner CA et al (2001) Molecular cloning and characterization of Atp6n1b: a novel fourth murine vacuolar H+-ATPase a-subunit gene. J Biol Chem 276:42382–42388
83. Feng NH, Lin HI, Wang JS et al (2005) Differential expression of a V-type ATPase C subunit gene, Atp6v1c2, during culture of rat lung type II pneumocytes. J Biomed Sci 12:899–911

Chapter 16
Eukaryotic V-ATPase and Its Super-complexes: From Structure and Function to Disease and Drug Targeting

Vladimir Marshansky, Masamitsu Futai, and Gerhard Grüber

Abstract The eukaryotic vacuolar-type ATPase (V-ATPase) is a multi-subunit membrane protein complex, which is evolutionarily conserved from yeast to human. It is also functionally conserved and operates as a rotary proton pumping nano-motor. In the first part of this chapter we discuss the structure and function of the yeast V-ATPase (V_1V_O) holoenzyme, We focus on the structural features of its subunits forming both catalytic V_1 and proton conducting V_O sectors. Particularly, the recently solved structure of DF-subunit complex is discussed in relation to the energy coupling and regulation of yeast V-ATPase. It is noteworthy that the structure could contribute to understanding the function and regulation of V-ATPases of eukaryotes including human, leading to the rational design of specific inhibitors for medical applications. In addition to the well characterized role as proton pump, V-ATPases have acquired alternative cellular functions during evolution. In the second part we analyze novel roles of V-ATPase in function, signaling, and vesicular trafficking of cellular receptors. Our recent studies have uncovered that V-ATPase

V. Marshansky (✉)
Kadmon Corporation, Molecular Signaling, Alexandria Center for Life Science,
450 East 29th Street, New York, NY 10016, USA

Center for Systems Biology, Program in Membrane Biology and Division of Nephrology,
Simches Research Center, Massachusetts General Hospital, Boston, MA 02114, USA

Department of Medicine, Harvard Medical School, Boston, MA 02114, USA
e-mail: Vladimir.Marshansky@kadmon.com

M. Futai
Department of Biochemistry, Faculty of Pharmaceutical Sciences, Iwate Medical University,
Iwate 028-3694, Japan

Institute of Scientific and Industrial Research, Osaka University, Osaka 567-0047, Japan

G. Grüber
School of Biological Sciences, Nanyang Technological University,
60 Nanyang Drive, Singapore 637551, Republic of Singapore

Bioinformatics Institute, Agency for Science, Technology and Research (A*STAR),
30 Biopolis Street, #07-01 Matrix, Singapore 138671, Republic of Singapore

S. Chakraborti, N.S. Dhalla (eds.), *Regulation of Ca^{2+}-ATPases,V-ATPases and F-ATPases*, Advances in Biochemistry in Health and Disease 14,
DOI 10.1007/978-3-319-24780-9_16

itself functions as an evolutionarily conserved pH-sensing and signaling receptor, which forms super-complex with aldolase/cytohesin-2/Arf1,6 small GTPases in early endosomes. On the other hand, V-ATPase forms a super-complex with mTORC1/Ragulator/Rag/Rheb small GTPases in late endosome/lysosomes and is involved in amino-acids sensing and monitoring nutritional state of cells. Finally, we discuss the role of V-ATPase in the development and progression of various diseases including cancer, diabetes, and osteopetrosis among others. We also present emerging approaches and future perspectives for specific drug targeting to V-ATPase and its super-complexes.

Keywords Eukaryotic V-ATPase • Holoenzyme • Acidification • pH-sensing - Receptor signaling • Super-complex • Vesicular trafficking • Human diseases - Drug targeting

Abbreviations

a2N	N-terminal cytosolic tail of a2-subunit V-ATPase
Arf1	ADP-ribosylation factor 1
Arf6	ADP-ribosylation factor 6
BafA1	*bafilomycin A1*
c/c″-ring	Ring composed by the c- and c″-subunits
ConA	*concanamycin A*
CRP	Calorie restriction pathway
cryo-EM	Cryo-Electron microscopy
CTH2	Cytohesin-2
dErbB	Dimeric EGFR/ErbB-receptor
EGF	Epidermal growth factor
EmGFP	Emerald green fluorescent protein
FKPB12	FK506/rapamycin binding protein
FRET	Fluorescence resonance energy transfer
Fz	Frizzled
GH	Growth hormone
HRG-1	Heme-responsive gene 1 protein
IGF-1R	Insulin-like growth factor-1 receptor
IR	Insulin receptor
LRP6	Low-density receptor-related protein
M. sexta	*Manduca sexta*
mErbB	Monomeric EGFR/ErbB-receptor
mTORC1	Mammalian target of rapamycin complex 1
mTORC2	Mammalian target of rapamycin complex 2
NMR	Nuclear magnetic resonance
NOE	Nuclear Overhauser effect
PAT1	Proton coupled amino acid transporter 1

PI3K	Phosphatidylinositol 3-kinase pathway
PKA	Protein kinase A
PPI	Protein–protein interaction interface inhibitors
RagA/C	Rag A/C GTPases
Ragulator	Ragulator complex
Ras	Rat sarcoma small GTPase
RAVE	Regulator of ATPase of vacuoles and endosomes
Rbcn-3	Rabconnectin-3A/B
Rheb GTPase	Ras homolog enriched in brain
S. cerevisiae	*Saccharomyces cerevisiae*
SAXS	Small-angle X-ray scattering
*Sc*DF1 and *Sc*DF2	Two conformations of subunit DF complex
TFEB	Transcription factor EB
TSC complex	Tuberous sclerosis complex
V-ATPase	V-type ATPase
ΔpH	Proton gradient
ΔΨ	Membrane potential

1 Introduction

Eukaryotic vacuolar-type ATPases (V-ATPases) are ATP-dependent proton pumps, which are localized in plasma membrane and the organelle membranes, and involved in various cellular processes [1–12]. This enzyme consists of a cytosolic V_1 and a membrane embedded V_O sectors. The subunit stoichiometry of the V_1 and V_O sectors are proposed to be A_3:B_3:C_1:D_1:E_3:F_1:G_3:H_1 and a_1:d_1:c_x:c'_y:c''_z, respectively [1–5]. Although yeast enzyme has only two isoforms (Vph1p and Stv1p) for a subunit, human and mice have multiple subunit isoforms including: (1) two for the B, E, H and d-subunits; (2) three for the C and G-subunits; and (3) four for a-subunit (a1, a2, a3, and a4). The expression and targeting of V-ATPase with these isoforms are specific for cells and organelles [1–5].

The hydrolysis of ATP into ADP and phosphate (Pi) in the A_3B_3 catalytic hexamer of V_1 sector drives the proton translocation by a ring of c, c′, and c″ subunits of V_O sector. The coupling of both events is mediated through the rotation of a complex of DFdcc′c″. The reversible assembly/disassembly of the V_1 and V_O is a crucial mechanism for the regulation of V-ATPase [13–16]. Originally, this mechanism was discovered in *Manduca sexta* (*M. sexta*) and *Saccharomyces cerevisiae* (*S. cerevisiae*) in response to ceased feeding [17, 18] and glucose depletion [13, 19], respectively. However, similar mechanism should be essential for mammalian V-ATPase [20–24].

V-ATPases play a central role in the maintenance of pH-homeostasis at the cellular and organism level in mammals [1–5]. This enzyme is also involved in the endosomal pH-sensing [1, 2, 25–30] and has most recently been uncovered as a

signaling receptor that modulates the activity of cytohesin-2 (CTH2) and Arf small GTPases [31]. In addition, V-ATPase is involved in sensing of amino acids and monitoring nutritional status of cells via its interaction with mTORC1/Ragulator/Rag and Rheb small GTPases [32–35]. An alternative direct role of eukaryotic ATPases in membrane fusion has been previously proposed [36–39] and the V_O has been implicated in this process during exocytosis and insulin secretion in mammalian pancreatic β-cells [2, 8]. Moreover, V-ATPase with a3 and d2 isoforms is assembled in the osteoclast plasma membrane, and a direct role of the d2 isoform in the fusion of osteoclast progenitors has been described [2, 40–43]. Here, we discuss the current understanding of the structure of eukaryotic V-ATPase, focusing on the recently determined crystal structure of *S. cerevisiae* DF-subunit complex [44]. The finding of their interaction interface could reveal functional insights into coupling and regulation of all eukaryotic V-ATPases. In addition, we describe the emerging novel roles of V-ATPases in acidification of compartments, modulation of the function of critical cellular receptors as well as pH and nutrient sensing and signaling via its super-complexes.

In recent years, the V-ATPase has been implicated in the pathophysiology of a variety of human diseases including primary distal renal tubular acidosis accompanied by sensorial deafness [45], autosomal recessive osteopetrosis [41, 46], and autosomal recessive cutis laxa [47–49]. In addition, a role of the V-ATPase in cancer has recently emerged, since its increased expression at the plasma membrane correlates with the invasive characteristics of various malignant cells [50–53]. Based on these findings, perspectives and strategies in drug targeting to V-ATPase in human disease is discussed.

2 Structure of the Multi-subunit Eukaryotic V-ATPase

2.1 The Two Sector Composition of V-ATPase

Eukaryotic V-ATPases are multi-protein complexes composed by 14 different subunits $A_3B_3CDE_3FG_3Hac_Xc'_Yc''_Zde$. V-ATPase holoenzyme have a bipartite structure formed by a cytoplasmic V_1 ($A_3B_3CDE_3FG_3H$) and a membrane-embedded V_O ($ac_xc'_yc''_zde$) sectors (Figs. 16.1 and 16.2). The stoichiometry of three V_O subunits ($c_Xc'_Yc''_Z$) is unknown, although they are multiple. Both sectors are linked by connecting regions that are important for coupling between ATP hydrolysis in V_1 and proton translocation in V_O. These connecting regions consist of a central (D,F,d) and three peripheral (E,G) stalks, which are also important for reversible disassembly/assembly of V-ATPase (Fig. 16.1a). Within two V_1V_O sectors, however, there are functionally identifiable "stator" ($A_3B_3EGCHae$) and "rotor" ($DFdc_Xc'_Yc''_Z$) subcomplexes responsible for implementation of rotary mechanism of V-ATPase nanomotor [1–5, 12].

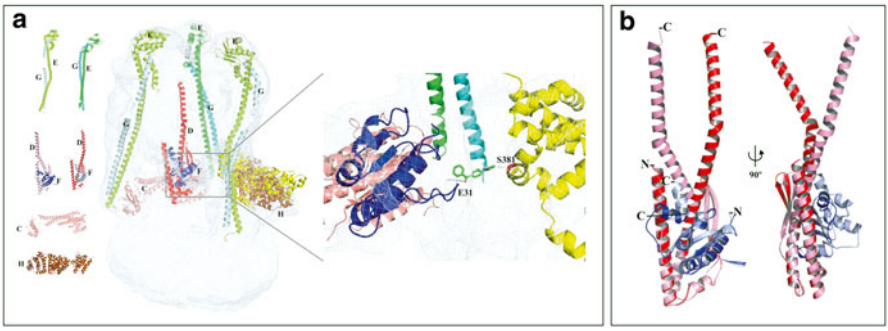

Fig. 16.1 Arrangement of the existing individual atomic subunit structures in the cryo-EM-map of the *S. cerevisiae* V-ATPase. (**a**) Subunits C (1U7L; *salmon*), H (1HO8, *brown*), and the D (4RND, *red*) and F assembly (4RND; *blue*) from *S. cerevisiae* were fitted into the cryo-EM map. The two conformations of EG subunits, the straight (4DL0; *green* and *cyan*) and more bent (4EFA; *lemo*n and *pale cyan*) are fitted to the three peripheral stalks. The crystallographic structure of two conformations of subunit D in ensemble with the stalk subunit F of *S. cerevisiae* (*Sc*DF1 and *Sc*DF2) V-ATPase are shown. (*Insert*) Region of the EM-map showing the interaction of modeled subunit H (S381) (*yellow*) through the sulfhydryl cross-linker 4-(*N*-maleimido)benzophenone (MBP) (stick; *green*) to the *S. cerevisiae* subunit F1-94 (E31) [44]. Cartoon representation of the structures of the individual *S. cerevisiae* subunits C (1U7L; *salmon*), F1-94 (4IX9, *blue*), H (1HO8, *brown*) and EG in two conformations, straight (4DL0; *green* and *cyan*) and bent (4EFA; *lemo*n and *pale cyan*). (**b**) Intermolecular interactions of the subunit DF-assembly. Superimposition of the *Sc*DF1 (*pink* and *blue*) with *Sc*DF2 molecule (*orange* and *grey*)

2.2 *Catalysis and Energy Coupling in V_1Sector*

V-ATPases exist in a dynamic equilibrium between fully assembled holoenzyme and reversibly disassembled V_1 and V_O [13–19]. Depending on the energy state of the cell, this equilibrium can be rapidly shifted [16, 54]. Recently, *S. cerevisiaeand M. sexta* V-ATPase holoenzymes have been isolated and its three-dimensional (3D) structure was shown using high resolution cryo-electron microscopy (cryo-EM) analysis [55–57]. The structure reveals that three A and B subunits form a hexagon with the nonhomologous regions at the top of subunit A [7, 55, 56, 58, 59]. The two nucleotide-binding subunits A and B alternate around a central cavity, which narrows toward its center and opens at both ends. Subunit D inside the cavity forms different interaction with domains of the three subunits A and B [12, 55, 56, 58]. The crystallographic structure of two conformations of subunit DF complex (*Sc*DF1 and *Sc*DF2) forming the central stalk of *S. cerevisiae* V-ATPase has been solved recently [44]. Subunit D in the complex consists of a long pair of α-helices, connected by a short helix ($_{79}$IGYQVQE$_{85}$) and a β-hairpin region, which is flanked by two flexible loops (Fig. 16.1b). The long pair of helices is composed of the N- and the C-terminal helix, respectively, and show structural alterations in the *Sc*DF1 and *Sc*DF2 structures. The subunit F consists of an N-terminal domain of four β-strands (β1-β4) connected by four α-helices (α1-α4). α1 and β2 are linked via the loop $_{26}$GQITPETQEK$_{35}$, which is unique in eukaryotic V-ATPases (Fig. 16.1a). Adjacent

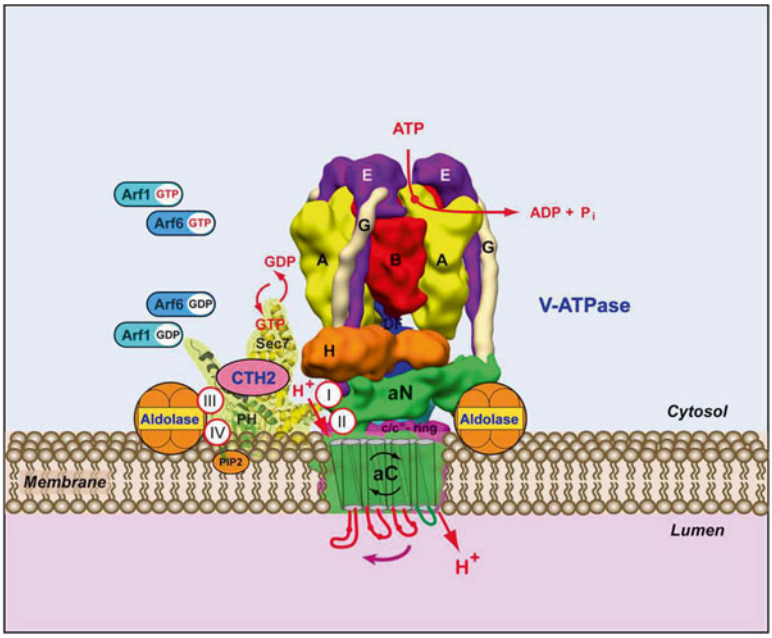

Fig. 16.2 Structure and composition of a novel V-ATPase/cytohesin-2/Arf1,6/aldolase signaling super-complex. The diagram shows the structure of the novel V-ATPase/cytohesin-2/aldolase/Arf1,6 super-complex localized on early endosomal (EE) membrane (see Fig. 16.3, *Complex 1*). It illustrates the binding site of cytohesin-2 (CTH2, in *yellow*) with an N-terminal tail of a2-subunit (a2N, in *green*) of V-ATPases [25, 29]. On the *left* is shown the CTH2 molecule interacting with a2N thorough Sec7-domain and with aldolase through PH-domain. *Roman numbers* indicate interfaces and affinities of interaction: (*I*) CTH2 with *a*2N(1–402) and (*II*) Sec7 domain with *a*2N(1–17) and *III*, *IV*) CTH2 with aldolase [28, 167]. On the *right* is shown the aldolase molecule interacting with a2N of V-ATPase

to the N-terminal domain is a flexible loop (P95-D106), followed by a C-terminal α5-helix. A perpendicular and extended conformation of the α5-helix was observed in the two crystal structures and in solution X-ray scattering experiments, respectively (Fig. 16.1a, left) [44]. The concerted interaction of the DF complex, including the P95-D106-loop with helix α5 of subunit F and bended C-terminal helix of subunit D, may activate ATP hydrolysis in the catalytic A_3B_3 hexamer [44, 60].

The $_{26}$GQITPETQEK$_{35}$-loop of the subunit F is facing to the C-terminal serine (S_{381}) of subunit H, revealed to be involved in cross-linking subunit F of the V_1 (Fig. 16.1a, right) [60, 61]. The unique stalk of subunit H is characterized by a large, primarily α-helical N-terminal domain, which is forming a shallow groove connected by a four-residue loop to the C-terminal domain [62]. This arrangement led to the proposal, that in the process of V_1 and V_O dissociation the flexible C-terminal domain of subunit H moves slightly closer to the exposed $_{26}$GQITPETQEK$_{35}$-loop of subunit F, where it causes conformational changes, leading to an inhibitory effect of ATPase activity in the V_1 [44, 60]. ^{15}N-[^{1}H]

heteronuclear NOE studies on the subunit F revealed a rigid core formed by β-strands, β1–β4, and α2–α4. In comparison, the N- and C-terminal helices α1 and α5 with their adjacent loops $_{26}$GQITPETQEK$_{35}$ and $_{94}$IPSKDHPYD$_{102}$, respectively, are more flexible in solution [60]. The N-terminal helix α1 of subunit F and the bottom segment of subunit D are in proximity to subunit *d*, forming the tip of the central stalk and being in direct neighborhood of the proton translocating ring of c-, c′-, c″-subunits of V_O [60]. This area might be modified during the process of reversible assembly/disassembly of the V_1 and V_O, as shown previously. The higher flexibility of α1 in subunit F would allow to transmit the conformational change of subunit *d* during dissociation from the DF-heterodimer and also the movement of subunit H closer to F, through the neighboring $_{26}$GQITPETQEK$_{35}$-loop [44, 60].

In addition to the central stalk, the catalytic A_3B_3 hexamer is connected to V_O by three peripheral stalks with a different degree of twisting in the C-terminal and/or middle part (Fig. 16.1a, left) [1]. The subunit E and G, forming the peripheral stalk, are arranged in a ~150 Å long complex. The peripheral stalk is connected to the A_3B_3 through the globular C-terminus of subunit E, formed by α-helices and β-sheets, arranged as β1:α1:β2:β3:β4:α2 [63, 64]. This C-terminus is connected by a flexible loop region with N-termini of both subunit E and G, which are folded in a noncanonical, right-handed coiled coil. The coiled coil is disrupted by a bulge of partially unfolded secondary structure in subunit G, which provides the necessary flexibility of the peripheral stalk during detachment and assembly of the V_1 from the V_O (Fig. 16.1a, left) [63].

The reversible disassembly of the V_1 and V_O is initiated by the dissociation of subunit C [65]. As shown for its hydrated [66] and crystallized form [67] subunit C is a boot-shaped protein with an upper head domain formed from α-helices and β-strands (residues 167–262) and a globular foot domain (residues 1–55 and 320–392). Both domains are connected by an elongated helical neck domain (Fig. 16.1a, left) [67]. Location and orientation of subunit C in the enzyme enables its binding to actin [67], ADP/ATP nucleotides [68], and WNT-kinase [69]. These interactions are taking place through the foot domain allocated in proximity to the N-termini of an EG-heterodimer, as well as in neighborhood to the N-terminal region of subunit *a* (Fig. 16.1a, left). It was suggested that binding of ATP/ADP [68] or WNT-kinase dependent phosphorylation [69] of subunit C could alter the stability of an subunit EGC assembly by affecting its binding properties with either EG-heterodimer or with actin.

2.3 Structure of the V_O Enabling Proton Conduction

The proton conducting V_O sector of V-ATPase may be formed by five or six subunits and two accessory proteins. Indeed, *S. cerevisiae* V_O consists of six different subunits (a, c, c′, c′′, d, and e). However, the c′ subunit gene was not found in mammalian genome, and thus, the mouse and human V_O are formed only by five subunits: a (a1, a2, a3, or a4), c, c′′, d (d1 or d2), and e (e1 or e2). In turn, the mammalian V_O

also contains the two additional accessory subunits Ac45 and M8-9 [1, 5, 70]. Structurally, the V_O is composed of a ring of *c*- and *c″*-subunits (c/c″ ring) and the adjacent single copies of the *a*, *e*, Ac45, and M8-9 subunits. As suggested by the 3D map of the V_O from bovine clathrin-coated vesicles V-ATPase, the accessory subunit Ac45 interacts with the c/c″ ring from the luminal side [71].

On the other hand, the N-terminal cytosolic tail of subunit *a* (aN) is oriented parallel to the cytoplasmic surface of the membrane in the close proximity to the N-terminus of subunit H (Fig. 16.2) [1, 55]. Recent small-angle X-ray scattering studies of the N-terminal tail $a_{104\text{-}363}$, suggested the connection between the cytoplasmic N-terminal (aN) and the transmembrane C-terminal (aC) domains of subunit *a* (Fig. 16.2) [72]. This arrangement makes the aN of V-ATPase accessible for cytohesin-2 (CTH2) and Arf1, Arf6 small GTPases (Fig. 16.2), which is essential for signaling and trafficking of various receptors, including EGFR/ErbB receptors (Fig. 16.3) [1, 31, 72]. Although the structure and orientation of the aN is available, the transmembrane topology of its aC remains controversial (Fig. 16.2) [1, 26]. In yeast a six [73, 74], eight [75, 76], and nine [77, 78] transmembrane helix models have been proposed. According to the model with eight helices, both N- and the C-termini of the a subunit (Vph1p) are located in the cytosol, which is supported by the results showing interaction of phosphofructokinase-1 with the C-terminal tail of the human a4- and a1-isoforms [79]. The moving membrane part of the yeast V-ATPase "rotor" is a ring composed by the c-, c′-, and c″-subunits. The c- and c′-subunits are 16 kDa proteins, proposed to contain four transmembrane helices with two loops exposed to the cytosol, while the c′′-subunit is a 23 kDa polypeptide with five putative transmembrane helices, two loops and a C-terminal tail exposed to the cytosol [80, 81]. Recently, cryo-EM observation of rotational states in *S. cerevisiae* V-ATPase has revealed the involvement of ten c-, c′-, and c″-subunits in the ring formation [56]. Each of these subunits is contributing two transmembrane helices to the inner ring and two helices to the outer ring. In addition, this study supported the eight transmembrane helices model of a-subunit [75, 76]. Remarkably, it was found that two of the helices are highly tilted and span the membrane where the a-subunit is in contact with the ring of ten c-, c′-, and c″-subunits, providing the new insights on the proton conducting mechanist of V_O sector [56]. The subunit composition and number of transmembrane helices in the c/c″-rings of mammalian V-ATPases are open questions. Recently, the first evidence for the position of subunit e within V_O has been provided [82].

The cryo-EM map of yeast V-ATPase revealed that a proton conducting channel is formed by the interface between transmembrane helixes of a-subunit and the ring of c-, c′-, c″-subunits. This channel is very narrow and occurs near the middle of the membrane region [12, 83]. It is important to note that the potent V-ATPase inhibitors *bafilomycin A1* (*BafA1*) and *concanamycin A* (*ConA*) bind to the interface between a-subunit and the ring of c-, c′-, c″-subunits inhibiting both rotary and proton-pumping mechanisms of yeast V-ATPase [84–86]. Although these compounds are very useful to analyze the role of V-ATPases in inside-acidic organelles of cultured mammalian cells [87, 88], they are unable to distinguish between V-ATPases with different isoforms, which are targeted to specific compartments.

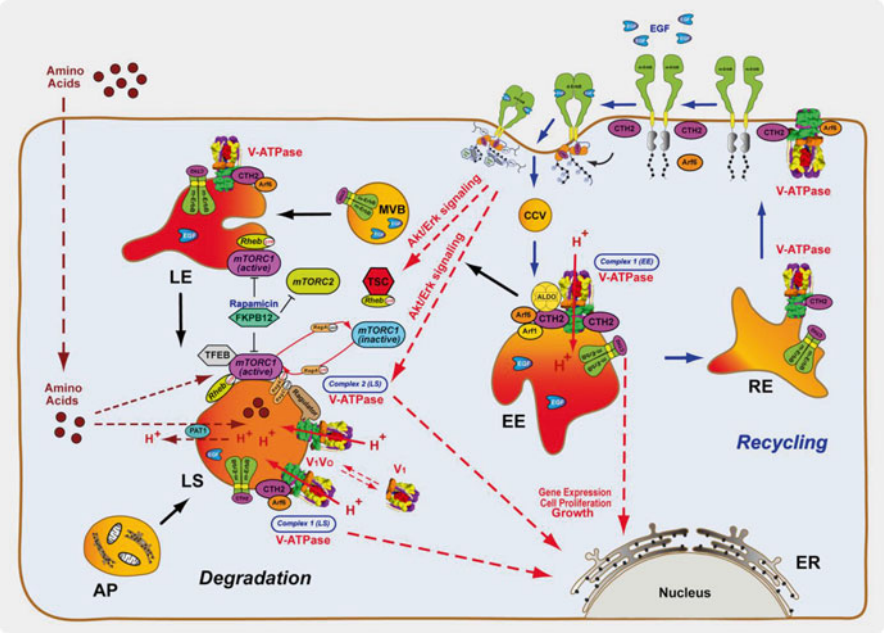

Fig. 16.3 Signaling and trafficking of EGFR/ErbB-receptors in endosomal/lysosomal pathway. Scheme shows signaling of epidermal growth factor (EGF) and trafficking of EGFR/ErbB-receptors in clathrin-dependent endocytosis and endosomal/lysosomal protein degradative pathway. The compartments are shown in yellow/red as follows: *CCV* clathrin-coated vesicles, *EE* early endosomes, *MVB* multi-vesicular bodies, *LE* late endosomes, *RE* recycling endosomes, *LS* lysosomes, *AP* autophagosomes, *ER* endoplasmic reticulum. Vesicular trafficking steps for the degradation branch are indicated with *black arrows* and for recycling branch with *blue arrows*. (*EE and super-complex-1*) Structure and composition of V-ATPase/CTH2/aldolase/Arf1,6 super-complex located in early endosomes. V-ATPase in this super-complex functions as pH-sensing and cytohesin-2/Arf1,6 signaling receptor which may regulate the trafficking and signaling EGFR/ErbB-receptors. (*LE/LS and super-complex-2*) Structure and composition of a novel V-ATPase/Ragulator/RagA/C/mTORC1/Rheb super-complex located in late endosomes and lysosomes. This complex is involved in sensing levels of amino acids and modulation of mTORC1-dependent downstream cellular programs and cell growth. Moreover, reversible association/dissociation of V_1V_O sectors of lysosomal V-ATPase is regulated by signaling of EGFR/ErbB-receptors through Akt/Erk pathway (*dashed red arrows*)

Therefore, there is an urgent need for the development of a new generation of inhibitors capable of selective inhibition of the subset of V-ATPases located at the specific compartments, such as Golgi, endosomes and lysosomes among others. Thus, an accumulating knowledge of high resolution structures of individual V-ATPase subunits as well as their interaction interfaces will be important for future developments of new generation of: (1) isoform and (2) organelle and/or (3) cell specific V-ATPase inhibitors (Figs. 16.1 and 16.2).

3 The Role of V-ATPases and Their Super-complexes in Acidification, Signaling, and Sensing

V-ATPase generates an electrochemical proton gradient, forming acidic intracellular compartments [1–5]. This enzyme is also targeted to the plasma membrane and is involved in extracellular acidification of specialized cells in kidney [89–91], epididymis [90, 92, 93], and bone [40, 74, 94–97]. It also acidifies extracellular environment in metastatic cancer cells [50–53]. The regulation of V-ATPase is achieved by the following three major processes: (1) modulation of acidification by the chemiosmotic mechanism; (2) targeting to specific organelles; and (3) regulation of the enzyme activity through reversible assembly/disassembly V_1 and V_O.

3.1 Chemiosmotic Process

The electrochemical proton gradient generated by V-ATPase consists of a proton gradient (ΔpH) and membrane potential (ΔΨ). Using a FRET approach, the values ΔpH = 2.2 units and ΔΨ = 27 mV were experimentally determined in intracellular organelles [98]. Acidification is predominant function of V-ATPase, which depends on its coupled function with Cl^-/H^+- and Na^+/H^+-exchangers as an important chemiosmotic mechanism regulating acidification of intracellular organelles [99–102].

3.2 Process of Subunit-Specific Targeting of V-ATPase

The *S. cerevisiae* V-ATPase is targeted by the two *a*-subunit isoforms Vph1p and Stv1p to the vacuole and Golgi/endosomes, respectively [103, 104]. Studies with chimeric proteins revealed that the targeting information is located in the cytosolic N-terminal domain of the a-subunit [104]. Similarly, in mammalian cells, localization of V-ATPase in endocytic and exocytic compartments and targeting to the plasma membrane depend on *a*-subunit isoforms (Figs. 16.2 and 16.3) [1–4, 94]. Of four subunit *a* isoforms (*a*1, *a*2, *a*3 and *a*4) [1–4], V-ATPase with a1 isoform is specifically targeted to presynaptic membranes and exocytic synaptic vesicles in mammalian neurons [105, 106]. Studies with neurosecretory PC12 cells revealed that both *a*1 and *a*2 regulate the acidification and neurotransmitter uptake and release by exocytic vesicles [107]. In contrast, V-ATPase with *a*1 is targeted to the endocytic pathway in brain microglial cells, and plays role in the fusion between phagosomes and lysosomes during phagocytosis, a process of microglial-mediated neuronal degeneration [108].

The *a*2 isoform targets V-ATPases to early endosomes of the endocytic pathway of kidney proximal tubule epithelial cells [25, 26, 30, 109, 110]. In these cells, the overexpressed recombinant *a*2-isoform (*a*2-EGFP) is also targeted V-ATPase to

endosomal compartments [31]. However, in cultured osteoclast cells and B16 cells, both endogenous *a*2 and a1 are targeted to secretory vesicles of Golgi complex in the exocytic pathway [94, 107]. Similarly, over-expression of recombinant *a*2 isoform (*a*2-EmGFP) in neuroendocrine PC12 cells targets V-ATPase to the Golgi apparatus [94, 107].

The V-ATPase with *a*3 is a lysosome specific enzyme of osteoclast progenitor. During differentiation, the V-ATPase with *a*3 is targeted and localized to the plasma membrane of osteoclasts. The osteoclast V-ATPase is involved in bone reabsorption and its defect caused infantile malignant osteopetrosis in humans [40, 74, 94–97]. V-ATPase with *a*3 is also targeted to the plasma membrane of breast cancer cells and plays an important role in metastatic processes [50–53]. Phagosomes in macrophage also acquire the same enzyme from lysosomes [111], whereas it is specifically targeted to insulin secretory granules of pancreatic β-cells [2, 94].

The V-ATPase with *a*4 is highly abundant in epididymis and kidney, where they are specifically targeted to the apical plasma membrane of epididymal clear cells and kidney collecting duct intercalated cells [89–93], indicting that this V-ATPase is involved in sperm-maturation [92, 93] and maintenance of acid-balance [90, 91], respectively. These results indicate that the *a*-subunit isoforms differentially target V-ATPase to the plasma membrane or intracellular compartments of the endocytic/exocytic pathways. In turn, the specific targeting and assembly of the enzyme may modulate acidification of extracellular milieu and intracellular organelles [1–4, 93, 112].

3.3 Reversible Assembly/Disassembly of V-ATPase

The regulation of V-ATPases by assembly/disassembly of the V_1V_O sectors was first described in response to ceased feeding in *M. sexta* [17, 18] and in response to glucose depletion in *S. cerevisiae* [13, 14, 19]. In *S. cerevisiae*, assembly/disassembly of the V_1V_O may be regulated by both *a*-isoform (Vph1 or Stv1) and E subunit. Evidence for the role of the E subunit in assembly was first obtained from yeast/mouse hybrid V-ATPase [113, 114]. A null mutant of yeast subunit E expressing the mouse (E1 or E2) is functional, indicating that this hybrid V-ATPase with E1 or E2 is functional as proton pump. However, assembly of the hybrid with E1 became less dependent on glucose [114]. Furthermore, a domain between residues K33 and K83 of *S. cerevisiae* subunit E could be replaced by the corresponding region of mouse E1 [114, 115]. Alanine scanning mutations revealed that the residue E44 of yeast subunit E is a key amino acid in regulation of subunit assembly and thus enzyme activity [115].

In *S. cerevisiae*, the reversible assembly and disassembly of V_1V_O sectors is controlled by two distinct mechanisms. While the assembly requires the cytosolic RAVE/Rab-Connectins complex (Rav-1, Rav-2, and Skp1), the disassembly process involves the cytosolic microtubular network [1, 2, 4, 5, 15, 116]. Recent study revealed, that RAVE/Rab-Connectins in yeast is an *a*-isoform specific complex, which is necessary for assembly of V-ATPase with Vph1p but not with Stv1p [117].

Moreover, the reversible assembly/disassembly of the yeast V_1 and V_O is also controlled by the direct interaction of V-ATPase with cytosolic aldolase, a central enzyme of the glycolysis (Fig. 16.2). The assembly/disassembly and interaction with aldolase is modulated by the Ras/cAMP/PKA pathway [118], suggesting that V-ATPases may act as a cytosolic glucose-sensor (Fig. 16.2) [119–121]. However, in mammalian kidney proximal tubule cells, glucose regulation on V-ATPase is modulated by the phosphatidylinositol 3-kinase (PI3K) pathway [21]. In dendritic cells, the assembly of V_1V_O is also regulated through the PI3K/mTOR-dependent pathway and is critical for lysosomal acidification, protein degradation, and antigen presentation (Fig. 16.3) [20, 24]. Thus, it is generally accepted that various regulatory pathways are involved in controlling assembly/disassembly of V-ATPase in eukaryotic cells and, therefore, in modulation of its function as well as acidification of intracellular organelles and extracellular milieu [22].

3.4 Novel Role of V-ATPases in Regulation of Signaling and Trafficking of Cellular Receptors

A novel role of V-ATPases in regulation of signaling, trafficking, and degradation of various cellular receptors has emerged recently. Endocytosis is an essential cellular process that is used by eukaryotic cells for the internalization of various receptors localized in the plasma membrane. As shown previously, the clathrin-dependent endocytosis pathway mediates internalization of Fz/LRP6, PRR, Notch, transferrin, megalin/cubilin, and EGFR/ErbB receptors among others (Fig. 16.3) [1, 31, 122]. Mounting evidence indicates that the V-ATPase is not only establishing the acidic pH in endocytic organelles but is also functioning as a cytohesin-2/Arf1,6 small GTPases signaling receptor (Fig. 16.2). Moreover, the V-ATPase is involved in direct interactions with critical cellular receptors, and thus, could modulate their signaling, traffic, and degradation along the endocytic pathway (Fig. 16.3). These emerging roles of V-ATPase will be discussed below.

3.5 V-ATPase and Epidermal Growth Factor Receptors (EGFR/ErbB's)

The epidermal growth factor receptor (EGFR) was among the first discovered growth receptors that regulate crucial cell biological processes including cell proliferation [123, 124]. The EGFR/ErbB-receptors (EGFR/ErbB's) family comprises four members (EGFR/ErbB1, ErbB-2, ErbB-3, and ErbB-4) and are involved in the development of a variety of cancers [124–127]. Activation of EGFR/ErbB-receptors by extracellular EGF ligand promotes their hetero-dimerization with subsequent activation of TK-domains and tyrosine trans-phosphorylation of the cytoplasmic tail.

However, the cytoplasmic proteins that could modulate EGF-induced activation and signaling of EGFR/ErbB-receptors were largely unknown.

Cytohesin-2 (CTH2) has been identified recently as a cytoplasmic activator of EGFR/ErbB-receptors (Fig. 16.3) [128, 129]. CTH2 enhances trans-dimerization and activation of EGFR/ErbB's by direct binding with TK-domains of dimerized receptors and by facilitating conformational changes and trans-phosphorylation of these domains. Figure 16.3 illustrates the signaling of the epidermal growth factor (EGF) through EGFR/ErbB's localized in the plasma membrane and early endosomes. The crucial role of CTH2 in hetero-dimerization of these receptors is also indicated. The figure also shows the V-ATPase dependent trafficking and signaling of EGFR/ErbB-receptors through the clathrin-dependent endocytosis endosomal/lysosomal protein degradation pathway. In particular, a novel important role of the assembly/disassembly of V_1V_O and V-ATPase-dependent late endosomal/lysosomal acidification in EGFR/ErbB-receptors function has been recently revealed [23]. It was demonstrated that EGF/EGFR-dependent signaling promotes the rapid recruiting of cytosolic V_1 sectors of the V-ATPase and increases its assembly with V_O on late endosomal/lysosomal compartments. This assembly in turn increases V-ATPase driven lysosomal acidification, protein degradation, and release of amino acids needed for Rheb(GTP) and mTORC1 activation (Fig. 16.3). V-ATPase is playing an indirect role in EGF-dependent activation of mTORC1 signaling pathway by modulating the assembly/disassembly of V_1 and V_O [32]. This is the first evidence showing the functional assembly of V-ATPase in response to the signaling of EGFR/ErbB-receptors. In this way, V-ATPase regulates mTORC1 signaling and trafficking EGFR/ErbB-receptors within the endosomal/lysosomal protein degradation pathway (Fig. 16.3) [23, 32]. Thus, V-ATPase-dependent acidification and cytohesin-2/Arf1,6 small GTPases signaling (Fig. 16.2) may play a key role in the modulation of EGFR/ErbB-receptors function, and is pivotal for the sustained signaling, recycling, or degradation (Fig. 16.3).

3.6 V-ATPase, Insulin-Like Growth Factor-1 Receptor (IGF-1R), and Heme-Responsive Gene 1 (HRG-1) Protein

Both the growth hormone (GH) and insulin-like growth factor 1 (IGF-1) exert powerful control over lipid, protein and glucose metabolism. The function of GH/IGF-I signaling pathway is associated with longevity, and thus, aging related morbidities including diabetes and cancer [130, 131]. This pathway also plays roles in maintenance and repair of muscles [132]. Signaling by insulin-like growth factor receptor (IGF-1R) controls expression of heme-responsive gene 1 (HRG-1) that encodes a 16 kDa transmembrane protein. A recent study revealed specific targeting of this protein to early endosomes and its direct interaction with V-ATPase *c*-subunit [133]. Increased expression of HGR-1 enhances V-ATPase activity in the plasma membrane, lowers the extracellular pH and activates pH-dependent matrix metalloproteinases. HRG-1 also increases endosomal V-ATPase activity, which promotes

trafficking of the IGF-1R, β1-integrin and glucose transporter-1 (GLUT-1) with concomitant increase of glucose uptake, cancer cell growth, migration and invasion. Thus, HRG-1 may represent a novel target for selectively disrupting V-ATPase activity and the metastatic potential of cancer cells [133, 134].

3.7 V-ATPase and Frizzled (Fz) and Low-Density Receptor-Related Protein (LRP6) Receptors

The Wnt/β-catenin, Wnt/PCP(planar cell polarity) and Wnt/Ca^{2+} signaling pathways are essential mechanisms that control embryonic tissue development, homeostasis, cell proliferation, polarity, and apoptosis [135, 136]. They are strongly linked to the development of a variety of human diseases including metastatic cancers [135, 136]. The direct role of V-ATPase in regulation of Wnt/β-catenin and Wnt/PCP signaling pathways has been uncovered recently [137, 138]. It was shown that signal transmission after association of Wnt ligands with Fz/LRP6 co-receptors requires direct interaction of LRP6 with an accessory M8-9 subunit of V-ATPase, also called V-ATPase lysosomal accessory protein-2 (ATP6AP2). This interaction takes place in early endosomes and the ATP6AP2 subunit acts as an adaptor that brings together V-ATPase and the Wnt/Fz/LRP6 receptor complex. Thus, both direct and electrochemical regulation by V-ATPases are involved in signaling of Wnt/Fz/LRP6 in endosomes involved in the protein degradation pathway.

3.8 V-ATPase and (Pro)renin Receptor (PRR)

The (pro)renin receptor (PRR), a single transmembrane cell surface receptor, plays a central role in activating the local renin-angiotensin system. Binding of prorenin to PRR induces its conformational change, allowing conversion of angiotensinogen to angiotensin-I, which is subsequently converted to angiotensin-II by an angiotensin-converting enzyme [139, 140]. However, an angiotensin-independent function of PRR has also been recently reported, which was identified as an accessory ATP6AP2 subunit of V-ATPase [137, 138, 140, 141]. Tissue-specific conditional knockout experiments confirmed a role of PRR/ATP6AP2 in assembly of V-ATPase in murine cardiomyocytes [142]. Importantly, the level of prorenin is elevated during diabetes and over-activation of PRR is associated with development of hypertension and diabetic kidney disease [122, 143]. The role of PRR in kidney function and its association with diabetes and hypertension has been recently reviewed [122, 140, 141, 143]. Thus, future studies in this area could lead to the novel therapeutic approaches for the treatment of hypertension, diabetes, and their complications [122].

3.9 V-ATPase and Notch Receptor

The cell-to-cell signaling by the Notch receptor pathway is critical during development and tissue regeneration for controlling the balance between cell proliferation and apoptosis. Pathological loss of regulation of Notch receptor signaling is also a hallmark of different cancers [144, 145]. Activation of the Notch receptor by ligands gives rise to its cleavage by γ-secretase-mediated intra-membrane proteolysis followed by activation of specific target genes. Surprisingly, recent studies revealed that V-ATPase driven acidification may control two opposite processes in the Notch signaling in *Drosophila*: (1) lysosomal degradation and loss of regulation of Notch receptors; and (2) γ-secretase-mediated Notch receptor activation in early endosomes [146]. Moreover, Notch receptor signaling is also controlled by Rabconnectin-3A/B (Rbcn-3) through regulating V-ATPase both in *Drosophila* and mammalian cells [147, 148]. It is noteworthy that mammalian Rbcn-3 protein is a homolog of yeast Rav-1, which forms a part of the RAVE (Rav-1, Rav-2, and Skp1) complex. Interaction of Rav-1 with V-ATPase is essential for reversible assembly/disassembly of the yeast V_1 and V_O [15, 116, 149]. Similar to Wnt-signaling, these studies also revealed two mechanisms of Notch-signaling modulation by V-ATPase in mammalian cells: (1) through subsequent Rbcn-3/V-ATPase interaction and (2) V-ATPase-driven acidification leading to activation of γ-secretase [138, 146–148].

3.10 V-ATPase as pH-Sensor and Cytohesin-2/Arf Small GTPases Signaling Receptor

The Arf-family small GTPases belong to the Ras-superfamily that are involved in regulation of a great variety of cellular pathways [150]. These GTPases function as "molecular switches" and the transition between "on" and "off" is mediated by a GDP/GTP cycle. In particular, activation of Arf small GTPases is accomplished by the cytohesin-family of guanine nucleotide exchange factors (GEFs). Cytohesin-family GEFs include cytohesin-1, cytohesin-2 (CTH2) (also known as ARNO), cytohesin-3 (also known as GRP1), and cytohesin-4. The generally accepted functions of cytohesin/Arf small GTPases are regulation of organelle biogenesis, modulation of vesicular trafficking, and actin cytoskeleton remodeling [151–153]. However, cytohesins have also emerged recently as central modulators of signaling and trafficking of plasma membrane receptors including: (1) EGFR/ErbB [128, 129], (2) insulin-receptor (IR) and insulin-like growth factor-1 receptor (IGF-1R) [154–158], (3) VEGF-2R [159], and (4) integrins [160, 161]. In particular, cytohesin-1 and -2 have been identified as activators of EGFR/ErbB's that are involved in regulation of cell proliferation and oncogenesis [128, 129]. Cytohesins are also crucial downstream effectors for the IR and IGF-1R signaling cascade involved in regulation of calorie restriction pathway, longevity, and aging process [154–158, 162–164].

Previously, our laboratory focused on studies of the functional interplay between V-ATPase and cytohesin-2/Arf1,6 small GTPases in endosomal/lysosomal protein degradation pathway [30, 109, 165, 166]. The cytohesin-2 and Arf1, Arf6 are specifically targeted to early endosomes of this pathway and co-localized with V-ATPase in kidney proximal tubule cells (Figs. 16.2 and 16.3) [30, 109]. Moreover, subsequent work from our laboratory revealed that V-ATPase itself functions as a novel long-sought pH-sensor or pH-sensing receptor. In particular, V-ATPase containing a2 isoform is specifically targeted to early endosomes and directly interacts with cytohesin-2 (CTH2) in acidification-dependent manner, suggesting that the a2 is a putative pH-sensing receptor (Fig. 16.2) [25, 26]. According to this concept, V-ATPase is not only responsible for proton pumping and the generation of a pH gradient but also involved in sensing the levels of acidification and transmitting this information through membrane. Moreover, other isoforms (a1, a3, and a4) were also found to interact with CTH2 [167]. Taken together, these results suggest that pH-sensing by V-ATPases and interaction with cytohesin-2/Arf1,6 small GTPase is a general phenomenon, which may take place in other acidic organelles of both the exocytotic and the endocytic pathways. We have uncovered the molecular details of unexpected function of V-ATPases, as an evolutionarily conserved pH-sensing and cytohesin-2/Arf1,6 small GTPases signaling receptor (Fig. 16.2) [1, 2, 25–27, 31, 167].

4 Functions of V-ATPase in Normal and Disease States

In this section, we discuss roles of V-ATPases in regulating vesicular trafficking and the development of various disease states. First, our focus is the role of V-ATPases in cancer development and metastasis process. Second, we analyze its role in modulation of exocytic/secretory pathway during pathogenesis of diabetes and bone diseases. Third, we discuss the roles of V-ATPases in regulating two novel super-complexes localized in endocytic or endosomal/lysosomal protein degradation pathway (Fig. 16.3). We also discuss their roles in cancer as well as aging and age-related diseases.

4.1 V-ATPase in Cancer Development and Metastasis

Human and mouse a1 and a2 are expressed ubiquitously under physiological conditions, whereas a3 and a4 are specifically expressed and targeted to the plasma membranes of bone osteoclast and kidney intercalated cells, respectively [73, 92, 93, 168, 169]. Previous studies suggested that the a subunit targets V-ATPase to different compartments and plasma membranes as well as senses the pH-gradient formed during acidification (Fig. 16.2) [1, 2]. V-ATPases with specific a-isoforms have been detected at the plasma membrane of the breast, ovarian, and prostate cancer cells. The role of V-ATPase dependent extracellular acidification was studied extensively in development and invasive phenotype of these metastatic tumors.

4.1.1 Breast Cancer

Early studies have demonstrated that V-ATPases are expressed in the plasma membrane of invasive cancer cells [170]. V-ATPase was found to be more prominently expressed in the highly metastatic MDA-MB231 breast cancer cells, which are more invasive and migratory than the less metastatic MCF-7 breast cancer cells. Moreover, inhibition of V-ATPase by *BafA1* significantly reduces the in vitro invasion of MDA-MB231 but not MCF7 cells [50]. These results indicate that targeting of V-ATPase to the plasma membrane is correlated with metastatic phenotype of the breast cancer cells. However, the mechanism of V-ATPase function and the subunits involved in its targeting to the plasma membrane remain obscure. Further studies have focused on the role of the a-subunit isoforms in cancer. Although all four isoforms are found in MDA-MB231 but not MCF7 cell lines, the expression levels of a3 and a4 are significantly higher in metastatic MDA-MB231 than in non-metastatic MCF-7 cells. In addition, siRNA knockdown experiments further demonstrated the role of a3 and a4 isoforms in targeting V-ATPase to the plasma membrane and invasive phenotype of MDA-MB231 cells [51]. Similar role of a3 was found in invasiveness of MCF10CA1 but not MCF10a breast cancer cells [52]. Finally, the recent studies demonstrated that invasiveness of breast cancer cells could be modulated by cell-impermeable molecules targeting extracellular parts of V-ATPase: (1) a biotin-conjugated *BafA1* or (2) the monoclonal antibody directed against the V5 epitope constructed on the extracellular loop of V_O c-subunit [53].

Other roles of V-ATPase in breast cancer development and metastasis have been revealed recently. First, V-ATPase is required for trafficking of Rab27B small GTPase dependent pro-invasive secretory vesicles which promote an invasive growth and metastasis in estrogen receptor (ER) alpha-positive breast cancer patients. Therefore, a role of V-ATPase in invasive growth and metastasis of ER-alpha-positive breast cancer has been suggested [171]. This study demonstrated that inhibiting V-ATPase by *BafA1* or silencing of a1 or d subunits might be an effective strategy for blocking Rab27B-dependent pro-invasive secretory vesicles which are involved in secretion of pro-invasive growth regulators. Second, V-ATPase driven acidosis of tumors may also control the pro-apoptotic protein Bnip3 death pathway [172]. Accordingly, it was reported that pharmacologic inhibition of V-ATPase with *BafA1* could effectively activate Bnip3 pathway, promote death of breast cancer cells and significantly reduced tumor growth in MCF7 and MDA-MB-231 mouse xenografts in vivo. Importantly, the combined treatment of mice bearing the breast MDA-MB-231 xenografts with *BafA1* and ERK1/2 inhibitor *sorafenib* has potentiated action of two inhibitors for tumor regression. These results present a novel mechanism to kill cancer cells and reverse resistance of breast hypoxic tumors. Third, breast cancer invasive cells are resistant to anoikis, a specific type of apoptosis promoted by loss of cell–matrix contact. A recent study demonstrated, that triggering of anoikis by V-ATPase inhibitor *archazolid* is promising therapeutic approach to reduce metastasis of breast cancer cells in mouse model in vivo [173]. Forth, very recent study has identified a novel tumor-metastasis related gene 1 (TMSG1) as a regulator of activity of V-ATPase and secreted metalloproteinase-2 in breast cancer cells [174].

All together, these studies suggest that V-ATPase could modulate invasiveness and breast tumor metastasis due to acidification of extracellular milieu and subsequent activation of metalloproteases. On the other hand, V-ATPase also controls apoptotic cell death and regulates vesicular trafficking and secretion of pro-invasive growth factors. Importantly, in breast cancer cells both invasiveness and metastasis could be controlled by targeting extracellular part of plasma membrane V-ATPase [175–177].

4.1.2 Ovarian Cancer

The role of V-ATPase in invasiveness and metastasis has also been recently addressed in ovarian carcinoma. Particularly, the expression, targeting, and function of a-subunit isoforms were studied in ovarian cancer tissues as well as in ovarian cancer A2780, SKOV-3, TOV-112D cell lines [178]. The a2-isoform is predominantly expressed in these cells and targeted V-ATPase to the plasma membrane. Under physiological conditions, a2-isoform is predominantly located in early endosomal compartment or Golgi and, thus, it relocates to the plasma membrane during tumorigenesis and metastasis. This study also reveals co-association of a2-isoform with cortactin, a protein involved in invasion of tumor cells. Targeting of a2 with monoclonal antibody reduces the activity of matrix MMP-2 and MMP-9 metalloproteinases and invasiveness of these ovarian cancer cells. These findings suggest that a2-isoform could be promising target for developing novel therapeutic anti-V-ATPase antibodies against ovarian carcinoma [178]. Finally, an important role of the a2-isoform derived secretory peptide in inflammation, angiogenesis, and tumorigenesis was also proposed [179–182].

4.1.3 Prostate Cancer and Tumor Angiogenesis

Angiogenesis is recognized as one of the hallmarks of cancer which enable tumor growth and metastatic dissemination [127]. Moreover, tumors are currently recognized as abnormal organs consisted of a complex mixture of the cells interacting and signaling with each other and required stable supply of nutrients and oxygen for their needs [183]. The cancer-induced neovascularization is triggered by pro-angiogenic signaling and cell-to-cell cross talk. In particular, plasma membrane V-ATPase was implicated in regulation of intracellular pH and migration of microvascular endothelial cells [184, 185]. Moreover, V-ATPase is taking part in cross talk and regulation of communication between microvascular endothelial and metastatic cells promoting acidification of extracellular space and favors protease activity [186]. A different mechanism of cross talk in metastatic prostate cancer cells involves regulation of V-ATPase by pigment epithelium-derived factor (PEDF), a potent endogenous inhibitor of angiogenesis. Thus, PEDF was identified as novel regulator of V-ATPase and suggested the mechanism of its inhibition of prostate tumor growth.

In summary, during last decade V-ATPase emerged as a crucial enzyme for tumorigenesis and metastatic phenotype of breast, ovarian, and prostate cancers. However, during last years the pathophysiological role of V-ATPase in the development of other tumors including: melanoma [187], hepatocellular carcinoma [188], oral squamous carcinoma [189], esophageal squamous carcinoma [190], non-small-cell lung cancer [191], gastric cancer [192], colon cancer [193], and pancreatic cancer [194] were also studied.

4.2 V-ATPase in Insulin Secretion and Diabetes Mellitus

V-ATPases play also essential roles in specific organelles of differentiated cells, especially those involved in exocytosis. The secretory granules have acidic luminal pH (5.0–5.5), important for condensation and maturation of their content. It has been suggested that the inside acidic pH or proton gradient across organelle membranes is involved in fusion of the vesicles to target membranes. Interesting question is which a-subunit isoform is expressed in secretory vesicles of mammalian cells. We have focused on the role of a-isoforms in insulin secretion, since previous studies suggested that V-ATPases may be pertinent for the insulin secretion [8, 195]. Of four isoforms, the a3 was detected in almost all cells in pancreatic Langerhans islet, and localized to the membranes of insulin containing granules in β-cells. Consistent with this finding, oc/oc mutant mice, homozygous 1.6 kb deletion of the a3-locus, exhibited reduced insulin secretion into blood upon glucose administration. However, the mutant β-cell contained essentially the same amount of mature insulin as the wild-type cell. Thus, the secretion of insulin was impaired in mutant β-cells. These results suggest that the a3-isoform has a direct function in exocytosis, possibly for fusion of the secretory vesicles to plasma membranes. The human ATP6i gene encoding the a3-isoform was mapped to a chromosome 11q13, and is located about 200 kb apart from LRP5 locus, which shows strong linkage to the disease. It is highly likely that alteration of ATP6i could also contribute to Type 1 diabetes [196]. We have identified that V-ATPase with a3 is highly expressed in endocrine tissues such as adrenal, parathyroid, thyroid and pituitary gland. Thus, a3 may be commonly involved in exocytosis of endocrine tissue and play an important role in the pathogenesis of endocrine and metabolic diseases including diabetes mellitus [8].

4.3 V-ATPase in Bone Homeostasis and Diseases

Bone homeostasis is maintained through the equilibrium between bone genesis and resorption by osteoblast and osteoclast, respectively. Defects of these cells are related to bone diseases such as osteopetrosis and osteoporosis. Osteoclast generates proton flux into bone resorption lacuna to mobilize bone calcium. This

acidification is carried out by V-ATPases, which are localized in the osteoclast plasma membrane. We have shown that a3 and d2 subunits are components of the osteoclast enzyme [40, 75]. Mammalian subunit d has two isoforms: ubiquitous d1 isoform and osteoclast/kidney/epididymis specific d2 isoform [40]. In contrast to the plasma membrane localization in osteoclast, the a3 isoform was found in late endosome/lysosome in NIH3T3 or RAW264.7 cells.

Murine macrophage line RAW264.7 can differentiate to multinuclear osteoclast-like cells. Upon stimulation with RANKL (Receptor Accepter Nuclear κB Ligand) from osteoblast, RAW264.7 cell differentiate into multinuclear osteoclast. During the differentiation, V-ATPase containing a3 isoform was transported to the cell periphery together with lysosome marker proteins, and finally assembled to the plasma membrane. The d2 isoform was also induced and assembled to the plasma membrane V-ATPase. Thus, secretory lysosomes should be involved in the formation of osteoclast plasma membranes. The splenic macrophage (from a3 knockout mice) lacking the a3-isoform could differentiate to multinuclear cells, which express osteoclast marker enzymes and V-ATPase with d2 and a1 or a2 isoforms [40, 197]. However, the multinuclear cell could not adsorb calcium phosphate, indicating that V-ATPase with d2/a2- or d2/a1-subunit isoforms could not perform the function of that with d2/a3-subunit isoforms containing V-ATPase.

In summary, we have studied the targeting and function of a3-isoform both in endocrine tissues and in bone osteoclasts. Remarkably, while in pancreatic β-cells a3 is targeting the V-ATPase to the membranes of insulin containing secretory granules of exocytic pathway, in bone osteoclast the V-ATPase with a3-isoform is expressed in plasma membrane and late endosomes/lysosomes of endocytic pathway. However, our results strongly suggest that V-ATPase a3 is localized into specialized secretory lysosomes in osteoclasts. These specialized lysosomes are not functioning as common endocytic lysosomes, but instead are transported to cell periphery and fused with plasma membrane, using the mechanism similar to exocytosis. In accordance with the pivotal role of V-ATPase in bone homeostasis, multiple mutations of the a3-isoform give rise to diseases of bone resorption and are associated with osteopetrosis in both mice models and humans [41, 46, 95, 198, 199].

4.4 V-ATPase and mTORC1/Ragulator/Rag/Rheb Small GTPases Super-complex in Cancer, Diabetes, and Age-Related Diseases

The mammalian target of rapamycin (mTOR) is a large cytosolic serine-threonine kinase that controls cellular growth and metabolism. Under physiological conditions both mTORC1 and mTORC2 are involved in neonatal autophagy and survival as well as development of obesity and aging processes in adulthood. Abnormal function of mTORC1 and mTORC2 are implicated in the pathogenesis of many diseases including cancer, diabetes, age-related diseases, aging, and

longevity [34, 35, 163, 200–204]. The mTOR belongs to the superfamily of phosphatidylinositol-3 kinase related-kinases (PI3KK) that forms the core of two functionally distinct complexes: mTORC1 and mTORC2. As mTORC1 primarily responds to the levels of amino acids, oxygen, energy and cellular stress stimuli, mTORC2 plays a central role in the growth factor and insulin signaling cascades (Fig. 16.3) [33–35]. mTORC2 also regulates cytoskeleton function, metabolism, and cell survival [35, 205]. V-ATPase has been identified recently as an important component of the mTORC1 regulatory super-complex and signaling pathway [32]. This super-complex, formed by V-ATPase, Ragulator, Rag, mTORC1, and Rheb, is associated with late endosomes and lysosomes of the protein degradation endocytic pathway (Fig. 16.3) [32, 206, 207]. Localization of mTORC1 on the late endosoaml/lysosomes membrane is also critical for its activation as a multi-functional serine–threonine kinase and is regulated by two types of small GTPases: (1) Rheb GTPase (Ras homolog enriched in brain); and (2) Rag GTPases. It is well recognized, that Rheb is a potent activator of mTORC1, which transmit signals of growth factors, oxygen, energy supply, and stress via the tuberous sclerosis complex (TSC), acting as a GTPase activating protein (GAP) for Rheb small GTPase.

Although amino acids are known to modulate cell growth and homeostasis, the molecular aspects of their regulation of mTORC1 function remained elusive. However, Sabatini and coworkers have shown recently that V-ATPase is a major player in the amino acids dependent recruitment, activation and signaling of mTORC1 [32]. V-ATPase is involved in sensing the levels of intra-lysosomal amino acids through the direct interaction with the Ragulator complex, that acts as a GTPase GTP/GDP-exchange factor for Rag small GTPases [33, 208]. They have proposed that the primary function of amino acid-dependent V-ATPase/Ragulator/Rag-signaling complex is to promote recruiting mTORC1 to lysosomal membrane, and thus trigger the TSC/Rheb-driven "ignition key" for the activation of the kinase activity of lysosomal mTORC1 complex. In their scenario, V-ATPase plays a direct role in intra-lysosomal sensing of amino acids and trans-membrane signaling to mTORC1.

Recent studies demonstrated, that mTORC1 is also activated by EGF via EGFR-receptor signaling pathway (Fig. 16.3). Then, the activation of mTORC1 involves in the Akt/Erk activation, TSC complex inhibition, and Rheb(GTP) formation. In contrast to amino acid-induction studies [32], EGF signaling pathway does not accompany mTORC1 recruitment from the cytosol and its translocation to the lysosomal membrane [23, 32]. Instead, the EGF signaling promoted the rapid recruitment of V_1 sectors and increased assembly of ATPase in late endosomal/lysosomal compartments. Thus, the novel role of V-ATPase in regulation of mTORC1 signaling and trafficking EGFR/ErbB-receptors within the endosomal/lysosomal protein degradation pathway is a crucial mechanism controlled by the assembly/disassembly of the V_1 and V_O (Fig. 16.3) [23, 32].

In summary, lysosomes and related organelles play a regulatory role in cellular protein degradation and energy production using V-ATPase/mTORC1 "sensing machinery" to monitor both lysosomal and cytosolic amino acid content as indicator of nutritional status of the cell. This physiological information is further

communicated to the nucleus to activate the gene expression programs allowing lysosomes to regulate their own function [209]. This quality control process is declining over life span, contributing to cancer and aging associated diseases, and thus, V-ATPase/mTORC1/Ragulator/Rag/Rheb small GTPases super-complex is considered as an important drug target.

4.5 V-ATPase and Cytohesin-2/aldolase/Arf1,6 Small GTPases Super-complex in Cancer, Diabetes, and Age-Related Diseases

Our recent studies uncovered, that in addition to its primary role as a proton-pump, V-ATPase also functions as a pH-sensing and cytohesin-2/Arf1,6 small GTPases signaling receptor (Fig. 16.2) [1, 2, 25, 27, 31]. However, the molecular mechanism of interaction between these proteins as well as functional significance of the signaling remain unclear. Thus, we also focused on the mechanism of interaction between N-terminal cytosolic tail of a2-subunit (*a*2N) of V-ATPase and cytohesin-2 (CTH2) [28]. The interaction sites between these two proteins were mapped using the combination of recombinant proteins/synthetic peptides pull-down and surface plasmon resonance (SPR) experiments. Two structural elements involved in specific and high affinity association of the a2 isoform with CTH2 were identified: (1) an N-terminal binding motif formed by the first 17 amino acids of the *a*2N (*a*2N1–17 peptide) and (2) the catalytic Sec7 domain of CTH2 [28, 31]. The SPR experiments further confirmed that these structural elements are major binding sites between *a*2N of V-ATPase and CTH2. Furthermore, this analysis revealed a strong binding affinity between this *a*2N1-17 peptide and the Sec7-domain of CTH2, with a dissociation constant of $K_D = 3.44 \times 10^{-7}$ M, similar to the binding affinity $K_D = 3.13 \times 10^{-7}$ M between full-length *a*2N and CTH2 proteins (Fig. 16.2, interfaces I and II). Analysis of enzyme activity confirmed that *a*2N1-17 peptide is crucial for V-ATPase/CTH2 signaling and regulate the cytohesin-2 enzymatic Arf-GEF activity. Indeed, these studies revealed that *a*2N1-17 peptide is a potent inhibitor of the GDP/GTP-exchange activity of CTH2, that is acting through its direct interaction with the catalytic Sec7 domain. The α-helical structure of *a*2N1-17 and its residues F5, M10, Q14 binding with the Sec7 domain were also identified by NMR spectroscopy analysis (Fig. 16.4a, b). In silico docking studies have shown that *a*2N1-17 epitope of V-ATPase competes with the switch-2 region of Arf1,6 for binding to the Sec7 domain of CTH2 (Fig. 16.4c, d). Together, these experiments revealed the structural basis and molecular details of mechanism of signaling between V-ATPase and CTH2/Arf1,6 small GTPases (Fig. 16.4).

Although our previous work uncovered a functional cross talk between V-ATPase, cytohesin-2, and Arf1,6 small GTPases, other downstream effectors and related cell biological events have not been unraveled. However, since V-ATPase interacts with both cytohesin-2 and aldolase, we suggested that these proteins could in turn interact with each other, forming V-ATPase/cytohesin-2/Arf1,6/aldolase super-complex.

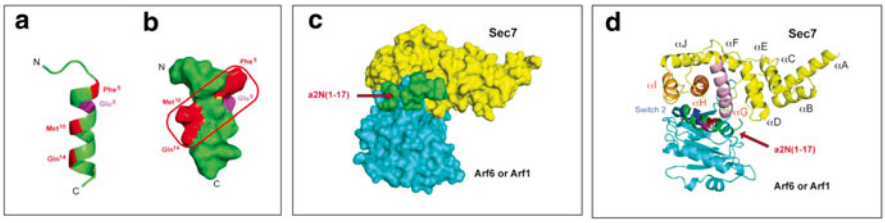

Fig. 16.4 The molecular features of the protein–protein interaction interface and signaling between V-ATPase and cytohesin-2/Arf1,6 small GTPases. (**a**) NMR structure *a*2N(1–17) peptide derived from V-ATPase and mapping of its interaction protein–protein binding interface (formed by amino acids F5, M10, Q14, shown in *red square*) involved in binding with catalytic Sec7 domain of cytohesin-2. (**b**) In silico docking experiments of the a2N(1–17) peptide at the interface between catalytic site of the Sec7-domain of cytohesin-2 and Arf1,6 small GTPases. (**c**) The binding of the *a*2N(1–17) peptide involves the αG, αH, and αI helixes of Sec7 and switch 2 of the Arf1,6 small GTPases

The super-complex coordinates endocytic vesicle trafficking and downstream signaling of receptors (Fig. 16.3). The direct interaction of aldolase with cytohesin-2 through its PH-domain was shown by the pull-down and SPR experiments (Fig. 16.2). This approach revealed a two-step interaction between these two proteins with $K_{D1} = 1.1 \times 10^{-4}$ M and $K_{D2} = 2.7 \times 10^{-6}$ M, clearly indicating a potential regulatory mechanism of this interaction (Fig. 16.2, interfaces III and IV). Moreover, using a cell fractionation approach, we demonstrated the association of aldolase with early endosomes and formation of V-ATPase/cytohesin-2/Arf1,6/aldolase super-complex (Figs. 16.2 and 16.3). The aldolase knockdown experiments further uncovered the functional significance of interactions within V-ATPase/cytohesin-2/Arf1,6/aldolase super-complex. It was shown that the direct interaction between aldolase and cytohesin-2 are important in: (1) gelsolin gene expression, (2) actin cytoskeletal rearrangement, and (3) redistribution of endosomal vesicles within endocytic protein-degradation pathway [167].

In summary, a novel V-ATPase/cytohesin-2/Arf1,6/aldolase super-complex identified on early endosomes may be involved in regulation of the signaling receptors and function of the protein degradation pathway (Figs. 16.2 and 16.3). Moreover, these data indicate that pH-dependent binding and signaling between V-ATPase and cytohesin-2 may modulate the interaction of the a-subunit isoforms with aldolase and/or the GE-heterodimer forming peripheral stalks and consequently modulate the reversible association/dissociation of the V_1 and V_O of V-ATPase (Fig. 16.2) [1, 2]. Thus, evolutionarily acquired pH-sensing and cytohesin-2/Arf1,6-signaling function of V-ATPase, and its interaction with aldolase, may be an integral part of the self-regulatory mechanism of the enzyme as a proton-pumping rotary nano-motor.

On the other hand, downstream effectors of V-ATPase/cytohesin-2/Arf1,6/aldolase super-complex have also recently emerged. Cytohesin-1/2 family Arf-GEFs are shown to play role in regulation of signaling and trafficking of EGFR/ErbB and IR/IGF-1R receptors [128, 129, 154, 156, 157]. In particular, these studies demonstrated

the direct interaction of cytohesin-2 with insulin receptor and regulation of the PI3K signaling pathway. Thus, both in mice and fly cytohesin-2 is essential for signaling of IR/IGF-1R, cell growth, regulation of metabolism, and function of calorie restriction pathway (CRP) during aging process [154, 156, 157, 162, 164, 202]. In cancer cells, cytohesin-2 serves as a cytoplasmic activator of EGFR/ErbB, that modulates phosphorylation-dependent dimerization, oncogenic signaling of these receptors, and development of cancer (Fig. 16.3) [128, 129]. In conclusion, cell biological insights of V-ATPase/cytohesin-2/Arf1,6/aldolase super-complex (Figs. 16.2 and 16.3) shed light on the regulation of endocytic protein degradation pathway, trafficking and signaling EGFR/ErbB and IR/EGF-1R receptors under both physiological (longevity and aging process) and pathological (cancer and diabetes) conditions.

5 Conclusions

5.1 Drug Design and Targeting to Diverse V-ATPases and Their Super-complexes

As discussed above, extensive research in the last few years made an astounding breakthrough in understanding the structure and function of V-ATPase [1–5, 7, 9–12]. The advances include following discoveries: (1) low resolution structure of V-ATPase using cryo-EM; (2) the crystal-structure of individual subunits and their protein–protein interfaces; (3) endosomal V-ATPase/cytohesin-2/Arf1,6/aldolase super-complex; (4) lysosomal V-ATPase/Ragulator/Rag/mTORC1/Rheb super-complex, (5) novel roles of V-ATPase in trafficking and signaling of receptors, and (6) critical role of V-ATPases in the development and pathogenesis of human diseases. Thus, V-ATPase could be considered as a potential target providing powerful approaches for the development of therapeutic agents. The seven different approaches could be considered as discussed below.

First, targeting to V-ATPases in diverse compartments with a large spectrum of subunit isoforms could be productive for pharmaceutical research. The expressions of these isoforms are specific for tissues, cells, and compartments. Recent experiments demonstrated that V-ATPases with unique combinations of subunit isoforms are localized in specific cell membranes which could dictate their functions [1–5, 8]. Thus, isoform-specific subunits of V-ATPase have been suggested as attractive targets for the treatment of human diseases. Targeting a-subunit and other isoforms by small molecule inhibitors is proposed in treating lytic bone disorders [210–212]. V-ATPase a-subunit isoforms are also potential targets for the treatment of metastatic cancers. Thus, the small molecule V-ATPase inhibitors and siRNA have been studied extensively with their potential application in cancer treatment and prevention of metastasis [213–217].

Secondly, targeting the extracellular domains of a- and c-subunits with specific antibodies has been recently successfully applied for selective inhibition of plasma

membrane V-ATPase and reduction of metastatic phenotype of the cancer cells [53, 178]. In addition, the first V-ATPase inhibitory peptide was also identified and its selectivity was demonstrated [82]. Thus, this approach should be considered for developing of novel anticancer pharmaceuticals including antibodies and peptides which have high specificity and low toxicity.

Third, unique mechanism of regulating V-ATPase is reversible assembly/disassembly, which could be a promising target in drug design. This approach would be even more fruitful if combined with targeting cell or tissue specific V-ATPase isoforms [13–15, 19].

Forth, V-ATPases in regulation of signaling, trafficking, and degradation of cellular receptors could be a potential target. As discussed above, endocytosis, signaling, and degradation of Fz/LRP6, PRR, and Notch receptors are regulated by the direct interaction with V-ATPase [1, 122]. Therefore, targeting to the interactions between V-ATPase and these receptors could provide a promising approach in treatment of diseases related to cellular trafficking such as cancer, diabetes, and neurodegenerative diseases.

Fifth, regulatory proteins interacting with V-ATPase could be a potential target. The V-ATPase dependent super-complexes in early endosomes (V-ATPase/cytohesin-2/Arf1,6/aldolase) and late endosomes/lysosomes (V-ATPase/Ragulator/Rag/mTORC1/Rheb) pathway have been discovered recently in our [1, 2, 25, 26, 28, 30, 31, 109, 167] and Sabatini [32–34, 208] laboratories, respectively. The specific cascade of different protein–protein interactions within these complexes could modulate pH and amino-acids sensing, targeting, assembly, and activity of V-ATPase, linked to the regulation of intravesicular acidification and trafficking. For example, mTOR-signaling pathway is critical for the pathogenesis of the cancer and age-related diseases [34, 35, 163, 200–204]. It is noteworthy that extensive studies in animal models and clinical trials have uncovered the beneficial action of *rapamycin*, a potent mTOR inhibitor approved by FDA for treatment of variety age-associated diseases including cancers, neurodegenerative disorders, aging, and longevity. However, due to its side effects caused by the action of *rapamycin* on both mTORC1 and mTORC2, there is growing necessity for pharmacological research producing more specific and efficient drugs targeting of these pathways. Therefore, small molecules specifically targeting of protein–protein interactions in V-ATPase/Ragulator/Rag/mTORC1/Rheb super-complex will provide an attractive therapeutic agents to control aberrant signaling of mTORC1 and mTORC2 complexes in cancer, diabetes, age-related diseases, aging, and longevity [34, 35, 163, 200–204].

Sixth, novel endosomal V-ATPase/cytohesin-2/Arf1,6/aldolase super-complex and especially its protein–protein interaction interfaces could be a potential therapeutic targets (Figs. 16.2, 16.3, and 16.4) [1, 2, 25, 26, 28, 31, 167]. We propose that this approach will develop novel protein–protein interaction (PPI) inhibitors including therapeutic peptides or small molecule drugs [218–220]. These compounds may be also used to regulate assembly/disassembly of V-ATPase and signaling of cytohesin-2/Arf1,6 small GTPases. Modulation of the function of EGFR/ErbB or IR/IGF-1R receptors by the similar approach may be useful for treating variety of cancers, age-related diseases, slowing aging process and extending human longevity [154–158, 162–164].

Seventh, in our recent study the V-ATPase interactome was mapped for the first time. This systematic approach, has revealed a novel interacting proteins involved in trafficking, folding, assembly, and phosphorylation of V-ATPase [221]. These cell biological processes regulate V-ATPase-dependent acidification, and thus, these pathways and proteins could serve as potential drug targets for the therapeutic regulation V-ATPase function in health and disease states.

Acknowledgements Original work in the authors' laboratories is supported by *NIH DK038452*, *BADERC DK057521-08* (Marshansky), Ministry of Education Tier 2 (MOE2011-T2-2-156; ARC 18/12), Singapore (Grüber), and Japan Science and Technology Agency (Futai).

References

1. Marshansky V, Rubinstein JL, Grüber G (2014) Eukaryotic V-ATPase: novel structural findings and functional insights. Biochim Biophys Acta 1837:857–879
2. Marshansky V, Futai M (2008) The V-type H^+-ATPase in vesicular trafficking: targeting, regulation and function. Curr Opin Cell Biol 20:415–426
3. Grüber G, Marshansky V (2008) New insights into structure-function relationships between archeal ATP synthase A1Ao and vacuolar type ATPase V1Vo. BioEssays 30:1–14
4. Nishi T, Forgac M (2002) The vacuolar H^+-ATPases—nature's most versatile proton pumps. Nat Rev Mol Cell Biol 3:94–103
5. Forgac M (2007) Vacuolar ATPases: rotary proton pumps in physiology and pathophysiology. Nat Rev Mol Cell Biol 8:917–929
6. Hinton A, Bond S, Forgac M (2009) V-ATPase functions in normal and disease processes. Pflugers Arch 457:589–598
7. Zhang Z, Zheng Y, Mazon H et al (2008) Structure of the yeast vacuolar ATPase. J Biol Chem 283:35983–35995
8. Sun-Wada GH, Tabata H, Kawamura N et al (2007) Differential expression of a subunit isoforms of the vacuolar-type proton pump ATPase in mouse endocrine tissues. Cell Tissue Res 329:239–248
9. Saroussi S, Nelson N (2009) Vacuolar H^+-ATPase-an enzyme for all seasons. Pflugers Arch 457:581–587
10. Muench SP, Huss M, Song CF et al (2009) Cryo-electron microscopy of the vacuolar ATPase motor reveals its mechanical and regulatory complexity. J Mol Biol 386:989–999
11. Maxson ME, Grinstein S (2014) The vacuolar-type H^+-ATPase at a glance – more than a proton pump. J Cell Sci 127:4987–4993
12. Rawson S, Phillips C, Huss M et al (2015) Structure of the vacuolar H^+-ATPase rotary motor reveals new mechanistic insights. Structure 23:461–471
13. Kane PM (2000) Regulation of V-ATPases by reversible disassembly. FEBS Lett 469:137–141
14. Kane PM (2006) The where, when, and how of organelle acidification by the yeast vacuolar H^+-ATPase. Microbiol Mol Biol Rev 70:177–191
15. Kane PM (2012) Targeting reversible disassembly as a mechanism of controlling V-ATPase activity. Curr Protein Pept Sci 13:117–123
16. Parra KJ, Chan CY, Chen J (2014) Saccharomyces cerevisiae vacuolar H^+-ATPase regulation by disassembly and reassembly: one structure and multiple signals. Eukaryot Cell 13:706–714
17. Sumner JP, Dow JA, Earley FG et al (1995) Regulation of plasma membrane V-ATPase activity by dissociation of peripheral subunits. J Biol Chem 270:5649–5653

18. Beyenbach KW, Wieczorek H (2006) The V-type H^+ ATPase: molecular structure and function, physiological roles and regulation. J Exp Biol 209:577–589
19. Kane PM (1995) Disassembly and reassembly of the yeast vacuolar H^+-ATPase in vivo. J Biol Chem 270:17025–17032
20. Trombetta ES, Ebersold M, Garrett W et al (2003) Activation of lysosomal function during dendritic cell maturation. Science 299:1400–1403
21. Sautin YY, Lu M, Gaugler A et al (2005) Phosphatidylinositol 3-kinase-mediated effects of glucose on vacuolar H^+-ATPase assembly, translocation, and acidification of intracellular compartments in renal epithelial cells. Mol Cell Biol 25:575–589
22. Lafourcade C, Sobo K, Kieffer-Jaquinod S et al (2008) Regulation of the V-ATPase along the endocytic pathway occurs through reversible subunit association and membrane localization. PLoS One 3, e2758
23. Xu Y, Parmar A, Roux E et al (2012) Epidermal growth factor-induced vacuolar H^+-ATPase assembly: a role in signaling via mTORC1 activation. J Biol Chem 287:26409–26422
24. Liberman R, Bond S, Shainheit MG et al (2014) Regulated assembly of the V-ATPase is increased during cluster disruption-induced maturation of dendritic cells through a phosphatidylinositol 3-kinase/mTOR-dependent pathway. J Biol Chem 289:1355–1363
25. Hurtado-Lorenzo A, Skinner M, El Annan J et al (2006) V-ATPase interacts with ARNO and Arf6 in early endosomes and regulates the protein degradative pathway. Nat Cell Biol 8:124–136
26. Marshansky V (2007) The V-ATPase a2-subunit as a putative endosomal pH-sensor. Biochem Soc Trans 35:1092–1099
27. Recchi C, Chavrier P (2006) V-ATPase: a potential pH sensor. Nat Cell Biol 8:107–109
28. Merkulova M, Bakulina A, Thaker YR et al (2010) Specific motifs of the V-ATPase a2-subunit isoform interact with catalytic and regulatory domains of ARNO. Biochim Biophys Acta 1797:1398–1409
29. Merkulova M, McKee M, Dip PV et al (2010) N-terminal domain of the V-ATPase a2-subunit displays integral membrane protein properties. Protein Sci 19:1850–1862
30. El-Annan J, Brown D, Breton S et al (2004) Differential expression and targeting of endogenous Arf1 and Arf6 small GTPases in kidney epithelial cells in situ. Am J Physiol Cell Physiol 286:C768–C778
31. Hosokawa H, Dip PV, Merkulova M et al (2013) The N termini of a-subunit isoforms are involved in signaling between vacuolar H^+-ATPase (V-ATPase) and cytohesin-2. J Biol Chem 288:5896–5913
32. Zoncu R, Bar-Peled L, Efeyan A et al (2011) mTORC1 senses lysosomal amino acids through an inside-out mechanism that requires the vacuolar H^+-ATPase. Science 334:678–683
33. Bar-Peled L, Sabatini DM (2012) SnapShot: mTORC1 signaling at the lysosomal surface. Cell 151:1390
34. Efeyan A, Zoncu R, Sabatini DM (2012) Amino acids and mTORC1: from lysosomes to disease. Trends Mol Med 18:524–533
35. Laplante M, Sabatini DM (2012) mTOR signaling in growth control and disease. Cell 149:274–293
36. Peters C, Bayer MJ, Buhler S, Andersen JS, Mann M, Mayer A (2001) Trans-complex formation by proteolipid channels in the terminal phase of membrane fusion. Nature 409:581–588
37. Bayer MJ, Reese C, Buhler S et al (2003) Vacuole membrane fusion: Vo functions after trans-SNARE pairing and is coupled to the $Ca2^+$-releasing channel. J Cell Biol 162:211–222
38. Baars TL, Petri S, Peters C, Mayer A (2007) Role of the V-ATPase in regulation of the vacuolar fission-fusion equilibrium. Mol Biol Cell 18:3873–3882
39. Strasser B, Iwaszkiewicz J, Michielin O, Mayer A (2011) The V-ATPase proteolipid cylinder promotes the lipid-mixing stage of SNARE-dependent fusion of yeast vacuoles. EMBO J 30:4126–4141
40. Matsumoto N, Daido S, Sun-Wada GH et al (2014) Diversity of proton pumps in osteoclasts: V-ATPase with a3 and d2 isoforms is a major form in osteoclasts. Biochim Biophys Acta 1837:744–749

41. Kornak U, Schulz A, Friedrich W et al (2000) Mutations in the a3 subunit of the vacuolar H(+)-ATPase cause infantile malignant osteopetrosis. Hum Mol Genet 9:2059–2063
42. Smith AN, Jouret F, Bord S et al (2005) Vacuolar H^+-ATPase d2 subunit: molecular characterization, developmental regulation, and localization to specialized proton pumps in kidney and bone. J Am Soc Nephrol 16:245–1256
43. Lee SH, Rho J, Jeong D et al (2006) V-ATPase Vo subunit d2-deficient mice exhibit impaired osteoclast fusion and increased bone formation. Nat Med 12:1403–1409
44. Balakrishna AM, Basak S, Manimekalai MS, Grüber G (2015) Crystal structure of subunits D and F in complex gives insight into energy transmission of the eukaryotic V-ATPase from Saccharomyces cerevisiae. J Biol Chem 290:3183–3196
45. Smith AN, Skaug J, Choate KA et al (2000) Mutations in ATP6N1B, encoding a new kidney vacuolar proton pump 116-kD subunit, cause recessive distal renal tubular acidosis with preserved hearing. Nat Genet 26:71–75
46. Frattini A, Orchard PJ, Sobacchi C et al (2000) Defects in TCIRG1 subunit of the vacuolar proton pump are responsible for a subset of human autosomal recessive osteopetrosis. Nat Genet 25:343–346
47. Kornak U, Reynders E, Dimopoulou A et al (2008) Impaired glycosylation and cutis laxa caused by mutations in the vesicular H^+-ATPase subunit ATP6V0A2. Nat Genet 40:32–34
48. Hucthagowder V, Morava E, Kornak U et al (2009) Loss-of-function mutations in ATP6V0A2 impair vesicular trafficking, tropoelastin secretion and cell survival. Hum Mol Genet 18:2149–2165
49. Morava E, Guillard M, Lefeber DJ, Wevers RA (2009) Autosomal recessive cutis laxa syndrome revisited. Eur J Hum Genet 17:1099–1110
50. Sennoune SR, Bakunts K, Martinez GM et al (2004) Vacuolar H^+-ATPase in human breast cancer cells with distinct metastatic potential: distribution and functional activity. Am J Physiol Cell Physiol 286:C1443–C1452
51. Hinton A, Sennoune SR, Bond S et al (2009) Function of a subunit isoforms of the V-ATPase in pH homeostasis and in vitro invasion of MDA-MB231 human breast cancer cells. J Biol Chem 284:16400–16408
52. Capecci J, Forgac M (2013) The function of vacuolar ATPase (V-ATPase) a subunit isoforms in invasiveness of MCF10a and MCF10CA1a human breast cancer cells. J Biol Chem 288:32731–32741
53. Cotter K, Capecci J, Sennoune S et al (2015) Activity of plasma membrane V-ATPases is critical for the invasion of MDA-MB231 breast cancer cells. J Biol Chem 290:3680–3692
54. Qi J, Forgac M (2007) Cellular environment is important in controlling V-ATPase dissociation and its dependence on activity. J Biol Chem 282:24743–24751
55. Benlekbir S, Bueler SA, Rubinstein JL (2012) Structure of the vacuolar-type ATPase from Saccharomyces cerevisiae at 11Å resolution. Nat Struct Mol Biol 19:1356–1362
56. Zhao J, Benlekbir S, Rubinstein JL (2015) Electron cryomicroscopy observation of rotational states in a eukaryotic V-ATPase. Nature 521:241–245
57. Muench SP, Scheres SH, Huss M et al (2014) Subunit positioning and stator filament stiffness in regulation and power transmission in the V1 motor of the Manduca sexta V-ATPase. J Mol Biol 426:286–300
58. Radermacher M, Ruiz T, Wieczorek H, Grüber G (2001) The structure of the V1-ATPase determined by three-dimensional electron microscopy of single particles. J Struct Biol 135:26–37
59. Hilario E, Gogarten JP (1998) The prokaryote-to-eukaryote transition reflected in the evolution of the V/F/A-ATPase catalytic and proteolipid subunits. J Mol Evol 46:703–715
60. Basak S, Lim J, Manimekalai MS, Balakrishna AM, Grüber G (2013) Crystal and NMR structures give insights into the role and dynamics of subunit F of the eukaryotic V-ATPase from Saccharomyces cerevisiae. J Biol Chem 288:11930–11939
61. Jefferies KC, Forgac M (2008) Subunit H of the vacuolar H^+-ATPase inhibits ATP hydrolysis by the free V1 domain by interaction with the rotary subunit F. J Biol Chem 283:4512–4519

62. Sagermann M, Stevens TM, Matthews BW (2001) Crystal structure of the regulatory subunit H of the V-type ATPase of Saccharomyces cerevisiae. Proc Natl Acad Sci U S A 98:7134–7139
63. Oot RA, Huang LS, Berry EA, Wilkens S (2012) Crystal structure of the yeast vacuolar ATPase heterotrimeric EGC(head) peripheral stalk complex. Structure 20:1881–1892
64. Rishikesan S, Grüber G (2011) Structural elements of the C-terminal domain of subunit E (E133-222) from the Saccharomyces cerevisiae V1Vo ATPase determined by solution NMR spectroscopy. J Bioenerg Biomembr 43:447–455
65. Vitavska O, Merzendorfer H, Wieczorek H (2005) The V-ATPase subunit C binds to polymeric F-actin as well as to monomeric G-actin and induces cross-linking of actin filaments. J Biol Chem 280:1070–1076
66. Armbrüster A, Svergun DI, Coskun U et al (2004) Structural analysis of the stalk subunit Vma5p of the yeast V-ATPase in solution. FEBS Lett 570:119–125
67. Drory O, Frolow F, Nelson N (2004) Crystal structure of yeast V-ATPase subunit C reveals its stator function. EMBO Rep 5:1148–1152
68. Ambrüster A, Hohn C, Hermesdorf A et al (2005) Evidence for major structural changes in subunit C of the vacuolar ATPase due to nucleotide binding. FEBS Lett 579:1961–1967
69. Hong-Hermesdorf A, Brux A, Grüber A, Grüber G, Schumacher K (2006) A WNK kinase binds and phosphorylates V-ATPase subunit C. FEBS Lett 580:932–939
70. Graham LA, Flannery AR, Stevens TH (2003) Structure and assembly of the yeast V-ATPase. J Bioenerg Biomembr 35:301–312
71. Wilkens S, Inoue T, Forgac M (2004) Three-dimensional structure of the vacuolar ATPase. Localization of subunit H by difference imaging and chemical cross-linking. J Biol Chem 279:41942–41949
72. Dip PV, Saw WG, Roessle M, Marshansky V, Grüber G (2012) Solution structure of subunit a, a104-363, of the Saccharomyces cerevisiae V-ATPase and the importance of its C-terminus in structure formation. J Bioenerg Biomembr 44:341–350
73. Smith AN, Finberg KE, Wagner CA et al (2001) Molecular cloning and characterization of Atp6n1b: a novel fourth murine vacuolar H^+-ATPase a-subunit gene. J Biol Chem 276:42382–42388
74. Ochotny N, van Vliet A, Chan N et al (2006) Effects of human a3 and a4 mutations that result in osteopetrosis and distal renal tubular acidosis on yeast V-ATPase expression and activity. J Biol Chem 281:26102–26111
75. Toyomura T, Oka T, Yamaguchi C et al (2000) Three subunit a isoforms of mouse vacuolar H^+-ATPase. Preferential expression of the a3 isoform during osteoclast differentiation. J Biol Chem 275:8760–8765
76. Toei M, Toei S, Forgac M (2011) Definition of membrane topology and identification of residues important for transport in subunit a of the vacuolar ATPase. J Biol Chem 286:35176–35186
77. Nishi T, Forgac M (2000) Molecular cloning and expression of three isoforms of the 100-kDa a subunit of the mouse vacuolar proton-translocating ATPase. J Biol Chem 275:6824–6830
78. Duarte AM, de Jong ER, Wechselberger R et al (2007) Segment TM7 from the cytoplasmic hemi-channel from V_O-H^+-V-ATPase includes a flexible region that has a potential role in proton translocation. Biochim Biophys Acta 1768:2263–2270
79. Su Y, Zhou A, Al-Lamki RS, Karet FE (2003) The a-subunit of the V-type H^+-ATPase interacts with phosphofructokinase-1 in humans. J Biol Chem 278:20013–20018
80. Flannery AR, Graham LA, Stevens TH (2004) Topological characterization of the c, c′, and c″ subunits of the vacuolar ATPase from the yeast Saccharomyces cerevisiae. J Biol Chem 279:39856–39862
81. Wang Y, Cipriano DJ, Forgac M (2007) Arrangement of subunits in the proteolipid ring of the V-ATPase. J Biol Chem 282:34058–34065
82. Muench SP, Rawson S, Eyraud V et al (2014) PA1b inhibitor binding to subunits c and e of the vacuolar ATPase reveals its insecticidal mechanism. J Biol Chem 289:16399–16408

83. Junge W, Nelson N (2005) Structural biology. Nature's rotary electromotors. Science 308:642–644
84. Wang Y, Inoue T, Forgac M (2005) Subunit a of the yeast V-ATPase participates in binding of bafilomycin. J Biol Chem 280:40481–40488
85. Bowman BJ, Bowman EJ (2002) Mutations in subunit C of the vacuolar ATPase confer resistance to bafilomycin and identify a conserved antibiotic binding site. J Biol Chem 277:3965–3972
86. Bowman EJ, Bowman BJ (2005) V-ATPases as drug targets. J Bioenerg Biomembr 37:431–435
87. Umata T, Moriyama Y, Futai M, Mekada E (1990) The cytotoxic action of diphtheria toxin and its degradation in intact Vero cells are inhibited by bafilomycin A1, a specific inhibitor of vacuolar-type H^+-ATPase. J Biol Chem 265:21940–21945
88. Yoshimori T, Yamamoto A, Moriyama Y et al (1991) Bafilomycin A1, a specific inhibitor of vacuolar-type H^+-ATPase, inhibits acidification and protein degradation in lysosomes of cultured cells. J Biol Chem 266:17707–17712
89. Brown D, Marshansky V (2004) Renal V-ATPase: physiology and pathophysiology. In: Futai M, Wada Y, Kaplan JH (eds) Handbook of ATPases. Wiley-VCH Verlag GmbH & Co. KGaA, Weinheim, pp 413–442
90. Brown D, Breton S, Ausiello DA, Marshansky V (2009) Sensing, signaling and sorting events in kidney epithelial cell physiology. Traffic 10:275–284
91. Brown D, Paunescu TG, Breton S, Marshansky V (2009) Regulation of the V-ATPase in kidney epithelial cells: dual role in acid–base homeostasis and vesicle trafficking. J Exp Biol 212:1762–1772
92. Shum WW, Da Silva N, Brown D, Breton S (2009) Regulation of luminal acidification in the male reproductive tract via cell-cell crosstalk. J Exp Biol 21:1753–1761
93. Breton S, Brown D (2013) Regulation of luminal acidification by the V-ATPase. Physiology (Bethesda) 28:318–329
94. Sun-Wada GH, Wada Y (2013) Vacuolar-type proton pump ATPases: acidification and pathological relationships. Histol Histopathol 28:208–215
95. Bhargava A, Voronov I, Wang Y, Glogauer M, Kartner N, Manolson MF (2012) Osteopetrosis mutation R444L causes endoplasmic reticulum retention and misprocessing of vacuolar H^+-ATPase a3 subunit. J Biol Chem 287:26829–26839
96. Kartner N, Manolson MF (2012) V-ATPase subunit interactions: the long road to therapeutic targeting. Curr Protein Pept Sci 13:164–179
97. Toro EJ, Ostrov DA, Wronski TJ, Holliday LS (2012) Rational identification of enoxacin as a novel V-ATPase-directed osteoclast inhibitor. Curr Protein Pept Sci 13:80–191
98. Steinberg BE, Touret N, Vargas-Caballero M, Grinstein S (2007) In situ measurement of the electrical potential across the phagosomal membrane using FRET and its contribution to the proton-motive force. Proc Natl Acad Sci U S A 104:9523–9528
99. Scheel O, Zdebik AA, Lourdel S, Jentsch TJ (2005) Voltage-dependent electrogenic chloride/proton exchange by endosomal CLC proteins. Nature 436:424–427
100. Jentsch TJ (2007) Chloride and the endosomal-lysosomal pathway: emerging roles of CLC chloride transporters. J Physiol 578:633–640
101. Stauber T, Weinert S, Jentsch TJ (2012) Cell biology and physiology of CLC chloride channels and transporters. Compr Physiol 2:1701–1744
102. Orlowski J, Grinstein S (2007) Emerging roles of alkali cation/proton exchangers in organellar homeostasis. Curr Opin Cell Biol 19:483–492
103. Manolson MF, Wu B, Proteau D et al (1994) STV1 gene encodes functional homologue of 95-kDa yeast vacuolar H^+-ATPase subunit Vph1p. J Biol Chem 269:14064–14074
104. Kawasaki-Nishi S, Bowers K, Nishi T et al (2001) The amino-terminal domain of the vacuolar proton-translocating ATPase a subunit controls targeting and in vivo dissociation, and the carboxyl-terminal domain affects coupling of proton transport and ATP hydrolysis. J Biol Chem 276:47411–47420

105. Morel N, Dedieu JC, Philippe JM (2003) Specific sorting of the a1 isoform of the V-H$^+$ATPase a subunit to nerve terminals where it associates with both synaptic vesicles and the presynaptic plasma membrane. J Cell Sci 116:4751–4762
106. Hiesinger PR, Fayyazuddin A, Mehta SQ et al (2005) The v-ATPase V_O subunit a1 is required for a late step in synaptic vesicle exocytosis in Drosophila. Cell 121:607–620
107. Saw NM, Kang SY, Parsaud L et al (2011) Vacuolar H$^+$-ATPase subunits Voa1 and Voa2 cooperatively regulate secretory vesicle acidification, transmitter uptake, and storage. Mol Biol Cell 22:3394–3409
108. Peri F, Nusslein-Volhard C (2008) Live imaging of neuronal degradation by microglia reveals a role for V_O-ATPase a1 in phagosomal fusion in vivo. Cell 133:916–927
109. Maranda B, Brown D, Bourgoin S et al (2001) Intra-endosomal pH-sensitive recruitment of the Arf-nucleotide exchange factor ARNO and Arf6 from cytoplasm to proximal tubule endosomes. J Biol Chem 276:18540–18550
110. Marshansky V, Ausiello DA, Brown D (2002) Physiological importance of endosomal acidification: potential role in proximal tubulopathies. Curr Opin Nephrol Hypertens 11:527–537
111. Sun-Wada GH, Tabata H, Kawamura K et al (2009) Direct recruitment of H$^+$-ATPase from lysosomes for phagosomal acidification. J Cell Sci 122:2504–2513
112. Toei M, Saum R, Forgac M (2010) Regulation and isoform function of the V-ATPases. Biochemistry 49:4715–4723
113. Sun-Wada GH, Imai-Senga Y, Yamamoto A, Murata Y, Hirata T, Wada Y, Futai M (2002) A proton pump ATPase with testis-specific E1-subunit isoform required for acrosome acidification. J Biol Chem 279:18098–18105
114. Hayashi K, Sun-Wada GH, Wada Y et al (2008) Defective assembly of a hybrid vacuolar H$^+$-ATPase containing the mouse testis-specific E1 isoform and yeast subunits. Biochim Biophys Acta 1777:1370–1377
115. Okamoto-Terry H, Umeki K, Nakanishi-Matsui M, Futai M (2013) Glu-44 in the amino-terminal alpha-helix of yeast vacuolar ATPase E subunit (Vma4p) has a role for VoV1 assembly. J Biol Chem 288:36236–36243
116. Smardon AM, Tarsio M, Kane PM (2002) The RAVE complex is essential for stable assembly of the yeast V-ATPase. J Biol Chem 277:13831–13839
117. Smardon AM, Diab HI, Tarsio M et al (2014) The RAVE complex is an isoform-specific V-ATPase assembly factor in yeast. Mol Biol Cell 25:356–367
118. Bond S, Forgac M (2008) The Ras/cAMP/protein kinase A pathway regulates glucose-dependent assembly of the vacuolar H+-ATPase in yeast. J Biol Chem 283:36513–36521
119. Lu M, Holliday LS, Zhang L et al (2001) Interaction between aldolase and vacuolar H$^+$-ATPase: evidence for direct coupling of glycolysis to the ATP-hydrolyzing proton pump. J Biol Chem 276:30407–30413
120. Lu M, Sautin YY, Holliday LS, Gluck SL (2004) The glycolytic enzyme aldolase mediates assembly, expression, and activity of vacuolar H$^+$-ATPase. J Biol Chem 279:8732–8739
121. Lu M, Ammar D, Ives H et al (2007) Physical interaction between aldolase and vacuolar H$^+$-ATPase is essential for the assembly and activity of the proton pump. J Biol Chem 282:24495–24503
122. Marshansky V (2014) Role of V-ATPase, cytohesin-2/Arf6 and aldolase in regulation of endocytosis: Implication for diabetic nephropathy. In: Nakamura S (ed) Handbook of H$^+$-ATPases. Pan Stanford Publishing Pte. Ltd, Singapore, pp 169–199
123. Cohen S (1962) Isolation of a mouse submaxillary gland protein accelerating incisor eruption and eyelid opening in the new-born animal. J Biol Chem 237:1555–1562
124. Cohen S, Carpenter G, King L (1980) Epidermal growth factor-receptor-protein kinase interactions: Co-purification of receptor and epidermal growth factor-enhanced phosphorylation activity. J Biol Chem 255:4834–4842
125. Normanno N, De Luca A, Bianco C, Strizzi L, Mancino M, Maiello MR, Carotenuto A, De Feo G, Caponigro F, Salomon DS (2006) Epidermal growth factor receptor (EGFR) signaling in cancer. Gene 366:2–16

126. Tomas A, Futter CE, Eden ER (2014) EGF receptor trafficking: consequences for signaling and cancer. Trends Cell Biol 24:26–34
127. Hanahan D, Weinberg RA (2011) Hallmarks of cancer: the next generation. Cell 144:646–674
128. Bill A, Schmitz A, Albertoni B et al (2010) Cytohesins are cytoplasmic ErbB receptor activators. Cell 143:201–211
129. Bill A, Schmitz A, Konig K et al (2013) Anti-proliferative effect of cytohesin inhibition in gefitinib-resistant lung cancer cells. PLoS One 7, e41179
130. Junnila RK, List EO, Berryman DE et al (2013) The GH/IGF-1 axis in ageing and longevity. Nat Rev Endocrinol 9:366–376
131. Berryman DE, Glad CA, List EO, Johannsson G (2013) The GH/IGF-1 axis in obesity: pathophysiology and therapeutic considerations. Nat Rev Endocrinol 9:346–356
132. Song YH, Song JL, Delafontaine P, Godard MP (2013) The therapeutic potential of IGF-I in skeletal muscle repair. Trends Endocrinol Metab 24:310–319
133. O'Callaghan KM, Ayllon V, O'Keeffe J et al (2010) Heme-binding protein HRG-1 is induced by insulin-like growth factor I and associates with the vacuolar H^+-ATPase to control endosomal pH and receptor trafficking. J Biol Chem 285:381–391
134. Fogarty FM, O'Keeffe J, Zhadanov A, Papkovsky D, Ayllon V, O'Connor R (2014) HRG-1 enhances cancer cell invasive potential and couples glucose metabolism to cytosolic/extracellular pH gradient regulation by the vacuolar-H^+-ATPase. Oncogene 33:4653–4663
135. Niehrs C (2012) The complex world of WNT receptor signaling. Nat Rev Mol Cell Biol 13:767–779
136. Niehrs C, Acebron SP (2012) Mitotic and mitogenic Wnt signaling. EMBO J 31:2705–2713
137. Cruciat CM, Ohkawara B, Acebron SP et al (2010) Requirement of prorenin receptor and vacuolar H+-ATPase-mediated acidification for Wnt signaling. Science 327:459–463
138. Niehrs C, Boutros M (2010) Trafficking, acidification, and growth factor signaling. Sci Signal 3:26
139. Nguyen G, Delarue F, Burckle C et al (2002) Pivotal role of the renin/prorenin receptor in angiotensin II production and cellular responses to renin. J Clin Invest 109:1417–1427
140. Danser AN (2009) (Pro)renin receptor and vacuolar H^+-ATPase. Hypertension 54:219–221
141. Ichihara A, Kinouchi K (2011) Current knowledge of (pro)renin receptor as an accessory protein of vacuolar H+-ATPase. J Renin Angiotensin Aldosterone Syst 12:638–640
142. Kinouchi K, Ichihara A, Sano M et al (2010) The (pro)renin receptor/ATP6AP2 is essential for vacuolar H+-ATPase assembly in murine cardiomyocytes. Circ Res 107:30–34
143. Danser AH, Deinum J (2005) Renin, prorenin and the putative (pro)renin receptor. Hypertension 46:1069–1076
144. Kopan R, Ilagan MX (2009) The canonical Notch signaling pathway: unfolding the activation mechanism. Cell 137:216–233
145. Wang Z, Li Y, Sarkar FH (2010) Notch signaling proteins: legitimate targets for cancer therapy. Curr Protein Pept Sci 11:398–408
146. Vaccari T, Duchi S, Cortese K et al (2010) The vacuolar ATPase is required for physiological as well as pathological activation of the Notch receptor. Development 137:1825–1832
147. Yan Y, Denef N, Schupbach T (2009) The vacuolar proton pump, V-ATPase, is required for notch signaling and endosomal trafficking in Drosophila. Dev Cell 17:387–402
148. Sethi N, Yan Y, Quek D, Schupbach T, Kang Y (2010) Rabconnectin-3 is a functional regulator of mammalian Notch signaling. J Biol Chem 285:34757–34764
149. Seol JH, Shevchenko A, Deshaies RJ (2001) Skp1 forms multiple protein complexes, including RAVE, a regulator of V-ATPase assembly. Nat Cell Biol 3:384–391
150. Bourne HR, Sanders DA, McCormick F (1990) The GTPase superfamily: a conserved switch for diverse cell functions. Nature 348:125–132
151. Donaldson JG, Jackson CL (2000) Regulators and effectors of the ARF GTPases. Curr Opin Cell Biol 12:475–482
152. Casanova JE (2007) Regulation of Arf activation: the Sec7 family of guanine nucleotide exchange factors. Traffic 8:1476–1485

153. D'Souza-Schorey C, Chavrier P (2006) ARF proteins: roles in membrane traffic and beyond. Nat Rev Mol Cell Biol 7:347–358
154. Hafner M, Schmitz A, Grune I et al (2006) Inhibition of cytohesins by SecinH3 leads to hepatic insulin resistance. Nature 444:941–944
155. Hafner M, Vianini E, Albertoni B et al (2008) Displacement of protein-bound aptamers with small molecules screened by fluorescence polarization. Nat Protoc 3:579–587
156. Fuss B, Becker T, Zinke I, Hoch M (2006) The cytohesin Steppke is essential for insulin signalling in Drosophila. Nature 444:945–948
157. Jackson C (2006) Diabetes: kicking off the insulin cascade. Nature 444:833–834
158. Lim J, Zhou M, Veenstra TD, Morrison DK (2010) The CNK1 scaffold binds cytohesins and promotes insulin pathway signaling. Genes Dev 24:1496–1506
159. Mannell HK, Pircher J, Chaudhry DI et al (2012) ARNO regulates VEGF-dependent tissue responses by stabilizing endothelial VEGFR-2 surface expression. Cardiovasc Res 93:111–119
160. Kolanus W, Nagel W, Schiller B et al (1996) Alpha L beta 2 integrin/LFA-1 binding to ICAM-1 induced by cytohesin-1, a cytoplasmic regulatory molecule. Cell 86:233–242
161. Kolanus W (2007) Guanine nucleotide exchange factors of the cytohesin family and their roles in signal transduction. Immunol Rev 218:102–113
162. Anisimov AN, Bartke A (2013) The key role of growth hormone-insulin-IGF-1 signaling in aging and cancer. Crit Rev Oncol Hematol 87:201–223
163. Anisimov AN (2015) Conservative growth hormone/IGF-1 and mTOR signaling pathways as a target for aging and cancer prevention: do we really have an antiaging drug? Interdiscip Top Gerontol 40:177–188
164. Blagosklonny MV (2013) Selective anti-cancer agents as anti-aging drugs. Cancer Biol Ther 14:1092–1097
165. Marshansky V, Bourgoin S, Londono I et al (1997) Identification of ADP-ribosylation factor-6 in brush-border membrane and early endosomes of human kidney proximal tubules. Electrophoresis 18:538–547
166. Marshansky V, Bourgoin S, Londono I et al (1997) Receptor-mediated endocytosis in kidney proximal tubules: recent advances and hypothesis. Electrophoresis 18:2661–2676
167. Merkulova M, Hurtado-Lorenzo A, Hosokawa H et al (2011) Aldolase directly interacts with ARNO and modulates cell morphology and acidic vesicle distribution. Am J Physiol Cell Physiol 300(6):1442–1455
168. Oka T, Murata Y, Namba M et al (2001) a4, a unique kidney-specific isoform of mouse vacuolar H+-ATPase subunit a. J Biol Chem 276:40050–40054
169. Pietrement C, Sun-Wada GH, Da Silva N et al (2006) Distinct expression patterns of different subunit isoforms of the V-ATPase in the rat epididymis. Biol Reprod 74:185–194
170. Martinez-Zaguilan R, Lynch RM, Martinez GM, Gillies RJ (1993) Vacuolar-type H^+-ATPases are functionally expressed in plasma membranes of human tumor cells. Am J Physiol 265:C1015–C1029
171. Hendrix A, Sormunen R, Westbroek W et al (2013) Vacuolar H^+ ATPase expression and activity is required for Rab27B-dependent invasive growth and metastasis of breast cancer. Int J Cancer 133:843–854
172. Graham RM, Thompson JW, Webster KA (2014) Inhibition of the vacuolar ATPase induces Bnip3-dependent death of cancer cells and a reduction in tumor burden and metastasis. Oncotarget 5:1162–1173
173. Schempp CM, von Schwarzenberg K, Schreiner L et al (2014) V-ATPase inhibition regulates anoikis resistance and metastasis of cancer cells. Mol Cancer Ther 13:926–937
174. Mei F, You J, Liu B et al (2015) LASS2/TMSG1 inhibits growth and invasion of breast cancer cell in vitro through regulation of vacuolar ATPase activity. Tumour Biol 36:2831–2844
175. Sennoune SR, Luo D, Martinez-Zaguilan R (2004) Plasmalemmal vacuolar-type H^+-ATPase in cancer biology. Cell Biochem Biophys 40:185–206
176. Sennoune SR, Martinez-Zaguilan R (2007) Plasmalemmal vacuolar H^+-ATPases in angiogenesis, diabetes and cancer. J Bioenerg Biomembr 39:427–433

177. Sennoune SR, Martinez-Zaguilan R (2012) Vacuolar H^+-ATPase signaling pathway in cancer. Curr Protein Pept Sci 13:152–163
178. Kulshrestha A, Katara GK, Ibrahim S et al (2015) Vacuolar ATPase 'a2' isoform exhibits distinct cell surface accumulation and modulates matrix metalloproteinase activity in ovarian cancer. Oncotarget 6:3797–3810
179. Ntrivalas E, Derks R, Gilman-Sachs A et al (2007) Novel role for the N-terminus domain of the a2 isoform of vacuolar ATPase in interleukin-1beta production. Hum Immunol 68:469–477
180. Ntrivalas E, Gilman-Sachs A, Kwak-Kim J, Beaman K (2007) The N-terminus domain of the a2 isoform of vacuolar ATPase can regulate interleukin-1beta production from mononuclear cells in co-culture with JEG-3 choriocarcinoma cells. Am J Reprod Immunol 57:201–209
181. Kwong C, Gilman-Sachs A, Beaman K (2011) Tumor-associated a2 vacuolar ATPase acts as a key mediator of cancer-related inflammation by inducing pro-tumorigenic properties in monocytes. J Immunol 186:1781–1789
182. Katara GK, Jaiswal MK, Kulshrestha A et al (2014) Tumor-associated vacuolar ATPase subunit promotes tumorigenic characteristics in macrophages. Oncogene 33:5649–5654
183. Ziyad S, Iruela-Arispe ML (2011) Molecular mechanisms of tumor angiogenesis. Genes Cancer 2:1085–1096
184. Rojas JD, Sennoune SR, Maiti D et al (2004) Plasmalemmal V-H^+-ATPases regulate intracellular pH in human lung microvascular endothelial cells. Biochem Biophys Res Commun 320:1123–1132
185. Rojas JD, Sennoune SR, Maiti D et al (2006) Vacuolar-type H^+-ATPases at the plasma membrane regulate pH and cell migration in microvascular endothelial cells. Am J Physiol Heart Circ Physiol 291:H1147–H1157
186. Sennoune SR, Arutunyan A, del Rosario C et al (2014) V-ATPase regulates communication between microvascular endothelial cells and metastatic cells. Cell Mol Biol (Noisy-le-grand) 60:19–25
187. Nishisho T, Hata K, Nakanishi M et al (2011) The a3 isoform vacuolar type H(+)-ATPase promotes distant metastasis in the mouse B16 melanoma cells. Mol Cancer Res 9:845–855
188. Xu J, Xie R, Liu X et al (2012) Expression and functional role of vacuolar H(+)-ATPase in human hepatocellular carcinoma. Carcinogenesis 33:2432–2440
189. Perez-Sayans M, Garcia-Garcia A, Reboiras-Lopez MD, Gandara-Vila P (2009) Role of V-ATPases in solid tumors: importance of the subunit C. Int J Oncol 34:1513–1520
190. Huang L, Lu Q, Han Y et al (2012) ABCG2/V-ATPase was associated with the drug resistance and tumor metastasis of esophageal squamous cancer cells. Diagn Pathol 7:180
191. Lu Q, Lu S, Huang L et al (2013) The expression of V-ATPase is associated with drug resistance and pathology of non-small-cell lung cancer. Diagn Pathol 8:145
192. Liu P, Chen H, Han L et al (2015) Expression and role of V1A subunit of V-ATPases in gastric cancer cells. Int J Clin Oncol 20(4):725–735
193. Lozupone F, Borghi M, Marzoli F et al (2015) TM9SF4 is a novel V-ATPase-interacting protein that modulates tumor pH alterations associated with drug resistance and invasiveness of colon cancer cells. Oncogene (PMID: 25659576)
194. Chung C, Mader CC, Schmitz JC et al (2011) The vacuolar-ATPase modulates matrix metalloproteinase isoforms in human pancreatic cancer. Lab Invest 91:732–743
195. Sun-Wada GH, Toyomura T, Murata Y et al (2006) The a3 isoform of V-ATPase regulates insulin secretion from pancreatic beta-cells. J Cell Sci 119:4531–4540
196. Twells RC, Mein CA, Payne F et al (2003) Linkage and association mapping of the LRP5 locus on chromosome 11q13 in type 1 diabetes. Hum Genet 113:99–105
197. Toyomura T, Murata Y, Yamamoto A et al (2003) From lysosomes to the plasma membrane: localization of vacuolar-type H^+-ATPase with the a3 isoform during osteoclast differentiation. J Biol Chem 278:22023–22030
198. Scimeca JC, Franchi A, Trojani C et al (2000) The gene encoding the mouse homologue of the human osteoclast-specific 116-kDa V-ATPase subunit bears a deletion in osteosclerotic (oc/oc) mutants. Bone 26:207–213

199. Kartner N, Yao Y, Bhargava A, Manolson MF (2013) Topology, glycosylation and conformational changes in the membrane domain of the vacuolar H^+-ATPase a subunit. J Cell Biochem 114:1474–1487
200. Efeyan A, Zoncu R, Chang S et al (2013) Regulation of mTORC1 by the Rag GTPases is necessary for neonatal autophagy and survival. Nature 493:679–683
201. Parkhitko AA, Favorova OO, Khabibullin DI et al (2014) Kinase mTOR: regulation and role in maintenance of cellular homeostasis, tumor development, and aging. Biochemistry (Mosc) 79:88–101
202. Blagosklonny MV (2010) Calorie restriction: decelerating mTOR-driven aging from cells to organisms (including humans). Cell Cycle 9:683–688
203. Blagosklonny MV (2011) Molecular damage in cancer: an argument for mTOR-driven aging. Aging (Albany NY) 3:1130–1141
204. Blagosklonny MV (2013) M(o)TOR of aging: mTOR as a universal molecular hypothalamus. Aging (Albany NY) 5:490–494
205. Lamming DW, Ye L, Katajisto P et al (2012) Rapamycin-induced insulin resistance is mediated by mTORC2 loss and uncoupled from longevity. Science 335:1638–1643
206. Flinn RJ, Backer JM (2010) mTORC1 signals from late endosomes: taking a TOR of the endocytic system. Cell Cycle 9:1869–1870
207. Flinn RJ, Yan Y, Goswami S et al (2010) The late endosome is essential for mTORC1 signaling. Mol Biol Cell 21:833–841
208. Bar-Peled L, Schweitzer LD, Zoncu R, Sabatini DM (2012) Ragulator is a GEF for the Rag GTPases that signal amino acid levels to mTORC1. Cell 150:1196–1208
209. Settembre C, Zoncu R, Medina DL et al (2012) A lysosome-to-nucleus signalling mechanism senses and regulates the lysosome via mTOR and TFEB. EMBO J 31:1095–1108
210. Xu J, Cheng T, Feng HT, Pavlos NJ, Zheng MH (2007) Structure and function of V-ATPases in osteoclasts: potential therapeutic targets for the treatment of osteolysis. Histol Histopathol 22:443–454
211. Qin A, Cheng TS, Pavlos NJ et al (2012) V-ATPases in osteoclasts: structure, function and potential inhibitors of bone resorption. Int J Biochem Cell Biol 44:1422–1435
212. Qin A, Cheng TS, Lin Z et al (2012) Prevention of wear particle-induced osteolysis by a novel V-ATPase inhibitor saliphenylhalamide through inhibition of osteoclast bone resorption. PLoS One 7, e34132
213. Lebreton S, Jaunbergs J, Roth MG et al (2008) Evaluating the potential of vacuolar ATPase inhibitors as anticancer agents and multigram synthesis of the potent salicylihalamide analog saliphenylhalamide. Bioorg Med Chem Lett 18:5879–5883
214. Perez-Sayans M, Somoza-Martin JM, Barros-Angueira F et al (2009) V-ATPase inhibitors and implication in cancer treatment. Cancer Treat Rev 35:707–713
215. You H, Jin J, Shu H, Yu B et al (2009) Small interfering RNA targeting the subunit ATP6L of proton pump V-ATPase overcomes chemoresistance of breast cancer cells. Cancer Lett 280:110–119
216. Niikura K (2006) Vacuolar ATPase as a drug discovery target. Drug News Perspect 19:139–144
217. Huss M, Wieczorek H (2009) Inhibitors of V-ATPases: old and new players. J Exp Biol 212:341–346
218. Pommier Y, Cherfils J (2005) Interfacial inhibition of macromolecular interactions: Nature's paradigm for drug discovery. Trends Pharmacol Sci 26:138–145
219. Mullard A (2012) Protein-protein interaction inhibitors get into the groove. Nat Rev Drug Discov 11:173–175
220. Azzarito V, Long K, Murphy NS, Wilson AJ (2013) Inhibition of alpha-helix-mediated protein-protein interactions using designed molecules. Nat Chem 5:161–173
221. Merkulova M, Păunescu TG, Azroyan A et al (2015) Mapping the H^+-V-ATPase interactome: identification of proteins involved in trafficking, folding, assembly and phosphorylation. Sci Rep 5:14827. (doi: 10.1038/srep14827)

Chapter 17
Vacuolar ATPase in Physiology and Pathology: Roles in Neurobiology, Infectious Disease, and Cancer

Colleen A. Fordyce, Martha M. Grimes, Yamhilette Licon-Munoz, Chun-Yuan Chan, and Karlett J. Parra

Abstract Vacuolar ATPase (V-ATPase) is an ATP-dependent proton pump present in all eukaryotic cells. V-ATPase is a critical regulator of intracellular pH across the endomembrane system and is essential for fundamental cellular functions including endocytosis and exocytosis, protein modification and maturation and loading of secretory vesicles. Here we describe the structure, regulation, and function of V-ATPase in pH regulation and the roles of V-ATPase in neurobiology, infectious disease, and cancer. V-ATPase is composed of two domains: a membrane-peripheral domain, V_1, and a membrane-integral domain, V_o. When extracellular glucose concentrations drop the V_1V_o complex disassembles to inhibit V-ATPase activity and prevent energy depletion; this ability allows yeast cells to quickly respond to alterations in energy state. Next, we present a body of growing new evidence that highlights the importance of V-ATPase in human health and disease. We discuss mechanisms by which V-ATPase participates in neurotransmission, neurodegeneration, and stroke-associated neuronal cell death. Then, we focus on the involvement of pH and V-ATPase in the pathogenesis of viruses, bacteria, and fungi and the processes necessary to ensure pathogen replication. In the last section, we capitalize upon a repertoire of studies in recent years that indicate that V-ATPase is a critical player in adaptation to cellular stress and that V-ATPase activity directly and indirectly contributes to many of the hallmarks of cancer.

Keywords V-ATPase • Proton pump • Membrane trafficking • Neurobiology • Infection • Cancer

C.A. Fordyce • M.M. Grimes • Y. Licon-Munoz • C.-Y. Chan • K.J. Parra (✉)
Department of Biochemistry and Molecular Biology,
University of New Mexico School of Medicine, Fitz Hall, Room 249, 1
University of New Mexico MSC 08, Albuquerque, NM 4670, USA
e-mail: kjparra@salud.unm.edu

S. Chakraborti, N.S. Dhalla (eds.), *Regulation of Ca^{2+}-ATPases,V-ATPases and F-ATPases*, Advances in Biochemistry in Health and Disease 14,
DOI 10.1007/978-3-319-24780-9_17

1 Introduction

1.1 V-ATPase Structure and Function

The V-type ATPase proton pump is a molecular motor structurally related to the F-type ATP synthase and the archaea A-type ATPase/synthase [1]. These three energy-converting biosystems operate by a similar mechanism of rotational catalysis, but only V-ATPase hydrolyzes ATP, which distinguishes V-ATPase from the F- and A-type enzymes that are ATP synthases. The V-ATPase multisubunit protein complex contains eight peripheral subunits (A, B, C, D, E, F, G, H) and six membrane-bound subunits (a, c, c′, c″, d, e); several of which are present in multiple copies (Table 17.1) [2–6]. The peripheral subunits form the V_1 domain. V_1 subunits A, B, and D form a catalytic globular protuberance from the membrane involved in the binding and hydrolysis of ATP (catalytic core). The other V_1 subunits play structural and regulatory roles. The membrane subunits form the V_o domain. V_o has a ring structure (c-ring) of proteolipid nature that captures cytosolic protons and transfers them across the membrane. ATP-driven V_1V_o proton transport sustains organelle, cellular, and extracellular pH homeostasis in lower eukaryotes and human cells. This chapter starts by describing the fundamental mechanism governing V-ATPase proton transport and regulation and the V-ATPase involvement in membrane trafficking processes.

1.2 V-ATPase Mechanisms of Action

Functional coupling of ATP hydrolysis and proton transport involves an intricate mechanism in which V_1 and V_o communicate in order to drive rotation of subunits D, F, d, and the c-ring (Fig. 17.1) [1, 7–9]. ATP hydrolysis occurs in the three A subunits of the V_1 catalytic core projecting from the cytosolic side of the membrane. The rotor consists of an elongated shaft that extends through the center of this globular structure (subunits D, F, and d). It connects with the hydrophobic c-ring in the membrane. A hemi-channel in the V_o subunit a accepts incoming protons at the cytosolic half-leaf of the membrane. From the V_o subunit a, protons are transferred to the c-ring. Each c-ring subunit (c, c′, c″) has a glutamic residue that is protonated during catalysis. Hydrolysis of three molecules of ATP drives 360° rotation of the rotor, during which all c-ring subunits are protonated. After one complete rotation each proton exits the membrane by passing through a second hemi-channel in V_o subunit a, at the luminal half-leaf of the membrane. Thus, the number of subunits forming the c-ring dictates the number of protons transferred per ATP-hydrolyzed against a concentration gradient. However, as we discuss subsequently, the ratio of protons transported in relation to ATP molecules hydrolyzed can be modified to regulate V-ATPase activity.

Table 17.1 Comparison of yeast and mammalian V-ATPase domains, subunits, and isoforms

Domain	Subunit (copies)	Yeast gene name	Mammalian gene name	Mammalian subunit isoform	Yeast subunit isoform	General function	Mammalian nucleotide accession	Yeast nucleotide accession
V_1 (peripheral domain)	A(3)	*VMA1*	ATP6V1A	A	A	Site of ATP hydrolysis; coupling; catalytic core	NM_001690	NM_001180245
	B(3)	*VMA2*	ATP6V1B1	B1	B	Non-catalytic/regulatory ATP site; binds to actin; catalytic core	NM_001692	NM_001178475
		–	ATP6V1B2	B2	–		NM_001693	–
	C(l)	*VMA5*	ATP6V1C1	C1	C	Regulatory; stator subunit; binds to actin	NM_001695	NM_001179646
		–	ATP6V1C2	C2	–		NM_001039362; NM_144583	–
	D(1)	*VMA8*	ATP6V1D	D	D	Rotary subunit; central stalk; catalytic core	NM_015994; AF100741	NM_001178866
	E(3)	*VMA4*	ATP6V1E1	El	E	Peripheral stalk subunit; stator; binds to RAVE complex and aldolase	NM_001696; NM_001039366; NM_001039367	NM_001183752
		–	ATP6V1E2	E2	–		NM_080653	–
	F(1)	*VMA7*	ATP6V1F	F	F	Rotary subunit; central stalk; catalytic core	NM_004231	NM_001181149
	G(3)	*VMA10*	ATP6V1G1	G1	G	Peripheral stalk subunit; stator subunit; binds to RAVE complex	NM_004888; BC008452	NM_001180027
		–	ATP6V1G2	G2	–		NM_130463; NM_138282	–
		–	ATP6V1G3	G3	–		NM_133262; NM_133326; BC101129	–
	H(1)	*VMA13*	ATP6V1H1	H	H	Regulatory subunit binds to negative replication factor	NM_015941; NM_213619; NM_213620	NM_001184133

(continued)

Table 17.1 (continued)

Domain	Subunit (copies)	Yeast gene name	Mammalian gene name	Mammalian subunit isoform	Yeast subunit isoform	General function	Mammalian nucleotide accession	Yeast nucleotide accession
V_0 (Membrane Domain)	a(1)	*VPH1*; *STV1*	ATP6VOA1	al	a	Involved in H^+ transport; membrane targeting; stator subunit; binds glycolytic enzymes, RAVE complex, ARNO and SNARE	NM_001130020; NM_001130021; NM_005177; DQ286422	NM_001183689; NM_001182552
			ATP6VOA2	a2			NM_012463; BC068531	
			ATP6VOA3	a3			NM_006019; NM_006053	
			ATP6VOA4	a4			NM_020632; NM_130840; NM_130841	
	c(n)	*VMA3*	ATP6VOC	c	c	H^+ transport; c-ring rotor subunit	NM_001694	NM_001178842
	c′(n)	*VMA11*	–	–	c′	H^+ transport; c-ring, rotor subunit	–	NM_001184048
	c″(n)	*VMA16*	ATP6V0B	c″	c″	H^+ transport; c-ring, rotor subunit	NM_004047; NM_001039457	NM_001179156
	d(l)	*VMA6*	ATP6V0D1	d1	d	Rotary subunit; coupling	NM_004691	NM_001182335
		–	ATP6VOD2	d2	–		NM_152565	–
	e(l)	*VMA9*	ATP6VOE1	el	e	(Unknown)	NM_003945	NM_001184518
		–	ATP6VOE2	e2	–		NM_145230; AK098362 NM_001100592	–

The table depicts the differences between the two V-ATPase domains, V_1 and V_o. All known yeast and mammalian V-ATPase subunits and their corresponding gene names are listed. A general function of each subunit is described. The corresponding nucleotide accession numbers are provided for both mammalian and yeast V-ATPase subunits

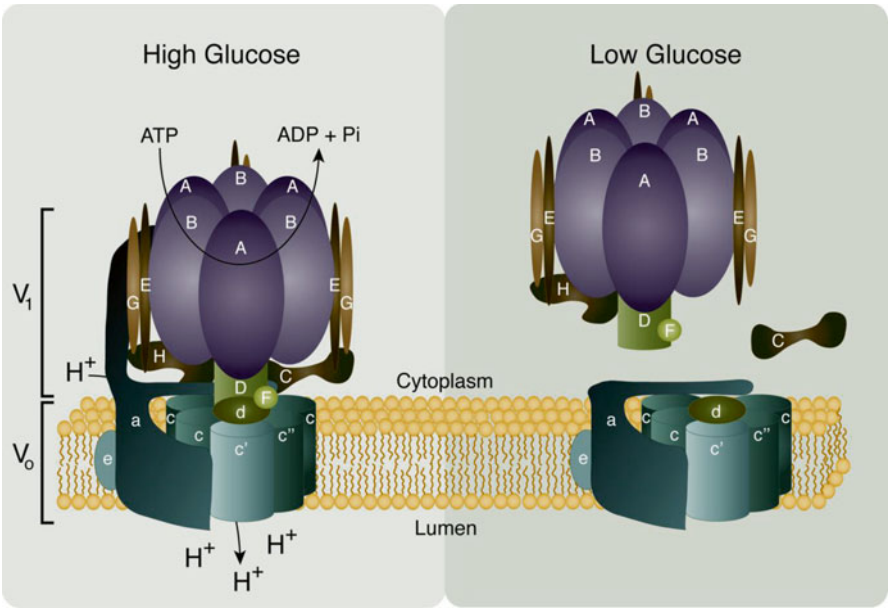

Fig. 17.1 V-ATPase structure and regulation. Vacuolar ATPase (V-ATPase) is composed of 14 proteins which are assembled into two functional domains: V_1 and V_o. V_1 is peripheral to the membrane and contains sites for ATP hydrolysis, thus this domain is often considered the catalytic domain. V_1 contains a hexameric core composed of alternating A and B subunits. The V_o domain is embedded within the membrane and contributes to proton transport through the central proteolipid ring of V_o which is composed of c, c′ and c″ in fungi (subunits c and c″ in higher eukaryotes). The proteolipid c-ring is adjacent to subunit a that also participates in proton transport. The V_1V_o domains are connected by a central stalk containing the D, F and d subunits of V-ATPase. V-ATPase also contains several subunits that contribute to forming the three peripheral stalks. These proteins include V_1 subunits C, E, G, H and the N-terminal of V_o subunit a. The C-terminal of V_o subunit a contains two hemi-channels (not shown) which are required for proton transport. When intracellular glucose concentrations are high, V_1 and V_o subunits assemble on the membrane and ATP-driven proton translocation is possible (*left*). However, when glucose concentration drops, the V_1 domain and subunit C disassemble from V_o and proton transport in V_o and ATP hydrolysis in V_1 are lost (*right*). The disassembly and rapid reassembly of V-ATPase is a critical mechanism for V-ATPase regulation

This elegant mechanism of catalysis generates and sustains the differential acidic luminal pH in the organelles of the endomembrane system (e.g., Golgi, endosome, lysosomes) [5, 6]. In addition to sustaining the organelle acidic pH, V-ATPase energizes membranes by generating an electrochemical proton gradient that drives secondary transport systems [6, 10] including the vacuolar Ca^{2+}/H^+ exchanger Vcx1p, and heavy metal transporters. A number of exchangers including Nhx1p, a $Na^+(K^+)/H^+$ exchanger, transport protons against the pH gradient created by the V-ATPase. As a result, V-ATPase proton transport contributes to pH homeostasis and supports many biological processes. Vesicle trafficking, protein glycosylation in the Golgi apparatus, zymogen activation in vacuoles and lysosomes, and loading of secretory vesicles require V-ATPase-dependent transport of protons.

The three elongated peripheral stalks, which include subunits E and G of V_1 serve as stators to allow rotation of the rotor-forming subunits relative to the immobile catalytic sites (Fig. 17.1). These peripheral stalk structures also distinguish V-ATPase from F-ATP and A-ATP synthases, which have one and two stators respectively. The V-ATPase stators are probably relatively more flexible than those found in F-ATP and A-ATP syntheses, because V-ATPase activity is regulated by reversible disassembly of V_1 and V_o [11]. This regulatory mechanism does not naturally occur in any other rotary machines.

V-ATPase activity is primarily regulated by adjusting the assembly state of the pump in response to environmental changes. Glucose levels, intracellular and extracellular pH changes, and osmotic stress modulate the levels of V_1V_o complexes assembled at the membrane [2, 11]. These external signals are communicated to V-ATPase by different pathways. A number of regulatory proteins including the Regulator of ATPase of Vacuoles and Endosomes complex (RAVE), Protein Kinase A (PKA), and glycolytic enzymes can regulate V-ATPase assembly in yeast. Although the cellular mechanisms and signals mediating V_1V_o reversible disassembly are not fully defined, it is clear that they vary in different cell types. The mechanisms governing V-ATPase regulation are discussed in more detail in the following sections.

2 Regulation of V-ATPase Activity

Given its critical role in fundamental cellular processes, it is not surprising that a number of mechanisms have evolved to precisely and efficiently regulate V-ATPase activity. Perhaps the best studied of these mechanisms is the reversible disassembly of the V_1 and V_o domains [2, 11]. However V-ATPase activity is also regulated by (i) reversible disulfide bond formation at the catalytic sites [12, 13], (ii) the coupling efficiency of proton transported per ATP hydrolyzed (i.e., the number of protons moved across the membrane per ATP molecule) [14, 15], (iii) changes in V-ATPase membrane localization [16, 17], and (iv) posttranslational modifications [2, 5, 6, 18–20]. There are many excellent reviews and research papers that address these topics; here we provide only a partial overview of V-ATPase regulation.

2.1 Control of V-ATPase Coupling Efficiency

Coupling efficiency describes the relationship between the number of protons transported across a membrane and ATP hydrolysis. Variations in the coupling efficiency of V-ATPase pumps have been proposed to regulate the acidification of intracellular compartments [6, 21–24]. In bovine clathrin-coated vesicles, coupling rates are reduced when ATP concentration is greater than 0.3 mM [23]. In plant cells, high levels of intracellular citrate and malate are associated with increased coupling efficiency [15].

Coupling efficiency is also dictated by V-ATPase subunit isoforms, which are membrane specific. In fungi there are two isoforms of the a subunit: Vph1p, at the vacuolar membrane and Stv1p, at the Golgi membrane [25, 26]. V-ATPase pumps containing Stv1p have a reduced coupling efficiency when compared to those containing Vph1p [27]. Site-directed mutation of conserved amino acids in V_1 subunit A and V_o subunit d have demonstrated that these subunits of V-ATPase are also critical for efficient coupling of ATP hydrolysis and proton transport [28, 29]. Overexpression of V_1 subunit H induces a unique uncoupling phenotype, preventing proton transport without decreasing ATP hydrolysis [30]. The discovery that certain mutations increase coupling efficiency, suggests that V-ATPase pumps may not be fully coupled in vivo [24]. Nevertheless, alterations in the coupling efficiency allow V-ATPase activity to be "fine tuned" to best meet not only the needs of a particular cell, but also a particular organelle.

2.2 *Modulation of Reversible Disulfide Bond Formation at the Catalytic Sites*

V-ATPase-dependent proton transport and ATP hydrolysis are inhibited by disulfide bond formation between Cys 254 and Cys 532 in the catalytic site of V_1A of the bovine V-ATPase [12, 13]. This observation in purified V-ATPase is consistent with studies in cortical collecting ducts [31] and Neurospora [32] where exposure to oxidizing agents inhibits V-ATPase activity. Yeast cells lacking *CYS4* cannot synthesize cysteine, have reduced glutathione levels and impaired V-ATPase activity, consistent with the concept that disulfide bond formation in V_1A is inhibitory [33]. Similarly, in insect cells, a disulfide bond forms between Cys-134 and Cys-186 of V_1 subunit E [34]. Thus, the redox state of the cytoplasm may regulate V-ATPase activity through the formation of reversible disulfide bonds.

2.3 *Reversible Disassembly of V-ATPase*

One of the most well studied mechanisms of V-ATPase regulation is the reversible disassembly of the V_1 and V_o domains. During disassembly of V-ATPase, the peripheral domain, V_1, detaches from the integral membrane domain, V_o, resulting in inhibition of both proton translocation and ATP hydrolysis [11, 35–38]. V_1V_o disassembly is a very quick process that can be detected in less than 5 min [11, 35, 39, 40] and is a particularly important regulatory mechanism since it allows cells to align V-ATPase assembly to cellular needs. For example, low glucose concentration triggers the rapid disassembly of V-ATPase, but the amount of assembled V_1V_o complexes is proportional to the amount of glucose [39, 41, 42].

In yeast, reassembly of V_1V_o in response to glucose requires the Regulator of ATPase of Vacuoles and Endosomes complex (RAVE complex). RAVE is a

three-component (Skp1p, Rav1p, and Rav2p) cytoplasmic V-ATPase assembly factor [43–45]. Loss of RAVE function is associated with impaired acidification of vacuoles at both steady state and after glucose readdition to glucose-deprived cells [46]. A mammalian homolog of Rav1p, rabconnectin 3, has been found to contribute to organelle acidification [47], suggesting that the requirement for RAVE to promote V_1V_o assembly is conserved in higher eukaryotes.

A number of glycolytic enzymes physically interact with V-ATPase, including aldolase and phosphofructokinase (PFK-1) [48–53]. In yeast, aldolase binding to V-ATPase is glucose dependent and disruption of this interaction leads to V_1V_o dissociation. V_o subunit a interacts with PFK-1 in both human kidney and yeast cells. Interestingly, mutations in the human V_o subunit a isoform a4, that inhibit V-ATPase interaction with PFK-1, are associated with distal renal tubular acidosis [49, 54]. In yeast, PFK-1 is required for V-ATPase activity and regulation [53]. Yeast cells lacking PFK-1 subunit genes display aberrant cytosolic and vacuolar pH homeostasis and cannot sufficiently reassemble V_1 and V_o after readdition of glucose to cells briefly deprived of glucose. It has been proposed that glycolytic enzymes form a super-complex with V-ATPase that promotes V-ATPase activity by acting as a glucose sensor or as a ready supplier of ATP [2, 48, 51, 54].

Protein kinase A (PKA) is, among other things, a key regulator of glucose metabolism. Not surprisingly, PKA and its upstream activators have been reported to promote V-ATPase assembly [41, 55–58]. In yeast, PKA constitutive activation prevents V_1V_o disassembly, even during glucose deprivation [41]. However, it has also been suggested that V-ATPase reactivation after V_1V_o reassembly promotes PKA signaling [40, 58]. These data suggest that the PKA pathway can regulate V-ATPase assembly and activity, and that V-ATPase itself can regulate PKA signaling. Finally, studies in yeast and higher eukaryotes suggest that V-ATPase activity may also be regulated by pH; V_o subunit a may sense pH changes [40, 59]. When extracellular pH is high, V-ATPase activity and assembly are also heightened, even during glucose deprivation [60, 61]. These findings suggest that during episodes of pH-related stress, V-ATPase activity is maintained, even when glucose concentrations are low.

3 V-ATPase Is Essential for Membrane Trafficking

Membrane trafficking mediates the distribution of macromolecules throughout the cell and their release to the extracellular space (endocytosis) or internalization from the microenvironment (exocytosis). As its name implies, membrane trafficking relies upon membrane-bound vesicles to mediate transport. Unfortunately, as we discuss in this chapter, pathogens also invade cells using the host membrane trafficking machinery [62–67] and defects in trafficking contribute to human pathologies such as cancer and neurodegeneration [5, 67–71]. Thus, the mechanisms of membrane trafficking play a central role in both physiological and pathological function in eukaryotic cells.

Membrane trafficking relies upon tight control of the differential pH of the cytosol and the compartments of the endomembrane system. Along the endocytic pathway, the luminal pH drops from approximately pH 6.5 within early endosomes to lower than pH 5.0 in lysosomes [72]. Secretory pathway compartments are also gradually acidified, displaying a near-cytosolic pH about 7.2 in the endoplasmic reticulum (ER) to value of pH 6.4–6.7 within the Golgi and a final pH of 5.2–5.4 in secretory granules. The V-ATPase pump is broadly localized in various organelle membranes including early endosomes, late endosomes, lysosomes, secretory vesicles, clathrin-coated vesicles, endocytotic vesicles, and vacuoles of fungi and plants [5, 73, 74]. Although a number of proteins contribute to the maintenance of organelle pH, V-ATPase is particularly important and its loss alters intracellular pH across the endomembrane system [3, 5].

Different isoforms of V-ATPase subunits assemble to yield V_1V_o complexes with unique catalytic and regulatory properties. As previously stated, fungi contain two types of V-ATPase pumps Vph1p or Stv1p [25, 26]. Complexes containing Vph1p and Stv1p differ in their kinetic properties and regulatory mechanisms. Except for V_o subunit a, each V-ATPase subunit is encoded by a single gene in fungi. However multiple isoforms for most V-ATPase subunits exist in mammalian cells [5, 75]. These isoforms combine to yield different populations of V-ATPase pumps that are membrane (e.g., lysosomal, endosomal, Golgi, or plasma membranes) and tissue specific [5, 75, 76]. Thus, V-ATPase has developed specialized organelle-specific roles and regulatory mechanisms that link it to diverse cellular and systemic processes.

In order to dissect the importance of organelle acidification, we must first discuss the role played by V-ATPase in membrane trafficking. Loss of V-ATPase function induced by knockout of the V_o subunit c, causes defective membrane trafficking and acidification during development [77]. Similarly, deletion of the V_o subunit a in *Caenorhabditis elegans* results in embryonic lethality [78]. Numerous studies have reported that inhibition of V-ATPase function is associated with defects in endocytosis or exocytosis of multiple proteins in a variety of cell types [71, 79–84]. Collectively these studies demonstrate that V-ATPase-dependent proton transport and V-ATPase-mediated organelle acidification play important roles in membrane trafficking, cell growth, and survival.

V-ATPase generates the acidic late endosomal pH required for dissociating ligands internalized through receptor-mediated endocytosis [5, 76, 85, 86]. The disruption of the acidic pH in endosomes by using V-ATPase specific inhibitors (concanamycin A or bafilomycin A), impairs ligand dissociation and receptor recycling during endocytosis. The fact that ionophores and weak bases have the same effect illustrates the importance of V-ATPase-mediated luminal acidification [79, 85–87]. By creating an acidic endosome, V-ATPase also activates the Wnt signaling pathway [87], which is important during development and contributes to diseases such as cancer [88]. Rabconnectin-3 interacts with the V_o subunit a (isoform a1). Deficiency of rabconnectin-3 or its binding partner, V-ATPase V_o subunit a (isoform a1), downregulates the Wnt signaling pathway by altering intracellular trafficking in zebrafish neural cells [89]. Inhibition of V-ATPase causes retention of several

pro-inflammatory cytokines (e.g., TNFα and IL-8) in the endoplasmic reticulum and impaired secretion of these proteins in human monocytes [83]. Thus, V-ATPase acidification of trafficking vesicles is fundamental for numerous and diverse processes, from embryonic development to signal transduction events and activation of inflammatory responses.

V-ATPase modulates endocytosis not only by controlling the intracellular pH but also by recruiting the small GTPase, Arf6, and its activator, ARNO, to early endosome compartments [79, 90]. Both ARNO and Arf6 are associated with endocytosis, participating in a number of important endocytic processes including actin cytoskeleton remodeling, lipid modification, and endosomal vesicle coat formation [91–93]. A seminal study in 2006 demonstrated that the V_oa isoform a2 and V_oc subunits of V-ATPase directly interact with cytosolic ARNO and Arf6, respectively. V-ATPase–Arf6–ARNO interaction facilitates the formation of early endosomes and is necessary for endocytosis. The recruitment of ARNO and Afr6 is dependent upon V-ATPase activity [79]. This study and others subsequent to it [94–98] demonstrate that V-ATPase is critical for endocytosis and, as described previously, is an important sensor of vesicle pH.

Exocytosis consists of three important steps: budding of vesicles from the ER or the trans-Golgi network (TGN), trafficking of vesicles to different compartments (lysosome, late endosomes), and the fusion of vesicles with acceptor compartments or the plasma membrane [99]. As we discuss in relation to neurotransmitter release, the V_o domain of V-ATPase has been suggested to directly participate in membrane fusion [100–103]. V-ATPase also plays a central role in exocytosis by generating the acidic environment necessary for protein modification and the activation of proproteins into their mature active form [104–106]. For example, acidic secretory vesicles containing the V_o subunit a (isoform a3) process pro-insulin to yield insulin in pancreatic cells [107]. Inhibition of V-ATPase induces extracellular accumulation of several immature lysosomal proteases [84, 108] and is likely dependent upon defects in receptor-dependent trafficking [84]. Thus, V-ATPase function is an important regulator of exocytosis.

In addition, V-ATPase activity is necessary for protein processing and sorting to various compartments. V-ATPase-mediated acidification of late endosomes is crucial for the maturation of lysosomal enzymes trafficked from the Golgi apparatus [5]. For example, those enzymes containing the glycosylated modification, mannose-6-phosphate (Man-6-P), recognized by the Man-6-p receptor in the TGN are delivered into the late endosome [109]. V-ATPase creates the low pH within the late endosome necessary to release the lysosomal enzymes from Man-6-p receptors, recycle the receptors back to the Golgi, and traffic the enzymes to the lysosomal compartment. Inhibiting V-ATPase activity with bafilomycin A alkalinizes the late endosomes and results in accumulation of Man-6-p receptors and their ligands in these vesicles [110] completely abrogating transport into lysosomes. These studies indicate that acidification of late endosomes, which is generated by V-ATPase proton transport, is required for membrane trafficking from the late endosome to lysosomes and the TGN.

4 V-ATPase in Neurobiology and Neuropathology

Neuron-to-neuron communication is essential for brain function and frequently relies upon electrochemical signaling through the release of neurotransmitters [111]. Exocytosis of neurotransmitters is a highly regulated process that allows synaptic vesicles or secretory granules to fuse with the plasma membrane and deposit their cargo in the synaptic cleft where neurotransmitters bind to their respective receptors on the surface of adjacent cells (Fig. 17.2). A growing body of evidence demonstrates that V-ATPase participates not only in neurotransmission, but also in neurodegeneration. Here we discuss this data.

4.1 Roles of V-ATPase in Neurotransmission

Following synthesis, neurotransmitters accumulate in vesicles (i.e., synaptic vesicles or synaptic granules) in the presynaptic neuron (Fig. 17.2). One to two V-ATPase molecules are present in each synaptic vesicle [112, 113]. The V-ATPase-dependent transport of protons to the lumen of synaptic vesicles generates and maintains an electrochemical gradient across the membrane [114] which is required for the uptake and subsequently storage of important neurotransmitters such as acetylcholine [115], glutamate [115], and monoamines (e.g., serotonin, dopamine) [114].

Preliminary studies demonstrated that exposure to bafilomycin A or loss of Rabconnectin 3 (Rbc3, homolog of Rav1p in yeast which promotes V_1 and V_o assembly [43]) decreases neurotransmitter release via exocytosis [116]. V-ATPase physically and functionally interacts with the soluble NSF attachment protein receptor (SNARE) family of proteins complexes, which mediates synaptic vesicle docking and fusion to the plasma membrane to regulate exocytosis of neurotransmitters. V-SNAREs, found on the synaptic vesicle, bind to t-SNAREs in the plasma membrane of the presynaptic neuron [117]. In *Drosophila*, the V_o subunit a (isoform a1) ortholog V100, interacts with t-SNARE [118]. Similarly, V_o subunit c has been reported to physically interact with a v-SNARE protein, VAMP2/synaptobrevin [116, 119]. Mutational studies of V_o subunit c indicate that the interaction with synaptobrevin is not required for V-ATPase-dependent proton transport, but is necessary for neurotransmitter release [119]. An elegant study using chromophore-assisted light inactivation of V_o subunit a isoform a1 further showed that V-ATPase is required for exocytosis of neurotransmitters [103]. Interestingly, the loss of V-ATPase-dependent proton gradients results in decreased exocytosis of neurotransmitters and the disassembly of V_1V_o [104], possibly freeing V_o for interaction with v-SNAREs. It is thought that the c-subunit of V_o assembles 5 to 6 v-SNARE molecules to act as a scaffold for fusion (pairing v-SNARES and t-SNARES; Fig. 17.2) of synaptic vesicles to the plasma membrane of the presynaptic neuron. Alternatively, two V_o domains (one in the synaptic vesicle and one in the plasma membrane) may combine to generate an aqueous fusion pore to promote neurotransmitter release (Fig. 17.2, [120–123]). Collectively these data suggest two distinct

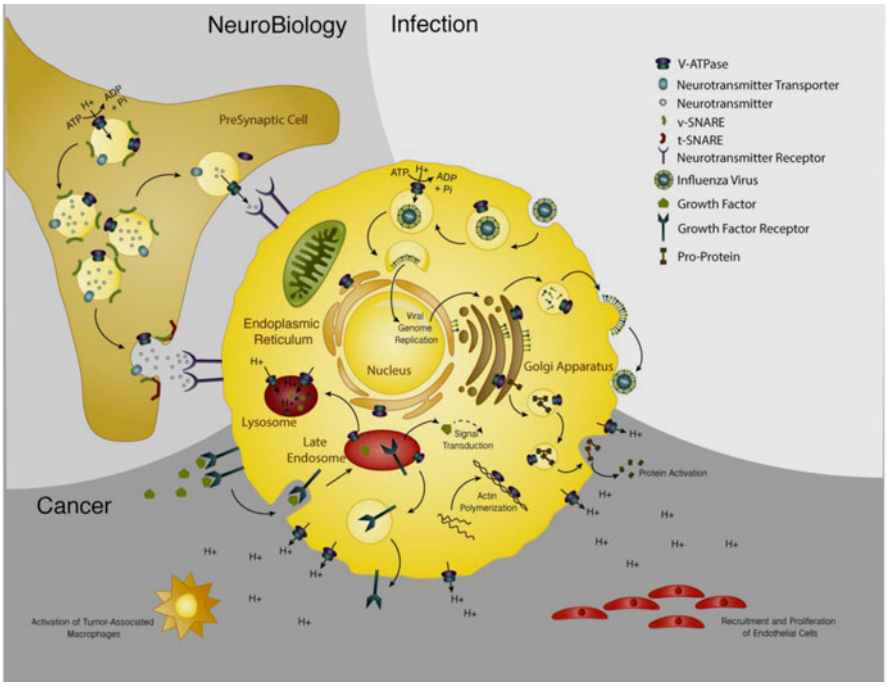

Fig. 17.2 V-ATPase function in neurobiology, infection and cancer. *Neurobiology* (*top left*): In presynaptic cells V-ATPase-dependent proton gradients are required for loading of neurotransmitters into synaptic vesicles. Fusion of synaptic vesicles with the plasma membrane may occur through two mechanisms. v-SNAREs may bind to t-SNAREs to mediate synaptic vesicle fusion and release of neurotransmitters or, alternatively, two V_o domains of V-ATPase may fuse to create a pore that allows neurotransmitters to move into the synaptic cleft. V-ATPase activity is also required for several aspects of viral, bacterial or fungal infection of host cells. *Infection* (*top right*): Here we outline the role of V-ATPase in influenza viral infection. Influenza viral particles enter the host cell through endocytosis. Once inside an endocytic vesicle, V-ATPase-dependent acidification triggers unpacking of the viral genome and fusion of viral proteins with the vesicle membrane to create a pore allowing the viral genome to exit the vesicle. Viral proteins rely upon the host cell's V-ATPase activity to transport them through the exocytic pathway to the plasma membrane. Once on the surface of the cell, viral proteins assemble with the replicated viral genome and bud from the cell. *Cancer* (*bottom*): V-ATPase function is necessary for endocytosis of receptor–ligand complexes and receptor recycling. It is also essential for proper transport of newly synthesized proteins through the exocytic pathway. In this way V-ATPase activity contributes to several important signal transduction pathways (e.g., HER2, Wnt, Rac, VEGF). V-ATPase activity is required for activation of pro-proteins including matrix metalloproteinases and cathepsins which degrade extracellular matrix and promote cell motility. The V_1 domain of V-ATPase may also directly promote cell motility by promoting assembly and enhancing polymerization of f-actin. V-ATPase activity is likely also required by endothelial cells to increase recruitment and proliferation and is associated with activation of tumor-associated macrophages

roles for V-ATPase in neurotransmitter release. First, V-ATPase acidifies vesicles, a process that is required for neurotransmitter uptake into vesicles. Secondly, although the exact mechanism remains unknown, interactions between V_o and SNARES can promote docking of vesicles to the plasma membrane and subsequently control neurotransmitter release into the synaptic cleft.

An additional role for V-ATPase in neurotransmission has been described at the synaptic cleft. After the arrival of an action potential in the presynaptic neuron, voltage-gated calcium channels open, allowing Ca^{2+} entrance into the cell. The resulting increase of intracellular Ca^{2+} triggers SNARE-dependent synaptic vesicle docking to the plasma membrane (Fig. 17.2, [111, 124]). Changes in the pH of the synaptic cleft can alter the activity of voltage-gated calcium channels, suggesting that the entrance of Ca^{2+} could be affected and modify neurotransmitter release [125]. In the horizontal cells of the vertebrate retina, this type of modulation is blocked in the presence of bafilomycin A, suggesting that acidification of the synaptic cleft is V-ATPase dependent [126, 127]. Additional studies are necessary to address the possibility that V-ATPase-dependent proton transport can modulate voltage-gated calcium channels in the brain.

Glucose-dependent reversible disassembly of V-ATPase may also contribute to neurotransmission independently of exocytosis. As described previously, V-ATPase disassembly and reassembly is intimately tied to glycolytic enzymes. At least two glycolytic enzymes, GAPDH and 3-phosphoglycerate kinase, are necessary for glutamate accumulation in presynaptic vesicles [128]. In theory, these enzymes could produce glycolytic ATP to drive the V-ATPase-dependent proton transport necessary for neurotransmitter uptake into synaptic vesicles. Consistent with this supposition, synaptic transmission is impaired during hypoglycemia [129]. Thus, it is possible that low intracellular glucose concentrations promote V-ATPase disassembly and reduced V-ATPase activity [11], decreasing neurotransmitter loading into synaptic vesicles.

4.2 Roles of V-ATPase in Neurodegeneration

Several chronic neurodegenerative disorders including: Alzheimer's, Parkinson's, and Huntington's diseases have a common etiology that involves the aggregation of misfolded proteins (e.g., presenilin, tau, α-synuclein) [130, 131]. Interestingly, mutations in presenilin 1 and 2 proteins, which cause familial early-onset alzheimer's disease, reduce V-ATPase localization to the lysosome, increase lysosomal pH [132], induce severe lysosomal pathology [133], and hinder autophagy [132]. Therefore, loss of V-ATPase function may indirectly contribute to these neurodegenerative diseases by inhibiting autophagy [131, 134, 135], a cellular process that degrades misfolded proteins [131, 134–136]. V-ATPases are required for autophagy since they facilitate the generation and maintenance of the acidic lysosomal pH needed for autophagosome formation [134, 137]. Abnormal autophagosomes accumulate in the brain tissues of patients affected with Alzheimer's [138] and Parkinson's diseases [139]. Likewise, the huntingtin protein collects in endosomes/lysosomes of patients with Huntington's disease [140]. In *Drosophila* neurons, loss of the V_oa1 ortholog, V100, causes autophagosomal accumulation [141] making neurons more susceptible to neurotoxicity of Alzheimer-related amyloid β and tau proteins [142].

Conversely, V-ATPase activity is required for neuronal cell death in models of stroke. In neurons of *Caenorhabditis elegans*, V-ATPase activity is required to generate the cytoplasmic acidification that leads to necrotic cell death [70]. V-ATPase inhibition also decreases matrix metalloproteinases (MMPs) presence in the extracellular fluid of cultured hippocampal neurons [143] which are needed to degrade neurovascular matrix and cause neuronal death [144]. Taken together these data suggest that V-ATPase inhibitors may be neuroprotective in some contexts [69, 70, 143].

In summary, V-ATPase is present in synaptic vesicles and in the plasma membrane of the presynaptic neurons and its activity is essential for neurotransmitter uptake into synaptic vesicles. V-ATPase subunits also associate with SNARE proteins to aid synaptic vesicle docking and fusion, modulating neurotransmitter release. Formation and maintenance of lysosomes by V-ATPase activity is essential for autophagosome formation and proper autophagy is required for clearance of misfolded proteins associated with age-related neurodegenerative diseases. Interestingly, V-ATPase acidification is required for neuronal cell death associated with stroke. Clearly, V-ATPase is extremely important in neuronal physiology and pathology; more studies are required to dissect the precise mechanisms involved in the roles described in this section. Those studies likely will elucidate novel functions of V-ATPase in neurobiology.

5 V-ATPase in Infectious Disease

Although many pathogenic organisms can infect their host without entering its cells, all viruses and many bacteria and fungi require an intracellular niche for growth and proliferation. Pathogens enter cells through a variety of mechanisms, many of which require V-ATPase activity. Once inside the host cell, V-ATPase activity can either suppress or support infectious processes and pathogen replication. Here we focus on the involvement of pH and V-ATPase in the entry of viruses, bacteria and fungi into the host cell and the processes necessary to ensure pathogen replication.

5.1 Roles of V-ATPase in Viral Infections

The roles of V-ATPase function in viral infection have been particularly well studied in influenza viruses, and thus we use this enveloped virus as an example. Influenza viral infection is initiated when the virus attaches itself to the surface of a host cell using hemagglutinin (HA) and is endocytosed [145]. The acidic pH of the endosome causes a conformational change in HA, which promotes the fusion of viral and endosomal membranes and release of the viral genome into the host cell (Fig. 17.2, [5, 146–148]). Importantly, the membrane fusion mediated by HA occurs in the narrow pH range of the late endosome: pH 4.5–5.5 [145, 147–150], which is generated and maintained by V-ATPase. V-ATPase activity is increased in host cells during influenza viral infection [148], suggesting that the virus is able to manipulate

host cell V-ATPase activity to support conditions that favor infection. The importance of V-ATPase in viral infection is further emphasized by the observations that increasing glucose concentration enhances viral infection in a bafilomycin A-dependent manner [148, 150] while loss of the V_1 subunit E (isoform E2) decreases viral titer [150]. Although the exact mechanisms vary, it is now clear that V-ATPase activity is required for endocytosis and subsequent infection of numerous viruses [5, 64, 147, 150–161].

5.2 *Roles of V-ATPase in Bacterial Infections*

Pathogenic bacteria often enter the host cell, either a macrophage or epithelial cell, through phagocytosis or endocytosis, respectively [155, 162–164]. As discussed previously, V-ATPase is critical for both processes [5, 147, 150–160, 162], and its inhibition, decreases bacterial infections [161, 163, 164]. Once inside the host cell, pathogenic bacteria must either escape from the phagosome/endocytic vesicle before fusion with a lysosome, or inhibit acidification of these vesicles. Both of these processes are intimately associated with V-ATPase.

While V-ATPase activity is necessary for acidification of the host phagosomal compartments [162], it also contributes to bacterial escape from host phagosome/endocytic vesicles. *Francisella tularenis* promotes fusion of lysosomes to the phagosome. The resulting V-ATPase-dependent acidification of the phagosome is required for bacterial escape into the cytosol [165]. *Listeria monocytogenes* and several other pathogenic bacteria secrete cytolysins, pH-dependent pore-forming proteins, allowing the bacterium to escape the phagosome and successfully complete infection [166–169].

Interestingly, the host's own immune response may modify V-ATPase activity. During mycobacterial infection, cytokine expression is altered resulting in (i) increased V-ATPase assembly and acidification of lysosomes, (ii) enhanced fusion between phagosomes and lysosomes, and (iii) increased mycobacterial escape into the host cell cytoplasm [170]. Although the exact mechanism mediating enhanced V-ATPase activity has not been fully elucidated in this model, the JAK-STAT pathway appears to be important [171]. Thus, pathogenic bacteria may capitalize upon a host cell's V-ATPase activity to promote escape from the phagosome/endocytic vesicle.

Other pathogenic bacteria have evolved mechanisms to inhibit acidification of the phagosome/endocytic vesicle and thus promote their own survival and replication [162, 172, 173]; many of these mechanisms result in V-ATPase inhibition [65, 66, 163, 165, 173–176]. *Yersinia pseudotuberculosis* and *Streptococcus pyogenes* inhibits V-ATPase-dependent acidification of the phagosome [65, 174, 176]. At least two pathogenic bacteria species, *Legionella pneumophila* and *Mycobacterium tuberculosis*, target the catalytic V_1 subunit A of V-ATPases to inhibit its activity [173, 176]. Notably, studies of V-ATPase inhibition in bacterial infections also suggest that the V_1 subunit H of V-ATPase helps coordinate phagosomal and lysosomal membrane fusion, thus enlarging the role of V-ATPase in endocytic processes [176]. To summarize, several bacterial pathogens have evolved specific and unique ways to elude destruction in acidic phagosomes/endocytic vesicles by inhibiting V-ATPase.

5.3 Roles of V-ATPase in Fungal Infections

Most fungal pathogens are commensal, yet in immunocompromised patients these organisms can cause severe systemic infections that are difficult to treat and can be fatal [177, 178]. Although there are many opportunistic fungi infecting immunocompromised patients (e.g., *Aspergillus fumigatus*, *Aspergillus nidulans*, *Cryptococcus neoformans*, *Histoplasma capsulatum*, and *Pneumocystis carinii*), the most prevalent is *Candida albicans* [179–181]. A remarkable feature of fungal pathogens is their ability to survive in a broad pH range [182, 183]. This capacity is dependent upon fungal V-ATPases. When fungal V-ATPase is inhibited, pH homeostasis cannot be maintained and fungal virulence is reduced [184–188].

Like other pathogens, some fungi modify the pH of the compartments in which they are enclosed to favor their survival [5]. *Histoplasma capsulatum* inhibits host V-ATPase accumulation in the phagosomal/endocytic vesicle membrane, which increases the pathogen's survival and replication [189, 190]. Interestingly, genetic inhibition of V_1 subunit A resulted in decreased virulence of *H. capsulatum* since the pathogen was unable to acquire necessary nutrients for replication [190].

5.4 V-ATPase as a Novel Antifungal Target

Given the difficulty of treating fungal infections, and their prevalence in health care settings, V-ATPase has become an attractive antifungal therapeutic target [181, 184, 185, 188, 191, 192]. Although there are similarities between mammalian and fungal V-ATPase, there are fungi-specific isoforms for the V_o subunit a: Vph1p and Stv1p. Additionally, fungi express the Vo subunit c′ and RAVE subunit Rav2p, which are absent in humans. Pharmaceutical targeting of Vph1p, Stv1p, or Rav2p could reduce fungal infections while maintaining host cell V-ATPase activity. Another possible antifungal therapeutic target could be the fungal specific protein, Pma1p, a plasma membrane ATPase that has reciprocal interactions with V-ATPases to control cytosolic pH in fungi [188, 193, 194].

6 V-ATPase Expression, Function, and Consequence in Cancer

Several "hallmarks of cancer" have been defined by Hanahan and Weinberg. These attributes include the ability to (i) sustain growth signals, (ii) evade growth-suppressive and apoptotic signals, (iii) induce angiogenesis, (iv) invade and proliferate in local and distant sites, (v) deregulate cellular metabolism, (vi) avoid immune destruction, and (vii) proliferate indefinitely [195]. Although tumors are adaptive and self-organizing systems, it has been postulated that these defining phenotypes may be derived from a small set of effector molecules [195]. Elucidating the

fundamental drivers of the hallmarks of cancer will revolutionize cancer detection, diagnosis and treatment.

V-ATPase activity directly and indirectly contributes to many of the hallmarks of cancer described above, including: resistance to growth suppressive and apoptotic signals [196–201], altered cellular metabolism [37, 40, 48, 49, 202], regulation of signal transduction pathways [83, 87, 201, 203–209], the proliferation and migration of endothelial cells [208, 209], and the activation of tumor-promoting macrophages [210]. V-ATPase is upregulated in solid tumors and in tumor cell lines, with the highest levels of expression associated with more aggressive phenotypes (i.e., higher grade, increased metastasis and invasion, and chemoresistance) [211–213]. As described previously, V-ATPase activity is regulated by a variety of factors including intracellular and extracellular pH [40, 215], PKA and AMPK [18, 56, 57], and glycolytic metabolism [37, 49, 50, 54], each of which is altered in tumor cells [195].

6.1 V-ATPase as a Regulator of Cellular Stress Responses

There is evidence indicating that V-ATPase is a critical player in adaptation to cellular stress including alterations in nutrient availability, acute or chronic hypoxia, reactive oxygen species (ROS) and DNA damage. In cardiomyocytes inhibition of V-ATPase increases DNA damage and results in a p53 and p21-dependent cell cycle arrest [216]. Reciprocally, DNA damage increases transcription of *ATP6L*, which encodes subunit c of the proton translocation V_o domain of V-ATPase [217]. V-ATPase inhibition is associated with increased ROS and oxidative [218] and endoplasmic reticulum stress [219]. Importantly, loss of V-ATPase function is associated with increased expression of Hypoxia Inducible Factor 1α (HIF1α), a key regulator of cellular stress response [220, 221] in both normoxic and hypoxic conditions. HIF1α regulates glycolytic metabolism, increasing glucose transport into cells and expression of several glycolytic enzymes as well as lactate dehydrogenase, the protein that generates lactate. These studies are reminiscent of work demonstrating that V-ATPase is regulated by nutrient deprivation and osmotic and oxidative stress in yeast and plants [222–223]. Collectively, they suggest that the elevated levels of V-ATPase observed in tumors and tumor cell lines may underlie an adaptive cell stress response that supports resistance to cell death or arrest and continued proliferation during poor conditions.

In vitro, tumor cells consume larger quantities of glucose than normal cells. This observation is the basis of PET scans, where the uptake of labeled glucose can be used to identify tumors and metastatic lesions in vivo. Once inside the tumor cell, glucose is converted to pyruvate and subsequently to lactate via glycolysis and lactate dehydrogenase A to generate ATP and NAD^+, respectively. The utilization of glucose to generate ATP in the absence of oxidative phosphorylation is termed the Warburg Effect [5, 195, 226]. It is postulated that the increased V-ATPase observed in tumor epithelial cells may be required for the rapid removal of H^+ gen-

erated by elevated rates of glycolysis to maintain a neutral cytoplasmic pH [5, 227, 228]. However, recent experiments employing co-culture of tumor epithelial cells and fibroblasts have reexamined the Warburg effect. In these heterotypic cultures the metabolic profiles of tumor epithelial cells are quite different than that observed in more traditional culture conditions. When co-cultured with tumor epithelial cells, fibroblasts appear to employ the Warburg Effect, and export lactate and ketones to adjacent tumor epithelial cells, which use these metabolic intermediates and oxidative phosphorylation (e.g., low lactate production) to fuel rapid cellular proliferation and expansion [228–230]. In this revised model, the requirement for V-ATPase may not be limited to the need to pump H^+ generated by glycolysis out of cells and further supports the idea that V-ATPase is a component of the cellular stress response.

6.2 V-ATPase Promotes Cell Motility and Invasion

V-ATPase expression and function is also intimately associated with increased cell motility, invasion, and tumor metastasis. Early observations in breast tumor cell lines found that invasive cell lines contained acidic phagosome [231]. Subsequent studies demonstrated that V-ATPase localization to the plasma membrane and acidification of the extracellular space was associated with invasion in vitro and metastasis in vivo and that pharmacologic inhibition of V-ATPase impaired these phenotypes [71, 213, 232–234]. The role of V-ATPase in tumor cell invasion was further confirmed in several studies using genetic approaches to target V-ATPase subunits. siRNA against V_o subunit a isoforms a3 and a4, demonstrated that V-ATPase activity at both the plasma membrane and intracellular compartments is required for in vitro invasion assays [17, 233]. Using a xenograph model of hepatocellular carcinoma, Lu and colleagues demonstrated that knock down of *ATP6L*, at the proton translocation domain of V-ATPase, impaired tumor growth and metastasis [235]. An analogous study of metastatic melanoma demonstrated that loss of V_o subunit a isoform a3 also decreased metastasis [236].

There are several possible mechanisms by which V-ATPase contributes to cell motility and invasion. In pancreatic tumors, V-ATPase is found at the leading edge of the tumor where it is closely associated with matrix metalloproteinases (MMPs) [104]. Several studies have shown that V-ATPase-dependent acidification of the extracellular environment facilitates activation of MMPs which can degrade and remodel the extracellular matrix [104, 236, 237]. V-ATPase activity may also directly contribute to motility and invasion by modulating cell morphology and cytoskeletal arrangement. For example, V_1 subunit C binding to filamentous actin (f-actin) increases its rate of polymerization and enhances stability, both of which are critical steps in cell motility [238]. Similarly, loss of V-ATPase function decreases activity of the Rho-GTPase, Rac1, and impairs signaling from EGFR [239]. Rac1 is a key regulator of cytoskeletal reorganization required for motility while epidermal growth factor receptor (EGFR) participates in directed migration [239].

Collectively these studies demonstrate that V-ATPase activity at both the plasma membrane and in intracellular compartments enhances cell motility and invasion by activating extracellular MMPs and signal transduction pathways associated with cytoskeletal rearrangement and cell motility.

6.3 V-ATPase Inhibitors as Novel Chemotherapeutics

Extracellular acidification and alterations in pH gradients between the intracellular and extracellular compartments can contribute to drug resistance. Lowering the extracellular pH decreases uptake and neutralization of weakly basic drugs and their sequestration in lysosomes [240–243]. Importantly, tumor cell lines that are most resistant to conventional therapies appear to have the highest levels of V-ATPase expression [243, 244] and *ATP6L* expression is increased following exposure to chemotherapeutics [217]. Genetic repression of *ATP6L*, increases caspase-dependent cell death in several tumor cell lines exposed to conventional chemotherapeutics [245]. Similarly, decreased V-ATPase activity increases the chemo-sensitivity of breast tumor cells in vitro and in mouse xenographs [246].

V-ATPase is expressed in nearly all cells, so complete loss of all V-ATPase activity would likely be associated with significant toxicity. Thus, efforts are underway to identify isoforms of specific V-ATPase subunits that are preferentially expressed in tumors. Current studies using proton pump inhibitors (PPIs), which target H^+/K^+-ATPases, have shown promise as adjuvant or sensitizing agents [247]. Treatment with PPIs decreases chemotherapeutic extrusion to patient plasma [248]. In vitro, PPIs increase extracellular, endosomal, and lysosomal pH in tumor cell lines, decrease cell proliferation and survival, and enhance chemosensitivity, recapitulating phenotypes associated with the loss of V-ATPase activity [247–252]. Pantoprazole, a PPI, increases uptake and tumor penetration of the DNA-damaging chemotherapeutic, doxorubicin, and decreases tumor growth in animal models of cancer [248]. Perhaps, most compellingly Kastelein and colleagues have recently demonstrated that PPIs decrease the risk of neoplastic progression in patients with Barret's esophagus [253, 254]. Thus, specific or nonspecific inhibition of V-ATPase activity may enhance the efficacy of existing chemotherapeutics and may suppress cancer progression.

While V-ATPase loss or inhibition can cooperate with conventional chemotherapeutics to enhance cell death, it can also directly contribute to the induction of cell death. V-ATPase-specific inhibitors neutralized lysosomal pH, induced cell cycle arrest, and triggered apoptosis in the breast tumor cell line, MCF-7 [199]. PPI exposure also induces cell death in human gastric cancer cells [206]. De Milito and colleagues demonstrated that PPIs altered lysosomal pH and induced cell death in primary cultures of leukemic cells in vitro and in vivo, in mice. In both models, cell death was associated with increased levels of ROS and mitochondrial depolarization [199, 201]. The role of ROS in V-ATPase-dependent cell death was further elucidated using transcriptional arrays. It was found that loss of V-ATPase function

is associated with increased expression of numerous cellular stress response genes including NRF2 (nuclear factor-erythroid 2-related factor 2), a mediator of the oxidative stress response. The induction of NRF2 is additional evidence that loss of V-ATPase increases ROS [218]. Subsequent work in multiple tumor cell lines confirmed and expanded upon these results, demonstrating that loss of V-ATPase function induced cell death via mitochondrial depolarization. Interestingly, prior to mitochondrial depolarization and cell death, HIF1α and autophagy were upregulated [198]. It seems that although cells try to adapt to the loss of V-ATPase function, ultimately its loss is insurmountable.

6.4 Signal Transduction in Tumor Cells and V-ATPase

The observation that V-ATPase inhibition is associated with the transcriptional upregulation of several genes including HIF1α, IGF, VEGF and COX-2 suggests that V-ATPase may participate in important signal transduction pathways [218]. Given its roles in fundamental cellular processes like protein sorting and maturation, endocytosis, and exocytosis, this is hardly surprising. Recently it has been shown that V-ATPase depletion impairs clathrin-mediated endocytosis, resulting in accumulation of clathrin-coated vesicles at the plasma membrane [80]. V-ATPase activity is required for receptor tyrosine kinase erbB-2 (HER2) localization to the plasma membrane in breast tumor cell lines [82] where HER2 dimerizes with other epidermal growth factor receptors to regulate proliferative and anti-apoptotic pathways. In prostate tumor cells, inhibition of V-ATPase decreases secretion of PSA (Prostate Specific Antigen) and its transcript, suggesting a defect in androgen receptor function since the androgen receptor is a potent transcriptional regulator of PSA [71]. Likewise, loss of V-ATPase function mediated by siRNA or pharmacologic inhibitors impairs endocytic activation of the Rho GTPase, Rac1, and decreases cell motility [239]. V-ATPase is also linked to Wnt signaling [255]. Wnt plays a critical role during embryogenesis where it helps regulate body axis patterning, cell fate determination, and cell motility. Wnt is also a potent oncogene. Loss of V-ATPase activity downregulates Wnt signaling in human cell lines and in vivo in *Xenopus* embryos [87, 256].

Recently, it has been shown that V-ATPase function is required for mammalian target of rapamycin (mTOR) activation [257, 258]. mTOR is part of a protein complex that senses nutrient and energy levels as well as signals from growth factor receptors to control numerous biosynthetic and catabolic processes; it is a key regulator of cellular energetics and metabolism [257, 259]. Xu and colleagues recently demonstrated that epidermal growth factor (EGF) binding to its receptor (EGFR) recruits the V_1 domain of V-ATPase to endosomes and lysosomes where it associates with the V_o domain to acidify these compartments [211]. EGFR is a key regulator of mTOR. Blockade of V-ATPase function with chemical inhibitors or siRNA can also directly inhibit mTOR signaling by preventing its localization to lysosomal membranes [258]. Interestingly, V-ATPase may itself be controlled by mTOR.

mTOR coordinately regulates phosphorylation and nuclear localization of the Transcription Factor EB (TFEB). TFEB increases the transcription of several V-ATPase subunits in vitro and in vivo in mice [260]. Hence, V-ATPase and mTOR participate in a positive feedback loop. This relationship may be of particular importance in cancer, where aberrant mTOR signaling can reduce apoptosis and enhance cell proliferation. A repertoire of studies in recent years has demonstrated that V-ATPase function underlies a number of fundamental cellular processes, many of which have been implicated in carcinogenesis. It is not surprising that V-ATPase can be so intimately linked to many of the hallmarks of cancer.

7 Conclusions

V-ATPase is an ATP-dependent proton pump. By moving protons against a concentration gradient, V-ATPase plays a critical role in pH homeostasis across the endomembrane system and creates the electrochemical proton gradient required for numerous secondary transport systems. V-ATPase is composed of 14 subunits that are assembled into two domains: V_1 and V_o. Isoforms of different V-ATPase subunits direct V-ATPase to different cellular membranes (e.g., Golgi complex, endosomes, lysosomes). Given its role in key cellular processes, it is not surprising that cells have evolved several mechanisms to regulate V-ATPase activity. The best studied of these is the reversible disassembly of the V_1V_o domains.

V-ATPase is necessary for both endocytosis and exocytosis because V-ATPase regulates and senses pH and interacts with several proteins in these pathways. Thus, V-ATPase indirectly contributes to numerous signal transduction pathways in both physiologic and pathologic settings. Here we have provided a brief overview of V-ATPase function in neurodegeneration, infectious disease and cancer. There are many excellent publications that address these topics, unfortunately, due to limitations in space, we have only been able to cite of few. It is both fascinating and humbling to acknowledge that this proton pump is capable of having such profound effects. We have no doubt that future studies will continue to elucidate as yet undiscovered functions of V-ATPase.

References

1. Muench SP, Trinick J, Harrison MA (2011) Structural divergence of the rotary ATPases. Q Rev Biophys 44:311–356
2. Parra KJ, Chan C-Y, Chen J (2014) Saccharomyces cerevisiae vacuolar H + -ATPase regulation by disassembly and reassembly: one structure and multiple signals. Eukaryot Cell 13:706–714
3. Marshansky V, Rubinstein JL, Grüber G (2014) Eukaryotic V-ATPase: novel structural findings and functional insights. Biochim Biophys Acta 1837:857–879
4. Zhao J, Rubinstein JL (2014) The study of vacuolar-type ATPases by single particle electron microscopy. Biochem Cell Biol 92:460–466

5. Forgac M (2007) Vacuolar ATPases: rotary proton pumps in physiology and pathophysiology. Nat Rev Mol Cell Biol 8:917–929
6. Kane PM (2006) The where, when, and how of organelle acidification by the yeast vacuolar H + -ATPase. Microbiol Mol Biol Rev 70:177–191
7. Nakanishi-Matsui M, Sekiya M, Nakamoto RK et al (2010) The mechanism of rotating proton pumping ATPases. Biochim Biophys Acta 1797:1343–1352
8. Futai M, Nakanishi-Matsui M, Okamoto H et al (2012) Rotational catalysis in proton pumping ATPases: from E. coli F-ATPase to mammalian V-ATPase. Biochim Biophys Acta 1817:1711–1721
9. Hirata T, Iwamoto-Kihara A, Sun-Wada G-H et al (2003) Subunit rotation of vacuolar-type proton pumping ATPase relative rotation of the G and c subunits. J Biol Chem 278:23714–23719
10. Nelson N, Perzov N, Cohen A et al (2000) The cellular biology of proton-motive force generation by V-ATPase. J Exp Biol 203:89–95
11. Kane PM (1995) Disassembly and reassembly of the yeast vacuolar H^+-ATPase in vivo. J Biol Chem 270:17025–17032
12. Feng Y, Forgac M (1992) A novel mechanism for regulation of vacuolar acidification. J Biol Chem 267:19769–19772
13. Feng Y, Forgac M (1994) Inhibition of vacuolar H(+)-ATPase by disulfide bond formation between cysteine 254 and cysteine 532 in subunit A. J Biol Chem 269:13224–13230
14. Müller ML, Jensen M, Taiz L (1999) The vacuolar H + -ATPase of lemon fruits is regulated by variable H+/ATP coupling and slip. J Biol Chem 274:10706–10716
15. Müller ML, Taiz L (2002) Regulation of the lemon-fruit V-ATPase by variable stoichiometry and organic acids. J Membr Biol 185:209–220
16. Toyomura T, Murata Y, Yamamoto A et al (2003) From lysosomes to the plasma membrane localization of vacuolar type H + -ATPase with the a3 isoform during osteoclast differentiation. J Biol Chem 278:22023–22030
17. Hinton A, Sennoune SR, Bond S et al (2009) Function of a subunit isoforms of the V-ATPase in pH homeostasis and in vitro invasion of MDA-MB231 human breast cancer cells. J Biol Chem 284:16400–16408
18. Alzamora R, Thali RF, Gong F et al (2010) PKA regulates vacuolar H + -ATPase localization and activity via direct phosphorylation of the A subunit in kidney cells. J Biol Chem 285:24676–24685
19. Lee M-R, Lee G-H, Lee H-Y et al (2014) BAX inhibitor-1-associated V-ATPase glycosylation enhances collagen degradation in pulmonary fibrosis. Cell Death Dis 5, e1113
20. Mulberg AE, Tulk BM, Forgac M (1991) Modulation of coated vesicle chloride channel activity and acidification by reversible protein kinase A-dependent phosphorylation. J Biol Chem 266:20590–20593
21. Nishi T, Forgac M (2002) The vacuolar (H+)-ATPases – nature's most versatile proton pumps. Nat Rev Mol Cell Biol 3:94–103
22. Nelson N (2003) A journey from mammals to yeast with vacuolar H + -ATPase (V-ATPase). J Bioenerg Biomembr 35:281–289
23. Arai H, Pink S, Forgac M (1989) Interaction of anions and ATP with the coated vesicle proton pump. Biochemistry (Mosc) 28:3075–3082
24. Shao E, Forgac M (2004) Involvement of the nonhomologous region of subunit A of the yeast V-ATPase in coupling and in vivo dissociation. J Biol Chem 279:48663–48670
25. Manolson MF, Wu B, Proteau D et al (1994) STV1 gene encodes functional homologue of 95-kDa yeast vacuolar H(+)-ATPase subunit Vph1p. J Biol Chem 269:14064–14074
26. Manolson MF, Proteau D, Preston RA et al (1992) The VPH1 gene encodes a 95-kDa integral membrane polypeptide required for in vivo assembly and activity of the yeast vacuolar H(+)-ATPase. J Biol Chem 267:14294–14303
27. Kawasaki-Nishi S, Nishi T, Forgac M (2001) Yeast V-ATPase complexes containing different isoforms of the 100-kDa a-subunit differ in coupling efficiency and in vivo dissociation. J Biol Chem 276:17941–17948

28. Shao E, Nishi T, Kawasaki-Nishi S, Forgac M (2003) Mutational analysis of the non-homologous region of subunit A of the yeast V-ATPase. J Biol Chem 278:12985–12991
29. Owegi MA, Pappas DL, Finch MW et al (2006) Identification of a domain in the Vo subunit d that is critical for coupling of the yeast vacuolar proton-translocating ATPase. J Biol Chem 281:30001–30014
30. Curtis KK, Kane PM (2002) Novel vacuolar H + -ATPase complexes resulting from overproduction of Vma5p and Vma13p. J Biol Chem 277:2716–2724
31. Tojo A, Guzman NJ, Garg LC et al (1994) Nitric oxide inhibits bafilomycin-sensitive H(+)-ATPase activity in rat cortical collecting duct. Am J Physiol 267:F509–F515
32. Dschida WJA, Bowman BJ (1995) The vacuolar ATPase: sulfite stabilization and the mechanism of nitrate inactivation. J Biol Chem 270:1557–1563
33. Oluwatosin YE, Kane PM (1997) Mutations in the CYS4 gene provide evidence for regulation of the yeast vacuolar H + -ATPase by oxidation and reduction in vivo. J Biol Chem 272:28149–28157
34. Grüber G, Radermacher M, Ruiz T et al (2000) Three-dimensional structure and subunit topology of the V1 ATPase from *Manduca sexta* midgut. Biochemistry (Mosc) 39:8609–8616
35. Sumner J-P, Dow JAT, Earley FGP et al (1995) Regulation of plasma membrane V-ATPase activity by dissociation of peripheral subunits. J Biol Chem 270:5649–5653
36. Trombetta ES, Ebersold M, Garrett W et al (2003) Activation of lysosomal function during dendritic cell maturation. Science 299:1400–1403
37. Nakamura S (2004) Glucose activates H + -ATPase in kidney epithelial cells. Am J Physiol Cell Physiol 287:C97–C105
38. Lafourcade C, Sobo K, Kieffer-Jaquinod S, Garin J, van der Goot FG (2008) Regulation of the V-ATPase along the endocytic pathway occurs through reversible subunit association and membrane localization. PLoS One 3(7), e2758
39. Parra KJ, Kane PM (1998) Reversible association between the V1 and V0 domains of yeast vacuolar H + -ATPase is an unconventional glucose-induced effect. Mol Cell Biol 18:7064–7074
40. Dechant R, Binda M, Lee SS et al (2010) Cytosolic pH is a second messenger for glucose and regulates the PKA pathway through V-ATPase. EMBO J 29:2515–2526
41. Bond S, Forgac M (2008) The Ras/cAMP/protein kinase A pathway regulates glucose-dependent assembly of the vacuolar (H+)-ATPase in yeast. J Biol Chem 283:36513–36521
42. Kane PM (2012) Targeting reversible disassembly as a mechanism of controlling V-ATPase activity. Curr Protein Pept Sci 13:117–123
43. Smardon AM, Tarsio M, Kane PM (2002) The RAVE complex is essential for stable assembly of the yeast V-ATPase. J Biol Chem 277:13831–13839
44. Smardon AM, Kane PM (2007) RAVE is essential for the efficient assembly of the c subunit with the vacuolar H + -ATPase. J Biol Chem 282:26185–26194
45. Smardon AM, Diab HI, Tarsio M et al (2014) The RAVE complex is an isoform-specific V-ATPase assembly factor in yeast. Mol Biol Cell 25:356–367
46. Seol JH, Shevchenko A, Shevchenko A, Deshaies RJ (2001) Skp1 forms multiple protein complexes, including RAVE, a regulator of V-ATPase assembly. Nat Cell Biol 3:384–391
47. Sethi N, Yan Y, Quek D et al (2010) Rabconnectin-3 is a functional regulator of mammalian notch signaling. J Biol Chem 285:34757–34764
48. Lu M, Holliday LS, Zhang L et al (2001) Interaction between aldolase and vacuolar H^+-ATPase evidence for direct coupling of glycolysis to the ATP-hydrolyzing proton pump. J Biol Chem 276:30407–30413
49. Su Y, Zhou A, Al-Lamki RS, Karet FE (2003) The a-subunit of the V-type H + -ATPase interacts with phosphofructokinase-1 in humans. J Biol Chem 278:20013–20018
50. Sautin YY, Lu M, Gaugler A et al (2005) Phosphatidylinositol 3-kinase-mediated effects of glucose on vacuolar H + -ATPase assembly, translocation, and acidification of intracellular compartments in renal epithelial cells. Mol Cell Biol 25:575–589

51. Lu M, Ammar D, Ives H et al (2007) Physical interaction between aldolase and vacuolar H + -ATPase is essential for the assembly and activity of the proton pump. J Biol Chem 282:24495–24503
52. Lu M, Sautin YY, Holliday LS, Gluck SL (2004) The glycolytic enzyme aldolase mediates assembly, expression, and activity of vacuolar H + -ATPase. J Biol Chem 279:8732–8739
53. Chan C-Y, Parra KJ (2014) Yeast phosphofructokinase-1 subunit Pfk2p is necessary for pH homeostasis and glucose-dependent vacuolar ATPase reassembly. J Biol Chem 289:19448–19457
54. Su Y, Blake-Palmer KG, Sorrell S et al (2008) Human H + ATPase a4 subunit mutations causing renal tubular acidosis reveal a role for interaction with phosphofructokinase-1. Am J Physiol Renal Physiol 295:F950–F958
55. Tiburcy F, Beyenbach KW, Wieczorek H (2013) Protein kinase A-dependent and -independent activation of the V-ATPase in Malpighian tubules of Aedes aegypti. J Exp Biol 216:881–891
56. Alzamora R, Al-Bataineh MM, Liu W et al (2013) AMP-activated protein kinase regulates the vacuolar H + -ATPase via direct phosphorylation of the A subunit (ATP6V1A) in the kidney. Am J Physiol Renal Physiol 305:F943–F956
57. Al-bataineh Mohammad M, Gong F, Marciszyn AL, Myerburg MM, Pastor-Soler NM (2014) Regulation of proximal tubule vacuolar H + -ATPase by PKA and AMP-activated protein kinase. Am J Physiol Renal Physiol 306:F981–F995
58. Dechant R, Saad S, Ibáñez AJ, Peter M (2014) Cytosolic pH regulates cell growth through distinct GTPases, Arf1 and Gtr1, to promote Ras/PKA and TORC1 activity. Mol Cell 55:409–421
59. Marshansky V (2007) The V-ATPase a2-subunit as a putative endosomal pH-sensor. Biochem Soc Trans 35:1092–1099
60. Diakov TT, Kane PM (2010) Regulation of vacuolar proton-translocating ATPase activity and assembly by extracellular pH. J Biol Chem 285:23771–23778
61. Padilla-López S, Pearce DA (2006) Saccharomyces cerevisiae lacking Btn1p modulate vacuolar ATPase activity to regulate pH imbalance in the vacuole. J Biol Chem 281:10273–10280
62. Hackstadt T (2000) Redirection of host vesicle trafficking pathways by intracellular parasites. Traffic 1:93–99
63. Méresse S, Steele-Mortimer O, Moreno E et al (1999) Controlling the maturation of pathogen-containing vacuoles: a matter of life and death. Nat Cell Biol 1:E183–E188
64. Suzuki T, Yamaya M, Sekizawa K et al (2001) Bafilomycin A1 inhibits rhinovirus infection in human airway epithelium: effects on endosome and ICAM-1. Am J Physiol Lung Cell Mol Physiol 280:L1115–L1127
65. Tsukano H, Kura F, Inoue S et al (1999) Yersinia pseudotuberculosis blocks the phagosomal acidification of B10.A mouse macrophages through the inhibition of vacuolar H + -ATPase activity. Microb Pathog 27:253–263
66. Wong D, Bach H, Sun J et al (2011) Mycobacterium tuberculosis protein tyrosine phosphatase (PtpA) excludes host vacuolar-H + –ATPase to inhibit phagosome acidification. Proc Natl Acad Sci 108:19371–19376
67. Aridor M, Hannan LA (2002) Traffic Jams II: an update of diseases of intracellular transport. Traffic 3:781–790
68. Olkkonen VM, Ikonen E (2000) Genetic defects of intracellular-membrane transport. N Engl J Med 343:1095–1104
69. Shacka JJ, Klocke BJ, Roth KA (2006) Autophagy, bafilomycin and cell death: the "A-B-Cs" of plecomacrolide-induced neuroprotection. Autophagy 2:228–230
70. Syntichaki P, Samara C, Tavernarakis N (2005) The vacuolar H + -ATPase mediates intracellular acidification required for neurodegeneration in C. elegans. Curr Biol 15:1249–1254
71. Michel V, Licon-Munoz Y, Trujillo K et al (2013) Inhibitors of vacuolar ATPase proton pumps inhibit human prostate cancer cell invasion and prostate-specific antigen expression and secretion. Int J Cancer 132:E1–E10

72. Mindell JA (2012) Lysosomal acidification mechanisms. Annu Rev Physiol 74:69–86. doi:10.1146/annurev-physiol-012110-142317
73. Beyenbach KW, Wieczorek H (2006) The V-type H+ ATPase: molecular structure and function, physiological roles and regulation. J Exp Biol 209:577–589
74. Gaxiola RA, Palmgren MG, Schumacher K (2007) Plant proton pumps. FEBS Lett 581:2204–2214
75. Toei M, Saum R, Forgac M (2010) Regulation and isoform function of the V-ATPases. Biochemistry (Mosc) 49:4715–4723
76. Marshansky V, Futai M (2008) The V-type H + -ATPase in vesicular trafficking: targeting, regulation and function. Curr Opin Cell Biol 20:415–426
77. Sun-Wada G-H, Murata Y, Yamamoto A et al (2000) Acidic endomembrane organelles are required for mouse postimplantation development. Dev Biol 228:315–325
78. Oka T, Toyomura T, Honjo K et al (2001) Four subunit a isoforms of Caenorhabditis elegans vacuolar H + -ATPase cell-specific expression during development. J Biol Chem 276:33079–33085
79. Hurtado-Lorenzo A, Skinner M, El Annan J et al (2006) V-ATPase interacts with ARNO and Arf6 in early endosomes and regulates the protein degradative pathway. Nat Cell Biol 8:124–136
80. Kozik P, Hodson NA, Sahlender DA et al (2013) A human genome-wide screen for regulators of clathrin-coated vesicle formation reveals an unexpected role for the V-ATPase. Nat Cell Biol 15:50–60
81. Sun-Wada G-H, Tabata H, Kawamura N et al (2009) Direct recruitment of H + -ATPase from lysosomes for phagosomal acidification. J Cell Sci 122:2504–2513
82 .Von Schwarzenberg K, Lajtos T, Simon L et al (2014) V-ATPase inhibition overcomes trastuzumab resistance in breast cancer. Mol Oncol 8:9–19
83. Scherer O, Steinmetz H, Kaether C et al (2014) Targeting V-ATPase in primary human monocytes by archazolid potently represses the classical secretion of cytokines due to accumulation at the endoplasmic reticulum. Biochem Pharmacol 91:490–500
84. Kubisch R, Fröhlich T, Arnold GJ et al (2014) V-ATPase inhibition by archazolid leads to lysosomal dysfunction resulting in impaired cathepsin B activation in vivo. Int J Cancer 134:2478–2488
85. Baravalle G, Schober D, Huber M et al (2005) Transferrin recycling and dextran transport to lysosomes is differentially affected by bafilomycin, nocodazole, and low temperature. Cell Tissue Res 320:99–113
86. Bayer N, Schober D, Prchla E et al (1998) Effect of bafilomycin A1 and nocodazole on endocytic transport in HeLa Cells: implications for viral uncoating and infection. J Virol 72:9645–9655
87. Cruciat C-M, Ohkawara B, Acebron SP et al (2010) Requirement of prorenin receptor and vacuolar H + -ATPase-mediated acidification for Wnt signaling. Science 327:459–463
88. Kim W, Kim M, Jho E (2013) Wnt/β-catenin signalling: from plasma membrane to nucleus. Biochem J 450:9–21
89. Tuttle AM, Hoffman TL, Schilling TF (2014) Rabconnectin-3a regulates vesicle endocytosis and canonical Wnt signaling in zebrafish neural crest migration. PLoS Biol 12, e1001852
90. Maranda B, Brown D, Bourgoin S et al (2001) Intra-endosomal pH-sensitive recruitment of the Arf-nucleotide exchange factor ARNO and Arf6 from cytoplasm to proximal tubule endosomes. J Biol Chem 276:18540–18550
91. Donaldson JG (2003) Multiple roles for Arf6: sorting, structuring, and signaling at the plasma membrane. J Biol Chem 278:41573–41576
92. Shmuel M, Santy LC, Frank S (2006) ARNO through its coiled-coil domain regulates endocytosis at the apical surface of polarized epithelial cells. J Biol Chem 281:13300–13308
93. Monier S, Chardin P, Robineau S, Goud B (1998) Overexpression of the ARF1 exchange factor ARNO inhibits the early secretory pathway and causes the disassembly of the Golgi complex. J Cell Sci 111(Pt 22):3427–3436

94. Hosokawa H, Dip PV, Merkulova M et al (2013) The N termini of a-subunit isoforms are involved in signaling between vacuolar H + -ATPase (V-ATPase) and cytohesin-2. J Biol Chem 288:5896–5913
95. Ernstrom GG, Weimer R, Pawar DRL et al (2012) V-ATPase V1 sector is required for corpse clearance and neurotransmission in Caenorhabditis elegans. Genetics 191:461–475
96. Yan Y, Denef N, Schüpbach T (2009) The vacuolar proton pump (V-ATPase) is required for Notch signaling and endosomal trafficking in Drosophila. Dev Cell 17:387–402
97. Brown D, Paunescu TG, Breton S, Marshansky V (2009) Regulation of the V-ATPase in kidney epithelial cells: dual role in acid–base homeostasis and vesicle trafficking. J Exp Biol 212:1762–1772
98. O'Callaghan KM, Ayllon V, O'Keeffe J et al (2010) Heme-binding protein HRG-1 is induced by insulin-like growth factor I and associates with the vacuolar H + -ATPase to control endosomal pH and receptor trafficking. J Biol Chem 285:381–391
99. Bonifacino JS, Glick BS (2004) The mechanisms of vesicle budding and fusion. Cell 116:153–166
100. Peri F, Nüsslein-Volhard C (2008) Live imaging of neuronal degradation by microglia reveals a role for v0-ATPase a1 in phagosomal fusion in vivo. Cell 133:916–927
101. Peters C, Bayer MJ, Bühler S et al (2001) Trans-complex formation by proteolipid channels in the terminal phase of membrane fusion. Nature 409:581–588
102. Strasser B, Iwaszkiewicz J, Michielin O, Mayer A (2011) The V-ATPase proteolipid cylinder promotes the lipid-mixing stage of SNARE-dependent fusion of yeast vacuoles. EMBO J 30:4126–4141
103. Poëa-Guyon S, Ammar MR, Erard M et al (2013) The V-ATPase membrane domain is a sensor of granular pH that controls the exocytotic machinery. J Cell Biol 203:283–298
104. Chung C, Mader CC, Schmitz J et al (2011) The vacuolar-ATPase (V-ATPase) modulates matrix metalloproteinase (MMP) isoforms in human pancreatic cancer. Lab Invest J Tech Methods Pathol 91:732–743
105. Xu X, Liu B, Zou P et al (2014) Silencing of LASS2/TMSG1 enhances invasion and metastasis capacity of prostate cancer cell. J Cell Biochem 115:731–743
106. Sun-Wada GH, Wada Y (2015) Role of vacuolar-type proton ATPase in signal transduction. Biochem Biophys Acat 10:1166–1172
107. Sun-Wada G-H, Toyomura T, Murata Y et al (2006) The a3 isoform of V-ATPase regulates insulin secretion from pancreatic β-cells. J Cell Sci 119:4531–4540
108. Tapper H, Sundler R (1995) Bafilomycin A1 inhibits lysosomal, phagosomal, and plasma membrane H(+)-ATPase and induces lysosomal enzyme secretion in macrophages. J Cell Physiol 163:137–144
109. Ghosh P, Dahms NM, Kornfeld S (2003) Mannose 6-phosphate receptors: new twists in the tale. Nat Rev Mol Cell Biol 4:202–212
110. Van Weert AW, Dunn KW, Geuze HJ et al (1995) Transport from late endosomes to lysosomes, but not sorting of integral membrane proteins in endosomes, depends on the vacuolar proton pump. J Cell Biol 130:821–834
111. Pereda AE (2014) Electrical synapses and their functional interactions with chemical synapses. Nat Rev Neurosci 15:250–263
112. Takamori S, Holt M, Stenius K et al (2006) Molecular anatomy of a trafficking organelle. Cell 127:831–846
113. Wilhelm BG, Mandad S, Truckenbrodt S et al (2014) Composition of isolated synaptic boutons reveals the amounts of vesicle trafficking proteins. Science 344:1023–1028
114. El Mestikawy S, Wallén-Mackenzie Å, Fortin GM et al (2011) From glutamate co-release to vesicular synergy: vesicular glutamate transporters. Nat Rev Neurosci 12:204–216
115. Maycox PR, Deckwerth T, Hell JW, Jahn R (1988) Glutamate uptake by brain synaptic vesicles. Energy dependence of transport and functional reconstitution in proteoliposomes J Biol Chem 263:15423–15428
116. Einhorn Z, Trapani JG, Liu Q, Nicolson T (2012) Rabconnectin3α promotes stable activity of the H+ pump on synaptic vesicles in hair cells. J Neurosci 32:11144–11156

117. Rizo J, Südhof TC (2002) Snares and munc18 in synaptic vesicle fusion. Nat Rev Neurosci 3:641–653
118. Hiesinger PR, Fayyazuddin A, Mehta SQ et al (2005) The v-ATPase V0 subunit a1 is required for a late step in synaptic vesicle exocytosis in Drosophila. Cell 121:607–620
119. Di Giovanni J, Boudkkazi S, Mochida S et al (2010) V-ATPase membrane sector associates with synaptobrevin to modulate neurotransmitter release. Neuron 67:268–279
120. Morel N (2003) Neurotransmitter release: the dark side of the vacuolar-H + ATPase. Biol Cell Auspices Eur Cell Biol Organ 95:453–457
121. El Far O, Seagar M (2011) SNARE, V-ATPase and neurotransmission. Méd Sci 27:28–31
122. Vavassori S, Mayer A (2014) A new life for an old pump: V-ATPase and neurotransmitter release. J Cell Biol 205:7–9
123. Morel N, Dunant Y, Israël M (2001) Neurotransmitter release through the V0 sector of V-ATPase. J Neurochem 79:485–488
124. Südhof TC (2013) A molecular machine for neurotransmitter release: synaptotagmin and beyond. Nat Med 19:1227–1231
125. Hirasawa H, Yamada M, Kaneko A (2012) Acidification of the synaptic cleft of cone photoreceptor terminal controls the amount of transmitter release, thereby forming the receptive field surround in the vertebrate retina. J Physiol Sci 62:359–375
126. Jouhou H, Yamamoto K, Homma A et al (2007) Depolarization of isolated horizontal cells of fish acidifies their immediate surrounding by activating V-ATPase. J Physiol 585:401–412
127. Wang T-M, Holzhausen LC, Kramer RH (2014) Imaging an optogenetic pH sensor reveals that protons mediate lateral inhibition in the retina. Nat Neurosci 17:262–268
128. Ikemoto A, Bole DG, Ueda T (2003) Glycolysis and glutamate accumulation into synaptic vesicles role of glyceraldehyde phosphate dehydrogenase and 3-phosphoglycerate kinase. J Biol Chem 278:5929–5940
129. Yamada KA, Rensing N, Izumi Y et al (2004) Repetitive hypoglycemia in young rats impairs hippocampal long-term potentiation. Pediatr Res 55:372–379
130. Ross CA, Poirier MA (2004) Protein aggregation and neurodegenerative disease. Nat Med 10:10–17
131. Nixon RA (2006) Autophagy in neurodegenerative disease: friend, foe or turncoat? Trends Neurosci 29:528–535
132. Lee J-H, Yu WH, Kumar A et al (2010) Lysosomal proteolysis and autophagy require presenilin 1 and are disrupted by Alzheimer-related PS1 mutations. Cell 141:1146–1158
133. Cataldo AM, Peterhoff CM, Schmidt SD et al (2004) Presenilin mutations in familial Alzheimer disease and transgenic mouse models accelerate neuronal lysosomal pathology. J Neuropathol Exp Neurol 63:821–830
134. Metcalf DJ, García-Arencibia M, Hochfeld WE, Rubinsztein DC (2012) Autophagy and misfolded proteins in neurodegeneration. Exp Neurol 238:22–28
135. Nixon RA (2013) The role of autophagy in neurodegenerative disease. Nat Med 19:983–997
136. Wong E, Cuervo AM (2010) Autophagy gone awry in neurodegenerative diseases. Nat Neurosci 13:805–811
137. Mehrpour M, Esclatine A, Beau I, Codogno P (2010) Overview of macroautophagy regulation in mammalian cells. Cell Res 20:748–762
138. Nixon RA, Wegiel J, Kumar A et al (2005) Extensive involvement of autophagy in Alzheimer disease: an immuno-electron microscopy study. J Neuropathol Exp Neurol 64:113–122
139. Anglade P, Vyas S, Javoy-Agid F et al (1997) Apoptosis and autophagy in nigral neurons of patients with Parkinson's disease. Histol Histopathol 12:25–31
140. Sapp E, Schwarz C, Chase K et al (1997) Huntingtin localization in brains of normal and Huntington's disease patients. Ann Neurol 42:604–612
141. Williamson WR, Wang D, Haberman AS, Hiesinger PR (2010) A dual function of V0-ATPase a1 provides an endolysosomal degradation mechanism in Drosophila melanogaster photoreceptors. J Cell Biol 189:885–899

142. Williamson WR, Hiesinger PR (2010) On the role of v-ATPase V0a1-dependent degradation in Alzheimer disease. Commun Integr Biol 3:604–607
143. Pamenter ME, Ryu J, Hua ST et al (2012) DIDS prevents ischemic membrane degradation in cultured hippocampal neurons by inhibiting matrix metalloproteinase release. PLoS One 7, e43995
144. Lo EH (2008) A new penumbra: transitioning from injury into repair after stroke. Nat Med 14:497–500
145. Sieczkarski SB, Brown HA, Whittaker GR (2003) Role of protein kinase C βII in influenza virus entry via late endosomes. J Virol 77:460–469
146. Pinto LH, Lamb RA (2006) The M2 proton channels of influenza A and B viruses. J Biol Chem 281:8997–9000
147. Adamson AL, Chohan K, Swenson J, LaJeunesse D (2011) A Drosophila model for genetic analysis of influenza viral/host interactions. Genetics 189:495–506
148. Kohio HP, Adamson AL (2013) Glycolytic control of vacuolar-type ATPase activity: a mechanism to regulate influenza viral infection. Virology 444:301–309
149. Hoekstra D, Klappe K (1993) Fluorescence assays to monitor fusion of enveloped viruses. In: Duzgunees N (ed) Methods enzymology. Academic, Waltham, MA, pp 261–276
150. Marjuki H, Gornitzky A, Marathe BM et al (2011) Influenza A virus-induced early activation of ERK and PI3K mediates V-ATPase-dependent intracellular pH change required for fusion. Cell Microbiol 13:587–601
151. Umata T, Moriyama Y, Futai M, Mekada E (1990) The cytotoxic action of diphtheria toxin and its degradation in intact Vero cells are inhibited by bafilomycin A1, a specific inhibitor of vacuolar-type H(+)-ATPase. J Biol Chem 265:21940–21945
152. Müller KH, Spoden GA, Scheffer KD et al (2014) Inhibition by cellular vacuolar ATPase impairs human papillomavirus uncoating and infection. Antimicrob Agents Chemother 58:2905–2911
153. Vidricaire G, Imbeault M, Tremblay MJ (2004) Endocytic host cell machinery plays a dominant role in intracellular trafficking of incoming human immunodeficiency virus type 1 in human placental trophoblasts. J Virol 78:11904–11915
154. Gruenberg J, van der Goot FG (2006) Mechanisms of pathogen entry through the endosomal compartments. Nat Rev Mol Cell Biol 7:495–504
155. Hunt SR, Hernandez R, Brown DT (2011) Role of the vacuolar-ATPase in Sindbis virus infection. J Virol 85:1257–1266
156. Miller ME, Adhikary S, Kolokoltsov AA, Davey RA (2012) Ebolavirus requires acid sphingomyelinase activity and plasma membrane sphingomyelin for infection. J Virol 86:7473–7483
157. Yip CW, Hon CC, Zeng F, Leung FCC (2012) Cell culture-adapted IBDV uses endocytosis for entry in DF-1 chicken embryonic fibroblasts. Virus Res 165:9–16
158. Chen H-W, Cheng JX, Liu M-T et al (2013) Inhibitory and combinatorial effect of diphyllin, a v-ATPase blocker, on influenza viruses. Antiviral Res 99:371–382
159. Silva-Ayala D, López T, Gutiérrez M et al (2013) Genome-wide RNAi screen reveals a role for the ESCRT complex in rotavirus cell entry. Proc Natl Acad Sci U S A 110:10270–10275
160. Arias CF, Silva-Ayala D, López S (2015) Rotavirus entry: a deep journey into the cell with several exits. J Virol 89:890–893
161. Abrami L, Reig N, van der Goot FG (2005) Anthrax toxin: the long and winding road that leads to the kill. Trends Microbiol 13:72–78
162. Flannagan RS, Jaumouillé V, Grinstein S (2012) The cell biology of phagocytosis. Annu Rev Pathol Mech Dis 7:61–98
163. Drecktrah D, Knodler LA, Howe D, Steele-Mortimer O (2007) Salmonella trafficking is defined by continuous dynamic interactions with the endolysosomal system. Traffic Cph Den 8:212–225
164. Arpaia N, Godec J, Lau L et al (2011) TLR signaling is required for virulence of an intracellular pathogen. Cell 144:675–688

165. Santic M, Asare R, Skrobonja I et al (2008) Acquisition of the vacuolar ATPase proton pum ad phagosome acidification are essential for escape of Francisella tularensis into the macrophage cytosol. Infect Immun 76:2671–2677
166. Birmingham CL, Canadien V, Kaniuk NA et al (2008) Listeriolysin O allows Listeria monocytogenes replication in macrophage vacuoles. Nature 451:350–354
167. Portnoy DA, Chakraborty T, Goebel W, Cossart P (1992) Molecular determinants of Listeria monocytogenes pathogenesis. Infect Immun 60:1263–1267
168. Tweten RK (2005) Cholesterol-dependent cytolysins, a family of versatile pore-forming toxins. Infect Immun 73:6199–6209
169. Petchampai N, Sunyakumthorn P, Guillotte ML et al (2014) Molecular and functional characterization of vacuolar-ATPase from the American dog tick Dermacentor variabilis. Insect Mol Biol 23:42–51
170. Mansilla Pareja ME, Colombo MI (2013) Autophagic clearance of bacterial pathogens: molecular recognition of intracellular microorganisms. Front Cell Infect Microbiol 3:54
171. Jung CW, Shih L-Y, Xiao Z et al (2014) Efficacy and safety of ruxolitinib in Asian patients with myelofibrosis. Leuk Lymphoma 1–8
172. Schwartz JT, Allen L-AH (2006) Role of urease in megasome formation and Helicobacter pylori survival in macrophages. J Leukoc Biol 79:1214–1225
173. Xu L, Shen X, Bryan A et al (2010) Inhibition of host vacuolar H + -ATPase activity by a Legionella pneumophila effector. PLoS Pathog 6:1000822
174. Nordenfelt P, Grinstein S, Björck L, Tapper H (2012) V-ATPase-mediated phagosomal acidification is impaired by Streptococcus pyogenes through Mga-regulated surface proteins. Microbes Infect 14:1319–1329
175. Tsukano H, Kura F, Inoues et al (1999) Yessernia pseudotuberculosis blocks the phagosomal acidification of B10A mouse macrophages through inhibition of vacuolar H (+) -ATPase acivity. Microb Pathog 4:253–263
176. Wong D, Bach H, Sun J et al (2011) Mycobacterium tuberculosis protein tyrosine phosphatase (PtpA) excludes host vacuolar H+-ATPase to inhibit phagosome acidifcation. Proc Natl Acad Sci USA 48:19371–19376
177. Moran C, Grussemeyer CA, Spalding JR et al (2009) Candida albicans and non-albicans bloodstream infections in adult and pediatric patients: comparison of mortality and costs. Pediatr Infect Dis J 28:433–435
178. Brissaud O, Guichoux J, Harambat J et al (2012) Invasive fungal disease in PICU: epidemiology and risk factors. Ann Intensive Care 2:6
179. Perlin DS (1998) Ion pumps as targets for therapeutic intervention: old and new paradigms. Electron J Biotechnol 1:55–64
180. Olsen I (2014) Attenuation of Candida albicans virulence with focus on disruption of its vacuole functions. J Oral Microbiol 6, PMC3974176
181. Davis DA (2009) How human pathogenic fungi sense and adapt to pH: the link to virulence. Curr Opin Microbiol 12:365–370
182. Sudbery P, Gow N, Berman J (2004) The distinct morphogenic states of Candida albicans. Trends Microbiol 12:317–324
183. Kabir MA, Hussain MA, Ahmad Z (2012) Candida albicans: a model organism for studying fungal pathogens. ISRN Microbiol 2012:Article ID 538694
184. Zhang Y-Q, Gamarra S, Garcia-Effron G et al (2010) Requirement for ergosterol in V-ATPase function underlies antifungal activity of azole drugs. PLoS Pathog 6(6):1000939
185. Patenaude C, Zhang Y, Cormack B et al (2013) Essential role for vacuolar acidification in Candida albicans virulence. J Biol Chem 288:26256–26264
186. Rane HS, Bernardo SM, Raines SM et al (2013) Candida albicans VMA3 is necessary for V-ATPase assembly and function and contributes to secretion and filamentation. Eukaryot Cell 12:1369–1382
187. Erickson T, Liu L, Gueyikian A et al (2001) Multiple virulence factors of Cryptococcus neoformans are dependent on VPH1. Mol Microbiol 42:1121–1131
188. Hayek SR, Lee SA, Parra KJ (2014) Advances in targeting the vacuolar proton-translocating ATPase (V-ATPase) for anti-fungal therapy. Front Pharmacol 5:4

189. Strasser JE, Newman SL, Ciraolo GM et al (1999) Regulation of the macrophage vacuolar ATPase and phagosome-lysosome fusion by Histoplasma capsulatum. J Immunol 162:6148–6154
190. Hilty J, Smulian AG, Newman SL (2008) The Histoplasma capsulatum vacuolar ATPase is required for iron homeostasis, intracellular replication in macrophages, and virulence in a murine model of histoplasmosis. Mol Microbiol 70:127–139
191. Parra KJ (2012) Vacuolar ATPase: a model proton pump for antifungal drug discovery. In: Tegos A, Mylonakis E (eds) Antimicrobial drug discovery: emerging strategies. CABI, Wallingford, CT, pp 89–100
192. Zhang Y-Q, Rao R (2010) Beyond ergosterol: linking pH to antifungal mechanisms. Virulence 1:551–554
193. Martínez-Muñoz GA, Kane P (2008) Vacuolar and plasma membrane proton pumps collaborate to achieve cytosolic pH homeostasis in yeast. J Biol Chem 283:20309–20319
194. Tarsio M, Zheng H, Smardon AM et al (2011) Consequences of loss of Vph1 protein-containing vacuolar ATPases (V-ATPases) for overall cellular pH homeostasis. J Biol Chem 286:28089–28096
195. Hanahan D, Weinberg RA (2011) Hallmarks of cancer: the next generation. Cell 144:646–674
196. Graham RM, Thompson JW, Webster KA (2014) Inhibition of the vacuolar ATPase induces Bnip3-dependent death of cancer cells and a reduction in tumor burden and metastasis. Oncotarget 5:1162–1173
197. Schempp CM, von Schwarzenberg K, Schreiner L et al (2014) V-ATPase inhibition regulates anoikis resistance and metastasis of cancer cells. Mol Cancer Ther 13:926–937
198. Von Schwarzenberg K, Wiedmann RM, Oak P et al (2013) Mode of cell death induction by pharmacological vacuolar H + -ATPase (V-ATPase) inhibition. J Biol Chem 288:1385–1396
199. McHenry P, Wang W-LW, Devitt E et al (2010) Iejimalides A and B inhibit lysosomal vacuolar H + -ATPase (V-ATPase) activity and induce S-phase arrest and apoptosis in MCF-7 cells. J Cell Biochem 109:634–642
200. Sasazawa Y, Futamura Y, Tashiro E, Imoto M (2009) Vacuolar H + -ATPase inhibitors overcome Bcl-xL-mediated chemoresistance through restoration of a caspase-independent apoptotic pathway. Cancer Sci 100:1460–1467
201. De Milito AD, Iessi E, Logozzi M et al (2007) Proton pump inhibitors induce apoptosis of human B-cell tumors through a caspase-independent mechanism involving reactive oxygen species. Cancer Res 67:5408–5417
202. Jewell JL, Kim YC, Russell RC et al (2015) Metabolism: differential regulation of mTORC1 by leucine and glutamine. Science 347:194–198
203. Horova V, Hradilova N, Jelinkova I et al (2013) Inhibition of vacuolar ATPase attenuates the TRAIL-induced activation of caspase-8 and modulates the trafficking of TRAIL receptosomes. FEBS J 280:3436–3450
204. Sennoune SR, Arutunyan A, del Rosario C et al (2014) V-ATPase regulates communication between microvasular endothelial cells and metastatic cells. Cell Mol Biol 60:19–25
205. Kobia F, Duchi S, Deflorian G, Vaccari T (2014) Pharmacologic inhibition of vacuolar H+ ATPase reduces physiologic and oncogenic Notch signaling. Mol Oncol 8:207–220
206. Shen W, Zou X, Chen M et al (2013) Effect of pantoprazole on human gastric adenocarcinoma SGC7901 cells through regulation of phospho-LRP6 expression in Wnt/β-catenin signaling. Oncol Rep 30:851–855
207. Han J, Sridevi P, Ramirez M et al (2013) β-Catenin-dependent lysosomal targeting of internalized tumor necrosis factor-α suppresses caspase-8 activation in apoptosis-resistant colon cancer cells. Mol Biol Cell 24:465–473
208. Rath S, Liebl J, Fürst R et al (2014) Regulation of endothelial signaling and migration by v-ATPase. Angiogenesis 17:587–601
209. Rojas JD, Sennoune SR, Maiti D et al (2006) Vacuolar-type H + -ATPases at the plasma membrane regulate pH and cell migration in microvascular endothelial cells. Am J Physiol Heart Circ Physiol 291:H1147–H1157

210. Katara GK, Jaiswal MK, Kulshrestha A et al (2014) Tumor-associated vacuolar ATPase subunit promotes tumorigenic characteristics in macrophages. Oncogene 33:5649–5654
211. Xu Y, Parmar A, Roux E et al (2012) Epidermal growth factor-induced vacuolar (H+)-ATPase assembly a role in signaling via mTORC1 activation. J Biol Chem 287:26409–26422
212. Liu P (2013) Effect of pantoprazole on human gastric adenocarcinoma SGC7901 cells through regulation of phospho-LRP6 expression in Wnt/β-catenin signaling. Oncol Rep 2524
213. Sennoune SR, Bakunts K, Martínez GM et al (2004) Vacuolar H + -ATPase in human breast cancer cells with distinct metastatic potential: distribution and functional activity. Am J Physiol Cell Physiol 286:C1443–C1452
214. Lu Q, Lu S, Huang L et al (2013) The expression of V-ATPase is associated with drug resistance and pathology of non-small-cell lung cancer. Diagn Pathol 8:145
215. Dechant R, Peter M (2011) The N-terminal domain of the V-ATPase subunit "a" is regulated by pH in vitro and in vivo. Channels 5:4–8
216. Long X, Crow MT, Sollott SJ et al (1998) Enhanced expression of p53 and apoptosis induced by blockade of the vacuolar proton ATPase in cardiomyocytes. J Clin Invest 101:1453–1461
217. Torigoe T, Izumi H, Ishiguchi H et al (2002) Enhanced expression of the human vacuolar H + -ATPase c subunit gene (ATP6L) in response to anticancer agents. J Biol Chem 277:36534–36543
218. Straud S, Zubovych I, De Brabander JK, Roth MG (2010) Inhibition of iron uptake is responsible for differential sensitivity to V-ATPase inhibitors in several cancer cell lines. PLoS One 5, e11629
219. Lee G-H, Kim D-S, Kim H-T et al (2011) Enhanced lysosomal activity is involved in bax inhibitor-1-induced regulation of the endoplasmic reticulum (ER) stress response and cell death against ER stress involvement of vacuolar H + -ATPASE (V-ATPASE). J Biol Chem 286:24743–24753
220. Lim J-H, Park J-W, Kim M-S et al (2006) Bafilomycin induces the p21-mediated growth inhibition of cancer cells under hypoxic conditions by expressing hypoxia-inducible factor-1α. Mol Pharmacol 70:1856–1865
221. Zhdanov AV, Dmitriev RI, Golubeva AV et al (2013) Chronic hypoxia leads to a glycolytic phenotype and suppressed HIF-2 signaling in PC12 cells. Biochim Biophys Acta 1830:3553–3569
222. Li SC, Diakov TT, Rizzo JM, Kane PM (2012) Vacuolar H + -ATPase works in parallel with the HOG pathway to adapt Saccharomyces cerevisiae cells to osmotic stress. Eukaryot Cell 11:282–291
223. Dietz KJ, Tavakoli N, Kluge C et al (2001) Significance of the V-type ATPase for the adaptation to stressful growth conditions and its regulation on the molecular and biochemical level. J Exp Bot 52:1969–1980
224. Lin M, Li SC, Kane PM, Höfken T (2012) Regulation of vacuolar H + -ATPase activity by the Cdc42 effector Ste20 in Saccharomyces cerevisiae. Eukaryot Cell 11:442–451
225. Seidel T, Scholl S, Krebs M et al (2012) Regulation of the V-type ATPase by redox modulation. Biochem J 448:243–251
226. Warburg O (1956) On the origin of cancer cells. Science 123:309–314
227. Sennoune SR, Martinez-Zaguilan R (2012) Vacuolar H + -ATPase signaling pathway in cancer. Curr Protein Pept Sci 13:152–163
228. Martinez-Outschoorn U, Sotgia F, Lisanti MP (2014) Tumor microenvironment and metabolic synergy in breast cancers: critical importance of mitochondrial fuels and function. Semin Oncol 41:195–216
229. Salem AF, Whitaker-Menezes D, Howell A et al (2012) Mitochondrial biogenesis in epithelial cancer cells promotes breast cancer tumor growth and confers autophagy resistance. Cell Cycle Georget, TX 11:4174–4180
230. Martinez-Outschoorn UE, Whitaker-Menezes D, Valsecchi M et al (2013) Reverse Warburg effect in a patient with aggressive B-cell lymphoma: is lactic acidosis a paraneoplastic syndrome? Semin Oncol 40:403–418

231. Montcourrier P, Mangeat PH, Valembois C et al (1994) Characterization of very acidic phagosomes in breast cancer cells and their association with invasion. J Cell Sci 107:2381–2391
232. Montcourrier P, Silver I, Farnoud R et al (1997) Breast cancer cells have a high capacity to acidify extracellular milieu by a dual mechanism. Clin Exp Metastasis 15:382–392
233. Capecci J, Forgac M (2013) The function of vacuolar ATPase (V-ATPase) a subunit isoforms in invasiveness of MCF10a and MCF10CA1a human breast cancer cells. J Biol Chem 288:32731–32741
234. Cotter K, Capecci J, Sennoune S et al (2015) Activity of plasma membrane V-ATPases is critical for the invasion of MDA-MB231 breast cancer cells. J Biol Chem 290:3680–3692
235. Lu X, Qin W, Li J et al (2005) The growth and metastasis of human hepatocellular carcinoma xenografts are inhibited by small interfering RNA targeting to the subunit ATP6L of proton pump. Cancer Res 65:6843–6849
236. Nishisho T, Hata K, Nakanishi M, Morita Y, Sun-Wada G-H, Wada Y, Yasui N, Yoneda T (2011) The a3 isoform vacuolar type H+-ATPase promotes distant metastasis in the mouse B16 melanoma cells. Mol Cancer Res 9:845–855. doi:10.1158/1541-7786.MCR-10-0449
237. Hendrix A, Sormunen R, Westbroek W et al (2013) Vacuolar H+ ATPase expression and activity is required for Rab27B-dependent invasive growth and metastasis of breast cancer. Int J Cancer 133:843–854
238. Feng S, Cai M, Liu P et al (2014) Atp6v1c1 may regulate filament actin arrangement in breast cancer cells. PLoS One 9, e84833
239. Wiedmann RM, von Schwarzenberg K, Palamidessi A et al (2012) The V-ATPase-inhibitor archazolid abrogates tumor metastasis via inhibition of endocytic activation of the Rho-GTPase Rac1. Cancer Res 72:5976–5987
240. Mahoney BP, Raghunand N, Baggett B, Gillies RJ (2003) Tumor acidity, ion trapping and chemotherapeutics. I. Acid pH affects the distribution of chemotherapeutic agents in vitro. Biochem Pharmacol 66:1207–1218
241. Simon SM, Schindler M (1994) Cell biological mechanisms of multidrug resistance in tumors. Proc Natl Acad Sci U S A 91:3497–3504
242. Martínez-Zaguilán R, Raghunand N, Lynch RM et al (1999) pH and drug resistance. I. Functional expression of plasmalemmal V-type H + -ATPase in drug-resistant human breast carcinoma cell lines. Biochem Pharmacol 57:1037–1046
243. Lebreton S, Jaunbergs J, Roth MG et al (2008) Evaluating the potential of vacuolar ATPase inhibitors as anticancer agents and multigram synthesis of the potent salicylihalamide analog saliphenylhalamide. Bioorg Med Chem Lett 18:5879–5883
244. Murakami T, Toda S, Fujimoto M et al (2001) Constitutive activation of Wnt/β-catenin signaling pathway in migration-active melanoma cells: role of LEF-1 in melanoma with increased metastatic potential. Biochem Biophys Res Commun 288:8–15
245. You H, Jin J, Shu H et al (2009) Small interfering RNA targeting the subunit ATP6L of proton pump V-ATPase overcomes chemoresistance of breast cancer cells. Cancer Lett 280:110–119
246. Fan S, Niu Y, Tan N et al (2013) LASS2 enhances chemosensitivity of breast cancer by counteracting acidic tumor microenvironment through inhibiting activity of V-ATPase proton pump. Oncogene 32:1682–1690
247. Patal KJ, Lee C, Tan Q et al (2013) Use of proton pump inhibitor pantoprazole to modify distribution and activity of doxorubcin a potential strategy to improve the therapy of solid tumors. Clin Cancer Res 19:6766–6776
248. Suzuki K, Doki K, Homma M et al (2009) Co-administration of proton pump inhibitors delays elimination of plasma methotrexate in high dose methotrexate therapy. Br J Clin Pharmacol 67:44–49
249. De Milito A, Canese R, Marino ML et al (2010) pH-dependent antitumor activity of proton pump inhibitors against human melanoma is mediated by inhibition of tumor acidity. Int J Cancer 127:207–219

250. Zhang S, Wang Y, Li SJ (2014) Lansoprazole induces apoptosis of breast cancer cells through inhibition of intracellular proton extrusion. Biochem Biophys Res Commun 448:424–429
251. De Milito A, Marino ML, Fais S (2012) A rationale for the use of proton pump inhibitors as antineoplastic agents. Curr Pharm Des 18:1395–1406
252. Huang S, Chen M, Ding X et al (2013) Proton pump inhibitor selectively suppresses proliferation and restores the chemosensitivity of gastric cancer cells by inhibiting STAT3 signaling pathway. Int Immunopharmacol 17:585–592
253. Kastelein F, Spaander MCW, Steyerberg EW et al (2013) Proton pump inhibitors reduce the risk of neoplastic progression in patients with Barrett's esophagus. Clin Gastroenterol Hepatol 11:382–388
254. Kastelein F, Spaander MCW, Biermann K et al (2011) Role of acid suppression in the development and progression of dysplasia in patients with Barrett's esophagus. Dig Dis Basel Switz 29:499–506
255. Krop M, Lu X, Danser AH et al (2013) The (Pro)renin receptor. A decade of research: what have we learned. Pflugers Arch 465:87–97
256. Kinouchi K, Ichihara A, Sano M et al (2010) The (Pro)renin receptor/ATP6AP2 is essential for vacuolar H + -ATPase assembly in murine cardiomyocytes. Circ Res 107:30–34
257. Jewell JL, Russell RC, Guan K-L (2013) Amino acid signalling upstream of mTOR. Nat Rev Mol Cell Biol 14:133–139
258. Zoncu R, Bar-Peled L, Efeyan A, Wang S, Sancak Y, Sabatini DM (2011) mTORC1 senses lysosomal amino acids through an inside-out mechanism that requires the vacuolar H^+-ATPase. Science 334:678–683
259. Laplante M, Sabatini DM (2012) mTOR signaling in growth control and disease. Cell 149:274–293
260. Peña-Llopis S, Vega-Rubin-de-Celis S, Schwartz JC et al (2011) Regulation of TFEB and V-ATPases by mTORC1. EMBO J 30:3242–3258

Chapter 18
Vacuolar H^+-ATPase Signaling in Cancer

Raul Martínez-Zaguilán and Souad R. Sennoune

Abstract The vacuolar H^+-ATPase (V-ATPase) is an electrogenic H^+ pump responsible for the regulation of pH in endomembranous compartments; and for the extrusion of H^+ across the plasma membrane in certain cell types, including metastatic cells. The study of the regulation of V-ATPase has been daunting. Regulation of V-ATPase by assembling and disassembling of V_1 and V_0 domain by glucose has emerged as one important mechanism. Tumor cells preferentially employ glycolysis to generate energy, even under well oxygenated conditions. This imposes in tumor cells the need to consume large amounts of glucose to generate energy via glycolysis. Elevated glycolysis produces lactic acid and cytosolic acidosis. To eliminate acid, metastatic cells use V-ATPase at the cell surface. Regulation of V-ATPase by glucose provides an exciting link between metabolism and tumor biology that warrants future studies. In addition to its widely accepted role of V-ATPase in regulating pH, a series of new noncanonical functions have emerged in the past few years, including cell signaling, metabolic sensing, and fusiogenic events. We provide a brief overview of past and new developments towards understanding the significance of this remarkable nanomotor for cell function, and its involvement in cancer biology.

Keywords V-ATPase • pH regulation • Glycolysis • Acidification • (P)RR/ATP6ap2 • Wnt pathway • Hypoxia-induced factor (HIF)

1 Introduction

In the first half of the twentieth century, Otto Warburg made the fundamental observation that cancer cells relied on glycolysis to obtain energy, suggesting altered cellular metabolism in cancer [1–4]. Cancer cells predominantly generate energy, i.e., ATP, via glycolysis even in the presence of oxygen. As a result of increased glycolysis cancer cells produce excessive lactic acid that contributes to an acidic

R. Martínez-Zaguilán • S.R. Sennoune (✉)
Department of Cell Physiology and Molecular Biophysics, Texas Tech University Health Sciences Center, Lubbock, TX 79430, USA
e-mail: Souad.Sennoune@ttuhsc.edu

S. Chakraborti, N.S. Dhalla (eds.), *Regulation of Ca^{2+}-ATPases,V-ATPases and F-ATPases*, Advances in Biochemistry in Health and Disease 14,
DOI 10.1007/978-3-319-24780-9_18

extracellular pH in tumor environments. This should be contrasted with normal cells that generate their energy by oxidative phosphorylation using the electron transport chain in the mitochondria. In normal cells, glycolysis in the cytosol is followed by oxidation of pyruvate in the mitochondria under aerobic conditions via the tricarboxylic acid cycle (TCA). It is paradoxical that cancer cells would use glycolysis to obtain their energy, since glycolysis only generates 4 molecules of ATP for each glucose molecule, whereas oxidation of pyruvate in the mitochondria via the TCA cycle generates 36 molecules of ATP. To compensate for the preferential use of glycolysis rather than oxidative phosphorylation, cancer cells utilize a huge amount of glucose to maintain cell proliferation and to avoid oxidative stress in the mitochondria.

Due to preferential utilization of glucose via glycolysis, the tumor extracellular pH is more acidic than normal tissue. It is a conundrum that the intracellular pH in tumor cells is more alkaline than in normal tissue, since the production of glucose 6 phosphate, the first step in glycolysis via hexokinase, generates intracellular acid because of its p*K*a of 0.94 and 6.11 [5]. Excessive acid is deleterious to cell function and leads to apoptosis in normal cells. We hypothesize that to survive this cytosolic acidification, tumor cells must employ unique pH regulatory mechanisms to extrude acid into the extracellular space. There are several pH regulatory mechanisms that all eukaryotic cells have evolved to regulate cytosolic pH (pH^{cyt}), including Na^+/H^+ exchangers (NHE), HCO_3^--based H^+-transporters, monocarboxylate transporters (MCTs), carbonic anhydrase (CAIX). Although these pH regulatory systems are sufficient to extrude acid in most normal cells, these mechanisms typically do not work at pH^{cyt} larger than 7.1; and most tumor cells maintain a pH^{cyt} higher than 7.1 favorable for cell grow. Thus, tumor cells require additional pH^{cyt} regulatory mechanisms such as the vacuolar H^+-ATPase (V-ATPase), a primary H^+-transporting mechanism that typically resides in endomembranous compartments. Importantly, in cancer cells, the V-ATPase is also located at the plasma membrane, where it plays an important role in extruding acid generated by excessive glycolysis (Fig. 18.1). The regulation of V-ATPase is a new and exciting field of research. V-ATPase activity is known to be sensitive to glucose availability. Its regulation by glucose is a well known, but poorly understood mechanism. In yeast, glucose withdrawal initiates the reversible dissociation of the V-ATPase shutting down its activity; addition of glucose triggers its reassembly, thus activating V-ATPase [6–8]. Since glycolysis is elevated in cancer, understanding the mechanisms by which glucose regulates V-ATPase is highly significant. Understanding this pathway will help to establish the significance of V-ATPase in cellular signaling pathways.

2 V-ATPase Structure

V-ATPase, a multi-subunit nanomotor pump, contains two coupled rotary motors consisting of two reversibly associated multi-subunit domains V_1 and V_0 domains. V-ATPase is an ATP-driven enzyme that transforms the energy of ATP hydrolysis to generate an electrochemical gradient, consisting of the membrane potential and the

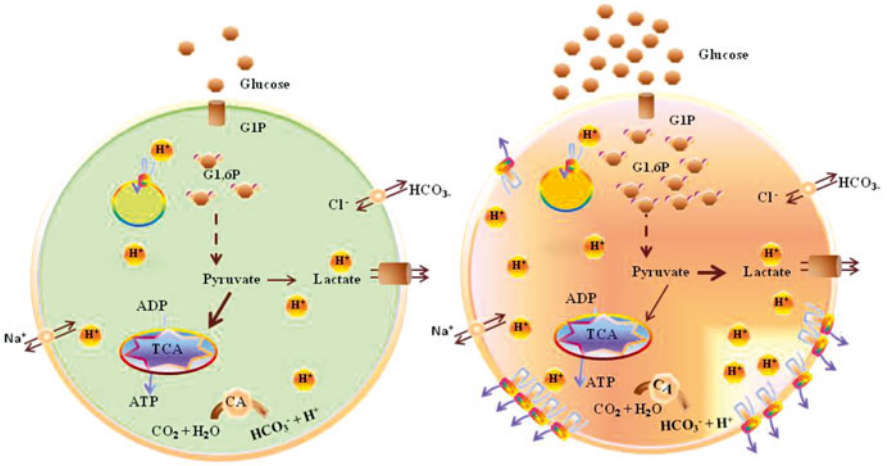

Fig. 18.1 Cancer cells are more glycolytic than normal cells. Cancer cells preferentially use glycolysis rather than oxidative phosphorylation to generate energy, even in the presence of oxygen. It is paradoxical that cancer cells use glycolysis since it generates only four moles of ATP per mole of glucose, whereas glucose metabolism via oxidative phosphorylation in the mitochondria generates 36 moles of ATP. To extrude excessive acid produced by glycolysis, tumor cells use V-ATPase located at the cell surface that allows them to maintain an alkaline intracellular pH optimal for growth and survival, while maintaining an acidic extracellular pH, optimal for the activity of proteases needed for invasion and metastasis

proton gradient across the membrane via the primary active transport of H^+. The electrochemical potential of H^+ is used to drive a variety of secondary active transport systems via H^+-dependent symporters, antiporters and channel-mediated transport systems [9–12].

The catalytic domain V_1 is composed of eight subunits (A–H). Three copies each of the A and B subunits are organized to form a hexamer. ATP hydrolysis occurs at the interface between the A and B subunits. One copy each of the C and H subunits and three copies each of the G and E subunits form peripheral stalks that act as stators. The D and F subunits form a central stalk that serves as a rotor, to couple the energy generated by ATP hydrolysis to the actual rotation of the proteolipid ring in the V_0 domain that transport protons.

The proton translocation domain V_0 is composed of six hydrophobic subunits (a, c, c′, c″, d, and e). In mammals, the trans-membrane V_0 domain contains five c and one c″, and single copy each of the other subunits. During rotation, protons are captured and translocated at the interface of the a- and c-subunits by consecutive binding to acidic residues.

In addition to V_1 and V_0 domains, two accessory proteins are associated with V-ATPase: ATP6ap1 and ATP6ap2. The ATP6ap1, also known as Ac45 co-purify with the V_0 domain from bovine adrenal chromaffin granules [13, 14]. Ac45 is associated with the V_0 domain subunits a3, c, and c″ and plays an important role in osteoclastic bone resorption [15]. Ac45 appears to be involved in regulating the

expression of the plasma membrane V-ATPase and increasing the efficiency of calcium-dependent secretion in neuro-endocrine cells [16]. These data suggest that Ac45 may contribute to the membrane fusion event during exocytosis. The ATP6ap2 gene codes for a protein with 350-amino acids and a mass of 37 kDa that can be divided into four different domains: an N-terminal signal peptide, an extracellular domain binding (pro)renin, a single trans-membrane domain, and a short cytoplasmic domain [17]. ATP6ap2 (also called (P)RR/ATP6ap2, ac8-9 or M8-9) has not been found as part of the V0 domain as Ac45. A furin cleavage site on the extracellular part of (P)RR/ATP6ap2 allows the release of a 28 kDa fragment during passage through the Golgi apparatus [18]. The cleavage leaves behind a short protein consisting of the trans-membrane and the intracellular domains, which corresponds to the M8-9 fragment of (P)RR/ATP6ap2 found to be associated with V-ATPase [18]. The significance of these accessory proteins is emphasized by the fact that Ac45 knockout in mice is lethal to embryos [19]; and ATP6ap2 knockout mice could not be generated [20, 21].

3 V-ATPase Functions

The first evidence for the physiological significance of the V-ATPases was shown by Eli Metchnikoff in 1905 [22]. He demonstrated vacuolar acidification in digestive vacuoles of unicellular organisms. Later, the V-ATPase was shown in various endomembranes of eukaryotic cells [23–29]. V-ATPase is now recognized as a key enzyme acidifying intracellular organelles and some extracellular milieus, localized in membranes of organelles of exocytic and endocytic pathways and at the cell surface. Maintenance of a luminal acidic environment in the exocytic and endocytic pathways is required in the processing and sorting of vesicle contents for a variety of signaling molecules, and ligand-receptor complexes [30, 31]. The significance of V-ATPases for cell growth and survival was first shown in yeast. Disruption of single-copy genes encoding the V_1 subunit B or the V_0 subunit c resulted in the inability of yeast cells to survive at pH values higher than 6.5 and they only grew well at pH values of 5.5. These observations indicate that V-ATPase is essential for survival at pH>6.5 [32]. Although first found in endo-membranes, the V-ATPase has also been found in the plasma membranes of various cell types, where it functions both in physiological and pathological processes [33–39]. This distinct subcellular localization of V-ATPase at the plasma membrane suggests its involvement in regulating unique cellular functions.

3.1 V-ATPase in Vesicular Trafficking

V-ATPase is ubiquitous on intracellular membranes (vacuoles, lysosomes, endosomes, secretory, Golgi, and synaptic vesicles) where it plays a major role in luminal acidification to provide optimal pH for multiple functions (protein degradation,

protein sorting, receptor recycling) [40]. In addition to control acidification of intracellular organelles, the V-ATPase also confers a voltage gradient. The proton potential across the membrane generated by V-ATPases provides a driving force to transport small molecules and ions into the lumen. The acidic luminal pH of intracellular organelles is a prerequisite for proper vesicular trafficking. V-ATPase recruits ARF6 (ADP ribosylation factor, a small GTPase) and ARNO (ADP ribosylation factor nucleotide site opener) to endosomal membranes via interaction of c-subunit with ARF6 and the a2-isoform with ARNO [41, 42]. The a2-isoform interacts with ARNO in a pH-dependent manner, suggesting its function as a pH sensor for controlling the recruitment of the GTPase activated by ARNO, ARF6, which in turn interacts with the V_0 domain [43]. Both ARF6 and ARNO have been implicated in regulation of endocytotic pathways, organelle biogenesis, and actin cytoskeleton remodeling [44]. The perturbation of these interactions with V-ATPase subunits leads to inhibition of endocytosis.

A role for V-ATPase in exocytosis is supported by the observation that the V_0 domain interacts with SNAREs (synaptobrevin and synaptophysin) and involves Ca^{2+}/calmodulin [45–47]. It has been also shown that the a- and c-subunits of V-ATPase bind syntaxin [48] and VAMP2 [49]. These data are consistent with a role for the a1-isoform at a late step in exocytosis [50, 51]. Several studies support the idea that the V_0 domain is involved in membrane fusion. It was suggested that two V_0 sectors in *trans* at the membrane interface between the two vacuoles destined to fuse, form a gap junction-like channel [52]. Studies from invertebrates showed that V_0 c-subunit participates in gap junction organization [53]. Peters and colleagues uncovered a crucial role of V_0 c-subunit in yeast vacuole fusion while searching for molecular partners of calmodulin, which acts as a Ca^{2+}-sensor [54]. The V_0 a-subunit has been shown to play a crucial role in exosome-mediated apical secretion of Hedgehog-related proteins in *C. elegans* [55]. It has also been shown that the V_0 a3-isoform regulates insulin secretion in pancreatic beta-cells [56]. Recently, Poëa-Guyon and colleagues have observed in neurosecretory PC12 cells that V_1 and V_0 domains associate on secretory granules in response to neutral pH and dissociate under acidified condition to aid in exocytosis [57]. V_0 serves as a sensor of intragranular pH that controls exocytosis and synaptic transmission via the reversible dissociation of V_1 at acidic pH. Altogether, these data supports an important role for V-ATPases in exocytosis in several cell models.

3.2 V-ATPase in the Plasma Membrane

In addition to its localization in intracellular compartments, V-ATPase is also present at the plasma membrane of some specialized cells, where it extrudes proton to the extracellular milieu to perform cell specific functions, such as, bone resorption [58], maturation and sperm storage in epididymal lumen [59], bicarbonate reabsorption in renal proximal tubes [60], renal acidification in distal nephron [61], as well as cytoplasmic pH regulation in microvascular endothelial cells and metastatic

cancer cells [37, 38, 62, 63]. We have characterized a number of human tumor cells, in terms of V-ATPase activity, and have determined that a subset of them translocated V-ATPases to the cell surface [37, 38, 64–66]. This was determined using bafilomycin and monitoring cytosolic pH recovery following acid loads in the absence of Na^+ and HCO_3^-, to inhibit two major cytosolic pH regulatory systems, i.e., NHE and HCO_3^--based H^+-transporting mechanisms. In the absence of Na^+ and HCO_3^-, only cells exhibiting an alternate cytosolic pH regulatory mechanism should recover from an acid load. Treatment of these cells with SCH28080, to block H^+/K^+-ATPase did not affect cytosolic pH regulation. Importantly, treatment of cells with bafilomycin, a V-ATPase inhibitor, decreases acid extrusion and inhibits pH regulation. We found that highly metastatic human melanoma cells exhibit higher pmV-ATPase than lowly metastatic human melanoma cells [38, 65, 66]. We have made similar observation in human breast cancer cells with high and low metastatic potential [63] as well as in pancreatic carcinoma and prostate cancer cells.

3.3 V-ATPase Regulation

Since the V-ATPase is located in several endo-membranes and at the cell surface, it might be expected that V-ATPase activity would be tightly regulated at different levels. However, the exact mechanisms that regulate V-ATPase activity remain to be elucidated. Little is known about the exact mechanism that modulates the differential coupling efficiency between ATP hydrolysis and proton translocation resulting in differential acidification along the exocytotic and endocytotic pathways. In yeast, it has been shown that the coupling efficiency is controlled by the C-terminal hydrophobic domain of a-subunit [67]. However, the best characterized mechanism of regulating V-ATPase activity described to date is the reversible dissociation of the V_1 and V_0 domains (Fig. 18.2).

The reversible dissociation of V_1 and V_0 domains for the regulation of V-ATPase was first observed in *Saccharomyces cerevisiae* and *Manduca sexta* following glucose deprivation and starvation, respectively [6, 68]. It is known that the V_0 free of V_1 is incompetent for proton translocation [69]. Similarly, cytoplasmic pools of V_1 appear to be unable to hydrolyze ATP. Therefore, the dissociation of V_1 and V_0 domain is an efficient mechanism of controlling the V-ATPase activity. In these organisms, however, dissociation appears as a survival mechanism to conserve the ATP stock upon conditions of energy limitation by glucose deprivation or starvation [7, 33]. When glucose becomes available again preexisting V_1 and V_0 domain reassociate. As expected, this process does not require de novo synthesis of proteins. Disassembly–reassembly process appears to be a way of regulating V-ATPase activity, and therefore regulating acidification. Changes in V_1 and V_0 association raise the questions of the mechanisms that regulate this process. Several signaling pathways that regulate reversible dissociation of the V-ATPase have been proposed.

Glucose causes assembly of the V-ATPase by activating the Ras/cAMP/ protein kinase A (PKA) pathway in yeast [70]. Elevated glucose concentration inhibits the

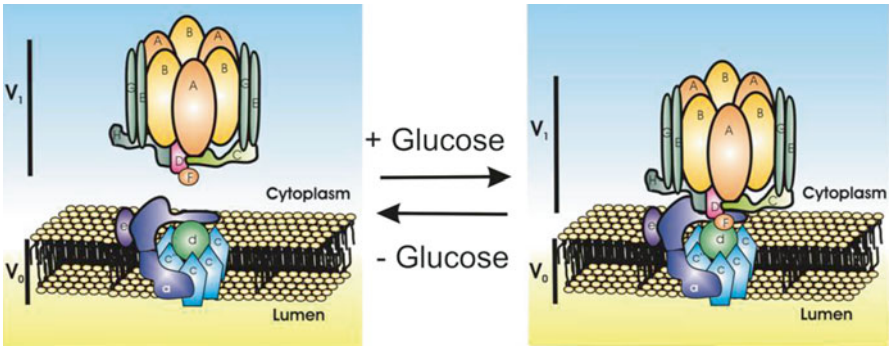

Fig. 18.2 The assembly–disassembly of V-ATPase into V_0 and V_1 domains is regulated by glucose. The composition of V-ATPase is described in text. The V_1 domain contains the catalytic sector responsible for ATP hydrolysis. The V_0 domain is embedded in the plasma membrane and is responsible for the translocation of H^+ via a rotary mechanism that is coupled to ATP hydrolysis. In the presence of glucose the V_0/V_1 domains associate, activating V-ATPase. In the absence of glucose the V_0 and V_1 dissociate, inhibiting V-ATPase

activity of the Ras GAPs Ira1p and Ira2p, which leads to an increase in the amount of GTP-bound Ras; and hence increased Ras activity. Activated Ras, in turn, activates adenylate cyclase and increases cAMP. Elevated cAMP levels causes dissociation of the regulatory subunits of PKA, that in turn is free to phosphorylate several protein targets, including the V-ATPase.

Transient phosphorylation of the V_1 C subunit during reassembly has been observed in *Manduca sexta*, and this may well be a critical target in the signaling pathways [71]. These studies suggest that C subunit binds to and serves as a substrate for PKA. These data also suggest that phosphorylation may be a regulatory switch for the formation of the active V_0/V_1 holoenzyme [71].

Sautin and colleagues have demonstrated an involvement of PI3K-dependent signaling in the control of V-ATPase trafficking, assembly, and function by glucose in renal epithelial cells [72]. In this study, glucose removal diminished V-ATPase dependent acidification, decreased ATP hydrolytic activity of V-ATPase, induced its disassembly and led to translocation of both V_1 and V_0 domains from plasma membrane and sub-membrane vesicles to intracellular vesicles (V_1 and V_0) and the cytoplasm (V_1). Glucose deprivation or replacement dramatically changed the pattern of V-ATPase localization. The effects of glucose on V-ATPase trafficking and assembly can be abolished by pretreatment with the PI3K inhibitor LY294002; and can be reproduced in glucose-deprived cells by adenoviral expression of the constitutively active catalytic subunit p110 of PI3K. These data provide evidence that, in renal epithelial cells, glucose plays an important role in the control of V-ATPase-dependent acidification of intracellular compartments and V-ATPase assembly and trafficking. The glucose effects on V-ATPase trafficking can be mediated by changes in the formation of microfilaments promoted by PI3K.

Dechant and colleagues assessed V-ATPase assembly in living cells, exposed to rapid shifts in glucose concentrations, by monitoring the subcellular localization of

GFP-tagged subunits of V-ATPase using microfluidic chips [73]. During conditions of high glycolytic flux, where there is increase in lactic acid production, the V_1 domain rapidly relocalizes to the vacuolar surface. Upon a shift to low glucose, the V_1 domain disassociates, limiting ATP consumption. Their results suggest that glucose metabolism and intracellular pH regulates the assembly of the V-ATPase. It has also been shown that in response to acidic pH caused by increased in glycolytic flux, V-ATPase functions as activator of PKA. Thus, the V-ATPase assembly responds to changes in intracellular pH and acts as a sensor. In addition, it has been shown that dissociation requires an intact microtubule network [74]; and reassembly of V_1 onto V_0 appears to be mediated by the RAVE complex (regulator of H^+-ATPase of vacuolar and endosomal membranes) and aldolase [75–77]. Tabke and colleagues have shown evidence that the V_1 C subunit directly interacts with microtubules; and that this is the sole component that dissociates during glucose withdrawal [78]. RAVE appears to stabilize the dissociated V_1 complex in an assembly competent form, and mediates assembly in both the normal biosynthetic pathway and the glucose-regulated process. In contrast, the glycolytic enzyme aldolase appears to be important in glucose induced V_0V_1 assembly. Mutations in aldolase prevent assembly of the V-ATPase [75]. Recently, Li and colleagues have shown that the membrane lipid, phosphatidylinositol (3,5)-bisphosphate (PtdIns(3,5)P2) is important for V-ATPase activity [79]. Vph1p (V_0 a-subunit) interacts with PtdIns(3,5)P2, and it is recruited from the cytosol to the membrane when PtdIns(3,5)P2 levels increase in endocytic compartments. Decreased V-ATPase activity and H^+ pumping in the absence of PtdIns(3,5)P2 are associated with reduced assembly of V_1 subunits in the endocytic pathway. Diakov and Kane have shown that extracellular pH also tightly regulates V-ATPase activity and assembly [80]. A novel regulatory mechanism of V-ATPase function has been identified by De Luca and colleagues [81]. In this study, the authors have shown that the Rab-interacting lysosomal protein (RILP) interacts with V-ATPase V_1 G_1-subunit. RILP was shown to recruit V_1 G_1-subunit to the late endosome, an interaction that is apparently necessary for endocytic acidification. RILP overabundance in the cytosol was associated with proteasomal degradation of V_1 G_1-subunit [81].

4 V-ATPase Inhibitors

The discovery of specific inhibitors of V-ATPase enables the study and significance of this enzyme for cellular functions. The first family of inhibitors identified in the 1980s was the plecomacrolides: bafilomycins and concanamycin. Since, new inhibitors have been identified including: the benzolactone enamides salicylihalamide, lobatamide, apicularen, oximidine, cruentaren, indolyls, and macrolactone archazolid (for review see ref. [82]). To date, V-ATPase inhibitors that selectively block V-ATPase located in the plasma membrane without affecting V-ATPase in endomembranous compartments have not been identified. It will be useful to develop such inhibitor for therapeutic purposes, since the plasma membrane V-ATPase has been shown to be involved in cancer metastasis and other diseases.

5 V-ATPase Targeting

One of the fundamental questions that need to be addressed is how the V-ATPase is translocated from the endo-membranes to the plasma membrane. Exocytosis could be one of the mechanisms for translocation of V-ATPase to the cell surface via vesicle trafficking and vesicle fusion with the plasma membrane. The other mechanism for V-ATPase translocation could be direct targeting since the a-subunit which is present in several isoforms (a1, a2, a3, and a4), contains information to target V-ATPases to different membranous locations [39, 67]. These a-isoforms are expressed in a tissue-specific manner. The a1-, a2-, and a3-isoforms have been shown to be ubiquitously expressed in mammalian cells, albeit their levels of expression are tissue-specific [39, 83]. The a4-isoform is expressed in renal intercalated cells and epididymal clear cells, where it is localized in the apical membrane [84, 85]; while the a3-isoform is expressed in osteoclasts, where it is translocated to the plasma membrane from the lysosome upon activation of osteoclasts [39, 84]. In the brain, the a1-isoform is present in both synaptic vesicles and the presynaptic plasma membrane of presynaptic nerve terminals; whereas the a2-isoform localizes only to the apical endosomes of the renal proximal tubule cells. It is also clear that a given cell type can express more than one a-isoform in the plasma membrane, as it has been demonstrated for rat vas deferens and epididymal cells [83, 84]. In our studies, we have shown that although all four isoforms are detectable in both highly (MB231) and lowly (MCF7) metastatic breast cancer cells, the levels of a3 and a4 are much higher in MB231 than in MCF7 cells [86]. Cytosolic pH was decreased only on knockdown of a3. The knockdown of either a3- or a4-isoforms significantly inhibited invasion of MB231 cells. We have found that the a1-isoform is downregulated and a4- is upregulated in highly metastatic cells compared to the lowly metastatic cells. Altogether, these data emphasize the significance of a3- and a4-isoforms for the acquisition of a more metastatic phenotype. Other studies have shown, that knockdown of the a3-isoform in the highly metastatic B16-F10 mouse melanoma cells reduces their ability to metastasize to the bone and lung in vivo [87]. More recently, a comparison of the noninvasive MCF10a breast epithelial cells with the highly invasive MCF10CA1a breast tumor cells revealed that invasion by MCF10CA1a cells is significantly inhibited by knockdown of either the a3- or more dramatically the a3- plus a4-isoforms. Importantly, overexpression of a3-isoform significantly increases both invasion and plasma membrane localization of V-ATPase in the noninvasive MCF10a cells [88]. To more directly assess the role of plasma membrane V-ATPases in tumor cell invasion, in our recent study, we inhibited specifically the plasma membrane V-ATPase activity. To do this, we have stably transfected the breast cancer line MDA-MB231 with a V5-tagged construct of the V-ATPase V_0 c-subunit that allows the extracellular expression of the V5 epitope. We show that monoclonal antibody against the V5 epitope causes cytosolic acidification and decrease of extracellular proton extrusion across the plasma membrane via V-ATPase. Importantly, anti-V5 antibody decreases breast cancer cell invasion in vitro. We have also observed that a membrane-impermeable form of the V-ATPase

inhibitor bafilomycin inhibits breast cancer cell invasion [89]. These studies clearly indicate the significance of developing therapeutic approaches to inhibit V-ATPase at the cell surface to inhibit cell invasion and cancer metastasis.

6 V-ATPase Signaling in Cancer

One of the hallmarks in cancer cells is a shift in glucose metabolism from oxidative phosphorylation to aerobic glycolysis (Warburg effect). However, the interactions between glucose homeostasis and V-ATPase activity in tumors are unclear. Glucose metabolism is required for maintaining V-ATPase assembly [69]. The reversible dissociation mechanism by glucose availability may be a mechanism of regulating V-ATPase activity in tumor cells. We hypothesize that glucose withdrawal in cancer cells initiates the reversible dissociation of the V-ATPase, shutting down its activity. To address this hypothesis, we incubated prostate cancer cells in medium without glucose. We observed that after 6 h in the absence of glucose there was a significant decrease of the V-ATPase activity, leading to cytosolic acidifying and cell death (unpublished observations).

V-ATPases are activated by glucose as well. Martinez-Munoz and Kane have shown in yeast that the change in pH is sensitive to glycolytic flux [34]. Paradoxically, they showed that cells in the presence of high glucose concentration have a more alkaline intracellular pH, whereas cells starved for glucose experience a more acidic intracellular pH. These data suggest that in response to elevated glucose that would cause increased in lactic acid production, there is upregulation of a pH regulatory mechanism, i.e., V-ATPase, to cope with excess acid that could kill the cells. Interestingly, the same phenomenon is observed in tumor cells. The high level of glycolysis leads the tumor cells to maintain a more alkaline intracellular pH (pH>7.1). In glucose starvation, the prostate cancer cells experience also a more acidic intracellular pH of ca. 6.8 (our unpublished observations). The high level of glycolysis leads also to an acidification of the tumor microenvironment that is caused by extrusion of H^+ via the V-ATPase at the cell surface in tumors. It has been well documented that the tumor microenvironment pH is more acidic (pH 6.6–6.8) than that in normal tissues, due to the high rate of glycolysis and large amount of lactic acid produced in tumor areas [90–93]. Importantly, the tumor cells are known to maintain a more alkaline intracellular pH (7.1–7.8) than normal tissue (6.9–7.1) and to be efficient at maintaining pH gradients [38]. Since mammalian cells can only survive at neutral intracellular pH, these data suggest that tumor cells have evolved mechanisms that allowed them to proliferate in a hostile acidic extracellular environment by strictly regulating their intracellular pH that allows for optimal functioning of glycolytic pathways. We hypothesize that such a mechanism is the V-ATPase.

It has been shown that in kidney, the V-ATPase E-subunit interacts directly with the glycolytic enzyme aldolase [75]; and the a-subunit interacts with phosphofructokinase-1 [94, 95], thereby providing a functional and spatial coupling of V-ATPase

with the glycolytic pathway. The interaction with aldolase is glucose-dependent in yeast and necessary for stable V_1V_0 assembly. Phosphofructokinase-1 co-localizes with the V_0 a4-isoform in the intercalated cells of the cortical collecting duct [94]. It is unclear whether glucose or any of its metabolites is responsible for the regulation of V-ATPase. However, due to the complexity of mammalian systems, it is expected that the regulation of V-ATPase by glucose is not limited to only its interaction with the glycolytic enzymes. Although the regulation of V-ATPase by glucose is a well known phenomenon, the underlying extracellular and intracellular signaling mechanisms that regulate V-ATPase are unclear. Cells are likely employing multiple signaling pathways to detect and respond to changes in glucose level [96]. Indeed, a recent study has shown that haeme-responsive gene (HRG-1) that is induced by insulin-like growth factor-1, is essential for V-ATPase activity, and that glucose-induced V-ATPase reassembly in endocytic compartments is reduced when HRG-1 is suppressed [97].

In this study, the authors investigated the significance of HRG-1 for cancer cell invasiveness and glucose metabolism. They showed that in highly invasive breast cancer cell MB231, HRG-1 and the V-ATPase are co-expressed at the plasma membrane, whereas in less invasive cell MCF-7, HRG-1 is located in intracellular compartments. They showed also that stable suppression of HRG-1 in MB-231 cells decreases extracellular pH, cell growth and invasion. Ectopic expression of HRG-1 in noninvasive MCF-7 cells enhances V-ATPase activity, and increases the extracellular pH. Their findings indicate that HRG-1 expression at the plasma membrane enhances V-ATPase activity, drives glycolytic flux and facilitates cancer cell growth and invasion [97].

6.1 V-ATPase Cross Talk with Wnt Signaling Pathway

Prominent in the signaling pathways leading to cell growth and differentiation is the Wnt pathway [98]. Currently, three different pathways appear to be activated upon activation of Wnt receptor: the canonical Wnt/β-catenin cascade, the noncanonical planar cell polarity (PCP) pathway, and the Wnt/Ca^{2+} pathway [99–101]. The best understood Wnt signal transduction cascade is the Wnt/β-catenin pathway.

The key to the transmission of canonical Wnt signals is the intracellular protein β-catenin, which is a transcriptional co-activator that also binds to cadherin proteins to form part of adherens junctions. The membrane-associated, cadherin-bound pool of β-catenin is highly stable. The cytosolic β-catenin is usually found in a protein complex with GSK3 (glycogen synthase kinase 3), Axin and APC (adenomatous polyposis coli). This leads to the phosphorylation of β-catenin by GSK3, which targets it for rapid ubiquitin-mediated degradation, thereby maintaining low levels of cytosolic β-catenin [102]. Activation of the canonical Wnt pathway involves the stabilization of β-catenin through the binding of Wnt ligands to cell surface receptors: Frizzled (Fz) family receptors and lipoprotein receptor-related protein 5 and 6 (LRP-5/6) [103]. The Fz proteins are members of the seven transmembrane domain

cell surface receptors that belong phylogenetically to the large family of G protein-coupled receptors. LRP-5/6 are co-receptors that are members of the family of low-density lipoprotein receptor-related protein (LRP) single transmembrane receptors. The binding of Wnts to cell-surface Fz receptors and LRP5/6 co-receptors results in a functional change in this complex such that GSK3 no longer phosphorylates β-catenin. The resultant accumulation of β-catenin in the cytoplasm leads to nuclear accumulation and binding to T cell/lymphoid enhancer-binding transcription factors to induce the expression of specific target genes [98–100]. The Wnt-signaling pathway is traditionally associated with regulation of development and differentiation, with defects in this pathway strongly associated with tumorigenesis [98–100]. It is known that tumors have greatly increased levels of glucose uptake, insulin/insulin growth factor and their respective receptors. It is becoming clear that the Wnt/β-catenin pathway is involved in the mechanisms regulating energy metabolism [104] and glucose metabolism [105]. These studies suggest that Wnt signaling is involved in the regulation of glucose homeostasis.

In the Wnt pathway, the endosomal acidic environment provided by V-ATPase, is essential for the phosphorylation of LRP6 involved in signal transduction leading to activation of β-catenin [106]. Since the V-ATPases are also located at the plasma membrane in certain cell types, including highly metastatic cells, several interesting questions emerge regarding the relationship between V-ATPase and Wnt signaling pathways; and the factors upstream/ downstream that regulate proton transport and vice versa. As we know, in cancer cells, there is a shift in energy production. It has been suggested that the activation of glycolysis favors tumor growth as well as tumor invasion and metastasis via acidification of the tumor microenvironment. As a consequence of the switch to glycolysis, cancer cells rapidly take up glucose and convert most of it to lactate and protons, leading to a more acidic cytosolic pH.

6.1.1 V-ATPase via (P)RR/ATP6ap2

(P)RR/ATP6ap2 was first discovered not as a (pro)renin binding protein but as a protein associated with the V-ATPase. Ludwig and colleagues, in 1998, described a truncated form of (P)RR/ATP6ap2 composed of the C-terminal part and the transmembrane domain, which co-purified with the V-ATPase in adrenal chromaffin cells and was later named ATP6ap2, for vacuolar H^+-ATPase associated protein 2 [107]. In 2002, Nguyen and colleagues, discovered the full-length (P)RR/ATP6ap2 [108]. The identity of the two proteins was not immediately obvious leading to two different names for the same protein. The subcellular localization of (P)RR/ATP6ap2 is unusual for a receptor. Sequence analysis predicted motifs in the cytosolic domain of (P)RR/ATP6ap2 targeting the protein to distinct intracellular vesicle compartments [21]. Indeed, the majority of (P)RR/ATP6ap2 is located on intracellular vesicles, although a significant amount of the protein is also found on the plasma membrane, possibly due to vesicle recycling. Interestingly, this distribution concurs with the localization of the V-ATPase in metastatic tumors that exhibit this enzyme both in acidic vesicles and at the cell surface [37, 38, 63]. The cellular

distribution of (P)RR/ATP6ap2 in tumors is unclear. Until recently, the only function assigned to renin and its precursor prorenin was the cleavage of angiotensinogen as a first step in the Renin-Angiotensin System (RAS) [17, 21, 109, 110]. The (P)RR/ATP6ap2 function in regulating the RAS pathway is well established, however its role in regulating V-ATPase is unclear. The signaling pathways involved in the regulation of (P)RR/ATP6ap2 and V-ATPase interactions are unclear. PRR/ATP6ap2 was been shown to serve as a scaffolding protein linking V-ATPase to the Wnt canonical and PCP signaling pathways [103, 106, 111].

Cruciat and colleagues characterized V-ATPase and (P)RR/ATP6ap2 as essential components of Wnt signaling in HEK293T cells and Xenopus embryos, which is crucial for several processes in embryonic development [106]. The authors show that phosphorylation of the Wnt co-receptor LRP6, and thereby activation of intracellular Wnt signaling, is dependent on its sequestration in vesicles, which are acidified by the V-ATPases. Because PRR/ATP6ap2 and other V-ATPase subunits also interacted physically with Fz and LRP6, this suggests a model that characterizes PRR/ATP6ap2 as an adaptor that links Fz and LRP6 to the V-ATPase complex [103, 111]. This adaptor function is predominantly carried out by the extracellular domain of PRR, which is also regarded as the prorenin and renin binding domain, and therefore seems to serve multiple purposes. Intriguingly, renin showed no effect on Wnt signaling [103, 111]. It was reported that full length ATP6ap2 represses Wnt signaling, perhaps by blocking proton pumping activity. Cleavage of ATP6ap2 by furin released this inhibition [112].

Taelman and colleagues showed that Wnt signaling triggers GSK3 sequestration in multivesicular bodies, a late endocytic compartment that harbors intralumenal vesicles highly enriched with V-ATPase [113]. The GSK3 sequestration in multivesicular bodies is one reason Wnt signaling requires endocytosis of Wnt receptor complexes. This could be regulated by acidification of multivesicular bodies via V-ATPase [102]. Endocytosis and V-ATPase may play other roles in Wnt signaling beyond the formation of multivesicular bodies. Experiments with a fusion protein of LRP6 and a pH reporter suggested that the V-ATPase mediates acidification of vesicles specialized for signalosome formation [114, 115]. This makes V-ATPase a unique component of the signalosome complex that could regulate activity and function of the complex via localized regulation of the pH microenvironment. The V-ATPase is critical to provide the driving force for vesicle trafficking, neurotransmitter uptake, and exocytosis. The lack of (P)RR/ATP6ap2 may impair neurotransmission. Contrepas and colleagues showed that the D4-(P)RR mutant have altered trafficking of this receptor to the neurite tips in vitro [110].

The biogenesis of V-ATPase complex requires the coordinated association of V_1 with V_0 domains. Studies in yeast have shown that several genes Vma12p, Vma21p, and Vma22p are required for V-ATPase assembly. This suggests that mammalian cells may have similar assembly mechanism. It is unclear however, what is the assembly chaperone of mammalian V-ATPase. A functional link between ATP6ap2 and assembly of V_0/V_1 to form V-ATPase has been suggested [116, 117]. Kinouchi and colleagues suggested that ATP6ap2 is essential for V-ATPase assembly in murine cardiomyocytes [116]. In their study, they generated a mouse with a cardiac-specific deficiency in ATP6ap2. These studies demonstrated for the first time that

ATP6ap2 might be an essential assembly chaperone of mammalian V-ATPase; and that genetic ablation of ATP6ap2 created a loss-of-function model for V-ATPase representing a function that is unique to mammalian cells. Interestingly, there is no yeast homolog to mammalian ATP6ap2. However, ATP6ap2 showed sequence and structural similarity to the yeast chaperone, Vma21p, needed for the V-ATPase assembly [107]. Assembly of V_0 and V_1 domains in yeast relies on glucose and needs chaperones. Because cancer cells also rely on glucose, they may need a chaperone to assemble V-ATPase. Whether (P)RR/ATP6ap2 operates as a chaperone or glucose sensor, and accordingly assembles/disassembles and targets the V-ATPase to specific compartments, is unclear and warrants further investigation. Kirsch and colleagues have recently demonstrated that high glucose induces (P)RR signal transduction in neuronal and epithelial cells [118]. We have shown that ATP6ap2 mRNA levels are upregulated in highly metastatic prostate cancer cells compared to the lowly metastatic prostate cancer cells [119]. Therefore, we hypothesize that (P)RR/ATP6ap2 is the pH sensor/glucose sensor, and accordingly assembles V-ATPase and targets it to specific compartments to regulate the pH gradient and/or initiates signaling pathways. Whether this is a direct effect of the (P)RR/ATP6ap2, or an indirect effect due to interactions with a-subunit, a putative pH sensor in V-ATPase [43], requires further investigation. Sreekumar and colleagues have recently showed that a functional V-ATPase is essential for Wnt/β-catenin signaling in human and murine models of pancreatic intraepithelial neoplasms. The activation of Wnt/β--catenin is V-ATPase dependent and necessary for pancreatic tumorigenesis [120].

6.2 *V-ATPase Cross Talk with Hypoxia-Induced Factor (HIF) Pathway*

In eukaryotic cells, the major routes of energy production in cells are glycolysis and oxidative phosphorylation. However, the biochemical hallmark of cancer cells is a shift in glucose metabolism to aerobic glycolysis that, in bioenergetic grounds, is less effective than oxidative phosphorylation. This conundrum raises the question of how cancer cells grow and survive. To further complicate this issue, the neovascularization is often inadequate leading to an insufficient supply of oxygen to the tumor, i.e., hypoxia. Hypoxia causes the induction of various genes that contribute to tumor cell invasion and metastasis [121–124]. Several studies suggest that activation of the hypoxia inducible factor (HIF) is a common consequence of cancer.

HIF has been shown as the sensor of oxygen and respond to various cellular stimuli by upregulating genes involved in glucose metabolism, angiogenesis, cell proliferation and survival [125, 126]. HIF-1 is a transcription factor composed of the subunits HIF-1α and HIF-1β. At normal oxygen tension, HIF-1α is hydroxylated by prolyl hydroxylases (PHD) in the oxygen dependent degradation domain. Hydroxylated HIF-1α is recognized by the Von Hippel-Lindau (VHL) protein, ubiquitinated and destined for degradation by proteasomes [121]. At low oxygen pressure stabilized HIF-1α subunits heterodimerize with β subunits to activate target genes after nuclear translocation.

In addition to directly upregulating glycolytic enzyme expression, HIF-1 directly contributes to downregulating the tricarboxylic acid (TCA) cycle and OXPHOS (oxidative phosphorylation). OXPHOS is governed by the availability of its two major substrates: pyruvate and oxygen. Pyruvate is the end product of glycolysis, after which it enters the mitochondria and is converted to acetyl-CoA by the pyruvate dehydrogenase (PDH) complex, allowing it to enter the TCA cycle. PDH activity is inhibited through phosphorylation by pyruvate dehydrogenase kinase (PDK). Pyruvate conversion to acetyl-CoA in the mitochondria is thought to be an irreversible step, making this a critical control point in cellular metabolism. Studies found that PDK is a HIF-1 target gene [123]. By inhibiting PDH via PDK, cells with activated HIF-1 will accumulate pyruvate, which is then converted into lactate by another HIF-1 target: lactate dehydrogenase (LDH). Lactate is then released into the extracellular space by the Mono Carboxylic Transporter (MCT), ultimately regenerating NAD^+ for another cycle of glycolysis. The MCT4 isoform was recently demonstrated to be a HIF-1 target [127], suggesting that activation of HIF-1 drives expression of every enzyme in the pathway from glucose import to lactate production and release. HIF also induces overexpression of carbonic anhydrase 9 that catalyzes the extracellular conversion of CO_2 and H_2O to HCO_3^- and H^+. The HCO_3^- exchangers import extracellular HCO_3^- into the cytosol to decrease intracellular acidification. To prevent intracellular acidification during glycolysis, HIFs also drive the expression of the Na^+/H^+ exchanger [121]. However, as indicate earlier, in metastatic tumors we hypothesize that the main H^+-transporting mechanism is the V-ATPase at the cell surface. Given the significance of V-ATPase for pH regulation, we hypothesize that HIF-1 interacts with V-ATPase and possibly regulates transcription of V-ATPase subunits, since regulated energy metabolism and pH are central for cell survival.

Sonveaux and colleagues showed that human cancer cells cultured under low oxygen conditions convert glucose to lactate and extrude it via MCT4, whereas aerobic cancer cells take up lactate via MCT1 and utilize it for oxidative phosphorylation. When MCT1 is inhibited, aerobic cancer cells take up glucose rather than lactate, and anaerobic cancer cells die due to glucose deprivation [127]. Since V-ATPase assembly relies on glucose, these data suggested that under conditions of low glucose, V-ATPase may be disassembled leading to cell death. Indeed, V-ATPase overexpression is an antiapoptotic signal and inhibition of V-ATPase triggers apoptosis.

Many tumors exhibit high HIF activity even under normoxic conditions. Importantly, HIF stabilization has been observed under conditions of cytosolic acidification. Mekhail and colleagues showed that normoxic acidosis neutralizes the function of VHL (Von Hippel-Lindau) by triggering its nucleolar sequestration that enables HIF to evade destruction in the presence of oxygen, thus activating its target genes [128]. Their findings suggest that cytosolic acidification elicits a transient and reversible loss of VHL function by promoting its nucleolar sequestration. Therefore, it is likely that increased acid production will further induce HIF activity and glycolysis. In this case, V-ATPase is suitable positioned at the plasma membrane of tumor cells to maintain extracellular acidosis, thus creating a positive feedback loop to enhance the tumor phenotype.

Interestingly, a study of the growth inhibition of tumor cells by bafilomycin revealed an induction of HIF-1α expression, subsequent p21 induction, and cell-cycle arrest [129]. In this study, the effect of V-ATPase inhibition by bafilomycin on tumor survival does not appear to be at the level of intracellular pH regulation. This interaction was confirmed in a follow-up study where it was demonstrated that the effect of bafilomycin on cell survival was not a result of intracellular pH acidification [130]. Instead it was found that bafilomycin enhances the binding of the V-ATPase V_0 c-subunit to the N-terminus of HIF-1α, altering protein structure to prevent pVHL binding and thus results in HIF-1α stabilization. Thus, it appears that in addition to its role in regulating pH, V-ATPase may have alternative important role in signaling mechanisms. The significance of V-ATPase in signal transduction pathways is clearly an emerging field of study in cell physiology and pathophysiology.

7 Conclusions

To conclude, after about four decades of studying the significance of V-ATPase for the regulation of cellular functions in physiological and pathological states, have led us to recognize that V-ATPase functions not only to regulate pH homeostasis, but also has emerged roles in signal pathways. The future studies related to V-ATPase will clearly bright since it will provide us with a wonderful opportunity to understand how this remarkable nanomotor controls not only proton pumping, but also cell metabolism, bioenergetics and signal transduction.

References

1. Warburg O (1956) On the origin of cancer cells. Science 123:309–314
2. Warburg O, Wind F, Negelein E (1927) The metabolism of tumors in the body. J Gen Physiol 8:519–530
3. Vander Heiden MG, Cantley LC, Thompson CB (2009) Understanding the Warburg effect: the metabolic requirements of cell proliferation. Science 324:1029–1033
4. Taubes G (2012) Cancer research. Ravenous for glucose. Science 335:31
5. Dawson RMC, Elliot DC, Elliot WH, Jones KM (eds) (1968) Data for biochemical research, 3rd edn. Oxford, Oxford Science Publications
6. Kane PM (1995) Disassembly and reassembly of the yeast vacuolar H(+)-ATPase in vivo. J Biol Chem 270:17025–17032
7. Kane PM (2012) Targeting reversible disassembly as a mechanism of controlling V-ATPase activity. Curr Protein Pept Sci 13:117–123
8. Kane PM, Smardon AM (2003) Assembly and regulation of the yeast vacuolar H+-ATPase. J Bioenerg Biomembr 35:313–321
9. Jefferies KC, Cipriano DJ, Forgac M (2008) Function, structure and regulation of the vacuolar (H+)-ATPases. Arch Biochem Biophys 476:33–42
10. Maxson ME, Grinstein S (2014) The vacuolar-type H+-ATPase at a glance – more than a proton pump. J Cell Sci 127:4987–4993

11. Nishi T, Forgac M (2002) The vacuolar (H+)-ATPases—nature's most versatile proton pumps. Nat Rev Mol Cell Biol 3:94–103
12. Sun-Wada GH, Wada Y (2010) Vacuolar-type proton pump ATPases: roles of subunit isoforms in physiology and pathology. Histol Histopathol 25:1611–1620
13. Supek F, Supekova L, Mandiyan S et al (1994) A novel accessory subunit for vacuolar H(+)-ATPase from chromaffin granules. J Biol Chem 269:24102–24106
14. Louagie E, Taylor NA, Flamez D et al (2008) Role of furin in granular acidification in the endocrine pancreas: identification of the V-ATPase subunit Ac45 as a candidate substrate. Proc Natl Acad Sci U S A 105:12319–12324
15. Feng H, Cheng T, Pavlos NJ et al (2008) Cytoplasmic terminus of vacuolar type proton pump accessory subunit Ac45 is required for proper interaction with V(0) domain subunits and efficient osteoclastic bone resorption. J Biol Chem 283:13194–13204
16. Jansen EJ, Hafmans TG, Martens GJ (2010) V-ATPase-mediated granular acidification is regulated by the V-ATPase accessory subunit Ac45 in POMC-producing cells. Mol Biol Cell 21:3330–3339
17. Nguyen G (2011) Renin, (pro)renin and receptor: an update. Clin Sci (Lond) 120:169–178
18. Cousin C, Bracquart D, Contrepas A et al (2009) Soluble form of the (pro)renin receptor generated by intracellular cleavage by furin is secreted in plasma. Hypertension 53:1077–1082
19. Schoonderwoert VT, Martens GJ (2002) Targeted disruption of the mouse gene encoding the V-ATPase accessory subunit Ac45. Mol Membr Biol 19:67–71
20. Amsterdam A, Nissen RM, Sun Z et al (2004) Identification of 315 genes essential for early zebrafish development. Proc Natl Acad Sci U S A 101:12792–12797
21. Sihn G, Rousselle A, Vilianovitch L et al (2010) Physiology of the (pro)renin receptor: Wnt of change? Kidney Int 78:246–256
22. Metchnikoff E (1905) Immunity in infectious diseases (Transl. Co M). Cambridge University Press Warehouse, Cambridge
23. Kirshner N (1962) Uptake of catecholamines by a particulate fraction of the adrenal medulla. J Biol Chem 237:2311–2317
24. Apps DK, Reid GA (1977) Adenosine triphosphatase and adenosine diphosphate/adenosine triphosphate isotope-exchange activities of the chromaffin-granule membrane. Biochem J 167:297–300
25. Ohkuma S, Moriyama Y, Takano T (1982) Identification and characterization of a proton pump on lysosomes by fluorescein-isothiocyanate-dextran fluorescence. Proc Natl Acad Sci U S A 79:2758–2762
26. Stone DK, Xie XS, Racker E (1983) An ATP-driven proton pump in clathrin-coated vesicles. J Biol Chem 258:4059–4062
27. Harikumar P, Reeves JP (1983) The lysosomal proton pump is electrogenic. J Biol Chem 258:10403–10410
28. Cidon S, Ben-David H, Nelson N (1983) ATP-driven proton fluxes across membranes of secretory organelles. J Biol Chem 258:11684–11688
29. Forgac M, Cantley L, Wiedenmann B et al (1983) Clathrin-coated vesicles contain an ATP-dependent proton pump. Proc Natl Acad Sci U S A 80:1300–1303
30. Beyenbach KW, Wieczorek H (2006) The V-type H+ ATPase: molecular structure and function, physiological roles and regulation. J Exp Biol 209:577–589
31. Futai M, Oka T, Sun-Wada G et al (2000) Luminal acidification of diverse organelles by V-ATPase in animal cells. J Exp Biol 203:107–116
32. Nelson H, Nelson N (1990) Disruption of genes encoding subunits of yeast vacuolar H(+)-ATPase causes conditional lethality. Proc Natl Acad Sci U S A 87:3503–3507
33. Forgac M (2007) Vacuolar ATPases: rotary proton pumps in physiology and pathophysiology. Nat Rev Mol Cell Biol 8:917–929
34. Martinez-Munoz GA, Kane P (2008) Vacuolar and plasma membrane proton pumps collaborate to achieve cytosolic pH homeostasis in yeast. J Biol Chem 283:20309–20319

35. Breton S, Brown D (2013) Regulation of luminal acidification by the V-ATPase. Physiology (Bethesda) 28:318–329
36. Marshansky V, Rubinstein JL, Gruber G (2014) Eukaryotic V-ATPase: novel structural findings and functional insights. Biochim Biophys Acta 1837:857–879
37. Martinez-Zaguilan R, Gillies RJ (1992) A plasma membrane V-type H(+)-ATPase may contribute to elevated intracellular pH (pHin) in some human tumor cells. Ann N Y Acad Sci 671:478–480
38. Martinez-Zaguilan R, Lynch RM, Martinez GM, Gillies RJ (1993) Vacuolar-type H(+)-ATPases are functionally expressed in plasma membranes of human tumor cells. Am J Physiol 265:C1015–C1029
39. Toyomura T, Murata Y, Yamamoto A et al (2003) From lysosomes to the plasma membrane: localization of vacuolar-type H+-ATPase with the a3 isoform during osteoclast differentiation. J Biol Chem 278:22023–22030
40. Marshansky V, Futai M (2008) The V-type H+-ATPase in vesicular trafficking: targeting, regulation and function. Curr Opin Cell Biol 20:415–426
41. Hurtado-Lorenzo A, Skinner M, El Annan J et al (2006) V-ATPase interacts with ARNO and Arf6 in early endosomes and regulates the protein degradative pathway. Nat Cell Biol 8:124–136
42. Merkulova M, Hurtado-Lorenzo A, Hosokawa H et al (2011) Aldolase directly interacts with ARNO and modulates cell morphology and acidic vesicle distribution. Am J Physiol Cell Physiol 300:C1442–C1455
43. Marshansky V (2007) The V-ATPase a2-subunit as a putative endosomal pH-sensor. Biochem Soc Trans 35:1092–1099
44. D'Souza-Schorey C, Chavrier P (2006) ARF proteins: roles in membrane traffic and beyond. Nat Rev Mol Cell Biol 7:347–358
45. El Far O, Seagar M (2011) A role for V-ATPase subunits in synaptic vesicle fusion? J Neurochem 117:603–612
46. Israel M, Morel N, Lesbats B et al (1986) Purification of a presynaptic membrane protein that mediates a calcium-dependent translocation of acetylcholine. Proc Natl Acad Sci U S A 83:9226–9230
47. Zhang W, Wang D, Volk E et al (2008) V-ATPase V0 sector subunit a1 in neurons is a target of calmodulin. J Biol Chem 283:294–300
48. Hiesinger PR, Fayyazuddin A, Mehta SQ et al (2005) The v-ATPase V0 subunit a1 is required for a late step in synaptic vesicle exocytosis in Drosophila. Cell 121:607–620
49. Di Giovanni J, Boudkkazi S, Mochida S et al (2010) V-ATPase membrane sector associates with synaptobrevin to modulate neurotransmitter release. Neuron 67:268–279
50. Di Giovanni J, Iborra C, Maulet Y et al (2010) Calcium-dependent regulation of SNARE-mediated membrane fusion by calmodulin. J Biol Chem 285:23665–23675
51. Quetglas S, Leveque C, Miquelis R et al (2000) $Ca2^{+}$-dependent regulation of synaptic SNARE complex assembly via a calmodulin- and phospholipid-binding domain of synaptobrevin. Proc Natl Acad Sci U S A 97:9695–9700
52. Brochier G, Morel N (1993) The same 15 kDa proteolipid subunit is a constituent of two different proteins in Torpedo, the acetylcholine releasing protein mediatophore and the vacuolar H^{+} ATPase. Neurochem Int 23:525–539
53. Levin M (2002) Isolation and community: a review of the role of gap-junctional communication in embryonic patterning. J Membr Biol 185:177–192
54. Peters C, Bayer MJ, Buhler S et al (2001) Trans-complex formation by proteolipid channels in the terminal phase of membrane fusion. Nature 409:581–588
55. Liegeois S, Benedetto A, Garnier JM et al (2006) The V0-ATPase mediates apical secretion of exosomes containing Hedgehog-related proteins in Caenorhabditis elegans. J Cell Biol 173:949–961
56. Sun-Wada GH, Toyomura T, Murata Y et al (2006) The a3 isoform of V-ATPase regulates insulin secretion from pancreatic beta-cells. J Cell Sci 119:4531–4540

57. Poea-Guyon S, Ammar MR, Erard M et al (2013) The V-ATPase membrane domain is a sensor of granular pH that controls the exocytotic machinery. J Cell Biol 203:283–298
58. Schlesinger PH, Blair HC, Teitelbaum SL, Edwards JC (1997) Characterization of the osteoclast ruffled border chloride channel and its role in bone resorption. J Biol Chem 272:18636–18643
59. Breton S, Smith PJ, Lui B, Brown D (1996) Acidification of the male reproductive tract by a proton pumping (H+)-ATPase. Nat Med 2:470–472
60. Wagner CA, Finberg KE, Breton S et al (2004) Renal vacuolar H+-ATPase. Physiol Rev 84:1263–1314
61. Al-Awqati Q (1996) Plasticity in epithelial polarity of renal intercalated cells: targeting of the H(+)-ATPase and band 3. Am J Physiol 270:C1571–C1580
62. Rojas JD, Sennoune SR, Maiti D et al (2006) Vacuolar-type H+-ATPases at the plasma membrane regulate pH and cell migration in microvascular endothelial cells. Am J Physiol Heart Circ Physiol 291:H1147–H1157
63. Sennoune SR, Bakunts K, Martinez GM et al (2004) Vacuolar H^+-ATPase in human breast cancer cells with distinct metastatic potential: distribution and functional activity. Am J Physiol Cell Physiol 286:C1443–C1452
64. Raghunand N, Martinez-Zaguilan R, Wright SH, Gillies RJ (1999) pH and drug resistance. II. Turnover of acidic vesicles and resistance to weakly basic chemotherapeutic drugs. Biochem Pharmacol 57:1047–1058
65. Martínez-Zaguilán R, Martinez GM, Gomez A et al (1998) Distinct regulation of pHin and [Ca2+]in in human melanoma cells with different metastatic potential. J Cell Physiol 176:196–205
66. Martínez-Zaguilán R, Raghunand N, Lynch RM et al (1999) pH and drug resistance. I. Functional expression of plasmalemmal V-type H+-ATPase in drug-resistant human breast carcinoma cell lines. Biochem Pharmacol 57:1037–1046
67. Kawasaki-Nishi S, Nishi T, Forgac M (2001) Yeast V-ATPase complexes containing different isoforms of the 100-kDa a-subunit differ in coupling efficiency and in vivo dissociation. J Biol Chem 276:17941–17948
68. Qi J, Forgac M (2007) Cellular environment is important in controlling V-ATPase dissociation and its dependence on activity. J Biol Chem 282:24743–24751
69. Parra KJ, Kane PM (1998) Reversible association between the V1 and V0 domains of yeast vacuolar H+-ATPase is an unconventional glucose-induced effect. Mol Cell Biol 18:7064–7074
70. Bond S, Forgac M (2008) The Ras/cAMP/protein kinase A pathway regulates glucose-dependent assembly of the vacuolar (H+)-ATPase in yeast. J Biol Chem 283:36513–36521
71. Voss M, Vitavska O, Walz B et al (2007) Stimulus-induced phosphorylation of vacuolar H(+)-ATPase by protein kinase A. J Biol Chem 282:33735–33742
72. Sautin YY, Lu M, Gaugler A et al (2005) Phosphatidylinositol 3-kinase-mediated effects of glucose on vacuolar H+-ATPase assembly, translocation, and acidification of intracellular compartments in renal epithelial cells. Mol Cell Biol 25:575–589
73. Dechant R, Binda M, Lee SS et al (2010) Cytosolic pH is a second messenger for glucose and regulates the PKA pathway through V-ATPase. EMBO J 29:2515–2526
74. Xu T, Forgac M (2001) Microtubules are involved in glucose-dependent dissociation of the yeast vacuolar [H+]-ATPase in vivo. J Biol Chem 276:24855–24861
75. Lu M, Ammar D, Ives H et al (2007) Physical interaction between aldolase and vacuolar H+-ATPase is essential for the assembly and activity of the proton pump. J Biol Chem 282:24495–24503
76. Seol JH, Shevchenko A, Deshaies RJ (2001) Skp1 forms multiple protein complexes, including RAVE, a regulator of V-ATPase assembly. Nat Cell Biol 3:384–391
77. Smardon AM, Diab HI, Tarsio M et al (2014) The RAVE complex is an isoform-specific V-ATPase assembly factor in yeast. Mol Biol Cell 25:356–367
78. Tabke K, Albertmelcher A, Vitavska O et al (2014) Reversible disassembly of the yeast V-ATPase revisited under in vivo conditions. Biochem J 462:185–197

79. Li SC, Diakov TT, Xu T et al (2014) The signaling lipid PI(3,5)P(2) stabilizes V(1)-V(o) sector interactions and activates the V-ATPase. Mol Biol Cell 25:1251–1262
80. Diakov TT, Kane PM (2010) Regulation of vacuolar proton-translocating ATPase activity and assembly by extracellular pH. J Biol Chem 285:23771–23778
81. De Luca M, Cogli L, Progida C et al (2014) RILP regulates vacuolar ATPase through interaction with the V1G1 subunit. J Cell Sci 127:2697–2708
82. Huss M, Wieczorek H (2009) Inhibitors of V-ATPases: old and new players. J Exp Biol 212:341–346
83. Toei M, Saum R, Forgac M (2010) Regulation and isoform function of the V-ATPases. Biochemistry 49:4715–4723
84. Pietrement C, Sun-Wada GH, Silva ND et al (2006) Distinct expression patterns of different subunit isoforms of the V-ATPase in the rat epididymis. Biol Reprod 74:185–194
85. Oka T, Murata Y, Namba M et al (2001) a4, a unique kidney-specific isoform of mouse vacuolar H+-ATPase subunit a. J Biol Chem 276:40050–40054
86. Hinton A, Sennoune SR, Bond S et al (2009) Function of a subunit isoforms of the V-ATPase in pH homeostasis and in vitro invasion of MDA-MB231 human breast cancer cells. J Biol Chem 284:16400–16408
87. Nishisho T, Hata K, Nakanishi M et al (2011) The a3 isoform vacuolar type H(+)-ATPase promotes distant metastasis in the mouse B16 melanoma cells. Mol Cancer Res 9:845–855
88. Capecci J, Forgac M (2013) The function of vacuolar ATPase a subunit isoforms in invasiveness of MCF10a and MCF10CA1a human breast cancer cells. J Biol Chem 288:32731–32741
89. Cotter K, Capecci J, Sennoune S et al (2014) Activity of plasma membrane V-ATPase is critical for the invasion of MDA-MB231 breast cancer cells. J Biol Chem 290(6):3680–3692
90. Racker E (1972) Bioenergetics and the problem of tumor growth. Am Sci 60:56–63
91. Gillies RJ, Martinez-Zaguilan R, Martinez GM et al (1990) Tumorigenic 3T3 cells maintain an alkaline intracellular pH under physiological conditions. Proc Natl Acad Sci U S A 87:7414–7418
92. Gillies RJ, Robey I, Gatenby RA (2008) Causes and consequences of increased glucose metabolism of cancers. J Nucl Med 49(Suppl 2):24S–42S
93. Spugnini EP, Sonveaux P, Stock C et al (2014) Proton channels and exchangers in cancer. Biochim Biophys Acta pii:S0005-2736(14)00350-2
94. Su Y, Zhou A, Al-Lamki RS, Karet FE (2003) The a-subunit of the V-type H+-ATPase interacts with phosphofructokinase-1 in humans. J Biol Chem 278:20013–20018
95. Chan CY, Parra KJ (2014) Yeast phosphofructokinase-1 subunit Pfk2p is necessary for pH homeostasis and glucose-dependent vacuolar ATPase reassembly. J Biol Chem 289:19448–19457
96. Rubenstein EM, Schmidt MC (2010) The glucose signal and metabolic p[H^+]lux. EMBO J 29:2473–2474
97. Fogarty FM, O'Keeffe J, Zhadanov A et al (2014) HRG-1 enhances cancer cell invasive potential and couples glucose metabolism to cytosolic/extracellular pH gradient regulation by the vacuolar-H(+) ATPase. Oncogene 33:4653–4663
98. Cadigan KM, Nusse R (1997) Wnt signaling: a common theme in animal development. Genes Dev 11:3286–3305
99. Clevers H (2006) Wnt/beta-catenin signaling in development and disease. Cell 127:469–480
100. Katoh M (2005) WNT/PCP signaling pathway and human cancer. Oncol Rep 14:1583–1588
101. Kohn AD, Moon RT (2005) Wnt and calcium signaling: beta-catenin-independent pathways. Cell Calcium 38:439–446
102. Kikuchi A, Yamamoto H (2007) Regulation of Wnt signalling by receptor-mediated endocytosis. J Biochem 141:443–451
103. Hermle T, Petzoldt AG, Simons M (2011) The role of proton transporters in epithelial Wnt signaling pathways. Pediatr Nephrol 26:1523–1527

104. Prestwich TC, Macdougald OA (2007) Wnt/beta-catenin signaling in adipogenesis and metabolism. Curr Opin Cell Biol 19:612–617
105. Fujino T, Asaba H, Kang MJ et al (2003) Low-density lipoprotein receptor-related protein 5 (LRP5) is essential for normal cholesterol metabolism and glucose-induced insulin secretion. Proc Natl Acad Sci U S A 100:229–234
106. Cruciat CM, Ohkawara B, Acebron SP et al (2010) Requirement of prorenin receptor and vacuolar H+-ATPase-mediated acidification for Wnt signaling. Science 327:459–463
107. Ludwig J, Kerscher S, Brandt U et al (1998) Identification and characterization of a novel 9.2-kDa membrane sector-associated protein of vacuolar proton-ATPase from chromaffin granules. J Biol Chem 273:10939–10947
108. Nguyen G, Delarue F, Burckle C et al (2002) Pivotal role of the renin/prorenin receptor in angiotensin II production and cellular responses to renin. J Clin Invest 109:1417–1427
109. Bader M (2007) The second life of the (pro)renin receptor. J Renin Angiotensin Aldosterone Syst 8:205–208
110. Contrepas A, Walker J, Koulakoff A et al (2009) A role of the (pro)renin receptor in neuronal cell differentiation. Am J Physiol Regul Integr Comp Physiol 297:R250–R257
111. Hermle T, Saltukoglu D, Grunewald J et al (2010) Regulation of frizzled-dependent planar polarity signaling by a V-ATPase subunit. Curr Biol 20:1269–1276
112. Bernhard SM, Seidel K, Schmitz J et al (2012) The (pro)renin receptor ((P)RR) can act as a repressor of Wnt signalling. Biochem Pharmacol 84:1643–1650
113. Taelman VF, Dobrowolski R, Plouhinec JL et al (2010) Wnt signaling requires sequestration of glycogen synthase kinase 3 inside multivesicular endosomes. Cell 143:1136–1148
114. Bilic J, Huang YL, Davidson G et al (2007) Wnt induces LRP6 signalosomes and promotes dishevelled-dependent LRP6 phosphorylation. Science 316:1619–1622
115. Niehrs C, Acebron SP (2010) Wnt signaling: multivesicular bodies hold GSK3 captive. Cell 143:1044–1046
116. Kinouchi K, Ichihara A, Sano M et al (2010) The (pro)renin receptor/ATP6AP2 is essential for vacuolar H+-ATPase assembly in murine cardiomyocytes. Circ Res 107:30–34
117. Kinouchi K, Ichihara A, Sano M et al (2013) The role of individual domains and the significance of shedding of ATP6AP2/(pro)renin receptor in vacuolar H^+-ATPase biogenesis. PLoS One 8, e78603
118. Kirsch S, Schrezenmeier E, Klare S et al (2014) The (pro)renin receptor mediates constitutive PLZF-independent pro-proliferative effects which are inhibited by bafilomycin but not genistein. Int J Mol Med 33:795–808
119. Sennoune SR, Bermudez LE, Lees JC et al (2014) Vacuolar H^+-ATPase is down-regulated by the angiogenesis-inhibitory pigment epithelium-derived factor in metastatic prostate cancer cells. Cell Mol Biol 60:45–52
120. Sreekumar BK, Belinsky GS, Einwachter H et al (2014) Polarization of the vacuolar adenosine triphosphatase delineates a transition to high-grade pancreatic intraepithelial neoplasm lesions. Pancreas 43:1256–1263
121. Aragones J, Fraisl P, Baes M, Carmeliet P (2009) Oxygen sensors at the crossroad of metabolism. Cell Metab 9:11–22
122. Semenza GL, Wang GL (1992) A nuclear factor induced by hypoxia via de novo protein synthesis binds to the human erythropoietin gene enhancer at a site required for transcriptional activation. Mol Cell Biol 12:5447–5454
123. Semenza GL (2010) HIF-1: upstream and downstream of cancer metabolism. Curr Opin Genet Dev 20:51–56
124. Robey IF, Stephen RM, Brown KS et al (2008) Regulation of the Warburg effect in early-passage breast cancer cells. Neoplasia 10:745–756
125. Kaelin WG Jr, Thompson CB (2010) Q&A: cancer: clues from cell metabolism. Nature 465:562–564
126. Maxwell PH (2005) The HIF pathway in cancer. Semin Cell Dev Biol 16:523–530
127. Sonveaux P, Vegran F, Schroeder T et al (2008) Targeting lactate-fueled respiration selectively kills hypoxic tumor cells in mice. J Clin Invest 118:3930–3942

128. Mekhail K, Gunaratnam L, Bonicalzi ME, Lee S (2004) HIF activation by pH-dependent nucleolar sequestration of VHL. Nat Cell Biol 6:642–647
129. Lim JH, Park JW, Kim MS et al (2006) Bafilomycin induces the p21-mediated growth inhibition of cancer cells under hypoxic conditions by expressing hypoxia-inducible factor-1alpha. Mol Pharmacol 70:1856–1865
130. Lim JH, Park JW, Kim SJ et al (2007) ATP6V0C competes with von Hippel-Lindau protein in hypoxia-inducible factor 1alpha binding and mediates HIF-1alpha expression by bafilomycin A1. Mol Pharmacol 71:942–948

Chapter 19
V-ATPases and Their Implication in Oral Cancer

Mônica Ghislaine Oliveira Alves, Abel García-García, and Mario Pérez-Sayáns

Abstract The control of intracellular and extracellular pH is extremely important for many biological functions and the condition of hypoxia is a frequent phenomenon during the development of oral squamous cell carcinoma (OSCC). The cellular acidosis appears to be controlled, mainly, by the vacuolar-type H+ ATPase (V-ATPase), which is clearly involved in cellular transformation during carcinogenesis and metastasis. The C subunit (ATP6V1C) of V1 intra-membrane domain of the V-ATPase is primarily responsible for its enzymatic function, through the control of a reversible dissociation of V0 and V1 domains. It is observed a high overexpression of the gene ATP6V1C1 in OSCC, this tumor cells exhibited high metabolic activity and the active mechanisms capable of pumping protons from the cell interior are necessary. The acidification of the extracellular environment resulting from poor vascularization and cell metabolism promotes the activity of proteolytic enzymes that contribute to tumor invasiveness and metastasis. In the future, V-ATPase inhibitor molecules could be used in cancer treatment through the mensuration of the overexpression of specific V-ATPase subunits in tumors to be treated and, then, using specific inhibitors for the subunits being expressed. This will allow clinicians to provide more specific treatment, while also minimizing adverse effects.

Keywords Oral squamous cell carcinoma • ATP6V1C1 • Cancer • V-ATPase inhibitors • Tumor metastasis • Chemoresistance

M.G.O. Alves
Department of Biosciences and Oral Diagnosis, Institute of Science and Technology, UNESP – Univ Estadual Paulista, 777 Engenheiro Francisco José Longo Avenue, São Dimas, São José dos Campos, SP, Brazil

M. Pérez-Sayáns (✉) • A. García-García
Faculty of Medicine and Dentistry, Oral Medicine, Oral Surgery and Implantology Unit, Entrerríos s/n 15782, Santiago de Compostela, ACoruña, Spain
e-mail: perezsayans@gmail.com

S. Chakraborti, N.S. Dhalla (eds.), *Regulation of Ca^{2+}-ATPases,V-ATPases and F-ATPases*, Advances in Biochemistry in Health and Disease 14,
DOI 10.1007/978-3-319-24780-9_19

1 Introduction

The control of intracellular and extracellular pH is extremely important for many biological functions such as cell proliferation, invasion, metastasis, drug resistance, and apoptosis. Since the hypoxia has a relationship with the extracellular decrease of pH, and the condition of hypoxia is a frequent phenomenon during the development of oral cancer [1], it is expected that the process of carcinogenesis is accompanied by metabolic disorders such as acidification of the extracellular medium and, therefore, the alkalinization of the intracellular medium [2, 3].

Tumor acid extracellular microenvironment is associated with increased invasiveness and progression of the lesion [3]. To survive in this hostile microenvironment, tumor cells must have a regulatory system in cytosolic pH which helps them in defense against H+ ions [4]. Some genes are related to the mechanism which regulates cytosolic pH and extracellular pH, like ATP6V0E, ATP6V1C1, ATP6V1G1, ATP6V0C, ATP6V1B1, ATP6V1A1, ATP6V1B2, ATP6V1E1, ATP6V1F, ATP6V0A1, ATP6V0B, and ATP6S1 [5].

The intracellular acidosis seems to be an early event in apoptosis [6]. In contrast, the intracellular pH is increased concomitantly with an increasing in DNA synthesis [7], leading to the raising of potential of neoplastic cells [8] and hence increasing of pathological disorders [1]. Reshkin et al. [8] showed that the alkalization is an early event for the establishment and maintenance of oncogenic transformation event.

The cellular acidosis appears to be controlled, mainly, by the vacuolar-type H+ ATPase (V-ATPase), which is clearly involved in cellular transformation during carcinogenesis and metastasis [1]. The pH regulation is mediated in squamous cell carcinoma (SCC) by vacuolar ATPase proton pump and, as well, it is involved in carcinogenesis [5].

The V-ATPase is a multi-subunit enzyme which reveals a great diversity of functions in eukaryotic organisms, such as acidification of a variety of intracellular compartments and the dispatch of protons to the extracellular medium through plasma membranes, conducting intracellular and extracellular ATP-dependent transport. Also, it is involved in receptor-mediated endocytosis [9], intracellular trafficking and acidification of late endosomes [10–13], the transport of lysosomal enzymes from the Golgi apparatus to lysosomes [13] and in the creation of the microenvironment necessary for proper protein transport, exchange and secretion [14]. This protein is also involved in the regulation of the acidity of the tumor microenvironment. Furthermore, there is evidence that it plays a fundamental role in resistance to chemotherapy [15].

V-ATPase is composed of a cytosolic V1 domain and a transmembrane V0 domain, and these domains are formed by subunits. Two alternative transcript variants encoding different isoforms have been found for the gene which controls the expression of the C subunit: ATP6V1C1 and ATP6V1C2a,b. While ATP6V1C1 is expressed continuously in all tissues, ATP6V1C2a,b is found only in the lungs, kidneys and epididymis, where it has an actin-binding function [5].

The C subunit is a 40-kDa protein located in the V1 domain of V-ATPase [16]. This subunit, which is essential for the proton secretion function of V-ATPases [17], is intimately involved in the reversible dissociation of the V1 and V0 domains [18, 19] and it is considered to be the unique responsible for regulating the dissociative mechanism of the enzyme [1, 20]. The crystal structure of the C subunit consists of two globular domains connected by a flexible connection [16].

Inoue and Forgac observed the importance of ATP6V1C1 for the reversible dissociation as a mechanism for monitoring the V-ATPase activity [21]. The authors described the connection of the subunit C with the G and E subunit of the V1 domain and the A subunit of the V0 domain, establishing the importance of this subunit as the main responsible for the enzyme control [21, 22]. Also, subunit C is involved in the reversible dissociation of the V0 and V1 domains [18, 23]. Moreover, the C subunit is crucial to the proton secretion function of the V-ATPases, since the ATP hydrolysis is blocked without it [17].

Puopolo et al. assert that subunit C speeds up the process but it is not essential for the formation of the complex V1V0 [24]. Beltran et al. [20] and Drory et al. [16], supported this theory, affirming that the C subunit is the only responsible for the in vivo dissociation of the V-ATPase [16, 20]. These results are discussed in other studies and, according to Voss et al., the C subunit is responsible for producing the dissociation of the V-ATPase in the cytosolic V1 complex and in the membranous V0 complex, through interaction with A-kinase protein. The C subunit serves as a substrate for the A-kinase protein and its phosphorylation may be the main mechanism to form the active V1V0 holoenzyme [19].

The C subunit seems to act as an anchor protein, allowing the connection between the V-ATPase and the actinic cytoskeleton. In addition, another mechanism of reversible dissociation regulated by the C subunit is the separation of V1V0 holoenzyme in V1 and V0 subcomplex, which is carried out through binding this holoenzyme to the F-actin next to the basement membrane of epithelial cells [25].

Without the C subunit, the assembly of the two domains occurred, but the V1V0 complex became highly unstable and the activity of the V-ATPase was extremely low, suggesting the exclusivity of the C subunit in the regulation of the complex V1V0 assembly [26]. In experimental models with different mutations in the gene of the C subunit, it was observed 48 % higher decrease in catalytic activity, without affecting the enzyme assembly [27].

2 Oral Squamous Cell Carcinoma

According to the World Health Organization (WHO), the oral and oropharyngeal carcinoma are the most frequent among malignant neoplasms of the head and neck [28], with about 600,000 new cases diagnosed per year worldwide [29]. The squamous cell carcinoma is the most common malignancy of the oral cavity [30], it is the sixth most common malignant tumor and its incidence is currently increasing worldwide [31].

The tongue and floor of mouth are the most common location, except in Southeast Asia, where the oral mucosa is a more common region to this carcinoma. Besides, it is strongly associated with environmental factors and the lifestyle play an important role in its development, among which we highlight the tobacco and alcohol [32].

The diagnosis, by clinical examination and histopathological studies, are commonly performed in advanced stages of the disease, resulting in a poor prognosis, a high cost treatment and a high mortality rate. Therefore, it is of utmost importance the early diagnosis [33].

Regardless of advances in reconstructive surgery the mortality remains high, with development of systemic metastases [34] or second malignancies [35]. The regional (neck) lymph node metastases have been recognized as an important prognostic factor, influencing the disease-specific survival rate [36], because of the treatment of the neck nodes, either therapeutic or prophylactic, which is an important aspect of the disease management [37, 38].

The treatment choice depends on the location of the primary tumor and of the stage of the disease. American Joint Committee on Cancer describes as early-stage oral SCC those usually treated with single-modality therapy, surgery or radiotherapy. The management of locally advanced disease generally requires various combinations of radiotherapy, surgery, and chemotherapy. The survival rates for all patients with oral SCC are, approximately, 40–60 % at 5 years [39].

3 Role of V-ATP-ases in Oral Cancer

The increased production and secretion of protons [H+], the acidification of the extracellular environment and the alkalization of the cytoplasm are metabolic disorders associated to the cell transformation and carcinogenesis processes, as well as to the increase of aggressiveness of the malignant tumors [40, 41].

The acid component of the intratumoral metabolic microenvironment increases the metastatic potential by promoting the angiogenesis [42, 43], the anchorage-independent growth, the genetic instability [44], the invasion, the infiltration, and the penetration of cancer cells into the normal tissue [3]. Equally, the angiogenesis is increased and the microvascular endothelial cells with the highest migratory capacity express V-ATPases in the plasma membrane [45].

The high increase of the invasiveness of tumor cells is the result of three complementary mechanisms: breaking of the cell-matrix interactions that arise because of the acid secretion increment, the protease activity (such as Cathepsin B) and the increased cell motility [3, 4, 46]. The degradation of the extracellular matrix during the metastatic invasion is performed by lysosomal enzymes that tumor cells secrete. These enzymes have a low optimum pH and the V-ATPases are the responsible for the microenvironment acidification [2, 10].

Cells must acquire motility and an invasive phenotype to become metastatically competent [3, 42]. A reduction of extracellular pH in the tumor microenvironment turns the cells into a more invasive cell and increases tumor cell motility through the

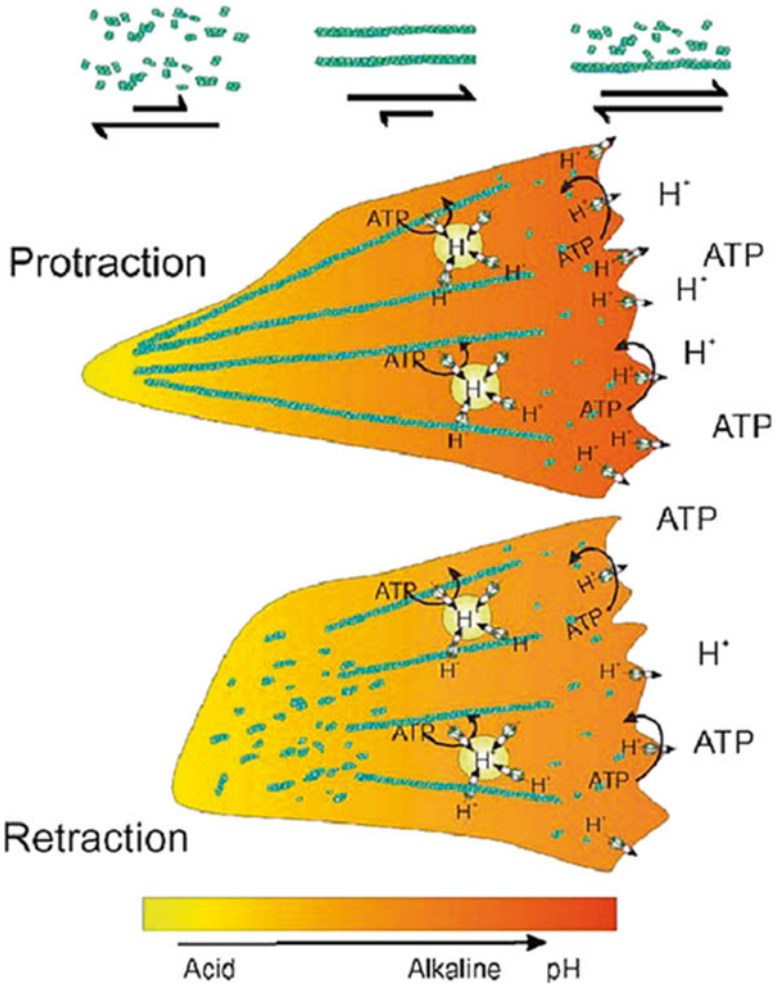

Fig. 19.1 Proposed mechanism by which overexpression of pmV-ATPase at the leading edge of the cell modulates cell migration/invasion. The proposed model should be viewed as a framework to explain how pmVATPases determine the acquisition of an invasive phenotype needed for angiogenesis and metastasis. Changes in pHcyt are critical for establishing cell polarity needed for cell movement. A critical step in directed motility and migration is the asymmetric actin polymerization at the leading edge. Reprinted from Ref. [42], with kind permission from Springer Science and Business Media

formation of pseudopodia. The extracellular acidification also induces an increase in the number and length of pseudopodia of metastatic cells [47], which are projected into the direction of movement of the tumor cells [48] (Fig. 19.1)

In addition, the hypoxic conditions are frequent phenomena during the OSCC development and they cause cellular acidosis. It seems to be a trigger for apoptosis and allows the endonuclease activation, which induces DNA fragmentation. Thus,

the pH regulators should be over-regulated in the tumor cells in order to avoid intracellular acidification under the abovementioned conditions [5].

It has been hypothesized that hypoxia and acidity may contribute to the transition from benign to malignant growth, inducing the selection of tumor cells capable to survive in an acidic, oxygen-deprived environment [49]. Indeed, alteration of the pH gradient between the extracellular environment and the cell cytoplasm has been suggested as a possible mechanism of resistance to cytotoxic drugs [50].

The pretreatment with proton pump inhibitors [PPIs] has been found to sensitize tumor cell lines to the effect of different chemotherapy drugs [50–52], triggering apoptotic mechanisms that lead to the inhibition of tumor growth [1]. The low pH levels are suitable for the complete activation of PPIs [53], suggesting that tumor alkalinization may be an extremely interesting target for future anticancer treatments [50, 51, 54].

V-ATPases are the key of the mechanisms that regulate this acidic tumor microenvironment and, therefore, they can be inhibited. While there are many pH regulator inhibitors, V-ATPase inhibitors have been proven to be the most efficient, since V-ATPases are the main regulators of pH [1, 4, 55]. Specific V-ATPase inhibitors such as concanamycin and bafilomycins are other candidates for investigation, not only to treat cancer but also to reduce multidrug resistance in tumors [1]

The V-ATPase is overexpressed in the plasma membrane of breast [2, 4, 56] and lung cancer cells [46, 56]; this occurs predominantly in the highly metastatic cells and, with less intensity, in the lowly metastatic cells [2, 4].

Otero-Rey et al. observed a high overexpression of the gene in ATP6V1C1 oral SCC biopsy samples. The authors found that ATP6V1C1 was overexpressed in 100 % of OSCC samples analyzed using real-time quantitative polymerase chain reaction and they argue that ATP6V1C1 plays a key role in the modification of the V-ATPase process and that the overexpression of ATP6V1C1 can explain the increase in extracellular pH observed in these tumors, even at early stages of the process [5]. They also state that the C1 subunit of V-ATPase allows that the union between the V0 component (membranous) and the V1 component [cytosolic catalytic] become stable [5]. Sayans-Perez et al. [57] ATP6V1C1 confirmed that the gene was significantly overexpressed, in oral SCC patients compared to healthy controls, using exfoliative cytology samples.

In normal epithelial cells, the staining of ATP6V1C1 was observed in the basal and parabasal layers, where there is more metabolic cell activity [58]. Besides, there were no signs of the C1 subunit on the keratinized surface of the epithelium. In the basal layer there is high production of protons, which must be eliminated by the cell to prevent destruction due the decrease of the pH [13].

The tumor cells in OSCC exhibited high metabolic activity and the active mechanisms capable of pumping protons from the cell interior are necessary to allow normal cell function. Moreover, the acidification of intercellular spaces, caused by disorderly growth of inadequately vascularized tumors and, by the deficient protons drainage through the environment requires active mechanisms in the cell membrane, such as the presence of V-ATPase, to pump protons against the gradient. Thus, acidification of the extracellular environment resulting from poor

vascularization and cell metabolism promotes the activity of proteolytic enzymes that contribute both to the destruction of intercellular protein architecture, such as collagen, and to tumor invasiveness and metastasis [2, 10].

4 V-ATP-ases as Protein Targeting

Tumor acidic microenvironment plays a key role in cancer development in terms of progression and metastasis [59]. The C subunit of V0 domain has been appointed as a possible target in the suppression of metastasis and tumor growth via V-ATPase inhibition, since it has a regulation function [4, 42, 60, 61]. However, Otero Rey et al. find that ATP6V0C is not overexpressed in OSCC in a statistically significant way. Therefore blocking this gene does not seem to be very useful in this type of tumors. Notwithstanding ATP6V1C1 was strongly overexpressed in oral squamous cell carcinoma [5].

Many possible targets were studied in the literature; however, it seems that none of these inhibitors has been proven useful in the OSCC. Thus, it is of high importance to carry out further research in order to determine the actual implication of V-ATPases in cancer development, as well to study the implementation of other inhibitors in the subunits responsible for enzyme assembly [4].

The inhibition of V-ATPase with PPIs allows the anticancer drugs enter and act within the tumor cells, triggering apoptotic mechanisms that lead to the inhibition of tumor growth [62].

5 V-ATPase Inhibitors and Implication in Cancer Treatment

As previously mentioned, the ability of tumor cells to secrete protons [H+] [2] to acidify the extracellular medium [3, 63], and it keeps the cytosolic pH alkaline [42], which is related with the increase of tumor aggressiveness [40, 41]. It is associated with degradation and remodeling through activation of proteolytic enzymes, which contribute to invasion and cancer metastasis [2, 64]. Thus, the V-ATPases in the plasma membrane are involved in the acquisition of a more metastatic phenotype. In this manner, the use of V-ATPase inhibitors allows distant metastasis to be minimized [62].

Further, scientific evidence suggests that the cells which express high levels of C subunit have an increased resistance to chemotherapeutic agents, so they may be a possible target in anticancer therapy [65]. There is overexpression of the ATP6C gene or C subunit in the cisplatin-resistant tumors [84].

Feng et al. indicated that ATP6V1C1 may be a viable target for breast cancer therapy and the silencing of ATP6V1C1 could be an innovative therapeutic approach for treatment and prevention of breast cancer growth and metastasis [56]. Lu et al. [67] observed that overexpression of V-ATPase was related to the pathological type

and grade of non-small-cell lung cancer. It was also likely the associated with chemotherapy drug resistance [67]. Huang et al. [68] observed that V-ATPase were overexpressed in esophageal squamous cancer cells, associated with pathological grade, TNM stage and tumor metastasis in esophageal squamous cancer cells. Their expression may be strongly associated with drug resistance and tumor metastasis [68].

Initial attempts to block V-ATPases were made with bafilomycin and concanamycin [69]. In addition, Moriyama et al. [70] described V-ATPase inhibition as a target for therapy, by blocking assembly and reducing H+ secretory activity with fusidic acid and suramin.

There are some classes of V-ATPase inhibitors: the first family is plecomacrolide antibiotics (concanamycin and bafilomycin), the second family is benzolactone namides (salicylihamide, apicularens, lobatamides, oximidines, and cruentaren); the third family is archazolid; the fourth family is indolyls; and, finally, the late-generation of V-ATPase inhibitors [62].

Lu et al. found that distant metastasis could be delayed and suppressed in human hepatocellular carcinoma in vitro by the inhibition of V-ATPase subunit C [ATP6L] [61], through bafilomycin and concanamycin [71].

The use of V-ATPase inhibitors, such as bafilomycin A1 or concanamycin A, also prevented conditions that favor metastatic dissemination in tyrosinase-positive amelanotic melanoma cells [72].

Cancer cells are more likely to express V-ATPase than normal cells, causing abnormalities in the acidic microenvironment and affecting cancer cell growth and infiltration significantly [4, 3, 63]. Moreover, neoplastic cells are more sensitive to bafilomycin A1 than normal cells, a fact that may be used in anticancer therapy [73].

Bafilomycin A1 inhibits cell proliferation and tumor growth. The precise mechanism remains unknown, notwithstanding, this effect has been attributed to the inhibition of intracellular acidosis by blocking V-ATPases [71]. Treatment with V-ATPase inhibitors lowers H+ extrusion, both in vitro and in vivo [74, 75]. It appears that bafilomycin may be a potential therapeutic agent for large solid tumors. Bafilomycin inhibits the growth of large tumors subject to elevated levels of hypoxia more than that of small ones [76].

V-ATPase inhibition has also been shown to trigger apoptosis through caspase-dependent and caspase-independent mechanisms [77], and bafilomycin and concanamycin induce apoptosis in other types of cells, including neutrophils [6] and osteoclasts [78]. In human, hepatoblastomas and bafilomycin A1 induced higher apoptotic cell ratios and diminished cell reproduction. Furthermore, cell growth inhibition in normal liver cells was insignificant, insofar as the inhibition of V-ATPase-specific genes have minimal effects on normal cells [79].

Bafilomycin A1 suppresses protein degradation pathway, which allows an increase in cell survival under stress and in cancer [80, 81] by preventing lysosome acidification [80–82].

Human pancreatic cancer cells treated with bafilomycin A1 in combination with Na+/H+ exchange pump inhibitors had delayed cell growth by reduces the intracellular pH and by increases the thermal sensitivity of cancer cells [83].

In tumor cells, V-ATPases can enhance resistance to antineoplastic drugs. Tumor cells with greater expression of V-ATPase subunits are related with drug-resistant tumor [84–86]. Thereby, V-ATPase inhibitors may enhance drug buildup in some tumors [52].

The chemotherapy for head and neck cancers reduces the number of patients requiring mandibulectomy and/or radiation therapy. However, chemotherapy had not improved, significantly, the survival of patients with oral SCC [87].

Kiyoshima et al. observed evidence that a VATPase inhibitor, concanamycin A1, can induce apoptosis in oral SCC cells. The authors also suggested that even in apparent concanamycin A1-resistant oral SCC cells, a combination of concanamycin A1 with a histone deacetylase inhibitor, suberoylanilide hydroxamic acid may allow an efficient cancer therapy [88].

There is multitude of V-ATPase inhibitor molecules, but its actual usefulness in clinical practice is still debated. The mechanism of action of some of these substances is not completely understood; hence, their use in humans should be restricted. However, in the future, these molecules could be used in cancer treatment through the mensuration of the overexpression of specific V-ATPase subunits in tumors to be treated and, then, using specific inhibitors for the subunits being expressed [89], as well as using several substances in a synergistic approach [90]. This will allow clinicians to provide more specific treatment, while also minimizing adverse effects [62].

6 Conclusions

The pH of the cell is important for several biological functions and it is clearly involved in cell transformation, carcinogenesis, and metastasis. The inhibition of V-ATPase, by anticancer drugs, can cause apoptotic mechanisms that lead to the inhibition of tumor growth. Therefore, the V-ATPases, which is, as stated above, related to the control of tissue acidosis, can be used as a target for treatment, especially the C subunit of the V1 domain in the enzymatic function of the V-ATPase, in case of OSCC. It is important highlight the need of further research of specific inhibitors for the above-mentioned subunit, in order to control the disastrous consequences of the cancer.

Acknowledgements We would like to thank all the personnel of the molecular biology laboratory of the IDIS, particularly to Elena Padín. And the Fundacion Publica Gallega de Medicina Genomica, especially to Francisco Barros.

References

1. Perez-Sayans M, Garcia-Garcia A, Reboiras-Lopez MD et al (2009) Role of V-ATPases in solid tumors: Importance of the subunit C (review). Int J Oncol 34:1513–1520
2. Martinez-Zaguilan R, Seftor EA, Seftor RE et al (1996) Acidic pH enhances the invasive behavior of human melanoma cells. Clin Exp Metastasis 14:176–186

3. Cardone RA, Casavola V, Reshkin SJ (2005) The role of disturbed pH dynamics and the Na+/H+ exchanger in metastasis. Nat Rev Cancer 5:786–795
4. Saroussi S, Nelson N (2009) Vacuolar H(+)-ATPase-an enzyme for all seasons. Pflugers Arch 57:581–587
5. Otero-Rey EM, Somoza-Martin M, Barros-Angueira F et al (2008) Intracellular pH regulation in oral squamous cell carcinoma is mediated by increased V-ATPase activity via over-expression of the ATP6V1C1 gene. Oral Oncol 44:193–199
6. Gottlieb RA, Giesing HA, Zhu JY et al (1995) Cell acidification in apoptosis: granulocyte colony-stimulating factor delays programmed cell death in neutrophils by up-regulating the vacuolar H(+)-ATPase. Proc Natl Acad Sci U S A 92:5965–5968
7. Reshkin SJ, Bellizzi A, Caldeira S et al (2000) Na+/H+ exchanger-dependent intracellular alkalinization is an early event in malignant transformation and plays an essential role in the development of subsequent transformation-associated phenotypes. FASEB J 14:2185–2197
8. Reshkin SJ, Bellizzi A, Albarani V et al (2000) Phosphoinositide 3-kinase is involved in the tumor-specific activation of human breast cancer cell Na(+)/H(+) exchange, motility, and invasion induced by serum deprivation. J Biol Chem 275:5361–5369
9. Forgac M (1998) Structure, function and regulation of the vacuolar (H+)-ATPases. FEBS Lett 440:258–263
10. Nishi T, Forgac M (2002) The vacuolar (H+)-ATPases—nature's most versatile proton pumps. Nat Rev Mol Cell Biol 3:94–103
11. Kawasaki-Nishi S, Nishi T, Forgac M (2003) Proton translocation driven by ATP hydrolysis in V-ATPases. FEBS Lett 545:76–85
12. Kane PM (1999) Introduction: V-ATPases 1992–1998. J Bioenerg Biomembr 31:3–5
13. Stevens TH, Forgac M (1997) Structure, function and regulation of the vacuolar (H+)-ATPase. Annu Rev Cell Dev Biol 13:779–808
14. Schoonderwoert VTG, Holthuis JCM, Tanaka S et al (2000) Inhibition of the vacuolar H+-ATPase perturbs the transport, sorting, processing and release of regulated secretory proteins. Eur J Biochem 267:5646–5654
15. Pérez-Sayáns M, Somoza-Martín JM, Barros-Angueira F et al (2010) Multidrug resistance in oral squamous cell carcinoma: the role of vacuolar ATPases. Cancer Lett 295:135–143
16. Drory O, Frolow F, Nelson N (2004) Crystal structure of yeast V-ATPase subunit C reveals its stator function. EMBO Rep 5:1148–1152
17. Peng S, Stone D, Xie X (1993) Reconstitution of recombinant 40-kDa subunit of the clathrin-coated vesicle H(+)-ATPase. J Biol Chem 268:23519–23523
18. Gruber G (2005) Structural features and nucleotide-binding capability of the C subunit are integral to the regulation of the eukaryotic V1Vo ATPases. Biochem Soc Trans 33:883–885
19. Voss M, Vitavska O, Walz B et al (2007) Stimulus-induced phosphorylation of vacuolar H(+)-ATPase by protein kinase A. J Biol Chem 282:33735–33742
20. Beltran C, Kopecky J, Pan YC et al (1992) Cloning and mutational analysis of the gene encoding subunit C of yeast vacuolar H(+)-ATPase. J Biol Chem 267:774–779
21. Inoue T, Forgac M (2005) Cysteine-mediated cross-linking indicates that subunit C of the V-ATPase is in close proximity to subunits E and G of the V1 domain and subunit a of the V0 domain. J Biol Chem 280:27896–27903
22. Forgac M (2007) Vacuolar ATPases: rotary proton pumps in physiology and pathophysiology. Nat Rev Mol Cell Biol 8:917–929
23. Armbruster A, Hohn C, Hermesdorf A et al (2005) Evidence for major structural changes in subunit C of the vacuolar ATPase due to nucleotide binding. FEBS Lett 579:1961–1967
24. Puopolo K, Sczekan M, Magner R et al (1992) The 40-kDa subunit enhances but is not required for activity of the coated vesicle proton pump. J Biol Chem 267:5171–5176
25. Vitavska O, Wieczorek H, Merzendorfer H (2003) A novel role for subunit C in mediating binding of the H+-V-ATPase to the actin cytoskeleton. J Biol Chem 278:18499–18505
26. Smardon AM, Kane PM (2007) RAVE is essential for the efficient assembly of the C subunit with the vacuolar H(+)-ATPase. J Biol Chem 282:26185–26194

27. Keenan Curtis K, Kane PM (2002) Novel vacuolar H+-ATPase complexes resulting from overproduction of Vma5p and Vma13p. J Biol Chem 277:2716–2724
28. Boyle P, Levin B (2008) World cancer report 2008. International Agency for Research on Cancer Press, Lyon, pp 304–307
29. Ferlay J, Soerjomataram I, Ervik M et al (2013) GLOBOCAN 2012 v1.0, cancer incidence and mortality worldwide: IARC CancerBase No. 11 [Internet]. Lyon, International Agency for Research on Cancer. http://globocan.iarc.fr. Accessed 13 Nov 2014
30. Jerjes W, Upile T, Petrie A et al (2010) Clinicopathological parameters, recurrence, locoregional and distant metastasis in 115T1-T2 oral squamous cell carcinoma patients. Head Neck Oncol 2:9
31. La Vecchia C, Tavani A, Franceschi S et al (1997) Epidemiology and prevention of oral cancer. Oral Oncol 33:302–312
32. Lambert R, Sauvaget C, de Camargo Cancela M et al (2011) Epidemiology of cancer from the oral cavity and oropharynx. Eur J Gastroenterol Hepatol 23:633–641
33. Fontes PC, Correa GHM, Issa PC et al (2008) Comparison of exfoliative Pap stain and AgNOR counts of the tongue in smokers and nonsmokers. Head Neck Pathol 2:157–162
34. Kyrgidis A, Nokolaou A, Rachvitsas D et al (2008) Demographic clinical and histopathological characteristics of oral cavity cancer: survival analysis in a single center retrospective study. Hell Otorhinolaryngol Head Neck Surg 33:8–18
35. Sudbo J, Reith A (2005) The evolution of predictive oncology and molecular-based therapy for oral cancer prevention. Int J Cancer 115:339–345
36. Woolgar J (1995) A pathologist's view of oral cancer in the north west. Br Dent Nurs J 54:14–16
37. Harish K (2005) Neck dissections: radical to conservative. World J Surg Oncol 3:21
38. Kowalski LP, Sanabria A (2007) Elective neck dissection in oral carcinoma: a critical review of the evidence. Acta Otorhinolaryngol Ital 27:113–117
39. Grégoire V, Lefebvre J-L, Licitra L et al (2010) Squamous cell carcinoma of the head and neck: EHNS–ESMO–ESTRO clinical practice guidelines for diagnosis, treatment and follow-up. Ann Oncol 21:v184–v186
40. Montcourrier P, Silver I, Farnoud R et al (1997) Breast cancer cells have a high capacity to acidify extracellular milieu by a dual mechanism. Clin Exp Metastasis 15:382–392
41. Parkins CS, Stratford MR, Dennis MF et al (1997) The relationship between extracellular lactate and tumour pH in a murine tumour model of ischaemia-reperfusion. Br J Cancer 75:319–323
42. Sennoune SR, Martinez-Zaguilan R (2007) Plasmalemmal vacuolar H+-ATPases in angiogenesis, diabetes and cancer. J Bioenerg Biomembr 39:427–433
43. Orive G, Reshkin SJ, Harguindey S et al (2003) Hydrogen ion dynamics and the Na+/H+ exchanger in cancer angiogenesis and antiangiogenesis. Br J Cancer 89:1395–1399
44. Gillies RJ, Raghunand N, Karczmar GS et al (2002) MRI of the tumor microenvironment. J Magn Reson Imaging 16:430–450
45. Rojas JD, Sennoune SR, Maiti D et al (2006) Vacuolar-type H+-ATPases at the plasma membrane regulate pH and cell migration in microvascular endothelial cells. Am J Physiol Heart Circ Physiol 291:H1147–H1157
46. Sennoune SR, Bakunts K, Martinez GM et al (2004) Vacuolar H+-ATPase in human breast cancer cells with distinct metastatic potential: distribution and functional activity. Am J Physiol Cell Physiol 286:C1443–C1452
47. Glunde K, Guggino SE, Solaiyappan M et al (2003) Extracellular acidification alters lysosomal trafficking in human breast cancer cells. Neoplasia 5:533–545
48. Condeelis J, Segall JE (2003) Intravital imaging of cell movement in tumours. Nat Rev Cancer 3:921–930
49. Raghunand N, Mahoney B, van Sluis R et al (2001) Acute metabolic alkalosis enhances response of C3H mouse mammary tumors to the weak base mitoxantrone. Neoplasia 3:227–235

50. De Milito A, Fais S (2005) Proton pump inhibitors may reduce tumour resistance. Expert Opin Pharmacother 6:1049–1054
51. Luciani F, Spada M, De Milito A et al (2004) Effect of proton pump inhibitor pretreatment on resistance of solid tumors to cytotoxic drugs. J Natl Cancer Inst 96:1702–1713
52. Sennoune SR, Luo D, Martinez-Zaguilan R (2004) Plasmalemmal vacuolar-type H+-ATPase in cancer biology. Cell Biochem Biophys 40:185–206
53. De Milito A, Iessi E, Logozzi M et al (2007) Proton pump inhibitors induce apoptosis of human B-cell tumors through a caspase-independent mechanism involving reactive oxygen species. Cancer Res 67:5408–5417
54. De Milito A, Fais S (2005) Tumor acidity, chemoresistance and proton pump inhibitors. Future Oncol 1:779–786
55. Ling V (1997) Multidrug resistance: molecular mechanisms and clinical relevance. Cancer Chemother Pharmacol 40:S3–S8
56. Feng S, Zhu G, McConnell M et al (2013) Silencing of atp6v1c1 prevents breast cancer growth and bone metastasis. Int J Biol Sci 9:853–862
57. Pérez-Sayáns M, Reboiras-López MD, Somoza-Martín JM et al (2010) Measurement of ATP6V1C1 expression in brush cytology samples as a diagnostic and prognostic marker in oral squamous cell carcinoma. Cancer Biol Ther 9:1057–1064
58. García-García A, Pérez-Sayáns García M, Rodríguez MJ et al (2012) Immunohistochemical localization of C1 subunit of V-ATPase (ATPase C1) in oral squamous cell cancer and normal oral mucosa. Biotech Histochem 87:133–139
59. Fais S, De Milito A, You H et al (2007) Targeting vacuolar H+-ATPases as a new strategy against cancer. Cancer Res 67:10627–10630
60. Germanov E, Berman JN, Guernsey DL et al (2006) Current and future approaches for the therapeutic targeting of metastasis (review). Int J Mol Med 18:1025–1036
61. Lu X, Qin W, Li J et al (2005) The growth and metastasis of human hepatocellular carcinoma xenografts are inhibited by small interfering RNA targeting to the subunit ATP6L of proton pump. Cancer Res 65:6843–6849
62. Pérez-Sayáns M, Somoza-Martín JM, Barros-Angueira F et al (2009) V-ATPase inhibitors and implication n in cancer treatment. Cancer Treat Rev 35:707–713
63. Perona R, Serrano R (1988) Increased pH and tumorigenicity of fibroblasts expressing a yeast proton pump. Nature 334:438–440
64. Rofstad EK, Mathiesen B, Kindem K et al (2006) Acidic extracellular pH promotes experimental metastasis of human melanoma cells in athymic nude mice. Cancer Res 66:6699–6707
65. Johnson LL, Pavlovsky AG, Johnson AR et al (2000) A rationalization of the acidic pH dependence for stromelysin-1 (matrix metalloproteinase-3) catalysis and inhibition. J Biol Chem 275:11026–11033
66. Kato Y, Lambert CA, Colige AC et al (2005) Acidic extracellular pH induces matrix metalloproteinase-9 expression in mouse metastatic melanoma cells through the phospholipase D-mitogen-activated protein kinase signaling. J Biol Chem 280:10938–10944
67. Lu Q, Lu S, Huang L et al (2013) The expression of V-ATPase is associated with drug resistance and pathology of non-small-cell lung cancer. Diagn Pathol 8:145
68. Huang L, Lu Q, Han Y et al (2012) ABCG2/V-ATPase was associated with the drug resistance and tumor metastasis of esophageal squamous cancer cells. Diagn Pathol 7:180
69. Bowman EJ, Siebers A, Altendorf K (1988) Bafilomycins: a class of inhibitors of membrane ATPases from microorganisms, animal cells, and plant cells. Proc Natl Acad Sci U S A 85:7972–7976
70. Moriyama Y, Nelson N (1988) Inhibition of vacuolar H+-ATPases by fusidic acid and suramin. FEBS Lett 234:383–386
71. Bowman EJ, Graham LA, Stevens TH et al (2004) The bafilomycin/concanamycin binding site in subunit c of the V-ATPases from Neurospora crassa and Saccharomyces cerevisiae. J Biol Chem 279:33131–33138

72. Halaban R, Patton RS, Cheng E et al (2002) Abnormal acidification of melanoma cells induces tyrosinase retention in the early secretory pathway. J Biol Chem 277:14821–14828
73. Ohta T, Arakawa H, Futagami F et al (1996) A new strategy for the therapy of pancreatic cancer by proton pump inhibitor. Gan To Kagaku Ryoho 23:1660–1664
74. Volk C, Albert T, Kempski OS (1998) A proton-translocating H+-ATPase is involved in C6 glial pH regulation. Biochim Biophys Acta 1372:28–36
75. McSheehy PM, Troy H, Kelland LR et al (2003) Increased tumour extracellular pH induced by bafilomycin A1 inhibits tumour growth and mitosis in vivo and alters 5-fluorouracil pharmacokinetics. Eur J Cancer 39:532–540
76. Lim JH, Park JW, Kim MS et al (2006) Bafilomycin induces the p21-mediated growth inhibition of cancer cells under hypoxic conditions by expressing hypoxia-inducible factor-1alpha. Mol Pharmacol 70:1856–1865
77. Aiko K, Tsujisawa T, Koseki T et al (2002) Involvement of cytochrome c and caspases in apoptotic cell death of human submandibular gland ductal cells induced by concanamycin A. Cell Signal 14:717–722
78. Xu J, Feng HT, Wang C et al (2003) Effects of bafilomycin A1: an inhibitor of vacuolar H (+)-ATPases on endocytosis and apoptosis in RAW cells and RAW cell-derived osteoclasts. J Cell Biochem 88:1256–1264
79. Morimura T, Fujita K, Akita M et al (2008) The proton pump inhibitor inhibits cell growth and induces apoptosis in human hepatoblastoma. Pediatr Surg Int 24:1087–1094
80. Meijer AJ, Codogno P (2004) Regulation and role of autophagy in mammalian cells. Int J Biochem Cell Biol 36:2445–2462
81. Mortimore GE, Hutson NJ, Surmacz CA (1983) Quantitative correlation between proteolysis and macro- and microautophagy in mouse hepatocytes during starvation and refeeding. Proc Natl Acad Sci U S A 80:2179–2183
82. Wu YC, Wu WK, Li Y et al (2009) Inhibition of macroautophagy by bafilomycin A1 lowers proliferation and induces apoptosis in colon cancer cells. Biochem Biophys Res Commun 382:451–456
83. Hayashi Y, Katayama K, Togawa T et al (2006) Effects of bafilomycin A1, a vacuolar type H+ ATPase inhibitor, on the thermosensitivity of a human pancreatic cancer cell line. Int J Hyperthermia 22:275–285
84. Murakami T, Shibuya I, Ise T et al (2001) Elevated expression of vacuolar proton pump genes and cellular PH in cisplatin resistance. Int J Cancer 93:869–874
85. Torigoe T, Izumi H, Ise T et al (2002) Vacuolar H(+)-ATPase: functional mechanisms and potential as a target for cancer chemotherapy. Anticancer Drugs 13:237–243
86. Torigoe T, Izumi H, Ishiguchi H et al (2002) Enhanced expression of the human vacuolar H+-ATPase c subunit gene (ATP6L) in response to anticancer agents. J Biol Chem 277:36534–36543
87. Licitra L, Grandi C, Guzzo M et al (2003) Primary chemotherapy in resectable oral cavity squamous cell cancer: a randomized controlled trial. J Clin Oncol 21:327–333
88. Kiyoshima T, Yoshida H, Wada H et al (2013) Chemoresistance to concanamycin A1 in human oral squamous cell carcinoma is attenuated by an HDAC inhibitor partly via suppression of Bcl-2 expression. PLoS One 8, e80998
89. Hinton A, Bond S, Forgac M (2009) V-ATPase functions in normal and disease processes. Pflugers Arch 457:589–598
90. Hilgenbrink AR, Low PS (2005) Folate receptor-mediated drug targeting: from therapeutics to diagnostics. J Pharm Sci 94:2135–2146

Chapter 20
The Vacuolar Proton ATPase (V-ATPase): Regulation and Therapeutic Targeting

Norbert Kartner and Morris F. Manolson

Abstract V-ATPases are highly conserved proton pumps that are found in all eukaryotic cells. They play vital housekeeping roles in cell physiological processes by performing their classical functions in acidifying luminal compartments of a variety of endomembrane organelles. Recently, it has become evident that V-ATPases also have nonclassical roles that require their direct interaction, apart from their proton translocating function. Moreover, V-ATPases can have specialized tissue-specific functions in organisms, where V-ATPase mutations or inappropriate expression can result in pathological conditions. Because of their multi-subunit structure and numerous subunit variants, V-ATPase expression and function may be uniquely fine-tuned for specific, biologically significant roles. From an interventionist point of view, these same traits potentially make V-ATPases uniquely selectively targetable, both within an organism and among different species. Recent examples, that have at least provided proof of principle for this notion, span fields ranging from medicine to agriculture. The study of V-ATPases in the last three decades has produced thousands of publications and many dozens of review articles. The present work seeks to provide a concise overview of the more recent works on structure and function of V-ATPases, their occurrence and importance, how they are regulated, and how they might be targeted. We focus on recent primary literature, but historical papers of interest and important reviews are also cited. In the areas of targeted pharmaceutical and pesticidal intervention we present published strategies for drug discovery and also provide relevant proofs of concept for targeting V-ATPases to the benefit human health and prosperity.

Keywords Biological membranes • Drug discovery • Drug screening • pH regulation • Proton transport • Regulation of expression • Small-molecule inhibitors • Species-targeted pesticides • Therapeutic targeting • Vacuolar-type proton pump

N. Kartner • M.F. Manolson (✉)
Dental Research Institute, Faculty of Dentistry, University of Toronto,
124 Edward Street, Toronto, ON, Canada, M5G 1G6
e-mail: m.manolson@dentistry.utoronto.ca

S. Chakraborti, N.S. Dhalla (eds.), *Regulation of Ca^{2+}-ATPases,V-ATPases and F-ATPases*, Advances in Biochemistry in Health and Disease 14,
DOI 10.1007/978-3-319-24780-9_20

1 Introduction

1.1 Classical V-ATPase Function

V-ATPases are highly conserved, multi-subunit molecular motors that hydrolyze ATP to pump protons across biological membranes against a pH gradient [1]. V-ATPases are found in all eukaryotes and manifestations of their activity that involve pH regulation or proton gradient formation are thought of as their "classical" functions as proton pumps. These functions can be subcategorized as "housekeeping" or "specialized." Without intracellular housekeeping functions of the V-ATPases, eukaryotic cells and organisms cannot survive in a native environment [2, 3]. Housekeeping functions include energizing membrane compartments to drive proton gradient (ΔH^+)-coupled transporters, and maintaining the acidic luminal pH required for the functions of the Golgi, lysosomes, and endomembrane organelles involved in vesicular trafficking, endocytosis, and secretion [3–5]. V-ATPases also contribute to intracellular pH homeostasis [6–8].

Specialized functions are not required for cell survival, but are crucial to the development and ongoing health of organisms. Apart from their ubiquitous housekeeping functions, intracellular V-ATPases perform tissue-specific functions, such as driving ΔH^+-coupled neurotransmitter loading of synaptic vesicles [9]. When they are localized to the plasma membrane, V-ATPases are involved in numerous tissue-specific functions involving acidification of extracellular compartments. Examples include osteoclast resorption lacunae involved in bone resorption [10, 11], luminal spaces of epididymal tubules involved in sperm maturation [10, 11], kidney tubules, where V-ATPases plays a role in systemic acid-base balance through proton secretion into the urine [12–15], and the coronary arterial endothelium, where V-ATPases maintain an acidic extracellular environment that enables lipid raft formation required for regulatory redox signaling crucial to endothelial function in the coronary circulation [16].

1.2 Nonclassical V-ATPase Function

V-ATPases are now recognized as having "nonclassical" functions that involve more than proton pumping activity. For example, V-ATPases are involved in regulation of vesicular trafficking and membrane fusion, which necessitates generation of vesicular pH gradients, but also requires the direct participation of some V-ATPase subunits [17–22]. V-ATPases have been shown to recruit cytohesin-2 in a luminal pH-sensitive manner, implying that they can act as pH sensors [22, 23]. V-ATPase-bound cytohesin-2 recruits ARF6 to the early endosomes and plasma membrane [24], where the complex may regulate endocytic vesicular trafficking, cytoskeletal organization, and cell adhesion [22]. Endosome recycling is dependent on the latter process, and it is thought that the V-ATPase undergoes conformational changes in

response to luminal pH to facilitate cytohesin-2 docking [25, 26]. V-ATPase apparently can also sense the pH of secretory vesicles that it acidifies, allowing discrimination of fully loaded and partially loaded vesicles [27]; however, whether the pH gradient, or direct involvement of V-ATPase components, is the primary factor governing subsequent membrane fusion, remains controversial [17, 28]. In receptor-mediated signaling, V-ATPase is required for acidification of early endosomes for ligand dissociation and receptor recycling, or lysosomal acidification for protein degradation. For Wnt signaling, however, a direct interaction of LRP6 co-receptor with V-ATPase is also required for signal transmission, and for Notch signaling V-ATPase assembly factors play an important role [29, 30].

V-ATPase appears also to be involved in regulation of autophagy and cell growth, by engaging in amino acid- and "ragulator complex"-dependent, recruitment of the mammalian target of rapamycin cytoplasmic 1 complex, mTORC1 [31]. The mTORC1 complex essentially ensures that an adequate supply of resources is available before the cell commits to proliferation. It senses cellular energy and redox status, and amino acid supply in late endosomal/lysosomal compartments, and inhibits growth and promotes autophagy if any one of these prerequisites is inadequate, operating essentially as an anabolic/catabolic switch that is also influenced by insulin and growth hormones [32–35]. Abnormal function has been implicated in pathologies including neurodegenerative diseases, diabetes, and cancer. V-ATPase plays an important role in sensing free amino acid status, and conveys this information by recruiting mTORC1 to the lysosomal membrane through its interaction with the multicomponent ragulator complex [36, 37]. Recent evidence suggests that amino acid sensing likely also requires the involvement of lysosomal amino acid transporters [38, 39]. Interestingly, mTORC1 coordinately regulates the activity of TFEB, a transcription factor that is a master regulator of lysosome biogenesis, thereby regulating expression of a host of mTORC1-responsive genes, including V-ATPase subunit genes [32]. All of this may be independent of the classical function of V-ATPase as a proton pump [36], although this notion remains controversial [40].

1.3 Overview of V-ATPase Structure

The default discussion in this review concerns human V-ATPases or, more generally, mammalian V-ATPases, and often examples will be taken from the field of bone research, especially osteoclasts, as this is the authors' area of expertise. Much of our understanding of V-ATPases, however, comes from work done in yeast (esp. *Saccharomyces cerevisiae*), insect (esp. *Manduca sexta*), and other nonmammalian systems; this will be noted where observations may not be generalized to mammalian V-ATPases.

The functional V-ATPase complex, the holoenzyme, comprises two subcomplexes: a peripherally bound cytoplasmic sector, V_1 (subunits A–H, empirically organized as $(AB)_3DF(EG)_3CH$), and an integral membrane sector, V_0 (subunits *a*, *c*, *c″*, *d*, and *e* (and accessory proteins *Ac45* and *M8-9* in vertebrates; yeast have an additional

subunit, *c′*), empirically organized as *aed(c$_5$c″)(Ac45, M8-9)*; *aed(c$_4$c′c″)* in yeast) [3, 41, 42]. The mammalian V-ATPase is depicted diagrammatically in Fig. 20.1 with 27 subunits, derived from at least 15 different genes. Many of the mammalian V-ATPase subunits have multiple isoforms encoded by paralogous genes [3, 43], and their post-transcriptional variants [44, 45]. These are listed in Table 20.1. Thus, many different combinations of subunit isoforms can potentially be found within a given holoenzyme, allowing the assembly and expression of many different isoenzymes, or "isocomplexes," of V-ATPase, which may have subtle influences on cellular organelle-specific, or tissue-specific, function or localization [3, 45–49].

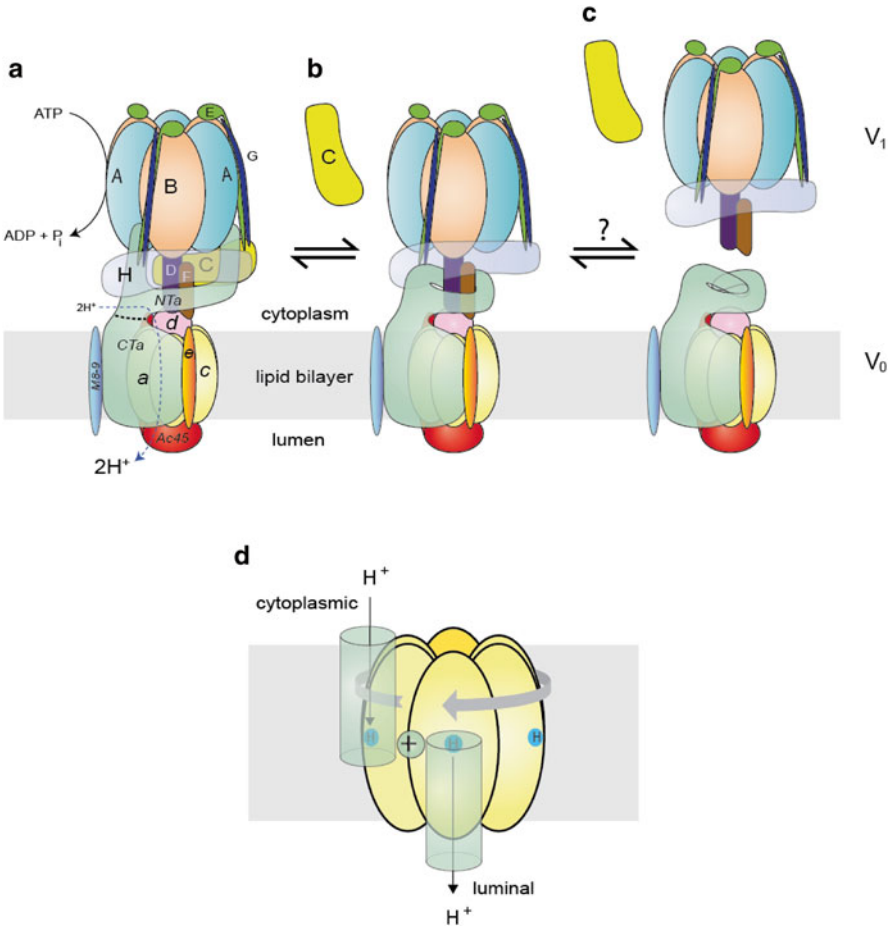

Fig. 20.1 Structure and function of V-ATPase. (**a**) Diagrammatic representation of the organization of a generic mammalian V-ATPase complex. The cytoplasmic V_1 sector consists of a catalytic headpiece (three each of alternating A and B subunit pairs forming a toroidal "barrel") that hydrolyzes ATP to drive a central rotor shaft (D and F subunits). The headpiece is held immobile against the torque that it generates by a stator complex (three pairs of E and G heterodimers attached to the

1.4 Health Impact of V-ATPases: Disease-Causing Mutations of Subunits

Why V-ATPases are of interest as therapeutic targets becomes clear when one realizes the astonishing range of important functions that they perform, many of which came to light when disease causing mutations were mapped to V-ATPase subunit genes. The first such report was for B1, by Karet et al. [50]. B1 is highly expressed in the kidney, where it is involved in systemic pH homeostasis, and the inner ear, where it maintains the pH of the fluid environment of sensory hair cells. Thus, the consequences of mutations are typically distal renal tubular acidosis (dRTA) with sensorineural deafness. Recently, loss of B1 function in a mouse model has also been shown to result in impaired olfactory function [51]. The majority of disease-causing mutations of V-ATPases, however, involve the *a* subunit. Knockout of *a1*, which plays a role in neural transmission, appears to be embryonic lethal [18], but loss of function of *a2* results in cutis laxa, characterized by aberrant Golgi function leading to glycosylation defects and abnormal elastin processing that affects the skin and other organs [52, 53]. Loss of function of *a3* in osteoclasts results in autosomal malignant osteopetrosis, characterized by dense, brittle bone due to diminished bone resorption [54]. Loss of *a4* function results in dRTA with occasional hearing loss [55, 56]. Loss of *d2* function in mice results in ineffective osteoclast

Fig. 20.1 (continued) catalytic headpiece, supported by a "collar" consisting of the C and H subunits and the N-terminal domain, *NTa*, of the *a* subunit) that is anchored to the membrane via continuity with the cytoplasmic domain, *CTa*, of the *a* subunit of the V_0 sector. The bifurcation of *NTa*, as shown here, is speculative [189]. The V_0 sector is largely inserted into the membrane bilayer, consisting of the rotor (a heterohexameric ring of 5 *c* subunits and a *c″* subunit; one of the *c* subunits is replaced with a *c′* subunit in yeast) and a *d* subunit, which couples the *c*-ring rotor to the ATP-driven DF central rotor shaft of the V_1 sector. The *a* subunit provides both a stator function, by interacting with the V_1 sector and anchoring it to the membrane, and a proton channel function. There are some additional subunits associated with the *a* subunit, whose locations and functions are as yet poorly understood, viz. the *e* subunit, and the accessory proteins *Ac45* (*AP1*) and *M8-9* (*AP2*) that are found in some specialized tissues. (**b**) One mechanism for control of V-ATPase activity is reversible disassembly, which at the least involves dissociation of the C subunit from the V_1V_0 complex and possibly also conformational changes in the *NTa* domain that destabilize the complex (depiction here is speculative) [136]. (**c**) Many published works have shown that regulatory reversible disassembly results in further dissociation of V_1 from V_0 [130]; however, this may be an in vitro experimental artifact, though overall conclusions regarding V-ATPase regulation likely remain reliable [136]. (**d**) The theory of V-ATPase transmembrane proton translocation suggests that protons diffuse into a cytoplasmic hemichannel formed by the *CTa* domain of the *a* subunit to protonate a glutamate residue (blue dot with proton, "H") on a subunit of the *c*-ring rotor. This is carried by ATP-driven rotation nearly 360° (clockwise as viewed from the cytoplasm, as indicated), until a luminal hemichannel is encountered where the proton can dissociate into the lumen [3]. A charged residue barrier within *CTa* (green sphere, "+") is thought to prevent carryover of the proton back into the cytoplasmic hemichannel. This latter event can, however, occur under some circumstances and is referred to a "slip" [172]. The orange subunit represents the single *c″* subunit of the mammalian *c*-ring. Modified from Ref. [189] with permission of ©The American Society for Biochemistry and Molecular Biology

Table 20.1 Mammalian V-ATPase subunit isoforms and splice variants[a]

Subunit isoforms	Human genes	Splice var.	No.	M_r (kDa)	Function; expression
V_1 sector					
A	*ATP6V1A*	1	3	70	Catalytic (stator); ubiquitous
B1	*ATP6V1B1*	1	3	58	Catalytic/regulatory (stator); B1 restricted, B2 ubiquitous
B2	*ATP6V1B2*	1		56	
C1	*ATP6V1C1*	1	1	42	Regulatory (stator); C1 ubiquitous, C2a/C2b restricted
C2	*ATP6V1C2*	2		48	
D	*ATP6V1D*	2	1	34	Primary rotor; ubiquitous
E1	*ATP6V1E1*	3	3	31	Stator arm with G subunit; E1 restricted, E2 ubiquitous[b]
E2	*ATP6V1E2*	1			
F	*ATP6V1F*	1	1	14	Rotor component; ubiquitous
G1	*ATP6V1G1*	2	3	13	Stator arm with E subunit; G1 ubiquitous, G2 restricted, G3 restricted
G2	*ATP6V1G2*	2			
G3	*ATP6V1G3*	3			
H	*ATP6V1H*	3	1	56	Regulatory (stator); ubiquitous
V_0 sector					
a1	*ATP6V0A1*	4	1	100–116[c]	Proton channel-forming (stator); *a1* ubiquitous, *a2* ubiquitous, *a3* ubiquitous (but highly expressed in osteoclasts), *a4* restricted
a2	*ATP6V0A2*	2			
a3	*ATP6V0A3*[d]	2			
a4	*ATP6V0A4*	3			
c”	*ATP6V0B*	2	1	21	Proton carrier (rotor); ubiquitous
c	*ATP6V0C*	1	5	16	Proton carrier (rotor); ubiquitous

d1	*ATP6V0D1*	1	1	38	Coupler (rotor); *d1* ubiquitous, *d2* restricted
d2	*ATP6V0D2*	1			
e1	*ATP6V0E1*	1	1	9	Unknown (stator); *e1* ubiquitous, *e2* restricted
e2	*ATP6V0E2*	3			
Ac45[e]	*ATP6AP1*	4	1	40[f]	Accessory[g] (stator); restricted
M8-9[h]	*ATP6AP2*	1[i]	1	9[j]	Accessory (stator); restricted

Molecular size (M_r) is given for the common human splice variant

[a]See also Fig. 20.1a. The number of known splice variants (Splice Var.) is shown here. Details of splice variants are cited in ref. [44]. The number of subunits per holoenzyme molecule is shown (No.); it is presently not known whether mixed isoforms of subunits B, E or G can coexist in the same holoenzyme. Function refers to role within the V-ATPase holoenzyme (stator or rotor localization in parentheses); expression refers to tissue localization, only insofar as whether distribution is ubiquitous or tissue restricted. A review of details of tissue distribution can be found in ref. [45]

[b]As a correction to ref. [44], E1 is expressed in spermatozoa (i.e., restricted), E2 is ubiquitous [210], as indicated here

[c]The *a* subunit is glycosylated [63, 189] with M_r of approximately 100–116 kDa. Predicted sizes are (*a1–a4*) 96, 98, 93, and 96 kDa, respectively

[d]Commonly and historically designated the T cell immune regulator 1 (*TCIRG1*; also *ATP6I*)

[e]Synonymous with accessory protein 1, *AP1*

[f]*Ac45* has a predicted size of 48 kDa, but is N-glycosylated, with an apparent size of 62 kDa. This is processed at a furin cleavage site, yielding the final V-ATPase-associated glycoprotein of approx. 40 kDa (27 kDa unglycosylated)

[g]The accessory proteins noted here are integral membrane proteins associated with the V_0 sector; their presence in the complex is required only in some tissues

[h]Synonymous with (pro)renin receptor and accessory protein 2, *AP2*

[i]There are six additional coding transcripts of *ATP6AP2* that do not include a transmembrane domain

[j]*M8-9* is processed from a 38 kDa precursor at a furin cleavage site

precursor fusion, resulting in mild osteopetrosis [57], but no equivalent mutations in human *d2* have been characterized. In rare cases of X-linked Parkinsonism with spasticity (XPDS) Korvatska et al. [58] reported the causative role of a variant transcript of the *M8-9* accessory protein. It displayed a high incidence of exon 4 skipping, yielding a protein with a 32 amino acid deletion and a consequent reduction in crucial V-ATPase function in autophagy in brain cells. A mutation with similar splicing consequences has also been reported that results in impaired ERK1/2 activation and resultant X-linked mental retardation with epilepsy [59].

2 Broader Disease-Related Implications

V-ATPases are even more generally implicated as potential targets in a wide variety of disease processes. Targeting the ruffled border V-ATPase in osteoclasts, for example, has been investigated as a means of controlling bone loss diseases, like osteoporosis [60–62]. Furthermore, the potential for intervention in rare cases of osteopetrosis, by targeting a protein-folding mutant *a3* subunit, has also been identified [63]. Gharanei et al. [64] have shown that the Wolfram syndrome 1 protein (WFS1), characteristic of that neurodegenerative disorder, binds the A subunit and destabilizes it, with consequences for granular acidification. This likely is a contributing factor for Wolfram syndrome, but whether targeting this association might alleviate symptoms is presently unknown. Inappropriate expression of plasma membrane V-ATPases containing *a3* or *a4* subunits in tumor cells may lead to tumor progression, metastasis and chemotherapy resistance [15, 34, 65–69], but their cell surface expression makes them potential therapeutic targets, as is discussed elsewhere within this volume.

There are also numerous correlations that require further investigation: V-ATPases containing *a3* isoform subunits are present in insulin-secretory granules of pancreatic β cells and appear to play a regulatory role in insulin secretion [21]. It has also been found that downregulation of H subunit expression correlates strongly with type 2 diabetes, though in what capacity remains to be determined [70, 71]. Loss of V-ATPase function in the autophagy-lysosome pathway has been implicated in aberrant metabolism of proteins that accumulate in neurodegenerative diseases, like Alzheimer's dementia and Parkinson's disease [72]. Loss of function of the VMA21 chaperone protein that is required for V-ATPase assembly, though it is not a part of the mature complex, also disrupts lysosomal acidification, leading to X-linked myopathy with excessive autophagy (XMEA) [73]. V-ATPase may also play a role in cardiovascular disease, possibly as an indirect consequence of excessive V-ATPase activity in osteoclasts, leading to calcification of arteries [74]. It is thought also that impaired endothelial cell plasma membrane V-ATPase function in diabetes may play a role in defective angiogenesis [75, 76].

V-ATPases of pathogenic organisms can also be of clinical importance. Parasitic nematodes, for example, place a significant burden on both human health and agriculture. It has been argued that V-ATPase, which performs many crucial functions within the *Caenorhabditis elegans* model parasitic organism, might serve as a useful

target for controlling them [77]. Similarly, the fungal V-ATPase appears to be essential for virulence and it has been suggested that it may be an appropriate target for controlling *Candida albicans* and other fungal pathogens [78]. Dengue fever is transmitted by mosquitoes and 100 million people are infected annually, with half the world population at risk. A mosquito V-ATPase has been identified as a required host factor in *Aedes aegypti*; its targeted inhibition could effectively control dengue virus transmission [79].

V-ATPases also play a role in viral infection. The H subunit binds the adaptor-related protein complex 2 (AP-2) μ2 chain (AP2M2) of coated endocytic vesicles and also the HIV Nef protein. Thus, the H subunit acts as a connector between HIV and the trafficking mechanism that carries endosomes to lysosomes, thereby contributing to HIV infectivity [80]. More generally, because of its involvement in viral processing, it has been suggested that targeting V-ATPase might provide an alternative means of preventing the spread of pandemic avian influenza, and a treatment modality that avoids selection for resistant strains [81].

2.1 Other Impacts

Agriculture has always been plagued by insect pests [82] and we consider in a following section ways that insect V-ATPases might be targeted to provide novel insecticides with high specificity for target species and the potential to significantly improve global agricultural yields. It is worth noting also that, globally, a considerable fraction of potentially arable land is inaccessible to high-yield agriculture due to excessive soil salt concentrations [83], and plant salt tolerance depends in part on V-ATPase expression [84]. Further understanding of this process, and engineering ways of exploiting the V-ATPase-dependent ion and osmotic stress response could improve agricultural yields, a growing concern as human population continues to expand.

3 Factors Affecting V-ATPase Activity

Expression is normally thought of as being under the control of promoters and transcription factors, which account for differential tissue distribution and assembly of V-ATPase isocomplexes with “customized” subunit isoform composition. However, differential sorting and trafficking, which determine subcellular localization, are also crucial to expression, as the V-ATPases have a uniquely diverse range of functions in various organelles. Additionally, modulation of function is an important acute form of regulation of in situ V-ATPase activity, in immediate response to various stimuli. Understanding V-ATPase regulation is a prerequisite for finding therapeutic solutions to diseases that involve a particular V-ATPase isocomplex, which will invariably be found in a background of vital housekeeping isocomplexes. The following is a brief survey of V-ATPase regulation, and there are many recent reviews of broader scope [3, 26, 45, 46, 85, 86].

3.1 Regulation of Transcription

Differential expression of V-ATPase isocomplexes is driven by the regulation of transcription of subunit isoform genes. Some V-ATPase isoforms, however, are ubiquitously expressed. For example, though the B2 subunit is one of the subunit isoforms characteristic of the osteoclast ruffled-border V-ATPase, it is widely expressed and its promoter contains a TATA-less, GC-rich regulatory region containing "CpG islands," with multiple Sp1 and AP-2-like binding sites [87, 88]. Similar promoter regions are seen for the C1, *c″*, and *c* subunits, where also Oct1 motifs are present [89, 90]. CpG islands are common in promoter regions of ubiquitously expressed genes, and genes expressed in early embryogenesis, though otherwise they are infrequent [91–93]. Thus, expression of ubiquitous V-ATPase subunits is regulated largely through such promoter regions [45, 94], and cytosine methylation in CpG islands may allow further epigenetic fine-tuning of expression [95].

There are examples also of regulation of tissue-restricted, specialized V-ATPase expression. In renal intercalated cells, the plasma membrane V-ATPase requires the B1 subunit isoform, whereas in osteoclasts it is the B2 isoform of the V_1 B subunit; these are paired with *a4*, or *a3*, respectively, of the V_0 *a* subunit. B1 expression is largely restricted to a family of forkhead-related epithelial (FORE) cells that occur in the kidney, epididymis and inner ear, where not only B1, but also E2 and *a4* subunits are under control of the forkhead box (FOX) transcription activator FOXI1, which acts as a master regulator of specialized plasma membrane V-ATPase expression in FORE cells [95–97]. It has been noted that some existing drugs may modulate expression of other FOX proteins [98]; whether FORE cell V-ATPase expression might be amenable to similar therapeutic manipulation is as yet unclear.

In osteoclasts, *a3* expression is under control of an NF-κB-induced transcription factor complex containing NFATC1, the master regulator of osteoclast differentiation [99, 100]. The *a3* subunit gene bears a RANKL-responsive NFATC1 promoter 1.6 kb upstream of the start codon. Basal transcription is downregulated by poly(ADP-ribose) polymerase-1 (PARP-1) binding to the promoter. RANKL stimulation results in PARP-1 degradation, causing upregulation of *a3* transcription [101]. A second PARP-1 site is a few hundred bases downstream, adjacent to an AP-1 site [102].

The *d2* isoform, which is part of the osteoclast ruffled border V-ATPase is also upregulated in osteoclasts, through the NFATC1 promoter [103] and co-activation by myocyte enhancer factor 2 (MEF2) and microphthalmia-associated transcription factor (MITF) [104]. RANKL-induced osteoclast differentiation, through NFATC1, turns on not just specific V-ATPase subunit isoform genes, but also a host of ancillary genes required for bone resorption, to express proteins like CLC7, the chloride counterion shunt without which V-ATPase could not effectively pump protons, and proteases like MMP9 and cathepsin K, required for degradation of the organic component of bone [100].

3.2 *Messenger RNA Stability*

Lee et al. [87] observed that in human macrophage/monocyte differentiation, where V-ATPase expression is upregulated, only B2 transcription is elevated. It was suggested that other subunits must be upregulated by post-transcriptional mechanisms. Furthermore, in kidney, transcript ratios do not equal their corresponding protein ratios for V-ATPase subunits [105], yet in osteoclasts the ratios are equal [106], suggesting that regulation in kidney must also involve mRNA stability, translation rates, or protein turnover rates. In a similar vein, Wang et al. [89] showed that promoter activity was similar for *c* subunit mRNA transcription in murine macrophage and fibroblast cell lines, despite a six- to eightfold difference in expression. In the high-expression macrophages, stability of mRNA was shown to be higher for B2, E1, F, *a1*, and *c* transcripts. Jeyaraj et al. [107] later showed that stability was determined by an AU-rich element (ARE), a common regulator of mammalian mRNA stability, near the 3′-UTR polyadenylation site [108]. AREs tend to be destabilizing, by involvement of microRNA binding; in contrast, HuR binding promotes transcript stability and translation efficiency [109, 110]. HuR has been shown, along with a second regulatory protein, hnRNP, to bind E1, G1, *c*, and *c″* mRNA [107, 111, 112]. Though regulation of mRNA stability may play an important role in V-ATPase isocomplex expression and subunit selection, a more complete understanding will require further investigation.

3.3 *MicroRNA Regulation*

MicroRNAs are conserved, short-hairpin RNAs that can bind mRNA targets and repress their expression, either by directly causing their cleavage, destabilizing them by shortening their polyA tail, or interfering with translation [113, 114]. It has been shown by Stark et al. [115] that the muscle microRNA, miR-1, binds human A, B2, C1, *a1*, and *c* subunit transcripts, and also *D. melanogaster* and *C. elegans* homologues of E, G, and *d*, possibly regulating the coordinated expression of ubiquitous subunits. In a specific example of relevance to human health, O'Connor et al. [116] showed that catestatin processing from the prohormone chromogranin A was variable, depending on a sequence polymorphism, T+3246C, residing in the 3′-UTR of the *a1* transcript. This C variant resulted in lowered plasma catestatin levels, leading to lower blood pressure and a reduced risk of hypertensive disease. This was later found to be due to regulation by the miR-637 microRNA, which preferentially binds the C variant *a1* mRNA, inhibiting its translation [117]. This causes a reduction in vacuolar V-ATPase activity, an increase in luminal pH, and a consequent decrease in chromogranin A processing to catestatin [116]. Although there is a great deal more to be learned about V-ATPase regulation by microRNAs, it seems evident that engineered microRNAs may have a future in therapeutic targeting of specific V-ATPase isocomplexes.

3.4 Splice Variants

The majority of V-ATPase subunit splice variant transcripts inferred in Table 20.1 remain uncharacterized, but their potential importance is highlighted by some examples: Poëa-Guyon et al. [118] characterized rat brain expression of subunit *a2* and four splice variants of subunit *a1*, *a1-I* (C variant), *a1-II* (N variant), *a1-III* (canonical), and *a1-IV* (N+C variant). The mRNA splice variants result in a seven amino acid insertion, peptide N, between the translated exons 4 and 5 (in the cytoplasmic *NTa* domain shown in Fig. 20.1a) and/or a six amino acid insertion, peptide C, between exons 17 and 18 (in the cytoplasmic loop between transmembrane helices 6 and 7 in the integral membrane domain, *CTa*, shown in Fig. 20.1a). Subunits *a2*, *a1-I* and *a1-II* were found to be endogenously co-expressed in rat hippocampal neurons. The peptide C-containing *a1* variants appeared to be specific to neuronal expression and were upregulated during neuronal synaptogenic differentiation. The three neuronal *a* subunit variants, epitope tagged and recombinantly expressed in cultured neuronal cells, were found to sort to different subcellular compartments; the ubiquitous *a2* to the soma, likely the Golgi, as is typical for *a2*, the *a1-I* variant to nerve terminals, and the *a1-IV* variant to dendritic processes. It appears that the peptide C insert determines sorting specific to neurotransmitter storage, and this may be modified by the addition of peptide N to target the plasma membrane. Peptide C also introduces a PEST motif that likely reduces the biological half-life of the *a1-I* and *a1-IV* subunit variants, but the significance of this remains unclear.

It has been shown that mouse and human *a4* have alternate first exons [119, 120]. In mouse, this results in differential embryonic and adult expression, though this has not been shown for human *a4*. The C2 subunit has an alternate exon [121, 122] resulting in lack of a 46 amino acid insert; C2+ (C2a) is expressed in lung, whereas C2– (C2b) is expressed in kidney. Additionally, there is an example of alternate start codon usage that results in non-V-ATPase expression of the *a3* subunit. The TIRC7 membrane protein involved in T cell activation is derived from an *a3* transcript utilizing a start codon within exon 5 of *ATP6V0A3* (historically, *TCIRG1*, *ATP6I*) [123]. TIRC7 is expressed on the surface of lymphocytes, whereas *a3* is highly expressed on the ruffled border of osteoclasts; alternate promoter usage must account for this differential expression. Thus, splice variants may account for differential tissue expression, sorting to various subcellular compartments, and proteins of alternate function.

3.5 Assembly and Reversible Disassembly

In yeast, the V_1 sector of V-ATPase appears to self-assemble in the cytoplasm [124]. For V_0 there are at least three ER chaperones, Vma12p, Vma21p, and Vma22p that are essential for assembly [124, 125]; there is also an ER-resident accessory chaperone, Pkr1p, that enhances V_0 assembly efficiency [126]. Vma21p additionally

escorts the V_0 sector to the Golgi, but is then recycled to the ER; none of the aforementioned proteins are retained as part of the functional V-ATPase complexes at their final destinations. In higher plants, the ER quality control chaperones, calnexin and BiP, have been coimmunoprecipitated with the full V-ATPase holoenzyme, suggesting that they too are involved as chaperones and in quality control of V-ATPase assembly and, moreover, that the entire V_1V_0 holoenzyme is assembled at the ER [127]. In humans the process of V_0 assembly appears to be conserved, but the chaperones have diverged considerably, although a putative ortholog of Vma21p has been identified [73].

Considerably more needs to be understood about assembly of mammalian V-ATPases before therapeutic intervention can be considered; however, their regulated disassembly may be more tractable. It has long been proposed that under certain types of stress, particularly cellular glucose deprivation, the V_1 sector of V-ATPase dissociates from the V_0 sector (Fig. 20.1c), resulting in V-ATPase inactivation (reviewed in Refs. [4, 128–130]). This process also results in the reversible loss of the C subunit from the V_1 sector (Fig. 20.1b, c). Regulation by reversible disassembly has been described most thoroughly in the yeast (*S. cerevisiae*) and in the insect (*M. sexta*) systems [85, 130–132]. Its evolutionary rationale may be to spare ATP for more immediately essential cellular processes, under starvation conditions. V-ATPase is known to associate with aldolase, by direct interaction with subunits B, E and *a*, which contributes to V-ATPase stability [23, 133–135] and is part of a glycolytic metabolon that dissociates on glucose starvation [136]. As part of this metabolon, V-ATPase also interacts with phosphofructokinase-1, which may also stabilize the complex [137]. This glycolytic metabolon senses and responds to metabolic status, making ATP and protons from glycolysis proximally available to the proton pump, but it also shuts down V-ATPase activity to regulate intracellular pH, or to respond to restricted cellular energy status.

V-ATPase disassembly in this process requires the involvement of microtubules, and it has been suggested that ATP/ADP binding and phosphorylation of the C subunit may destabilize V-ATPase structure in a regulatory manner by altering its affinity for actin, or components of the V-ATPase stator [26, 138, 139]. The *NTa* domain of the *a* subunit recruits cytohesin-2 in a pH-dependent manner, which in turn recruits ARF6. It has been speculated that the activity of this cytohesin guanine nucleotide exchange factor (GEF) signaling complex, which may be further modulated by aldolase binding, affects the interaction of *NTa* with stator EG heterodimers, resulting in instability leading to the regulatory disassembly of the C subunit and of V_1–V_0 [26].

For V-ATPase reassembly, Chan and Parra [140] have shown in *S. cerevisiae* that reassociation of the C subunit is dependent on the Pfk2p subunit of the glycolytic enzyme, phosphofructokinase-1. V_1V_0 reassembly is modulated by glucose-sensitive association of V-ATPase with aldolase [134, 141], and with the yeast "regulator of H^+-ATPase of vacuolar and endosomal membranes" (RAVE; or equivalent rabconnectins in mammalian cells), a complex that interacts with EG heterodimers and the C subunit. RAVE-dependent assembly in yeast may be specific to the *a* subunit isoform, required for V-ATPases containing Vph1p and not for those containing Stv1p [142].

Similarly, Tuttle et al. [143] have suggested that different rabconnectins may pair with specific *a* subunit isoforms to influence cell type-specific trafficking and signal processing in vertebrates. Signaling pathways dependent on cytosolic pH, as determined by glycolytic activity [144], and involving phosphatidylinositol 3-kinase (PKI3) [145] and protein kinase A (PKA) [146], have been shown to be involved in recruitment and assembly of V-ATPases. Reassembly or stability also seem to be promoted by high extracellular pH [147]. Both disassembly and reassembly are rapidly reversible, and the catalytic ATPase and proton translocation activities of the isolated V_1 and V_0 sectors, respectively, are inhibited [132, 148, 149]. The H subunit inhibits the ATPase activity of the V_1 sector, likely by interaction with the F subunit of the DF "crankshaft," which protrudes from the catalytic headpiece of dissociated V_1 [148, 150, 151]. Interestingly, in *S. cerevisiae* it has been shown that the V_0 *a* subunit lysosomal isoform, Vph1p, is more responsive for reversible disassembly than the Golgi-localized Stv1p, with both V-ATPase subunit composition and local membrane environment contributing to the difference [152, 153].

The first mammalian report of V_1V_0 disassembly was for dendritic cells responding to maturation signals [154]. In immature dendritic cells, lysosomal acidification is depressed by V-ATPase dissociation to preserve antigen integrity. On maturation, V-ATPase reassembles, the lysosome is acidified, and antigen is processed. Recent evidence suggests that this reassembly is controlled by the PI3K/mTOR signaling pathway [155]. Type II alveolar cells stimulated with surfactant secretagogues also disassemble *a1*/B2-containing lamellar body V-ATPase [156]. These examples are not the result of glucose deprivation, and their mechanisms are poorly understood. The first evidence of mammalian glucose-dependent reassembly was found in cultured kidney cells [145, 157]. Glucose treatment promotes both reassembly of V_1V_0 after starvation and translocation of V-ATPase to the apical plasma membrane from a cytoplasmic vesicle pool, and both of these processes are dependent on PI3K activity. Reversible disassembly also appears to be regulated by extracellular pH [144, 147], by salt stress in plants [158] and, in insect cells, transient phosphorylation of the C subunit might mediate reassociation of the C subunit with V_1 and consequent reassembly of V_1V_0 [159].

Tabke et al. [136] have suggested recently that in vivo disassembly of V_1V_0 into independent sectors does not occur, but rather only the C subunit dissociates from the complex, rendering it reversibly inactive. Their in vivo FRET analyses, using fluorescent protein-tagged V-ATPase subunit expression in *S. cerevisiae* show that yeast V_1 and V_0 sectors remain in close proximity to the vacuolar membrane upon cellular glucose starvation. Instead of V_1 dissociation, dissociation of the C subunit alone is observed, and this appears to depend on direct interaction of microtubules with the C subunit, though reassembly is microtubule-independent. Tabke et al. [136] further argue that when the C subunit dissociates, the V_1V_0 holoenzyme is destabilized to the extent that further in vitro histo/cytochemical or biochemical manipulation results in artifactual V_1V_0 dissociation, in proportion to the prior loss of C subunit. These FRET analyses also reveal a change in distance between the B and *a* subunits during glucose starvation, in a manner that suggests conformational changes in the V-ATPase that could plausibly account for its apparent concurrent instability upon C subunit loss. One might perhaps think of in vitro V_1–V_0 dissociation

as an assay for in vivo C subunit dissociation, with few conclusions in the published literature being substantially affected by the distinction. Regardless of the precise in vivo mechanism of "reversible disassembly," it results in regulatory inactivation/reactivation of V-ATPase as an ATP hydrolytic enzyme and as a proton pump. Tapping into this regulatory mechanism by way of therapeutic intervention will, however, require a more detailed understanding relevant to human tissues.

3.6 Regulation by Localization: Recruitment and Redistribution

V-ATPases depend on vesicular trafficking to arrive at the various destination membrane compartments where they perform their functions. Failure to target correctly, whether in a regulatory manner, as a result of pathology, or due to therapeutic intervention, negates the intended V-ATPase function. How normal targeting is regulated remains obscure, but in at least some cases it is likely that the V-ATPase subunit composition encodes signals that predetermine its localization. In yeast, for example, the two *a* subunit isoforms Vph1p and Stv1p are localized to the vacuole and the Golgi apparatus, respectively, by virtue of polypeptide targeting signals within their *NTa* domains [47–49, 160].

A tissue-specific example of targeting is seen in the mammalian intestine, where luminal $Cl^-/HCO3^-$ equilibrium requires proton secretion mediated by V-ATPase. Here it is the cystic fibrosis transmembrane-conductance regulator, CFTR, that regulates V-ATPase activity by providing a variable chloride counterion shunt. CFTR itself is regulated by the cAMP-dependent protein kinase, PKA, not just in its chloride channel activity, but also in its recruitment to the enterocyte brush border membrane. This recruitment appears to apply to V-ATPase as well, by direct interaction with CFTR, resulting in translocation of the former from the basolateral membrane to the apical brush border [161]. In other examples, it has been shown that cAMP/PKA and Rab11b regulate trafficking of V-ATPase into apical membranes of epithelial cells in the kidney, salivary glands and epididymis by recruitment from subapical endosomal compartments [146, 162, 163]. In mouse cortical collecting duct, angiotensin II initiates a similar redistribution of V-ATPase to apical plasma membranes from subapical vesicles [164]. The A subunit appears to play a direct role in regulation of V-ATPase redistribution, as it has been noted that it can be transiently phosphorylated by PKA at serine 175, resulting in upregulated activity in kidney and epididymal epithelia [165–168]. The A subunit can also be phosphorylated by the 5′-AMP-activated protein kinase, AMPK, at serine 384 [166, 168], although this appears to be inhibitory for plasma membrane V-ATPase activity in kidney. In osteoclasts, V-ATPase is translocated to the ruffled border upon osteoclast activation, from a pool of intracellular lysosomal vesicles. This requires interaction with actin microfilaments that bind the N-terminal domain of V-ATPase B subunits [169, 170]. Therapeutically targeting the interaction of F-actin and V-ATPase B subunits and other specific protein-protein interactions within the osteoclast V-ATPase, to inhibit osteoclastic bone resorption, is discussed further, below.

3.7 Coupling Efficiency

Kawasaki-Nishi et al. [153] showed that yeast V-ATPases with the *a* subunits Stv1p or Vph1p have similar enzyme kinetic properties, yet Stv1p realizes a four- to fivefold lower coupling efficiency of protons transported per ATP molecule hydrolyzed than Vph1p. It has been suggested that this difference in coupling efficiency accounts for the higher pH observed in the Golgi, compared to the vacuole, and that differences in subunit isoform composition of mammalian V-ATPase isocomplexes may regulate differences in steady state pH within the organelles to which they are targeted. Electrophysiological studies of active transporters have revealed a common "lack of precision" in predicted solute output per molecule of ATP hydrolyzed [171]. For V-ATPases, one possibility for this lack of precision is referred to as "slip," which may be due to the inability of protons to dissociate into the lumen against a large ΔH^+, resulting in carryover, past what is usually an effective charge barrier between the luminal and cytoplasmic proton hemichannels (Fig. 20.1d), and release back into the cytoplasm instead [172]. Slippage, or more generally, proton "shunting," depends on the current–voltage properties of the proton pump, the transmembrane electrical charge and pH gradient. Shunting alone may account for all of the variable coupling efficiencies that have been observed for V-ATPases and may represent transient thermodynamic behavior of the V-ATPase as an open proton channel [173]. Whether slippage, or shunting, is completely intrinsic to V-ATPase structure, or is influenced by other regulatory elements, or can be pharmaceutically manipulated, is presently not known.

3.8 Lipid Microenvironment

It has recently been shown that the signaling lipid, phosphatidylinositol 3,5-bisphosphate, $PI(3,5)P_2$, directly interacts with the V-ATPase V_0 sector and promotes assembly and stability of V-ATPase, possibly by altering the conformation of the N-terminal domain of the *a* subunit, Vph1p, in yeast [174]. C26 acyl sphingolipids also affect yeast V-ATPase activity, but surprisingly it is the cytosolic V_1 sector that is inactive without them. It has been suggested that these lipids support V_1 activity indirectly, by affecting the RAVE complex that is required for V_1 assembly [175]. In mammalian cells the simple sphingolipid, glucosylceramide, appears to be required to support high levels of V-ATPase activity in melanocyte endomembranes, a necessity for protein sorting and melanosome biogenesis [176]. In plants, tonoplast V-ATPase activity is enhanced in vitro by tonoplast phospholipids, but depressed by tonoplast glycolipids [177]. Yoshida et al. [178] have shown further that in *Arabidopsis thaliana* vacuoles the organellar membrane consists of microdomains that are characterized by either detergent sensitivity or detergent resistance. V-ATPase was found to associate with detergent resistant microdomains, which have elevated proportions of saturated fatty acids in their phosphatidyl choline and phosphatidyl ethanolamine phospholipids, compared with total vacuolar phospholipids. The authors speculate that since plasma membrane microdomains play a role

in signal transduction, vacuolar microdomains may be involved in regulation of membrane transport and signal processing at the vacuolar level; however, direct evidence of this remains lacking.

Although the concept has been largely unexplored in mammalian systems, there is some indication that manipulation of the membrane lipid microenvironment in which V-ATPases find themselves might have therapeutic value. In yeast, membrane ergosterol (which is not found in animal cells) is required for V-ATPase function. V-ATPase is crucial to virulence of pathogenic fungi, and the azole class of antifungal drugs exploits this by inhibiting ergosterol biosynthesis [179].

3.9 Ancillary Enzymes

V-ATPases cannot function without a number of supporting enzymes and transport proteins, often also having tissue-specific expression. Intracellular carbonic anhydrase II (CA II) is expressed to rapidly equilibrate the reaction of CO_2 and water to produce protons and bicarbonate ions. Though widely distributed, CA II is especially important in highly active acid-secreting cells, like osteoclasts and specialized kidney ductal epithelial cells, to provide a readily accessible pool of protons to the V-ATPase. It also provides bicarbonate ions to power cellular chloride uptake via Cl^-/HCO_3^- exchange. In osteoclasts, the latter role is performed specifically by the anion exchange protein 2 (AE2) with which CA II directly interacts [180]. Electrogenic proton pumping by V-ATPase would come to a quick halt if the charge gradient were not neutralized by a counterion shunt [181–183]; in the osteoclast this is provided by the chloride channel 7 (CLC7), an electrogenic $H^+/2Cl^-$ exchanger, which utilizes the chloride ions provided by AE2. Depending on the tissue and subcellular compartment, other isozymes and H^+/ion exchangers can take on the roles of those specifically highlighted here.

Mutations in the above ancillary enzymes illustrate their importance to V-ATPase activity. Mutations in *CA2*, the gene coding for CA II, which is highly expressed in both osteoclasts and kidney, cause combined osteopetrosis and dRTA, similar to what is seen separately for mutations in the V-ATPase subunits *a3* and *a4*, which are also highly expressed in the respective tissues [56, 184]. Mutations in *SLC4A2*, which codes for AE2 have not been described in humans, but a deletion mutation in bovine *SLC4A2* results in osteopetrosis in cattle [185]. Interestingly, mutations in the anion exchange protein 1 (AE1), which is a kidney-specific form, cause a dominant variation of dRTA that is otherwise similar to what is seen for mutations in the kidney-specific V-ATPase B1 and *a4* subunit isoforms. Mutations in *CLCN7*, which codes for the chloride channel CLC7, also cause osteopetrosis, much like mutations in the V-ATPase *a3* subunit [186], and a specific inhibitor of CLC7 has been shown to prevent bone loss in ovariectomized rats [187]. Apart from mutations, there is also the observation, as was noted above, that V-ATPase proton extrusion into the gut lumen depends on a specialized, tissue-specific association with CFTR [161]. These examples illustrate the potential for indirect manipulation of V-ATPases by targeting the ancillary proteins upon which their activity depends.

4 Targeting Inhibition of V-ATPase

It is tempting to think that manipulating specific endogenous regulatory mechanisms for V-ATPase expression and function, including those described above, might achieve precise therapeutic targeting. While this may 1 day be the case in some applications, a great deal more needs to be understood regarding these regulatory mechanisms before such an approach can be realized. Furthermore, many of the regulatory molecules described are widely distributed throughout the organism, making a "magic bullet" solution unlikely. Historically, numerous small molecule inhibitors, mostly natural products, have been used to experimentally inhibit V-ATPases, the plecomacrolides bafilomycin A1 and concanamycin A being the most commonly used [188]. These generally are not selective among V-ATPase isocomplexes. Some inhibitors have been described that may be selective for osteoclast V-ATPases, but clinical utility has proved elusive. We briefly review here illustrative examples of strategies used towards trying to achieve specific V-ATPase targeting, with applications ranging from pharmaceutical to agrochemical.

4.1 Novel V-ATPase Inhibitors: Discovery Strategies and Applications

The ultimate goal in targeting V-ATPases clearly is to be able to manage a "surgical strike" against a specific isocomplex without affecting V-ATPases of alternative subunit isoform composition. Recently, strategies have been designed to discover inhibitors of protein interactions that are required for the functions of specific V-ATPase isocomplexes, and RNAi methods to knock down expression of specific subunit isoforms.

4.1.1 Small Molecule Inhibitors of V-ATPase Quaternary Subunit Interaction

Kartner et al. [189] characterized interactions between mouse V-ATPase *a* and B subunits, using yeast two hybrid screening and pulldown assays of recombinant fusion proteins. They further characterized the interactions between all of the mouse *a* and B subunit isoform pairs using an ELISA system to generate relative binding curves. This assay lent itself to modification to achieve high-throughput screening for small molecule inhibitors of the *a3*–B2 interaction, an interaction that has some specificity for osteoclast ruffled-border V-ATPase [190, 191]. Screening of small synthetic compound and natural product libraries led to the discovery of a small synthetic molecule, 3,4-dihydroxy-*N*′-(2-hydroxybenzylidene)benzohydrazide, that was able to inhibit in vitro osteoclastic bone resorption with an IC_{50} of 1.2 μM [189].

Crasto et al. [192] used a similar strategy to discover the natural product small molecule inhibitor, luteolin, a plant flavonoid that inhibits the *a3–d2* interaction that also occurs in osteoclast ruffled-border V-ATPases. Luteolin inhibited in vitro osteoclast

bone resorption with an IC_{50} of 2.5 μM. Shin et al. [193] have independently shown in vivo that luteolin inhibits prosthetic wear particle osteolysis in mice.

For either of the above compounds, the precise mechanisms of action remain speculative, and metabolic lability and intellectual property issues have impacted on their further development [61, 62]. Nevertheless, these proof-of-concept examples suggest that targeting sites of subunit interaction within the V-ATPase complex may be a viable means of obtaining inhibitors of specific isocomplexes, in these cases those of the osteoclast ruffled border for the purpose of limiting bone-loss diseases like osteoporosis. They also highlight a novel and simple ELISA-based approach to high-throughput random drug screening that can be generalized to potentially identify highly targeted inhibitors of important tertiary, quaternary, or quinary protein structure interactions that can be modeled in vitro. Furthermore, so long as the interacting pair of proteins or appropriate polypeptide segments can be produced or isolated in sufficient quantity, such a screening method can be performed even in the absence of structural information or a precise knowledge of the protein interaction sites.

4.1.2 Small Molecule Inhibitors of V-ATPase Quinary Protein Interaction

In a different screening strategy, Toro et al. [194] exploited the knowledge that V-ATPases bind actin filaments in osteoclasts via an interaction between F-actin and the B2 subunit [195]. This interaction is crucial for cycling of ruffled border V-ATPase between bone resorptive activity at the ruffled-border plasma membrane and "storage" in cytoplasmic vesicles. Using computer modeling of the docking sites for this interaction, Ostrov et al. [196] were able to perform virtual screening for small molecule inhibitors, the most promising hit being enoxacin, a fluoroquinolone antibiotic. Enoxacin appears to inhibit the vesicular trafficking of the osteoclast ruffled-border V-ATPase, which is dependent on its interaction with the actin cytoskeleton, thus making it a promising candidate for osteoporosis treatment [197]. A bone-targeted enoxacin–bisphosphonate conjugate has been shown to inhibit in vivo orthodontic tooth movement in rats [198]. What separates this work to identify inhibitors of protein interaction from the previous examples is the use of virtual screening, where both the site of protein interaction and the library of compounds screened are computer models. Such methods clearly are highly cost effective, and this proof-of-concept example highlights their potential. With regard specifically to therapeutic V-ATPase targeting, a broader application of virtual drug screening must await broader databases of high-resolution 3D subunit structures and their interactions, both intra-V-ATPase isocomplex interactions and their, as yet poorly defined, extra-complex quinary interactomes.

4.1.3 RNAi and Gene Therapy Approaches

In periodontal disease, inflammation induces local osteoclastogenesis and consequent bone loss [199, 200]. In activated osteoclasts, expression of V-ATPase containing the *a3* subunit is upregulated. Additionally, the *a3* splice-variant, TIRC7, plays a role in T cell activation [123, 201]. Jiang et al. [202] proposed that regulating

a3/TIRC7 could be a means of stemming both bone loss and inflammation in periodontal disease, simultaneously. In a mouse *Porphyromonas gingivalis* maxillary infection model, they used local injection of adeno-associated virus (AAV) to deliver short hairpin RNA (shRNA) constructs designed for RNA interference (RNAi) targeting of both *Atp6i* and *Tirc7* transcripts. Knockdown of *a3*/Tirc7 expression caused reduced osteoclast formation and maturation, resulting in a reduction of maxillary bone loss by over 85 % relative to controls, and a similar reduction in gingival inflammation in the infected mice.

In a similar approach, Feng et al. [203] demonstrated that the C1 subunit isoform predominates in the V-ATPase of the osteoclast ruffled border. As with the *a3* subunit, C1 is highly upregulated during osteoclastogenesis and is required for formation of the actin-ring sealing zone of activated osteoclasts, and for the subsequent lacunar acidification required for bone resorption. Unlike the RNAi knockdown of *a3* described above [202], knockdown of C1 expression using Lentivirus-mediated siRNA delivery in vitro did not affect osteoclast formation or maturation, although actin sealing-rings were also completely disrupted.

Gene therapy is commonly regarded as a gain-of-function modality, and such approaches may, in the future, have utility for relatively rare diseases of V-ATPase subunit mutations [63]. As the above proofs of concept suggest, gene-silencing approaches have broader clinical utility using, for example, localized periarticular or periodontal injections of viral RNAi vectors for treating bone-loss disease. For the present, however, safety and cost remain major issues, and systemic gene therapy for bone loss treatment or prevention, such as for osteoporosis, will likely be a long time coming. More acutely life-threatening diseases, such as metastatic cancers, however, may see the first applications of such V-ATPase targeting approaches.

4.2 Novel V-ATPase Targeting Strategies in Agriculture

It is worth pointing out that the potential for V-ATPase targeting transcends human medicine, with wide applicability as well to veterinary medicine and agriculture, all of which ultimately impact human well-being. Examples of strategies and applications follow.

4.2.1 RNAi by dsDNA Dusting

Much early and ongoing work on V-ATPases has been accomplished in insect models. In insects, V-ATPases play a particularly important role in maintaining the pH gradient of the gut, which is vital for nutrient acquisition. Consequently, insect V-ATPases have long been recognized as targets for potentially highly specific RNAi-based insecticides [204]. The corn planthopper, *Peregrinus maidis*, is a major pest that feeds on maize crops, and is a mold and plant virus vector. Yao et al. [205] observed significant knockdown of V-ATPase activity in *P. maidis* that were fed dsRNA to achieve RNAi for V-ATPase A and D subunits, with a resultant decrease in nymph survival and female fecundity.

4.2.2 RNAi by Crop Transgenics

In a small-scale screen, Baum et al. [206] fed Western corn rootworm larvae (*Diabrotica virgifera*) 290 different dsRNA constructs and found 14 causing significant mortality at low doses. One, a dsRNA targeting the V-ATPase A subunit, was transformed into corn, which then showed significant resistance to *D. virgifera* feeding damage. In these examples, simple ingestion of dsRNA was likely successful because the RNAi target is the V-ATPase of the gut epithelium. This strategy, using carefully selected and relatively short dsRNA sequences could be useful in producing transgenic crops with insecticidal qualities only against pest species, without collateral effects. Off-target effects of traditional insecticides are of growing public concern, but the utility of RNAi methods will depend on public acceptance of the transgenic crops, or enhanced methods of production of dsRNA for large-scale crop spraying, and will require the availability of complete genomic sequences for both pest target and beneficial nontarget insect species.

4.2.3 Peptide Inhibition of the V_0 Rotor

The small (37-mer) polypeptide, pea albumin 1b (PA1b), is a potent *M. sexta* V-ATPase inhibitor that binds *c* subunits, possibly interfering with rotor movement, by jamming against the *e* subunit within the proton-translocating V_0 sector, or by binding a *c* and an *e* subunit simultaneously [207, 208]. The extracellular termini and loops available on the *c* subunit for PA1b binding are the least conserved regions of the otherwise highly conserved *c* subunit polypeptide. Consequently, though PA1b has potent insecticidal properties toward *M. sexta*, it has little effect on yeast or mammalian V-ATPases, or even some other insect species. These observations support the notion that species selectivity is possible in strategies aimed at eliminating pests and parasites by targeting the non-conserved sequences of the V_0 rotor. Furthermore, it points to the possibility that peptides may offer exquisitely engineered selectivity, where small molecules fail.

4.2.4 A Gain of Function V-ATPase Strategy: Genetic Engineering of Salt Resistance

While inhibitory strategies are foremost in current agricultural research targeting V-ATPases, gain of function approaches have had some traction for crop improvement. For example, it has been shown that salt stress causes upregulation of V-ATPase subunit expression in wheat, resulting in enhanced Na^+ sequestration in the central vacuole. Furthermore, overexpression of wheat V-ATPase subunit genes in *A. thaliana* results in improved salt and osmotic stress tolerance [84, 209]. Genetic engineering of salt stress resistance in crop species has significant potential for improving worldwide food production.

5 Conclusions

5.1 V-ATPases Represent an Emerging Target of Broad Significance

We have described here the wide variety of impacts that V-ATPases have on human health and welfare. This is unique among potential pharma/agro targets and has recently been a considerable source of motivation for drug discovery. It seems likely that this interest will drive research into V-ATPase structure and function at an accelerating pace into the foreseeable future. Furthermore, new knowledge acquired for any of the diverse areas of application that we have described will enhance the development of V-ATPase targeting as a whole. The most pressing issue for targeting of V-ATPases is the matter of specificity: how to distinguish specialized V-ATPases whose inhibition would be of benefit from those V-ATPases that are vital to survival. Presently, knowledge of the structure of any V-ATPase holoenzyme at atomic resolution is lacking, as is a detailed knowledge of its interactome. Advances in these areas have been slow due to the complexity of the V-ATPase holoenzyme, but it is not unreasonable to think that a complete V-ATPase structure and a list of many more fully characterized functional interactions might be at hand within a decade. Whether V-ATPase targeting breakthroughs come in the form of novel small molecule inhibitors, engineered peptides, RNAi methods, or gene therapy, the potential for health, welfare and economic impact is great.

Acknowledgements The authors wish to acknowledge research funding from the Canadian Institutes of Health Research (CIHR). The authors declare no conflict of interest.

References

1. Futai M, Nakanishi-Matsui M, Okamoto H et al (2012) Rotational catalysis in proton pumping ATPases: from *E. coli* F-ATPase to mammalian V-ATPase. Biochim Biophys Acta 1817:1711–1721
2. Kane PM (2007) The long physiological reach of the yeast vacuolar H^+-ATPase. J Bioenerg Biomembr 39:415–421
3. Toei M, Saum R, Forgac M (2010) Regulation and isoform function of the V-ATPases. Biochemistry 49:4715–4723
4. Forgac M (2007) Vacuolar ATPases: rotary proton pumps in physiology and pathophysiology. Nat Rev Mol Cell Biol 8:917–929
5. Beyenbach KW, Wieczorek H (2006) The V-type H^+ ATPase: molecular structure and function, physiological roles and regulation. J Exp Biol 209:577–589
6. Nordström T, Rotstein OD, Romanek R et al (1995) Regulation of cytoplasmic pH in osteoclasts: contribution of proton pumps and a proton-selective conductance. J Biol Chem 270:2203–2212
7. Schewe B, Schmälzlin E, Walz B (2008) Intracellular pH homeostasis and serotonin-induced pH changes in *Calliphora* salivary glands: the contribution of V-ATPase and carbonic anhydrase. J Exp Biol 211:805–815

8. Grinstein S, Nanda A, Lukacs G et al (1992) V-ATPases in phagocytic cells. J Exp Biol 172:179–192
9. Saw NMN, Kang S-YA, Parsaud L et al (2011) Vacuolar H^+-ATPase subunits Voa1 and Voa2 cooperatively regulate secretory vesicle acidification, transmitter uptake, and storage. Mol Biol Cell 22:3394–3409
10. Manolson MF, Yu H, Chen W et al (2003) The a3 isoform of the 100-kDa V-ATPase subunit is highly but differentially expressed in large (≥10 nuclei) and small (≤5 nuclei) osteoclasts. J Biol Chem 278:49271–49278
11. Henriksen K, Sørensen MG, Jensen VK et al (2008) Ion transporters involved in acidification of the resorption lacuna in osteoclasts. Calcif Tissue Int 83:230–242
12. Brown D, Smith PJS, Breton S (1997) Role of V-ATPase-rich cells in acidification of the male reproductive tract. J Exp Biol 200:257–262
13. Breton S, Brown D (2013) Regulation of luminal acidification by the V-ATPase. Physiology 28:318–329
14. Brown D, Paunescu TG, Breton S et al (2009) Regulation of the V-ATPase in kidney epithelial cells: dual role in acid–base homeostasis and vesicle trafficking. J Exp Biol 212:1762–1772
15. Hinton A, Sennoune SR, Bond S et al (2009) Function of a subunit isoforms of the V-ATPase in pH homeostasis and in vitro invasion of MDA-MB231 human breast cancer cells. J Biol Chem 284:16400–16408
16. Xu M, Xia M, Li X-X et al (2012) Requirement of translocated lysosomal V1 H^+-ATPase for activation of membrane acid sphingomyelinase and raft clustering in coronary epithelial cells. Mol Biol Cell 23:1546–1557
17. Strasser B, Iwaszkiewicz J, Michielin O et al (2011) The V-ATPase proteolipid cylinder promotes the lipid-mixing stage of SNARE-dependent fusion of yeast vacuoles. EMBO J 30:4126–4141
18. Hiesinger PR, Fayyazuddin A, Mehta SQ et al (2005) The v-ATPase V_0 subunit a1 is required for a late step in synaptic vesicle exocytosis in *Drosophila*. Cell 121:607–620
19. Schumacher K (2006) Endomembrane proton pumps: connecting membrane and vesicle transport. Curr Opin Plant Biol 9:595–600
20. Sabota JA, Bäck N, Eipper BA et al (2009) Inhibitors of the V_0 subunit of the vacuolar H^+-ATPase prevent segregation of lysosomal- and secretory-pathway proteins. J Cell Sci 122:3542–3553
21. Sun-Wada G-H, Toyomura T, Murata Y et al (2006) The *a*3 isoform of V-ATPase regulates insulin secretion from pancreatic β-cells. J Cell Sci 119:4531–4540
22. Hurtado-Lorenzo A, Skinner M, El Annan J et al (2006) V-ATPase interacts with ARNO and Arf6 in early endosomes and regulates the protein degradative pathway. Nat Cell Biol 8:124–136
23. Merkulova M, Bakulina A, Thaker YR et al (2010) Specific motifs of the V-ATPase a2-subunit isoform interact with catalytic and regulatory domains of ARNO. Biochim Biophys Acta 1797:1398–1409
24. Hofmann I, Thompson A, Sanderson CM et al (2007) The Arl4 family of small G proteins can recruit the cytohesin Arf6 exchange factors to the plasma membrane. Curr Biol 17:711–716
25. Hosokawa H, Dip PV, Merkulova M et al (2013) The N termini of a-subunit isoforms are involved in signaling between vacuolar H^+-ATPase (V-ATPase) and cytohesin-2. J Biol Chem 288:5896–5913
26. Marshansky V, Rubinstein JL, Grüber G (2014) Eukaryotic V-ATPase: novel structural findings and functional insights. Biochim Biophys Acta 1837:857–879
27. Poëa-Guyon S, Ammar MR, Erard M et al (2013) The V-ATPase membrane domain is a sensor of granular pH that controls the exocytic machinery. J Cell Biol 203:283–298
28. Coonrod EM, Graham LA, Carpp LN et al (2013) Homotypic vacuole fusion in yeast requires organelle acidification and not the V-ATPase membrane domain. Dev Cell 27:462–468
29. Yan Y, Denef N, Schüpbach T (2009) The vacuolar proton pump (V-ATPase) is required for Notch signaling and endosomal trafficking in Drosophila. Dev Cell 17:387–402

30. Cruciat C-M, Ohkawara B, Acebron SP et al (2010) Requirement of prorenin receptor and vacuolar H^+-ATPase-mediated acidification for Wnt signaling. Science 327:459–463
31. Jewell JL, Russel RC, Guan K-L (2013) Amino acid signalling upstream of mTOR. Nat Rev Mol Cell Biol 14:133–139
32. Peña-Llopis S, Vega-Rubin-de-Celis S, Schwartz JC et al (2011) Regulation of TFEB and V-ATPases by mTORC1. EMBO J 30:3242–3258
33. Laplante M, Sabatini DM (2013) Regulation of mTORC1 and its impact on gene expression at a glance. J Cell Sci 126:1713–1719
34. Efeyan A, Zoncu R, Sabatini DM (2012) Amino acids and mTORC1: from lysosomes to disease. Trends Mol Med 18:524–533
35. Sancak Y, Sabatini DM (2009) Rag proteins regulate amino acid-induced mTORC1 signaling. Biochem Soc Trans 37:289–290
36. Zoncu R, Bar-Peled L, Efeyan A et al (2011) mTORC1 senses lysosomal amino acids through an inside-out mechanism that requires the vacuolar H^+-ATPase. Science 334:678–683
37. Bar-Peled L, Schweitzer LD, Zoncu R et al (2012) Ragulator is a GEF for the Rag GTPases that signal amino acid levels to mTORC1. Cell 150:1196–1208
38. Abraham RT (2015) Making sense of amino acid sensing. Science 347:128–129
39. Wang S, Tsun Z-Y, Wolfson RL et al (2015) Lysosomal amino acid transporter SLC38A9 signals arginine sufficiency to mTORC1. Science 347:188–194
40. Xu Y, Parmar A, Roux E et al (2012) Epidermal growth factor-induced vacuolar (H^+)-ATPase assembly: a role in signaling via mTORC1 activation. J Biol Chem 287:26409–26422
41. Muench SP, Trinick J, Harrison MA (2011) Structural divergence of the rotary ATPases. Q Rev Biophys 44:311–356
42. Zhang Z, Zheng Y, Mazon H et al (2008) Structure of the yeast vacuolar ATPase. J Biol Chem 283:35983–35995
43. Smith AN, Lovering RC, Futai M et al (2003) Revised nomenclature for mammalian vacuolar-type H^+-ATPase subunit genes. Mol Cell 12:801–803
44. Miranda KC, Karet FE, Brown D (2010) An extended nomenclature for mammalian V-ATPase subunit genes and splice variants. PLoS One 5, e9531
45. Lee BS (2012) Regulation of V-ATPase expression in mammalian cells. Curr Protein Peptide Sci 13:107–116
46. Holliday LS (2014) Vacuolar H^+-ATPase: an essential multitasking enzyme in physiology and pathophysiology. New J Sci 2014:1–21. doi:10.1155/2014/675430
47. Finnigan GC, Hanson-Smith V, Houser BD et al (2011) The reconstructed ancestral subunit a functions as both V-ATPase isoforms Vph1p and Stv1p in *Saccharomyces cerevisiae*. Mol Biol Cell 22:3176–3191
48. Manolson MF, Wu B, Proteau D et al (1994) *STV1* gene encodes functional homologue of 95-kDa yeast vacuolar H^+-ATPase subunit Vph1p. J Biol Chem 269:14064–14074
49. Kawasaki-Nishi S, Bowers K, Nishi T et al (2001) The amino-terminal domain of the vacuolar proton-translocating ATPase a subunit controls targeting and *in vivo* dissociation, and the carboxyl-terminal domain affects coupling of proton transport and ATP hydrolysis. J Biol Chem 276:47411–47420
50. Karet FE, Finberg KE, Nelson RD et al (1999) Mutations in the gene encoding B1 subunit of H^+-ATPase cause renal tubular acidosis with sensorineural deafness. Nat Genet 21:84–90
51. Păunescu TG, Rodriguez S, Benz E et al (2012) Loss of the V-ATPase B1 subunit isoform expressed in non-neuronal cells of the mouse olfactory epithelium impairs olfactory function. PLoS One 7, e45395
52. Guillard M, Dimopoulou A, Fischer B et al (2009) Vacuolar H^+-ATPase meets glycosylation in patients with cutis laxa. Biochim Biophys Acta 1792:903–914
53. Fischer B, Dimopoulou A, Egerer J et al (2012) Furher characterization of *ATP6V0A2*-related autosomal recessive cutis laxa. Hum Genet 131:1761–1773
54. Sobacchi C, Schulz A, Coxon FP et al (2013) Osteopetrosis: genetics, treatment and new insights into osteoclast function. Nat Rev Endocrinol 9:522–536

55. Stover EH, Borthwick KJ, Bavalia C et al (2002) Novel *ATP6V1B1* and *ATP6V0A4* mutations in autosomal recessive distal renal tubular acidosis with new evidence for hearing loss. J Med Genet 39:796–803
56. Batlle D, Haque SK (2012) Genetic causes and mechanisms of distal renal tubular acidosis. Nephrol Dial Transplant 27:3691–3704
57. Lee S-H, Rho J, Jeong D et al (2006) v-ATPase V_0 subunit d2-deficient mice exhibit impaired osteoclast fusion and increased bone formation. Nat Med 12:1403–1409
58. Korvatska O, Strand NS, Berndt JD et al (2013) Altered splicing of ATP6AP2 causes X-linked parkinsonism with spasticity (XPDS). Hum Mol Genet 22:3259–3268
59. Ramser J, Abidi FE, Burckle CA et al (2005) A unique exonic splice enhancer mutation in a family with X-linked mental retardation and epilepsy points to a novel role of the renin receptor. Hum Mol Genet 14:1019–1027
60. Holliday LS (2012) Vacuolar H^+-ATPase: Targeting a "housekeeping" enzyme for drug development. Curr Protein Peptide Sci 13:105–106
61. Kartner N, Manolson MF (2014) Novel techniques in the development of osteoporosis drug therapy: the osteoclast ruffled-border vacuolar H^+-ATPase as an emerging target. Expert Opin Drug Discov 9:505–522
62. Kartner N, Manolson MF (2012) V-ATPase subunit interactions: the long road to therapeutic targeting. Curr Protein Peptide Sci 13:164–179
63. Bhargava A, Voronov I, Wang Y et al (2012) Osteopetrosis mutation R444L causes ER retention and misprocessing of vacuolar H^+-ATPase *a3* subunit. J Biol Chem 287:26829–26839
64. Gharanei S, Zatyka M, Astuti D et al (2013) Vacuolar-type H^+-ATPase V1A subunit is a molecular partner of Wolfram syndrome 1 (WFS1) protein, which regulates its expression and stability. Hum Mol Genet 22:203–217
65. Capecci J, Forgac M (2013) Function of vacuolar ATPase (V-ATPase) a subunit isoforms in invasiveness of MCF10a and MCF10CA1a human breast cancer cells. J Biol Chem 288:3271–32741
66. Nishisho T, Hata K, Nakanishi M et al (2011) The a3 isoform vacuolar type H^+-ATPase promotes distant metastasis in the mousse B16 melanoma cells. Mol Cancer Res 9:845–855
67. Sennoune SR, Luo D, Martinez-Zaguilán R (2004) Plasmalemmal vacuolar-type H^+-ATPase in cancer biology. Cell Biochem Biophys 40:185–206
68. Sennoune SR, Bakunts K, Martínez GM et al (2004) Vacuolar H^+-ATPase in human breast cancer cells with distinct metastatic potential: distribution and functional activity. Am J Physiol Cell Physiol 286:C1443–C1452
69. Pérez-Sayáns M, Somoza-Martín JM, Barros-Angueira F et al (2010) Multidrug resistance in oral squamous cell carcinoma: the role of vacuolar ATPases. Cancer Lett 295:135–143
70. Olsson AH, Yang BT, Hall E et al (2011) Decreased expression of genes involved in oxidative phosphorylation in human pancreatic islets from patients with type 2 diabetes. Eur J Endocrinol 165:589–595
71. Molina MF, Qu H-Q, Rentfro AR et al (2011) Decreased expression of ATP6V1H in type 2 diabetes: a pilot report on the diabetes risk study of Mexican Americans. Biochem Biophys Res Commun 412:728–731
72. Mangieri LR, Mader BJ, Thomas CE et al (2014) ATP6V0C knockdown in neuroblastoma cell alters autophagy-lysosome pathway function and metabolism of proteins that accumulate in neurodegenerative disease. PLoS One 9, e93257
73. Ramachandran N, Munteanu I, Wang P et al (2013) VMA21 deficiency prevents vacuolar ATPase assembly and causes autophagic vacuolar myopathy. Acta Neuropathol (Berl) 125:439–457
74. Price PA, June HH, Buckley JR et al (2002) SB 242784, a selective inhibitor of the osteoclastic V-H^+-ATPase, inhibits arterial calcification in the rat. Circ Res 91:547–552
75. Rojas JD, Sennoune SR, Martinez GM et al (2004) Plasmalemmal vacuolar H^+-ATPase is decreased in microvascular endothelial cells from a diabetic model. J Cell Physiol 201: 190–200

76. Rojas JD, Sennoune SR, Maita D et al (2006) Vacuolar-type H^+-ATPases at the plasma membrane regulate pH and cell migration in microvascular endothelial cells. Am J Physiol Heart Circ Physiol 291:H1147–H1157
77. Knight AJ, Behm CA (2012) Minireview: the role of the vacuolar ATPase in nematodes. Exp Parasitol 132:47–55
78. Jia C, Yu Q, Zhang B et al (2014) Role of *TFP1* in vacuolar acidification, oxidative stress and filamentous development in *Candida albicans*. Fungal Genet Biol 71:58–67
79. Kang S, Shields AR, Jupatanakul N et al (2014) Supressing dengue-2 infection by chemical inhibition of *Aedes aegypti* host factors. PLoS Negl Trop Dis 8, e3084
80. Geyer M, Yu H, Mandic R et al (2002) Subunit H of the V-ATPase binds to the medium chain of adaptor protein complex 2 and connects Nef to the endocytic machinery. J Biol Chem 277:28521–28529
81. Müller KH, Kainov DE, El Bakkouri K et al (2011) The proton translocation domain of cellular vacuolar ATPase provides a target for the treatment of influenza A virus infections. Br J Pharmacol 164:344–357
82. Dhaliwal GS, Jindal V, Dhawan AK (2010) Insect pest problems and crop losses: changing trends. Indian J Ecol 37:1–7
83. Rahdari P, Hoseini SM (2011) Salinity stress: a review. Tech J Eng Appl Sci 1:63–66
84. He X, Huang X, Shen Y et al (2014) Wheat V-H^+-ATPase subunit genes significantly affect salt tolerance in *Arapidopsis thaliana*. PLoS One 9, e86982
85. Parra KJ (2014) Saccharomyces cerevisiae vacuolar H^+-ATPase regulation by disassembly and reassembly: One structure and multiple signals. Eukaryot Cell 13:706–714
86. Maxson ME, Grinstein S (2014) The vacuolar-type H^+-ATPase at a glance – more than a proton pump. J Cell Sci 127:4987–4993
87. Lee BS, Underhill DM, Crane MK et al (1995) Transcriptional regulation of the vacuolar H^+-ATPase B2 subunit gene in differentiating THP-1 cells. J Biol Chem 270:7320–7329
88. Lee BS, Krits I, Crane-Zelkovic MK et al (1997) A novel transcription factor regulates expression of the vacuolar H^+-ATPase B2 subunit through AP-2 sites during monocytic differentiation. J Biol Chem 272:174–181
89. Wang S-P, Krits I, Bai S et al (2002) Regulation of enhanced vacuolar H^+-ATPase expression in macrophages. J Biol Chem 277:8827–8834
90. Izumi H, Ise T, Murakami T et al (2003) Structural and functional characterization of two human V-ATPase subunit gene promoters. Biochim Biophys Acta 1628:97–104
91. Gardiner-Garden M, Frommer M (1987) CpG islands in vertebrate genomes. J Mol Biol 196:261–282
92. Robinson PN, Böhme U, Lopez R et al (2004) Gene-ontology analysis reveals association of tissue-specific 5′CpG-island genes with development and embryogenesis. Hum Mol Genet 13:1969–1978
93. Illingworth RS, Bird AP (2009) CpG islands – 'a rough guide'. FEBS Lett 583:1713–1720
94. Chatterjee R, Vinson C (2012) CpG methylation recruits sequence specific transcription factors essential for tissue specific gene expression. Biochim Biophys Acta 1819:763–770
95. Jaenisch R, Bird A (2003) Epigenetic regulation of gene expression: how the genome integrates intrinsic and environmental signals. Nat Genet 33:245–254
96. Vidarsson H, Westergren R, Heglind M et al (2009) The forkhead transcription factor Foxi1 is a master regulator of vacuolar H^+-ATPase proton pump subunits in the inner ear, kidney and epididymis. PLoS One 4, e4471
97. Blomqvist SR, Vidarsson H, Fitzgerald S et al (2004) Distal renal tubular acidosis in mice that lack the forkhead transcription factor Foxi1. J Clin Invest 113
98. Jackson BC, Carpenter C, Nebert DW et al (2010) Update of human and mouse forkead box (FOX) gene families. Hum Genomics 4:345–352
99. Lacey DL, Timms E, Tan HL et al (1998) Osteoprotegerin ligand is a cytokine that regulates osteoclast differentiation and activation. Cell 93:165–176
100. Song I, Kim JH, Kim K et al (2009) Regulatory mechanism of NFATc1 in RANKL-induced osteoclast activation. FEBS Lett 583:2435–2440

101. Beranger GE, Momier D, Rochet N et al (2006) RANKL treatment releases the negative regulation of the poly(ADP-ribose) polymerase-1 on Tcirg1 gene expression during osteoclastogenesis. J Bone Miner Res 21:1757–1769
102. Beranger GE, Momier D, Guigonis J-M et al (2007) Differential binding of poly(ADP-ribose) polymerase-1 and JunD/Fra2 accounts for RANKL-induced *Tcirg1* gene expression during osteoclastogenesis. J Bone Miner Res 22:975–983
103. Takayanagi H (2007) The role of NFAT in osteoclast formation. Ann N Y Acad Sci 116:227–237
104. Feng H, Cheng T, Steer JH et al (2009) Myocyte enhancer factor 2 and microphthalmia-associated transcription factor cooperate with NFATc1 to transactivate the V-ATPase d2 promoter during RANKL-induced osteoclastogenesis. J Biol Chem 284:14667–14676
105. Jouret F, Auzanneau C, Debaix H et al (2005) Ubiquitous and kidney-specific subunits of vacuolar H^+-ATPase are differentially expressed during nephrogenesis. J Am Soc Nephrol 16:3235–3246
106. Lee BS, Holliday LS, Krits I et al (1999) Vacuolar H^+-ATPase activity and expression in mouse bone marrow cultures. J Bone Miner Res 14:2127–2136
107. Jeyaraj S, Dakhlallah D, Hill SR et al (2005) HuR stabilizes vacuolar H^+-translocating ATPase mRNA during cellular energy depletion. J Biol Chem 280:37957–37964
108. Khabar KSA, Bakheet T, Williams BRG (2005) AU-rich transient response transcripts in the human genome: expressed sequence tag clustering and gene discovery approach. Genomics 85:165–175
109. Peng SS-Y, Chen C-YA XN et al (1998) RNA stabilization by the AU-rich element binding protein, HuR, an ELAV protein. EMBO J 17:3461–3470
110. Fan XC, Steitz JA (1998) Overexpression of HuR, a nuclear-cytoplasmic shuttling protein, increases the *in vivo* stability of ARE-containing mRNAs. EMBO J 17:3448–3460
111. Jeyaraj S, Dakhlallah D, Hill SR et al (2006) Expression and distribution of HuR during ATP depletion and recovery in proximal tubule cells. Am J Physiol Renal Physiol 291: F1255–F1263
112. López de Silanes I, Zhan M, Lal A et al (2004) Identification of a target RNA motif for RNA-binding protein HuR. Proc Natl Acad Sci U S A 101:2987–2992
113. Hobert O (2008) Gene regulation by transcription factors and microRNAs. Science 319:1785–1786
114. Bartel DP (2009) MicroRNAs: target recognition and regulatory functions. Cell 136:215–233
115. Stark A, Brennecke J, Bushati N et al (2005) Animal microRNAs confer robustness to gene expression and have a significant impact on 3'UTR evolution. Cell 123:1133–1146
116. O'Connor DT, Zhu G, Rao F et al (2008) Heritability and genome-wide linkage in US and Australian twins identify novel genomic regions controlling chromogranin A: implications for secretion and blood pressure. Circulation 118:247–257
117. Wei Z, Biswas N, Courel M et al (2011) A common genetic variant in the 3′-UTR of vacuolar H^+-ATPase *ATP6V0A1* creates a micro-RNA motif to alter chromogranin A processing and hypertension risk. Circ Cardiovasc Genet 4:381–389
118. Poëa-Guyon S, Amar M, Fossier P et al (2006) Alternative splicing controls neuronal expression of V-ATPase subunit a1 and sorting to nerve terminals. J Biol Chem 281:17164–17172
119. Kawasaki-Nishi S, Yamaguchi A, Forgac M et al (2007) Tissue specific expression of the splice variants of the mouse vacuolar proton-translocating ATPase a4 subunit. Biochem Biophys Res Commun 364:1032–1036
120. Smith AN, Skaug J, Choate KA et al (2000) Mutations in *ATP6N1B*, encoding a new kidney vacuolar proton pump 116-kD subunit, cause recessive distal renal tubular acidosis with preserved hearing. Nat Genet 26:71–75
121. Smith AN, Borthwick KJ, Karet FE (2002) Molecular cloning and characterization of novel tissue-specific isoforms of the human vacuolar H^+-ATPase C, G and d subunits, and their evaluation in autosomal recessive distal renal tubular acidosis. Gene 297:169–177
122. Sun-Wada G-H, Murata Y, Namba M et al (2003) Mouse proton pump ATPase *C* subunit isoforms (*C*2-a and *C*2-b) specifically expressed in kidney and lung. J Biol Chem 278: 44843–44851

123. Heinemann T, Bulwin G-C, Randall J et al (1999) Genomic organization of the gene coding for TIRC7, a novel membrane protein essential for T cell activation. Genomics 57:398–406
124. Kane PM (1999) Biosynthesis and regulation of the yeast vacuolar H+-ATPase. J Bioenerg Biomembr 31:49–56
125. Graham LA, Flannery AR, Stevens TH (2003) Structure and assembly of the yeast V-ATPase. J Bioenerg Biomembr 35:301–312
126. Davis-Kaplan SR, Compton MA, Flannery AR et al (2006) *PKR1* encodes an assembly factor for the yeast V-type ATPase. J Biol Chem 281:32025–32035
127. Li X, Su RTC, H-t H et al (1998) The molecular chaperone calnexin associates with the vacuolar H+-ATPase from oat seedlings. Plant Cell 10:119–130
128. Kane PM, Smardon AM (2003) Assembly and regulation of the yeast vacuolar H+-ATPase. J Bioenerg Biomembr 35:313–322
129. Merzendorfer H, Gräf R, Huss M et al (1997) Regulation of proton-translocating V-ATPases. J Exp Biol 200:225–235
130. Kane PM (2012) Targeting reversible disassembly as a mechanism of controlling V-ATPase activity. Curr Protein Peptide Sci 13:117–123
131. Sumner J-P, Dow JAT, Earley FGP et al (1995) Regulation of plasma membrane V-ATPase activity by dissociation of peripheral subunits. J Biol Chem 270:5649–5653
132. Kane PM (1995) Disassembly and reassembly of the yeast vacuolar H+-ATPase *in vivo*. J Biol Chem 270:17025–17032
133. Merkulova M, Hurtado-Lorenzo A, Hosokawa H et al (2011) Aldolase directly interacts with ARNO and modulates cell morphology and acidic vesicle distribution. Am J Physiol Cell Physiol 2011:C1442–C1455
134. Lu M, Ammar D, Ives H et al (2007) Physical interaction between aldolase and vacuolar H+-ATPase is essential for the assembly and activity of the proton pump. J Biol Chem 282: 24495–24503
135. Marshansky V, Futai M (2008) The V-type H+-ATPase in vesicular trafficking: targeting, regulation and function. Curr Opin Cell Biol 20:415–426
136. Tabke K, Albertmelcher A, Vitavska O et al (2014) Reversible disassembly of the yeast V-ATPase revisited under *in vivo* conditions. Biochem J 462:185–197
137. Su Y, Blake-Palmer KG, Sorrell S et al (2008) Human H+ATPase a4 subunit mutations causing renal tubular acidosis reveal a role for interaction with phosphofructokinase-1. Am J Physiol Renal Physiol 295:F950–F958
138. Hong-Hermesdorf A, Brüx A, Grüber A et al (2006) A WNK kinase binds and phosphorylates V-ATPase subunit C. FEBS Lett 580:932–939
139. Armbrüster A, Hohn C, Hermesdorf A et al (2005) Evidence for major structural changes in subunit C of the vacuolar ATPase due to nucleotide binding. FEBS Lett 579:1961–1967
140. Chan C-Y, Parra KJ (2014) Yeast phosphofructokinase-1 subunit Pfk2p is necessary for pH homeostasis and glucose-dependent vacuolar ATPase reassembly. J Biol Chem 289:19448–19457
141. Lu M, Sautin YY, Holliday S et al (2004) The glycolytic enzyme aldolase mediates assembly, expression, and activity of vacuolar H+-ATPase. J Biol Chem 279:8732–8739
142. Smardon AM, Diab HI, Tarsio M et al (2014) The RAVE complex is an isoform-specific V-ATPase assembly factor in yeast. Mol Biol Cell 25:356–367
143. Tuttle AM, Hoffman TL, Schilling TF (2014) Rabconnectin-3a regulates vesicle endocytosis and canonical Wnt signaling in zebrafish neural crest migration. PLoS Biol 12, e1001852
144. Dechant R, Binda M, Lee SS et al (2010) Cytosolic pH is a second messenger for glucose and regulates the PKA pathway through V-ATPase. EMBO J 29:2515–2526
145. Sautin YY, Lu M, Gaugler A et al (2005) Phosphatidylinositol 3-kinase-mediated effects of glucose on vacuolar H+-ATPase assembly, translocation, and acidification of intracellular compartments in renal epithelial cells. Mol Cell Biol 25:575–589
146. Oehlke O, Schlosshardt C, Feuerstein M et al (2012) Acidosis-induced V-ATPase trafficking in salivary ducts is initiated by cAMP/PKA/CREB pathway via regulation of Rab11b expression. Int J Biochem Cell Biol 44:1254–1265

147. Diakov TT, Kane PM (2010) Regulation of vacuolar proton-translocating ATPase activity and assembly by extracellular pH. J Biol Chem 285:23771–23778
148. Parra KJ, Keenan KL, Kane PM (2000) The H subunit (Vma13p) of the yeast V-ATPase inhibits the ATPase activity of cytosolic V_1 complexes. J Biol Chem 275:21761–21767
149. Gräf R, Harvey WR, Wieczorek H (1996) Purification and properties of a cytosolic V_1-ATPase. J Biol Chem 271:20908–20913
150. Diab H, Ohira M, Liu M et al (2009) Subunit interactions and requirements for inhibition of the yeast V_1-ATPase. J Biol Chem 284:13316–13325
151. Jefferies KC, Forgac M (2008) Subunit H of the vacuolar (H^+) ATPase inhibits ATP hydrolysis by the free V_1 domain by interaction with thte rotary subunit F. J Biol Chem 283: 4512–4519
152. Qi J, Forgac M (2007) Cellular environment is important in controlling V-ATPase dissociation and its dependency on activity. J Biol Chem 282:24743–24751
153. Kawasaki-Nishi S, Nishi T, Forgac M (2001) Yeast V-ATPase complexes containing different isoforms of the 100-kDa a-subunit differ in coupling efficiency and *in vivo* dissociation. J Biol Chem 276:17941–17948
154. Trombetta ES, Ebersold M, Garrett W et al (2003) Activation of lysosomal function during dendritic cell maturation. Science 299:1400–1403
155. Liberman R, Bond S, Shainheit MG et al (2014) Regulated assembly of vacuolar ATPase is increased during cluster disruption-induced maturation of dendritic cells through a phosphatidyl 3-kinase/mTOR-dependent pathway. J Biol Chem 289:1355–1363
156. Chintagari NR, Mishra A, Su L et al (2010) Vacuolar ATPase regulates surfactant secretion in rat alveolar typeII cells by modulating lamellar body calcium. PLoS One 5, e9228
157. Nakamura S (2004) Glucose activates H^+-ATPase in kidney epithelial cells. Am J Physiol Cell Physiol 287:C97–C105
158. Silva P, Gerós H (2009) Regulation by salt of vacuolar H^+-ATPase and H^+-pyrophosphatase activities and Na^+/H^+ exchange. Plant Signal Behav 4:718–726
159. Voss M, Vitavska O, Walz B et al (2007) Stimulus-induced phosphorylation of vacuolar H^+-ATPase by protein kinase A. J Biol Chem 282:33735–33742
160. Finnigan GC, Cronan GE, Park HJ et al (2012) Sorting of the yeast vacuolar-type, proton-translocating ATPase enzyme complex (V-ATPase). J Biol Chem 287:19487–19500
161. Collaco AM, Geibel P, Lee BS et al (2013) Functional vacuolar ATPase (V-ATPase) proton pumps traffic to the enterocyte brush border membrane and require CFTR. Am J Physiol Cell Physiol 305:C981–C996
162. Păunescu TG, Ljubojevic M, Russo LM et al (2010) cAMP stimulates apical V-ATPase accumulation, microvillar elongation and proton extrusion in kidney collecting duct A-intercalated cells. Am J Physiol Renal Physiol 298:F643–F654
163. Pastor-Soler NM, Hallows KR, Smolak C et al (2008) Alkaline pH- and cAMP-induced V-ATPase membrane accumulation is mediated by protein kinase A in epididymal clear cells. Am J Physiol Cell Physiol 294:C488–C494
164. Pech V, Pham TD, Verlander JW et al (2008) Angiotensin II activates H^+-ATPase in type A intercalated cells. J Am Soc Nephrol 19:84–91
165. Alzamora R, Thali RF, Gong F et al (2010) PKA regulates vacuolar H^+-ATPase localization and activity via direct phosphorylation of the A subunit in kidney cells. J Biol Chem 285:24676–24685
166. Rieg T, Rieg JD (2013) Connecting type A intercalated cell metabolic state to V-ATPase function: phosphorylation does matter! Am J Physiol Renal Physiol 305:F1105–F1106
167. Hallows KR, Alzamora R, Li H et al (2009) AMP-activated protein kinase inhibits alkaline pH- and PKA-induced apical vacuolar H^+-ATPase accumulation in epididymal clear cells. Am J Physiol Cell Physiol 296:C672–C681
168. Alzamora R, Al-Bataineh M, Liu W et al (2013) AMP-activated protein kinase regulates the vacuolar H^+-ATPase via direct phosphorylation of the A subunit (ATP6V1A) in the kidney. Am J Physiol Renal Physiol 305:F943–F956

169. Lee BS, Gluck SL, Holliday LS (1999) Interaction between vacuolar H+-ATPase and microfilaments during osteoclast activation. J Biol Chem 274:29164–29171
170. Chen S-H, Bubb MR, Yarmola EG et al (2004) Vacuolar H^+-ATPase binding to microfilaments: regulation in response to phosphatidylinositol 3-kinase activity and detailed characterization of the actin-binding site in subunit B. J Biol Chem 279:7988–7998
171. Nelson N, Sacher A, Nelson H (2002) The significance of molecular slips in transport systems. Nat Rev Mol Cell Biol 3:876–881
172. Grabe M, Wang H, Oster G (2000) The mechanochemistry of V-ATPase proton pumps. Biophys J 78:2798–2813
173. Kettner C, Bertl A, Obermeyer G et al (2003) Electrophysiological analysis of the yeast V-type proton pump: variable coupling ratio and proton shunt. Biophys J 85:3730–3738
174. Li SC, Diakov TT, Xu T et al (2014) The signaling lipid $PI(3,5)P_2$ stabilizes V_1–V_o sector interactions and activates the V-ATPase. Mol Biol Cell 25:1251–1262
175. Chung J-H, Lester RL, Dickson RC (2003) Sphingolipid requirement for generation of a functional V_1 component of vacuolar ATPase. J Biol Chem 278:28872–28881
176. van der Poel S, Wolthoorn J, van den Heuvel D et al (2011) Hyperacidification of *trans*-Golgi network and endo/lysosomes in melanocytes by glucosylceramide-dependent V-ATPase activity. Traffic 12:1634–1647
177. Yamaguchi M, Kasamo K (2001) Modulation in the activity of purified tonoplast H^+-ATPase by tonoplast glycolipids prepared from cultured rice (*Oryza sativa* L. var. Boro) cells. Plant Cell Physiol 42:516–523
178. Yoshida K, Ohnishi M, Fukao Y et al (2013) Studies on vacuolar membrane microdomains isolated from *Arabidopsis* suspension-cultured cells: local distribution of vacuolar membrane proteins. Plant Cell Physiol 54:1571–1584
179. Zhang Y-Q, Gamarra S, Garcia-Effron G et al (2010) Requirement for ergosterol in V-ATPase function underlies antifungal activity of azole drugs. PLoS Pathog 6, e1000939
180. Sterling D, Reithmeier RAF, Casey JR (2001) A transport metabolon: functional interaction of carbonic anhydrase II and chloride/bicarbonate exchangers. J Biol Chem 276:47886–47894
181. Mindell JA (2012) Lysosomal acidification mechanisms. Annu Rev Physiol 74:69–86
182. Kasper D, Planells-Cases R, Fuhrmann JC et al (2005) Loss of the chloride channel ClC-7 leads to lysosomal storage disease and neurodegeneration. EMBO J 24:1079–1091
183. Graves AR, Curran PK, Smith CL et al (2008) The Cl^-/H^+ antiporter ClC-7 is the primary chloride permeation pathway in lysosomes. Nature 453:788–792
184. Venta PJ, Welty RJ, Johnson TM et al (1991) Carbonic anhydrase II deficiency syndrome in a Belgian family is caused by a point mutation at an invariant histidine residue (107 His → Tyr): complete structure of the normal human CA II gene. Am J Hum Gene 49:1082–1090
185. Meyers SN, McDaneld TG, Swist SL et al (2010) A deletion in bovine *SLC4A2* is associated with osteopetrosis in Red Angus cattle. BMC Genomics 11:337
186. Kornak U, Kasper D, Bösl MR et al (2001) Loss of the ClC-7 chloride channel leads to osteopetrosis in mice and man. Cell 104:205–215
187. Schaller S, Henriksen K, Sveigaard C et al (2004) The chloride channel inhibitor N53736 prevents bone resorption in ovariectomized rats without changing bone formation. J Bone Miner Res 19:1144–1153
188. Thudium CS, Jensen VK, Karsdal MA et al (2012) Disruption of the V-ATPase functionality as a way to uncouple bone formation and resorption – a novel target for treatment of osteoporosis. Curr Protein Peptide Sci 13:141–151
189. Kartner N, Yao Y, Li K et al (2010) Inhibition of osteoclast bone resorption by disrupting vacuolar H^+-ATPase *a3*–B2 subunit interaction. J Biol Chem 285:37476–37490
190. Toyomura T, Oka T, Yamaguchi C et al (2000) Three subunit *a* isoforms of mouse vacuolar H^+-ATPase: preferential expression of the *a*3 isoform during osteoclast differentiation. J Biol Chem 275:8760–8765
191. Bartkiewicz M, Hernando N, Reddy SV et al (1995) Characterization of the osteoclast vacuolar H(+)-ATPase B-subunit. Gene 160:157–164

192. Crasto GJ, Kartner N, Yao Y et al (2013) Luteolin inhibition of V-ATPase *a3–d2* interaction decreases osteoclast resorptive activity. J Cell Biochem 114:929–941
193. Shin D-K, Kim M-H, Lee S-H et al (2012) Inhibitory effects of luteolin on titanium particle-induced osteolysis in a mouse model. Acta Biomater 8:3524–3531
194. Toro EJ, Ostrov DA, Wronski TJ et al (2012) Rational identification of enoxacin as a novel V-ATPase-directed osteoclast inhibitor. Curr Protein Peptide Sci 13:180–191
195. Holliday LS, Lu M, Lee BS et al (2000) The amino-terminal domain of the B subunit of vacuolar H^+-ATPase contains a filamentous actin binding site. J Biol Chem 275:32331–32337
196. Ostrov DA, Magis AT, Wronski TJ et al (2009) Identification of Enoxacin as an inhibitor of osteoclast formation and bone resorption by structure-based virtual screening. J Med Chem 52:5144–5151
197. Toro EJ, Zuo J, Ostrov DA et al (2012) Enoxacin directly inhibits osteoclastogenesis without inducing apoptosis. J Biol Chem 287:17894–17904
198. Toro EJ, Zuo J, Guiterrez A et al (2013) Bis-enoxacin inhibits bone resorption and orthodontic tooth movement. J Dent Res 92:925–931
199. Lin X, Han X, Kawai T et al (2011) Antibody to receptor activator of NF-κB ligand ameliorates T cell-mediated periodontal bone resorption. Infect Immun 79:911–917
200. Kawai T, Matsuyama T, Hosokawa Y et al (2006) B and T lymphocytes are the primary source of RANKL in the bone resorptive lesion of periodontal disease. Am J Pathol 169:987–998
201. Utku N, Heinemann T, Tullius SG et al (1998) Prevention of acute allograft rejection by antibody targeting of TIRC7, a novel T cell membrane protein. Immunity 9:509–518
202. Jiang H, Chen W, Zhu G et al (2013) RNAi-mediated silencing of Atp6i and Atp6i haploinsufficiency prevents both bone loss and inflammation in a mouse model of periodontal disease. PLoS One 8, e58599
203. Feng S, Deng L, Chen W et al (2009) Atp6v1c1 is an essential component of the osteoclast proton pump and in F-actin ring formation in osteoclasts. Biochem J 417:195–203
204. Whyard S, Singh AD, Wong S (2009) Ingested double-stranded RNAs can act as species-specific insecticides. Insect Biochem Mol Biol 39:824–832
205. Yao J, Rotenberg D, Afsharifar A et al (2013) Development of RNAi methods for *Peregrinus maidis*, the corn planthopper. PLoS One 8, e70243
206. Baum JA, Bogaert T, Clinton W et al (2007) Control of colepteran insect pests through RNA interference. Nat Biotechnol 25:1322–1326
207. Chouabe C, Eyraud V, Da Silva P et al (2011) New mode of action for a knottin protein bioinsecticide: pea albumin 1 subunit b (PA1b) is the first peptidic inhibitor of V-ATPase. J Biol Chem 286
208. Muench SP, Rawson S, Eyraud V et al (2014) PA1b inhibitor binding to subunits *c* and *e* of the vacuolar ATPase reveals its insecticidal mechanism. J Biol Chem 289:16399–16408
209. Zhang X-H, Li B, Hu Y-G et al (2014) The wheat E subunit of V-type H^+-ATPase is involved in the plant response to osmotic stress. Int J Mol Sci 15:16196–16210
210. Sun-Wada G-H, Imai-Senga Y, Yamamoto A et al (2002) A proton pump ATPase with testis-specific *E*1-subunit isoform required for acrosome acidification. J Biol Chem 277:18098–18105

Part IV
F_1F_o-and Other ATPases

Chapter 21
Thiol-Related Regulation of the Mitochondrial F_1F_O-ATPase Activity

Alessandra Pagliarani, Salvatore Nesci, Fabiana Trombetti, and Vittoria Ventrella

Abstract The ATP synthase or F_1F_O-ATPase is the key enzyme in cell bioenergetics, due to its main role to build ATP, but it can also work "in reverse" to hydrolyze ATP. The enzyme complex, increasingly involved as key molecular switch between life and death, is finely tuned by multiple and only partially known mechanisms, widely operative in health and disease. Among them, the enzyme regulation through the chemical modification of protein thiols, namely cysteine side chains, is thought to play a prominent role. Thiols are known to have high biological impact, to be easily oxidized, susceptive to multiple post-translational oxidative modifications and to occur both in the catalytic sector F_1 and in the membrane-embedded rotor F_O which form the F_1F_O complex. Even if thiol properties mirror the chemical attitudes of sulfur, not all cysteine thiols are equally prone to chemical modifications, being strongly influenced by their molecular environment. Cysteine thiol modifications, which, according to the ambient, may be reversible, interchangeable and even irreversible, not only modulate the enzyme catalytic and proton channeling activities, but also its response to co-occurring effectors. Additionally, they mirror the ambient redox state and the availability of reactive species involved in cell signaling. In short, within the F_1F_O complex, thiols act as chemical interface between the environment and the enzyme function. In this chapter the knowledge on the thiol-related F_1F_O-ATPase modulation is reviewed, with special focus on mammalian mitochondria, aiming at contributing to shed light on a key molecular mechanism under physiological and pathological conditions.

Keywords Cysteine • F_1F_O-ATPase • Mitochondria • Macrolides • Organotins • Post-translational modifications • Thiol oxidation • Thiol reagents

A. Pagliarani (✉) • S. Nesci • F. Trombetti • V. Ventrella
Department of Veterinary Medical Sciences, University of Bologna,
via Tolara di Sopra, 50, 40064 Ozzano Emilia, Bologna, Italy
e-mail: alessandra.pagliarani@unibo.it

S. Chakraborti, N.S. Dhalla (eds.), *Regulation of Ca^{2+}-ATPases,V-ATPases and F-ATPases*, Advances in Biochemistry in Health and Disease 14,
DOI 10.1007/978-3-319-24780-9_21

1 Introduction

The ATP synthase or F_1F_O-ATPase (EC 3.6.3.14) is the key enzyme in cell bioenergetics, due to its main role to convert the transmembrane electrochemical gradient in ATP synthesis, the energy currency of all living organisms. In heterotrophic bacterial membranes as well as in mitochondria, the ATP synthase converts the electrochemical transmembrane gradient built by respiratory complexes into ATP, to satisfy cell energy demand. Bacterial and mitochondrial ATP synthases share the same mushroom-like structure with a bulky cap protruding outside the membrane embedding a cylindric stalk, even if they slightly differ in subunit composition/nomenclature [1]. While in eukaryotes the F_1F_O-ATPase is inserted in the inner mitochondrial membrane by the F_O moiety and protrudes with its hydrophilic portion F_1 in the mitochondrial matrix, the bacterial homologue displays a similar subunit arrangement with F_O embedded in the plasma membrane and F_1 protruding in the cytoplasm. The two sectors F_1 and F_O are connected by a peripheral stalk and a central stalk (γ subunit). In all cases the membrane-bound F_1F_O complex stands at the interface between two aqueous environments with different electrochemical features and performs its catalytic function in the same way. As unique bifunctional enzyme mechanism in biology, under physiological conditions the F_1F_O complex exploits the downhill proton flux from the positive to the negative side of the membrane to drive ATP synthesis from ADP and inorganic phosphate (Pi). Conversely, by acting in the "reverse" mode, the F_1F_O complex exploits the free energy from ATP hydrolysis to pump protons and re-energize the membrane. The "reverse" mode, which leads to ATP waste, is usually associated with oxygen lack as during myocardial ischemia [2]. The two opposite functions of ATP synthesis and hydrolysis imply opposite rotary directions of the two matched sectors F_1 and F_O which, through a complex electromechanical mechanism, rotate clockwise (as viewed from the intermembrane space side) during ATP synthesis and counterclockwise in ATP hydrolysis [3] (Fig. 21.1). The same enzyme complex, in its dimeric form, has been recently involved in cell death, by promoting the mitochondrial permeability transition (MPT) and leading to apoptosis [4–6]. The *c*-ring, which constitutes the core of F_O, would even coincide with the MTP pore [6, 7]. Increasing evidence highlights the F_1F_O-ATPase as key molecular and enzymatic switch between cell life and death. The enzyme complex is very tightly regulated and posttranslational modifications play a relevant role in the enzyme modulation in eukaryotes [8]. In mammals slight differences in the amino acid composition and protein structure can lead to mitochondrial dysfunctions and huge damage to the cell [9]. In recent years, the mitochondrial F_1F_O-ATPase has been involved in neurodegenerative disorders, cardiovascular diseases, and other pathologies [10], stressing its attractiveness in pharmacology as drug target [11] as well as in clinical research.

Among posttranslational modifications, thiol-oxidations are especially suitable to modulate protein function [12]. In turn the thiol redox state mirrors the oxidant status of the cell [13]. Mitochondria per se contain about 15 % of the modified thiols of cellular proteins [8]. As many cellular proteins and the neighbor respiratory chain

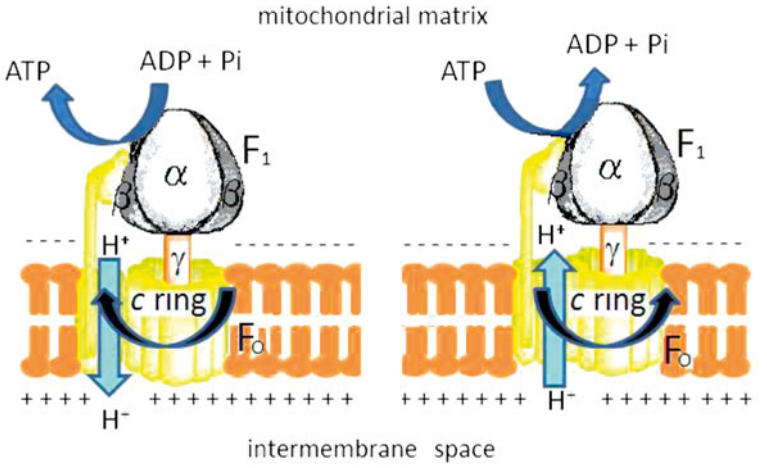

Fig. 21.1 The two opposite functions of the mitochondrial F_1F_O ATP synthase, namely ATP synthesis (*left*) and ATP hydrolysis (*right*). The two functions are associated with opposite H^+ fluxes across the inner mitochondrial membrane, namely downhill and uphill respectively, and opposite directions of rotation of the *c*-ring rotor, in turn transmitted through the central stalk (γ) to the catalytic sector F_1

complexes [12, 14], the mitochondrial F_1F_O-ATPase activity and functioning mode are modulated by thiol redox state [8, 15–17]. Sulfur-containing amino acids such as cysteine (Cys) and methionine (Met) are especially susceptive to oxidation. Of great interest, as widely exploited post-translational modification, is the oxidation of their side chains when they are bound in proteins [18] and especially when these residues contain thiols, long known to react faster than the other amino acid side chains with oxidizing species [13] and to be crucial in biology [19, 20]. Thus, in practice Cys oxidation means oxidation of its thiol (sulfhydrylic) group (–SH), which features its side chain. In most cases, the maintenance of Cys thiol in the reduced form (–SH) is essential for protein structure, since non native disulfide bonds to form Cystine (Cys–Cys) can lead to protein unfolding and inactivation. Accordingly, Cys thiol oxidation as well as mutations involving Cys substitutions has been also exploited to investigate the structural arrangement of mitochondrial ATPase subunits [21].

However, Cys thiol oxidation, initially only considered as detrimental symptom of oxidative damage, soon revealed multiple intriguing facets. Above all there are different modes of reversible and irreversible thiol oxidation associated with different posttranslational modifications [8], in turn often interrelated and involved in a variety of cellular processes. A main Cys role is to sense the redox environment. Accordingly, Cys thiols have been recently defined as nanoswitches to sense microenvironmental effects and modulate enzyme activities in variegated cellular physiological and pathological events [8, 12, 22]. At present, Cys thiols are considered as the major interface between environmental oxidants and cellular signaling pathways [12]. In this chapter the knowledge on the thiol-related modulation of the activity of

key enzyme complex in bioenergetics is reviewed, with special focus on mammalian mitochondria, aiming at contributing to shed light on a molecular mechanism of increasing and widespread impact. We see here that Cys modifications are widely operative in health and disease as well as in the enzyme response to environmental contaminants and drugs.

2 Chemistry and Oxidative Modifications of Cysteine Thiols

2.1 Biological Chemistry of Cys Thiol

Cys is unique among the 20 coded proteinogenic amino acids in having a thiol-containing side chain. This side-chain thiol defines Cys chemical reactivity, which can be synthesized in terms of nucleophilicity, redox activity, and metal binding properties, three features which can also coincide in proteins [23]. Due to its properties, Cys is often among the key catalytic components of enzyme proteins. Thiol is a sulfur analogue of alcohol, but the smaller difference in electronegativity between the sulfur atom and the hydrogen atom makes the S-H bond less polarized than the O-H bond, leading to a poor propensity to form hydrogen bonds. In contrast, thiols are much more acidic than alcohols, due to the weakness of the S-H bond and the possible distribution within sulfur 3d orbitals of the negative charge of thiolate anion ($R\text{-}S^-$) obtained from proton dissociation (Fig. 21.2). In the thiol group, the electron-rich sulfur atom, thanks to its *d* orbitals, can shift to multiple oxidation states (−2 to +4), in turn associated with a variety of post-translational oxidative modifications [8] and also, last but not least, with its metal-binding properties [23]. The thiol/thiolate form (Fig. 21.2) can undergo different reactions featured by a variety of mechanisms such as nucleophilic attack, electron transfer, hydride transfer, hydrogen radical transfer and oxygen atom transfer [23]. Assumed that in

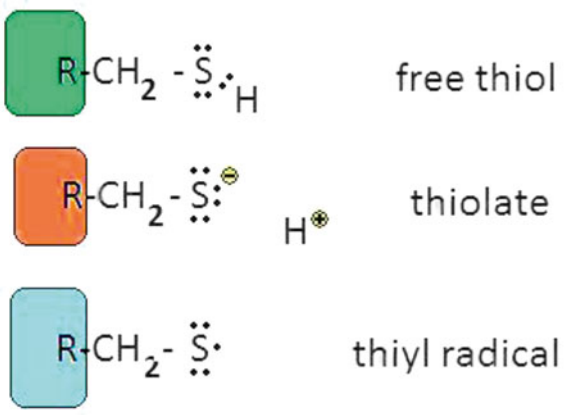

Fig. 21.2 Changes in cysteine sulfur: thiol, thiolate, and thiyl radical as Lewis dot structures

general Cys thiols behave as mild acids, the protein microenvironment can dramatically influence their p*K*a value. As a matter of fact for only partially known reasons not all Cys residues are equally reactive and reactivity most frequently coincides with acidity [8]. While most Cys have p*K*a values between 8 and 9 and are fully protonated under physiological conditions, thus poorly susceptive to oxidation, oxidation-sensitive thiols often have much lower p*K*a values and are deprotonated to form the much more reactive and nucleophilic thiolate. To sum up, the lower is the thiol's p*K*a, the higher is its reactivity. When attacked by two-electron oxidants, such as hydrogen peroxide (H_2O_2), thiolate anions rapidly form sulfenic acids (R-S-OH) and water, according to the reaction:

$$R-SH+HO-OH \rightarrow R-S-OH+H_2O$$

Most sulfenic acids are short-lived intermediates and react with other protein thiols to form disulfide (R-S-S-R′) bonds or with non-protein thiols such as reduced glutathione (GSH) or free Cys to form mixed disulfide bonds [22]. Thiol–disulfide interconversions are long known to play a crucial role in biological systems [20]. In turn sulfenic acids may also react with nearby amino groups yielding cyclic sulfenamides (sulfenylamides) (Fig. 21.3). All these oxidative thiol modifications are fully reversible. Finally, in the presence of strong oxidants such as hydrogen

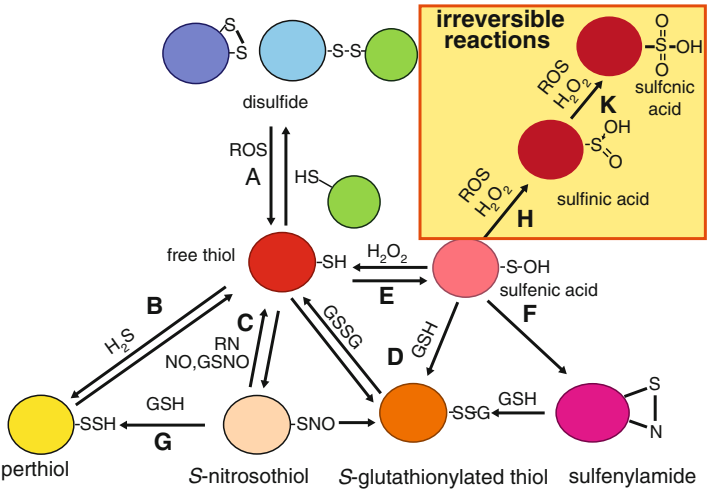

Fig. 21.3 Oxidative modifications on Cys side chains and mutual interrelations, modified and redrawn according to previously depicted models [8, 13, 24]. Disulfide formation (A) can lead to intermolecular (cystine) or intramolecular bonds. Oxidations in the presence of small molecules can lead to perthiolation (B), *S*-nitrosylation (nitrosation) (C), *S*-glutathionylation (D) and production of sulfenic acid (E), which in turn can produce cyclic sulfenylamide (F) or be further irreversibly oxidized to sulfinic (H) and sulfonic acids (K), both in the upper right rectangle. Different Cys modifications on the same protein can yield mixed forms [13], here not shown. Radical intermediates are not shown. ROS, reactive oxygen species; RNS, reactive nitrogen species. Other acronyms are explained in the text

peroxide (H_2O_2), sulfenic acid and sulfenamides can be further oxidized to yield sulfinic ($–SO_2H$) or sulfonic acids ($–SO_3H$) [22], both with a higher oxidation state of sulfur [8] (Fig. 21.3).

2.2 Cysteine Post-translational Modifications

Post-translational Cys modifications, related to the multiple oxidation states of sulfur [23], can be reversible or irreversible. The main pathways are shown in Fig. 21.3. The most common modifications are *S*-nitrosylation (also called *S*-nitrosation) (SNO), sulfhydration (R-SSH), *S*-glutathionylation (RS-SG), disulfide bonds (R-S-S-R′), sulfenylation (R-SOH), and finally sulfinic (R-SO-OH) and sulfonic (RSO_2OH) acid formation which correspond to the highest oxidation state of sulfur [24]. Even if these extreme oxidations can be reversed enzymatically, they are widely considered as irreversible [8]. Some of the reversible post-translational Cys modifications are mutually interchangeable and mediated by small molecules available in the cellular environment such as hydrogen sulfide (H_2S), nitric oxide (NO) [25], and the tripeptide glutathione, both in the reduced form (GSH) and in the oxidized glutathione-disulfide form (GSSG). Accordingly, sulfhydration or perthiolation results into the formation of a persulfide bond in which two sulfur atoms are bound together (R-SSH). S-glutathionylation, which comes from the reaction of GSSG or S-nitrosoglutathione (GSNO) with thiol group via single or dual electron pathways, usually leads to protein functional changes (either inactivation or activation) [13, 26]. It is essential to bear in mind that all these modifications are interconnected. For example, H_2O_2 can convert a thiol to a sulfenic acid, which can be a posttranslational modification itself, or react with GSH to form a *S*-glutathionylated protein or with an adjacent thiol to form a disulfide. Thus, the extent of glutathionylation on a particular mitochondrial thiol can mirror changes in the GSH/GSSG ratio or even occur independently [26]. *S*-glutathionylation, which may protect thiols against oxidative stress and also act as a storage form of GSH, has been involved in cellular signaling [13] and also implicated in several mammalian diseases [8]. Up to now its role in non mammalian organisms is less considered and documented [13]. *S*-nitrosylation (SNO), which can be mediated by nitric oxide (NO) itself, nitrite, S-nitrosothiols such as GSNO or higher N-oxides (NO_x) and also be catalyzed by transition metals [13], is a major signaling pathway by which NO exerts its widespread effects [25]. Even if the mechanism of formation of *S*-nitrosothiols in vivo is still obscure [26], in vitro studies pointed out that *S*-nitrosothiols may be formed through the direct reaction of thiols with dinitrogen trioxide (N_2O_3) and less commonly with NO or by trans-nitrosylation with an NO-donor. NO can directly produce SNO if the thiol residue is in the form of thiyl (cysteinyl) radical (–S•) (Fig. 21.2) [25]. Accordingly, the low redox negative potential of Cys, between −270 and −125 mV in most proteins, allows the rapid electron transfer to produce the thiyl radical [23] by detachment of the H atom from the sulfhydryl group. Under physiological pHs, thiyl radicals are unstable and reactive [8]. However they are quite rare and large amount of SNO are likely to stem from the reaction of thiols/

thiolates with N_2O_3 or directly with nitrosonium ion (NO^+) which can be transferred between different SNO through a reaction defined trans-nitrosation or trans-nitrosylation [25]. The latter results in the NO group transfer from one molecular species to another and can be catalyzed by protein-bound transition metals such as Cu^{2+} or Fe^{2+} in close proximity to a target thiol. GSNO, derived from GSH, is the main non-protein S-nitrosothiol [27]. SNO, which due to its reversibility, is the prototype mechanism of redox signaling, depends on many factors such as environmental hydrophobicity, net charges, hindrance of the Cys-containing microenvironment and oxygen availability [25]. Accordingly, SNOs are relatively unstable modifications and can undergo exchange reactions. *S*-denitrosylation reactions can reduce back to thiol group. There is a complex interplay between oxidative and nitrosative (or nitroxidative) pathways. They represent interconnected facets of the same redox state of the cell involving both reactive oxygen species (ROS) and reactive nitrogen species (RNS). Traditionally, ROS have been strictly associated with oxidative stress, aging and various diseases. However, increasing evidence points out that controlled ROS generation has a key role in intracellular signaling. In particular ROS can react with Cys residues and with NO, limiting its bioavailability and competing with NO for binding to the same Cys [28].

Disulfide bonds, often involved in protein folding and stabilization, may be intermolecular (between two different proteins) or intramolecular (within the same protein). Disulfide formation usually comes from radical reactions, through the highly reactive thiyl radical intermediate, between two adjacent thiols or between sulfenic acid and thiolates [8, 13]. For instance, two thiyl radicals tend to combine forming disulfide bonds [13]. The presence of a disulfide bond imposes conformational rigidity on the protein. The disulfide bond can have either a left- or a right-handed spiral conformation with a dihedral angle of +90 or −90°, respectively [29].

As stated above, sulfenic acids, long considered as deleterious but recently re-evaluated for their essential role in signaling, are also highly unstable and reactive and in turn can lead to other reversible post-translational modifications such as *S*-glutathionylation and disulfide bond formation, which could protect sulfur against further oxidation, or irreversibly lead to sulfinic and sulfonic acids [8].

Increasing evidence suggests that the reversible modification of Cys thiols plays a key role in redox regulation and signaling, while irreversible modifications lead to cell damage and death [30]. However the whole pattern is quite complicated and the danger of oversimplification is behind the corner. Accordingly, since most post-translational *S*-modifications are interchangeable, not only irreversible *S*-modifications but also reversible reactions under certain conditions can lead to protein unfolding, misfolding, or aggregation and produce damage [27].

2.3 Factors Affecting Cys Reactivity

It is clear that not all Cys behave the same way. In other words, Cys susceptibility to redox changes is highly affected by the molecular environment. Neighboring amino acid residues can vary Cys thiol's p*K*a from 3.5 to 10.0. Of course, the lower

is the p*K*a, the easier is proton dissociation to yield the thiolate anion ($–S^-$). The latter bears a negative charge and is stabilized by positively charged residues or protonated (neutral) acid residues and *vice versa* destabilized by negative side chains [8]. Therefore, a cationic environment makes Cys thiols especially susceptive to *S*-glutathionylation. Additionally other factors such as helix-dipole effects, and hydrogen bonding of Cys residues which charged side chains of Ser or His are thought to lower the Cys p*K*a. Cys susceptible to SNO are most frequently located between an acidic and a basic amino acid and require a consensus motif [28]. Also adjacent aromatic residues can favor SNO [13]. Therefore changes in the adjacent amino acids, due to mutations or posttranslational modifications, can substantially and selectively modify the p*K*a of individual Cys thiols and alter their reactivity. Other than thiol p*K*a, steric factors, local hydrophobicity and other still unknown factors may contribute to determine the accessibility and reactivity of a specific thiol [8, 26]. Additionally, since the pH of the mitochondrial matrix is higher than that of the cytosol (7.8–8.0 against 7.2), free thiols may be up to sixfold more reactive in mitochondria than in the cytosol [26]. If not all Cys are equally prone to oxidative post-translational modifications, even the stability of thiol modifications is in turn modulated by different variables. The stability of SNO is favored by low oxygen concentrations, while thiolate formation increases at increasing oxygen concentrations. SNO is tightly regulated both at the level of formation and decomposition of S–NO bonds. In turn denitrosylating enzymes are coupled to cellular antioxidant redox systems [28]. Moreover SNO can promote or inhibit the formation of disulfide bonds within or between proteins, depending on thiol proximity and orientation. The influence of one kind of oxidative post-translational modification of Cys on another one is dictated by changes in protein conformation that alter the electrostatic environment, hydrophobicity, contiguity and orientation of aromatic side chains and the proximity of target thiols to transition metals which act as catalyst or redox centers [27].

Structural alterations produced by thiol mediated modifications such as glutathionylation, disulfide formation or SNO can potentially have a great or moderate impact on protein function, mainly depending on the Cys localization and role. However, up to now in only a few cases have detailed structural analyses clearly depicted the molecular mechanism involved [26].

3 Thiols in the Mitochondrial F_1F_O-ATPase

Bacterial F_OF_1 ATP synthase contain less Cys than the mitochondrial enzyme and these Cys are apparently not essential for the enzyme functions. Accordingly, when in *Escherichia coli* isolated membranes all the 21 native Cys were replaced by alanines its functionality was fully maintained [31]. Post-translational modifications are poorly documented in bacteria and probably confined to some proteins and species [13].

Conversely, the mitochondrial F_OF_1 ATP synthase is a hot spot for oxidative post-translational modifications involving thiols. As far as we are aware, only few Cys residues have been identified as susceptive to oxidative post-translational modifications and usually the same thiols can undergo multiple modifications [8]. The hydrophilic catalytic sector F_1 is a hexamer which consists of three α subunits alternated with three β subunits [1]. In mammalian F_1 ATP synthase only α and γ subunits contain Cys: two in α and one in γ subunit (the central stalk). In detail the Cys at the interface between α and β subunits is close to the glycine-rich loop and is a suitable candidate for SNO. These Cys modifications may affect subunit interaction and/or promote conformational changes that affect the F_1F_O-ATPase activity [8].

Oxidative stress features many cardiovascular diseases [30]. During heart failure the α subunit of F_1 forms disulfide bonds between Cys294 on neighboring α subunits as well as between Cys294 and Cys103 on γ-subunit. The same Cys294 can also be *S*-glutathionylated and *S*-nitrosylated. The formation of disulfide bonds and RS-SG at these regulatory sites inhibits the ATPase activity, thus suggesting that these bonds trigger conformational changes in the enzyme structure which prevent its catalytic activity. Pharmacological manipulations of oxidative and nitrosative pathways are known to be beneficial in patients with heart failure [28]. Moreover, an adequate resynchronization therapy has been reported to reverse the disulfide bond formation and replace it by SNO, resulting in the recovery of the ATPase activity. According to the authors [8], the cardiac resynchronization therapy is likely to stimulate the mitochondrial antioxidant defense systems or enhance the reducing status in the molecular environment. Reversible Cys oxidations may protect against permanent oxidative damage to the ATPase which would lower ATP production [8]. On the other hand, during heart failure the ATPase inhibition would have positive implications by limiting ATP consumption, contributing to ATP homeostasis and reducing the mitochondrial membrane potential ($\Delta\psi$) and consequently the driving force for Ca^{2+} uptake [32].

According to an intriguing model, Cys294 in the α subunit of the F_1F_O-ATPase, localized on the enzyme surface and surrounded by several basic amino acids residues, works as a redox switch. Under physiological conditions it is probably deprotonated and susceptive to oxidants. Most likely, at first Cys294 is oxidized to sulfenic acid, thus causing conformational changes which in turn expose other side chains such as Cys103 of γ subunit. When *S*-glutathionylated or involved in disulfide bonds between two Cys in adjacent α subunits as well as between Cys294 and Cys103 of the γ subunit, these cross-links block the enzyme activity and inhibit ATP production. It seems reasonable to think that under such conditions the enzyme cannot rotate to perform its catalytic activity. The therapy would stimulate the cellular antioxidant efficiency. As a result, disulfide bonds break, thus favoring SNO, which is apparently compatible with the catalytic activity of the enzyme [8]. Thus, this single modifiable Cys in the F_1F_O complex can act as a redox modulator of cellular ATP concentration [33].

However, since an increase in SNO of α_1 subunits of F_1 causes a dose-dependent decrease of the enzyme activity in GSNO-treated cardiomyocytes [25] and SNO inhibits the ATPase activity during ischemia/reperfusion [28], it seems reasonable

to conclude that SNO effects on the catalytic activity of the F_1F_O complex may depend on the targeted Cys and many other variables, most of which are still to be defined. It is not clear if SNO under some conditions can also lead to S-glutathionylation [30].

If F_1 thiols are sufficiently known and documented, thiols in the F_O sector are only partially known. There is a set of thiol or dithiol groups of Fo long known to be involved in the coupling mechanism between F_O and F_1 [34]. F_1 was claimed to protect F_O against oxidation. Subunit b of F_O, which is essential for binding F_1 to F_O, contains only one Cys residue [35]. As illustrated in Fig. 21.4, the *c* subunits of the mitochondrial F_1F_O complex contain conserved Cys residues which are absent in the homologous bacterial enzyme [17]. Each *c* subunit has a hairpin-like structure with the N-terminal α-helix which protrudes towards the center of the *c*-ring and the C-terminus transmembrane α-helix which constitutes the external annulus of the cylinder [1]. After the loss of the transit peptide, which transports the nuclearly encoded *c* subunit to mitochondria, the unique Cys in the mature *c*-subunit is close to the proton binding site, which contains a carboxyl group from Glu or Asp and is approximately at the midpoint of C-terminal region of the hairpin (Fig. 21.4). Interestingly, a single-amino acid mutation in *Saccharomyces cerevisiae* strains (Cys65Ser) in the C-terminal α-helix of *c* subunit, induces oligomycin-resistance [36].

4 Thiol Oxidation in the Mitochondrial F_1F_O Complex Induced by Xenobiotics

Due to the nucleophilic properties of thiol sulfur, some electrophilic groups from exogenous compounds can easily bind to thiols and modulate the activity of the F_1F_O complex. Additionally, the unique metal binding ability of Cys sulfur allows the thiolate to act as monodentate or bidentate ligand to bind metal ions, thus producing different oxidized forms, resulting in very diverse structures with the same metal [24].

4.1 Thiol Reagents

A wide definition of thiol reagent is that of a reagent which modifies the native redox state of thiols. A huge variety of organic compounds is known to inhibit the catalytic activity of the F_1F_O complex by modifying Cys residues. Most of these thiol reagents are currently employed for research purposes, other compounds are almost exclusively used in therapy. Some of them act selectively on different F_1F_O complexes and in some cases produce different effects on catalysis and proton conductance, thus indicating they target different Cys thiols. Other reagents have quite broad and aspecific targets. The structures of the most common thiol reagents are

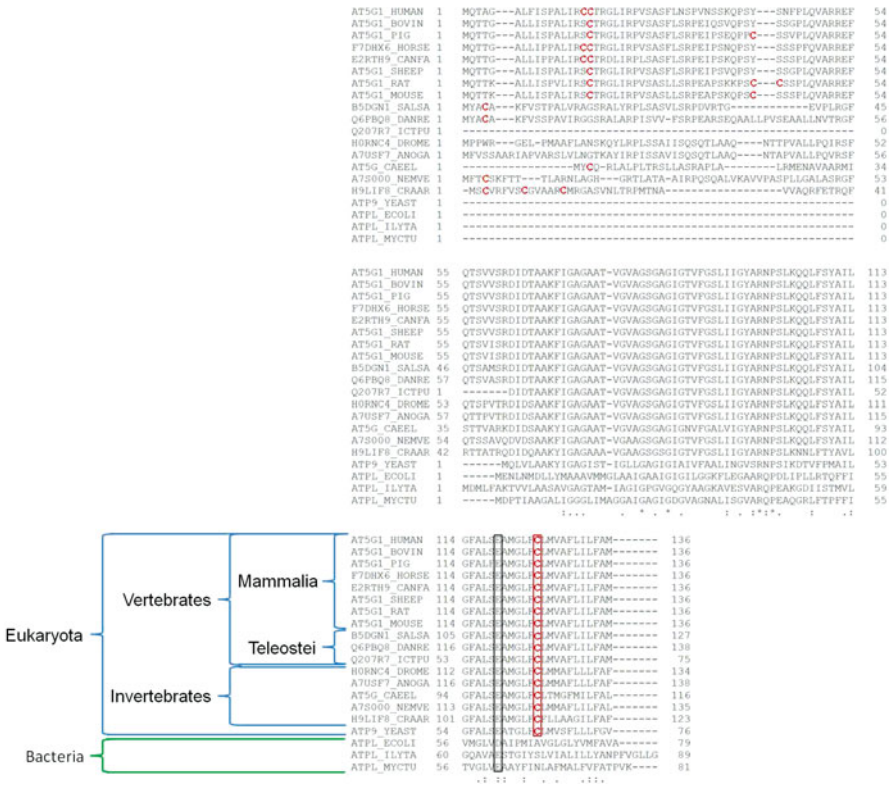

Fig. 21.4 Multiple sequence alignment for *c* subunit of the F_1F_O-ATP synthase in eukaryotic and bacterial species. Entry names of protein sequences: AT5G1_HUMAN *Homo sapiens* (Human): AT5G1_BOVIN *Bos taurus* (Bovine); AT5G1_PIG *Sus scrofa* (Pig); F7DHX6_HORSE *Equus caballus* (Horse); E2RTH9_CANFA *Canis familiaris* (Dog); AT5G1_SHEEP *Ovis aries* (Sheep); AT5G1_RAT *Rattus norvegicus* (Rat); AT5G1_MOUSE *Mus musculus* (Mouse); B5DGN1_SALSA *Salmo salar* (Atlantic salmon); Q6PBQ8_DANRE *Danio rerio* (Zebrafish); Q207R7_ICTPU *Ictalurus punctatus* (Channel catfish); H0RNC4_DROME *Drosophila melanogaster* (Fruit fly); A7USF7_ANOGA *Anopheles gambiae* (African malaria mosquito); AT5G_CAEEL *Caenorhabditis elegans*; A7S000_NEMVE *Nematostella vectensis* (Starlet sea anemone); H9LIF8_CRAAR *Crassostrea ariakensis* (Suminoe oyster); ATP9_YEAST *Saccharomyces cerevisiae* (Baker's yeast); ATPL_ECOLI *Escherichia coli* (strain K12); ATPL_ILYTA *Ilyobacter tartaricus*; ATPL_MYCTU *Mycobacterium tuberculosis* (strain ATCC 25618/H37Rv). All cysteines are in red. In the C-terminal region the *red rectangular shape* embraces the highly conserved Cys close to the acidic residue (*black rectangle*) which binds protons

illustrated in Fig. 21.5. Specifically, *N*-ethylmaleimide (NEM), a cyclic imide of maleic acid, irreversibly inhibits the ATPase activity of F_1 from fungi, some bacteria and yeasts, while it has no effect on *E. coli* and bovine heart mitochondria [10]. NEM forms a strong thioether bond by selectively reacting with isolated Cys thiols [15], preferentially in the thiolate form, in the pH range 6.5–7.5. Therefore NEM sensitive thiols are believed to lie in a polar aqueous environment. Other than binding to F_1, NEM also binds to various Cys in F_O, such as peripheral Cys in the *a* subunit, and inhibits proton flux [37].

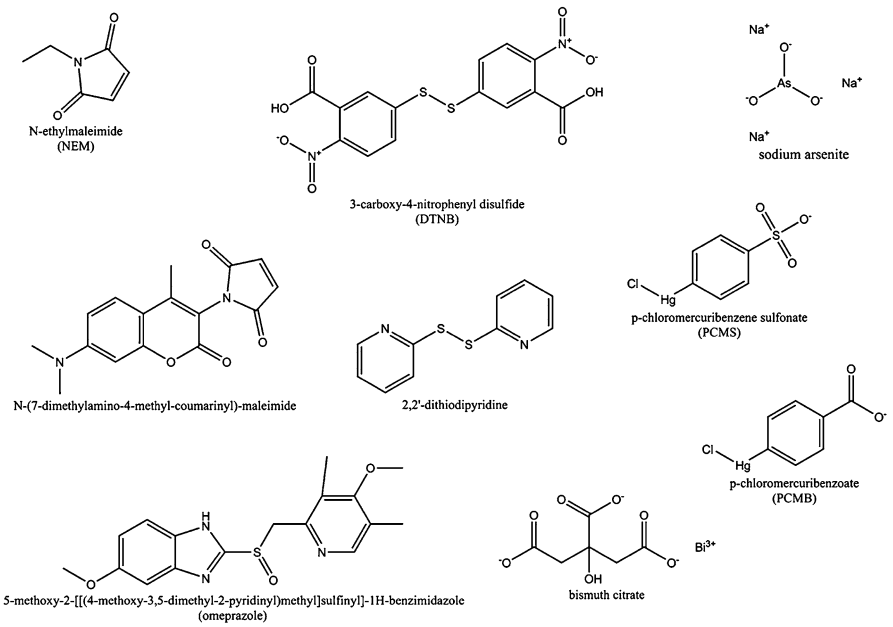

Fig. 21.5 Structures of commonly employed thiol reagents

The antiulcer drugs bismuth subcitrate and omeprazole bind to thiol groups of F_1 from *Helicobacter pylori* and form stable complexes, but the reaction can be reversed by GSH. At low pH, omeprazole forms a cyclic sulfonamide, a more powerful inhibitor of F_1 [10].

5,5′-Dithiobis(2-nitrobenzoic acid) (DTNB) only inhibits the ATPase activity of F_1 in the absence of adenylic nucleotides [10]. Due to its selective covalent binding to thiols, DTNB in Ellman's reagent was the early reagent widely used for estimating the number of thiol groups. To this aim an increasing variety of thiol-binding compounds have been built [29].

The high affinity of mercury for sulfur, causing an efficient binding to Cys residues in proteins, which perturbs their functions, is a main cause of mercury toxicity. Accordingly, historically thiols were also called mercaptans from the Latin "mercurium captans," namely "able to bind mercury." Polar organic mercurials such as *p*-chloromercuribenzoate (PCMB), *p*-chloromercuribenzene sulfonate (PCMS) and mersalyl acid target F_O [10]. Both PCMB and PCMS inhibit the ATP synthesis and ATPase activities of bovine heart ATP synthase by targeting different thiols from NEM and such inhibition can be partially reversed by dithiothreitol (DTT) which protects thiol groups. Mersalyl acid, long known as a diuretic, is much more effective than PCMB and PCMS in blocking proton conductivity by F_O from bovine heart mitochondria. The sulfhydryl-reactive agents 2,2′-dithiobispyridine and *N*-(7-dimethylamino-4-methyl-coumarinyl)-maleimide also inhibit proton conductivity by F_O from bovine heart mitochondria [10].

Trivalent arsenic species, including inorganic and organic arsenic compounds, are known to have high affinity for the thiol groups. As(III)-containing compounds exist as trigonal pyramidal structures which are maintained upon binding of arsenic ions to cellular proteins in vivo where the sulfur atoms of thiolate groups act as coordinating ligands. The resulting arsenic-thiol linkages are mainly responsible for arsenic toxicity [38]. Arsenic-containing compounds can react with monothiols and dithiols. The inorganic salt sodium meta-arsenite, primarily used as pesticide, and its organic derivatives preferentially bind to vicinal thiols [15, 39] through the trivalent arsenic to form stable complexes.

4.2 Metals and Organometals

Other than mercury, other heavy metals can easily bind thiols and some of them are known to affect the mitochondrial F_1F_O complex. The capability of Cys to chelate heavy metals such as Ag^+ and Cd^{2+} has been exploited to investigate the function and localization of specific Cys or mutated Cys in the whole F_1F_O machinery. Accordingly, if the metal binding to Cys simply blocks proton translocation, then function can be restored by thiol reagents upon removal of the blocking metal. The thiolates of the reduced forms of these thiol reagents compete with protein Cys residues for the Ag^+ or Cd^{2+} ions causing the inhibition. Conversely, when the metal binding disrupts the interactions between F_O and F_1 causing the uncoupling of proton flux to the catalytic activity, the effect is irreversible [40].

In general organometals are membrane-active toxicants because they match the lipophilicity of the organic moiety which allows their penetration in the hydrophobic membranous sectors of the enzyme to a metal core which enables chelation, most commonly by thiols [41]. The action mechanisms of some organomercury compounds (mercurials), widely exploited to explore Cys thiols, are considered in Sect. 4.1.

Both in mammals and in invertebrates [41–43], the mitochondrial F_1F_O-complex is highly susceptive to the environmental pollutant tributyltin (TBT), long known as mitochondrial poison as other trisubstituted organotin species [41]. The interaction with TBT causes a dramatic inhibition of the enzyme activity [44]. The effects on the enzyme are related to the capability of the enzyme complex to bind TBT. Recent studies from our lab pointed out that there are at least two different enzyme sites able to bind the pollutant: a high affinity site, presumptively hydrophobic and main responsible for the inhibition of the catalytic activity, and a thiol-containing low-affinity site [15]. The latter exploits the metal binding properties of Cys sulfur to bind TBT. When TBT binds covalently to biomolecules, it may onset various geometrical arrangements. It generally maintains its tetrahedral arrangement if the Sn(IV) binds to single atoms such as sulfur of isolated thiol groups. Alternatively, if TBT binds to two or three nucleophilic ligands, it forms a trigonal bipyramidal pentacoordinate complex or an octahedral hexacoordinate complex [41]. In the presence of vicinal thiols (dithiols) the central tin may form a S-Sn-S bridge after

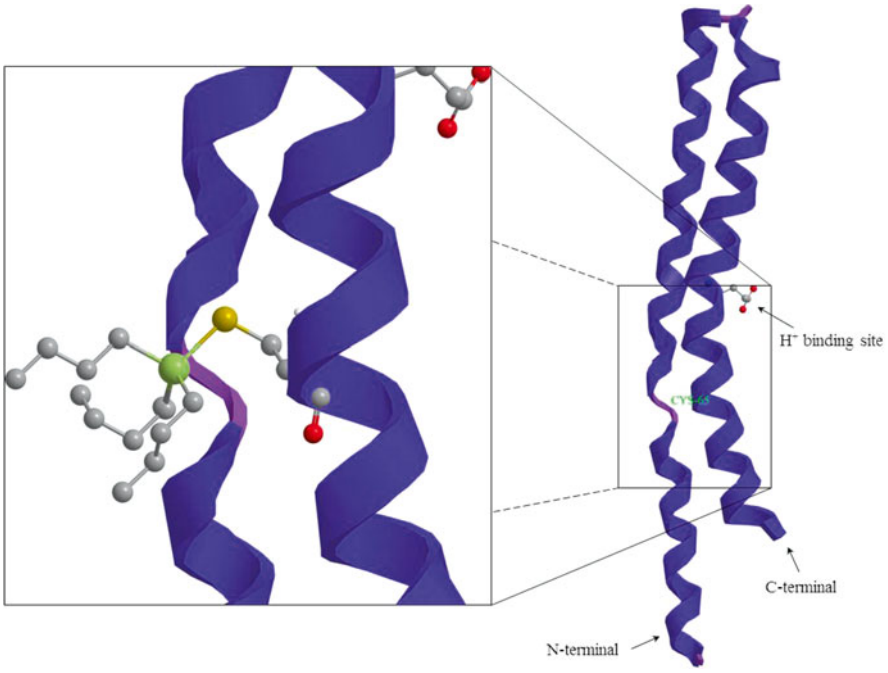

Fig. 21.6 Model of the TBT binding to the low affinity site on *c* subunit. The hairpin-shaped *c* subunit is in violet; the tin atom (*green*) is bound to sulfur (*yellow*), most likely of Cys65. Carbon atoms are in *gray*, oxygen atoms are in *red*

debutylation and the dealkylated toxicant may rearrange in a distorted tetrahedral structure bound to the protein [45]. When TBT at micromolar concentrations interacts with the mitochondrial F_1F_O-complex, it binds to the low-affinity site within F_O, likely localized on *c* subunits at the a/*c* interface. TBT acts as electrophile and oxidizes the cysteine thiols, namely it changes R-SH to R-S-Sn by the onset of a covalent tin-sulfur bond [46]. Within the *c* subunit amino acid sequence, the unique Cys hypothesized as candidate to provide suitable thiol group for TBT binding is highly conserved in eukaryotic ATP synthases (Fig. 21.4) and absent in the prokaryotic proteolipid. It seems reasonable to think that the binding of TBT to Cys through tin-sulfur bond (Fig. 21.6) would alter the interhelical packing of *c* subunit, thus destabilizing a common binding site of macrolide drugs [16]. Accordingly, TBT binding strikingly decreases the enzyme sensitivity to its selective inhibitor oligomycin, as shown by an impressive increase in the oligomycin-insensitive ATPase activity at higher than 1 μM TBT concentrations. In detail, the tin-sulfur bond would promote conformational changes within F_O which modify the oligomycin-blocked F_O conformation, which prevents proton flux within F_O, allowing proton translocation recovery [16]. As proton conduction is essential for both ATP synthesis and ATP hydrolysis, this mechanism allows the recovery of the catalytic activity of the enzyme even in the presence of powerful F_O inhibitors which block proton pathway.

The removal of oligomycin inhibition of the F_1F_O complex is a peculiar feature of TBT [47], tightly related to its structural features and its capability to bind thiols, and it is not shared by other butyltins [48].

4.3 Macrolide Antibiotics

The F_1F_O sensitivity to oligomycin and other macrolide inhibitors is modulated by the redox state of some Cys thiols of F_O. Accordingly, some macrolide antibiotics and other antimicrobial drugs specifically bind to the *c*-ring, thus blocking ion translocation through F_O which is essential for both ATP synthesis and ATP hydrolysis. Once bound to F_O, probably through different binding sites on a common binding region, the macrolide antibiotics oligomycin, venturicidin and bafilomycin inhibit the catalytic activity of the F_1F_O complex. Conversely, if crucial cysteine thiols in the *c*-subunits, highly conserved among vertebrates and absent in bacteria, are oxidized, the common drug binding site of the enzyme is somehow destabilized, thus weakening the enzyme–drug interactions and making the F_1F_O complex refractory to the drug. This effect is unrelated to the occurrence of ROS [16, 17]. As far as we are aware, it is not known if other thiol-binding xenobiotics, other than TBT, can exert the same enzyme desensitization to macrolide inhibitors. However, once established that the F_1F_O-ATPase can be exploited as drug target to counteract cancer and other diseases [49], the possibility of switching on and off specific thiols within the enzyme complex by pharmacological manipulations, could significantly implement the available therapeutic tools to fight pathogens [17].

5 Conclusions

The oxidation of Cys thiols on the mitochondrial F_1F_O-ATP synthase is a powerful tool to modulate the enzyme catalytic activity, proton channeling function and response to xenobiotics. In a few words, the redox state of Cys thiols really constitutes a sort of chemical interface between the cell environment and the mitochondrial enzyme function. The involvement of Cys thiols of the mitochondrial F_1F_O complex in health and diseases stimulates efforts to clarify some still unsolved questions. Accordingly, the Cys role in the enzyme machinery is not fully clarified yet and that of post-translational modifications of the F_1F_O complex under physiological and pathological conditions is merely at the embryo stage. In the next future, the definition of the relationship between post-translational modification of thiols and effects on the structure and functionality of the key enzyme in bioenergetics is an intriguing challenge for researchers to improve life quality.

Acknowledgement Work financed by RFO (Fundamental and Oriented Research) grant from the University of Bologna, Italy.

References

1. Walker JE (2013) The ATP synthase: the understood, the uncertain and the unknown. Biochem Soc Trans 41:1–16
2. Grover GJ, Malm J (2009) Pharmacological profile of the selective mitochondrial F_1F_O ATP hydrolase inhibitor BMS-1999264 in myocardial ischemia. Cardiovasc Ther 26:287–296
3. Watanabe R, Noji H (2013) Chemomechanical coupling mechanism of F_1-ATPase: catalysis and torque generation. FEBS Lett 587:1030–1035
4. Giorgio V, Von Stockum S, Antoniel M et al (2013) Dimers of the mitochondrial ATP synthase form the permeability transition pore. PNAS 110:5887–5892
5. Bonora M, Wieckowski MR, Chinopoulos C et al (2014) Molecular mechanisms of cell death: central implication of ATP synthase in mitochondrial permeability transition. Oncogene 34(12):1608
6. Morciano G, Giorgi C, Bonora M et al (2015) Molecular identity of the mitochondrial permeability transition pore and its role in ischemia/reperfusion injury. J Mol Cell Cardiol 78:142–153
7. Alavian KN, Beutner G, Lazrove E et al (2014) An uncoupling channel within the c-subunit ring of the F_1F_O ATP synthase is the mitochondrial permeability transition pore. PNAS 111:10580–10585
8. Chung HS, Wang SB, Venkatraman V et al (2013) Cysteine oxidative posttranslational modifications: emerging regulation in the cardiovascular system. Circ Res 112:382–392
9. Johnson JA, Ogbi M (2011) Targeting the F_1F_O ATP Synthase: modulation of the body's powerhouse and its implications for human disease. Curr Med Chem 18:4684–4714
10. Hong S, Pedersen PL (2008) ATP synthase and the actions of inhibitors utilized to study its roles in human health, disease, and other scientific areas. Microbiol Mol Biol Rev 72(4):590–641
11. Sakthivel S (2012) ATP-ase as a potential drug target for cancer, tumor growth and cellular functions. Int J Hum Genet 12:151–156
12. Drose S, Brandt U, Wittig I (2014) Mitochondrial respiratory chain complexes as sources and targets of thiol-based regulation. Biochim Biophys Acta 1844:1344–1354
13. Dalle-Donne I, Rossi R, Colombo G et al (2009) Protein *S*-glutathionylation: a regulatory device from bacteria to humans. Trends Biochem Sci 34:85–95
14. Nesci S, Ventrella V, Trombetti F, Pirini M, Pagliarani A (2011) Tributyltin (TBT) and mitochondrial respiration in mussel digestive gland. Toxicol in Vitro 25:951–959
15. Nesci S, Ventrella V, Trombetti F et al (2014) The mitochondrial F_1F_O-ATPase desensitization to oligomycin is due to thiol oxidation. Biochimie 97:128–137
16. Nesci S, Ventrella V, Trombetti F et al (2014) Thiol oxidation is crucial in the desensitization of the mitochondrial F_1F_O-ATPase to oligomycin and other macrolide antibiotics. Biochim Biophys Acta 1840:1882–1891
17. Nesci S, Ventrella V, Trombetti F et al (2014) Thiol oxidation of mitochondrial F_O-*c* subunits: a way to switch off antimicrobial drug targets of the mitochondrial ATP synthase. Med Hypotheses 83:160–165
18. Drazic A, Winter J (2014) The physiological role of reversible methionine oxidation. Biochim Biophys Acta 1844:1837–1382
19. Haugaard N (2000) Reflections on the role of thiol groups in biology. Ann N Y Acad Sci 899:148–158
20. Leichert LI, Jakob U (2004) Protein thiol modifications visualized *in vivo*. PLoS Biol 2, e333. doi:10.1371/journal.pbio.0020333
21. Velours J, Poumard P, Soubonnier V et al (2000) Organization of the yeast ATP synthase F_O: a study based on cysteine mutants, thiol modifications and cross-linking reagents. Biochim Biophys Acta 1458:443–456
22. Groitl B, Jakob U (2014) Thiol based redox switches. Biochim Biophys Acta 1844:1335–1343

23. Giles NM, Watts AB, Giles GI et al (2003) Metal and redox modulation of cysteine protein function. Chem Biol 10:677–693
24. Chang AHK, Sancheti H, Garcia J et al (2014) Respiratory substrates regulate *S*-nitrosylation of mitochondrial proteins through a thiol-dependent pathway. Chem Res Toxicol 27:794–804
25. Di Giacomo G, Rizza S, Montagna C et al (2012) Established principles and emerging concepts on the interplay between mitochondrial physiology and *S*-(de)nitrosylation: implications in cancer and neurodegeneration. Int J Cell Biol 2012, Article ID 361872, 20p doi: 10.1155/2012/361872
26. Murphy MP (2012) Mitochondrial thiols in antioxidant protection and redox signaling: distinct roles for glutathionylation and other thiol modifications. Antiox Red Sign 16:476–485
27. Hess DT, Matsumoto A, Kim AO et al (2005) Protein *S*-nitrosylation: purview and parameters. Nat Rev 6:150–166
28. Schulman I, Hare JM (2012) Regulation of cardiovascular cellular processes by *S*-nitrosylation. Biochim Biophys Acta 1820:752–762
29. Trivedi MV, Lawrence S, Siahaan JJ (2009) The role of thiols and disulfides in protein chemical and physical stability. Curr Protein Pept Sci 10:614–625
30. Zweier JL, Chen CA, Talukder H (2011) Cardiac resynchronization therapy and reverse molecular remodelling: importance of mitochondrial redox signalling. Circ Res 109:716–719
31. Kuo PH, Ketchum C, Nakamoto RK (1998) Stability and functionality of cysteine-less F_OF_1-ATP synthase from *Escherichia coli*. FEBS Lett 426:217–220
32. Sun J, Murphy E (2010) Protein *S*-nitrosylation and cardioprotection. Circ Res 106:285–296
33. Wang SB, Murray CI, Chung HS et al (2013) Redox regulation of mitochondrial ATP synthase. Trends Cardiovasc Med 23:11–18
34. Yagi T, Hatefi Y (1987) Thiols in oxidative phosphorylation: thiols in the F_O of ATP synthase essential for the ATPase activity. Arch Biochem Biophys 254:102–109
35. Lippe G, Dabbeni-Sala F, Sorgato K (1988) ATP synthase from beef heart mitochondria. Role of the thiol group of the 25-KDa subunit of F_O in the coupling mechanism between F_O and F_1. J Biol Chem 263:18627–18634
36. Sebald W, Wachter E, Tzagoloff A (1979) Identification of amino acid substitutions in the dicyclohexylcarbodiimide-binding subunit of the mitochondrial ATPase complex from oligomycin-resistant mutants of *Saccharomyces cerevisiae*. Eur J Biochem 100:599–60
37. Fillingame RH, Angevine CM, Dmitriev OY (2003) Mechanism of coupling proton movements to *c*-ring rotation in ATP synthase. FEBS Lett 555:29–34
38. Spuches AM, Kruszyna G, Rich AM et al (2005) Thermodynamics of the As (III)-thiol interactions: arsenite and monomethyl arsenite complexes with glutathione, dihydrolipoic acid and other thiol ligands. Inorg Chem 44:2964–2972
39. Baqui TK, Ghosh M, Datta AK (1996) Two conformationally vicinal thiols at the active site of *Leishmania donovani* adenosine kinase. Biochem J 316:439–445
40. Steed PR, Fillingame RH (2014) Residue in the polar loop of subunit *c* in Escherichia coli ATP synthase function in gating proton transport to the cytoplasm. J Biol Chem 289:2127–2138
41. Pagliarani A, Nesci S, Trombetti F et al (2010) Chapter 6: Organotin effects on membrane-bound ATPase activities". In: Chin HF (ed) Organometallic compounds: preparation, structure and properties. Nova Science Publishers Inc, New York NY, pp 225–253. ISBN 978-1-60741-917-4
42. Nesci S, Ventrella V, Trombetti F et al (2011) Multisite TBT binding skews the inhibition of oligomycin on the mitochondrial Mg-ATPase in *Mytilus galloprovincialis*. Biochimie 93:1157–1164
43. Nesci S, Ventrella V, Trombetti F et al (2012) Tri-*n*-butyltin binding to a low-affinity site decreases the F_OF_1–ATPase sensitivity to oligomycin in mussel mitochondria. Appl Organomet Chem 26:593–599
44. Pagliarani A, Bandiera P, Ventrella V et al (2008) Tributyltin (TBT) inhibition of oligomycin-sensitive Mg-ATPase activity in mussel mitochondria. Toxicol in Vitro 22(4):827–836
45. Buck-Koehntop B, Porcelli F, Lewin JL et al (2006) Biological chemistry of organotin compounds: Interactions and dealkylation by dithiols. J Organomet Chem 691:1748–1755

46. Munguia T, Cervantes-Lee F, Parkànyi L et al (2006) Organotin-sulfur intramolecular interactions: an overview of current and past compounds and the biological implications of SneS interactions, in: Modern Aspects of Main Group Chemistry. ACS Publications, pp. 422e435 (Chapter 30)
47. Pagliarani A, Nesci S, Ventrella V (2013) Modifiers of the oligomycin sensitivity of the mitochondrial F_1F_O-ATPase. Mitochondrion 13:312–319
48. Nesci S, Ventrella V, Pagliarani A (2013) Modulation of F_1F_0-ATPase function by butyltin compounds. Appl Org Chem 27:199–205
49. Ahmad Z, Okafor F, Azim S et al (2013) The ATP synthase: a molecular therapeutic drug target for antimicrobial and antitumor peptides. Curr Med Chem 20:1956–1957

Chapter 22
F_1F_0-ATPase Functions Under Markedly Acidic Conditions in Bacteria

Yirong Sun

Abstract ATP synthase (F_1F_0-ATPase), consisting of a water-soluble F1 portion and a transmembrane FO portion, is present in bacterial cytoplasmic membranes and the inner membranes of mitochondria and chloroplasts. This enzyme plays a central role in biological energy transduction. F_1F_0-ATPase is bifunctional, being involved in ATP synthesis and hydrolysis. When bacteria are subjected to specific environmental challenges, F_1F_0-ATPase changes its operation to overcome the challenges. F_1F_0-ATPase synthesizes ATP using energy released from proton movement in oxidative phosphorylation under aerobic conditions at a near-neutral pH. This enzyme exports protons coupled with ATP hydrolysis as a reverse reaction in some specific environments. Recent research has indicated that F_1F_0-ATPase plays an important role in bacterial survival in markedly acidic environments. In this chapter, the roles of F_1F_0-ATPase in bacteria subjected to marked acidic stress are discussed.

Keywords F_1F_0-ATPase • ATP synthesis • pHi regulation • Survival at acidic pH

1 Introduction

F_1F_0-ATPase is present in bacterial cytoplasmic membranes and the inner membranes of mitochondria and chloroplasts. It is a well-established proton transporter in cell membranes [1]. This enzyme is ubiquitous, as the basic structure and mechanism are conserved throughout the biological kingdom. It comprises two sub-complexes referred to as F_1 and F_O [2, 3]. The hydrophilic membrane-associated F1 portion houses the catalytic sites and consists of α, β, γ, δ, and ε subunits at a ratio of 3:3:l:l:l [4]. The hydrophobic membrane-integrated part (F_O) has three subunits, a, b, and c, at a ratio of 1:2:6–15 [5]. Another report suggested that the copy number of the c subunit is 10–15 [6].

Y. Sun (✉)
Guangzhou Institutes of Biomedicine and Health, Chinese Academy of Sciences Guangzhou, 190 Kaiyuan Road, Science Park, Guangzhou 510530, P. R. China
e-mail: sunyr1206@163.com

S. Chakraborti, N.S. Dhalla (eds.), *Regulation of Ca^{2+}-ATPases,V-ATPases and F-ATPases*, Advances in Biochemistry in Health and Disease 14,
DOI 10.1007/978-3-319-24780-9_22

F_1F_0-ATPase is bifunctional, catalyzing ATP synthesis and hydrolysis. This enzyme uses the energy released from proton movement across cell membranes for the generation of ATP from ADP and Pi under aerobic conditions at a near-neutral pH [7]. When bacteria are subjected to specific environmental stress, such as acidic conditions and hypoxia, F_1F_0-ATPase transports protons across membranes coupled with ATP hydrolysis as a reverse reaction [7]. In this chapter, the recent findings concerning the roles of F_1F_0-ATPase under markedly acidic conditions are summarized, and the possible mechanisms are discussed.

2 Bacterial Resistance to Markedly Acidic Environments

Since the normal human stomach averages a pH of 2 for approximately 2 h after it becomes empty, both commensal and enteric bacteria have to develop a mechanism to protect themselves against acidic stress. Although many neutrophils are unable to grow in extremely acidic environments, they can survive for a certain period under such harsh conditions, and hence they can pass through the stomach without the loss of viability. Examples of such microorganisms are *Salmonella typhimurium*, *Vibrio cholerae*, pathogenic *Escherichia coli* (*E. coli*), *Yersinia enterocolitica*, and *Helicobacter* [8].

The main mechanism for survival under acidic conditions is now thought to be the maintenance of a cytoplasmic pH (pHi) at around 5 [9], and several systems for such maintenance have been proposed.

A large number of systems for achieving resistance against acidic stress have been reported in *E. coli* and *Salmonellae* [9]. It has been suggested that acid resistance system 1 (AR1), one of the major systems proposed to date, is induced in cells grown to a stationary growth phase in moderately acidic medium, and requires the sigma factor RpoS [10] and the cyclic AMP receptor protein CRP [11], but its mechanism remains unclear. Amino acid-dependent systems proposed in *E. coli* and *Salmonellae*, AR2, AR3, and AR4, are dependent on amino acid decarboxylation. The most potent amino acid-dependent system is the glutamate-dependent system (AR2) that requires two glutamate decarboxylases, GadA and GadB, and a putative glutamate/γ-aminobutyric acid antiporter [12]. The arginine-dependent system (AR3) is induced at a low pH under anaerobic conditions, and requires arginine decarboxylase and an arginine/agmatine antiporter [13]. The lysine-dependent system (AR4) requires lysine decarboxylase and a lysine/cadaverine antiporter [14]. Recent data showed that adenosine deamination increases the survival of *E.coli* [15]. It has been suggested that amino acid decarboxylation and adenosine deamination alkalinize the intracellular space and alkalization increases resistance against acidic stress (AR), but the increase in pHi is not the sole factor explaining the increase in the AR of *E. coli*.

The deletion of *purA* or *purB*, which encode enzymes producing AMP from inosine phosphate by the addition of adenine, markedly decreased the ATP content and survival rate under acidic conditions in *E.coli* [16]. An *E. coli* mutant deficient

in *hemA* encoding glutamyl-tRNA reductase, which synthesizes glutamate 1-semialdehyde, a metabolic precursor for heme synthesis, also showed a decrease in the intracellular ATP content and survival rate at pH 2.5 [17], probably due to the deficiency in oxidative phosphorylation.

Helicobacter pylori has been reported to use the pH-gated urea channel UreI to promote the movement of external urea to periplasmic spaces, where urease produces carbon dioxide from urea, and a membrane-anchored periplasmic carbonic anhydrase regulates the periplasmic pH at around 6 using carbon dioxide in acidic media [8].

In addition to the many systems reported to date in different bacteria, F_1F_0-ATPase has been suggested to be important for all of these bacteria to survive under markedly acidic conditions.

3 Survival under Markedly Acidic Conditions of Bacterial Mutants Deficient in F_1F_0-ATPase

F_1F_0-ATPase plays a central role in energy metabolism, and it can be argued that this enzyme is important for bacterial survival under markedly acidic conditions, because survival requires energy. F_1F_0-ATPase was reported to be essential for the growth of *Helicobacter pylori* and *Lactobacillus* under acidic conditions [18, 19]. A recent study showed that the deletion of F_1F_0-ATPase decreases the survival by hundreds of fold, and the intracellular pH of these mutants was decreased faster than that of the wild-type [17]. It was reported that the ATP level markedly decreased under highly acidic conditions in F_1F_0-ATPase mutants [17]. The results indicate that F_1F_0-ATPase participates in pHi regulation and the maintenance of the ATP content at a high level under acidic conditions, both of which enhance the AR of *E. coli*.

4 Effect of pH on ATP Synthesis Mediated by F_1F_0-ATPase

The sum of ΔpH and ΔΨ is the PMF, usually −140 to −180 mV in growing *E. coli*, which is generated by the respiratory chain and drives ATP synthesis via F_1F_0-ATPase [20]. ΔΨ is always negative inside growing neutrophils, and ΔΨ decreases as ΔpH (internal pH—external pH) increases to maintain a stable PMF value. ΔpH decreases below zero in an alkaline medium, and the PMF is solely due to an internally negative ΔΨ. In contrast to an alkaline pH, ΔΨ decreases with an increase in ΔpH in an acidic medium.

E. coli growing at pH 7 under modestly aerobic conditions maintains ΔΨ at approximately −90 mV. ΔΨ was reported to be approximately −50 mV in cells in the stationary growth phase [9]. When such cells were transferred to pH 2.5 medium, ΔΨ decreased to near 0. Acidophils, such as *Bacillus acidocaldarius* and

Thiobacillus acidophilus, which grow at an external pH of 3 or less, have an inverted $\Delta\Psi$ (internally positive), with an internal pH close to neutral, namely a large ΔpH is present [21]. If the internal pH is kept at neutral in a medium of pH 3, ΔpH is calculated to be approximately −250 mV. To prevent an excessive PMF, a reverse $\Delta\Psi$ may be generated. An excessive PMF could create rapid proton movement, like a short spark from a battery. It is suggested that an internally negative $\Delta\Psi$ is a force that attracts protons, which are charged positively, into the cell [22], and an internally positive $\Delta\Psi$ can repel protons.

Asp 61 of the c subunit and Arg 210 of the a subunit are involved in proton translocation through FO [22–25], and the area constructed by these amino acid residues may be a hydrophilic access pathway from both sides of the membrane [26]. Proton binding and release at a conserved carboxylate side chain in the center of the membrane has been proposed to drive the rotation of the c oligomer [27]. Structural analysis showed that the morphology of subunit c was different between pH 8 and 5 [24]. The morphological difference of subunit c at different pH values is still enigmatic (Fig. 22.1a).

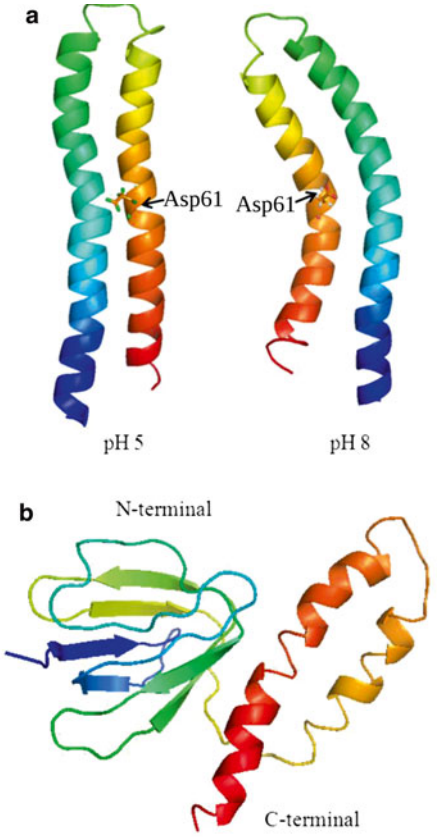

Fig. 22.1 (**a**) The structural change of the c subunit at pH 5 and pH 8. (**b**) The structure of the ε subunit. Drawn from data in Protein Data Bank http://www.rcsb.org/pdb/home/home.do)

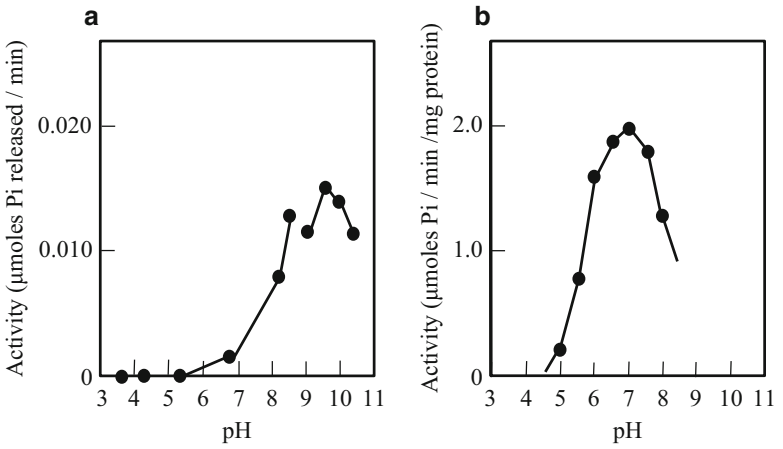

Fig. 22.2 The ATP hydrolysis activity of F_1F_0-ATPase at different pH values in *E. coli* (**a**) and *E. hirae* (**b**). Drawn from data in Refs. [28] and [29]

These data suggest that the ATP-synthesizing activity is affected by the pH, but detailed observations are still limited.

The ATP hydrolysis activity of F_1F_0-ATPase in *E.coli* was approximately 0.5–0.6 μmol Pi/min/mg membrane protein at pH 9.0 [17, 28], and the activity reduced gradually as the pH of the assay medium decreased from pH 9.0 in vitro (Fig. 22.2a). A decrease in ATP hydrolysis activity at an acidic pH was also reported in *Streptococcus faecalis*, which is now referred to as *Enterococcus hirae* (Fig. 22.2b, [29]). Similar pH-dependent activities were reported in other bacteria [25]. If the ATP hydrolysis activity of F_1F_0-ATPase is low in vivo, the proton extrusion activity coupled with ATP hydrolysis mediated by this enzyme could be very low in an acidic medium. It is, however, possible that the high proton extrusion activity is preserved by an unknown regulatory mechanism(s) under acidic conditions in vivo.

5 F_1F_0-ATPase as a pH Regulator

Since F_1F_0-ATPase is able to hydrolyze ATP to transfer protons outside cells, this enzyme can be considered as a potent regulator of cytosolic pH homeostasis to prevent internal acidification. In enterococci, which lack oxidative phosphorylation due to the absence of the respiratory chain, F_1F_0-ATPase has been reported to regulate pHi, and this regulation is essential for the growth of these bacteria under acidic conditions [30]. Recently research showed that pHi in mutants deficient in F_1F_0-ATPase was lower than that of the wild-type in *E. coli* when the cells were challenged by markedly acidic stress [17], indicating that the pHi-regulating activity declines in F_1F_0-ATPase mutants.

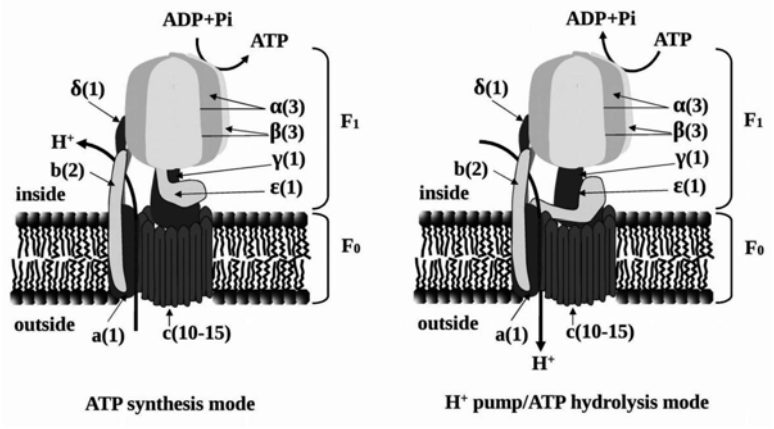

Fig. 22.3 Two hypothetical modes of F_1F_0-ATPase. Drawn from the proposal in Ref. [20]

Bacteria have other types of enzyme which hydrolyze ATP and pump protons to maintain a higher pHi. In some bacteria, F_1F_0-ATPase generates a membrane potential via pumping sodium ions across the membranes into the external surroundings. The use of sodium ions instead of protons as coupling ions may be an essential adaptation strategy of F_1F_0-ATPase to highly alkaline environments, where protons are less available. An interesting example is highlighted in the anaerobic thermos-alkaliphilus *Clostridium paradoxum*, in which ATP is generated via the fermentation of glucose to acetate and CO_2 [31]. Acetate production maintains a near-neutral cytoplasmic pH under alkaline environments.

How is the function of F_1F_0-ATPase changed in neutrophilic aerobic bacteria, such as *E. coli*? When the PMF falls below a threshold level, F_1F_0-ATPase may function as a proton exporter, and this change may be caused by the reorientation of the ε subunit toward FO and away from the β subunit of F1 [20]. This rearrangement may enable the F1 part to hydrolyze ATP and export protons (Fig. 22.3, [20]). The ε subunit has an N-terminal part, which forms a flattened 10-stranded β sandwich structure, and a C-terminal domain, which forms two α-helices running antiparallel to one another (Fig. 22.2b, [32]). Studies with the chloroplast F_1F_0-ATP synthase have shown that the C-terminal domain of the ε subunit is a regulator of ATP hydrolysis, and this activity can be attributed mainly to the last 45 C-terminal amino acids [33]. Another report also suggested that the regulatory function of the ε subunit is mediated by the C-terminal α helical domain [34, 35].

6 Gene Expression of the *atp* Operon at an Acidic pH

The *atp* operon contains 8 genes encoding subunits of F_1F_0-ATPase and one gene whose function is still unknown in many bacteria [6] It was reported that the expression of the *atp* operon showed upregulation at an alkaline pH and

downregulation at pH 5 [36]. The results showed that the expressions of *atpA, B, C, D, E, F, G,* and *I* were induced at a high pH, but decreased at a low pH, and only the expression of *atpH* was induced at a low pH [36]. Western blotting analysis showed that the levels of most F_1F_0-ATPase subunits were almost the same at both pH 7.5 and 5.5 [17]. As described above, F_1F_0-ATPase was shown to be important for bacterial survival under markedly acidic conditions, but expression of the *atp* operon was correlated negatively at an acidic pH. The content of the c subunit varies in bacteria. The copy number of the c subunit was reported to be 10 in membranes of growing cells at a near-neutral pH, and it increased to 12 under acidic stress [24, 37, 38], but the effect of this change is still unclear.

In enterococci, the mRNA level of the *atp* operon was not affected by the pH, but the amount of the enzyme in the membranes was increased at an acidic pH, probably due to enhancement of the enzyme assembly to construct an active enzyme complex [39]. This increase in the membrane level of F_1F_0-ATPase is advantageous for its function to regulate pHi under acidic conditions [29, 40].

7 Possible Mechanisms of F_1F_0-ATPase Functioning under Markedly Acidic Conditions in *E. coli*

There are two hypotheses to account for why F_1F_0-ATPase is important for bacterial survival under such acidic conditions. One is that ATP synthesis mediated by F_1F_0-ATPase is indispensable for bacterial survival under these conditions. It was shown that the ATP level decreased markedly in very acidic environments in mutants deficient in F_1F_0-ATPase [17].

It has been reported that ATP is essential for bacterial survival at an acidic pH, even though bacteria do not grow. During the adaptation processes, many systems for survival at an acidic pH were induced, and such induced systems consume ATP. Mutants deficient in *recB* showed poor survival at an acidic pH [16]. Furthermore, a triple *recB*, *recC*, and *sbcB* mutation led to a lower survival rate at pH 2.5 [16]. The DNA repair system containing RecB requires ATP as an energy source [41]. The other systems which require ATP as the energy source may also take a role under markedly acidic stress [42, 43].

The ATP content increased when cells were adapted in a moderately acidic medium at pH 5 to 6, and the level decreased rapidly after cells were challenged at pH 2 to 3 [16]. The magnitude of PMF was, however, low at a low pH [22]. The increase in the ATP level may also be caused by a decline in metabolic processes consuming ATP, such as the biosynthesis of macromolecules. In fact, the growth rate was low at pH 5.5.

Another hypothesis, which may be more likely, is that F_1F_0-ATPase functions as a pHi regulator under acidic environments. The main pump for proton extrusion is the respiratory chain in *E. coli*, and respiration decreased at an acidic pH [44, 45]. To compensate for the decrease, F_1F_0-ATPase may hydrolyze ATP to pump protons from the intracellular spaces under acidic conditions, and the cytoplasmic pH is maintained at a higher value, which promotes bacterial survival.

The published data revealed that F_1F_0-ATPase has an important role in the protection of cells via AR1 [17]. However, AR1 was entirely independent from F_1F_0-ATPase [22]. Furthermore, F_1F_0-ATPase shows no participation in AR2 or AR3 [9].

8 Conclusions

It is now generally accepted that F_1F_0-ATPase has various roles in bacteria to promote survival in the presence of environmental stresses. The published data showed that a large number of systems function for bacterial growth and survival under acidic conditions, and F_1F_0-ATPase is an enzyme required under such harsh conditions, although the mechanism still remains unclear. One possible explanation would be that F_1F_0-ATPase provides ATP, which is an essential energy source for survival at an acidic pH. Alternatively, F_1F_0-ATPase extrudes protons to maintain a higher cytoplasmic pH for survival under highly acidic conditions. Further investigations will be indispensable for our improved understanding of bacterial survival under markedly acidic conditions, and the mechanisms of F_1F_0-ATPase for switching between the two roles under different conditions should be clarified.

Acknowledgements The author would like to express thanks to Hiroshi Kobayashi (Chiba University) for his valuable suggestions.

References

1. Elston T, Wang H, Oster G (1998) Energy transduction in ATP synthase. Nature 391:510–513
2. Sorgen PL, Bubb MR, Cain BD (1999) Lengthening the second stalk of F_1F_O -ATP synthase in Escherichia coli. J Biol Chem 274:36261–36266
3. Capaldi RA, Schulenberg B, Murray J, Aggeler R (2000) Cross-linking and electron microscopy studies of the structure and functioning of the Escherichia coli ATP synthase. J Exp Biol 203: 29–33
4. Wang H, Oster G (1998) Energy transduction in the F1 motor of ATP synthase. Nature 396:279–282
5. Foster DL, Fillingame RH (1982) Stoichiometry of subunits in the H+-ATPase complex of Escherichia coli. J Biol Chem 257:2009–2015
6. von Ballmoos C, Cook GM, Dimroth P (2008) Unique rotary ATP synthase and its biological diversity. Annu Rev Biophys 37:43–64
7. Bulygin VV, Milgrom YM (2009) A bi-site mechanism for Escherichia coli F1-ATPase accounts for the observed positive catalytic cooperativity. Biochim Biophys Acta 1787:1016–1023
8. Sachs G, Weeks DL, Wen Y et al (2005) Acid acclimation by Helicobacter pylori. Physiology 20:429438
9. Richard H, Foster JW (2004) Escherichia coli glutamate- and arginine-dependent acid resistance systems increase internal pH and reverse transmembrane potential. J Bacteriol 186:60326041
10. Castanie-Cornet MP, Penfound TA, Smith D et al (1999) Control of acid resistance in Escherichia coli. J Bacteriol 181:3525–3535
11. Castanie-Cornet MP, Foster JW (2001) *Escherichia coli* acid resistance: cAMP receptor protein and a 20 bp cis-acting sequence control pH and stationary phase expression of the *gadA* and *gadBC* glutamate decarboxylase genes. Microbiology 147:709–715

12. Hersh BM, Farooq FT, Barstad DN et al (1996) A glutamate-dependent acid resistance gene in *Escherichia coli*. J Bacteriol 178:3978–3981
13. Iyer R, Williams C, Miller C (2003) Arginine-agmatine antiporter in extreme acid resistance in *Escherichia coli*. J Bacteriol 185:6556–6561
14. Meng SY, Bennett GN (1992) Nucleotide sequence of the *Escherichia coli* cad operon: a system for neutralization of low extracellular pH. J Bacteriol 174:2659–2669
15. Sun Y, Fukamachi T, Saito H et al (2012) Adenosine deamination increases the survival under acidic conditions in *Escherichia coli*. J Appl Microbiol 112:775–781
16. SunY FT, Saito H et al (2011) ATP requirement for acidic resistance in *Escherichia coli*. J Bacteriol 193:3072–3077
17. Sun Y, Fukamachi T, Saito H et al (2012) Respiration and the F_1F_0-ATPase enhance survival under acidic conditions in *Escherichia coli*. PLoS One 7, e52577
18. Bijlsma JJ, Lie-A-Ling M, Nootenboom IC et al (2000) Identification of loci essential for the growth of *Helicobacter pylori* under acidic conditions. J Infect Dis 182:1566–1569
19. Kullen MJ, Klaenhammer TR (1999) Identification of the pH-inducible, proton-translocating F_1F_0-ATPase (*atpBEFHAGDC*) operon of *Lactobacillus acidophilus* by differential display: gene structure, cloning and characterization. Mol Microbiol 33:1152–1161
20. Suzuki T, Murakami T, Iino R et al (2003) F_1F_0-ATPase/synthase is geared to the synthesis mode by conformational rearrangement of epsilon subunit in response to proton motive force and ADP/ATP balance. J Biol Chem 278:46840–46846
21. Matin A, Zychlinsky E, Keyhan M et al (1996) Capacity of *Helicobacter pylori* to generate ionic gradients at low pH is similar to that of bacteria which grow under strongly acidic conditions. Infect Immun 64:1434–1436
22. Foster JW (2004) *Escherichia coli* acid resistance: tales of an amateur acidophile. Nat Rev Microbiol 2:898–907
23. Cain BD, Simoni RD (1989) Proton translocation by the F_1F_0-ATPase of *Escherichia coli*. Mutagenic analysis of the a subunit. J Biol Chem 264:3292–3300
24. Rastogi VK, Girvin ME (1999) Structural changes linked to proton translocation by subunit c of the ATP synthase. Nature 402:263–268
25. von Ballmoos C, Dimroth P (2007) Two distinct proton binding sites in the ATP synthase family. Biochemistry 46:11800–11809
26. Fillingame RH (1997) Coupling H^+ transport and ATP synthesis in F_1F_0-ATP synthases: glimpses of interacting parts in a dynamic molecular machine. J Exp Biol 200:217–224
27. Fillingame RH, Angevine CM, Dmitriev OY (2003) Mechanics of coupling proton movements to c-ring rotation in ATP synthase. FEBS Lett 555:29–34
28. Kobayashi H, Anraku Y (1972) Membrane-bound adenosine triphosphatase of *Escherichia coli*. I Partial purification and properties. J Biol Chem 71:387–399
29. Kobayashi H, Suzuki T, Kinoshita N et al (1984) Amplification of the *Streptococcus faecalis* proton-translocating ATPase by a decrease in cytoplasmic pH. J Bacteriol 158:1157–1160
30. Kobayashi H (1985) A proton-translocating ATPase regulates pH of the bacterial cytoplasm. J Biol Chem 260:72–76
31. Ferguson SA, Keis S, Cook GM (2006) Biochemical and molecular characterization of a Na^+ translocating F_1F_0-ATPase from the thermoalkaliphilic bacterium *Clostridium paradoxum*. J Bacteriol 188:5045–5054
32. Cingolani G, Duncan TM (2011) Structure of the ATP synthase catalytic complex (F1) from *Escherichia coli* in an autoinhibited conformation. Nat Struct Mol Biol 18:701–707
33. Nowak KF, McCarty RE (2004) Regulatory role of the C-terminus of the epsilon subunit from the chloroplast ATP synthase. Biochemistry 43:3273–3279
34. Feniouk BA, Suzuki T, Yoshida M (2006) The role of subunit epsilon in the catalysis and regulation of F_1F_0-ATP synthase. Biochim Biophys Acta 1757:326–338
35. Nakanishi-Matsui M, Sekiya M, Yano S et al (2014) Inhibition of F1-ATPase rotational catalysis by the carboxyl-terminal domain of the subunit. J Biol Chem 289:30822–30831
36. Maurer LM, Yohannes E, Bondurant SS et al (2005) pH regulates genes for flagellar motility, catabolism, and oxidative stress in *Escherichia coli* K-12. J Bacteriol 187:304–319

37. Aris JP, Klionsky DJ, Simoni RD (1985) The Fo subunits of the *Escherichia coli* F_1F_0-ATP synthase are sufficient to form a functional proton pore. J Biol Chem 260:11207–11215
38. Krebstakies T, Aldag I, Altendorf K et al (2008) The stoichiometry of subunit c of *Escherichia coli* ATP synthase is independent of its rate of synthesis. Biochemistry 47:6907–6916
39. Arikado E, Ishihara H, Ehara T et al (1999) Enzyme level of enterococcal F_1F_0-ATPase is regulated by pH at the step of assembly. Eur J Biochem 259:262–268
40. Suzuki T, Unemoto T, Kobayashi H (1988) Novel streptococcal mutants defective in the regulation of H^+-ATPase biosynthesis and in FO complex. J Biol Chem 263:11840–11843
41. Wu CG, Bradford C, Lohman TM (2010) *Escherichia coli* RecBC helicase has two translocase activities controlled by a single ATPase motor. Nat Struct Mol Biol 17:1210–1217
42. Naseem R, Wann KT, Holland IB et al (2009) ATP regulates calcium efflux and growth in *E. coli*. J Mol Biol 391:42–56
43. Yan H, Fukamachi T, Saito H et al (2011) Expression and activity of Kdp under acidic conditions in *Escherichia coli*. Biol Pharm Bull 34:426–429
44. Ingledew WJ, Poole RK (1984) The respiratory chains of *Escherichia coli*. Microbiol Rev 48: 222–271
45. Kinoshita N, Unemoto T, Kobayashi H (1984) Proton motive force is not obligatory for growth of *Escherichia coli*. J Bacteriol 160:1074–1077

Chapter 23
"Tuning" the ATPase Activity of Hsp90

Chrisostomos Prodromou and Rhodri M.L. Morgan

Abstract The Hsp90 chaperone is responsible for the activation and maturation of an eclectic set of proteins. These are often key regulatory proteins that include protein kinases, steroid hormone receptors and transcription factors. Consequently, Hsp90 has become one of the most important anti-cancer targets of our time, as well as a target for other diseases, such a neurodegenerative, parasitic and viral diseases. The ATPase activity of Hsp90 is central to its mechanistic action and the binding and hydrolysis of ATP drives a conformational cycle that brings about activation and maturation of client proteins. The structurally diverse clientele of Hsp90 necessitates that Hsp90 co-operates with a variety of co-chaperones that modulate and tune its activity and thus its conformational cycle. Delivering client proteins is one role that specific co-chaperones play, while others stabilize client complex or provide directionality and alterations to the ATP-coupled conformational cycle of Hsp90. The formation of a catalytically active unit, able to hydrolyze ATP, involves all regions of Hsp90. This complexity has facilitated the evolution of a variety of co-chaperones that regulate Hsp90 by modulating different molecular switches within the chaperone. It has also allowed the evolution of Hsp90 orthologues that are kinetically different. Furthermore, it appears that the conformational switches of Hsp90 are not always coupled. Here, we describe the known Hsp90-co-chaperone complexes, the role that specific co-chaperones play in these complexes and, briefly, post-translational modifications that affect the ATPase activity of Hsp90.

Keywords Hsp90 • Heat shock protein 90 • Chaperones • Co-chaperone • Stress response • ATPase activity • Conformational cycle • Activation

C. Prodromou (✉) • R.M.L. Morgan
Genome Damage and Stability Centre, University of Sussex,
Science Park Rd, Falmer, Brighton, East Sussex BN1 9RQ, UK
e-mail: chris.prodromou@sussex.ac.uk

S. Chakraborti, N.S. Dhalla (eds.), *Regulation of Ca^{2+}-ATPases,V-ATPases and F-ATPases*, Advances in Biochemistry in Health and Disease 14,
DOI 10.1007/978-3-319-24780-9_23

1 Introduction

Hsp90 is a molecular chaperone that is involved in the activation and maturation of a structurally diverse eclectic group of proteins (see http://www.picard.ch/Downloads/Hsp90interactors.pdf). These are often key regulatory proteins that include protein kinases [1] as well as phosphatidylinositol-3-kinase-like kinases such as mTOR and SMG1 [2, 3], steroid hormone receptors [4] and transcription factors [5]. Consequently, Hsp90 has become a major anti-cancer target [6–8], as well as being involved in a variety of other disease processes, such as Alzheimer's and other neurodegenerative diseases [9–11], parasitic disease such as malaria [12] and viral disease [13]. However, because of the structural diversity of client proteins that Hsp90 has to deal with, it has evolved into a number of homologues that are each suited to their precise role. In the cytoplasm there are two homologues, Hsp90α and Hsp90β, while in the endoplasmic reticulum and mitochondria there is Grp94/Gp96 and Trap1, respectively [14–17]. Hsp90 has many regulatory switches that allow a variety of co-chaperones to modulate precisely its ATPase activity [16] and consequently its conformational cycle, upon which activation and maturation of the client protein depends. In fact, the system is so versatile that viruses have also recruited Hsp90 for their own purposes [18].

A single unvaried conformational cycle in Hsp90 would severely limit the array of client proteins that it could activate. Consequently, and in addition to the variety of Hsp90 homologues, a whole host of co-chaperones have evolved that specifically regulate the conformational cycle of Hsp90 by controlling a limited number of Hsp90 molecular switches. These include co-chaperones that inhibit the ATPase activity of Hsp90, often silencing the chaperone machine in order to allow client proteins to be loaded onto the chaperone. They include proteins such as Sti1p/Hop and Cdc37 [16]. Other, such as p23 and RAR1, may help stabilize client protein complexes resulting in long-lived client protein-Hsp90 complex. Slowing the cycle might increase the time allowed for small molecule binding to the client protein [19, 20]. Others still help to drive the conformational cycle forward by activating the ATPase activity of Hsp90. The best, and perhaps the only example of this is Aha1 and the closely related protein, Hch1 [21].

Understanding the mechanism of Hsp90 activation and maturation of client proteins needs an in depth understanding of the molecular details of the various co-chaperone-Hsp90 complexes. In this review we will initially discuss the complex structural changes that occur in Hsp90 that bring about its activation. We will then describe the role that co-chaperones play in regulating its ATPase activity by modulating the conformational switches within Hsp90.

2 Hsp90, ATP and the Formation of a Catalytically Active Conformation

The binding of ATP to Hsp90 helps to stabilize a series of conformational changes that lead to a catalytically active unit that is able to hydrolyze ATP [16]. ATP itself binds deep within a pocket found in the N-terminal domains of Hsp90 [22] (Fig. 23.1a).

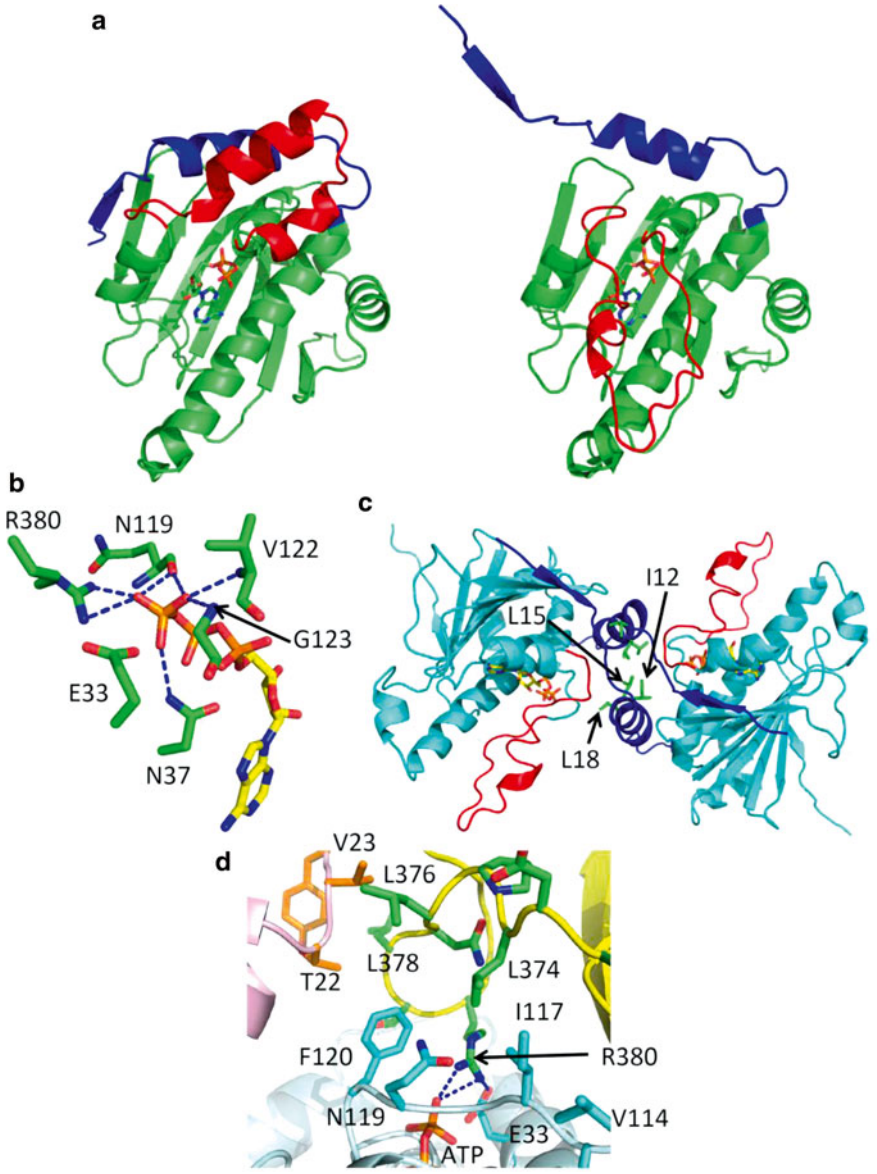

Fig. 23.1 Pymol cartoons showing the formation of the catalytically active unit of Hsp90. (**a**) The *left* and *right panels* show the open and closed conformation of the ATP lid (*red*). The structure in *blue* represents the N-terminal domain sequence involved in the β-strand exchange and dimerization of the N-terminal domains. (**b**) Details showing the interaction of the base of the ATP lid and the γ -phosphate of ATP. (**c**) Cartoon showing the dimerization interfaces between the N-terminal domains of Hsp90. The red fragments represent the ATP lids. The *blue coloured* elements represent the N-terminal sequences of the N-terminal domains that change conformation during the β-strand exchange. (**d**) Cartoon showing the interaction of the γ-phosphate of ATP with the catalytic Arg 380 of the catalytic loop (*yellow loop, green residue*). The catalytic loop is stabilized by interactions with the N-terminal domain (especially Ile 117), within the same monomer (*cyan*), and with the neighbouring N-terminal domain (salmon with orange residue), especially Thr 22

Once ATP is bound the ATP "lid" of the N-terminal domain is able to close over the entrance to the ATP-binding pocket, thus helping to trap the ATP. The movement of the ATP lid is permitted because of two flexible positions, Gly 94 and Gly 121 (*Saccharomyces cerevisiae* numbering), at the base of the ATP lid. The ATP lid is stabilized by a series of hydrogen bonds that interact with the γ-phosphate of ATP (Fig. 23.1b). The restructuring of the ATP lid in turn destabilizes helix 1 of the N-terminal domain as it is normally packed against the open conformation of the ATP lid (Fig. 23.1c). This α-helix is now mobile and moves together with β-strand 1 of the N-terminal domain. In all, residues 1–27 of each Hsp90 monomer remodels as part of a β-strand exchange between the N-terminal domains of Hsp90 that leads to N-dimerization [19]. In particular repositioning of α-helix 1 provides a dimerization interface (Fig. 23.1c).

Although the bound ATP is now trapped in the N-terminal domain and the protein has undergone dimerization, the hydrolysis of ATP is still dependent on modulation of the catalytic loop of the middle domain. This involves association of the N-terminal domains of Hsp90 with its middle domains. This enables the catalytic loop of each middle domain to reach into the active site of each Hsp90 N-terminal domain within the same monomer. Thus, the Arg 380 residue of the catalytic loop can now directly interact with the γ-phosphate of ATP (Fig. 23.1d). Stabilization of the active conformation of the catalytic loop is achieved by making a hydrophobic contact between Ile 117 of the N-terminal domain and Leu 374 of the catalytic loop (Fig. 23.1d). Further stabilization is also achieved through an interaction between Thr 22 of the repositioned α-helix 1 and Leu378 of the catalytic loop from the neighbouring Hsp90 monomer (Fig. 23.1d).

3 Hsp90 Kinetic Models

The rate-limiting step for the turnover of ATP by Hsp90 has been controversial. Kinetic experiments [23, 24] now agree that it is the complex set of conformational changes [25] that limit ATP turnover rather than ATP hydrolysis "per se" [26]. The kinetic model for yeast [24] suggest that following binding of ATP the conformational changes leading to the catalytically active state involve a transition towards two intermediate conformations (Fig. 23.2). The first of these, I1, is thought to derive from ATP lid closure and the release of the N-terminal segment of the N-terminal domain, and appears to have the lowest rate constant. The second state, I2, is then formed through the dimerization of the N-domains. Finally, the catalytically active state occurs following transition to a state that involves the association of the N- and middle-domains and presumably interaction of ATP with Arg 380 of the catalytic loop. The ATP is now trapped within the N-terminal domains and is committed to hydrolysis. It is thought that in this model Aha1 may bypass the formation of the I1 state, thus accelerating the rate-limiting step of the reaction. In contrast, for *Escherichia coli* HtpG, ATP binding leads to a two-phase transition where a rapid change to an intermediate state is followed by a slower transition to

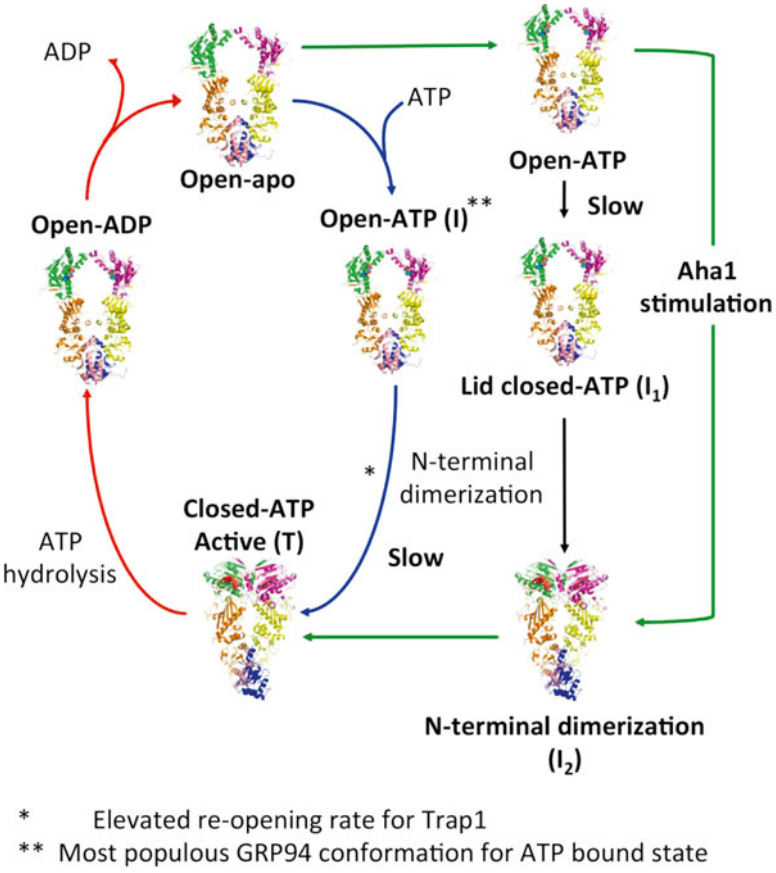

Fig. 23.2 The kinetic cycles of the Hsp90s. In the yeast cycle (*red* and *green arrows*), transition via two intermediate conformations (I1 and I2) leads to the catalytically closed ATP-state, and Aha1 accelerates the cycle by bypassing the I1 sate. Alternatively, for the *E. coli* cycle (*red* and *blue arrows*), the closed active state (T) is reached by a two-phase transition via an intermediate state (I). Conformational change represents the slowest step in both cycles and is indicated in the figure (slow). The state of Hsp90, open, closed and active, including the nucleotide state are indicated throughout the cycle

the T (closed) state [23] (Fig. 23.2). Interestingly, to date an equivalent Aha1 homologue for HtpG has not been identified, which might account for this difference, assuming all states have been identified.

The above model suggests that Aha1 can accelerate the rate-limiting step of the cycle by modulating the early conformational changes that lead to the formation of a catalytically active unit of Hsp90. However, the story cannot be so simplistic. For example, the activation of Hsp90 ATPase activity by full-length Aha1 is significantly more potent than that of its N-terminal domain alone (or Hch1). However, both full-length Aha1 and the N-terminal domain of Aha1 modulate the position of the catalytic domain of the middle domain. This modulation to an open active state

of the catalytic loop appears to be a late step in the cycle, because its interactions with the bound ATP and N-terminal domain occur later in the cycle following the association of the middle and N-domains of Hsp90. Clearly, activation by Aha1 might involve other mechanisms that we do not yet understand.

However, in contrast to these models those for Grp94 and Trap1 appear to be very different. For Trap1 the rate-limiting step for ATP turnover has still not been settled. Furthermore, both TRAP1 and Grp94 do not show trapping of ATP and commitment to hydrolysis [27, 28]. While at first sight these differences may seem surprising, when taking into account the different client proteins with which these homologues have to work with, and the different cellular environments they encounter, it is perhaps understandable why a common conformational cycle is regulated in different ways.

4 Client Protein Hsp90 Chaperone Cycles

Without co-chaperones the Hsp90 cycle is stochastic and does not support an efficient activation of client proteins [29]. Thus co-chaperones, as well as a variety of post-translational modifications, give directionality to the cycle and increase the efficiency of client protein activation. Perhaps the best described Hsp90—client-protein chaperone cycle is that for steroid hormone receptors. Early studies identified many of the interacting co-chaperones [30–32] (Fig. 23.3) and early-, intermediate- and late-stage complexes of the cycle, which characterize the specific co-chaperone within the complex. Early stage complexes see the association of Hsp70-steroid hormone receptor complex with Hsp90, which is achieved through HOP binding to both Hsp70 and Hsp90. Thus HOP acts as a scaffold utilizing distinct tetratricopeptide repeat (TPR) domains to hold together two chaperone complexes in close vicinity. However, HOP is more than a simple scaffold protein, at least for the homologous yeast Sti1p, as it simultaneously inhibits the ATPase cycle of Hsp90 [33]. Furthermore, both HOP and Sti1p have been shown to activate the ATPase activity of Hsp70 and Ssa1, respectively [34, 35]. The inactive Hsp90 forms a stable complex that can accept the client while active Hsp70 would allow it to release the client to Hsp90. The complex then needs to progress and this appears to occur by the binding of an immunophillin, such as FKBP51 or 52, which displaces HOP and Hsp70. Mixed Hsp90 complexes with the yeast Cpr6 and Sti1p, have been reported [36]. The release of Hsp70 and HOP from the complex establishes the intermediate stage. This stage is now competent to bind ATP and undergo N-terminal dimerization, which then signals the binding of p23 [37]. This late stage complex converts the steroid hormone receptor to a high hormone binding state thus allowing efficient activation of the steroid hormone receptor.

The other major chaperone cycle that has been described is that of kinases, which probably represent the largest class of client protein [1] (Fig. 23.4). Delivery of protein kinase to Hsp90, as for steroid hormone receptors, occurs via an adaptor protein, the co-chaperone $Cdc37^{p50}$. Like Sti1p, $Cdc37^{p50}$ silences the ATPase

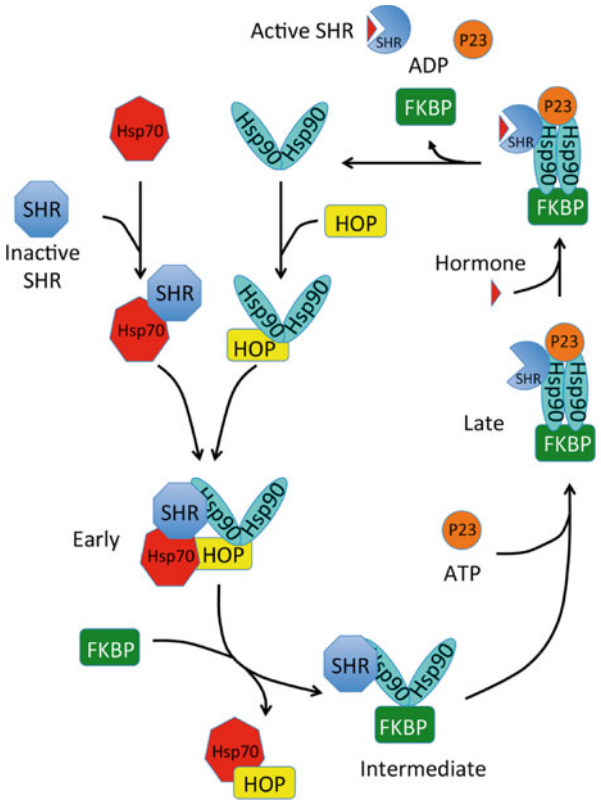

Fig. 23.3 Activation cycle for steroid hormone receptors by Hsp90. Hsp90 and HOP form a complex and HOP inactivates Hsp90, while simultaneously acting as a scaffold that recruits Hsp70 and bound steroid hormone receptor (SHR). This establishes the early Hsp90-SHR complex. The SHR is then transferred to Hsp90. Subsequently, HOP and Hsp70 are displaced following binding of an immunophillin, such as FKBP51 or 52. This establishes the intermediate chaperone complex that is able to bind ATP and then p23. Binding of p23 is ATP dependent and results in slowing of the chaperone cycle. The complex now represents the late stage, which allows efficient activation of the SHR by binding hormone. Eventually ATP is hydrolyzed and the complex dismantles

activity of Hsp90 [38], but in this case also that of the kinase [39]. Association of the kinase with Cdc37^{p50} is favoured by the phosphorylation of Ser 13 of Cdc37^{p50} in humans and Ser 14 and 17 in yeast [40–42]. Once the Hsp90-kinase complex is established by interaction of Cdc37^{p50} With Hsp90, PP5 enters the complex and dephosphorylates Cdc37^{p50} [43]. This in turn primes the complex for phosphorylation by the kinase YES [44]. YES phosphorylates Tyr 298 or Tyr 4 on Cdc37^{p50}, which appears to weaken the interaction between the kinase and Cdc37^{p50}. Finally, phosphorylation at Tyr 197 on Hsp90 by YES kinase causes the dissociation of Cdc37^{p50} from the complex. Consequently and with subsequent phosphorylation on Tyr 313 of Hsp90, a conformational change is induced that promotes the recruitment of Aha1 [44] and stimulation of the ATPase activity of Hsp90 [21].

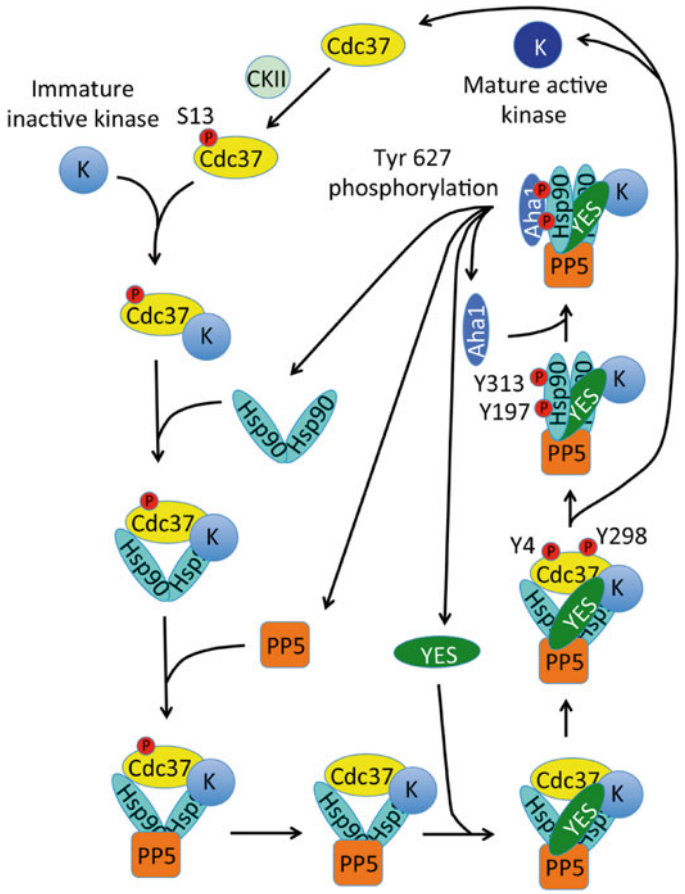

Fig. 23.4 Activation cycle of protein kinase by Hsp90. Cdc37^{p50} is phosphorylated by casein kinase II (CKII) at Ser 13. This efficiently binds Hsp90-dependent kinases and recruits them to Hsp90 where they can interact with the chaperone. PP5 then dephosphorylates Cdc37^{p50} and primes the complex for phosphorylation by the YES kinase. YES kinase then phosphorylates Cdc37 at Tyr4 and 298, weakening the interaction with Cdc37^{p50}. Finally, phosphorylation of Tyr 197 of Hsp90 results in the dissociation of Cdc37^{p50}. A subsequent phosphorylation by YES kinase at Tyr313 of Hsp90 signals recruitment of Aha1, which stimulates the ATPase chaperone cycle that may drive the maturation of the kinase. Finally, phosphorylation at Tyr 627 of Hsp90 results in dissociation of the Hsp90-kinase complex

Finally, Hsp90 phosphorylation at Tyr 627 leads to a dissociation of the complex. However, although YES kinase is depicted here, other tyrosine kinases may also be able to carry out these phosphorylations, as the knockdown of YES kinase does not lead to a cessation of the kinase cycle [44]. The recycling of Hsp90 and Cdc37^{p50} by dephosphorylation results via as yet unknown phosphatase(s).

Comparing the chaperone cycles of steroid hormone receptor and kinases demonstrates how specific client proteins have their own requirements for activation,

and highlights the versatility of the Hsp90 chaperone cycle. While these two cycles remain the best described to date it is not unreasonable to expect to see differences in the chaperone cycle, the co-chaperone requirement and the post-translational modifications imposed by other structurally unrelated client proteins.

5 Modulation of the Catalytic Unit of Hsp90 by Client Delivering co-Chaperones

There are a number of Hsp90 co-chaperones that have been implicated in delivering client proteins to Hsp90. These include Hop/Sti1p, Cdc37^{p50}, Sgt1 as part of a Sgt1-Rar1 complex and Tah1 as part of the R2TP complex (RVBL1, RVBL2, Tah1 and RPAP3). Hop/Sti1p is responsible for delivering steroid hormone receptors to the Hsp90 complex that have been bound by Hsp70 and was the first co-chaperone shown to be able to inhibit the ATPase activity of Hsp90 [33]. Recruitment of the steroid hormone receptor is achieved by acting as a scaffold between Hsp90 and Hsp70 by binding both proteins simultaneously, through highly conserved peptide motifs, IEEVD (Hsp70) and MEEVD (Hsp90) [45]. The domains that bind such conserved peptides are known as tetratricopeptide (TPR) domains. Hop/Sti1p consists of three TPR modules, TPR1, TPR2A and TPR2B (Fig. 23.5). The former is responsible for binding the IEEVD motif of Hsp70, while the TPR2A domain is predominantly required for binding the MEEVD peptide of Hsp90. Although Hop/Sti1p was the first co-chaperone shown to be able to regulate the ATPase activity of Hsp90 [33], structural details showing how this is achieved have been elusive. However, various studies suggest that Hop has multiple interaction sites with the C-terminal, middle- and N-terminal-domains of Hsp90 [46]. Noteworthy, is the

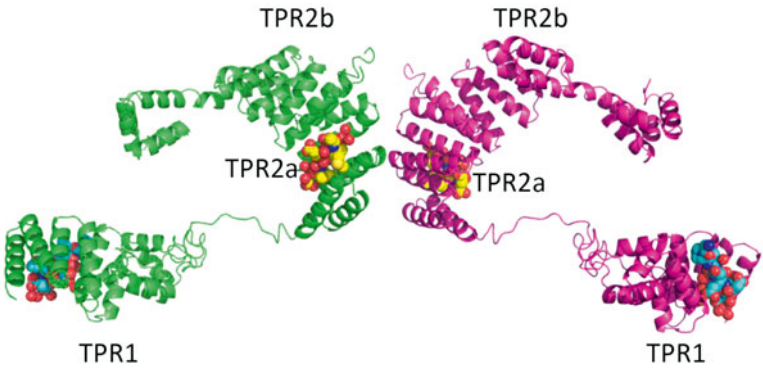

Fig. 23.5 A model of the structure of Hop. In solution HOP/Sti1 appear to be dimeric. However, monomers of Hop/Sti1 may interact with Hsp90 independently when in complex with the chaperone. The conserved IEEVD of Hsp70 and the MEEVD peptide motif of Hsp90 are shown as spheres bound to the TPR1 and TPR2a domains, respectively. Co-ordinates obtained as a kind gift from J. Guenter Grossmann

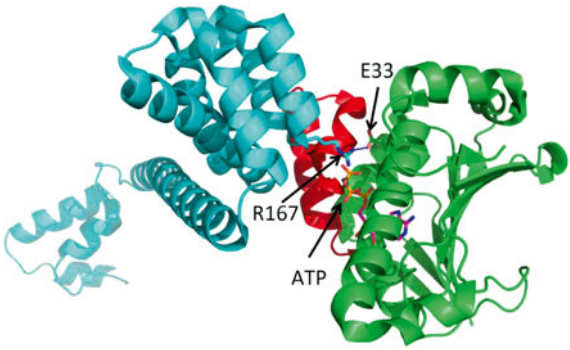

Fig. 23.6 Inhibition of the ATPase activity of Hsp90 by the co-chaperone Cdc37^{p50}. The ATP lid of the N-terminal domain of Hsp90 is shown in *red*. Cdc37^{p50} (*cyan*) binds the N-terminal domain of Hsp90 (*green*) by interacting with its ATP lid. This prevents the lid from moving to the closed state and also prevents direct N-terminal dimerization. Furthermore, the interaction between Arg 167 of Cdc37^{p50} and the catalytic Glu 33 of Hsp90 prevents the chaperone from hydrolyzing ATP. AMPPNP (the non-hydrolyzable analogue of ATP) is shown in *magent*a. Hydrogen bonds are shown as *dotted blue lines*

observation that Sti1p is able to prevent Hsp90 N-terminal dimerization by interacting with the first 24 amino acid residues of the N-terminal domain [47].

Cdc37^{p50} is a co-chaperone that specifically delivers protein kinases to Hsp90 [1]. Like Hop/Sti1p, Cdc37 has also been shown to inhibit the ATPase activity of Hsp90 [38]. Structural details show that human Cdc37 binds between the N-terminal domains of Hsp90, thus preventing their association and therefore the formation of the catalytically active closed state of Hsp90 [48]. In fact, Cdc37 binds to the ATP lids themselves directly while also interacting with the catalytic Glu 33 of Hsp90, thus preventing it from carrying out ATP hydrolysis (Fig. 23.6).

Sgt1, and perhaps in complex with Rar1, is a co-chaperone that acts as a hub and is responsible for delivering client proteins to Hsp90 [20, 49]. In particular, Sgt1 and Rar1 are involved in the activation of innate immunity receptors in plants [50] and the animal related Nod-like receptors. Sgt1 is a multi-domain protein consisting of an N-terminal TPR domain that interacts with SKP1 [51], a middle CS-domain that interacts with the N-terminal domains of Hsp90 [20] and a C-terminal SGS domain that is essential for innate immunity receptor stability and therefore likely interacts with such receptor proteins [52]. The CS domain of Sgt1 is structurally similar to that of Sba1p/p23, another co-chaperone of Hsp90. However, the binding sites for such CS-domains vary. Consequently, unlike Sba1p/p23, Sgt1 alone does not inhibit the ATPase activity of Hsp90 [53]. Although Sgt1 does not affect the ATPase activity of Hsp90, it does recruit a co-chaperone known as Rar1 in plants, or Chp1 or melusin in mammals, which, at least for Rar1, can weakly stimulate the ATPase activity of Hsp90 [20] and convert it to an ADP bound state. Hydrolysis of the bound ATP was shown to be carried out by the CHORD II domain of Rar1 and this is thought to lead to the formation of a stable Sgt1-Hsp90-Rar1 complex. This presumably results in a long-lived association with the client protein, but without

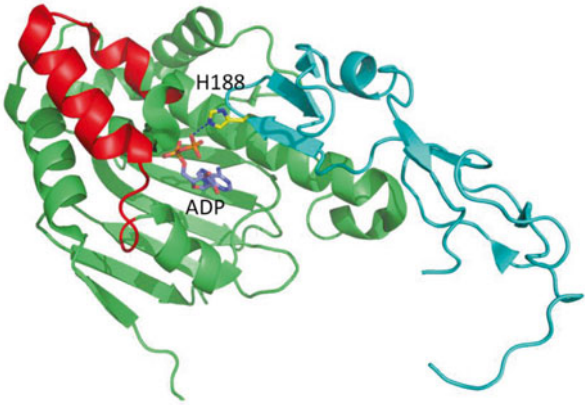

Fig. 23.7 Stabilization of the Hsp90-Rar1 complex. Pymol cartoon showing the interaction of the Rar1 CHORD II domain (*cyan*) with the N-terminal domain of Hsp90 (*green* with *red* ATP lid). ADP is shown in *pale blue* and is hydrogen bonded to His 188 from the CHORD II domain of Rar1. Hydrogen bonds are shown as *dotted blue lines*

promoting a closed state (N-terminal dimerization) in Hsp90 (Fig. 23.7). This may be important where long-lived Hsp90 complexes are required to act as sensors for small molecules from invasive organisms. Such complexes would be activated immediately following infection, representing a "standby" option, without the need to elicit transcription of these proteins in the first instance [16]. Thus, for client proteins entering this complex a stable inactive platform is offered that includes bound ADP brought about by Sgt1-Rar1 binding [20].

Finally, Tah1 of the R2TP complex is known to act as a scaffold that connects the Hsp90 complex to the R2TP (RuvBL1, RuvBL2, Tah1 and Pih1) complex. In turn, the R2TP complex recruits the TTT complex (TEL2 TTI1 and TTI2),which interacts with phosphatidylinositol-3-kinase-like kinases (PIKKs), such as mTOR and SMG1 [2, 3]. Activation of the ATPase activity of Hsp90 by Tah1 has been shown to be weak [54, 55]. However, a Tah1-Pih1 complex appears to inhibit the ATPase activity of Hsp90 [54, 55]. Although there is good structural detail describing the interaction of the Hsp90-Tah1-Pih1 complex [2, 55], the mechanism by which this weak inhibition of Hsp90 activity is achieved remains elusive.

6 Modulation of the Catalytic Unit of Hsp90 by p23/Sba1p

p23/Sba1p is a small acidic protein that consists of a CS domain and an extended unstructured C-terminus [19, 56]. p23 is part of the Hsp90-steroid hormone receptor complexes and enters these complexes at the late stage of complex formation [57, 58]. The binding to Hsp90 is favoured by an ATP-bound N-terminally dimerized Hsp90 conformation [37, 59]. The binding of p23 to Hsp90 results in the inhibition of Hsp90-ATPase activity [21, 59]. However, unlike Sti1p and Cdc37p50, inhibition

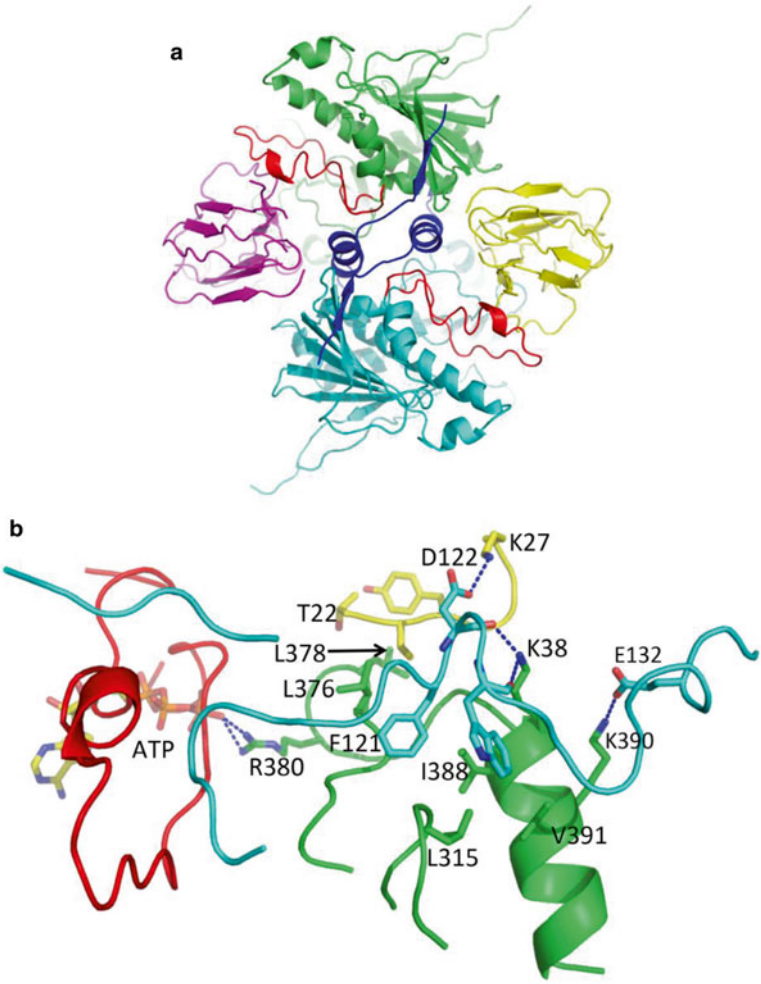

Fig. 23.8 Regulation of the ATPase activity of Hsp90 by Sba1. (**a**) The "inhibited" state of Sba1 bound Hsp90. Sba1, shown in *yellow* and *magenta*, is bound between the N-terminal domains of Hsp90 (*cyan* and *green*). The bound Sba1 domains prevent movement of the ATP lids (*red*) of Hsp90 and help to stabilize the closed state. Consequently, the chaperone cycle is inhibited. (**b**) Sba1 modulation of the catalytic loop of Hsp90. The C-terminal unstructured region of Sba1 (*cyan*) interacts with the middle domain of Hsp90 (*green*) causing the catalytic loop of the middle domain to move to its open active-state. This allows Arg 380 of Hsp90 to interact with the ϒ-phosphate of ATP (*yellow*)

by the yeast protein, Sba1p, does not completely abolish the ATPase activity of Hsp90 [21]. This remained a point of contention until the structure of Sba1p in complex with the full-length Hsp90 was determined [19] (Fig. 23.8). The structure showed that Sba1p bound the N-terminal domains of Hsp90 thus locking the closed

N-terminally dimerized state. In fact, Sba1p binds directly to the ATP lids preventing their movement and thus stabilizing a closed complex (Fig. 23.8a). While this explains how Sba1p inhibits, or more precisely slows, the chaperone cycle and therefore the ATPase activity of Hsp90, it does not in itself explain why the turnover of ATP is only partially inhibited. On closer inspection, it was found that the unstructured C-terminal fragment of Sba1p interacts with the catalytic loop in the Hsp90 middle domain (Fig. 23.8b). Consequently, Hsp90 is fully competent to hydrolyze ATP, which explains why Sba1p cannot completely inhibit the ATPase activity of HSp90. It appears that Sba1p/p23 acts to slow the cycle, perhaps aiding a slow folding step or providing additional time for hormone to bind the steroid hormone receptor protein.

7 NudC Proteins

The archetypal NudC (nuclear distribution) gene from *Aspergillus nidulans* is involved in the maintenance of nuclear migration [60–65]. Three paralogues of NudC exist in vertebrates: NudC, NudC-like (NudCL), and NudC-like 2 (NudCL2) [66–69]. The fourth is a distantly related family member, CML66, and contains a NudC-like domain [70, 71]. The *NudC* gene has been implicated in a number of functions from cell division to the regulation of cytoplasmic dynein, and human NudC in the migration and proliferation of tumour cells as well as inflammatory responses and thrombopoisis [72]. NudC, which contains a CS domain [73] in common with p23/Sba1p, has also been reported to inhibit the ATPase activity of Hsp90 [74]. However, unlike p23/Sba1p the molecular details have not yet been established.

8 Modulation of the Catalytic Unit of Hsp90 by Aha1

Aha1 is the only potent activator of the Hsp90 ATPase activity that has been described to date [21, 75]. The molecular detail by which the N-terminal domain of Aha1 modulates the catalytic loop of Hsp90 has been determined [75]. The structure shows that the loop is released from its closed to an open state that allows Arg 380 to interact with the bound ATP [75] and thus promote ATP hydrolysis (Fig. 23.9). However, full-length Aha1 is significantly more potent than the N-terminal domain of Aha1 alone [75]. It is thought that the C-terminal domain of Aha1 binds between the dimerized N-terminal domains of Hsp90 [76], in a similar fashion to the Sba1p interaction. Thus, it is possible that the C-terminal domain of Aha1 might promote N-terminal dimerization or the association of the N- and Middle-domains of Hsp90. Further biochemical and structural work is required to categorically show the exact mechanism.

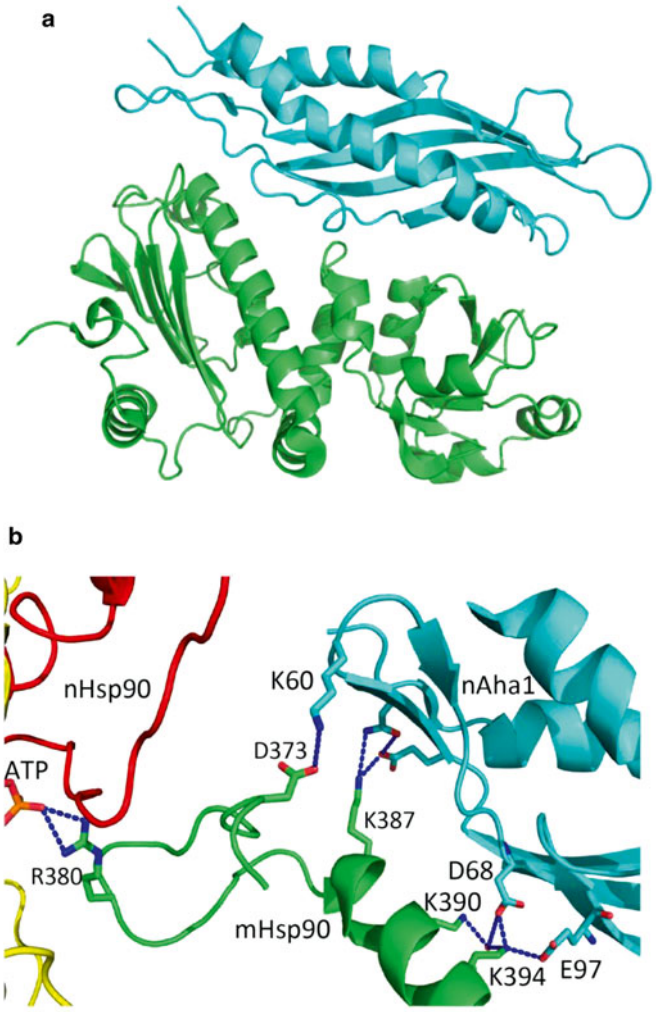

Fig. 23.9 Regulation of the ATPase activity of Hsp90 by Aha1. (**a**) The interaction between the N-terminal domain of Aha1 (*cyan*) and the middle domain of Hsp90 (*green*). (**b**), Catalytic-loop activation of Hsp90 by the N-terminal domain of Aha1. The interaction of Aha1 (*cyan*) with the middle domain of Hsp90 (*green*) causes the catalytic loop to move to the open active-state. This allows the catalytic Arg 380 of Hsp90 to interact with the ϒ-phosphate of ATP. Hydrogen bonds are shown as *dotted blue lines*

9 Modulation of the Catalytic Unit of Hsp90 by Immunophillins and Client Proteins

The only immunophillin known to influence the ATPase activity of Hsp90 is Cpr6 [21]. However, the stimulation seen was weak and has not been confirmed. FKBP52 was shown to potentiate the activation of GR receptor when hormone levels are

limiting, while the closely related FKBP51 protein blocks potentiation. The activation was found to require both Hsp90 binding and the propyl isomerase activity of FKBP52 [77]. Thus it appears that for FKBP, the efficiency at which GR is activated is increased. Whether this is a common theme for specific client protein-immunophillin combinations is currently unknown and the lack of an immunophillin-Hsp90 structural complex means that the mechanism by which immunophillins act remains unknown. However, it appears that immunophillins may play a role in the progression of Hsp90 complex. For steroid hormone receptors at least, immunophillins enter the Hsp90 complex at an intermediate stage, after Hop binding and prior to p23 stabilization of the complex. Their binding helps to displace HOP and consequently allow ATP and p23 binding. Thus, it appears that they are required to help the complex progress from the early stage to the late stage, where hormone is known to bind the steroid hormone receptor. In this respect they may be acting in a similar fashion to Aha1 in progressing the cycle and thus altering the conformation of the client protein in some way [16, 21]. However, due to the lack of structural and biochemical detail, the exact mechanism remains elusive.

The only client protein known to affect the ATPase activity of Hsp90 is Glucocorticoid receptor. This receptor was found to stimulate the ATPase activity of Hsp90 [78]. However, the glucocorticoid DNA binding domain used in this study was found to be dimeric rather than monomeric, which is the normal state of the receptor when bound to Hsp90. Whether ATPase activation of Hsp90 by client proteins is a common feature of the system is currently unknown.

10 Post-translation Modifications Affecting the ATPase Activity

Post-translational modification of Hsp90 has been extensively covered in a recent review [79]. Mutation of Tyr 24 in yeast (Tyr 38 in humans) to the phosphorylation mimetic glutamate resulted in the inhibition of Hsp90 ATPase activity [80]. In fact Y24E and Y24D as a sole source of Hsp90 in yeast could not support viability probably due to their very low ATPase activity. Furthermore, using Y24F and Y38F mutants it was shown that phosphorylation at these sites was required for productive chaperoning of kinases and for suppression of heat shock factor activity [80]. Thr 22 (yeast) and Thr 36 (human) are also subject to phosphorylation [81, 82]. Thr 22 is critical for stabilization of the catalytic loop in the open active-state, and consequently mutation to a possible phospho-mimetic state (T22E) results in decreased Hsp90 ATPase activity. The T22E mutant was seen to decrease the activation of v-Src and Ste11, enhance the activation of glucocorticoid receptor [82] and increase the stability of the cystic transmembrane regulator. This appeared to be mirrored in the human system where loss of interaction with v-Src, Raf1, ErbB2, Cdk4 and GR was seen, whereas there was an increase in CFTR protein levels.

The phosphorylation of Hsp90 may not just affect its ATPase activity, but may also influence its association with co-chaperones and client proteins. In a Swe1Δ

background with Y24F and wild-type Hsp90, the association of Aha1 was abolished [80]. In contrast, Sba1p interaction was reduced while Cdc37^{p50} and Sti1p/Hop association was unaffected, and these results were similarly reflected for the human Y38F mutant. For T22A and T22E mutants the association of Aha1 was completely abolished, while interaction with Cdc37^{p50} was reduced. In contrast, the association with Sti1p and Sba1p were unaffected. Again the human T38A and T38E mutants reflected these results. Thus, Aha1 interaction was completely diminished, Cdc37^{p50} was mainly reduced with the T38E mutant, Hop association was unaffected while p23 interaction was slightly reduced.

Apart from phosphorylation other post-translational modifications of Hsp90 have also been reported [83–88]. While acetylation of yeast Hsp90 Lys 294 has been shown, its effects on the ATPase activity remain unknown [85]. However, K294Q and K294A show altered interactions with co-chaperones suggesting that the chaperone cycle of Hsp90, and therefore its ATP turnover would be affected. S-nitrosylation of Cys 598 in human Hsp90α has been shown to inhibit its ATPase activity. Similarly the equivalent yeast mutation, A577I or A557N, also inhibited the ATPase activity of Hsp90.

11 Conclusions

Hsp90 is a molecular chaperone that is responsible for the activation of an eclectic set of client proteins that are often key signalling protein [1, 89–92]. Its role in cancer progression and disease are now well documented [6–13]. The chaperone cycle is central to the activation of client protein and is driven by the binding and hydrolysis of ATP. Because of the very diverse structural proteins that Hsp90 deals with it has evolved a number of orthologues that are tuned to their own specific needs. The orthologues of Hsp90 show differing kinetic properties, and for some, are regulated by their own set of co-chaperones that allow the efficient activation of their specific client proteins. These appear to fall into four broad classes. The first are involved in loading the client protein onto the Hsp90 platform. Perhaps the simplest is Cdc37^{p50}, which binds both the client protein and Hsp90 directly. Sgt1 also appears to be able to deliver client protein to Hsp90 complex by binding the client and Hsp90 directly. In contrast, Hop/Sti1p delivers clients by acting as a scaffold between Hsp90 and Hsp70-client protein complex. Others rely on a more complex set of proteins such as the R2TP complex.

The second class of co-chaperone appears to be those that aid progression of the chaperone cycle from the loading stage. These include proteins such as immunophillins and Aha1. Yet another class is represented by p23/Sba1p, which helps to stabilize protein complex. Perhaps Rar1 could also be viewed as a co-chaperone that stabilizes client-Hsp90 complex as it itself does not bind client but helps to stabilize the association of Sgt1 bound with client protein. The final class of co-chaperone represents proteins that bring about changes to the chaperone cycle by post-translational modification of the Hsp90 complex. These are likely to include proteins

such as PP5 and CHIP [93, 94], which modify the cycle and fate of individual client proteins as required by the cell.

However, a further layer of complexity is present in that specific co-chaperones are often associated with the activation of a particular client protein class. For example $Cdc37^{p50}$ is intimately associated with protein kinase delivery to the Hsp90 chaperone machine. In contrast, Hop appears to be involved in steroid hormone receptor activation, while Sgt1 recruits innate immunity receptors. Perhaps the complexity of the R2TP system is a reflection of its recruitment to deliver a number of structurally diverse proteins for activation and maturation. These include RNA polymerase 2 [95, 96], small nucleolar ribonucleoproteins (snoRNPs) [97–100] and phosphatidylinositol-3-kinase-like kinases [2, 3]. p23 has also been seen to associate with a variety of structurally diverse client protein–Hsp90 complexes, such as steroid hormone receptors and telomerase [89, 101–106].

The vast array of client proteins that Hsp90 deals with means that Hsp90 has evolved a number of conformational switches within its structure. This most likely enables the chaperone cycle to be modulated so that it suits the particular client protein's requirement. These switches include an ATP lid, an N-terminal section of structure involved in β-strand exchange and dimerization of the N-terminus, and a catalytic loop found in the middle domain of Hsp90. The advantage of having these switches is that a variety of co-chaperones can regulate Hsp90 at various points through structural changes that occur over the whole of the chaperone cycle. This increases the flexibility and diversity of the Hsp90 chaperone cycle so that Hsp90 is able to deal with its structurally diverse clientele.

References

1. Pearl LH (2005) Hsp90 and Cdc37—a chaperone cancer conspiracy. Curr Opin Genet Dev 15:55–61
2. Horejsi Z, Takai H, Adelman CA et al (2010) CK2 phospho-dependent binding of R2TP complex to TEL2 is essential for mTOR and SMG1 stability. Mol Cell 39:839–850
3. Takai H, Xie Y, de Lange T, Pavletich NP (2010) Tel2 structure and function in the Hsp90-dependent maturation of mTOR and ATR complexes. Genes Dev 24:2019–2030
4. Pratt WB, Morishima Y, Murphy M, Harrell M (2006) Chaperoning of glucocorticoid receptors. Handb Exp Pharmacol 172:111–138
5. Pratt WB (1998) The hsp90-based chaperone system: involvement in signal transduction from a variety of hormone and growth factor receptors. Proc Soc Exp Biol Med 217:420–434
6. Miyata Y, Nakamoto H, Neckers L (2013) The therapeutic target Hsp90 and cancer hallmarks. Curr Pharm Des 19:347–365
7. Workman P, Burrows F, Neckers L, Rosen N (2007) Drugging the cancer chaperone HSP90: combinatorial therapeutic exploitation of oncogene addiction and tumor stress. Ann N Y Acad Sci 1113:202–216
8. Wang X, Chen M, Zhou J, Zhang X (2014) HSP27, 70 and 90, anti-apoptotic proteins, in clinical cancer therapy (Review). Int J Oncol 45:18–30
9. Ou JR, Tan MS, Xie AM et al (2014) Heat shock protein 90 in Alzheimer's disease. BioMed Res Int 2014:796869. doi:10.1155/2014/796869

10. Pratt WB, Gestwicki JE, Osawa Y, Lieberman AP (2014) Targeting Hsp90/Hsp70-based protein quality control for treatment of adult onset neurodegenerative diseases. Annu Rev Pharmacol Toxicol. doi:10.1146/annurev-pharmtox-010814-124332
11. Ebrahimi-Fakhari D, Saidi LJ, Wahlster L (2013) Molecular chaperones and protein folding as therapeutic targets in Parkinson's disease and other synucleinopathies. Acta Neuropathol Commun 1:79. doi:10.1186/2051-5960-1-79
12. Ramdhave AS, Patel D, Ramya I et al (2013) Targeting heat shock protein 90 for malaria. Mini Rev Med Chem 13:1903–1920
13. Geller R, Taguwa S, Frydman J (2012) Broad action of Hsp90 as a host chaperone required for viral replication. Biochim Biophys Acta 1823:698–706. doi:10.1016/j.bbamcr.2011.11.007
14. Altieri DC, Stein GS, Lian JB, Languino LR (2012) TRAP-1, the mitochondrial Hsp90. Biochim Biophys Acta 1823:767–773
15. Marzec M, Eletto D, Argon Y (2012) GRP94: An HSP90-like protein specialized for protein folding and quality control in the endoplasmic reticulum. Biochim Biophys Acta 1823:774–787
16. Prodromou C (2012) The 'active life' of Hsp90 complexes. Biochim Biophys Acta 1823:614–623
17. Jackson SE (2013) Hsp90: structure and function. Top Curr Chem 328:155–240
18. Nagy PD, Wang RY, Pogany J et al (2011) Emerging picture of host chaperone and cyclophilin roles in RNA virus replication. Virology 411:374–382
19. Ali MM, Roe SM, Vaughan CK et al (2006) Crystal structure of an Hsp90-nucleotide-p23/Sba1 closed chaperone complex. Nature 440:1013–1017
20. Zhang M, Kadota Y, Prodromou C et al (2010) Structural basis for assembly of Hsp90-Sgt1-CHORD protein complexes: implications for chaperoning of NLR innate immunity receptors. Mol Cell 39:269–281
21. Panaretou B, Siligardi G, Meyer P et al (2002) Activation of the ATPase activity of hsp90 by the stress-regulated cochaperone aha1. Mol Cell 10:1307–1318
22. Prodromou C, Roe SM, O'Brien R et al (1997) Identification and structural characterisation of the ATP/ADP binding site in the Hsp90 molecular chaperone. Cell 90:65–75
23. Graf C, Stankiewicz M, Kramer G, Mayer MP (2009) Spatially and kinetically resolved changes in the conformational dynamics of the Hsp90 chaperone machine. EMBO J 28:602–613
24. Hessling M, Richter K, Buchner J (2009) Dissection of the ATP-induced conformational cycle of the molecular chaperone Hsp90. Nat Struct Mol Biol 16:287–293
25. Prodromou C, Panaretou B, Chohan S et al (2000) The ATPase cycle of Hsp90 drives a molecular 'clamp' via transient dimerization of the N-terminal domains. EMBO J 19:4383–4392
26. Weikl T, Muschler P, Richter K et al (2000) C-terminal Regions of Hsp90 are Important for Trapping the Nucleotide during the ATPase Cycle. J Mol Biol 303:583–592
27. Frey S, Leskovar A, Reinstein J, Buchner J (2007) The ATPase cycle of the endoplasmic chaperone Grp94. J Biol Chem 282:35612–35620
28. Leskovar A, Wegele H, Werbeck ND et al (2008) The ATPase cycle of the mitochondrial Hsp90 analog Trap1. J Biol Chem 283:11677–11688
29. Ratzke C, Berkemeier F, Hugel T (2012) Heat shock protein 90's mechanochemical cycle is dominated by thermal fluctuations. Proc Natl Acad Sci U S A 109:161–166
30. Smith DF (1993) Dynamics of heat-shock protein 90-progesterone receptor binding and the disactivation loop model for steroid receptor complexes. Mol Endocrinol 7:1418–1429
31. Smith DF, Toft DO (1993) Steroid receptors and their associated proteins. Mol Endocrinol 7:4–11
32. Smith DF, Whitesell L, Nair SC et al (1995) Progesterone receptor structure and function altered by geldanamycin, an Hsp90 binding agent. Mol Cell Biol 15:6804–6812
33. Prodromou C, Siligardi G, O'Brien R et al (1999) Regulation of Hsp90 ATPase activity by tetratricopeptide repeat (TPR)-domain co-chaperones. EMBO J 18:754–762

34. Gross M, Hessefort S (1996) Purification and characterisation of a 66-kDa protein from rabbit reticulocyte lysate which promotes the recycling of hsp70. J Biol Chem 271: 16833–16841
35. Johnson BD, Schumacher RJ, Ross ED, Toft DO (1998) Hop modulates hsp70/hsp90 interactions in protein folding. J Biol Chem 273:3679–3686
36. Li J, Richter K, Buchner J (2011) Mixed Hsp90-cochaperone complexes are important for the progression of the reaction cycle. Nat Struct Mol Biol 18:61–66
37. Siligardi G, Hu B, Panaretou B et al (2004) Co-chaperone regulation of conformational switching in the Hsp90 ATPase cycle. J Biol Chem 279(50):51989–51998
38. Siligardi G, Panaretou B, Meyer P et al (2002) Regulation of Hsp90 ATPase activity by the co-chaperone Cdc37p/p50cdc37. J Biol Chem 277(23):20151–20159
39. Polier S, Samant RS, Clarke PA et al (2013) ATP-competitive inhibitors block protein kinase recruitment to the Hsp90-Cdc37 system. Nat Chem Biol 9:307–312. doi:10.1038/nchembio.1212
40. Bandhakavi S, McCann RO, Hanna DE, Glover CV (2003) A positive feedback loop between protein kinase CKII and Cdc37 promotes the activity of multiple protein kinases. J Biol Chem 278:2829–2836
41. Shao J, Prince T, Hartson SD, Matts RL (2003) Phosphorylation of serine 13 is required for the proper function of the Hsp90 co-chaperone, Cdc37. J Biol Chem 278:38117–38120
42. Miyata Y, Nishida E (2004) CK2 controls multiple protein kinases by phosphorylating a kinase-targeting molecular chaperone, Cdc37. Mol Cell Biol 24:4065–4074
43. Vaughan CK, Gohlke U, Sobott F et al (2006) Structure of an Hsp90-Cdc37-Cdk4 complex. Mol Cell 23:697–707
44. Xu W, Mollapour M, Prodromou C et al (2012) Dynamic tyrosine phosphorylation modulates cycling of the HSP90-P50(CDC37)-AHA1 chaperone machine. Mol Cell 47:434–443
45. Scheufler C, Brinker A, Bourenkov G et al (2000) Structure of TPR domain-peptide complexes: critical elements in the assembly of the Hsp70-Hsp90 multichaperone machine. Cell 101:199–210
46. Southworth DR, Agard DA (2011) Client-loading conformation of the Hsp90 molecular chaperone revealed in the cryo-EM structure of the human Hsp90:Hop complex. Mol Cell 42:771–781
47. Richter K, Muschler P, Hainzl O et al (2003) Sti1 is a noncompetitive inhibitor of the Hsp90 ATPase. Binding prevents the N-terminal dimerization reaction during the ATPase cycle. J Biol Chem 278:10328–10333
48. Roe SM, Ali MM, Meyer P et al (2004) The Mechanism of Hsp90 regulation by the protein kinase-specific cochaperone p50(cdc37). Cell 116:87–98
49. Zhang M, Boter M, Li K et al (2008) Structural and functional coupling of Hsp90- and Sgt1-centred multi-protein complexes. EMBO J 27(20):2789–2798
50. Kadota Y, Amigues B, Ducassou L et al (2008) Structural and functional analysis of SGT1-HSP90 core complex required for innate immunity in plants. EMBO Rep 9:1209–1215
51. Rodrigo-Brenni MC, Thomas S, Bouck DC, Kaplan KB (2004) Sgt1p and Skp1p modulate the assembly and turnover of CBF3 complexes required for proper kinetochore function. Mol Biol Cell 15:3366–3378. doi:10.1091/mbc.E03-12-0887
52. Boter M, Amigues B, Peart J et al (2007) Structural and functional analysis of SGT1 reveals that its interaction with HSP90 is required for the accumulation of Rx, an R protein involved in plant immunity. Plant Cell 19:3791–3804. doi:10.1105/tpc.107.050427
53. Catlett MG, Kaplan KB (2006) Sgt1p is a unique co-chaperone that acts as a client adaptor to link Hsp90 to Skp1p. J Biol Chem 281:33739–33748
54. Eckert K, Saliou JM, Monlezun L et al (2010) The Pih1-Tah1 cochaperone complex inhibits Hsp90 molecular chaperone ATPase activity. J Biol Chem 285:31304–31312. doi:10.1074/jbc.M110.138263
55. Pal M, Morgan M, Phelps SE et al (2014) Structural basis for phosphorylation-dependent recruitment of Tel2 to Hsp90 by Pih1. Structure 22:805–818

56. Weaver AJ, Sullivan WP, Felts SJ et al (2000) Crystal structure and activity of human p23, a heat shock protein 90 co- chaperone. J Biol Chem 275:23045–23052
57. Freeman BC, Felts SJ, Toft DO, Yamamoto KR (2000) The p23 molecular chaperones act at a late step in intracellular receptor action to differentially affect ligand efficacies. Genes Dev 14:422–434
58. Young JC, Hartl FU (2000) Polypeptide release by Hsp90 involves ATP hydrolysis and is enhanced by the co-chaperone p23. EMBO J 19:5930–5940
59. McLaughlin SH, Sobott F, Yao ZP et al (2006) The co-chaperone p23 arrests the Hsp90 ATPase cycle to trap client proteins. J Mol Biol 356:746–758
60. Morris NR (1975) Mitotic mutants of Aspergillus nidulans. Genet Res 26:237–254
61. Morris NR, Xiang X, Beckwith SM (1995) Nuclear migration advances in fungi. Trends Cell Biol 5:278–282
62. Xiang X, Beckwith SM, Morris NR (1994) Cytoplasmic dynein is involved in nuclear migration in Aspergillus nidulans. Proc Natl Acad Sci U S A 91:2100–2104
63. Xiang X, Osmani AH, Osmani SA et al (1995) NudF, a nuclear migration gene in Aspergillus nidulans, is similar to the human LIS-1 gene required for neuronal migration. Mol Biol Cell 6:297–310
64. Willins DA, Xiang X, Morris NR (1995) An alpha tubulin mutation suppresses nuclear migration mutations in Aspergillus nidulans. Genetics 141:1287–1298
65. Beckwith SM, Roghi CH, Morris NR (1995) The genetics of nuclear migration in fungi. Genet Eng 17:165–180
66. Miller BA, Zhang MY, Gocke CD et al (1999) A homolog of the fungal nuclear migration gene nudC is involved in normal and malignant human hematopoiesis. Exp Hematol 27:742–750
67. Matsumoto N, Ledbetter DH (1999) Molecular cloning and characterization of the human NUDC gene. Hum Genet 104:498–504
68. Zhou T, Zimmerman W, Liu X, Erikson RL (2006) A mammalian NudC-like protein essential for dynein stability and cell viability. Proc Natl Acad Sci U S A 103:9039–9044
69. Yang Y, Yan X, Cai Y et al (2010) NudC-like protein 2 regulates the LIS1/dynein pathway by stabilizing LIS1 with Hsp90. Proc Natl Acad Sci U S A 107:3499–3504
70. Garcia-Ranea JA, Mirey G, Camonis J, Valencia A (2002) p23 and HSP20/alpha-crystallin proteins define a conserved sequence domain present in other eukaryotic protein families. FEBS Lett 529:162–167
71. Wang Q, Li M, Wang Y et al (2008) RNA interference targeting CML66, a novel tumor antigen, inhibits proliferation, invasion and metastasis of HeLa cells. Cancer Lett 269:127–138
72. Riera J, Lazo PS (2009) The mammalian NudC-like genes: a family with functions other than regulating nuclear distribution. Cell Mol Life Sci 66:2383–2390
73. Zheng M, Cierpicki T, Burdette AJ et al (2011) Structural features and chaperone activity of the NudC protein family. J Mol Biol 409:722–741
74. Zhu XJ, Liu X, Jin Q et al (2010) The L279P mutation of nuclear distribution gene C (NudC) influences its chaperone activity and lissencephaly protein 1 (LIS1) stability. J Biol Chem 285:29903–29910
75. Meyer P, Prodromou C, Liao C et al (2004) Structural basis for recruitment of the ATPase activator Aha1 to the Hsp90 chaperone machinery. EMBO J 23:511–519
76. Retzlaff M, Hagn F, Mitschke L et al (2010) Asymmetric activation of the hsp90 dimer by its cochaperone aha1. Mol Cell 37:344–354
77. Riggs DL, Roberts PJ, Chirillo SC et al (2003) The Hsp90-binding peptidylprolyl isomerase FKBP52 potentiates glucocorticoid signaling in vivo. EMBO J 22:1158–1167
78. McLaughlin SH, Smith HW, Jackson SE (2002) Stimulation of the weak ATPase activity of human Hsp90 by a client protein. J Mol Biol 315:787–798
79. Mollapour M, Neckers L (2012) Post-translational modifications of Hsp90 and their contributions to chaperone regulation. Biochim Biophys Acta 1823:648–655
80. Mollapour M, Tsutsumi S, Donnelly AC et al (2010) Swe1Wee1-dependent tyrosine phosphorylation of Hsp90 regulates distinct facets of chaperone function. Mol Cell 37:333–343

81. Mollapour M, Tsutsumi S, Kim YS et al (2011) Casein kinase 2 phosphorylation of Hsp90 threonine 22 modulates chaperone function and drug sensitivity. Oncotarget 2:407–417
82. Mollapour M, Tsutsumi S, Truman AW et al (2011) Threonine 22 phosphorylation attenuates Hsp90 interaction with cochaperones and affects its chaperone activity. Mol Cell 41:672–681
83. Yu X, Guo ZS, Marcu MG et al (2002) Modulation of p53, ErbB1, ErbB2, and Raf-1 expression in lung cancer cells by depsipeptide FR901228. J Natl Cancer Inst 94:504–513
84. Yang Y, Rao R, Shen J et al (2008) Role of acetylation and extracellular location of heat shock protein 90alpha in tumor cell invasion. Cancer Res 68:4833–4842
85. Scroggins BT, Robzyk K, Wang D et al (2007) An acetylation site in the middle domain of Hsp90 regulates chaperone function. Mol Cell 25(1):151–159. doi:10.1016/j.molcel.2006.12.008
86. Kovacs JJ, Murphy PJ, Gaillard S et al (2005) HDAC6 regulates Hsp90 acetylation and chaperone-dependent activation of glucocorticoid receptor. Mol Cell 18:601–607
87. Martinez-Ruiz A, Villanueva L, Gonzalez de Orduna C et al (2005) S-nitrosylation of Hsp90 promotes the inhibition of its ATPase and endothelial nitric oxide synthase regulatory activities. Proc Natl Acad Sci U S A 102:8525–8530
88. Retzlaff M, Stahl M, Eberl HC et al (2009) Hsp90 is regulated by a switch point in the C-terminal domain. EMBO Rep 10:1147–1153
89. Holt SE, Aisner DL, Baur J et al (1999) Functional requirement of p23 and Hsp90 in telomerase complexes. Genes Dev 13:817–826
90. Garcia-Cardena G, Fan R, Shah V et al (1998) Dynamic activation of endothelial nitric oxide synthase by Hsp90. Nature 392:821–824
91. Pratt WB, Toft DO (2003) Regulation of signaling protein function and trafficking by the hsp90/hsp70-based chaperone machinery. Exp Biol Med (Maywood) 228:111–133
92. Park SJ, Suetsugu S, Takenawa T (2005) Interaction of HSP90 to N-WASP leads to activation and protection from proteasome-dependent degradation. EMBO J 24:1557–1570
93. Zhang M, Windheim M, Roe SM et al (2005) Chaperoned ubiquitylation--crystal structures of the CHIP U box E3 ubiquitin ligase and a CHIP-Ubc13-Uev1a complex. Mol Cell 20:525–538
94. Das AK, Cohen PTW, Barford D (1998) The structure of the tetratricopeptide repeats of protein phosphatase 5: implications for TPR-mediated protein-protein interactions. EMBO J 17:1192–1199
95. Boulon S, Pradet-Balade B, Verheggen C et al (2010) HSP90 and its R2TP/Prefoldin-like cochaperone are involved in the cytoplasmic assembly of RNA polymerase II. Mol Cell 39:912–924
96. Forget D, Lacombe AA, Cloutier P et al (2010) The protein interaction network of the human transcription machinery reveals a role for the conserved GTPase RPAP4/GPN1 and microtubule assembly in nuclear import and biogenesis of RNA polymerase II. Mol Cell Proteomics 9:2827–2839
97. Gonzales FA, Zanchin NI, Luz JS, Oliveira CC (2005) Characterization of Saccharomyces cerevisiae Nop17p, a novel Nop58p-interacting protein that is involved in Pre-rRNA processing. J Mol Biol 346:437–455
98. Kurokawa M, Zhao C, Reya T, Kornbluth S (2008) Inhibition of apoptosome formation by suppression of Hsp90beta phosphorylation in tyrosine kinase-induced leukemias. Mol Cell Biol 28:5494–5506
99. Samarsky DA, Fournier MJ, Singer RH, Bertrand E (1998) The snoRNA box C/D motif directs nucleolar targeting and also couples snoRNA synthesis and localization. EMBO J 17:3747–3757
100. Kakihara Y, Houry WA (2012) The R2TP complex: discovery and functions. Biochim Biophys Acta 1823:101–107
101. Hu J, Toft D, Anselmo D, Wang X (2002) In vitro reconstitution of functional hepadnavirus reverse transcriptase with cellular chaperone proteins. J Virol 76(1):269–279

102. Nair SC, Toran EJ, Rimerman RA et al (1996) A pathway of multi-chaperone interactions common to diverse regulatory proteins: estrogen receptor, Fes tyrosine kinase, heat shock transcription factor Hsf1, and the aryl hydrocarbon receptor. Cell Stress Chaperones 1:237–250
103. Felts SJ, Toft DO (2003) p23, a simple protein with complex activities. Cell Stress Chaperones 8:108–113
104. Grad I, McKee TA, Ludwig SM et al (2006) The Hsp90 cochaperone p23 is essential for perinatal survival. Mol Cell Biol 26:8976–8983
105. Lovgren AK, Kovarova M, Koller BH (2007) cPGES/p23 is required for glucocorticoid receptor function and embryonic growth but not prostaglandin E2 synthesis. Mol Cell Biol 27:4416–4430
106. Tanioka T, Nakatani Y, Semmyo N et al (2000) Molecular identification of cytosolic prostaglandin E2 synthase that is functionally coupled with cyclooxygenase-1 in immediate prostaglandin E2 biosynthesis. J Biol Chem 275:32775–32782

Chapter 24
Role of ATPases in Disease Processes

Swatilekha Ghosh and Parimal C. Sen

Abstract In the course of evolution, a number of agents have emerged as carriers of signals that are essential for the correct functioning of cell life. Ca^{2+} is the most versatile of all of them; other messengers are normally committed to the regulation of a single cell function, or at most a few of them. Ca^{2+} instead regulates a plethora of cellular processes, beginning with the origin of new cell life, its growth, proliferation and differentiation and ending with its termination in the process of programmed cell death. Thus, precise regulation of calcium within the cellular compartments is of utmost importance to maintain proper cellular function. Calcium balance is finely regulated within the cell by the coordinated action of the calcium pumps and the channels. As calcium ions play such critical role in regulation of varied cellular functions, malfunction of the calcium pumps is associated with different disease progression. In the present review, we have discussed the properties and functioning of the calcium pumps and also highlighted its association with different malfunction and diseases. This knowledge might be effective in using the calcium pumps as therapeutic targets for drug development in the near future.

Keywords Calcium signalling • Ca^{2+}-transporting proteins • Plasma membrane • Ca^{2+} ATPase • Sarco(endo)plasmic reticulum ATPase • Ca^{2+} pump

1 Introduction

ATPases play a crucial role in regulating chemical gradients across cell membranes, thereby maintaining cellular homeostasis and are vital for all kingdoms of life. There are different types of ATPase which differ in function, structure and the types of ions they transport. F-ATPases (F1FO-ATPases) are found mainly in the mitochondria, chloroplasts and bacterial plasma membranes and are the prime

S. Ghosh • P.C. Sen (✉)
Division of Molecular Medicine, Bose Institute,
P-1/12, Calcutta Improvement Trust Scheme VII M, Kolkata 700 054, India
e-mail: parimalsen.boseinst@gmail.com

S. Chakraborti, N.S. Dhalla (eds.), *Regulation of Ca^{2+}-ATPases,V-ATPases and F-ATPases*, Advances in Biochemistry in Health and Disease 14,
DOI 10.1007/978-3-319-24780-9_24

producers of ATP, using the proton gradient generated by oxidative phosphorylation (mitochondria) or photosynthesis (chloroplasts). V-ATPases (vacuolar ATPases) are primarily found in eukaryotic vacuoles, catalysing ATP hydrolysis to transport solutes and lower pH in organelles like proton pump of lysosome. P-ATPases are found in bacteria, in fungi and in eukaryotic plasma membranes and organelles and function to transport a variety of different ions across membranes. The P-ATPases are distinct from the others in forming an intermediate phosphorylated intermediate during their ion transport cycle [1]. The Na+ K+ ATPase is located in the plasma membrane and maintains plasma membrane potential in eukaryotic cells. The pump drives three sodium ions out of the cell and two potassium ions into the cell against stiff concentration gradient. The activity of this enzyme is required for diverse functions like maintenance of cellular osmotic balance, generation of neuronal membrane potentials and intestinal handling of solutes [2]. The pump comprises of two subunits, a 100 kDa α-subunit and a heavily glycosylated 55 kDa β-subunit. The H+ K+ ATPase acidifies the stomach, and the heavy metal ATPases are required for trace metal homeostasis. The Ca^{2+} ATPases are crucial for muscle function and transport of calcium into secretory vesicles. Thus, a clear understanding of the functioning of these ATPases might be important to determine their role in regulation of various life processes. Dysfunction of these ATPases has been found to be associated with different disease development in humans and other animals. Malfunction of the Na+ K+ ATPase has been found to be associated with various neurodegenerative disorders [3, 4] and henceforth provide an important target for medicinal research. On the other hand, Ca^{2+} ATPase dysfunction has been found to be associated with Brody's disease, heart failure and even cancer [5]. Thus, it can be stated that ATPases play a vital role regulation of disease development and progression. In the present review, we have discussed the role of ATPases, especially the Ca^{2+} ATPase, regarding their structure, function, mutations and role in disease progression and subsequently consider that this information might be useful to target these ATPases for extensive biological research for application in biotechnology and medicine.

2 Calcium Signalling

In the furnaces of the stars, the elements have been evolved from hydrogen. When oxygen and neon captured successive α-particles, the element calcium was born. Roughly ten billion years later, cell membranes began to parse the world by charge, temporarily and locally defying relentless entropy. To adapt with the changing environments, cells must signal, and signalling requires messengers whose concentration varies with time. Filling this role, calcium ions (Ca^{2+}) have come to rule cell signalling. Among the other signalling molecules, Ca^{2+} is the most versatile: other messengers are normally committed to the regulation of a single cell function, or at most a few of them. Ca^{2+} instead regulates a very large list of essential functions, beginning with the origin of new cell life at fertilisation

and ending with its termination in the process of programmed cell death. Between these two events, Ca^{2+} transmits signals to functions as fundamental as gene transcription, muscle contraction (and motility in general), secretion (including that of neurotransmitters) and generation of fuels in various metabolic pathways [6]. The involvement of Ca^{2+} in so many fundamental cell processes naturally demands its efficient and precise control. Ca^{2+} signalling requires the strict cooperation among the different cellular compartments and organelles, being in fact a highly sophisticated way of communication to maintain homeostasis and functionality of the whole cell. Failure of the mechanisms devoted to maintain Ca^{2+} homeostasis (Fig. 24.1) produces generalised Ca^{2+} alterations, in turn producing rough cell damage, without involving specific signalling, i.e. when strong, Ca^{2+} alterations cause cell death by necrosis [7–11]. The concentration of Ca^{2+} in the cytosol is normally maintained at 100–200 nM. To maintain this cytosolic Ca^{2+} level, evolution has created numerous proteins that are able to bind Ca^{2+} and/or to transport it out of the cytosol, reducing its free concentration in the surrounding environment

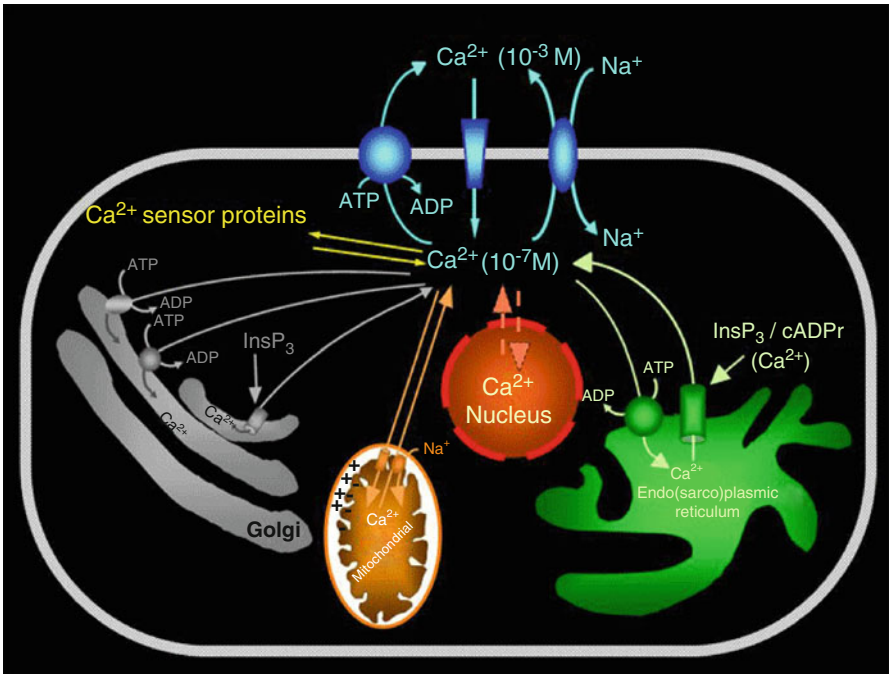

Fig. 24.1 Representation of cellular calcium homeostasis in a single cell. Extracellular Ca^{2+} enters the cell through plasma membrane Ca^{2+} channels and leaves the cell using Ca^{2+} pumps and Na+/Ca^{2+} exchangers. Endoplasmic reticulum (ER) is a major site for sequestered Ca^{2+} ions. Ca^{2+} is accumulated in intracellular stores by means of Ca^{2+} pumps and released by inositol 1,4,5- trisphosphate (IP3) via IP3 receptors (IP3R) and by cyclic adenosine diphosphate ribose (cADPr) via ryanodine receptors (RyR) (Adapted from Carafoli et al. (2004) Biol Res 34: 497–505). Reproduced with permission from Biol Res

to the limits that are necessary for its signalling function. This has been made possible by the peculiar coordination chemistry of Ca^{2+}, which allows it to be bound by cavities of irregular shapes, such as those that are normally offered by the tertiary structure of proteins. The proteins that bind or interact with Ca^{2+} can be divided into two broad classes—those that only bind or interact with Ca^{2+} to regulate its concentration (Ca^{2+}-buffering and Ca^{2+}-transporting proteins) and those that bind Ca^{2+} to decode its signal (Ca^{2+} sensors) thereby by critically regulating the cellular homeostasis.

3 Ca^{2+}-Buffering and Ca^{2+}-Transporting Proteins

Proteins that regulate the intracellular Ca^{2+} concentration can reside in the cytosol, in organelles, or they can be intrinsic to membranes. Soluble Ca^{2+}-buffering proteins in the cytosol and organelles are acidic proteins that can store large amounts of Ca^{2+}. As a rule, they have a low Ca^{2+} affinity. An important Ca^{2+}-buffering protein in the sarco(endo)plasmic reticulum is calsequestrin, and an interesting Ca^{2+}-buffering protein in the cytosol is parvalbumin, which belongs to the family of EF-hand Ca^{2+}-sensor proteins [6].

Membrane-intrinsic proteins can create and shape Ca^{2+} signals by functioning as channels, ATPases (pumps) or exchangers that transport Ca^{2+} across membranes. Ca^{2+} channels mediate the penetration of Ca^{2+} into the cell and its exit from the sarco(endo)plasmic reticulum. In the plasma membrane, Ca^{2+} channels are gated by voltage changes, by ligand interactions or by a poorly understood mechanism that is linked to the emptying of intracellular Ca^{2+} stores. The voltage-gated channels have several subtypes [12] of which the L-type, which is the target of widely used Ca^{2+} antagonists, is the best characterised. The most important ligand-operated channels are gated by neurotransmitters, and, among them, the glutamate-operated channels are the most intensively studied [13] In the sarco(endo)plasmic reticulum, the opening of Ca^{2+} channels is regulated by Ca^{2+} itself—the process of Ca^{2+}-induced Ca^{2+} release [14]—but this opening also requires ligands like inositol-(1,4,5)-trisphosphate ($Ins(1,4,5)P_3$) [15] or, in selected cell types, another endogenous ligand, cyclic ADP ribose [16], which releases Ca^{2+} through channels that are known as ryanodine receptors. Both the plasma membrane and the inner mitochondrial membrane also contain Na+/Ca^{2+} exchangers (NCX and MNCX, respectively) that export Ca^{2+} from the cell and the mitochondrial matrix [17], respectively. The high capacity plasma-membrane NCX is particularly active in excitable cells, which demand the periodic ejection of large Ca^{2+} loads. The less well-characterised mitochondrial exchanger (MNCX) is also particularly active in excitable cells. Whereas the plasma-membrane NCX exchanges three Na+ per one Ca^{2+} and therefore responds both to the Na+ and Ca^{2+} transmembrane gradients and to the voltage difference across the plasma membrane, MNCX seems to exchange two Na+ per one Ca^{2+}.

4 Calcium Pumps

4.1 The Plasma Membrane Ca^{2+}ATPase (PMCA)

The Ca^{2+} ATPases of the plasma membrane (PMCA pumps) export Ca^{2+} from all eukaryotic cells (Fig. 24.2). The PMCA pumps belong to the superfamily of P-type pumps, which are so defined because they conserve temporarily the energy of the ATP due to the hydrolysis of a phosphorylated aspartic acid residue [1]. The structure of the PMCA pump, modelled on the template of the SERCA pump, repeats as expected the essential properties of the latter. Even if subtler differences, e.g. the presence of only one instead of two Ca^{2+}-binding sites, are not revealed by the modelling, it is reasonable to assume that the molecular transitions that occur in the SERCA pump also occur in the PMCA pump. However, the PMCA pump differs from the SERCA pump in a number of more significant aspects, which will only be understood when its own three-dimensional structure is solved.

In mammals, four genes encode four basic PMCA pumps: isoforms 1 and 4 are widely distributed in tissues and until shortly ago had been considered housekeeping isoforms. Recently, however, the housekeeping role has come into question, particularly for PMCA4, as this isoform has been found to have specific Ca^{2+} signalling roles not exclusively linked to its Ca^{2+} exporting function [18]. As for PMCA1, it is expressed in the tissues of the embryo from the earliest times of development. At variance with PMCA 1 and 4, PMCA 2 and 3 are expressed in a very limited number of tissues, the most important being the nervous system (the mammary gland also expresses significant amounts of PMCA2 and skeletal muscles of PMCA3).

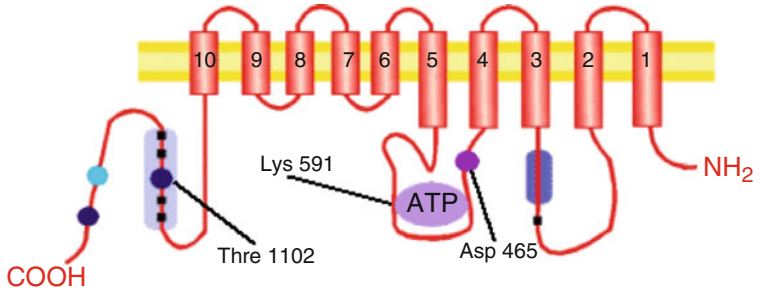

Fig. 24.2 Structure of the PMCA pump showing the ten transmembrane domains with the ATP-binding site (Monteith GR, Roufogalis BD. (1995) Cell Calcium 18: 459–470). Reproduced with permission from Elsevier

4.2 *The Sarco(endo)plasmic Reticulum Ca^{2+} ATPase (SERCA)*

The sarcoplasmic reticulum (SR) is an intracellular membranous network found in muscle cells. Although it is analogous to the endoplasmic reticulum (ER), it can store millimolar amounts of calcium. It serves to initiate muscle contraction by releasing calcium through the ryanodine receptors (RyR) into the cytosol and facilitates muscle relaxation by active reuptake of calcium by the sarco(endo)-plasmic reticulum Ca^{2+} ATPase (SERCA) (Fig. 24.3). The SERCA pump serves a dual function: (1) to cause muscle relaxation by lowering the cytosolic calcium and (2) at the same time to restore SR calcium store necessary for muscle contraction. Alterations in Ca^{2+} transport and intracellular calcium levels have been implicated in many types of pathological processes, including cancer and heart disease [19].

The SERCA pump has ten transmembrane spanning domains, and its three-dimensional structure has been recently solved at atomic resolution in both the Ca^{2+}-bound and the Ca^{2+}-free states [20, 21]. The structure has permitted the identification of the location of all important domains, including the ATP-binding site and the catalytic aspartyl residue, which are located in a large globular domain protruding between the fourth and fifth transmembrane sectors. All ten transmembrane domains and the cavity that forms the Ca^{2+}-binding sites have also

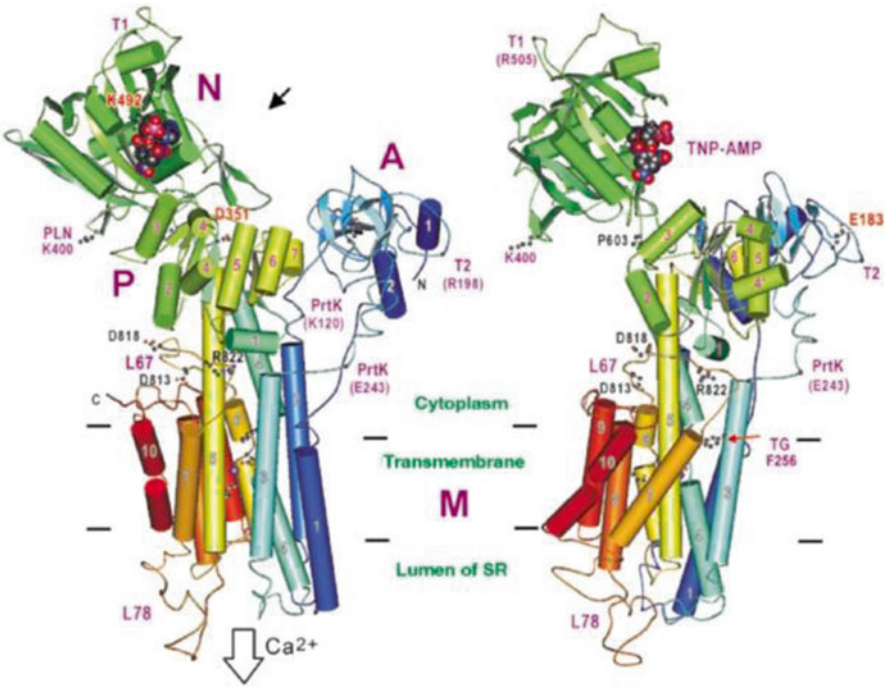

Fig. 24.3 Structure of the SERCA pump (Toyoshima et al. (2000) Nature 405: 647–655). Reproduced with permission from Nature

been located. In human, SERCA-type Ca^{2+} pumps are encoded by three genes (ATP2A1-3), which generate multiple isoforms of SERCA, i.e. SERCAla, b, SERCA2a–c and SERCA3a–f by developmental or tissue-specific alternative splicing [22]. The changes in the expression pattern of the variants during development and tissue differentiation indicate that each isoform is adapted to specific functions. Whereas SERCA1 is expressed in skeletal muscle, and the SERCA2a isoform is found in cardiac muscle, SERCA2b expression is ubiquitous. In several cell types such as T lymphocytes, myeloid cells, megakaryocytes and platelets, as well as in colon and gastric epithelial cells, SERCA2b is co-expressed with SERCA3 [23–30]. Whereas the basic biochemical function (i.e. calcium transport into the ER) is shared among SERCA2 and SERCA3 isoenzymes, the calcium affinity of SERCA3 is significantly inferior to that of SERCA2b [31–35]. The co-expression of SERCA2b and SERCA3 within the same cell is thus involved in the fine regulation of the calcium uptake characteristics of the ER in a cell type-dependent manner.

4.3 The Calcium Transport Cycle by the Ca^{2+} ATPases

A simplified reaction scheme forms the basic line which is valid for all the Ca^{2+} ATPases. Originally, the scheme envisaged two conformational states of the pumps: the E1 state, in which the enzyme has high Ca^{2+} affinity and interacts with Ca^{2+} at one side of the membrane, and the E2 state, in which the lower Ca^{2+} affinity leads to the release of the ion at the opposite side [36]. More recent structural work on the SERCA pump has increased the complexity of the conformational transitions that occur during the catalytic cycle. Upon binding of Ca^{2+}, a series of structural changes occur that involve both the protruding cytoplasmic sector and the transmembrane domains, permitting the phosphorylation of the catalytic D-residue by the γ-phosphate of ATP. The dissociation of Ca^{2+} from the enzyme follows the transition of the high Ca^{2+} affinity E1~P(Ca^{2+}) enzyme to the lower affinity E2~P enzyme, the hydrolysis of which then regenerates the Ca^{2+}-free E2 ATPase, completing the catalytic cycle (Fig. 24.4).

4.4 Calcium Signalling in Cell Survival and Death

Ca^{2+} deregulation is a consequence of many different insults that end up altering Ca^{2+} homeostasis, causing an increased damage to cells; for this reason, it may be defined as an "intrinsic stress", meaning that it is auto-induced by the cells as a consequence of an extrinsic stress of a different nature. Recent developments have emphasised the central role of the calcium ion in the regulation of cell death. Similar to the conductor of an orchestra, it can activate distinct parts of the cell death programme, which can then function alone or in conjunction with other subprogrammes to kill the cell [37].

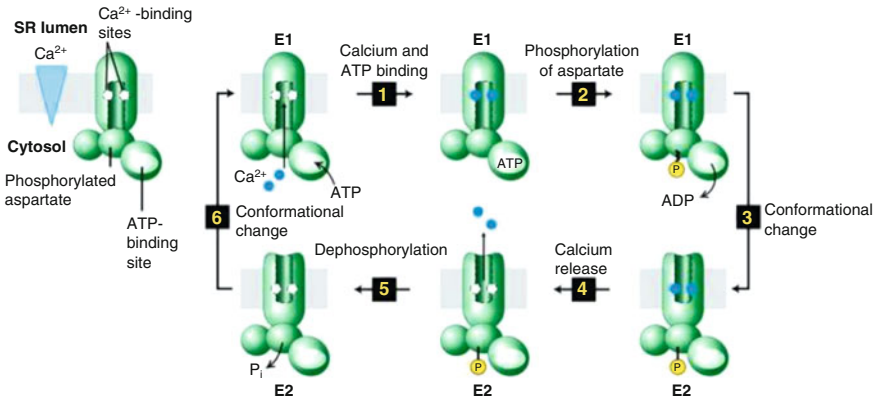

Fig. 24.4 A simplified reaction scheme of the transport cycle of Ca^{2+} ATPases showing the two conformational states of the pump associated with the binding and release of calcium (Molecular Cell Biology, 6th edition). Reproduced with permission from the publisher

However, on the other hand, Ca^{2+} is involved in pro-survival or anti-apoptotic pathways, such as the activation of protein kinase C, whose many isoforms play pivotal roles in coordinating survival cell responses [38]. This versatility of the calcium signalling is emphasised by growing evidence that Ca^{2+} controls cellular processes as diverse as cell proliferation and the neuronal plasticity that is responsible for learning and memory. But at any moment, any of these orderly signalling events can be switched to activate a programme that leads to cell death—a big challenge for the future is to understand how Ca^{2+} suddenly transforms from a signal for life to a signal of death. Thus, exploitation of the calcium signalling pathways may be very important in discerning various disease processes and also for searching better therapeutic options for targeted therapies.

5 Calcium Pumps and Diseases

5.1 The SERCA)Pump in Disease Process

Two major human genetic disorders, Brody's and Darier's disease, have been known to be associated with mutations in the SERCA pump genes. Brody's disease is a rare recessive muscular condition characterised by impaired relaxation, painless cramps and stiffness following exercise [39]. Reduced activity of the SERCA pump is mainly thought to be associated with this disorder. In fact, decreased SERCA1 expression has been observed in many cases [40, 41]. However, some compensation is provided by ectopic expression of SERCA2 or SERCA3 and/or by Ca^{2+} removal from the cytosol by the PMCA pump. Darier's disease (or Darier-White's disease)

is a rare autosomal dominant skin disorder characterised by loss of adhesion between epidermal cells and abnormal keratinisation [42]. The disease is characterised by keratotic papules in seborrheic areas of the skin and in the skin flexures which can then form confluent plaques. Reports suggest that more than 130 mutations of the SERCA2 gene have been observed in human patients with this disease. Apart from the above-mentioned genetic disorders, dysfunction of the SERCA pump is associated with other disease progression also. The SERCA pump has been observed to be functionally decreased in nearly all models of heart failure [43], and a decline in the SR Ca^{2+} transport and SR Ca^{2+} content have been also detected in animal heart failure models.

Although heterogeneity in the expression level of the SERCA pump has been observed in failing hearts, it is generally accepted that a reduction of the SERCA2a protein levels (and/or activity) plays a role in the development of the failure condition. The SERCA) pump has been also suggested to exhibit a strong relationship with cancer. Accumulating evidence indicates that the altered cellular homeostasis of Ca^{2+} may be involved in the abnormal cell proliferation that is a hallmark of the malignant transformation. The matter has aspects that are seemingly paradoxical: on one hand, the increase of cytosolic Ca^{2+}, e.g. by hyperactivated plasma membrane channels, promotes cell proliferation. On the other hand, situations of Ca^{2+} overload trigger apoptotic death pathways. A remodelling of Ca^{2+} homeostasis is thus increasingly considered important in the process of malignant transformation [22], and it is thus only to be expected that alterations of the expression and/or function of Ca^{2+} regulators such as the Ca^{2+} pumps should have a role in the process of tumorigenesis.

The SERCA) pump has been also associated with different types of cancer. Colon carcinoma cells have shown a prominent decline in the SERCA3 expression level, whereas the SERCA3 expression is normally elevated in healthy colonic epithelium. Thus, decreased SERCA3 expression can be considered as an early marker of colon cancer. SERCA3 expression has been also found to be prominently declined in early breast tumours, whereas normal breast acinar tissue showed distinctly elevated SERCA3 expression. Thus, it can be stated that SERCA3 expression is inversely co-related with tumour differentiation and aggressiveness of breast cancer. Thus, it can be suggested that the SERCA pump may act as a potential target for cancer treatment and therapeutics. SERCA pumps have also shown to play important role in the lymphocyte activation process. Downregulation of SERCA3 expression has been found to be associated with T-lymphocyte activation [44]. The expression of the SERCA3 pump in pancreatic β-cells and the association of sequence variants of the pump with type II diabetes [45] as well as the finding that SERCA pumping activity was impaired in diabetic rats model [46] have suggested that the SERCA3 pump could be involved in the Ca^{2+} deregulation linked to the onset of diabetes and that it could contribute to the genetic susceptibility to type II diabetes. Thus, drugs designed to target the SERCA pump may play a significant role in providing benefits against a diverse group of diseases and also provides a major platform for intensive research in disease progression and drug development.

5.2 The PMCA Pump and Disease Processes

Several genetic pathologies have been known to be related with the PMCA pump dysfunction. Among them, the only spontaneous human disease related to a PMCA pump defect so far identified is a form of hereditary deafness [47, 48]. The defect involves the PMCA2 pump, which is abundantly expressed in the brain, particularly in the Purkinje cell of the cerebellum and in the hair cells of the Corti organ of the inner ear. The role of the PMCA pump in the hearing process becomes more evident from the fact that PMCA2 knocked out mice showed impairment in the hearing process. In addition to the inner ear, PMCA2 is also prominently expressed in other brain regions, and its dysfunction is also correlated with neurodegenerative disorders. Transcriptional downregulation of PMCA2 in brains of mouse models has been found to be associated with Huntington disease [49]. The dysfunction may contribute to the alteration of the homeostasis of Ca^{2+} which is widely considered to have a role in the aetiology of the disease. PMCA2 null mice have also shown significant reduction in the spinal cord motor neuron [50] and abnormalities in Purkinje neurons [51]. PMCA2 is also prominently expressed in the epithelial cells of the mammary gland and has an important role in the regulation of the concentration of Ca^{2+} in the milk. Recent report suggests that a missense mutation in the PMCA3 gene is associated with human pancreatic cancer [52]. The PMCA4 gene has rather housekeeping functions, but dysfunction of the PMCA4 gene has been found to be associated with male infertility. Sperms of PMCA4 null mice were still able to fertilise eggs [53] but were incapable of achieving hyperactivated motility and thus could not reach them to perform the fertilisation. PMCA4 also plays important roles in maintenance of cardiac physiology. Ablation of the PMCA4 gene has been found to be associated with cardiac hypertrophy. The PMCA pump also has a specific role in regulation of calcium homeostasis in β cells of the pancreas [54, 55] and thus also plays a unique role in diabetes. Thus, mostly all defects associated with the PMCA pump involve alteration of cellular calcium homeostasis, and targeting the PMCA pump provides a unique approach to targeted therapy against many disease types.

6 Conclusion

The calcium pumps play major roles in regulation of cellular homeostasis of calcium. As calcium acts as a ubiquitous cellular signal molecule, it regulates a varied type of cellular process, and thus alterations in this calcium homeostasis are often associated with disorders. As highlighted above, the SERCA pump has been found to be associated with disease like cancer, whereas malfunctioning of the PMCA pump leads to cardiovascular disorders, diabetes, infertility, cancer, etc. (Fig. 24.5). Thus, detailed study about the involvement of the calcium pumps in disease processes and also identification of small molecules to target these pumps

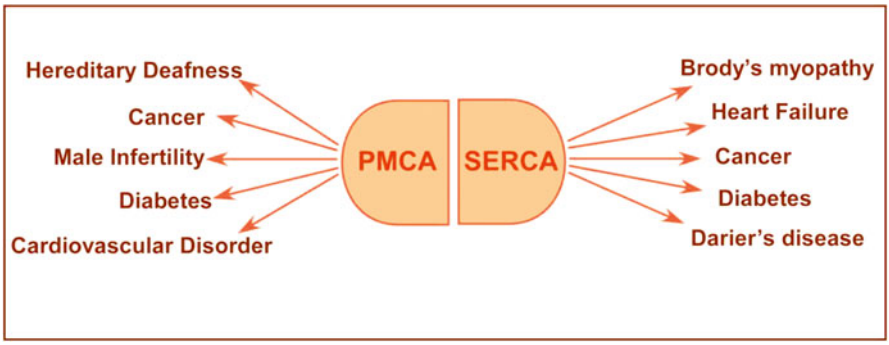

Fig. 24.5 Schematic representation of the diseases associated with calcium pumps (PMCA and SERCA) disorders

might be useful to provide improved therapeutic options for many key diseases. In the present study, we have provided an overview of the importance of calcium signalling in life processes and also highlighted its importance in disease development. Enhancement of research in this field might prove successful for development of therapeutic agents in the future.

Acknowledgements The authors sincerely acknowledge Department of Atomic Energy for financial assistance and Bose Institute for providing facilities.

References

1. Pedersen PL, Carafoli E (1987) Ion motive ATPases. I. Ubiquity, properties, and significance to cell function. Trends Biochem Sci 12:146–150
2. Sen PC (2011) Endogenous modulators in the regulation of ion transporting enzymes: structure, function, interactions, recent advancements and future perspectives. Adv Biol Chem 1:74–92
3. de Carvalho AP, Sweadner KJ, Penniston JT et al (2004) Mutations in the Na^+/K^+ - ATPase alpha3 gene ATP1A3 are associated with rapid-onset dystonia parkinsonism. Neuron 43:169–175
4. Riant F, De FM, Aridon P et al (2005) ATP1A2 mutations in 11 families with familial hemiplegic migraine. Hum Mutat 26:281
5. Brini M, Carafoli E (2009) Calcium pumps in health and disease. Physiol Rev 89:1341–1378
6. Carafoli E (2003) The calcium-signalling saga: tap water and protein crystals. Nat Rev Mol Cell Biol 4:326–332
7. Kaiser N, Edelman IS (1977) Calcium dependence of glucocorticoid induced lymphocytolysis. Proc Natl Acad Sci U S A 74:638–642
8. Kaiser N, Edelman IS (1978) Calcium dependence of ionophore A23187 induced lymphocyte cytotoxicity. Cancer Res 38:3599–3603
9. de Leiris J, Boucher F (1990) Ischemic myocardial cell necrosis: calcium overload or oxygen free-radicals? Rev Port Cardiol 9:153–158
10. Richter C (1993) Pro-oxidants and mitochondrial Ca2+: their relationship to apoptosis and oncogenesis. FEBS Lett 325:104–107

11. Qian T, Herman B, Lemasters JJ (1999) The mitochondrial permeability transition mediates both necrotic and apoptotic death of hepatocytes exposed to Br- A23187. Toxicol Appl Pharmacol 154:117–125
12. Tsein RW (1987) Multiple types of calcium channels in excitable cells. Soc Gen Physiol Ser 41:167–187
13. Watkins JC (1989) NMDA agonists and antagonists. In: Watkins JC, Collingridge GL (eds) NMDA receptor. Oxford Univ. Press, New York, 1–17
14. Endo M (1970) Calcium induced release of calcium from the sarcoplasmic reticulum of skinned skeletal muscle fibres. Nature 228:34–36
15. Streb H (1983) Release of Ca2+ from a nonmitochondrial intracellular store in pancreatic acinar cells by inositol-1,4,5-trisphosphate. Nature 306:67–69
16. Lee HC (1997) Mechanisms of calcium signaling by cyclic ADP ribose and NAADP. Physiol Rev 77:1133–1164
17. Carafoli E (1974) The release of calcium from heart mitochondria by sodium. J Mol Cell Cardiol 6:361–371
18. Cartwright EJ, Oceandy D, Neyses L (2009) Physiological implications of the interaction between the plasma membrane calcium pump and nNOS. Pflugers Arch 457:665–671
19. Periasamy M, Kalyanasundaram A (2006) SERCA pump isoforms: their role in calcium transport and disease. Muscle Nerve 35:430–442
20. MacLennan DH, Loke J, Odermatt A, Carafoli E, Klee CB (eds) (1999) Calcium as a cellular regulator. Oxford Univ Press, New York, pp 610–630
21. Sakuntabhai A (1999) Mutations in ATP2A2, encoding a Ca2+ pump, cause Darier disease. Nat Genet 21:271–277
22. Monteith GR, Mc Andrew D, Faddy HM et al (2007) Calcium and cancer: targeting Ca2+ transport. Nat Rev Cancer 7:519–530
23. Brouland JP, Gélébart P, Kovàcs T et al (2005) The loss of sarco/endoplasmic reticulum calcium transport ATPase 3 expression is an early event during the multistep process of colon carcinogenesis. Am J Pathol 167:233–242
24. Papp B, Brouland JP, Gélébart P et al (2004) Endoplasmic reticulum calcium transport ATPase expression during differentiation of colon cancer and leukaemia cells. Biochem Biophys Res Commun 322:1223–1236
25. Gélébart P, Martin V, Enouf J et al (2003) Identification of a new SERCA2 splice variant regulated during monocytic differentiation. Biochem Biophys Res Commun 303:676–684
26. Gélébart P, Kovàcs T, Brouland JP et al (2002) Expression of endomembrane calcium pumps in colon and gastric cancer cells. Induction of SERCA3 expression during differentiation. J Biol Chem 277:26310–26320
27. Launay S, Giannì M, Kovàcs T et al (1999) Lineage-specific modulation of calcium pump expression during myeloid differentiation. Blood 93:4395–4405
28. Launay S, Bobe R, Lacabaratz-Porret C et al (1997) Modulation of endoplasmic reticulum calcium pump expression during T lymphocyte activation. J Biol Chem 272:10746–10750
29. Wuytack F, Papp B, Verboomen H et al (1994) A sarco/endoplasmic reticulum Ca(2+)-ATPase 3-type Ca2+ pump is expressed in platelets, in lymphoid cells, and in mast cells. J Biol Chem 269:1410–1416
30. Papp B, Enyedi A, Kovàcs T et al (1991) Demonstration of two forms of calcium pumps by thapsigargin inhibition and radioimmunoblotting in platelet membrane vesicles. J Biol Chem 266:14593–14596
31. Wuytack F, Raeymaekers L, Missiaen L (2002) Molecular physiology of the SERCA and SPCA pumps. Cell Calcium 32:279–305
32. Dode L, Vilsen B, Van Baelen K et al (2002) Dissection of the functional differences between sarco(endo)plasmic reticulum Ca2+-ATPase (SERCA) 1 and 3 isoforms by steady-state and transient kinetic analyses. J Biol Chem 277:45579–45591
33. Poch E, Leach S, Snape S et al (1998) Functional characterization of alternatively spliced human SERCA3 transcripts. Am J Physiol 275:1449–1458

34. Wuytack F, Dode L, Baba-Aissa F et al (1995) The SERCA3- type of organellar Ca2+ pumps. Biosci Rep 15:299–306
35. Chandrasekera PC, Kargacin ME, Deans JP et al (2009) Determination of apparent calcium affinity for endogenously expressed human sarco/endoplasmic reticulum calcium ATPase isoform, SERCA3. Am J Physiol Cell Physiol 296(5):C1105–C1114
36. De Meis L, Vianna AL (1979) Energy interconversion by the Ca2+- dependent ATPase of the sarcoplasmic reticulum. Annu Rev Biochem 48:275–292
37. Orrenius S, Zhivotovsky B, Nicotera P (2003) Regulation of cell death: The calcium–apoptosis link. Nat Rev 4:522–565
38. Miyawaki H, Zhou X, Ashraf M (1996) Calcium preconditioning elicits strong protection against ischemic injury via protein kinase C signaling pathway. Circ Res 79:137–146
39. BrodyI A (1969) Muscle contracture induced by exercise. A syndrome attributable to decreased relaxing factor. N Engl J Med 281:187–192
40. Benders AA, Veerkamp JH, Oosterhof A, Jongen PJ, Bindels RJ, Smit LM, Busch HF, Wevers RA (1994) Ca2+ homeostasis in Brody's disease. A study in skeletal muscle and cultured muscle cells and the effects of dantrolene an verapamil. J Clin Invest 94:741–748
41. Karpati G, Charuk J, Carpenter S, Jablecki C, Holland P (1986) Myopathy caused by a deficiency of Ca2_-adenosine triphosphatase in sarcoplasmic reticulum (Brody's disease). Ann Neurol 20:38–49
42. Burge SM, Wilkinson JD (1992) Darier-White disease: a review of the clinical features in 163 patients. J Am Acad Dermatol 27:40–50
43. Kranias EG, Bers DM (2007) Calcium and cardiomyopathies. Subcell Biochem 45:523–537
44. Ghosh S, Adhikary A, Chakraborty S et al (2012) Nifetepimine, a dihydropyrimidone, ensures CD4+ T cell survival in tumor micro-environment by maneuvering Sarco(endo)plasmic reticulum Ca2+ ATPase (SERCA). J Biol Chem 287:32881–32896
45. Varadi A, Lebel L, Hashim Y et al (1999) Sequence variants of the sarco(endo)plasmic reticulum Ca(2+)- transport ATPase 3 gene (SERCA3) in Caucasian type II diabetic patients (UK Prospective Diabetes Study 48). Diabetologia 42:1240–1243
46. Levy J, Zhu Z, Dunbar JC (1998) The effect of glucose and calcium on Ca2+- adenosine triphosphatase in pancreatic islets isolated from a normal and a non-insulin-dependent diabetes mellitus rat model. Metabolism 47:185–189
47. Ficarella R, Di Leva F, Bortolozzi M et al (2007) A functional study of plasma-membrane calcium-pump isoform 2 mutants causing digenic deafness. Proc Natl Acad Sci U S A 104:1516–1521
48. Schultz JM, Yang Y, Caride AJ et al (2005) Modification of human hearing loss by plasma-membrane calcium pump PMCA2. N Engl J Med 352:1557–1564
49. Kuhn A, Goldstein DR, Hodges A et al (2007) Mutant Huntingtin's effects on striatal gene expression in mice recapitulate changes observed in human Huntington's disease brain and do not differ with mutant huntingtin length or wild-type huntingtin dosage. Hum Mol Genet 16:1845–1861
50. Kurnellas MP, Shull GE, Elkabes S (2005) Plasma membrane calcium ATPase deficiency causes neuronal pathology in the spinal cord: a potential mechanism for neurodegeneration in multiple sclerosis and spinal cord injury. FASEB J 19:298–300
51. Kurnellas MP, Li H et al (2007) Molecular alterations in the cerebellum of the plasma membrane calcium ATPase 2 (PMCA2)-null mouse indicate abnormalities in Purkinje neurons. Mol Cell Neurosci 34:178–188
52. Jones S, Zhang X, Parsons DW et al (2008) Core signaling pathways in human pancreatic cancers revealed by global genomic analyses. Science 321:1801–1806
53. Schuh K, Cartwright EJ, Jankevics E et al (2004) Plasma membrane Ca2+ ATPase 4 is required for sperm motility and male fertility. J Biol Chem 279:28220–28226
54. Kamagate A, Herchuelz A, Bollen A et al (2000) Expression of multiple plasma membrane Ca(2+)-ATPases in rat pancreatic islet cells. Cell Calcium 27:231–246
55. Varadi A, Molnar E, Ashcroft SJ (1996) A unique combination of plasma membrane Ca2+-ATPase isoforms is expressed in islets of Langerhans and pancreatic beta-cell lines. Biochem J 314:663–669

Chapter 25
Renal H^+-ATPase Function, Regulation, and Role in Distal Renal Tubular Acidosis

Ira Kurtz, Irina Rogova, Vladimir Turygin, Jingbo Huang, Natalia Abuladze, and Alexander Pushkin

Abstract The kidney plays an important role in systemic acid–base balance by maintaining the blood HCO_3^- concentration within narrow limits. Various H^+/base transport processes and metabolic pathways have evolved that orchestrate in a coordinated fashion, the absorption of the filtered bicarbonate load and the generation of new HCO_3^-. The impairment of either of these processes in the nephron can result in a decrease in the blood HCO_3^- concentration with concomitant metabolic acidosis. In the renal proximal tubule and the collecting duct, secretion of protons by the vacuolar H^+-ATPase is one of the key transport steps involved in both the reclamation of filtered HCO_3^- and the generation of new HCO_3^-. The activity of the vacuolar H^+-ATPase is dynamically regulated by various local and systemic factors. Naturally occurring mutations in specific subunits of the vacuolar H^+-ATPase cause the disease distal renal tubular acidosis.

Keywords Distal renal tubular acidosis • H^+-ATPase • Bicarbonate • Acid–base • Transport

1 Introduction

In spite of the fact that dietary metabolism typically generates a net H^+ load which would in the absence of compensatory mechanisms titrate extracellular and intracellular buffers over time, systemic acid–base parameters are maintained constant [1]. With regard to the most prevalent buffer, the HCO_3^- buffer system, dietary H^+ combines with

I. Kurtz (✉)
Division of Nephrology, David Geffen School of Medicine, UCLA,
7-155 Factor Bldg, 10833 Le Conte Avenue, Los Angeles, CA 90035, USA

Brain Research Institute, UCLA, Los Angeles, CA, USA
e-mail: ikurtz@mednet.ucla.edu

I. Rogova • V. Turygin • J. Huang • N. Abuladze • A. Pushkin
Division of Nephrology, David Geffen School of Medicine, UCLA,
7-155 Factor Bldg, 10833 Le Conte Avenue, Los Angeles, CA 90035, USA

S. Chakraborti, N.S. Dhalla (eds.), *Regulation of Ca^{2+}-ATPases,V-ATPases and F-ATPases*, Advances in Biochemistry in Health and Disease 14,
DOI 10.1007/978-3-319-24780-9_25

HCO_3^- extracellularly and intracellularly where $H^+ + HCO_3^- \rightarrow CO_2 + H_2O$. The kidneys are responsible for the generation and delivery to the renal veins, the required quantity of HCO_3^- to prevent the systemic HCO_3^- concentration from changing [2, 3]. In addition to generating new HCO_3^-, the kidney must absorb essentially all the HCO_3^- from the glomerular filtrate to prevent its loss in the urine [4]. In the proximal tubule, it is estimated that the brush border H^+-ATPase contributes to ~35 % of H^+ secretion and transepithelial bicarbonate absorption [5, 6]. In the collecting duct, H^+ secretion acidifies the urine that results in the titration of luminal NH_3, HPO_4^- creatinine, and other organic anions, and the generation of new intracellular bicarbonate [6].

2 Structural Properties and Regulation of the Vacuolar H^+-ATPase

The vacuolar H^+-ATPase consists of two separate domains: the V_1 cytoplasmic domain (ATP6V1) and the V_o transmembrane domain (Fig. 25.1) [7–10]. The V_1 domain is assembled from eight different subunits, and the four subunits comprise the V_o domain. ATP is hydrolyzed at the B/A subunit interface in the V_1 domain. The V_o domain mediates H^+ translocation between the a and c rings. Various functions in addition to transcellular and organelle H^+ transport have been ascribed in to the vacuolar H^+-ATPase including notch signaling [11], regulation of GTPase activity [12], and modulation of Wnt [13].

In general, several factors are involved in regulating H^+-ATPase activity including: recycling of cytoplasmic H^+-ATPase-containing vesicles, modulation of the interaction between the V_1 and V_o domains [14–18], and potential changes in their coupling efficiency. In the kidney, recycling of vesicles is thought to be an important mechanism for altering the cell surface expression of the H^+-ATPase [19, 20]. Subunits B1, B2, and C are known bind to the actin cytoskeleton [21–23]. RhoA inhibition by depolymerizing actin results in an increase in plasma membrane H^+-ATPase expression [24]. Exocytosis involves direct interaction of the H^+-ATPase with the SNARE complex [25]. Intracellular vesicles coated with H^+-ATPase are involved in recruiting coat proteins to endosomes [26] or directly regulate the recycling process [27]. Whether modulation of the interaction between the V_1 and V_o domains plays an important role in the kidney is unknown.

3 Role of the H^+-ATPase Pump in Proximal Tubule HCO_3^- Transport

Approximately 75 % of the filtered HCO_3^- load is reabsorbed in the proximal tubule. This tubule segment is further divided into convoluted and straight segments that have different capacities to absorb HCO_3^- [28–30]. The absorption of HCO_3^- across the apical membrane is indirect and is mediated by secreted H^+ ions that react with

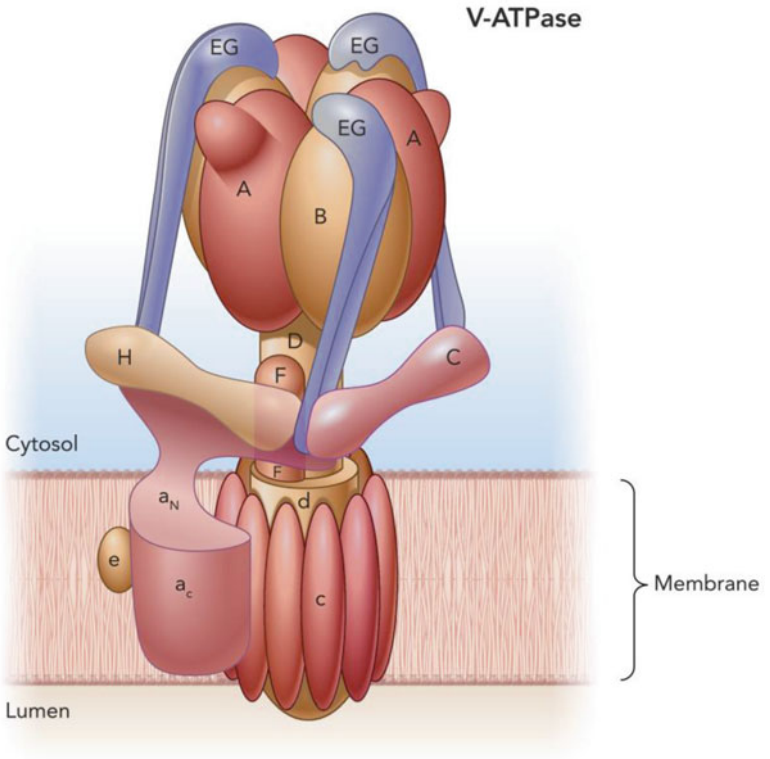

Fig. 25.1 The subunit structure of the vacuolar H+-ATPase. The V_o transmembrane domain is composed of the a, c, d, and e subunits. The V_1 domain is composed of the A, B, C, D, E, F, G, and H subunits (Ref. 7 with permission)

luminal HCO_3^- to form CO_2+H_2O; the latter are absorbed passively across the apical membrane recombining to form H^+ and HCO_3^- intracellularly (Fig. 25.2). HCO_3^- is transported across the basolateral membrane by an electrogenic Na^+–HCO_3^- cotransporter, NBCe1-A [31]. Both membrane-associated and intracellular carbonic anhydrase isoforms play an important role in accelerating proximal tubule transepithelial HCO_3^- absorption [6].

Apical membrane H^+ secretion is mediated predominantly by the Na^+/H^+ exchanger NHE3 and, to a lesser extent, the vacuolar H+-ATPase [31]. Immunohistochemistry studies have demonstrated that the largest expression of the H+-ATPase is at base of the brush border microvilli [32]. In neonates, the NHE8 Na^+/H^+ exchanger accounts for the majority of apical NHE activity. Using the H+-ATPase inhibitor DCCD, Bank et al. were able to block ~21 % of proximal tubule HCO_3^- absorption; however, it was unclear that all activity was inhibited [5]. There are no studies of proximal tubular bicarbonate absorption in mice lacking apical H+-ATPase activity. Conversely, assessing the contribution of NHE3 to bicarbonate absorption is made difficult by the fact that disruption of the NHE3 *Slc9a3* gene

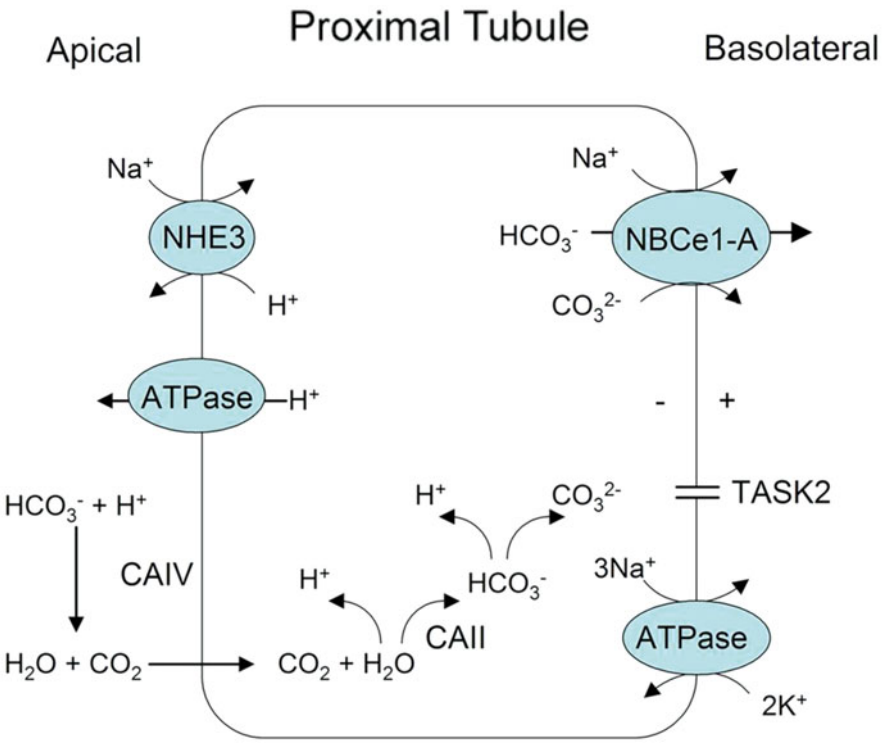

Fig. 25.2 Cell model of acid–base transport processes in the proximal tubule. Approximately 1/3 of apical proton secretion is mediated by the apical H^+-ATPase

may result in compensatory changes in H^+-ATPase activity and other NHE isoforms [33, 34]. In addition to bicarbonate absorption, a further role has been attributed to intracellular H^+-ATPase in the endosomal pathway. Accordingly, in mice lacking the H^+-ATPase a4 subunit, there are additional proximal tubule transport abnormalities that have been reported: accumulation of material in lysosomes, proteinuria, phosphaturia, and abnormal endocytic trafficking [35].

4 Regulation of Proximal Tubule H^+-ATPase Activity

4.1 Cl^- and PKA

In the proximal tubule, Cl^- modulates H^+-ATPase activity [36, 37], and CFTR and ClC-5 may play a role [38]. Fusion of H^+-ATPase-containing vesicles with the plasma membrane is also Cl^- -dependent [39]. The exact Cl^--dependent mechanism is unclear since Cl^- channel activity detected in more distal nephron segments [40–42], has not been demonstrated in the native proximal tubule. Interestingly, the

ClC-5 Cl^- channel colocalizes with the apical H^+-ATPase in type A ICs; however, it may be involved in endocytosis rather than luminal H^+ secretion [42]. In proximal tubule cells, apical H^+-ATPase expression is increased by PKA, whereas AMP-activated protein kinase (AMPK) blocks this effect [43]. GPR4 may also be involved in the signaling pathway as a mechanism for increasing cAMP [44, 45].

5 Role of the H^+-ATPase Pump in Collecting Duct Urinary Acidification

The collecting duct is the region of the nephron ultimately responsible for achieving the minimum urine pH that plays a key role in the process of effective new HCO_3^- generation via the protonation of luminal NH_3, HPO_4^{2-}, creatinine, and other organic anions. The collecting duct segment is subdivided into the cortical collecting duct (CCD), the outer medullary collecting duct (OMCD), and inner medullary collecting ducts (IMCD); each segment having unique apical and basolateral H^+/base transport properties. In the CCD, ~60 % of the cells are principal cells (PCs) that are responsible for Na^+ absorption, K^+ secretion, and water absorption in response to AVP [46]. Approximately 40 % of the cells are intercalated cells (ICs). These cells are subdivided into type A and type B ICs (also named alpha and beta ICs, respectively) (Fig. 25.3) [47–49]. Type A ICs have an apical vacuolar H^+-ATPase and a basolateral AE1, a Cl^-/HCO_3^- exchanger. Type B ICs express the Cl^-/HCO_3^- exchanger pendrin apically and basolateral or diffuse H^+-ATPase expression [32, 50–55]. These IC cell properties are best distinguished and characterized in the rat. Cells not fitting these classic IC cell models have also been described and are called γ or G cells [56, 57] and non-A non-B ICs [58, 59]. In the OMCD, there is a lumen-positive transepithelial voltage due to electrogenic apical H^+ secretion by type A ICs with basolateral HCO_3^- efflux mediated by the AE1 coupled to Cl^- recycling [60]. Cl^- enters the lumen paracellularly driven by the positive luminal transtubular potential. In the IMCD, species differences exist. Specifically, the rat IMCD secretes H^+ via an undefined Na^+-independent mechanism [61, 62]; however, unlike type A ICs, IMCD cells lack staining for the H^+-ATPase. There is no evidence for luminal H^+ secretion in the rabbit IMCD [63].

6 Regulation of Collecting Duct H^+-ATPase Activity

6.1 Acid–Base Status, Ions, Hormones, and Prostaglandins

During respiratory acidosis, an increase in pCO_2 stimulates vesicles containing H^+-ATPase that fuse with the plasma membrane; the process is inhibited by colchicine [64]. It is currently thought that in collecting duct ICs, soluble adenylyl cyclase (sAC) senses the changes in intracellular pH [65]. Accordingly, intracellular HCO_3^- modulates cAMP activity resulting in PKA phosphorylation that may involve the A subunit

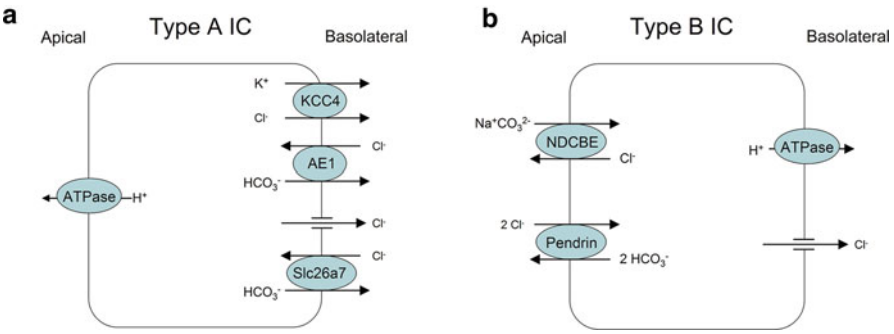

Fig. 25.3 Cell models of acid–base transport processes in the type A intercalated cell (**a**) and type B intercalated cell (**b**). Type A intercalated cells secrete H^+, whereas type B intercalated cells secrete bicarbonate. These cells differ with regard to the specific membrane targeting of the H^+-ATPase

and changes in membrane H^+-ATPase expression [65–69]. Signaling through PKC doesn't appear to be involved [44, 65–67, 70].

An increase in apical membrane PC Na^+ transport in the CCD without concomitant charge compensation by transported anions (particularly in the presence of aldosterone) results in an increased transepithelial voltage [71, 72]. In this setting, the apical membrane of type A ICs depolarizes due to circular intraepithelial current loops creating an increased driving for enhanced H^+ secretion. Accordingly, as has been shown in the $OMCD_{os}$ [73], blocking ENaC in the apical membrane of CCD PCs would be predicted to hyperpolarize the apical membrane of ICs leading to decreased electrogenic H^+ secretion and HCO_3^- absorption [74] and a voltage-dependent hyperkalemic dRTA. K^+ is also thought to modulate collecting duct H^+/base transport although its direct role is difficult to demonstrate because, clinically, disorders of K^+ balance are often accompanied by changes in aldosterone levels and acid–base abnormalities that can independently modulate tubule transport. K^+ depletion is associated with increased apical H^+-ATPase expression, basolateral AE1, basolateral *Slc26a7* [75, 76], and increased collecting duct H^+-K^+-ATPase activity [77]. In the OMCD, H^+-ATPase activity is significantly enhanced by Ca^{2+} (5.0 mM) and the CaSR agonist neomycin [78]. It has been hypothesized that increased luminal Ca^{2+} concentration in the DCT and collecting duct could stimulate H^+-ATPase activity lowering urinary pH and preventing stone formation [78].

The (pro)renin receptor, (P)RR, colocalizes in the collecting duct [79] and is an accessory protein of the H^+-ATPase [80]. When prorenin binds to (P)RR, renin-angiotensin activity is induced. H^+-ATPase activity and (P)RR are required for activation of ERK1/2 via prorenin [79]. H^+-ATPase activation by angiotensin II and aldosterone is also dependent on ERK1/2 [81]. (P)RR appears to be required for both prorenin-dependent and prorenin-independent activation of the H^+-ATPase [82]; however, its role in vivo remains unclear. The effect of angiotensin II on collecting duct H^+/base transport is complex and species-dependent. In the rabbit CCD, angiotensin II increases HCO_3^- secretion [83] and type B IC H^+-ATPase activity in

the mouse CNT and CCD [84]. In rat, HCO_3^- absorption is increased [85]. In the mouse, angiotensin II stimulates the plasma membrane expression of type A IC H^+-ATPase [86, 87], and type B IC HCO_3^- secretion is secondarily increased [54]. Angiotensin II stimulates the plasma membrane insertion of cytoplasmic H^+-ATPase-containing vesicles [81, 84, 87]. Following angiotensin II binding to the AT1 receptors, PKC signaling is involved [81]. In the OMCD, HCO_3^- absorption is decreased by angiotensin II [88].

Mineralocorticoids stimulate luminal H^+ secretion in the collecting duct. In the CCD, mineralocorticoids indirectly depolarize the apical membrane of type A ICs inducing an increase in H^+ secretion via stimulation of PC ENaC Na^+ transport [89]. In both the CCD and $OMCD_{is}$, mineralocorticoids also have a direct effect on type IC H^+-ATPase transport [71, 90]. Mineralocorticoids also stimulate H^+ secretion in the rat IMCD [91]. Acutely aldosterone stimulates collecting duct H^+ secretion non-genomically through MAPK kinase, Gαq, PKC, Ca^{2+}, and ERK1/2 [92, 93]. More prolonged aldosterone exposure increases H^+-ATPase membrane expression [92]. In the absence of aldosterone signaling, patients have hyperkalemic dRTA [94]. In vasopressin receptor $V1a^{-/-}$ mice that develop type 4 RTA, fludrocortisone appears to ameliorate the acidosis by increasing H^+-K^+-ATPase and RhCG expression associated with enhanced urinary ammonium excretion and decrease H^+-ATPase expression [95]. In vivo ET-1 administration increases acidification in the DCT by stimulating H^+ secretion and by decreasing HCO_3^- secretion (following HCO_3^- loading) [96], and inhibition of the ET_B receptor blocks aldosterone-induced stimulation of H^+ secretion [97]. H^+-ATPase inactivation in type B ICs induces PGE2 release via Ca^{2+}-coupled purinergic receptor activation [98]. In the $OMCD_{is}$, PGE_2 inhibits HCO_3^- absorption [99].

7 Isolated Familial Distal RTA (dRTA): Mutations in H^+-ATPase Subunits

Isolated familial dRTA is caused by mutations in CAII [100–103], AE1 [104–110], and specific H^+-ATPase subunits. In general, patients with dRTA have a urine pH that is elevated in comparison to controls on a similar diet. In addition, they can have decreased urinary ammonium excretion, hypercalciuria with or without calcium phosphate stones, and nephrocalcinosis [100]. Patients are often hypokalemic with an elevated fractional excretion of potassium [100].

Karet et al. first described patients with mutations in the *ATP6V1B1* gene encoding the H^+-ATPase B1 subunit who had autosomal recessive dRTA and sensorineural hearing loss [111]. The patients have nephrocalcinosis with hypokalemia and may have rickets and hypercalciuria. Their hearing loss is typically sensorineural; however, a conductive component can be present with enlarged vestibular aqueducts [112]. Mutations in the *ATP6V0A1* gene encoding the a4 subunit were also reported by Karet et al. The patients had dRTA, normal hearing, hypokalemia, and nephrocalcinosis and may have hypercalciuria [113]. Subsequent studies showed that

patients with *ATP6V0A1* gene mutations may have hearing loss [114–116]. Depending on the specific mutation, impaired collecting duct H^+-ATPase activity may be due to impaired pump function, abnormal pump assembly, abnormal targeting to the plasma membrane, and loss of interaction with the enzyme phosphofructokinase-1(PFK-1) [117–119]. $B1^{-/-}$ mice do not have dRTA, and it has been hypothesized that in patients with homozygous B1 subunit, unlike in mice, adaptive formation of B2 subunit containing H^+-ATPase transporters fails to occur [120, 121]. Mutations in the a4 subunit also cause autosomal recessive hypokalemic dRTA [122]. It has been suggested based on studies in $a4^{-/-}$ mice that ATP6V0A4 gene mutations in patients cause both proximal and distal acidification defects [35, 123]. Loss of the a4 subunit has the additional effect of downregulating other H^+-ATPase subunits, thereby potentially perturbing the overall assembly of the H^+-ATPase [35]. In a separate context, $Fox1^{-/-}$ mice lacking the transcription factor Fox1 have loss of the a4 subunit in addition to other key H^+/base transporters including pendrin and AE1 [124, 125].

8 Conclusions

In the renal proximal tubule and the collecting duct, the vacuolar H^+-ATPase in concert with other transport proteins plays a role in overall renal modulation of systemic acid–base chemistry such that despite the fact that the average human diet typically generates a net acid load, the pH of blood is maintained at approximately 7.4. In this regard, the vacuolar H^+-ATPase helps contribute to two key functions in the kidney: (1) reabsorption of filtered HCO_3^-, thereby preventing its urinary excretion, and (2) generating new HCO_3^- to compensate for the loss of HCO_3^- resulting from metabolic H^+ production and HCO_3^- consumption in the urea cycle. H^+-ATPase activity is regulated in specific nephron segments by factors that alter its intrinsic function and/or membrane expression. The disease distal renal tubular acidosis (dRTA) resulting from mutations in specific H^+-ATPase subunits demonstrates its essential role in the renal regulation of system acid–base balance.

Acknowledgment The preparation of this article was supported in part by funds from the NIH (R01-DK077162), the Allan Smidt Charitable Fund, the Factor Family Foundation, and the Arvey Foundation.

References

1. Kurtz I, Maher T, Hulter HN et al (1983) Effect of diet on plasma acid–base composition in normal humans. Kidney Int 24:670–680
2. Halperin ML, Kamel KS (1990) Ammonium metabolism: emphasis on energy considerations. Miner Electrolyte Metab 16:277–282
3. Kurtz I, Dass PD, Cramer S (1990) The importance of renal ammonia metabolism to whole body acid–base balance: a reanalysis of the pathophysiology of renal tubular acidosis. Miner Electrolyte Metab 16:331–340

4. Relman AS, Lennon EJ, Lemann J Jr (1961) Endogenous production of fixed acid and the measurement of the net balance of acid in normal subjects. J Clin Invest 40:1621–1630
5. Bank N, Aynedjian HS, Mutz BF (1989) Proximal bicarbonate absorption independent of Na^+-H^+ exchange: effect of bicarbonate load. Am J Physiol 256:F577–F582
6. Kurtz I (2014) Molecular mechanisms and regulation of urinary acidification. Compr Physiol 4:1737–1774
7. Breton S, Brown D (2013) Regulation of luminal acidification by the V-ATPase. Physiology (Bethesda) 28:318–329
8. Cipriano DJ, Wang Y, Bond S et al (2008) Structure and regulation of the vacuolar ATPases. Biochim Biophys Acta 1777:599–604
9. Forgac M (2007) Vacuolar ATPases: rotary proton pumps in physiology and pathophysiology. Nat Rev Mol Cell Biol 8:917–929
10. Wagner CA, Finberg KE, Breton S et al (2004) Renal vacuolar H^+-ATPase. Physiol Rev 84:1263–1314
11. Yan Y, Denef N, Schupbach T (2009) The vacuolar proton pump, V-ATPase, is required for notch signaling and endosomal trafficking in Drosophila. Dev Cell 17:387–402
12. Hosokawa H, Dip PV, Merkulova M et al (2013) The N termini of a-subunit isoforms are involved in signaling between vacuolar H^+-ATPase (V-ATPase) and cytohesin-2. J Biol Chem 288:5896–5913
13. Cruciat CM, Ohkawara B, Acebron SP et al (2010) Requirement of prorenin receptor and vacuolar H^+-ATPase-mediated acidification for Wnt signaling. Science 327:459–463
14. Diakov TT, Kane PM (2010) Regulation of vacuolar proton-translocating ATPase activity and assembly by extracellular pH. J Biol Chem 285:23771–23778
15. Kane PM (1995) Disassembly and reassembly of the yeast vacuolar H^+-ATPase in vivo. J Biol Chem 270:17025–17032
16. Kane PM (2012) Targeting reversible disassembly as a mechanism of controlling V-ATPase activity. Curr Protein Pept Sci 13:117–123
17. Moriyama Y, Nelson N (1989) Cold inactivation of vacuolar proton-ATPases. J Biol Chem 264:3577–3582
18. Voss M, Schmidt R, Walz B et al (2009) Stimulus-induced translocation of the protein kinase A catalytic subunit to the apical membrane in blowfly salivary glands. Cell Tissue Res 335:657–662
19. Brown D, Paunescu TG, Breton S et al (2009) Regulation of the V-ATPase in kidney epithelial cells: dual role in acid–base homeostasis and vesicle trafficking. J Exp Biol 212: 1762–1772
20. Madsen KM, Tisher CC (1984) Response of intercalated cells of rat outer medullary collecting duct to chronic metabolic acidosis. Lab Invest 51:268–276
21. Chen SH, Bubb MR, Yarmola EG et al (2004) Vacuolar H^+-ATPase binding to microfilaments: regulation in response to phosphatidylinositol 3-kinase activity and detailed characterization of the actin-binding site in subunit B. J Biol Chem 279:7988–7998
22. Holliday LS, Lu M, Lee BS et al (2000) The amino-terminal domain of the B subunit of vacuolar H^+-ATPase contains a filamentous actin binding site. J Biol Chem 275:32331–32337
23. Vitavska O, Wieczorek H, Merzendorfer H (2003) A novel role for subunit C in mediating binding of the H^+-V-ATPase to the actin cytoskeleton. J Biol Chem 278:18499–18505
24. Shum WW, Da Silva N, Belleannee C et al (2011) Regulation of V-ATPase recycling via a RhoA- and ROCKII-dependent pathway in epididymal clear cells. Am J Physiol Cell Physiol 301:C31–C43
25. Banerjee A, Shih T, Alexander EA et al (1999) SNARE proteins regulate H^+-ATPase redistribution to the apical membrane in rat renal inner medullary collecting duct cells. J Biol Chem 274:26518–26522
26. Merkulova M, Bakulina A, Thaker YR et al (2010) Specific motifs of the V-ATPase a2-subunit isoform interact with catalytic and regulatory domains of ARNO. Biochim Biophys Acta 1797:1398–1409

27. Brown D, Breton S, Ausiello DA et al (2009) Sensing, signaling and sorting events in kidney epithelial cell physiology. Traffic 10:275–284
28. Bernstein H, Atherton LJ, Deen WM (1986) Axial heterogeneity and filtered-load dependence of proximal bicarbonate reabsorption. Biophys J 50:239–252
29. Liu FY, Cogan MG (1984) Axial heterogeneity in the rat proximal convoluted tubule. I. Bicarbonate, chloride, and water transport. Am J Physiol 247:F816–F821
30. Liu FY (1987) Cogan MG (1987) Kinetics of bicarbonate transport in the early proximal convoluted tubule. Am J Physiol 253:F912–F916
31. Kurtz I (2014) NBCe1 as a model carrier for understanding the structure-function properties of Na^+ -coupled SLC4 transporters in health and disease. Pflugers Arch 466(8):1501–1516
32. Brown D, Hirsch S, Gluck S (1988) Localization of a proton-pumping ATPase in rat kidney. J Clin Invest 82:2114–2126
33. Choi JY, Shah M, Lee MG et al (2000) Novel amiloride-sensitive sodium-dependent proton secretion in the mouse proximal convoluted tubule. J Clin Invest 105:1141–1146
34. Wang T, Yang CL, Abbiati T et al (2001) Essential role of NHE3 in facilitating formate-dependent NaCl absorption in the proximal tubule. Am J Physiol Renal Physiol 281:F288–F292
35. Hennings JC, Picard N, Huebner AK et al (2012) A mouse model for distal renal tubular acidosis reveals a previously unrecognized role of the V-ATPase a4 subunit in the proximal tubule. EMBO Mol Med 4:1057–1071
36. Kurtz I (1987) Apical Na^+/H^+ antiporter and glycolysis-dependent H^+-ATPase regulate intracellular pH in the rabbit S3 proximal tubule. J Clin Invest 80:928–935
37. Zimolo Z, Montrose MH, Murer H (1992) H^+ extrusion by an apical vacuolar-type H^+-ATPase in rat renal proximal tubules. J Membr Biol 126:19–26
38. Carraro-Lacroix LR, Lessa LM, Bezerra CN et al (2010) Role of CFTR and ClC-5 in modulating vacuolar H^+-ATPase activity in kidney proximal tubule. Cell Physiol Biochem 26:563–576
39. Malnic G, Geibel JP (2000) Cell pH and H^+ secretion by S3 segment of mammalian kidney: role of H^+-ATPase and Cl^-. J Membr Biol 178:115–125
40. Koeppen BM (1985) Conductive properties of the rabbit outer medullary collecting duct: inner stripe. Am J Physiol 248:F500–F506
41. Koeppen BM (1986) Conductive properties of the rabbit outer medullary collecting duct: outer stripe. Am J Physiol 250:F70–F76
42. Sakamoto H, Sado Y, Naito I et al (1999) Cellular and subcellular immunolocalization of ClC-5 channel in mouse kidney: colocalization with H^+-ATPase. Am J Physiol 277:F957–F965
43. Al-Bataineh MM, Gong F, Marciszyn A et al (2014) Regulation of the proximal tubule vacuolar H+-ATPase by PKA and AMP-activated protein kinase. Am J Physiol Renal Physiol 306(9):F981–F995
44. Gong F, Alzamora R, Smolak C et al (2010) Vacuolar H^+-ATPase apical accumulation in kidney intercalated cells is regulated by PKA and AMP-activated protein kinase. Am J Physiol Renal Physiol 298:F1162–F1169
45. Paunescu TG, Ljubojevic M, Russo LM et al (2010) cAMP stimulates apical V-ATPase accumulation, microvillar elongation, and proton extrusion in kidney collecting duct A-intercalated cells. Am J Physiol Renal Physiol 298:F643–F654
46. O'Neil RG, Hayhurst RA (1985) Functional differentiation of cell types of cortical collecting duct. Am J Physiol 248:F449–F453
47. Madsen KM, Tisher CC (1986) Structural-functional relationships along the distal nephron. Am J Physiol 250:F1–F15
48. Verlander JW, Madsen KM, Tisher CC (1987) Effect of acute respiratory acidosis on two populations of intercalated cells in rat cortical collecting duct. Am J Physiol 253:F1142–F1156
49. Verlander JW, Madsen KM, Tisher CC (1991) Structural and functional features of proton and bicarbonate transport in the rat collecting duct. Semin Nephrol 11:465–477
50. Alper SL, Natale J, Gluck S et al (1989) Subtypes of intercalated cells in rat kidney collecting duct defined by antibodies against erythroid band 3 and renal vacuolar H^+-ATPase. Proc Natl Acad Sci U S A 86:5429–5433

51. Brown D, Hirsch S, Gluck S (1988) An H^+-ATPase in opposite plasma membrane domains in kidney epithelial cell subpopulations. Nature 331:622–624
52. Kim YH, Kwon TH, Frische S et al (2002) Immunocytochemical localization of pendrin in intercalated cell subtypes in rat and mouse kidney. Am J Physiol Renal Physiol 283: F744–F754
53. Milton AE, Weiner ID (1997) Intracellular pH regulation in the rabbit cortical collecting duct A-type intercalated cell. Am J Physiol 273:F340–F347
54. Milton AE, Weiner ID (1998) Regulation of B-type intercalated cell apical anion exchange activity by CO_2/HCO_3. Am J Physiol 274:F1086–F1094
55. Verlander JW, Madsen KM, Low PS et al (1988) Immunocytochemical localization of band 3 protein in the rat collecting duct. Am J Physiol 255:F115–F125
56. Emmons C, Kurtz I (1994) Functional characterization of three intercalated cell subtypes in the rabbit outer cortical collecting duct. J Clin Invest 93:417–423
57. Weiner ID, Weill AE, New AR (1994) Distribution of Cl^-/HCO_3^- exchange and intercalated cells in rabbit cortical collecting duct. Am J Physiol 267:F952–F964
58. Kim J, Kim YH, Cha JH et al (1999) Intercalated cell subtypes in connecting tubule and cortical collecting duct of rat and mouse. J Am Soc Nephrol 10:1–12
59. Madsen KM, Verlander JW, Kim J et al (1991) Morphological adaptation of the collecting duct to acid–base disturbances. Kidney Int Suppl 33:S57–S63
60. Schuster VL, Fejes-Toth G, Naray-Fejes-Toth A et al (1991) Colocalization of H^+-ATPase and band 3 anion exchanger in rabbit collecting duct intercalated cells. Am J Physiol 260: F506–F517
61. Wall SM, Sands JM, Flessner MF et al (1990) Net acid transport by isolated perfused inner medullary collecting ducts. Am J Physiol 258:F75–F84
62. Wall SM, Truong AV, DuBose TD Jr (1996) H^+-K^+-ATPase mediates net acid secretion in rat terminal inner medullary collecting duct. Am J Physiol 271:F1037–F1044
63. Ishibashi K, Sasaki S, Yoshiyama N et al (1987) Generation of pH gradient across the rabbit collecting duct segments perfused in vitro. Kidney Int 31:930–936
64. Schwartz GJ, Al-Awqati Q (1985) Carbon dioxide causes exocytosis of vesicles containing H^+ pumps in isolated perfused proximal and collecting tubules. J Clin Invest 75:1638–1644
65. Paunescu TG, Da Silva N, Russo LM et al (2008) Association of soluble adenylyl cyclase with the V-ATPase in renal epithelial cells. Am J Physiol Renal Physiol 294:F130–F138
66. Pastor-Soler N, Beaulieu V, Litvin TN et al (2003) Bicarbonate-regulated adenylyl cyclase (sAC) is a sensor that regulates pH-dependent V-ATPase recycling. J Biol Chem 278:49523–49529
67. Pastor-Soler NM, Hallows KR, Smolak C et al (2008) Alkaline pH- and cAMP-induced V-ATPase membrane accumulation is mediated by protein kinase A in epididymal clear cells. Am J Physiol Cell Physiol 294:C488–C494
68. Alzamora R, Thali RF, Gong F et al (2010) PKA regulates vacuolar H^+-ATPase localization and activity via direct phosphorylation of the a subunit in kidney cells. J Biol Chem 285:24676–24685
69. Hallows KR, Alzamora R, Li H et al (2009) AMP-activated protein kinase inhibits alkaline pH- and PKA-induced apical vacuolar H^+-ATPase accumulation in epididymal clear cells. Am J Physiol Cell Physiol 296:C672–C681
70. Hays SR, Baum M, Kokko JP (1987) Effects of protein kinase C activation on sodium, potassium, chloride, and total CO_2 transport in the rabbit cortical collecting tubule. J Clin Invest 80:1561–1570
71. Koeppen BM, Helman SI (1982) Acidification of luminal fluid by the rabbit cortical collecting tubule perfused in vitro. Am J Physiol 242:F521–F531
72. Laski ME, Kurtzman NA (1983) Characterization of acidification in the cortical and medullary collecting tubule of the rabbit. J Clin Invest 72:2050–2059
73. Koeppen BM (1987) Electrophysiological identification of principal and intercalated cells in the rabbit outer medullary collecting duct. Pflugers Arch 409:138–141
74. O'Neil RG, Sansom SC (1984) Characterization of apical cell membrane Na^+ and K^+ conductances of cortical collecting duct using microelectrode techniques. Am J Physiol 247:F14–F24

75. Barone S, Amlal H, Kujala M et al (2007) Regulation of the basolateral chloride/base exchangers AE1 and SLC26A7 in the kidney collecting duct in potassium depletion. Nephrol Dial Transplant 22:3462–3470
76. Stetson DL, Wade JB, Giebisch G (1980) Morphologic alterations in the rat medullary collecting duct following potassium depletion. Kidney Int 17:45–56
77. Doucet A, Marsy S (1987) Characterization of K-ATPase activity in distal nephron: stimulation by potassium depletion. Am J Physiol 253:F418–F423
78. Renkema KY, Velic A, Dijkman HB et al (2009) The calcium-sensing receptor promotes urinary acidification to prevent nephrolithiasis. J Am Soc Nephrol 20:1705–1713
79. Advani A, Kelly DJ, Cox AJ et al (2009) The (Pro)renin receptor: site-specific and functional linkage to the vacuolar H^+-ATPase in the kidney. Hypertension 54:261–269
80. Ludwig J, Kerscher S, Brandt U et al (1998) Identification and characterization of a novel 9.2-kDa membrane sector-associated protein of vacuolar proton-ATPase from chromaffin granules. J Biol Chem 273:10939–10947
81. Rothenberger F, Velic A, Stehberger PA et al (2007) Angiotensin II stimulates vacuolar H^+-ATPase activity in renal acid-secretory intercalated cells from the outer medullary collecting duct. J Am Soc Nephrol 18:2085–2093
82. Lu X, Garrelds IM, Wagner CA et al (2013) (Pro)renin receptor is required for prorenin-dependent and -independent regulation of vacuolar H^+-ATPase activity in MDCK.C11 collecting duct cells. Am J Physiol Renal Physiol 305:F417–F425
83. Weiner ID, New AR, Milton AE et al (1995) Regulation of luminal alkalinization and acidification in the cortical collecting duct by angiotensin II. Am J Physiol 269:F730–F738
84. Wagner CA, Mohebbi N, Uhlig U et al (2011) Angiotensin II stimulates H^+-ATPase activity in intercalated cells from isolated mouse connecting tubules and cortical collecting ducts. Cell Physiol Biochem 28:513–520
85. Wang T, Giebisch G (1996) Effects of angiotensin II on electrolyte transport in the early and late distal tubule in rat kidney. Am J Physiol 271:F143–F149
86. Pech V, Kim YH, Weinstein AM et al (2007) Angiotensin II increases chloride absorption in the cortical collecting duct in mice through a pendrin-dependent mechanism. Am J Physiol Renal Physiol 292:F914–F920
87. Pech V, Zheng W, Pham TD et al (2008) Angiotensin II activates H+-ATPase in type A intercalated cells. J Am Soc Nephrol 19:84–91
88. Wall SM, Fischer MP, Glapion DM et al (2003) ANG II reduces net acid secretion in rat outer medullary collecting duct. Am J Physiol Renal Physiol 285:F930–F937
89. Patel AB, Frindt G, Palmer LG (2013) Feedback inhibition of ENaC during acute sodium loading in vivo. Am J Physiol Renal Physiol 304:F222–F232
90. Stone DK, Seldin DW, Kokko JP et al (1983) Mineralocorticoid modulation of rabbit medullary collecting duct acidification. A sodium-independent effect. J Clin Invest 72:77–83
91. DuBose TD Jr, Caflisch CR (1988) Effect of selective aldosterone deficiency on acidification in nephron segments of the rat inner medulla. J Clin Invest 82:1624–1632
92. Winter C, Kampik NB, Vedovelli L et al (2011) Aldosterone stimulates vacuolar H^+-ATPase activity in renal acid-secretory intercalated cells mainly via a protein kinase C-dependent pathway. Am J Physiol Cell Physiol 301:C1251–C1261
93. Winter C, Schulz N, Giebisch G et al (2004) Nongenomic stimulation of vacuolar H^+-ATPases in intercalated renal tubule cells by aldosterone. Proc Natl Acad Sci U S A 101:2636–2641
94. Kurtzman NA (2000) Renal tubular acidosis syndromes. South Med J 93:1042–1052
95. Izumi Y, Hori K, Nakayama Y et al (2011) Aldosterone requires vasopressin V1a receptors on intercalated cells to mediate acid–base homeostasis. J Am Soc Nephrol 22:673–680
96. Wesson DE, Dolson GM (1997) Endothelin-1 increases rat distal tubule acidification in vivo. Am J Physiol 273:F586–F594
97. Khanna A, Simoni J, Wesson D (2005) Endothelin-induced increased aldosterone activity mediates augmented distal nephron acidification as a result of dietary protein. J Am Soc Nephrol 16:1929–1935

98. Gueutin V, Vallet M, Jayat M et al (2013) Renal β-intercalated cells maintain body fluid and electrolyte balance. J Clin Invest 123:4219–4231
99. Hays S, Kokko JP, Jacobson HR (1986) Hormonal regulation of proton secretion in rabbit medullary collecting duct. J Clin Invest 78:1279–1286
100. Batlle D, Haque SK (2012) Genetic causes and mechanisms of distal renal tubular acidosis. Nephrol Dial Transplant 27:3691–3704
101. Fathallah DM, Bejaoui M, Sly WS et al (1994) A unique mutation underlying carbonic anhydrase II deficiency syndrome in patients of Arab descent. Hum Genet 94:581–582
102. Shah GN, Bonapace G, Hu PY et al (2004) Carbonic anhydrase II deficiency syndrome (osteopetrosis with renal tubular acidosis and brain calcification): novel mutations in CA2 identified by direct sequencing expand the opportunity for genotype-phenotype correlation. Hum Mutat 24:272
103. Muzalef A, Alshehri M, Al-Abidi A et al (2005) Marble brain disease in two Saudi Arabian siblings. Ann Trop Paediatr 25:213–218
104. Bruce LJ, Cope DL, Jones GK et al (1997) Familial distal renal tubular acidosis is associated with mutations in the red cell anion exchanger (Band 3, AE1) gene. J Clin Invest 100:1693–1707
105. Karet FE, Gainza FJ, Gyory AZ et al (1998) Mutations in the chloride-bicarbonate exchanger gene AE1 cause autosomal dominant but not autosomal recessive distal renal tubular acidosis. Proc Natl Acad Sci U S A 95:6337–6342
106. Jarolim P, Palek J, Amato D et al (1991) Deletion in erythrocyte band 3 gene in malaria-resistant Southeast Asian ovalocytosis. Proc Natl Acad Sci U S A 88:11022–11026
107. Bruce LJ, Wrong O, Toye AM et al (2000) Band 3 mutations, renal tubular acidosis and South-East Asian ovalocytosis in Malaysia and Papua New Guinea: loss of up to 95% band 3 transport in red cells. Biochem J 350(Pt 1):41–51
108. Alper SL (2010) Familial renal tubular acidosis. J Nephrol 23(Suppl 16):S57–S76
109. Yenchitsomanus PT, Kittanakom S, Rungroj N et al (2005) Molecular mechanisms of autosomal dominant and recessive distal renal tubular acidosis caused by SLC4A1 (AE1) mutations. J Mol Genet Med 1:49–62
110. Chu CY, King JC, Berrini M et al (2013) Functional rescue of a kidney anion exchanger 1 trafficking mutant in renal epithelial cells. PLoS One 8:e57062
111. Karet FE, Finberg KE, Nelson RD et al (1999) Mutations in the gene encoding B1 subunit of H+-ATPase cause renal tubular acidosis with sensorineural deafness. Nat Genet 21:84–90
112. Joshua B, Kaplan DM, Raveh E et al (2008) Audiometric and imaging characteristics of distal renal tubular acidosis and deafness. J Laryngol Otol 122:193–198
113. Karet FE, Finberg KE, Nayir A et al (1999) Localization of a gene for autosomal recessive distal renal tubular acidosis with normal hearing (rdRTA2) to 7q33-34. Am J Hum Genet 65: 1656–1665
114. Miura K, Sekine T, Takahashi K et al (2013) Mutational analyses of the ATP6V1B1 and ATP6V0A4 genes in patients with primary distal renal tubular acidosis. Nephrol Dial Transplant 28:2123–2130
115. Stover EH, Borthwick KJ, Bavalia C et al (2002) Novel ATP6V1B1 and ATP6V0A4 mutations in autosomal recessive distal renal tubular acidosis with new evidence for hearing loss. J Med Genet 39:796–803
116. Vargas-Poussou R, Houillier P, Le Pottier N et al (2006) Genetic investigation of autosomal recessive distal renal tubular acidosis: evidence for early sensorineural hearing loss associated with mutations in the ATP6V0A4 gene. J Am Soc Nephrol 17:1437–1443
117. Fuster DG, Zhang J, Xie XS et al (2008) The vacuolar-ATPase B1 subunit in distal tubular acidosis: novel mutations and mechanisms for dysfunction. Kidney Int 73:1151–1158
118. Su Y, Blake-Palmer KG, Sorrell S et al (2008) Human H+ATPase a4 subunit mutations causing renal tubular acidosis reveal a role for interaction with phosphofructokinase-1. Am J Physiol Renal Physiol 295:F950–F958

119. Yang Q, Li G, Singh SK et al (2006) Vacuolar H^+ -ATPase B1 subunit mutations that cause inherited distal renal tubular acidosis affect proton pump assembly and trafficking in inner medullary collecting duct cells. J Am Soc Nephrol 17:1858–1866
120. Finberg KE, Wagner CA, Bailey MA et al (2005) The B1-subunit of the H^+ ATPase is required for maximal urinary acidification. Proc Natl Acad Sci U S A 102:13616–13621
121. Paunescu TG, Russo LM, Da Silva N et al (2007) Compensatory membrane expression of the V-ATPase B2 subunit isoform in renal medullary intercalated cells of B1-deficient mice. Am J Physiol Renal Physiol 293:F1915–F1926
122. Smith AN, Skaug J, Choate KA et al (2000) Mutations in ATP6N1B, encoding a new kidney vacuolar proton pump 116-kD subunit, cause recessive distal renal tubular acidosis with preserved hearing. Nat Genet 26:71–75
123. Norgett EE, Golder ZJ, Lorente-Canovas B (2012) Atp6v0a4 knockout mouse is a model of distal renal tubular acidosis with hearing loss, with additional extrarenal phenotype. Proc Natl Acad Sci U S A 109:13775–13780
124. Blomqvist SR, Vidarsson H, Fitzgerald S et al (2004) Distal renal tubular acidosis in mice that lack the forkhead transcription factor Foxi1. J Clin Invest 113:1560–1570
125. Vidarsson H, Westergren R, Heglind M et al (2009) The forkhead transcription factor Foxi1 is a master regulator of vacuolar H-ATPase proton pump subunits in the inner ear, kidney and epididymis. PLoS One 4:e4471

Chapter 26
Plasma Membrane ATPase: Potential Target for Antifungal Drug Therapy

Nikhat Manzoor

Abstract Fungal plasma membrane H^+-ATPase (PM-ATPase) is crucial to cell physiology as it maintains an electrochemical proton gradient across cell membranes required for the uptake of nutrients. It regulates intracellular pH and dimorphic transition that is directly linked with growth and pathogenicity of the fungus. Opportunistic fungal pathogens, mainly *Candida* spp., lead to complications in HIV-infected and other immunocompromised patients. Due to the eukaryotic nature of fungal cells, it is difficult to identify unique antifungal targets not shared with human hosts. Also the currently available drugs have low efficacy and high toxicity and frequently lead to drug resistance. They have undesirable side effects and are ineffective against reemerging fungi. Treatment options for invasive infections are limited and almost always involve the use of nephrotoxic amphotericin B and azoles, which lead to resistance on prolonged use probably due to their fungistatic nature. There is thus a critical need to develop more effective therapies to deal with such infections, and natural products offer a safer alternative. PM-ATPase is unique and crucial to fungal cells and hence is a promising antifungal target. It will help in the development of new mechanism-based drugs. Intracellular pH and glucose-induced H^+ efflux, consequences of PM-ATPase activity, are inhibited by natural compounds to the same extent in both susceptible and resistant *Candida* strains. Several plant essential oil constituents inhibit PM-ATPase activity significantly and hence may be considered as good candidates for designing specific surface active antifungal drugs that target the PM-ATPase and will ultimately help in curbing drug resistance in pathogenic fungi.

Keywords PM-ATPase • *Candida* • Pathogenicity • Reaction kinetics • Natural compounds • Antifungal target

N. Manzoor (✉)
College of Applied Medical Sciences, Taibah University,
Al-Madinah Al-Munnawara, Kingdom of Saudi Arabia

Medical Mycology Lab, Department of Biosciences, Jamia Millia Islamia, New Delhi, India
e-mail: nikhatmanzoor@yahoo.co.in

S. Chakraborti, N.S. Dhalla (eds.), *Regulation of Ca^{2+}-ATPases,V-ATPases and F-ATPases*, Advances in Biochemistry in Health and Disease 14,
DOI 10.1007/978-3-319-24780-9_26

1 Introduction

Fungal infections have increased tremendously in the past few decades, especially in immunocompromised patients [1, 2] contributing to morbidity and mortality, the main reason being an increase in antimicrobial resistance and limited number of antifungal drugs. Also, most of these conventional drugs have undesirable side effects. *Candida* species are major human fungal pathogens that cause both superficial and systemic infections [1]. *Candida albicans*, the fourth most common cause of hospital-acquired infections, is believed to be an obligate associate of warm-blooded animals. Normally present as a harmless asymptomatic commensal, it can manifest as a pathogen due to its capacity to induce germ tube formation. Besides morphological transition, there are several other virulence factors like adhesion, biofilm formation, and invasion of host responses [3].

The fungal cell membrane possesses an H^+-ATPase (PM-ATPase) that plays a critical role in fungal cell growth and physiology. It is essential for maintaining a proton electrochemical gradient necessary for the secondary transport of nutrients. This membrane protein is also associated with regulation of intracellular pH (pHi 7.0) and dimorphism and pathogenicity of the fungus. Several studies have shown that the inhibition of enzyme activity correlates with cessation of cell growth [4–10] and hence endorse PM-ATPase to be a desirable molecular target for antifungal drug therapy [11, 12].

Several important antifungal drugs in clinical use today are fungistatic. These drugs prevent additional growth of cells but have little effect on existing cell populations. Thus, the immune system is required to clear an infection which is not possible in the case of severely immunocompromised individuals, and large cell populations often remain as potential sources of new infection. It is desirable that antifungal agents be fungicidal and be able to kill existing cells. The PM-ATPase is an essential enzyme that is needed for both new growth and stable cell maintenance in the absence of growth. Due to its slow turnover in the membrane, it is likely that specific inhibitors of this membrane protein will be fungicidal [13].

Medicinal plants and bioactive natural products offer an unlimited source of unique molecules that serve as an unparalleled source of therapeutic agents to treat infectious diseases. Interestingly, around 80 % of all available clinically used antibiotics are directly or indirectly derived from natural products [14]. Several of these molecules have shown binding affinity to other related ATPases [15–17]. There are only a few antifungal drugs available largely due to the eukaryotic nature of fungal cells and hence the difficulty in identifying unique antifungal targets not shared with human hosts. PM-ATPase is unique and crucial to fungal cells and hence is a promising antifungal target. It will help in the development of new mechanism-based drugs, and natural compounds that are able to target this crucial protein will serve a good purpose for the same.

2 PM-ATPase: Structure and Function

The fungal PM-ATPase is a 100 kD single polypeptide constituting ~25 % of the total plasma membrane protein. Like all P-type ATPases, it has both N- and C-terminal domains in the cytoplasm and traverses the lipid bilayer 8–10 times.

This proton pump shares only ~30 % of its sequence identity with P-type ATPase family members from animal cells, while they show a high degree of sequence similarity among diverse fungal PMA gene [18]. The enzyme appears highly asymmetric with nearly 70 % of the mass exposed to the cytoplasm and only ~5 % exposed to the extra-cytoplasmic compartment. The considerable structural conservation within the P-type ATPases occurs most strongly in a set of six sequences found in the cytoplasmic catalytic domains [19] located within the putative transduction and kinase domains which contain the ATP-binding site and site of phosphorylation. The secondary structure and its interaction with the lipid bilayer are strongly conserved. A notable structural difference between the various P-type ATPases with differing cation specificity is the sets of relatively short extracellular turns (~4–20 amino acid residues) [19] that are expected to provide extracellular recognition elements that could help target drugs to cell surface. Therefore, an understanding of the functional properties of the transmembrane loops and the accessibility of their extracellular turns may be invaluable for developing specific targets among the P-type ATPases.

The fungal PM-ATPase is a high-capacity proton pump that plays a critical role in fungal cell physiology by helping to regulate intracellular pH [20, 21] and maintain transmembrane electrochemical proton gradients necessary for nutrient uptake [22, 23]. The gene encoding this enzyme, PMA1, has been cloned from diverse fungi and has been shown to be highly conserved [18]. PM-ATPase plays important roles in the maintenance of cell homeostasis by regulating intracellular pH. This mechanism creates a membrane potential and an electrochemical gradient that allows the uptake of ions and nutrients required for cellular physiology [24–27]. The PM-ATPase is one of the few antifungal targets that have been demonstrated to be essential by gene disruption [28]. In addition to its role in cell growth, it has been implicated in fungal pathogenicity through its effects on dimorphism, nutrient uptake, and medium acidification.

The regulation of PM-ATPase is a complex process that operates at several levels. Apart from transcriptional regulation [29], enzyme activity is autoregulated through the generation of membrane potential [30] and intracellular Ca^{2+} metabolism. The enzyme contains a carboxyl-terminal regulatory domain that includes a phosphorylation site for a calmodulin-dependent multiprotein kinase. This domain governs the response of the enzyme-to-glucose metabolism/starvation. Mutations in the carboxyl-terminal phosphorylation site can retard or even stop fungal cell growth. The carboxyl-terminal domain is a negative regulator that is believed to interact with the ATP-binding region of the enzyme [31].

3 Kinetic Studies on Fungal PM-ATPase

The mechanism of PM-ATPase has been studied in *C. albicans* using fast reaction kinetics in a stopped flow spectrophotometer [32]. A distinct pre-steady-state phase of ATP hydrolysis was recorded on rapid mixing of ATP with ATPase. Around two protons per ATPase molecule were released, of which around ~1.3

were absorbed back. While the rapid mixing of inorganic phosphate and ATPase produced no transient pH changes, the mixing of ADP led to the release of one proton per ATPase molecule. The magnitudes of both proton release and absorption were found to be independent of ATP concentration. The rate of proton release showed ATP dependence, while the rate of proton absorption was independent of ATP concentration. The low rate of proton liberation with ADP in comparison to ATP indicates low affinity of the ATPase for ADP. No change in the difference spectrum was observed with ADP. The stoichiometry of ATP binding to PM-ATPase was found to be unity from UV-difference spectrum studies. The rates of proton release and appearance of a difference spectrum following the addition of ATP were found to be similar beyond an ATP: ATPase ratio of 1:1. The mechanism of ATP hydrolysis is summarized in a four-step kinetic scheme [32].

Similar kinetic studies were done in the presence of some nutrients (glucose, glutamic acid, proline, lysine, arginine) and two glucose analogs (2-deoxy D-GLUCOSE and xylose). In the presence of glucose, proton absorption to release ratio was exceptionally high (0.92) in comparison to other nutrients which was in the range 0.25–0.36 [33]. Although no UV difference spectrum was observed with ADP, mixing of ATP with ATPase led to a large conformational change. Exposure to different nutrients restricted the magnitude of the conformational change; the analogs of glucose were found to be ineffective. This suppression was maximal in the case of glucose (80 %), while with other nutrients, magnitude of suppression was in the range 40–50 %. The rate of H^+ absorption showed positive correlation with suppression of conformational change only in the case of glucose and no other nutrient/analog. Mode of interaction of glucose with PM-ATPase thus appeared to be strikingly distinct in comparison to other nutrients/analogs tested [33].

Mechanism of glucose stimulation of H^+ efflux by PM-ATPase remains a mystery despite extensive research [5, 32–36]. Studies on mechanism of ATP hydrolysis and H^+ efflux including its nutrient regulation by PM-ATPase are crucial for the design of mechanism-based drugs for this vital target. In a study conducted by the same group, the rate of proton efflux and its stimulation by nutrients/analogs was quantitated in cells and spheroplasts of *C. albicans* [5, 36]. Glucose showed a striking stimulation of 7.5-fold in the rate of H^+ efflux, while the rest of the nutrients/analogs were noneffective. Glucose stimulation was not observed much in the case of spheroplasts probably due to slow transport of nutrients and loss of interaction between PM-ATPase and other membrane proteins [5, 34]. Since intracellular ATP remains almost unused in both cells and spheroplasts, there is a possibility that glucose exposure leads to increase in intracellular ATP concentration due to its metabolism, but most of it is consumed by the highly active pump. Therefore, ATP does not appear to be the cause for glucose stimulation of PM-ATPase. A decreased intracellular ATP concentration on exposure to glucose is due to the high utilization of ATP by the stimulated ATPase [36].

4 Fungal PM-ATPase as a Potential Target for Antifungal Therapy

The development of an effective target remains a critical part of the drug discovery process, and fungal PM-ATPase is a highly desirable target for the development of novel antifungal therapeutics. It has well-defined properties that facilitate drug discovery. The enzyme is very crucial to fungal cell physiology, being required for the formation of a large electrochemical proton gradient and maintenance of intracellular pH. Complete inhibition of the proton pump will definitely be lethal; thus, an effective antagonist of the proton pump will be fungicidal, which is an important attribute for a drug being developed to treat opportunistic infections in severely immunocompromised patients. Well-characterized biochemical studies and genetics of this enzyme will facilitate detailed analysis of the interaction of model compounds with the enzyme [12]. Detailed genetic analysis suggests that modification of amino acids in the first two transmembrane segments can either enhance or diminish the drug sensitivity of the PM-ATPase, depending on the nature and location of the amino acid substitution. This region in mammalian P-type enzymes has been implicated in the interaction of cardiac glycosides and reversible gastric pump inhibitors [12]. Hence, it is suggested that this region in the PM-ATPase may be valuable as a potential interaction domain for antifungal agents. Also, a number of primary and secondary screens are available to identify compounds that target the PM-ATPase and affect one or more of its functional properties. These screens assess function of the enzyme and have already yielded promising PM-ATPase-directed antagonists [12]. Like other P-type ATPases, the N- and C-termini and the extracellular surface of the pump show the highest divergence; this contributes to its unique catalytic and regulatory features. PM-ATPase antagonists that are selective for the fungal proton pump over related animal cell ion pumps should display broad-spectrum activity on diverse fungal enzymes because of the high degree of primary sequence similarity found among these enzymes.

It has been observed that inhibition of PM-ATPase leads to intracellular acidification and cell death. Inhibition of cell growth and H^+ efflux by certain natural and synthetic compounds suggests that their antifungal properties are related to their inhibitory effects on PM-ATPase. It has been reported that PM-ATPase activity increases in both bud and germ tube forming populations after 135 min of fungal growth. This is the time at which morphological transition is initiated [37]. PM-ATPase regulates dimorphism in *C. albicans*. Its activity is regulated by a large number of environmental factors at both transcriptional and posttranslational levels. Diverse numbers of PM-ATPase genes have been cloned both in fungi and plants [31, 38]. There has been rapid progress on the molecular basis of reaction mechanism and regulation of the proton pump.

Studies with Omeprazole, a sulfhydryl-reactive compound, indicated that PM-ATPase can be inhibited from its extracellular membrane surface [4, 12] and that its inhibition is closely correlated with inhibition of fungal cell growth that is fungicidal [11]. Genetic studies also demonstrated that perturbations of extracellular

protein structure of the PM-ATPase can reduce the catalytic activity of the enzyme [39]. These results were also consistent with the known behavior of antagonists to the Na, K-ATPase and H, K-ATPase which have binding sites on the extracellular surface of the membrane.

The importance of PM-ATPase as an antifungal target has been demonstrated by several studies. *Cryptococcus neoformans* PM-ATPase is an established and viable target for antifungal drug discovery [13]. Ebselen, a nonspecific PM-ATPase antagonist, is also fungicidal and inhibits ATP hydrolysis and medium acidification by whole cells [40, 41]. NC1175, a novel thiol-blocking conjugated styryl ketone, exhibits activity against a wide spectrum of pathogenic fungi. NC1175 inhibited glucose-induced acidification of external medium by *Candida*, *Saccharomyces*, and *Aspergillus* species in a concentration-dependent manner. Vanadate-inhibited ATP hydrolysis by membrane fractions of *C. albicans* was completely inhibited by 50 μM NC1175, suggesting that one of the targets for NC1175 in these fungi may be PM-ATPase [42]. Studies have demonstrated that bafilomycin inhibits ATPase activity with high specificity and potency [43]. Although PMA1 is also present in the human transcriptome, several domains are exclusive to fungi, and gene deletion has been demonstrated to be lethal for some of those microorganisms. As ATPases are promising targets for the development of antimycotics, the differences between fungal and mammalian proteins need to be further investigated [44].

5 Natural Compounds as Potential Inhibitors of PM-ATPase

Natural products play an important role in drug discovery and development [45, 46]. More than 75 % of the drugs used in therapy for infectious diseases are of natural origin [47]. The fungal PM-ATPase is an ideal antifungal target as it is an essential enzyme not found in animals, and an important functional part of the protein is exposed to the cell exterior. Natural plant products have shown potential in having inhibitory effects on this antifungal target. Several of these natural products available may be effective pump inhibitors and should be sought for in plant extracts by screening for their effect on PM-ATPase activity. This enzyme when co-crystallized with identified inhibitors will provide information on inhibitor binding segments in the pump and offer a crucial foundation for the development of novel efficient and specific antifungals.

Plant-derived substances have recently become of great interest owing to their versatile applications [45, 48]. The initial stages of drug development include identification of active principles, meticulously designed biological assays, and dosage formulations, followed by clinical studies to establish safety, efficacy, and pharmacokinetic profile of the new drug [49]. Several studies have shown the antifungal potential of natural plant products and showed that the inhibition of the proton pump activity is correlated with termination of fungal cell growth. A direct relation between intracellular pH (pHi) and functioning of PM-ATPase has been established by several studies [6, 10, 50, 51].

The pathogenicity of *Candida albicans* is due to its capacity to induce germ tube formation [52]. These hyphae penetrate host tissues to extract nutrients required for cell growth. A wide range of biochemical factors have been implicated in a variety of dimorphic fungi as being central to the control of yeast dimorphism [53]. It is however possible to invoke mechanisms which incorporate changes in intracellular pH with the modulation of biochemical activities as a regulatory switch. A rapid but transient increase in pHi has been observed around the time of evagination of germ tubes, and the magnitude of increase in pHi of the population destined to form buds was more sensitive to orthovanadate, an inhibitor of the PM-ATPase [50]. Change in pHi, which has a direct relationship with PM-ATPase, is widely regarded as of crucial importance [6, 50].

High-energy phosphates play an important role in regulating fungal PM-ATPase activity. Phosphocreatine (PCr) is a phosphorylated creatine (Cr) molecule that serves as a rapidly mobilizable backup of high-energy phosphates in skeletal muscles and the brain. It has been shown to influence ATP-dependent enzymes [6] and is found in association with virtually all types of ATPases in vertebrate cells. PCr/Cr ratio in cells is a better reflection of energy status compared to ATP/ADP ratio [50, 52]. Studies report that *Candida* infections are held in check mostly by immunologic factors in healthy human hosts. A number of situations however expose the yeast to other cellular constituents. Our group investigated the effect of PCr on the rate of H^+ extrusion, pHi, and dimorphism in *C. albicans* [6, 7]. H^+ efflux by PM-ATPase of *C. albicans* and intracellular pH pattern of cells undergoing morphogenesis were profoundly affected by PCr at concentrations present in vertebrate tissues. In comparison to control cells, PCr-exposed cells showed only 10 % yeast to hyphal transition after 120 min at the same concentration range of 20–40 mM, while the number of hyphae producing cells was not more than 40 %. Exposure to PCr also decreased hyphal length to a large extent [6], and the magnitude of inhibition was comparable to vanadate, a potent inhibitor of PM-ATPase. This indicates that both of them may have binding sites on the ATPase and bring protein conformational changes in a similar manner. Cr alone has no effect on H^+ extrusion. Since the structure of vanadate is analogous to the structure of phosphate (Fig. 26.1), it may be speculated that PCr may bind to the ATP-binding site via its phosphoryl group. When *Candida* cells were exposed to both vanadate and PCr together, a cumulative effect was produced. Both of them may be having more than one binding sites [7]. Similar studies showed that ATP synthesis and PM-ATPase activity were significantly affected by sodium nitroprusside (SNP), a nitric oxide (NO) donor. A decrease in ATP concentration was observed in SNP-treated cells, the decrease being more in the presence of sugars and amino acids. Hence, NO, not only inhibits mitochondrial electron transport chain but also alters PM-ATPase conformation resulting in a decrease in its activity [54, 55].

Plant essential oils (EOs) possess a broad spectrum of antimicrobial properties due to the presence of bioactive natural molecules. Although several studies demonstrate their antifungal potential [56–59], there are very few reports that clearly reveal their mode of action. The antifungal activity of EOs is basically credited to their ability to cross fungal cell walls and penetrate between fatty acyl chains of the lipid

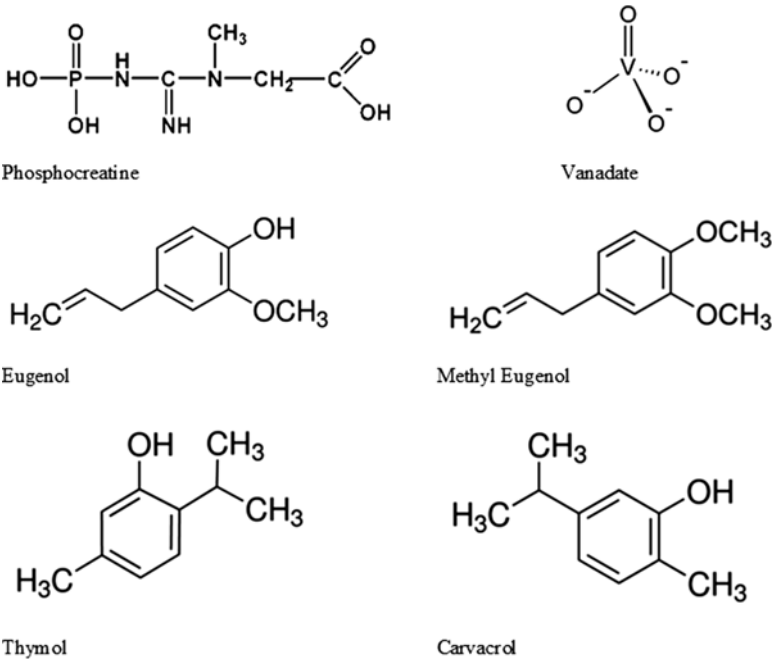

Fig. 26.1 The structure of some antifungal compounds discussed in this chapter that inhibit PM-ATPase activity

bilayer, altering membrane fluidity and permeability and damaging membrane proteins, leading to degradation of the cytoplasmic membrane and to cell death. Loss of cell homeostasis, leakage of cell contents, and lysis are the critical consequences of these induced alterations in membrane structure and function [56]. Most of the studies claim that the antifungal activity of these compounds is due to their ability to destroy the integrity of cell membranes, release cellular components, and drastically inhibit mycelial growth of fungal pathogens [59].

Excellent anti-*Candida* activity has been demonstrated by several studies [58, 60, 61]. PM-ATPase has been explored as a potential antifungal target for several of these natural products. Eugenol, methyl eugenol, thymol, and carvacrol are some of the natural compounds (Fig. 26.1) that showed inhibition of PM-ATPase activity to encouraging levels, i.e., up to 70 % inhibition in both sensitive and resistant *Candida* strains [51] (Table 26.1). Eugenol is a phenylpropanoid present in the essential oil of clove, cinnamon, nutmeg, basil, star anise, and dill. Methyl eugenol, methyl ether of this compound, is also present in various essential oils. Carvacrol and thymol are monoterpene phenols present as major constituents in the essential oils of *Origanum vulgare* and thyme, respectively.

Glucose-induced acidification of the extracellular medium by yeast cells is a convenient measure of PM-ATPase-mediated H^+ pumping [62]. Table 26.1 gives the average percentage inhibition of PM-ATPase-mediated H^+ efflux by *Candida*

Table 26.1 Percentage inhibition of glucose-induced H^+ efflux by *Candida* spp. at pH 7.0 in the presence of some natural compounds at their respective MICs

	Percentage inhibition of H^+ efflux w.r.t. control		
Compounds	Standard	Clinical	Resistant
Phosphocreatine (25 mM)	83	–	–
Eugenol (500 µg/ml)	44	46	39
Methyl eugenol (350 µg/ml)	49	42	43
Thymol (100 µg/ml)	60	54	46
Carvacrol (50 µg/ml)	69	61	67
Fluconazole (5 µg/ml)	24	19	25
Amphotericin B (2 µg/ml)	16	16	17
Vanadate (5 mM)	100	91	96

Cells were suspended in 0.1 mM $CaCl_2$ and 0.1 M KCl at 25 °C along with 5 mM glucose
– = not evaluated

species in the presence of some natural compounds at their respective MIC values. The rate of proton extrusion by *Candida* cells was calculated in nmoles min/mg yeast cells by titrating the cell suspension with 0.01 N NaOH [7]. Eugenol, methyl eugenol, thymol, and carvacrol (Fig. 26.1) showed the most significant inhibition of more than 50 % in both clinical and resistant *Candida* stains. Moreover, H^+ extrusion in every case was inhibited by 91–100 % in the presence of orthovanadate (5 mM), a specific inhibitor of H^+-ATPase, whereas neither fluconazole nor amphotericin B had any significant effect on the acidification of the extracellular medium (Table 26.1). The intracellular pH (pHi) of yeast cells is maintained between 6.0 and 7.5, and any change in pHi is regarded as of crucial importance as it has a direct relationship with PM-ATPase [6, 50]. A significant decrease in pHi was observed in treated *Candida* cells. In comparison to the control cells (untreated), the decrease in pHi in cells was in the order given: Control > EUG > MEUG > THY > CARV [51].

On exposing *Candida* cells for a short duration, the effect of these bioactive compounds was rapid, irreversible, and lethal which suggests the presence of a cellular target that is accessible to the compounds externally. Since PM-ATPase is present in plasma membranes of pathogenic fungi, there is a possibility that these compounds bind to it externally. Significant inhibition of PM-ATPase-mediated proton pumping activity at MIC values of bioactive compounds suggests that these compounds can be considered as potential ATPase inhibitors. The fact that they have low MIC values and negligible toxicity in comparison to conventional drugs makes them even better candidates. It has been reported that vanadate inhibits H^+ efflux in *Candida* cells by 91–100 %, while conventional antifungal drugs like FLC and AmB had no significant effect on the PM-ATPase activity [51]. These antifungal drugs are known to interact with the sterol components of the membrane, [63] and there are no reports of their interaction with the proton pumps. Besides these commercially available antifungals have low efficacy and high toxicity and frequently lead to drug resistance. There is thus a critical need to develop more effective therapies to deal with such infection, and natural compounds offer a safer alternative.

6 Conclusion

Fungal infections occur as a result of a complex interaction between the host, pathogen, and the environment. Antibiotics have helped in the treatment of infections to a great extent, but their indiscriminate use has led to the development of drug-resistant pathogens. The emergence of azole resistance in *Candida albicans* and other *Candida* species is a huge crisis today. The antimicrobial activity of plant essential oils and their components is well established against a wide range of microorganisms. Plants and plant products can assist in confronting the issue of infection and provide a better understanding of mechanisms for the designing and development of novel and more effective antimicrobial agents. The discovery of new antifungal therapeutic agents based on natural compounds as scaffolds for molecular targets will help in the management and treatment of fungal and other microbial infections. Fungicidal natural compounds having low MIC values and negligible cytotoxicity have a profound effect on PM-ATPase of *Candida* and other fungal species, suggesting that the PM-ATPase can be explored as a potential surface active antifungal target for these and other potential drugs.

References

1. Sardi JCO, Scorzoni L, Bernardi T et al (2013) *Candida* species: current epidemiology, pathogenicity, biofilm formation, natural antifungal products and new therapeutic options. J Med Microbiol 62:10–24
2. Zheng X, Zhang G (2014) Imaging pulmonary infectious diseases in immunocompromised patients. Radiol Infect Dis 1:37–41
3. Calderone RA, Fonzi WA (2001) Virulence factors of *Candida albicans*. Trends Microbiol 9:327–335
4. Seto-Young D, Monk BC, Mason AB et al (1997) Exploring an antifungal target in the plasma membrane H^+-ATPase of fungi. Biochim Biophys Acta 1326:249–256
5. Manzoor N, Khan LA, Amin M (2000) Nutrient associated changes in plasma membrane H^+-ATPase activity of permeabilized *Candida albicans* cells. Indian J Biochem Biophys 37:241–244
6. Manzoor N, Khan LA, Amin M (2002) Effect of Phosphocreatine on H^+-extrusion, pHi and dimorphism in *Candida albicans*. Indian J Exp Biol 40:785–790
7. Manzoor N, Haque MM, Khan LA (2004) Inhibition of H^+ extrusion by Phosphocreatine in *Candida albicans*. J Plant Biochem Biotech 13:65–67
8. Ahmad A, Khan A, Khan LA et al (2010) *In vitro* synergy of eugenol and methyl eugenol with fluconazole against clinical *Candida* isolates.". J Med Microbiol 59:1178–1184
9. Shreaz S, Maurya IK, Bhatia R et al (2013) Influences of cinnamic aldehydes on plasma membrane H^+ ATPase activity and ultrastructure of *Candida*. J Med Microbiol 62:232–240
10. Bhatia R, Shreaz S, Muralidhar S et al (2012) Proton pumping ATPase mediated fungicidal activity of two essential oil components. J Basic Microbiol 52:504–512
11. Monk BC, Mason AB, Abramochkin G et al (1995) The yeast plasma membrane proton pumping ATPase is a viable antifungal target. I Effects of the cysteine-modifying reagent omeprazole. Biochim Biophys Acta 1239:81–90
12. Perlin DS, Seto-Young D, Monk BC (1997) The plasma membrane H^+-ATPase of fungi. A candidate drug target? Ann N Y Acad Sci 834:609–617

13. Soteropoulos P, Vaz T, Santangelo R et al (2000) Molecular characterization of the plasma membrane H^+-ATPase, an antifungal target in *Cryptococcus neoformans*. Antimicrob Agents Chemother 44:2349–2355
14. Roemer T, Xu D, Singh SB et al (2011) Confronting the challenges of natural product-based antifungal discovery. Chem Biol 18:148–164
15. Gledhill JR, Montgomery MG, Leslie AG et al (2007) How the regulatory protein, IF(1), inhibits F(1)-ATPase from bovine mitochondria. Proc Natl Acad Sci U S A 104:15671–15676
16. Hong S, Pedersen LP (2008) ATP synthase and the actions of inhibitors utilized to study its roles in human health, disease, and other scientific areas. Microbiol Mol Biol Rev 72:590–741
17. Laughlin TM, Ahmad Z (2010) Inhibition of Escherichia coli ATP synthase by amphibian antimicrobial peptides. Int J Biol Macromol 46:367–374
18. Wach A, Schlesser A, Goffeau A (1992) An alignment of 17 deduced protein sequences from plant, fungi, and ciliate H^+-ATPase genes. J Bioenerg Biomemb 24:309–317
19. Monk BC, Perlin DS (1994) Fungal plasma membrane proton pumps as promising new antifungal targets. Crit Rev Microbiol 20:209–223
20. Sanders D, Hansen UP, Slayman CL (1981) Role of the plasma membrane proton pump in pH regulation in non-animal cells. Proc Natl Acad Sci U S A 78:5903–5907
21. Vallejo CG, Serrano R (1989) Physiology of mutants with reduced expressions of plasma membrane H^+-ATPase. Yeast 5:307–319
22. Serrano R (1989) Structure and function of plasma membrane ATPase. Annu Rev Plant Physiol Plant Mol Biol 40:61–94
23. Prasad R (1991) The Plasma Membrane of Candida albicans: Its Relevance to Transport Phenomenon. In: Prasad R (eds) *Candida albicans.* Springer, Berlin. pp 108–127
24. Burghoorn HP, Soteropoulos P, Paderu P et al (2002) Molecular evaluation of the plasma membrane proton pump from *Aspergillus fumigatus*. Antimicrob Agents Chemother 46:615–624
25. Lee MCS, Hamamoto S, Schekman R (2002) Ceramide biosynthesis is required for the formation of oligomeric H^+-ATPase, Pma1p, in the yeast endoplasmic reticulum. J Biol Chem 277:22395–22401
26. Wang Q, Chang A (2002) Sphingoid base synthesis is required for oligomerization and cell surface stability of the yeast plasma membrane ATPase, Pma1. Proc Natl Acad Sci U S A 99: 12853–12858
27. Pizzirusso M, Chang A (2004) Ubiquitin-mediated targeting of a mutant plasma membrane ATPase, Pma1-7, to the endosomal/vacuolar system in yeast. Mol Biol Cell 5:2401–2409
28. Serrano R, Kielland-Brandt MC, Fink GR (1986) Yeast plasma membrane ATPase is essential for growth and has homology with (Na^+K^+), K^+-and Ca^{2+}-ATPase. Nature 319:689–693
29. Capieaux E, Vignais ML, Sentenac A et al (1989) The yeast H^+-ATPase gene is controlled by the promoter binding factor TUF. J Biol Chem 264:7437–7446
30. Seto-Young D, Perlin DS (1991) Effect of membrane voltage on the plasma membrane H^+-ATPase of Saccharomyces cerevisiae. J Biol Chem 266:1383–1389
31. Monk BC, Kurtz MB, Marrinan JA et al (1991) Cloning and characterization of the plasma membrane H^+-ATPase from *Candida albicans*. J Bacteriol 173:6826–6836
32. Manzoor N, Khan LA, Amin M (1999) Pre steady state kinetic studies on H^+- ATPase from *Candida albicans*. J Biochem 126:776–780
33. Rashid B, Manzoor N, Khan LA et al (2004) Effect of glucose, its analogs and some amino acids on pre-steady state kinetics of ATP hydrolysis by PM-ATPase of *Candida albicans*. Korean J Biol Sci 8:307–312
34. Serrano R (1984) Plasma membrane ATPase of fungi and plants as a novel type of proton pump. Curr Top Cell Regul 23:87–126
35. Ramos S, Balbin M, Raposo M et al (1989) The mechanism of intracellular acidification induced by glucose in *Saccharomyces cerevisiae*. J Gen Microbiol 135:2413–2422
36. Rashid B, Manzoor N, Khan LA (2007) Kinetic analysis of nutrient stimulated H^+ efflux by PM-ATPase of *Candida albicans*. Rev Latinoam Microbiol 49:55–59

37. Kaur S, Mishra P (1991) Dimorphism-associated changes in plasma membrane H^+-ATPase activity of *Candida albicans*. Arch Microbiol 156:412–415
38. Zhang X, Wang H, Liu S et al (2014) Cloning and characterization of a plasma membrane H^+-ATPase (PMA) gene from a salt-tolerant plant *Chloris virgata*. Mol Soil Biol 5:16–22
39. Na S, Perlin DS, Seto-Young D et al (1993) Characterization of yeast plasma membrane H^+-ATPase mutant pma1-A135V and its revertants. J Biol Chem 268:11792–11797
40. Billack B, Pietka-Ottlik M, Santoro M et al (2010) Evaluation of the antifungal and plasma membrane H^+-ATPase inhibitory action of ebselen and two ebselen analogs in *S. cerevisiae* cultures. J Enzyme Inhib Med Chem 25:312–317
41. Chan G, Hardej D, Santoro M et al (2007) Evaluation of the antimicrobial activity of ebselen: role of the yeast plasma membrane H^+-ATPase. J Biochem Mol Toxicol 21:252–264
42. Manavathu EK, Dimmock JR, Vashishtha SC et al (1999) Proton-pumping-ATPase-targeted antifungal activity of a novel conjugated styryl ketone. Antimicrob Agents Chemother 43:2950–2959
43. Bowman BJ, Bowman EJ (2002) Mutations in subunit C of the vacuolar ATPase confer resistance to bafilomycin and identify a conserved antibiotic binding site. J Biol Chem 277:3965–3972
44. Georgopapadakou NH, Walsh TJ (1996) Antifungal agents: chemotherapeutic targets and immunologic strategies. Antimicrob Agents Chemother 40:279–291
45. Harvey A (2010) The role of natural products in drug discovery and development in the new millennium. IDrugs 13:70–72
46. Newman DJ, Cragg GM (2012) Natural products as sources of new drugs over the 30 years from 1981 to 2010. J Nat Prod 75:311–335
47. Sun L, Liao K, Wang D (2015) Effects of magnolol and honokiol on adhesion, yeast-hyphal transition and formation of Biofilm by Candida albicans. PLOS One. doi:10.1371/journal.pone.0117695
48. Fürst R, Zündorf I (2014) Plant-derived anti-inflammatory compounds: hopes and disappointments regarding the translation of preclinical knowledge into clinical progress. Mediators Inflamm 2014:146832
49. Iwu MW, Duncan AR, Okunji CO (1999) Perspectives on new crops and new uses. In: Janick J (eds) New antimicrobials of plant origin. Alexandria: ASHS Press. pp 457–462
50. Kaur S, Mishra P, Prasad R (1988) Dimorphism-associated changes in intracellular pH of Candida albicans. Biochim Biophys Acta 972:277–282
51. Ahmad A, Khan A, Yousuf S et al (2010) Proton translocating ATPase mediated fungicidal activity of Eugenol and Thymol. Fitoterapia 81:1157–1162
52. Shepherd MG, Poulter RT, Sullivan PA (1985) *Candida albicans*: biology, genetics, and pathogenicity. Annu Rev Microbiol 39:579–614
53. Odds FC (1985) Morphogenesis in *Candida albicans*. Crit Rev Microbiol 12:45–93
54. Haque MM, Manzoor N, Hussain E et al (2004) Effect of nitric oxide on H^+-efflux in the presence of various nutrients in *Candida albicans*. J Exp Biol 42:86–90
55. Haque MM, Pooja, Manzoor N et al (2005) Effect of Sodium nitroprusside on H^+-ATPase activity and ATP concentration in *Candida albicans*. Indian J Exp Biol 43:873–879
56. Bakkali F, Averbeck S, Averbeck D et al (2008) Biological effects of essential oils – a review. Food Chem Toxicol 46:446–475
57. Delaquis PJ, Stanich K, Girard B et al (2002) Antimicrobial activity of individual and mixed fractions of dill, cilantro, coriander and eucalyptus essential oils. Int J Food Microbiol 74:101–109
58. Zore GB, Thakre AD, Rathod V et al (2011) Evaluation of anti-*Candida* potential of geranium oil constituents against clinical isolates of *Candida albicans* differentially sensitive to fluconazole: inhibition of growth, dimorphism and sensitization. Mycoses 54:e99–e109
59. Seow YX, Yeo CR, Chung HL et al (2014) Plant essential oils as active antimicrobial agents. Crit Rev Food Sci Nutr 54:625–644
60. Agarwal V, Lal P, Pruthi V (2008) Prevention of *Candida albicans* biofilm by plant oils. Mycopathologia 165:13–19
61. Devkatte AN, Zore GB, Karuppayil SM (2005) Potential of plant oils as inhibitors of *Candida albicans* growth. FEMS Yeast Res 5:867–873
62. Ben-Josef AM, Manavathu EK, Platt D et al (2000) Proton translocating ATPase mediated fungicidal activity of a novel complex carbohydrate: CAN-296. Int J Antimicrob Agents 13:287–295
63. Onyewu C, Blankenship JR, Del Poeta M et al (2003) Ergosterol biosynthesis inhibitors become fungicidal when combined with calcineurin inhibitors against *Candida albicans*, *Candida glabrata*, and *Candida krusei*. Antimicrob Agents Chemother 47:956–964

Chapter 27
The Yeast Ca^{2+}-ATPases and Ca^{2+}/H^{+} Exchangers of the Secretory Pathway and Their Regulation

Lev A. Okorokov

Abstract We propose a new model for yeast Ca^{2+} homeostasis that considers the roles of different Ca^{2+}/H^{+} exchangers and Ca^{2+}-ATPases which function in all secretory organelles. Majority of these Ca^{2+}-ATPases are blocked by cyclopiazonic acid and thapsigargin in a similar fashion as SERCA. The exchangers and Ca^{2+}-ATPases are activated ~7- and ~2-fold by extracellular glucose and contribute ~80 % and 20 %, respectively, to Ca^{2+} efflux from the cytosol. Vacuoles do not represent major storage organelles, contributing 20–35 % in Ca^{2+} uptake (an efflux from the cytosol). *VCX1* and *PMC1* and their respective vacuolar transporters positively regulate both types of transporters from all secretory organelles, whereas *PMR1* and Pmr1p negatively regulate Ca^{2+} pumps from the ER and NE. Calcineurin is a positive regulator of Ca^{2+}-ATPases and the exchangers from secretory organelles, whose capacity is modulated depending on the energy supply. Calcineurin activates Ca^{2+}-ATPases and the exchangers under normal growth conditions and under high Ca^{2+} stress in the absence of glucose. Glucose and high Ca^{2+} together additively stimulate Ca^{2+}-ATPases, whereas Ca^{2+}/H^{+} exchangers demonstrate higher activity than that observed under Ca^{2+} stress in the absence of glucose but lower activity than that observed with glucose alone. Modulation of the exchanger activities under Ca^{2+} stress correlates with that of V H^{+}-ATPase, suggesting indirect regulation of the exchangers by calcineurin via regulation of this H^{+} pump. The presence of Ca^{2+}-ATPases and exchangers in all secretory organelles is discussed from the point of view of local and specific Ca^{2+} signaling.

Keywords Ca^{2+}-ATPases • Ca^{2+}/H^{+} exchangers • Regulation • Yeast secretory pathway • Glucose • Calcineurin • SERCA • Ca^{2+} signaling

L.A. Okorokov (✉)
Laboratório de Fisiologia e Bioquímica de Microrganismos, Centro de Biociência e Biotecnologia, Universidade Estadual do Norte Fluminense Darcy Ribeiro, Campos dos Goytacazes, RJ 28013-602, Brazil
e-mail: okorokov@uenf.br

S. Chakraborti, N.S. Dhalla (eds.), *Regulation of Ca^{2+}-ATPases,V-ATPases and F-ATPases*, Advances in Biochemistry in Health and Disease 14,
DOI 10.1007/978-3-319-24780-9_27

1 Introduction

Ca^{2+} signaling includes the activation of Ca^{2+}-release channels, which increase the local concentration of free Ca^{2+} in the cytosol by an influx of these cations from intracellular organelles and extracellular medium in response to a stimulus [1]. Ca^{2+} signaling continues until the transporters responsible for Ca^{2+} efflux can restore the initial low free Ca^{2+} concentration (commonly 50–100 nM), transporting Ca^{2+} back to intracellular organelles and the extracellular medium. In yeast, fungi and plants, whose membranes are energized by H^+ gradients, the Ca^{2+} efflux is brought about by Ca^{2+}/H^+ exchangers (antiporters) and Ca^{2+}-ATPases. The amplitude, duration and form of the signals (spikes), and therefore their specificity, are determined by the coordinated activities of the influx and efflux transport systems. The local signaling is due to the specificity and localization of both the release channels and the efflux systems to different organelles and most likely even to distinct membrane rafts. This paper presents new insights on yeast Ca^{2+} homeostasis by briefly revising the current view of the properties, localization and regulation of the Ca^{2+}-ATPases and Ca^{2+}/H^+ exchangers from the yeast secretory pathway.

2 Intrinsic Ca^{2+} Transporters Along the Yeast Secretory Pathway

It is currently accepted that the yeast *Saccharomyces cerevisiae* possesses only two Ca^{2+} pumps, Pmc1p in the vacuolar membrane [2] and Pmr1p in the Golgi membrane [3–7], whereas only one VH^+-ATPase-dependent Ca^{2+}/H^+ exchanger, Vcx1p/Hum1p, is localized to vacuolar membranes [8–13]). This exchanger generates the difference in membrane potentials formed by Ca^{2+} [14] that can be used for the accumulation of anions such as citrate and α-ketoglutarate, among others [15]. Due to a lack of experimental evidence, the presence of a Ca^{2+}-ATPase in the yeast plasma membrane (PM) was doubtful following these insights [10, 16]. However, the separation of the PM following its modification with concanavalin A from intracellular membranes decreased Ca^{2+} uptake by total membranes (TMs) by ~20 %, suggesting the presence of a Ca^{2+} pump in the yeast PM [17]. It was also supposed that the endoplasmic reticulum (ER) does not possess a genuine Ca^{2+}-ATPase [16]. Several lines of evidence suggest that yeast secretory pathway organelles are equipped with more than two Ca^{2+}-ATPases and additional Ca^{2+}/H^+ exchangers apart from Vcx1p. Moreover, each organelle of the secretory pathway likely possesses a genuine Ca^{2+}-ATPase and Ca^{2+}/H^+ exchanger. *First*, TMs were separated in a sucrose density gradient for several membrane populations exhibiting both Ca^{2+}-ATPase and Ca^{2+}/H^+ exchanger activities in addition to marker enzymatic activities typical for the ER, Golgi and vacuoles (Fig. 27.1 and [17, 18, 20–25]). Additionally, the activities of both Ca^{2+} transporters were found in membrane vesicles exhibiting

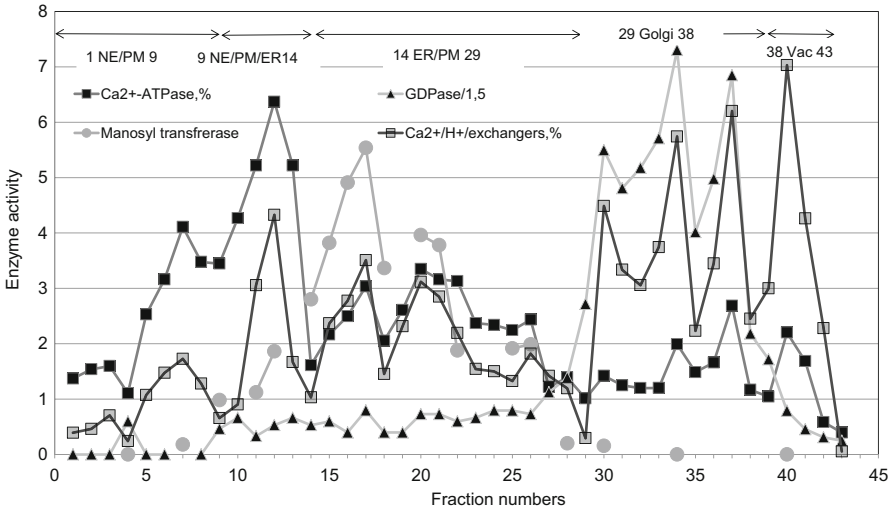

Fig. 27.1 Separation of the yeast total membranes (TMs) on a sucrose density gradient. TMs were isolated from spheroplasts of the *S. cerevisiae* SEY 6210 strain and separated on a sucrose density gradient according to [18]. Ca^{2+}-ATPase and Ca^{2+}/H^{+} transport activities were determined after 10 min of membrane incubation with $^{45}Ca^{2+}$ as FCCP-insensitive and FCCP-sensitive Ca^{2+} uptake, respectively, and are presented in % from total activity of each type of transporter. Protein mannosyltransferase (PMT) was determined according to [19] and represented in cpm:2000; GDPase shown in % from 50 % of its total activity. Fractions 1–14, 14–28, 28–38 and 38–43 are enriched with NE/ER, ER/PMs, Golgi and vacuolar membrane vesicles, respectively. The representative experiment of two is shown

a higher density than that of the ER and co-migrating PM, which are likely derived from the nuclear envelope (NE) (Fig. 27.1, fractions 1–14 and [22, 25]). *Second*, Ca^{2+}-ATPase activities responsible for Ca^{2+} uptake by vesicles derived from the NE, ER/PM, Golgi and vacuoles exhibit considerable differences in their sensitivity to vanadate, with IC_{50} values of 15, 610, 130, and 30 μM, respectively [22, 25]. Subsequent analysis revealed that the ATP hydrolytic activity and Ca^{2+} transport driven by respective Ca^{2+}-ATPases in these membranes exhibit a similar sensitivity to vanadate [25]. Interestingly, the selective sensitivity to vanadate of Ca^{2+} pumps from the yeast secretory pathway is partially reminiscent of SERCA from mammalian cells [26]. *Third*, a *pmr1* mutant demonstrates an approximately 50 % decrease in the Ca^{2+}-ATPase activity from Golgi membranes, indicating that Pmr1p is localized to these membranes and that the Golgi possesses a second putative Ca^{2+} pump [18] that is distinct from Pmc1p, since the efficient separation of the Golgi from vacuolar membrane vesicles and ER (Figs. 27.1, 27.2 and [25, 27]. *Fourth,* in contrast to the suggestion that the yeast ER does not possess a Ca^{2+}-ATPase and that the yeast ER can be provided with Ca^{2+} by Pmr1p [28], the ER demonstrated a high contribution to the total Ca^{2+}-ATPase activity of TMs, particularly in wild-type SEY6210 and X2180 strains, which exhibit enhanced growth compared with

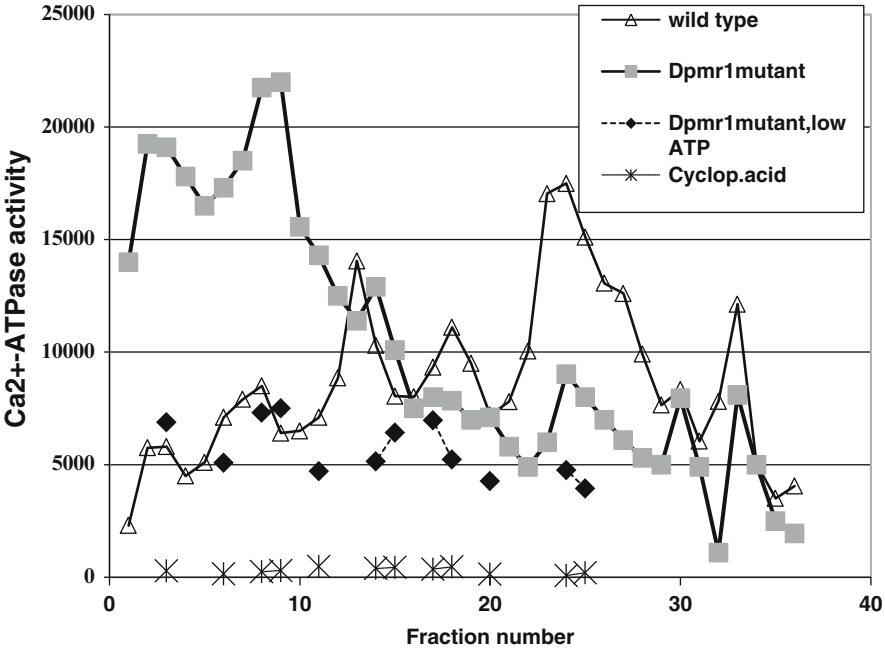

Fig. 27.2 Cyclopiazonic acid inhibits Ca^{2+}-ATPase activities in membranes from NE, ER/PM, and the Golgi of the *pmr1* mutant. TMs were isolated from spheroplasts of the wild-type strain (AA255) and *pmr1* mutant (AA274) and fractionated on a sucrose density gradient according to [18]. In experiments with cyclopiazonic acid the Ca^{2+}-ATPase activity (cpm/mg protein of TMs) in the *pmr1* mutant membranes was determined using 20 μM ATP (low ATP) instead of commonly used concentration of 0.5 mM (wild-type strain). The representative experiment of three is shown

AA255 and K601. The facts that the ER-enriched membranes were not contaminated with Golgi, vacuolar and NE-like membranes (Fig. 27.1 and [27]), exhibited high resistance to vanadate and demonstrated high Ca^{2+}-ATPase and Ca^{2+}/H^+ exchanger activities suggest that these membranes possess genuine Ca^{2+} transporters. Additionally, spheroplast homogenization and subsequent membrane fractionation in the presence or absence of 1 mM Mg^{2+} or in the presence of 1 mM EDTA revealed a shift of both Ca^{2+}-ATPase and Ca^{2+}/H^+ exchanger activities from the rough ER to the smooth ER simultaneously with a similar shift in the ER marker NADPH cytochrome *c* oxidoreductase [25]. Moreover, the high resistance of the ER Ca^{2+}-ATPase to vanadate [22, 25] distinguishes it from the Ca^{2+}-ATPases of other organelles, including the Golgi, vacuoles and NE. The relatively high resistance of the ER Ca^{2+}-ATPase activity to vanadate may be attributed to an accumulation of the $E_1 \sim P$ state during the catalytic cycle, with a lower level in the E_2 state. Indeed, it has been shown that the E_2 state of the catalytic cycle of P-type ion-transporting ATPases is critical for the binding of vanadate and, therefore, for inhibition of the enzyme [29]. From this point of view Spf1p in *S. cerevisiae* is the

relevant Ca^{2+}-ATPase for the ER because it accumulates in the $E_1 \sim P$ state of the catalytic cycle and its turnover is extremely low [30]. This suggestion and the possibility that Cta4p, NCA-1 and Eca1p are localized in the ER of fission yeast, *Neurospora crassa* and *Ustilago maydis* fungi, respectively [31–33], require further investigation. Deletion of *cta4*$^+$ has been already reported to result in decreased Ca^{2+}-ATPase activity in the ER of fission yeast [31], suggesting that Cta4p may function as the relevant Ca^{2+}-ATPase. *Fifth*, a comparison of the Ca^{2+}-ATPase activities in the *pmr1* mutant (strain AA274) and wild-type AA255 strain revealed an increase in the Ca^{2+}-ATPase activity in the NE-like membranes and in the ER simultaneously with its decrease in the Golgi (Fig. 27.2 and [18]). This increase indicates that a Ca^{2+}-ATPase other than Pmr1p is recruited to the ER and NE membranes of the *pmr1* mutant, which may be due to upregulation of the genuine NE and ER Ca^{2+} pumps and/or Ca^{2+}-ATPases of organelles located downstream of the Golgi in the secretory pathway. These last proteins were hypothetically recruited to the ER and NE membranes because they cannot be properly targeted to their own organelles due to the defective Ca^{2+} status of the Golgi [18]. For example, this increase may result from partial relocalization of the second Ca^{2+}-ATPase of the Golgi, which remains active following PMR1 deletion and/or Pmc1p [18]. The possibility of the relocalization of Pmc1p has been verified by Marchi et al. [16], who have claimed that Pmc1p can relocate to the ER and other dense membranes in the *pmr1* mutant or even in the wild-type strain under high concentrations of extracellular Ca^{2+}. However, their assertion was based on results obtained from membrane fractionation of the spheroplasts homogenate in a sucrose density gradient without preliminary separation of the soluble and membrane proteins by membrane sedimentation. Subsequent quantification of Ca^{2+}-ATPase activity and Pmc1p immunoreactivity was based on the protein content in each fraction despite the fact that soluble proteins dominated membrane proteins in the light membrane fractions. The predominance of the soluble proteins from the cytosol of the *pmr1* mutant was even higher for the vacuolar and Golgi fractions because the protein content in their membranes was decreased by ~50 and ~33 %, respectively, as a result of the *pmr1* mutation [18]. Consequently, the Ca^{2+}-ATPase activities and immunoreactivity of Pmc1p in the lightest membrane fractions were strongly underestimated (particularly for vacuolar membranes) compared with those in dense membranes. It most likely accounts for the uncommon distribution of enzymes along the sucrose gradient, i.e., Pmc1p was not detected in vacuolar membranes from the wild-type strain but "co-migrated" with membranes that are denser than Golgi membranes in this report, whereas Pmr1p was detected in light membranes that did not exhibit maximal GDPase (a Golgi marker) activity even in the wild-type strain under normal growth conditions [16]. The appearance of stronger Pmc1p immunoreactivity in dense membranes (an artifact?) is consistent with the high content of membrane proteins used in the immunoblot analysis [16]. Indeed, we found high immunoreactivity in vacuolar membranes and very low immunoreactivity for Pmc1p in the Golgi, ER and NE membranes when a low protein content of membranes preliminarily separated by centrifugation from soluble proteins was used in such studies [27]. The loading of a higher amount of membrane protein exhibited an increase in the immunoreactivity

in membranes denser than vacuolar membranes, whereas the vacuolar membranes exhibited a saturation of the signals [27]. Therefore, the relocalization of Pmc1p to the ER and NE membranes in the *pmr1* mutant is unlikely or does not significantly contribute to the higher Ca^{2+} transport activity in the NE and ER (Fig. 27.2). This explanation increases the possibility that the putative Ca^{2+}-ATPase(s) of the NE and ER can be upregulated in the *pmr1* mutant. The nature of this activity was analyzed by determining its sensitivity to cyclopiazonic acid, which is a known SERCA inhibitor [34]. This analysis revealed that the Ca^{2+}-ATPase activity in the dense membrane fractions of the *pmr1* mutant and in its Golgi membranes was inhibited at relatively low ATP concentration (Fig. 27.2), conditions that were found for SERCA-type pumps [34]. The strong inhibition of the yeast Ca^{2+}-pump activities in the ER and the NE-like membranes of the *pmr1* mutant indicates the presence of Ca^{2+} pump(s) that are similar to SERCA in membranes from both the mutant and wild-type strains. It is also correct for the Golgi Ca^{2+} pump in the mutant. Considering that Pmc1p is closely related to PM-type Ca^{2+}-ATPases [2, 10], these results (Fig. 27.2) also suggest that the localization of Pmc1p was not altered from vacuoles to the ER and the Golgi by the *pmr1* mutation.

Some attempts, which were made to support the assertion of the absence of a genuine Ca^{2+}-ATPase in the ER and to explain how the yeast ER lumen can be supplied with Ca^{2+} in this case, require additional discussion. The first argument is the finding that the "steady-state free Ca^{2+} concentration in the yeast endoplasmic reticulum reaches only 10 μM" [28], suggesting a low Ca^{2+} gradient for its influx into the cytosol and weak, if any, Ca^{2+} transport activity of the ER membranes. However, the concentration of free Ca^{2+} in the yeast vacuolar lumen (which is supplied by the Ca^{2+}-ATPase and Ca^{2+}/H^{+} exchanger) was found to be approximately 30 μM [35], which is close to that in the ER. The importance of bound Ca^{2+} in the organelle lumen has been demonstrated for the effective influx of Ca^{2+} when the free Ca^{2+} concentration in the Ca^{2+} storage organelles was maintained at approximately 25 μM [36]. Most of the Ca^{2+} in the lumen of these organelles is in the bound form [36], as is the majority of Ca^{2+}, Mg^{2+} and Mn^{2+} in yeast vacuoles [35, 37–39] and, most likely, in other organelles. Following a stimulus, the influx of Ca^{2+} into the cytosol does not decrease the free Ca^{2+} concentration in the organelle lumen because bound Ca^{2+} can be released, dissociating from its binding molecules [36]. Therefore, bound Ca^{2+} may buffer free Ca^{2+}. Notably, the influx of Ca^{2+} is accompanied by an efflux of K^{+}, which can replace bound Ca^{2+} in the organelle lumen, and this Ca^{2+}/K^{+} exchange can be reversed following the completion of signaling [36]. The second argument that the ER plays an insignificant role in yeast Ca^{2+} homeostasis and that the yeast ER lacks its own Ca^{2+}-ATPase is based on the finding that 5 μM thapsigargin did not decrease free Ca^{2+} in the ER lumen of yeast cells [28]. However, the actual capacity of the inhibitor remains unclear because its efficacy was determined in control experiments using a concentration of approximately 500 μM rather than 5 μM [28]. The third argument is based on the observed decrease in free Ca^{2+} in the ER of the *pmr1* mutant (approximately 30 %), which led to the conclusion that Pmr1p can supply the ER lumen with Ca^{2+} [28]. This interpretation contradicts experimental results that demonstrate an increase in Ca^{2+}-ATPase activity

in the dense membranes (including ER membranes) of the *pmr1* mutant ([18] and Fig. 27.2). The decrease in free Ca^{2+} in the ER lumen of the *pmr1* mutant is most likely due to more efficient Ca^{2+} binding resulting from the higher protein content in the ER and NE of this mutant [18].

Therefore, experimental evidence allows us to propose a model of Ca^{2+} homeostasis in *S. cerevisiae* with the participation of more than two Ca^{2+}-ATPases, i.e., Pmc1p in vacuoles [2], Pmr1p [3–7] and the second pump in the Golgi [18], a pump in the ER ([17, 25] and this review, likely Spf1p/Cod1p [30, 40, 41]), a putative Ca^{2+}-ATPase in the PM [17] and in NE-like membranes ([25] and Fig. 27.1). Additionally, Ca^{2+}/H^{+} exchangers from the same organelles are important participants of homeostasis, contributing up to 80 % to the total Ca^{2+} uptake by TMs (see below). This activity is detected in those organelles following membrane fractionation, which prevents contamination of the NE-like membranes, ER and Golgi by vacuolar membranes (Fig. 27.1, [27]). The presence of Ca^{2+}/H^{+} exchanger(s) in these organelles also follows from a finding that bafilomycin A_1 treatment of *vcx1*mutant cells additionally reduced their ability to properly normalize/diminish the free cytosolic Ca^{2+} concentration [9, 42]. Interestingly, the low residual Ca^{2+}/H^{+} activity in TMs from the *vcx1* mutant ([43] and Fig. 27.3) is

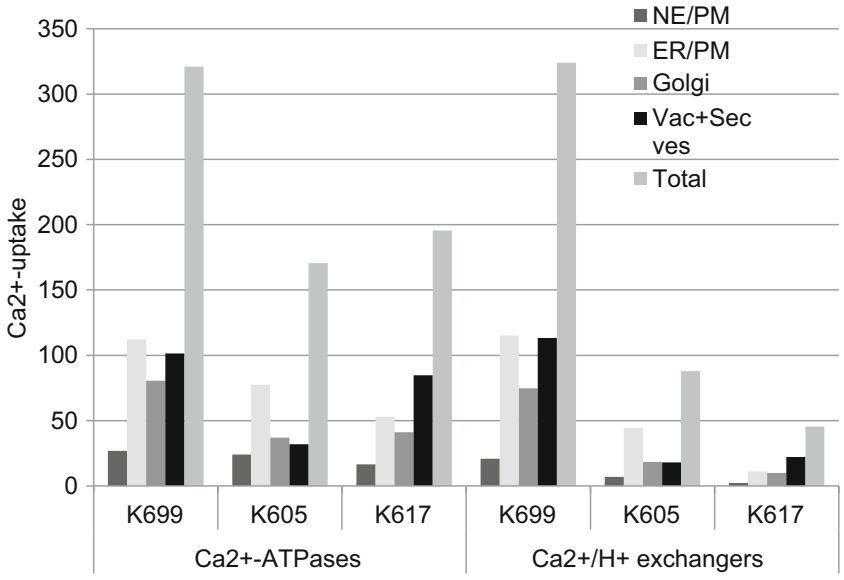

Fig. 27.3 *VCX1* and *PMC1* positively regulate all Ca^{2+} transporters of the yeast secretory pathway. Membrane vesicles from the spheroplast homogenates from wild-type strain K699 (PMC::HA), the *pmc1* mutant K605 and the *vcx1* mutant K617 were separated on a sucrose density gradient. Ca^{2+} transport activity was determined as described in the legend for Fig. 27.1 and is represented for the sums of the respective membrane populations in pmol × (mg protein of the spheroplast homogenates)$^{-1}$. Representative experiment of four is shown

consistent with the relatively small negative effect of bafilomycin A_1 on the recovery of the free cytosolic Ca^{2+} in the *vcx1* mutant [9, 42] but contradicts biochemical studies that the contribution of Ca^{2+}/H^+ activity from all organelles distinct from vacuoles reached 65–80 % in different wild-type strains, whereas that of the vacuolar exchanger does not exceed 35 %.

3 *VCX1*, *PMC1* and Their Products Are Important Regulatory Determinants of the Yeast Ca^{2+} Homeostasis

We therefore hypothesize that Vcx1p positively controls the activities of Ca^{2+}/H^+ exchangers in different organelles of the yeast secretory pathway that are distinct from vacuoles. Interestingly, Pmc1p demonstrates a similar property. Indeed, the Ca^{2+}-ATPase activity of the organelles distinct from vacuole including the Golgi equipped with Pmr1p and another Ca^{2+} pump (see above) was diminished in the *pmc1* mutant simultaneously with the disappearance of Pmc1p in vacuolar membranes ([43] and Fig. 27.3); the residual Ca^{2+}-ATPase activity in vacuolar membrane fractions is likely due to the co-migrating secretory vesicles. Moreover, the vacuolar Vcx1p controls the activities of Ca^{2+}-ATPases in the entire secretory pathway, whereas Pmc1p regulates the activities of all Ca^{2+}/H^+ exchangers along the pathway (Fig. 27.3). For example, the *VCX1* deletion causes ~50 % decrease in Ca^{2+}-ATPases from the ER/PM and Golgi, whereas the *PMC1* inactivation diminishes the Ca^{2+}/H^+ exchanger activities in the NE, ER, Golgi and vacuoles by 67, 61, 75 and 84 %, respectively ([43] and Fig. 27.3). This strong inhibition of the transport activity of another type of Ca^{2+} transporter is even more effective than the inhibition of the same type of the transporter (Ca^{2+}-ATPases). Indeed, the decrease of Ca^{2+}-ATPase activities in those membranes from the *pmc1* mutant was 11, 31, 54 and 68 %, respectively. These findings show the positive cross-control between Ca^{2+}-ATPases and Ca^{2+}/H^+ exchangers. Moreover, they confirm the existence of additional Ca^{2+} transporters together with Pmc1p, Pmr1p and Vcx1p along the secretory pathway.

These findings indicate the important properties of vacuolar Ca^{2+} transporters and their respective genes as positive regulators of the same type of Ca^{2+} transporters in distinct secretory organelles and also different types of Ca^{2+} transporters along the yeast secretory pathway. Interestingly, although the Golgi Pmr1p negatively regulates Ca^{2+}-ATPase activity in NE and ER membranes (Fig. 27.2 and [18]), Pmc1p and Vcx1p are positive regulators of all Ca^{2+} transporters along the secretory pathway. It is likely that in the case of their low activity or the absence of *PMC1* and/or *VCX1*, all other Ca^{2+} transporters receive a signal to decrease their activities. Both vacuolar Ca^{2+} transporters and their genes can be considered feedback regulators of Ca^{2+} yeast homeostasis. One should remind that the conclusions on the dominant or even exclusive role of Pmc1p and Vcx1p and the insignificant role of the ER in Ca^{2+} homeostasis were primarily based on analysis of the physiological consequences observed in vivo for the respective mutants (e.g., the growth inhibition by

high Ca^{2+}). The significant changes in the mutant physiology and a decrease of Ca^{2+} pumps activity in the *pmc1*, *pmr1* and *cnb1* mutants were interpreted by a simplified manner. It was concluded that the physical absence of the respective pumps is solely responsible for the significant decrease of Ca^{2+}-ATPase activity in those mutants. It was even claimed that "…all of the observed Ca^{2+} pump activity in yeast is derived from two Ca^{2+}-ATPases, Pmr1 and Pmc1" [16]. Unfortunately, the additional regulatory interplay of the vacuolar transporters and those from other secretory organelles as well as of their respective genes was not taken into account. At present time we know two examples of the interplay between the secretory organelles responsible for the Ca^{2+} homeostasis. First one is the increased Ca^{2+}-ATPase activity in NE and ER membranes from *pmr1* mutant ([16, 18] and Fig. 27.2) which can be attributed to the increased level of the free Ca^{2+} in cytosol as well as upregulation of the Ca^{2+} pumps in those organelles. The second one we reveal for the *vcx1* and *pmc1* mutants when the activities of Ca^{2+}/H^{+} exchangers and Ca^{2+}-ATPases were unexpectedly diminished in all secretory organelles instead of their expectable activation in result of the most likely increase in free cytosolic Ca^{2+} (this report and [43]). The mechanism of the activity decrease of the Ca^{2+} transporters in those mutants needs to be explored. Additionally, the conclusions on the dominant role of Pmc1p and Vcx1p and the insignificant role of the ER in Ca^{2+} homeostasis were influenced by the claim that ~90 % of the cellular Ca^{2+} in yeast is located in vacuoles [10, 11, 44]. This assertion was based on the finding that most of the intracellular Ca^{2+} was released following vacuole lysis from osmotic shock of the cells in which the PMs were permeabilized [44]. However, the lysis of other intracellular organelles/membrane vesicles was not considered (Fig. 27.1. in [5] and our unpublished results). Considering the biochemical results, including the high contribution of the Ca^{2+} transporters from the ER/PM and NE to the total Ca^{2+} uptake compared with that of the vacuolar transporters (see below), the well separation of the membrane vesicles derived from NE, ER, Golgi and vacuole, as well as the positive regulation of the Ca^{2+} transporters in the NE, RE/PM and Golgi by those from vacuolar membranes (Figs. 21.1, 27.3 and [25, 27, 43], we propose a clarification of the regulatory role of the vacuolar transporters in yeast Ca^{2+} homeostasis. Our supposition includes the nearly equivalent participation of different secretory organelles equipped with proper Ca^{2+} transporters in Ca^{2+} efflux ([18, 22–25] and see below) and the moderate contribution of the vacuolar transporters from wild-type strains, which has been previously overestimated [2, 8, 10, 11, 16, 44].

4 The Yeast Ca^{2+}-ATPases Are Similar to SERCA

The available data on the nature of the yeast Ca^{2+} pumps are controversial. It was shown [17] that the formation of a phosphorylated intermediate (acyl phosphate) by yeast TMs can be efficiently blocked by cyclopiazonic acid, which is a specific inhibitor of SERCA (sarco/endoplasmic reticulum calcium ATPases). However, the

insensitivity of Pmr1p to cyclopiazonic acid and thapsigargin, which is another specific SERCA inhibitor, was subsequently reported [7]. This report together with the finding that Pmc1p exhibits ~40 % identity with Ca^{2+}-ATPases from the mammalian PMs [2] was used to make a generalized conclusion that "*S. cerevisiae* and other budding yeasts do not retain SERCA family Ca^{2+} pumps" [10]. However, the assertion that Pmr1p exhibits very weak sensitivity to cyclopiazonic acid [7] was based on results obtained under experimental conditions (0.5 mM ATP) that do not permit the inhibition of even genuine SERCA [34]. Indeed, we also found that 0.5 and 1.0 mM ATP prevent cyclopiazonic acid inhibition of both the yeast Ca^{2+}-ATPases from TMs and the Ca^{2+}-ATPases from the rabbit sarcoplasmic reticulum (data not shown). Moreover, the strong inhibition of the formation of the acyl phosphate intermediate and Ca^{2+} uptake by cyclopiazonic acid at low ATP concentrations was well reproducible ([17, 25] and Fig. 27.2). Additionally, the inability of thapsigargin to inhibit Pmr1p activity that was reported in [7] can be explained by inhibitor inactivation, which was not verified using genuine SERCA as it was made in other studies [25, 45]. Therefore, we conclude that the yeast Ca^{2+}-ATPases are similar to SERCA at least from the point of view of their sensitivity to specific inhibitors of these mammalian pumps. This finding clearly indicates an evolutionary link of the yeast Ca^{2+}-ATPases with mammalian SERCAs, suggesting their common ancestor and that certain kinetic differences between these ATPases [7] have arisen during evolution. Therefore, we believe that the yeast Ca^{2+} homeostasis model is useful to better understand mammalian Ca^{2+} homeostasis.

5 Regulation of the Yeast Ca^{2+} Transporters by Extracellular Glucose

Extracellular glucose stimulates the activities of Ca^{2+}-ATPases and Ca^{2+}/H^+ exchangers of TMs by ~2- and ~7-fold, respectively [25]. This stimulation was found for both types of Ca^{2+} transporters from all secretory organelles, exhibiting a selective activation for different organelles, particularly for exchangers. Ca^{2+}-ATPases of the NE/PM, NE/ER/PM, ER/PM, Golgi and vacuoles were stimulated 3.1-, 1.7-, 1.5-, 1.2- and 1.7-fold by extracellular glucose, respectively, whereas the Ca^{2+}/H^+ exchangers from these membranes increased their activities by 11.2-, 7.3-, 7.7-, 6.8-10.5-fold, respectively [25].

The impressive efficacy of Ca^{2+}/H^+ exchangers to rapidly decrease the free cytosolic Ca^{2+} concentration, which was sharply increased by high extracellular Ca^{2+} or high osmolality [9, 42], called into question the two-decade-long opinion on the low Ca^{2+} affinity of the exchangers [10, 11, 46]. Reinvestigation of the kinetic properties of the Ca^{2+} transporters of TMs using the free Ca^{2+} values instead of the previously used nominal (total) Ca^{2+} concentrations revealed that the K_M values of the nonactivated and extracellular glucose-activated exchangers from TMs are 61 ± 27 nM and 99 ± 13 nM, while V_{max} are 0.52 ± 0.17 nmol/min × mg and 4.3 ± 0.5 nmol/min × mg protein, respectively [25, 47]. The Ca^{2+}-ATPase activity of TMs exhibits K_M values

of 46 ± 3 nM and 51 ± 11 nM for nonactivated and activated states, whereas V_{max} are 0.29 ± 0.03 nmol/min × mg protein and 1.22 ± 0.12 nmol/min mg protein, respectively [25, 47]. Therefore, Ca^{2+} affinity of exchangers is similar to that of Ca^{2+}-ATPases, but they transport Ca^{2+} with higher velocity.

Given that Ca^{2+} uptake by vesicles of intracellular membranes reflects the capacity of the respective organelles for Ca^{2+} efflux from the cytosol, a potential contribution of Ca^{2+} transporters in this efflux was evaluated considering the glucose-activated transporters [25]. Ca^{2+}-ATPases of the NE/PM, PM/ER, ER/PM, Golgi and vacuoles contributed ~14, 16, 33, 23 and 14 % from total Ca^{2+}-ATPase activity. It means that the Ca^{2+} pumps of the NE/PM, PM/ER and ER/PM membranes contributed more (63 %, including 33 % from ER/PM) to the potential efflux than the Ca^{2+}-ATPases of the Golgi and vacuolar membranes combined (37 %). Moreover, the potential efflux mediated by exchanger(s) on the Golgi and vacuoles (46 %) is less in comparison with that mediated by the exchanger(s) on the NE/PM, PM/ER and ER/PM membranes (54 %), further demonstrating the importance of organelles other than vacuoles and Golgi for yeast Ca^{2+} homeostasis [25]. Notably, the ratio of the exchanger to Ca^{2+} pump activities is higher in vacuolar, Golgi and ER/PM membranes of *S. cerevisiae* X2180 (6.4, 7.6, 4.7-fold, respectively), and diminishes in NE/PM and PM/ER (2.4- and 2.4 fold, respectively) [25]. We found such increase of the ratio from NE/PM to vacuolar membranes for different *S. cerevisiae* wild-type strains (not shown). This difference between various Ca^{2+} storage organelles can most likely be used to generate the distinct shapes of Ca^{2+} signals by these differentially located compartments.

6 Regulation of Ca^{2+} Transporters in Response to High Extracellular Ca^{2+} Under Different Energy Supply Conditions

The available data on the regulation of the yeast Ca^{2+} transporters under high Ca^{2+} stress are primarily based on the investigation of their gene expression. This analysis has shown an increase in the expression of *PMC1* and *PMR1* as a result of this stress, whereas *VCX1* expression was diminished compared with normal growth conditions (YPD medium). This regulation was attributed to the positive regulation of these Ca^{2+}-ATPases and to negative regulation of Vcx1p by calcineurin [8–10]. Our biochemical analyses of the activities of transporters are consistent with these findings. It was shown that TMs isolated from yeast growing in the high-Ca^{2+} YPD medium exhibited activation of Ca^{2+}-ATPases and inhibition of Ca^{2+}/H^+ exchangers compared with normal growth conditions [48]. Membrane fractionation revealed the activation of Ca^{2+}-ATPases from vacuoles and the Golgi, which is consistent with results on the increase in the expression of *VCX1* and *PMR1* [8–10, 16]. Additionally, Ca^{2+} pumps from membrane fractions enriched with the ER/PM and NE were also stimulated, indicating the coordinated and collective response of Ca^{2+}-ATPases from all secretory organelles to the high Ca^{2+} stress. Ca^{2+}/H^+

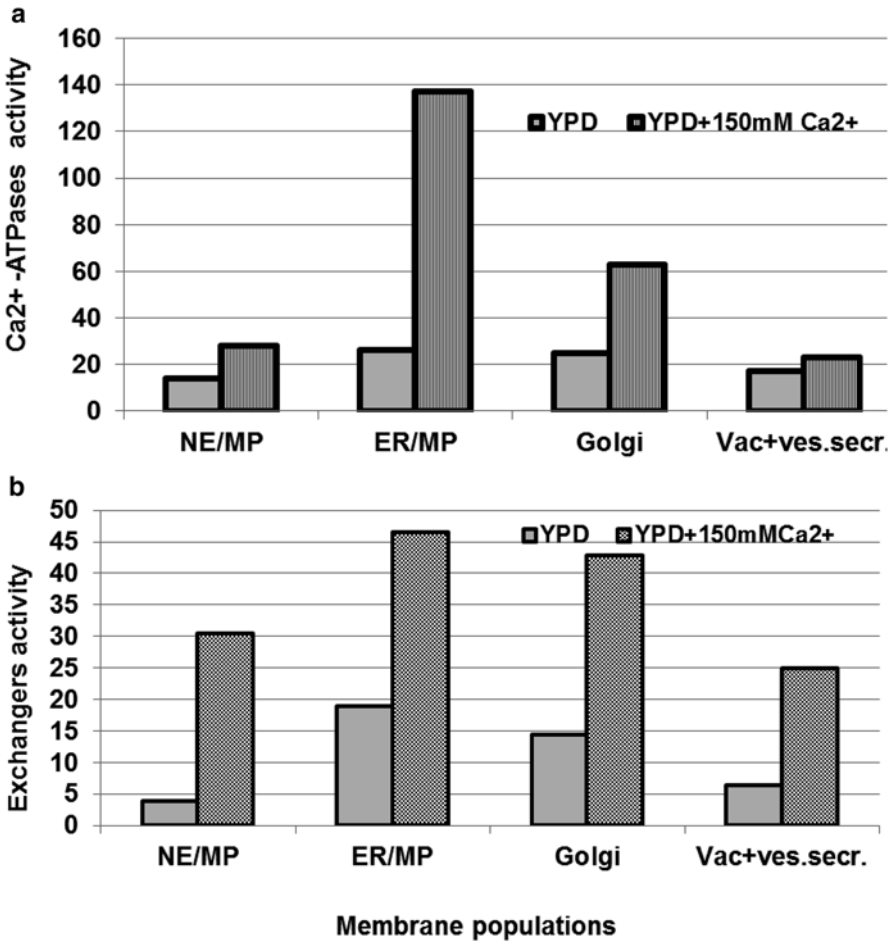

Fig. 27.4 The preliminary Ca^{2+} stress stimulates all Ca^{2+}-ATPases and Ca^{2+}/H^{+} exchangers of secretory pathway when extracellular glucose is depleted. Cells of the wild-type strain AA255 were grown in YPD or YPD + 150 mM $CaCl_2$. Spheroplasts were isolated in the absence of Ca^{2+} and glucose. TMs were fractionated on a sucrose density gradient as described in legend of Fig. 27.1. The sum of the respective Ca^{2+} transport activities for each membrane population is represented in cpm $\times 10^{-3} \times$ (mg TM protein)$^{-1}$. (**a**) Ca^{2+}-ATPase and (**b**) Ca^{2+}/H^{+} exchanger activities. The representative experiment of three is shown

exchangers also collectively responded to this stress, although through the coordinated decrease in their activities in all secretory organelles [48] including vacuoles (which is consistent with the decrease in *VCX1* expression [8–10].

Notably, that in the described experiments, TMs were isolated from spheroplasts obtained from cells growing with 150 mM Ca^{2+} and pretreated for 10 min with 100 mM glucose. Unexpectedly, when spheroplasts were preincubated without glucose, the response of the Ca^{2+} transporters to the preliminary Ca^{2+} stress was altered.

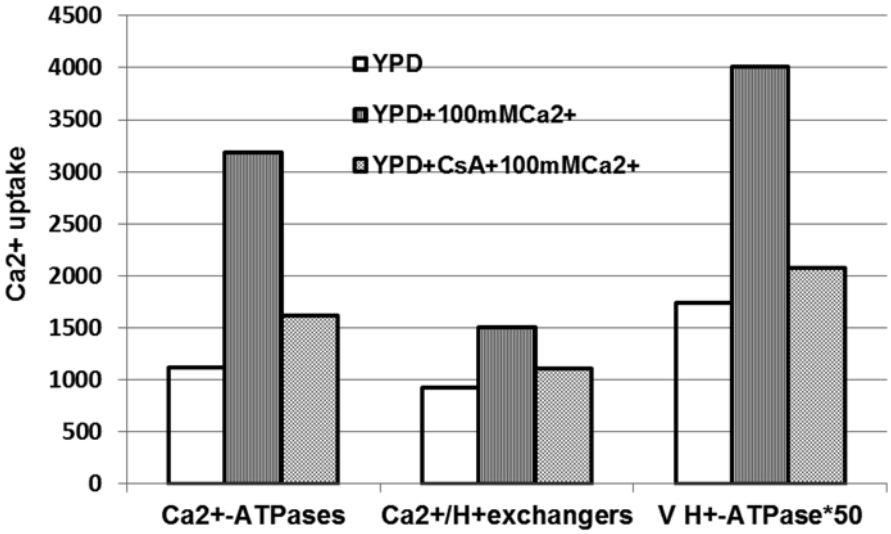

Fig. 27.5 Cyclosporine A prevents the stimulation of Ca^{2+}-ATPases, Ca^{2+}/H^+ exchangers, and V H^+-ATPase during preliminary Ca^{2+} stress when glucose is then depleted. Yeast cells of wild-type strain AA255 were grown to OD_{600} 3.0, divided into three parts: two parts were allowed to continue their growth in YPD, while cyclosporine A (10 μg/ml) was added to the third one. After 2.5 h, $CaCl_2$ was added to second and third part cultures to a final concentration of 100 mM. After 2.5 h growth the spheroplasts were isolated from yeast cells, preliminary washed with water, and used for TMs isolation. H^+ transport activity (steady state) was determined according to [13–15, 24] and represented in % of fluorescent quinching × 50 × (mg protein of TMs)$^{-1}$. See also legend of Fig. 27.1. Ca^{2+} transport activity is represented in pmol × (mg protein of TMs)$^{-1}$

Although the Ca^{2+}-ATPases continued to be activated, Ca^{2+}/H^+ exchangers were also activated (Fig. 27.4a, b), in contrast to the previously observed decrease in the activity. This activation of the exchangers was also reproduced following the incubation of cells with 100 mM $CaCl_2$ for 2.5 h (Fig. 27.5). Once again, Ca^{2+}-ATPases and exchangers were activated under identical conditions. Notably, activation of both types of Ca^{2+} transporters was prevented to a considerable extent by the calcineurin antagonist cyclosporine A (Fig. 27.5), indicating calcineurin-dependent modulation of the activities of these Ca^{2+} transporters. Interestingly, the activation of Ca^{2+}/H^+ exchangers in the absence of glucose and its prevention by cyclosporine A was accompanied by the similar modulation of VH^+-ATPase activity (Fig. 27.5). Given the direct dependence of the exchanger activities from V H^+-ATPase, this data assume that calcineurin indirectly controls the exchanger activities via the H^+ pump regulation (see also below).

Unexpectedly, only the removal of glucose, which is used in a 10-min preincubation of spheroplasts prior to membrane isolation, from the medium while maintaining all other experimental conditions identical increases the exchanger activity after preliminary Ca^{2+} stress (Figs. 27.4 and 27.5). In summary, Ca^{2+} stress in the absence of glucose activates Ca^{2+}-ATPases and Ca^{2+}/H^+ exchangers (Fig. 27.6). Glucose also

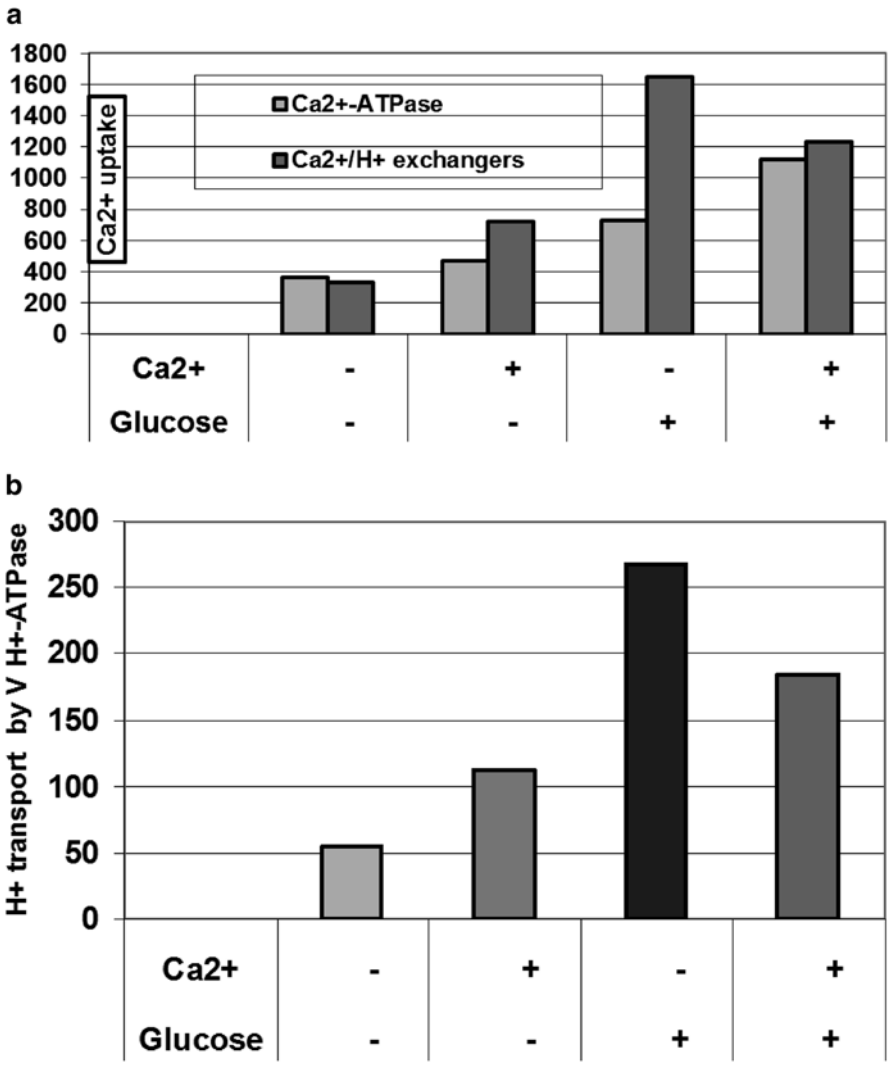

Fig. 27.6 Modulation of Ca^{2+}-ATPase, Ca^{2+}/H^+ exchanger (**a**) and V H^+-ATPase (**b**) activities of TMs by extracellular Ca^{2+} and glucose. Spheroplasts were isolated from wild-type strain AA255 cells exposed or not to 100 mM $CaCl_2$ stress and then incubated or not with 100 mM glucose for 10 min before the TM isolation. Determination of Ca^{2+} and H^+ transport activities is described in Figs. 27.1 and 27.5, respectively. Ca^{2+} transport is represented in pmol × (mg protein of TMs)$^{-1}$ and H^+ transport is shown in % of fluorescent quinching × (mg protein of TMs)$^{-1}$. (**a**) Ca^{2+}-ATPase and Ca^{2+}/H^+ exchanger and (**b**) V H^+-ATPase activities

activates both types of Ca^{2+} transporters, if extracellular Ca^{2+} is low. However, when Ca^{2+} stress is applied in the presence of glucose, Ca^{2+}-ATPases are additionally activated, but the exchangers operate with lower capacity although with higher capacity compared with that observed in the absence of glucose (Fig. 27.6). Therefore, calcineurin most likely positively regulates both Ca^{2+}-ATPases and $Ca^{2+}/$

H^+ exchangers of the yeast secretory pathway under deficient energy and carbon source conditions. When glucose is supplied, Ca^{2+}-ATPases are additively stimulated; however, the exchanger activity is moderately limited but is higher than in the presence of Ca^{2+} alone (Fig. 27.6). These observations allow us to suggest that calcineurin is only a moderate negative regulator of the glucose-dependent activation of Ca^{2+}/H^+ exchangers under the Ca^{2+} stress conditions. The modulation of the exchanger activities under different concentrations of the extracellular Ca^{2+} and glucose is accompanied by the similar modulation of the VH^+-ATPase activity (Fig. 27.6). Therefore, it is very likely that the regulation of the exchangers by calcineurin is achieved by the modulation of the V H^+-ATPase activities in yeast secretory organelles (Figs. 27.5, 27.6 and [48]). Interestingly, the partial inhibition of Ca^{2+}/H^+ exchangers was observed in preconditions of the Ca^{2+} stress and its subsequent abolition during cell washing and spheroplast isolation (collectively ~60–75 min) and the subsequent 10-min incubation with glucose. This inhibition correlates with the decrease in *VCX1* expression observed in vivo at continuous high extracellular Ca^{2+} concentrations in the presence of glucose [8–10]. We suppose that when the extracellular Ca^{2+} stress was removed prior to membrane isolation, the cytosol remained under stress from the Ca^{2+} accumulated by intracellular organelles. To prevent an uncontrolled increase in free cytosolic Ca^{2+} as a result of the Ca^{2+} diffusion from its intracellular stores, Ca^{2+}-ATPases were activated and the capacity of Ca^{2+}/H^+ exchangers was moderately diminished compared with that found in the presence of glucose alone. We therefore suggest that the regulation of both Ca^{2+} transporters by calcineurin when Ca^{2+} stress is applied can be achieved by two steps. The first step is achieved by utilizing endogenous energy sources, and the second step operates additionally if an extracellular energy source is available. In this case, the capacities of both transporters are higher compared with those of the first step (Fig. 27.6).

Moreover, it was found that calcineurin deletion decreased Ca^{2+} uptake by TMs by approximately 60 %, inhibiting Ca^{2+}-ATPases (~70 %) and Ca^{2+}/H^+ exchangers (~50 %) when the *cnb* mutant cells were grown under normal conditions in the absence of high Ca^{2+} stress [48]. This decrease was observed for both the Ca^{2+}-ATPase and the Ca^{2+}/H^+ exchanger of vacuolar membranes and for transporters of the NE/PM, PM/ER, ER/PM and Golgi membranes (Fig. 27.7). These data collaborate well with the results presented above (Figs. 27.5, 27.6 and 27.7). Taken together they suggest the positive and flexible regulation of all Ca^{2+} transporters from the secretory pathway by calcineurin under various conditions of yeast growth (Figs. 27.5, 27.6 and 27.7 and [48]).

Under common laboratory conditions (~1 μM of free Ca^{2+} in YPD medium [5]) and even under conditions of high Ca^{2+} stress and glucose deficiency, all Ca^{2+} transporters are positively regulated by calcineurin. This positive regulation of Ca^{2+}-ATPases exists even under conditions of Ca^{2+} stress and a glucose supply, when additive stimulation of the pumps by Ca^{2+} and glucose occurs. Under identical conditions, the high capacity and high affinity Ca^{2+}/H^+ exchangers are moderately restricted by calcineurin, demonstrating their apparent negative regulation by calcineurin compared with the exchanger activities observed when the Ca^{2+} stress is not applied but glucose is supplied. However, these activities remain significantly higher than those observed under Ca^{2+} stress in the absence of glucose, revealing the relative

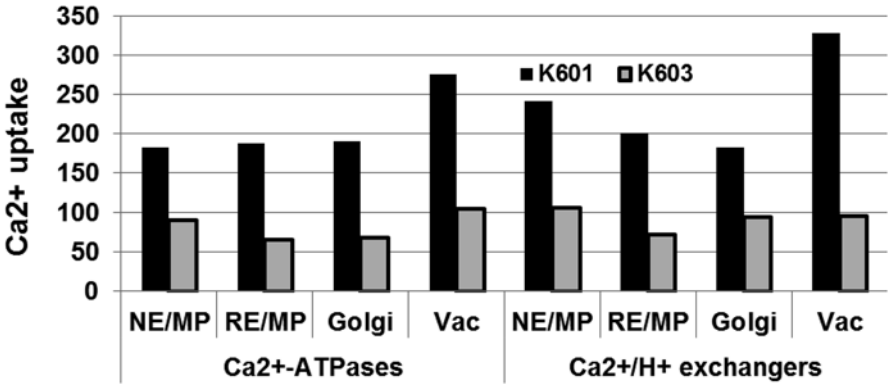

Fig. 27.7 Calcineurin positively regulates all Ca^{2+} transporters of the secretory pathway under normal growth conditions. Yeast cells of wild-type K601 and the calcineurin mutant K603 (*cnb1*) strains were grown in YPD. Homogenates were isolated from spheroplasts preincubated for 10 min with 100 mM glucose and then fractionated on a sucrose density gradient. Ca^{2+} transport activity was determined as described in the legend for Fig. 27.1 and is represented for the sums of the respective membrane populations in pmol × (mg protein of the homogenates of spheroplasts)$^{-1}$. See legends of Figs. 27.1 and 27.3

positive regulation of the exchangers by calcineurin. Notably, the level of the Ca^{2+}/H^+ exchanger activity in TMs regulated by calcineurin under different conditions correlates well with the respective activity of the VH^+-ATPase (Fig. 27.6), suggesting that calcineurin regulation of the exchanger activity is primarily achieved via calcineurin modulation of the VH^+-ATPase rather than by its direct interaction with the exchangers. This attractive insight offers new possibilities for the investigation of the role of calcineurin in the regulation of the VH^+-ATPase and numerous processes with the participation of this ubiquitous H^+ pump that include the regulation of the cytosolic H^+ concentration and the participation of various cation/H^+ exchangers in the homeostasis of cations such as K^+, Na^+, Mg^{2+}, and Zn^{2+}, among others.

7 Conclusions

The participation of a set of secretory organelles in Ca^{2+} homeostasis protects cells from uncontrolled alterations in the free Ca^{2+} concentration in the cytosol and guarantees the local nature of Ca^{2+} signaling. If the respective Ca^{2+}-release channels determine the signal amplitude and the microdomain size [49], i.e., the number of released Ca^{2+} ions in the cytosol near the respective Ca^{2+} storage organelle, the different velocities of Ca^{2+} efflux mediated by the Ca^{2+} transporters in various secretory organelles can generate distinct shapes for the Ca^{2+} signals. Therefore, the presence of Ca^{2+}-ATPases and Ca^{2+}/H^+ exchanger on the same membrane appears to be physiologically significant. A variable ratio between the number of Ca^{2+} pumps and Ca^{2+}/H^+

exchangers between secretory organelles can also contribute to differences in the resulting signals. However, we propose that in yeast and fungi, the key role in the formation of the signal shape is mainly played by the exchangers, not Ca^{2+}-ATPases, because the exchangers modulate the duration and shape of the signals [9, 42]. Also, the presence of Ca^{2+}-ATPases in the same membrane is important because they can operate under an energy deficit. For example, the non-glucose-activated Ca^{2+}-ATPase of the yeast Golgi exhibits a K_M of 5 μM [5], whereas the nonactivated VH^+-ATPase exhibits a K_M of 100 μM (based on membrane potential formation; Kulakovskaia TV and Okorokov LA, unpublished) or 127 μM (based on ATP hydrolysis) [50]. Additionally, Ca^{2+}-ATPases, at least Pmr1p, can use ATP produced from ADP due to myokinase activity [5] and, therefore, can operate much better than VH^+-ATPase-dependent exchangers under an energy deficit.

Acknowledgments The different parts of this work were supported by the former Academy of Science of USSR, DFG (Deutsche Forschungsgemeinschaft, Germany), CNPq (Conselho Nacional de Pesquisa e Desenvolvimento), and FAPERJ (Fundação de Amparo à Pesquisa do Estado do Rio de Janeiro). I thank Drs. L. Lehle, W. Tanner, H. K. Rudolph, and K. Cunningham for kindly providing yeast strains and Dr. M. Gentzsch for the determination of the protein mannosyltransferase activity. I am grateful to my former and actual colleagues and students in Russia, Germany, and Brazil, who have contributed to our collective attempts to better understand the exciting construction of the yeast Ca^{2+} homeostasis created by nature.

References

1. Berridge MJ, Bootman MD, Roderick HL (2003) Calcium signalling: dynamics, homeostasis and remodeling. Nat Rev Mol Cell Biol 4:517–529
2. Cunningham KW, Fink GR (1994) Calcineurin-dependent growth control in *Saccharomyces cerevisiae* mutants lacking *PMC1*, a homolog of plasma membrane Ca^{2+} ATPases. J Cell Biol 124:351–363
3. Rudolph HK, Antebi A, Fink GR et al (1989) The yeast secretory pathway is perturbed by mutations in PMR1, a member of a Ca2+ ATPase family. Cell 58:133–145
4. Antebi A, Fink GR (1992) The yeast Ca^{2+}-ATPase homologue, PMR1, is required for normal Golgi function and localizes in a novel Golgi-like distribution. Mol Biol Cell 3:633–654
5. Okorokov LA, Tanner W, Lehle L (1993) A novel primary Ca^{2+}-transport system from *Saccharomyces cerevisiae*. Eur J Biochem 216:573–577
6. Okorokov LA, Lehle, L (1995) The PMR1 gene encodes a Ca^{2+}-ATPase which services Golgi and Golgi-related compartments in yeast: biochemical evidence. In: Proceedings 10th International Workshop on Plant Membrane Biology. Regensburg, 10: 54
7. Sorin A, Rosas G, Rao R (1997) PMR1, a Ca2 + -ATPase in yeast Golgi, has properties distinct from sarco/endoplasmic reticulum and plasma membrane calcium pumps. J Biol Chem 272:9895–9901
8. Cunningham KW, Fink GR (1996) Calcineurin inhibits *VCX1*-dependent H^+/Ca^{2+} exchange and induces Ca^{2+}-ATPases in *Saccharomyces cerevisiae*. Mol Cell Biol 16:2226–2237
9. Pozos TC, Sekler I, Cyert MS (1996) The product of *HUM1*, a novel yeast gene, is required for vacuolar Ca^{2+}/H^+ exchange and is related to mammalian Na^+/Ca^{2+} exchangers. Mol Cell Biol 16:3730–3741
10. Cunningham KW (2011) Acidic calcium stores of *Saccharomyces cerevisiae*. Cell Calcium 50:129–138

11. Pittman JK (2011) Vacuolar Ca^{2+} uptake. Cell Calcium 50:139–146
12. Ohsumi Y, Anraku Y (1983) Calcium transport driven by a proton motive force in vacuolar membrane vesicles of *Saccharomyces cerevisiae*. J Biol Chem 258:5614–5617
13. Okorokov LA, Kulakovskayaya TV, Lichko LP et al (1985) H^+/ion antiport as the principal mechanism of transport systems in the vacuolar membrane of the yeast *Saccharomyces carlsbergensis*. FEBS Lett 192:303–306
14. Okorokov LA, Lichko LP, Kulakovskayaya TV (1985) Biochemistry and function of vacuolar adenosine triphosphatase in fungi and plants. Springer, Berlin, pp 203–212
15. Kulakovskaya TV, Matys SV, Okorokov LA (1991) Transport of organic acid anions and guanosine into vacuoles of *Saccharomyces pastorianus*. Yeast 7:495–501
16. Marchi V, Sorin A, Wei Y, Rao R (1999) Induction of vacuolar Ca2+-ATPase and H+/Ca2+ exchange activity in yeast mutants lacking Pmr1, the Golgi Ca2+- ATPase. FEBS Lett 454: 181–186
17. Okorokov LA, Kuranov AJ, Kuranova EV et al (1997) Ca^{2+} transporting ATPase(s) of the reticulum type in intracellular membranes of *Saccharomyces cerevisiae*: biochemical identification. FEMS Microbiol Lett 146:39–46
18. Okorokov LA, Lehle L (1998) Ca^{2+}-ATPases of *Saccharomyces cerevisiae*: diversity and possible role in protein sorting. FEMS Microbiol Lett 162:83–91
19. Gentzsch M, Tanner W (1997) Protein-O-glycosylation in yeast: protein-specific mannosyl transferases. Glycobiol 7:481–486
20. Okorokov L (1995) Various compartments of the protein secretory pathway of yeast possess Ca^{2+}/H^+ antiporter (s) and V_1V_0 H^+ - ATPase(s). In: Proceedings of 10th International Workshop on Plant Membrane Biology. Regensburg 10: 56
21. Okorokov LA, Prasad R, Zviagilskaia RA et al (1996) Manual on membrane lipids, 16th edn. Springer, Heidelberg, pp 16–36
22. Okorokov LA (1997) Diversity of Ca^{2+} transporters and Ca^{2+} store compartments in yeast: possible role in protein targeting and in signal transduction. Folia Microbiol 42:244–245
23. Okorokov LA (1994) Several compartments of *Saccharomyces cerevisiae* are equipped with Ca^{2+}-ATPase(s). FEMS Microbiol Lett 117:311–318
24. Okorokov LA, Silva FE, Okorokova-Façanha AL (2001) Ca^{2+} and H^+ homeostasis in fission yeast: a role of Ca^{2+}/H^+ exchange and distinct V-H^+-ATPases of the secretory pathway organelles. FEBS Lett 505:321–324
25. Ribeiro CC, Silva FE, Okorokova-Façanha AL, Okorokov LA (submitted) Ca^{2+} homeostasis in the yeast *Saccharomyces cerevisiae*: new insights
26. Lytton J, Westlin M, Burk SE et al (1992) Functional comparison between isoforms of the sarcoplasmic or endoplasmic reticulum family of calcium pumps. J Biol Chem 267:14483–14489
27. Samarão SS, Teodoro CES, Silva FE, Ribeiro CC et al (2008) V H^+-ATPase along the yeast secretory pathway: energization of the ER and Golgi membranes. Biochim Biophys Acta 1788:303–313
28. Strayle J, Pozzan T, Rudolph H (1999) Steady-state free Ca^{2+} in the yeast endoplasmic reticulum reaches only 10 μM and is mainly controlled by the secretory pathway pump Pmr1. EMBO J 18:4733–4743
29. Wang X, Qian X, Stumpf B et al (2013) Modulatory ATP binding to the E_2 state of maize plasma membrane H^+-ATPase indicated by the kinetics of vanadate inhibition. FEBS J 280:4793–4806
30. Corradi GR, Pinto FT, Mazzitelli LR, Adamo HP (2012) Shadows of an absent partner: ATP hydrolysis and phosphoenzyme turnover of the Spf1 (Sensitivity to *Pichia farinosa killer toxin)*. J Biol Chem 287:30477–30484
31. Lustoza ACDM, Palma LM, Façanha AR et al (2011) P5A-type ATPase Cta4p is essential for Ca^{2+} transport in the endoplasmic reticulum of *Schizosaccharomyces pombe*. PLoS ONE 6:e27843. doi:10.1371/journal.pone.0027843
32. Bowman BJ, Draskovic M, Freita M et al (2009) Structure and distribution of organelles and cellular location of calcium transporters in *Neurospora crassa*. Eukaryot Cell 8:1845–1855

33. Adamicova L, Straube A, Schuz I, Steinberg G (2004) Calcium signaling is involved in dynein-dependent microtubule organization. Mol Biol Cell 15:1969–1980
34. Seidler NW, Jona I, Vegh M, Martonosi A (1989) Cyclopiazonic acid is a specific inhibitor of the Ca2+-ATPase of sarcoplasmic reticulum. J Biol Chem 264:17816–17823
35. Dunn T, Gable K, Beeler T (1994) Regulation of cellular Ca^{2+} by yeast vacuoles. J Biol Chem 269:7273–7278
36. Nguyen T, Chin WC, Verdugo P (1998) Role of Ca^{2+}/K^{+} ion exchange in intracellular storage and release of Ca^{2+}. Nature 395:908–912
37. Okorokov L, Lichko LP, Kulaev IS (1980) Vacuoles: main compartments of potassium, magnesium and phosphate ions in *Saccharomyces carlsbergensis* cells. J Bacteriol 144:661–665
38. Lichko LP, Okorokov L, Kulaev IS (1980) Role of vacuolar ion pool in *Saccharomyces carlsbergensis*: potassium efflux from vacuoles is coupled with manganese or magnesium influx. J Bacteriol 144:666–671
39. Lichko LP, Okorokov L, Kulaev IS (1982) Participation of vacuoles in regulation of levels of K^{+}, Mg^{2+} and orthophosphate ions in cytoplasm of the yeast *Saccharomyces*. Arch Microbiol 132:289–293
40. Suzuki C, Shimma Y (1999) P-type ATPase spf1 mutants show a novel resistance mechanism for the killer toxin SMKT. Mol Microbiol 32:813–823
41. Cronin SR, Rao R, Hampton RY (2002) Cod1p/Spf1p is a P-type ATPase involved in ER function and Ca^{2+} homeostasis. J Cell Biol 57:1017–1028
42. Miseta A, Kellermayer R, Aiello DP et al (1999) The vacuolar Ca^{2+}/H^{+} exchanger Vcx1p/Hum1p tightly controls cytosolic Ca^{2+} levels in *S. cerevisiae*. FEBS Lett 451:132–136
43. Silva FE, Ribeiro CC, Palma LM et al. (in preparation) *VCX1, PMC1* and their products positively control Ca^{2+}/H^{+} exchangers and Ca^{2+}-ATPases of the yeast secretory pathway
44. Eilam Y, Lavy H, Grossowicz N (1985) Cytoplasmic Ca^{2+} homeostasis maintained by a vacuolar Ca^{2+} transport system in the yeast *Saccharomyces cerevisiae*. J Gen Microbiol 131:623–629
45. Almeida AJC, Benchimol M, Souza W, Okorokov L (2003) Ca^{2+} sequestering in the early-branching amitochondriate protozoan *Tritrichomonas foetus*: an important role of the Golgi complex and its Ca^{2+}-ATPase. Biochim Biophys Acta 1615:60–68
46. Belde PJM, Vossen JH, Borst-Pauwels GWFH, Theuvenet APR (1993) Inositol 1,4,5-trisphosphate releases Ca^{2+} from vacuolar membrane vesicles of *Saccharomyces cerevisiae*. FEBS Lett 323:113–118
47. Ribeiro CC, Bernardes NR, Silva FE et al. (2007) Regulation of V H+-ATPases and Ca2+ transporters by extracellular glucose. In: 25th small meeting on yeast transport and energetics, SMYTE 25, Arraial d'Ájuda, Bahia, Brasil, 25:29
48. Silva FE, Ribeiro CC, Okorokova-Façanha AL, Okorokov LA (in preparation). Regulation of the yeast Ca^{2+} transporters in response to high extracellular Ca^{2+} under different energy supply conditions
49. Berridge MJ (2006) Calcium microdomains: organization and function. Cell Calcium 40: 405–412
50. Ribeiro CC, Monteiro RM, Freitas FP et al (2012) Extracellular glucose increases the coupling capacity of the yeast V H^{+}-ATPase and the resistance of its H^{+} transport activity to nitrate inhibition. PLoS ONE 7:e49580. doi:10.1371/journal.pone.0049580

Chapter 28
Role of P_{5A}-Type ATPase in Ion Homeostasis and Signaling: Shedding Light on Obscure Pump

Anna L. Okorokova-Façanha, Antônio Jesus Dorighetto Cogo, and Lívia Marini Palma

Abstract Despite the substrate specificity has not yet been clarified for the putative cation pumps belonging to the P_{5A}-type ATPase subfamily, compelling evidences have increasingly been accumulated about its crucial physiological role in Ca^{2+} homeostasis and signal transduction. The aim of this review is to discuss some of the most relevant functional data available, which establish a clear relationship among different phenomena underlying or depending on tightly modulations of cellular Ca^{2+} changes and the functional expression of P_{5A}-ATPases. Issues related to the different substrate propositions and structural analysis will only be mentioned, since they have thoroughly been explored in recent reviews. The relevance of critical biochemical characterizations in the completion of the most frequent molecular approaches in the elucidation of the key physiological role of the P_{5A}-type ATPases will be highlighted, whose evolution seems to be tightly integrated to the origin of eukaryotes.

Keywords Membrane transport • Ion pump • Calcium signaling • Manganese • Endoplasmic reticulum • Oxidative stress • Cell wall integrity

A.L. Okorokova-Façanha (✉)
Laboratório Fisiologia e Bioquímica de Microrganismos, Centro de Biociências e Biotecnologia, Universidade Estadual do Norte Fluminense Darcy Ribeiro, Av. Alberto Lamego 2000, Campos dos Goytacazes, RJ 28013-602, Brazil
e-mail: anna@uenf.br

A.J.D. Cogo • L.M. Palma
Laboratório Fisiologia e Bioquímica de Microrganismos, Centro de Biociências e Biotecnologia, Universidade Estadual do Norte Fluminense Darcy Ribeiro, Av. Alberto Lamego 2000, Campos dos Goytacazes, RJ 28013-602, Brazil

Laboratório de Biologia Celular e Tecidual, Centro de Biociências e Biotecnologia, Universidade Estadual do Norte Fluminense Darcy Ribeiro, Av. Alberto Lamego 2000, Campos dos Goytacazes, RJ 28013-602, Brazil

S. Chakraborti, N.S. Dhalla (eds.), *Regulation of Ca^{2+}-ATPases,V-ATPases and F-ATPases*, Advances in Biochemistry in Health and Disease 14,
DOI 10.1007/978-3-319-24780-9_28

1 Introduction

The flow of ions across cellular membranes is mediated by the coordinated function of ion transporters and channels. Primary pumps transport ions generating the electrochemical gradients on the expense of ATP hydrolysis, which energize secondary transporters, and this integrated system orchestrates the ion and metabolite's acquisitions, exclusions, and compartmentalizations and the ion homeostasis and signaling. In accordance with such relevance for the cellular development, multiple ion ATPases evolved during the earlier events of prokaryote and eukaryote evolution, differing in their amino acid sequences, biochemical properties, and subcellular localizations. The three main types of ion-motive ATPases include the multimeric F-type and V-type ATPases, which translocate H^+, and the P-type ATPases mostly composed by single polypeptides [1, 2]. The latter are also much more diverse in terms of ion translocation and functions and can be found in plasmalemma and endomembranes as well. The formation of a phosphorylated intermediate during the catalytic cycle is a key characteristic of P-type ATPases that distinguishes them from V-ATPases and F-ATPases [1, 2]. They share five highly conserved regions within two hydrophilic cytosolic loops, which include phosphorylation (also a site for irreversible vanadate binding) and ATP-binding domains [3–5]. The sequencing of the genomes from Bacteria, Archaea, and Eukarya has allowed the identification of hundreds of genes encoding for P-type ATPases and phylogenetic analysis of the main ion pumps belonging to this superfamily [6]. P-type ATPases are distributed in five subfamilies depending on substrate specificity. Among the substrates transported by these pumps are protons, calcium, sodium, potassium, and heavy metals such as manganese, iron, copper, zinc, and also aminophospholipids.

The genes encoded for novel uncharacterized P-type ATPases were initially identified during the first complete inventory of the P-type ATPases in a unicellular eukaryotic microorganism, which was carried out in the budding yeast *Saccharomyces cerevisiae* by a group headed by Prof. A. Goffeau [7]. The members of this novel subfamily, with unknown substrate specificity, have been further revealed in the genomes of plant *Arabidopsis thaliana* [8] and the archiascomycete fungus *Schizosaccharomyces pombe* [9] and other eukaryotic organisms and were classified as P_5-type ATPases [6]. Based on sequence analysis of P_5-type ATPases from diverse eukaryotic genomes, they can be divided in two groups, namely, P_{5A} and P_{5B} [9, 10]. Contrasting with P_{5A}-type ATPases which are present in all eukaryotic genomes, P_{5B}-type ATPases are absent in some multicellular eukaryotes including land plants [10]. The degree of sequence variation between two subclasses of P5-type ATPases may reflect distinct substrate specificity, mode of regulation, and cellular localization. Indeed, P_{5A}-type ATPases have been localized to the endoplasmic reticulum [11–14], while P_{5B}-type ATPases to the vacuole/Golgi/lysosomal membrane [15, 16]. Sequence and structural differences between P_{5A}- and P_{5B}-ATPases have been discussed in [17].

So far, even after 16 years of intense investigations since the first phenotypic characterization of deletion mutant of P_{5A}-type ATPase in *S. cerevisiae*, there is no

definition and agreement regarding the substrate specificity of P_{5A}-type ATPase and complete understanding of its molecular functions. Our current knowledge on physiological functions of these unique and enigmatic pumps is based essentially on genetic and biochemical characterization of P_{5A}-type ATPases from yeast and plant cells. The loss of P_{5A}-type ATPases has a profound effect on several processes including the establishment and maintenance of cell polarity, cytokinesis, ion homeostasis, and protein glycosylation, folding, and secretion [11–13, 18–20].P5A-type ATPase is also important for reproduction since the absence of its expression results in *Arabidopsis* plants with decreased fertility [13] and fission yeast with impaired formation of the forespore membrane [14]. However, many questions remain to be explored, such as: (1) why the expression of this unique kind of pump in the endoplasmic reticulum has such a profound effect on cell functioning? (2) Do P_{5A}-type ATPases represent primary ancient pumps serving the endoplasmic reticulum? How does the evolution of function and regulation of P_{5A}-type ATPase accompany the evolution of the signaling pathways irradiating from the endoplasmic reticulum to reach the development of complex signaling networks characteristic of the eukaryotic cells? Such complex issues have to be addressed integrating advanced molecular analysis with basic functional characterization toward the accomplishment of effective system biology approaches.

2 P_{5A}-Type ATPase, Cell Wall Integrity, and Endoplasmic Reticulum Stresses

The analysis of *S. cerevisiae* mutants sensitive to *Pichia farinosa* killer toxin provided the first clue in understanding a potential physiological function of P_{5A}-type ATPases. It was found that the deletion of gene encoding P_{5A}-type Spf1 ATPase conferred resistance to *Pichia farinosa*, salt-mediated killer toxin (SMKT) [21]. The effect of SMKT was also investigated on fission yeast cells lacking P_{5A}-type Cta4, revealing that *cta4Δ* cells were also resistant to the toxin [12]. It has been shown that SMKT interacts with the plasma membrane of wild type but not with that of mutant *spf1* cells [18], raising thus a possibility that a structure and/or targeting of some cell wall component, which binds the toxin, is similarly affected in *S. cerevisiae spf1* and *S. pombe cta4Δ* mutant cells.

In line with this notion, we found that mutants *cta4Δ* and *spf1* are more resistant to cell wall enzymatic hydrolysis using lytic enzymes from *Trichoderma*, when compared to wild-type cells (Fig. 28.1). The lytic enzymes are endowed with β-1,3-glucanase with some cellulase, protease, and chitinase activities. Interestingly, the lack of Pmr1 Golgi Ca^{2+}-ATPase, belonging to P_2-type subfamily, also resulted in cells with altered cell wall which was sensitive to lytic enzymes [22]. These findings point toward specific roles for these pumps in signaling the cell wall integrity.

In addition, the disruption of the *cta4*$^+$ gene resulted in clumpy multiseptated cells with aberrant morphology suggesting further problems in cell wall remodeling [12].

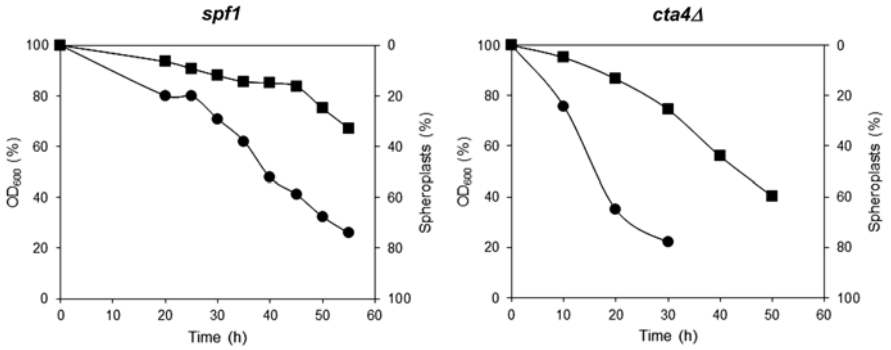

Fig. 28.1 Sensitivity of *Saccharomyces cerevisiae* mutant lacking P_{5A} Spf1 ATPase and *Schizosaccharomyces pombe* mutant lacking P_{5A} Cta4 ATPase to cell wall degradation with lyticase. Wild-type (*filled circle*) and mutant strains *spf1* and *cta4Δ* (*filled square*) were grown to mid-log phase in YPD medium and collected and treated with lyticase in spheroplast buffer containing 1.4 M sorbitol, 50 mM tris-HCl pH 7.4, and 30 mM β-mercaptoethanol. The 10 μl aliquots were removed at the indicated times, diluted in 1 ml of water, and used for OD_{600} determination after 1–2 min. The decay in OD_{600} was taken as an indication of the lysis of spheroplasts. The optical density of cell suspensions at time 0, for each respective strain, was set to 100 %

Mutant *spf1* cells also showed several phenotypes expected for yeast cells with defects in cell wall, such as aggregated cells; hypersensitivity to calcofluor-white, which interferes with cell wall assembly; and hygromycin B, characteristic for yeast mutants with defective N-glycosylation [23]. In fact, mutant cells lacking *SPF1* display glycosylation defects [18] and altered processing of protein-linked oligosaccharides [19]. The enzymes involved in the glycosylation process require Ca^{2+} and Mn^{2+} for their activity [24–26] and are located to the endoplasmic reticulum and Golgi, thus the luminal environment of these organelles is perturbed in yeast cells lacking P_{5A}-type ATPases. The resistance of mutant *cta4Δ* and *spf1* cells to enzymatic hydrolysis of cell wall could thus be explained by changes in cell wall structure/organization due to alteration in activity of proteins and luminal ion homeostasis to maintain cell wall integrity.

This trait seems to be evolutionary conserved since *Arabidopsis thaliana* plants with disruption in P_{5A} MIA ATPase exhibited decreased expression of a large number of genes encoding cell wall-modifying enzymes [13].

Further investigations of the role of P_{5A} type in cell wall revealed that the dimorphic fungi *Candida albicans spf1Δ/Δ* mutant cells lacking homologous P_{5A}-type Spf1 ATPase exhibited abnormal cell wall composition with decreased levels of both β-(1,3)-glucan and β-(1,6)-glucan, delayed cell wall reconstitution after enzymatic removal of cell wall, and decreased flocculation and adherence, reinforcing the notion that cell wall integrity signaling relies on P_{5A}-type ATPase [20].

It is now well established that the cell wall integrity is under a control of mitogen-activated protein kinase cascade and that the response is coordinately regulated with an endoplasmic reticulum stress response [27].

Endoplasmic reticulum stress is a condition resulted from the impairment of Ca^{2+} homeostasis in endoplasmic reticulum and the accumulation of unfolded proteins, which in turn leads to the induction of unfolded protein response (UPR) [28]. The cells under severe endoplasmic reticulum stress became susceptible to apoptosis, activating specific apoptotic pathway. Over the past two decades, there have been significant advances in our understanding of endoplasmic reticulum stress machinery and pathological consequences of dysregulation of unfolded protein response. Dysfunction of the UPR is a main pathological characteristic in neurodegenerative, metabolic, and inflammatory diseases, as well as cancer, prompting increased research focus on the mechanisms controlling endoplasmic reticulum homeostasis [28, 29].

Yeast and plant P_{5A}-type ATPases were localized to the endoplasmic reticulum, by means of immunochemical analysis of subcellular membrane fractionation and immune microscopy [11–14, 18, 19]. Thus, it is not surprising that the loss of P5A-type ATPase function would have a drastic effect on endoplasmic reticulum homeostasis and processes that depend on the endoplasmic reticulum functioning.

Indeed, the degradation of endoplasmic reticulum membrane protein HMG-CoA reductase is defective in budding yeast mutants deficient of P_{5A}-type ATPase Spf1 [30]. Furthermore, both budding and fission null yeast mutants lacking P_{5A}-type ATPases Spf1 and Cta4, respectively, are very sensitive to UPR activators tunicamycin and DTT (inhibitors of protein glycosylation) and exhibited induced expression of chaperone protein BiP, indicator of BiP, indicating that the absence of P_{5A}-type ATPase results in endoplasmic reticulum stress [11, 12, 18]. Among thousands of *S. cerevisiae* mutants, *spf1* null mutant exhibited very strong unfolded protein response [31]. Moreover, BiP was found also in Golgi and vacuole membranes in *cta4Δ* mutant [12]. The disruption of *cta4*$^+$ gene may affect not only the BiP distribution but also that of other proteins of the secretory pathway.

The inhibition of endoplasmic reticulum Ca^{2+}-ATPases in animal cells also leads to an increase of mRNA levels for the marker proteins BiP/GRP78 [32]. Similarly, the phenotypes of yeast *pmr1* mutant lacking Golgi Ca^{2+}-ATPase are that of mutants defective in UPR pathway [19, 33]. A critical role of P_{5A}-ATPases in maintaining the endoplasmic reticulum environment likely occurs through controlling Ca^{2+} and Mn^{2+} homeostasis.

3 P_{5A}-Type ATPase and Ca^{2+} Homeostasis

There is a body of evidence showing that a loss of P_{5A}-type ATPase leads to severe disturbance of cellular Ca^{2+} homeostasis, supporting a hypothesis that Ca^{2+} is a possible substrate of the pump:

1. The growth of null mutants lacking *cta4*$^+$ and *SPF1* genes encoded for P5A-ATPases in yeast cells is sensitive to Ca^{2+} and to Ca^{2+}-preferring chelator ethylene glycol tetra acetic acid (EGTA). The growth of *S. pombe cta4Δ* strain was partially inhibited already by the addition of 10 mM $CaCl_2$ and completely inhibited

by the addition of 50 mM $CaCl_2$ [12]; the growth of *S. cerevisiae spf1* mutant was abolished at 125 mM $CaCl_2$ [11], while the growth of *Candida albicans spf1*Δ/Δ mutant was reduced 30 % in the presence of 160 mM $CaCl_2$ [34]. It should be noted that *S. cerevisiae* mutants lacking known P_2-type Ca^{2+}-ATPases exhibit deficient growth on Ca^{2+}-containing medium; however, the sensitivity differs between mutant yeast cells: *pmr1* requires low Ca^{2+} for optimal growth [33], and the growth of *pmc1* mutant is only inhibited at high Ca^{2+} concentrations [35].

2. Fluorescence resonance energy transfer (FRET) experiments in living fission yeast cells using the fluorescent yellow cameleon indicator for Ca^{2+} indicated that a deletion of *cta4*$^+$ causes an elevation of nuclear Ca^{2+} levels [12].
3. Fission yeast cells lacking Cta4 ATPase exhibited sixfold increase in total $^{45}Ca^{2+}$ accumulation as compared to wild-type cells [36] indicating that loss of this P5A-type ATPase leads to enhanced calcium influx, which occurs in response to the depletion of Ca^{2+} from the endoplasmic reticulum, as a result of induction of endoplasmic reticulum stress response.

   The activation of Ca^{2+} entry using high-affinity calcium system (HACS) is a major response to defects in the secretory, endosomal, and vacuolar protein-trafficking pathways [37] and resembles a mechanism of capacitative calcium entry (CCE) into the cytoplasm through plasma membrane channels upon inhibition of sarco/endoplasmic reticulum calcium ATPases (SERCA) in animal cells [38].

   The genome-wide approach allowed the identification of two groups of yeast mutants regarding HACS activation. Group A mutants display spontaneous HACS activation and defects in endomembrane trafficking system, and group B mutants require external stimuli (tunicamycin or α-factor) to activate Ca^{2+} influx [37]. *S. cerevisiae* mutant lacking Golgi Ca^{2+}-ATPase Pmr1 belongs to group A [37], as well as *S. pombe* mutant lacking P_{5A}-type Cta4 ATPase [36], while *spf1* and *pmc1* mutants belong to group B [37], indicating that each ATPase has specific functions in the regulation of Ca^{2+} influx survival system.
4. The deletion of *S. cerevisiae SPF1* gene resulted in induced expression of calcium-responsive genes with calcium-dependent response element (CDRE) such as *PMC1*, *ENA1*, and *FKS2* encoding vacuolar Ca^{2+}-ATPase, Na^+-ATPase, and β-1,3-glucanase, respectively (demonstrated using ß-galactosidase reporter plasmid in [11]). This induction was mostly dependent on calcineurin, the Ca^{2+}/CaM-dependent protein phosphatase 2B. In line with these observations, the deletion of Spf1 in *C. albicans* led to increased (threefold) expression of gene encoding calcium channel HACS CCH1, which was mainly dependent on calcineurin [34]. In *S. pombe*, vacuolar Ca^{2+}-ATPase Pmc1p assumes a leading role in calcium homeostasis in cells with *cta4Δ* genetic background, a phenomenon likely modulated by calcineurin [36].
5. Ca^{2+} entry in *S. pombe* cells lacking P_{5A}-type Cta4 ATPase is strongly induced upon the inhibition of calcineurin by cyclosporin A, reaching nearly 30-fold higher levels than in wild-type strain grown in standard conditions [36].
6. Direct biochemical measurements of calcineurin phosphatase activity revealed its tenfold stimulation upon *cta4*$^+$ gene deletion [36]. In this regard, it is of note that mutant lacking Cta4 ATPase was sensitive to inhibition of calcineurin

by cyclosporin A [12] indicating that activated calcineurin and consequently calcineurin signaling are essential for the survival of *cta4Δ* cells, as it has been previously demonstrated for other yeast mutants with activated Ca^{2+} influx via HACS.

These evidences reinforce the argument that P_{5A}-ATPase might transport Ca^{2+} or, at least, regulates Ca^{2+} transport in the endoplasmic reticulum by influencing P_2 Ca^{2+}-ATPases.

4 P_{5A}-Type ATPase and Mn^{2+} Homeostasis

There is growing evidence suggesting that calcium homeostasis has a profound effect on proton homeostasis and other ions like copper, iron, and zinc. Thus, it is not surprising that *S. cerevisiae spf1* mutant was identified among 212 mutant strains (out of 4385 mutants generated by the genome deletion project) exhibiting changes in yeast ionome as revealed by using inductively coupled plasma atomic emission spectroscopy [39]. This ionome analysis revealed that Spf1 ATPase is critical to the homeostatic control of several elements such as calcium, cobalt, copper, iron, magnesium, manganese, nickel, phosphorus, potassium, selenium, sodium, sulfur, and zinc [39].

In this regard, contrasting elemental susceptibilities have been found among different fungal species, for instance, low manganese concentrations were found to be toxic to *S. pombe* cells lacking Cta4 ATPase [12], while deletion of *SPF1* in *S. cerevisiae* did not affect manganese sensitivity [11].

Recent study analyzed metal ion content in total membrane vesicles isolated from *spf1* mutant cells using inductively coupled plasma mass spectrometer [40]. It was found that the only ion that showed decreased levels was Mn^{2+}. In addition, membrane vesicles isolated from cells overexpressing Spf1 ATPase exhibited increased Mn^{2+} levels. Since Mn^{2+} is required for the normal function of several enzymes including those involved in lipid biosynthesis and glycosylation [24, 26], diversity of phenotypes observed in the absence of *SPF1* can be also accounted for by changes in activity of Mn^{2+}-dependent enzymes in the ER lumen and cytosol. Indeed, the levels of different sphingolipids were reduced in *spf1* cells comparing wild type indicating the reduced activity of inositol phosphoceramide (IPC) synthase upon lack of Spf1 pump [40]. Although these data are not sufficient to conclude that Spf1 ATPase uses Mn^{2+} as a transporting ion or as co-factor, they clearly demonstrate that loss of Spf1 results in impaired luminal Mn^{2+} homeostasis. It is possible that the activity of P_{5A}-type Spf1 ATPase may be essential for the proper activity of Mn^{2+} transporters (such as Smf1 and Smf2) residing within the yeast membrane network.

A possibility that P_{5A}-type ATPase might transport Mn^{2+} has overshadowed the previous proposition that these pumps might function as P_4-type ATPases (flippases) which transport aminophospholipids [41].

5 Biochemical Characterization of P_{5A}-type ATPase

Seminal kinetic studies revealed two clearly distinct states in the catalytic cycle of the P-ATPases, originally designated as E and E* or E1 and E2 that have become the most common notation to distinguish the enzyme dephosphorylated from the phosphorylated form, respectively [42]. Although lately it became clear that the enzymatic cycle involves multiple intermediate states [43], the E1/E2 nomenclature is almost universally accepted and remains useful for identifying particular states [44], which have different affinities for the nucleotide and the transported ions. The enzyme phosphorylation by ATP at the invariant aspartate residue in the highly conserved phosphorylation sequence DKTGLT, which resides in the beginning of major cytoplasmic loop, results in conformational transitions that culminate with the release of ion/substrate at another side of the membrane, followed by P_i release. The phosphorylation is prevented by orthovanadate, the specific inhibitor of P-type ATPase, which binds covalently and irreversibly to invariant aspartate residue at the phosphorylation site [45]. The enzymatic cycle assures that ATP hydrolysis occurs only when ion is bound and transported by pump. This reaction is influenced by pH, temperature, and water activity [46]. Commonly, the presence of ion/substrate to be transported by pump in the reaction medium promotes an induction in its activity. The activity of P-type ATPases can be determined by monitoring the ATP hydrolysis, formation of phosphorylated intermediate, and vanadate-sensitive ATP-dependent ion transport in isolated cellular membranes or by purified enzyme. These activities have been measured with higher precision by using radioisotopes making possible to study in detail the mechanistic features characteristic of this pump family.

In spite of the previously described evidences indicating that P_{5A}-ATPases are clearly involved in Ca^{2+} homeostasis, the sequence and structural analysis failed in finding characteristic Ca^{2+}-binding site motifs previously identified in P_2 Ca^{2+} pumps [47], which has maintained the substrate specificity of these pumps unassigned. Nonetheless, one more step toward the biochemical characterization of P_{5A}-type ATPases was performed by the measurements of ATP-dependent and FCCP-insensitive $^{45}Ca^{2+}$ transport activity in native *S. pombe* yeast membranes and the comparison between wild-type and mutant *cta4Δ* cells lacking P_{5A} Cta4 ATPase [36]. It was found that $^{45}Ca^{2+}$ transport mediated by Ca^{2+}-ATPase was fourfold lower in *cta4Δ* total cellular membranes than in wild type and that 50 % of this activity was sensitive to orthovanadate, the specific inhibitor of P-type ATPases, with $IC_{50} \sim 200$ μM vanadate. The same range of concentrations of vanadate (500 μM) blocked the Spf1 ATPase activity [11]. Importantly, this biochemical property of vanadate inhibition clearly differentiates P_{5A}-type ATPases and P_4-type ATPases since flippases exhibit a very high sensitivity to vanadate with $IC_{50} = 1–5$ μM [48, 49].

Further fractionation of cellular membranes and subsequent analysis of Ca^{2+} transport showed that ATP-dependent FCCP-insensitive $^{45}Ca^{2+}$ transport was strongly reduced in the endoplasmic reticulum and nucleus membranes isolated from *cta4Δ* cells [36]. These biochemical data clearly indicated that *cta4*$^+$ gene is

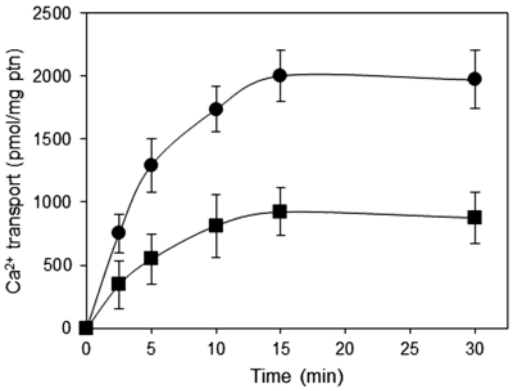

Fig. 28.2 Loss of P_{5A} Spf1 ATPase resulted in strong reduction of ATP-dependent protonophore-insensitive $^{45}Ca^{2+}$ transport in *S. cerevisiae* membranes. $^{45}Ca^{2+}$ uptake in total membrane vesicles isolated from wild-type (*circle*) and *spf1* (*square*) cells grown in YPD was measured in the presence of 1 mM ATP and 2 μM FCCP

required for Ca^{2+}-ATPase activity and Ca^{2+} sequestering in fission yeast endoplasmic reticulum membranes.

Remarkably, the decrease in $^{45}Ca^{2+}$ transport was also found in membrane vesicles isolated from *S. cerevisiae spf1* mutant cells (Fig. 28.2) indicating the crucial role of Spf1 ATPase in maintenance of ATP-dependent Ca^{2+} gradients across membranes and replenishment of intracellular Ca^{2+} stores in budding yeast cells.

The first assay on ATPase activity in vitro was performed using purified His-tagged Spf1p [11]. Ca^{2+} and several other cations such as Sr^{2+}, Ba^{2+}, Mn^{2+}, Fe^{2+}, Fe^{3+}, Co^{2+}, Ni^{2+}, Cu^{2+}, Zn^{2+}, and Cd^{2+} were tested in the reaction medium; however, they all failed to stimulate hydrolytic activity, as one would expected for putative substrate. No stimulation of enzyme hydrolytic activity was found above the basal levels already observed in the presence of Mg^{2+}, which is usually added to the reaction medium together with ATP. At 5 mM Mg^{2+}, His-tagged Spf1p exhibited $K_m \sim 15$ μM for ATP hydrolysis and $V_{max} \sim 150$ nmol $P_i.min^{-1}.mg^{-1}$. This activity was sensitive to 500 μM vanadate. Free Ca^{2+} concentrations higher than 10 μM inhibited ATP hydrolysis. The lack of ion which induced Spf1 ATPase led the authors to suggest that the factors coupling Spf1p/Cod1p to a specific ion might be lost during the purification of the enzyme from *S. cerevisiae* membranes [11]. In addition, it appears that the *S. cerevisiae* Spf1p/Cod1p ATPase forms an oligomeric endomembrane complex [50].

In another study, the hydrolytic activity of vector-expressed and purified GFP-Spf1 was quantified [51]; the ATPase activity of 0.3–1.2 μmol $P_i.mg^{-1}.min^{-1}$ was higher than that reported in [11]. Two ATP-binding sites were identified: a high-affinity site of $K_{m1} \sim 3$ μM and a regulatory site of $K_{m2} \sim 280$ μM for ATP. The regulatory effect of Ca^{2+}, as a putative substrate, on ATP hydrolysis was also verified; however, the addition of 0.5 mM EGTA or 10 μM free Ca^{2+} did not change the ATPase activity of GFP-Spf1. On the other hand, ATPase activity was positively modulated in the presence of Mg^{2+}, with half-maximal activity at 45 μM Mg^{2+}, and decreased by ~40 % in the presence of 150 μM Mn^{2+} [51].

Purified GFP-Spf1 was also able to undergo a phosphorylation in the presence of 30 μM [γ-^{32}P] ATP and 2 mM $MgCl_2$, resulting in $E_1 \sim P$ conformation [51]. The formation of phosphorylated intermediate was abolished by preincubating the

enzyme with 1 mM EDTA. Although the addition of 10 μM $CaCl_2$ had no significant effect on the amount of phosphoenzyme formed by the GFP-Spf1 protein, reduced levels of phosphoenzyme were observed in the presence of 5 mM $CaCl_2$, indicating that Ca^{2+} might positively regulate its decay. It should be mentioned, however, that these high Ca^{2+} concentrations are in a range above physiological cytoplasmic Ca^{2+} concentrations (50 to 200 nM) [52] and free Ca^{2+} (<1 μM) used for analysis of Ca^{2+}-ATPases [53]. The authors suggested that the phosphorylation medium already contained a transported ion/substrate and/or that GFP-SPf1 protein is phosphorylated spontaneously and does not require the binding of ion/substrate for this reaction. High abundance of $E_1 \sim P$ state for GFP-Spf1 and its low turnover is quite different from what is commonly observed for many other P-type ATPases with prevalence of E2 state [42, 51, 54].

The formation of phosphorylated intermediate by barley P_{5A}-ATPase has been also investigated [47]. The prevalence of stable $E_1 \sim P$ conformation was observed for RGS-His_6-tagged HvP5A1, expressed in yeast cells. Likewise *S. cerevisiae* GFP-Spf1 protein, barley HvP5A1-RGS-His_6 underwent slow spontaneous phosphorylation in the presence of 7 μM [γ-^{32}P] ATP and 1 mM $MgCl_2$. The phosphoenzyme was formed even in the presence of 1 mM EGTA, indicating that the formation of $E1 \sim P$ occurred independently of substrate binding. The decay of barley phosphoenzyme (dephosphorylation) was dependent on Ca^{2+}, with $K_{0.5}$ of approximately 200 μM. Mutations in specific amino acid residues located in M4 transmembrane domain, which are known to bind the transported substrates (calcium in Ca^{2+}-ATPases), had no effect on the Ca^{2+}-dependent phosphoenzyme degradation. These results led the authors to conclude that barley HvP5A1 ATPase does not transport Ca^{2+} but is modulated by Ca^{2+} that could influence phosphoenzyme stability or might mediate cation binding directly at the site of phosphorylation [47].

Unfortunately, the hydrolytic activity of barley HvP5A1 ATPase was not detected, probably because of enzyme slow turnover rate or its inability to undergo the full catalytic cycle [47].

The above-described findings obtained using yeast and plant P_{5A}-ATPases also led to the suggestion that P_{5A}-type ATPase might require another factor for its activity that is only present in native membranes and lost during enzyme preparation [47, 51] or might differ in catalytic cycle from other classical P-type ATPases.

6 P_{5A}-Type ATPase and Oxidative Stress

Loss of P_{5A}-type ATPases results in endoplasmic reticulum stress and UPR induction [11, 13, 18, 36, 40]. It is well established that the inability of cell to cope with endoplasmic reticulum stress results in chronic activation of UPR signaling, which could in turn lead to the induction of cell death responses [28, 29].

Recent studies suggest that endoplasmic reticulum homeostasis is closely related to the cellular redox potential. However, the mechanisms and signaling pathways that

link endoplasmic reticulum stress and oxidative stress remain to be fully characterized. The increase in cytosolic Ca^{2+}, as a result of activated Ca^{2+} influx in response to the depletion of endoplasmic reticulum luminal Ca^{2+}, can stimulate mitochondrial ROS production through multiple mechanisms. Interrelationships between Ca^{2+} and ROS signaling, integrating Ca^{2+} and ROS metabolism and the activation of their respective effectors, have been reported as occurring in SR/ER-mitochondrial junctions [55]. The most common molecular targets of ROS are the cysteine thiol groups and disulfide bonds of proteins, including Ca^{2+}-ATPases that have the Ca^{2+} pumping activity differently affected by ROS, according to their position, accessibility, and reactivity of their thiol groups [56]. Defects in the activity of endoplasmic reticulum Ca^{2+}-ATPases have been implicated in several pathologies, and it has been found that a reduction in SERCA expression and Ca^{2+} transport activity potently activated ER stress [57]. Indeed, distinct functional changes of Ca^{2+}-ATPases could be evoked by mild and harsh oxidative conditions, in which graded ROS elevations can serve both as signaling events and a harmful stress condition acting through a single protein [58].

Modulation of ER calcium homeostasis contributes to oxidative stress-induced neuronal apoptosis, involving the impairment of membrane ion-motive ATPases and glucose transporters, and thereby renders neurons vulnerable to excitotoxicity [59].

In animals, P_{5A}-type ATPase encoded by ATP13A1 gene seems to play an important role in the nervous system since its expression peaks at the height of neurogenesis and is strongest in several brain regions of adult mouse. It has been recently demonstrated that the human ATP13A1 is an orthologue of yeast P_{5A}-type Spf1 ATPase [40]. Thus, the studies using yeasts as model organisms should provide a platform for future studies assessing a role of P_{5A}-type ATPases in health and disease of the nervous system.

In this direction, the occurrence of oxidative stress was investigated in fission yeast cells lacking endoplasmic reticulum Cta4 ATPase. As shown in Fig. 28.3, *cta4Δ* deleted mutant cells exhibited strong induction of ROS production comparing with wild-type cells indicating the importance of P_{5A}-ATPase in integrating ER and oxidative stress signaling pathways.

7 Conclusions

The long-standing open question concerning the ion specificity of the members of P_{5A}-ATPase subfamily will probably require a precise description of geometry of the side chains in the ion-binding sites by advanced structural studies like that culminated in the first high-resolution X-ray structures of the P-type family prototype, the SERCA Ca^{2+}-ATPase. However, it is not certain when this level of detail would be achieved with such large, inherently flexible membrane proteins [44].

Nevertheless, from an evolutionary point of view, a rationale is emerging taking altogether the biochemical data we have discussed in this chapter, establishing a functional correlation between the P_5-type ATPases and two other families that are

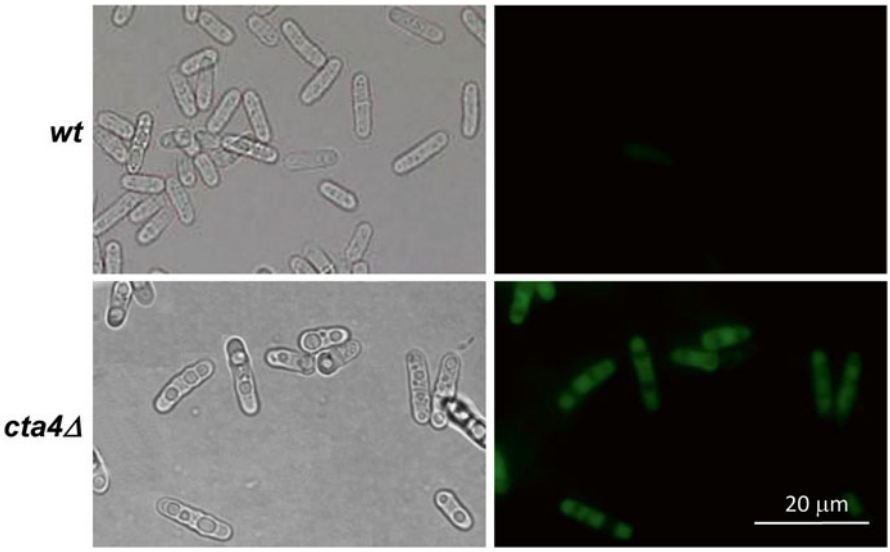

Fig. 28.3 Increased production of reactive oxygen species (ROS) in the fission yeast *S. pombe* cells lacking P_{5A} Cta4 ATPase. Yeast cells were incubated with fluorescent indicator of ROS, H_2DCFDA (2.5 μg.ml^{-1}), for 2 h and visualized by epifluorescence microscopy

also exclusively found in eukaryotes, the P_2-ATPases (Ca^{2+}-ATPases) and the P4-ATPases (aminophospholipid flippases). Clearly, P_5-type ATPases have proved to share many of the physiological roles related to P_{2B}- and P_4-ATPases, and it is tempting to speculate that the P_5 subfamily could encompass reminiscents of a common ancestral of these subfamilies. In this hypothetical scenario, a P_5-like ancestral molecule had evolved in protoeukaryotic cells as a key element providing a higher level of Ca^{2+} signaling and homeostasis and lipid translocation that made possible the endomembrane emergence and ion signal transductions compatible to a compartmentalized cell. Future studies integrating functional characterizations and data on molecular evolution of the P_5-, P_2-, and P_4-ATPases should be directed to clarify whether the last two subfamilies could be a result of molecular specializations of a P_5 ancestor evolved at the earlier stages of the eukaryotic speciation. Such landscape would become still more exciting if the modern P_5 subfamily could represent enzymes in transitional stages of evolution, a feature that may account for the broader array of substrates (e.g., Ca^{2+}, Mn^{2+}, Fe^{2+}).

Acknowledgments This work was supported by CNPq (Conselho Nacional de Pesquisa e Desenvolvimento) and FAPERJ (Fundação de Amparo à Pesquisa do Estado do Rio de Janeiro). L. M. P. received a Ph.D. fellowship from CAPES (Coordenação de Aperfeiçoamento de Pessoal no Nível Superior); L. M. P and A. J. D. C. are recipients of FAPERJ postdoc and Ph.D. fellowships, respectiviely. The authors would like to thank Arnoldo R. Façanha (UENF) for a careful and critical reading of this work.

References

1. Pedersen PL, Carafoli E (1987) Ion motive ATPases. I. Ubiquity, properties, and significance for cell function. Trends Biochem Sci 12:146–150
2. Pedersen PL, Carafoli E (1987) Ion motive ATPases. II. Energy coupling and work output. Trends Biochem Sci 12:186–189
3. Serrano R (1989) Structure and function of plasma membrane ATPase. Annu Rev Plant Physiol Plant Mol Biol 40:61–94
4. Fagan MJ, Saier MH Jr (1994) P-type ATPases of eukaryotes and bacteria: sequence analyses and construction of phylogenetic trees. J Mol Evol 38:57–99
5. Møller JV, Juul B, le Maire M (1996) Structural organization, ion transport, and energy transduction of P-type ATPases. Biochim Biophys Acta 1286:1–51
6. Axelsen KB, Palmgren MG (1998) Evolution of substrate specificities in the P-type ATPase superfamily. J Mol Evol 46:84–101
7. Catty P, de Kerchoved'Exaerde A, Goffeau A (1997) The complete inventory of the yeast Saccharomyces cerevisiae P-type transport ATPases. FEBS Lett 409:325–332
8. Axelsen KB, Palmgren MG (2001) Inventory of the superfamily of P-type ion pumps in Arabidopsis. Plant Physiol 126:696–706
9. Okorokova-Façanha AL, Okorokov LA, Ekwall K (2003) An inventory of the P-type ATPases in the fission yeast Schizosaccharomyces pombe. Curr Genet 43(4):273–280
10. Møller AB, Asp T, Holm PB et al (2008) Phylogenetic analysis of P5 P-type ATPases, a eukaryotic lineage of secretory pathway pumps. Mol Phylogenet Evol 46:619–634
11. Cronin SR, Rao R, Hampton RY (2002) Cod1p/Spf1 is a P-type ATPase involved in ER function and Ca2+ homeostasis. J Cell Biol 157:1017–1028
12. Okorokova-Façanha AL, Appelgren H, Tabish M et al (2002) The endoplasmic reticulum cation P-type ATPase Cta4p is required for control of cell shape and microtubule dynamics. J Cell Biol 157:1029–1039
13. Jakobsen MK, Poulsen LR, Schulz A et al (2005) Pollen development and fertilization in Arabidopsis is dependent on the MALE GAMETOGENESIS IMPAIRED ANTHERS gene encoding a type V P-type ATPase. Genes Dev 19:2757–2769
14. Yoshida SH, Nakamura T, Shimoda C (2005) The cation-transporting P-type ATPase Cta4 is required for assembly of the forespore membrane in fission yeast. Genes Genet Syst 80:317–324
15. Furune T, Hashimoto K, Ishiguro J (2008) Characterization of a fission yeast P5-type ATPase homologue that is essential for Ca2+/Mn2+ homeostasis in the absence of P2-type ATPases. Genes Genet Syst 83:373–381
16. van Veen S, Sørensen DM, Holemans T et al (2014) Cellular function and pathological role of ATP13A2 and related P-type transport ATPases in Parkinson's disease and other neurological disorders. Front Mol Neurosci 7:48
17. Sørensen DM, Buch-Pedersen MJ, Palmgren MG (2010) Structural divergence between the two subgroups of P5 ATPases. Biochim Biophys Acta 1797:846–855
18. Suzuki C (2001) Immunochemical and mutational analyses of P-type ATPase Spf1p involved in the yeast secretory pathway. Biosci Biotechnol Biochem 65:2405–2411
19. Vashist S, Frank CG, Jakob CA, Ng DT (2002) Two distinctly localized p-type ATPases collaborate to maintain organelle homeostasis required for glycoprotein processing and quality control. Mol Biol Cell 13:3955–3966
20. Yu Q, Ding X, Zhang B et al (2013) The P-type ATPase Spf1 is required for endoplasmic reticulum functions and cell wall integrity in Candida albicans. Int J Med Microbiol 303:257–266
21. Suzuki C, Shimma Y (1999) P-type ATPase spf1 mutants show a novel resistance mechanism for the killer toxin SMKT. Mol Microbiol 32:813–823
22. Okorokov LA, Lehle L (1998) Ca2+-ATPases of Saccharomyces cerevisiae: diversity and possible role in protein sorting. FEMS Microbiol Lett 162:83–91

23. Dean N (1995) Yeast glycosylation mutants are sensitive to aminoglycosides. Proc Natl Acad Sci U S A A92:1287–1291
24. Kaufman RJ, Swaroop M, Murtha-Riel P (1994) Depletion of manganese within the secretory pathway inhibits O-linked glycosylation in mammalian cells. Biochemistry 33:9813–9819
25. Dean N (1999) Asparagine-linked glycosylation in the yeast Golgi. Biochim Biophys Acta 1426:309–322
26. Reddi AR, Jensen LT, Culotta VC (2009) Manganese homeostasis in Saccharomyces cerevisiae. Chem Rev 109:4722–4732
27. Krysan DJ (2009) The cell wall and endoplasmic reticulum stress responses are coordinately regulated in Saccharomyces cerevisiae. Commun Integr Biol 2:233–235
28. Wu H, Ng BS, Thibault G (2014) Endoplasmic reticulum stress response in yeast and humans. Biosci Rep 34:e00118
29. Wang S, Kaufman RJ (2012) The impact of the unfolded protein response on human disease. J Cell Biol 197:857–867
30. Cronin SR, Khoury A, Ferry DK, Hampton RY (2000) Regulation of HMG-CoA reductase degradation requires the P-Type ATPase Cod1p/Spf1p. J Cell Biol 148:915–924
31. Jonikas MC, Collins SR, Denic V et al (2009) Comprehensive characterization of genes required for protein folding in the endoplasmic reticulum. Science 323:1693–1697
32. Price BD, Mannheim-Rodman LA, Calderwood SK (1992) Brefeldin A, thapsigargin and AIF4 stimulate the accumulation of GRP78 mRNA in a cycloheximide dependent manner, whilst induction by hypoxia is independent of protein synthesis. J Cell Physiol 152:545–552
33. Dürr G, Strayle J, Plemper R et al (1998) The medial-Golgi ion pump Pmr1 supplies the yeast secretory pathway with Ca2+ and Mn2+ required for glycosylation, sorting, and endoplasmic reticulum-associated protein degradation. Mol Biol Cell 9:1149–1162
34. Yu Q, Wang H, Xu N, Cheng X et al (2012) Spf1 strongly influences calcium homeostasis, hyphal development, biofilm formation and virulence in Candida albicans. Microbiology 158:2272–2282
35. Cunningham KW, Fink GR (1994) Calcineurin-dependent growth control in Saccharomyces cerevisiae mutants lacking PMC1, a homolog of plasma membrane Ca2+ ATPases. J Cell Biol 124:351–363
36. Lustoza ACDM, Palma LM, Façanha AR et al (2011) P5A-type ATPase Cta4p is essential for Ca2+ transport in the endoplasmic reticulum of Schizosaccharomyces pombe. PloS One 6:e27843
37. Martin DC, Kim H, Mackin NA et al (2011) New regulators of a high affinity Ca2+ influx system revealed through a genome-wide screen in yeast. J Biol Chem 286:10744–10754
38. Putney JW (2009) Capacitative calcium entry: from concept to molecules. Immunol Rev 231:10–22
39. Eide DJ, Clark S, Nair TM et al (2005) Characterization of the yeast ionome: a genome-wide analysis of nutrient mineral and trace element homeostasis in Saccharomyces cerevisiae. Genome Biol 6:R77
40. Cohen Y, Megyeri M, Oscar CW et al (2013) The yeast P5 type ATPase, Spf1, regulates manganese transport into the endoplasmic reticulum. PLoS ONE 8(12):e85519
41. Poulsen LR, Lo´pez-Marque´s RL, Palmgren MG (2008) Flippases: still more questions than answers. Cell Mol Life Sci 65:3119–3125
42. de Meis L, Vianna AL (1979) Energy interconversion by the Ca2+-dependent ATPase of the sarcoplasmic reticulum. Annu Rev Biochem 48:275–292
43. Scarborough GA (2003) Rethinking the P-type ATPase problem. Trends Biochem Sci 28:581–584
44. Kühlbrandt W (2004) Biology, structure and mechanism of P-type ATPases. Nat Rev 5:282–295
45. Pick U (1982) The interaction of vanadate ions with the Ca-ATPase from sarcoplasmic reticulum. J Biol Chem 257:6111–6119

46. De Meis L, Martins OB, Alves EW (1980) Role of water, hydrogen ion, and temperature on the synthesis of adenosine triphosphate by the sarcoplasmic reticulum adenosine triphosphatase in the absence of a calcium ion gradient. Biochemistry 19:4252–4261
47. Sørensen DM, Møller AB, Jakobsen MK et al (2012) Ca2+ induces spontaneous dephosphorylation of a novel P5A-type ATPase. J Biol Chem 287:28336–28348
48. Zhou X, Graham TR (2009) Reconstitution of phospholipid translocase activity with purified Drs2p, a type-IV P-type ATPase from budding yeast. Proc Natl Acad Sci U S A 106:16586–16591
49. Eckford PD, Sharom FJ (2005) The reconstituted P-glycoprotein multidrug transporter is a flippase for glucosylceramide and other simple glycosphingolipids. Biochem J 389:517–526
50. Thever MD, Saier MH (2009) Bioinformatic characterization of P-type ATPases encoded within the fully sequenced genomes of 26 eukaryotes. J Membr Biol 229:115–130
51. Corradi GR, Pinto FT, Mazzitelli LR, Adamo HP (2012) Shadows of an absent partner: ATP hydrolysis and phosphoenzyme turnover of the Spf1 (sensitivity to Pichia farinosa killer toxin) P5-ATPase. J Biol Chem 287:30477–30484
52. Cui J, Kaandorp JA, Sloot PMA et al (2009) Calcium homeostasis and signaling in yeast cells and cardiac myocytes. FEMS Yeast Res 9:1137–1147
53. Okorokov LA, Tanner W, Lehle L (1993) A novel primary Ca2+ transport system from Saccharomyces cerevisiae. Eur J Biochem 216:573–577
54. Froehlich JP, Heller PF (1985) Transient-state kinetics of the ADP-insensitive phosphoenzyme in sarcoplasmic reticulum: implications for transient-state calcium translocation. Biochemistry 24:126–136
55. Csordás CG, Hajnóczky G (2009) SR/ER–mitochondrial local communication: calcium and ROS. Biochim Biophys Acta 1787:1352–1362
56. Hidalgo C, Donoso P (2008) Crosstalk between calcium and redox signaling: from molecular mechanisms to health implications. Antioxid Redox Signal 10:1275–1312
57. Fu S, Yang L, Li P et al (2011) Aberrant lipid metabolism disrupts calcium homeostasis causing liver endoplasmic reticulum stress in obesity. Nature 473:528–531
58. Li Y, Camacho P (2004) Ca2+-dependent redox modulation of SERCA 2b by ERp57. J Cell Biol 164:35–46
59. Yu Z, Luo H, Fu W, Mattson MP (1999) The endoplasmic reticulum stress-responsive protein GRP78 protects neurons against excitotoxicity and apoptosis: suppression of oxidative stress and stabilization of calcium homeostasis. Exp Neurol 155:302–314

Chapter 29
Role and Significance of Various ATPases of Nematode Parasites

Meghna S. Dhaka, Shriya Srivastava, and Shailja-Misra Bhattacharya

Abstract ATPases in nematodes are involved in a variety of functions which mainly include movement of metabolites, membrane potential maintenance and energy generation for metabolic processes. The enzymes are located mostly in mitochondria, cytosol and microsomes in a nematode organism. Nematode ATPases are active at varied pH range and under different biochemical conditions as required by the parasite and its host. Sequence studies show that nematode ATPases show much similarity in their DNA sequences and share conserved domains. Na^+-K^+ ATPases have also been explored for their potential in generating immune response against parasitic nematodes in the host. A few ATPase-dependent helicase enzymes also show high protective efficacy against parasitic infections. Overall, ATPases carry a great deal of information about nematodes, their behaviour and infections. More studies are needed to evaluate their potential and come up with their use in prevention of parasitic infections in the host.

Keywords ATPase • Anti-helminthic • Nematodes • Helicases • Na^+-K^+-ATPase • AAA-type ATPase • Vaccine • Parasitic infection • Gene silencing

1 Introduction

Nematodes include a large group of organisms, which survive either as free living or parasitic species on animals, humans and plants. ATPases in nematodes constitute one of the most common clusters of enzymes responsible for a majority of cellular process like signal transduction, trans-membrane movement of ions, cell metabolism and cell membrane potential. ATPases are responsible for outflux of many

M.S. Dhaka • S. Srivastava
IMS Engineering College, Ghaziabad, Uttar Pradesh, India

S.-M. Bhattacharya (✉)
Division of Parasitology, CSIR-Central Drug Research Institute,
Sector 10, Jankipuram Extension, Sitapur Road, Lucknow 226031, Uttar Pradesh, India
e-mail: shailja_bhattacharya@rediffmail.com

S. Chakraborti, N.S. Dhalla (eds.), *Regulation of Ca^{2+}-ATPases,V-ATPases and F-ATPases*, Advances in Biochemistry in Health and Disease 14,
DOI 10.1007/978-3-319-24780-9_29

metabolites, toxins and wastes that interfere with normal cellular process of parasitic cell [1–4]. Besides this, ATPases also provide energy from ATP hydrolysis, used by many special ion pumps present on cell membrane to carry out the ionic movement across membrane against the electrochemical gradient [2, 5–9]. According to their function, there are different kinds of ATPases explored in nematodes which broadly include Na^+-K^+ ATPases, H^+-K^+ ATPase, Mg^{2+}-Ca^{2+} dependent ATPases, Mn^{2+} ATPases, vacuolar-type ATPases (V-ATPases) and recently discovered AAA (ATPase associated with various activities) superfamily ATPases [2, 10].

2 Structure, Types and Localization of ATPase in Nematodes

The prokaryotic and yeast cells contain ATPase bound to cell membrane or organelles like mitochondria and plasma membranes [5, 11]. Higher plants, on the other hand, show ATPase activity mostly in mitochondria, thylakoid membrane and chloroplast region [12]. Nematodes in contrast contain ATPases concentrated in mitochondria, cytosol and microsomes. The pyrolic appendages inhabiting parasites, *Bothriocephalus scorpii* and *Myoxocephalus brandti*, show majority of ATPase activity in mitochondria, cytoplasm and microsomes. Nematodes have major ATPase functioning centres in mitochondria and microsomes. *Strongyloides stercoralis* larvae contain a major cluster of Na^+-K^+ ATPases in cuticles, esophagus-surrounding glands and muscular regions as evident by binding of anti-Na^+-K^+ ATPase human IgG antibody. Na^+-K^+ ATPase in *Setaria cervi* is involved in ionic gradient management and muscle contractions in tegument and caracass region [13]. If specifically considered, Na^+-K^+ ATPases are hetero-dimeric integral membrane proteins, consisting of alpha and beta subunits, that couple ATP hydrolysis to Na^+ and K^+ ion transport and maintenance of the electrochemical gradients across the plasma membrane [14].

An interesting class of ATPase enzymes is vacuolar ATPase complex (V-ATPase) which pumps protons across membranes using ATP hydrolysis energy. The proton transfer process catalyzed by V-ATPases leads to acidification required in various intracellular processes such as activation of zymogen, release of ligands from receptors, degradation of macromolecules, accumulation of neurotransmitters in secretary vesicles and sorting of nascent polypeptides [10]. It is involved in many physiological processes and any defect in V-ATPase may cause disease in an organism. V-ATPase is mostly located in plasma membrane, renal intercalated cells and epithelial cells of seminal ducts. They contain two segments; one is responsible for ATP hydrolysis and the other one for proton translocation across membrane. These V-ATPases consist of five different subunits (a, d, c, c′ and c″) which work together to facilitate proton movement [10]. *Caenorhabditis elegans* contains an intestine-specific a-subunit of the H^+-K^+ ATPase complex (V-ATPase) VHA-6 that resides in the apical membrane of the intestinal epithelial cells and is required for luminal acidification. Disruption of the vha-6 gene leads to early developmental arrest in the free-living nematode [3].

The involvement of V-ATPase in nematodes is not well deciphered. However, a few reports suggest its crucial role in nematode nutrition, osmoregulation, cuticle synthesis, neuronal and reproduction process. Based on multiple roles played by of V-ATPase enzymes, they are emerging as potential drug target against nematode parasites. However, the challenge is to develop a high-throughput assay with which to test potential inhibitors against these ATPases.

Another recently discovered class of ATPase is AAA (ATPase associated with various activities) which possesses either one or two conserved AAA domains in its C terminus and uses the energy derived from ATP hydrolysis mediated by the AAA domain. They perform various biological functions in parasitic nematodes including major processes as protein unfolding, nucleosome remodeling and microtubule disassembly. AAA ATPase enzyme activates by assembly of subunits into ring-shaped hexamers through AAA domain interaction. This marvellous category of ATPase is mostly located within the membrane and mitochondrial region of a cell subunit. In *C. elegans*, the AAA domain of gene CeFIGL-1 displays unusually high ATPase activity due to its charge interaction mediated by two acidic residues in helix α9a [4]. The proteins of this family form a hexameric ring forming ATP-binding pocket, which consists of three functionally important motifs: Walker A, Walker B and second region of homology (SRH). Highly conserved arginine residues in the SRH function as arginine fingers, which interact with the γ-phosphate of bound ATP. Mutational studies have shown that ATP binding to these proteins induces conformational changes in Walker motifs, resulting in proper orientation of arginine residues required for hydrolysis of ATP [15].

A flippase family P-type ATPase TAT-2 in *C. elegans* is being implicated to play a crucial role in regulation of specific fatty acids and creation of phospholipid bilayer asymmetry [16]. A CATP-5 is the first P (5)-type ATPase associated with the plasma membrane of *C. elegans*. It is expressed in the apical membrane region of intestinal and the excretory cells. CATP-5 is involved in polyamine synthesis and the reduced levels of polyamine lead to retarded postembryonic development, reduced brood size, shortened lifespan and small body size in the free-living nematode [17].

The differing localization of ATPase in nematodes suggests that ATPases have a wide distribution network within different cells. Their existence traces back to early evolution stages of life, which makes the enzyme more important for revealing information about evolution of parasitic nematodes.

3 Biochemical Activity of Nematode ATPase

ATPases work in a wide range of conditions in different parasitic cells. In *B. scorpii* and *Hymenolepis diminuta*, ATPases are active at an optimal pH range of 8–9 in the mitochondrial fractions [6]. *E. pancreaticum* has pH optima at 8.4 while *Ascaris suum* ATPases work best between 8 and 8.2 pH ranges [2, 18]. On the other hand, *Schistosoma mansoni*, *F. hepatica*, *C. ijimai*, *Bunostomum trigonocephalum* and *Schistocephalus solidus* work best between 7.2 and 7.4 [19].

Besides pH, ATPase enzymes also demonstrate quick response to the presence or absence of metal ions in their activity. In *B. scorpii* the absence of metal ions in the incubation medium halts ATP hydrolysis in cytosol and occurs at minimal rate in mitochondria and microsomes. Further addition of K^+ and Na^+ ions enhances ATPase activity in mitochondria and microsomes, while HCO_3^- anions increase the ATP hydrolysis only in microsomal fraction. The combination of bicarbonate ions with Mg^{2+} and Mn^{2+} increases ATPase activity in both the organelles while inhibits in combination with Ca^{2+}. In both microsomal and mitochondrial fractions of *B. scorpii* the ATPase activity is higher with Ca^{2+} and Mn^{2+} than with Mg^{2+}. Parasitic nematodes *F. hepatica*, *Trichinella spiralis*, *A. suum*, *S. mansoni*, *C. ijimai*, *E. pancreaticum* and *H. diminuta* also contain Mg^{2+}- and Ca^{2+}-dependent ATPases in most of the tissues [7, 8, 20, 21]. The presence of Ca^{2+} ions stimulates the muscle ATPase of digestive and sexual tracts of *A. suum* whereas Mg^{2+} inhibits the same [22]. Sodium azide, dinitrophenol, thiocyanate and sodium fluoride strongly inhibit the microsomal ATPase activity in *B. scorpii*. Mg^{2+}-independent Ca^{2+}-ATPase is also well characterized in a bovine filarial parasite, *Setaria cervi*. These Ca^{2+}-ATPase carry out transport of ATP-assisted Ca^{2+} ion through plasma membrane and regulate Ca^{2+} homeostasis in the cells [24]. Ca^{2+} ATPases are equally distributed through the cuticle-muscular hypodermis layer, genital organs and gastrointestinal tissue of *S. cervi*. Ca^{2+}-ATPases are most active in the presence of $CaCl_2$ while lower concentration of EGTA completely inhibits their activity. Once in soluble form, the processivity of Ca^{2+}-ATPases increases by fourfold. On the other hand, activation by calmodulin leads to twofold increased activity of Ca^{2+}-ATPases in *S. cervi*. Phenothiazines and anti-helminthics specifically inhibit the Ca^{2+}-ATPase activity when tested in *S. cervi*. Trifluoperazine is observed to be the most potent inhibitor of enzyme activity followed by promethazine and chlorpromazine. Significant inhibition of filarial Ca^{2+}-ATPase by some anti-helminthics as DEC, centperazine, levamisole and suramine is also reported. Of these, diethylcarbamazine with IC_{50} value of 22 μM and centperazine with IC_{50} value—55 μM are found to be more potent inhibitors of the enzyme as compared to levamisol and suramine. The enzyme shows a Km value of 3.33 mM as obtained by Lineweaver–Burk plot [1]. The varied range of optimal pH for ATPases in different parasitic nematodes suggests the great adaptation behaviour of ATPases as per the parasite requirement in different organelles, hosts and conditions.

4 Genomic Properties of Nematode ATPases

This genomic information is of much significance to understand the biology of nematodes. This helps to understand nematode-specific control targets such as mitochondria, which plays crucial role in parasite survival and infections [23]. The mitochondrial genomes of *C. elegans* (13.8 kbp) and *A. suum* (14.3 kbp) contain genes Fo ATPase complex (ATPase 6 and ATPase 8). Unique features of mitochondrial genomes of some nematodes from class Chromodorea, *C. elegans* and *A. Suum*, *O. volvulus*, *S. stercoralis* and *Steinernema carpocapsae* are reported

[24–26]. They lack the gene for ATPase subunit 8, commonly found in other metazoan mitochondrial DNAs.

The mitochondrial genome of human hookworms *Ancylostoma duodenale* (13,721 bp) and *Necator americanus* (13,604 bp) compared with *C. elegans*, *A. suum* and *O. volvulus* contains ATPase complex subunit six sequences; however, the ATP synthetase subunit eight gene sequences are lacking. The ATPase sequence homology of the two hookworms was tested using translation initiation and termination codons of the protein genes and it revealed that ATPase protein of *N. americanus* is one amino acid shorter than that of both *A. duodenale* and *C. elegans*. The ATPase enzyme amino acid sequence of hookworms is more similar to *C. elegans* as compared to *A. suum* and *O. volvulus*.

Muhammad Amjad Ali et al. in 2013 [27] carried out studies on the role of ATPase gene involved in syncytium development and abiotic stress responses. Syncytium is a condition induced in the roots of *Arabidopsis thaliana* by the beet cyst nematode, *Heterodera schachtii*. At1g64110 gene is found to be strongly upregulated in syncytia. This gene encodes AAA+-type ATPase, which forms a large superfamily of proteins containing a P-loop NTPase domain. They perform various functions such as molecular chaperons involved in unfolding of macromolecules [28], as subunit of proteases, etc. At1g64110/DAA1 gene has been proved to be important for the development of syncytia and abiotic stress responses. The complete mitochondrial genome of plant parasitic nematode, *Radopholus similis* (16.8 kbp), shows some unique features such as small transfer RNAs, truncated RNAs and unidirectional transcription in Chromadorean nematodes. *R. similis* has been reported to have the most AT-rich mitochondrial genome until date (85.4 % AT) with 12 protein-coding genes and absence of any ATPase subunit.

Molecular characterization and phylogenetic analysis of animal infecting parasites, *Toxocara canis* and *Toxocara vitulorum* (infecting dogs and buffaloes), reveal that nucleotide and amino acid sequences of ATPase 6 gene of species is similar to *Toxocara cati* and *Toxocara malaysiensis* species. Analyses of the ITS-2 and 28S regions revealed that the 28S region was more conserved (95 % nucleotide similarity between *T. canis* and *T. vitulorum*) than the ITS-2 region (85 %). The conserved nature of ATPase 6 genes in *Toxocara* species could be used for discrimination of species and molecular phylogenetics [29]. Further genomic studies should be done in nematodes so as to identify more ATPases and to reveal their phylogenetic similarity with other worms. This would also allow cloning cDNA sequences encoding various ATPases and explore their regulated mechanism of expression. All this information is helpful towards finding a new control strategy against parasitic nematodes [30].

5 Potential of ATPases as Vaccine Candidates

Keeping in mind the crucial role played by ATPases in various metabolic processes, their immune system eliciting property against infecting parasite has also been studied in detail. Once the parasite infects the host, it attacks its defence system and

inhabits the host immune organs for many years making parasitic infection life threatening [31]. Much research has been focused on different proteins/antigens as drug or vaccine targets but none of them is able to demonstrate complete clearance. Hence, ATPases raise a hope for its use as vaccine candidate against nematode parasitic infections.

In intestinal nematode parasite *S. stercoralis* three genes were identified which provide protective efficacy against the parasite in mice; one of these genes codes for Na^+-K^+ ATPase (*Sseat-6*) enzyme [32–35]. Na^+-K^+ ATPases are heterodimeric integral membrane proteins, consisting of alpha and beta subunits, that couple ATP hydrolysis to Na^+ and K^+ ion transport and maintenance of the electrochemical gradients across the plasma membrane [11]. DNA immunization with Na^+-K^+ ATPase (*Sseat-6*) resulted in induced protective immunity to larval *S. stercoralis* in mice. On the other hand, serum from mice immunized with DNA encoding Na^+-K^+ ATPase transferred to naive mice resulted in partial protective immunity. Immunization with Na^+-K^+ ATPase leads to generation of antibody response against *S. stercoralis*, which in turn causes partial killing of larvae. The mechanism behind larval killing by Na^+-K^+ ATPase antibodies is still not very clear. Localization studies using human IgG reveal that Na^+-K^+ ATPases are located in cuticle, esophagus surrounding glands and muscles of *S. stercoralis* L3. When mice are vaccinated with Na^+-K^+ ATPase plasmids, the parasite regions harbouring these enzymes generate antibodies against larval parasites in the host. Further studies suggest that anti-Na^+-K^+ ATPase antibodies alter the ion concentration gradient in the pharyngeal and cuticle region, thus leading to death of worm [9, 35]. Also in *C. elegans* mutation of *eat-6* gene encoding alpha subunit of Na^+-K^+ ATPase results in slow contraction, relaxation and abnormal feeding behaviour of pharyngeal muscle [9, 36]. Also, the Na^+-K^+ ATPase location may be the target site for the neutrophils to mediate larval killing by human IgG and mouse IgG [37].

Other parasitic nematodes such as *Ascaris suum* and *Haemonchus contortus* are also targeted via mechanism of muscle paralysis using anti-Na^+-K^+ ATPase antibodies. One of the anti-parasitic drugs ivermectin is reported to halt the Na^+-K^+ ATPase activity by inducing paralysis of the pharyngeal muscles in *A. suum* and *H. contortus* [37]. Thus, Na^+-K^+ ATPase is the first defined antigen against *S. stercoralis* in mice and a promising vaccine candidate [35].

Other than these, ATPase activity is also associated with helicase enzyme and provides them energy by ATP hydrolysis so as to carry various metabolic processes in a cell. Helicases are crucial enzymes for all DNA/RNA-related processes including metabolism, synthesis, replication and gene silencing. In nematodes ATPase-dependent helicases are highly characterized for their involvement in different processes such as germ line development in *C. elegans*, RNA silencing as Dicer protein and embryogenesis in *Brugia malayi* [38–41]. The ATPase-dependent DExD/H box RNA helicase family enzymes are multifunctional proteins involved in unwinding of inter- and intra-molecular base-paired regions. Successful knockdown of DEAD box RNA helicase gene (BmL3-Helicase) of human lymphatic filarial parasite *Brugia malayi* using specifically designed and chemically synthesized siRNAs of <20 bp resulted in decreased parasite motility, viability (97 %) and

release of microfilariae (81.0 % reduction) from adult females in vitro. The specific gene knockdown also resulted into death of adult male worms in addition to phenotypic deformities in female worm intrauterine stages as shown in Fig. 29.1. Recombinant BmL3-Helicase also generates immune response in *Mastomys coucha* resulting in a 67.4 % reduction in adult parasite recovery, 86.7 % decrease in the microfilarial density and profound sterility of the recovered female worms [39–41]. The study presents positive response of filarial ATPase-associated helicase enzyme in generating immune response against the parasite infection in animal host. This again emphasizes the importance of ATPases in parasitic infection control strategies.

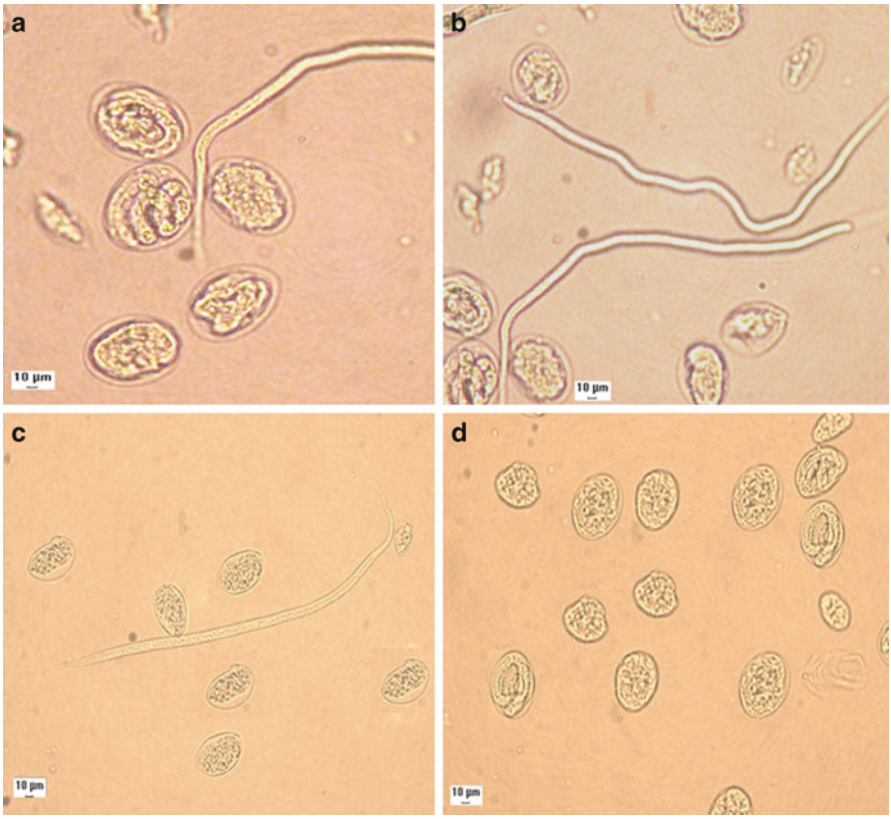

Fig. 29.1 Effect on embryos and pretzel stages of adult female parasite after siRNA-induced silencing of *Brugia malayi* ATPase-dependent RNA helicase. The embryos of helicase-specific siRNA-exposed group (**c** and **d**) appeared degenerated and granular when compared with embryos of parasites exposed to culture medium (**a**) and scrambled siRNA (**b**). The embryos have distorted shape and eggshell visible due to contraction of embryo, which later diminished (**c** and **d**)

6 Conclusion

ATPases in nematode parasites are emerging as a new target because of their abundance, involvement in multiple processes and unique structures. Many research findings discussed in this chapter show that ATPases are highly functional under various physiological conditions and play a crucial role in supporting parasitic nematodes after infecting a host cell. However, more focussed studies of different ATPases are required to reveal their mechanism and functions in nematode parasites. Their use as vaccine candidates or development as a drug target against infection in human, plant and animal hosts is also not explored much when compared with other organisms. It is therefore suggested to escalate research on these marvellous enzymes to reveal more information about parasitism.

Acknowledgements We are thankful to Prof. Sajal Chakraborti, Department of Biochemistry and Biophysics, University of Kalyani, and Prof. Naranjan S. Dhalla, Distinguished Professor, Institute of Cardiovascular Sciences, University of Manitoba, Canada, for inviting us to write this chapter. We also express gratitude to Elsevier for accepting our work. We would also like to remember Prof. Ernesto Carafoli, to whom this book is dedicated. His contributions in this field will always enlighten us.

References

1. Abha A, Onkar PS, Babu LT (1992) Characterization of Ca^{2+} ATPase of *Setaria cervi* (nematoda: filarioidea): effect of phenothiazines and anthelmintics. Int J Biochem 24(9):1447–1452
2. Burenina EA (2007) Adenosine triphosphatases of cestodes *Bothriocephalus scorpii*. J Evol Biochem Physiol 43(3):287–294
3. Allman E, Johnson D, Nehrke K (2009) Loss of the apical V-ATPase a-subunit VHA-6 prevents acidification of the intestinal lumen during a rhythmic behaviour in C. elegans. Am J Physiol Cell Physiol 297(5):C1071–C1081
4. Peng W, Lin Z, Li W et al (2013) Structural insights into the unusually strong ATPase activity of the AAA domain of the Caenorhabditis elegans fidgetin-like 1(FIGL-1) protein. J Biol Chem 288(41):29305–29312
5. Ishida M, Mizushima S (1969) Membrane ATPase of *Bacillus megaterium.* I. Properties of membrane ATPase and its solubilised form. J Biochem 66(1):33–43
6. Rahman M, Mettrick DF, Prodesta RB (1981) Properties of a Mg^{2+} dependent and Ca^{2+} inhibited ATPase localized in the brush border of the surface epithelial syncytium of a parasitic flatworm. Can J Zool 59:918–923
7. Podesta RB, McDiarmid SS (1982) Enrichment and partial enzyme characterization of ATPase activity associated with the outward-facing membrane complex and inward-acing membrane of the surface epithelial syncytium of *Schistosoma mansoni*. Mol Biochem Parasitol 6(4):225–236
8. Savchenko AV (1983) Phosphorylase and ATPase activity of *Fasciola hepatica* mitochondria. Bull VIGIS 35:67–68
9. Davis MW, Somerville D, Lee RY, Lockery S, Avery L, Fambrough DM (1995) Mutations in the *Caenorhabditis elegans* Na, K-ATPase alpha-subunit gene, eat-6, disrupt excitable cell function. J Neurosci 15:8408–8418

10. Oka T, Toyomura T, Honjo K, Wada Y, Futai M (2001) Four subunits a-isoforms of *Caenorhabditis elegans* vacuolar H^+ ATPase: cell-specific expression during development. J Biol Chem 276(35):33079–33085
11. Ryrie IJ (1975) Purification and partial characterization of the oligomycin-sensitive ATPase from yeast mitochondria. Arch Biochem Biophys 168:712–719
12. Nelson N, Nelson H, Racker E (1972) Partial resolution of the enzymes catalyzing phosphorylation. J Biol Chem 247(20):6506–6510
13. Fetterer RH, Pax RA, Bennett J (1981) Na^+, K^+-transport, motility and tegumental membrane potential in adult male *Schistosoma mansoni*. Parasitology 82:97–109
14. Shima Y, Tada Y, Furuki M, Hara Y et al (1998) A missense mutation of the gene for Na+, K(+)-ATPase alpha-subunit causes abnormal feeding behavior in *Caenorhabditis elegans*. Biochem Biophys Res Commun 248:778–782
15. Yasufumi Y, Shingo N, Kunitoshi Y, Teru O (2006) Mutational analysis of the functional motifs in the ATPase domain of *Caenorhabditis elegans* fidgetin homologue FIGL-1: firm evidence for an intersubunit catalysis mechanism of ATP hydrolysis by AAA ATPases. J Struct Biol 156(1):93–100
16. Seamen E, Blanchette JM, Han M (2009) P-type ATPase TAT-2 negatively regulates monomethyl branched-chain fatty acid mediated function in post-embryonic growth and development in C. elegans. PLoS Genet 5(8):e1000589
17. Heinick A, Urban K, Roth S et al (2010) *Caenorhabditis elegans* P5B-type ATPase CATP-5 operates in polyamine transport and is crucial for norspermidine-mediated suppression of RNA interference. FASEB J 24(1):206–217
18. Povyakel LI (1968) Adenosine triphosphate activity in muscle tissue mitochondria of the round worm (*Ascaris suum* Goeze 1758). Med Parasitol Parasit Dis 37:530–533
19. Shaw MK (1987) *Schistosoma mansoni*: fine structural localization of tegumental adenosine triphosphatases. Exp Parasitol 64:310–321
20. Agosin M, Aravena LC (1959) Anaerobic glycolysis in homogenates of *Trichinella spiralis* larvae. Exp Parasitol 8(1):10–30
21. Moczon T (1973) Histochemical studies on the enzymes of *Hymenolepis diminuta.* II. Nonspecific and specific phosphatases in oncospheres and cysticercoids. Acta Parasitol Pol 21(1–10):99–106
22. Carafoli E (1987) Intracellular calcium homeostasis. Annu Rev Biochem 56:395–433
23. Jacob JE, Vanholme B, Leeuwen TV et al (2009) A unique genetic code change in the mitochondrial genome of the parasitic nematode *Radopholus similis*. BMC Res Notes 2:192
24. Okimoto R, Macfarlane JL, Clary DO et al (1992) The mitochondrial genomes of two nematodes, Caenorhabditis elegans and Ascaris suum. Genetics 130(3):471–498
25. Keddie EM, Higazi T, Unnasch TR (1998) The mitochondrial genome of Onchocerca volvulus: sequences, structure and phylogenetic analysis. Mol Biochem Parasitol 95:111–127
26. Hu M, Chilton NB, Gasser RB (2003) The mitochondrial genome of Strongyloides stercoralis (Nematoda)—idiosyncratic gene order and evolutionary implications. Int J Parasitol 33:1393–1408
27. Amjad M, Plattner S, Radakovic Z et al (2013) An Arabidopsis ATPase gene involved in nematode-induced syncytium development and abiotic stress responses. Plant J 74:852–866
28. Iyer LM, Leipe DD, Koonin EV, Aravind L (2004) Evolutionary history and higher order classification of AAA plus ATPases. J Struct Biol 146:11–31
29. Susiji W, Lalani Y, Rajapakse RPVJ et al (2009) Toxocara canis and Toxocara vitulorum: molecular characterization, discrimination, and phylogenetic analysis based on mitochondrial (ATP synthase subunit 6 and 12S) and nuclear ribosomal (ITS-2 and 28S) genes. Parasitol Res 104:1425–1430
30. Dawei L, Lijie C, Yuxi D (2011) Differential proteomic analysis of the resistant soybean infected by soybean cyst nematode, *Heterodera glycines* race 3. J Agric Sci 3(4)
31. Singh U, Misra S, Murthy PK et al (1997) Immunoreactive molecules of Brugia malayi and their diagnostic potential. Serodiagn Immunother Infect Dis 8:207–212

32. Genta RM (1989) Global prevalence of strongyloidiasis: critical review with epidemiologic insights into the prevention of disseminated disease. Rev Infect Dis 11:755–767
33. Grove DI (1996) Human strongyloidiasis. Adv Parasitol 38:251–309
34. Adedayo AO, Grell GA, Bellot P (2001) Case study: fatal strongyloidiasis associated with human T-cell lymphotropic virus type 1 infection. Am J Trop Med Hyg 65:650–651
35. Kerepesi LA, Keiser PB, Nolan TJ (2005) DNA immunization with Na^+-K^+ ATPase (*Sseat-6*) induces protective immunity to larval *Strongyloides stercoralis* in mice. Infect Immun 73(4):2298–2305
36. Tarrab-Hazdai R, Camacho M, Mendelovic F (1997) An association between activity of the Na/K-pump and resistance of *Schistosoma mansoni* towards complement-mediated killing. Parasite Immunol 19:395–400
37. Ligas JA, Kerepesi LA, Galioto AM, Lustigman S et al (2003) Specificity and mechanism of immunoglobulin M (IgM)- and IgG-dependent protective immunity to larval *Strongyloides stercoralis* in mice. Infect Immun 71:6835–6843
38. Matranga C, Pyle AM (2010) Double-stranded RNA-dependent ATPase DRH-3: insight into its role in RNAsilencing in Caenorhabditis elegans. J Biol Chem 285(33):25363–25371
39. Singh M, Shrivastava N, Saquib U, Siddiqui MI, Misra-Bhattacharya S (2013) Structural modelling studies and immunoprophylactic potential of Brugia malayi DEAD Box RNA helicase. Parasitology 140(8):1016–1025
40. Singh M, Singh PK, Misra-Bhattacharya S (2012) RNAi mediated silencing of ATPase RNA helicase gene in adult filarial parasite *Brugia malayi* impairs in vitro microfilaria release and adult parasite viability. J Biotechnol 157(3):351–358
41. Singh M, Srivastava KK, Bhattacharya SM (2008) Molecular cloning and characterization of a novel immunoreactive ATPase/RNA helicase in human filarial parasite Brugia malayi. Parasitol Res 104(4):753–761

Index

S. Chakraborti, N.S. Dhalla (eds.), *Regulation of Ca^{2+}-ATPases,V-ATPases and F-ATPases*, Advances in Biochemistry in Health and Disease 14,
DOI 10.1007/978-3-319-24780-9